ANL/RTR/TM-18/18 Rev. 0

Verification and Validation of the PLTEMP/ANL Code for Thermal-Hydraulic Analysis of Experimental and Test Reactors

Code Version 4.3

Nuclear Science and Engineering Division

About Argonne National Laboratory

Argonne is a U.S. Department of Energy laboratory managed by UChicago Argonne, LLC under contract DE-AC02-06CH11357. The Laboratory's main facility is outside Chicago, at 9700 South Cass Avenue, Argonne, Illinois 60439. For information about Argonne and its pioneering science and technology programs, see www.anl.gov.

DOCUMENT AVAILABILITY

Online Access: U.S. Department of Energy (DOE) reports produced after 1991 and a growing number of pre-1991 documents are available free at OSTI.GOV (http://www.osti.gov/), a service of the U.S. Dept. of Engery's Office of Scientific and Technical Information.

Reports not in digital format may be purchased by the public from the National Technical Information Service (NTIS):

U.S. Department of Commerce
National Technical Information Service
5301 Shawnee Rd
Alexandria, VA 22312
www.ntis.gov
Phone: (800) 553-NTIS (6847) or (703)
605-6000 Fax: (703) 605-6900
Email: **orders@ntis.gov**

Reports not in digital format are available to DOE and DOE contractors from the Office of Scientific and Technical Information (OSTI):

U.S. Department of Energy
Office of Scientific and Technical Information
P.O. Box 62
Oak Ridge, TN 37831-0062
www.osti.gov
Phone: (865) 576-8401
Fax: (865) 576-5728
Email: **reports@osti.gov**
Disclaimer

Disclaimer

This report was prepared as an account of work sponsored by an agency of the United States Government. Neither the United States Government nor any agency thereof, nor UChicago Argonne, LLC, nor any of their employees or officers, makes any warranty, express or implied, or assumes any legal liability or responsibility for the accuracy, completeness, or usefulness of any information, apparatus, product, or process disclosed, or represents that its use would not infringe privately owned rights. Reference herein to any specific commercial product, process, or service by trade name, trademark, manufacturer, or otherwise, does not necessarily constitute or imply its endorsement, recommendation, or favoring by the United States Government or any agency thereof. The views and opinions of document authors expressed herein do not necessarily state or reflect those of the United States Government or any agency thereof, Argonne National Laboratory, or UChicago Argonne, LLC.

ANL/RTR/TM-18/18 Rev. 0

Verification and Validation of the PLTEMP/ANL Code for Thermal-Hydraulic Analysis of Experimental and Test Reactors

Code Version 4.3

by
M. Kalimullah, A. P. Olson, E. E. Feldman, N. Hanan, and S. H. Pham
Nuclear Science and Engineering Division, Argonne National Laboratory

November 2018

(This page left intentionally blank)

TABLE OF CONTENTS

Chapter Title Page

1 Overview of Code Verification and Script for Routine Verification 1
1.1 Description and History of the Code 1
1.2 Overview of Code Verification and Validation 2
1.2.1 Temperature Calculation Using User-specified Channel Flow Rates in an Assembly Made of Multiple Three-layer Fuel Plates 3
1.2.2 Temperature Calculation Using User-specified Channel Flow Rates in an Assembly Made of Multiple Five-layer Fuel Tubes 5
1.2.3 Calculation of Channel Flow Rates for an Input Pressure Drop in a Fuel Assembly..... 6
1.2.4 Modeling of a Solid Fuel Rod at the Center of a Fuel Assembly Made of Multiple Coaxial Fuel Tubes 7
1.2.5 Calculation of Natural Circulation Flow Rate and the Resulting Temperatures 7
1.2.6 Hot Channel Factors (HCFs) to Account for the Fuel Plate Manufacturing Tolerances and the Uncertainties in Thermal-hydraulic Modeling 8
1.2.7 ONBR Based on Bergles-Rohsenow Correlation 9
1.2.8 OFIR Based on Whittle and Forgan Criterion 9
1.2.9 CHFR Based on Extended Groeneveld 2006 CHF Table..... 10
1.2.10 CHFR based for Low Flow and Atmospheric Pressure..... 11
1.2.11 CHFR based on Bernath Correlation 12
1.2.12 CHFR based on Labuntsov Correlation..... 12
1.2.13 CHFR Based on Sudo-Kaminaga Correlation 13
1.2.14 Search Capability..... 13
1.2.15 Longitudinal Fins on Fuel Plates 14
1.2.16 Coolant Thermal Properties 15
1.3 Other Publications on PLTEMP/ANL Verification and Validation 15
1.4 Verification Script for PLTEMP/ANL Code..... 16
1.5 REFERENCES 19
2 Verification of Exact and Broyden Solutions for Temperature Distribution in an Assembly Made of Multiple Three-layer Fuel Plates..... 36
2.1 Comparison of PLTEMP/ANL Exact Solution with RELAP5 Code 37
2.2 Heat-up of Non-adjacent Coolant Channels Due to Heat Source in a Fuel Plate..... 37
2.3 Equilibration of Coolant Channel Temperatures in the Axial Direction 37
2.4 Verification of Implementation of Heat Source in Cladding and Coolant Channels 38

2.5 List of Standard Problems 39

APPENDIX A IRT-1 LEU Steady State Analysis with Inner Channel Blocked RELAP5/Mod3.2.1.2 Vs. PLTEMP w/Exact Solution 67

3 Verification Tests of PLTEMP/ANL V3.0 Code Performed in Conjunction with the Solution to the KFKI Benchmark Problem 71

3.1 Introduction 71

3.2 Consistency Tests 71

3.3 Code Corrections 72

3.4 Discussion and Conclusions 72

APPENDIX B Steady-State Thermal Analysis for a Benchmark Problem Specified by KFKI for the Budapest Research Reactor 73

4 Verification of the Radial Geometry Exact Solution Method in PLTEMP/ANL Version 3.2 90

4.1 Radial Geometry Problem 1: 90

4.1.1 Hand Calculation for Problem 1 90

4.1.2 Solution of Problem 1 by Standalone Routine SLICEHTR 91

4.1.3 Solution of Modified Problem 1 by PLTEMP/ANL Version 3.2 92

4.2 Radial Geometry Problem 2: 92

4.2.1 Hand Calculation for Problem 2 93

4.2.2 Solution of Problem 2 by Standalone Routine SLICEHTR 94

4.2.3 Solution of Modified Problem 2 by PLTEMP Code Version 3.2 95

4.3 Calculation of Heat Coefficient in the Broyden Method 95

4.4 Radial Geometry Problem 3 96

4.4.1 Solution of Problem 3 by PLTEMP Code Version 3.2 96

4.4.2 Hand Calculation for Problem 3 97

4.5 Radial Geometry Problem 4: 99

4.5.1 Solution of Problem 4 by PLTEMP Code Version 3.1 99

4.5.2 Solution of Problem 4 by PLTEMP Code Version 3.2 99

4.6 Slab Geometry Problem 5 100

4.6.1 Hand Calculation for Problem 5 100

4.6.2 Comparison of Solutions of Problem 5 by Slab Geometry Exact Method and Radial Geometry Exact Method 101

4.7 Hungarian Reactor Benchmark Problem with a Power of 90 kW 102

4.8 ASTRA2 Six-Tube Assembly Problem 3 Case 1 102

4.9 Conclusions 104

4.10 REFERENCES 105

APPENDIX C Enthalpy of Liquid Water Used in the PLTEMP Code 156

5 Numbering the Outermost Fuel Tube as the First When Using the Radial Geometry Exact Method in PLTEMP – Implementation and Verification 159

5.1 Introduction 159

5.2 Technique Used if Input Data Has the Outermost Tube First 159

5.3 Verification of the Implementation of the Technique 159

5.4 Historical Perspective on PLTEMP/ANL Code Versions 162

5.5 REFERENCES 163

6 Verification of Carnavos Correlation Implemented in PLTEMP/ANL for Heat Transfer Coefficient and Friction Factor in Finned Coolant Channels 179

6.1 Introduction 179

6.2 Carnavos Correlation and its Implementation 179

6.3 Verification of Carnavos Correlation Implemented in PLTEMP/ANL 182

6.3.1 Verification of Friction Factor and Flow Rate in Finned Coolant Channels 183

6.3.2 Verification of Heat Transfer Coefficient 185

6.3.3 Comparison of Zero-Height Fin Option with No Fin Option 186

6.4 Code Output for Finned Coolant Channels 186

6.5 REFERENCES 189

7 Verification and Validation of Babelli-Ishii Flow Instability Criterion with 75 Tests Performed by Whittle and Forgan 195

7.1 Babelli-Ishii Criterion for Flow Instability 195

7.2 Liquid-Phase Pressure Drop in a Channel Heated by a Given Power 198

7.3 Application of Babelli-Ishii Criterion to the Channel Heated by a Given Power 198

7.4 Application of Babelli-Ishii Flow Instability Criterion to Whittle and Forgan Tests 199

7.4.1 Application of Flow Instability Criterion of Equation (7.1) 199

7.4.2 Application of Flow Instability Criterion of Eq. (7.5) 200

7.4.3 Approach to Flow Instability 201

7.5 Value of Parameter η According to the Instability Criterion of Equation (7.5) 202

7.6 A Program for Applying the Instability Criteria to Whittle and Forgan Tests 203

7.7 Conclusions 203

7.8 REFERENCES 206

APPENDIX D Derivation of Babelli and Ishii Flow Instability Equation 227

APPENDIX E *Babelli.WFtests.f* Program for Applying Flow Instability Criteria of Eq. (7.1) or Eq. (7.5) to Whittle and Forgan Tests. 228

8 Verification of Colburn Heat Transfer Correlation 234
8.1 Verification of the Corrected Code 234
8.2 Conclusion 235
9 Verification of the Natural Circulation Option Implemented in the PLTEMP/ANL V3.5 Code 238
9.1 Introduction 238
9.2 Hand Calculation for a Natural Circulation Test Problem 238
9.3 Frictional Pressure Drop Calculation in the Heated Section Without Dividing it into Sub-sections 243
9.4 *Mathematica* Calculations Using Three Sets of Coolant Properties 244
9.5 NATCON Code Calculation 244
9.6 RELAP5-3D Code Calculation 244
9.7 PLTEMP/ANL Version 3.5 Code Calculation 247
9.8 Conclusion 248
9.9 REFERENCES 249
APPENDIX F *Mathematica* Program for Solving Sample Problem 20, Using Coolant Properties of the PLTEMP/ANL Code 259
APPENDIX G Natural Convective Test Case for PLEMP/ANL Solved with RELAP5 262
10 Verification of the Chimney Model in Natural Circulation Calculation Implemented in the PLTEMP/ANL V3.6 Code 264
10.1 Introduction 264
10.2 A Test Problem with Chimney 264
10.3 *Mathematica* Calculations 265
10.4 NATCON Code Calculation 265
10.5 PLTEMP/ANL Version 3.6 Code Calculation 266
10.6 Conclusion 267
10.7 REFERENCES 269
APPENDIX H *Mathematica* Program for Solving Test Problem 22 281
11 Verification of the Hot Channel Factors Option in Natural Circulation Calculation by PLTEMP/ANL V3.6 284
11.1 Introduction 284
11.2 Test Problem Used in Verification 285
11.3 *Mathematica* Calculations 285
11.4 PLTEMP/ANL Version 3.6 Code Calculation 286
11.5 Conclusions 287
11.6 REFERENCES 288

APPENDIX I *Mathematica* Program for Solving Test Problem 21 301

12 Verification of the Search Capability in PLTEMP/ANL V3.7 304

12.1 Introduction 304

12.2 History Data and Search Capability 304

12.3 Implementation of the Search Capability 305

12.4 Verification for a Test Problem without Hot Channel Factors 306

12.5 Verification for a Test Problem Using Hot Channel Factors 307

12.6 Conclusions 308

12.7 REFERENCES 309

13 Verification and Validation of the Sudo-Kaminaga CHF Correlation for Rectangular Channels as Implemented in the PLTEMP/ANL Code 326

13.1 Introduction 326

13.2 Sudo-Kaminaga CHF Correlation 326

13.3 Validation of the Sudo-Kaminaga CHF Correlation Implemented in PLTEMP/ANL 328

13.3.1 Validation at Lower Coolant Velocities 328

13.3.2 Verification at Higher Coolant Velocities 329

13.4 Parametric Studies of Sudo-Kaminaga CHF Correlation 330

13.4.1 Sensitivity of Sudo-Kaminaga CHF Correlation to Coolant Channel Thickness 330

13.4.2 Continuity of Sudo-Kaminaga CHF Correlation as a Function of Mass Velocity 330

13.5 Conclusions 331

13.6 REFERENCES 332

APPENDIX J PLTEMP/ANL Input Data Files for 11 CHF Tests Done by Mirshak, Durant, and Towell 343

14 Comparison between PLTEMP/ANL and Hand Calculation for Interpolating the Groeneveld 2006 CHF Tables 353

14.1 Introduction 353

14.2 PLTEMP/ANL-Calculated CHF for a Standard Test Problem 353

14.3 Hand Calculation of CHF 353

14.4 Comparison between Hand and PLTEMP/ANL Calculations 355

14.5 REFERENCES 355

15 Verification of Pressure Drops during Subcooled Nucleate Boiling by Comparison with the RELAP5 Code 358

15.1 Background 358

15.2 Test Case 359

15.3 Solution Procedure and Results 359

15.4 Analysis 360
15.5 Conclusions 361
15.6 REFERENCES 362
16 Verification of the PLTEMP/ANL Capability to Model a Solid Fuel Rod at the Center of a Fuel Assembly of Nested Fuel Tubes 363
16.1 Introduction 363
16.2 Comparison of PLTEMP with an Independent Method 363
16.2.1 An Independent Method of Calculating Steady-State Temperature Distribution in a Fuel Assembly Consisting of Six Fuel Tubes 364
16.2.2 Solution of Test Problems with Six Fuel Tubes by an Independent Method 366
16.2.3 Verification of PLTEMP against Solution Obtained by an Independent Method 367
16.3 Comparison of Two PLTEMP Solutions of a Six-Tube Test Problem 3 with its Spreadsheet Solution 368
17 Verification of H_2O and D_2O Coolant Properties Calculated by the Code Version 4.2 388
17.1 Introduction and Summary 388
17.2 Verification of Coolant Thermal Properties 388
17.2.1 Verification of Liquid H_2O Thermal Properties 389
17.2.2 Verification of Liquid D_2O Thermal Properties 389
17.3 Conclusions 390
17.4 REFERENCES 390
18 Implementation and Verification of Carnavos Correlations for Heat Transfer Coefficient and Friction Factor in Channels Having Longitudinal Fins in the Radial Geometry Option of PLTEMP/ANL Code 425
18.1 Introduction and Summary 425
18.2 Carnavos Correlation and its Implementation 426
18.3 Verification of Carnavos Correlation in Radial Geometry 433
18.3.1 Plan of Testing and Verification 433
18.3.2 Verification of Geometrical Parameters for Test Problem 34 435
18.3.3 Comparison of Code Results for Two Models of Test Problem 34 435
18.3.4 Comparison of Code Results for Test Problem 34 Modified to Have No Fins 435
18.3.5 Hand Calculation of Heat Transfer Coefficient for Test Problem 34 with Fins 436
18.4 REFERENCES 440
19 Comparison of PLTEMPANL_4.2_r80_160720 Calculation with Carnavos' Experimental Data of Internally Finned Tubes 463
19.1 Introduction 463
19.2 Carnavos Experiment 463

19.3 PLTEMP/ANL Modeling 464
19.4 Comparison of Calculation Results and Experimental Data 464
19.4.1 Data of $Nu/Pr^{0.4}$ 464
19.4.2 Friction Factor 465
19.5 Conclusion 465
19.6 REFERENCES 465
20 Testing of Carnavos Correlations for Heat Transfer Coefficient and Friction Factor with Longitudinal Fins over a Part of the Coolant Channel Perimeter in the PLTEMP/ANL Version 4.2_r80_160720 Code 472
20.1 Introduction and Summary 472
20.2 Verification for Standard Test Problem 36 472
20.3 Conclusion 473
20.3 REFERENCES 473
21 Verification of PLTEMPANL_4.2_r80_160720 for Finned Pin Problems 478
21.1 Introduction 478
21.2 Finned Fuel Pin Test Problems 478
21.3 PLTEMP/ANL Model 478
21.4 Hand Calculation Procedure 479
21.5 Comparison between Code and Hand Calculations 480
21.6 REFERENCES 480
22 Verification of the Heat Transfer Method for Fuel Assemblies Made of Multiple Five-Layer Plates and the Calculation of ONBR and OFIR in PLTEMP/ANL 485
22.1 Introduction and Executive Summary 485
22.2 Development of a Spreadsheet for Calculating Temperature Distribution in Fuel Assemblies Made of Five-Layer Plates with Plate-by-Plate Axial Power Shape 487
22.2.1 Method Used in the Spreadsheet to Calculate Temperature Distribution 487
22.2.2 D_2O Coolant Thermal Properties Used in the Spreadsheet 490
22.3 Verification of PLTEMP/ANL Heat Transfer Method for an Assembly of Five-Layer Fuel Plates 491
22.3.1 Problem 38 with Symmetrical Fuel Plates and Linear Axial Power Shape 492
22.3.2 Problem 39 with Unsymmetrical Plate 1 in Assembly 1 and Linear Axial Power Shape 492
22.3.3 Problem 40 with Unsymmetrical Plates in Assembly 1 and Linear Axial Power Shape 493
22.3.4 Problem 41 with Unsymmetrical Plates in Both Assemblies and Plate-by-Plate Axial Power Shape 494

22.3.5 Problem 42 with Unsymmetrical and Unequal Power Plates in Both Assemblies and Plate-by-Plate Axial Power Shape 494
22.4 Verification of Onset of Nucleate Boiling Ratio 495
22.5 Verification of Onset of Flow Instability Ratio 498
22.6 Conclusions 499
22.7 REFERENCES 502
23 Verification of Flow Rate Calculation for a Specified Frictional Pressure Drop ... 543
23.1 Flow Rate Calculation Method in PLTEMP/ANL 543
23.2 Problems Used in Verification of the PLTEMP/ANL Flow Rate Calculation 545
23.3 Verification of Code-Calculated Flow Rates by Comparison with the Spreadsheet 545
23.3.1 Verification of Code-Calculated Flow Rates 546
23.3.2 Comparison of Channel Exit Temperatures 547
23.4 Channel Flow Rate Error due to Lack of Thermal-Hydraulic Iteration 547
23.5 Conclusions 550
APPENDIX K Spreadsheet for Calculating Flow Rate to Verify PLTEMP/ANL 551
APPENDIX L Calculation of Channel Flow Rates in the PLTEMP/ANL Code 559
24 Verification of the Bernath and the Labuntsov CHF Correlations in PLTEMP/ANL 587
24.1 Introduction 587
24.2 Verification of Bernath Critical Heat Flux Correlation 587
24.3 Verification of Labuntsov Critical Heat Flux Correlation 589
24.4 REFERENCES 592
25 Verification of Newly Implemented Hot Channel Factors for Coolant Velocity and Channel Heated Diameter 600
25.1 Step 1 - Verification of Correct Reading of Input Data for the Two New HCFs 601
25.2 Step 2 - Verification of Correct Calculation of Flow Instability Ratio for Each Channel 602
25.3 Step 3 - Verification of CHF and CHFR by the Checker Program for the Limiting FIR Channel and the Limiting CHF Channel 603
25.4 Conclusions 605
25.5 REFERENCES 605
26 Verification and Validation of Heat Transfer with Lateral Conduction Option in PLTEMP/ANL Code V4.3 607
26.1 Introduction 607
26.2 Test Problem and Models 607
26.3 Comparison between PLTEMP/ANL and COMSOL Calculations 607
26.4 Checking the Search Option of the Code 608

26.5 Conclusion 608
26.6 REFERENCE ……...…….. 608
27 Closing Remarks …….….….613

LIST OF FIGURES

Figure Page

Figure 1.1 Cross Section of a Typical Fuel Assembly Having Six Fuel Plates Modeled by the PLTEMP/ANL Code 22

Figure 1.2 Pressure Drop and its Frictional Component in Multiple Axial Regions of a Fuel Assembly. Region 1 is the Assembly Inlet Section, Region 2 is the Fueled Length, and Region 3 is the Assembly Exit Section..... 23

Figure 1.3 Coolant Flow Path in a Fuel Assembly and Chimney Modeled in PLTEMP/ANL (Multiple Axial Regions Downstream of the Heated Section are Allowed) 24

Figure 1.4 Fig. 1.4. Comparison of Extended Groeneveld Table and Hall-Mudawar ICC Correlation to Mirshak's Measured 65 CHF Data Points..... 25

Figure 1.5 Input Filename *input.A2.p3.c3r* Used as Standard Problem 1 in PLTEMP/ANL Verification Script 26

Figure 1.6 Input Filename *input.12assemblies* Used as Standard Problem 2 in PLTEMP/ANL Verification Script 27

Figure 1.7 Input Filename *input.2assemblies* Used as Standard Problem 3 in PLTEMP/ANL Verification Script 28

Figure 1.8 Input Filename *input.2subassTypes* Used as Standard Problem 4 in PLTEMP/ANL Verification Script 29

Figure 1.9 Input Filename *input.DeltaPloop_Powerloop* Used as Standard Problem 5 in PLTEMP/ANL Verification Script..... 30

Figure 1.10 Input Filename *input.fixedflows* Used as Standard Problem 6 in PLTEMP/ANL Verification Script 31

Figure 1.11 Input Filename *input.Powerloop* Used as Standard Problem 7 in PLTEMP/ANL Verification Script 32

Figure 1.12 Input Filename *input.pressuredriven* Used as Standard Problem 8 in PLTEMP/ANL Verification Script 33

Figure 2.1 PLTEMP/ANL V3.0 Input Data for Standard Problem 10, a Assembly With Heat Source in Fuel Plate 1 Only 41

Figure 2.2 Exact Solution by PLTEMP/ANL V3.0 for a Assembly With Heat Source in Fuel Plate 1 Only, Heat Transfer to Farther Channels Using Actual Thermal Conductivity of Water..... 42

Figure 2.3 Exact Solution by PLTEMP/ANL V3.0 for a Assembly With Heat Source in Fuel Plate 1 Only, Heat Transfer to Farther Channels With Water Thermal Conductivity Multiplied by 10..... 43

Figure 2.4 Exact Solution by PLTEMP/ANL V3.0 for a Assembly With Heat Source in Fuel Plate 1 Only, Heat Transfer to Farther Channels With Water Thermal Conductivity Multiplied by 100..... 44

Figure 2.5 Exact Solution by PLTEMP/ANL V3.0 for a Assembly With Heat Source in Fuel Plate 1 Only, Heat Transfer to Farther Channels With Water Thermal Conductivity Multiplied by 1000 45

Figure 2.6 PLTEMP/ANL V3.0 Input Data for Standard Problem 11 – Equilibration of Coolant Channel Temperatures over Unheated Axial Length 46

Figure 2.7 Exact Solution by PLTEMP/ANL V3.0 for Standard Problem 11 – Equilibration of Coolant Channel Temperatures over Unheated Axial Length 47

Figure 2.8 Standard Problem 12 Input Data for PLTEMP/ANL V3.0: Practically Zero Cladding Thickness, Heat Source in Fuel, and No Heat Source in Cladding and Coolant (Fuel Meat Thickness = 2.0 mm) 49

Figure 2.9 Exact Solution of Standard Problem 12: Practically Zero Cladding Thickness, Heat Source in Fuel, No Heat Source in Cladding and Coolant (Fuel Meat Thickness = 2.0 mm) 50

Figure 2.10 Standard Problem 13 Input Data for PLTEMP/ANL V3.0: 50% of Reactor Power Produced in Fuel and 50% in Cladding, No Heat Source in Coolant (Cladding Thickness = 0.5 mm) 51

Figure 2.11 Exact Solution of Standard Problem 13: 50% of Reactor Power Produced in Fuel and 50% in Cladding, No Heat Source in Coolant (Cladding Thickness = 0.5 mm) 52

Figure 2.12 Standard Problem 14 Input Data for PLTEMP/ANL V3.0: 10% of Reactor Power Produced in Fuel and 90% in Cladding, No Heat Source in Coolant (Cladding Thickness = 0.9 mm) 53

Figure 2.13 Exact Solution of Standard Problem 14: 10% of Reactor Power Produced in Fuel and 90% in Cladding, No Heat Source in Coolant (Cladding Thickness = 0.9 mm) 54

Figure 2.14 Standard Problem 15 Input Data for PLTEMP/ANL V3.0: 100% of Reactor Power Directly Deposited in Coolant (No Heat Source in Fuel and Cladding) 55

Figure 2.15 Exact Solution of Standard Problem 15: 100% of Reactor Power Directly Deposited in Coolant (No Heat Source in Fuel and Cladding) 56

Figure 4.1 Solution of Radial Geometry Problem 1 Obtained by the Standalone Routine SLICEHTR 106

Figure 4.2 Solution of Radial Geometry Problem 1 Slightly Modified by Setting $h_1 = 10^{-6}$ W/m^2-°C, Obtained by the Standalone Routine SLICEHTR 106

Figure 4.3 PLTEMP/ANL Version 3.2 Code Input Data for Radial Geometry Problem 1 Slightly Modified by Setting $h_1 = 10^{-6}$ W/m^2-°C 107

Figure 4.4 Solution of Radial Geometry Problem 1 Slightly Modified by Setting $h_1 = 10^{-6}$ W/m^2-°C, Obtained by the Exact Method in PLTEMP/ANL Version 3.2 108

Figure 4.5 Solution of Radial Geometry Problem 2 Obtained by the Standalone Routine SLICEHTR 109

Figure 4.6 Solution of Radial Geometry Problem 2 Slightly Modified by Setting $h_1 = 10^{-6}$ W/m^2-°C, Obtained by the Standalone Routine SLICEHTR 109

Figure 4.7 PLTEMP/ANL Version 3.2 Code Input Data for Radial Geometry Problem 2 Slightly Modified by Setting $h_1 = 10^{-6}$ W/m^2-°C 110

Figure 4.8 Solution of Radial Geometry Problem 2 Slightly Modified by Setting $h_1 = 10^{-6}$ W/m^2-°C, Obtained by the Broyden Method in PLTEMP/ANL Version 3.2 111

Figure 4.9 Solution of Radial Geometry Problem 2 Slightly Modified by Setting $h_1 = 10^{-6}$ W/m^2-°C, Obtained by the Exact Method in PLTEMP/ANL Version 3.2 112

Figure 4.10 Comparison of Solutions of Problem 2 by the Broyden Method with Improved Film Coefficient and the Exact Method (For Each Axial Node the Broyden Method is Followed by Exact Method) 113

Figure 4.11 PLTEMP/ANL Version 3.2 Code Input Data for Radial Geometry Problem 3... 114

Figure 4.12 Solution of Radial Geometry Problem 3 by the Broyden Method in PLTEMP/ANL Version 3.2 115

Figure 4.13 Solution of Radial Geometry Problem 3 by the Exact Method in PLTEMP/ANL Version 3.2 116

Figure 4.14 Input Data for Radial Geometry Problem 4 for PLTEMP Versions 3.1 and 3.2 117

Figure 4.15 Solution of Radial Geometry Problem 4 by the Broyden Method in PLTEMP/ANL Version 3.1 118

Figure 4.16 Solution of Radial Geometry Problem 4 by the Broyden Method in PLTEMP/ANL Version 3.2 119

Figure 4.17 Solution of Radial Geometry Problem 4 by the Exact Method in PLTEMP/ANL Version 3.2 120

Figure 4.18 PLTEMP/ANL Version 3.2 Code Input Data for Slab Geometry Problem 5 Using the Slab Geometry Exact Method 121

Figure 4.19 PLTEMP/ANL Version 3.2 Code Input Data for Slab Geometry Problem 5 Using the Radial Geometry Exact Method with a Mean Tube Radius of 1000 m 122

Figure 4.20 Solution of Slab Geometry Problem 5 by the Slab Geometry Exact Method in PLTEMP/ANL Version 3.2 123

Figure 4.21 Solution of Slab Geometry Problem 5 by the Radial Geometry Exact Method in PLTEMP/ANL Version 3.2 (Using a Mean Tube Radius of 1000 m) 124

Figure 4.22 Input Data File for the Hungarian Reactor Benchmark Problem for PLTEMP/ANL Code Versions 3.1 and 3.2 125

Figure 4.23 Comparison of Solutions of Hungarian Reactor Benchmark Problem Using Constant Coolant Specific Heat Option ICP = 1 by PLTEMP/ANL Version 3.2 (For Each Axial Node Broyden Method is Followed by Exact Method) 126

Figure 4.24 Solution of Hungarian Reactor Benchmark Problem by the Broyden Method in PLTEMP/ANL Version 3.1 (Using Actual Coolant Properties) 130

Figure 4.25 Solution of Hungarian Reactor Benchmark Problem by the Broyden Method in PLTEMP/ANL Version 3.2 (Using Actual Coolant Properties) 132

Figure 4.26 Solution of Hungarian Reactor Benchmark Problem by the Exact Method in PLTEMP/ANL Version 3.2 (Using Actual Coolant Properties) 134

Figure 4.27 ASTRA2 Problem 3 Case 1 Input Data File for PLTEMP/ANL Code Versions 3.1 and 3.2 (Using C_p = 4180 J/kg-°C, and ρ = 1000 kg/m^3, Same as ASTRA2 Code Input) 136

Figure 4.28 Solution of ASTRA2 Problem 3 Case 1 by PLTEMP/ANL of May 22 2003 (From PLTEMP/ANL Output File output.astra2p3c1r.1) 137

Figure 4.29 Solution of ASTRA2 Problem 3 Case 1 by the Broyden Method in PLTEMP/ANL Version 3.1 (Using Coolant C_p = 4180 J/kg-°C, and ρ = 1000 kg/m^3, Same as ASTRA2 Code Input) 139

Figure 4.30 Solution of ASTRA2 Problem 3 Case 1 by the Broyden Method in PLTEMP/ANL Version 3.2 (Using Coolant C_p = 4180 J/kg-°C, and ρ = 1000 kg/m^3, Same as ASTRA2 Code Input) 143

Figure 4.31 Solution of ASTRA2 Problem 3 Case 1 by the Radial Geometry Exact Method in PLTEMP/ANL Version 3.2 (Using Coolant C_p = 4180 J/kg-°C, and ρ = 1000 kg/m^3, Same as ASTRA2 Code Input) 147

Figure 5.1 Input Data for Standard Problem 17 Having the Outermost Tube Numbered First in the Input Data 163

Figure 5.2 Input Data for Standard Problem 18 Having the Innermost Tube Numbered First in the Input Data 164

Figure 6.1 Reactor Coolant Channels with Longitudinal Inner Fins: 190

Figure 6.2 Fin Geometry Used in Calculating Coolant Flow Area in a Circular Tube Having Longitudinal Internal Fins 191

Figure 6.3 Input Data for Test Problem 16 Having MITR-Type Finned Coolant Channels . 192

Figure 7.1 Schematic Diagram of a Heated Coolant Channel with Downward Flow 207

Figure 7.2 Dependence of Total Pressure Drop on Inlet Velocity for a Coolant Channel with Downflow of Water at a Given Power of 7 kW 208

Figure 7.3 Dependence of Total Pressure Drop on Inlet Velocity for a Coolant Channel with Upflow of Water at a Given Power of 7 kW 209

Figure 7.4 Comparison of Coolant Inlet Velocity at OFI Calculated Using Eq. (7.1) Versus its Measured Value in 75 Tests Reported by Whittle and Forgan 210

Figure 7.5 Comparison of Coolant Inlet Velocity at OFI Calculated Using Eq. (7.5) Versus its Measured Value in 75 Tests Reported by Whittle and Forgan 211

Figure 7.6 Variation of Ratio N_{sub}/N_{zub} and Right Hand Side of Eq. (7.1) Over the Heated Length of Channel in Whittle and Forgan Test 1..... 212

Figure 8.1 Input Data File of the Sample Test Problem *input.file.sai.chi.inp3* Used in Verifying the Colburn Heat Transfer Coefficient 236

Figure 9.1 Geometry of a Coolant Channel in a Four-Plate Fuel Assembly Used in Sample Problem 20 250

Figure 9.2 NATCON Input Data for Sample Problem 20 Used in the Verification of Natural Circulation Calculation of PLTEMP/ANL Version 3.5..... 251

Figure 9.3 PLTEMP/ANL Input Data for Sample Problem 20 Used in the Verification of Natural Circulation Calculation by the Code..... 252

Figure 10.1 Coolant Flow Path in a Fuel Assembly and Chimney Modeled in PLTEMP/ANL (Multiple Axial Regions Downstream of the Heated Section Are Allowed)..... 270

Figure 10.2 Locations of Coolant Pressure in a Group of Fuel Assemblies Exiting into a Common Chimney 271

Figure 10.3 Geometry of a Coolant Channel in a Four-Plate Fuel Assembly Used in Test Problem 22 272

Figure 10.4 NATCON Input Data for Test Problem 22 Used in the Verification of the Chimney Model 273

Figure 10.5 PLTEMP/ANL Input Data for Test Problem 22 Used in the Verification of the Chimney Model..... 274

Figure 11.1 Coolant Flow Path in a Fuel Assembly and Chimney Modeled in PLTEMP/ANL (Multiple Axial Regions Downstream of the Heated Section Are Allowed)..... 289

Figure 11.2 Locations of Coolant Pressure in a Group of Fuel Assemblies Exiting into a Common Chimney 290

Figure 11.3 Geometry of a Coolant Channel in a Four-Plate Fuel Assembly Used in Test Problem 22 291

Figure 11.4 PLTEMP/ANL Input Data for Test Problem 21 Used in the Verification of Hot Channel Factors Treatment in Case of Natural Circulation..... 292

Figure 11.5 Solution of Test Problem 21 Assembly 1 by PLTEMP/ANL V3.6 Code – Nominal Case 293

Figure 11.6 Solution of Test Problem 21 Assembly 1 by PLTEMP/ANL V3.6 Code – Global Hot Channel Factors Applied FPOWER = 1.20, FFLOW = 1.20, FNUSLT = 1.15..... 294

Figure 11.7 Solution of Test Problem 21 Assembly 1 by PLTEMP/ANL V3.6 Code – All Six Hot Channel Factors Applied FPOWER = 1.20, FFLOW = 1.20, FNUSLT = 1.15, FBULK = 1.15, FFILM = 1.18, FFLUX = 1.22 295

Figure 12.1 Logical Flow Diagram of the Main Program of PLTEMP/ANL V3.7 Code..... 310

Figure 12.2 Input File for Test Problem 27 without Hot Channel Factors That Uses Double Search Type 21 311

Figure 12.3 Converged Input File for Test Problem 27 without the Search Option..... 312

Figure 12.4 Comparison of Key Results for Test Problem 27 Obtained by PLTEMP/ANL V3.7 and V3.6..... 313

Figure 12.5 Input File for Test Problem 28 with Hot Channel Factors Option 2 That Uses Double Search Type 21 314

Figure 12.6 Converged Input File for Test Problem 28 with Hot Channel Factors Option 2 Without the Search Option..... 315

Figure 12.7 Comparison of Key Results for Test Problem 28 Calculated by PLTEMP/ANL V3.7 and V3.6..... 316

Figure 12.8 Input File for Test Problem 29 Using Double Search Type 21 for 40 Target Values 317

Figure 12.9 History Data Printed by PLTEMP/ANL V3.7 for the Test Problem 29 318

Figure 12.10 Reactor Operation Diagram Showing the Relationship among Nominal Reactor Power, Nominal Core Flow, and the Minimum ONBR with Global and Local Hot Channel Factors 320

Figure 12.11 Reactor Operation Diagram Showing the Relationship among True Reactor Power, True Core Flow, and the Minimum ONBR with Global and Local Hot Channel Factors Applied..... 321

Figure 12.12 Reactor Operation Diagram Showing the Relationship among Nominal Core Flow, Maximum Cladding Surface Temperature, and the Minimum ONBR with Global and Local Hot Channel Factors Applied..... 322

Figure 12.13 Reactor Operation Diagram Showing the Relationship among Nominal Core Flow, Maximum Coolant Temperature, and the Minimum ONBR with Global and Local Hot Channel Factors Applied 323

Figure 12.14 Reactor Operation Diagram Showing the Relationship among Nominal Core Flow, Minimum Flow Instability Power Ratio, and the Minimum ONBR with Global and Local Hot Channel Factors Applied..... 324

Figure 13.1 Illustration of Sudo-Kaminaga Correlation for Upward and Downward Flows .. 333

Figure 13.2 Geometry of the Test Section Used by Sudo and Kaminaga for Measuring CHF 334

Figure 13.3 PLTEMP/ANL Input Data for the Test Section Used by Sudo and Kaminaga for Measuring CHF 335

Figure 13.4 Spreadsheet for Calculating the Effect of Varying Channel Thickness or Mass Velocity on the Sudo-Kaminaga CHF Correlation 336

Figure 14.1 A Part of the PLTEMP/ANL Output File Showing the CHFs for Fuel Assembly 1 of Standard Problem 12 356

Figure 15.1 Pressure Drop vs. Flow at 200 kW per Channel and 5.0 bar Exit Pressure 360

Figure 16.1 Vertical Section of an Experimental Reactor Fuel Assembly Consisting of Multiple Coaxial Fuel Tubes 369

Figure 16.2 PLTEMP Input Data File of Test Problem 1 370

Figure 16.3 PLTEMP Input Data File of Test Problem 2 371

Figure 16.4 PLTEMP Version 42bta_r65_131030 Calculated Results for Problem 1 Without Pinhole 372

Figure 16.5 PLTEMP Version 42bta_r65_131030 Calculated Results for Problem 2 With a Pinhole 373

Figure 16.6 PLTEMP Version 42bta_r65_131030 Calculated Areal Fractions for Problem 2 With a Pinhole 374

Figure 16.7 PLTEMP Input Data File of Test Problem 3 with Increasing Tube Radii 375

Figure 16.8 PLTEMP Input Data File of Test Problem 3 with Decreasing Tube Radii 376

Figure 16.9 PLTEMP/ANL V4.2 Output File for Test Problem 3 with Pinhole with Increasing RMID 377

Figure 16.10 PLTEMP/ANL V4.2 Output File for Test Problem 3 with Pinhole with Decreasing RMID 380

Figure 17.1 Liquid H_2O Enthalpy Calculated by PLTEMP/ANL Code as a Function of Temperature and Pressure 391

Figure 17.2 Liquid H_2O Enthalpy Calculated by PLTEMP/ANL Code as a Function of Temperature and Pressure (Enlarged View) 392

Figure 17.3 Liquid D_2O Enthalpy Calculated by PLTEMP/ANL Code as a Function of Temperature and Pressure 393

Figure 17.4 Liquid D_2O Enthalpy Calculated by PLTEMP/ANL Code as a Function of Temperature and Pressure (Enlarged View) 394

Figure 18.1 A Typical Fuel Assembly Made of Two Fuel Tubes Having Longitudinal Fins on the Inside and Outside of the Tubes (Input Option IGOM = 1) 441

Figure 18.2 Radial Geometry Used in Calculating Coolant Flow Area in an Assembly Made of Multiple Fuel Tubes Having Longitudinal Fins (Fuel tube radii entered in increasing order) 442

Figure 18.3 Input Data File of Standard Test Problem 34 Having Finned Channels with Fuel Tubes Radii in the Increasing Order 443

Figure 18.4 Input Data File of Standard Test Problem 34 Having Finned Channels with Fuel Tubes Radii in the Decreasing Order 444

Figure 18.5 Input Data File of Test Problem 34 of Fig. 18.3 Modified to Set the Fin Size to Zero While Using the Finned Channels Heat Transfer Correlation 445

Figure 18.6 Input Data File of Test Problem 34 of Fig. 18.3 Modified to Have No Fins While Using the Dittus-Boelter Heat Transfer Correlation 446

Figure 18.7 Part of Code Output Showing the Temperature Distribution Calculated Using the Input Data File of Fig. 18.3 (Radii of Fuel Tubes in the Increasing Order) 447

Figure 18.8 Part of Code Output Showing the Temperature Distribution Calculated Using the Input Data File of Fig. 18.4 (Radii of Fuel Tubes in the Decreasing Order) 450

Figure 18.9 Part of Code Output Showing the Temperature Distribution Calculated Using the Input Data File of Fig. 18.5 (Fin Size Set to Zero While Using the Carnavos Correlation) 453

Figure 18.10 Part of Code Output Showing the Temperature Distribution Calculated Using the Input Data File of Fig. 18.6 (Without Fins While Using the Dittus-Boelter Correlation) 456

Figure 19.1 Diagram of Carnavos Heat Transfer Experiment 466

Figure 19.2 Experimental Data Plot 467

Figure 19.3 PLTEMP/ANL Model of Carnavos Experiment Test-section 468

Figure 19.4 Sample Input Data (Tube #10 and Re = 17000) 468

Figure 19.5 Data of $Nu/Pr^{0.4}$ 469

Figure 19.6 Data of Friction Factor 469

Figure 20.1 Geometry of the Fuel Assembly in Standard Test Problem 36 474

Figure 20.2 PLTEMP/ANL Input Data File of Standard Test Problem 36 Used in Verification 475

Figure 21.1 Representative Cross Section of Finned Fuel Pin Geometry 481

Figure 21.2 Original Finned Fuel Pin (a) is Simulated by Tube Geometry of PLTEMP/ANL (b) 481

Figure 21.3 Sample Input Data (Case A) 482

Figure 22.1 Geometry and Thermal Conductivity of Fuel Assemblies in Problem 38 - Symmetrical Plates and Linear Axial Power Shape 503

Figure 22.2 Geometry and Thermal Conductivity of Fuel Assemblies in Problem 39 - Unsymmetrical Plate 1 in Assembly 1 and Linear Axial Power Shape 504

Figure 22.3 Geometry and Thermal Conductivity of Fuel Assemblies in Problem 40 - Unsymmetrical Plates in Assembly 1 and Linear Axial Power Shape 505

Figure 22.4 Geometry and Thermal Conductivity of Fuel Assemblies in Problem 41 - Unsymmetrical Plates in Both Assemblies and Plate-by-Plate Axial Power Shape 506

Figure 22.5 Geometry and Thermal Conductivity of Fuel Assemblies in Problem 42 - Unsymmetrical and Unequal Power Plates in Both Assemblies and Plate-by-Plate Axial Power Shape 507

Figure 22.6 Geometrical Representation of ONB Ratio for a Fuel Plate Axial Node in PLTEMP/ANL Code. 508

Figure 22.7 Comparison between PLTEMP/ANL- and Spreadsheet-Calculated ONBR by the First Approach for Fuel Assembly 1 of Problem 42 509

Figure 22.8 Comparison between PLTEMP/ANL- and Spreadsheet-Calculated ONBR by the First Approach for Fuel Assembly 2 of Problem 42 510

Figure 22.9 Comparison between PLTEMP/ANL- and Spreadsheet-Calculated ONBR by the Second Approach *before Code Correction* for Fuel Assembly 1 of Problem 42 511

Figure 22.10 Comparison between PLTEMP/ANL- and Spreadsheet-Calculated ONBR by the Second Approach *before Code Correction* for Fuel Assembly 2 of Problem 42 512

Figure 22.11 Comparison between PLTEMP/ANL- and Spreadsheet-Calculated ONBR by the Second Approach *after Code Correction* for Fuel Assembly 1 of Problem 42 513

Figure 22.12 Comparison between PLTEMP/ANL- and Spreadsheet-Calculated ONBR by the Second Approach *after Code Correction* for Fuel Assembly 2 of Problem 42 514

Figure 22.13 Part of PLTEMP/ANL Output File Showing the Values of OFIR for Test Problem 42..... 515

Figure 23.1 Pressure Drop and its Frictional Component in Several Axial Regions of a Fuel Assembly..... 562

Figure 23.2 Dependence of the Spreadsheet-Calculated Flow Rate in Fuel Assemblies of Problem 3C with Increasing Power 563

Figure 23.3 PLTEMP/ANL Input File *input.2Assemblies.stdprob3* for Standard Problem 3 Used to Verify the Flow Calculation Method Implemented in the Code..... 564

Figure 23.4 PLTEMP/ANL Input File *input.2Assemblies.stdprob3B* for Standard Problem 3B Used to Verify the Flow Calculation Method Implemented in the Code..... 565

Figure 23.5 PLTEMP/ANL Input File *input.2Assemblies.stdprob3C* for Standard Problem 3C Used to Verify the Flow Calculation Method Implemented in the Code..... 566

Figure 23.6 PLTEMP/ANL Input File *input.2Assemblies.stdprob43* for Standard Problem 43 Used to Verify the Flow Calculation Method Implemented in the Code 567

Figure 23.7 PLTEMP/ANL Input File *input.2Assemblies.stdprob44* for Standard Problem 44 Used to Verify the Flow Calculation Method Implemented in the Code 568

Figure 23.8 PLTEMP/ANL Input File *input.2Assemblies.stdprob45* for Standard Problem 45 Used to Verify the Flow Calculation Method Implemented in the Code 569

Figure 24.1 Comparison between PLTEMP/ANL- and Spreadsheet-Calculated Critical Heat Flux by Heat Balance Method using the Bernath Correlation for Fuel Assembly 1 of Problem 38 591

Figure 24.2 Comparison between PLTEMP/ANL- and Spreadsheet-Calculated Critical Heat Flux by Heat Balance Method using the Bernath Correlation for Fuel Assembly 2 of Problem 38 592

Figure 24.3 Comparison between PLTEMP/ANL- and Spreadsheet-Calculated Critical Heat Flux by Direct Substitution Method using the Labuntsov Correlation for Fuel Assembly 2 of Problem 38 593

Figure 24.4 Comparison between PLTEMP/ANL- and Spreadsheet-Calculated Critical Heat Flux by Direct Substitution Method using the Labuntsov Correlation for Fuel Assembly 2 of Problem 38 594

Figure 26.1 Test Problem Geometry 606

Figure 26.2 Cross-section of (a) PLTEMP/ANL Model and (b) COMSOL Model 606

Figure 26.3 Power Distribution 607

Figure 26.4 Comparison of Temperature Profiles 607

LIST OF TABLES

Table	Page
Table 1.1	Comparison of Spreadsheet and PLTEMP/ANL Solutions for Five Test Problems ... 33
Table 1.2	Comparison of PLTEMP/ANL- and Spreadsheet-Calculated Flow Rates for Three Problems ... 34
Table 1.3	Solution of the Standard Test Problem 20 by Different Codes Used to Verify the Natural Circulation Optionof the PLTEMP/ANL Code* ... 35
Table 1.4	Comparison of Thermal Properties of H_2O over 1 to 145 bar Pressure and 4 to 339 ºC Temperature between PLTEMP/ANL and NIST Data ... 35
Table 1.5	Comparison of Thermal Properties of D_2O over 1 to 150 bar Pressure and 5 to 341 ºC Temperature between PLTEMP/ANL and NIST Data ... 35
Table 2.1	Heat Transfer to Farther Channels in Standard Problem 10 Using the Exact Solution by PLTEMP/ANL V3.0 Code ... 57
Table 2.2	Comparison of PLTEMP/ANL Versions 3.0 and 2.14 for Standard Problem 1... 57
Table 2.3	Comparison of PLTEMP/ANL Versions 3.0 and 2.14 for Standard Problem 2... 57
Table 2.4	Comparison of PLTEMP/ANL Versions 3.0 and 2.14 for Standard Problem 3... 58
Table 2.5	Comparison of PLTEMP/ANL Versions 3.0 and 2.14 for Standard Problem 4... 58
Table 2.6	Comparison of PLTEMP/ANL Versions 3.0 and 2.14 for Standard Problem 5... 59
Table 2.7	Comparison of PLTEMP/ANL Versions 3.0 and 2.14 for Standard Problem 6... 64
Table 2.8	Comparison of PLTEMP/ANL Versions 3.0 and 2.14 for Standard Problem 7... 65
Table 2.9	Comparison of PLTEMP/ANL Versions 3.0 and 2.14 for Standard Problem 8... 66
Table 4.1	Comparison of Results by Four Methods for Radial Geometry Problem 1 ... 151
Table 4.2	Comparison of Results by Five Methods for Radial Geometry Problem 2 ... 151
Table 4.3	Pressure Derivative of Water Enthalpy at 1.5 bar and 50 °C Calculated From PLTEMP Code ... 152
Table 4.4	Summary of PLTEMP/ANL Code Results for Problem 4 ... 152
Table 4.5	Solution of Flat Plate Problem 5 by the Radial Geometry Exact Method Using Increasing Values of the Input Mean Radius of the Fuel Tube ... 153
Table 4.6	Comparison of Three Solutions for the Hungarian Reactor Benchmark Problem (Using Actual Coolant Properties) ... 153
Table4.7	Comparison of Solutions for ASTRA2 Radial Geometry Problem 3 Case 1 (Using the Constant Coolant C_p Option) ... 154
Table 4.8	Temperature Distribution in ASTRA2 Radial Geometry Problem 3 Case 1 With the Innermost Fuel Tube as the First ... 155

Table 5.1 Comparison of Six Solutions of Standard Problem 17 to Verify PLTEMP/ANL V3.4 165

Table 5.2 PLTEMP V3.2 Output for Problem 17 Having the Outermost Tube First in Input Data – Broyden Method 166

Table 5.3 PLTEMP V3.2 Output for Problem 18 Having the Innermost Tube First in Input Data – Broyden Method 168

Table 5.4 PLTEMP V3.4 Output for Problem 17 Having the Outermost Tube First in Input Data – Broyden Method 170

Table 5.5 PLTEMP V3.4 Output for Problem 18 Having the Innermost Tube First in Input Data – Broyden Method 172

Table 5.6 PLTEMP V3.4 Output for Problem 17 Having the Outermost Tube First in Input Data – Exact Method 174

Table 5.7 PLTEMP V3.4 Output for Problem 18 Having the Innermost Tube First in Input Data – Exact Method 176

Table 5.8 Comparison of Solutions by Different PLTEMP/ANL Versions for Standards Problems 17 and 18 178

Table 6.1 Comparison of PLTEMP Calculations With and Without Fins in Internal Coolant Channels of Test Problem 16 193

Table 6.2 Portion of PLTEMP/ANL V3.3 Output for Test Problem 16 Having MITR-Type Finned Coolant Channels 194

Table 7.1 Critical Value of Dimensionless Non-boiling Length $(L_{nvg}/L)_{critical}$ as Function of Subcooling Number 213

Table 7.2 Application of Babelli and Ishii Flow Instability Criterion to a Channel With Downflow 214

Table 7.3 Application of Babelli and Ishii Flow Instability Criterion to a Channel with Upflow 216

Table 7.4 Geometry and Operating Data for 75 Flow Instability Tests Performed by Whittle and Forgan 218

Table 7.5 Exit Temperature and Pressure Drop at Different Inlet Velocities Calculated in the Application ofBabelli and Ishii Flow Instability Criterion to a Typical Whittle and Forgan Test (Number 1) 220

Table 7.6 Application of Babelli and Ishii Flow Instability Criterion to a Typical Whittle and Forgan Test (Number 1) 222

Table 7.7 Comparison of Coolant Inlet Velocity at OFI Calculated Using Eq. (7.1) Versus its Measured Value in 75 Tests Reported by Whittle and Forgan 223

Table 7.8 Comparison of Coolant Inlet Velocity at OFI Calculated Using Eq. (7.5) Versus its Measured Value in 75 Tests Reported by Whittle and Forgan 225

Table 8.1 Comparison between Versions 3.4 and 3.0 of PLTEMP/ANL Code in Calculating Colburn Heat Transfer Coefficient 237

Table 9.1 Solution of Sample Problem 20 by Different Codes Used to Verify the Natural Circulation Option of PLTEMP/ANL Version 3.5 253

Table 9.2 Water Properties Used in the NATCON Code, RELAP5-3D Code, and PLTEMP/ANL Code 254

Table 9.3 *Mathematica* Solution of Standard Problem 20, Using Coolant Properties of NATCON Code 255

Table 9.4 *Mathematica* Solution of Standard Problem 20, Using Coolant Properties of PLTEMP/ANL Code 256

Table 9.5 *Mathematica* Solution of Standard Problem 20, Using Coolant Properties of RELAP5-3D Code 257

Table 9.6 RELAP5-3D-Calculated Solution of Sample Problem 20 and Two Analyses of the Solution 258

Table 10.1 Solution of Test Problem 22 by Different Codes Used to Verify the Chimney Model in Natural Circulation Calculation in PLTEMP/ANL V3.6 275

Table 10.2 Water Properties Used in the NATCON Code and PLTEMP/ANL Code 276

Table 10.3 Solution of Test Problem 22 with a Chimney by *Mathematica* Using PLTEMP/ANL Coolant Properties and Laminar and Transition Flow Friction Factor Correlations of PLTEMP/ANL 277

Table 10.4 Solution of Test Problem 22 with a Chimney by *Mathematica* Using NATCON Coolant Properties and Laminar and Transition Flow Friction Factor Correlations of PLTEMP/ANL 278

Table 10.5 Solution of Test Problem 22 with Chimney by NATCON Code Using its Built-in Coolant Properties and Friction Factor 279

Table 10.6 Solution of Test Problem 22 with a Chimney by PLTEMP/ANL V3.6 Code Using its Laminar and Transition Flow Friction Factor Correlations 280

Table 11.1 Comparison of PLTEMP/ANL V3.6 and *Mathematica* Solutions of Test Problem 21 Fuel Assembly 1, With and Without Global Hot Channel Factors . 296

Table 11.2 PLTEMP/ANL Results for Sample Problem 21 with Six Hot Channel Factors 297

Table 11.3 Solution of Test Problem 21 Fuel Assembly 1 by *Mathematica* Using PLTEMP/ANL Coolant Properties, ... 298

Table 11.4 Solution of Test Problem 21 Fuel Assembly 1 by *Mathematica* Using PLTEMP/ANL Coolant Properties, with Global Hot Channel Factors 299

Table 11.5 Temperature Distribution in Test Problem 21 Fuel Assembly 1 at the Channel Flow Rate Obtained byApplying Global Hot Channel Factors 300

Table 12.1 List of Searches Implemented in PLTEMP/ANL V3.7 325

Table 13.1 Test Section Used by Sudo and Kaminaga for Measuring CHF [Ref. 1] 337

Table 13.2 Comparison of PLTEMP/ANL with the Sudo and Kaminaga Experimental CHF Data for Upflow (Inlet Subcooling is 20 to 36 °C) 337

Table 13.3 Comparison of PLTEMP/ANL with the Sudo and Kaminaga Experimental CHF Data for Downflow (Inlet Subcooling is 69 to 78 °C) 337

Table 13.4 Spreadsheet Calculation of 11 CHF Tests Done by Mirshak, Durant, and Towell to Find the Geometry, Power, and Flow Data Required for Preparing PLTEMP/ANL Input Data Files 338

Table 13.5 Comparison of PLTEMP/ANL-Calculated CHF Using the Sudo-Kaminaga Correlation with Measured CHF for 11 CHF Tests Done by Mirshak, Durant, and Towell 339

Table 13.6 Effect of Varying Channel Thickness for a Fixed Coolant Mass Velocity on the Sudo-Kaminaga CHF Correlation (Mass Velocity = 10141.5 kg/m^2-s downflow)..... 340

Table 13.7 Effect of Varying Upward Mass Velocity for a Fixed Channel Thickness on the Sudo-Kaminaga CHF Correlation..... 341

Table 13.8 Effect of Varying Downward Mass Velocity for a Fixed Channel Thickness on the Sudo-Kaminaga CHF Correlation..... 342

Table 14.1 Part of Groeneveld 2006 CHF Table and Results of Inperpolation by Hand Calculation of CHF at Channel 1 Exit … ..... ……. 357

Table 15.1 Key Parameters 358

Table 15.2 Pressure Drop vs. Flow 359

Table 16.1 Geometry and Operating Data for a 6-Tube Radial Geometry Problem without a Pinhole - Test Problem 1..... 383

Table 16.2 Geometry and Operating Data for a 6-Tube Radial Geometry Problem with a Pinhole - Test Problem 2..... 384

Table 16.3 Excel Spreadsheet Calculated Results for Test Problem 1 385

Table 16.4 Results for Test Problem 1 Calculated by PLTEMP Versions 42bta_r65_131030 and 4.2 with Hard-Coded Values of Heat Transfer Coefficients..... 385

Table 16.5 Excel Spreadsheet Calculated Results for Test Problem 2 with Pinhole..... 386

Table 16.6 Results for Test Problem 2 Calculated by PLTEMP Versions 42bta_r65_131030 and 4.2 with Hard-Coded Values of Heat Transfer Coefficients..... 386

Table 16.7 Comparison of PLTEMP/ANL Version 4.2 Results for Test Problem 3 with Increasing versus Decreasing Fuel Tube Radii..... 387

Table 17.1 Comparison of Liquid H_2O Properties at 1 bar between PLTEMP/ANL Version 4.2 and NIST Data..... 395

Table 17.2 Comparison of Liquid H_2O Properties at 2 bar between PLTEMP/ANL Version 4.2 and NIST Data..... 396

Table 17.3 Comparison of Liquid H_2O Properties at 3 bar between PLTEMP/ANL Version 4.2 and NIST Data..... 397

Table 17.4 Comparison of Liquid H_2O Properties at 4 bar between PLTEMP/ANL Version 4.2 and NIST Data 398

Table 17.5 Comparison of Liquid H_2O Properties at 5 bar between PLTEMP/ANL Version 4.2 and NIST Data 399

Table 17.6 Comparison of Liquid H_2O Properties at 10 bar between PLTEMP/ANL Version 4.2 and NIST Data 400

Table 17.7 Comparison of Liquid H_2O Properties at 20 bar between PLTEMP/ANL Version 4.2 and NIST Data 401

Table 17.8 Comparison of Liquid H_2O Properties at 30 bar between PLTEMP/ANL Version 4.2 and NIST Data 402

Table 17.9 Comparison of Liquid H_2O Properties at 40 bar between PLTEMP/ANL Version 4.2 and NIST Data 403

Table 17.10 Comparison of Liquid H_2O Properties at 50 bar between PLTEMP/ANL Version 4.2 and NIST Data 404

Table 17.11 Comparison of Liquid H_2O Properties at 75 bar between PLTEMP/ANL Version 4.2 and NIST Data 405

Table 17.12 Comparison of Liquid H_2O Properties at 100 bar between PLTEMP/ANL Version 4.2 and NIST Data 406

Table 17.13 Comparison of Liquid H_2O Properties at 125 bar between PLTEMP/ANL Version 4.2 and NIST Data 407

Table 17.14 Comparison of Liquid H_2O Properties at 145 bar between PLTEMP/ANL Version 4.2 and NIST Data 408

Table 17.15 Comparison of Thermal Properties of H_2O over 1 to 145 bar Pressure and 4 to 339 ºC Temperature between PLTEMP/ANL Version 4.2 and NIST Data 409

Table 17.16 Comparison of Liquid D_2O Properties at 1 bar between PLTEMP/ANL Version 4.2 and NIST Data 410

Table 17.17 Comparison of Liquid D_2O Properties at 2 bar between PLTEMP/ANL Version 4.2 and NIST Data 411

Table 17.18 Comparison of Liquid D_2O Properties at 3 bar between PLTEMP/ANL Version 4.2 and NIST Data 412

Table 17.19 Comparison of Liquid D_2O Properties at 4 bar between PLTEMP/ANL Version 4.2 and NIST Data 413

Table 17.20 Comparison of Liquid D_2O Properties at 5 bar between PLTEMP/ANL Version 4.2 and NIST Data 414

Table 17.21 Comparison of Liquid D_2O Properties at 10 bar between PLTEMP/ANL Version 4.2 and NIST Data 415

Table 17.22 Comparison of Liquid D_2O Properties at 20 bar between PLTEMP/ANL Version 4.2 and NIST Data 416

Table 17.23 Comparison of Liquid D_2O Properties at 30 bar between PLTEMP/ANL Version 4.2 and NIST Data 417

Table 17.24 Comparison of Liquid D_2O Properties at 40 bar between PLTEMP/ANL Version 4.2 and NIST Data 418

Table 17.25 Comparison of Liquid D_2O Properties at 50 bar between PLTEMP/ANL Version 4.2 and NIST Data 419

Table 17.26 Comparison of Liquid D_2O Properties at 75 bar between PLTEMP/ANL Version 4.2 and NIST Data 420

Table 17.27 Comparison of Liquid D_2O Properties at 100 bar between PLTEMP/ANL Version 4.2 and NIST Data 421

Table 17.28 Comparison of Liquid D_2O Properties at 125 bar between PLTEMP/ANL Version 4.2 and NIST Data 422

Table 17.29 Comparison of Liquid D_2O Properties at 150 bar between PLTEMP/ANL Version 4.2 and NIST Data 423

Table 17.30 Comparison of Thermal Properties of D_2O over 1 to 150 bar Pressure and 5 to 341 ºC Temperature between PLTEMP/ANL Version 4.2 and NIST Data 424

Table 19.1 Geometry Data Calculated on Spreadsheet from the Input Data for Standard Test Problem 34 459

Table 18.2 Geometry Data Calculated on PLTEMP/ANL from the Input Data for Standard Test Problem 34 460

Table 18.3 Comparison of Channel Coolant Exit Temperatures Calculated Using the Input File of Fig. 18.3 with Those Calculated Using the Input File of Fig. 18.4 461

Table 18.4 Comparison of Channel Coolant Exit Temperatures Calculated Using the Input File of Fig. 18.5 with Those Calculated Using the Input File of Fig. 18.6 462

Table 19.1 Internally Finned Tube Dimension 470

Table 19.2 Comparison of $Nu/Pr^{0.4}$ 470

Table 19.3 Comparison of Friction Factor 471

Table 20.1 Fuel Assembly Design in Standard Test Problem 36 Used in PLTEMP/ANL Verification 476

Table 20.2 Comparison between PLTEMP/ANL and Spreadsheet Calculations of Heat Transfer Coefficient and Friction Factor in Finned Channels for Standard Test Problem 36 477

Table 21.1 Specifications of Finned Pin Test Problems 483

Table 22.1 Fuel Assembly Input Data for Test Problems 37, 38, 39, and 40 Used in Verification of Capability 2 of PLTEMP/ANL 516

Table 22.2 Coefficients of Fitted Equations for D_2O Coolant Thermal Properties at 0.36 MPa System pressure Used in the Spreadsheet 517

Table 22.3 Axial Power Shape by Fuel Plate in Problems 38, 39, and 40..... 518

Table 22.4 Axial Power Shape by Fuel Plate in Problems 41 and 42..... 518

Table 22.5 Comparison of PLTEMP/ANL and Spreadsheet-Calculated Position (X_{left}) of Peak Meat Temperature in Meat Thickness - Problem 38 519

Table 22.6 Spreadsheet-Calculated Temperature Distribution in Problem 38 520

Table 22.7 PLTEMP/ANL-Calculated Temperature Distribution in Problem 38..... 521

Table 22.8 Comparison of PLTEMP/ANL and Spreadsheet-Calculated Position (X_{left}) of Peak Meat Temperature in Meat Thickness - Problem 39 522

Table 22.9 Spreadsheet-Calculated Temperature Distribution in Problem 39 523

Table 22.10 PLTEMP/ANL-Calculated Temperature Distribution in Problem 39..... 523

Table 22.11 Comparison of PLTEMP/ANL and Spreadsheet-Calculated Position (X_{left}) of Peak Meat Temperature in Meat Thickness - Problem 40 525

Table 22.12 Spreadsheet-Calculated Temperature Distribution in Problem 40 526

Table 22.13 PLTEMP/ANL-Calculated Temperature Distribution in Problem 40..... 527

Table 22.14 Comparison of PLTEMP/ANL and Spreadsheet-Calculated Position (X_{left}) of Peak Meat Temperature in Meat Thickness - Problem 41 528

Table 22.15 Spreadsheet-Calculated Temperature Distribution in Problem 41 529

Table 22.16 PLTEMP/ANL-Calculated Temperature Distribution in Problem 41..... 530

Table 22.17 Comparison of PLTEMP/ANL and Spreadsheet-Calculated Position (X_{left}) of Peak Meat Temperature in Meat Thickness - Problem 42 531

Table 22.18 Spreadsheet-Calculated Temperature Distribution in Problem 42 532

Table 22.19 PLTEMP/ANL-Calculated Temperature Distribution in Problem 42..... 533

Table 22.20 Wall Temperatures and Heat Fluxes Calculated by Spreadsheet for Fuel Assembly 1 of Problem 42..... 534

Table 22.21 Wall Temperatures and Heat Fluxes Calculated by Spreadsheet for Fuel Assembly 2 of Problem 42..... 535

Table 22.22 Comparison of ONBR Calculated by the *First Approach* between PLTEMP/ANL and Spreadsheet for Fuel Assembly 1 of Problem 42 536

Table 22.23 Comparison of ONBR Calculated by the *First Approach* between PLTEMP/ANL and Spreadsheet for Fuel Assembly 2 of Problem 42 537

Table 22.24 Comparison of ONBR Calculated by the *Second Approach* between PLTEMP/ANL and Spreadsheet for Fuel Assembly 1 of Problem 42 – Using H_2O Saturation Temperature 538

Table 22.25 Comparison of ONBR Calculated by the *Second Approach* between PLTEMP/ANL and Spreadsheet for Fuel Assembly 2 of Problem 42 - Using H_2O Saturation Temperature 539

Table 22.26 Comparison of ONBR Calculated by the *Second Approach* between PLTEMP/ANL and Spreadsheet for Fuel Assembly 1 of Problem 42 – Using D_2O Saturation Temperature 540

Table 22.27 Comparison of ONBR Calculated by the *Second Approach* between PLTEMP/ANL and Spreadsheet for Fuel Assembly 2 of Problem 42 – Using D_2O Saturation Temperature 541

Table 22.28 Comparison of OFIR between PLTEMP/ANL and Spreadsheet for Fuel Assemblies 1 and 2 of Problem 42 542

Table 23.1 Spreadsheet Solution of Equations (K.16) to (K.18) to Find Channel Flow Rates in Assembly 2 of Problem 3 579

Table 23.2 Spreadsheet Calculation of Parameters in Eq. (K.12) to Find the Assembly Flow Rate for Problem 3C 580

Table 23.3 Spreadsheet Solution of Equations (K.16) to (K.18) to Find Channel Flow Rates in Assembly 1 of Problem 3C 581

Table 23.4 Spreadsheet Solution of Equations (K.16) to (K.18) to Find Channel Flow Rates in Assembly 2 of Problem 3C 582

Table 23.5 PLTEMP/ANL-Calculated Fraction of Fuel Plate Power Deposited in the Left Coolant Channel 583

Table 23.6 Change in Channel Flow Rates due to the Second T/H Iteration in Problem 3 (Coolant Velocity ~ 3 m/s) 584

Table 23.7 Change in Channel Flow Rates due to the Second T/H Iteration in Problem 43 (Coolant Velocity ~11 m/s) 584

Table 23.8 Change in Channel Flow Rates due to the Second T/H Iteration in Problem 44 (Coolant Velocity ~ 11 m/s) 585

Table 23.9 Change in Channel Flow Rates due to the Second T/H Iteration in Problem 45 (Coolant Velocity ~11 m/s) 585

Table 23.10 Spreadsheet-Calculated Flow in Standard Problem 3C at Different Reactor Powers 586

Table 24.1 Comparison between PLTEMP/ANL and Spreadsheet of CHF by Direct Substitution Method Using the Bernath Correlation for Problem 38 595

Table 24.2 Comparison between PLTEMP/ANL and Spreadsheet of CHF by Heat Balance Method Using the Bernath Correlation for Problem 38 596

Table 24.3 Detailed Comparison between PLTEMP/ANL and Spreadsheet of CHF by Heat Balance Method Using the Bernath Correlation For Axial Segment 10, Problem 38, Fuel Assembly 1, Plate 1 Left Side 597

Table 24.4 Comparison between PLTEMP/ANL and Spreadsheet of CHF by Direct Substitution Method Using the Labuntsov Correlation for Problem 38 598

Table 24.5 Comparison between PLTEMP/ANL and Spreadsheet of CHF by Heat Balance Method Using the Labuntsov Correlation for Problem 38 599

Table 25.1 Key Files Used in the Verification of Two New HCFs 606

Table 26.1 Test Problem Specifications .. ……..…….. 608

Table 26.2 Input Parameter Used for the Search Option of PLTEMP/ANL Model …… 608

Table 26.3 Heat Balance…….…….……. 609

Table 26.4 Comparision Between the Peak Fuel Temperatures and its Locations ……..…. 609

Table 26.5 Comparison Between PLTEMP/ANL Models With and Without the Search Option …….. …… 609

ACKNOWLEDGEMENT

The authors appreciate and acknowledge the encouragement of J. E. Matos and E. H. Wilson of the NSE Division to complete the report. Over the years 2006 to 2016, J. E. Matos pointed out, from time to time, the importance of verification and validation of the PLTEMP/ANL code, and as a result, several chapters were written during this decade. During the last two years, E. H. Wilson and H. M. Connaway of the NSE Division emphasized the importance of finishing the report to make it publishable. The first author is very grateful to E. E. Feldman, J. J. Sienicki, and A. P. Olson of the NSE Division for a thorough and critical review and for the numerous suggestions for improvement of the report. The incorporation of these suggestion greatly improved the clarity and readability of the report. The report would not have been complete without the help of K. R. Grudzinski and L. A. Bromberek who worked hard to prepare the table of contents, the list of figures and the list of tables, for which the authors are thankful to them. J. R. Licht and H. M. Connaway did a very valuable final review of the report, and the inclusion of their comments made the report more useful and understandable to the users of the current version of the code. The authors also thank former Argonne staff member Benoit Dionne for his valuable contributions to this technical work and to the development of this report.

This work was sponsored by the U.S. Department of Energy, Office of Material Management and Minimization in the U.S. National Nuclear Security AdministrationOffice of Defense Nuclear Nonproliferation under Contract DE-AC02-06CH11357.

Verification and Validation of the PLTEMP/ANL Code for Thermal-Hydraulic Analysis of Experimental and Test Reactors

M. Kalimullah, Arne P. Olson, E. E. Feldman, N. Hanan, and S. H. Pham
Argonne National Laboratory
Argonne, Illinois 60439 USA

ABSTRACT

The document compiles in a single volume the verification and validation works done for the PLTEMP/ANL code during the years of its development and improvement. The verification of sixteen capabilities of the PLTEMP/ANL Version 4.3 code that were identified by research reactor analysts as frequently used in their thermal-hydraulic analysis are described and documented. Each chapter of the document deals with the verification or validation of a specific model. The model verification is usually done by comparing the code with hand calculation, Microsoft spreadsheet calculation, or *Mathematica* calculation. The model validation is done by comparing the code with experimental data or a widely tested code like the RELAP5 code. In addition, some PLTEMP/ANL verification works that are available in the open literature are simply referenced and not included in the document. PLTEMP/ANL has been used in conversion safety analysis reports of several US and foreign research reactors that have been licensed and converted. A list of such reactors is given.

1 Overview of Code Verification and Script for Routine Verification

This report documents the verification and validation (V&V) of the PLTEMP/ANL Version 4.3 code. A brief description of the code and its history are given in Section 1.1. Section 1.2 provides an overview of PLTEMP/ANL verification and validation work done to date. Section 1.3 lists some publications by other authors on PLTEMP/ANL verification and validation. Section 1.4 describes a UNIX script developed to routinely verify the code after a code modification. The V&V work documented in this report was performed over several years, as code development progressed. In each verification/validation testing discussion, the version of PLTEMP/ANL which was initially used for the V&V work is referenced, but all of the testing presented in this report is applicable to current release version 4.3 of the code.

1.1 Description and History of the Code

Description: PLTEMP/ANL is a thermal-hydraulics code for calculating single-phase steady-state flow, temperature distribution, and safety margins to the onset nucleate boiling, static flow instability and critical heat flux, for a nuclear research reactor core consisting of one or more fuel assemblies of different types. The code is intended for thermal-hydraulic analysis of research reactor performance in the sub-cooled boiling regime. It is based on an evolutionary sequence of codes originally used for **pl**ate **temp**eratures, hence the name "PLTEMP", developed at Argonne National Laboratory over several decades. Fueled and non-fueled regions are modeled. Bypass flow through non-fueled channels is modeled. Each fuel assembly consists of one or more plates or tubes separated by coolant channels. The fuel plates may have one to five layers of different materials, each with heat generation. The width of a fuel plate may be divided into multiple longitudinal stripes, each with its own axial power shape. The temperature solution is effectively 2-dimensional. Axial thermal conduction in the fuel plates is ignored. Lateral coolant flow and intermixing over the width of a channel is ignored. It begins with a one-dimensional simultaneous solution across all coolant channels and fuel plates or tubes within a given fuel assembly, at the entrance to the assembly. The temperature solution is repeated for each axial node along the length of the fuel assembly. The geometry may be either slab or radial, corresponding to fuel assemblies made of a series of flat (or slightly curved) plates, or of nested tubes. A variety of thermal-hydraulic correlations are available with which to determine the cladding-to-coolant heat transfer, and the safety margins such as onset-of-nucleate boiling ratio (ONBR), departure from nucleate boiling ratio (DNBR), and onset of flow instability ratio (OFIR). Coolant properties for either light or heavy water are obtained from built-in FORTRAN functions rather than from tables. Both turbulent and laminar flow regimes can be modeled. Options to calculate both forced flow and natural circulation are available. A general search capability is available to greatly reduce the reactor analyst's time.

The code has been used in the approved conversion safety analysis reports (SAR) of research reactors regulated by the U.S. Nuclear Regulatory Commission. It has also been used in approved conversion safety analysis reports of the Portuguese research reactor (RPI) reviewed by the IAEA as well as other foreign research reactors.

History: PLTEMP/ANL was developed originally by Mishima, *et al.* [1, 2] in 1980 at the Argonne National Laboratory (ANL) under the sponsorship of the U.S. Department of Energy to analyze

the steady-state thermal-hydraulic conditions in the Kyoto University Research Reactor (KUR). It then had only 14 subroutines with a total of 2066 lines of FORTRAN and modeled a single thermal-hydraulic node without any axial power profile. Since then it has been improved to model assemblies made of up to 49 fuel plates or nested fuel tubes, cooled by up to 50 coolant channels with light or heavy water (see Fig. 1.1), and using multiple axial power profiles, and has 127 subroutines with a total of 26378 lines of FORTRAN. PLTEMP/ANL Version 4.3 is the current release version of the code.

The original PLTEMP was created to obtain a 1-dimensional steady-state temperature solution for a nuclear reactor core consisting of a group of fuel assemblies, each comprised of multiple flat plates separated by coolant channels. It was intended for analysis of "MTR-type" fuel assemblies. Bypass flow was modeled. The original PLTEMP was designed to represent flow and temperature conditions in a single hot channel, a single fuel assembly, or a reactor core consisting of up to five different types of fuel assemblies, and up to 30 fuel assemblies of each type. It was assumed that the coolant temperature was that at the outlet. This assumption gave conservative estimates for the peak fuel temperature and clad surface temperature, and for the safety margin to critical heat flux. The code was first applied to the Kyoto University Reactor (KUR), which is a light water-moderated, tank-type research reactor consisting of enriched uranium fuel of MTR-type, with a power of 5 MWt and a mean thermal neutron flux of 3.2×10^{13}n/cm^2/s.

<u>Code Limitations</u>: PLTEMP/ANL is based on single-phase (liquid phase) thermal-hydraulics and does not model boiling, axial thermal conduction in the fuel plates is ignored, and lateral coolant flow and intermixing over the width of a channel is ignored. When a coolant temperature greater than the saturation temperature is encountered (e.g., during a search iteration), it is reset equal to the saturation temperature. The code is still applicable to the steady-state analysis of research and test reactors because they all operate with a safety margin to the onset of nucleate boiling. The maximum pressure that can be used is 16.79 MPa for light or heavy water provided that the maximum coolant temperature does not exceed the smaller of the saturation temperature (T_{sat}) and 340 ºC. The saturation pressure at 340 C is 14.60 MPa. During power searches (for achieving a desired value of ONBR, OFIR, CHFR, or any other reactor parameter), the code will permit reaching T_{sat}. If the converged problem solution for coolant temperature does not exceed T_{sat}, then the solution is correct. If the converged problem solution has a coolant temperature that was reset to T_{sat}, then the solution is in a two-phase regime that the code cannot evaluate correctly.

1.2 Overview of Code Verification and Validation

Sixteen capabilities of the code that were identified by research reactor analysts as frequently used in their thermal-hydraulic analysis are described below, with verification for each. Verification means demonstrating that the code does what it was designed to do. Validation means that the code predictions are shown to agree with experimental data within an acceptable tolerance. These 16 capabilities were verified and documented over the last decade. The verification was done by comparing the results of the code for dozens of test problems with those obtained by hand calculation, Excel spreadsheet, *Mathematica*, and other computer codes. The model validation was done by comparing the code with experimental data.

In additioin to the 16 capabilities documented in this report, there are some code capabilities which were tested and verified during code development by the code developer but their verification is

not documented in this report, e.g., Babelli-Ishii flow instability criterion, heat transfer coefficient correlations in turbulent flow, laminar flow and mixed flow regimes (altogether 12 correlations), Forster-Grief ONB correlation, Russian modified Forster-Grief ONB correlation, Mirshak-Durant-Towell CHF correlation, Waterhead CHF correlation, Shah CHF correlation, the use of hot channel factors in a search problem using the newly implemented heat transfer method with lateral conduction, etc. These additional capabilities are presented in the User Guide. The analysts wishing to use those capabilities are responsible for their own V&V.

A procedure recommended to guard against modeling error in thermal-hydraulic analysis is to carry out the following five steps:

(1) Prepare a PLTEMP/ANL input data file including all the modeling features that are important for the problem in the analyst's engineering judgement.

(2) Then remove as many features of the problem as needed in order to simplify the problem so that the analyst is able to solve the simplified problem analytically, *without running the PLTEMP/ANL code*. For example, the analyst may assume that all fuel assemblies are identical having the same geometry, power and flow; all fuel plates are indentical; all coolant channels are identical and have the same flow; the axial power shape is flat; coolant properties are constant (temperature-independent), etc.,

(3) Solve the simplified problem analytically, *without running the code*. Run the code for the simplified problem. These two solutions of the simplified problem must be identical. The analyst has full confidence in the solution of the simplified problem.

(4) Now add one feature of the actual problem (a feature that was removed during simplification in Step 2), at a time, to the simplified problem to get an updated input data file, run the code for this updated input data file, try to understand and make sure that the change in results of the updated input file compared to those of the simplified problem are reasonable.

(5) Go on adding one feature at a time, running the run the code for this updated input data file, making sure that the change in the results of this updated input file compared to the results of the prior updated input file are reasonable. Adding a feature at a time in this way, arrive at the actual problem and its solution by the code, with full confidence in the solution.

The 16 capabilities addressed in this report include the calculation of channel flow rates in forced flow or in natural circulation. The code has a variety of correlations, described in Appendix IV of [3], to predict liquid-phase heat transfer, a variety of correlations to determine safety margins to Onset of Nucleate Boiling (ONB), Critical Heat Flux (CHF), and Onset of Flow Instability (OFI), including the effect of six user-input hot channel factors (HCFs). The six HCFs account for all manufacturing tolerances and modeling uncertainties, as described in Appendix V of [3]. A generalized search capability is available to the reactor designer as an aid to achieve a desired value of a chosen safety parameter, by adjusting the reactor power or the driving pressure drop. The chosen safety parameter could be the minimum ONBR (margin to ONB), the minimum DNBR (margin to CHF), the minimum FIR (margin to FI), the maximum cladding surface temperature, the maximum fuel temperature, or the maximum coolant temperature.

1.2.1 Temperature Calculation Using User-specified Channel Flow Rates in an Assembly Made of Multiple Three-layer Fuel Plates

This capability is used to calculate the coolant, cladding and fuel steady-state temperature distribution in one or more fuel assemblies, each made of up to 49 three-layer fuel plates.

Specifying the channel flow rates (rather than calculating the flow rates from a specified pressure drop) is useful for inter-code comparison of thermal modeling (i.e., calculation of temperatures) because the effect of inter-code hydraulic modeling differences is then eliminated. This capability permits only one axial power distribution shape for all fuel plates of the reactor.

Method: The code has three methods for this capability.
Method 1 (Broyden Method): The heated length of a fuel assembly is divided into a series of axial segments. Axial conduction is ignored and therefore the thermal solution for an axial segment depends only on that of the upstream segment. The segment at the core inlet is solved first, using the input coolant inlet temperature. Each segment is solved, simultaneously for all fuel plates and coolant channels in the assembly, in succession until the assembly exit. The fuel meat of all fuel plates have the same thickness and thermal conductivity. The claddings of all fuel plates have the same thickness and thermal conductivity. All fuel plates have the same axial power shape.

The temperature distribution in a fuel assembly made of K three-layer (fuel meat between two cladding layers) flat fuel plates is calculated by assuming a position ($X_{left,k}$ k=1, 2, 3, … K) of the peak temperature in the meat thickness of each plate of the fuel assembly, and then iteratively minimizing the difference between (i) the peak temperature in the meat thickness of a plate calculated from the coolant channel on the left side of the plate, and (ii) that calculated from the coolant channel on the right side of the plate, as described in Section 3.1 of [3]. The minimization is done by the Broyden method [4].

Method 2 (Exact Method): The first paragraph in Method 1 also applies here. All material layers of each fuel plate and all coolant channels may have a heat source to model fission and γ-heating in Method 2. This method for calculating axial and radial temperature distribution in an assembly made of K three-layer fuel plates cooled by K+1 coolant channels is documented in detail in Appendix VI of [3]. The method sets up (and solves by tridiagonal matrix inversion) K+1 simultaneous linear equations, Eq. (1.1), in K+1 bulk coolant temperatures, $T_{bc,k,n}$ for k = 1 to K+1, at the mid-height of an axial segment, n, of the fuel assembly.

$$a_k T_{bc,k-1,n} + b_k T_{bc,k,n} + c_k T_{bc,k+1,n} = d_k \quad \text{(for channels k = 1 through K+1)} \tag{1.1}$$

where the coefficients a_k , b_k , c_k and d_k are obtained from *closed-form* solutions of slab-geometry heat conduction differential equations in all 3K fuel tube material layers, *as complicated algebraic expressions* (with the aid of *Mathematica*) of the thicknesses, thermal conductivities, film coefficients, and power densities in the material layers and coolant channels. A similar method in cylindrical geometry, used for an assembly made of K three-layer nested fuel tubes cooled by K+1 annular coolant channels, is documented in detail in Appendix VIII of [3].

A similar exact method for calculating axial and radial temperature distribution in an assembly made of multiple *five-layer* fuel tubes/plates is documented in detail in Appendix XIII of [3].

Method 3 (Numerical Method with Lateral Heat Conduction): A method for calculating axial and radial temperature distribution, accounting for lateral heat conduction along the width of fuel plates, in an assembly made of K five-layer fuel plates cooled by K+1 coolant channels is documented in detail in Appendix XV of [3].

Verification: Using 18 test problems, Chapters 2 and 3 describe the verification of the Broyden method and the exact method (slab geometry), by comparison with RELAP5, by studying physical trends of PLTEMP/ANL results, and by comparison of different solutions by PLTEMP/ANL of physically the same problem using different modeling techniques in the input data. These 18 problems are included in the set of standard test problems in an automated code verification script that is run after every code modification.

Using 9 other test problems, Chapters 4 and 5 describe the verification of the exact method (radial geometry), by comparison of several solutions of the same problem by different methods (e.g. hand calculation aided by Mathematica, Broyden method, exact method for slab geometry, standalone programs).

A verification of Method 3 by comparison with an exact analytical series solution is given in Appendix XV of [3]. Another verification and validation of Method 3 by comparison with COMSOL is given in Chapter 26.

1.2.2 Temperature Calculation Using User-specified Channel Flow Rates in an Assembly Made of Multiple Five-layer Fuel Tubes

This capability is used to calculate the coolant, cladding and fuel steady-state temperature distribution in one or more fuel assemblies, each made of multiple 5-layer fuel tubes (or flat plates by specifying a large radius of curvature for the fuel tube, e.g., 50 m). The plate width is divided into multiple axial stripes. The axial power distribution shape can vary from plate to plate, and from axial stripe to stripe within a fuel plate.

Method: This method for calculating axial and radial temperature distribution in an assembly made of K different nested coaxial five-layer fuel tubes cooled by K+1 coolant channels of annular cross section is documented in detail in Appendix XIII of [3]. The normalization of reactor power distribution is documented in Appendix XIV of [3]. All the 5K material layers of K fuel tubes have different thicknesses, different thermal conductivities, and different axial power shapes. All material layers of each fuel tube and all coolant channels may have a heat source to model fission and γ-heating. Ignoring axial heat conduction in the tubes, the method sets up (and solves by tridiagonal matrix inversion) K+1 simultaneous linear equations, same as Eq. (1.1), in K+1 bulk coolant temperatures, $T_{bc,k,n}$ for k = 1 to K+1, at the mid-height of an axial segment, n, of the fuel assembly. The coefficients a_k , b_k , c_k and d_k of Eq. (1.1) are obtained from *closed-form* solutions of radial heat conduction differential equations in all 5K fuel tube material layers, *as even more complicated algebraic expressions* (with the aid of *Mathematica*) of the thicknesses, thermal conductivities, film coefficients, and power densities in the material layers and coolant channels.

Verification and/or Validation: Chapter 22 documents in detail the verification of this capability for fuel assemblies cooled by D_2O with user-input flow rates, by comparing the code with a spreadsheet developed (purely for the verification purpose) to calculate the axial and radial (across fuel plate thicknesses) temperature distribution in test problems having two fuel assemblies, with two plates in each assembly. The verification was done using a series of five standard test problems (Problems 38, 39, 40, 41 and 42) exercising an increasing number of code features. Problem 42 (that exercises most features of this capability) is included in the standard test problems of the

automated verification script. These were solved as slab geometry problems (IGOM=0) on the spreadsheet whereas they were solved by the code as radial geometry problems (IGOM=1) using a large radius of curvature of 50 m. This verifies that this capability can also be used to solve slab geometry problems by setting the radius of curvature to an artificially large value. The temperatures in these problems vary from 35 to 1605 °C, and the film coefficients are ~7500 W/m^2-C. Table 1.1 shows the temperature differences and film coefficient differences that are relatively small and demonstrate a good agreement between the spreadsheet and PLTEMP/ANL. The comparison also showed similarly good agreement for the locations of peak fuel temperatures, the margins to onset of nucleate boiling, and the margins to onset of flow instability.

1.2.3 Calculation of Channel Flow Rates for an Input Pressure Drop in a Fuel Assembly

The flow rates in each fuel assembly and in its coolant channels are calculated for a user-input frictional pressure drop in the assembly using the model shown in Fig. 1.2 and documented in Chapter 23.

Method: The fuel assembly is divided into an inlet region (region 1), a fueled region (region 2), and a series of one or more consecutive outlet regions (regions 3, 4, etc.). The fueled region consists of a number of parallel coolant channels of equal length. Each region is characterized by a flow area, a hydraulic diameter, a form-loss factor, and an axial length. All parallel channels in region 2 of an assembly are initially represented by a single equivalent channel having the total flow area, total wetted perimeter, and total flow rate of all the parallel channels. A starting guess for the assembly flow rate is used to get the coolant exit temperature in the assembly. The coolant temperature in region 1 is uniformly the inlet temperature; the coolant temperature in the fueled length is assumed to be the average of the inlet temperature and the calculated assembly exit temperature; the coolant temperature in region 3 and downstream is uniformly the assembly exit temperature. The coolant properties, the Reynolds number, and the friction factor are calculated for each region. Finally, a new value for the assembly flow rate is obtained by equating the input assembly frictional pressure drop to the sum of the frictional pressure drops in all axial regions, as shown by Eq. (1.2).

$$\Delta P_{fric} = \frac{W_f^2}{2} \sum_{n=1}^{3} \frac{K_n + f_n \, L_n / D_{h,n}}{\rho_n \, A_{f,n}^2} \tag{1.2}$$

The guessed assembly flow rate is adjusted iteratively to arrive at a converged flow-rate solution. The converged assembly flow rate is used to determined the frictional pressure drop in region 2 of the assembly, that is used to iteratively calculate the flow rate in each coolant channel of region 2. The coolant properties in each channel is calculated at the average temperature in the channel. For this purpose, the coolant temperature rise in each channel is calculated using the power deposited in each coolant channel, which is estimated by asuming that the power generated in each fuel plate is split equally between the two adjacent channels. After obtaining the solution for all channels, the converged flow rates of all channels are summed to obtain the assembly flow rate.

Verification and/or Validation: Chapter 23 documents the verification of this capability in detail by comparing the code-calculated flow rates for three standard problems (Problems 23, 23B, and 23C) with a spreadsheet developed for this purpose. The development and checking of the

spreadsheet itself is documented in Appendix K. Each problem models two fuel assemblies with 5 channels in each assembly, with a total power of 0.0001 MW, 1.0 MW, and 4.0 MW in Problems 23, 23B, and 23C, respectively. Table 1.2 shows a comparison between the code and the spreadsheet. The maximum absolute difference in channel flow rate in Problem 23B is 0.074%, that in Problem 23 is 0.097%, and that in assembly 1 of Problem 23C is 0.097%. These are good agreements. The maximum absolute difference in channel flow rate in assembly 2 of Problem 23C (having an unrealistic high power resulting in a channel temperature rise of 144 ºC whereas research reactors have a rise of about 20 ºC) is 1.361%. This is an acceptable agreement.

1.2.4 Modeling of a Solid Fuel Rod at the Center of a Fuel Assembly Made of Multiple Coaxial Fuel Tubes

This capability is used to model a central solid fuel rod with or without multiple coaxial fuel tubes around the fuel rod. Since the basic structure of the code requires a coolant channel on both sides of each fuel tube, the modeling of a central solid fuel rod requires a special attention described in Section 3.11 of [3].

Method: A central solid fuel rod is modeled by PLTEMP/ANL as a special case of the heat transfer method (described in Section 2.2 above) for an assembly made of five-layer nested fuel tubes. In this special case to model a *solid* fuel rod, the flow area of the innermost channel must be specified to be less than 10^{-15} m^2, the inner cladding thickness must be zero, and the code then internally sets the convective heat transfer coefficient to be 1.0 W/m^2-ºC for the innermost channel.

Verification and/or Validation: Section 16.2.3 documents the verification of this capability using a test problem (named Problem 2 with pinhole) for a fuel assembly having six fuel tubes of which the central one is a solid fuel rod with pinhole. The verification was done by comparing the code results (temperatures and safety margins) with an independent analytical solution developed for this purpose and numerically evaluated on a spreadsheet. The results of the comparison are:

Maximum Absolute Temperature Difference	= 0.131 ºC
RMS Temperature Difference	= 0.048 ºC

A verification of this capability in the case of natural circulation flow was done for the Ghana Research Reactor (GHARR-1), by comparing the code-calculated temperature drop in the fuel meat (118.293 ºC) with the hand-calculated value (118.343 ºC) using analytical equations.

1.2.5 Calculation of Natural Circulation Flow Rate and the Resulting Temperatures

This capability is used to calculate the buoyancy-induced steady-state flow rate (and the resulting temperature distribution) upwards through the fuel assemblies into a chimney and downwards in the cross sectional area outside the core within the reactor vessel. The flow through the fuel assemblies could be laminar or turbulent.

Method: The method of calculating the natural circulation flow rate, based on the flow resistances shown in Fig. 1.3, is documented in detail in Appendix XI of [3]. The solution strategy uses (i) inner iterations to find channel flow rates for a given set of coolant channel temperature profiles, and (ii) outer iterations to make the hydraulic calculation and the heat transfer calculation

consistent with each other. In computing the buoyancy head and frictional pressure drop, the method accounts for (i) the channel-to-channel variation of coolant temperature profiles, and (ii) the axial variation of coolant temperature, density, viscosity, Reynolds number, and friction factor.

Verification and/or Validation: A verification of this capability for a test Standard Problem 20 for a fuel assembly with each fuel plate producing equal power was done by comparing the code with hand calculation aided by Mathematica and the RELAP5-3D code [5]. As shown in Table 1.3, the natural circulation flow rate of 0.1093 kg/s in a channel compares well with 0.1086 kg/s calculated earlier by a hand calculation using *Mathematica* and confirmed by the NATCON [32] and RELAP5-3D [33] codes.

1.2.6 Hot Channel Factors (HCFs) to Account for the Fuel Plate Manufacturing Tolerances and the Uncertainties in Thermal-hydraulic Modeling

All manufacturing tolerances and modeling uncertainties are combined, outside of PLTEMP/ANL, into the following six (three global and three local) hot channel factors (HCFs) that are input to the code. The six HCFs are defined and the method of using them in the code are described in Section 3.5 of [3]. The six HCFs are usually the same for all channels, but they could be channel-dependent in PLTEMP/ANL.

Global (reactor system-wide) factors:

1. F_{power} = A factor to account for uncertainty in total reactor power measurement.
2. F_{flow} = A factor to account for uncertainty in total reactor flow measurement.
3. F_{Nuslt} = A factor to account for uncertainty in Nu number correlation.

Local (random hot spot) factors:

4. F_{bulk} = A factor for local bulk coolant temperature rise.
5. F_{film} = A factor for local temperature rise across the coolant film.
6. F_{flux} = A factor for local heat flux from cladding surface.

The method of combining the uncertainties depends on whether the flow is forced by an applied pressure drop (as described in Appendix V of [3]) or by natural circulation which depends on the assembly power (as described in [6]).

Two new local hot channel factors were implemented in the code in the year 2018, i.e., F_{dhtd} a factor for coolant channel heated diameter, and F_{velc} a factor for channel coolant velocity. Chapter 25 describes these HCFs and documents a verification of their implementation.

Method: The code incorporates the effect of these uncertainties into the calculated temperatures and safety margins, by performing the following three calculations: (1) Nominal or best estimate calculation, (2) A calculation that incorporates only the reactor-wide uncertainties in power, flow, and (3) A final calculation that incorporates the effects of local random uncertainties into the 2nd. calculation. The resulting bulk coolant temperature rise, film temperature rise, and heat flux in the final calculation are given by the following equations:

$$T_{b,hc} - T_{in} = F_{bulk}\,(T_{b,op} - T_{in}) \tag{1.3}$$
$$T_{w,hc} - T_{b,hc} = F_{film}\,(T_{w,op} - T_{b,op}) \tag{1.4}$$
$$q''_{hc} = F_{flux}\,q''_{op} \tag{1.5}$$

Verification and/or Validation: Using a standard test Problem 21 with natural circulation flow in a 1.05 m long vertical rectangular duct (3 mm × 30 mm), Table 11.2 in Chapter 11 documents the verification of how the hot channel factors are incorporated into the temperature distribution. All three calculations (nominal without any HCF, results with three global HCFs, results with all six HCFs) are printed by the code. This aids in verification by hand calculation.

1.2.7 ONBR Based on Bergles-Rohsenow Correlation

This capability is used to estimate the safety margin to the onset of nucleate boiling (ONB), i.e., the power that would cause the onset of nucleate boiling at any location on the cladding surface in the reactor core, divided by the operating power of the reactor.

Method: The Bergles-Rohsenow Correlation [7] for ONB can be written as Eq. (1.6).

$$T_{onb} = T_{sat} + \frac{1}{1.8}\left[\frac{q_{onb}}{0.0010829\ \ P^{1.156}}\right]^{(P^{0.0234}/2.16)} \tag{1.6}$$

where

P = Coolant absolute pressure, bar

q_{onb} = Cladding-to-coolant heat flux (MW/m^2) that causes onset of nucleate boiling at a location with cladding surface temperature T_{onb} (ºC) and absolute pressure P (bar)

T_{sat} = Coolant saturation temperature at the ONB location, °C

T_{onb} = Cladding surface temperature (ºC) at which the designed operating heat flux q_{op} will cause onset of nucleate boiling at the axial location.

Verification and/or Validation: Chapter 22 documents in detail the verification of this capability for a standard test Problem 42 having fuel assemblies made of five-layer fuel plates, and cooled by D_2O with input flow rates. The ONBR values obtained by the code and by a spreadsheet developed for this purpose were compared for all 10 axial segments of all 8 fuel plate surfaces in Problem 42 (see Tables 22.22 to 22.27 in Chapter 22). The code calculates ONBR by Bergles-Rohsenow correlation using two approaches, the first based on the cladding-surface-to-coolant-inlet temperature difference, and the second based on the cladding-surface heat flux. The ONBR calculated by each approach was verified. The maximum absolute difference in ONBR obtained by either approach, between the code and the spreadsheet is found to be 0.83%.

1.2.8 OFIR Based on Whittle and Forgan Criterion

This capability is used to estimate the safety margin to the onset of excursive flow instability (OFI), i.e., the power that would cause the onset of flow instability in any coolant channel of the core, divided by the operating power of the reactor.

Method: According to the Whittle and Forgan criterion, the flow instability occurs when the ratio of the bulk coolant temperature rise ($T_{out} - T_{in}$) to the difference (T_{sat} - T_{in}) between the inlet temperature and the saturation temperature at the exit, equals a value determined purely by the channel geometry, as shown below by Eq. (1.7).

$$\frac{T_{out,OFI} - T_{in}}{T_{sat} - T_{in}} = \frac{1}{1 + \left(\eta D_h / L_h\right)} \tag{1.7}$$

where

T_{in} = Coolant inlet temperature, ºC

$T_{out,op}$ = Designed operating coolant exit temperature at the axial location where OFIR is being calculated, ºC

$T_{out,OFI}$ = Coolant exit temperature (at the axial location where OFIR is being calculated) that will cause onset of flow instability, ºC

T_{sat} = Saturation temperature at the axial location where OFIR is being calculated, ºC

D_h = Heated diameter of the coolant channel, m
= 4(Flow area in a channel)/(Heated perimeter in the channel).

L_h = Heated length to the axial location where OFIR is being calculated, m

η = An experimentally determined dimensionless parameter. The parameter η was set to 32.5 in the verification work.

Verification and/or Validation: Olson [8] and Feldman ([9] and Chapter 15 herein) taken together have analyzed and reported about the ability of the code to predict flow instability in five sets of electrically heated tests done by Croft [10], Waters [11], Whittle and Forgan [12], and Siman-Tov, et al. [13, 14]. In this work, Olson calibrated the value of the parameter η in the Whittle and Forgan OFI criterion from measured test data. In his work, Feldman compared with RELAP5 and verified the PLTEMP/ANL-calculated coolant channel flow during bubble nucleation on cladding surface with the approach of flow instability (prior to its occurrence). It was found that the code-calculated flow instability ratio based on the Whittle and Forgan criterion reliably predicts the OFI. Another paper [34] provides an additional verification of the Whittle and Forgan criterion by comparing it with four other OFI criteria, using a stand-alone program developed for this purpose.

Chapter 22 documents in detail the verification of this capability for a standard test Problem 42 having fuel assemblies made of five-layer fuel plates, and cooled by D_2O with input flow rates. The OFIR values obtained by the code and a spreadsheet developed for this purpose were compared for all six coolant channels in the test problem (see Table 22.28 in Chapter 22). The maximum absolute difference in OFIR between the code and the spreadsheet is 0.00445.

1.2.9 CHFR Based on Extended Groeneveld 2006 CHF Table

This capability is one of the options in the code to estimate the safety margin to burnout by critical heat flux, i.e., the power that would cause critical heat flux at any cladding surface location in the core, divided by the operating power of the reactor.

Method: This option for calculating CHF is given by Eq. (1.8) and is described in [15]. It is an extension of the Groeneveld 2006 look-up table [16] that is derived from a world-class database of ~32500 measured CHF data points. Compared to other CHF correlations, it is applicable to the *widest range* of thermal-hydraulic conditions.

$$q_c(D,P,G,X_o) = q_c(0.008,P,G,X_o)\left(\frac{0.008}{D}\right)^n \left\{\left(\frac{G}{8000}\right)^{0.376} \text{ if } G > 8000\right\} \tag{1.8}$$

The range of application is:

$3 < D < 25$ mm,	$L/D > 25$ for subcooled CHF,	$T_i > 0.01$ °C,
$1000 < G < 30{,}000$ kg/m^2-s ,	$L/D > 50$ for saturated CHF,	$-0.5 < X_o < 1.0$,
$1.0 \le P \le 210$ bar		

The extension for higher mass flux is based on an evaluation of 12 newer CHF correlations published during the last 20 years. The 12 correlations were compared at six pressures: 1, 5, 10, 20, 30, and 50 bar. It is found that two authors, Groeneveld et al. [16] and Hall and Mudawar [17], have assembled all the CHF measured data from the world literature dating back to 1949, have checked each data point by heat balance for error, and have independently developed two world-class CHF databases, each containing nearly 32500 data points. Only two CHF prediction methods are based on practically all the measured CHF data in the world: the Hall-Mudawar inlet conditions correlation (ICC) and the Groeneveld 2006 CHF table. A close agreement between these two was found. Based on the work of Celata, et al. [18], Tanase et al. [19] and the Hall-Mudawar ICC, (i) the Groeneveld 2006 table is extended to a maximum mass flux (G) of 30,000 kg/m^2-s by multiplying the tabulated CHF at 8000 kg/m^2-s by a factor of $(G/8000)^{0.376}$, and (ii) the recommended diameter correction factor is $(0.008/D_h)^{0.312}$ where D_h is in meters.

Verification and Validation: A validation of the extended Groeneveld lookup table by comparison to the Mirshak's measured CHF data is documented in [15]. A comparison of the measured and calculated CHF values is shown in Fig. 1.4 with each prediction method's trend-line passing through the origin. The calculated CHF data points of the Groeneveld table and Hall-Mudawar ICC are in close agreement. The RMS error over Mirshak's 65 CHF data points, of the Groeneveld 2006 table and the Hall-Mudawar ICC are 13.4% and 15.0%, respectively, about the same as their RMS error over the AECL-IPPE database or the PUBTPFL database from which the prediction method was derived. In conclusion, the extended Groeneveld 2006 CHF table and the Hall-Mudawar ICC give acceptably accurate values of CHF for channels of rectangular and annular cross sections, with one-sided heating.

1.2.10 CHFR based for Low Flow and Atmospheric Pressure

This capability [20] is one of the options available in the code for estimating CHF, and is applicable only at near atmospheric pressure for coolant mass flux less than 400 kg/m^2-s.

Method: Mishima performed CHF tests at near-atmospheric pressure for water flowing in annular, rectangular, and round ducts. The mass velocity (G) in these tests varies from 0 to 350 kg/m^2-s for down-flow, and from 0 to 70 kg/m^2-s for up-flow. Mishima's fit to his CHF data gives much smaller CHF values for G < ~350 kg/m^2-s than do the Mirshak and the Labuntsov correlations, which are based on CHF test data for G > ~1500 kg/m^2-s. Mishima's fit to his CHF data for rectangular ducts was combined with the Mirshak and the Labuntsov correlations valid for G > ~1500 kg/m^2-s, in order to provide CHF for G from 0 to ~1500 kg/m^2-s, for up-flow, down-flow, and for one-sided and two-sided heating.

Verification and/or Validation: Ref. [20] documents the verification of this capability. It was verified that PLTEMP/ANL calculations agree with both Mishima's and Mirshak's CHF test data, and reproduce the plot of CHF versus coolant velocity for an MTR-type 2-MW test reactor studied in the IAEA TECDOC- 233.

1.2.11 CHFR based on Bernath Correlation

This capability is one of the options available in the code for estimating CHF. It is based on a database of ~374 measured CHF data points and, compared to the extended Groeneveld 2006 table described above, is applicable to a *smaller range* of thermal-hydraulic conditions.

Method: The Bernath CHF correlation [21] is given below.

$$q_c = 5.679 \times 10^{-6} \left(\frac{10890\,D}{D + \xi/\pi} + \frac{48\,V}{D^{0.6}} \right) \left\{ 57 \ln(P) - \frac{54\,P}{P+15} - \frac{V}{4} - T_b \right\} \tag{1.9}$$

where

q_c = Critical heat transfer coefficient at burnout, MW/m^2
V = Coolant velocity, ft/s
P = Coolant pressure, psia
D = Hydraulic diameter, ft
ξ = Heated perimeter, ft
T_b = Local bulk coolant temperature (at axial segment exit), °C

Verification and/or Validation: Using a standard test Problem 38, Section 24.2 in Chapter 24 describes the verification of Bernath CHF correlation by comparing the code-calculated CHF values with those obtained by an Excel spreadsheet developed to calculate CHF by the direct substitution method (DSM) and the heat balance method (HBM) using the Bernath correlation. The mean absolute difference in CHF by calculated by the direct substitution method is 0.161%. The maximum absolute difference in CHF by the heat balance method is 0.185%.

1.2.12 CHFR based on Labuntsov Correlation

This capability is one of the options available in the code for estimating CHF. It is based on CHF data from 9 *Russian* sources and, compared to the extended Groeneveld 2006 table described above, is applicable to a *smaller range* of thermal-hydraulic conditions.

Method: The Labuntsov CHF correlation [22] is given below.

$$q_c = 1.454\ \theta(P)[1+2.5\ U^2 / \theta(P)]^{1/4}\ [1 + (15.1/ P^{1/2})\ (Cp\ \Delta T_{sub} / \lambda)], \tag{1.10}$$

where

$\theta(P)$ = $0.99531\ P^{1/3}(1 - P/P_c)^{4/3}$
C_p = Specific heat of the coolant, kJ/kg-°C
λ = Latent heat of vaporization, kJ/kg
= An average value of 1959.35 kJ/kg, over the pressure range 3.6 to 3.8 bar in the problem, was obtained from PLTEMP/ANL output and used in the spreadsheet.

P	= Pressure at the axial location of CHF, bar
P_c	= Critical pressure of the coolant, bar
	= 221.14 bar is hard-coded in PLTEMP/ANL and used in the spreadsheet.
ΔT_{sub}	= Coolant subcooling at the axial location of CHF (i.e., the heated length exit), °C
U	= Coolant velocity, m/s

Verification and/or Validation: Using a standard test Problem 38, Section 24.3 in Chapter 24 describes the verification of Labuntsov CHF correlation by comparing the code-calculated CHF values with those obtained by an Excel spreadsheet developed to calculate CHF by the DSM and the HBM using the Labuntsov correlation. The mean absolute difference in CHF calculated by the direct substitution method is 0.181%. The maximum absolute difference in CHF by the heat balance method is 0.211%.

1.2.13 CHFR Based on Sudo-Kaminaga Correlation

This capability [23] is one of the newer options available in the code for estimating CHF. It is based on a database of 596 measured CHF data points from 8 sources covering the following geometrical and thermal-hydraulic conditions, and is applicable to channels of rectangular cross section at near atmospheric pressure.

Channel gap: 2.25 to 5.0 mm
Ratio of heated length to hydraulic diameter: 8 to 240
Mass velocity: Downflow of 25,800 to stagnant flow to upflow of 6250 kg/m^2-s
System pressure: 0.1 to 0.72 MPa (only a small number of data points at greater than 0.1 MPa)
Inlet subcooling: 1 to 213 °C
Outlet condition: From subcooling of 0 to 74 °C to quality of 0 to 1.0

Method: The correlation is documented in Chapter 13.

Verification and/or Validation: Chapter 13 also documents the verification of the Sudo-Kaminaga CHF correlation implemented in the code by comparing it (i) with some measured CHF data reported by Sudo and Kaminaga [24] at coolant velocities less than 1.0 m/s, (ii) with some measured CHF data reported by Mirshak, Durant, and Towell [25] at coolant velocities greater than 1.0 m/s, and (iii) parametric studies of the Sudo-Kaminaga CHF correlation for its dependence on channel thickness and coolant mass velocity. The comparison provided a verification of the implementation of the correlation in the code. Parametric studies of the correlation showed that (i) the correlation is very sensitive to the channel thickness at channel thicknesses smaller than 2.25 mm, and (ii) the correlation is a continuous function of coolant mass velocity.

1.2.14 Search Capability

This is a capability used in reactor design to adjust a design parameter (such as reactor power, core flow, etc.) in order to achieve a user-specified value of a specific safety margin (such as ONBR, maximum heat flux, maximum coolant temperature, etc.). In a **single** search problem, one design parameter is adjusted to achieve a user-specified value of a **single** safety margin. In a **double** search

problem, two design parameters are adjusted to achieve user-specified values of **two** safety margins. The achieved value of a safety margin includes the effect of hot channel factors.

Method: The method for implementing the search capability is documented in detail in Section 3.10 of [3]. Basically, the whole pre-search version of the PLTEMP/ANL code is turned into a subroutine that is called as needed by a newly developed main program. In a single search, the to-be-adjusted design parameter (an input datum) is first set at its lower limit XLOW (a user-specified value); an input data file is written on a scratch file; and the *pre-search* code is run to find the corresponding value Y1 for the safety margin (an output of the code). The to-be-adjusted design parameter is then reset at its upper limit XHIGH (another user-specified value); another input data file is written on the scratch file; and the *pre-search* code is re-run to find the corresponding value Y2 for the safety margin. The interval between XLOW and XHIGH is then halved, and the to-be-adjusted design parameter is reset at the arithmetic mean X3 of its lower and upper limits, and the *pre-search* code is re-run to find the corresponding value Y3 for the safety margin. The to-be-adjusted design parameter is repeatedly adjusted by interval halving until the corresponding value of the safety margin equals its user-specified value within a specified tolerance.

Verification and/or Validation: The verification was done by comparing the PLTEMP/ANL code version having the search capability with an older pre-search code version 3.6 not having the search capability. Chapter 12 documents the verification of this capability, using 6 standard test problems (Problems 23, 24, 25, 27, 28, 29). The verification was done for single search problems (Problems 23, 24, 25) and for double search problems (Problems 27, 28, 29). The verification was done for a test Problem 27 without hot channel factors (i.e. equal to 1.0), and for a test Problem 28 with hot channel factors.

1.2.15 Longitudinal Fins on Fuel Plates

The code can model the increase in cladding-to-coolant heat transfer coefficient and the increase in friction factor due to longitudinal fins of trapezoidal cross section in coolant channels between multiple fuel plates or multiple nested tubes. The model is based on Carnavos correlations [26]. The code can model coolant channels having fins on only part of the wetted perimeter.

Method: The Carnavos correlations for heat transfer coefficient and friction factor in a tube with longitudinal fins of trapezoidal cross section is documented in Appendix IX of [3]. These correlations represent the measured data to within ±10%. Closed-form analytical equations are developed for the cross-sectional area of nominally trapezoidal fins on the inner or outer surface of a circular fuel tube or flat fuel plate in Appendix IX of [3].

Verification and/or Validation: Section 6.3 in Chapter 6 documents a verification of this capability for an MITR-type finned channel (flat fuel plates) using a standard test Problem 16. The code-calculated heat transfer coefficient and friction factor were compared with hand-calculated values. Chapter 18 documents a verification of this capability in the radial geometry using a standard test Problem 34 that models six nested fuel tubes. These results are summarized below.

Standard Test Problem	Heat Transfer Coeff., kW/m^2-ºC		Frictional Pressure Drop, MPa	
	Hand Calc.	PLTEMP/ANL	Hand Calc.	PLTEMP/ANL
Problem 16 (MITR-type plates)	43.1303	43.130	0.099975	0.1
Problem 34, channel 1 (6 nested fuel tubes)	97.6507	97.878		
Problem 34, channel 2	1072.2226	1072.2		

A verification of the capability for modeling *partly finned* channels in slab geometry is documented in Chapter 20. It was done by comparing the code with spreadsheet calculations for a standard test Problem 36 having 4 fuel plates and 5 channels. The maximum difference in heat transfer coefficient was 0.086%. The maximum difference in friction factor was 0.037%.
Using a test problem modeling a finned solid fuel rod, Chapter 21 documents a verification of the capability for modeling a *partly finned* channel in the radial geometry by comparing the code with spreadsheet calculations. The difference between the code and spreadsheet calculations was found to be negligible.

1.2.16 Coolant Thermal Properties

The code has built-in thermal properties of two coolants, liquid H_2O and liquid D_2O. These properties are calculated using FORTRAN subroutines obtained from the IAPWS-1977 (revised 1983) [27].

Verification and/or Validation: Using the PLTEMP/ANL input files at 14 different pressures for each coolant, the thermal properties of liquid H_2O and liquid D_2O calculated by the code are verified in Chapter 17 by comparison with the National Institute of Standards and Technology (NIST) data [28] on the NIST web site on the world wide web. Table 1.4 shows the maximum percent difference in five properties of H_2O over the pressure range of 1 to 145 bar and temperature range of 4 to 339 ºC. The maximum difference in enthalpy is 0.6%, in thermal conductivity 2.2%, in density 0.12%, in dynamic viscosity 21.4%, and in specific heat 3.7%. All the properties are in reasonable agreement with the NIST data except for the dynamic viscosity near saturation temperature at pressures above 100 bar. Table 1.5 shows the maximum percent difference in five properties of D_2O over the pressure range of 1 to 150 bar and temperature range of 5 to 341 ºC. The maximum difference is 2.8% in enthalpy, 4.8% in thermal conductivity, 3.4% in specific heat, 0.5% in density, and 1.8% in liquid D_2O dynamic viscosity. The fact that the NIST data for D_2O enthalpy is consistently greater than the code's data (by 1.0 to 2.8%) suggests that the enthalpy changes of interest in calculating temperatures are actually more accurate than 2.8%.

In conclusion, a verification and validation of 16 necessary capabilities currently identified by reactor analysts in their applications of the PLTEMP/ANL code to research reactors has been satisfactorily completed and documented here.

1.3 Other Publications on PLTEMP/ANL Verification and Validation

Three other publications [29-31] on PLTEMP/ANL verification and validation are available in the open literature and hence are not described in this document. Additional confidence in PLTEMP/ANL is gained by its use in the licensing of the following research reactors in USA and other countries.

List of US Research Reactors Converted and Licensed by the U.S. Nuclear Regulatory Commission, Based on Conversion Safety Analysis Reports in Which the PLTEMP/ANL Code was used:

(1) University of Florida Training Reactor (UFTR)
(2) Purdue University Reactor (PUR-1)
(3) Georgia institute of Technology Research Reactor (GTRR)
(4) University of Massachusetts Lowell Research Reactor (UMLRR)
(5) University of Michigan Ford Nuclear Reactor (FNR)
(6) Rhode Island Nuclear Science Center (RINSC) Research Reactor
(7) University of Virginia Reactor (UVAR)
(8) University of Missouri-Rolla Nuclear Reactor (UMRR)

List of Non-US Research Reactors Converted and Licensed by Other Regulatory Agencies, Based on Conversion Safety Analysis Reports in Which the PLTEMP/ANL Code was used:

(1) Portuguese research reactor (RPI) (reviewed by the International Atomic Energy Agency)

Research reactors of Russian design:
(2) Sophia research reactor in Bulgaria (IRT-200)
(3) Tajoura reactor in Libya (IRT-1)
(4) INP Tashkent in Uzbekistan (WWR-CM Tashkent)
(5) Dalat Nuclear Research Reactor in Vietnam (DNRR)

1.4 Verification Script for PLTEMP/ANL Code

The verification work reported here was done in March 2006. In order to routinely verify the PLTEMP/ANL code after a code modification, a UNIX script *verify.pltemp.csh* has been developed that runs the new executable for a set of standard test problems (whose accepted outputs from an older PLTEMP/ANL code executable are saved for comparison purposes) and compares each new output with the old, and saves the differences (using the program *differ.x* that finds the maximum temperature difference for each fuel plate) in a file for the code developer to examine. The input filenames of the standard test problems with a brief description of the problem are:

Sample Problem 1 Input File *input.A2.p3.c3r*
This input file (shown in Fig. 1.5) models one fuel assembly of a single fuel type in radial geometry, with a power of 0.80811 MW. The assembly has 6 fuel tubes and 7 coolant channels. The fueled length of 0.58 meter is divided into 11 axial nodes. The code is run in the flow-driven mode, i.e., using input fixed flow rates (1.943 kg/s, 1.577 kg/s, 1.542 kg/s, 1.411 kg/s, 1.168 kg/s, 1.151 kg/s and 0.914 kg/s) in coolant channels. One bypass channel is modeled. Hot channel factors are not used.

Sample Problem 2 Input File *input.12assemblies*
This input file (shown in Fig. 1.6) models 12 fuel assemblies of a single fuel type in slab geometry, with a total power of 1.0 MW. Each assembly has 4 fuel plates (made of 1.0 mm thick fuel meat with 0.5 mm thick cladding on both sides) and 5 coolant channels (each 3.0 mm thick and 20.0 cm wide). The fueled length of 0.75 meter is divided into 10 equal-length axial nodes. The code is run

in the flow-driven mode, i.e., using input fixed flow rates in coolant channels. Bypass channel or hot channel factors are not used.

Sample Problem 3 Input File *input.2assemblies*

This input file (shown in Fig. 1.7) models 2 fuel assemblies of a single fuel type in slab geometry, with a total power of 1.0 MW. Each assembly has 4 fuel plates (made of 1.0 mm thick fuel meat with 0.5 mm thick cladding on both sides) and 5 coolant channels (each 3.0 mm thick and 20.0 cm wide). The fuel plates have an un-fueled length of 0.15 meter above (minor loss factor 8.0) and an un-fueled length of 0.15 meter below (minor loss factor 8.0) the fueled length of 0.75 meter which is divided into 10 equal-length axial nodes. The code is run in the pressure-driven mode with a pressure drop of 0.10 MPa and an inlet pressure of 1.4 MPa. Bypass channel or hot channel factors are not used.

Sample Problem 4 Input File *input.2subassTypes*

This input file (shown in Fig. 1.8) models 4 fuel assemblies, with 2 assemblies of one type and 2 of another type, in slab geometry, with a total power of 2.0 MW. Each assembly has 4 fuel plates (made of 1.0 mm thick fuel meat with 0.5 mm thick cladding on both sides) and 5 coolant channels (each 3.0 mm thick and 20.0 cm wide). The fuel plates have an un-fueled length of 0.15 meter above (minor loss factor 8.0) and an un-fueled length of 0.15 meter below (minor loss factor 8.0) the fueled length of 0.75 meter which is divided into 10 equal-length axial nodes. The code is run in the pressure-driven mode with a pressure drop of 0.10 MPa and an inlet pressure of 1.4 MPa. Bypass channel or hot channel factors are not used.

Sample Problem 5 Input File *input.DeltaPloop_Powerloop*

This input file (shown in Fig. 1.9) models 2 fuel assemblies of a single fuel type in slab geometry. It runs the code in pressure-driven mode. It exercises the power loop and the pressure drop loop features of the code. In a single run, the code does 45 steady-state calculations by increasing the total power from 1.0 MW to 3.8 MW in steps of 0.2 MW (thus assuming 15 values of total power), and by assuming 3 values of pressure drop (0.10 MPa, 0.14 MPa and 0.18 MPa) for each value of total power. The pressure drop is increased in steps of 0.04 MPa, starting from 0.10 MPa, the inlet pressure always being 1.4 MPa. The total power and pressure drop loops are set up using the input data on card type 0600. Each assembly has 4 fuel plates (made of 1.0 mm thick fuel meat with 0.5 mm thick cladding on both sides) and 5 coolant channels (each 3.0 mm thick and 20.0 cm wide). The fuel plates have an un-fueled length of 0.15 meter above and an un-fueled length of 0.15 meter below the fueled length of 0.75 meter which is divided into 10 axial nodes. Bypass channel or hot channel factors are not used. The total number of tables (of coolant, cladding and fuel temperatures) in its output is 360 (2 x 4 x 45).

Sample Problem 6 Input File *input.fixedflows*

This input file (shown in Fig. 1.10) models 2 fuel assemblies of a single fuel type in slab geometry, with a total power of 1.0 MW. Each assembly has 4 fuel plates (made of 1.0 mm thick fuel meat with 0.5 mm thick cladding on both sides) and 5 coolant channels (each 3.0 mm thick and 20.0 cm wide). The fuel plates have an un-fueled length of 0.15 meter above and an un-fueled length of 0.15 meter below the fueled length of 0.75 meter which is divided into 10 axial nodes. The code is run in flow-driven mode, i.e., using an input fixed flow rate of 0.50 kg/s in each coolant channel. Bypass channel or hot channel factors are not used.

Sample Problem 7 Input File *input.Powerloop*

This input file (shown in Fig. 1.11) models 2 fuel assemblies of a single fuel type in slab geometry. It exercises the code's power loop feature using the input data on card type 0600. In a single run, the code does 11 steady-state calculations by increasing the total power from 1.0 MW to 3.0 MW in steps of 0.2 MW (i.e., using the values 1.0 MW, 1.2 MW, 1.4 MW … 2.8 MW and 3.0 MW). The code is run in pressure-driven mode using a pressure drop of 0.1 MPa and an inlet pressure of 1.4 MPa. Each assembly has 4 fuel plates (made of 1.0 mm thick fuel meat with 0.5 mm thick cladding on both sides) and 5 coolant channels (each 3.0 mm thick and 20.0 cm wide). The fuel plates have an un-fueled length of 0.15 meter above and an un-fueled length of 0.15 meter below the fueled length of 0.75 meter which is divided into 10 axial nodes. Bypass channel or hot channel factors are not used.

Sample Problem 8 Input File *input.pressuredriven*

This input file (shown in Fig. 1.12) models 2 fuel assemblies of a single fuel type in slab geometry. It is identical to the input file for Sample Problem 3 except for more skewed radial power factors now input on card type 0309.

1.5 REFERENCES

1. W. L. Woodruff and K. Mishima, "Neutronics and Thermal-Hydraulics Analysis of KUHFR," ANL/RERTR/TM-3, CONF-801144, p. 579, 1980.
2. K. Mishima, K. Kanda and T. Shibata, "Thermal-Hydraulic Analysis for Core Conversion to the Use of Low-Enriched Uranium Fuels in the KUR," ANL/RERTR/TM-6, CONF-8410173, p. 375 (1984).
3. M. Kalimullah, A. P. Olson and E. E. Feldman, "A User's Guide to the PLTEMP/ANL Code," ANL/RTR/TM-18/17 Version 4.3, Revision 0, Argonne National Laboratory, Argonne, 9700 South Cass Avenue, IL 60439, USA (November 2018).
4. William H. Press, Saul A. Teukolsky, William T. Vetterling, and Brian P. Flannery, "Numerical Recipes in FORTRAN, The Art of Scientific Computing, Second Ed., Cambridge University Press, Chapter 9 (1992).
5. M. Kalimullah, A. P. Olson, and E. E. Feldman, "Natural Circulation Flow Rate Calculation in PLTEMP/ANL Code," RERTR 2008, 30th. International Meeting on Reduced Enrichment for Research and Test Reactors, Washington D.C., USA (October 5-9, 2008).
6. M. Kalimullah, B. Dionne, E. E. Feldman, J. E. Matos, and A. P. Olson, "Estimating Hot Channel Factors for a Generic MNSR Using Rodded Fuel Cooled by Natural Circulation," RERTR 2011, 33rd. International Meeting on Reduced Enrichment for Research and Test Reactors, Santiago, Chile (October 23-27, 2011).
7. A. E. Bergles and W. M. Rohsenow, "The Determination of Forced-Convection Surface-Boiling Heat Transfers," Trans. ASME, J. Heat Transfer **86**, 365 (1964).
8. A. P. Olson, "Analysis of Flow Excursion Experiments Relevant To Research Reactors: Revisited," 2006 RERTR Conference, Cape Town, South Africa, RERTR Program, Nuclear Engineering Division, Argonne National Laboratory, Argonne, IL USA (October 29 – November 3, 2006).
9. Feldman, E. E., "Comparison of the PLTEMP Code Flow Instability Predictions with Measurements Made with Electrically Heated Channels for the Advanced Test Reactor," ANL/RERTR/TM-11-23, Nuclear Engineering Division, Argonne National Laboratory, Argonne, IL, USA (June 9, 2011).
10. W. M. Croft, "Advanced Test Reactor Burnout Heat Transfer Tests," USAEC Report IDO-24465, ATR-FE-102, Ca-2, Babcock & Wilcox Company (January 1964).
11. E. D. Waters, "Heat Transfer Experiments for the Advanced Test Reactor," USAEC Report BNWL-216, UC-80, Reactor Technology (TID-4500), Pacific Northwest Laboratory, Richland, Washington (May 1966).
12. R. H. Whittle and R. Forgan, "A Correlation for the Minima in the Pressure Drop Versus Flow-Rate Curves for Sub-Cooled Water Flowing in Narrow Heated Channels," Nuclear Engineering and Design 6, pp. 89-99 (1967).
13. M. Siman-Tov, D. K. Felde, G. Farquharson, J. L. McDuffee, M. T. McFee, A. E. Ruggles, M. W. Wendel, and G. L. Yoder, FY 1995 Progress Report on the ANS Thermal-Hydraulic Test Loop Operation and Results, ORNL/TM-12972, Oak Ridge National Laboratory (July 1997).
14. M. Siman-Tov, D. K. Felde, J. L. McDuffee, and G. L. Yoder, Experimental Study of Static Flow Instability in Sub-cooled Flow Boiling in Parallel Channels, 4th ASME/JSME Thermal Engineers Joint Conference, Maui, Hawaii, CONF-950113-1,Oak Ridge National Laboratory (January 1995).

15. M. Kalimullah, E. E. Feldman, A. P. Olson, B. Dionne, J. G. Stevens, and J. E. Matos, "An Evaluation of Subcooled CHF Correlations and Databases For Research Reactors Operating at 1 to 50 bar Pressure," RERTR 2012 – 34th International Mtg. on Reduced Enrichment for Research and Test Reactors, Warsaw, Poland (October 14-17, 2012).
16. D. C. Groeneveld et al., "The 2006 CHF Look-up Table," Nuclear Engineering and Design, 237, pp. 1909-1922 (2007).
17. D. D. Hall and I. Mudawar, "Critical Heat Flux for Water Flow in Tubes – I. Compilation and Assessment of World CHF Data," Intern. J. Heat and Mass Transfer, Vol. 43, pp. 2573-2604 (2000).
18. G. P. Celata, M. Cumo, and A. Mariani, "The Effect of the Tube Diameter on the Critical Heat Flux in Subcooled Flow Boiling," Intern. J. of Heat and Mass Transfer, Vol. 39, pp. 1755-1757 (1996).
19. A. Tanase, S. C. Cheng, D. C. Groeneveld, and J. Q. Shan, "Diameter Effect on Critical Heat Flux," Nucl. Eng. Des., Vol. 239, pp. 289-294 (2009).
20. M. Kalimullah, E. E. Feldman, and A. P. Olson, "Implementation and Verification of Mishima's CHF Data at Low Flow and Atmospheric Pressure in the PLTEMP/ANL Code," RERTR 2009 – 31st. International Meeting on Reduced Enrichment for Research and Test Reactors, Beijing, China (November 1-5, 2009).
21. L. Bernath, "A Theory of Local Boiling Burnout and Its Application to Existing Data," Chem. Eng. Prog. Symp. Series, **56** (30), 95 (1960).
22. D. A. Labuntsov, "Critical Thermal Loads in Forced Motion of Water Which is Heated to a Temperature Below the Saturation Temperature," Soviet J. of Atomic Energy (English Translation) Vol. 10, No. 5, pp. 516-518 (May 1961).
23. M. Kaminaga, K. Yamamoto, and Y. Sudo, "Improvement of Critical Heat Flux Correlation for Research Reactors Using Plate-Type Fuel," J. Nuclear Sci. and Technol., Vol. 35, No. 12, pp. 943-951 (1998).
24. M. Kaminaga, Y. Sudo, Y. Murayama, and T. Usui, "Experimental Study of Critical Heat Flux in a Narrow Vertical Rectangular Channel," Heat Transfer – Japanese Research, Vol. 20(1), pp. 72-85 (1991).
25. S. Mirshak, W. S. Durant, and R. H. Towell, "Heat Flux at Burnout," DP-355, U.S. Atomic Energy Commission (1959).
26. T. C. Carnavos, "Heat Transfer Performance of Internally Finned Tubes in Turbulent Flow," AIChE Paper presented at the 18th National Heat Transfer Conference, San Diego, CA (Aug. 1979).
27. "International Association for the Properties of Steam (IAPS)," H. J. White, Secretary, National Bureau of Standards, Washington, D.C., 1977 (revised 1983).
28. National Institute of Standards and Technology (NIST), webbook.nist.gov/chemistry/, 100 Bureau Drive, Gaithersburg, MD 20899, USA (2011).
29. E. E. Feldman, "Comparison of the PLTEMP Code Flow Instability Predictions with Measurements Made with Electrically Heated Channels for the Advanced Test Reactor," ANL/RERTR/TM-11-23, Global Threat Reduction Initiative (GTRI) - Conversion Program, Nuclear Engineering Division, Argonne National Laboratory, Argonne, USA (June 9, 2011).
30. M. Kalimullah, A. P. Olson, and E. E. Feldman, "Natural Circulation Flow Rate Calculation in PLTEMP/ANL Code," RERTR 2008 – 30th. International Meeting on Reduced Enrichment for Research and Test Reactors, Washington, D.C., USA (October 5-9, 2008).

31. M. Kalimullah, N. A. Hanan, E. E. Feldman, and A. P. Olson, "Implementation and Verification of Mishima's CHF Data at Low Flow and Atmospheric Pressure in the PLTEMP/ANL Code," RERTR 2009 – 31st. International Meeting on Reduced Enrichment for Research and Test Reactors, Beijing, China (November 1-5, 2009).
32. R. S. Smith and W. L. Woodruff, "A Computer Code, NATCON, for the Analysis of Steady-State Thermal-Hydraulics and Safety Margins in Plate-Type Research Reactors Cooled by Natural Convection," ANL/RERTR/TM-12, Argonne National Laboratory, Argonne, Illinois, USA (December 1988).
33. The RELAP5-3D© Code Development Team, RELAP5-3D© Code Manual, Version 2.3, INEEL-EXT-98-00834, Idaho National Laboratory, Idaho, USA April 2005.
34. M. Kalimullah, E. E. Feldman, A. P. Olson, and J. R. Licht, "Comparison of Moritz, Fabrega, Saha-Zuber, and Whittle-Forgan Criteria for OFI with 75 Experiments," RERTR 2017 - 38th International Meeting on Reduced Enrichment for Research and Test Reactors, Chicago, Illinois, USA (November 12-15, 2017).

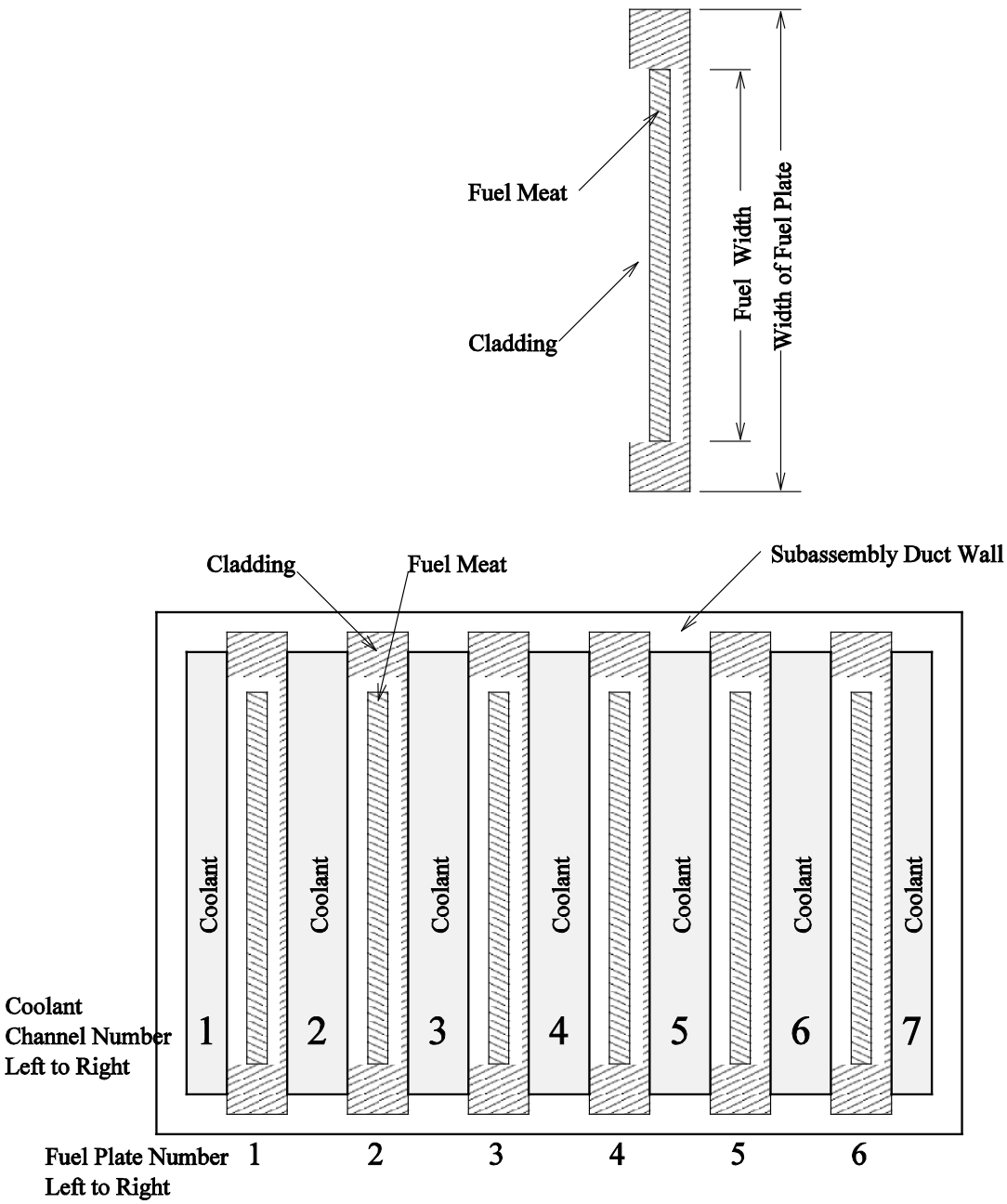

Figure 1.1 Cross Section of a Typical Fuel Assembly Having Six Fuel Plates Modeled by the PLTEMP/ANL Code

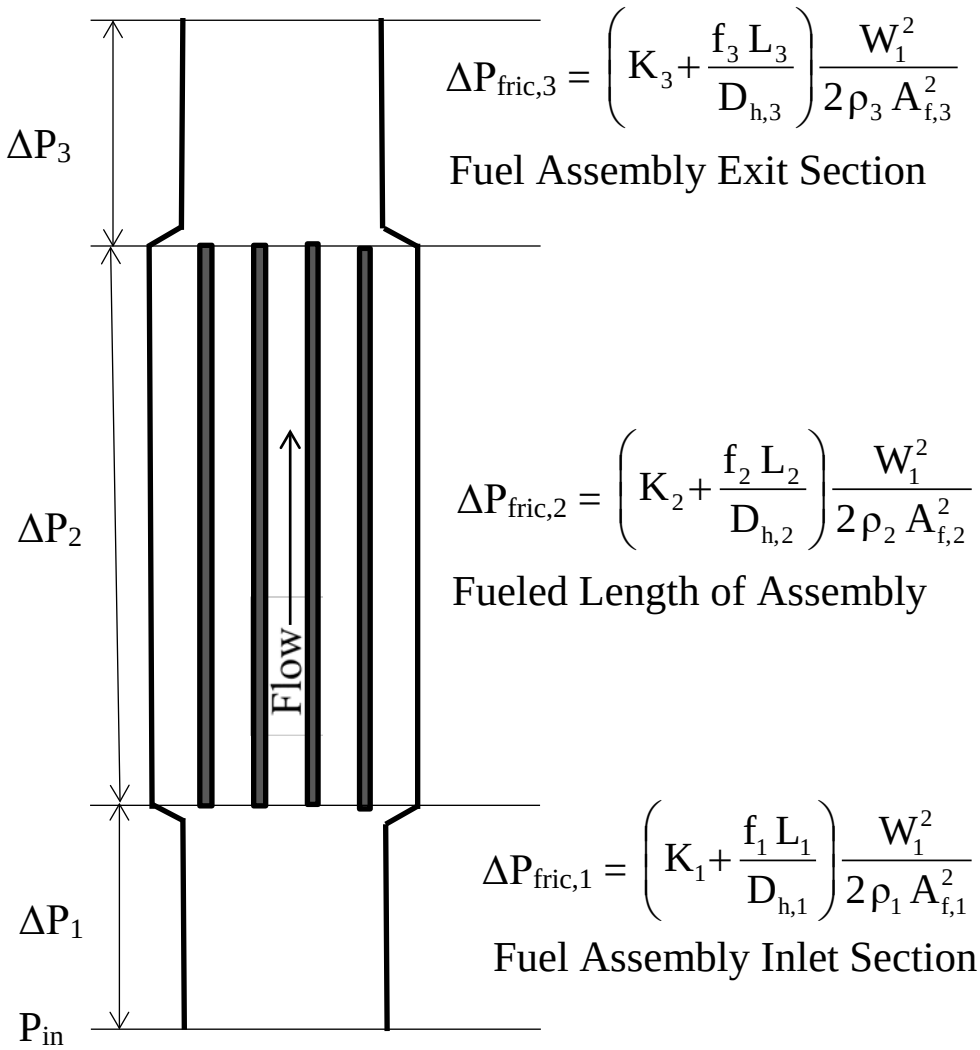

Figure 1.2 Pressure Drop and its Frictional Component in Multiple Axial Regions of a Fuel Assembly. Region 1 is the Assembly Inlet Section, Region 2 is the Fueled Length, and Region 3 is the Assembly Exit Section.

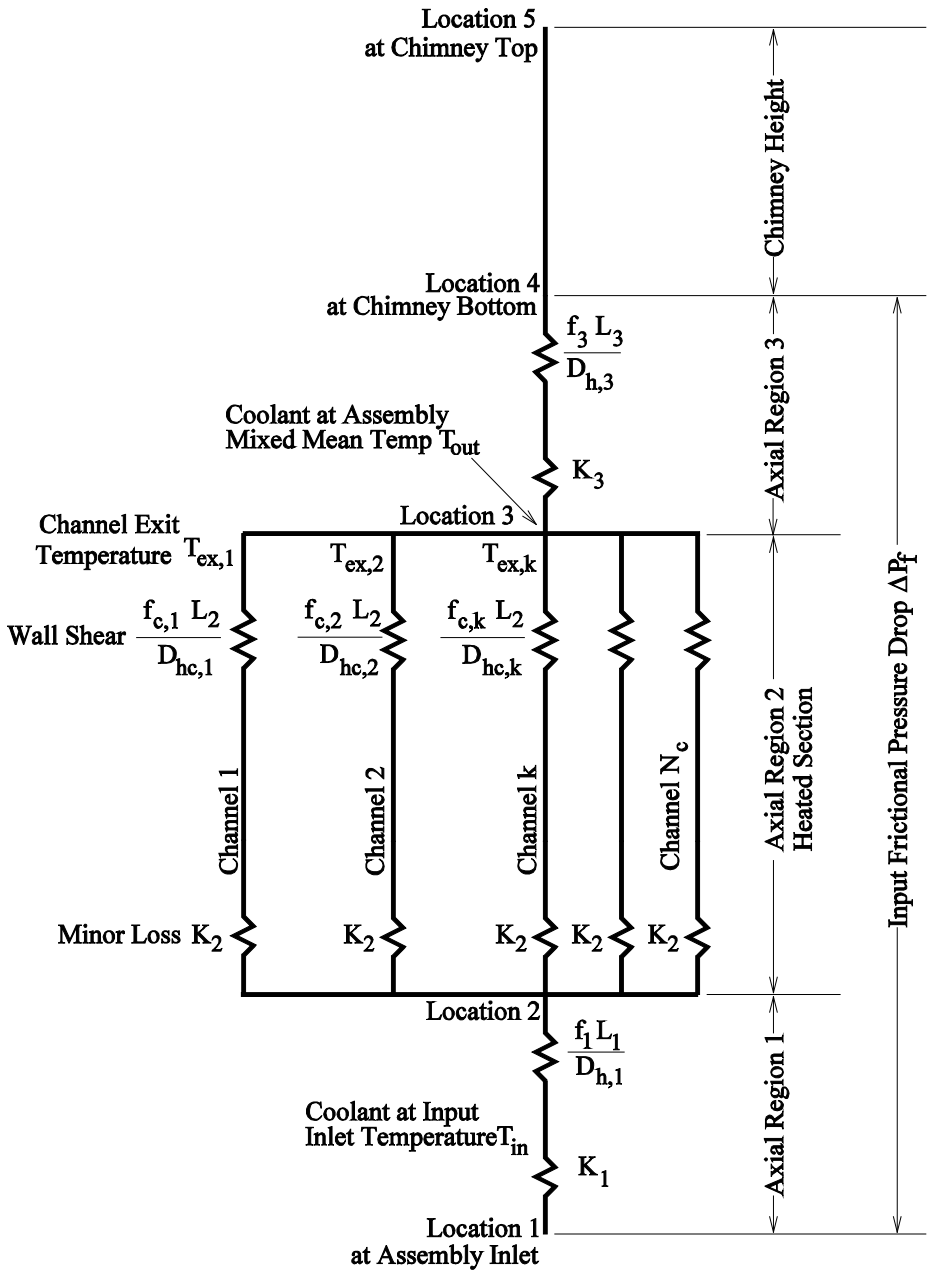

Figure 1.3 Coolant Flow Path in a Fuel Assembly and Chimney Modeled in PLTEMP/ANL (Multiple Axial Regions Downstream of the Heated Section are Allowed)

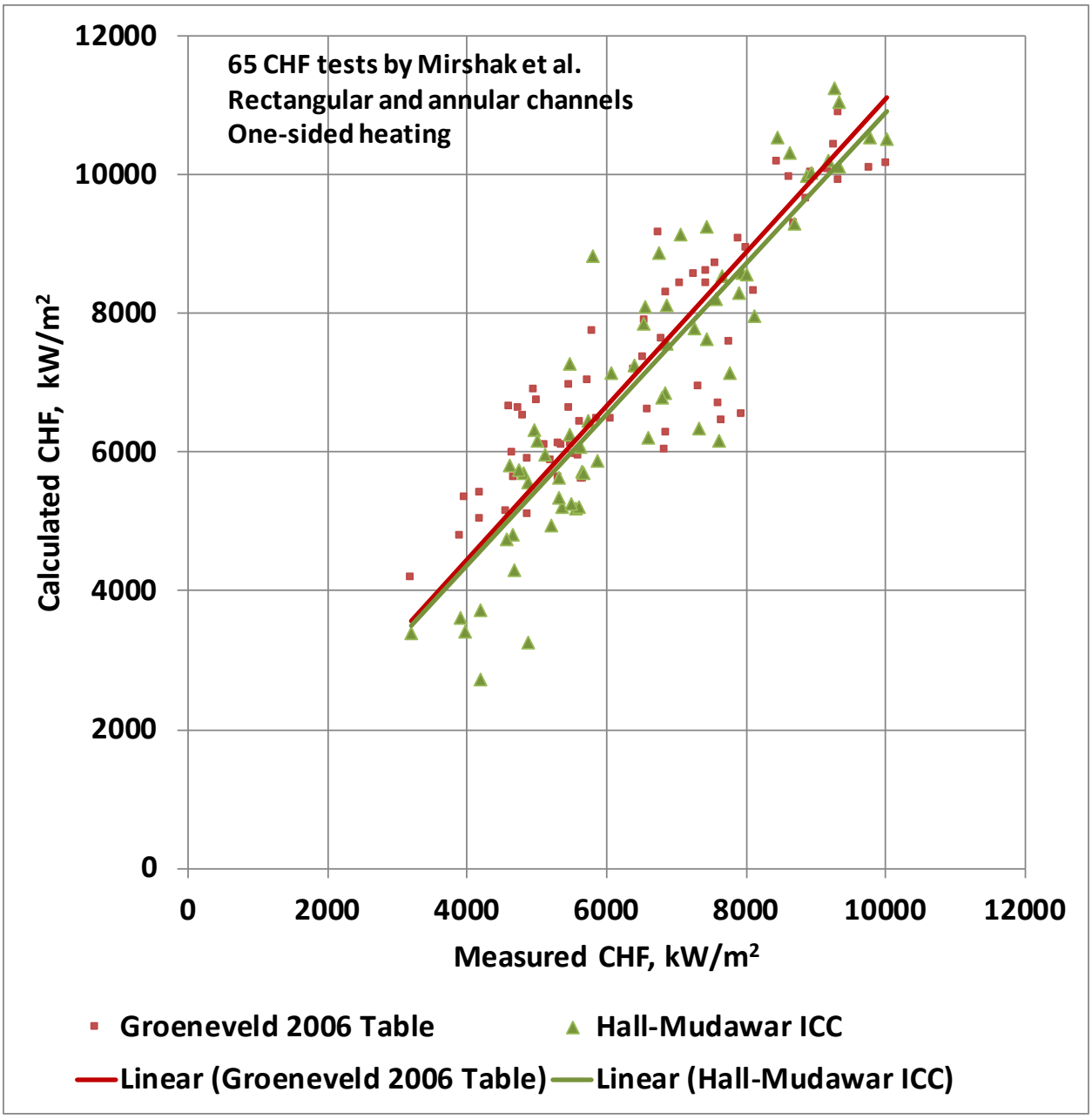

Figure 1.4 **Fig. 1.4. Comparison of Extended Groeneveld Table and Hall-Mudawar ICC Correlation to Mirshak's Measured 65 CHF Data Points**

Figure 1.5 Input Filename *input.A2.p3.c3r* Used as Standard Problem 1 in PLTEMP/ANL Verification Script

```
IRT-3M 36% Enr FA; 6 Tubes 0.58 m Height - ASTRA2 P3 true->plate
! input.A2.p3.c3r
! Notes by Kalim, Jan 12, 2006
! NFTYP=1,   Only one type of assembly in the problem
! NELF(1)=1, A single assembly in type 1
   4   2   2   1   1   0   1   0   1   1                                        Card(1)0200
   1   3  0.0        1.00        1.000       1.00                              Card(1)0300
   7   7  1.000                                                                 Card(1)0301
   1   2   1                                                                    Card(1)0302
 1.3135                                                                         Card(1)0303
 0.0043433  0.038540    0.10        0.5                                         Card(3)0304
 0.0        0.0         0.580       0.0                                         Card(3)0304
 0.0043433  0.038540    0.035       1.0                                         Card(3)0304
 0.316      0.250                                                               Card(1)0305
   7  0 0.0         0.580         0.450E-03  170.        0.500E-03  100.       Card(1)0306
  6.0524E-04 4.46024E-03  0.27139    0.27139                                    Card(7)0307
  5.2931E-04 4.17778E-03  0.50679    0.50679                                    Card(7)0307
  4.7273E-04 4.18729E-03  0.45159    0.45159                                    Card(7)0307
  4.1615E-04 4.19944E-03  0.39639    0.39639                                    Card(7)0307
  3.5957E-04 4.21553E-03  0.34119    0.34119                                    Card(7)0307
  3.0299E-04 4.23783E-03  0.28599    0.28599                                    Card(7)0307
  2.4641E-04 4.27080E-03  0.23079    0.23079                                    Card(7)0307
 0.267193   0.239593    0.211993    0.184393    0.156793    0.129193           Card(1)0308
  .0340      .03055      .02710       .02365     .02020      .01675
 1.1696     1.0901      1.0234      0.9579      0.90175     0.85731            Card(1)0309
1.94282     1.57675     1.54174     1.41065     1.16807     1.15058
0.91358
   1   1         1.0
  1.1545E-04    3.00E-03    0.680           1.4
       0.316    0.25
 .100633     .0005        .12540     0.80811      45.0        .135             Card(1)0500
 100 1.00000E-04   25.0        0.0000        0.80811
 -12
0.00000      0.025       0.52323
0.05000      0.100       0.62029
0.15         0.20        0.85886
0.25         0.30        1.06336
0.35         0.40        1.24058
0.45         0.50        1.34964
0.55         0.60        1.36328
0.65         0.70        1.27466
0.75         0.80        1.09062
0.85         0.90        0.85886
0.95         0.975       0.75662
1.00000
   0
```

Figure 1.6 Input Filename *input.12assemblies* Used as Standard Problem 2 in PLTEMP/ANL Verification Script

```
Test Problem: 12 assemblies (of identical geometry) producing 1 MWt
! Each assembly has 4 fuel plates and 5 coolant channels
! H2O coolant, Flow = 6.0 kg/s, All hot channel factors = 1.0
! No bypass flow, NCTYP=0
! 10 axial heat transfer nodes in the heated length of fuel plates
!  1   2   3   4   5   6   7   8   9  10  11  12  13                          Card 0200 indeces
   0   0   0   1   0   1   1   1   0   0   0   0   0                          Card(1)0200
  12   3 0.00       1.00        1.00        1.00           3                 Card(1)0300
! Using pressure driven mode
! 12   3 0.45       1.00        1.00        1.00           3                 Card(1)0300
   1  20 1.00                                                                Card(1)0301
   1   1   1                                                                 Card(1)0302
1.20        1.20        1.20        1.20        1.20        1.20             Card(2)0303
1.20        1.20        1.20        1.20        1.20        1.20             Card(2)0303
30.0E-04    0.02955665  0.15        1.0                                      Card(3)0304
30.0E-04    0.02955665  0.15        1.0                                      Card(3)0304
30.0E-04    0.02955665  0.15        1.0                                      Card(3)0304
! Use code's correlation for friction factor
0.00        0.00        0.00                                                 Card(1)0305
   5   3 0.00       0.75        0.50E-03    0.00        1.00E-03    100.00   Card(1)0306
6.00E-04    5.91133E-03 0.4060      0.20        0.20        3.00E-03         Card(5)0307
6.00E-04    5.91133E-03 0.4060      0.40        0.20        3.00E-03         Card(5)0307
6.00E-04    5.91133E-03 0.4060      0.40        0.20        3.00E-03         Card(5)0307
6.00E-04    5.91133E-03 0.4060      0.40        0.20        3.00E-03         Card(5)0307
6.00E-04    5.91133E-03 0.4060      0.20        0.20        3.00E-03         Card(5)0307
0.20        0.20        0.20        0.20                                     Card(1)0308
! Card 0308a not required
! Radial power peaking factor data by fuel plate for each assembly. Input flow data by
! channel for each assembly on Cards 0310 not required because WFGES(1) is non-zero
0.90        0.95        1.05        1.10                                     Card(12)0309
0.09        0.09        0.09        0.09        0.09                         Card(12)0310
0.901       0.951       1.049       1.099                                    Card(12)0309
0.09        0.09        0.09        0.09        0.09                         Card(12)0310
0.902       0.952       1.048       1.098                                    Card(12)0309
0.09        0.09        0.09        0.09        0.09                         Card(12)0310
0.903       0.953       1.047       1.097                                    Card(12)0309
0.09        0.09        0.09        0.09        0.09                         Card(12)0310
0.904       0.954       1.046       1.096                                    Card(12)0309
0.09        0.09        0.09        0.09        0.09                         Card(12)0310
0.905       0.955       1.045       1.095                                    Card(12)0309
0.09        0.09        0.09        0.09        0.09                         Card(12)0310
0.906       0.956       1.044       1.094                                    Card(12)0309
0.09        0.09        0.09        0.09        0.09                         Card(12)0310
0.907       0.957       1.043       1.093                                    Card(12)0309
0.09        0.09        0.09        0.09        0.09                         Card(12)0310
0.908       0.958       1.042       1.092                                    Card(12)0309
0.09        0.09        0.09        0.09        0.09                         Card(12)0310
0.909       0.959       1.041       1.091                                    Card(12)0309
0.09        0.09        0.09        0.09        0.09                         Card(12)0310
0.910       0.960       1.040       1.090                                    Card(12)0309
0.09        0.09        0.09        0.09        0.09                         Card(12)0310
0.911       0.961       1.039       1.089                                    Card(12)0309
0.09        0.09        0.09        0.09        0.09                         Card(12)0310
! DP0       DDP         DPMAX       POWER       TIN         PIN
0.10        0.10        0.20        1.00        45.0        1.40             Card(1)0500
  50 0.0001     25.0        0.00        1.00                                 Card(1)0600
  11                                                                         Card(1)0700
0.00        1.00                                                             Card(11)0701
0.10        1.00                                                             Card(11)0701
0.20        1.00                                                             Card(11)0701
0.30        1.00                                                             Card(11)0701
0.40        1.00                                                             Card(11)0701
0.50        1.00                                                             Card(11)0701
0.60        1.00                                                             Card(11)0701
0.70        1.00                                                             Card(11)0701
0.80        1.00                                                             Card(11)0701
0.90        1.00                                                             Card(11)0701
1.00        1.00                                                             Card(11)0701
   0                                                                         Card(11)0702
```

Figure 1.7 Input Filename *input.2assemblies* Used as Standard Problem 3 in PLTEMP/ANL Verification Script

```
 Test Problem: 2 assemblies (of identical geometry) producing 1 MWt
! Each assembly has 4 fuel plates and 5 coolant channels
! H2O coolant, Flow is calculated from input pressure drop
! All hot channel factors = 1.0
! No bypass flow, NCTYP=0
! 10 axial heat transfer nodes in the heated length of fuel plates
!  1   2   3   4   5   6   7   8   9  10  11  12  13                  Indices on Card 0200
   0   0   0   1   0   1   1   1   0   0   0   0   0                           Card(1)0200
   2   3 0.50       1.00        1.00        1.00           3                  Card(1)0300
! Using pressure driven mode
   1  20 1.00                                                                  Card(1)0301
   1   1   1                                                                   Card(1)0302
1.20        1.20                                                               Card(2)0303
30.0E-04    0.02955665  0.15        8.00        0.20        15.0E-03           Card(3)0304
30.0E-04    0.02955665  0.75        0.00        0.20        15.0E-03           Card(3)0304
30.0E-04    0.02955665  0.15        8.00        0.20        15.0E-03           Card(3)0304
! Use the code's built-in correlation for friction factor
0.00        0.00        0.00                                                   Card(1)0305
   5   3 0.00       0.75        0.50E-03    0.00        1.00E-03    100.00     Card(1)0306
6.00E-04    5.91133E-03 0.4060      0.20        0.20        3.00E-03           Card(5)0307
6.00E-04    5.91133E-03 0.4060      0.40        0.20        3.00E-03           Card(5)0307
6.00E-04    5.91133E-03 0.4060      0.40        0.20        3.00E-03           Card(5)0307
6.00E-04    5.91133E-03 0.4060      0.40        0.20        3.00E-03           Card(5)0307
6.00E-04    5.91133E-03 0.4060      0.20        0.20        3.00E-03           Card(5)0307
0.20        0.20        0.20        0.20                                       Card(1)0308
! Card 0308a not required
! Radial power peaking factor data by fuel plate for each assembly. Input flow data by
! channel for each assembly on Cards 0310 not required because WFGES(1) is non-zero
0.900       0.950       1.050       1.100                                      Card(2)0309
0.901       0.951       1.049       1.099                                      Card(2)0309
! DP0       DDP         DPMAX       POWER       TIN         PIN
0.10        0.04        0.10        1.00        45.0        1.40               Card(1)0500
  50 0.0001     25.0        0.50        1.00                                   Card(1)0600
  11                                                                           Card(1)0700
0.00        0.80                                                               Card(11)0701
0.10        0.88                                                               Card(11)0701
0.20        0.96                                                               Card(11)0701
0.30        1.04                                                               Card(11)0701
0.40        1.12                                                               Card(11)0701
0.50        1.20                                                               Card(11)0701
0.60        1.12                                                               Card(11)0701
0.70        1.04                                                               Card(11)0701
0.80        0.96                                                               Card(11)0701
0.90        0.88                                                               Card(11)0701
1.00        0.80                                                               Card(11)0701
   0                                                                           Card(11)0702
```

Figure 1.8 Input Filename *input.2subassTypes* Used as Standard Problem 4 in PLTEMP/ANL Verification Script

```
 Test Problem: 4 assemblies (of identical geometry) producing 2 MWt
! Each assembly has 4 fuel plates and 5 coolant channels
! H2O coolant, Flow is calculated from input pressure drop
! All hot channel factors = 1.0
! No bypass flow, NCTYP=0
! 10 axial heat transfer nodes in the heated length of fuel plates
!  1   2   3   4   5   6   7   8   9  10  11  12  13                  Indices on Card 0200
   0   0   0   2   0   1   1   1   0   0   0   0   0                                Card(1)0200
!-----------------------------------------------------------------------------------------
! Data for Type 1 fuel assemblies
   2   3 0.50       1.00        1.00        1.00           3                     Card(1)0300
! Using pressure driven mode
   1  20 1.00                                                                     Card(1)0301
   1   1   1                                                                      Card(1)0302
1.20        1.20                                                                  Card(2)0303
30.0E-04    0.02955665  0.15        8.00        0.20        15.0E-03              Card(3)0304
30.0E-04    0.02955665  0.75        0.00        0.20        15.0E-03              Card(3)0304
30.0E-04    0.02955665  0.15        8.00        0.20        15.0E-03              Card(3)0304
! Use the code's built-in correlation for friction factor
0.00        0.00        0.00                                                      Card(1)0305
   5   3 0.00       0.75        0.50E-03    0.00        1.00E-03    100.00        Card(1)0306
6.00E-04    5.91133E-03 0.4060      0.20        0.20        3.00E-03              Card(5)0307
6.00E-04    5.91133E-03 0.4060      0.40        0.20        3.00E-03              Card(5)0307
6.00E-04    5.91133E-03 0.4060      0.40        0.20        3.00E-03              Card(5)0307
6.00E-04    5.91133E-03 0.4060      0.40        0.20        3.00E-03              Card(5)0307
6.00E-04    5.91133E-03 0.4060      0.20        0.20        3.00E-03              Card(5)0307
0.20        0.20        0.20        0.20                                          Card(1)0308
! Card 0308a not required
! Radial power peaking factor data by fuel plate for each assembly. Input flow data by
! channel for each assembly on Cards 0310 not required because WFGES(1) is non-zero
0.700       0.800       0.900       1.000                                         Card(2)0309
1.000       1.100       1.200       1.300                                         Card(2)0309
!-----------------------------------------------------------------------------------------
! Data for Type 2 fuel assemblies
   2   3 0.50       1.00        1.00        1.00           3                     Card(1)0300
! Using pressure driven mode
   1  20 1.00                                                                     Card(1)0301
   1   1   1                                                                      Card(1)0302
1.20        1.20                                                                  Card(2)0303
30.0E-04    0.02955665  0.15        8.00        0.20        15.0E-03              Card(3)0304
30.0E-04    0.02955665  0.75        0.00        0.20        15.0E-03              Card(3)0304
30.0E-04    0.02955665  0.15        8.00        0.20        15.0E-03              Card(3)0304
! Use the code's built-in correlation for friction factor
0.00        0.00        0.00                                                      Card(1)0305
   5   3 0.00       0.75        0.50E-03    0.00        1.00E-03    100.00        Card(1)0306
6.00E-04    5.91133E-03 0.4060      0.20        0.20        3.00E-03              Card(5)0307
6.00E-04    5.91133E-03 0.4060      0.40        0.20        3.00E-03              Card(5)0307
6.00E-04    5.91133E-03 0.4060      0.40        0.20        3.00E-03              Card(5)0307
6.00E-04    5.91133E-03 0.4060      0.40        0.20        3.00E-03              Card(5)0307
6.00E-04    5.91133E-03 0.4060      0.20        0.20        3.00E-03              Card(5)0307
0.20        0.20        0.20        0.20                                          Card(1)0308
! Card 0308a not required
! Radial power peaking factor data by fuel plate for each assembly. Input flow data by
! channel for each assembly on Cards 0310 not required because WFGES(1) is non-zero
0.700       0.800       0.900       1.000                                         Card(2)0309
2.000       2.100       2.200       2.300                                         Card(2)0309
!-----------------------------------------------------------------------------------------
! DP0       DDP         DPMAX       POWER       TIN         PIN
0.10        0.04        0.10        2.00        45.0        1.40                  Card(1)0500
  50 0.0001     25.0        0.50        1.00                                      Card(1)0600
  11                                                                              Card(1)0700
0.00        0.80                                                                  Card(11)0701
0.10        0.88                                                                  Card(11)0701
0.20        0.96                                                                  Card(11)0701
0.30        1.04                                                                  Card(11)0701
0.40        1.12                                                                  Card(11)0701
0.50        1.20                                                                  Card(11)0701
0.60        1.12                                                                  Card(11)0701
0.70        1.04                                                                  Card(11)0701
0.80        0.96                                                                  Card(11)0701
0.90        0.88                                                                  Card(11)0701
1.00        0.80                                                                  Card(11)0701
   0                                                                              Card(11)0702
```

Figure 1.9 Input Filename *input.DeltaPloop_Powerloop* Used as Standard Problem 5 in PLTEMP/ANL Verification Script

```
 Test Problem: 2 assemblies (of identical geometry) producing 1 MWt
! Each assembly has 4 fuel plates and 5 coolant channels
! H2O coolant, Flow is calculated from input pressure drop
! All hot channel factors = 1.0
! No bypass flow, NCTYP=0
! 10 axial heat transfer nodes in the heated length of fuel plates
!  1   2   3   4   5   6   7   8   9  10  11  12  13                  Indices on Card 0200
   0   0   0   1   0   1   1   1   0   0   0   0   0                           Card(1)0200
   2   3 0.50       1.00        1.00        1.00           3                  Card(1)0300
! Using pressure driven mode
   1  20 1.00                                                                  Card(1)0301
   1   1   1                                                                   Card(1)0302
1.20        1.20                                                               Card(2)0303
30.0E-04    0.02955665  0.15        8.00        0.20        15.0E-03           Card(3)0304
30.0E-04    0.02955665  0.75        0.00        0.20        15.0E-03           Card(3)0304
30.0E-04    0.02955665  0.15        8.00        0.20        15.0E-03           Card(3)0304
! Use the code's built-in correlation for friction factor
0.00        0.00        0.00                                                   Card(1)0305
   5   3 0.00       0.75        0.50E-03    0.00        1.00E-03    100.00     Card(1)0306
6.00E-04    5.91133E-03 0.4060      0.20        0.20        3.00E-03           Card(5)0307
6.00E-04    5.91133E-03 0.4060      0.40        0.20        3.00E-03           Card(5)0307
6.00E-04    5.91133E-03 0.4060      0.40        0.20        3.00E-03           Card(5)0307
6.00E-04    5.91133E-03 0.4060      0.40        0.20        3.00E-03           Card(5)0307
6.00E-04    5.91133E-03 0.4060      0.20        0.20        3.00E-03           Card(5)0307
0.20        0.20        0.20        0.20                                       Card(1)0308
! Card 0308a not required
! Radial power peaking factor data by fuel plate for each assembly. Input flow data by
! channel for each assembly on Cards 0310 not required because WFGES(1) is non-zero
0.900       0.950       1.050       1.100                                      Card(2)0309
0.600       0.800       1.200       1.400                                      Card(2)0309
! DP0       DDP         DPMAX       POWER       TIN         PIN
0.10        0.04        0.20        1.00        45.0        1.40               Card(1)0500
!     CONV       ETA        DPWR        PWRM
 -50 0.0001     25.0        0.20        6.00                                   Card(1)0600
  11                                                                            Card(1)0700
0.00        0.80                                                               Card(11)0701
0.10        0.88                                                               Card(11)0701
0.20        0.96                                                               Card(11)0701
0.30        1.04                                                               Card(11)0701
0.40        1.12                                                               Card(11)0701
0.50        1.20                                                               Card(11)0701
0.60        1.12                                                               Card(11)0701
0.70        1.04                                                               Card(11)0701
0.80        0.96                                                               Card(11)0701
0.90        0.88                                                               Card(11)0701
1.00        0.80                                                               Card(11)0701
   0                                                                            Card(11)0702
```

Figure 1.10 Input Filename *input.fixedflows* Used as Standard Problem 6 in PLTEMP/ANL Verification Script

```
 Test Problem: 2 assemblies (of identical geometry) producing 1 MWt
! Each assembly has 4 fuel plates and 5 coolant channels
! H2O coolant, Input coolant flow = 2.5 kg/s per coolant channel
! All hot channel factors = 1.0
! No bypass flow, NCTYP=0
! 10 axial heat transfer nodes in the heated length of fuel plates
!  1   2   3   4   5   6   7   8   9  10  11  12  13                  Indices on Card 0200
   0   0   0   1   0   1   1   1   0   0   0   0   0                           Card(1)0200
   2   3 0.00       1.00        1.00        1.00           3                  Card(1)0300
! Using pressure driven mode
   1  20 1.00                                                                  Card(1)0301
   1   1   1                                                                   Card(1)0302
1.20        1.20                                                               Card(2)0303
30.0E-04    0.02955665  0.15        8.00        0.20        15.0E-03           Card(3)0304
30.0E-04    0.02955665  0.75        0.00        0.20        15.0E-03           Card(3)0304
30.0E-04    0.02955665  0.15        8.00        0.20        15.0E-03           Card(3)0304
! Use the code's built-in correlation for friction factor
0.00        0.00        0.00                                                   Card(1)0305
   5   3 0.00       0.75        0.50E-03    0.00        1.00E-03    100.00     Card(1)0306
6.00E-04    5.91133E-03 0.4060      0.20        0.20        3.00E-03           Card(5)0307
6.00E-04    5.91133E-03 0.4060      0.40        0.20        3.00E-03           Card(5)0307
6.00E-04    5.91133E-03 0.4060      0.40        0.20        3.00E-03           Card(5)0307
6.00E-04    5.91133E-03 0.4060      0.40        0.20        3.00E-03           Card(5)0307
6.00E-04    5.91133E-03 0.4060      0.20        0.20        3.00E-03           Card(5)0307
0.20        0.20        0.20        0.20                                       Card(1)0308
! Card 0308a not required
! Radial power peaking factor data by fuel plate for each assembly. Input flow data by
! channel for each assembly on Cards 0310 not required because WFGES(1) is non-zero
0.900       0.950       1.050       1.100                                      Card(2)0309
0.50        0.50        0.50        0.50        0.50                           Card(2)0310
0.600       0.800       1.200       1.400                                      Card(2)0309
0.50        0.50        0.50        0.50        0.50                           Card(2)0310
! DP0       DDP         DPMAX       POWER       TIN         PIN
0.10        0.04        0.10        1.00        45.0        1.40               Card(1)0500
  50 0.0001     25.0        0.50        1.00                                   Card(1)0600
  11                                                                           Card(1)0700
0.00        0.80                                                               Card(11)0701
0.10        0.88                                                               Card(11)0701
0.20        0.96                                                               Card(11)0701
0.30        1.04                                                               Card(11)0701
0.40        1.12                                                               Card(11)0701
0.50        1.20                                                               Card(11)0701
0.60        1.12                                                               Card(11)0701
0.70        1.04                                                               Card(11)0701
0.80        0.96                                                               Card(11)0701
0.90        0.88                                                               Card(11)0701
1.00        0.80                                                               Card(11)0701
   0                                                                           Card(11)0702
```

Figure 1.11 Input Filename *input.Powerloop* Used as Standard Problem 7 in PLTEMP/ANL Verification Script

```
 Test Problem: 2 assemblies (of identical geometry) producing 1 MWt
! Each assembly has 4 fuel plates and 5 coolant channels
! H2O coolant, Flow is calculated from input pressure drop
! All hot channel factors = 1.0
! No bypass flow, NCTYP=0
! 10 axial heat transfer nodes in the heated length of fuel plates
!  1   2   3   4   5   6   7   8   9  10  11  12  13                  Indices on Card 0200
   0   0   0   1   0   1   1   1   0   0   0   0   0                           Card(1)0200
   2   3 0.50       1.00        1.00        1.00           3                  Card(1)0300
! Using pressure driven mode
   1  20 1.00                                                                  Card(1)0301
   1   1   1                                                                   Card(1)0302
1.20        1.20                                                               Card(2)0303
30.0E-04    0.02955665  0.15        8.00        0.20        15.0E-03           Card(3)0304
30.0E-04    0.02955665  0.75        0.00        0.20        15.0E-03           Card(3)0304
30.0E-04    0.02955665  0.15        8.00        0.20        15.0E-03           Card(3)0304
! Use the code's built-in correlation for friction factor
0.00        0.00        0.00                                                   Card(1)0305
   5   3 0.00       0.75        0.50E-03    0.00        1.00E-03    100.00     Card(1)0306
6.00E-04    5.91133E-03 0.4060      0.20        0.20        3.00E-03           Card(5)0307
6.00E-04    5.91133E-03 0.4060      0.40        0.20        3.00E-03           Card(5)0307
6.00E-04    5.91133E-03 0.4060      0.40        0.20        3.00E-03           Card(5)0307
6.00E-04    5.91133E-03 0.4060      0.40        0.20        3.00E-03           Card(5)0307
6.00E-04    5.91133E-03 0.4060      0.20        0.20        3.00E-03           Card(5)0307
0.20        0.20        0.20        0.20                                       Card(1)0308
! Card 0308a not required
! Radial power peaking factor data by fuel plate for each assembly. Input flow data by
! channel for each assembly on Cards 0310 not required because WFGES(1) is non-zero
0.900       0.950       1.050       1.100                                      Card(2)0309
0.600       0.800       1.200       1.400                                      Card(2)0309
! DP0       DDP         DPMAX       POWER       TIN         PIN
0.10        0.04        0.10        1.00        45.0        1.40               Card(1)0500
!     CONV       ETA        DPWR        PWRM
 -50 0.0001     25.0        0.20        6.00                                   Card(1)0600
  11                                                                            Card(1)0700
0.00        0.80                                                               Card(11)0701
0.10        0.88                                                               Card(11)0701
0.20        0.96                                                               Card(11)0701
0.30        1.04                                                               Card(11)0701
0.40        1.12                                                               Card(11)0701
0.50        1.20                                                               Card(11)0701
0.60        1.12                                                               Card(11)0701
0.70        1.04                                                               Card(11)0701
0.80        0.96                                                               Card(11)0701
0.90        0.88                                                               Card(11)0701
1.00        0.80                                                               Card(11)0701
   0                                                                            Card(11)0702
```

Figure 1.12 Input Filename *input.pressuredriven* Used as Standard Problem 8 in PLTEMP/ANL Verification Script

```
 Test Problem: 2 assemblies (of identical geometry) producing 1 MWt
! Each assembly has 4 fuel plates and 5 coolant channels
! H2O coolant, Flow is calculated from input pressure drop
! All hot channel factors = 1.0
! No bypass flow, NCTYP=0
! 10 axial heat transfer nodes in the heated length of fuel plates
!  1   2   3   4   5   6   7   8   9  10  11  12  13                  Indices on Card 0200
   0   0   0   1   0   1   1   1   0   0   0   0   0                                Card(1)0200
   2   3 0.50       1.00        1.00        1.00           3                     Card(1)0300
! Using pressure driven mode
   1  20 1.00                                                                     Card(1)0301
   1   1   1                                                                      Card(1)0302
1.20        1.20                                                                  Card(2)0303
30.0E-04    0.02955665  0.15        8.00        0.20        15.0E-03              Card(3)0304
30.0E-04    0.02955665  0.75        0.00        0.20        15.0E-03              Card(3)0304
30.0E-04    0.02955665  0.15        8.00        0.20        15.0E-03              Card(3)0304
! Use the code's built-in correlation for friction factor
0.00        0.00        0.00                                                      Card(1)0305
   5   3 0.00       0.75        0.50E-03    0.00        1.00E-03    100.00       Card(1)0306
6.00E-04    5.91133E-03 0.4060      0.20        0.20        3.00E-03              Card(5)0307
6.00E-04    5.91133E-03 0.4060      0.40        0.20        3.00E-03              Card(5)0307
6.00E-04    5.91133E-03 0.4060      0.40        0.20        3.00E-03              Card(5)0307
6.00E-04    5.91133E-03 0.4060      0.40        0.20        3.00E-03              Card(5)0307
6.00E-04    5.91133E-03 0.4060      0.20        0.20        3.00E-03              Card(5)0307
0.20        0.20        0.20        0.20                                          Card(1)0308
! Card 0308a not required
! Radial power peaking factor data by fuel plate for each assembly. Input flow data by
! channel for each assembly on Cards 0310 not required because WFGES(1) is non-zero
0.900       0.950       1.050       1.100                                         Card(2)0309
0.600       0.800       1.200       1.400                                         Card(2)0309
! DP0       DDP         DPMAX       POWER       TIN         PIN
0.10        0.04        0.10        1.00        45.0        1.40                  Card(1)0500
  50 0.0001     25.0        0.50        1.00                                      Card(1)0600
  11                                                                              Card(1)0700
0.00        0.80                                                                  Card(11)0701
0.10        0.88                                                                  Card(11)0701
0.20        0.96                                                                  Card(11)0701
0.30        1.04                                                                  Card(11)0701
0.40        1.12                                                                  Card(11)0701
0.50        1.20                                                                  Card(11)0701
0.60        1.12                                                                  Card(11)0701
0.70        1.04                                                                  Card(11)0701
0.80        0.96                                                                  Card(11)0701
0.90        0.88                                                                  Card(11)0701
1.00        0.80                                                                  Card(11)0701
   0                                                                              Card(11)0702
```

Table 1.1 Comparison of Spreadsheet and PLTEMP/ANL Solutions for Five Test Problems

Problem	Temperature Difference* (ΔT), °C		Film Coefficient Difference‡ (Δh), W/m^2-C	
	Max. |ΔT|	RMS†	Max. |Δh|	RMS†
38	0.18	0.14	25.3	19.2
39	0.20	0.12	39.5	20.7
40	0.20	0.12	41.5	20.0
41	0.61	0.18	60.6	27.4
42	0.61	0.14	44.3	18.3

*Includes all bulk coolant, clad surface, interface, and peak fuel temperatures
†Root-mean-square of all ΔT's or Δh's
‡Includes all 80 (4 plates × 2 surfaces × 10 axial levels) film coefficients

Table 1.2 Comparison of PLTEMP/ANL- and Spreadsheet-Calculated Flow Rates for Three Problems

Input Data	Standard Problem 23B Flow Rate, kg/s				Standard Problem 23 Flow Rate, kg/s				Standard Problem 23C Flow Rate, kg/s			
Reactor Power, MW	0.0001				1.0				4.0			
Fuel Plate No.	1	2	3	4	1	2	3	4	1	2	3	4
Radial Power Factors of Plates in Assembly 1	0.900	0.950	1.050	1.100	0.900	0.950	1.050	1.100	0.2250	0.2375	0.2625	0.2750
Radial Power Factors of Plates in Assembly 2	0.901	0.951	1.049	1.099	0.901	0.951	1.049	1.099	1.0000	2.5000	2.5000	1.0000
	Comparison of Results											
Geometrical Region	Power Deposited in Channels W	Spread-sheet Flow kg/s	PLTEMP Flow kg/s	% Diff. in Flow	Power Deposited in Channels W	Spread-sheet Flow kg/s	PLTEMP Flow kg/s	% Diff. in Flow	Power Deposited in Channels W	Spread-sheet Flow kg/s	PLTEMP Flow kg/s	% Diff. in Flow
Assembly 1, Estimate	50.00	9.66577	9.6634	0.025	500000	9.66262	9.6697	0.073	500000	9.66262	9.6697	0.073
Assembly 1	50.00	9.65676	9.6639	0.074	500000	9.66254	9.6694	0.071	500000	9.66254	9.6694	0.071
Assembly 1, Channel 1	5.63	1.93135	1.93277	0.073	56250	1.92185	1.92371	0.097	56250	1.92185	1.92371	0.097
Assembly 1, Channel 2	11.56	1.93135	1.93278	0.074	115625	1.93636	1.93758	0.063	115625	1.93636	1.93758	0.063
Assembly 1, Channel 3	12.50	1.93135	1.93278	0.074	125000	1.93857	1.93966	0.056	125000	1.93857	1.93966	0.056
Assembly 1, Channel 4	13.44	1.93135	1.93278	0.074	134375	1.94076	1.94172	0.049	134375	1.94076	1.94172	0.049
Assembly 1, Channel 5	6.88	1.93135	1.93277	0.073	68750	1.92498	1.92673	0.091	68750	1.92498	1.92673	0.091
Max. Abs. % Diff.				**0.074**				**0.097**				**0.097**
Assembly 2, Estimate	50.00	9.65676	9.6634	0.069	500000	9.66262	9.6697	0.073	3500000	9.6227	9.6169	0.060
Assembly 2	50.00	9.65676	9.6639	0.074	500000	9.66254	9.6694	0.071	3500000	9.61921	9.5705	0.509
Assembly 2, Channel 1	5.63	1.93135	1.93277	0.073	56313	1.92187	1.92372	0.096	250000	1.85672	1.86167	0.266
Assembly 2, Channel 2	11.56	1.93135	1.93278	0.074	115750	1.9364	1.93761	0.062	875000	1.95561	1.93968	0.821
Assembly 2, Channel 3	12.50	1.93135	1.93278	0.074	125000	1.93858	1.93966	0.056	1250000	1.99455	1.96776	1.361
Assembly 2, Channel 4	13.44	1.93135	1.93278	0.074	134250	1.94073	1.94169	0.049	875000	1.95561	1.93969	0.821
Assembly 2, Channel 5	6.88	1.93135	1.93277	0.073	68688	1.92497	1.92671	0.090	250000	1.85672	1.86167	0.266
Max. Abs. % Diff.				**0.074**				**0.096**				**1.361**

Table 1.3 Solution of the Standard Test Problem 20 by Different Codes Used to Verify the Natural Circulation Optionof the PLTEMP/ANL Code*

Input or Calculated Quantity	Hand Calculation Using NATCON Properties	*Mathematica* Calculation			NATCON Code Solution	RELAP5 Code Solution **	PLTEMP/ANL Solution	
		Using NATCON Coolant Properties	Using PLTEMP Coolant Properties	Using RELAP5 Coolant Properties			General Method, Friction Factor = 96/Re	General Method, Friction Factor = 94.717/Re
Inlet Temp, °C	25	25	25	25	25	25	25	25
Power per Channel, W	25000	25000	25000	25000	25000	25000	25000	25000
Loss Coeff. at Inlet	0.5	0.5	0.5	0.5	0.5	0.5	0.5	0.5
Loss Coeff. at Exit	1.0	1.0	1.0	1.0	1.0	1.0	1.0	1.0
CALCULATED QUANTITIES								
Flow per Channel, kg/s	0.1086	0.1088	0.1088	0.1113	0.1087	0.1140	0.1088	0.1093
Exit Temp, °C	79.967	79.900	79.891	78.727	79.970	77.432	79.891	79.646
BUOYANCY ΔP_{buoy} , Pa								
Axial Region 1	0.0	0.0	0.0	0.0	0.0	0.0	0.0	0.0
Axial Region 2	75.716	75.761	75.793	79.094	75.783	82.591	75.786	75.342
Axial Region 3	36.040	36.001	36.009	36.334	36.034	35.157	36.015	35.785
Channel ΔP_{buoy}	111.756	111.762	111.802	115.428	111.817	117.748	111.801	111.127
FRICTIONAL PRESSURE DROP ΔP_f , Pa								
Inlet Loss	3.652	3.664	3.667	3.830	3.659	4.022	3.667	3.700
Axial Region 1	22.268	22.307	22.300	22.514	22.348	23.074	22.300	22.101
Axial Region 2	68.970	69.239	69.276	71.500	69.275	71.385	69.275	68.758
Axial Region 3	9.015	9.037	9.041	9.340	9.033	9.630	9.042	8.894
Exit Loss	7.487	7.513	7.518	7.855	7.503	8.243	7.518	7.585
Momentum Flux Term	0.368	0.0	0.0	0.389	0.0	0.395	0.0	0.0
Channel ΔP_f	111.760	111.761	111.802	115.428	111.817	116.749	111.803	111.126

* Laminar friction factor = 96/Re, except as noted in the last column.

** The RELAP5-3D solution is not accurate because the nodal coolant temperatures at node exit are treated by the code as node-centered temperatures in calculating buoyancy and frictional pressure drop.

Table 1.4 Comparison of Thermal Properties of H_2O over 1 to 145 bar Pressure and 4 to 339 ºC Temperature between PLTEMP/ANL and NIST Data

Phase & Pressure	% Diff. H	% Diff. K	% Diff. Cp	% Diff. ρ	% Diff. μ
Liquid, 1 bar	0.619	2.175	1.251	0.070	3.160
Liquid, 2 bar	0.522	2.110	1.109	0.096	3.590
Liquid, 3 bar	0.518	2.101	1.107	0.106	3.563
Liquid, 4 bar	0.510	2.050	1.041	0.106	3.540
Liquid, 5 bar	0.505	2.057	1.036	0.107	3.511
Liquid, 10 bar	0.489	2.043	0.960	0.109	3.372
Liquid, 20 bar	0.463	1.965	2.606	0.111	3.098
Liquid, 30 bar	0.438	1.843	2.821	0.113	3.288
Liquid, 40 bar	0.400	1.778	3.687	0.113	3.825
Liquid, 50 bar	0.371	1.718	3.057	0.115	4.050
Liquid, 75 bar	0.310	1.621	2.602	0.113	4.420
Liquid, 100 bar	0.262	1.527	2.426	0.113	6.747
Liquid, 125 bar	0.214	1.422	2.456	0.113	14.332
Liquid, 145 bar	0.177	1.380	2.174	0.121	21.414
Max. % Error All Pressures	**0.619**	**2.175**	**3.687**	**0.121**	**21.414**

Table 1.5 Comparison of Thermal Properties of D_2O over 1 to 150 bar Pressure and 5 to 341 ºC Temperature between PLTEMP/ANL and NIST Data

Phase & Pressure	% Diff. H	% Diff. K	% Diff. Cp	% Diff. ρ	% Diff. μ
Liquid, 1 bar	2.710	1.941	3.411	0.476	1.793
Liquid, 2 bar	2.728	1.854	3.285	0.468	1.353
Liquid, 3 bar	2.730	1.853	3.283	0.463	1.346
Liquid, 4 bar	2.726	1.779	3.167	0.454	0.969
Liquid, 5 bar	2.728	1.770	3.167	0.449	0.957
Liquid, 10 bar	2.688	1.608	2.965	0.422	0.592
Liquid, 20 bar	2.770	1.526	2.869	0.406	0.629
Liquid, 30 bar	2.786	1.444	2.783	0.396	0.617
Liquid, 40 bar	2.805	1.366	2.703	0.385	0.583
Liquid, 50 bar	2.804	1.298	2.630	0.364	0.750
Liquid, 75 bar	2.831	1.204	2.615	0.356	0.853
Liquid, 100 bar	2.828	1.134	2.603	0.336	0.828
Liquid, 125 bar	2.824	2.699	2.585	0.323	0.926
Liquid, 150 bar	2.814	4.839	2.605	0.307	0.983
Max. % Diff., All Pressures	2.831	4.839	3.411	0.476	1.793

2 Verification of Exact and Broyden Solutions for Temperature Distribution in an Assembly Made of Multiple Three-layer Fuel Plates

The Exact and Broyden solution methods for calculating temperature distribution are briefly described in Section 1.2.1 and documented in the code users guide [Ref. 3 in Chapter 1]. The Exact method is far more robust and faster. However, the Broyden method been maintained because it provides an important bridge to the newer method. It is used for checking the newer method. The Exact method was implemented due to a limitation of the Broyden method. It does not converge when the location of peak fuel temperature is locatred at one of the fuel-cladding interfaces, and the fuel temperature in meat thickness has a non-zero gradient at that location. A calculated parameter in the Broyden method, that is used in the code verification reported below, is the mismatch T_{diff} between (1) the fuel maximum temperature calculated starting from the coolant channel temperature on the right side of the fuel plate and (2) that calculated starting from the coolant channel temperature on the left side of the fuel plate.

The verification work reported here was done in June 2006. The verification script described in Chapter 1 was run for the version 3.0 code. The verification script ran the code executable for the 8 standard problems listed in Section 1.4 of Chapter 1 and compared each problem's output with the stored output obtained by code version 2.14 for the problem. Tables 2.2 to 2.9 summarize the mismatch T_{diff} of fuel maximum temperature, and the changes in calculated temperatures. The column 4 shows the biggest mismatch T_{diff} in current code output, searched over all axial nodes of a fuel plate. The column 5 shows the similar mismatch in the old saved output of the standard problem. It is found that there is a marked improvement in code convergence as shown by a decrease in mismatch T_{diff} of fuel maximum temperature (column 4 compared to column 5). For all 8 standard problems, the current T_{diff} is small and acceptable (maximum 0.5 C).

The maximum temperature difference shown in column 2 of each table (of Tables 2.2 to 2.9) is the biggest change in coolant, cladding and fuel temperatures, searched over all axial nodes of a fuel plate, between the current output and the saved output. The column 2 basically gives the error in the old calculation.

<u>Four special types of test problems</u> (standard problems 9 to 15, listed in Section 2.5) were solved to test the robustness of the Exact method, and these are described in the next four sections. In the first special type described in Section 2.1, a fuel assembly is analyzed in which one of the channels has a flow blockage that is represented by a significant reduction in flow. The results of the PLTEMP/ANL solutions are compared with those obtained with the RELAP5/Mod3.2.1.2 code. In Section 2.2, in a four-plate fuel assembly having five coolant channels, the first fuel plate is heated while the other three are not. The purpose here is to study the distribution of temperature among the four fuel plates and five coolant channels. In order to exaggerate the effect, in some of the test cases the coolant thermal conductivity is artificially substantially increased.

In Section 2.3, a four-plate fuel assembly is unrealistically long (10 m). It is heated only over the first 2.5 m of only the middle two fuel plates. The purpose here is to study the distribution of temperature over the whole length and from channel to channel of the fuel assembly. In Section 2.4, large volumetric heat generation rates are assumed in the cladding and in the coolant in order to test the new capabilities to model heat generation in the cladding and the coolant.

2.1 Comparison of PLTEMP/ANL Exact Solution with RELAP5 Code

Appendix A provides a comparison of a safety analysis (blocked inner channel) for the Libyan research reactor IRT-1 using two codes, RELAP5/Mod3.2.1.2 and the exact solution obtained by PLTEMP/ANL V2.21. The results obtained by the two codes, shown in Appendix A, are in good agreement. This provides a verification of the exact solution method implemented in the PLTEMP/ANL code. The PLTEMP/ANL input data file for this analysis has been saved as standard problem 9 (filename: *input.blockage.hanan*) for code verification in the future.

2.2 Heat-up of Non-adjacent Coolant Channels Due to Heat Source in a Fuel Plate

To verify whether or not the heat transfer from a fuel plate to farther non-adjacent coolant channels in a fuel assembly is modeled in the exact solution method implemented in PLTEMP/ANL code, the version 3.0 was run for an assembly having 4 fuel plates and 5 coolant channels, producing 0.5 MWt power, with all power being generated in plate 1. The input data file given in Fig. 2.1 (standard problem 10) shows the radial power factors of the 4 fuel plates as 1.0, 10^{-8}, 10^{-8}, 10^{-8}. The coolant inlet temperature is 25 C. Coolant channels 1 and 2 are in direct contact with fuel plate 1. Coolant channels 3, 4 and 5 are the non-adjacent channels. Of interest is the heat-up of the coolant channel 5 which is located the farthest from plate 1.

Since water thermal conductivity is very low compared to fuel and cladding conductivities, four cases were run using water conductivity artificially increased by a factor of 1.0, 10.0, 100.0, or 1000.0. To run these cases, a Fortran card (e.g., ZTHCL=ZTHCL*10.0) was put just before RETURN in the source code of the function routine ZTHCL which calculates the thermal conductivity of coolant, and four different executables of PLTEMP/ANL V3.0 were created using each of the four factors. The four outputs obtained by running these executables for the input data given in Fig. 2.1 are shown in Figs. 2.2 to 2.5. The coolant channel outlet temperatures in Figs. 2.2 to 2.5 are summarized in Table 2.1.

The coolant channel 5 (the farthest from fuel plate 1) does not heat much in case 1 that uses the actual water thermal conductivity. The temperature rise is only 0.136 C. Only channel 3 among the non-adjacent channels in this case has a considerable heat-up (temperature rise 15.214 C). But there is considerable temperature rise in coolant channel 5 in cases 2, 3 and 4, being 16.052, 52.427, and 56.340 C respectively. In case 4, the coolant channel 5 (outlet temperature 81.340 C) is almost as hot as channel 2 (outlet temperature 85.578 C) that is adjacent to fuel plate 1. This verifies that the exact solution method implemented in PLTEMP/ANL V3.0 code models the heat transfer from a fuel plate to farther non-adjacent coolant channels in a fuel assembly.

2.3 Equilibration of Coolant Channel Temperatures in the Axial Direction

To verify whether or not the heat transfer between coolant channels in a assembly is modeled in the exact solution method, the PLTEMP/ANL V3.0 code was run for a problem that models a assembly consisting of four fuel plates, each 10 meters long, of which the fuel meat in the lower 2.5 meters of only two plates (plates 2 and 3) have heat source. The upper 7.5 meters of plates 2 and 3, and the whole length of plates 1 and 4 do not have any heat source. Figure 2.6 shows the input data for the problem (standard problem 11). The coolant inlet temperature is 25 C. The whole

10-meter plate length is divided into 40 axial nodes to calculate the equilibration of the five coolant channel temperatures.

Figure 2.7 shows the code output. At the top of the axial length having heat source, i.e., the axial node 11, the five coolant channel temperatures are 50.83, 78.98, 97.97, 97.97, 78.98, 50.83 C. These coolant channel temperatures are symmetric as expected. There is a wide temperature variation from channel 1 to channel 3, i.e., from 50.83 C to 97.97 C. At the outlet of the assembly, the five channel temperatures are 72.76, 72.84, 72.90, 72.84, 72.76 C, all within a fraction of a degree of each other. This equilibration occurs over the upper 7.5 meters of unheated plate length. It verifies that the heat transfer between coolant channels in a assembly is modeled in the exact solution method.

2.4 Verification of Implementation of Heat Source in Cladding and Coolant Channels

The exact method, implemented in PLTEMP/ANL version 3.0 for calculating temperature distribution in a fuel assembly, allows for heat generation sources in the cladding on left and right sides of fuel plates, and for heat source in coolant channels. A verification of this implementation was performed by running the code and comparing the results for three problems (standard problems 12, 13 and 14) which are identical except for the differences in (i) cladding thickness and (ii) the fraction of reactor power produced in cladding, as discussed here. The cladding thickness expressed as a fraction of plate thickness is kept equal to the power produced in cladding expressed as a fraction of reactor power. This makes all three standard problems physically identical (from heat transfer point of view) since the input thermal conductivities of fuel and cladding are equal (10.0 W/m-K) in these problems. Hence all calculated temperatures (of coolant channels, cladding surfaces, fuel) are expected to be the same in these three problems.

The input data and outputs of problems 12, 13 and 14 are given in Figs. 2.8 through 2.13. The standard problem 12 has a heat source of 350 MW/m^3 in fuel meat only (no heat source in cladding and coolant); the fuel meat is 2.0 mm thick and the cladding thickness is negligible (0.5×10^{-6} mm). In problem 13, the cladding is 0.5 mm thick with a power density of 350 MW/m^3, producing 50% of reactor power. The fuel meat thickness is reduced from 2.0 mm to 1.0 mm, keeping the plate thickness fixed at 2.0 mm. In problem 14, the cladding is 0.9 mm thick with a power density of 350 MW/m^3, producing 90% of reactor power. The fuel meat thickness is further reduced to 0.2 mm, keeping the plate thickness fixed at 2.0 mm.

The outputs of these problems given in Figs. 2.9, 2.11 and 2.13 show that all coolant channel temperatures, cladding surface temperatures, and fuel peak temperatures are equal, thus verifying the implementation of cladding heat source in PLTEMP/ANL version 3.0 code.

A verification of the implementation of heat source in coolant channels was performed by running the code for standard problem 15 in which 100% of reactor power is generated in coolant channels. There is no heat source in fuel and cladding in this problem. The input data for the problem (given in Fig. 2.14) shows that the radial power factors (on input card 0309) of all four fuel plates in a assembly are 1.0, and the coolant flow rate (0.25 kg/s) in the first or last channel is half of the flow rate (0.50 kg/s) in an internal channel, i.e., channels 2, 3 or 4. These flow rates were selected to heat up each channel equally, based on the reason discussed here. It is because the volumetric heat source in coolant channels is found (in the implementation) from the input fraction QFCOOL (on

card 0500) by depositing half of QFCOOL*(power in a fuel plate node) in the two coolant channels on the left and right of the plate. Thus the volumetric heat source in the first and last coolant channels (116.67 MW/m^3 as shown in Fig. 2.15) turns out to be half of the heat source (233.33 MW/m^3 as shown in Fig. 2.15) in coolant channels 2, 3 or 4.

The output of problem 15 given in Fig. 2.15 shows that, in any axial node, all 5 coolant channel temperatures are equal as expected. The nodal fuel and cladding temperatures are also equal to the coolant nodal temperature. This is because the fuel and cladding have no heat source, and are in steady-state equilibrium with the coolant. This verifies the implementation of heat source in coolant channels.

A further verification is that the mixed mean coolant temperature is the same (104.46 C) in these four standard problems (see Figs. 2.9, 2.11, 2.13 and 2.15), irrespective of the heat source distribution in fuel, cladding and coolant channels. The mixed mean temperature is fixed because these four problems have the same reactor power and coolant flow rate.

2.5 List of Standard Problems

Eight standard problems were documented in Chapter 1. An additional 7 standard problems were developed to verify the exact solution method and its new capabilities. These are listed below:

(9) Standard problem 9 (input data filename *input.blockage.hanan*): It was developed for analyzing an event (blocked inner channel) in the Libyan research reactor.

(10) Standard problem 10 (input data filename *input.Stdproblem10*): It is a problem modeling a four-fuel plate assembly, producing 0.5 MWt power, with all power being generated in only one fuel plate, i.e., plate 1. It was developed to verify coolant temperature equilibration in the radial direction.

(11) Standard problem 11 (input data filename *input.Stdproblem11.channTemp.long*): It is a problem modeling an assembly consisting of four plates, each 10 meters long, of which the fuel meat in the lower 2.5 meters of only plates 2 and 3 have heat source. It was developed to verify coolant temperature equilibration in the axial direction.

(12) Standard problem 12 (input data filename *input.Stdproblem12.HEATinCladandFuel*): This problem models 2 four-plate assemblies with a total power of 1.0 MWt. None of this power is generated in the cladding, and the cladding thickness is practically zero (0.5×10^{-6} mm) compared to the total fuel plate thickness (2.0 mm). The fuel plate (and coolant) temperature distribution in this problem must be identical to that in standard problems 13 and 14, since the input thermal conductivities of fuel and cladding are equal (10 W/m-K).

(13) Standard problem 13 (input data filename *input.Stdproblem13.HEATinCladandFuel*): This problem models 2 four-plate assemblies with a total power of 1.0 MWt. A fraction 0.5 of this power is assumed to be generated in the cladding, and the two cladding thicknesses (each 0.5 mm) add up to 0.5 times the total fuel plate thickness (2 mm). The fuel plate (and coolant) temperature distribution in this problem must be identical to that in standard problems 12 and 14, since the input thermal conductivities of fuel and cladding are equal (10 W/m-K).

(14) Standard problem 14 (input data filename *input.Stdproblem14.HEATinCladandFuel*): This problem models 2 four-plate assemblies with a total power of 1.0 MWt. A fraction 0.9 of this power is assumed to be generated in the cladding, and the two cladding thicknesses (each 0.9 mm) add up to 0.9 times the total fuel plate thickness (2 mm). The fuel plate (and coolant) temperature distribution in this problem must be identical to that in standard problems 12 and 13, since the input thermal conductivities of fuel and cladding are equal (10 W/m-K).

(15) Standard problem 15 (input data filename *input.Stdproblem15.HEATinCoolant*): This problem models 2 four-plate assemblies with a total power of 1.0 MWt. All this power is assumed to be generated in coolant channels. There is no heat source in fuel and cladding in this problem. With the input radial power factors of all four plates equal to 1.0, and the coolant flow in the first and the last channel each being half of the flow in an internal channel, each channel must heat up identically.

Figure 2.1 PLTEMP/ANL V3.0 Input Data for Standard Problem 10, a Assembly With Heat Source in Fuel Plate 1 Only

```
 Standard Problem 10: 1 assembly producing 0.5 MWt; All power in Plate 1
! The assembly has 4 fuel plates and 5 coolant channels
! H2O coolant, Input coolant flow = 3.16 kg/s per coolant channel
! All hot channel factors = 1.0
! No bypass flow, NCTYP=0
! 10 axial heat transfer nodes in the heated length of fuel plates
!  1   2   3   4   5   6   7   8   9  10  11  12  13                   Indices on Card 0200
   0   0   0   1   0   1   1   1   0   0   0   0   0                            Card(1)0200
   1   3 0.00       1.00        1.00        1.00           3                   Card(1)0300
   1  20 1.00                                                                  Card(1)0301
   1   1   1                                                                   Card(1)0302
1.20        1.20                                                               Card(2)0303
30.0E-04    0.02955665  0.15        8.00        0.20        15.0E-03           Card(3)0304
30.0E-04    0.02955665  0.75        0.00        0.20        15.0E-03           Card(3)0304
30.0E-04    0.02955665  0.15        8.00        0.20        15.0E-03           Card(3)0304
! Use the code's biult-in correlation for friction factor
0.00        0.00        0.00                                                   Card(1)0305
   5   3 0.00       0.75        0.50E-03    0.00        1.00E-03    100.00     Card(1)0306
6.00E-04    5.91133E-03 0.4060      0.20        0.20        3.00E-03           Card(5)0307
6.00E-04    5.91133E-03 0.4060      0.40        0.20        3.00E-03           Card(5)0307
6.00E-04    5.91133E-03 0.4060      0.40        0.20        3.00E-03           Card(5)0307
6.00E-04    5.91133E-03 0.4060      0.40        0.20        3.00E-03           Card(5)0307
6.00E-04    5.91133E-03 0.4060      0.20        0.20        3.00E-03           Card(5)0307
0.20        0.20        0.20        0.20                                       Card(1)0308
! Card 0308a not required
! Radial power peaking factor data by fuel plate for each assembly. Input flow data by
! channel for each assembly on Cards 0310 not required because WFGES(1) is non-zero
1.000       1.0E-08     1.0E-08     1.0E-08                                    Card(2)0309
3.0         0.4E-01     0.4E-01     0.4E-01     0.4E-01                        Card(2)0310
! DP0       DDP         DPMAX       POWER       TIN         PIN
0.10        0.04        0.10        0.50        25.0        1.40               Card(1)0500
                                                                               Card(2)0500
  50 0.0001     25.0        0.50        1.00                                   Card(1)0600
  11                                                                           Card(1)0700
0.00        1.00                                                               Card(11)0701
0.10        1.00                                                               Card(11)0701
0.20        1.00                                                               Card(11)0701
0.30        1.00                                                               Card(11)0701
0.40        1.00                                                               Card(11)0701
0.50        1.00                                                               Card(11)0701
0.60        1.00                                                               Card(11)0701
0.70        1.00                                                               Card(11)0701
0.80        1.00                                                               Card(11)0701
0.90        1.00                                                               Card(11)0701
1.00        1.00                                                               Card(11)0701
   0                                                                           Card(11)0702
!234567890123456789012345678901234567890123456789012345678901234567890123456789 0
```

Figure 2.2 Exact Solution by PLTEMP/ANL V3.0 for a Assembly With Heat Source in Fuel Plate 1 Only, Heat Transfer to Farther Channels Using Actual Thermal Conductivity of Water

FUEL PLATE 1 (ExactSoln)

NODE	COOLANTl (C)	CladSl (C)	FUEL PEAK (C)	CladSr (C)	COOLANTr (C)	HCOFl W/C-m^2	HCOFr W/C-m^2	ONBRl [F Note 1]	ONBRr	ETA'l K-cm^3/J	ETA'r K-cm^3/J
	25.000				25.000						
1	26.927	155.029	179.424	179.064	30.370	2.5072E+04	8.1729E+02	0.75	0.52	1.138E+02	4.003E+01
2	30.778	154.555	178.937	178.573	40.967	2.5939E+04	8.9123E+02	0.75	0.52	1.079E+02	3.359E+01
3	34.627	154.458	178.847	178.486	51.201	2.6799E+04	9.5865E+02	0.75	0.52	1.018E+02	2.787E+01
4	38.475	154.708	179.123	178.768	60.935	2.7646E+04	1.0181E+03	0.75	0.52	9.572E+01	2.265E+01
5	42.324	155.264	179.715	179.369	70.076	2.8477E+04	1.0713E+03	0.75	0.51	8.961E+01	1.773E+01
6	46.174	156.105	180.601	180.267	78.575	2.9290E+04	1.1152E+03	0.74	0.51	8.350E+01	1.304E+01
7	50.026	157.196	181.741	181.419	86.418	3.0082E+04	1.1523E+03	0.73	0.51	7.739E+01	8.477E+00
8	53.880	158.503	183.095	182.785	93.632	3.0851E+04	1.1849E+03	0.73	0.50	7.129E+01	3.989E+00
9	57.736	160.005	184.644	184.345	100.245	3.1597E+04	1.2119E+03	0.72	0.50	6.521E+01	-4.227E-01
10	61.595	161.726	186.429	186.146	106.232	3.2322E+04	1.2119E+03	0.71	0.49	5.911E+01	-4.786E+00
	63.525				109.060						

FUEL PLATE 2 (ExactSoln)

	25.000				25.000						
1	30.370	27.764	27.758	27.731	25.093	8.0318E+02	7.9354E+02	99.99	27.60	9.999E+03	2.381E+03
2	40.967	33.388	33.371	33.291	25.457	8.2103E+02	7.9422E+02	99.99	9.15	9.999E+03	7.973E+02
3	51.201	39.210	39.182	39.051	26.170	8.5452E+02	7.9555E+02	99.99	5.42	9.999E+03	4.795E+02
4	60.935	45.407	45.367	45.184	27.218	9.2270E+02	7.9748E+02	99.99	3.79	9.999E+03	3.380E+02
5	70.076	51.614	51.563	51.331	28.583	9.8570E+02	7.9997E+02	99.99	2.91	9.999E+03	2.611E+02
6	78.575	57.662	57.601	57.324	30.231	1.0402E+03	8.0293E+02	99.99	2.38	9.999E+03	2.134E+02
7	86.418	63.472	63.402	63.083	32.126	1.0877E+03	8.0627E+02	99.99	2.02	9.999E+03	1.809E+02
8	93.632	69.026	68.948	68.593	34.229	1.1311E+03	8.0991E+02	99.99	1.77	9.999E+03	1.572E+02
9	100.245	73.994	73.909	73.517	36.517	1.1671E+03	8.2805E+02	99.99	1.59	9.999E+03	1.378E+02
10	106.232	78.208	78.117	77.696	38.960	1.1751E+03	8.5017E+02	99.99	1.47	9.999E+03	1.232E+02
	109.060				40.214						

FUEL PLATE 3 (ExactSoln)

	25.000				25.000						
1	25.093	25.047	25.047	25.047	25.002	7.9354E+02	7.9337E+02	99.99	******	9.999E+03	1.390E+05
2	25.457	25.236	25.235	25.233	25.011	7.9422E+02	7.9338E+02	99.99	321.52	9.999E+03	2.834E+04
3	26.170	25.608	25.607	25.602	25.038	7.9555E+02	7.9344E+02	99.99	124.69	9.999E+03	1.116E+04
4	27.218	26.165	26.163	26.152	25.094	7.9748E+02	7.9354E+02	99.99	65.21	9.999E+03	5.937E+03
5	28.583	26.902	26.899	26.882	25.188	7.9997E+02	7.9372E+02	99.99	39.99	9.999E+03	3.704E+03
6	30.231	27.809	27.803	27.778	25.328	8.0293E+02	7.9398E+02	99.99	27.13	9.999E+03	2.554E+03
7	32.126	28.868	28.861	28.827	25.521	8.0627E+02	7.9434E+02	99.99	19.72	9.999E+03	1.887E+03
8	34.229	30.066	30.056	30.013	25.771	8.0991E+02	7.9481E+02	99.99	15.07	9.999E+03	1.465E+03
9	36.517	31.392	31.380	31.327	26.082	8.1377E+02	7.9539E+02	99.99	11.96	9.999E+03	1.179E+03
10	38.960	32.831	32.817	32.753	26.457	8.1780E+02	7.9608E+02	99.99	9.77	9.999E+03	9.764E+02
	40.214				26.661						

FUEL PLATE 4 (ExactSoln)

	25.000				25.000						
1	25.002	25.001	25.001	25.001	25.000	7.9337E+02	6.6514E+02	99.99	******	9.999E+03	8.631E+06
2	25.011	25.006	25.006	25.006	25.000	7.9338E+02	6.6516E+02	99.99	******	9.999E+03	1.291E+06
3	25.038	25.021	25.021	25.021	25.001	7.9344E+02	6.6519E+02	99.99	******	9.999E+03	3.725E+05
4	25.094	25.053	25.053	25.052	25.003	7.9354E+02	6.6528E+02	99.99	******	9.999E+03	1.524E+05
5	25.188	25.106	25.106	25.105	25.007	7.9372E+02	6.6541E+02	99.99	711.57	9.999E+03	7.683E+04
6	25.328	25.186	25.186	25.185	25.015	7.9398E+02	6.6564E+02	99.99	405.52	9.999E+03	4.435E+04
7	25.521	25.297	25.297	25.295	25.029	7.9434E+02	6.6595E+02	99.99	254.03	9.999E+03	2.814E+04
8	25.771	25.443	25.442	25.439	25.048	7.9481E+02	6.6639E+02	99.99	170.61	9.999E+03	1.915E+04
9	26.082	25.626	25.625	25.620	25.076	7.9539E+02	6.6695E+02	99.99	120.84	9.999E+03	1.374E+04
10	26.457	25.848	25.847	25.841	25.114	7.9608E+02	6.6766E+02	99.99	89.23	9.999E+03	1.028E+04
	26.661				25.136						

[1] The ONB ratio is here defined as (Tonb - Tinlet)/(Tsurf - Tinlet). If the heat flux is negative (the coolant is hotter than the adjacent cladding surface), then the ONB ratio is arbitrarily set to 99.99 .

Figure 2.3 Exact Solution by PLTEMP/ANL V3.0 for a Assembly With Heat Source in Fuel Plate 1 Only, Heat Transfer to Farther Channels With Water Thermal Conductivity Multiplied by 10

FUEL PLATE 1 (ExactSoln)

NODE	COOLANTl (C)	CladSl (C)	FUEL PEAK (C)	CladSr (C)	COOLANTr (C)	HCOFl W/C-m^2	HCOFr W/C-m^2	ONBRl [F Note 1]	ONBRr	ETA'l K-cm^3/J	ETA'r K-cm^3/J
	25.000				25.000						
1	26.811	54.827	76.885	75.863	37.297	1.0776E+05	8.1507E+03	3.23	1.62	1.213E+02	1.393E+01
2	30.491	58.281	81.515	80.844	55.163	1.1217E+05	8.4188E+03	2.91	1.45	1.116E+02	1.445E+01
3	34.252	61.346	85.076	84.542	63.973	1.1655E+05	8.5308E+03	2.67	1.35	1.041E+02	1.427E+01
4	38.046	64.316	88.276	87.804	69.569	1.2092E+05	8.5953E+03	2.47	1.28	9.751E+01	1.347E+01
5	41.855	67.280	91.359	90.918	73.896	1.2532E+05	8.6415E+03	2.29	1.21	9.120E+01	1.229E+01
6	45.671	70.293	94.436	94.011	77.657	1.2961E+05	8.6792E+03	2.14	1.16	8.504E+01	1.087E+01
7	49.488	73.356	97.533	97.117	81.143	1.3383E+05	8.7121E+03	2.01	1.11	7.895E+01	9.330E+00
8	53.306	76.469	100.662	100.251	84.488	1.3796E+05	8.7419E+03	1.89	1.06	7.291E+01	7.718E+00
9	57.122	79.629	103.829	103.419	87.760	1.4200E+05	8.7692E+03	1.78	1.02	6.689E+01	6.072E+00
10	60.935	82.832	107.031	106.621	91.000	1.4595E+05	8.7945E+03	1.68	0.98	6.090E+01	4.413E+00
	62.841				92.615						

FUEL PLATE 2 (ExactSoln)

	25.000				25.000						
1	37.297	32.319	32.206	31.688	26.592	8.1507E+03	7.9633E+03	99.99	11.60	9.999E+03	1.204E+02
2	55.163	44.257	44.002	42.829	31.424	8.4188E+03	8.0504E+03	99.99	4.43	9.999E+03	4.968E+01
3	63.973	51.901	51.615	50.299	37.674	8.5308E+03	8.1569E+03	99.99	3.13	9.999E+03	4.024E+01
4	69.569	57.473	57.184	55.855	43.247	8.5953E+03	8.2461E+03	99.99	2.57	9.999E+03	3.627E+01
5	73.896	61.989	61.703	60.388	48.018	8.6415E+03	8.3182E+03	99.99	2.24	9.999E+03	3.355E+01
6	77.657	65.929	65.646	64.346	52.196	8.6792E+03	8.3780E+03	99.99	2.01	9.999E+03	3.117E+01
7	81.143	69.541	69.260	67.969	55.978	8.7121E+03	8.4297E+03	99.99	1.84	9.999E+03	2.888E+01
8	84.488	72.961	72.681	71.393	59.504	8.7419E+03	8.4756E+03	99.99	1.71	9.999E+03	2.663E+01
9	87.760	76.268	75.988	74.700	62.868	8.7692E+03	8.5175E+03	99.99	1.59	9.999E+03	2.440E+01
10	91.000	79.511	79.230	77.939	66.131	8.7945E+03	8.5563E+03	99.99	1.50	9.999E+03	2.218E+01
	92.615				67.744						

FUEL PLATE 3 (ExactSoln)

	25.000				25.000						
1	26.592	25.942	25.928	25.861	25.209	7.9633E+03	7.9376E+03	99.99	87.98	9.999E+03	9.608E+02
2	31.424	28.968	28.913	28.660	26.175	8.0504E+03	7.9556E+03	99.99	20.97	9.999E+03	2.485E+02
3	37.674	33.267	33.167	32.707	28.210	8.1569E+03	7.9929E+03	99.99	10.05	9.999E+03	1.329E+02
4	43.247	37.562	37.432	36.833	31.005	8.2461E+03	8.0430E+03	99.99	6.58	9.999E+03	9.791E+01
5	48.018	41.571	41.422	40.736	34.113	8.3182E+03	8.0971E+03	99.99	4.96	9.999E+03	8.171E+01
6	52.196	45.292	45.132	44.392	37.296	8.3780E+03	8.1507E+03	99.99	4.03	9.999E+03	7.208E+01
7	55.978	48.791	48.623	47.848	40.462	8.4297E+03	8.2022E+03	99.99	3.42	9.999E+03	6.532E+01
8	59.504	52.132	51.959	51.160	43.588	8.4756E+03	8.2514E+03	99.99	2.99	9.999E+03	5.999E+01
9	62.868	55.369	55.192	54.376	46.679	8.5175E+03	8.2983E+03	99.99	2.67	9.999E+03	5.545E+01
10	66.131	58.541	58.361	57.531	49.747	8.5563E+03	8.3433E+03	99.99	2.41	9.999E+03	5.137E+01
	67.744				51.277						

FUEL PLATE 4 (ExactSoln)

	25.000				25.000						
1	25.209	25.140	25.139	25.132	25.024	7.9376E+03	5.0537E+03	99.99	569.10	9.999E+03	9.191E+03
2	26.175	25.806	25.798	25.761	25.181	7.9556E+03	5.0556E+03	99.99	99.25	9.999E+03	1.698E+03
3	28.210	27.264	27.243	27.146	25.653	7.9929E+03	5.0612E+03	99.99	35.41	9.999E+03	6.545E+02
4	31.005	29.374	29.337	29.169	26.583	8.0430E+03	5.0722E+03	99.99	18.32	9.999E+03	3.724E+02
5	34.113	31.861	31.810	31.577	27.994	8.0971E+03	5.0887E+03	99.99	11.66	9.999E+03	2.627E+02
6	37.296	34.550	34.488	34.201	29.821	8.1507E+03	5.1097E+03	99.99	8.36	9.999E+03	2.086E+02
7	40.462	37.348	37.277	36.951	31.975	8.2022E+03	5.1339E+03	99.99	6.45	9.999E+03	1.772E+02
8	43.588	40.210	40.133	39.777	34.376	8.2514E+03	5.1604E+03	99.99	5.22	9.999E+03	1.566E+02
9	46.679	43.116	43.034	42.656	36.957	8.2983E+03	5.1881E+03	99.99	4.37	9.999E+03	1.418E+02
10	49.747	46.054	45.969	45.575	39.668	8.3433E+03	5.2164E+03	99.99	3.75	9.999E+03	1.302E+02
	51.277				41.052						

[1] The ONB ratio is here defined as (Tonb - Tinlet)/(Tsurf - Tinlet). If the heat flux is negative (the coolant is hotter than the adjacent cladding surface), then the ONB ratio is arbitrarily set to 99.99 .

Figure 2.4 Exact Solution by PLTEMP/ANL V3.0 for a Assembly With Heat Source in Fuel Plate 1 Only, Heat Transfer to Farther Channels With Water Thermal Conductivity Multiplied by 100

FUEL PLATE 1 (ExactSoln)

NODE	COOLANTl (C)	CladSl (C)	FUEL PEAK (C)	CladSr (C)	COOLANTr (C)	HCOFl W/C-m^2	HCOFr W/C-m^2	ONBRl [F Note 1]	ONBRr	ETA'l K-cm^3/J	ETA'r K-cm^3/J
	25.000				25.000						
1	26.634	32.419	51.114	48.863	41.446	4.7084E+05	8.2179E+04	12.87	3.56	1.348E+02	6.704E+00
2	30.116	36.390	59.209	58.418	55.443	4.9135E+05	8.4225E+04	8.49	2.44	1.134E+02	1.238E+01
3	33.785	39.721	62.001	61.050	57.553	5.1178E+05	8.4504E+04	6.56	2.28	1.090E+02	1.000E+01
4	37.465	43.296	66.389	65.678	63.004	5.3254E+05	8.5191E+04	5.29	2.00	1.007E+02	1.129E+01
5	41.185	46.802	69.920	69.217	66.580	5.5320E+05	8.5615E+04	4.44	1.84	9.459E+01	1.028E+01
6	44.919	50.380	73.810	73.195	70.872	5.7376E+05	8.6095E+04	3.82	1.68	8.782E+01	1.010E+01
7	48.669	53.953	77.453	76.857	74.610	5.9405E+05	8.6489E+04	3.35	1.56	8.165E+01	9.043E+00
8	52.427	57.558	81.192	80.632	78.522	6.1402E+05	8.6876E+04	2.98	1.45	7.537E+01	8.088E+00
9	56.192	61.170	84.852	84.306	82.250	6.3362E+05	8.7222E+04	2.68	1.36	6.927E+01	6.807E+00
10	59.959	64.798	88.541	88.011	86.019	6.5286E+05	8.7548E+04	2.44	1.28	6.316E+01	5.483E+00
	61.843				87.845						

FUEL PLATE 2 (ExactSoln)

	25.000				25.000						
1	41.446	38.487	37.811	34.704	31.686	8.2179E+04	8.0550E+04	99.99	8.39	9.999E+03	1.869E+01
2	55.443	51.819	50.971	47.070	43.370	8.4225E+04	8.2480E+04	99.99	3.72	9.999E+03	1.233E+01
3	57.553	55.260	54.722	52.247	49.927	8.4504E+04	8.3459E+04	99.99	2.96	9.999E+03	1.716E+01
4	63.004	60.564	59.987	57.331	54.861	8.5191E+04	8.4147E+04	99.99	2.50	9.999E+03	1.441E+01
5	66.580	64.644	64.184	62.067	60.113	8.5615E+04	8.4833E+04	99.99	2.17	9.999E+03	1.595E+01
6	70.872	68.967	68.512	66.417	64.497	8.6095E+04	8.5371E+04	99.99	1.94	9.999E+03	1.433E+01
7	74.610	72.915	72.508	70.635	68.928	8.6489E+04	8.5881E+04	99.99	1.75	9.999E+03	1.401E+01
8	78.522	76.873	76.475	74.644	72.984	8.6876E+04	8.6320E+04	99.99	1.61	9.999E+03	1.244E+01
9	82.250	80.694	80.318	78.584	77.020	8.7222E+04	8.6730E+04	99.99	1.49	9.999E+03	1.115E+01
10	86.019	84.496	84.126	82.422	80.892	8.7548E+04	8.7098E+04	99.99	1.39	9.999E+03	9.400E+00
	87.845				82.860						

FUEL PLATE 3 (ExactSoln)

	25.000				25.000						
1	31.686	30.513	30.251	29.044	27.861	8.0550E+04	7.9866E+04	99.99	19.54	9.999E+03	5.082E+01
2	43.370	41.019	40.481	38.003	35.617	8.2480E+04	8.1226E+04	99.99	6.21	9.999E+03	2.208E+01
3	49.927	48.023	47.581	45.551	43.625	8.3459E+04	8.2520E+04	99.99	3.90	9.999E+03	2.357E+01
4	54.861	53.287	52.919	51.227	49.639	8.4147E+04	8.3418E+04	99.99	3.04	9.999E+03	2.524E+01
5	60.113	58.655	58.311	56.729	55.259	8.4833E+04	8.4200E+04	99.99	2.51	9.999E+03	2.398E+01
6	64.497	63.233	62.934	61.555	60.284	8.5371E+04	8.4855E+04	99.99	2.17	9.999E+03	2.440E+01
7	68.928	67.722	67.435	66.112	64.900	8.5881E+04	8.5419E+04	99.99	1.93	9.999E+03	2.244E+01
8	72.984	71.878	71.613	70.393	69.282	8.6320E+04	8.5921E+04	99.99	1.74	9.999E+03	2.126E+01
9	77.020	75.948	75.689	74.501	73.425	8.6730E+04	8.6366E+04	99.99	1.60	9.999E+03	1.885E+01
10	80.892	79.868	79.621	78.482	77.455	8.7098E+04	8.6773E+04	99.99	1.48	9.999E+03	1.664E+01
	82.860				79.411						

FUEL PLATE 4 (ExactSoln)

	25.000				25.000						
1	27.861	27.475	27.390	26.996	26.387	7.9866E+04	5.0699E+04	99.99	38.71	9.999E+03	1.589E+02
2	35.617	34.571	34.335	33.249	31.594	8.1226E+04	5.1297E+04	99.99	9.55	9.999E+03	5.357E+01
3	43.625	42.540	42.292	41.148	39.431	8.2520E+04	5.2139E+04	99.99	4.89	9.999E+03	4.498E+01
4	49.639	48.826	48.638	47.772	46.490	8.3418E+04	5.2839E+04	99.99	3.44	9.999E+03	5.244E+01
5	55.259	54.511	54.336	53.531	52.351	8.4200E+04	5.3378E+04	99.99	2.74	9.999E+03	5.020E+01
6	60.284	59.620	59.463	58.743	57.696	8.4855E+04	5.3838E+04	99.99	2.31	9.999E+03	4.976E+01
7	64.900	64.294	64.150	63.489	62.534	8.5419E+04	5.4227E+04	99.99	2.03	9.999E+03	4.792E+01
8	69.282	68.710	68.573	67.945	67.045	8.5921E+04	5.4567E+04	99.99	1.81	9.999E+03	4.435E+01
9	73.425	72.886	72.757	72.163	71.316	8.6366E+04	5.4870E+04	99.99	1.65	9.999E+03	4.073E+01
10	77.455	76.933	76.808	76.229	75.409	8.6773E+04	5.5141E+04	99.99	1.52	9.999E+03	3.580E+01
	79.411				77.427						

[1] The ONB ratio is here defined as (Tonb - Tinlet)/(Tsurf - Tinlet). If the heat flux is negative (the coolant is hotter than the adjacent cladding surface), then the ONB ratio is arbitrarily set to 99.99 .

Figure 2.5 Exact Solution by PLTEMP/ANL V3.0 for a Assembly With Heat Source in Fuel Plate 1 Only, Heat Transfer to Farther Channels With Water Thermal Conductivity Multiplied by 1000

FUEL PLATE 1 (ExactSoln)

NODE	COOLANTl (C)	CladSl (C)	FUEL PEAK (C)	CladSr (C)	COOLANTr (C)	HCOFl W/C-m^2	HCOFr W/C-m^2	ONBRl [F Note 1]	ONBRr	ETA'l K-cm^3/J	ETA'r K-cm^3/J
	25.000				25.000						
1	26.547	27.746	44.889	41.941	41.023	2.1523E+06	8.2112E+05	34.58	5.08	1.425E+02	5.458E+00
2	29.936	31.305	53.976	53.143	52.830	2.2428E+06	8.3869E+05	15.33	2.90	1.142E+02	1.251E+01
3	33.579	34.865	56.791	55.727	55.341	2.3387E+06	8.4211E+05	9.78	2.68	1.104E+02	9.556E+00
4	37.266	38.557	62.146	61.573	61.353	2.4362E+06	8.4989E+05	7.15	2.21	9.969E+01	1.437E+01
5	41.017	42.247	65.498	64.832	64.581	2.5343E+06	8.5381E+05	5.61	2.04	9.453E+01	1.146E+01
6	44.776	45.979	69.801	69.292	69.097	2.6318E+06	8.5900E+05	4.62	1.81	8.716E+01	1.277E+01
7	48.552	49.707	73.333	72.772	72.559	2.7280E+06	8.6275E+05	3.92	1.69	8.157E+01	1.034E+01
8	52.328	53.450	77.309	76.810	76.619	2.8224E+06	8.6691E+05	3.41	1.55	7.509E+01	9.795E+00
9	56.106	57.190	80.932	80.402	80.202	2.9150E+06	8.7034E+05	3.01	1.45	6.930E+01	7.822E+00
10	59.881	60.935	84.785	84.284	84.095	3.0055E+06	8.7384E+05	2.70	1.36	6.311E+01	6.587E+00
	61.771				85.578						

FUEL PLATE 2 (ExactSoln)

	25.000				25.000						
1	41.023	40.539	39.436	34.361	33.870	8.2112E+05	8.0929E+05	99.99	8.89	9.999E+03	1.107E+01
2	52.830	52.404	51.413	46.853	46.422	8.3869E+05	8.2945E+05	99.99	3.79	9.999E+03	9.972E+00
3	55.341	55.133	54.646	52.406	52.197	8.4211E+05	8.3780E+05	99.99	2.94	9.999E+03	1.810E+01
4	61.353	61.114	60.551	57.956	57.716	8.4989E+05	8.4526E+05	99.99	2.45	9.999E+03	1.381E+01
5	64.581	64.432	64.081	62.463	62.315	8.5381E+05	8.5107E+05	99.99	2.13	9.999E+03	1.972E+01
6	69.097	68.916	68.485	66.503	66.322	8.5900E+05	8.5585E+05	99.99	1.93	9.999E+03	1.436E+01
7	72.559	72.420	72.089	70.566	70.427	8.6275E+05	8.6047E+05	99.99	1.75	9.999E+03	1.638E+01
8	76.619	76.459	76.074	74.302	74.141	8.6691E+05	8.6440E+05	99.99	1.62	9.999E+03	1.229E+01
9	80.202	80.063	79.729	78.191	78.052	8.7034E+05	8.6831E+05	99.99	1.50	9.999E+03	1.199E+01
10	84.095	83.943	83.576	81.885	81.733	8.7384E+05	8.7175E+05	99.99	1.40	9.999E+03	9.046E+00
	85.578				83.946						

FUEL PLATE 3 (ExactSoln)

	25.000				25.000						
1	33.870	33.624	33.069	30.516	30.267	8.0929E+05	8.0299E+05	99.99	14.66	9.999E+03	2.322E+01
2	46.422	46.091	45.328	41.817	41.482	8.2945E+05	8.2185E+05	99.99	4.87	9.999E+03	1.415E+01
3	52.197	52.044	51.686	50.044	49.890	8.3780E+05	8.3454E+05	99.99	3.18	9.999E+03	2.588E+01
4	57.716	57.566	57.215	55.599	55.449	8.4526E+05	8.4226E+05	99.99	2.60	9.999E+03	2.336E+01
5	62.315	62.197	61.918	60.635	60.517	8.5107E+05	8.4884E+05	99.99	2.22	9.999E+03	2.606E+01
6	66.322	66.215	65.960	64.789	64.682	8.5585E+05	8.5393E+05	99.99	1.98	9.999E+03	2.550E+01
7	70.427	70.322	70.070	68.910	68.804	8.6047E+05	8.5868E+05	99.99	1.80	9.999E+03	2.272E+01
8	74.141	74.044	73.811	72.739	72.642	8.6440E+05	8.6284E+05	99.99	1.65	9.999E+03	2.151E+01
9	78.052	77.952	77.709	76.591	76.491	8.6831E+05	8.6678E+05	99.99	1.53	9.999E+03	1.770E+01
10	81.733	81.638	81.408	80.353	80.258	8.7175E+05	8.7040E+05	99.99	1.42	9.999E+03	1.568E+01
	83.946				82.088						

FUEL PLATE 4 (ExactSoln)

	25.000				25.000						
1	30.267	30.164	29.935	28.879	28.717	8.0299E+05	5.0970E+05	99.99	20.31	9.999E+03	5.739E+01
2	41.482	41.309	40.914	39.096	38.823	8.2185E+05	5.2076E+05	99.99	5.67	9.999E+03	2.858E+01
3	49.890	49.801	49.597	48.655	48.516	8.3454E+05	5.3030E+05	99.99	3.32	9.999E+03	4.639E+01
4	55.449	55.381	55.222	54.490	54.384	8.4226E+05	5.3557E+05	99.99	2.65	9.999E+03	5.286E+01
5	60.517	60.451	60.294	59.574	59.469	8.4884E+05	5.3983E+05	99.99	2.26	9.999E+03	4.765E+01
6	64.682	64.632	64.514	63.971	63.892	8.5393E+05	5.4332E+05	99.99	1.99	9.999E+03	5.622E+01
7	68.804	68.749	68.617	68.008	67.921	8.5868E+05	5.4631E+05	99.99	1.81	9.999E+03	4.452E+01
8	72.642	72.594	72.480	71.956	71.881	8.6284E+05	5.4908E+05	99.99	1.65	9.999E+03	4.520E+01
9	76.491	76.440	76.318	75.755	75.676	8.6678E+05	5.5158E+05	99.99	1.53	9.999E+03	3.641E+01
10	80.258	80.210	80.095	79.564	79.489	8.7040E+05	5.5395E+05	99.99	1.42	9.999E+03	3.243E+01
	82.088				81.340						

[1] The ONB ratio is here defined as (Tonb - Tinlet)/(Tsurf - Tinlet). If the heat flux is negative (the coolant is hotter than the adjacent cladding surface), then the ONB ratio is arbitrarily set to 99.99 .

Figure 2.6 PLTEMP/ANL V3.0 Input Data for Standard Problem 11 – Equilibration of Coolant Channel Temperatures over Unheated Axial Length

```
 Standard Problem 11: 1 assembly producing 0.04 MWt
! Each assembly has 4 fuel plates and 5 coolant channels
! H2O coolant, Input coolant flow = 0.2 kg/s per coolant channel
! All hot channel factors = 1.0
! No bypass flow, NCTYP=0
! 10 axial heat transfer nodes in the heated length of fuel plates
!  1   2   3   4   5   6   7   8   9  10  11  12  13  14  15  16  17  18        Indices on Card 0200
   0   0   0   1   0   1   1   1   0   0   0   0   0       1       0            Card(1)0200
   1   3 0.00       1.00        1.00        1.00           3                   Card(1)0300
   1  20 1.00                                                                  Card(1)0301
   1   1   1                                                                   Card(1)0302
1.20        1.20                                                               Card(2)0303
30.0E-04    0.02955665  0.15        8.00        0.20        15.0E-03           Card(3)0304
30.0E-04    0.02955665  0.75        0.00        0.20        15.0E-03           Card(3)0304
30.0E-04    0.02955665  0.15        8.00        0.20        15.0E-03           Card(3)0304
! Use the code's biult-in correlation for friction factor
0.00        0.00        0.00                                                   Card(1)0305
   5   6 0.00       10.00        1.00E-03    120.00      1.00E-03    120.00     Card(1)0306
6.00E-04    5.91133E-03 0.4060      0.20        0.20        3.00E-03           Card(5)0307
6.00E-04    5.91133E-03 0.4060      0.40        0.20        3.00E-03           Card(5)0307
6.00E-04    5.91133E-03 0.4060      0.40        0.20        3.00E-03           Card(5)0307
6.00E-04    5.91133E-03 0.4060      0.40        0.20        3.00E-03           Card(5)0307
6.00E-04    5.91133E-03 0.4060      0.20        0.20        3.00E-03           Card(5)0307
0.20        0.20        0.20        0.20                                       Card(1)0308
! Card 0308a not required
! Radial power peaking factor data by fuel plate for each assembly. Input flow data by
! channel for each assembly on Cards 0310 not required because WFGES(1) is non-zero
1.0E-04     1.0         1.0         1.0E-04                                    Card(2)0309
0.4E-01     0.4E-01     0.4E-01     0.4E-01     0.4E-01                        Card(2)0310
! DP0       DDP         DPMAX       POWER       TIN         PIN
0.30        0.10        0.40        0.04        25.0        0.40               Card(1)0500
                                                                               Card(2)0500
  50 0.0001     25.0        0.04        0.04                                   Card(1)0600
  41                                                                           Card(1)0700
0.000       1.00                                                               Card(11)0701
0.025       1.00                                                               Card(11)0701
0.050       1.00                                                               Card(11)0701
0.075       1.00                                                               Card(11)0701
0.100       1.00                                                               Card(11)0701
0.125       1.00                                                               Card(11)0701
0.150       1.00                                                               Card(11)0701
0.175       1.00                                                               Card(11)0701
0.200       1.00                                                               Card(11)0701
0.225       1.00                                                               Card(11)0701
0.250       1.00                                                               Card(11)0701
0.275       1.00E-03                                                           Card(11)0701
0.300       1.00E-03                                                           Card(11)0701
0.325       1.00E-03                                                           Card(11)0701
0.350       1.00E-03                                                           Card(11)0701
0.375       1.00E-03                                                           Card(11)0701
0.400       1.00E-03                                                           Card(11)0701
0.425       1.00E-03                                                           Card(11)0701
0.450       1.00E-03                                                           Card(11)0701
0.475       1.00E-03                                                           Card(11)0701
0.500       1.00E-03                                                           Card(11)0701
0.525       1.00E-03                                                           Card(11)0701
0.550       1.00E-03                                                           Card(11)0701
0.575       1.00E-03                                                           Card(11)0701
0.600       1.00E-03                                                           Card(11)0701
0.625       1.00E-03                                                           Card(11)0701
0.650       1.00E-03                                                           Card(11)0701
0.675       1.00E-03                                                           Card(11)0701
0.700       1.00E-03                                                           Card(11)0701
0.725       1.00E-03                                                           Card(11)0701
0.750       1.00E-03                                                           Card(11)0701
0.775       1.00E-03                                                           Card(11)0701
0.800       1.00E-03                                                           Card(11)0701
0.825       1.00E-03                                                           Card(11)0701
0.850       1.00E-03                                                           Card(11)0701
0.875       1.00E-03                                                           Card(11)0701
0.900       1.00E-03                                                           Card(11)0701
0.925       1.00E-03                                                           Card(11)0701
0.950       1.00E-03                                                           Card(11)0701
0.975       1.00E-03                                                           Card(11)0701
1.000       1.00E-03                                                           Card(11)0701
   0                                                                           Card(11)0702
!234567890123456789012345678901234567890123456789012345678901234567890123456789
```

Figure 2.7 Exact Solution by PLTEMP/ANL V3.0 for Standard Problem 11 – Equilibration of Coolant Channel Temperatures over Unheated Axial Length

FUEL PLATE 1 (ExactSoln)

NODE	COOLANTl (C)	CladSl (C)	FUEL PEAK (C)	CladSr (C)	COOLANTr (C)	HCOFl W/C-m^2	HCOFr W/C-m^2	ONBRl [F Note 1]	ONBRr	ETA'l K-cm^3/J	ETA'r K-cm^3/J
	25.000				25.000						
1	25.146	26.605	26.621	26.629	27.846	6.6952E+02	7.9875E+02	74.01	99.99	8.107E+03	9.999E+03
2	25.721	29.914	29.962	29.985	33.507	6.8010E+02	8.0878E+02	24.15	99.99	2.756E+03	9.999E+03
3	26.832	33.397	33.473	33.511	39.078	6.9431E+02	8.1809E+02	14.12	99.99	1.705E+03	9.999E+03
4	28.434	37.032	37.134	37.185	44.584	7.1185E+02	8.2677E+02	9.84	99.99	1.250E+03	9.999E+03
5	30.496	40.911	41.038	41.101	50.050	7.3272E+02	8.5234E+02	7.43	99.99	9.823E+02	9.999E+03
6	33.002	45.016	45.167	45.243	55.429	7.5678E+02	8.9225E+02	5.90	99.99	8.044E+02	9.999E+03
7	35.926	49.228	49.402	49.489	60.685	7.8355E+02	9.3065E+02	4.87	99.99	6.814E+02	9.999E+03
8	39.225	53.516	53.710	53.807	65.806	8.1261E+02	9.6750E+02	4.13	99.99	5.912E+02	9.999E+03
9	42.858	57.865	58.076	58.182	70.790	8.4351E+02	1.0038E+03	3.58	99.99	5.219E+02	9.999E+03
10	46.777	62.244	62.470	62.583	75.642	8.7575E+02	1.0370E+03	3.15	99.99	4.673E+02	9.999E+03
11	50.833	65.825	66.052	66.165	78.982	9.0685E+02	1.0606E+03	2.87	99.99	4.444E+02	9.999E+03
12	54.681	67.714	67.917	68.018	79.427	9.3350E+02	1.0665E+03	2.73	99.99	4.742E+02	9.999E+03
13	58.010	68.630	68.799	68.883	78.415	9.5445E+02	1.0634E+03	2.67	99.99	5.456E+02	9.999E+03
14	60.767	69.360	69.499	69.569	77.442	9.7141E+02	1.0602E+03	2.62	99.99	6.385E+02	9.999E+03
15	63.029	69.957	70.071	70.128	76.583	9.8510E+02	1.0571E+03	2.58	99.99	7.564E+02	9.999E+03
20	69.372	71.710	71.750	71.770	74.054	1.0237E+03	1.0478E+03	2.45	99.99	1.945E+03	9.999E+03
25	71.579	72.384	72.397	72.404	73.202	1.0364E+03	1.0447E+03	2.38	99.99	5.306E+03	9.999E+03
30	72.354	72.639	72.644	72.647	72.932	1.0409E+03	1.0438E+03	2.34	99.99	1.441E+04	9.999E+03
35	72.636	72.744	72.745	72.746	72.854	1.0425E+03	1.0436E+03	2.31	99.99	3.709E+04	9.999E+03
40	72.748	72.795	72.795	72.796	72.843	1.0431E+03	1.0436E+03	2.28	99.99	8.352E+04	9.999E+03
	72.755				72.843						

FUEL PLATE 2 (ExactSoln)

	25.000				25.000						
1	27.846	52.827	53.037	52.851	30.406	7.9875E+02	8.0336E+02	4.30	4.29	3.917E+02	4.313E+02
2	33.507	60.249	60.481	60.315	40.708	8.0878E+02	8.3421E+02	3.39	3.38	3.430E+02	4.312E+02
3	39.078	66.600	66.849	66.699	50.092	8.3451E+02	9.0430E+02	2.86	2.85	3.059E+02	4.257E+02
4	44.584	72.445	72.715	72.583	58.604	8.7931E+02	9.6469E+02	2.51	2.49	2.710E+02	4.295E+02
5	50.050	78.041	78.329	78.212	66.254	9.2216E+02	1.0180E+03	2.24	2.23	2.423E+02	4.313E+02
6	55.429	83.386	83.690	83.584	73.174	9.6270E+02	1.0634E+03	2.03	2.02	2.183E+02	4.298E+02
7	60.685	88.482	88.798	88.702	79.487	1.0009E+03	1.1028E+03	1.86	1.85	1.978E+02	4.239E+02
8	65.806	93.345	93.672	93.584	85.301	1.0371E+03	1.1377E+03	1.73	1.72	1.800E+02	4.130E+02
9	70.790	97.987	98.323	98.241	90.708	1.0726E+03	1.1697E+03	1.62	1.60	1.642E+02	3.977E+02
10	75.642	102.471	102.815	102.738	95.786	1.1049E+03	1.2000E+03	1.52	1.51	1.500E+02	3.763E+02
11	78.982	96.918	97.171	97.179	97.973	1.1131E+03	1.2006E+03	1.63	99.99	2.106E+02	9.999E+03
12	79.427	87.414	87.560	87.633	95.101	1.1005E+03	1.1719E+03	1.87	99.99	4.730E+02	9.999E+03
13	78.415	84.558	84.670	84.725	90.537	1.0911E+03	1.1468E+03	1.95	99.99	6.281E+02	9.999E+03
14	77.442	82.279	82.366	82.409	87.020	1.0827E+03	1.1274E+03	2.03	99.99	8.134E+02	9.999E+03
15	76.583	80.449	80.518	80.552	84.257	1.0755E+03	1.1118E+03	2.09	99.99	1.035E+03	9.999E+03
20	74.054	75.424	75.448	75.460	76.777	1.0544E+03	1.0679E+03	2.27	99.99	3.039E+03	9.999E+03
25	73.202	73.705	73.714	73.718	74.183	1.0471E+03	1.0520E+03	2.32	99.99	8.279E+03	9.999E+03
30	72.932	73.126	73.129	73.131	73.289	1.0447E+03	1.0465E+03	2.32	99.99	2.109E+04	9.999E+03
35	72.854	72.941	72.942	72.943	72.993	1.0439E+03	1.0446E+03	2.30	99.99	4.651E+04	9.999E+03
40	72.843	72.892	72.892	72.892	72.905	1.0438E+03	1.0441E+03	2.27	99.99	8.045E+04	9.999E+03
	72.843				72.901						

[1] The ONB ratio is here defined as (Tonb - Tinlet)/(Tsurf - Tinlet). If the heat flux is negative (the coola than the adjacent cladding surface), then the ONB ratio is arbitrarily set to 99.99 .

Figure 2.7 Cont'd

FUEL PLATE 3 (ExactSoln)

NODE	COOLANTl (C)	CladSl (C)	FUEL PEAK (C)	CladSr (C)	COOLANTr (C)	HCOFl W/C-m^2	HCOFr W/C-m^2	ONBRl [F Note 1]	ONBRr	ETA'l K-cm^3/J	ETA'r K-cm^3/J
	25.000				25.000						
1	30.406	52.851	53.037	52.827	27.846	8.0336E+02	7.9875E+02	4.29	4.30	4.313E+02	3.917E+02
2	40.708	60.315	60.481	60.249	33.507	8.3421E+02	8.0878E+02	3.38	3.39	4.312E+02	3.430E+02
3	50.092	66.699	66.849	66.600	39.078	9.0430E+02	8.3451E+02	2.85	2.86	4.257E+02	3.059E+02
4	58.604	72.583	72.715	72.445	44.584	9.6469E+02	8.7931E+02	2.49	2.51	4.295E+02	2.710E+02
5	66.254	78.212	78.329	78.041	50.050	1.0180E+03	9.2216E+02	2.23	2.24	4.313E+02	2.423E+02
6	73.174	83.584	83.690	83.386	55.429	1.0634E+03	9.6270E+02	2.02	2.03	4.298E+02	2.183E+02
7	79.487	88.702	88.798	88.482	60.685	1.1028E+03	1.0009E+03	1.85	1.86	4.239E+02	1.978E+02
8	85.301	93.584	93.672	93.345	65.806	1.1377E+03	1.0371E+03	1.72	1.73	4.130E+02	1.800E+02
9	90.708	98.241	98.323	97.987	70.790	1.1697E+03	1.0726E+03	1.60	1.62	3.977E+02	1.642E+02
10	95.786	102.738	102.815	102.471	75.642	1.2000E+03	1.1049E+03	1.51	1.52	3.763E+02	1.500E+02
11	97.973	97.179	97.171	96.918	78.982	1.2006E+03	1.1131E+03	99.99	1.63	9.999E+03	2.106E+02
12	95.101	87.633	87.560	87.414	79.427	1.1719E+03	1.1005E+03	99.99	1.87	9.999E+03	4.730E+02
13	90.537	84.725	84.670	84.558	78.415	1.1468E+03	1.0911E+03	99.99	1.95	9.999E+03	6.281E+02
14	87.020	82.409	82.366	82.279	77.442	1.1274E+03	1.0827E+03	99.99	2.03	9.999E+03	8.134E+02
15	84.257	80.552	80.518	80.449	76.583	1.1118E+03	1.0755E+03	99.99	2.09	9.999E+03	1.035E+03
20	76.777	75.460	75.448	75.424	74.054	1.0679E+03	1.0544E+03	99.99	2.27	9.999E+03	3.039E+03
25	74.183	73.718	73.714	73.705	73.202	1.0520E+03	1.0471E+03	99.99	2.32	9.999E+03	8.279E+03
30	73.289	73.131	73.129	73.126	72.932	1.0465E+03	1.0447E+03	99.99	2.32	9.999E+03	2.109E+04
35	72.993	72.943	72.942	72.941	72.854	1.0446E+03	1.0439E+03	99.99	2.30	9.999E+03	4.651E+04
40	72.905	72.892	72.892	72.892	72.843	1.0441E+03	1.0438E+03	99.99	2.27	9.999E+03	8.045E+04
	72.901				72.843						

FUEL PLATE 4 (ExactSoln)

	25.000				25.000						
1	27.846	26.629	26.621	26.605	25.146	7.9875E+02	6.6952E+02	99.99	74.01	9.999E+03	8.107E+03
2	33.507	29.985	29.962	29.914	25.721	8.0878E+02	6.8010E+02	99.99	24.15	9.999E+03	2.756E+03
3	39.078	33.511	33.473	33.397	26.832	8.1809E+02	6.9431E+02	99.99	14.12	9.999E+03	1.705E+03
4	44.584	37.185	37.134	37.032	28.434	8.2677E+02	7.1185E+02	99.99	9.84	9.999E+03	1.250E+03
5	50.050	41.101	41.038	40.911	30.496	8.5234E+02	7.3272E+02	99.99	7.43	9.999E+03	9.823E+02
6	55.429	45.243	45.167	45.016	33.002	8.9225E+02	7.5678E+02	99.99	5.90	9.999E+03	8.044E+02
7	60.685	49.489	49.402	49.228	35.926	9.3065E+02	7.8355E+02	99.99	4.87	9.999E+03	6.814E+02
8	65.806	53.807	53.710	53.516	39.225	9.6750E+02	8.1261E+02	99.99	4.13	9.999E+03	5.912E+02
9	70.790	58.182	58.076	57.865	42.858	1.0038E+03	8.4351E+02	99.99	3.58	9.999E+03	5.219E+02
10	75.642	62.583	62.470	62.244	46.777	1.0370E+03	8.7575E+02	99.99	3.15	9.999E+03	4.673E+02
11	78.982	66.165	66.052	65.825	50.833	1.0606E+03	9.0685E+02	99.99	2.87	9.999E+03	4.444E+02
12	79.427	68.018	67.917	67.714	54.681	1.0665E+03	9.3350E+02	99.99	2.73	9.999E+03	4.742E+02
13	78.415	68.883	68.799	68.630	58.010	1.0634E+03	9.5445E+02	99.99	2.67	9.999E+03	5.456E+02
14	77.442	69.569	69.499	69.360	60.767	1.0602E+03	9.7141E+02	99.99	2.62	9.999E+03	6.385E+02
15	76.583	70.128	70.071	69.957	63.029	1.0571E+03	9.8510E+02	99.99	2.58	9.999E+03	7.564E+02
20	74.054	71.770	71.750	71.710	69.372	1.0478E+03	1.0237E+03	99.99	2.45	9.999E+03	1.945E+03
25	73.202	72.404	72.397	72.384	71.579	1.0447E+03	1.0364E+03	99.99	2.38	9.999E+03	5.306E+03
30	72.932	72.647	72.644	72.639	72.354	1.0438E+03	1.0409E+03	99.99	2.34	9.999E+03	1.441E+04
35	72.854	72.746	72.745	72.744	72.636	1.0436E+03	1.0425E+03	99.99	2.31	9.999E+03	3.709E+04
40	72.843	72.796	72.795	72.795	72.748	1.0436E+03	1.0431E+03	99.99	2.28	9.999E+03	8.352E+04
	72.843				72.755						

[1] The ONB ratio is here defined as (Tonb - Tinlet)/(Tsurf - Tinlet). If the heat flux is negative (the coola than the adjacent cladding surface), then the ONB ratio is arbitrarily set to 99.99 .

Figure 2.8 Standard Problem 12 Input Data for PLTEMP/ANL V3.0: Practically Zero Cladding Thickness, Heat Source in Fuel, and No Heat Source in Cladding and Coolant (Fuel Meat Thickness = 2.0 mm)

```
 Standard Problem 12: 2 assemblies (of identical geometry) producing 1 MWt
! Each assembly has 4 fuel plates and 5 coolant channels
! Each fuel plate has equal power all of which is directly deposited in
! coolant channels. See card(2) 0500.
! H2O coolant, Input coolant flow = 0.50 kg/s in channel 2, 3, or 4
!                                 = 0.25 kg/s in channel 1, or 5
! All hot channel factors = 1.0
! No bypass flow, NCTYP=0
! 10 axial heat transfer nodes in the heated length of fuel plates
!  1   2   3   4   5   6   7   8   9  10  11  12  13  14  15  16  17  18        Indices Card 0200
   0   0   5   1   0   1   1   1   0   0   0   0   0           1                Card(1)0200
   2   3 0.00       1.00        1.00        1.00           3                   Card(1)0300
! Using pressure driven mode
   1  20 1.00                                                                  Card(1)0301
   1   1   1                                                                   Card(1)0302
1.20        1.20                                                               Card(2)0303
30.0E-04    0.02955665  0.15        8.00        0.20        15.0E-03           Card(3)0304
30.0E-04    0.02955665  0.75        0.00        0.20        15.0E-03           Card(3)0304
30.0E-04    0.02955665  0.15        8.00        0.20        15.0E-03           Card(3)0304
! Use the code's biult-in correlation for friction factor
0.00        0.00        0.00                                                   Card(1)0305
   5   3 0.00       0.75        0.50E-09    10.00       2.00E-03    10.00       Card(1)0306
6.00E-04    5.91133E-03 0.4060      0.20        0.20        3.00E-03           Card(5)0307
6.00E-04    5.91133E-03 0.4060      0.40        0.20        3.00E-03           Card(5)0307
6.00E-04    5.91133E-03 0.4060      0.40        0.20        3.00E-03           Card(5)0307
6.00E-04    5.91133E-03 0.4060      0.40        0.20        3.00E-03           Card(5)0307
6.00E-04    5.91133E-03 0.4060      0.20        0.20        3.00E-03           Card(5)0307
0.20        0.20        0.20        0.20                                       Card(1)0308
! Card 0308a not required
! Radial power peaking factor data by fuel plate for each assembly. Input flow data by
! channel for each assembly on Cards 0310 not required because WFGES(1) is non-zero
1.000       1.000       1.000       1.000                                      Card(2)0309
0.25        0.50        0.50        0.50        0.25                           Card(2)0310
1.000       1.000       1.000       1.000                                      Card(2)0309
0.25        0.50        0.50        0.50        0.25                           Card(2)0310
! DP0       DDP         DPMAX       POWER       TIN         PIN
0.32336     0.04        0.36136     1.00        45.0        0.12               Card(2)0500
0.0         0.0                                                                Card(2)0500
  50 0.0001     25.0        0.50        1.00                                   Card(1)0600
  11                                                                           Card(1)0700
0.00        0.80                                                               Card(11)0701
0.10        0.88                                                               Card(11)0701
0.20        0.96                                                               Card(11)0701
0.30        1.04                                                               Card(11)0701
0.40        1.12                                                               Card(11)0701
0.50        1.20                                                               Card(11)0701
0.60        1.12                                                               Card(11)0701
0.70        1.04                                                               Card(11)0701
0.80        0.96                                                               Card(11)0701
0.90        0.88                                                               Card(11)0701
1.00        0.80                                                               Card(11)0701
   0                                                                           Card(11)0702
```

Figure 2.9 Exact Solution of Standard Problem 12: Practically Zero Cladding Thickness, Heat Source in Fuel, No Heat Source in Cladding and Coolant (Fuel Meat Thickness = 2.0 mm)

```
Input Power Densities (MW/m**3) in Axial Node   1 of Assembly   1 of Type   1:
FUEL PLATE  COOLANTl    CLADDINGl   FUEL MEAT   CLADDINGr   COOLANTr
     1      0.0000E+00  0.0000E+00  3.5000E+02  0.0000E+00  0.0000E+00
     2      0.0000E+00  0.0000E+00  3.5000E+02  0.0000E+00  0.0000E+00
     3      0.0000E+00  0.0000E+00  3.5000E+02  0.0000E+00  0.0000E+00
     4      0.0000E+00  0.0000E+00  3.5000E+02  0.0000E+00  0.0000E+00

 FUEL PLATE   1 (ExactSoln)
 NODE    COOLANTl  CladSl  FUEL PEAK   CladSr  COOLANTr   HCOFl      HCOFr    ONBRl  ONBRr  ETA'l     ETA'r
         (C)       (C)       (C)       (C)       (C)     W/C-m^2    W/C-m^2    [F Note 1]  K-cm^3/J  K-cm^3/J
         45.000                                  45.000
    1    47.083   117.096   129.129   105.142    47.725 4.1454E+03 7.1368E+03  1.37  1.65 1.364E+02 1.919E+02
    2    51.462   125.641   139.015   113.016    53.420 4.3167E+03 7.4915E+03  1.22  1.46 1.173E+02 1.645E+02
    3    56.269   134.230   148.979   121.013    59.605 4.4969E+03 7.8614E+03  1.10  1.30 1.008E+02 1.406E+02
    4    61.504   143.113   159.201   129.215    66.278 4.6626E+03 8.2540E+03  1.00  1.18 8.661E+01 1.190E+02
    5    67.161   152.388   169.802   137.778    73.436 4.8140E+03 8.6473E+03  0.91  1.06 7.404E+01 9.956E+01
    6    73.049   156.523   174.243   142.631    80.814 4.9581E+03 8.9424E+03  0.88  1.01 6.692E+01 8.821E+01
    7    78.783   155.384   172.267   143.344    87.889 5.0887E+03 9.2002E+03  0.88  1.00 6.434E+01 8.307E+01
    8    84.164   154.345   170.350   144.052    94.408 5.2037E+03 9.4298E+03  0.88  0.98 6.192E+01 7.792E+01
    9    89.184   153.281   168.369   144.636   100.377 5.3060E+03 9.6380E+03  0.89  0.97 5.969E+01 7.277E+01
   10    93.838   152.109   166.250   145.033   105.803 5.3992E+03 9.8237E+03  0.89  0.96 5.766E+01 6.763E+01
         96.073                                 108.381

 FUEL PLATE   2 (ExactSoln)
         45.000                                  45.000
    1    47.725    97.260   114.732    97.204    47.513 7.0601E+03 7.0492E+03  1.90  1.90 2.249E+02 2.250E+02
    2    53.420   105.018   124.097   104.842    52.781 7.4123E+03 7.3801E+03  1.65  1.65 1.921E+02 1.926E+02
    3    59.605   112.957   133.635   112.646    58.531 7.7807E+03 7.7283E+03  1.45  1.46 1.635E+02 1.645E+02
    4    66.278   121.078   143.360   120.642    64.760 8.1720E+03 8.0915E+03  1.30  1.30 1.381E+02 1.396E+02
    5    73.436   129.502   153.353   128.868    71.469 8.5642E+03 8.4759E+03  1.16  1.17 1.154E+02 1.173E+02
    6    80.814   134.602   158.354   133.769    78.420 8.9085E+03 8.8077E+03  1.09  1.11 1.018E+02 1.042E+02
    7    87.889   136.309   158.298   135.281    85.137 9.1875E+03 9.0767E+03  1.07  1.08 9.527E+01 9.829E+01
    8    94.408   137.955   158.190   136.749    91.383 9.4298E+03 9.3174E+03  1.04  1.06 8.883E+01 9.241E+01
    9   100.377   139.454   157.955   138.112    97.156 9.6380E+03 9.5237E+03  1.02  1.04 8.242E+01 8.663E+01
   10   105.803   140.698   157.484   139.256   102.456 9.8237E+03 9.7068E+03  1.00  1.02 7.603E+01 8.096E+01
        108.381                                 104.988

FUEL PLATE   3 (ExactSoln)
         45.000                                  45.000
    1    47.513    97.204   114.732    97.260    47.725 7.0492E+03 7.0601E+03  1.90  1.90 2.250E+02 2.249E+02
    2    52.781   104.842   124.097   105.018    53.420 7.3801E+03 7.4123E+03  1.65  1.65 1.926E+02 1.921E+02
    3    58.531   112.646   133.635   112.957    59.605 7.7283E+03 7.7807E+03  1.46  1.45 1.645E+02 1.635E+02
    4    64.760   120.642   143.360   121.078    66.278 8.0915E+03 8.1720E+03  1.30  1.30 1.396E+02 1.381E+02
    5    71.469   128.868   153.353   129.502    73.436 8.4759E+03 8.5642E+03  1.17  1.16 1.173E+02 1.154E+02
    6    78.420   133.769   158.354   134.602    80.814 8.8077E+03 8.9085E+03  1.11  1.09 1.042E+02 1.018E+02
    7    85.137   135.281   158.298   136.309    87.889 9.0767E+03 9.1875E+03  1.08  1.07 9.829E+01 9.527E+01
    8    91.383   136.749   158.190   137.955    94.408 9.3174E+03 9.4298E+03  1.06  1.04 9.241E+01 8.883E+01
    9    97.156   138.112   157.955   139.454   100.377 9.5237E+03 9.6380E+03  1.04  1.02 8.663E+01 8.242E+01
   10   102.456   139.256   157.484   140.698   105.803 9.7068E+03 9.8237E+03  1.02  1.00 8.096E+01 7.603E+01
        104.988                                 108.381

 FUEL PLATE   4 (ExactSoln)
         45.000                                  45.000
    1    47.725   105.142   129.129   117.096    47.083 7.1368E+03 4.1454E+03  1.65  1.37 1.919E+02 1.364E+02
    2    53.420   113.016   139.015   125.641    51.462 7.4915E+03 4.3167E+03  1.46  1.22 1.645E+02 1.173E+02
    3    59.605   121.013   148.979   134.230    56.269 7.8614E+03 4.4969E+03  1.30  1.10 1.406E+02 1.008E+02
    4    66.278   129.215   159.201   143.113    61.504 8.2540E+03 4.6626E+03  1.18  1.00 1.190E+02 8.661E+01
    5    73.436   137.778   169.802   152.388    67.161 8.6473E+03 4.8140E+03  1.06  0.91 9.956E+01 7.404E+01
    6    80.814   142.631   174.243   156.523    73.049 8.9424E+03 4.9581E+03  1.01  0.88 8.821E+01 6.692E+01
    7    87.889   143.344   172.267   155.384    78.783 9.2002E+03 5.0887E+03  1.00  0.88 8.307E+01 6.434E+01
    8    94.408   144.052   170.350   154.345    84.164 9.4298E+03 5.2037E+03  0.98  0.88 7.792E+01 6.192E+01
    9   100.377   144.636   168.369   153.281    89.184 9.6380E+03 5.3060E+03  0.97  0.89 7.277E+01 5.969E+01
   10   105.803   145.033   166.250   152.109    93.838 9.8237E+03 5.3992E+03  0.96  0.89 6.763E+01 5.766E+01
        108.381                                  96.073
[1] The ONB ratio is here defined as (Tonb - Tinlet)/(Tsurf - Tinlet). If the heat flux is negative (the
    coolant is hotter than the adjacent cladding surface), then the ONB ratio is arbitrarily set to 99.99 .


MIXED MEAN TEMP. (CORE FLOW ONLY)=   104.456
 WORK: TBAR RETURNED FROM FINLED= 104.459
```

Figure 2.10 Standard Problem 13 Input Data for PLTEMP/ANL V3.0: 50% of Reactor Power Produced in Fuel and 50% in Cladding, No Heat Source in Coolant (Cladding Thickness = 0.5 mm)

```
 Standard Problem 13: 2 assemblies (of identical geometry) producing 1 MWt
! Each assembly has 4 fuel plates and 5 coolant channels
! Each fuel plate has equal power all of which is directly deposited in
! coolant channels. See card(2) 0500.
! H2O coolant, Input coolant flow = 0.50 kg/s in channel 2, 3, or 4
!                                 = 0.25 kg/s in channel 1, or 5
! All hot channel factors = 1.0
! No bypass flow, NCTYP=0
! 10 axial heat transfer nodes in the heated length of fuel plates
!  1   2   3   4   5   6   7   8   9  10  11  12  13  14  15  16  17  18        Indices Card 0200
   0   0   5   1   0   1   1   1   0   0   0   0   0           1                Card(1)0200
   2   3 0.00       1.00        1.00        1.00           3                  Card(1)0300
! Using pressure driven mode
   1  20 1.00                                                                  Card(1)0301
   1   1   1                                                                   Card(1)0302
1.20        1.20                                                               Card(2)0303
30.0E-04    0.02955665  0.15        8.00        0.20        15.0E-03           Card(3)0304
30.0E-04    0.02955665  0.75        0.00        0.20        15.0E-03           Card(3)0304
30.0E-04    0.02955665  0.15        8.00        0.20        15.0E-03           Card(3)0304
! Use the code's biult-in correlation for friction factor
0.00        0.00        0.00                                                   Card(1)0305
   5   3 0.00       0.75        0.50E-03    10.00       1.00E-03    10.00      Card(1)0306
6.00E-04    5.91133E-03 0.4060      0.20        0.20        3.00E-03           Card(5)0307
6.00E-04    5.91133E-03 0.4060      0.40        0.20        3.00E-03           Card(5)0307
6.00E-04    5.91133E-03 0.4060      0.40        0.20        3.00E-03           Card(5)0307
6.00E-04    5.91133E-03 0.4060      0.40        0.20        3.00E-03           Card(5)0307
6.00E-04    5.91133E-03 0.4060      0.20        0.20        3.00E-03           Card(5)0307
0.20        0.20        0.20        0.20                                       Card(1)0308
! Card 0308a not required
! Radial power peaking factor data by fuel plate for each assembly. Input flow data by
! channel for each assembly on Cards 0310 not required because WFGES(1) is non-zero
1.000       1.000       1.000       1.000                                      Card(2)0309
0.25        0.50        0.50        0.50        0.25                           Card(2)0310
1.000       1.000       1.000       1.000                                      Card(2)0309
0.25        0.50        0.50        0.50        0.25                           Card(2)0310
! DP0       DDP         DPMAX       POWER       TIN         PIN
0.32336     0.04        0.36136     1.00        45.0        0.12               Card(2)0500
0.5         0.0                                                                Card(2)0500
  50 0.0001     25.0        0.50        1.00                                   Card(1)0600
  11                                                                           Card(1)0700
0.00        0.80                                                               Card(11)0701
0.10        0.88                                                               Card(11)0701
0.20        0.96                                                               Card(11)0701
0.30        1.04                                                               Card(11)0701
0.40        1.12                                                               Card(11)0701
0.50        1.20                                                               Card(11)0701
0.60        1.12                                                               Card(11)0701
0.70        1.04                                                               Card(11)0701
0.80        0.96                                                               Card(11)0701
0.90        0.88                                                               Card(11)0701
1.00        0.80                                                               Card(11)0701
   0                                                                           Card(11)0702
```

Figure 2.11 Exact Solution of Standard Problem 13: 50% of Reactor Power Produced in Fuel and 50% in Cladding, No Heat Source in Coolant (Cladding Thickness = 0.5 mm)

```
Input Power Densities (MW/m**3) in Axial Node   1 of Assembly   1 of Type   1:
FUEL PLATE  COOLANTl    CLADDINGl   FUEL MEAT   CLADDINGr   COOLANTr
     1      0.0000E+00  3.5000E+02  3.5000E+02  3.5000E+02  0.0000E+00
     2      0.0000E+00  3.5000E+02  3.5000E+02  3.5000E+02  0.0000E+00
     3      0.0000E+00  3.5000E+02  3.5000E+02  3.5000E+02  0.0000E+00
     4      0.0000E+00  3.5000E+02  3.5000E+02  3.5000E+02  0.0000E+00

 FUEL PLATE   1 (ExactSoln)
 NODE    COOLANTl  CladSl  FUEL PEAK   CladSr  COOLANTr   HCOFl      HCOFr    ONBRl  ONBRr  ETA'l     ETA'r
         (C)       (C)       (C)       (C)       (C)     W/C-m^2    W/C-m^2    [F Note 1]  K-cm^3/J  K-cm^3/J
         45.000                                 45.000
    1    47.083   117.096   129.129   105.142    47.725 4.1454E+03 7.1368E+03  1.37  1.65 1.364E+02 1.919E+02
    2    51.462   125.641   139.015   113.016    53.420 4.3167E+03 7.4915E+03  1.22  1.46 1.173E+02 1.645E+02
    3    56.269   134.230   148.979   121.013    59.605 4.4969E+03 7.8614E+03  1.10  1.30 1.008E+02 1.406E+02
    4    61.504   143.113   159.201   129.215    66.278 4.6626E+03 8.2540E+03  1.00  1.18 8.661E+01 1.190E+02
    5    67.161   152.388   169.802   137.778    73.436 4.8140E+03 8.6473E+03  0.91  1.06 7.404E+01 9.956E+01
    6    73.049   156.523   174.243   142.631    80.814 4.9581E+03 8.9424E+03  0.88  1.01 6.692E+01 8.821E+01
    7    78.783   155.384   172.267   143.344    87.889 5.0887E+03 9.2002E+03  0.88  1.00 6.434E+01 8.307E+01
    8    84.164   154.345   170.350   144.052    94.408 5.2037E+03 9.4298E+03  0.88  0.98 6.192E+01 7.792E+01
    9    89.184   153.281   168.369   144.636   100.377 5.3060E+03 9.6380E+03  0.89  0.97 5.969E+01 7.277E+01
   10    93.838   152.109   166.250   145.033   105.803 5.3992E+03 9.8237E+03  0.89  0.96 5.766E+01 6.763E+01
         96.073                                 108.381

 FUEL PLATE   2 (ExactSoln)
         45.000                                 45.000
    1    47.725    97.260   114.732    97.204    47.513 7.0601E+03 7.0492E+03  1.90  1.90 2.249E+02 2.250E+02
    2    53.420   105.018   124.097   104.842    52.781 7.4123E+03 7.3801E+03  1.65  1.65 1.921E+02 1.926E+02
    3    59.605   112.957   133.635   112.646    58.531 7.7807E+03 7.7283E+03  1.45  1.46 1.635E+02 1.645E+02
    4    66.278   121.078   143.360   120.642    64.760 8.1720E+03 8.0915E+03  1.30  1.30 1.381E+02 1.396E+02
    5    73.436   129.502   153.353   128.868    71.469 8.5642E+03 8.4759E+03  1.16  1.17 1.154E+02 1.173E+02
    6    80.814   134.602   158.354   133.769    78.420 8.9085E+03 8.8077E+03  1.09  1.11 1.018E+02 1.042E+02
    7    87.889   136.309   158.298   135.281    85.137 9.1875E+03 9.0767E+03  1.07  1.08 9.527E+01 9.829E+01
    8    94.408   137.955   158.190   136.749    91.383 9.4298E+03 9.3174E+03  1.04  1.06 8.883E+01 9.241E+01
    9   100.377   139.454   157.955   138.112    97.156 9.6380E+03 9.5237E+03  1.02  1.04 8.242E+01 8.663E+01
   10   105.803   140.698   157.484   139.256   102.456 9.8237E+03 9.7068E+03  1.00  1.02 7.603E+01 8.096E+01
        108.381                                 104.988

FUEL PLATE   3 (ExactSoln)
 NODE
         45.000                                 45.000
    1    47.513    97.204   114.732    97.260    47.725 7.0492E+03 7.0601E+03  1.90  1.90 2.250E+02 2.249E+02
    2    52.781   104.842   124.097   105.018    53.420 7.3801E+03 7.4123E+03  1.65  1.65 1.926E+02 1.921E+02
    3    58.531   112.646   133.635   112.957    59.605 7.7283E+03 7.7807E+03  1.46  1.45 1.645E+02 1.635E+02
    4    64.760   120.642   143.360   121.078    66.278 8.0915E+03 8.1720E+03  1.30  1.30 1.396E+02 1.381E+02
    5    71.469   128.868   153.353   129.502    73.436 8.4759E+03 8.5642E+03  1.17  1.16 1.173E+02 1.154E+02
    6    78.420   133.769   158.354   134.602    80.814 8.8077E+03 8.9085E+03  1.11  1.09 1.042E+02 1.018E+02
    7    85.137   135.281   158.298   136.309    87.889 9.0767E+03 9.1875E+03  1.08  1.07 9.829E+01 9.527E+01
    8    91.383   136.749   158.190   137.955    94.408 9.3174E+03 9.4298E+03  1.06  1.04 9.241E+01 8.883E+01
    9    97.156   138.112   157.955   139.454   100.377 9.5237E+03 9.6380E+03  1.04  1.02 8.663E+01 8.242E+01
   10   102.456   139.256   157.484   140.698   105.803 9.7068E+03 9.8237E+03  1.02  1.00 8.096E+01 7.603E+01
        104.988                                 108.381

 FUEL PLATE   4 (ExactSoln)
         45.000                                 45.000
    1    47.725   105.142   129.129   117.096    47.083 7.1368E+03 4.1454E+03  1.65  1.37 1.919E+02 1.364E+02
    2    53.420   113.016   139.015   125.641    51.462 7.4915E+03 4.3167E+03  1.46  1.22 1.645E+02 1.173E+02
    3    59.605   121.013   148.979   134.230    56.269 7.8614E+03 4.4969E+03  1.30  1.10 1.406E+02 1.008E+02
    4    66.278   129.215   159.201   143.113    61.504 8.2540E+03 4.6626E+03  1.18  1.00 1.190E+02 8.661E+01
    5    73.436   137.778   169.802   152.388    67.161 8.6473E+03 4.8140E+03  1.06  0.91 9.956E+01 7.404E+01
    6    80.814   142.631   174.243   156.523    73.049 8.9424E+03 4.9581E+03  1.01  0.88 8.821E+01 6.692E+01
    7    87.889   143.344   172.267   155.384    78.783 9.2002E+03 5.0887E+03  1.00  0.88 8.307E+01 6.434E+01
    8    94.408   144.052   170.350   154.345    84.164 9.4298E+03 5.2037E+03  0.98  0.88 7.792E+01 6.192E+01
    9   100.377   144.636   168.369   153.281    89.184 9.6380E+03 5.3060E+03  0.97  0.89 7.277E+01 5.969E+01
   10   105.803   145.033   166.250   152.109    93.838 9.8237E+03 5.3992E+03  0.96  0.89 6.763E+01 5.766E+01
        108.381                                 96.073
[1] The ONB ratio is here defined as (Tonb - Tinlet)/(Tsurf - Tinlet). If the heat flux is negative (the
    coolant is hotter than the adjacent cladding surface), then the ONB ratio is arbitrarily set to 99.99 .


MIXED MEAN TEMP. (CORE FLOW ONLY)=   104.456
 WORK: TBAR RETURNED FROM FINLED= 104.459
```

Figure 2.12 Standard Problem 14 Input Data for PLTEMP/ANL V3.0: 10% of Reactor Power Produced in Fuel and 90% in Cladding, No Heat Source in Coolant (Cladding Thickness = 0.9 mm)

```
 Standard Problem 14: 2 assemblies (of identical geometry) producing 1 MWt
! Each assembly has 4 fuel plates and 5 coolant channels
! Each fuel plate has equal power all of which is directly deposited in
! coolant channels. See card(2) 0500.
! H2O coolant, Input coolant flow = 0.50 kg/s in channel 2, 3, or 4
!                                 = 0.25 kg/s in channel 1, or 5
! All hot channel factors = 1.0
! No bypass flow, NCTYP=0
! 10 axial heat transfer nodes in the heated length of fuel plates
!  1   2   3   4   5   6   7   8   9  10  11  12  13  14  15  16  17  18        Indices Card 0200
   0   0   5   1   0   1   1   1   0   0   0   0   0           1                Card(1)0200
   2   3 0.00       1.00        1.00        1.00           3                  Card(1)0300
! Using pressure driven mode
   1  20 1.00                                                                  Card(1)0301
   1   1   1                                                                   Card(1)0302
1.20        1.20                                                               Card(2)0303
30.0E-04    0.02955665  0.15        8.00        0.20        15.0E-03           Card(3)0304
30.0E-04    0.02955665  0.75        0.00        0.20        15.0E-03           Card(3)0304
30.0E-04    0.02955665  0.15        8.00        0.20        15.0E-03           Card(3)0304
! Use the code's biult-in correlation for friction factor
0.00        0.00        0.00                                                   Card(1)0305
   5   3 0.00       0.75        0.90E-03    10.00       0.20E-03    10.00      Card(1)0306
6.00E-04    5.91133E-03 0.4060      0.20        0.20        3.00E-03           Card(5)0307
6.00E-04    5.91133E-03 0.4060      0.40        0.20        3.00E-03           Card(5)0307
6.00E-04    5.91133E-03 0.4060      0.40        0.20        3.00E-03           Card(5)0307
6.00E-04    5.91133E-03 0.4060      0.40        0.20        3.00E-03           Card(5)0307
6.00E-04    5.91133E-03 0.4060      0.20        0.20        3.00E-03           Card(5)0307
0.20        0.20        0.20        0.20                                       Card(1)0308
! Card 0308a not required
! Radial power peaking factor data by fuel plate for each assembly. Input flow data by
! channel for each assembly on Cards 0310 not required because WFGES(1) is non-zero
1.000       1.000       1.000       1.000                                      Card(2)0309
0.25        0.50        0.50        0.50        0.25                           Card(2)0310
1.000       1.000       1.000       1.000                                      Card(2)0309
0.25        0.50        0.50        0.50        0.25                           Card(2)0310
! DP0       DDP         DPMAX       POWER       TIN         PIN
0.32336     0.04        0.36136     1.00        45.0        0.12               Card(2)0500
0.9         0.0                                                                Card(2)0500
  50 0.0001     25.0        0.50        1.00                                   Card(1)0600
  11                                                                           Card(1)0700
0.00        0.80                                                               Card(11)0701
0.10        0.88                                                               Card(11)0701
0.20        0.96                                                               Card(11)0701
0.30        1.04                                                               Card(11)0701
0.40        1.12                                                               Card(11)0701
0.50        1.20                                                               Card(11)0701
0.60        1.12                                                               Card(11)0701
0.70        1.04                                                               Card(11)0701
0.80        0.96                                                               Card(11)0701
0.90        0.88                                                               Card(11)0701
1.00        0.80                                                               Card(11)0701
   0                                                                           Card(11)0702
```

Figure 2.13 Exact Solution of Standard Problem 14: 10% of Reactor Power Produced in Fuel and 90% in Cladding, No Heat Source in Coolant (Cladding Thickness = 0.9 mm)

```
Input Power Densities (MW/m**3) in Axial Node   1 of Assembly   1 of Type   1:
FUEL PLATE  COOLANTl    CLADDINGl   FUEL MEAT   CLADDINGr   COOLANTr
     1      0.0000E+00  3.5000E+02  3.5000E+02  3.5000E+02  0.0000E+00
     2      0.0000E+00  3.5000E+02  3.5000E+02  3.5000E+02  0.0000E+00
     3      0.0000E+00  3.5000E+02  3.5000E+02  3.5000E+02  0.0000E+00
     4      0.0000E+00  3.5000E+02  3.5000E+02  3.5000E+02  0.0000E+00

 FUEL PLATE   1 (ExactSoln)
 NODE    COOLANTl  CladSl  FUEL PEAK   CladSr  COOLANTr   HCOFl      HCOFr    ONBRl  ONBRr  ETA'l     ETA'r
         (C)       (C)       (C)       (C)       (C)     W/C-m^2    W/C-m^2    [F Note 1]  K-cm^3/J  K-cm^3/J
         45.000                                  45.000
    1    47.083   117.096   129.041   105.142    47.725 4.1454E+03 7.1368E+03  1.37  1.65 1.364E+02 1.919E+02
    2    51.462   125.641   138.934   113.016    53.420 4.3167E+03 7.4915E+03  1.22  1.46 1.173E+02 1.645E+02
    3    56.269   134.230   148.908   121.013    59.605 4.4969E+03 7.8614E+03  1.10  1.30 1.008E+02 1.406E+02
    4    61.504   143.113   159.134   129.215    66.278 4.6626E+03 8.2540E+03  1.00  1.18 8.661E+01 1.190E+02
    5    67.161   152.388   169.738   137.778    73.436 4.8140E+03 8.6473E+03  0.91  1.06 7.404E+01 9.956E+01
    6    73.049   156.523   174.197   142.631    80.814 4.9581E+03 8.9424E+03  0.88  1.01 6.692E+01 8.821E+01
    7    78.783   155.384   172.241   143.344    87.889 5.0887E+03 9.2002E+03  0.88  1.00 6.434E+01 8.307E+01
    8    84.164   154.345   170.338   144.052    94.408 5.2037E+03 9.4298E+03  0.88  0.98 6.192E+01 7.792E+01
    9    89.184   153.281   168.366   144.636   100.377 5.3060E+03 9.6380E+03  0.89  0.97 5.969E+01 7.277E+01
   10    93.838   152.109   166.250   145.033   105.803 5.3992E+03 9.8237E+03  0.89  0.96 5.766E+01 6.763E+01
         96.073                                  108.381

 FUEL PLATE   2 (ExactSoln)
         45.000                                  45.000
    1    47.725    97.260   114.732    97.204    47.513 7.0601E+03 7.0492E+03  1.90  1.90 2.249E+02 2.250E+02
    2    53.420   105.018   124.097   104.842    52.781 7.4123E+03 7.3801E+03  1.65  1.65 1.921E+02 1.926E+02
    3    59.605   112.957   133.635   112.646    58.531 7.7807E+03 7.7283E+03  1.45  1.46 1.635E+02 1.645E+02
    4    66.278   121.078   143.360   120.642    64.760 8.1720E+03 8.0915E+03  1.30  1.30 1.381E+02 1.396E+02
    5    73.436   129.502   153.353   128.868    71.469 8.5642E+03 8.4759E+03  1.16  1.17 1.154E+02 1.173E+02
    6    80.814   134.602   158.354   133.769    78.420 8.9085E+03 8.8077E+03  1.09  1.11 1.018E+02 1.042E+02
    7    87.889   136.309   158.298   135.281    85.137 9.1875E+03 9.0767E+03  1.07  1.08 9.527E+01 9.829E+01
    8    94.408   137.955   158.190   136.749    91.383 9.4298E+03 9.3174E+03  1.04  1.06 8.883E+01 9.241E+01
    9   100.377   139.454   157.955   138.112    97.156 9.6380E+03 9.5237E+03  1.02  1.04 8.242E+01 8.663E+01
   10   105.803   140.698   157.484   139.256   102.456 9.8237E+03 9.7068E+03  1.00  1.02 7.603E+01 8.096E+01
        108.381                                  104.988

FUEL PLATE   3 (ExactSoln)
         45.000                                  45.000
    1    47.513    97.204   114.732    97.260    47.725 7.0492E+03 7.0601E+03  1.90  1.90 2.250E+02 2.249E+02
    2    52.781   104.842   124.097   105.018    53.420 7.3801E+03 7.4123E+03  1.65  1.65 1.926E+02 1.921E+02
    3    58.531   112.646   133.635   112.957    59.605 7.7283E+03 7.7807E+03  1.46  1.45 1.645E+02 1.635E+02
    4    64.760   120.642   143.360   121.078    66.278 8.0915E+03 8.1720E+03  1.30  1.30 1.396E+02 1.381E+02
    5    71.469   128.868   153.353   129.502    73.436 8.4759E+03 8.5642E+03  1.17  1.16 1.173E+02 1.154E+02
    6    78.420   133.769   158.354   134.602    80.814 8.8077E+03 8.9085E+03  1.11  1.09 1.042E+02 1.018E+02
    7    85.137   135.281   158.298   136.309    87.889 9.0767E+03 9.1875E+03  1.08  1.07 9.829E+01 9.527E+01
    8    91.383   136.749   158.190   137.955    94.408 9.3174E+03 9.4298E+03  1.06  1.04 9.241E+01 8.883E+01
    9    97.156   138.112   157.955   139.454   100.377 9.5237E+03 9.6380E+03  1.04  1.02 8.663E+01 8.242E+01
   10   102.456   139.256   157.484   140.698   105.803 9.7068E+03 9.8237E+03  1.02  1.00 8.096E+01 7.603E+01
        104.988                                  108.381

 FUEL PLATE   4 (ExactSoln)
         45.000                                  45.000
    1    47.725   105.142   129.041   117.096    47.083 7.1368E+03 4.1454E+03  1.65  1.37 1.919E+02 1.364E+02
    2    53.420   113.016   138.934   125.641    51.462 7.4915E+03 4.3167E+03  1.46  1.22 1.645E+02 1.173E+02
    3    59.605   121.013   148.908   134.230    56.269 7.8614E+03 4.4969E+03  1.30  1.10 1.406E+02 1.008E+02
    4    66.278   129.215   159.134   143.113    61.504 8.2540E+03 4.6626E+03  1.18  1.00 1.190E+02 8.661E+01
    5    73.436   137.778   169.738   152.388    67.161 8.6473E+03 4.8140E+03  1.06  0.91 9.956E+01 7.404E+01
    6    80.814   142.631   174.197   156.523    73.049 8.9424E+03 4.9581E+03  1.01  0.88 8.821E+01 6.692E+01
    7    87.889   143.344   172.241   155.384    78.783 9.2002E+03 5.0887E+03  1.00  0.88 8.307E+01 6.434E+01
    8    94.408   144.052   170.338   154.345    84.164 9.4298E+03 5.2037E+03  0.98  0.88 7.792E+01 6.192E+01
    9   100.377   144.636   168.366   153.281    89.184 9.6380E+03 5.3060E+03  0.97  0.89 7.277E+01 5.969E+01
   10   105.803   145.033   166.250   152.109    93.838 9.8237E+03 5.3992E+03  0.96  0.89 6.763E+01 5.766E+01
        108.381                                  96.073
[1] The ONB ratio is here defined as (Tonb - Tinlet)/(Tsurf - Tinlet). If the heat flux is negative (the
    coolant is hotter than the adjacent cladding surface), then the ONB ratio is arbitrarily set to 99.99 .


MIXED MEAN TEMP. (CORE FLOW ONLY)=   104.456

 WORK: TBAR RETURNED FROM FINLED= 104.459
```

Figure 2.14 Standard Problem 15 Input Data for PLTEMP/ANL V3.0: 100% of Reactor Power Directly Deposited in Coolant (No Heat Source in Fuel and Cladding)

```
 Standard Problem 15: 2 assemblies (of identical geometry) producing 1 MWt
! Each assembly has 4 fuel plates and 5 coolant channels
! Each fuel plate has equal power all of which is directly deposited in
! coolant channels. See card(2) 0500.
! H2O coolant, Input coolant flow = 0.50 kg/s in channel 2, 3, or 4
!                                 = 0.25 kg/s in channel 1, or 5
! All hot channel factors = 1.0
! No bypass flow, NCTYP=0
! 10 axial heat transfer nodes in the heated length of fuel plates
!  1   2   3   4   5   6   7   8   9  10  11  12  13  14  15  16  17  18        Indices Card 0200
   0   0   5   1   0   1   1   1   0   0   0   0   0           1                Card(1)0200
   2   3 0.00       1.00        1.00        1.00           3                   Card(1)0300
! Using pressure driven mode
   1  20 1.00                                                                  Card(1)0301
   1   1   1                                                                   Card(1)0302
1.20        1.20                                                               Card(2)0303
30.0E-04    0.02955665  0.15        8.00        0.20        15.0E-03           Card(3)0304
30.0E-04    0.02955665  0.75        0.00        0.20        15.0E-03           Card(3)0304
30.0E-04    0.02955665  0.15        8.00        0.20        15.0E-03           Card(3)0304
! Use the code's biult-in correlation for friction factor
0.00        0.00        0.00                                                   Card(1)0305
   5   3 0.00       0.75        0.50E-03    10.00       1.00E-03    10.00       Card(1)0306
6.00E-04    5.91133E-03 0.4060      0.20        0.20        3.00E-03           Card(5)0307
6.00E-04    5.91133E-03 0.4060      0.40        0.20        3.00E-03           Card(5)0307
6.00E-04    5.91133E-03 0.4060      0.40        0.20        3.00E-03           Card(5)0307
6.00E-04    5.91133E-03 0.4060      0.40        0.20        3.00E-03           Card(5)0307
6.00E-04    5.91133E-03 0.4060      0.20        0.20        3.00E-03           Card(5)0307
0.20        0.20        0.20        0.20                                       Card(1)0308
! Card 0308a not required
! Radial power peaking factor data by fuel plate for each assembly. Input flow data by
! channel for each assembly on Cards 0310 not required because WFGES(1) is non-zero
1.000       1.000       1.000       1.000                                      Card(2)0309
0.25        0.50        0.50        0.50        0.25                           Card(2)0310
1.000       1.000       1.000       1.000                                      Card(2)0309
0.25        0.50        0.50        0.50        0.25                           Card(2)0310
! DP0       DDP         DPMAX       POWER       TIN         PIN
0.32336     0.04        0.36136     1.00        45.0        0.12               Card(2)0500
0.0         .99999999999                                                       Card(2)0500
  50 0.0001     25.0        0.50        1.00                                   Card(1)0600
  11                                                                           Card(1)0700
0.00        0.80                                                               Card(11)0701
0.10        0.88                                                               Card(11)0701
0.20        0.96                                                               Card(11)0701
0.30        1.04                                                               Card(11)0701
0.40        1.12                                                               Card(11)0701
0.50        1.20                                                               Card(11)0701
0.60        1.12                                                               Card(11)0701
0.70        1.04                                                               Card(11)0701
0.80        0.96                                                               Card(11)0701
0.90        0.88                                                               Card(11)0701
1.00        0.80                                                               Card(11)0701
   0                                                                           Card(11)0702
```

Figure 2.15 Exact Solution of Standard Problem 15: 100% of Reactor Power Directly Deposited in Coolant (No Heat Source in Fuel and Cladding)

```
Input Power Densities (MW/m**3) in Axial Node   1 of Assembly   1 of Type   1:
FUEL PLATE  COOLANTl    CLADDINGl   FUEL MEAT   CLADDINGr   COOLANTr
     1      1.1667E+02  0.0000E+00  7.0000E-09  0.0000E+00  2.3333E+02
     2      2.3333E+02  0.0000E+00  7.0000E-09  0.0000E+00  2.3333E+02
     3      2.3333E+02  0.0000E+00  7.0000E-09  0.0000E+00  2.3333E+02
     4      2.3333E+02  0.0000E+00  7.0000E-09  0.0000E+00  1.1667E+02

 FUEL PLATE   1 (ExactSoln)
 NODE    COOLANTl  CladSl  FUEL PEAK   CladSr  COOLANTr   HCOFl      HCOFr    ONBRl  ONBRr  ETA'l     ETA'r
         (C)       (C)       (C)       (C)       (C)     W/C-m^2    W/C-m^2    [F Note 1]  K-cm^3/J  K-cm^3/J
         45.000                                  45.000
    1    47.511    47.511    47.511    47.511    47.511 3.7008E+03 6.4434E+03 37.75 37.75 1.375E+13 1.907E+13
    2    52.771    52.771    52.771    52.771    52.771 3.8824E+03 6.7597E+03 12.15 12.15 1.166E+13 1.647E+13
    3    58.503    58.503    58.503    58.503    58.503 4.0745E+03 7.0940E+03  6.97  6.97 9.874E+12 1.419E+13
    4    64.705    64.705    64.705    64.705    64.705 4.2757E+03 7.4444E+03  4.75  4.75 8.315E+12 1.215E+13
    5    71.376    71.376    71.376    71.376    71.376 4.4908E+03 7.8190E+03  3.54  3.54 6.939E+12 1.030E+13
    6    78.275    78.275    78.275    78.275    78.275 4.6928E+03 8.1706E+03  2.79  2.79 6.118E+12 9.252E+12
    7    84.926    84.926    84.926    84.926    84.926 4.8756E+03 8.4888E+03  2.32  2.32 5.722E+12 8.849E+12
    8    91.093    91.093    91.093    91.093    91.093 5.0391E+03 8.7735E+03  2.00  2.00 5.341E+12 8.448E+12
    9    96.776    96.776    96.776    96.776    96.776 5.1903E+03 9.0368E+03  1.77  1.77 4.972E+12 8.054E+12
   10   101.979   101.979   101.979   101.979   101.979 5.3290E+03 9.2783E+03  1.60  1.60 4.618E+12 7.669E+12
        104.459                                 104.459

 FUEL PLATE   2 (ExactSoln)
         45.000                                  45.000
    1    47.511    47.511    47.511    47.511    47.511 6.4434E+03 6.4434E+03 37.75 37.75 2.255E+13 2.250E+13
    2    52.771    52.771    52.771    52.771    52.771 6.7597E+03 6.7597E+03 12.15 12.15 1.938E+13 1.924E+13
    3    58.503    58.503    58.503    58.503    58.503 7.0940E+03 7.0940E+03  6.97  6.97 1.660E+13 1.642E+13
    4    64.705    64.705    64.705    64.705    64.705 7.4444E+03 7.4444E+03  4.75  4.75 1.414E+13 1.394E+13
    5    71.376    71.376    71.376    71.376    71.376 7.8190E+03 7.8190E+03  3.54  3.54 1.193E+13 1.172E+13
    6    78.275    78.275    78.275    78.275    78.275 8.1706E+03 8.1706E+03  2.79  2.79 1.065E+13 1.042E+13
    7    84.926    84.926    84.926    84.926    84.926 8.4888E+03 8.4888E+03  2.32  2.32 1.012E+13 9.847E+12
    8    91.093    91.093    91.093    91.093    91.093 8.7735E+03 8.7735E+03  2.00  2.00 9.591E+12 9.283E+12
    9    96.776    96.776    96.776    96.776    96.776 9.0368E+03 9.0368E+03  1.77  1.77 9.072E+12 8.733E+12
   10   101.979   101.979   101.979   101.979   101.979 9.2783E+03 9.2783E+03  1.60  1.60 8.566E+12 8.201E+12
        104.459                                 104.459

FUEL PLATE   3 (ExactSoln)
         45.000                                  45.000
    1    47.511    47.511    47.511    47.511    47.511 6.4434E+03 6.4434E+03 37.75 37.75 2.250E+13 2.255E+13
    2    52.771    52.771    52.771    52.771    52.771 6.7597E+03 6.7597E+03 12.15 12.15 1.924E+13 1.938E+13
    3    58.503    58.503    58.503    58.503    58.503 7.0940E+03 7.0940E+03  6.97  6.97 1.642E+13 1.660E+13
    4    64.705    64.705    64.705    64.705    64.705 7.4444E+03 7.4444E+03  4.75  4.75 1.394E+13 1.414E+13
    5    71.376    71.376    71.376    71.376    71.376 7.8190E+03 7.8190E+03  3.54  3.54 1.172E+13 1.193E+13
    6    78.275    78.275    78.275    78.275    78.275 8.1706E+03 8.1706E+03  2.79  2.79 1.042E+13 1.065E+13
    7    84.926    84.926    84.926    84.926    84.926 8.4888E+03 8.4888E+03  2.32  2.32 9.846E+12 1.012E+13
    8    91.093    91.093    91.093    91.093    91.093 8.7735E+03 8.7735E+03  2.00  2.00 9.282E+12 9.592E+12
    9    96.776    96.776    96.776    96.776    96.776 9.0368E+03 9.0368E+03  1.77  1.77 8.733E+12 9.073E+12
   10   101.979   101.979   101.979   101.979   101.979 9.2783E+03 9.2783E+03  1.60  1.60 8.200E+12 8.567E+12
        104.459                                 104.459

 FUEL PLATE   4 (ExactSoln)
         45.000                                  45.000
    1    47.511    47.511    47.511    47.511    47.511 6.4434E+03 3.7008E+03 37.75 37.75 1.907E+13 1.375E+13
    2    52.771    52.771    52.771    52.771    52.771 6.7597E+03 3.8824E+03 12.15 12.15 1.647E+13 1.166E+13
    3    58.503    58.503    58.503    58.503    58.503 7.0940E+03 4.0745E+03  6.97  6.97 1.419E+13 9.874E+12
    4    64.705    64.705    64.705    64.705    64.705 7.4444E+03 4.2757E+03  4.75  4.75 1.215E+13 8.315E+12
    5    71.376    71.376    71.376    71.376    71.376 7.8190E+03 4.4908E+03  3.54  3.54 1.030E+13 6.939E+12
    6    78.275    78.275    78.275    78.275    78.275 8.1706E+03 4.6928E+03  2.79  2.79 9.252E+12 6.118E+12
    7    84.926    84.926    84.926    84.926    84.926 8.4888E+03 4.8756E+03  2.32  2.32 8.849E+12 5.722E+12
    8    91.093    91.093    91.093    91.093    91.093 8.7735E+03 5.0391E+03  2.00  2.00 8.449E+12 5.340E+12
    9    96.776    96.776    96.776    96.776    96.776 9.0368E+03 5.1903E+03  1.77  1.77 8.054E+12 4.972E+12
   10   101.979   101.979   101.979   101.979   101.979 9.2783E+03 5.3290E+03  1.60  1.60 7.669E+12 4.617E+12
        104.459                                 104.459
[1] The ONB ratio is here defined as (Tonb - Tinlet)/(Tsurf - Tinlet). If the heat flux is negative (the
    coolant is hotter than the adjacent cladding surface), then the ONB ratio is arbitrarily set to 99.99 .


MIXED MEAN TEMP. (CORE FLOW ONLY)=   104.459

 WORK: TBAR RETURNED FROM FINLED= 104.459
```

Table 2.1 Heat Transfer to Farther Channels in Standard Problem 10 Using the Exact Solution by PLTEMP/ANL V3.0 Code

Case	Water Thermal Conductivity Multiplier	Coolant Temperature at Core Outlet, C					
		Channel 1	Channel 2	Channel 3	Channel 4	Channel 5	Mixed Mean
1	1	63.53	109.06	40.21	26.66	25.14	62.85
2	10	62.84	92.62	67.74	51.28	41.05	62.86
3	100	61.84	87.85	82.86	79.41	77.43	62.86
4	1000	61.77	85.58	83.95	82.09	81.34	62.86

Table 2.2 Comparison of PLTEMP/ANL Versions 3.0 and 2.14 for Standard Problem 1

Table Number	Max Temp Diff	Occurs in Axial Node	Max Tdiff Current Output	Max Tdiff Saved Output
1	1.420	11	0.000	3.060
2	0.358	11	0.000	0.770
3	0.146	11	0.010	0.330
4	0.428	11	0.010	0.920
5	0.271	11	0.010	0.590
6	0.006	5	0.000	0.010

Note: Table number here simply counts the tables of steady-state temperatures printed for each fuel plate by PLTEMP/ANL. If results for the same plate is printed again in the code output, it is counted again.

Table 2.3 Comparison of PLTEMP/ANL Versions 3.0 and 2.14 for Standard Problem 2

Table Number	Max Temp Diff	Occurs in Axial Node	Max Tdiff Current Output	Max Tdiff Saved Output
1	2.873	10	0.000	5.640
2	0.315	9	0.030	0.530
3	0.152	10	0.040	0.150
4	1.866	10	0.010	3.680
5	2.872	10	0.000	5.630
6	0.565	10	0.000	0.870
7	0.238	10	0.000	0.320
8	1.867	10	0.000	3.670
9	2.871	10	0.000	5.480
10	1.585	9	0.010	3.160
11	0.605	9	0.010	1.120
12	1.868	10	0.000	3.740
13	2.863	10	0.010	5.410
14	4.166	10	0.590	8.350
15	1.842	10	0.360	3.390
16	2.081	10	0.000	4.150
17	2.870	10	0.000	5.480
18	1.935	9	0.000	3.870
19	0.329	9	0.000	0.560
20	1.868	10	0.000	3.710
21	2.869	10	0.000	5.550
22	1.870	10	0.000	3.530
23	1.262	10	0.000	2.340
24	1.869	10	0.000	3.660

25	2.870	10	0.000	5.500
26	1.743	9	0.000	3.430
27	0.440	9	0.000	0.790
28	1.873	10	0.000	3.680
29	2.869	10	0.000	5.480
30	4.140	10	0.100	8.290
31	1.831	10	0.020	3.430
32	2.092	10	0.000	4.180
33	2.867	10	0.000	5.620
34	0.440	8	0.000	0.860
35	0.455	8	0.000	0.920
36	1.871	10	0.000	3.630
37	2.867	10	0.000	5.570
38	2.684	10	0.030	5.260
39	1.141	10	0.010	2.110
40	1.871	10	0.000	3.710
41	2.865	10	0.000	5.290
42	8.487	10	0.000	17.040
43	4.803	10	0.000	9.320
44	1.872	10	0.000	3.540
45	2.865	10	0.000	5.600
46	1.182	10	0.000	2.150
47	0.486	10	0.000	0.810
48	1.873	10	0.000	3.690

Table 2.4 Comparison of PLTEMP/ANL Versions 3.0 and 2.14 for Standard Problem 3

Table Number	Max Temp Diff	Occurs in Axial Node	Max Tdiff Current Output	Max Tdiff Saved Output
1	0.448	10	0.000	0.960
2	0.365	10	0.000	0.770
3	0.069	10	0.000	0.140
4	0.145	10	0.000	0.310
5	0.446	10	0.000	0.940
6	0.179	10	0.000	0.380
7	0.121	10	0.000	0.260
8	0.012	10	0.000	0.010

Table 2.5 Comparison of PLTEMP/ANL Versions 3.0 and 2.14 for Standard Problem 4

Table Number	Max Temp Diff	Occurs in Axial Node	Max Tdiff Current Output	Max Tdiff Saved Output
1	0.568	10	0.000	1.200
2	0.076	8	0.000	0.160
3	0.078	8	0.000	0.170
4	0.008	10	0.000	0.000
5	0.609	10	0.040	1.280
6	0.067	8	0.150	0.040
7	0.084	8	0.180	0.050
8	0.013	8	0.030	0.000
9	0.568	10	0.000	1.200
10	0.018	10	0.000	0.010
11	0.010	9	0.000	0.020
12	0.008	10	0.000	0.000
13	1.277	10	0.000	2.710
14	0.054	10	0.000	0.030
15	0.019	10	0.000	0.010
16	0.317	10	0.000	0.690

Table 2.6 Comparison of PLTEMP/ANL Versions 3.0 and 2.14 for Standard Problem 5

Table Number	Max Temp Diff	Occurs in Axial Node	Max Tdiff Current Output	Max Tdiff Saved Output
1	0.447	10	0.000	0.950
2	0.130	10	0.110	0.270
3	0.044	10	0.030	0.100
4	0.013	10	0.000	0.020
5	2.761	10	0.000	5.750
6	0.328	10	0.000	0.660
7	2.360	10	0.000	5.080
8	0.211	10	0.000	0.410
9	0.065	10	0.000	0.140
10	0.185	9	0.070	0.400
11	0.094	9	0.020	0.200
12	0.010	10	0.000	0.000
13	1.298	10	0.000	2.730
14	0.874	10	0.120	1.920
15	0.386	10	0.260	0.840
16	0.327	10	0.000	0.720
17	0.008	10	0.000	0.000
18	0.022	8	0.050	0.000
19	0.031	8	0.070	0.000
20	0.008	10	0.000	0.000
21	1.007	10	0.000	2.150
22	0.039	10	0.010	0.030
23	0.009	1	0.020	0.000
24	0.010	10	0.000	0.000
25	0.656	10	0.000	1.390
26	0.397	10	0.000	0.840
27	0.042	10	0.010	0.080
28	0.070	10	0.010	0.150
29	2.166	10	0.000	4.490
30	0.717	9	0.000	1.560
31	0.390	9	0.000	0.850
32	0.195	9	0.000	0.420
33	0.191	10	0.000	0.410
34	0.009	10	0.000	0.010
35	0.005	10	0.000	0.000
36	0.012	10	0.000	0.000
37	1.571	10	0.000	3.330
38	0.161	6	0.030	0.340
39	0.136	9	0.010	0.290
40	0.032	9	0.000	0.060
41	0.010	10	0.000	0.000
42	0.009	3	0.020	0.000
43	0.006	3	0.010	0.000
44	0.010	10	0.000	0.000
45	1.214	10	0.010	2.590
46	0.079	10	0.000	0.140
47	0.046	10	0.000	0.100
48	0.012	10	0.000	0.010
49	0.894	10	0.000	1.900
50	0.232	4	0.000	0.500
51	0.095	4	0.000	0.200
52	0.147	10	0.000	0.310
53	2.570	10	0.010	5.360
54	0.259	9	0.020	0.530
55	0.087	3	0.010	0.190
56	0.030	10	0.000	0.010
57	0.326	10	0.000	0.670
58	0.386	9	0.000	0.830
59	0.354	9	0.030	0.780
60	0.078	7	0.000	0.170
61	1.859	10	0.000	3.920
62	0.084	10	0.000	0.080
63	0.014	10	0.000	0.000
64	0.018	10	0.000	0.020
65	0.010	10	0.000	0.000

66	0.004	10	0.000	0.000
67	0.006	10	0.000	0.000
68	0.012	10	0.000	0.000
69	1.432	10	0.000	3.060
70	0.149	9	0.010	0.310
71	0.185	1	0.000	0.400
72	0.019	9	0.000	0.030
73	1.154	10	0.000	2.450
74	0.052	10	0.000	0.050
75	0.202	10	0.000	0.420
76	0.369	10	0.000	0.790
77	3.016	10	0.000	6.280
78	0.161	10	0.100	0.110
79	4.425	10	0.030	9.640
80	0.157	10	0.050	0.060
81	0.479	10	0.000	1.040
82	0.130	10	0.000	0.260
83	0.351	10	0.000	0.780
84	0.035	4	0.000	0.080
85	2.160	10	0.030	4.560
86	0.361	10	0.020	0.680
87	0.388	10	0.020	0.860
88	0.171	9	0.000	0.360
89	0.086	10	0.000	0.190
90	0.011	10	0.000	0.010
91	0.007	10	0.000	0.010
92	0.014	10	0.000	0.000
93	1.658	10	0.000	3.540
94	0.436	10	0.000	0.890
95	0.043	10	0.000	0.100
96	0.045	10	0.000	0.090
97	1.447	10	0.000	3.060
98	0.060	10	0.020	0.030
99	0.019	10	0.020	0.000
100	0.627	10	0.010	1.340
101	3.459	10	0.110	7.190
102	0.365	10	0.500	0.660
103	0.243	1	0.520	0.340
104	0.174	10	0.040	0.350
105	0.656	10	0.000	1.420
106	0.031	10	0.010	0.030
107	0.012	10	0.000	0.010
108	0.020	10	0.000	0.000
109	2.478	10	0.000	5.260
110	0.371	10	0.000	0.780
111	2.424	10	0.000	5.350
112	0.131	4	0.000	0.290
113	0.194	10	0.000	0.430
114	0.014	10	0.010	0.000
115	0.009	10	0.010	0.000
116	0.016	10	0.020	0.000
117	1.898	10	0.000	4.050
118	0.256	10	0.000	0.480
119	0.036	10	0.000	0.070
120	0.170	10	0.000	0.380
121	1.767	10	0.400	3.730
122	0.085	10	0.060	0.000
123	0.164	1	0.340	0.030
124	0.924	10	0.120	1.990
125	3.919	10	0.000	8.140
126	0.594	10	0.000	1.150
127	0.303	10	0.000	0.600
128	0.178	10	0.000	0.390
129	0.851	10	0.000	1.840
130	0.041	10	0.010	0.040
131	0.031	6	0.000	0.050
132	0.021	10	0.000	0.040
133	2.827	10	0.000	5.960
134	0.141	10	0.000	0.040
135	0.163	10	0.000	0.360
136	0.026	10	0.000	0.010

137	0.321	10	0.000	0.710
138	0.048	9	0.000	0.100
139	0.332	9	0.000	0.750
140	0.019	10	0.000	0.000
141	2.164	10	0.000	4.600
142	0.421	10	0.000	0.890
143	0.243	10	0.000	0.500
144	0.024	10	0.000	0.010
145	2.123	10	0.000	4.500
146	0.095	10	0.010	0.070
147	0.050	10	0.010	0.020
148	1.281	10	0.000	2.750
149	4.394	10	0.000	9.120
150	0.858	10	0.030	1.740
151	0.071	10	0.010	0.030
152	0.041	10	0.000	0.030
153	1.064	10	0.010	2.290
154	0.050	10	0.020	0.040
155	0.022	10	0.060	0.050
156	0.200	10	0.010	0.450
157	3.170	10	0.000	6.690
158	0.194	9	0.010	0.370
159	2.837	10	0.010	6.320
160	0.093	10	0.000	0.020
161	0.463	10	0.000	1.020
162	0.027	10	0.000	0.030
163	0.014	10	0.000	0.020
164	0.031	10	0.000	0.060
165	2.433	10	0.000	5.180
166	0.110	10	0.000	0.080
167	0.057	10	0.000	0.120
168	0.023	10	0.000	0.000
169	2.512	10	0.000	5.320
170	0.112	10	0.010	0.010
171	0.067	10	0.010	0.000
172	1.673	10	0.000	3.610
173	4.880	10	0.000	10.140
174	1.161	10	0.010	2.390
175	0.169	10	0.010	0.250
176	0.053	10	0.000	0.020
177	1.306	10	0.000	2.800
178	0.240	1	0.000	0.520
179	0.730	10	0.000	1.630
180	0.426	10	0.000	0.950
181	3.525	10	0.010	7.420
182	0.187	10	0.000	0.270
183	0.035	10	0.010	0.000
184	0.034	10	0.000	0.000
185	0.617	10	0.470	1.350
186	0.041	10	0.030	0.010
187	0.027	2	0.050	0.000
188	0.035	2	0.080	0.000
189	2.707	10	0.000	5.750
190	0.244	10	0.080	0.450
191	0.183	10	0.050	0.380
192	0.026	10	0.010	0.020
193	2.940	10	0.000	6.230
194	0.141	10	0.010	0.170
195	0.148	10	0.010	0.210
196	2.270	10	0.000	4.810
197	5.390	10	0.000	11.200
198	1.470	10	0.000	3.070
199	0.221	10	0.000	0.350
200	0.352	10	0.000	0.760
201	1.566	10	0.000	3.380
202	0.090	10	0.080	0.050
203	0.129	10	0.090	0.130
204	0.676	10	0.000	1.500
205	3.885	10	0.000	8.160
206	2.082	10	0.030	4.670
207	0.109	10	0.050	0.130

208	0.043	10	0.000	0.020
209	0.788	10	0.000	1.730
210	0.082	10	0.000	0.130
211	0.074	10	0.000	0.140
212	0.029	10	0.000	0.010
213	2.985	10	0.000	6.390
214	0.386	10	0.000	0.690
215	0.235	10	0.000	0.500
216	0.071	10	0.000	0.140
217	3.392	10	0.000	7.030
218	3.395	5	0.020	7.520
219	3.445	5	0.020	7.600
220	2.651	10	0.000	5.830
221	5.919	10	0.000	12.280
222	1.860	10	0.000	3.900
223	0.134	10	0.000	0.010
224	0.757	10	0.000	1.700
225	1.854	10	0.000	4.000
226	0.087	10	0.150	0.060
227	0.047	10	0.010	0.010
228	0.968	10	0.000	2.140
229	4.262	10	0.000	8.990
230	0.593	10	0.000	1.160
231	0.090	2	0.170	0.050
232	0.050	10	0.020	0.060
233	0.983	10	0.000	2.150
234	0.250	10	0.010	0.510
235	0.107	10	0.000	0.230
236	0.078	10	0.000	0.160
237	3.269	10	0.000	6.980
238	0.163	10	0.000	0.320
239	0.121	7	0.000	0.240
240	0.037	10	0.000	0.020
241	3.949	10	0.000	8.520
242	0.257	10	0.000	0.340
243	0.126	10	0.000	0.050
244	3.158	10	0.000	6.720
245	6.477	10	0.000	13.410
246	2.242	10	0.050	4.840
247	0.145	10	0.030	0.210
248	1.331	10	0.000	2.940
249	2.192	10	0.060	4.680
250	0.129	10	0.520	0.380
251	0.059	10	0.010	0.020
252	1.401	10	0.000	3.060
253	4.650	10	0.000	9.810
254	0.824	10	0.000	1.680
255	0.065	10	0.000	0.040
256	0.058	10	0.000	0.070
257	1.192	10	0.000	2.610
258	0.440	10	0.000	0.920
259	0.181	10	0.000	0.340
260	0.270	10	0.000	0.620
261	3.574	10	0.000	7.630
262	0.190	10	0.060	0.090
263	0.050	9	0.020	0.050
264	0.064	9	0.000	0.110
265	4.700	10	0.000	9.850
266	0.249	10	0.000	0.030
267	0.146	10	0.010	0.000
268	3.671	10	0.000	7.830
269	7.050	10	0.000	14.530
270	4.963	10	0.000	11.100
271	1.989	10	0.000	4.190
272	2.194	10	0.000	4.920
273	2.509	10	0.000	5.410
274	0.358	10	0.000	0.670
275	0.144	10	0.000	0.200
276	1.718	10	0.000	3.710
277	5.054	10	0.000	10.640
278	1.183	10	0.000	2.500

279	0.096	10	0.000	0.010
280	0.274	10	0.000	0.510
281	1.424	10	0.000	3.120
282	0.073	10	0.000	0.060
283	0.037	10	0.000	0.010
284	0.498	10	0.000	1.140
285	3.883	10	0.000	8.290
286	0.237	10	0.040	0.360
287	0.052	10	0.060	0.010
288	0.045	10	0.010	0.010
289	5.225	10	0.000	10.990
290	0.298	10	0.010	0.140
291	0.202	9	0.000	0.370
292	4.232	10	0.000	9.060
293	7.658	10	0.000	15.850
294	3.078	10	0.040	6.580
295	2.183	10	0.010	4.570
296	3.022	10	0.020	6.600
297	2.877	10	0.030	6.280
298	0.643	10	0.000	1.320
299	0.101	10	0.020	0.080
300	2.047	10	0.000	4.440
301	5.473	10	0.000	11.520
302	1.422	10	0.010	3.040
303	0.134	1	0.000	0.270
304	0.135	10	0.000	0.230
305	1.677	10	0.000	3.670
306	0.085	10	0.010	0.010
307	0.049	10	0.010	0.030
308	0.843	10	0.000	1.860
309	4.201	10	0.000	8.950
310	0.424	10	0.010	0.790
311	0.160	10	0.000	0.290
312	0.050	10	0.000	0.030
313	5.802	10	0.000	12.200
314	0.328	10	0.000	0.080
315	0.611	10	0.000	1.080
316	4.949	10	0.000	10.650
317	8.284	10	0.010	16.360
318	29.514	10	0.190	64.740
319	5.813	10	0.040	11.450
320	3.845	10	0.000	8.360
321	3.455	10	0.000	7.400
322	0.154	10	0.000	0.090
323	0.095	10	0.000	0.010
324	2.413	10	0.000	5.230
325	5.906	10	0.010	12.430
326	1.680	10	0.010	3.610
327	0.224	9	0.000	0.420
328	0.618	10	0.000	1.420
329	1.949	10	0.000	4.270
330	0.097	10	0.000	0.040
331	0.047	10	0.000	0.010
332	1.073	10	0.000	2.370
333	4.532	10	0.010	9.660
334	0.620	10	0.030	1.230
335	0.071	10	0.000	0.040
336	0.055	10	0.000	0.020
337	6.418	10	0.000	13.500
338	0.439	9	0.010	0.860
339	0.272	10	0.010	0.470
340	5.868	10	0.000	12.710
341	8.942	10	0.000	18.530
342	4.224	10	0.000	9.010
343	1.875	10	0.000	3.680
344	4.651	10	0.000	10.270
345	3.873	10	0.000	8.240
346	0.202	10	0.000	0.260
347	0.108	10	0.000	0.080
348	2.826	10	0.000	6.120
349	6.356	10	0.000	13.340

350	1.912	10	0.000	4.220
351	0.962	9	0.000	2.170
352	1.358	10	0.000	3.090
353	2.242	10	0.000	4.970
354	0.113	4	0.000	0.220
355	0.436	4	0.000	0.960
356	1.328	10	0.000	2.950
357	4.873	10	0.000	10.410
358	0.829	10	0.000	1.780
359	0.642	9	0.000	1.450
360	0.074	9	0.000	0.080

Table 2.7 Comparison of PLTEMP/ANL Versions 3.0 and 2.14 for Standard Problem 6

Table Number	Max Temp Diff	Occurs in Axial Node	Max Tdiff Current Output	Max Tdiff Saved Output
1	1.988	10	0.000	4.060
2	0.463	10	0.000	0.940
3	0.308	10	0.000	0.610
4	1.353	10	0.000	2.810
5	3.535	10	0.000	7.320
6	1.328	10	0.140	2.640
7	0.957	10	0.190	1.960
8	0.772	10	0.000	1.600

Table 2.8 Comparison of PLTEMP/ANL Versions 3.0 and 2.14 for Standard Problem 7

Table Number	Max Temp Diff	Occurs in Axial Node	Max Tdiff Current Output	Max Tdiff Saved Output
1	0.447	10	0.000	0.950
2	0.130	10	0.110	0.270
3	0.044	10	0.030	0.100
4	0.013	10	0.000	0.020
5	2.761	10	0.000	5.750
6	0.328	10	0.000	0.660
7	2.360	10	0.000	5.080
8	0.211	10	0.000	0.410
9	0.656	10	0.000	1.370
10	0.312	5	0.000	0.670
11	0.218	5	0.000	0.470
12	0.015	10	0.000	0.030
13	2.167	10	0.030	4.520
14	0.111	10	0.030	0.090
15	0.046	8	0.090	0.000
16	0.036	8	0.060	0.020
17	0.896	10	0.000	1.890
18	0.088	7	0.000	0.180
19	0.198	7	0.250	0.430
20	0.134	10	0.000	0.300
21	2.570	10	0.000	5.390
22	0.484	9	0.000	0.980
23	0.085	9	0.000	0.180
24	0.200	9	0.000	0.420
25	1.158	10	0.000	2.450
26	0.183	10	0.000	0.360
27	0.261	3	0.000	0.560
28	0.367	10	0.000	0.810
29	3.015	10	0.000	6.280
30	0.161	10	0.000	0.220
31	0.091	10	0.000	0.180
32	0.027	10	0.000	0.000
33	1.446	10	0.000	3.060
34	0.060	10	0.000	0.020
35	0.030	10	0.000	0.030
36	0.625	10	0.000	1.340
37	3.459	10	0.000	7.210
38	0.329	10	0.000	0.600
39	0.190	9	0.000	0.400
40	0.039	9	0.000	0.050
41	1.765	10	0.000	3.730
42	0.074	10	0.130	0.010
43	0.091	1	0.180	0.000
44	0.926	10	0.110	1.990
45	3.919	10	0.000	8.120
46	0.579	10	0.000	1.160
47	0.505	9	0.100	1.110
48	0.062	9	0.000	0.090
49	2.126	10	0.040	4.500
50	0.241	2	0.510	0.020
51	0.245	10	0.230	0.460
52	1.281	10	0.000	2.750
53	4.393	10	0.000	9.120
54	0.847	10	0.000	1.730
55	0.375	10	0.000	0.790
56	0.043	10	0.000	0.020
57	2.511	10	0.000	5.320
58	0.113	10	0.000	0.000

59	0.067	10	0.010	0.000
60	1.672	10	0.000	3.600
61	4.880	10	0.010	10.140
62	1.152	10	0.000	2.380
63	0.234	10	0.010	0.420
64	0.053	10	0.000	0.010
65	2.938	10	0.000	6.230
66	0.131	10	0.000	0.110
67	0.086	10	0.000	0.030
68	2.268	10	0.000	4.820
69	5.389	10	0.010	11.180
70	1.494	10	0.010	3.110
71	0.524	10	0.000	0.990
72	0.351	10	0.000	0.760
73	3.393	10	0.050	7.220
74	0.207	10	0.060	0.240
75	0.870	10	0.070	1.780
76	2.693	10	0.000	5.700
77	5.924	10	0.000	12.280
78	1.852	10	0.000	3.900
79	0.126	10	0.000	0.010
80	0.765	10	0.000	1.700
81	3.946	10	0.000	8.520
82	0.214	10	0.000	0.190
83	0.127	10	0.000	0.040
84	3.157	10	0.000	6.720
85	6.476	10	0.000	13.410
86	2.246	10	0.000	4.840
87	0.146	10	0.000	0.130
88	1.329	10	0.000	2.930

Table 2.9 Comparison of PLTEMP/ANL Versions 3.0 and 2.14 for Standard Problem 8

Table Number	Max Temp Diff	Occurs in Axial Node	Max Tdiff Current Output	Max Tdiff Saved Output
1	0.447	10	0.000	0.950
2	0.130	10	0.110	0.270
3	0.044	10	0.030	0.100
4	0.013	10	0.000	0.020
5	2.761	10	0.000	5.750
6	0.328	10	0.000	0.660
7	2.360	10	0.000	5.080
8	0.211	10	0.000	0.410

APPENDIX A IRT-1 LEU Steady State Analysis with Inner Channel Blocked RELAP5/Mod3.2.1.2 Vs. PLTEMP w/Exact Solution

One of the events to be analyzed for the IRT-1 LEU safety analysis is a blocked inner channel for the 8-tube fuel assembly with the highest power peak. This analysis was first performed using the RELAP5/Mod3.2.1.2 code because the existing version of PLTEMP/ANL at that time (V2.1) had a convergence problem. Recently, an analytical solution for the problem with parallel plates has been implemented. Note that this code can use only one axial power distribution for all the parallel plates (in this analysis the tubes are modeled as parallel plates). In RELAP, calculated distributions can be used for each of the plates, and this is a small modification that should be implemented in a future version of PLTEMP code.

The results are presented below for two cases:

1. Figures A.1a/1c: Results for the outer tube (tube 8) and for the two inner tubes (tube 7 and tube 8) are presented for the case in which RELAP uses the calculated axial distributions for each tube. These figures show that even in this (not consistent) case both codes yield essentially the same results. Small differences do exist mainly at the ends of the fuel assembly because of the different axial power shapes for the inner tubes.
2. Figures A.2a/2c: The RELAP input was modified to use the same axial distribution for all tubes as in PLTEMP. These figures show that the results are in very good agreement.

It is concluded that the analytical solution implemented in the new PLTEMP is performing correctly.

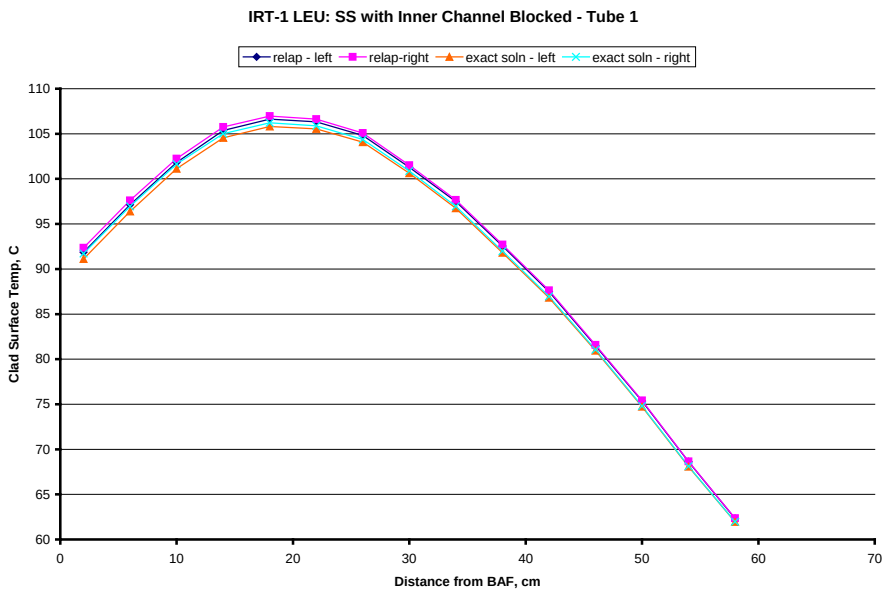

Figure A.1 Tube 8 (Outer Tube) Comparison: RELAP w/Calculated Axial Power Distributions for Each Tube and PLTEMP (Exact Solution) with All Tubes Using Axial Power Distribution from Tube 1

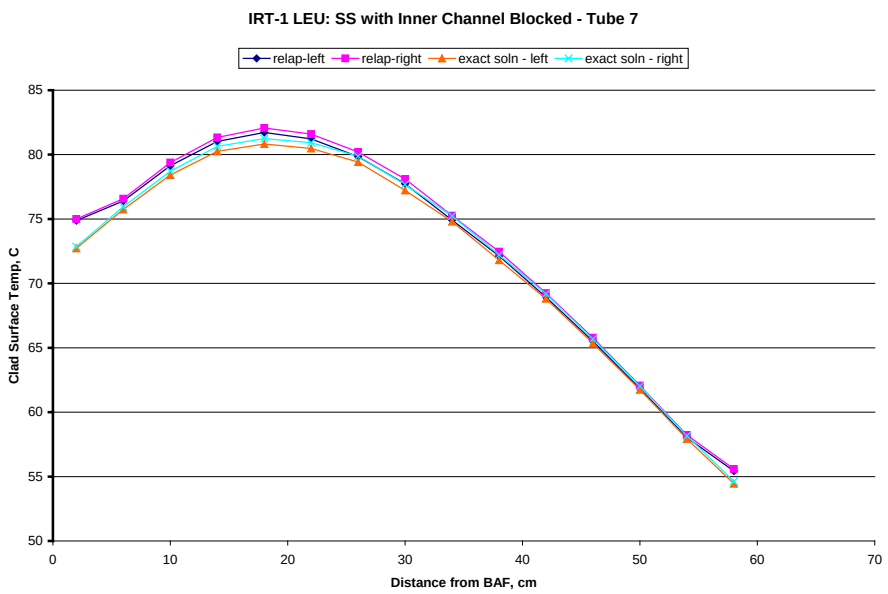

Figure A.1b Tube 7 Comparison: RELAP w/Calculated Axial Power Distributions for Each Tube and PLTEMP (Exact Solution) with All Tubes Using Axial Power Distribution from Tube 1

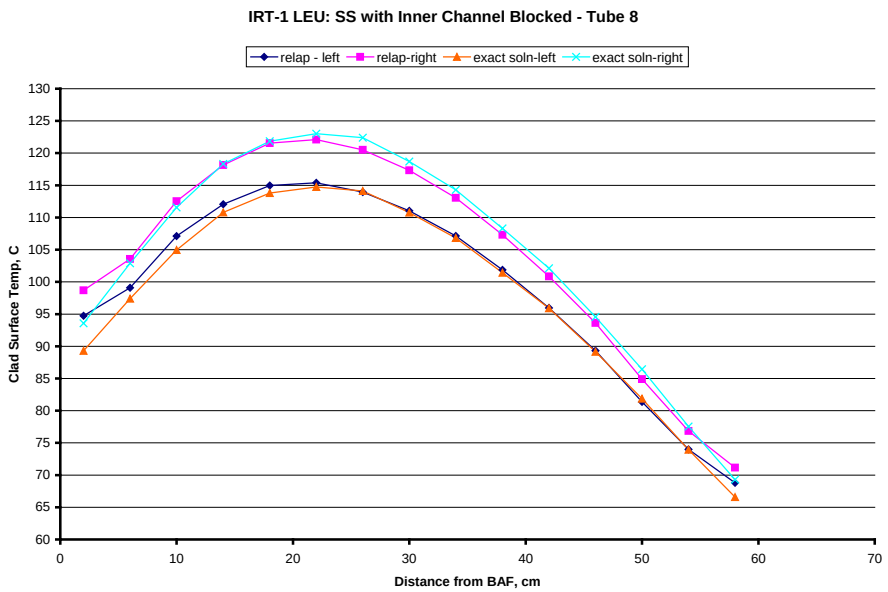

Figure A.1c Tube 8 (Inner Tube) Comparison: RELAP w/Calculated Axial Power Distributions for Each Tube and PLTEMP (Exact Solution) with All Tubes Using Axial Power Distribution from Tube 1

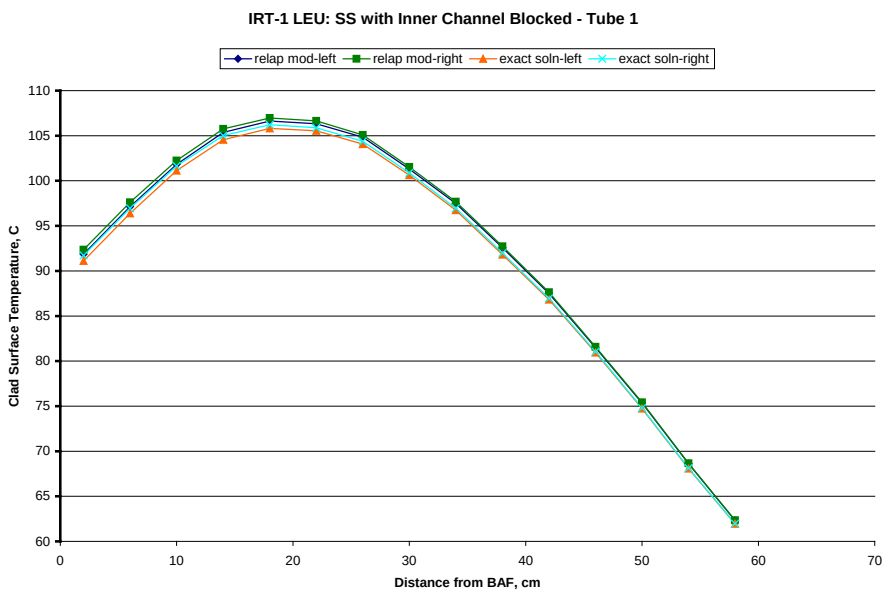

Figure A.2a Tube 1 (Outer Tube) Comparison: Same Axial Power Distribution in All Tubes

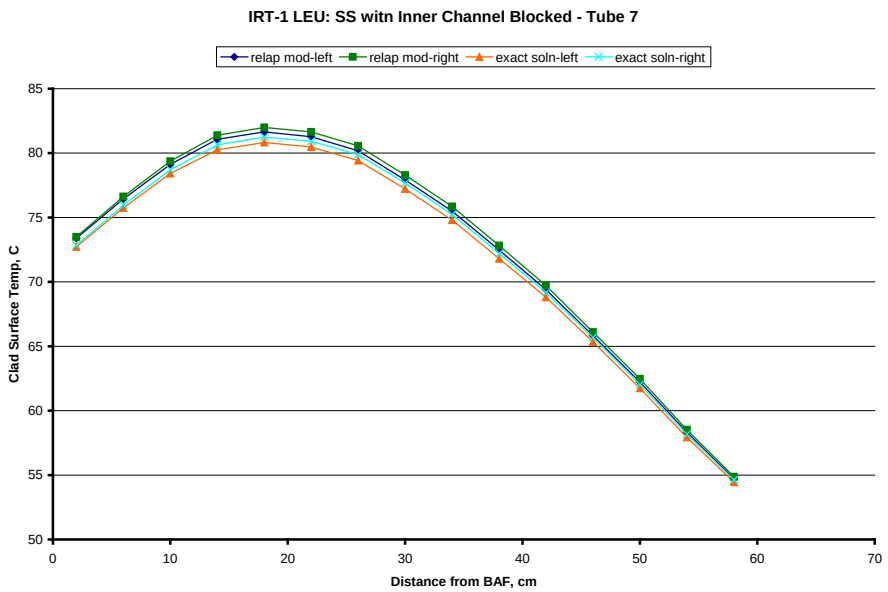

Figure A.2b Tube 7 Comparison: Same Axial Power Distribution in All Tubes

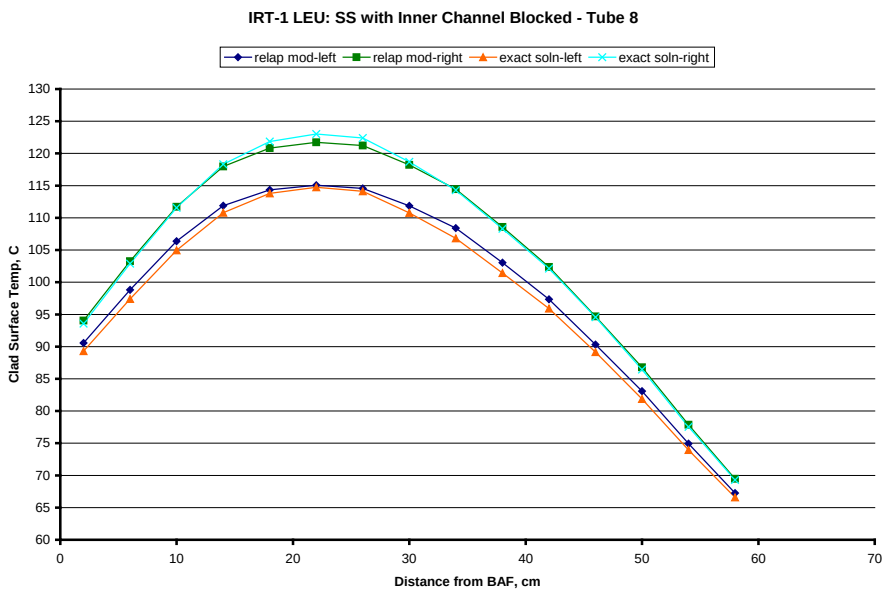

Figure A.2c Tube 8 (Inner Tube) Comparison: Same Axial Power Distribution in All Tubes

3 Verification Tests of PLTEMP/ANL V3.0 Code Performed in Conjunction with the Solution to the KFKI Benchmark Problem

3.1 Introduction

The verification work reported here was done in November 2006. While the thermal analysis of the KFKI benchmark problem (see Appendix B) was being performed with the PLTEMP/ANL V3.0, tests were made on the internal consistency of the analytical results. The benchmark problem is an assembly with three coaxial fueled tubes. The assembly was analyzed at three power levels, but only the 90 kW results were used in the consistency tests. The tests uncovered shortcomings in the code in the treatment of fuel tubes. These shortcomings were not visible in cases where the effects of tube curvature were small enough to make the tube and flat-plate solutions essentially the same. After the shortcomings were fixed, the consistency tests were repeated and consistent results were obtained. Improving on the release version PLTEMP/ANL V3.0, the corrections were provided in PLTEMP/ANL V3.1. The thermal solution is obtained by the Broyden method, which is described in Chapter 2, because the Exact solution method for cylindrical geometry was not added to the code until PLTEMP/ANL V3.2. Although this problem is called a benchmark problem, we have no benchmark results to compare with.

3.2 Consistency Tests

The following consistency tests were performed:

1. For each of the three tubes, the heat flux of each tube, as provided by PLTEMP, was integrated over the surface area of the tube to obtain the total power of the tube. This agreed very well with the power generated by the tube, which was deduced from PLTEMP inputs.

2. For both the inner and outer sides of the fifth axial level of each tube, two methods for determining power per unit length were used and the results were compared. For the first method a closed-form analytical solution was used to determine the power per unit length exiting each fuel meat surface. This required the values of the coolant temperatures and the film coefficients at both clad surfaces, which were obtained from the PLTEMP code output. Since no power is generated in the clad, the power per unit length exiting each fuel meat surface also exits the outer surface of its adjacent clad. For the second method the power per unit length exiting a clad surface was determined from the heat flux exiting the clad surface, which is a PLTEMP code output.

3. For the fifth axial level of each tube, the power per unit length exiting each surface of the fuel, as determined in the previous test, was used to determine the radius at which the peak temperature occurs. This is possible because all of the power must flow away from the location of the highest fuel temperature. The calculated location of the peak fuel temperature in each was found to be totally consistent with the PLTEMP output.

4. For the fifth axial level of each tube, another closed-form analytical solution was used to determine the radius at which the peak fuel temperature occurs in a fuel tube. This solution uses the temperatures at the fuel meat surfaces as the boundary conditions rather than the

coolant temperatures and the film coefficients at the clad outer surfaces. The results were totally consistent with the PLTEMP results.

5. In the PLTEMP code coaxial tubes can be ordered from biggest to smallest or from smallest to biggest. The code determines which it is, based on whether the radii are increasing or decreasing in size. When there is only one tube, the code assumes that the first of the two coolant channels is the outer channel. As an additional check, the 90 kW case was run twice – once with each way of ordering the tubes. The temperatures, heat fluxes, film coefficients, and locations of the peak fuel temperature for each tube were manually compared. Although the results were essentially the same for both runs, the run with the tubes ordered smallest to biggest seemed to produce slightly better results and in fewer iterations. The run with the smallest tube first produced a solution in 200 iterations with all values of "TDIFF" at 0.00. The other run had two non-zero values of TDIFF after 800 iterations. These were −0.07 and 0.02 at the first and second axial levels, respectively, of the middle tube. However, it is not reasonable to make a general conclusion using only a single comparison.

3.3 Code Corrections

The following corrections were made to the PLTEMP/ANL V3.0 code, and are available in versions 3.1 and later (including the current version 4.3:

1. The code was modified so that when the radial tube geometry is used, the code output identifies the tube surfaces as "inner" and "outer" instead of "left" and "right".

2. Subroutine FUNCV was originally correct as coded to a first order in the curvature correction term, Δ. By simply replacing terms like $(1 + \Delta)$ with $1/(1 - \Delta)$, full accuracy was produced in computing the tube surface heat fluxes. Here $\Delta = (t_{clad} + t_{meat}/2) / R_{mid}$, where t_{clad} is the clad thickness, t_{meat} is the fuel meat thickness, and R_{mid} is the radius of the tube centerline.

3.4 Discussion and Conclusions

In the PLTEMP code, the quantity "FUEL X" is a ratio of two fuel cross-sectional areas. The numerator for this ratio is the area between the first edge of the fuel meat (i.e., the edge nearest to the lower numbered coolant channel) and the location at which the peak fuel temperature occurs. The denominator for this ratio is the total tube meat cross-sectional area. Thus, for the tube solution, the ratio is the ratio of the areas of the appropriate two fuel annuli. For a flat plate this area ratio is also equal to the distance from the first edge of the fuel meat to the location of the peak temperature divided by the total fuel meat thickness.

The above consistency tests enabled shortcomings in the tube solution of the PLTEMP/ANL V3.0 code to be uncovered and fixed before final results for the KFKI benchmark problem were obtained. The shortcomings have no impact on the PLTEMP flat-plate solution and no impact on the PLTEMP tube solution when the effects of tube curvature were small enough to make the tube and flat-plate solutions essentially the same.

APPENDIX B Steady-State Thermal Analysis for a Benchmark Problem Specified by KFKI for the Budapest Research Reactor

SUMMARY

Steady-state thermal analysis has been performed for a benchmark problem specified by KFKI that is related to the WWR-M2 fuel assembly used in the Budapest Research Reactor. The analyses were done using the PLTEMP/ANL V3.0 code [1]. The WWR-M2 fuel assembly consists of three concentric fueled tubes. Three assembly power levels were requested. Axial distribution of clad surface temperature and heat transfer coefficient for each surface of each tube, the axial distribution of peak fuel temperature for each fuel tube, and the axial distribution of coolant temperature and coolant density for each coolant channel are provided.

B.1 INTRODUCTION

The KFKI specifications for the benchmark problem are shown in Table B.1. The assembly to be analyzed consists of three concentric fueled tubes, as shown in Figutre B-1. The outer most tube is hexagonal with rounded corners. The inner two tubes are circular. The wall of each tube is 2.5 mm thick, with a 0.98 mm thick fuel meat and 0.76 mm thick cladding. The assembly is assumed to be inside an infinite array of identical assemblies that are all on a 35 mm hexagonal pitch. The assembly can be thought of as being located at the center of a unit cell that is 35 mm across flats.

The calculations do not include any hot channel factors or other means of accounting for manufacturing tolerances or uncertainties in the analytical models.

B.2 POWER AND POWER DISTRIBUTION

The relative axial distribution of power of each tube is the same – a cosine shape with zero values at the beginning and the end of the 58-cm fuel length. In the analysis the fuel length is to be divided into eight equal axial levels. The equation for the normalized axial power shape, $P(x)/P_0$ is:

$$\frac{P(x)}{P_0} = \frac{4\pi}{L}\sin\left(\pi\frac{x}{L}\right) \qquad (1)$$

where L is the length and x is the axial location from the inlet of the fuel. For the eight segments the relative average power is obtained by integrating equation (B.1) over each segment. Then the relative power over each segment, P_i/P_0 is given by:

$$\frac{P_i}{P_0} = 4\left[\cos\left(i\frac{\pi}{8}\right) - \cos\left((i-1)\frac{\pi}{8}\right)\right], \text{ for } i = 1, 8 \qquad (2)$$

Equation (B.2) was evaluated to produce the axial power distribution given in Table B.2. The sum of all eight relative values equals 8.00.

The benchmark problem is to be solved for assembly powers of 90, 140, and 190 kW.

B.3 KEY PARAMETERS AND CORRELATIONS

The flow areas, perimeters, and hydraulic diameters that are needed to perform the required analysis can be calculated from a few key tube dimensions. Table B.3 shows the values of key dimensions in bold type. A computer spreadsheet was used to perform the calculations. Needed quantities are listed in the table essentially in the order that they were produced. The calculations start at the outside of the assembly near the top of the table and proceed to the innermost tube. Some of the thick horizontal lines in the table tend to separate the data for each tube from those of the other two.

The value of flow velocity for each of the four coolant channels was provided, as shown in bold type in Table B.4. The first channel is at the center of the assembly. The fourth one is between the outer perimeter of the hexagonal outer tube and the boundary of the hexagonal unit cell. As indicated in the table the volumetric flow rate for each channel is deduced from the flow area and the velocity. The total volumetric flow rate is also shown in bold type in the table. This value is only 0.86% greater than the 6.0 m^3/h value that was specified as part of the benchmark problem definition. The channel velocities are assumed to correspond to the channel inlet where the temperature is 50º C and the local pressure is 1.3 bar. For these conditions the coolant water density is 988.08 kg/m^3. With this density and the volumetric flow rates shown in the table, one can deduce the mass flow rates in kg/s that are shown in the table and were used as inputs to the PLTEMP code. Some of the data in Table B.2 is repeated in Table B.5, where it is used to determine quantities for the three fuel tubes that are used in the PLTEMP code input.

In the PLTEMP code, there are several choices of correlations for Nusselt number, Nu, for turbulent flow. For the analysis the Sieder-Tate correlation, $Nu = 0.027\ Re^{0.8}\ Pr^{0.4}\ (\mu/\mu_w)^{0.14}$, was used. Here Re is Reynolds number, Pr is Prandtl number, μ is the dynamic viscosity of the bulk fluid, and μ_w is the dynamic viscosity of the fluid at the surface of the clad.

The inlet of the assembly is assumed to be at an absolute pressure of 1.3 bar and the fluid is assumed to be at its inlet velocity. Over the 58-cm length of the fuel, the pressure in the reactor vessel increases by about 5600 Pa due solely to the change in the depth of the water. However, within the coolant channels it is estimated that the friction pressure drop along the 58-cm length is about 8700 Pa. Thus, there is a net loss in pressure of about 3000 Pa, or 0.03 bar. Therefore, in the PLTEMP code the inlet pressure is taken to be 1.30 bar and the outlet is taken to be 1.27 bar. The local pressure between the inlet and the outlet is assumed to vary linearly. Small differences in local pressure are not important in the current calculations because the margin to the onset of nuclear boiling is not included in the results.

B.4 RESULTS

The requested results are:

- the axial distribution of clad outer surface temperature and heat transfer coefficient for each surface of each tube,
- the axial distribution of fuel centerline temperature for each fuel tube, and
- the axial distribution of coolant temperature and coolant density for each coolant channel.

The PLTEMP/ANL code computes the peak temperature in the fuel meat, which may not occur at the fuel meat centerline. As a result, peak temperatures are provided in this report instead of centerline temperatures.

Tables B.6a, B.6b, and B.6c provide all of the required results for the innermost, center, and outmost tubes, respectively, for an assembly power of 90 KW. Similarly, Tables B.7a, B.7b, and B.7c provide the results for 140 kW and Tables B.8a, B.8b, and B.8c provide the results for 190 kW.

It is worth noting that the PLTEMP results indicate that for the highest power (190 kW) case, there is no bulk boiling, but the Bergles and Rohsenow correlation indicates that the onset of nucleate boiling occurs at the surface of the clad at some locations.

B.5 CONCLUSIONS

The requested calculations have been performed and input quantities and the required analytical results are provided in tables.

B.6 REFERENCES

1. Arne P. Olson and Kalimullah, “A User’s Guide to the PLTEMP/ANL Code,” ANL/RERTR/TM-11-22, Version 4.1, Argonne National Laboratory, 9700 South Cass Avenue, Argonne, IL 60439, USA (April 6, 2011).

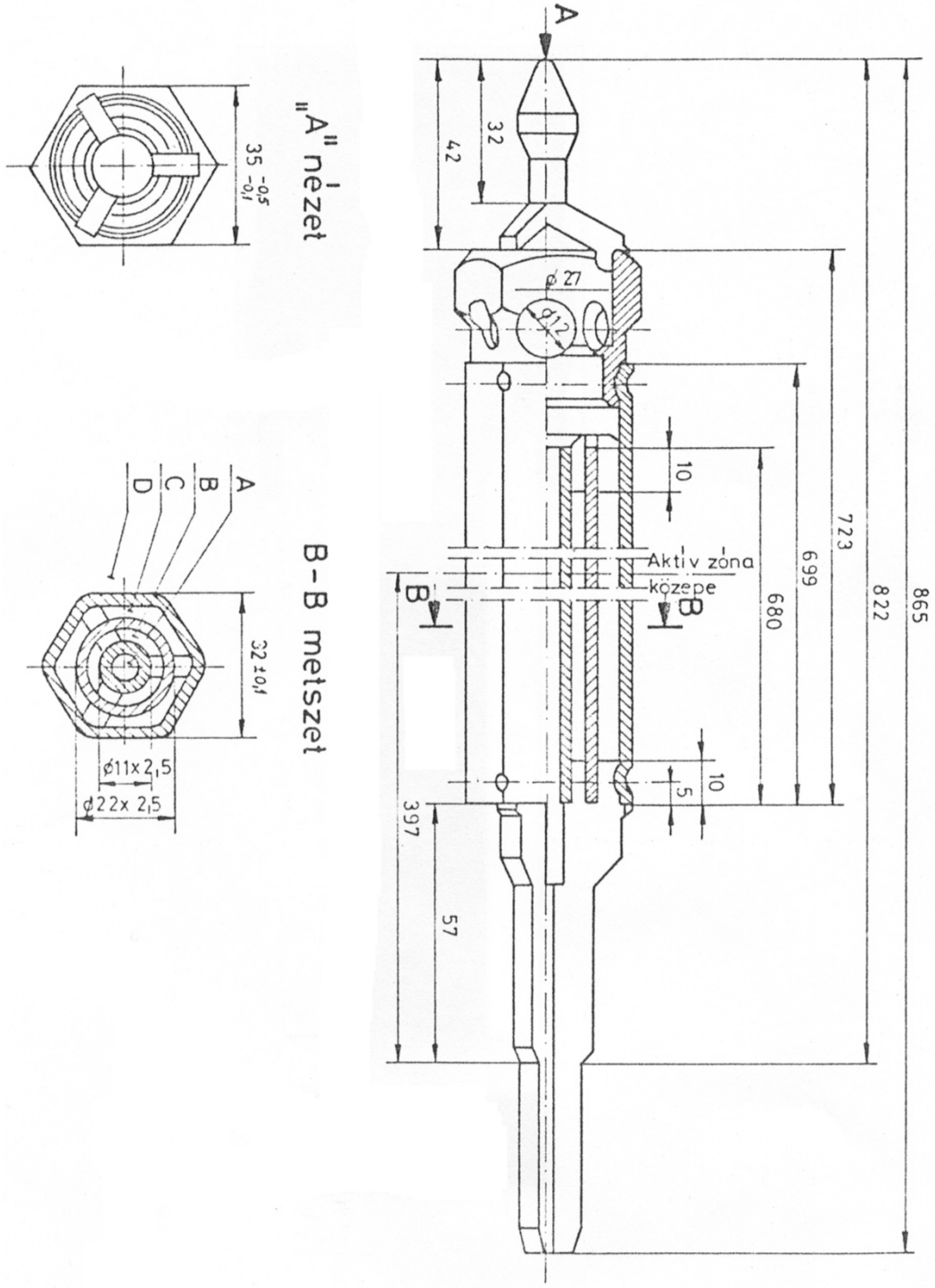

Figure B.1 WWR-M2 Fuel Assembly

Table B.1 KFKI Benchmark Specifications*

Stationary test problems for VVRSzM type thermohydraulics at different assembly power values:

The middle active length of the fuel, 58 cm, is to be calculated.

Inlet temperature: 50 ºC
(The inlet is at the top.)

Total inlet flow to the 4 concentric channels: 6 m^3/h

Inlet velocities equivalent for each sub-channel

Pressure at the inlet:1,3 bar

Assembly power values: 90 kW, 140kW, 190 kW

Power distribution: Flat in radial direction, cosinus type in axial direction, with zero values at the edge of the 58 cm active length

Meat thickness: 0.98 mm

Thermal data for the meat:
Cp= 633 J/kg/K
` LAMBDA: 180 W/m/K
RO: 3534 kg/m3

Thermal data for cladding:
Cp= 860 J/kg/K
` LAMBDA: 206 W/m/K
RO: 2700 kg/m3

Output quantities to be computed in 8 axial meshes:

- Axial distribution of the azimuth average cladding surface temperature on the 6 radial surface elements
- Axial distribution of the azimuth average heat transfer coefficients on the 6 radial surface elements
- Axial distribution of the azimuth average fuel centerline temperature of the 3 fuel meet layers
- Coolant temperature and density axial and radial distribution

---

*In addition to the above, the following was sent by email:

The velocities at 6m3/h from a very old calculation starting from the innermost sub-channel are

2.7943 m/s
2.7931 m/s
2.8529 m/s
2.8870 m/s.

Table B.2 Power Distribution

Axial Level	Relative Power
1	0.30448
2	0.86709
3	1.29769
4	1.53073
5	1.53073
6	1.29769
7	0.86709
8	0.30448

Table B.3 Key Geometric Parameters

Item	Value
total fuel length, m	**0.58**
number of axial fuel segments (nodes)	**8**
length of one segment, m	0.0725
thickness of all fuel tubes, mm	**2.5**
meat thickness of all tubes, mm	**0.98**
clad thickness of all tubes, mm	0.76
hexagonal pitch between assemblies, mm	**35**
area inside hexagonal unit cell of assembly, mm^2	1060.9
flat-to-flat outer dimension of hex tube, mm	**32**
flat-to flat midline dimension of hex tube, mm	29.5
flat-to-flat inner dimension of hex tube, mm	27
outer corner radius of hex tube, mm	**4.3**
midline corner radius of hex tube, mm	3.05
inner corner radius of hex tube, mm	1.8
outer perimeter of hex tube, mm	108.08
midline circumference of hex tube, mm	100.22
inner perimeter of hex tube, mm	92.370
area inside outer circumference of hex tube, mm^2	880.85
area inside inner circumference of hex tube, mm^2	630.29
equivalent radius of hex tube based on midline circumference, mm	15.951
flow area outside of hex tube, mm^2	180.03
hydraulic diameter between assemblies, mm	6.6631
outer diameter of middle tube, which is circular, mm	**22**
midline diameter of middle tube, which is circular, mm	19.5
inner diameter of middle tube, which is circular, mm	17
outer perimeter of middle tube, mm	69.115
midline circumference of middle tube, mm	61.261
inner perimeter of middle tube, mm	53.407
area inside outer perimeter of middle tube, mm^2	380.13
area inside inner perimeter of middle tube, mm^2	226.98
outer diameter of inner tube, which is circular, mm	**11**
midline diameter of inner tube, which is circular, mm	8.5
inner diameter of inner tube, which is circular, mm	6
outer perimeter of inner tube, mm	34.558
midline circumference of inner tube, mm	26.704
inner perimeter of inner tube, mm	18.850
area inside outer perimeter of inner tube, mm^2	95.033
area inside inner perimeter of inner tube, mm^2	28.274
flow area between hex tube and middle tube, mm^2	250.15
wetted perimeter of channel between hex & middle tubes, mm	161.48
hydraulic diameter of channel between hex & middle tubes, mm	6.1964
flow area between middle and center tubes, mm^2	131.95
wetted perimeter of channel between middle & inner tubes, mm	87.965
hydraulic diameter of channel between middle & inner tubes, mm	6

Table B.4 Coolant Channel Parameters

	Channel Number				
Item	**1 (center)**	**2**	**3**	**4**	**Total**
flow area, m^2	2.8274E-05	1.3195E-04	2.5015E-04	1.8003E-04	
hydraulic diameter, m	6.0000E-03	6.0000E-03	6.1964E-03	6.6631E-03	
wetted perimeter, m	1.8850E-02	8.7965E-02	1.6148E-01	1.0808E-01	
heated perimeter, m	1.8850E-02	8.7965E-02	1.6148E-01	1.0808E-01	
velocity, m/s	**2.7943**	**2.7931**	**2.8529**	**2.8870**	
volumetric flow rate,m^3/h	0.28443	1.32675	2.56920	1.87113	**6.05151**
mass flow rate, kg/s	0.07807	0.36415	0.70516	0.51356	1.66094

Table B.5 Fuel Tube Parameters

	Tube Number			
Item	**1 (center)**	**2**	**3**	**Total**
centerline arc length, m	2.6704E-02	6.1261E-02	1.0022E-01	
centerline radius, m	0.00425	0.00975	0.0159511	
fuel volume, m^3	1.5178E-05	3.4821E-05	5.6967E-05	1.0697E-04
fraction of total fuel volume	0.14190	0.32553	0.53257	1.00000
heat transfer area, m^2	0.03098	0.07106	0.11626	0.21830

Table B.6a 90 kW Results for Innermost Tube

	Temperature, C				
	Inner		Maximum	Outer	
Level	**Coolant**	**Clad**	**Fuel**	**Clad**	**Coolant**
inlet	50.0				50.0
1	50.3	57.6	58.1	57.4	50.3
2	51.3	71.4	72.9	70.8	51.3
3	53.2	82.3	84.6	81.4	53.1
4	55.7	89.1	91.8	88.1	55.6
5	58.4	91.2	93.8	90.1	58.2
6	60.9	88.4	90.6	87.4	60.6
7	62.8	81.1	82.6	80.5	62.5
8	63.8	70.2	70.7	69.9	63.5
outlet	64.0				63.7

	Coolant Density, kg/m^3		Heat Transfer Coefficient, W/m^2-C	
Level	**Inner**	**Outer**	**Inner**	**Outer**
inlet				
1	988.4	988.4	17,481	17,465
2	987.7	987.7	18,152	18,121
3	986.6	986.7	18,750	18,706
4	985.4	985.4	19,255	19,200
5	984.0	984.1	19,623	19,561
6	982.8	983.0	19,805	19,741
7	982.0	982.2	19,765	19,704
8	981.8	981.9	19,468	19,417
outlet				

Table B.6b 90 kW Results for Center Tube

	Temperature, C				
	Inner		Maximum	Outer	
Level	**Coolant**	**Clad**	**Fuel**	**Clad**	**Coolant**
inlet	50.0				50.0
1	50.3	57.5	58.0	57.4	50.3
2	51.3	71.0	72.7	70.7	51.2
3	53.1	81.7	84.2	81.3	53.0
4	55.6	88.4	91.3	87.9	55.3
5	58.2	90.4	93.3	89.9	57.8
6	60.6	87.6	90.1	87.1	60.1
7	62.5	80.4	82.0	80.1	61.9
8	63.5	69.6	70.2	69.5	62.8
outlet	63.7				63.1

	Coolant Density, kg/m^3		Heat Transfer Coefficient, W/m^2-C	
Level	**Inner**	**Outer**	**Inner**	**Outer**
inlet				
1	988.4	988.4	17,469	17,647
2	987.7	987.7	18,128	18,300
3	986.7	986.8	18,716	18,878
4	985.4	985.6	19,209	19,361
5	984.1	984.4	19,568	19,710
6	983.0	983.3	19,745	19,878
7	982.2	982.5	19,702	19,831
8	981.9	982.3	19,406	19,536
outlet				

Table B.6c 90 kW Results for Outermost (Hexagonal) Tube

	Temperature, C				
	Inner		Maximum	Outer	
Level	**Coolant**	**Clad**	**Fuel**	**Clad**	**Coolant**
inlet	50.0				50.0
1	50.3	57.4	58.0	57.3	50.2
2	51.2	70.8	72.6	70.7	51.1
3	53.0	81.4	84.0	81.2	52.7
4	55.3	88.0	91.0	87.7	54.8
5	57.8	89.8	92.8	89.5	57.1
6	60.1	86.9	89.5	86.6	59.3
7	61.9	79.6	81.3	79.4	60.9
8	62.8	68.8	69.4	68.7	61.8
outlet	63.1				62.1

	Coolant Density, kg/m^3		Heat Transfer Coefficient, W/m^2-C	
Level	**Inner**	**Outer**	**Inner**	**Outer**
inlet				
1	988.4	988.4	17,648	17,553
2	987.7	987.8	18,303	18,186
3	986.8	986.9	18,881	18,738
4	985.6	985.9	19,363	19,191
5	984.4	984.7	19,708	19,512
6	983.3	983.8	19,872	19,659
7	982.5	983.1	19,818	19,598
8	982.3	982.8	19,513	19,298
outlet				

Table B.7a 140 kW Results for Innermost Tube

	Temperature, C				
	Inner		Maximum	Outer	
Level	Coolant	Clad	Fuel	Clad	Coolant
inlet	50.0				50.0
1	50.4	61.7	62.5	61.4	50.4
2	52.0	82.5	84.8	81.6	52.0
3	55.0	98.6	102.1	97.2	54.9
4	58.9	108.4	112.6	106.8	58.6
5	63.0	111.5	115.6	109.8	62.7
6	66.9	107.1	110.6	105.7	66.5
7	69.9	96.7	99.0	95.7	69.4
8	71.4	80.8	81.6	80.5	70.9
outlet	71.9				71.3

	Coolant Density, kg/m^3		Heat Transfer Coefficient, W/m^2-C	
Level	Inner	Outer	Inner	Outer
inlet				
1	988.2	988.2	17,670	17,650
2	987.2	987.2	18,624	18,582
3	985.5	985.6	19,483	19,420
4	983.4	983.5	20,200	20,161
5	981.2	981.4	20,679	20,630
6	979.2	979.4	21,095	21,011
7	977.8	978.1	21,060	20,971
8	977.3	977.6	20,672	20,600
outlet				

Table B.7b 140 kW Results for Center Tube

	Temperature, C				
	Inner		Maximum	Outer	
Level	Coolant	Clad	Fuel	Clad	Coolant
inlet	50.0				50.0
1	50.4	61.5	62.4	61.3	50.4
2	52.0	81.9	84.5	81.5	51.9
3	54.9	97.7	101.6	97.1	54.6
4	58.6	107.4	111.9	106.6	58.2
5	62.7	110.3	114.8	109.5	62.1
6	66.5	106.0	109.8	105.2	65.7
7	69.4	95.6	98.2	95.1	68.5
8	70.9	80.0	80.8	79.7	70.0
outlet	71.3				70.3

	Coolant Density, kg/m^3		Heat Transfer Coefficient, W/m^2-C	
Level	Inner	Outer	Inner	Outer
inlet				
1	988.2	988.3	17,654	17,831
2	987.2	987.3	18,592	18,759
3	985.6	985.7	19,434	19,585
4	983.5	983.8	20,162	20,309
5	981.4	981.7	20,630	20,770
6	979.4	979.9	21,018	21,125
7	978.1	978.7	20,969	21,072
8	977.6	978.2	20,585	20,691
outlet				

Table B.7c 140 kW Results for Outermost (Hexagonal) Tube

	Temperature, C				
	Inner		Maximum	Outer	
Level	Coolant	Clad	Fuel	Clad	Coolant
inlet	50.0				50.0
1	50.4	61.4	62.3	61.3	50.4
2	51.9	81.7	84.4	81.4	51.7
3	54.6	97.3	101.3	96.9	54.2
4	58.2	106.7	111.4	106.3	57.5
5	62.1	109.4	114.1	108.9	61.1
6	65.7	105.0	109.0	104.5	64.4
7	68.5	94.5	97.1	94.1	67.0
8	70.0	78.8	79.6	78.5	68.4
outlet	70.3				68.7

	Coolant Density, kg/m^3		Heat Transfer Coefficient, W/m^2-C	
Level	Inner	Outer	Inner	Outer
inlet				
1	988.3	988.3	17,834	17,733
2	987.3	987.4	18,764	18,632
3	985.7	986.0	19,591	19,417
4	983.8	984.2	20,313	20,096
5	981.7	982.4	20,770	20,528
6	979.9	980.7	21,118	20,814
7	978.7	979.6	21,054	20,765
8	978.2	979.1	20,659	20,381
outlet				

Table B.8a 190 kW Results for Innermost Tube

	Temperature, C				
	Inner		Maximum	Outer	
Level	Coolant	Clad	Fuel	Clad	Coolant
inlet	50.0				50.0
1	50.6	65.7	66.8	65.3	50.6
2	52.7	93.2	96.4	91.9	52.7
3	56.8	114.4	119.2	112.5	56.6
4	62.0	127.9	133.5	125.6	61.7
5	67.7	131.5	137.1	129.3	67.3
6	73.0	125.7	130.5	123.8	72.4
7	77.0	111.6	114.7	110.3	76.3
8	79.1	91.2	92.3	90.7	78.4
outlet	79.7				79.0

	Coolant Density, kg/m^3		Heat Transfer Coefficient, W/m^2-C	
Level	Inner	Outer	Inner	Outer
inlet				
1	988.1	988.1	17,851	17,826
2	986.6	986.7	19,053	19,000
3	984.3	984.4	19,997	19,964
4	981.3	981.5	20,654	20,606
5	978.1	978.4	21,304	21,243
6	975.2	975.6	21,804	21,734
7	973.2	973.6	22,120	22,044
8	972.5	972.9	21,760	21,669
outlet				

Table B.8b 190 kW Results for Center Tube

	Temperature, C				
	Inner		Maximum	Outer	
Level	**Coolant**	**Clad**	**Fuel**	**Clad**	**Coolant**
inlet	50.0				50.0
1	50.6	65.4	66.7	65.2	50.5
2	52.7	92.4	96.0	91.9	52.6
3	56.6	113.3	118.5	112.4	56.3
4	61.7	126.4	132.6	125.4	61.2
5	67.3	130.0	136.1	128.9	66.5
6	72.4	124.2	129.4	123.2	71.4
7	76.3	110.2	113.6	109.5	75.1
8	78.4	90.1	91.2	89.7	77.1
outlet	79.0				77.6

	Coolant Density, kg/m^3		Heat Transfer Coefficient, W/m^2-C	
Level	**Inner**	**Outer**	**Inner**	**Outer**
inlet				
1	988.1	988.1	17,832	18,007
2	986.7	986.8	19,014	19,175
3	984.4	984.6	19,964	20,126
4	981.5	981.9	20,606	20,747
5	978.4	978.9	21,243	21,366
6	975.6	976.3	21,734	21,844
7	973.6	974.5	22,044	22,147
8	972.9	973.8	21,650	21,738
outlet				

Table B.8c 190 kW Results for Outermost (Hexagonal) Tube

	Temperature, C				
	Inner		Maximum	Outer	
Level	Coolant	Clad	Fuel	Clad	Coolant
inlet	50.0				50.0
1	50.5	65.3	66.6	65.2	50.5
2	52.6	92.1	95.8	91.8	52.3
3	56.3	112.7	118.1	112.2	55.7
4	61.2	125.6	132.0	125.0	60.2
5	66.5	128.9	135.3	128.2	65.1
6	71.4	122.8	128.2	122.2	69.6
7	75.1	108.6	112.2	108.1	73.0
8	77.1	88.4	89.6	88.1	74.9
outlet	77.6				75.4

	Coolant Density, kg/m^3		Heat Transfer Coefficient, W/m^2-C	
Level	Inner	Outer	Inner	Outer
inlet				
1	988.1	988.2	18,011	17,905
2	986.8	986.9	19,182	19,034
3	984.6	985.0	20,126	19,936
4	981.9	982.5	20,747	20,505
5	978.9	979.9	21,366	21,078
6	976.3	977.5	21,844	21,527
7	974.5	975.8	22,147	21,817
8	973.8	975.2	21,698	21,367
outlet				

4 Verification of the Radial Geometry Exact Solution Method in PLTEMP/ANL Version 3.2

The verification work reported here was done in March 2007. To verify the implementation in PLTEMP/ANL code [1] of the radial geometry Exact solution method for calculating temperature distribution in a fuel assembly made of multiple coaxial fuel tubes, 7 sample test problems (with assemblies having 1 to 6 fuel tubes) and their solution by the following four methods are documented:

(1) Hand calculation aided by *Mathematica*
(2) Standalone routine SLICEHTR
(3) Broyden method of PLTEMP/ANL code
(4) Newly-implemented Exact method in PLTEMP/ANL code

The first four problems have a single *fuel tube* with two coolant channels. The fifth problem consists of a flat *fuel plate* with two coolant channels. The flat plate is modeled both as a flat plate and as fuel tube with a very large radius. The sixth test problem, the Hungarian reactor benchmark problem, consists of a fuel assembly made of three coaxial fuel tubes. The seventh test problem, an ASTRA2 assembly problem, consists of a fuel assembly made of six coaxial fuel tubes. Some selected results are printed to 12 or more significant digits and compared to check the code because such small differences, although of no practical significance in reactor analysis, may be indicative of a coding error.

In version 3.2 of the code, the radial geometry Exact method requires that the input data be prepared numbering the fuel tubes in the order of increasing radii.

4.1 Radial Geometry Problem 1:

Find the temperature difference across the thickness of a 60 cm long tube which is generating a power of 9 kW. The inner surface of the tube is perfectly insulated. The inner radius of the tube is 0.5 cm, the outer radius is 4.5 cm, and the thermal conductivity is 7 W/m-°C. What is the coolant (water) temperature rise in the outer channel with a flow rate of 0.05 kg/s and C_p = 4180.0 J/kg-°C.

4.1.1 Hand Calculation for Problem 1

Input data given: r_a = 0.005 m, r_d = 0.045 m, L = 0.6 m, K = 7 W/m-°C

Volumetric heat source $q = \dfrac{9000.0}{\pi(r_d^{\,2} - r_a^{\,2})\,L} = \dfrac{9000.0}{\pi(0.045^2 - 0.005^2)\,0.6}$

$$= 2.3873{,}2414{,}6378{,}4300 \times 10^6 \text{ W/m}^3 \qquad (4.1)$$

The solution of the steady-state heat conduction equation in a tube with a uniform heat source gives the temperature distribution T(r).

$$T(r) = A_2 + A_1 \mathrm{Log}(r/r_d) - \frac{q r^2}{4K}$$ (A_1 and A_2 are constants of integration)

Putting $r = r_a$ and $r = r_d$ in the above equation for T(r), and getting the difference we get

$$\text{Temperature difference across tube thickness} = T(r_a) - T(r_d) = A_1 \mathrm{Log}(r_a/r_d) + \frac{q(r_d^{\,2} - r_a^{\,2})}{4K} \qquad (4.2)$$

A_1 is found by setting the temperature derivative to zero at radius r_a

$$\frac{dT}{dr} = \frac{A_1}{r} - \frac{q\,r}{2K} = 0 \text{ at } r = r_a \qquad \text{This boundary condition gives } A_1 = \frac{q\,r_a^{\,2}}{2K} \qquad (4.3)$$

Substituting Eq. (4.3) and the input data into Eq. (4.2), the temperature difference becomes

$$T(r_a) - T(r_d) = \frac{q\,r_a^{\,2}}{2K} \mathrm{Log}(r_a/r_d) + \frac{q(r_d^{\,2} - r_a^{\,2})}{4K} = \mathbf{161.1562,1172,6154,12\ °C} \qquad (4.4)$$

$$\text{Coolant temperature rise} = \frac{9000}{4180 \times 0.05} = \mathbf{43.0622,0095,6937,80\ °C} \qquad (4.5)$$

4.1.2 Solution of Problem 1 by Standalone Routine SLICEHTR

This routine is based on the radial geometry Exact solution described in Appendix VIII of PLTEMP/ANL Users Guide. It has been implemented in the PLTEMP/ANL version 3.2 code but it can also be used as a standalone program. The standalone routine was run for this calculation. In order to use the routine, the total thickness of the tube (r_a = 0.005 m, r_d = 0.045 m) was conceptually divided into 3 layers (to correspond to the inner cladding, fuel meat, and outer cladding in a reactor fuel tube) of equal thermal conductivity (7 W/m-°C) with r_a = 0.005 m, r_b = 0.015 m, r_c = 0.035 m, r_d = 0.045 m. The heat source in each of the 3 layers was set to the value in Eq. (4.1). The film coefficient at the inner surface of the tube was set exactly to zero. The whole length (0.6 m) of the tube was treated as a single axial node because the standalone routine can handle only one node. A small main program was written to define these input data and to call the routine. The output of the routine is shown in Fig. 4.1. The temperature drop across the tube thickness and the coolant temperature rise in the outer channel are noted below. All 16 digits in these values agree with the above hand calculated results in Eqs. (4.4) and (4.5).

Temperature difference across tube thickness From Fig. 4.1 = 161.1562,1172,6154,1 °C (4.6)
Node-center coolant temperature from Fig. 4.1 = 71.5311,0047,8468,90 °C
Coolant temperature rise = 2 x (71.53110047846890 - 50) = 43.0622,0095,6937,80 °C (4.7)

If the problem is slightly modified, i.e., the film coefficient at the inner surface of the tube is set to 10^{-6} W/m^2-°C instead of exactly zero, then the routine's output is shown in Fig. 4.2. These results are slightly different from those in Eqs. (4.4) and (4.5). Only 8 or 9 significant digits agree. The results changed presumably due to the slight change in the inner surface boundary condition.

Temperature difference across tube thickness from Fig. 4.2 = 161.1562,1235,9536,1 °C (4.8)
Node-center coolant temperature from Fig. 4.2 = 71.5311,0046,9959,36 °C
Coolant temperature rise = 2 x (71.53110046995936 – 50) = 43.0622,0093,9918,72 °C (4.9)

The modified problem is useful (for comparing the Broyden and Exact methods in the PLTEMP/ANL code) because the Broyden method is not designed to handle zero film coefficient on the inner surface of the innermost or the outer surface of the outermost fuel tube of an assembly. The routine SLICEHTR based on the Exact method is designed to handle zero film coefficient.

4.1.3 Solution of Modified Problem 1 by PLTEMP/ANL Version 3.2

Only the Exact method of the code could be used to solve this problem because of heat generation in the cladding. In order to apply the code, the total thickness of the tube (r_a = 0.005 m, r_d = 0.045 m) was again conceptually divided into 3 layers (inner cladding, fuel meat, and outer cladding) of equal thermal conductivity (7 W/m-°C) as above: r_a = 0.005 m, r_b = 0.015 m, r_c = 0.035 m, r_d = 0.045 m. In order to have a uniform heat source in the whole thickness of the tube, the input data QFCLAD on card 500 (i.e., the cladding power fraction) is set to 0.5 because the combined inner and outer cladding cross sectional area equals the fuel cross sectional area. The film coefficient at the inner surface was set to 1.0^{-6} W/m^2-°C. The input data has 10 axial nodes (with axially uniform heat source) in the 0.6 meter length of the tube. The constant coolant specific heat option (ICP = 1 on input card 200) is used (C_p = 4180.0 J/kg-°C). The input data file used is shown in Fig. 4.3. The relevant parts of the PLTEMP output are shown in Fig. 4.4. For comparison, the results of all four methods are summarized in Table 4.1.

Each axial node has practically the same temperature difference between the inner and outer surfaces of the tube, as expected. For all axial nodes, the temperature difference is found to be **161.15621**$^{0}_{3}$ **°C** (meaning that the 9th digit varies from 0 to 3). This agrees to 8 significant digits with the value in Eq. (4.8) obtained by the standalone routine SLICEHTR for the modified problem. As indicated in Section 4.1.2, a comparison of the results of Eqs. (4.4) and (4.6) shows that the routine SLICEHTR is capable of an accuracy to 16 significant digits. The accuracy of the PLTEMP Exact method is limited to 8 digits presumably because the accuracy of the input data (especially the tube circumference CIRCF) to the code is limited to 10 digits due to the 12-column data fields.

The coolant temperature rise calculated by PLTEMP/ANL is **43.0622,0093,9**615,2 °C. The highlighted 11 digits of this value agree with the more accurate value given in Eq. (4.9) that was obtained by the standalone routine SLICEHTR for the modified problem.

In summary, the PLTEMP Exact method calculated coolant temperature rise is good to 11 significant digits, and the temperature difference across the tube thickness is good to 8 digits for problem 1.

4.2 Radial Geometry Problem 2:

Find the temperature difference across the thickness of a 60 cm long fuel tube whose fuel meat is generating a power of 9 kW (no power in the cladding). The inner surface of the tube is perfectly insulated. The tube inner radius is 0.5 cm, the meat inner radius is 1.5 cm, the meat outer radius is 3.5 cm, the tube outer radius is 4.5 cm, and the thermal conductivities of cladding and meat are 7 and 8 W/m-°C. What is the coolant (water) temperature rise in the outer channel with a flow rate of 0.05 kg/s and C_p = 4180.0 J/kg-°C.

4.2.1 Hand Calculation for Problem 2

Input data given: r_a = 0.005 m, r_b = 0.015 m, r_c = 0.035 m, r_d = 0.045 m,
L = 0.6 m, K_c = 7 W/m-°C, K_f = 8 W/m-°C

Volumetric heat source $q = \dfrac{9000.0}{\pi(r_c^2 - r_b^2)L} = \dfrac{9000.0}{\pi(0.035^2 - 0.015^2)0.6}$

$$= 4.7746,4829,2756,8601\text{x}10^6 \text{ W/m}^3 \tag{4.10}$$

There is no radial heat flux in the inner cladding, and therefore the temperature difference across its thickness is zero.

$$T(r_a) - T(r_b) = 0 \tag{4.11}$$

The solution of the steady-state heat conduction equation in the meat with a uniform heat source gives the temperature distribution T(r).

$T(r) = A_4 + A_3 \text{Log}(r/r_c) - \dfrac{qr^2}{4K_f}$ (A_3 and A_4 are constants of integration)

Putting r = r_b and r = r_c in the above equation for T(r), and getting the difference we get

Temperature difference across meat thickness = $T(r_b) - T(r_c) = A_3 \text{Log}(r_b/r_c) + \dfrac{q(r_c^2 - r_b^2)}{4K_f}$ (4.12)

A_3 is found by setting the temperature derivative to zero at radius r_b

$\dfrac{dT}{dr} = \dfrac{A_3}{r} - \dfrac{qr}{2K_f} = 0$ at r = r_b The boundary condition gives $A_3 = \dfrac{q r_b^2}{2K_f}$ (4.13)

Substituting Eq. (4.13) and the input data into Eq. (4.12), the temperature difference across the meat thickness becomes

$$T(r_b) - T(r_c) = \frac{q r_b^2}{2K_f}\text{Log}(r_b/r_c) + \frac{q(r_c^2 - r_b^2)}{4K_f} = 92.3172,2236,2732,004 \text{ °C} \tag{4.14}$$

The solution of heat conduction equation in the outer cladding *without heat source* is given by

$T_c(r) = A_6 + A_5 \text{Log}(r/r_d)$ (A_5 and A_6 are constants of integration) (4.15)

The temperature difference across the outer cladding thickness is given

$$T(r_c) - T(r_d) = A_5 \text{Log}(r_c/r_d) \tag{4.16}$$

The constant A_5 can be evaluated using the heat flux boundary condition at the outer surface of the tube. The power generated in the meat (9000 W) flows radially outwards in the outer cladding, giving the following heat flux at the tube outer surface.

$$q''(r_d) = \frac{9000}{2\pi r_d L} \text{ W/m}^2 \tag{4.17}$$

The heat flux obtained from Eq.(4.15), i.e., $-K_c\, dT_c/dr$ at $r = r_d$ becomes $-K_c A_5/r_d$ which is equated to the value in Eq. (4.17). This gives the following value of A_5.

$$A_5 = -\frac{9000}{2\pi K_c L} \tag{4.18}$$

Putting the value of A_5 into Eq. (4.16), the temperature difference across the outer cladding thickness becomes

$$T(r_c) - T(r_d) = \frac{9000}{2\pi K_c L} \text{Log}(r_d/r_c) = 85.7098{,}5756{,}6899{,}611 \text{ °C} \tag{4.19}$$

The sum of Eqs. (4.11), (4.14) and (4.19) gives the total temperature difference across the tube thickness.

$T(r_a) - T(r_d)$ = **178.0270,7992,9631,615 °C** (4.20)

The coolant temperature rise is the same as that in problem 1.

Coolant temperature rise = $\frac{9000}{4180 \times 0.05}$ = **43.0622,0095,6937,80 °C** (4.21)

4.2.2 Solution of Problem 2 by Standalone Routine SLICEHTR

The standalone routine was run for this calculation. The heat source in the meat was set to the value in Eq. (4.10), and that in the cladding was set to zero. The film coefficient at the inner surface of the tube was set exactly to zero. The whole length (0.6 m) of the tube was treated as a single axial node because the standalone routine can handle only one node. A small main program was written to define these input data and to call the routine. The output of the routine is shown in Fig. 4.5. The temperature drop across the tube thickness and the coolant temperature rise in the outer channel are noted below. All 16 digits in these values agree with the hand calculated results in Eqs. (4.20) and (4.21).

Temperature difference across tube thickness from Fig. 4.5 = 178.0270,7992,9631,6 °C (4.22)
Node-center coolant temperature from Fig. 4.5 = 71.5311,0047,8468,90 °C
Coolant temperature rise = 2 x (71.53110047846890 - 50) = 43.0622,0095,6937,80 °C (4.23)

If the problem is slightly modified, i.e., the film coefficient at the inner surface of the tube is set to 10^{-6} W/m^2-°C instead of exactly zero, then the routine's output is shown in Fig. 4.6. These results are slightly different from those in Eqs. (4.20) and (4.21). Only 8 or 9 significant digits agree. The results changed presumably due to the slight change in the inner surface boundary condition.

Temperature difference across tube thickness from Fig. 4.6 = 161.1562,1235,9536,1 °C (4.24)
Node-center coolant temperature from Fig. 4.6 = 71.5311,0046,9198,58 °C
Coolant temperature rise = 2 x (71.53110046919858 – 50) = 43.0622,0093,8397,16 °C (4.25)

4.2.3 Solution of Modified Problem 2 by PLTEMP Code Version 3.2

The problem was solved by the Broyden method and the newly-implemented Exact method. The input data file (for the Broyden method) used is shown in Fig. 4.7. The film coefficient at the inner surface was set to 1.0^{-6} W/m^2-°C. The input data has 10 axial nodes (with axially uniform heat source) in the 0.6 meter length of the tube. The constant coolant specific heat option (ICP = 1 on card 200) was used (C_p = 4180.0 J/kg-°C). The code was run for the input file shown in Fig. 4.7. The relevant part of the output for the Broyden solution is shown in Fig. 4.8, and that for the Exact solution is shown in Fig. 4.9. For comparison, the results of all five methods are summarized in Table 4.2.

For the PLTEMP Broyden method, each axial node gives practically the same temperature difference between the inner and outer surfaces of the tube, as expected. For all axial nodes, the temperature difference is found to be **178.0270,782**$^{2}_{8}$ **°C** (meaning that the 11th digit varies from 2 to 8**)**. This can be compared with the hand-calculated value in Eq. (4.20) or the routine SLICEHTR-calculated value in Eq. (4.22) for the *unmodified* problem 2. But more appropriately, the Broyden method calculated value should be compared with the routine SLICEHTR-calculated value in Eq. (4.24) for the *modified* problem 2. There is an agreement to 8 significant digits with the value in Eq. (4.24).

The coolant temperature rise calculated by the Broyden method is **43.0622,0093,8**102,2 °C. The highlighted 11 digits of this value agree with the more accurate value given in Eq. (4.25) that was obtained by the standalone routine SLICEHTR for the modified problem.

For the PLTEMP Exact method, each axial node gives practically the same temperature difference between the inner and outer surfaces of the tube, as expected. For all axial nodes, the temperature difference is found to be **178.0270,79**$^{59}_{64}$ **°C** (meaning that the 10th and 11th digits vary from 59 to 64**)**. This can be compared with the hand-calculated value in Eq. (4.20) or the routine SLICEHTR-calculated value in Eq. (4.22) for the *unmodified* problem 2. But more appropriately, the Exact method calculated value should be compared with the routine SLICEHTR-calculated value in Eq. (4.24) for the *modified* problem 2. There is agreement to 9 significant digits with the value in Eq. (4.24). As indicated in Section 4.2.2, a comparison of the results of Eqs. (4.20) and (4.22) shows that the routine SLICEHTR is capable of an accuracy to 16 significant digits. The accuracy of the Exact method is here limited to 9 digits presumably because the accuracy of the input data (especially the tube circumference CIRCF) to the code is limited to 10 digits due to the 12-column data fields.

The coolant temperature rise calculated by the Exact method is **43.0622,0093,8**093,5 °C. The highlighted 11 digits of this value agree with the more accurate value given in Eq. (4.25) that was obtained by the standalone routine SLICEHTR for the modified problem.

4.3 Calculation of Heat Coefficient in the Broyden Method

Figures 4.8 and 4.9 (solutions of the same problem by the Broyden and Exact methods) show a difference in film coefficient in channel 2. The film coefficient to channel 2 calculated in the Broyden and Exact methods are not in good agreement, in spite of a precise agreement (to 11

significant digits) in the channel 2 coolant temperature rise calculated by the two methods. This agreement in coolant temperature is shown in Figs. 4.8 and 4.9 and was discussed in Section 4.2. An example of the disagreement in film coefficient to channel 2 is 5029.9 versus 4963.8 W/m^2-°C in axial mesh interval 1 in the Broyden and Exact methods respectively, also shown in Figs. 4.8 and 4.9.

The reason for this disagreement was traced to the use (in routine FUNCV) of coolant thermal properties at the *outlet* of an axial mesh interval (rather than the mesh *center*) in film coefficient calculation in the Broyden method. This was subsequently changed to use the coolant properties at the mesh center. After this improvement, problem 2 was solved again by the Broyden method, and the results are compared with the Exact solution in Fig. 4.10 (printed to 13 digits using the option KPRINT = 1). The film coefficients for the axial nodes 1 to 9 now agree to 13 digits for this problem. The agreement in the axial node 10 is only to 5 digits (i.e., 6348.184 versus 6348.170 W/m^2-°C). This is unexpected because the coolant temperatures in all axial nodes (1 to 10) agree to 13 digits.

4.4 Radial Geometry Problem 3

Find the temperature difference across the thickness of a 60 cm long fuel tube whose fuel meat is generating a power of 9 kW (no power in the cladding). Use a film coefficient of 10^{-6} W/m^2-°C on the inner surface of the fuel tube, and the Sieder-Tate correlation of film coefficient on the outer surface. The tube inner radius is 0.5 cm, the meat inner radius is 1.5 cm, the meat outer radius is 3.5 cm, the tube outer radius is 4.5 cm, and the thermal conductivities of cladding and meat are 7 and 8 W/m-°C. What is the coolant (water) temperature rise using the actual enthalpy and specific heat of the coolant (water) with a flow rate of 0.05 kg/s in each channel?

4.4.1 Solution of Problem 3 by PLTEMP Code Version 3.2

Since the actual enthalpy and specific heat of the coolant are used in problem 3, a comparison of the solutions by the Broyden and the Exact methods shows the differences actually experienced in reactor conversion analyses. The input data for the problem is shown in Fig. 4.11. This input file is obtained from that for problem 2 simply by setting the option ICP to zero (on input card 200). All other data remain unchanged. The solutions obtained by the Broyden and Exact methods are shown in Figs. 4.11 and 4.12.

The total temperature difference across the fuel tube thickness for each axial node is the same as that in problem 2, i.e., **178.0270,782$\frac{2}{8}$ °C** by the Broyden method (see Fig. 4.12) and **178.0270,79$\frac{59}{64}$ °C** by the Exact method (see Fig. 4.13). The temperature differences across the tube thickness calculated by the two methods agree to 8 significant digits. The coolant temperatures do not agree this accurately although their difference is less than **0.127 °C** which is investigated below in items 1 and 2. The film coefficients of the first axial node in the two solutions agree to 5 significant digits (4987.77 versus 4987.84 W/m^2-°C) but the difference between the film coefficients grows in the flow direction due to the growing coolant temperature difference. In the last axial node, the film coefficients in the two solutions agree to only 3 digits (6425.53 versus 6421.81 W/m^2-°C).

The following differences between the coolant temperatures calculated by the two methods and their explanation are noted:

(1) The coolant outlet temperature in channel 2 found by the Broyden method is 92.9923 °C compared to 92.8645 °C found by the Exact method (i.e., a difference of 0.1268 °C). In order to determine which of these values is more accurate, a hand calculation was done based on the coolant enthalpy used by the PLTEMP/ANL code. The hand calculation reported in Section 4.4.2 below gives a value of 92.8624 °C. This implies that the Exact method calculated value is more accurate. The difference between the values obtained by hand calculation and the Exact method is 0.0021 °C. The reason for this difference is believed to be related to the uncertainty (or jumps shown below in Table 4.3) in the values of $\partial h/\partial P$ evaluated using different values of ΔP in the enthalpy routine ZHLIQ of the PLTEMP/ANL code.

(2) The coolant outlet temperature in channel 1 found by the Broyden method is 50.0000 °C compared to 50.0199 °C found by the Exact method (i.e., a difference of 0.0199 °C). The film coefficient to coolant channel 1 is input to be $1.0\text{x}10^{-6}$ W/m^2-°C, and hence the heat transfer to the coolant in channel 1 is very small. The coolant temperature rise in channel 1 is found in Section 4.4.2 to be less than $2.0\text{x}10^{-8}$ °C if the pressure-dependence of coolant enthalpy is ignored. This agrees with the result by the Broyden method.

In Section 4.4.2, the coolant temperature rise in channel 1 is also estimated accounting for the pressure-dependence of coolant enthalpy, and found to be about 0.0214 °C. The coolant temperature rise in channel 1 is 0.0199 °C in the Exact method due to the fact that the pressure dependence of coolant enthalpy is accounted for by the method.

4.4.2 Hand Calculation for Problem 3

<u>Coolant Temperature Rise in Channel 1:</u> The film coefficient to coolant channel 1 is input to be $1.0\text{x}10^{-6}$ W/m^2-°C, and the heat transfer to the coolant in channel 1 is very small. Hence the temperature rise is very small if the pressure-dependence of coolant enthalpy is not accounted for. Therefore, the temperature rise is calculated in two ways, first ignoring the pressure-dependence of enthalpy, and then accounting for the pressure-dependence of enthalpy.

<u>Temperature Rise in Channel 1 Ignoring Pressure-Dependence of Enthalpy:</u>

Input data: $h_1 = 1.0\text{x}10^{-6}$ W/m^2-°C, $r_a = 0.005$ m, $T_s \leq 277$ °C (see Fig. 4.12), $L = 0.6$ m, $T_{in} = 50$ °C, $W = 0.05$ kg/s, $C_p = 4180$ J/kg-°C,

$$\text{Coolant temperature rise in channel 1} \leq \frac{2\pi r_a L h_1 (T_s - T_{in})}{W C_p} = 2.0\text{x}10^{-8}\ °\text{C}$$

<u>Temperature Rise in Channel 1 Accounting for Pressure-Dependence of Enthalpy:</u>
The value of C_T, i.e., the partial derivative $\partial h/\partial P$ at constant temperature varies from 74.6 to 104.6 J/kg-°C-bar over the coolant temperature and pressure range of the problem (50 to 90 °C

and 1 to 2 bar). It is assumed to have a mean value of 89.6 J/kg-bar in the estimation of the coolant temperature rise ΔT in channel 1, *without any heat addition*, due only to the pressure drop from the channel inlet to outlet (i.e., 2 bar to 1 bar). Setting the enthalpy change from the inlet to outlet to zero, we get

$$C_p \, \Delta T + C_T \, \Delta P = 0 \tag{4.26}$$

Equation (4.26) can be rewritten as

$$\Delta T = - C_T \, \Delta P \, / \, C_p \tag{4.27}$$

Putting $\Delta P = -1.0$ bar and $C_p = 4180$ J/kg-°C, we get from Eq. (4.27)

Coolant temperature rise in channel 1 = $\Delta T \approx -89.6 \times (-1.0)/4180 =$ **0.0214 °C** (4.28)

<u>Coolant Outlet Temperature in Channel 2</u>: In the code, the enthalpy and specific heat of water is treated as a function of temperature and pressure. The enthalpy of water used by the code (calculated in the subroutine ZHLIQ) is tabulated in Appendix C for the temperature range 1 to 100 °C and the pressure range 1 to 10 bars. In problem 3, the input inlet and outlet pressures are 2 bar and 1 bar respectively. Almost all the heat generated in the fuel goes to coolant channel 2 because the film coefficient to channel 1 is 10^{-6} W/m^2-°C, i.e., very small compared to the values of ~5000 W/m^2-°C in channel 2. Hence the channel 2 outlet temperature can be found by equating the total power (9000 W) generated in the fuel to the heat removal rate by the coolant in channel 2, as follows.

$$W \, [\, h(T_{out}, 1\text{bar}) - h(T_{in}, 2\text{bar}) \,] = 9000 \tag{4.29}$$

where $W = 0.05$ kg/s
$T_{in} = 50$ °C
$h(T_{in}, 2\text{bar}) = 208{,}844.8334$ J/kg (from Appendix C)

Equation (4.29) gives the channel 2 outlet enthalpy.

$$h(T_{out}, 1\text{bar}) = 208{,}844.8334 + 9000/0.05 = 388{,}844.8334 \text{ J/kg} \tag{4.30}$$

The outlet enthalpy in Eq. (4.30) lies between the following enthalpy data given in Appendix C at the outlet pressure of 1 bar.

h(92 °C,1bar) = 385,204.5441 J/kg
h(93 °C,1bar) = 389,425.7355 J/kg
Change Δh = 4221.1914 J/kg
Using the above data and the channel 2 outlet enthalpy of Eq. (4.30), the outlet temperature in channel 2 is interpolated as follows.

$$T_{out} = 92 + (388{,}844.8334 - 385{,}204.5441) / 4221.1914 = \mathbf{92.8624\ °C} \tag{4.31}$$

4.5 Radial Geometry Problem 4:

Find the temperature difference across the thickness of a 60 cm long fuel tube whose fuel meat is generating a power of 9000 W (no power in the cladding). Use a film coefficient of 1000 W/m^2-°C on the inner and outer surfaces of the fuel tube. The tube inner radius is 0.5 cm, the meat inner radius is 1.5 cm, the meat outer radius is 3.5 cm, the tube outer radius is 4.5 cm, and the thermal conductivities of cladding and meat are 7 and 8 W/m-°C. What is the coolant (water) temperature rise using the enthalpy and specific heat of the coolant (water) with a flow rate of 0.05 kg/s in each channel?

4.5.1 Solution of Problem 4 by PLTEMP Code Version 3.1

Problem 4 is identical to problem 3 in all respects except that the film coefficients on the inner and outer surfaces of the tube are different. This problem has an input film coefficient of 1000 W/m^2-°C on each side of the tube whereas problem 3 had an input value of 10^{-6} W/m^2-°C on the inner surface and a film coefficient calculated by the code using the Sieder-Tate correlation on the outer surface. Figure 4.14 shows the input file for problem 4 (same for versions 3.1 and 3.2 of PLTEMP/ANL). This input file was obtained by changing only two data on card 300, i.e., by setting the flag IBCA to 3, and the film coefficient HBC to 1000.

Figure 4.15 shows the results of running 200 iterations of the Broyden method in the version 3.1 of PLTEMP/ANL. The results are not good because the calculation did not converge as indicated by the large values of temperature mismatch T_{diff} (> 100 °C) in all axial nodes (see Fig. 4.15). The lack of convergence is due to an unsuitable initial guess for the location of the peak fuel temperature in meat thickness. The initial guess is unsuitable because it is provided by the *slab geometry* Exact solution of the problem in this version of the code (because it does not have a radial geometry Exact method). The Broyden method in this version converges in the radial geometry for many actual reactor assemblies (e.g., the ASTRA2 six-tube assembly problem 3 reported below) using the initial guess provided by the slab geometry Exact solution when the fuel areal fraction (called X) inside the peak fuel temperature, $(r_{\max}^2 - r_b^2)/(r_c^2 - r_b^2)$, is close to 0.5 in each fuel tube. The code may not converge if X is far from 0.5 in any tube, i.e., X < 0.2 or X > 0.8.

4.5.2 Solution of Problem 4 by PLTEMP Code Version 3.2

The input file given in Fig. 4.14 was also used in the version 3.2 of the code. Figure 4.16 shows the results of running 200 iterations of the Broyden method, and Fig. 4.17 shows the results of running the newly implemented Exact method in the version 3.2. Although no change was made in the iteration strategy of the Broyden method, the method converged this time as indicated by negligible T_{diff} shown in Fig. 4.16, and the results are good. This is because the initial guess for the peak fuel temperature location in meat thickness is good. The initial guess is good because it is provided by the Exact solution of the actual radial geometry problem (after the implementation of the radial geometry Exact method in version 3.2 of the code).

Table 4.4 shows a comparison of temperatures calculated by the two methods for problem 4. Using a previously developed utility *differ.x*, it is found that the maximum difference between the two solutions in all coolant, cladding, and fuel temperatures given in Figs. 4.16 and 4.17 is 0.055 °C

that occurs in the outer channel outlet temperature. The agreement between the two methods provides a verification of the implementation of the Exact method.

4.6 Slab Geometry Problem 5

Turn the radial geometry problem 3 into a slab geometry problem by just setting the option IGOM to 0 (on the input card 200), and solve the resulting problem for a fuel plate of width 5π cm, length 60 cm, generating a power of 9 kW (no power in the cladding). Use a film coefficient of 10^{-6} W/m^2-°C on the left surface of the fuel plate, and the Sieder-Tate correlation of film coefficient on the right surface. The thicknesses of cladding and meat remain unchanged, i.e., 1.0 cm and 2.0 cm respectively, and the thermal conductivities of cladding and meat are 7 and 8 W/m-°C. What is the coolant (water) temperature rise using the actual enthalpy and specific heat of the coolant (water) with a flow rate of 0.05 kg/s in each channel?

The purpose in this section is to solve the flat fuel plate problem 5 in two ways: first by the slab geometry Exact method in the PLTEMP/ANL version 3.2 code and then by the radial geometry Exact method in the code by using a practically infinite mean radius for the fuel tube. The solution obtained by the radial geometry Exact method should approach the solution by the slab geometry Exact method, thus proving a verification of the newly implemented radial geometry Exact method.

4.6.1 Hand Calculation for Problem 5

Input data given: t_c = 0.01 m, t_f = 0.02 m, w = 0.05π m,
K_c = 7 W/m-°C, K_f = 8 W/m-°C, L = 0.6 m, P = 9000 W

The left fuel-cladding interface is practically adiabatic due to the negligible film coefficient on the left surface of the fuel plate. Hence there is no temperature difference across the left cladding thickness. The volumetric heat source in the meat and the temperature drop across the meat thickness are given by

$$q''' = \frac{P}{L\,w\,t_f} = 4.77464829275686\text{x}10^6 \text{ W/m}^3 \tag{4.32}$$

$$\Delta T_f = \frac{q'''\,t_f^{\,2}}{2\,K_f} = 119.3662073189215 \text{ °C} \tag{4.33}$$

All the power conducts through the right side cladding, and therefore the heat flux and temperature difference across the right cladding thickness are given by

$$q'' = \frac{P}{Lw} = 95492.9658551372 \text{ W/m}^2 \tag{4.34}$$

$$\Delta T_c = \frac{q''\,t_c}{K_c} = 136.418522650196 \text{ °C} \tag{4.35}$$

The sum of Eqs. (4.33) and (4.35) gives the total temperature drop across the plate thickness, from the right cladding surface to the left cladding surface.

$$T_{csr} - T_{csl} = 255.7847299691175\ °C \tag{4.36}$$

where T_{csr} and T_{csl} are the temperatures at the right and left cladding surfaces, respectively.

4.6.2 Comparison of Solutions of Problem 5 by Slab Geometry Exact Method and Radial Geometry Exact Method

Figure 4.18 shows the PLTEMP input data file for problem 5 that was obtained by setting the input flag IGOM to 0 (on the input card 200) in the input file of problem 3 shown in Fig. 4.11. It is the only difference between these input files. On the other hand, Fig. 4.19 shows the input data file to solve problem 5 using the radial geometry Exact method. This input file was obtained by setting the mean tube radius to 1000 m instead of 0.025 m in the input file for problem 3 (input RMID on card 308A). It is the only difference between the input files shown in Figs. 4.11 and 4.19.

The PLTEMP/ANL version 3.2 code was run for these two input files (Figs. 4.18 and 4.19), and the results are shown in Figs. 4.20 and 4.21 respectively. By running the latter input file using mean radii smaller than 1000 m it was found that 1000 m is practically infinite. Using a previously developed utility *differ.x*, it is found that the maximum difference in all coolant, cladding, and fuel temperatures between the two solutions given in Figs. 4.20 and 4.21 is 0.004 °C that occurs in axial node 1 of the left side cladding. This provides a verification of the radial geometry Exact method implemented in the version 3.2 of the code.

Setting the print option KPRINT = 1, the total temperature drop across the fuel plate thickness was obtained to 13 significant digits for comparison with the accurate hand calculation given in Eq. (4.36). The total temperature drop in the solution by the slab geometry Exact method gives 255.784728^{5}_{3} °C (meaning that the 10th digit varies from 3 to 5 for the 10 axial nodes used). This agrees with the hand calculation of Eq. (4.36) to 8 significant digits (the 9th digit in the PLTEMP solution should be 9 instead of 8), verifying the result of the slab geometry Exact method. The total temperature drop in the solution of problem 5 by the radial geometry Exact method gives 255.781891^{8}_{6} °C (meaning that the 10th digit varies from 6 to 8 for the 10 axial nodes used). This agrees with the hand calculation of Eq. (4.36) *only to 5 significant digits*, and has an error of 0.0028 °C.

Table 4.5 summarizes several solutions of problem 5 by the radial geometry Exact method using increasing values of the input mean radius for the fuel tube. It is noted that the most accurate solution (with an error of 0.0006 °C in the temperature drop across the fuel plate thickness) is obtained by using a tube radius of 10000 m. The solution deteriorates (presumably due to round-ff error) if the input tube radius is increased beyond 10000 m. However, this comparison shows that the solution of a slab geometry problem by the radial geometry Exact method approaches the actual solution as the fuel tube radius is made very large (practically infinite). This provides a verification of the radial geometry Exact method.

4.7 Hungarian Reactor Benchmark Problem with a Power of 90 kW

The temperature distribution in the Hungarian reactor benchmark problem was calculated using the PLTEMP/ANL version 3.1 code. Figure 4.22 shows the input data file used. The fuel assembly in this problem consists of 3 fuel tubes. For a verification of the newly implemented radial geometry Exact method in PLTEMP/ANL version 3.2, five solutions to this problem obtained by the following methods are compared in this section.

(1) The Broyden method in version 3.2 using the constant coolant C_p option
(2) The radial geometry Exact method in version 3.2 using the constant C_p option
(3) The Broyden method in version 3.1 using the actual coolant properties, i.e., the coolant properties that are based on the steam tables that are built into the code
(4) The Broyden method in version 3.2 using the actual coolant properties
(5) The radial geometry Exact method in version 3.2 using the actual coolant properties

The first two solutions (i.e., the Broyden and Exact methods using constant C_p) give identical standard output files that are printed to 4 decimal digits using the print flag KPRINT = 0. The two solutions were then printed to 13 significant digits by setting the print flag KPRINT = 1, and are compared in Fig. 4.23. All coolant, cladding, and meat temperatures and film coefficients (except 3 temperatures highlighted with bold characters in Fig. 4.23) agree to 6 significant digits. The three exceptions are the fuel peak temperatures in axial nodes 2 and 3 of fuel tube 1, and in axial node 2 of fuel tube 3. By entering more digits in the input data, an agreement better than this was shown for problem 2 in Section 4.3.

The three calculations performed using the actual coolant properties (shown in Figs. 4.24, 4.25, and 4.26) are compared in Table 4.6 by reporting the maximum difference ΔT_{max} between a (selected) pair of solutions for all coolant, cladding, and fuel temperatures of a fuel tube and its two adjacent channels. A previously developed utility *differ.x* was used to find the difference ΔT_{max}.

The maximum difference between the solutions 3 and 4 (i.e., the solution by the Broyden method in version 3.1 and the solution by the Broyden method in version 3.2) is about 0.25 °C (as shown in Table 4.6). This difference is due to using the coolant *node center* temperature for calculating film coefficient in version 3.2 instead of using the coolant *node outlet* temperature for calculating film coefficient in version 3.1.

The maximum difference between the solutions 4 and 5 (i.e., the solution by the Broyden method in version 3.2 and the solution by the radial geometry Exact method in version 3.2) is about 0.007 °C. This difference is because the Exact method accounts for the pressure derivative of coolant enthalpy whereas the Broyden method does not. This provides a verification of the Exact method.

4.8 ASTRA2 Six-Tube Assembly Problem 3 Case 1

The temperature distribution in a six-tube radial geometry problem (called ASTRA2 Problem 3 Case 1) was calculated earlier by Russian authors using their ASTRA2 code and provided to ANL [2, 3]. For comparison purposes, a solution to this problem was calculated using the PLTEMP/ANL code version of May 22, 2003. The fuel tubes were arranged in the order of

decreasing mean radii in this calculation. Since the radial geometry Exact method implemented in PLTEMP/ANL version 3.2 requires the tubes to be arranged in the order of increasing radii, the input card types 307, 308, 308A, 309, and 310 were rearranged in the reverse order. The resulting input data file is shown in Fig. 4.27, and the May 2003 results (rearranged accordingly) are shown in Fig. 4.28.

Using this input file (Fig. 4.27), the temperature distribution in the ASTRA2 radial geometry problem 3 case 1 was recalculated by the Broyden method using the current versions 3.1 and 3.2 of the PLTEMP/ANL code (using 200 iterations), and by the radial geometry Exact method in version 3.2 of the code. The results of the three recalculations are shown in Figs. 4.29, 4.30, and 4.31. The Broyden solution using version 3.1 has fuel peak temperature mismatches (i.e., T_{diff} which is a measure of convergence) of 0.19 to 0.61 °C in 4 of the 66 axial nodes used in the problem (11 nodes per tube × 6 tubes). The Broyden solution using version 3.2 has temperature mismatches T_{diff} of 0.01 °C in only 2 of the 66 axial nodes used in the problem.

Table 4.7 compares these three recalculations with the older May 2003 results by reporting the maximum difference ΔT_{max} in the coolant, cladding, and fuel temperatures of *all channels and tubes* between a pair of solutions. Selected results of all four PLTEMP/ANL calculations are compared in Table 4.8 with the results obtained by Russian authors using their ASTRA2 code.

Based on Table 4.7, the following observations are made in numbered paragraphs. A verification of the radial geometry Exact method is provided in paragraph number 2.

(1) Comparing the Broyden solutions obtained by PLTEMP/ANL versions 3.1 and 3.2 (shown in Figs. 4.29 and 4.30), it is found that the maximum temperature difference ΔT_{max} is 0.171 °C. This difference is due to using node outlet versus node center coolant temperature in calculating film coefficient in the versions 3.1 and 3.2. The latter solution is considered to be more accurate. The solution obtained by the newly implemented radial geometry Exact method is therefore compared (in paragraph number 2) with the latter solution (PLTEMP/ANL version 3.2).

(2) Comparing the radial geometry Exact solution and the Broyden solution by PLTEMP/ANL version 3.2 (Fig. 30 and Fig. 4.31), it is found that the maximum temperature difference ΔT_{max} is 0.089 °C. This difference is not due to the lack of accounting for $\partial h/\partial P$ in the Broyden method because the constant coolant C_p option (ICP = 1 on input card 200) is used in this problem, and $\partial h/\partial P$ is zero in both methods when this option is used (as shown by the comparison given in Fig. 4.23 for the Hungarian reactor benchmark problem in Section 4.7). The reason for this difference is not clear. However, the difference ΔT_{max} is small, and the comparison for the ASTRA2 problem provides a verification of the radial geometry Exact method.

(3) Comparing the radial geometry Exact solution with the Broyden solution by PLTEMP/ANL version 3.1, it is found that the maximum temperature difference ΔT_{max} is 0.203 °C. This difference is due to using node outlet versus node center coolant temperature in calculating film coefficient in the versions 3.1 and 3.2. This temperature difference is not due to the lack of accounting for $\partial h/\partial P$ in the Broyden method, as discussed above.

(4) Comparing the May 2003 results with the Broyden solution by PLTEMP/ANL version 3.1, the maximum temperature difference ΔT_{max} is found to be 5.987 °C which occurs in axial node 11 of the meat of tube 6 (outermost). This difference is significantly large. It is due to the code improvements done after May 2003, and also perhaps because the solution converged only approximately. The version 3.1 solution had temperature mismatches T_{diff} (a measure of convergence) of 0.11 to 0.77 °C in 29 of the 66 axial nodes used in the problem. The Broyden solution of May 2003 is less accurate than the current Broyden solutions.

As a side remark, it is noted that the Broyden method in PLTEMP/ANL *version 3.1* converges for this radial geometry problem. The convergence of the Broyden method in version 3.1 shows that the initial guess for fuel areal fraction (called X) inside the peak fuel temperature, i.e., $(r_{\max}^2 - r_b^2)/(r_c^2 - r_b^2)$, in each fuel tube is suitable for convergence. The initial guess in the version 3.1 is provided by the *slab geometry* Exact method. The radial geometry Exact method is not available in this version. However, the Broyden method converges because the fuel areal fraction X in each tube is close to 0.5 (in the range 0.35 to 0.60). The Broyden method in PLTEMP/ANL *version 3.1* may not converge for some other radial geometry problems, as it did not for problem 4 discussed in Section 4.5.1.

4.9 Conclusions

In summary, for the constant coolant specific heat option in the code (ICP = 1 on input card 200), the coolant temperature rise calculated by the Exact method in PLTEMP/ANL code is good to 11 significant digits, and the temperature difference across the tube thickness is good to 8 digits in problem 1. The coolant temperature rise calculated by the Exact method is good to 11 significant digits, and the temperature difference across the tube thickness is good to 9 digits in problem 2.

When using the actual thermal properties of the coolant in problem 3 (otherwise identical to problem 2), there is a difference of 0.0021 °C in the coolant temperature rise calculated by the Exact method and hand calculation, and the temperature difference across the tube thickness is good to 9 digits. There is a difference of 0.13 °C in the coolant temperature rise calculated by the Broyden method and hand calculation.

The solution of a slab geometry problem by the radial geometry Exact method approaches the actual solution as the fuel tube radius (input RMID on card 308A) is made very large (~ 1000 m).

For the Hungarian reactor benchmark problem, the radial geometry Exact solution and the Broyden solution by PLTEMP/ANL version 3.2 were compared to find that the maximum difference in the coolant, cladding, and fuel temperatures of *all channels and tubes* is 0.007 °C.

For the ASTRA2 six-tube assembly, the radial geometry Exact solution and the Broyden solution by PLTEMP/ANL version 3.2 were compared to find that the maximum difference in the coolant, cladding, and fuel temperatures of *all channels and tubes* is 0.089 °C.

4.10 REFERENCES

1. A. P. Olson and M. Kalimullah, "A User's Guide to the PLTEMP/ANL Code," ANL/RERTR/TM-11-22, Version 4.1, Argonne National Laboratory, 9700 South Cass Avenue, Argonne, IL 60439, USA (April 6, 2011).

2. A. P. Olson, Argonne National Laboratory, private communication, February 26, 2007.

3. Pavel Egorenkov, Kurchatov Institute, Kurchatov Square 1, 123182, Moscow, private communication of Results to J. E. Matos of Argonne National Laboratory, 2002.

Figure 4.1 Solution of Radial Geometry Problem 1 Obtained by the Standalone Routine SLICEHTR

```
Coolant Temperatures (C) of All Channels at the Center of Axial Node (Exact Solution by SLICE1):
             50.0000000000000000     71.5311004784689000

SLICEHTR: Power source in fuel+clad+coolant vs Power removed by coolant  9.000000D+03 9.000000D+03 W

q1``, q2``   =    0.0000000000000000D+00  5.3051647697298440D+04

Temp diff across tube thickness = 161.1562117261541

CHECKING BOUNDARY AND INTERFACE CONDITIONS ON TEMPERATURE (C) AND HEAT FLUX (W/cm**2) FOR FUEL TUBE  1:
                    Inner Cladding              Fuel Meat                 Fuel Meat                Outer Cladding
                    Inner Surface             Inner Surface             Outer Surface              Outer Surface
Temp Conds:    238.7041  =  238.7041      226.3353  =  226.3353      144.6858  =  144.6858       77.5479  =   77.5479
Flux Conds:   0.00000D+00=-9.09495D-13   1.59155D+04= 1.59155D+04   4.09256D+04= 4.09256D+04   5.30516D+04= 5.30516D+04
Temp diff across tube thickness = 161.1562117261541

Here, positive heat flux means it is directed radially outward.
```

Figure 4.2 Solution of Radial Geometry Problem 1 Slightly Modified by Setting $h_1 = 10^{-6}$ W/m^2-°C, Obtained by the Standalone Routine SLICEHTR

```
Coolant Temperatures (C) of All Channels at the Center of Axial Node (Exact Solution by SLICE1):
             50.0000000085095400     71.5311004699593600

SLICEHTR: Power source in fuel+clad+coolant vs Power removed by coolant  9.000000D+03 9.000000D+03 W

q1``, q2``   =    1.8870414803855670D-04  5.3051647676331310D+04

Temp diff across tube thickness = 161.1562123595361

CHECKING BOUNDARY AND INTERFACE CONDITIONS ON TEMPERATURE (C) AND HEAT FLUX (W/cm**2) FOR FUEL TUBE  1:
                    Inner Cladding              Fuel Meat                 Fuel Meat                Outer Cladding
                    Inner Surface             Inner Surface             Outer Surface              Outer Surface
Temp Conds:    238.7041  =  238.7041      226.3353  =  226.3353      144.6858  =  144.6858       77.5479  =   77.5479
Flux Conds:  -1.88704D-04=-1.88704D-04   1.59155D+04= 1.59155D+04   4.09256D+04= 4.09256D+04   5.30516D+04= 5.30516D+04
Temp diff across tube thickness = 161.1562123595361

Here, positive heat flux means it is directed radially outward.
```

Figure 4.3 PLTEMP/ANL Version 3.2 Code Input Data for Radial Geometry Problem 1 Slightly Modified by Setting $h_1 = 10^{-6}$ W/m^2-°C

```
  Radial Geometry Test Problem 1: One fuel tube, Total power=9 kW, Length=60 cm  Card 100
! Tube radii: Ra=0.5 cm, Rb=1.5 cm, Rc=3.5 cm, Rd=4.5 cm
!234567890123456789012345678901234567890123456789012345678901234567890123456789
!  1   2   3   4   5   6   7   8   9  10  11  12  13  14  15  16  17  18
   0   0   5   1   0   0   1   1   1   1   0   0   0   0   2   1   0   0         Card 200
         1.0         1.0         1.0                                           Card 201
   1   3         0.0         1.0         1.0         1.0   0   1     1.0D-06    Card 300
         1.0         1.0         1.0                                           Card 300A
   1   2         1.0                                                           Card 301
   1   1   1                                                                   Card 302
        1.00                                                                   Card 303
         1.0         1.0         1.0         1.0         1.0         1.0       Card 304
         0.0         0.0        0.60         0.0         0.0         0.0       Card 304
         1.0         1.0         1.0         1.0         1.0         1.0       Card 304
         0.0         0.0         0.0                                           Card 305
   2   0         0.0        0.60         .01         7.0       0.020         7.0 Card 306
7.8539816D-5        0.01 .0314159265 .0314159265         1.0         1.0       Card 307
7.8539816D-5        0.01 .2827433388 .2827433388         1.0         1.0       Card 307
.15707963268                                                                   Card 308
.02500000000                                                                   Card 308A
         1.0                                                                   Card 309
      5.0D-2      5.0D-2                                                       Card 310
       0.1D0       0.001       0.2D0      9.0D-3      50.0D0                    Card 500
      0.50D0       0.0D0                                                       Card 500
   1      0.0001        36.8         0.0         1.0                           Card 600
  11                                                                           Card 700
      0.00D0      1.00D0                                                       Card 701
      0.10D0      1.00D0                                                       Card 701
      0.20D0      1.00D0                                                       Card 701
      0.30D0      1.00D0                                                       Card 701
      0.40D0      1.00D0                                                       Card 701
      0.50D0      1.00D0                                                       Card 701
      0.60D0      1.00D0                                                       Card 701
      0.70D0      1.00D0                                                       Card 701
      0.80D0      1.00D0                                                       Card 701
      0.90D0      1.00D0                                                       Card 701
      1.00D0      1.00D0                                                       Card 701
   0                                                                           Card 702
```

Figure 4.4 Solution of Radial Geometry Problem 1 Slightly Modified by Setting $h_1 = 10^{-6}$ W/m^2-°C, Obtained by the Exact Method in PLTEMP/ANL Version 3.2

```
NPH = 7, Temp diff across tube thickness =  1.6115621122278600D+02
NPH = 7, Temp diff across tube thickness =  1.6115621018189140D+02
NPH = 7, Temp diff across tube thickness =  1.6115621332971350D+02
NPH = 7, Temp diff across tube thickness =  1.6115621087903860D+02
NPH = 7, Temp diff across tube thickness =  1.6115621258905200D+02
NPH = 7, Temp diff across tube thickness =  1.6115621156698840D+02
NPH = 7, Temp diff across tube thickness =  1.6115621220764980D+02
NPH = 7, Temp diff across tube thickness =  1.6115621008530520D+02
NPH = 7, Temp diff across tube thickness =  1.6115621127580810D+02
NPH = 7, Temp diff across tube thickness =  1.6115621105099810D+02
```

FUEL PLATE 1 (ExactSoln)

NODE	COOLANT inner(C)	CladSurf inner(C)	FUEL PEAK (C)	CladSurf outer(C)	COOLANT outer(C)	HCOFinner W/C-m^2	HCOFouter W/C-m^2	ONBRin [F Note 1]	ONBRout	ETAin K-cm^3/J	ETAout K-cm^3/J	COOLNT at NodeOutlet inner(C)	outer(C)
	50.000				50.000								
1	50.000	223.997	211.628	62.841	52.153	1.0000E-06	4.9638E+03	0.40	5.59	2.540E+11	8.074E+02	50.000	54.306
2	50.000	227.938	215.569	66.782	56.459	1.0000E-06	5.1395E+03	0.38	4.19	2.425E+11	7.359E+02	50.000	58.612
3	50.000	231.915	219.547	70.759	60.766	1.0000E-06	5.3085E+03	0.36	3.30	2.312E+11	6.636E+02	50.000	62.919
4	50.000	235.922	223.553	74.766	65.072	1.0000E-06	5.4726E+03	0.35	2.70	2.200E+11	5.902E+02	50.000	67.225
5	50.000	239.944	227.576	78.788	69.378	1.0000E-06	5.6377E+03	0.33	2.26	2.090E+11	5.158E+02	50.000	71.531
6	50.000	244.003	231.634	82.846	73.684	1.0000E-06	5.7902E+03	0.31	1.92	1.981E+11	4.401E+02	50.000	75.837
7	50.000	248.084	235.715	86.928	77.990	1.0000E-06	5.9361E+03	0.29	1.66	1.872E+11	3.630E+02	50.000	80.144
8	50.000	252.183	239.815	91.027	82.297	1.0000E-06	6.0765E+03	0.28	1.44	1.763E+11	2.843E+02	50.000	84.450
9	50.000	256.297	243.929	95.141	86.603	1.0000E-06	6.2133E+03	0.26	1.26	1.654E+11	2.038E+02	50.000	88.756
10	50.000	260.422	248.053	99.266	90.909	1.0000E-06	6.3482E+03	0.24	1.10	1.543E+11	1.211E+02	50.000	93.062
	50.000				93.062								

Coolant temp rise (out - in) in channels = 1.73227761024464D-08 4.30622009396152D+01
Temp diff across plate thickness(node10) = 1.61156211050998D+02 L&R surf temps = 2.60422300386202D+02 9.92660893352038D+01

[1] The ONB ratio is here defined as (Tonb - Tinlet)/(Tsurf - Tinlet). If the heat flux is negative (the coolant is hotter than the adjacent cladding surface), then the ONB ratio is arbitrarily set to 99.99 .

FUEL PLATE 1 (ExactSoln) AREAL

NODE	FLUX inner MW/m^2	FLUX outer MW/m^2	FUEL X inner	Tsat (C)	Tdiff (C)	FUEL-CLADinterface inner (C)	outer (C)	Pressure (bar)	Z-mid	Z-int
1	1.7400E-10	5.3052E-02	0.0000	119.432		211.628	129.979	1.95000	0.0500	0.1000
2	1.7794E-10	5.3052E-02	0.0000	117.784		215.569	133.919	1.85000	0.1500	0.2000
3	1.8192E-10	5.3052E-02	0.0000	116.061		219.547	137.897	1.75000	0.2500	0.3000
4	1.8592E-10	5.3052E-02	0.0000	114.256		223.553	141.904	1.65000	0.3500	0.4000
5	1.8994E-10	5.3052E-02	0.0000	112.359		227.576	145.926	1.55000	0.4500	0.5000
6	1.9400E-10	5.3052E-02	0.0000	110.358		231.634	149.984	1.45000	0.5500	0.6000
7	1.9808E-10	5.3052E-02	0.0000	108.241		235.715	154.065	1.35000	0.6500	0.7000
8	2.0218E-10	5.3052E-02	0.0000	105.990		239.815	158.165	1.25000	0.7500	0.8000
9	2.0630E-10	5.3052E-02	0.0000	103.585		243.929	162.279	1.15000	0.8500	0.9000
10	2.1042E-10	5.3052E-02	0.0000	101.001		248.053	166.404	1.05000	0.9500	1.0000

Figure 4.5 Solution of Radial Geometry Problem 2 Obtained by the Standalone Routine SLICEHTR

```
Coolant Temperatures (C) of All Channels at the Center of Axial Node (Exact Solution by SLICE1):
            50.0000000000000000     71.5311004784689000

SLICEHTR: Power source in fuel+clad+coolant vs Power removed by coolant  9.000000D+03 9.000000D+03 W

q1``, q2``   =    0.0000000000000000D+00  5.3051647697298460D+04

Temp diff across tube thickness = 178.0270799296316

CHECKING BOUNDARY AND INTERFACE CONDITIONS ON TEMPERATURE (C) AND HEAT FLUX (W/cm**2) FOR FUEL TUBE  1:
                    Inner Cladding              Fuel Meat                 Fuel Meat               Outer Cladding
                    Inner Surface             Inner Surface             Outer Surface             Outer Surface
Temp Conds:    255.5750  =  255.5750      255.5750  =  255.5750      163.2578  =  163.2578       77.5479  =   77.5479
Flux Conds:   0.00000D+00= 0.00000D+00   0.00000D+00= 0.00000D+00   6.82093D+04= 6.82093D+04   5.30516D+04= 5.30516D+04

Here, positive heat flux means it is directed radially outward.
```

Figure 4.6 Solution of Radial Geometry Problem 2 Slightly Modified by Setting $h_1 = 10^{-6}$ W/m^2-°C, Obtained by the Standalone Routine SLICEHTR

```
Coolant Temperatures (C) of All Channels at the Center of Axial Node (Exact Solution by SLICE1):
            50.0000000092703300     71.5311004691985800

SLICEHTR: Power source in fuel+clad+coolant vs Power removed by coolant  9.000000D+03 9.000000D+03 W

q1``, q2``   =    2.0557501622937420D-04  5.3051647674456790D+04

Temp diff across tube thickness = 178.0270796225448

CHECKING BOUNDARY AND INTERFACE CONDITIONS ON TEMPERATURE (C) AND HEAT FLUX (W/cm**2) FOR FUEL TUBE  1:
                    Inner Cladding              Fuel Meat                 Fuel Meat               Outer Cladding
                    Inner Surface             Inner Surface             Outer Surface             Outer Surface
Temp Conds:    255.5750  =  255.5750      255.5750  =  255.5750      163.2578  =  163.2578       77.5479  =   77.5479
Flux Conds:  -2.05575D-04=-2.05575D-04  -6.85250D-05=-6.85250D-05   6.82093D+04= 6.82093D+04   5.30516D+04= 5.30516D+04

Here, positive heat flux means it is directed radially outward.
```

Figure 4.7 PLTEMP/ANL Version 3.2 Code Input Data for Radial Geometry Problem 2 Slightly Modified by Setting $h_1 = 10^{-6}$ W/m^2-°C

```
  Radial Geometry Test Problem 2: One fuel tube, Total power=9 kW, Length=60 cm  Card 100
! Tube radii: Ra=0.5 cm, Rb=1.5 cm, Rc=3.5 cm, Rd=4.5 cm
!234567890123456789012345678901234567890123456789012345678901234567890123456789 0
!  1   2   3   4   5   6   7   8   9  10  11  12  13  14  15  16  17  18
   0   0   5   1   0   0   1   1   1   1   0   0   0   0   2   1   0 200         Card 200
         1.0         1.0         1.0                                           Card 201
   1   3         0.0         1.0         1.0         1.0   0   1     1.0D-06    Card 300
         1.0         1.0         1.0                                           Card 300A
   1   2         1.0                                                           Card 301
   1   1   1                                                                   Card 302
        1.00                                                                   Card 303
         1.0         1.0         1.0         1.0         1.0         1.0       Card 304
         0.0         0.0        0.60         0.0         0.0         0.0       Card 304
         1.0         1.0         1.0         1.0         1.0         1.0       Card 304
         0.0         0.0         0.0                                           Card 305
   2   0         0.0        0.60         .01         7.0       0.020         8.0 Card 306
7.8539816D-5        0.01 .0314159265 .0314159265         1.0         1.0       Card 307
7.8539816D-5        0.01 .2827433388 .2827433388         1.0         1.0       Card 307
.15707963268                                                                   Card 308
.02500000000                                                                   Card 308A
         1.0                                                                   Card 309
      5.0D-2      5.0D-2                                                       Card 310
       0.1D0       0.001       0.2D0      9.0D-3      50.0D0                    Card 500
       0.0D0       0.0D0                                                       Card 500
   1      0.0001        36.8         0.0         1.0                           Card 600
  11                                                                           Card 700
      0.00D0      1.00D0                                                       Card 701
      0.10D0      1.00D0                                                       Card 701
      0.20D0      1.00D0                                                       Card 701
      0.30D0      1.00D0                                                       Card 701
      0.40D0      1.00D0                                                       Card 701
      0.50D0      1.00D0                                                       Card 701
      0.60D0      1.00D0                                                       Card 701
      0.70D0      1.00D0                                                       Card 701
      0.80D0      1.00D0                                                       Card 701
      0.90D0      1.00D0                                                       Card 701
      1.00D0      1.00D0                                                       Card 701
   0                                                                           Card 702
```

Figure 4.8 Solution of Radial Geometry Problem 2 Slightly Modified by Setting $h_1 = 10^{-6}$ W/m^2-°C, Obtained by the Broyden Method in PLTEMP/ANL Version 3.2

```
Node  1, Temp diff across plate thickness =  1.78027078280832D+02 L&R surf temps =  2.40727374372441D+02  6.27002960916090D+01
Node  2, Temp diff across plate thickness =  1.78027078274102D+02 L&R surf temps =  2.44681152384974D+02  6.66540741108715D+01
Node  3, Temp diff across plate thickness =  1.78027078268861D+02 L&R surf temps =  2.48669935856409D+02  7.06428575875474D+01
Node  4, Temp diff across plate thickness =  1.78027078263333D+02 L&R surf temps =  2.52675969763550D+02  7.46488915002179D+01
Node  5, Temp diff across plate thickness =  1.78027078256786D+02 L&R surf temps =  2.56718787261212D+02  7.86917090044256D+01
Node  6, Temp diff across plate thickness =  1.78027078250659D+02 L&R surf temps =  2.60786683822159D+02  8.27596055715000D+01
Node  7, Temp diff across plate thickness =  1.78027078244552D+02 L&R surf temps =  2.64875941026020D+02  8.68488627814688D+01
Node  8, Temp diff across plate thickness =  1.78027078238480D+02 L&R surf temps =  2.68982450728101D+02  9.09553724896214D+01
Node  9, Temp diff across plate thickness =  1.78027078232276D+02 L&R surf temps =  2.73101560972909D+02  9.50744827406335D+01
Node 10, Temp diff across plate thickness =  1.78027078226028D+02 L&R surf temps =  2.77229672643710D+02  9.92025944176820D+01
```

FUEL PLATE 1 (BroydenSoln)

NODE	COOLANT inner(C)	CladSurf inner(C)	FUEL PEAK (C)	CladSurf outer(C)	COOLANT outer(C)	HCOFinner W/C-m^2	HCOFouter W/C-m^2	ONBRin [F Note 1]	ONBRout	ETAin K-cm^3/J	ETAout K-cm^3/J	COOLNT at NodeOutlet inner(C)	outer(C)
	50.000				50.000								
1	50.000	240.727	240.727	62.700	52.153	1.0000E-06	5.0299E+03	0.36	5.66	2.318E+11	8.074E+02	50.000	54.306
2	50.000	244.681	244.681	66.654	56.459	1.0000E-06	5.2038E+03	0.35	4.22	2.217E+11	7.359E+02	50.000	58.612
3	50.000	248.670	248.670	70.643	60.766	1.0000E-06	5.3711E+03	0.33	3.32	2.117E+11	6.636E+02	50.000	62.919
4	50.000	252.676	252.676	74.649	65.072	1.0000E-06	5.5394E+03	0.32	2.71	2.018E+11	5.902E+02	50.000	67.225
5	50.000	256.719	256.719	78.692	69.378	1.0000E-06	5.6961E+03	0.30	2.27	1.920E+11	5.158E+02	50.000	71.531
6	50.000	260.787	260.787	82.760	73.684	1.0000E-06	5.8457E+03	0.29	1.93	1.823E+11	4.401E+02	50.000	75.837
7	50.000	264.876	264.876	86.849	77.990	1.0000E-06	5.9888E+03	0.27	1.66	1.726E+11	3.630E+02	50.000	80.144
8	50.000	268.982	268.982	90.955	82.297	1.0000E-06	6.1270E+03	0.26	1.44	1.628E+11	2.843E+02	50.000	84.450
9	50.000	273.102	273.102	95.074	86.603	1.0000E-06	6.2623E+03	0.24	1.26	1.529E+11	2.038E+02	50.000	88.756
10	50.000	277.230	277.230	99.203	90.909	1.0000E-06	6.3968E+03	0.22	1.10	1.429E+11	1.211E+02	50.000	93.062
	50.000				93.062								

Coolant temp rise (out - in) in channels = 1.88355713248711D-08 4.30622009381022D+01

[1] The ONB ratio is here defined as (Tonb - Tinlet)/(Tsurf - Tinlet). If the heat flux is negative (the coolant is hotter than the adjacent cladding surface), then the ONB ratio is arbitrarily set to 99.99 .

FUEL PLATE 1 (BroydenSoln) AREAL

NODE	FLUX inner MW/m^2	FLUX outer MW/m^2	FUEL X inner	Tsat (C)	Tdiff (C)	FUEL-CLADinterface inner (C)	outer (C)	Pressure (bar)	Z-mid	Z-int
1	1.9073E-10	5.3052E-02	0.0000	119.432	0.00	240.727	148.410	1.95000	0.0500	0.1000
2	1.9468E-10	5.3052E-02	0.0000	117.784	0.00	244.681	152.364	1.85000	0.1500	0.2000
3	1.9867E-10	5.3052E-02	0.0000	116.061	0.00	248.670	156.353	1.75000	0.2500	0.3000
4	2.0268E-10	5.3052E-02	0.0000	114.256	0.00	252.676	160.359	1.65000	0.3500	0.4000
5	2.0672E-10	5.3052E-02	0.0000	112.359	0.00	256.719	164.402	1.55000	0.4500	0.5000
6	2.1079E-10	5.3052E-02	0.0000	110.358	0.00	260.787	168.469	1.45000	0.5500	0.6000
7	2.1488E-10	5.3052E-02	0.0000	108.241	0.00	264.876	172.559	1.35000	0.6500	0.7000
8	2.1898E-10	5.3052E-02	0.0000	105.990	0.00	268.982	176.665	1.25000	0.7500	0.8000
9	2.2310E-10	5.3052E-02	0.0000	103.585	0.00	273.102	180.784	1.15000	0.8500	0.9000
10	2.2723E-10	5.3052E-02	0.0000	101.001	0.00	277.230	184.912	1.05000	0.9500	1.0000

Figure 4.9 Solution of Radial Geometry Problem 2 Slightly Modified by Setting $h_1 = 10^{-6}$ W/m^2-°C, Obtained by the Exact Method in PLTEMP/ANL Version 3.2

```
NPH = 7, Temp diff across tube thickness =  1.7802707964393580D+02
NPH = 7, Temp diff across tube thickness =  1.7802707963804910D+02
NPH = 7, Temp diff across tube thickness =  1.7802707963210740D+02
NPH = 7, Temp diff across tube thickness =  1.7802707962612240D+02
NPH = 7, Temp diff across tube thickness =  1.7802707962011370D+02
NPH = 7, Temp diff across tube thickness =  1.7802707961405150D+02
NPH = 7, Temp diff across tube thickness =  1.7802707960795520D+02
NPH = 7, Temp diff across tube thickness =  1.7802707960183100D+02
NPH = 7, Temp diff across tube thickness =  1.7802707959568550D+02
NPH = 7, Temp diff across tube thickness =  1.7802707958952400D+02
```

FUEL PLATE 1 (ExactSoln)

NODE	COOLANT inner(C)	CladSurf inner(C)	FUEL PEAK (C)	CladSurf outer(C)	COOLANT outer(C)	HCOFinner W/C-m^2	HCOFouter W/C-m^2	ONBRin [F Note 1]	ONBRout	ETAin K-cm^3/J	ETAout K-cm^3/J	COOLNT at inner(C)	NodeOutlet outer(C)
	50.000				50.000								
1	50.000	240.868	240.868	62.841	52.153	1.0000E-06	4.9638E+03	0.36	5.59	2.316E+11	8.074E+02	50.000	54.306
2	50.000	244.809	244.809	66.782	56.459	1.0000E-06	5.1395E+03	0.35	4.19	2.215E+11	7.359E+02	50.000	58.612
3	50.000	248.786	248.786	70.759	60.766	1.0000E-06	5.3085E+03	0.33	3.30	2.116E+11	6.636E+02	50.000	62.919
4	50.000	252.793	252.793	74.766	65.072	1.0000E-06	5.4726E+03	0.32	2.70	2.017E+11	5.902E+02	50.000	67.225
5	50.000	256.815	256.815	78.788	69.378	1.0000E-06	5.6377E+03	0.30	2.26	1.920E+11	5.158E+02	50.000	71.531
6	50.000	260.874	260.874	82.846	73.684	1.0000E-06	5.7902E+03	0.29	1.92	1.822E+11	4.401E+02	50.000	75.837
7	50.000	264.955	264.955	86.928	77.990	1.0000E-06	5.9361E+03	0.27	1.66	1.725E+11	3.630E+02	50.000	80.144
8	50.000	269.054	269.054	91.027	82.297	1.0000E-06	6.0765E+03	0.26	1.44	1.627E+11	2.843E+02	50.000	84.450
9	50.000	273.168	273.168	95.141	86.603	1.0000E-06	6.2133E+03	0.24	1.26	1.529E+11	2.038E+02	50.000	88.756
10	50.000	277.293	277.293	99.266	90.909	1.0000E-06	6.3482E+03	0.22	1.10	1.428E+11	1.211E+02	50.000	93.062
	50.000				93.062								

Coolant temp rise (out - in) in channels = 1.88443181059483D-08 4.30622009380935D+01

[1] The ONB ratio is here defined as (Tonb - Tinlet)/(Tsurf - Tinlet). If the heat flux is negative (the coolant is hotter than the adjacent cladding surface), then the ONB ratio is arbitrarily set to 99.99 .

FUEL PLATE 1 (ExactSoln)

NODE	FLUX inner MW/m^2	FLUX outer MW/m^2	AREAL FUEL X inner	Tsat (C)	Tdiff (C)	FUEL-CLADinterface inner (C)	outer (C)	Pressure (bar)	Z-mid	Z-int
1	1.9087E-10	5.3052E-02	0.0000	119.432		240.868	148.551	1.95000	0.0500	0.1000
2	1.9481E-10	5.3052E-02	0.0000	117.784		244.809	152.491	1.85000	0.1500	0.2000
3	1.9879E-10	5.3052E-02	0.0000	116.061		248.786	156.469	1.75000	0.2500	0.3000
4	2.0279E-10	5.3052E-02	0.0000	114.256		252.793	160.476	1.65000	0.3500	0.4000
5	2.0682E-10	5.3052E-02	0.0000	112.359		256.815	164.498	1.55000	0.4500	0.5000
6	2.1087E-10	5.3052E-02	0.0000	110.358		260.874	168.556	1.45000	0.5500	0.6000
7	2.1495E-10	5.3052E-02	0.0000	108.241		264.955	172.637	1.35000	0.6500	0.7000
8	2.1905E-10	5.3052E-02	0.0000	105.990		269.054	176.737	1.25000	0.7500	0.8000
9	2.2317E-10	5.3052E-02	0.0000	103.585		273.168	180.851	1.15000	0.8500	0.9000
10	2.2729E-10	5.3052E-02	0.0000	101.001		277.293	184.976	1.05000	0.9500	1.0000

Figure 4.10 Comparison of Solutions of Problem 2 by the Broyden Method with Improved Film Coefficient and the Exact Method (For Each Axial Node the Broyden Method is Followed by Exact Method)

```
FUEL PLATE   1 (BroydenSoln)
FUEL PLATE   1 (ExactSoln)
NODE    COOLANT             CladSurf            FUEL PEAK           CladSurf            COOLANT             HCOFinner           HCOFouter
        inner(C)            inner(C)               (C)              outer(C)            outer(C)            W/C-m^2             W/C-m^2
        50.000                                                                          50.000
   1  5.000000000086D+01  2.408679387878D+02  2.408679327685D+02  6.284084816924D+01  5.215311004699D+01  1.000000000000D-06  4.963786263200D+03
   1  5.000000000086D+01  2.408679278132D+02  2.408679279630D+02  6.284084816924D+01  5.215311004699D+01  1.000000000000D-06  4.963786263200D+03

   2  5.000000000260D+01  2.448086636406D+02  2.448086705129D+02  6.678159880489D+01  5.645933014094D+01  1.000000000000D-06  5.139533701612D+03
   2  5.000000000260D+01  2.448086784429D+02  2.448086785958D+02  6.678159880489D+01  5.645933014094D+01  1.000000000000D-06  5.139533701612D+03

   3  5.000000000437D+01  2.487863241341D+02  2.487863180811D+02  7.075923344748D+01  6.076555023486D+01  1.000000000000D-06  5.308518045486D+03
   3  5.000000000437D+01  2.487863130796D+02  2.487863132356D+02  7.075923344748D+01  6.076555023486D+01  1.000000000000D-06  5.308518045486D+03

   4  5.000000000619D+01  2.527928575830D+02  2.527928590708D+02  7.476578197768D+01  6.507177032874D+01  1.000000000000D-06  5.472620582252D+03
   4  5.000000000619D+01  2.527928616038D+02  2.527928617629D+02  7.476578197768D+01  6.507177032874D+01  1.000000000000D-06  5.472620582252D+03

   5  5.000000000803D+01  2.568152834519D+02  2.568152863527D+02  7.878821067221D+01  6.937799042259D+01  1.000000000000D-06  5.637662697246D+03
   5  5.000000000803D+01  2.568152902923D+02  2.568152904546D+02  7.878821067221D+01  6.937799042259D+01  1.000000000000D-06  5.637662697246D+03

   6  5.000000000992D+01  2.608735837414D+02  2.608735801704D+02  8.284649801797D+01  7.368421051640D+01  1.000000000000D-06  5.790218617854D+03
   6  5.000000000992D+01  2.608735776320D+02  2.608735777975D+02  8.284649801797D+01  7.368421051640D+01  1.000000000000D-06  5.790218617854D+03

   7  5.000000001184D+01  2.649545967321D+02  2.649546013745D+02  8.692752743504D+01  7.799043061017D+01  1.000000000000D-06  5.936116471920D+03
   7  5.000000001184D+01  2.649546070430D+02  2.649546072117D+02  8.692752743504D+01  7.799043061017D+01  1.000000000000D-06  5.936116471920D+03

   8  5.000000001379D+01  2.690543622609D+02  2.690543566559D+02  9.102727246865D+01  8.229665070391D+01  1.000000000000D-06  6.076502808431D+03
   8  5.000000001379D+01  2.690543520705D+02  2.690543522424D+02  9.102727246865D+01  8.229665070391D+01  1.000000000000D-06  6.076502808431D+03

   9  5.000000001579D+01  2.731683636709D+02  2.731683554766D+02  9.514126869991D+01  8.660287079761D+01  1.000000000000D-06  6.213302340719D+03
   9  5.000000001579D+01  2.731683482956D+02  2.731683484707D+02  9.514126869991D+01  8.660287079761D+01  1.000000000000D-06  6.213302340719D+03

  10  5.000000001782D+01  2.772931714088D+02  2.772931601897D+02  9.926607038775D+01  9.090909089127D+01  1.000000000000D-06  6.348184495870D+03
  10  5.000000001782D+01  2.772931689230D+02  2.772931691013D+02  9.926608933346D+01  9.090909089127D+01  1.000000000000D-06  6.348170104237D+03
        50.000                                                                          93.062
Coolant temp rise (out - in) in channels =  1.88442825788115D-08  4.30622009380935D+01
Coolant temp rise (out - in) in channels =  1.88443181059483D-08  4.30622009380935D+01
```

Figure 4.11 PLTEMP/ANL Version 3.2 Code Input Data for Radial Geometry Problem 3

```
  Radial Geometry Test Problem 3: One fuel tube, Total power=9 kW, Length=60 cm  Card 100
! Tube radii: Ra=0.5 cm, Rb=1.5 cm, Rc=3.5 cm, Rd=4.5 cm
!234567890123456789012345678901234567890123456789012345678901234567890123456789
!  1   2   3   4   5   6   7   8   9  10  11  12  13  14  15  16  17  18
   0   0   5   1   0   0   1   1   1   0   0   0   0   0   2   0   0  20         Card 200
         1.0         1.0         1.0                                           Card 201
   1   3         0.0         1.0         1.0         1.0   0   1     1.0D-06     Card 300
         1.0         1.0         1.0                                           Card 300A
   1   2         1.0                                                           Card 301
   1   1   1                                                                   Card 302
        1.00                                                                   Card 303
         1.0         1.0         1.0         1.0         1.0         1.0       Card 304
         0.0         0.0        0.60         0.0         0.0         0.0       Card 304
         1.0         1.0         1.0         1.0         1.0         1.0       Card 304
         0.0         0.0         0.0                                           Card 305
   2   0         0.0        0.60         .01         7.0       0.020         8.0 Card 306
7.8539816D-5        0.01 .0314159265 .0314159265         1.0         1.0       Card 307
7.8539816D-5        0.01 .2827433388 .2827433388         1.0         1.0       Card 307
.15707963268                                                                   Card 308
.02500000000                                                                   Card 308A
         1.0                                                                   Card 309
      5.0D-2      5.0D-2                                                       Card 310
       0.1D0       0.001       0.2D0      9.0D-3      50.0D0                    Card 500
       0.0D0       0.0D0                                                       Card 500
   1      0.0001        36.8         0.0         1.0                           Card 600
  11                                                                           Card 700
      0.00D0      1.00D0                                                       Card 701
      0.10D0      1.00D0                                                       Card 701
      0.20D0      1.00D0                                                       Card 701
      0.30D0      1.00D0                                                       Card 701
      0.40D0      1.00D0                                                       Card 701
      0.50D0      1.00D0                                                       Card 701
      0.60D0      1.00D0                                                       Card 701
      0.70D0      1.00D0                                                       Card 701
      0.80D0      1.00D0                                                       Card 701
      0.90D0      1.00D0                                                       Card 701
      1.00D0      1.00D0                                                       Card 701
   0                                                                           Card 702
```

Figure 4.12 Solution of Radial Geometry Problem 3 by the Broyden Method in PLTEMP/ANL Version 3.2

```
FUEL PLATE   1 (BroydenSoln)
NODE    COOLANT             CladSurf            FUEL PEAK           CladSurf            COOLANT             HCOFinner           HCOFouter
        inner(C)            inner(C)               (C)              outer(C)            outer(C)            W/C-m^2             W/C-m^2
        50.000                                                                          50.000
   1  5.000000000086D+01  2.408130311637D+02  2.408130313135D+02  6.278595288319D+01  5.214961306879D+01  1.000000000000D-06  4.987772918283D+03
   2  5.000000000259D+01  2.447422928116D+02  2.447422929644D+02  6.671521453693D+01  5.644883920635D+01  1.000000000000D-06  5.167514918088D+03
   3  5.000000000437D+01  2.487081790474D+02  2.487081792034D+02  7.068110077871D+01  6.074806534387D+01  1.000000000000D-06  5.340930073497D+03
   4  5.000000000617D+01  2.527025488215D+02  2.527025489806D+02  7.467547055880D+01  6.504729148136D+01  1.000000000000D-06  5.510039566974D+03
   5  5.000000000802D+01  2.567127611149D+02  2.567127612771D+02  7.868568285812D+01  6.934651761881D+01  1.000000000000D-06  5.680555629409D+03
   6  5.000000000990D+01  2.607584455871D+02  2.607584457525D+02  8.273136733630D+01  7.364574375623D+01  1.000000000000D-06  5.839076119120D+03
   7  5.000000001181D+01  2.648267104676D+02  2.648267106362D+02  8.679963222306D+01  7.794496989360D+01  1.000000000000D-06  5.991380100041D+03
   8  5.000000001377D+01  2.689135127894D+02  2.689135129613D+02  9.088643455104D+01  8.224419603095D+01  1.000000000000D-06  6.138646549671D+03
   9  5.000000001575D+01  2.730144349952D+02  2.730144351702D+02  9.498735676285D+01  8.654342216825D+01  1.000000000000D-06  6.282811298215D+03
  10  5.000000001778D+01  2.771261083709D+02  2.771261085491D+02  9.909903014458D+01  9.084264830552D+01  1.000000000000D-06  6.425532237486D+03
        50.000                                                                          92.992
Coolant temp rise (out - in) in channels =  1.88038029591553D-08  4.29922613741454D+01
```

```
FUEL PLATE   1 (BroydenSoln) AREAL                      FUEL-CLADinterface
NODE FLUX inner FLUX outer  FUEL X   Tsat     Tdiff     inner     outer    Pressure  Z-mid     Z-int
       MW/m^2     MW/m^2     inner   (C)       (C)       (C)       (C)      (bar)
   1 1.9081E-10 5.3052E-02  0.0000 119.432     0.00    240.813   148.496   1.95000   0.0500    0.1000
   2 1.9474E-10 5.3052E-02  0.0000 117.784     0.00    244.742   152.425   1.85000   0.1500    0.2000
   3 1.9871E-10 5.3052E-02  0.0000 116.061     0.00    248.708   156.391   1.75000   0.2500    0.3000
   4 2.0270E-10 5.3052E-02  0.0000 114.256     0.00    252.703   160.385   1.65000   0.3500    0.4000
   5 2.0671E-10 5.3052E-02  0.0000 112.359     0.00    256.713   164.396   1.55000   0.4500    0.5000
   6 2.1076E-10 5.3052E-02  0.0000 110.358     0.00    260.758   168.441   1.45000   0.5500    0.6000
   7 2.1483E-10 5.3052E-02  0.0000 108.241     0.00    264.827   172.509   1.35000   0.6500    0.7000
   8 2.1891E-10 5.3052E-02  0.0000 105.990     0.00    268.914   176.596   1.25000   0.7500    0.8000
   9 2.2301E-10 5.3052E-02  0.0000 103.585     0.00    273.014   180.697   1.15000   0.8500    0.9000
  10 2.2713E-10 5.3052E-02  0.0000 101.001     0.00    277.126   184.809   1.05000   0.9500    1.0000
```

Figure 4.13 Solution of Radial Geometry Problem 3 by the Exact Method in PLTEMP/ANL Version 3.2

FUEL PLATE 1 (ExactSoln)

NODE	COOLANT inner(C)	CladSurf inner(C)	FUEL PEAK (C)	CladSurf outer(C)	COOLANT outer(C)	HCOFinner W/C-m^2	HCOFouter W/C-m^2
	50.000				50.000		
1	5.000082986697D+01	2.408146262689D+02	2.408146264186D+02	6.278754662484D+01	5.215135742965D+01	1.000000000000D-06	4.987843550196D+03
2	5.000248959589D+01	2.447455662490D+02	2.447455664018D+02	6.671848661085D+01	5.645238559675D+01	1.000000000000D-06	5.167652997241D+03
3	5.000497916546D+01	2.487106748134D+02	2.487106749694D+02	7.068359518122D+01	6.075080931948D+01	1.000000000000D-06	5.341064270742D+03
4	5.000746872476D+01	2.527010494421D+02	2.527010496012D+02	7.467396981584D+01	6.504567660604D+01	1.000000000000D-06	5.509974251779D+03
5	5.000912842336D+01	2.567028724349D+02	2.567028725971D+02	7.867579281461D+01	6.933602948623D+01	1.000000000000D-06	5.680191864493D+03
6	5.001078811219D+01	2.607373849617D+02	2.607373851270D+02	8.271030534740D+01	7.362338697539D+01	1.000000000000D-06	5.838244111127D+03
7	5.001244779101D+01	2.647904765363D+02	2.647904767049D+02	8.676339692812D+01	7.790677928927D+01	1.000000000000D-06	5.990057360108D+03
8	5.001410745980D+01	2.688581330139D+02	2.688581331857D+02	9.083105341180D+01	8.218605489029D+01	1.000000000000D-06	6.136686725952D+03
9	5.001576711883D+01	2.729357841035D+02	2.729357842785D+02	9.490870450748D+01	8.646105771571D+01	1.000000000000D-06	6.280050406940D+03
10	5.001825658304D+01	2.770190455049D+02	2.770190456831D+02	9.899196591498D+01	9.073079758482D+01	1.000000000000D-06	6.421809307311D+03
	50.020				92.865		

Coolant temp rise (out - in) in channels = 1.99162201240739D-02 4.28645368259166D+01

FUEL PLATE 1 (ExactSoln)

NODE	FLUX inner MW/m^2	FLUX outer MW/m^2	AREAL FUEL X inner	Tsat (C)	Tdiff (C)	FUEL-CLADinterface inner (C)	outer (C)	Pressure (bar)	Z-mid	Z-int
1	1.9081E-10	5.3052E-02	0.0000	119.432		240.815	148.497	1.95000	0.0500	0.1000
2	1.9474E-10	5.3052E-02	0.0000	117.784		244.746	152.428	1.85000	0.1500	0.2000
3	1.9871E-10	5.3052E-02	0.0000	116.061		248.711	156.393	1.75000	0.2500	0.3000
4	2.0269E-10	5.3052E-02	0.0000	114.256		252.701	160.384	1.65000	0.3500	0.4000
5	2.0669E-10	5.3052E-02	0.0000	112.359		256.703	164.386	1.55000	0.4500	0.5000
6	2.1073E-10	5.3052E-02	0.0000	110.358		260.737	168.420	1.45000	0.5500	0.6000
7	2.1478E-10	5.3052E-02	0.0000	108.241		264.790	172.473	1.35000	0.6500	0.7000
8	2.1884E-10	5.3052E-02	0.0000	105.990		268.858	176.541	1.25000	0.7500	0.8000
9	2.2292E-10	5.3052E-02	0.0000	103.585		272.936	180.619	1.15000	0.8500	0.9000
10	2.2700E-10	5.3052E-02	0.0000	101.001		277.019	184.702	1.05000	0.9500	1.0000

Figure 4.14 Input Data for Radial Geometry Problem 4 for PLTEMP Versions 3.1 and 3.2

```
  Radial Geometry Test Problem 4: One fuel tube, Total power=9 kW, Length=60 cm  Card 100
! Tube radii: Ra=0.5 cm, Rb=1.5 cm, Rc=3.5 cm, Rd=4.5 cm
!234567890123456789012345678901234567890123456789012345678901234567890123456789 0
!  1   2   3   4   5   6   7   8   9  10  11  12  13  14  15  16  17  18
   0   0   5   1   0   0   1   1   1   0   0   0   0   0   2   0   0   0         Card 200
         1.0         1.0         1.0                                           Card 201
   1   3         0.0         1.0         1.0         1.0   0   3     1.0D+03     Card 300
         1.0         1.0         1.0                                           Card 300A
   1   2         1.0                                                           Card 301
   1   1   1                                                                   Card 302
        1.00                                                                   Card 303
         1.0         1.0         1.0         1.0         1.0         1.0       Card 304
         0.0         0.0        0.60         0.0         0.0         0.0       Card 304
         1.0         1.0         1.0         1.0         1.0         1.0       Card 304
         0.0         0.0         0.0                                           Card 305
   2   0         0.0        0.60         .01         7.0       0.020         8.0 Card 306
7.8539816D-5        0.01 .0314159265 .0314159265         1.0         1.0         Card 307
7.8539816D-5        0.01 .2827433388 .2827433388         1.0         1.0         Card 307
.15707963268                                                                   Card 308
.02500000000                                                                   Card 308A
         1.0                                                                   Card 309
      5.0D-2      5.0D-2                                                       Card 310
       0.1D0       0.001       0.2D0      9.0D-3      50.0D0                    Card 500
       0.0D0       0.0D0                                                       Card 500
   1      0.0001        36.8         0.0         1.0                           Card 600
  11                                                                           Card 700
      0.00D0      1.00D0                                                       Card 701
      0.10D0      1.00D0                                                       Card 701
      0.20D0      1.00D0                                                       Card 701
      0.30D0      1.00D0                                                       Card 701
      0.40D0      1.00D0                                                       Card 701
      0.50D0      1.00D0                                                       Card 701
      0.60D0      1.00D0                                                       Card 701
      0.70D0      1.00D0                                                       Card 701
      0.80D0      1.00D0                                                       Card 701
      0.90D0      1.00D0                                                       Card 701
      1.00D0      1.00D0                                                       Card 701
   0                                                                           Card 702
```

Figure 4.15 Solution of Radial Geometry Problem 4 by the Broyden Method in PLTEMP/ANL Version 3.1

FUEL PLATE 1 (BroydenSoln)

NODE	COOLANT outer(C)	CladSurf outer(C)	FUEL PEAK (C)	CladSurf inner(C)	COOLANT inner(C)	HCOFouter W/C-m^2	HCOFinner W/C-m^2	ONBRout [F Note 1]	ONBRin	ETAout K-cm^3/J	ETAin K-cm^3/J	COOLNT at outer(C)	NodeOutlet inner(C)
	50.000				50.000								
1	51.505	88.641	257.304	193.884	50.645	1.0000E+03	1.0000E+03	1.85	0.51	1.184E+03	3.108E+02	53.009	51.290
2	54.514	91.650	259.454	195.174	51.935	1.0000E+03	1.0000E+03	1.68	0.49	1.103E+03	2.976E+02	56.019	52.580
3	57.524	94.660	261.603	196.464	53.224	1.0000E+03	1.0000E+03	1.53	0.48	1.020E+03	2.839E+02	59.028	53.869
4	60.533	97.669	263.753	197.754	54.514	1.0000E+03	1.0000E+03	1.39	0.46	9.364E+02	2.700E+02	62.038	55.159
5	63.543	100.679	265.903	199.043	55.804	1.0000E+03	1.0000E+03	1.28	0.45	8.508E+02	2.556E+02	65.047	56.449
6	66.552	103.688	268.052	200.333	57.094	1.0000E+03	1.0000E+03	1.17	0.43	7.635E+02	2.407E+02	68.057	57.739
7	69.561	106.698	270.202	201.623	58.383	1.0000E+03	1.0000E+03	1.07	0.41	6.742E+02	2.253E+02	71.066	59.028
8	72.571	109.707	272.352	202.913	59.673	1.0000E+03	1.0000E+03	0.98	0.40	5.825E+02	2.093E+02	74.076	60.318
9	75.580	112.717	274.501	204.202	60.963	1.0000E+03	1.0000E+03	0.90	0.38	4.881E+02	1.926E+02	77.085	61.608
10	78.590	115.726	276.651	205.492	62.253	1.0000E+03	1.0000E+03	0.82	0.36	3.906E+02	1.751E+02	80.095	62.898
	80.095				62.898								

[1] The ONB ratio is here defined as (Tonb - Tinlet)/(Tsurf - Tinlet). If the heat flux is negative (the coolant is hotter than the adjacent cladding surface), then the ONB ratio is arbitrarily set to 99.99 .

FUEL PLATE 1 (BroydenSoln)

NODE	AREAL FLUX outer MW/m^2	FLUX inner MW/m^2	FUEL X outer	Tsat (C)	Tdiff (C)	FUEL-CLADinterface outer (C)	inner (C)	Pressure (bar)	Z-mid	Z-int
1	3.7136E-02	1.4324E-01	0.7000	119.432	-141.19	148.638	306.288	1.95000	0.0500	0.1000
2	3.7136E-02	1.4324E-01	0.7000	117.784	-139.47	151.647	307.577	1.85000	0.1500	0.2000
3	3.7136E-02	1.4324E-01	0.7000	116.061	-137.75	154.657	308.867	1.75000	0.2500	0.3000
4	3.7136E-02	1.4324E-01	0.7000	114.256	-136.03	157.666	310.157	1.65000	0.3500	0.4000
5	3.7136E-02	1.4324E-01	0.7000	112.359	-134.31	160.676	311.447	1.55000	0.4500	0.5000
6	3.7136E-02	1.4324E-01	0.7000	110.358	-132.59	163.685	312.736	1.45000	0.5500	0.6000
7	3.7136E-02	1.4324E-01	0.7000	108.241	-130.87	166.695	314.026	1.35000	0.6500	0.7000
8	3.7136E-02	1.4324E-01	0.7000	105.990	-129.15	169.704	315.316	1.25000	0.7500	0.8000
9	3.7136E-02	1.4324E-01	0.7000	103.585	-127.43	172.713	316.606	1.15000	0.8500	0.9000
10	3.7136E-02	1.4324E-01	0.7000	101.001	-125.71	175.723	317.896	1.05000	0.9500	1.0000

Figure 4.16 Solution of Radial Geometry Problem 4 by the Broyden Method in PLTEMP/ANL Version 3.2

FUEL PLATE 1 (BroydenSoln)

NODE	COOLANT inner(C)	CladSurf inner(C)	FUEL PEAK (C)	CladSurf outer(C)	COOLANT outer(C)	HCOFinner W/C-m^2	HCOFouter W/C-m^2	ONBRin [F Note 1]	ONBRout	ETAin K-cm^3/J	ETAout K-cm^3/J	COOLNT at inner(C)	NodeOutlet outer(C)
	50.000				50.000								
1	50.402	139.628	218.919	94.886	51.748	1.0000E+03	1.0000E+03	0.81	1.60	5.008E+02	1.016E+03	50.803	53.496
2	51.210	141.466	221.761	98.262	55.239	1.0000E+03	1.0000E+03	0.78	1.45	4.774E+02	9.410E+02	51.616	56.982
3	52.027	143.306	224.599	101.631	58.721	1.0000E+03	1.0000E+03	0.74	1.32	4.541E+02	8.649E+02	52.438	60.460
4	52.854	145.148	227.435	104.990	62.194	1.0000E+03	1.0000E+03	0.71	1.21	4.306E+02	7.874E+02	53.269	63.928
5	53.689	146.993	230.267	108.342	65.657	1.0000E+03	1.0000E+03	0.68	1.11	4.070E+02	7.082E+02	54.109	67.387
6	54.534	148.839	233.097	111.685	69.112	1.0000E+03	1.0000E+03	0.65	1.02	3.831E+02	6.271E+02	54.958	70.837
7	55.387	150.688	235.923	115.020	72.558	1.0000E+03	1.0000E+03	0.62	0.94	3.590E+02	5.439E+02	55.816	74.278
8	56.250	152.539	238.746	118.347	75.994	1.0000E+03	1.0000E+03	0.58	0.86	3.344E+02	4.584E+02	56.683	77.710
9	57.121	154.391	241.566	121.666	79.422	1.0000E+03	1.0000E+03	0.55	0.79	3.092E+02	3.702E+02	57.559	81.134
10	58.002	156.246	244.382	124.977	82.841	1.0000E+03	1.0000E+03	0.52	0.72	2.833E+02	2.790E+02	58.444	84.548
	58.444				84.548								

[1] The ONB ratio is here defined as (Tonb - Tinlet)/(Tsurf - Tinlet). If the heat flux is negative (the coolant is hotter than the adjacent cladding surface), then the ONB ratio is arbitrarily set to 99.99 .

FUEL PLATE 1 (BroydenSoln) AREAL

NODE	FLUX inner MW/m^2	FLUX outer MW/m^2	FUEL X inner	Tsat (C)	Tdiff (C)	FUEL-CLADinterface inner (C)	FUEL-CLADinterface outer (C)	Pressure (bar)	Z-mid	Z-int
1	8.9226E-02	4.3138E-02	0.1869	119.432	0.00	209.645	164.578	1.95000	0.0500	0.1000
2	9.0256E-02	4.3023E-02	0.1890	117.784	0.00	212.292	167.770	1.85000	0.1500	0.2000
3	9.1279E-02	4.2910E-02	0.1912	116.061	0.00	214.934	170.955	1.75000	0.2500	0.3000
4	9.2295E-02	4.2797E-02	0.1933	114.256	0.00	217.574	174.132	1.65000	0.3500	0.4000
5	9.3304E-02	4.2685E-02	0.1954	112.359	0.00	220.210	177.303	1.55000	0.4500	0.5000
6	9.4306E-02	4.2573E-02	0.1975	110.358	0.00	222.843	180.466	1.45000	0.5500	0.6000
7	9.5301E-02	4.2463E-02	0.1996	108.241	0.00	225.472	183.623	1.35000	0.6500	0.7000
8	9.6289E-02	4.2353E-02	0.2017	105.990	0.00	228.099	186.772	1.25000	0.7500	0.8000
9	9.7270E-02	4.2244E-02	0.2037	103.585	0.00	230.722	189.915	1.15000	0.8500	0.9000
10	9.8245E-02	4.2136E-02	0.2058	101.001	0.00	233.341	193.051	1.05000	0.9500	1.0000

Figure 4.17 Solution of Radial Geometry Problem 4 by the Exact Method in PLTEMP/ANL Version 3.2

FUEL PLATE 1 (ExactSoln)

NODE	COOLANT inner(C)	CladSurf inner(C)	FUEL PEAK (C)	CladSurf outer(C)	COOLANT outer(C)	HCOFinner W/C-m^2	HCOFouter W/C-m^2	ONBRin [F Note 1]	ONBRout	ETAin K-cm^3/J	ETAout K-cm^3/J	COOLNT at inner(C)	NodeOutlet outer(C)
	50.000				50.000								
1	50.403	139.629	218.921	94.888	51.750	1.0000E+03	1.0000E+03	0.81	1.60	5.008E+02	1.016E+03	50.806	53.500
2	51.214	141.470	221.766	98.268	55.245	1.0000E+03	1.0000E+03	0.78	1.45	4.774E+02	9.409E+02	51.622	56.990
3	52.034	143.313	224.606	101.638	58.728	1.0000E+03	1.0000E+03	0.74	1.32	4.540E+02	8.648E+02	52.445	60.467
4	52.862	145.156	227.441	104.996	62.199	1.0000E+03	1.0000E+03	0.71	1.21	4.306E+02	7.873E+02	53.278	63.931
5	53.700	147.000	230.271	108.344	65.659	1.0000E+03	1.0000E+03	0.68	1.11	4.069E+02	7.081E+02	54.122	67.386
6	54.547	148.846	233.097	111.682	69.108	1.0000E+03	1.0000E+03	0.65	1.02	3.831E+02	6.271E+02	54.973	70.830
7	55.403	150.693	235.918	115.010	72.546	1.0000E+03	1.0000E+03	0.62	0.94	3.589E+02	5.441E+02	55.833	74.261
8	56.268	152.541	238.732	118.325	75.971	1.0000E+03	1.0000E+03	0.58	0.86	3.343E+02	4.588E+02	56.703	77.680
9	57.141	154.389	241.542	121.631	79.384	1.0000E+03	1.0000E+03	0.55	0.79	3.091E+02	3.708E+02	57.580	81.089
10	58.023	156.238	244.346	124.925	82.786	1.0000E+03	1.0000E+03	0.52	0.72	2.832E+02	2.798E+02	58.466	84.484
	58.466				84.484								

[1] The ONB ratio is here defined as (Tonb - Tinlet)/(Tsurf - Tinlet). If the heat flux is negative (the coolant is hotter than the adjacent cladding surface), then the ONB ratio is arbitrarily set to 99.99 .

FUEL PLATE 1 (ExactSoln)

NODE	FLUX inner MW/m^2	FLUX outer MW/m^2	AREAL FUEL X inner	Tsat (C)	Tdiff (C)	FUEL-CLADinterface inner (C)	outer (C)	Pressure (bar)	Z-mid	Z-int
1	8.9226E-02	4.3138E-02	0.1869	119.432		209.647	164.581	1.95000	0.0500	0.1000
2	9.0257E-02	4.3023E-02	0.1890	117.784		212.297	167.776	1.85000	0.1500	0.2000
3	9.1279E-02	4.2910E-02	0.1912	116.061		214.942	170.962	1.75000	0.2500	0.3000
4	9.2294E-02	4.2797E-02	0.1933	114.256		217.580	174.138	1.65000	0.3500	0.4000
5	9.3300E-02	4.2685E-02	0.1954	112.359		220.215	177.305	1.55000	0.4500	0.5000
6	9.4299E-02	4.2574E-02	0.1975	110.358		222.845	180.465	1.45000	0.5500	0.6000
7	9.5290E-02	4.2464E-02	0.1996	108.241		225.469	183.614	1.35000	0.6500	0.7000
8	9.6273E-02	4.2355E-02	0.2016	105.990		228.088	186.753	1.25000	0.7500	0.8000
9	9.7248E-02	4.2246E-02	0.2037	103.585		230.702	189.884	1.15000	0.8500	0.9000
10	9.8216E-02	4.2139E-02	0.2057	101.001		233.311	193.004	1.05000	0.9500	1.0000

Figure 4.18 PLTEMP/ANL Version 3.2 Code Input Data for Slab Geometry Problem 5 Using the Slab Geometry Exact Method

```
  Slab Geometry Test Problem 5: One fuel tube, Total power=9 kW, Length=60 cm    Card 100
! Tube radii: Ra=0.5 cm, Rb=1.5 cm, Rc=3.5 cm, Rd=4.5 cm
!234567890123456789012345678901234567890123456789012345678901234567890123456789
!  1   2   3   4   5   6   7   8   9  10  11  12  13  14  15  16  17  18
   0   0   5   1   0   0   1   1   0   0   0   0   0   0   2   0   0   0         Card 200
         1.0         1.0         1.0                                           Card 201
   1   3         0.0         1.0         1.0         1.0   0   1     1.0D-06     Card 300
         1.0         1.0         1.0                                           Card 300A
   1   2         1.0                                                           Card 301
   1   1   1                                                                   Card 302
        1.00                                                                   Card 303
         1.0         1.0         1.0         1.0         1.0         1.0       Card 304
         0.0         0.0        0.60         0.0         0.0         0.0       Card 304
         1.0         1.0         1.0         1.0         1.0         1.0       Card 304
         0.0         0.0         0.0                                           Card 305
   2   0         0.0        0.60         .01         7.0       0.020         8.0 Card 306
7.8539816D-5        0.01 .0314159265 .0314159265         1.0         1.0       Card 307
7.8539816D-5        0.01 .2827433388 .2827433388         1.0         1.0       Card 307
.15707963268                                                                   Card 308
.02500000000                                                                   Card 308A
         1.0                                                                   Card 309
      5.0D-2      5.0D-2                                                       Card 310
       0.1D0       0.001       0.2D0      9.0D-3      50.0D0                    Card 500
       0.0D0       0.0D0                                                       Card 500
   1      0.0001        36.8         0.0         1.0                           Card 600
  11                                                                           Card 700
      0.00D0      1.00D0                                                       Card 701
      0.10D0      1.00D0                                                       Card 701
      0.20D0      1.00D0                                                       Card 701
      0.30D0      1.00D0                                                       Card 701
      0.40D0      1.00D0                                                       Card 701
      0.50D0      1.00D0                                                       Card 701
      0.60D0      1.00D0                                                       Card 701
      0.70D0      1.00D0                                                       Card 701
      0.80D0      1.00D0                                                       Card 701
      0.90D0      1.00D0                                                       Card 701
      1.00D0      1.00D0                                                       Card 701
   0                                                                           Card 702
```

Figure 4.19 PLTEMP/ANL Version 3.2 Code Input Data for Slab Geometry Problem 5 Using the Radial Geometry Exact Method with a Mean Tube Radius of 1000 m

```
  Slab Geometry Test Problem 5: One fuel tube, Total power=9 kW, Length=60 cm    Card 100
! Using Radial Geometry Exact Method with Infinite Tube Radius
! Tube radii: Ra=0.5 cm, Rb=1.5 cm, Rc=3.5 cm, Rd=4.5 cm
!234567890123456789012345678901234567890123456789012345678901234567890123456789
!  1   2   3   4   5   6   7   8   9  10  11  12  13  14  15  16  17  18
   0   0   5   1   0   0   1   1   1   0   0   0   0   0   2   0   0   0         Card 200
         1.0         1.0         1.0                                           Card 201
   1   3         0.0         1.0         1.0         1.0   0   1     1.0D-06    Card 300
         1.0         1.0         1.0                                           Card 300A
   1   2         1.0                                                           Card 301
   1   1   1                                                                   Card 302
        1.00                                                                   Card 303
         1.0         1.0         1.0         1.0         1.0         1.0       Card 304
         0.0         0.0        0.60         0.0         0.0         0.0       Card 304
         1.0         1.0         1.0         1.0         1.0         1.0       Card 304
         0.0         0.0         0.0                                           Card 305
   2   0         0.0        0.60         .01         7.0       0.020         8.0 Card 306
7.8539816D-5        0.01 .0314159265 .0314159265         1.0         1.0       Card 307
7.8539816D-5        0.01 .2827433388 .2827433388         1.0         1.0       Card 307
.15707963268                                                                   Card 308
1000.0000000                                                                   Card 308A
         1.0                                                                   Card 309
      5.0D-2      5.0D-2                                                       Card 310
       0.1D0       0.001       0.2D0      9.0D-3      50.0D0                    Card 500
       0.0D0       0.0D0                                                       Card 500
   1      0.0001        36.8         0.0         1.0                           Card 600
  11                                                                           Card 700
      0.00D0      1.00D0                                                       Card 701
      0.10D0      1.00D0                                                       Card 701
      0.20D0      1.00D0                                                       Card 701
      0.30D0      1.00D0                                                       Card 701
      0.40D0      1.00D0                                                       Card 701
      0.50D0      1.00D0                                                       Card 701
      0.60D0      1.00D0                                                       Card 701
      0.70D0      1.00D0                                                       Card 701
      0.80D0      1.00D0                                                       Card 701
      0.90D0      1.00D0                                                       Card 701
      1.00D0      1.00D0                                                       Card 701
   0                                                                           Card 702
```

Figure 4.20 Solution of Slab Geometry Problem 5 by the <u>Slab Geometry</u> Exact Method in PLTEMP/ANL Version 3.2

FUEL PLATE 1 (ExactSoln)

NODE	COOLANTl (C)	CladSl (C)	FUEL PEAK (C)	CladSr (C)	COOLANTr (C)	HCOFl W/C-m^2	HCOFr W/C-m^2	ONBRl [F Note 1]	ONBRr	ETA'l K-cm^3/J	ETA'r K-cm^3/J	COOLNT at NodeOutlet left(C)	right(C)
	50.000				50.000								
1	50.001	326.776	326.776	70.991	52.151	1.0000E-06	5.0688E+03	0.25	3.46	3.231E+12	4.560E+02	50.002	54.303
2	50.002	330.454	330.454	74.669	56.452	1.0000E-06	5.2420E+03	0.24	2.88	3.113E+12	4.157E+02	50.003	58.602
3	50.005	334.184	334.184	78.399	60.751	1.0000E-06	5.4109E+03	0.23	2.44	2.994E+12	3.749E+02	50.007	62.900
4	50.007	337.957	337.957	82.172	65.046	1.0000E-06	5.5757E+03	0.22	2.10	2.874E+12	3.336E+02	50.008	67.192
5	50.009	341.750	341.750	85.965	69.336	1.0000E-06	5.7426E+03	0.21	1.83	2.753E+12	2.916E+02	50.010	71.480
6	50.011	345.598	345.598	89.814	73.623	1.0000E-06	5.8981E+03	0.20	1.61	2.630E+12	2.490E+02	50.012	75.767
7	50.012	349.479	349.479	93.694	77.907	1.0000E-06	6.0487E+03	0.19	1.42	2.505E+12	2.056E+02	50.013	80.047
8	50.014	353.385	353.385	97.600	82.186	1.0000E-06	6.1951E+03	0.18	1.26	2.377E+12	1.613E+02	50.015	84.325
9	50.016	357.313	357.313	101.528	86.461	1.0000E-06	6.3379E+03	0.17	1.12	2.246E+12	1.161E+02	50.017	88.597
10	50.018	361.345	361.345	105.560	90.731	1.0000E-06	6.4396E+03	0.16	1.00	2.110E+12	6.961E+01	50.020	92.865
	50.020				92.865								

[1] The ONB ratio is here defined as (Tonb - Tinlet)/(Tsurf - Tinlet). If the heat flux is negative (the coolant is hotter than the adjacent cladding surface), then the ONB ratio is arbitrarily set to 99.99 .

FUEL PLATE 1 (ExactSoln)

NODE	FLUX left MW/m^2	FLUX right MW/m^2	AREAL FUEL X left	Tsat (C)	Tdiff (C)	FUEL-CLADinterface left (C)	right (C)	Pressure (bar)	Z-mid	Z-int
1	2.7677E-10	9.5493E-02	0.0000	119.432		326.776	207.409	1.95000	0.0500	0.1000
2	2.8045E-10	9.5493E-02	0.0000	117.784		330.454	211.088	1.85000	0.1500	0.2000
3	2.8418E-10	9.5493E-02	0.0000	116.061		334.184	214.818	1.75000	0.2500	0.3000
4	2.8795E-10	9.5493E-02	0.0000	114.256		337.957	218.591	1.65000	0.3500	0.4000
5	2.9174E-10	9.5493E-02	0.0000	112.359		341.750	222.384	1.55000	0.4500	0.5000
6	2.9559E-10	9.5493E-02	0.0000	110.358		345.598	226.232	1.45000	0.5500	0.6000
7	2.9947E-10	9.5493E-02	0.0000	108.241		349.479	230.113	1.35000	0.6500	0.7000
8	3.0337E-10	9.5493E-02	0.0000	105.990		353.385	234.019	1.25000	0.7500	0.8000
9	3.0730E-10	9.5493E-02	0.0000	103.585		357.313	237.946	1.15000	0.8500	0.9000
10	3.1133E-10	9.5493E-02	0.0000	101.001		361.345	241.978	1.05000	0.9500	1.0000

Figure 4.21 Solution of Slab Geometry Problem 5 by the <u>Radial Geometry</u> Exact Method in PLTEMP/ANL Version 3.2 (Using a Mean Tube Radius of 1000 m)

FUEL PLATE 1 (ExactSoln)

NODE	COOLANT inner(C)	CladSurf inner(C)	FUEL PEAK (C)	CladSurf outer(C)	COOLANT outer(C)	HCOFinner W/C-m^2	HCOFouter W/C-m^2	ONBRin [F Note 1]	ONBRout	ETAin K-cm^3/J	ETAout K-cm^3/J	COOLNT at inner(C)	NodeOutlet outer(C)
	50.000				50.000								
1	50.001	326.772	326.772	70.990	52.151	1.0000E-06	5.0688E+03	0.25	3.46	1.624E+11	4.560E+02	50.002	54.303
2	50.002	330.451	330.451	74.669	56.452	1.0000E-06	5.2420E+03	0.24	2.88	1.564E+11	4.157E+02	50.003	58.602
3	50.005	334.181	334.181	78.399	60.751	1.0000E-06	5.4109E+03	0.23	2.44	1.505E+11	3.749E+02	50.007	62.900
4	50.007	337.954	337.954	82.172	65.046	1.0000E-06	5.5757E+03	0.22	2.10	1.444E+11	3.336E+02	50.008	67.192
5	50.009	341.747	341.747	85.965	69.336	1.0000E-06	5.7425E+03	0.21	1.83	1.383E+11	2.916E+02	50.010	71.480
6	50.011	345.595	345.595	89.813	73.623	1.0000E-06	5.8981E+03	0.20	1.61	1.321E+11	2.490E+02	50.012	75.767
7	50.012	349.476	349.476	93.694	77.907	1.0000E-06	6.0487E+03	0.19	1.42	1.259E+11	2.056E+02	50.013	80.047
8	50.014	353.382	353.382	97.600	82.186	1.0000E-06	6.1951E+03	0.18	1.26	1.194E+11	1.613E+02	50.015	84.325
9	50.016	357.310	357.310	101.528	86.461	1.0000E-06	6.3379E+03	0.17	1.12	1.128E+11	1.161E+02	50.017	88.597
10	50.018	361.341	361.341	105.559	90.731	1.0000E-06	6.4396E+03	0.16	1.00	1.060E+11	6.962E+01	50.020	92.865
	50.020				92.865								

[1] The ONB ratio is here defined as (Tonb - Tinlet)/(Tsurf - Tinlet). If the heat flux is negative (the coolant is hotter than the adjacent cladding surface), then the ONB ratio is arbitrarily set to 99.99 .

FUEL PLATE 1 (ExactSoln)

NODE	FLUX inner MW/m^2	FLUX outer MW/m^2	AREAL FUEL X inner	Tsat (C)	Tdiff (C)	FUEL-CLADinterface inner (C)	outer (C)	Pressure (bar)	Z-mid	Z-int
1	2.7677E-10	9.5491E-02	0.0000	119.432		326.772	207.407	1.95000	0.0500	0.1000
2	2.8045E-10	9.5491E-02	0.0000	117.784		330.451	211.085	1.85000	0.1500	0.2000
3	2.8418E-10	9.5491E-02	0.0000	116.061		334.181	214.815	1.75000	0.2500	0.3000
4	2.8795E-10	9.5491E-02	0.0000	114.256		337.954	218.588	1.65000	0.3500	0.4000
5	2.9174E-10	9.5491E-02	0.0000	112.359		341.747	222.381	1.55000	0.4500	0.5000
6	2.9558E-10	9.5491E-02	0.0000	110.358		345.595	226.230	1.45000	0.5500	0.6000
7	2.9946E-10	9.5491E-02	0.0000	108.241		349.476	230.110	1.35000	0.6500	0.7000
8	3.0337E-10	9.5491E-02	0.0000	105.990		353.382	234.017	1.25000	0.7500	0.8000
9	3.0729E-10	9.5491E-02	0.0000	103.585		357.310	237.944	1.15000	0.8500	0.9000
10	3.1132E-10	9.5491E-02	0.0000	101.001		361.341	241.976	1.05000	0.9500	1.0000

Figure 4.22 Input Data File for the Hungarian Reactor Benchmark Problem for PLTEMP/ANL Code Versions 3.1 and 3.2

```
! September 13, 2006
Hungarian Reactor Benchmark Problem;  90 kW                                    Card 100
   0   0   5   1   0   0   0   0   1   0   0   0   0   0   1   1   0 200       Card 200
   1   3        0.0        1.0        1.0        1.0   0   0                 Card 300
   1   2        1.0                                                           Card 301
   1   1   1                                                                  Card 302
        1.53                                                                  Card 303
        1.0        1.0        1.0        1.0        1.0        1.0           Card 304
        1.0        1.0        1.0        1.0        1.0        1.0           Card 304
        1.0        1.0        1.0        1.0        1.0        1.0           Card 304
        0.0        0.0        0.0                                             Card 305
   4   0        0.0        0.58     0.76e-3        206.     0.98e-3        180. Card 306
  2.8274E-05  6.0000E-03  1.8850E-02  1.8850E-02        1.0        1.0         Card 307
  1.3195E-04  6.0000E-03  8.7965E-02  8.7965E-02        1.0        1.0         Card 307
  2.5015E-04  6.1964E-03  1.6148E-01  1.6148E-01        1.0        1.0         Card 307
  1.8003E-04  6.6631E-03  1.0808E-01  1.0808E-01        1.0        1.0         Card 307
  2.6704E-02  6.1261E-02  1.0022E-01                                            Card 308
   0.0042500   0.0097500   0.0159511                                            Card 308A
        1.0        1.0        1.0                                             Card 309
  7.8065E-02  3.6415E-01  7.0516E-01  5.1356E-01                                Card 310
      0.127       0.001       0.130      90.e-3        50.                     Card 500
        0.0        0.0                                                         Card 500
   1      0.0001        36.8        0.0        1.0                            Card 600
  -9                                                                          Card 700
      0.000      0.0625     0.30448                                            Card 701
      0.125      0.1875     0.86709                                            Card 701
      0.250      0.3125     1.29769                                            Card 701
      0.375      0.4375     1.53073                                            Card 701
      0.500      0.5625     1.53073                                            Card 701
      0.625      0.6875     1.29769                                            Card 701
      0.750      0.8125     0.86709                                            Card 701
      0.875      0.9375     0.30448                                            Card 701
      1.000                                                                    Card 701
   0                                                                          Card 702
```

Figure 4.23 Comparison of Solutions of Hungarian Reactor Benchmark Problem Using Constant Coolant Specific Heat Option ICP = 1 by PLTEMP/ANL Version 3.2 (For Each Axial Node Broyden Method is Followed by Exact Method)

```
FUEL PLATE   1 (BroydenSoln)
FUEL PLATE   1 (ExactSoln)
NODE    COOLANT             CladSurf            FUEL PEAK           CladSurf            COOLANT             HCOFinner           HCOFouter
        inner(C)            inner(C)               (C)              outer(C)            outer(C)            W/C-m^2             W/C-m^2
        50.000                                                                          50.000
   1  5.026788168178D+01  5.763033403660D+01  5.815674542593D+01  5.741790622196D+01  5.026207746876D+01  1.737546797787D+04  1.736044227160D+04
   1  5.026788168178D+01  5.763033403660D+01  5.815674238644D+01  5.741790622196D+01  5.026207746876D+01  1.737546797787D+04  1.736044227160D+04

   2  5.129912585683D+01  7.156699603522D+01  7.306725519855D+01  7.096425694763D+01  5.127033738507D+01  1.798617003496D+04  1.795706158604D+04
   2  5.129912585683D+01  7.156699603522D+01  7.306724654413D+01  7.096425694763D+01  5.127033738507D+01  1.798617003496D+04  1.795706158604D+04

   3  5.320520901445D+01  8.264683041186D+01  8.489275304379D+01  8.174596745034D+01  5.313286079191D+01  1.853507502551D+04  1.849488203967D+04
   3  5.320520899932D+01  8.264683000694D+01  8.489274004557D+01  8.174596776521D+01  5.313286089371D+01  1.853507502551D+04  1.849488203967D+04

   4  5.569575227254D+01  8.955443068083D+01  9.220342425820D+01  8.849130790231D+01  5.556537428244D+01  1.900985134219D+04  1.895945257020D+04
   4  5.569575224228D+01  8.955443065057D+01  9.220340906724D+01  8.849130810591D+01  5.556537448604D+01  1.900985134219D+04  1.895945257020D+04

   5  5.839057541372D+01  9.159689947923D+01  9.424397306363D+01  9.053012017051D+01  5.819669872016D+01  1.937148707849D+04  1.931350829851D+04
   5  5.839057538346D+01  9.159689944897D+01  9.424395787045D+01  9.053012037411D+01  5.819669892377D+01  1.937148707849D+04  1.931350829851D+04

   6  6.087764969365D+01  8.869923970638D+01  9.093898179580D+01  8.778660352537D+01  6.062521504470D+01  1.956892568815D+04  1.950877827538D+04
   6  6.087764966339D+01  8.869923967612D+01  9.093896892377D+01  8.778660372897D+01  6.062521524831D+01  1.956892568815D+04  1.950877827538D+04

   7  6.277640973990D+01  8.129552158824D+01  8.278486831557D+01  8.067198223197D+01  6.248008601000D+01  1.956401945259D+04  1.950665141504D+04
   7  6.277640970964D+01  8.129552155798D+01  8.278485973500D+01  8.067198243557D+01  6.248008621360D+01  1.956401945259D+04  1.950665141504D+04

   8  6.379638748880D+01  7.025584218194D+01  7.076691989025D+01  7.001410016907D+01  6.347782810713D+01  1.931725037000D+04  1.926862574114D+04
   8  6.379638745854D+01  7.025584215168D+01  7.076691691857D+01  7.001410037267D+01  6.347782831073D+01  1.931725037000D+04  1.926862574114D+04

Coolant temp rise (out - in) in channels =  1.40576789239336D+01  1.37340636570114D+01
Coolant temp rise (out - in) in channels =  1.40576788936754D+01  1.37340638606144D+01

FUEL PLATE   2 (BroydenSoln)
FUEL PLATE   2 (ExactSoln)
NODE    COOLANT             CladSurf            FUEL PEAK           CladSurf            COOLANT             HCOFinner           HCOFouter
        inner(C)            inner(C)               (C)              outer(C)            outer(C)            W/C-m^2             W/C-m^2
      50.000                                                                          50.000
   1  5.026207746876D+01  5.749962056227D+01  5.808350216372D+01  5.740004408121D+01  5.024996183759D+01  1.736347889400D+04  1.754227608636D+04
   1  5.026207746876D+01  5.749962056227D+01  5.808350232547D+01  5.740004408121D+01  5.024996183759D+01  1.736347889400D+04  1.754227608636D+04

   2  5.127033738507D+01  7.118980820391D+01  7.285235283615D+01  7.090580945633D+01  5.121152245339D+01  1.796426073518D+04  1.813835351449D+04
   2  5.127033738507D+01  7.118980820391D+01  7.285235329679D+01  7.090580945633D+01  5.121152245339D+01  1.796426073518D+04  1.813835351449D+04

   3  5.313286079191D+01  8.206102033617D+01  8.454766215957D+01  8.163298620280D+01  5.298758123502D+01  1.850358710542D+04  1.867058756623D+04
   3  5.313286089371D+01  8.206102462578D+01  8.454766330259D+01  8.163298280415D+01  5.298758104346D+01  1.850358710542D+04  1.867058756623D+04
```

```
   4  5.556537428244D+01  8.882483962945D+01  9.175503764515D+01  8.831405418463D+01  5.530685251994D+01  1.896834187896D+04  1.912537186204D+04
   4  5.556537448604D+01  8.882483983305D+01  9.175503836874D+01  8.831405380151D+01  5.530685213682D+01  1.896834187896D+04  1.912537186204D+04

   5  5.819669872016D+01  9.080064373893D+01  9.372545891293D+01  9.027928317303D+01  5.781527826289D+01  1.932084927442D+04  1.946778118060D+04
   5  5.819669892377D+01  9.080064394254D+01  9.372545963668D+01  9.027928278991D+01  5.781527787977D+01  1.932084927442D+04  1.946778118060D+04

   6  6.062521504470D+01  8.791505833827D+01  9.038576312458D+01  8.745570239806D+01  6.012990332273D+01  1.951232651802D+04  1.965101395700D+04
   6  6.062521524831D+01  8.791505854187D+01  9.038576372476D+01  8.745570201494D+01  6.012990293961D+01  1.951232651802D+04  1.965101395700D+04

   7  6.248008601000D+01  8.059770820383D+01  8.223475363207D+01  8.026353728310D+01  6.189725682700D+01  1.950443939117D+04  1.963771512444D+04
   7  6.248008621360D+01  8.059770840744D+01  8.223475400378D+01  8.026353689998D+01  6.189725644388D+01  1.950443939117D+04  1.963771512444D+04

   8  6.347782810713D+01  6.970724168720D+01  7.025874076289D+01  6.954356476011D+01  6.284729445379D+01  1.925783984674D+04  1.938933953762D+04
   8  6.347782831073D+01  6.970724189081D+01  7.025874083613D+01  6.954356437699D+01  6.284729407067D+01  1.925783984674D+04  1.938933953762D+04

Coolant temp rise (out - in) in channels =  1.37340636570114D+01  1.30909891747219D+01
Coolant temp rise (out - in) in channels =  1.37340638606144D+01  1.30909887916010D+01

FUEL PLATE   3 (BroydenSoln)
FUEL PLATE   3 (ExactSoln)
NODE    COOLANT             CladSurf            FUEL PEAK           CladSurf            COOLANT             HCOFinner           HCOFouter
        inner(C)            inner(C)               (C)              outer(C)            outer(C)            W/C-m^2             W/C-m^2
      50.000                                                                          50.000
   1  5.024996183759D+01  5.744292780031D+01  5.804989826450D+01  5.738904377431D+01  5.022806893706D+01  1.754390501053D+04  1.745152848655D+04
   1  5.024996183759D+01  5.744292780031D+01  5.804990461580D+01  5.738904377431D+01  5.022806893706D+01  1.754390501053D+04  1.745152848655D+04

   2  5.121152245339D+01  7.100791169903D+01  7.273504855628D+01  7.085174311896D+01  5.110598465145D+01  1.814162159711D+04  1.803335901499D+04
   2  5.121152245339D+01  7.100791169903D+01  7.273506664426D+01  7.085174311896D+01  5.110598465145D+01  1.814162159711D+04  1.803335901499D+04

   3  5.298758123502D+01  8.173809939468D+01  8.431925145590D+01  8.149709551110D+01  5.272935168345D+01  1.867355577266D+04  1.854294322766D+04
   3  5.298758104346D+01  8.173809257182D+01  8.431927805860D+01  8.149710141168D+01  5.272935187660D+01  1.867355577266D+04  1.854294322766D+04

   4  5.530685251994D+01  8.836406625288D+01  9.140269181829D+01  8.806782640925D+01  5.485279457261D+01  1.912670569428D+04  1.897026637291D+04
   4  5.530685213682D+01  8.836406586976D+01  9.140272375898D+01  8.806782679554D+01  5.485279495890D+01  1.912670569428D+04  1.897026637291D+04

   5  5.781527826289D+01  9.021424927870D+01  9.324330732332D+01  8.989909062739D+01  5.715513182533D+01  1.946598591476D+04  1.928488498526D+04
   5  5.781527787977D+01  9.021424889557D+01  9.324333927102D+01  8.989909101368D+01  5.715513221161D+01  1.946598591476D+04  1.928488498526D+04

   6  6.012990332273D+01  8.722277060633D+01  8.977611313126D+01  8.692674483760D+01  5.928831594404D+01  1.964453198255D+04  1.944433432213D+04
   6  6.012990293961D+01  8.722277022321D+01  8.977614022690D+01  8.692674522389D+01  5.928831633033D+01  1.964453198255D+04  1.944433432213D+04

   7  6.189725682700D+01  7.983033829728D+01  8.151441046396D+01  7.958881284154D+01  6.093017532097D+01  1.962464281158D+04  1.941422500136D+04
   7  6.189725644388D+01  7.983033791416D+01  8.151442858897D+01  7.958881322782D+01  6.093017570726D+01  1.962464281158D+04  1.941422500136D+04

   8  6.284729445379D+01  6.890809185249D+01  6.946289762652D+01  6.874982373794D+01  6.183308349649D+01  1.936669056720D+04  1.915698572822D+04
   8  6.284729407067D+01  6.890809146937D+01  6.946290404128D+01  6.874982412423D+01  6.183308388278D+01  1.936669056720D+04  1.915698572822D+04

Coolant temp rise (out - in) in channels =  1.30909891747219D+01  1.20749017955535D+01
Coolant temp rise (out - in) in channels =  1.30909887916010D+01  1.20749021818406D+01
```

Figure 4.23 Continued

```
FUEL PLATE   1 (BroydenSoln) AREAL
FUEL PLATE   1 (ExactSoln)   AREAL                          FUEL-CLADinterface
NODE FLUX inner FLUX outer  FUEL X   Tsat     Tdiff     inner     outer    Pressure  Z-mid     Z-int
       MW/m^2     MW/m^2     inner   (C)       (C)       (C)       (C)      (bar)
   1 1.2793E-01 1.2423E-01  0.3597 107.091     0.00     58.051    57.911   1.29812   0.0625    0.1250
   2 3.6454E-01 3.5364E-01  0.3599 107.006     0.00     72.766    72.368   1.29438   0.1875    0.2500
   3 5.4570E-01 5.2920E-01  0.3600 106.921     0.00     84.441    83.847   1.29062   0.3125    0.3750
   4 6.4365E-01 6.2426E-01  0.3600 106.836     0.00     91.671    90.970   1.28688   0.4375    0.5000
   5 6.4326E-01 6.2447E-01  0.3597 106.751     0.00     93.712    93.010   1.28313   0.5625    0.6250
   6 5.4444E-01 5.2989E-01  0.3592 106.666     0.00     90.490    89.890   1.27938   0.6875    0.7500
   7 3.6231E-01 3.5486E-01  0.3577 106.580     0.00     82.487    82.081   1.27562   0.8125    0.8750
   8 1.2478E-01 1.2594E-01  0.3508 106.495     0.00     70.666    70.514   1.27188   0.9375    1.0000

   1 1.2793E-01 1.2423E-01  0.3597 107.091              58.051    57.911   1.29812   0.0625    0.1250
   2 3.6454E-01 3.5364E-01  0.3599 107.006              72.766    72.368   1.29438   0.1875    0.2500
   3 5.4570E-01 5.2920E-01  0.3600 106.921              84.441    83.847   1.29062   0.3125    0.3750
   4 6.4365E-01 6.2426E-01  0.3600 106.836              91.671    90.970   1.28688   0.4375    0.5000
   5 6.4326E-01 6.2447E-01  0.3597 106.751              93.712    93.010   1.28313   0.5625    0.6250
   6 5.4444E-01 5.2989E-01  0.3592 106.666              90.490    89.890   1.27938   0.6875    0.7500
   7 3.6231E-01 3.5486E-01  0.3577 106.580              82.487    82.081   1.27562   0.8125    0.8750
   8 1.2478E-01 1.2594E-01  0.3508 106.495              70.666    70.514   1.27188   0.9375    1.0000

FUEL PLATE   2 (BroydenSoln) AREAL
FUEL PLATE   2 (ExactSoln)   AREAL                          FUEL-CLADinterface
NODE FLUX inner FLUX outer  FUEL X   Tsat     Tdiff     inner     outer    Pressure  Z-mid     Z-int
       MW/m^2     MW/m^2     inner   (C)       (C)       (C)       (C)      (bar)
   1 1.2567E-01 1.2543E-01  0.4364 107.091     0.00     57.944    57.880   1.29812   0.0625    0.1250
   2 3.5784E-01 3.5722E-01  0.4363 107.006     0.00     72.454    72.271   1.29438   0.1875    0.2500
   3 5.3527E-01 5.3483E-01  0.4361 106.921     0.00     83.952    83.678   1.29062   0.3125    0.3750
   4 6.3088E-01 6.3128E-01  0.4357 106.836     0.00     91.054    90.727   1.28688   0.4375    0.5000
   5 6.2994E-01 6.3200E-01  0.4351 106.751     0.00     93.027    92.695   1.28313   0.5625    0.6250
   6 5.3249E-01 5.3698E-01  0.4338 106.666     0.00     89.797    89.509   1.27938   0.6875    0.7500
   7 3.5337E-01 3.6067E-01  0.4309 106.580     0.00     81.846    81.642   1.27562   0.8125    0.8750
   8 1.1997E-01 1.2984E-01  0.4166 106.495     0.00     70.131    70.040   1.27188   0.9375    1.0000

   1 1.2567E-01 1.2543E-01  0.4364 107.091              57.944    57.880   1.29812   0.0625    0.1250
   2 3.5784E-01 3.5722E-01  0.4363 107.006              72.454    72.271   1.29438   0.1875    0.2500
   3 5.3527E-01 5.3483E-01  0.4361 106.921              83.952    83.678   1.29062   0.3125    0.3750
   4 6.3088E-01 6.3128E-01  0.4357 106.836              91.054    90.727   1.28688   0.4375    0.5000
   5 6.2994E-01 6.3200E-01  0.4351 106.751              93.027    92.695   1.28313   0.5625    0.6250
   6 5.3249E-01 5.3698E-01  0.4338 106.666              89.797    89.509   1.27938   0.6875    0.7500
   7 3.5337E-01 3.6067E-01  0.4309 106.580              81.846    81.642   1.27562   0.8125    0.8750
   8 1.1997E-01 1.2984E-01  0.4166 106.495              70.131    70.040   1.27188   0.9375    1.0000
```

Figure 4.23 Continued

FUEL PLATE 3 (BroydenSoln) AREAL
FUEL PLATE 3 (ExactSoln) AREAL

NODE	FLUX inner MW/m^2	FLUX outer MW/m^2	FUEL X inner	Tsat (C)	Tdiff (C)	FUEL-CLADinterface inner (C)	FUEL-CLADinterface outer (C)	Pressure (bar)	Z-mid	Z-int
1	1.2619E-01	1.2497E-01	0.4632	107.091	0.00	57.897	57.861	1.29812	0.0625	0.1250
2	3.5914E-01	3.5608E-01	0.4629	107.006	0.00	72.300	72.195	1.29438	0.1875	0.2500
3	5.3687E-01	5.3344E-01	0.4624	106.921	0.00	83.669	83.510	1.29062	0.3125	0.3750
4	6.3228E-01	6.3010E-01	0.4617	106.836	0.00	90.638	90.445	1.28688	0.4375	0.5000
5	6.3068E-01	6.3146E-01	0.4605	106.751	0.00	92.483	92.282	1.28313	0.5625	0.6250
6	5.3223E-01	5.3741E-01	0.4584	106.666	0.00	89.137	88.955	1.27938	0.6875	0.7500
7	3.5193E-01	3.6224E-01	0.4537	106.580	0.00	81.096	80.956	1.27562	0.8125	0.8750
8	1.1738E-01	1.3250E-01	0.4309	106.495	0.00	69.330	69.250	1.27188	0.9375	1.0000
1	1.2619E-01	1.2497E-01	0.4632	107.091		57.897	57.861	1.29812	0.0625	0.1250
2	3.5914E-01	3.5608E-01	0.4629	107.006		72.300	72.195	1.29438	0.1875	0.2500
3	5.3687E-01	5.3344E-01	0.4624	106.921		83.669	83.510	1.29062	0.3125	0.3750
4	6.3228E-01	6.3010E-01	0.4617	106.836		90.638	90.445	1.28688	0.4375	0.5000
5	6.3068E-01	6.3146E-01	0.4605	106.751		92.483	92.282	1.28313	0.5625	0.6250
6	5.3223E-01	5.3741E-01	0.4584	106.666		89.137	88.955	1.27938	0.6875	0.7500
7	3.5193E-01	3.6224E-01	0.4537	106.580		81.096	80.956	1.27562	0.8125	0.8750
8	1.1738E-01	1.3250E-01	0.4309	106.495		69.330	69.250	1.27188	0.9375	1.0000

Figure 4.24 Solution of Hungarian Reactor Benchmark Problem by the Broyden Method in PLTEMP/ANL Version 3.1 (Using Actual Coolant Properties)

FUEL PLATE 1 (BroydenSoln)

NODE	COOLANT inner(C)	CladSurf inner(C)	FUEL PEAK (C)	CladSurf outer(C)	COOLANT outer(C)	HCOFinner W/C-m^2	HCOFouter W/C-m^2	ONBRin [F Note 1]	ONBRout	ETAin K-cm^3/J	ETAout K-cm^3/J	COOLNT at NodeOutlet inner(C)	NodeOutlet outer(C)
	50.000				50.000								
1	50.267	57.586	58.113	57.374	50.262	1.7481E+04	1.7465E+04	8.11	8.34	1.246E+03	1.281E+03	50.535	50.523
2	51.297	71.384	72.885	70.782	51.268	1.8152E+04	1.8121E+04	3.01	3.09	4.287E+02	4.414E+02	52.060	52.013
3	53.201	82.312	84.559	81.413	53.128	1.8750E+04	1.8706E+04	2.03	2.09	2.761E+02	2.847E+02	54.342	54.243
4	55.688	89.126	91.776	88.065	55.557	1.9255E+04	1.9200E+04	1.70	1.74	2.229E+02	2.301E+02	57.034	56.871
5	58.379	91.169	93.817	90.104	58.184	1.9623E+04	1.9561E+04	1.61	1.65	2.109E+02	2.178E+02	59.724	59.497
6	60.863	88.359	90.599	87.447	60.609	1.9805E+04	1.9741E+04	1.71	1.75	2.360E+02	2.434E+02	62.001	61.720
7	62.759	81.092	82.582	80.469	62.461	1.9765E+04	1.9704E+04	2.05	2.09	3.393E+02	3.482E+02	63.516	63.201
8	63.777	70.186	70.697	69.944	63.457	1.9468E+04	1.9417E+04	3.02	3.06	9.607E+02	9.569E+02	64.038	63.713
	64.038				63.713								

FUEL PLATE 2 (BroydenSoln)

NODE	COOLANT inner(C)	CladSurf inner(C)	FUEL PEAK (C)	CladSurf outer(C)	COOLANT outer(C)	HCOFinner W/C-m^2	HCOFouter W/C-m^2	ONBRin [F Note 1]	ONBRout	ETAin K-cm^3/J	ETAout K-cm^3/J	COOLNT at NodeOutlet inner(C)	NodeOutlet outer(C)
	50.000				50.000								
1	50.262	57.456	58.040	57.357	50.250	1.7469E+04	1.7647E+04	8.25	8.36	1.266E+03	1.296E+03	50.523	50.499
2	51.268	71.011	72.674	70.728	51.210	1.8128E+04	1.8300E+04	3.06	3.10	4.361E+02	4.468E+02	52.013	51.920
3	53.128	81.735	84.222	81.308	52.983	1.8716E+04	1.8878E+04	2.07	2.10	2.814E+02	2.885E+02	54.243	54.046
4	55.557	88.407	91.338	87.898	55.299	1.9209E+04	1.9361E+04	1.72	1.75	2.276E+02	2.335E+02	56.871	56.551
5	58.184	90.383	93.308	89.863	57.803	1.9568E+04	1.9710E+04	1.64	1.66	2.159E+02	2.215E+02	59.497	59.055
6	60.609	87.582	90.053	87.124	60.114	1.9745E+04	1.9878E+04	1.74	1.76	2.422E+02	2.480E+02	61.720	61.173
7	62.461	80.398	82.035	80.064	61.879	1.9702E+04	1.9831E+04	2.10	2.12	3.496E+02	3.545E+02	63.201	62.584
8	63.457	69.638	70.189	69.474	62.827	1.9406E+04	1.9536E+04	3.10	3.13	1.005E+03	9.618E+02	63.713	63.070
	63.713				63.070								

FUEL PLATE 3 (BroydenSoln)

NODE	COOLANT inner(C)	CladSurf inner(C)	FUEL PEAK (C)	CladSurf outer(C)	COOLANT outer(C)	HCOFinner W/C-m^2	HCOFouter W/C-m^2	ONBRin [F Note 1]	ONBRout	ETAin K-cm^3/J	ETAout K-cm^3/J	COOLNT at NodeOutlet inner(C)	NodeOutlet outer(C)
	50.000				50.000								
1	50.250	57.401	58.008	57.347	50.228	1.7648E+04	1.7553E+04	8.31	8.37	1.288E+03	1.316E+03	50.499	50.455
2	51.210	70.835	72.563	70.680	51.104	1.8303E+04	1.8186E+04	3.08	3.10	4.443E+02	4.542E+02	51.920	51.753
3	52.983	81.425	84.007	81.185	52.724	1.8881E+04	1.8738E+04	2.09	2.10	2.873E+02	2.940E+02	54.046	53.696
4	55.299	87.962	91.002	87.668	54.844	1.9363E+04	1.9191E+04	1.75	1.76	2.331E+02	2.388E+02	56.551	55.992
5	57.803	89.811	92.841	89.498	57.142	1.9708E+04	1.9512E+04	1.66	1.68	2.219E+02	2.273E+02	59.055	58.292
6	60.114	86.901	89.454	86.605	59.271	1.9872E+04	1.9659E+04	1.77	1.79	2.501E+02	2.552E+02	61.173	60.250
7	61.879	79.636	81.320	79.394	60.910	1.9818E+04	1.9598E+04	2.15	2.17	3.633E+02	3.647E+02	62.584	61.570
8	62.827	68.840	69.394	68.681	61.812	1.9513E+04	1.9298E+04	3.23	3.27	1.065E+03	9.752E+02	63.070	62.054
	63.070				62.054								

[1] The ONB ratio is here defined as (Tonb - Tinlet)/(Tsurf - Tinlet). If the heat flux is negative (the coolant is hotter than the adjacent cladding surface), then the ONB ratio is arbitrarily set to 99.99 .

Figure 4.24. Continued

FUEL PLATE 1 (BroydenSoln) AREAL

NODE	FLUX inner MW/m^2	FLUX outer MW/m^2	FUEL X inner	Tsat (C)	Tdiff (C)	FUEL-CLADinterface inner (C)	FUEL-CLADinterface outer (C)	Pressure (bar)	Z-mid	Z-int
1	1.2794E-01	1.2422E-01	0.3597	107.091	0.00	58.007	57.867	1.29812	0.0625	0.1250
2	3.6462E-01	3.5360E-01	0.3600	107.006	0.00	72.583	72.186	1.29438	0.1875	0.2500
3	5.4586E-01	5.2911E-01	0.3601	106.921	0.00	84.107	83.514	1.29062	0.3125	0.3750
4	6.4385E-01	6.2415E-01	0.3601	106.836	0.00	91.243	90.543	1.28688	0.4375	0.5000
5	6.4344E-01	6.2437E-01	0.3598	106.751	0.00	93.285	92.583	1.28313	0.5625	0.6250
6	5.4456E-01	5.2982E-01	0.3592	106.666	0.00	90.149	89.551	1.27938	0.6875	0.7500
7	3.6235E-01	3.5484E-01	0.3577	106.580	0.00	82.284	81.878	1.27562	0.8125	0.8750
8	1.2476E-01	1.2596E-01	0.3508	106.495	0.00	70.596	70.444	1.27188	0.9375	1.0000

FUEL PLATE 2 (BroydenSoln) AREAL

NODE	FLUX inner MW/m^2	FLUX outer MW/m^2	FUEL X inner	Tsat (C)	Tdiff (C)	FUEL-CLADinterface inner (C)	FUEL-CLADinterface outer (C)	Pressure (bar)	Z-mid	Z-int
1	1.2568E-01	1.2542E-01	0.4364	107.091	0.00	57.900	57.836	1.29812	0.0625	0.1250
2	3.5790E-01	3.5717E-01	0.4364	107.006	0.00	72.276	72.093	1.29438	0.1875	0.2500
3	5.3540E-01	5.3473E-01	0.4362	106.921	0.00	83.627	83.353	1.29062	0.3125	0.3750
4	6.3103E-01	6.3116E-01	0.4358	106.836	0.00	90.637	90.311	1.28688	0.4375	0.5000
5	6.3008E-01	6.3189E-01	0.4352	106.751	0.00	92.609	92.279	1.28313	0.5625	0.6250
6	5.3258E-01	5.3691E-01	0.4339	106.666	0.00	89.464	89.176	1.27938	0.6875	0.7500
7	3.5341E-01	3.6065E-01	0.4309	106.580	0.00	81.647	81.443	1.27562	0.8125	0.8750
8	1.1995E-01	1.2985E-01	0.4165	106.495	0.00	70.062	69.970	1.27188	0.9375	1.0000

FUEL PLATE 3 (BroydenSoln) AREAL

NODE	FLUX inner MW/m^2	FLUX outer MW/m^2	FUEL X inner	Tsat (C)	Tdiff (C)	FUEL-CLADinterface inner (C)	FUEL-CLADinterface outer (C)	Pressure (bar)	Z-mid	Z-int
1	1.2620E-01	1.2496E-01	0.4633	107.091	0.00	57.855	57.818	1.29812	0.0625	0.1250
2	3.5921E-01	3.5602E-01	0.4630	107.006	0.00	72.128	72.023	1.29438	0.1875	0.2500
3	5.3702E-01	5.3331E-01	0.4625	106.921	0.00	83.356	83.198	1.29062	0.3125	0.3750
4	6.3246E-01	6.2994E-01	0.4618	106.836	0.00	90.237	90.045	1.28688	0.4375	0.5000
5	6.3083E-01	6.3134E-01	0.4606	106.751	0.00	92.080	91.880	1.28313	0.5625	0.6250
6	5.3230E-01	5.3735E-01	0.4585	106.666	0.00	88.815	88.633	1.27938	0.6875	0.7500
7	3.5192E-01	3.6225E-01	0.4536	106.580	0.00	80.902	80.761	1.27562	0.8125	0.8750
8	1.1732E-01	1.3255E-01	0.4307	106.495	0.00	69.262	69.181	1.27188	0.9375	1.0000

Figure 4.25 Solution of Hungarian Reactor Benchmark Problem by the Broyden Method in PLTEMP/ANL Version 3.2 (Using Actual Coolant Properties)

FUEL PLATE 1 (BroydenSoln)

NODE	COOLANT inner(C)	CladSurf inner(C)	FUEL PEAK (C)	CladSurf outer(C)	COOLANT outer(C)	HCOFinner W/C-m^2	HCOFouter W/C-m^2	ONBRin [F Note 1]	ONBRout	ETAin K-cm^3/J	ETAout K-cm^3/J	COOLNT at NodeOutlet inner(C)	NodeOutlet outer(C)
	50.000				50.000								
1	50.267	57.599	58.125	57.387	50.262	1.7450E+04	1.7435E+04	8.10	8.32	1.246E+03	1.281E+03	50.535	50.523
2	51.297	71.479	72.979	70.876	51.268	1.8065E+04	1.8035E+04	2.99	3.07	4.288E+02	4.414E+02	52.059	52.013
3	53.200	82.510	84.756	81.610	53.128	1.8620E+04	1.8579E+04	2.02	2.07	2.762E+02	2.847E+02	54.341	54.242
4	55.687	89.383	92.033	88.321	55.556	1.9103E+04	1.9052E+04	1.68	1.73	2.230E+02	2.301E+02	57.033	56.870
5	58.378	91.412	94.059	90.346	58.183	1.9474E+04	1.9415E+04	1.60	1.64	2.110E+02	2.178E+02	59.723	59.496
6	60.861	88.527	90.767	87.615	60.608	1.9681E+04	1.9619E+04	1.70	1.74	2.360E+02	2.434E+02	61.999	61.720
7	62.757	81.165	82.655	80.542	62.460	1.9683E+04	1.9624E+04	2.05	2.09	3.394E+02	3.482E+02	63.514	63.200
8	63.775	70.194	70.705	69.952	63.456	1.9440E+04	1.9390E+04	3.02	3.06	9.607E+02	9.570E+02	64.036	63.712
	64.036				63.712								

FUEL PLATE 2 (BroydenSoln)

NODE	COOLANT inner(C)	CladSurf inner(C)	FUEL PEAK (C)	CladSurf outer(C)	COOLANT outer(C)	HCOFinner W/C-m^2	HCOFouter W/C-m^2	ONBRin [F Note 1]	ONBRout	ETAin K-cm^3/J	ETAout K-cm^3/J	COOLNT at NodeOutlet inner(C)	NodeOutlet outer(C)
	50.000				50.000								
1	50.262	57.468	58.052	57.369	50.250	1.7438E+04	1.7618E+04	8.24	8.35	1.266E+03	1.296E+03	50.523	50.499
2	51.268	71.102	72.765	70.818	51.210	1.8042E+04	1.8217E+04	3.04	3.08	4.362E+02	4.467E+02	52.013	51.920
3	53.128	81.925	84.412	81.498	52.983	1.8588E+04	1.8755E+04	2.06	2.08	2.814E+02	2.885E+02	54.242	54.045
4	55.556	88.656	91.586	88.145	55.298	1.9061E+04	1.9218E+04	1.71	1.74	2.276E+02	2.335E+02	56.870	56.551
5	58.183	90.618	93.543	90.097	57.803	1.9423E+04	1.9569E+04	1.63	1.65	2.159E+02	2.215E+02	59.496	59.054
6	60.608	87.745	90.216	87.286	60.113	1.9623E+04	1.9761E+04	1.73	1.75	2.422E+02	2.480E+02	61.720	61.173
7	62.460	80.470	82.107	80.136	61.878	1.9622E+04	1.9754E+04	2.09	2.12	3.496E+02	3.545E+02	63.200	62.583
8	63.456	69.646	70.197	69.482	62.826	1.9379E+04	1.9509E+04	3.10	3.13	1.005E+03	9.619E+02	63.712	63.070
	63.712				63.070								

FUEL PLATE 3 (BroydenSoln)

NODE	COOLANT inner(C)	CladSurf inner(C)	FUEL PEAK (C)	CladSurf outer(C)	COOLANT outer(C)	HCOFinner W/C-m^2	HCOFouter W/C-m^2	ONBRin [F Note 1]	ONBRout	ETAin K-cm^3/J	ETAout K-cm^3/J	COOLNT at NodeOutlet inner(C)	NodeOutlet outer(C)
	50.000				50.000								
1	50.250	57.412	58.019	57.358	50.228	1.7619E+04	1.7526E+04	8.30	8.36	1.288E+03	1.316E+03	50.499	50.455
2	51.210	70.920	72.648	70.764	51.104	1.8220E+04	1.8112E+04	3.07	3.09	4.443E+02	4.542E+02	51.920	51.753
3	52.983	81.604	84.185	81.363	52.725	1.8758E+04	1.8627E+04	2.08	2.09	2.873E+02	2.939E+02	54.045	53.697
4	55.298	88.197	91.236	87.901	54.845	1.9219E+04	1.9061E+04	1.73	1.75	2.331E+02	2.387E+02	56.551	55.993
5	57.803	90.035	93.064	89.720	57.143	1.9568E+04	1.9383E+04	1.65	1.67	2.220E+02	2.273E+02	59.054	58.294
6	60.113	87.056	89.610	86.761	59.273	1.9754E+04	1.9551E+04	1.76	1.78	2.502E+02	2.551E+02	61.173	60.252
7	61.878	79.705	81.389	79.464	60.912	1.9741E+04	1.9526E+04	2.15	2.17	3.633E+02	3.647E+02	62.583	61.572
8	62.826	68.849	69.403	68.690	61.814	1.9486E+04	1.9272E+04	3.23	3.27	1.064E+03	9.753E+02	63.070	62.055
	63.070				62.055								

[1] The ONB ratio is here defined as (Tonb - Tinlet)/(Tsurf - Tinlet). If the heat flux is negative (the coolant is hotter than the adjacent cladding surface), then the ONB ratio is arbitrarily set to 99.99 .

Figure 4.25 Continued

FUEL PLATE 1 (BroydenSoln) AREAL

NODE	FLUX inner MW/m^2	FLUX outer MW/m^2	FUEL X inner	Tsat (C)	Tdiff (C)	FUEL-CLADinterface inner (C)	FUEL-CLADinterface outer (C)	Pressure (bar)	Z-mid	Z-int
1	1.2793E-01	1.2422E-01	0.3597	107.091	0.00	58.020	57.880	1.29812	0.0625	0.1250
2	3.6457E-01	3.5363E-01	0.3599	107.006	0.00	72.677	72.280	1.29438	0.1875	0.2500
3	5.4575E-01	5.2917E-01	0.3600	106.921	0.00	84.305	83.711	1.29062	0.3125	0.3750
4	6.4370E-01	6.2423E-01	0.3600	106.836	0.00	91.500	90.799	1.28688	0.4375	0.5000
5	6.4332E-01	6.2444E-01	0.3598	106.751	0.00	93.528	92.825	1.28313	0.5625	0.6250
6	5.4449E-01	5.2986E-01	0.3592	106.666	0.00	90.318	89.719	1.27938	0.6875	0.7500
7	3.6234E-01	3.5485E-01	0.3577	106.580	0.00	82.357	81.951	1.27562	0.8125	0.8750
8	1.2477E-01	1.2595E-01	0.3508	106.495	0.00	70.604	70.452	1.27188	0.9375	1.0000

FUEL PLATE 2 (BroydenSoln) AREAL

NODE	FLUX inner MW/m^2	FLUX outer MW/m^2	FUEL X inner	Tsat (C)	Tdiff (C)	FUEL-CLADinterface inner (C)	FUEL-CLADinterface outer (C)	Pressure (bar)	Z-mid	Z-int
1	1.2567E-01	1.2543E-01	0.4364	107.091	0.00	57.912	57.848	1.29812	0.0625	0.1250
2	3.5785E-01	3.5721E-01	0.4363	107.006	0.00	72.367	72.184	1.29438	0.1875	0.2500
3	5.3529E-01	5.3481E-01	0.4361	106.921	0.00	83.817	83.542	1.29062	0.3125	0.3750
4	6.3091E-01	6.3125E-01	0.4358	106.836	0.00	90.885	90.558	1.28688	0.4375	0.5000
5	6.2997E-01	6.3198E-01	0.4351	106.751	0.00	92.844	92.513	1.28313	0.5625	0.6250
6	5.3251E-01	5.3696E-01	0.4339	106.666	0.00	89.627	89.339	1.27938	0.6875	0.7500
7	3.5339E-01	3.6066E-01	0.4309	106.580	0.00	81.718	81.514	1.27562	0.8125	0.8750
8	1.1995E-01	1.2985E-01	0.4165	106.495	0.00	70.070	69.978	1.27188	0.9375	1.0000

FUEL PLATE 3 (BroydenSoln) AREAL

NODE	FLUX inner MW/m^2	FLUX outer MW/m^2	FUEL X inner	Tsat (C)	Tdiff (C)	FUEL-CLADinterface inner (C)	FUEL-CLADinterface outer (C)	Pressure (bar)	Z-mid	Z-int
1	1.2619E-01	1.2497E-01	0.4632	107.091	0.00	57.866	57.830	1.29812	0.0625	0.1250
2	3.5914E-01	3.5608E-01	0.4629	107.006	0.00	72.212	72.108	1.29438	0.1875	0.2500
3	5.3689E-01	5.3343E-01	0.4624	106.921	0.00	83.535	83.376	1.29062	0.3125	0.3750
4	6.3230E-01	6.3008E-01	0.4617	106.836	0.00	90.471	90.278	1.28688	0.4375	0.5000
5	6.3070E-01	6.3144E-01	0.4605	106.751	0.00	92.303	92.102	1.28313	0.5625	0.6250
6	5.3224E-01	5.3740E-01	0.4584	106.666	0.00	88.971	88.788	1.27938	0.6875	0.7500
7	3.5193E-01	3.6224E-01	0.4536	106.580	0.00	80.971	80.831	1.27562	0.8125	0.8750
8	1.1735E-01	1.3252E-01	0.4308	106.495	0.00	69.271	69.190	1.27188	0.9375	1.0000

Figure 4.26 Solution of Hungarian Reactor Benchmark Problem by the Exact Method in PLTEMP/ANL Version 3.2 (Using Actual Coolant Properties)

FUEL PLATE 1 (ExactSoln)

NODE	COOLANT inner(C)	CladSurf inner(C)	FUEL PEAK (C)	CladSurf outer(C)	COOLANT outer(C)	HCOFinner W/C-m^2	HCOFouter W/C-m^2	ONBRin [F Note 1]	ONBRout	ETAin K-cm^3/J	ETAout K-cm^3/J	COOLNT at inner(C)	NodeOutlet outer(C)
	50.000				50.000								
1	50.268	57.599	58.125	57.387	50.261	1.7450E+04	1.7435E+04	8.10	8.32	1.246E+03	1.281E+03	50.536	50.523
2	51.298	71.479	72.979	70.877	51.268	1.8065E+04	1.8035E+04	2.99	3.07	4.288E+02	4.414E+02	52.061	52.014
3	53.202	82.511	84.757	81.611	53.129	1.8620E+04	1.8580E+04	2.02	2.07	2.762E+02	2.847E+02	54.343	54.245
4	55.689	89.385	92.034	88.322	55.559	1.9103E+04	1.9052E+04	1.68	1.73	2.229E+02	2.300E+02	57.035	56.873
5	58.378	91.413	94.060	90.347	58.185	1.9474E+04	1.9416E+04	1.60	1.64	2.110E+02	2.178E+02	59.722	59.497
6	60.859	88.526	90.766	87.614	60.608	1.9681E+04	1.9619E+04	1.70	1.74	2.360E+02	2.434E+02	61.996	61.718
7	62.753	81.162	82.652	80.539	62.457	1.9682E+04	1.9624E+04	2.05	2.09	3.394E+02	3.482E+02	63.510	63.196
8	63.770	70.189	70.700	69.947	63.451	1.9439E+04	1.9389E+04	3.02	3.06	9.607E+02	9.571E+02	64.030	63.707
	64.030				63.707								

FUEL PLATE 2 (ExactSoln)

NODE	COOLANT inner(C)	CladSurf inner(C)	FUEL PEAK (C)	CladSurf outer(C)	COOLANT outer(C)	HCOFinner W/C-m^2	HCOFouter W/C-m^2	ONBRin [F Note 1]	ONBRout	ETAin K-cm^3/J	ETAout K-cm^3/J	COOLNT at inner(C)	NodeOutlet outer(C)
	50.000				50.000								
1	50.261	57.468	58.052	57.369	50.250	1.7438E+04	1.7618E+04	8.24	8.35	1.266E+03	1.296E+03	50.523	50.499
2	51.268	71.103	72.765	70.819	51.210	1.8042E+04	1.8217E+04	3.04	3.08	4.362E+02	4.467E+02	52.014	51.921
3	53.129	81.927	84.413	81.499	52.984	1.8588E+04	1.8756E+04	2.06	2.08	2.814E+02	2.884E+02	54.245	54.047
4	55.559	88.657	91.587	88.146	55.299	1.9061E+04	1.9218E+04	1.71	1.74	2.276E+02	2.335E+02	56.873	56.552
5	58.185	90.618	93.543	90.097	57.802	1.9423E+04	1.9569E+04	1.63	1.65	2.159E+02	2.215E+02	59.497	59.053
6	60.608	87.744	90.215	87.285	60.111	1.9623E+04	1.9761E+04	1.73	1.75	2.422E+02	2.480E+02	61.718	61.169
7	62.457	80.466	82.103	80.132	61.873	1.9622E+04	1.9754E+04	2.09	2.12	3.497E+02	3.545E+02	63.196	62.576
8	63.451	69.640	70.191	69.476	62.819	1.9378E+04	1.9508E+04	3.10	3.13	1.005E+03	9.619E+02	63.707	63.061
	63.707				63.061								

FUEL PLATE 3 (ExactSoln)

NODE	COOLANT inner(C)	CladSurf inner(C)	FUEL PEAK (C)	CladSurf outer(C)	COOLANT outer(C)	HCOFinner W/C-m^2	HCOFouter W/C-m^2	ONBRin [F Note 1]	ONBRout	ETAin K-cm^3/J	ETAout K-cm^3/J	COOLNT at inner(C)	NodeOutlet outer(C)
	50.000				50.000								
1	50.250	57.412	58.019	57.358	50.228	1.7619E+04	1.7527E+04	8.30	8.36	1.288E+03	1.316E+03	50.499	50.455
2	51.210	70.921	72.648	70.765	51.104	1.8221E+04	1.8112E+04	3.07	3.09	4.443E+02	4.542E+02	51.921	51.753
3	52.984	81.604	84.186	81.363	52.725	1.8759E+04	1.8627E+04	2.08	2.09	2.873E+02	2.939E+02	54.047	53.697
4	55.299	88.197	91.236	87.901	54.845	1.9220E+04	1.9061E+04	1.73	1.75	2.331E+02	2.387E+02	56.552	55.992
5	57.802	90.034	93.063	89.719	57.142	1.9568E+04	1.9383E+04	1.65	1.67	2.220E+02	2.273E+02	59.053	58.291
6	60.111	87.054	89.607	86.758	59.270	1.9754E+04	1.9550E+04	1.76	1.78	2.502E+02	2.551E+02	61.169	60.248
7	61.873	79.701	81.385	79.459	60.907	1.9740E+04	1.9525E+04	2.15	2.17	3.633E+02	3.647E+02	62.576	61.566
8	62.819	68.842	69.396	68.683	61.807	1.9485E+04	1.9271E+04	3.23	3.27	1.064E+03	9.755E+02	63.061	62.047
	63.061				62.047								

[1] The ONB ratio is here defined as (Tonb - Tinlet)/(Tsurf - Tinlet). If the heat flux is negative (the coolant is hotter than the adjacent cladding surface), then the ONB ratio is arbitrarily set to 99.99 .

Figure 4.26 Continued

FUEL PLATE 1 (ExactSoln) AREAL FUEL-CLADinterface

NODE	FLUX inner MW/m^2	FLUX outer MW/m^2	FUEL X inner	Tsat (C)	Tdiff (C)	inner (C)	outer (C)	Pressure (bar)	Z-mid	Z-int
1	1.2793E-01	1.2423E-01	0.3597	107.091		58.020	57.880	1.29812	0.0625	0.1250
2	3.6456E-01	3.5363E-01	0.3599	107.006		72.678	72.281	1.29438	0.1875	0.2500
3	5.4575E-01	5.2917E-01	0.3600	106.921		84.306	83.712	1.29062	0.3125	0.3750
4	6.4371E-01	6.2422E-01	0.3600	106.836		91.502	90.801	1.28688	0.4375	0.5000
5	6.4332E-01	6.2444E-01	0.3598	106.751		93.528	92.826	1.28313	0.5625	0.6250
6	5.4450E-01	5.2985E-01	0.3592	106.666		90.317	89.718	1.27938	0.6875	0.7500
7	3.6235E-01	3.5484E-01	0.3577	106.580		82.354	81.948	1.27562	0.8125	0.8750
8	1.2478E-01	1.2594E-01	0.3508	106.495		70.599	70.447	1.27188	0.9375	1.0000

FUEL PLATE 2 (ExactSoln) AREAL FUEL-CLADinterface

NODE	FLUX inner MW/m^2	FLUX outer MW/m^2	FUEL X inner	Tsat (C)	Tdiff (C)	inner (C)	outer (C)	Pressure (bar)	Z-mid	Z-int
1	1.2568E-01	1.2542E-01	0.4364	107.091		57.912	57.848	1.29812	0.0625	0.1250
2	3.5785E-01	3.5721E-01	0.4363	107.006		72.367	72.184	1.29438	0.1875	0.2500
3	5.3529E-01	5.3481E-01	0.4361	106.921		83.818	83.543	1.29062	0.3125	0.3750
4	6.3089E-01	6.3126E-01	0.4358	106.836		90.886	90.560	1.28688	0.4375	0.5000
5	6.2995E-01	6.3199E-01	0.4351	106.751		92.844	92.513	1.28313	0.5625	0.6250
6	5.3250E-01	5.3697E-01	0.4338	106.666		89.626	89.338	1.27938	0.6875	0.7500
7	3.5336E-01	3.6068E-01	0.4309	106.580		81.715	81.510	1.27562	0.8125	0.8750
8	1.1992E-01	1.2987E-01	0.4164	106.495		70.064	69.972	1.27188	0.9375	1.0000

FUEL PLATE 3 (ExactSoln) AREAL FUEL-CLADinterface

NODE	FLUX inner MW/m^2	FLUX outer MW/m^2	FUEL X inner	Tsat (C)	Tdiff (C)	inner (C)	outer (C)	Pressure (bar)	Z-mid	Z-int
1	1.2619E-01	1.2497E-01	0.4632	107.091		57.866	57.829	1.29812	0.0625	0.1250
2	3.5914E-01	3.5608E-01	0.4629	107.006		72.213	72.108	1.29438	0.1875	0.2500
3	5.3688E-01	5.3344E-01	0.4624	106.921		83.536	83.376	1.29062	0.3125	0.3750
4	6.3229E-01	6.3009E-01	0.4617	106.836		90.472	90.279	1.28688	0.4375	0.5000
5	6.3069E-01	6.3145E-01	0.4605	106.751		92.303	92.102	1.28313	0.5625	0.6250
6	5.3224E-01	5.3740E-01	0.4584	106.666		88.969	88.786	1.27938	0.6875	0.7500
7	3.5193E-01	3.6224E-01	0.4537	106.580		80.967	80.826	1.27562	0.8125	0.8750
8	1.1736E-01	1.3252E-01	0.4308	106.495		69.264	69.183	1.27188	0.9375	1.0000

Figure 4.27 ASTRA2 Problem 3 Case 1 Input Data File for PLTEMP/ANL Code Versions 3.1 and 3.2 (Using C_p = 4180 J/kg-°C, and ρ = 1000 kg/m^3, Same as ASTRA2 Code Input)

```
IRT-3M 36% Enr. FA - 6 0.58 m Height - ASTRA2 P3, INCREASING RADII, astra2p3c1r
! Input card types 307, 308, 308A, 309, 310 were rearranged
!234567890123456789012345678901234567890123456789012345678901234567890123456789012345678901234567890
!  1   2   3   4   5   6   7   8   9  10  11  12  13  14  15  16  17  18
   4   1   2   1   1   1   1   0   1   1   0   0   0   0   2   0   0  20        Card(1)0200
 1.0        1.0         1.0                                                   Card(1)0201
   1   3  0.0        1.00        1.000       1.00                             Card(1)0300
 1.0        1.0         1.0                                                   Card(1)300A
   7   7  1.000                                                               Card(1)0301
   1   2   1                                                                  Card(1)0302
 1.3135                                                                       Card(1)0303
 0.0043433  0.038540    0.10        0.5                                       Card(3)0304
 0.0        0.0         0.580       0.0                                       Card(3)0304
 0.0043433  0.038540    0.035       1.0                                       Card(3)0304
 0.316      0.250                                                             Card(1)0305
   7  0 0.0         0.580         0.450E-03  170.        0.500E-03  100.     Card(1)0306
  1.9353E-04  0.0         0.18881    0.18881                                 Card(1)0307
  2.3797E-04  0.0         0.23216    0.23216                                 Card(2)0307
  2.8241E-04  0.0         0.27552    0.27552                                 Card(3)0307
  3.2684E-04  0.0         0.31887    0.31887                                 Card(4)0307
  3.7128E-04  0.0         0.36223    0.36223                                 Card(5)0307
  4.1572E-04  0.0         0.40558    0.40558                                 Card(6)0307
  5.1808E-04 4.60000E-03  0.22525    0.22525                                 Card(7)0307
 0.105243   0.126920    0.148597    0.170274    0.191951    0.213628         Card(1)0308
  .0188      .02225      .0257       .02915      .0326       .0363            Card(1)308A
0.85731     0.90175     0.9579      1.0234      1.0901      1.1696           Card(1)0309
0.717522    0.903667    0.917400    1.10792     1.21088     1.23838          Card(1)0310
1.663038                                                                      Card(2)0310
   1   1         1.0                                                          Card(1)0400
  1.1545E-04    3.00E-03    0.680           1.4                               Card(1)0401
       0.316    0.25                                                          Card(1)0402
 .100633     .0005        .12540     0.662880     45.0        .135            Card(1)0500
 0.0         0.0                                                              Card(2)0500
 100 1.00000E-04   25.0        0.0000        0.66288                          Card(1)0600
 -12                                                                          Card(1)0700
0.00000      0.025       0.52323                                             Card(1)0701
0.05000      0.100       0.62029                                             Card(2)0701
0.15         0.20        0.85886                                             Card(3)0701
0.25         0.30        1.06336                                             Card(4)0701
0.35         0.40        1.24058                                             Card(5)0701
0.45         0.50        1.34964                                             Card(6)0701
0.55         0.60        1.36328                                             Card(7)0701
0.65         0.70        1.27466                                             Card(8)0701
0.75         0.80        1.09062                                             Card(9)0701
0.85         0.90        0.85886                                             Card(10)701
0.95         0.975       0.75662                                             Card(11)701
1.00000                                                                       Card(12)701
0
```

Figure 4.28 Solution of ASTRA2 Problem 3 Case 1 by PLTEMP/ANL of May 22 2003 (From PLTEMP/ANL Output File output.astra2p3c1r.1)

FUEL PLATE 1 (BroydenSoln)

NODE	COOLANT inner(C)	CladSurf inner(C)	FUEL PEAK (C)	CladSurf outer(C)	COOLANT outer(C)
	45.000				45.000
1	45.128	57.615	58.441	56.668	45.233
2	45.552	59.783	60.890	59.749	46.032
3	46.269	66.000	67.356	65.369	47.368
4	47.207	70.933	72.881	70.975	49.103
5	48.334	75.772	78.077	75.883	51.189
6	49.615	79.394	81.943	79.595	53.526
7	50.957	80.431	84.373	82.318	55.982
8	52.285	81.165	83.695	81.592	58.359
9	53.480	77.160	83.041	81.397	60.468
10	54.438	73.284	80.065	78.770	62.212
11	55.045	71.723	79.077	77.936	63.333
	55.231				63.681

FUEL PLATE 2 (BroydenSoln)

NODE	COOLANT inner(C)	CladSurf inner(C)	FUEL PEAK (C)	CladSurf outer(C)	COOLANT outer(C)
	45.000				45.000
1	45.233	58.213	59.474	58.653	45.282
2	46.032	61.419	62.682	61.563	46.217
3	47.368	67.938	69.856	68.478	47.791
4	49.103	74.184	76.368	74.467	49.830
5	51.189	79.856	82.414	80.205	52.253
6	53.526	84.254	87.051	84.662	54.975
7	55.982	86.789	89.628	87.227	57.825
8	58.359	87.196	89.882	87.667	60.592
9	60.468	84.178	88.992	87.278	63.081
10	62.212	81.333	85.251	83.932	65.149
11	63.333	80.854	83.451	82.347	66.463
	63.681				66.861

FUEL PLATE 3 (BroydenSoln)

NODE	COOLANT inner(C)	CladSurf inner(C)	FUEL PEAK (C)	CladSurf outer(C)	COOLANT outer(C)
	45.000				45.000
1	45.282	60.267	61.176	59.437	45.293
2	46.217	63.251	64.476	63.163	46.288
3	47.791	71.205	72.700	70.003	47.957
4	49.830	77.377	79.485	77.242	50.129
5	52.253	83.653	86.118	83.509	52.740
6	54.975	88.526	91.217	88.387	55.677
7	57.825	91.341	94.069	91.220	58.755
8	60.592	91.837	94.403	91.754	61.751
9	63.081	89.217	92.634	90.665	64.453
10	65.149	86.523	88.418	86.800	66.688
11	66.463	85.482	87.129	85.680	68.086
	66.861				68.503

Figure 4.28 Continued

FUEL PLATE 4 (BroydenSoln)

NODE	COOLANT inner(C)	CladSurf inner(C)	FUEL PEAK (C)	CladSurf outer(C)	COOLANT outer(C)
	45.000				45.000
1	45.293	60.825	61.929	60.737	45.326
2	46.288	64.359	65.729	64.379	46.428
3	47.957	72.428	74.085	71.975	48.273
4	50.129	79.321	81.684	79.383	50.671
5	52.740	85.991	88.756	86.080	53.553
6	55.677	91.185	94.204	91.304	56.792
7	58.755	94.218	97.283	94.368	60.185
8	61.751	94.824	97.710	95.004	63.482
9	64.453	92.836	95.454	93.287	66.425
10	66.688	89.464	91.516	89.798	68.840
11	68.086	87.118	91.324	89.895	70.372
	68.503				70.840

FUEL PLATE 5 (BroydenSoln)

NODE	COOLANT inner(C)	CladSurf inner(C)	FUEL PEAK (C)	CladSurf outer(C)	COOLANT outer(C)
	45.000				45.000
1	45.326	62.525	63.801	62.627	45.373
2	46.428	66.478	67.982	66.579	46.612
3	48.273	75.105	77.195	75.261	48.669
4	50.671	82.955	85.546	83.155	51.323
5	53.553	90.247	93.277	90.495	54.477
6	56.792	95.890	99.196	96.178	57.993
7	60.185	99.150	102.501	99.464	61.637
8	63.482	99.738	102.886	100.060	65.130
9	66.425	97.032	100.713	98.621	68.331
10	68.840	93.427	96.321	94.702	71.061
11	70.372	91.017	96.234	94.715	72.792
	70.840				73.320

FUEL PLATE 6 (BroydenSoln)

NODE	COOLANT inner(C)	CladSurf inner(C)	FUEL PEAK (C)	CladSurf outer(C)	COOLANT outer(C)
	45.000				45.000
1	45.373	64.486	65.593	63.492	45.156
2	46.612	67.991	69.461	67.815	45.694
3	48.669	76.975	78.878	76.465	46.611
4	51.323	84.764	87.207	84.304	47.815
5	54.477	91.941	94.745	91.309	49.277
6	57.993	97.232	100.223	96.421	50.939
7	61.637	99.889	102.830	98.904	52.706
8	65.130	99.635	102.284	98.501	54.457
9	68.331	100.938	103.159	91.022	55.982
10	71.061	97.247	99.026	84.809	57.173
11	72.792	94.691	96.156	83.606	57.934
	73.320				58.176

Figure 4.29 Solution of ASTRA2 Problem 3 Case 1 by the Broyden Method in PLTEMP/ANL Version 3.1 (Using Coolant C_p = 4180 J/kg-°C, and ρ = 1000 kg/m^3, Same as ASTRA2 Code Input)

FUEL PLATE 1 (BroydenSoln)

NODE	COOLANT inner(C)	CladSurf inner(C)	FUEL PEAK (C)	CladSurf outer(C)	COOLANT outer(C)	HCOFinner W/C-m^2	HCOFouter W/C-m^2	ONBRin [F Note 1]	ONBRout	ETAin K-cm^3/J	ETAout K-cm^3/J	COOLNT at inner(C)	NodeOutlet outer(C)
	45.000				45.000								
1	45.123	57.164	58.086	57.110	45.239	2.0902E+04	2.1314E+04	6.11	6.14	8.959E+02	9.110E+02	45.247	45.478
2	45.542	59.802	60.911	59.770	46.043	2.1167E+04	2.1618E+04	5.06	5.06	7.366E+02	7.609E+02	45.838	46.608
3	46.252	65.698	67.255	65.695	47.388	2.1714E+04	2.2222E+04	3.68	3.67	5.151E+02	5.370E+02	46.665	48.168
4	47.183	70.962	72.915	71.009	49.131	2.2216E+04	2.2791E+04	2.96	2.95	4.010E+02	4.203E+02	47.701	50.094
5	48.311	75.805	78.115	75.921	51.214	2.2654E+04	2.3300E+04	2.52	2.49	3.298E+02	3.463E+02	48.921	52.335
6	49.593	79.430	81.983	79.635	53.551	2.2992E+04	2.3712E+04	2.25	2.22	2.891E+02	3.041E+02	50.265	54.766
7	50.955	81.296	83.928	81.607	55.989	2.3201E+04	2.3988E+04	2.13	2.09	2.712E+02	2.871E+02	51.644	57.212
8	52.303	81.203	83.734	81.627	58.350	2.3270E+04	2.4113E+04	2.11	2.05	2.730E+02	2.941E+02	52.962	59.487
9	53.544	79.165	81.409	79.676	60.453	2.3193E+04	2.4074E+04	2.20	2.12	2.971E+02	3.340E+02	54.127	61.418
10	54.607	75.910	77.801	76.544	62.170	2.3010E+04	2.3917E+04	2.37	2.26	3.470E+02	4.233E+02	55.087	62.922
11	55.305	74.728	76.460	75.408	63.253	2.2945E+04	2.3863E+04	2.43	2.30	3.717E+02	4.808E+02	55.524	63.585
	55.524				63.585								

FUEL PLATE 2 (BroydenSoln)

	45.000				45.000								
1	45.239	58.385	59.446	58.496	45.276	2.1429E+04	1.8926E+04	5.60	5.51	8.182E+02	7.876E+02	45.478	45.552
2	46.043	61.435	62.697	61.576	46.205	2.1765E+04	1.9233E+04	4.59	4.51	6.740E+02	6.516E+02	46.608	46.859
3	47.388	68.114	69.869	68.324	47.764	2.2443E+04	1.9849E+04	3.32	3.26	4.696E+02	4.549E+02	48.168	48.668
4	49.131	74.206	76.386	74.479	49.788	2.3040E+04	2.0395E+04	2.65	2.60	3.627E+02	3.518E+02	50.094	50.907
5	51.214	79.879	82.436	80.223	52.213	2.3590E+04	2.0902E+04	2.24	2.19	2.948E+02	2.857E+02	52.335	53.518
6	53.551	84.279	87.075	84.682	54.938	2.4038E+04	2.1319E+04	1.99	1.94	2.547E+02	2.467E+02	54.766	56.357
7	55.989	86.802	89.646	87.247	57.789	2.4347E+04	2.1613E+04	1.86	1.81	2.352E+02	2.279E+02	57.212	59.221
8	58.350	87.204	89.891	87.673	60.559	2.4500E+04	2.1765E+04	1.82	1.77	2.335E+02	2.271E+02	59.487	61.896
9	60.453	85.454	87.789	85.925	63.038	2.4483E+04	2.1764E+04	1.86	1.81	2.525E+02	2.486E+02	61.418	64.180
10	62.170	82.344	84.228	82.801	65.076	2.4344E+04	2.1650E+04	1.96	1.90	2.963E+02	2.998E+02	62.922	65.971
11	63.253	81.557	82.974	81.466	66.365	2.4322E+04	2.1608E+04	1.97	1.93	3.133E+02	3.346E+02	63.585	66.759
	63.585				66.759								

FUEL PLATE 3 (BroydenSoln)

	45.000				45.000								
1	45.276	59.884	60.916	59.806	45.296	1.9034E+04	1.9690E+04	5.03	5.06	7.087E+02	7.195E+02	45.552	45.592
2	46.205	63.259	64.486	63.174	46.294	1.9362E+04	2.0034E+04	4.13	4.15	5.834E+02	5.935E+02	46.859	46.996
3	47.764	70.647	72.348	70.534	47.968	2.0016E+04	2.0716E+04	2.99	3.01	4.053E+02	4.129E+02	48.668	48.940
4	49.788	77.379	79.493	77.256	50.145	2.0587E+04	2.1316E+04	2.39	2.40	3.118E+02	3.178E+02	50.907	51.349
5	52.213	83.661	86.131	83.523	52.755	2.1114E+04	2.1871E+04	2.02	2.02	2.519E+02	2.567E+02	53.518	54.161
6	54.938	88.538	91.232	88.402	55.691	2.1549E+04	2.2332E+04	1.79	1.80	2.160E+02	2.199E+02	56.357	57.221
7	57.789	91.352	94.084	91.236	58.768	2.1857E+04	2.2662E+04	1.67	1.68	1.978E+02	2.013E+02	59.221	60.315
8	60.559	91.848	94.417	91.768	61.763	2.2015E+04	2.2836E+04	1.63	1.64	1.946E+02	1.981E+02	61.896	63.210
9	63.038	90.006	92.207	89.944	64.451	2.2010E+04	2.2840E+04	1.67	1.67	2.086E+02	2.137E+02	64.180	65.691
10	65.076	86.636	88.404	86.656	66.671	2.1888E+04	2.2733E+04	1.75	1.75	2.438E+02	2.523E+02	65.971	67.650
11	66.365	85.772	87.112	85.352	68.081	2.1878E+04	2.2688E+04	1.76	1.77	2.572E+02	2.760E+02	66.759	68.512
	66.759				68.512								

Figure 4.29 Continued

FUEL PLATE 4 (BroydenSoln)

NODE	COOLANT inner(C)	CladSurf inner(C)	FUEL PEAK (C)	CladSurf outer(C)	COOLANT outer(C)	HCOFinner W/C-m^2	HCOFouter W/C-m^2	ONBRin [F Note 1]	ONBRout [F Note 1]	ETAin K-cm^3/J	ETAout K-cm^3/J	COOLNT at inner(C)	NodeOutlet outer(C)
	45.000				45.000								
1	45.296	60.786	61.938	60.795	45.327	1.9769E+04	1.9171E+04	4.77	4.76	6.713E+02	6.666E+02	45.592	45.654
2	46.294	64.372	65.743	64.392	46.429	2.0128E+04	1.9527E+04	3.92	3.90	5.516E+02	5.493E+02	46.996	47.205
3	47.968	72.200	74.104	72.239	48.279	2.0836E+04	2.0226E+04	2.84	2.83	3.823E+02	3.811E+02	48.940	49.353
4	50.145	79.352	81.712	79.406	50.683	2.1455E+04	2.0840E+04	2.27	2.26	2.930E+02	2.922E+02	51.349	52.012
5	52.755	86.019	88.785	86.108	53.564	2.2027E+04	2.1411E+04	1.92	1.90	2.357E+02	2.347E+02	54.161	55.115
6	55.691	91.214	94.234	91.333	56.803	2.2504E+04	2.1890E+04	1.70	1.69	2.010E+02	1.997E+02	57.221	58.491
7	58.768	94.246	97.312	94.396	60.195	2.2847E+04	2.2238E+04	1.59	1.58	1.827E+02	1.812E+02	60.315	61.900
8	61.763	94.851	97.738	95.031	63.493	2.3028E+04	2.2425E+04	1.55	1.53	1.782E+02	1.767E+02	63.210	65.085
9	64.451	92.982	95.480	93.191	66.448	2.3029E+04	2.2445E+04	1.58	1.56	1.894E+02	1.886E+02	65.691	67.810
10	66.671	89.541	91.539	89.766	68.880	2.2914E+04	2.2330E+04	1.65	1.63	2.188E+02	2.211E+02	67.650	69.950
11	68.081	88.529	90.215	88.576	70.421	2.2889E+04	2.2297E+04	1.67	1.64	2.310E+02	2.382E+02	68.512	70.891
	68.512				70.891								

FUEL PLATE 5 (BroydenSoln)

	45.000				45.000								
1	45.327	62.543	63.807	62.619	45.368	1.9306E+04	1.7966E+04	4.32	4.28	5.947E+02	5.822E+02	45.654	45.736
2	46.429	66.480	67.984	66.582	46.602	1.9700E+04	1.8342E+04	3.55	3.52	4.878E+02	4.788E+02	47.205	47.467
3	48.279	75.117	77.204	75.266	48.657	2.0422E+04	1.9028E+04	2.58	2.55	3.370E+02	3.310E+02	49.353	49.847
4	50.683	82.966	85.558	83.167	51.309	2.1061E+04	1.9637E+04	2.07	2.04	2.573E+02	2.524E+02	52.012	52.771
5	53.564	90.264	93.294	90.510	54.464	2.1657E+04	2.0206E+04	1.75	1.73	2.058E+02	2.014E+02	55.115	56.156
6	56.803	95.906	99.212	96.192	57.981	2.2162E+04	2.0689E+04	1.56	1.54	1.742E+02	1.700E+02	58.491	59.805
7	60.195	99.167	102.518	99.479	61.626	2.2523E+04	2.1035E+04	1.46	1.43	1.570E+02	1.528E+02	61.900	63.447
8	63.493	99.756	102.903	100.075	65.120	2.2709E+04	2.1221E+04	1.42	1.40	1.518E+02	1.474E+02	65.085	66.794
9	66.448	97.641	100.340	97.925	68.189	2.2716E+04	2.1216E+04	1.45	1.42	1.598E+02	1.557E+02	67.810	69.584
10	68.880	93.761	95.916	94.042	70.639	2.2573E+04	2.1079E+04	1.52	1.49	1.836E+02	1.803E+02	69.950	71.693
11	70.421	92.543	94.363	92.633	72.144	2.2538E+04	2.1033E+04	1.53	1.51	1.934E+02	1.924E+02	70.891	72.594
	70.891				72.594								

FUEL PLATE 6 (BroydenSoln)

	45.000				45.000								
1	45.368	64.032	65.294	63.927	45.160	1.8065E+04	1.8713E+04	3.98	4.02	5.352E+02	5.555E+02	45.736	45.319
2	46.602	67.997	69.468	67.822	45.702	1.8440E+04	1.9047E+04	3.32	3.36	4.447E+02	4.556E+02	47.467	46.084
3	48.657	76.878	78.884	76.572	46.620	1.9126E+04	1.9685E+04	2.43	2.48	3.105E+02	3.174E+02	49.847	47.156
4	51.309	84.773	87.218	84.315	47.826	1.9727E+04	2.0220E+04	1.97	2.01	2.392E+02	2.458E+02	52.771	48.496
5	54.464	91.953	94.758	91.323	49.287	2.0285E+04	2.0700E+04	1.68	1.72	1.929E+02	2.008E+02	56.156	50.077
6	57.981	97.244	100.237	96.435	50.948	2.0747E+04	2.1080E+04	1.51	1.56	1.649E+02	1.746E+02	59.805	51.819
7	61.626	99.901	102.844	98.918	52.714	2.1058E+04	2.1313E+04	1.42	1.48	1.509E+02	1.621E+02	63.447	53.608
8	65.120	99.646	102.297	98.514	54.464	2.1197E+04	2.1377E+04	1.41	1.47	1.494E+02	1.614E+02	66.794	55.319
9	68.189	96.483	98.623	95.239	56.075	2.1135E+04	2.1266E+04	1.46	1.54	1.642E+02	1.738E+02	69.584	56.832
10	70.639	91.506	93.039	90.192	57.458	2.0935E+04	2.1037E+04	1.56	1.67	2.036E+02	2.006E+02	71.693	58.083
11	72.144	89.615	90.876	88.257	58.368	2.0862E+04	2.0953E+04	1.59	1.72	2.275E+02	2.133E+02	72.594	58.652
	72.594				58.652								

Figure 4.29 Continued

FUEL PLATE 1 (BroydenSoln) AREAL — FUEL-CLADinterface

NODE	FLUX inner MW/m^2	FLUX outer MW/m^2	FUEL X inner	Tsat (C)	Tdiff (C)	inner (C)	outer (C)	Pressure (bar)	Z-mid	Z-int
1	2.5168E-01	2.5302E-01	0.4801	105.939	0.00	57.823	57.788	1.24781	0.0250	0.0500
2	3.0183E-01	2.9675E-01	0.4856	105.504	0.00	60.591	60.564	1.22923	0.1000	0.1500
3	4.2227E-01	4.0683E-01	0.4907	104.915	0.00	66.803	66.785	1.20447	0.2000	0.2500
4	5.2829E-01	4.9863E-01	0.4958	104.317	0.00	72.343	72.345	1.17970	0.3000	0.3500
5	6.2285E-01	5.7568E-01	0.5011	103.708	0.00	77.434	77.463	1.15493	0.4000	0.4500
6	6.8599E-01	6.1850E-01	0.5073	103.088	0.00	81.224	81.291	1.13017	0.5000	0.5500
7	7.0395E-01	6.1452E-01	0.5153	102.457	0.00	83.136	83.252	1.10540	0.6000	0.6500
8	6.7249E-01	5.6130E-01	0.5265	101.814	0.00	82.961	83.131	1.08063	0.7000	0.7500
9	5.9422E-01	4.6278E-01	0.5438	101.158	0.03	80.719	80.915	1.05586	0.8000	0.8500
10	4.9019E-01	3.4380E-01	0.5696	100.490	0.00	77.192	77.465	1.03110	0.9000	0.9500
11	4.4564E-01	2.9005E-01	0.5878	99.980	0.01	75.893	76.185	1.01252	0.9750	1.0000

FUEL PLATE 2 (BroydenSoln) AREAL — FUEL-CLADinterface

NODE	FLUX inner MW/m^2	FLUX outer MW/m^2	FUEL X inner	Tsat (C)	Tdiff (C)	inner (C)	outer (C)	Pressure (bar)	Z-mid	Z-int
1	2.8170E-01	2.5021E-01	0.5139	105.939	0.00	59.123	59.165	1.24781	0.0250	0.0500
2	3.3502E-01	2.9562E-01	0.5155	105.504	0.00	62.313	62.366	1.22923	0.1000	0.1500
3	4.6517E-01	4.0810E-01	0.5170	104.915	0.00	69.333	69.415	1.20447	0.2000	0.2500
4	5.7774E-01	5.0358E-01	0.5186	104.317	0.00	75.719	75.825	1.17970	0.3000	0.3500
5	6.7620E-01	5.8547E-01	0.5203	103.708	0.00	81.651	81.788	1.15493	0.4000	0.4500
6	7.3864E-01	6.3412E-01	0.5224	103.088	0.00	86.214	86.377	1.13017	0.5000	0.5500
7	7.5021E-01	6.3668E-01	0.5253	102.457	0.00	88.767	88.949	1.10540	0.6000	0.6500
8	7.0692E-01	5.9014E-01	0.5294	101.814	0.00	89.056	89.250	1.08063	0.7000	0.7500
9	6.1213E-01	4.9811E-01	0.5357	101.158	0.00	87.058	87.256	1.05586	0.8000	0.8500
10	4.9111E-01	3.8375E-01	0.5458	100.490	0.00	83.630	83.826	1.03110	0.9000	0.9500
11	4.4517E-01	3.2631E-01	0.5616	99.980	0.61	82.723	82.338	1.01252	0.9750	1.0000

FUEL PLATE 3 (BroydenSoln) AREAL — FUEL-CLADinterface

NODE	FLUX inner MW/m^2	FLUX outer MW/m^2	FUEL X inner	Tsat (C)	Tdiff (C)	inner (C)	outer (C)	Pressure (bar)	Z-mid	Z-int
1	2.7805E-01	2.8572E-01	0.4796	105.939	0.00	60.613	60.569	1.24781	0.0250	0.0500
2	3.3020E-01	3.3818E-01	0.4804	105.504	0.00	64.126	64.077	1.22923	0.1000	0.1500
3	4.5802E-01	4.6747E-01	0.4813	104.915	0.00	71.848	71.782	1.20447	0.2000	0.2500
4	5.6802E-01	5.7789E-01	0.4821	104.317	-0.01	78.869	78.798	1.17970	0.3000	0.3500
5	6.6402E-01	6.7293E-01	0.4831	103.708	0.00	85.404	85.319	1.15493	0.4000	0.4500
6	7.2406E-01	7.3051E-01	0.4842	103.088	0.00	90.437	90.352	1.13017	0.5000	0.5500
7	7.3358E-01	7.3581E-01	0.4856	102.457	0.00	93.276	93.201	1.10540	0.6000	0.6500
8	6.8883E-01	6.8520E-01	0.4877	101.814	0.00	93.655	93.597	1.08063	0.7000	0.7500
9	5.9358E-01	5.8228E-01	0.4912	101.158	0.03	91.563	91.499	1.05586	0.8000	0.8500
10	4.7189E-01	4.5433E-01	0.4959	100.490	0.00	87.874	87.869	1.03110	0.9000	0.9500
11	4.2459E-01	3.9184E-01	0.5064	99.980	0.52	86.886	86.398	1.01252	0.9750	1.0000

Figure 4.29 Continued

FUEL PLATE 4 (BroydenSoln) AREAL

NODE	FLUX inner MW/m^2	FLUX outer MW/m^2	FUEL X inner	Tsat (C)	Tdiff (C)	FUEL-CLADinterface inner (C)	FUEL-CLADinterface outer (C)	Pressure (bar)	Z-mid	Z-int
1	3.0622E-01	2.9655E-01	0.4960	105.939	0.00	61.590	61.586	1.24781	0.0250	0.0500
2	3.6387E-01	3.5076E-01	0.4972	105.504	0.00	65.328	65.327	1.22923	0.1000	0.1500
3	5.0491E-01	4.8462E-01	0.4982	104.915	0.00	73.526	73.532	1.20447	0.2000	0.2500
4	6.2663E-01	5.9859E-01	0.4994	104.317	0.01	80.998	81.003	1.17970	0.3000	0.3500
5	7.3270E-01	6.9679E-01	0.5006	103.708	0.00	87.943	87.967	1.15493	0.4000	0.4500
6	7.9942E-01	7.5585E-01	0.5020	103.088	0.00	93.313	93.349	1.13017	0.5000	0.5500
7	8.1059E-01	7.6054E-01	0.5039	102.457	0.00	96.375	96.424	1.10540	0.6000	0.6500
8	7.6195E-01	7.0724E-01	0.5066	101.814	0.00	96.852	96.917	1.08063	0.7000	0.7500
9	6.5705E-01	6.0025E-01	0.5106	101.158	-0.01	94.708	94.792	1.05586	0.8000	0.8500
10	5.2406E-01	4.6637E-01	0.5171	100.490	0.00	90.918	91.010	1.03110	0.9000	0.9500
11	4.6803E-01	4.0480E-01	0.5243	99.980	0.21	89.758	89.656	1.01252	0.9750	1.0000

FUEL PLATE 5 (BroydenSoln) AREAL

NODE	FLUX inner MW/m^2	FLUX outer MW/m^2	FUEL X inner	Tsat (C)	Tdiff (C)	FUEL-CLADinterface inner (C)	FUEL-CLADinterface outer (C)	Pressure (bar)	Z-mid	Z-int
1	3.3237E-01	3.0992E-01	0.5067	105.939	0.00	63.417	63.445	1.24781	0.0250	0.0500
2	3.9500E-01	3.6648E-01	0.5080	105.504	0.00	67.519	67.558	1.22923	0.1000	0.1500
3	5.4810E-01	5.0631E-01	0.5091	104.915	0.00	76.558	76.615	1.20447	0.2000	0.2500
4	6.7993E-01	6.2559E-01	0.5101	104.317	0.00	84.753	84.834	1.17970	0.3000	0.3500
5	7.9483E-01	7.2834E-01	0.5111	103.708	0.00	92.354	92.451	1.15493	0.4000	0.4500
6	8.6661E-01	7.9054E-01	0.5122	103.088	0.00	98.184	98.299	1.13017	0.5000	0.5500
7	8.7777E-01	7.9623E-01	0.5136	102.457	0.00	101.474	101.601	1.10540	0.6000	0.6500
8	8.2353E-01	7.4177E-01	0.5154	101.814	0.00	101.921	102.052	1.08063	0.7000	0.7500
9	7.0859E-01	6.3088E-01	0.5183	101.158	0.03	99.504	99.606	1.05586	0.8000	0.8500
10	5.6164E-01	4.9333E-01	0.5217	100.490	0.00	95.238	95.357	1.03110	0.9000	0.9500
11	4.9859E-01	4.3096E-01	0.5257	99.980	0.19	93.853	93.782	1.01252	0.9750	1.0000

FUEL PLATE 6 (BroydenSoln) AREAL

NODE	FLUX inner MW/m^2	FLUX outer MW/m^2	FUEL X inner	Tsat (C)	Tdiff (C)	FUEL-CLADinterface inner (C)	FUEL-CLADinterface outer (C)	Pressure (bar)	Z-mid	Z-int
1	3.3716E-01	3.5119E-01	0.4802	105.939	0.00	64.918	64.862	1.24781	0.0250	0.0500
2	3.9452E-01	4.2132E-01	0.4739	105.504	0.00	69.035	68.944	1.22923	0.1000	0.1500
3	5.3977E-01	5.8961E-01	0.4683	104.915	0.00	78.298	78.143	1.20447	0.2000	0.2500
4	6.6017E-01	7.3781E-01	0.4626	104.317	0.00	86.510	86.280	1.17970	0.3000	0.3500
5	7.6046E-01	8.7014E-01	0.4568	103.708	0.00	93.953	93.640	1.15493	0.4000	0.4500
6	8.1461E-01	9.5886E-01	0.4498	103.088	0.00	99.387	98.988	1.13017	0.5000	0.5500
7	8.0600E-01	9.8476E-01	0.4406	102.457	0.00	102.021	101.541	1.10540	0.6000	0.6500
8	7.3184E-01	9.4168E-01	0.4278	101.814	0.00	101.571	101.022	1.08063	0.7000	0.7500
9	5.9799E-01	8.3284E-01	0.4086	101.158	0.00	98.056	97.457	1.05586	0.8000	0.8500
10	4.3685E-01	6.8864E-01	0.3790	100.490	0.00	92.655	92.026	1.03110	0.9000	0.9500
11	3.6448E-01	6.2626E-01	0.3590	99.980	0.00	90.574	89.925	1.01252	0.9750	1.0000

Figure 4.30 Solution of ASTRA2 Problem 3 Case 1 by the Broyden Method in PLTEMP/ANL Version 3.2 (Using Coolant C_p = 4180 J/kg-°C, and ρ = 1000 kg/m^3, Same as ASTRA2 Code Input)

FUEL PLATE 1 (BroydenSoln)

NODE	COOLANT inner(C)	CladSurf inner(C)	FUEL PEAK (C)	CladSurf outer(C)	COOLANT outer(C)	HCOFinner W/C-m^2	HCOFouter W/C-m^2	ONBRin [F Note 1]	ONBRout	ETAin K-cm^3/J	ETAout K-cm^3/J	COOLNT at inner(C)	NodeOutlet outer(C)
	45.000				45.000								
1	45.123	57.170	58.092	57.116	45.239	2.0895E+04	2.1301E+04	6.11	6.14	8.958E+02	9.111E+02	45.247	45.478
2	45.542	59.817	60.926	59.785	46.043	2.1151E+04	2.1587E+04	5.05	5.06	7.363E+02	7.611E+02	45.838	46.608
3	46.252	65.726	67.283	65.724	47.387	2.1693E+04	2.2179E+04	3.67	3.66	5.149E+02	5.372E+02	46.666	48.167
4	47.184	71.002	72.956	71.051	49.130	2.2189E+04	2.2738E+04	2.96	2.94	4.008E+02	4.205E+02	47.701	50.093
5	48.312	75.857	78.168	75.975	51.214	2.2621E+04	2.3240E+04	2.51	2.49	3.296E+02	3.464E+02	48.922	52.334
6	49.595	79.488	82.043	79.696	53.550	2.2956E+04	2.3647E+04	2.25	2.22	2.890E+02	3.043E+02	50.267	54.765
7	50.957	81.353	83.987	81.666	55.988	2.3165E+04	2.3925E+04	2.13	2.08	2.712E+02	2.872E+02	51.647	57.211
8	52.306	81.252	83.784	81.678	58.349	2.3236E+04	2.4055E+04	2.11	2.05	2.729E+02	2.941E+02	52.965	59.486
9	53.547	79.188	81.445	79.725	60.452	2.3162E+04	2.4027E+04	2.19	2.11	2.972E+02	3.338E+02	54.128	61.418
10	54.609	75.933	77.823	76.567	62.170	2.2985E+04	2.3881E+04	2.37	2.25	3.471E+02	4.232E+02	55.089	62.921
11	55.307	74.732	76.467	75.419	63.250	2.2934E+04	2.3847E+04	2.43	2.29	3.718E+02	4.806E+02	55.525	63.578
	55.525				63.578								

FUEL PLATE 2 (BroydenSoln)

	45.000				45.000								
1	45.239	58.394	59.455	58.505	45.276	2.1416E+04	1.8912E+04	5.59	5.51	8.182E+02	7.877E+02	45.478	45.552
2	46.043	61.458	62.721	61.601	46.205	2.1734E+04	1.9201E+04	4.58	4.50	6.740E+02	6.516E+02	46.608	46.859
3	47.387	68.156	69.912	68.367	47.764	2.2401E+04	1.9805E+04	3.31	3.25	4.696E+02	4.550E+02	48.167	48.668
4	49.130	74.265	76.447	74.542	49.788	2.2988E+04	2.0342E+04	2.65	2.60	3.627E+02	3.518E+02	50.093	50.907
5	51.214	79.956	82.513	80.301	52.213	2.3530E+04	2.0840E+04	2.23	2.18	2.948E+02	2.858E+02	52.334	53.518
6	53.550	84.365	87.162	84.769	54.938	2.3974E+04	2.1253E+04	1.98	1.94	2.546E+02	2.467E+02	54.765	56.357
7	55.988	86.886	89.730	87.330	57.789	2.4284E+04	2.1548E+04	1.86	1.81	2.352E+02	2.279E+02	57.211	59.221
8	58.349	87.273	89.961	87.743	60.559	2.4442E+04	2.1707E+04	1.82	1.77	2.335E+02	2.271E+02	59.486	61.896
9	60.452	85.504	87.839	85.974	63.037	2.4436E+04	2.1715E+04	1.86	1.80	2.525E+02	2.486E+02	61.418	64.179
10	62.170	82.374	84.258	82.831	65.075	2.4307E+04	2.1613E+04	1.96	1.90	2.963E+02	2.998E+02	62.921	65.970
11	63.250	81.301	82.990	81.758	66.364	2.4286E+04	2.1610E+04	1.99	1.92	3.182E+02	3.283E+02	63.578	66.758
	63.578				66.758								

FUEL PLATE 3 (BroydenSoln)

	45.000				45.000								
1	45.276	59.895	60.927	59.817	45.296	1.9021E+04	1.9675E+04	5.03	5.06	7.087E+02	7.195E+02	45.552	45.592
2	46.205	63.289	64.515	63.203	46.294	1.9330E+04	1.9998E+04	4.12	4.15	5.833E+02	5.936E+02	46.859	46.996
3	47.764	70.698	72.400	70.586	47.968	1.9972E+04	2.0667E+04	2.98	3.00	4.053E+02	4.130E+02	48.668	48.940
4	49.788	77.456	79.568	77.327	50.145	2.0533E+04	2.1256E+04	2.39	2.40	3.118E+02	3.178E+02	50.907	51.349
5	52.213	83.757	86.225	83.616	52.755	2.1053E+04	2.1803E+04	2.01	2.02	2.519E+02	2.567E+02	53.518	54.160
6	54.938	88.642	91.336	88.507	55.691	2.1484E+04	2.2260E+04	1.79	1.79	2.160E+02	2.199E+02	56.357	57.221
7	57.789	91.455	94.185	91.335	58.768	2.1793E+04	2.2591E+04	1.67	1.67	1.978E+02	2.013E+02	59.221	60.314
8	60.559	91.932	94.501	91.853	61.762	2.1956E+04	2.2771E+04	1.63	1.63	1.946E+02	1.981E+02	61.896	63.210
9	63.037	90.050	92.267	90.020	64.451	2.1961E+04	2.2787E+04	1.66	1.66	2.088E+02	2.136E+02	64.179	65.692
10	65.075	86.673	88.441	86.693	66.671	2.1850E+04	2.2691E+04	1.75	1.74	2.438E+02	2.523E+02	65.970	67.651
11	66.364	85.541	87.116	85.593	68.083	2.1846E+04	2.2684E+04	1.77	1.76	2.607E+02	2.722E+02	66.758	68.515
	66.758				68.515								

Figure 4.30 Continued

FUEL PLATE 4 (BroydenSoln)

NODE	COOLANT inner(C)	CladSurf inner(C)	FUEL PEAK (C)	CladSurf outer(C)	COOLANT outer(C)	HCOFinner W/C-m^2	HCOFouter W/C-m^2	ONBRin [F Note 1]	ONBRout [F Note 1]	ETAin K-cm^3/J	ETAout K-cm^3/J	COOLNT at inner(C)	NodeOutlet outer(C)
	45.000				45.000								
1	45.296	60.798	61.951	60.809	45.327	1.9754E+04	1.9155E+04	4.77	4.75	6.713E+02	6.666E+02	45.592	45.654
2	46.294	64.405	65.776	64.425	46.430	2.0092E+04	1.9489E+04	3.91	3.89	5.515E+02	5.493E+02	46.996	47.205
3	47.968	72.259	74.163	72.299	48.279	2.0788E+04	2.0174E+04	2.83	2.82	3.823E+02	3.812E+02	48.940	49.353
4	50.145	79.432	81.797	79.495	50.683	2.1395E+04	2.0776E+04	2.27	2.25	2.931E+02	2.922E+02	51.349	52.013
5	52.755	86.125	88.892	86.217	53.564	2.1958E+04	2.1338E+04	1.91	1.90	2.357E+02	2.347E+02	54.160	55.116
6	55.691	91.332	94.353	91.451	56.803	2.2432E+04	2.1813E+04	1.70	1.69	2.010E+02	1.997E+02	57.221	58.491
7	58.768	94.358	97.426	94.510	60.196	2.2776E+04	2.2163E+04	1.59	1.57	1.827E+02	1.812E+02	60.314	61.900
8	61.762	94.946	97.833	95.125	63.493	2.2963E+04	2.2357E+04	1.55	1.53	1.782E+02	1.767E+02	63.210	65.086
9	64.451	93.053	95.548	93.256	66.447	2.2975E+04	2.2388E+04	1.58	1.56	1.894E+02	1.886E+02	65.692	67.809
10	66.671	89.582	91.581	89.808	68.879	2.2872E+04	2.2286E+04	1.65	1.63	2.188E+02	2.210E+02	67.651	69.950
11	68.083	88.450	90.230	88.686	70.420	2.2865E+04	2.2284E+04	1.67	1.64	2.322E+02	2.369E+02	68.515	70.891
	68.515				70.891								

FUEL PLATE 5 (BroydenSoln)

	45.000				45.000								
1	45.327	62.558	63.822	62.634	45.368	1.9290E+04	1.7949E+04	4.31	4.28	5.947E+02	5.822E+02	45.654	45.736
2	46.430	66.522	68.025	66.622	46.601	1.9662E+04	1.8303E+04	3.54	3.51	4.877E+02	4.789E+02	47.205	47.467
3	48.279	75.189	77.276	75.338	48.656	2.0370E+04	1.8974E+04	2.57	2.55	3.370E+02	3.310E+02	49.353	49.845
4	50.683	83.069	85.659	83.266	51.306	2.0998E+04	1.9571E+04	2.06	2.04	2.572E+02	2.525E+02	52.013	52.768
5	53.564	90.391	93.420	90.635	54.460	2.1584E+04	2.0132E+04	1.74	1.72	2.057E+02	2.014E+02	55.116	56.152
6	56.803	96.043	99.349	96.329	57.976	2.2085E+04	2.0612E+04	1.55	1.53	1.742E+02	1.700E+02	58.491	59.799
7	60.196	99.300	102.648	99.605	61.620	2.2448E+04	2.0960E+04	1.45	1.43	1.570E+02	1.528E+02	61.900	63.440
8	63.493	99.868	103.016	100.188	65.113	2.2641E+04	2.1147E+04	1.42	1.40	1.518E+02	1.474E+02	65.086	66.786
9	66.447	97.702	100.413	98.010	68.182	2.2658E+04	2.1164E+04	1.45	1.42	1.599E+02	1.556E+02	67.809	69.577
10	68.879	93.805	95.958	94.084	70.632	2.2529E+04	2.1040E+04	1.52	1.49	1.836E+02	1.803E+02	69.950	71.687
11	70.420	92.471	94.378	92.736	72.139	2.2514E+04	2.1022E+04	1.53	1.51	1.942E+02	1.915E+02	70.891	72.591
	70.891				72.591								

FUEL PLATE 6 (BroydenSoln)

	45.000				45.000								
1	45.368	64.044	65.306	63.939	45.160	1.8048E+04	1.8706E+04	3.98	4.01	5.353E+02	5.554E+02	45.736	45.319
2	46.601	68.031	69.501	67.854	45.702	1.8399E+04	1.9030E+04	3.31	3.35	4.450E+02	4.554E+02	47.467	46.085
3	48.656	76.939	78.943	76.629	46.621	1.9071E+04	1.9660E+04	2.43	2.47	3.107E+02	3.172E+02	49.845	47.157
4	51.306	84.859	87.302	84.396	47.827	1.9661E+04	2.0189E+04	1.97	2.01	2.394E+02	2.456E+02	52.768	48.498
5	54.460	92.061	94.863	91.423	49.289	2.0210E+04	2.0664E+04	1.68	1.72	1.931E+02	2.006E+02	56.152	50.080
6	57.976	97.362	100.352	96.547	50.951	2.0669E+04	2.1041E+04	1.51	1.55	1.651E+02	1.744E+02	59.799	51.823
7	61.620	100.013	102.955	99.027	52.718	2.0983E+04	2.1273E+04	1.42	1.48	1.510E+02	1.621E+02	63.440	53.613
8	65.113	99.746	102.396	98.611	54.468	2.1122E+04	2.1340E+04	1.41	1.47	1.495E+02	1.613E+02	66.786	55.324
9	68.182	96.549	98.689	95.305	56.081	2.1081E+04	2.1232E+04	1.46	1.54	1.643E+02	1.737E+02	69.577	56.837
10	70.632	91.545	93.079	90.233	57.463	2.0896E+04	2.1010E+04	1.56	1.67	2.035E+02	2.006E+02	71.687	58.088
11	72.139	89.629	90.892	88.274	58.372	2.0845E+04	2.0940E+04	1.59	1.72	2.275E+02	2.133E+02	72.591	58.657
	72.591				58.657								

Figure 4.30 Continued

FUEL PLATE 1 (BroydenSoln) AREAL — FUEL-CLADinterface

NODE	FLUX inner MW/m^2	FLUX outer MW/m^2	FUEL X inner	Tsat (C)	Tdiff (C)	inner (C)	outer (C)	Pressure (bar)	Z-mid	Z-int
1	2.5172E-01	2.5299E-01	0.4801	105.939	0.00	57.828	57.793	1.24781	0.0250	0.0500
2	3.0192E-01	2.9666E-01	0.4858	105.504	0.00	60.606	60.580	1.22923	0.1000	0.1500
3	4.2243E-01	4.0668E-01	0.4909	104.915	0.00	66.830	66.813	1.20447	0.2000	0.2500
4	5.2850E-01	4.9843E-01	0.4960	104.317	0.00	72.384	72.386	1.17970	0.3000	0.3500
5	6.2310E-01	5.7544E-01	0.5013	103.708	0.00	77.486	77.516	1.15493	0.4000	0.4500
6	6.8625E-01	6.1827E-01	0.5075	103.088	0.00	81.283	81.351	1.13017	0.5000	0.5500
7	7.0414E-01	6.1435E-01	0.5155	102.457	0.00	83.194	83.312	1.10540	0.6000	0.6500
8	6.7260E-01	5.6119E-01	0.5266	101.814	0.00	83.011	83.181	1.08063	0.7000	0.7500
9	5.9391E-01	4.6307E-01	0.5435	101.158	0.00	80.741	80.965	1.05586	0.8000	0.8500
10	4.9015E-01	3.4383E-01	0.5696	100.490	0.00	77.215	77.488	1.03110	0.9000	0.9500
11	4.4548E-01	2.9020E-01	0.5876	99.980	0.00	75.897	76.196	1.01252	0.9750	1.0000

FUEL PLATE 2 (BroydenSoln) AREAL — FUEL-CLADinterface

NODE	FLUX inner MW/m^2	FLUX outer MW/m^2	FUEL X inner	Tsat (C)	Tdiff (C)	inner (C)	outer (C)	Pressure (bar)	Z-mid	Z-int
1	2.8173E-01	2.5018E-01	0.5139	105.939	0.00	59.132	59.174	1.24781	0.0250	0.0500
2	3.3503E-01	2.9561E-01	0.5156	105.504	0.00	62.336	62.391	1.22923	0.1000	0.1500
3	4.6523E-01	4.0805E-01	0.5170	104.915	0.00	69.375	69.457	1.20447	0.2000	0.2500
4	5.7779E-01	5.0354E-01	0.5186	104.317	0.00	75.778	75.888	1.17970	0.3000	0.3500
5	6.7630E-01	5.8537E-01	0.5203	103.708	0.00	81.728	81.866	1.15493	0.4000	0.4500
6	7.3876E-01	6.3401E-01	0.5225	103.088	0.00	86.301	86.464	1.13017	0.5000	0.5500
7	7.5033E-01	6.3656E-01	0.5253	102.457	0.00	88.851	89.032	1.10540	0.6000	0.6500
8	7.0698E-01	5.9009E-01	0.5294	101.814	0.00	89.125	89.321	1.08063	0.7000	0.7500
9	6.1216E-01	4.9808E-01	0.5358	101.158	0.00	87.108	87.306	1.05586	0.8000	0.8500
10	4.9111E-01	3.8375E-01	0.5458	100.490	0.00	83.660	83.856	1.03110	0.9000	0.9500
11	4.3840E-01	3.3266E-01	0.5531	99.980	0.00	82.450	82.647	1.01252	0.9750	1.0000

FUEL PLATE 3 (BroydenSoln) AREAL — FUEL-CLADinterface

NODE	FLUX inner MW/m^2	FLUX outer MW/m^2	FUEL X inner	Tsat (C)	Tdiff (C)	inner (C)	outer (C)	Pressure (bar)	Z-mid	Z-int
1	2.7807E-01	2.8570E-01	0.4796	105.939	0.00	60.625	60.579	1.24781	0.0250	0.0500
2	3.3023E-01	3.3815E-01	0.4805	105.504	0.00	64.155	64.106	1.22923	0.1000	0.1500
3	4.5805E-01	4.6744E-01	0.4813	104.915	0.00	71.900	71.834	1.20447	0.2000	0.2500
4	5.6813E-01	5.7778E-01	0.4822	104.317	0.00	78.947	78.869	1.17970	0.3000	0.3500
5	6.6409E-01	6.7286E-01	0.4831	103.708	0.00	85.499	85.413	1.15493	0.4000	0.4500
6	7.2410E-01	7.3048E-01	0.4842	103.088	0.00	90.541	90.457	1.13017	0.5000	0.5500
7	7.3368E-01	7.3572E-01	0.4857	102.457	0.01	93.380	93.299	1.10540	0.6000	0.6500
8	6.8883E-01	6.8520E-01	0.4877	101.814	0.00	93.739	93.682	1.08063	0.7000	0.7500
9	5.9321E-01	5.8263E-01	0.4909	101.158	0.00	91.606	91.575	1.05586	0.8000	0.8500
10	4.7192E-01	4.5431E-01	0.4959	100.490	0.00	87.911	87.906	1.03110	0.9000	0.9500
11	4.1894E-01	3.9719E-01	0.4997	99.980	0.00	86.640	86.653	1.01252	0.9750	1.0000

Figure 4.30 Continued

FUEL PLATE 4 (BroydenSoln) AREAL

NODE	FLUX inner MW/m^2	FLUX outer MW/m^2	FUEL X inner	Tsat (C)	Tdiff (C)	FUEL-CLADinterface inner (C)	FUEL-CLADinterface outer (C)	Pressure (bar)	Z-mid	Z-int
1	3.0622E-01	2.9656E-01	0.4960	105.939	0.00	61.602	61.600	1.24781	0.0250	0.0500
2	3.6390E-01	3.5073E-01	0.4972	105.504	0.00	65.361	65.361	1.22923	0.1000	0.1500
3	5.0496E-01	4.8457E-01	0.4983	104.915	0.00	73.586	73.591	1.20447	0.2000	0.2500
4	6.2661E-01	5.9861E-01	0.4994	104.317	0.00	81.078	81.092	1.17970	0.3000	0.3500
5	7.3276E-01	6.9673E-01	0.5006	103.708	0.00	88.049	88.075	1.15493	0.4000	0.4500
6	7.9950E-01	7.5577E-01	0.5021	103.088	0.00	93.432	93.467	1.13017	0.5000	0.5500
7	8.1063E-01	7.6050E-01	0.5039	102.457	0.00	96.487	96.539	1.10540	0.6000	0.6500
8	7.6199E-01	7.0720E-01	0.5066	101.814	0.00	96.947	97.012	1.08063	0.7000	0.7500
9	6.5712E-01	6.0019E-01	0.5106	101.158	0.00	94.778	94.856	1.05586	0.8000	0.8500
10	5.2401E-01	4.6642E-01	0.5171	100.490	0.00	90.958	91.052	1.03110	0.9000	0.9500
11	4.6569E-01	4.0703E-01	0.5216	99.980	0.00	89.673	89.771	1.01252	0.9750	1.0000

FUEL PLATE 5 (BroydenSoln) AREAL

NODE	FLUX inner MW/m^2	FLUX outer MW/m^2	FUEL X inner	Tsat (C)	Tdiff (C)	FUEL-CLADinterface inner (C)	FUEL-CLADinterface outer (C)	Pressure (bar)	Z-mid	Z-int
1	3.3239E-01	3.0990E-01	0.5068	105.939	0.00	63.432	63.460	1.24781	0.0250	0.0500
2	3.9506E-01	3.6643E-01	0.5081	105.504	0.00	67.560	67.598	1.22923	0.1000	0.1500
3	5.4815E-01	5.0626E-01	0.5091	104.915	0.00	76.630	76.687	1.20447	0.2000	0.2500
4	6.8003E-01	6.2550E-01	0.5102	104.317	0.00	84.856	84.933	1.17970	0.3000	0.3500
5	7.9489E-01	7.2828E-01	0.5111	103.708	0.00	92.481	92.576	1.15493	0.4000	0.4500
6	8.6662E-01	7.9053E-01	0.5122	103.088	0.00	98.321	98.436	1.13017	0.5000	0.5500
7	8.7782E-01	7.9619E-01	0.5137	102.457	0.01	101.607	101.727	1.10540	0.6000	0.6500
8	8.2357E-01	7.4173E-01	0.5154	101.814	0.00	102.033	102.165	1.08063	0.7000	0.7500
9	7.0816E-01	6.3128E-01	0.5180	101.158	0.00	99.564	99.693	1.05586	0.8000	0.8500
10	5.6155E-01	4.9342E-01	0.5216	100.490	0.00	95.281	95.399	1.03110	0.9000	0.9500
11	4.9647E-01	4.3299E-01	0.5234	99.980	0.00	93.776	93.890	1.01252	0.9750	1.0000

FUEL PLATE 6 (BroydenSoln) AREAL

NODE	FLUX inner MW/m^2	FLUX outer MW/m^2	FUEL X inner	Tsat (C)	Tdiff (C)	FUEL-CLADinterface inner (C)	FUEL-CLADinterface outer (C)	Pressure (bar)	Z-mid	Z-int
1	3.3707E-01	3.5127E-01	0.4801	105.939	0.00	64.931	64.874	1.24781	0.0250	0.0500
2	3.9429E-01	4.2154E-01	0.4737	105.504	0.00	69.068	68.977	1.22923	0.1000	0.1500
3	5.3940E-01	5.8997E-01	0.4680	104.915	0.00	78.358	78.200	1.20447	0.2000	0.2500
4	6.5968E-01	7.3829E-01	0.4623	104.317	0.00	86.595	86.362	1.17970	0.3000	0.3500
5	7.5992E-01	8.7066E-01	0.4565	103.708	0.00	94.060	93.742	1.15493	0.4000	0.4500
6	8.1408E-01	9.5937E-01	0.4495	103.088	0.00	99.503	99.103	1.13017	0.5000	0.5500
7	8.0560E-01	9.8514E-01	0.4403	102.457	0.00	102.132	101.650	1.10540	0.6000	0.6500
8	7.3152E-01	9.4199E-01	0.4277	101.814	0.00	101.670	101.120	1.08063	0.7000	0.7500
9	5.9801E-01	8.3282E-01	0.4086	101.158	0.00	98.122	97.523	1.05586	0.8000	0.8500
10	4.3699E-01	6.8850E-01	0.3791	100.490	0.00	92.694	92.067	1.03110	0.9000	0.9500
11	3.6459E-01	6.2615E-01	0.3591	99.980	0.00	90.588	89.941	1.01252	0.9750	1.0000

Figure 4.31 Solution of ASTRA2 Problem 3 Case 1 by the Radial Geometry Exact Method in PLTEMP/ANL Version 3.2 (Using Coolant C_P = 4180 J/kg-°C, and ρ = 1000 kg/m^3, Same as ASTRA2 Code Input)

FUEL PLATE 1 (ExactSoln)

NODE	COOLANT inner(C)	CladSurf inner(C)	FUEL PEAK (C)	CladSurf outer(C)	COOLANT outer(C)	HCOFinner W/C-m^2	HCOFouter W/C-m^2	ONBRin [F Note 1]	ONBRout	ETAin K-cm^3/J	ETAout K-cm^3/J	COOLNT at inner(C)	NodeOutlet outer(C)
	45.000				45.000								
1	45.123	57.172	58.127	57.114	45.239	2.0895E+04	2.1301E+04	6.11	6.14	8.956E+02	9.113E+02	45.247	45.478
2	45.542	59.818	60.967	59.784	46.043	2.1151E+04	2.1587E+04	5.05	5.06	7.362E+02	7.612E+02	45.838	46.607
3	46.252	65.727	67.339	65.723	47.387	2.1693E+04	2.2179E+04	3.67	3.66	5.148E+02	5.372E+02	46.666	48.167
4	47.184	71.002	73.026	71.051	49.130	2.2189E+04	2.2738E+04	2.96	2.94	4.008E+02	4.204E+02	47.702	50.093
5	48.312	75.855	78.249	75.977	51.213	2.2621E+04	2.3240E+04	2.51	2.48	3.296E+02	3.464E+02	48.922	52.334
6	49.595	79.484	82.131	79.699	53.549	2.2956E+04	2.3647E+04	2.25	2.22	2.891E+02	3.042E+02	50.267	54.764
7	50.957	81.346	84.076	81.672	55.987	2.3165E+04	2.3925E+04	2.13	2.08	2.712E+02	2.872E+02	51.646	57.210
8	52.305	81.242	83.867	81.686	58.348	2.3235E+04	2.4056E+04	2.11	2.05	2.730E+02	2.940E+02	52.964	59.485
9	53.545	79.174	81.515	79.736	60.451	2.3161E+04	2.4028E+04	2.19	2.11	2.974E+02	3.336E+02	54.127	61.417
10	54.607	75.916	77.879	76.580	62.169	2.2984E+04	2.3882E+04	2.37	2.25	3.473E+02	4.228E+02	55.087	62.920
11	55.305	74.713	76.516	75.433	63.249	2.2932E+04	2.3848E+04	2.43	2.29	3.721E+02	4.800E+02	55.523	63.578
	55.523				63.578								

FUEL PLATE 2 (ExactSoln)

	45.000				45.000								
1	45.239	58.392	59.485	58.507	45.276	2.1416E+04	1.8912E+04	5.59	5.50	8.183E+02	7.875E+02	45.478	45.552
2	46.043	61.456	62.757	61.603	46.205	2.1734E+04	1.9202E+04	4.58	4.50	6.741E+02	6.515E+02	46.607	46.859
3	47.387	68.153	69.962	68.371	47.764	2.2400E+04	1.9806E+04	3.31	3.25	4.696E+02	4.549E+02	48.167	48.669
4	49.130	74.260	76.509	74.547	49.789	2.2988E+04	2.0342E+04	2.65	2.59	3.628E+02	3.517E+02	50.093	50.908
5	51.213	79.950	82.586	80.308	52.214	2.3529E+04	2.0841E+04	2.23	2.18	2.948E+02	2.857E+02	52.334	53.520
6	53.549	84.358	87.241	84.777	54.939	2.3973E+04	2.1254E+04	1.98	1.94	2.547E+02	2.466E+02	54.764	56.359
7	55.987	86.877	89.810	87.340	57.791	2.4284E+04	2.1549E+04	1.86	1.81	2.352E+02	2.279E+02	57.210	59.223
8	58.348	87.265	90.036	87.753	60.561	2.4442E+04	2.1707E+04	1.82	1.77	2.335E+02	2.270E+02	59.485	61.898
9	60.451	85.496	87.904	85.985	63.040	2.4435E+04	2.1716E+04	1.86	1.80	2.526E+02	2.485E+02	61.417	64.182
10	62.169	82.366	84.310	82.841	65.078	2.4307E+04	2.1613E+04	1.96	1.90	2.964E+02	2.996E+02	62.920	65.974
11	63.249	81.293	83.036	81.769	66.367	2.4286E+04	2.1611E+04	1.99	1.92	3.183E+02	3.281E+02	63.578	66.761
	63.578				66.761								

FUEL PLATE 3 (ExactSoln)

	45.000				45.000								
1	45.276	59.897	60.955	59.815	45.296	1.9021E+04	1.9675E+04	5.02	5.06	7.086E+02	7.196E+02	45.552	45.592
2	46.205	63.291	64.549	63.201	46.294	1.9331E+04	1.9998E+04	4.12	4.15	5.832E+02	5.936E+02	46.859	46.995
3	47.764	70.701	72.446	70.584	47.968	1.9972E+04	2.0667E+04	2.98	3.00	4.053E+02	4.130E+02	48.669	48.940
4	49.789	77.459	79.625	77.324	50.144	2.0534E+04	2.1256E+04	2.38	2.40	3.118E+02	3.179E+02	50.908	51.349
5	52.214	83.759	86.292	83.614	52.754	2.1053E+04	2.1803E+04	2.01	2.02	2.519E+02	2.567E+02	53.520	54.160
6	54.939	88.645	91.409	88.504	55.690	2.1484E+04	2.2260E+04	1.79	1.79	2.160E+02	2.200E+02	56.359	57.220
7	57.791	91.456	94.259	91.335	58.767	2.1793E+04	2.2591E+04	1.67	1.67	1.978E+02	2.013E+02	59.223	60.314
8	60.561	91.935	94.570	91.851	61.762	2.1956E+04	2.2771E+04	1.63	1.63	1.945E+02	1.982E+02	61.898	63.210
9	63.040	90.052	92.326	90.019	64.450	2.1961E+04	2.2787E+04	1.66	1.66	2.087E+02	2.136E+02	64.182	65.691
10	65.078	86.674	88.488	86.694	66.670	2.1850E+04	2.2691E+04	1.75	1.74	2.438E+02	2.523E+02	65.974	67.650
11	66.367	85.542	87.157	85.593	68.082	2.1847E+04	2.2684E+04	1.77	1.76	2.607E+02	2.722E+02	66.761	68.514
	66.761				68.514								

Figure 4.31 Continued

FUEL PLATE 4 (ExactSoln)

NODE	COOLANT inner(C)	CladSurf inner(C)	FUEL PEAK (C)	CladSurf outer(C)	COOLANT outer(C)	HCOFinner W/C-m^2	HCOFouter W/C-m^2	ONBRin [F Note 1]	ONBRout [F Note 1]	ETAin K-cm^3/J	ETAout K-cm^3/J	COOLNT at inner(C)	NodeOutlet outer(C)
	45.000				45.000								
1	45.296	60.798	61.977	60.808	45.327	1.9754E+04	1.9155E+04	4.77	4.76	6.713E+02	6.666E+02	45.592	45.654
2	46.294	64.405	65.807	64.426	46.429	2.0092E+04	1.9490E+04	3.91	3.89	5.516E+02	5.493E+02	46.995	47.205
3	47.968	72.259	74.206	72.299	48.279	2.0787E+04	2.0174E+04	2.83	2.82	3.823E+02	3.812E+02	48.940	49.353
4	50.144	79.432	81.850	79.495	50.683	2.1395E+04	2.0776E+04	2.27	2.25	2.931E+02	2.922E+02	51.349	52.013
5	52.754	86.125	88.955	86.216	53.564	2.1958E+04	2.1338E+04	1.91	1.90	2.357E+02	2.347E+02	54.160	55.115
6	55.690	91.330	94.421	91.452	56.803	2.2432E+04	2.1813E+04	1.70	1.69	2.010E+02	1.997E+02	57.220	58.491
7	58.767	94.357	97.494	94.511	60.195	2.2776E+04	2.2162E+04	1.59	1.57	1.827E+02	1.812E+02	60.314	61.899
8	61.762	94.943	97.897	95.127	63.492	2.2963E+04	2.2357E+04	1.55	1.53	1.782E+02	1.767E+02	63.210	65.085
9	64.450	93.049	95.602	93.258	66.447	2.2975E+04	2.2388E+04	1.58	1.56	1.894E+02	1.886E+02	65.691	67.808
10	66.670	89.579	91.624	89.809	68.879	2.2872E+04	2.2287E+04	1.65	1.63	2.188E+02	2.210E+02	67.650	69.949
11	68.082	88.445	90.267	88.689	70.419	2.2865E+04	2.2284E+04	1.67	1.64	2.322E+02	2.368E+02	68.514	70.890
	68.514				70.890								

FUEL PLATE 5 (ExactSoln)

	45.000				45.000								
1	45.327	62.557	63.847	62.635	45.368	1.9290E+04	1.7949E+04	4.31	4.27	5.947E+02	5.822E+02	45.654	45.736
2	46.429	66.521	68.055	66.623	46.602	1.9662E+04	1.8303E+04	3.54	3.51	4.877E+02	4.788E+02	47.205	47.467
3	48.279	75.187	77.317	75.340	48.656	2.0370E+04	1.8974E+04	2.57	2.54	3.370E+02	3.310E+02	49.353	49.846
4	50.683	83.066	85.711	83.269	51.307	2.0998E+04	1.9572E+04	2.06	2.04	2.572E+02	2.524E+02	52.013	52.769
5	53.564	90.388	93.481	90.640	54.461	2.1584E+04	2.0132E+04	1.74	1.72	2.058E+02	2.014E+02	55.115	56.153
6	56.803	96.040	99.415	96.333	57.978	2.2085E+04	2.0612E+04	1.55	1.53	1.742E+02	1.700E+02	58.491	59.802
7	60.195	99.294	102.714	99.613	61.622	2.2448E+04	2.0961E+04	1.45	1.43	1.570E+02	1.528E+02	61.899	63.443
8	63.492	99.865	103.079	100.193	65.117	2.2641E+04	2.1147E+04	1.42	1.40	1.518E+02	1.474E+02	65.085	66.791
9	66.447	97.700	100.468	98.016	68.187	2.2658E+04	2.1164E+04	1.45	1.42	1.599E+02	1.556E+02	67.808	69.582
10	68.879	93.802	96.002	94.090	70.638	2.2529E+04	2.1041E+04	1.52	1.49	1.836E+02	1.802E+02	69.949	71.693
11	70.419	92.471	94.418	92.742	72.145	2.2514E+04	2.1022E+04	1.53	1.51	1.942E+02	1.915E+02	70.890	72.597
	70.890				72.597								

FUEL PLATE 6 (ExactSoln)

	45.000				45.000								
1	45.368	64.046	65.333	63.937	45.160	1.8048E+04	1.8705E+04	3.98	4.02	5.352E+02	5.555E+02	45.736	45.319
2	46.602	68.034	69.534	67.851	45.702	1.8400E+04	1.9029E+04	3.31	3.35	4.449E+02	4.554E+02	47.467	46.085
3	48.656	76.944	78.988	76.624	46.621	1.9072E+04	1.9660E+04	2.43	2.47	3.106E+02	3.172E+02	49.846	47.156
4	51.307	84.867	87.358	84.389	47.827	1.9661E+04	2.0189E+04	1.97	2.01	2.393E+02	2.457E+02	52.769	48.498
5	54.461	92.070	94.929	91.416	49.288	2.0210E+04	2.0663E+04	1.68	1.72	1.930E+02	2.007E+02	56.153	50.079
6	57.978	97.375	100.424	96.536	50.950	2.0670E+04	2.1040E+04	1.50	1.55	1.650E+02	1.745E+02	59.802	51.822
7	61.622	100.029	103.028	99.013	52.716	2.0984E+04	2.1272E+04	1.42	1.48	1.509E+02	1.621E+02	63.443	53.611
8	65.117	99.764	102.464	98.595	54.466	2.1124E+04	2.1339E+04	1.41	1.47	1.494E+02	1.614E+02	66.791	55.322
9	68.187	96.569	98.748	95.288	56.078	2.1083E+04	2.1231E+04	1.46	1.54	1.641E+02	1.738E+02	69.582	56.834
10	70.638	91.566	93.128	90.215	57.459	2.0897E+04	2.1008E+04	1.56	1.67	2.033E+02	2.007E+02	71.693	58.084
11	72.145	89.651	90.936	88.256	58.368	2.0847E+04	2.0939E+04	1.59	1.72	2.272E+02	2.134E+02	72.597	58.653
	72.597				58.653								

Figure 4.31 Continued

FUEL PLATE 1 (ExactSoln) AREAL FUEL-CLADinterface

NODE	FLUX inner MW/m^2	FLUX outer MW/m^2	FUEL X inner	Tsat (C)	Tdiff (C)	inner (C)	outer (C)	Pressure (bar)	Z-mid	Z-int
1	2.5176E-01	2.5295E-01	0.4802	105.939		57.830	57.791	1.24781	0.0250	0.0500
2	3.0195E-01	2.9663E-01	0.4858	105.504		60.608	60.578	1.22923	0.1000	0.1500
3	4.2245E-01	4.0667E-01	0.4909	104.915		66.831	66.812	1.20447	0.2000	0.2500
4	5.2849E-01	4.9844E-01	0.4960	104.317		72.383	72.386	1.17970	0.3000	0.3500
5	6.2305E-01	5.7549E-01	0.5012	103.708		77.484	77.518	1.15493	0.4000	0.4500
6	6.8614E-01	6.1837E-01	0.5074	103.088		81.278	81.355	1.13017	0.5000	0.5500
7	7.0397E-01	6.1450E-01	0.5154	102.457		83.187	83.317	1.10540	0.6000	0.6500
8	6.7236E-01	5.6142E-01	0.5264	101.814		83.000	83.190	1.08063	0.7000	0.7500
9	5.9359E-01	4.6337E-01	0.5432	101.158		80.726	80.977	1.05586	0.8000	0.8500
10	4.8978E-01	3.4417E-01	0.5691	100.490		77.197	77.502	1.03110	0.9000	0.9500
11	4.4509E-01	2.9057E-01	0.5871	99.980		75.877	76.211	1.01252	0.9750	1.0000

FUEL PLATE 2 (ExactSoln) AREAL FUEL-CLADinterface

NODE	FLUX inner MW/m^2	FLUX outer MW/m^2	FUEL X inner	Tsat (C)	Tdiff (C)	inner (C)	outer (C)	Pressure (bar)	Z-mid	Z-int
1	2.8167E-01	2.5023E-01	0.5139	105.939		59.129	59.176	1.24781	0.0250	0.0500
2	3.3498E-01	2.9566E-01	0.5155	105.504		62.333	62.394	1.22923	0.1000	0.1500
3	4.6515E-01	4.0812E-01	0.5170	104.915		69.371	69.462	1.20447	0.2000	0.2500
4	5.7768E-01	5.0364E-01	0.5185	104.317		75.773	75.893	1.17970	0.3000	0.3500
5	6.7617E-01	5.8549E-01	0.5202	103.708		81.722	81.873	1.15493	0.4000	0.4500
6	7.3859E-01	6.3417E-01	0.5224	103.088		86.293	86.472	1.13017	0.5000	0.5500
7	7.5012E-01	6.3676E-01	0.5252	102.457		88.842	89.042	1.10540	0.6000	0.6500
8	7.0680E-01	5.9026E-01	0.5293	101.814		89.117	89.331	1.08063	0.7000	0.7500
9	6.1196E-01	4.9826E-01	0.5356	101.158		87.099	87.317	1.05586	0.8000	0.8500
10	4.9093E-01	3.8392E-01	0.5456	100.490		83.652	83.867	1.03110	0.9000	0.9500
11	4.3822E-01	3.3284E-01	0.5528	99.980		82.441	82.659	1.01252	0.9750	1.0000

FUEL PLATE 3 (ExactSoln) AREAL FUEL-CLADinterface

NODE	FLUX inner MW/m^2	FLUX outer MW/m^2	FUEL X inner	Tsat (C)	Tdiff (C)	inner (C)	outer (C)	Pressure (bar)	Z-mid	Z-int
1	2.7810E-01	2.8567E-01	0.4797	105.939		60.626	60.578	1.24781	0.0250	0.0500
2	3.3027E-01	3.3811E-01	0.4805	105.504		64.158	64.103	1.22923	0.1000	0.1500
3	4.5809E-01	4.6740E-01	0.4814	104.915		71.903	71.832	1.20447	0.2000	0.2500
4	5.6818E-01	5.7773E-01	0.4822	104.317		78.950	78.867	1.17970	0.3000	0.3500
5	6.6413E-01	6.7283E-01	0.4831	103.708		85.502	85.411	1.15493	0.4000	0.4500
6	7.2415E-01	7.3042E-01	0.4842	103.088		90.545	90.454	1.13017	0.5000	0.5500
7	7.3366E-01	7.3573E-01	0.4857	102.457		93.381	93.299	1.10540	0.6000	0.6500
8	6.8886E-01	6.8517E-01	0.4877	101.814		93.742	93.680	1.08063	0.7000	0.7500
9	5.9322E-01	5.8263E-01	0.4909	101.158		91.609	91.574	1.05586	0.8000	0.8500
10	4.7187E-01	4.5435E-01	0.4958	100.490		87.911	87.907	1.03110	0.9000	0.9500
11	4.1892E-01	3.9722E-01	0.4997	99.980		86.641	86.653	1.01252	0.9750	1.0000

Figure 4.31 Continued

FUEL PLATE 4 (ExactSoln) AREAL FUEL-CLADinterface

NODE	FLUX inner MW/m^2	FLUX outer MW/m^2	FUEL X inner	Tsat (C)	Tdiff (C)	inner (C)	outer (C)	Pressure (bar)	Z-mid	Z-int
1	3.0623E-01	2.9655E-01	0.4960	105.939		61.602	61.599	1.24781	0.0250	0.0500
2	3.6390E-01	3.5073E-01	0.4972	105.504		65.361	65.361	1.22923	0.1000	0.1500
3	5.0496E-01	4.8458E-01	0.4983	104.915		73.585	73.591	1.20447	0.2000	0.2500
4	6.2661E-01	5.9861E-01	0.4994	104.317		81.078	81.092	1.17970	0.3000	0.3500
5	7.3277E-01	6.9672E-01	0.5006	103.708		88.050	88.074	1.15493	0.4000	0.4500
6	7.9947E-01	7.5580E-01	0.5020	103.088		93.430	93.468	1.13017	0.5000	0.5500
7	8.1061E-01	7.6053E-01	0.5039	102.457		96.486	96.539	1.10540	0.6000	0.6500
8	7.6193E-01	7.0726E-01	0.5066	101.814		96.944	97.014	1.08063	0.7000	0.7500
9	6.5705E-01	6.0025E-01	0.5106	101.158		94.774	94.859	1.05586	0.8000	0.8500
10	5.2396E-01	4.6647E-01	0.5170	100.490		90.955	91.053	1.03110	0.9000	0.9500
11	4.6561E-01	4.0711E-01	0.5215	99.980		89.668	89.775	1.01252	0.9750	1.0000

FUEL PLATE 5 (ExactSoln) AREAL FUEL-CLADinterface

NODE	FLUX inner MW/m^2	FLUX outer MW/m^2	FUEL X inner	Tsat (C)	Tdiff (C)	inner (C)	outer (C)	Pressure (bar)	Z-mid	Z-int
1	3.3237E-01	3.0992E-01	0.5067	105.939		63.431	63.461	1.24781	0.0250	0.0500
2	3.9504E-01	3.6645E-01	0.5080	105.504		67.559	67.599	1.22923	0.1000	0.1500
3	5.4812E-01	5.0629E-01	0.5091	104.915		76.628	76.689	1.20447	0.2000	0.2500
4	6.7998E-01	6.2555E-01	0.5101	104.317		84.854	84.936	1.17970	0.3000	0.3500
5	7.9481E-01	7.2836E-01	0.5111	103.708		92.477	92.581	1.15493	0.4000	0.4500
6	8.6656E-01	7.9059E-01	0.5122	103.088		98.318	98.440	1.13017	0.5000	0.5500
7	8.7768E-01	7.9632E-01	0.5136	102.457		101.601	101.735	1.10540	0.6000	0.6500
8	8.2353E-01	7.4177E-01	0.5154	101.814		102.030	102.170	1.08063	0.7000	0.7500
9	7.0813E-01	6.3132E-01	0.5180	101.158		99.561	99.699	1.05586	0.8000	0.8500
10	5.6151E-01	4.9346E-01	0.5215	100.490		95.278	95.405	1.03110	0.9000	0.9500
11	4.9646E-01	4.3300E-01	0.5234	99.980		93.775	93.896	1.01252	0.9750	1.0000

FUEL PLATE 6 (ExactSoln) AREAL FUEL-CLADinterface

NODE	FLUX inner MW/m^2	FLUX outer MW/m^2	FUEL X inner	Tsat (C)	Tdiff (C)	inner (C)	outer (C)	Pressure (bar)	Z-mid	Z-int
1	3.3711E-01	3.5124E-01	0.4801	105.939		64.933	64.872	1.24781	0.0250	0.0500
2	3.9435E-01	4.2149E-01	0.4737	105.504		69.072	68.974	1.22923	0.1000	0.1500
3	5.3950E-01	5.8987E-01	0.4681	104.915		78.363	78.195	1.20447	0.2000	0.2500
4	6.5982E-01	7.3815E-01	0.4624	104.317		86.602	86.355	1.17970	0.3000	0.3500
5	7.6010E-01	8.7049E-01	0.4566	103.708		94.070	93.734	1.15493	0.4000	0.4500
6	8.1434E-01	9.5912E-01	0.4496	103.088		99.517	99.090	1.13017	0.5000	0.5500
7	8.0591E-01	9.8484E-01	0.4405	102.457		102.149	101.636	1.10540	0.6000	0.6500
8	7.3187E-01	9.4166E-01	0.4279	101.814		101.689	101.103	1.08063	0.7000	0.7500
9	5.9837E-01	8.3248E-01	0.4088	101.158		98.143	97.505	1.05586	0.8000	0.8500
10	4.3735E-01	6.8816E-01	0.3795	100.490		92.717	92.048	1.03110	0.9000	0.9500
11	3.6494E-01	6.2581E-01	0.3594	99.980		90.611	89.922	1.01252	0.9750	1.0000

Table 4.1 Comparison of Results by Four Methods for Radial Geometry Problem 1

Method	Temperature Difference Across Tube Thickness, °C	Coolant Temperature Rise, °C	Comments
Hand Calculation	161.1562,1172,6154,12	43.0622,0095,6937,80	All digits good
Standalone Routine SLICEHTR	161.1562,1172,6154,1	43.0622,0095,6937,80	All digits good
Standalone Routine SLICEHTR for the Modified Problem	161.1562,1235,9536,1	43.0622,0093,9918,72	All digits presumed good
Exact Method in PLTEMP/ANL Version 3.2 for the Modified Problem	161.1562,1008,5305,20 [a] 161.1562,1332,9713,50 [b]	43.0622,0093,9615,2	Agrees to 8 digits

a. The smallest value in the 10 axial nodes used over the length of fuel tube.
b. The largest value in the 10 axial nodes used over the length of fuel tube.

Table 4.2 Comparison of Results by Five Methods for Radial Geometry Problem 2

Method	Temperature Difference Across Tube Thickness, °C	Coolant Temperature Rise, °C	Comments
Hand Calculation	178.0270,7992,9631,615	43.0622,0095,6937,80	All digits good
Standalone Routine SLICEHTR	178.0270,7992,9631,6	43.0622,0095,6937,80	All digits good
Standalone Routine SLICEHTR for the Modified Problem	178.0270,7962,2544,8	43.0622,0093,8397,16	All digits presumed good
Broyden Method in PLTEMP v3.2 for the Modified Problem	178.0270,7822,6028 [a] 178.0270,7828,0832 [b]	43.0622,0093,8102,2	Agrees to 8 digits or more
Exact Method in PLTEMP v3.2 for the Modified Problem	178.0270,7958,9524,00 [a] 178.0270,7964,3935,80 [b]	43.0622,0093,8093,5	Agrees to 9 digits

a. The smallest value in the 10 axial nodes used over the length of fuel tube.
b. The largest value in the 10 axial nodes used over the length of fuel tube.

Table 4.3 Pressure Derivative of Water Enthalpy at 1.5 bar and 50 °C Calculated From PLTEMP Code

Case No.	ΔP, bar	ΔT, °C	∂h/∂P, J/kg-bar
Method: ∂h/∂P at (T,P) = **{**h(T, P+0.5ΔP) - h(T, P-0.5ΔP)**}**/ ΔP			
1	0.1		138.9
2	0.2		69.43
3	0.5		83.31
∂h/∂P at (T,P) = **{**h(T+0.5ΔT, P+0.5ΔP) - h(T-0.5ΔT, P-0.5ΔP) – ΔT C_p(T,P)**}**/ ΔP			
4	0.05	2.0	131.5
5	0.1	2.0	131.5
6	0.1	4.0	65.75
7	0.25	2.0	81.84
8	0.5	2.0	82.58

Table 4.4 Summary of PLTEMP/ANL Code Results for Problem 4

PLTEMP/ANL Version and Method	**Temperature of Coolant Outlet or Fuel Tube Axial Node 10, °C**					Comments
	Inner Coolant	Inner Clad Surface	Meat Maximum	Outer Clad Surface	Outer Coolant	
Broyden Method in Version 3.1	80.095	115.726	276.651	205.492	62.898	Results did not converge
Broyden Method in Version 3.2	58.444	156.246	244.382	124.977	84.548	Good results
Exact Method in Version 3.2	58.466	156.238	244.346	124.925	84.484	Good results

Table 4.5 Solution of Flat Plate Problem 5 by the Radial Geometry Exact Method Using Increasing Values of the Input Mean Radius of the Fuel Tube

Calculation Method	Input Tube Radius, m	Temperature Drop Across Plate Thickness, °C	Comments
Hand Calculation	Not used	255.7847299691175	All digits good
Slab Geometry Exact Method	Not used	255.784728^{5}_{3}	Agrees to 8 digits
Radial Geometry Exact Method	500	255.779054^{1}_{0}	Error = 0.0057 °C
	10^3	255.781891^{8}_{6}	Error = 0.0028 °C
	10^4	255.78410^{80}_{78}	Error = 0.0006 °C
	10^5	255.861963^{3}_{0}	Error = 0.0772 °C
	5×10^5	255.330459^{7}_{0}	Error = 0.4543 °C
	10^6	219.21695^{4}_{1}	Error = 36.5678 °C

Table 4.6 Comparison of Three Solutions for the Hungarian Reactor Benchmark Problem (Using Actual Coolant Properties)

Calculation Methods Compared	ΔT_{max} Maximum Temperature Difference, °C			Location of ΔT_{max}	Comments
	Tube 1	Tube 2	Tube 3		
Broyden Method in PLTEMP/ANL Version 3.1 versus Broyden Method in Version 3.2	0.257	0.249	0.235	Meat in Axial Node 4	Due to node outlet vs node center coolant temperature used in film coefficient
Broyden Method in PLTEMP/ANL Version 3.2 versus Radial Geometry Exact Method in Version 3.2	0.005	0.007	0.007	Coolant in Axial Node 8	Due to not accounting for $\partial h/\partial P$ in Broyden method

Table4.7 Comparison of Solutions for ASTRA2 Radial Geometry Problem 3 Case 1 (Using the Constant Coolant C_p Option)

Calculation Methods Compared	ΔT_{max} Maximum Temperature Difference, °C	Location of ΔT_{max}	Comments
Broyden Method in Version 3.1 versus Broyden Method in Version 3.2	0.171	Inner Cladding of Tube 5 in Axial Node 11	(1) Due to node outlet vs. node center coolant temperature used in film coefficient
Broyden Method in Version 3.2 versus Radial Geometry Exact Method in Version 3.2	0.089	Meat of Tube 1 in Axial Node 7	(2) The reason for this difference is not clear.
Broyden Method in Version 3.1 versus Radial Geometry Exact Method in Version 3.2	0.203	Meat of Tube 5 in Axial Node 6	Comments 1 and 2
PLTEMP/ANL of May 2003 versus Broyden Method in Version 3.1	5.987	Meat of Tube 6 in Axial Node 10	Code improvements after May 2003

Table 4.8 Temperature Distribution in ASTRA2 Radial Geometry Problem 3 Case 1 With the Innermost Fuel Tube as the First

	Tube	ASTRA2 Code	PLTEMP/ANL of May 22, 2003 [a]	PLTEMP/ANL Version 3.1 Broyden Method	PLTEMP/ANL Version 3.2 Broyden Method	PLTEMP/ANL Version 3.2 Exact Method
Geometry		Cylinder	Cylinder	Cylinder	Cylinder	Cylinder
Power, MW		0.66288	0.66288	0.66288	0.66288	0.66288
Flow, kg/s		7.7588	7.7588	7.7588	7.7588	7.7588
Fuel Heated Area, m^2		1.1097	1.1097	1.1097	1.1097	
Velocity in Channel 7, m/s		3.21	3.21	3.21	3.21	3.21
Tube 6 Power Fraction		0.25486	0.25486	0.25486	0.25486	0.25486
Coolant ΔT, °C		20.4392	20.4398	20.439	20.439	20.4392
Peak Fuel Temperature, °C		103.0	103.159 In Tube 6	102.903 In Tube 5	103.016 In Tube 5	103.079 In Tube 5
Location of Temperature		**Coolant Channel Outlet Temperature or Fuel Tube Last Axial Node Temperature, °C**				
Channel 1 Outlet		55.4	55.231	55.524	55.525	55.305
Inner Clad Surface	1		71.723	74.728	74.732	74.713
Peak Fuel			79.077	76.460	76.467	76.516
Outer Clad Surface			77.936	75.408	75.419	75.433
Channel 2 Outlet		63.6	63.681	63.585	63.578	63.578
Inner Clad Surface	2		80.854	81.557	81.301	81.293
Peak Fuel			83.451	82.974	82.990	83.036
Outer Clad Surface			82.347	81.466	81.758	81.769
Channel 3 Outlet		66.8	66.861	66.759	66.758	66.761
Inner Clad Surface	3		85.482	85.772	85.541	85.542
Peak Fuel			87.129	87.112	87.116	87.157
Outer Clad Surface			85.680	85.352	85.593	85.593
Channel 4 Outlet		68.5	68.503	68.512	68.515	68.514
Inner Clad Surface	4		87.118	88.529	88.450	88.445
Peak Fuel			91.324	90.215	90.230	90.267
Outer Clad Surface			89.895	88.576	88.686	88.689
Channel 5 Outlet		70.9	70.840	70.891	70.891	70.890
Inner Clad Surface	5		91.017	92.543	92.471	92.471
Peak Fuel			96.234	94.363	94.378	94.418
Outer Clad Surface			94.715	92.633	92.736	92.742
Channel 6 Outlet		72.8	73.320	72.594	72.591	72.597
Inner Clad Surface	6		94.691	89.615	89.629	89.651
Peak Fuel			96.156	90.876	90.892	90.936
Outer Clad Surface			83.606	88.257	88.274	88.256
Channel 7 Outlet		58.5	58.176	58.652	58.657	58.653

Note a. Output File: output.astra2p3c1r.1

APPENDIX C Enthalpy of Liquid Water Used in the PLTEMP Code

T ,C	h(T, 1bar) J/kg	h(T, 2bar) J/kg	h(T, 3bar) J/kg	h(T, 4bar) J/kg	h(T, 5bar) J/kg	h(T, 6bar) J/kg	h(T, 7bar) J/kg	h(T, 8bar) J/kg	h(T, 9bar) J/kg	h(T,10bar) J/kg
1.00	4554.4434	4658.5846	4755.7831	4859.9243	4957.1228	5061.2640	5158.4625	5262.6038	5359.8022	5463.9435
2.00	8713.1500	8810.3485	8914.4897	9011.6882	9108.8867	9213.0280	9317.1692	9414.3677	9511.5662	9615.7074
3.00	12864.9139	12962.1124	13066.2537	13163.4521	13267.5934	13364.7919	13468.9331	13566.1316	13663.3301	13767.4713
4.00	17016.6779	17120.8191	17218.0176	17315.2161	17419.3573	17516.5558	17620.6970	17717.8955	17815.0940	17919.2352
5.00	21175.3845	21272.5830	21369.7815	21473.9227	21571.1212	21675.2625	21772.4609	21869.6594	21973.8007	22070.9991
6.00	25327.1484	25431.2897	25528.4882	25632.6294	25729.8279	25827.0264	25924.2249	26028.3661	26125.5646	26222.7631
7.00	29485.8551	29583.0536	29687.1948	29784.3933	29881.5918	29978.7903	30082.9315	30180.1300	30284.2712	30381.4697
8.00	33644.5618	33741.7603	33838.9587	33936.1572	34040.2985	34137.4969	34234.6954	34338.8367	34436.0352	34533.2336
9.00	37796.3257	37900.4669	37997.6654	38094.8639	38199.0051	38296.2036	38393.4021	38490.6006	38587.7991	38684.9976
10.00	41955.0323	42059.1736	42156.3721	42253.5706	42350.7690	42447.9675	42545.1660	42649.3073	42746.5057	42843.7042
11.00	46113.7390	46210.9375	46315.0787	46412.2772	46509.4757	46606.6742	46703.8727	46808.0139	46905.2124	47002.4109
12.00	50272.4457	50376.5869	50473.7854	50570.9839	50668.1824	50765.3809	50862.5793	50959.7778	51056.9763	51154.1748
13.00	54431.1523	54528.3508	54632.4921	54729.6906	54826.8890	54924.0875	55021.2860	55118.4845	55215.6830	55312.8815
14.00	58596.8018	58694.0002	58791.1987	58888.3972	58985.5957	59082.7942	59179.9927	59277.1912	59374.3896	59471.5881
15.00	62755.5084	62852.7069	62949.9054	63047.1039	63144.3024	63241.5009	63338.6993	63435.8978	63533.0963	63630.2948
16.00	66914.2151	67011.4136	67108.6121	67205.8105	67303.0090	67400.2075	67497.4060	67594.6045	67691.8030	67789.0015
17.00	71079.8645	71177.0630	71274.2615	71371.4600	71468.6584	71565.8569	71656.1127	71753.3112	71850.5096	71947.7081
18.00	75238.5712	75335.7697	75432.9681	75530.1666	75627.3651	75724.5636	75821.7621	75918.9606	76009.2163	76106.4148
19.00	79404.2206	79501.4191	79591.6748	79688.8733	79786.0718	79883.2703	79980.4688	80077.6672	80174.8657	80272.0642
20.00	83562.9272	83660.1257	83757.3242	83854.5227	83951.7212	84048.9197	84146.1182	84236.3739	84333.5724	84430.7709
21.00	87728.5767	87825.7751	87922.9736	88020.1721	88117.3706	88207.6263	88304.8248	88402.0233	88499.2218	88589.4775
22.00	91894.2261	91991.4246	92088.6230	92178.8788	92276.0773	92373.2758	92470.4742	92560.7300	92657.9285	92755.1270
23.00	96059.8755	96157.0740	96247.3297	96344.5282	96441.7267	96538.9252	96629.1809	96726.3794	96823.5779	96920.7764
24.00	100225.5249	100322.7234	100412.9791	100510.1776	100607.3761	100697.6318	100794.8303	100892.0288	100989.2273	101079.4830
25.00	104391.1743	104488.3728	104578.6285	104675.8270	104773.0255	104863.2812	104960.4797	105057.6782	105154.8767	105245.1324
26.00	108556.8237	108654.0222	108751.2207	108841.4764	108938.6749	109028.9307	109126.1292	109223.3276	109313.5834	109410.7819
27.00	112722.4731	112819.6716	112916.8701	113007.1259	113104.3243	113194.5801	113291.7786	113388.9771	113479.2328	113576.4313
28.00	116895.0653	116985.3210	117082.5195	117179.7180	117269.9738	117367.1722	117457.4280	117554.6265	117644.8822	117742.0807
29.00	121060.7147	121157.9132	121248.1689	121345.3674	121435.6232	121532.8217	121623.0774	121720.2759	121817.4744	121907.7301
30.00	125233.3069	125323.5626	125420.7611	125511.0168	125608.2153	125698.4711	125795.6696	125885.9253	125983.1238	126073.3795
31.00	129398.9563	129496.1548	129586.4105	129683.6090	129773.8647	129871.0632	129961.3190	130058.5175	130148.7732	130245.9717
32.00	133571.5485	133661.8042	133759.0027	133849.2584	133946.4569	134036.7126	134133.9111	134224.1669	134314.4226	134411.6211
33.00	137744.1406	137834.3964	137931.5948	138021.8506	138119.0491	138209.3048	138299.5605	138396.7590	138487.0148	138577.2705
34.00	141916.7328	142006.9885	142104.1870	142194.4427	142284.6985	142381.8970	142472.1527	142562.4084	142659.6069	142749.8627
35.00	146089.3250	146179.5807	146269.8364	146367.0349	146457.2906	146547.5464	146644.7449	146735.0006	146825.2563	146922.4548
36.00	150261.9171	150352.1729	150449.3713	150539.6271	150629.8828	150720.1385	150817.3370	150907.5928	150997.8485	151088.1042
37.00	154434.5093	154524.7650	154615.0208	154712.2192	154802.4750	154892.7307	154989.9292	155080.1849	155170.4407	155267.6392
38.00	158607.1014	158697.3572	158794.5557	158884.8114	158975.0671	159072.2656	159162.5214	159252.7771	159343.0328	159433.2886
39.00	162786.6364	162876.8921	162967.1478	163057.4036	163154.6021	163244.8578	163335.1135	163425.3693	163515.6250	163612.8235
40.00	166959.2285	167049.4843	167139.7400	167236.9385	167327.1942	167417.4500	167507.7057	167597.9614	167695.1599	167785.4156
41.00	171138.7634	171229.0192	171319.2749	171409.5306	171499.7864	171590.0421	171680.2979	171777.4963	171867.7521	171958.0078
42.00	175311.3556	175401.6113	175498.8098	175589.0656	175679.3213	175769.5770	175859.8328	175950.0885	176040.3442	176130.6000
43.00	179490.8905	179581.1462	179671.4020	179761.6577	179851.9135	179942.1692	180039.3677	180122.6807	180219.8792	180310.1349
44.00	183670.4254	183760.6812	183850.9369	183941.1926	184031.4484	184121.7041	184211.9598	184302.2156	184392.4713	184482.7271
45.00	187849.9603	187940.2161	188030.4718	188120.7275	188210.9833	188301.2390	188391.4948	188481.7505	188572.0062	188662.2620

T ,C	h(T, 1bar) J/kg	h(T, 2bar) J/kg	h(T, 3bar) J/kg	h(T, 4bar) J/kg	h(T, 5bar) J/kg	h(T, 6bar) J/kg	h(T, 7bar) J/kg	h(T, 8bar) J/kg	h(T, 9bar) J/kg	h(T,10bar) J/kg
46.00	192029.4952	192119.7510	192210.0067	192300.2625	192390.5182	192480.7739	192571.0297	192661.2854	192751.5411	192841.7969
47.00	196209.0302	196299.2859	196389.5416	196479.7974	196570.0531	196660.3088	196750.5646	196840.8203	196924.1333	197021.3318
48.00	200395.5078	200478.8208	200569.0765	200659.3323	200749.5880	200839.8437	200930.0995	201020.3552	201103.6682	201200.8667
49.00	204575.0427	204665.2985	204755.5542	204838.8672	204929.1229	205019.3787	205109.6344	205199.8901	205290.1459	205380.4016
50.00	208754.5776	208844.8334	208935.0891	209025.3448	209115.6006	209198.9136	209289.1693	209379.4250	209469.6808	209559.9365
51.00	212941.0553	213031.3110	213114.6240	213204.8798	213295.1355	213385.3912	213475.6470	213558.9600	213649.2157	213739.4714
52.00	217127.5330	217210.8459	217301.1017	217391.3574	217481.6132	217571.8689	217655.1819	217745.4376	217835.6934	217919.0063
53.00	221307.0679	221397.3236	221487.5793	221577.8351	221661.1481	221751.4038	221841.6595	221931.9153	222015.2283	222105.4840
54.00	225500.4883	225583.8013	225674.0570	225764.3127	225847.6257	225937.8815	226028.1372	226111.4502	226201.7059	226291.9617
55.00	229680.0232	229770.2789	229860.5347	229943.8477	230034.1034	230124.3591	230207.6721	230297.9279	230388.1836	230471.4966
56.00	233873.4436	233956.7566	234047.0123	234137.2681	234220.5811	234310.8368	234394.1498	234484.4055	234567.7185	234657.9742
57.00	238059.9213	238150.1770	238233.4900	238316.8030	238407.0587	238497.3145	238580.6274	238670.8832	238761.1389	238844.4519
58.00	242246.3989	242336.6547	242419.9677	242510.2234	242593.5364	242683.7921	242774.0479	242857.3608	242940.6738	243030.9296
59.00	246439.8193	246523.1323	246613.3881	246696.7010	246786.9568	246870.2698	246960.5255	247043.8385	247134.0942	247217.4072
60.00	250626.2970	250716.5527	250799.8657	250890.1215	250973.4344	251063.6902	251147.0032	251230.3162	251320.5719	251410.8276
61.00	254819.7174	254909.9731	254993.2861	255076.5991	255166.8549	255250.1678	255340.4236	255423.7366	255507.0496	255597.3053
62.00	259013.1378	259096.4508	259186.7065	259270.0195	259353.3325	259443.5883	259526.9012	259617.1570	259700.4700	259783.7830
63.00	263206.5582	263289.8712	263380.1270	263463.4399	263546.7529	263637.0087	263720.3217	263803.6346	263893.8904	263977.2034
64.00	267399.9786	267483.2916	267573.5474	267656.8604	267740.1733	267823.4863	267913.7421	267997.0551	268087.3108	268170.6238
65.00	271593.3990	271683.6548	271766.9678	271850.2808	271933.5937	272016.9067	272107.1625	272190.4755	272280.7312	272364.0442
66.00	275793.7622	275877.0752	275960.3882	276043.7012	276127.0142	276217.2699	276300.5829	276383.8959	276474.1516	276557.4646
67.00	279987.1826	280070.4956	280153.8086	280237.1216	280327.3773	280410.6903	280494.0033	280584.2590	280667.5720	280750.8850
68.00	284180.6030	284270.8588	284354.1718	284437.4847	284520.7977	284604.1107	284694.3665	284777.6794	284860.9924	284944.3054
69.00	288380.9662	288464.2792	288554.5349	288637.8479	288721.1609	288804.4739	288887.7869	288971.0999	289054.4128	289137.7258
70.00	292581.3293	292664.6423	292747.9553	292831.2683	292914.5813	292997.8943	293088.1500	293171.4630	293254.7760	293338.0890
71.00	296781.6925	296865.0055	296948.3185	297031.6315	297114.9445	297198.2574	297281.5704	297371.8262	297455.1392	297538.4521
72.00	300982.0557	301065.3687	301148.6816	301231.9946	301315.3076	301398.6206	301481.9336	301565.2466	301648.5596	301731.8726
73.00	305182.4188	305265.7318	305349.0448	305432.3578	305515.6708	305598.9838	305682.2968	305765.6097	305848.9227	305932.2357
74.00	309382.7820	309466.0950	309549.4080	309632.7209	309716.0339	309799.3469	309882.6599	309965.9729	310049.2859	310132.5989
75.00	313590.0879	313673.4009	313756.7139	313840.0269	313923.3398	314006.6528	314089.9658	314173.2788	314256.5918	314332.9620
76.00	317797.3938	317880.7068	317964.0198	318040.3900	318123.7030	318207.0160	318290.3290	318373.6420	318456.9550	318540.2679
77.00	321997.7570	322081.0699	322164.3829	322247.6959	322331.0089	322414.3219	322490.6921	322574.0051	322657.3181	322740.6311
78.00	326205.0629	326288.3759	326371.6888	326455.0018	326531.3721	326614.6851	326697.9980	326781.3110	326864.6240	326947.9370
79.00	330412.3688	330495.6818	330578.9948	330662.3077	330738.6780	330821.9910	330905.3040	330988.6169	331071.9299	331148.3002
80.00	334626.6174	334702.9877	334786.3007	334869.6136	334945.9839	335029.2969	335112.6099	335195.9229	335279.2358	335355.6061
81.00	338833.9233	338917.2363	338993.6066	339076.9196	339153.2898	339236.6028	339319.9158	339403.2288	339486.5417	339562.9120
82.00	343041.2292	343124.5422	343207.8552	343284.2255	343367.5385	343443.9087	343527.2217	343610.5347	343693.8477	343770.2179
83.00	347255.4779	347331.8481	347415.1611	347498.4741	347574.8444	347658.1573	347734.5276	347817.8406	347901.1536	347984.4666
84.00	351469.7266	351546.0968	351629.4098	351705.7800	351789.0930	351872.4060	351948.7762	352032.0892	352108.4595	352191.7725
85.00	355677.0325	355760.3455	355843.6584	355920.0287	356003.3417	356079.7119	356163.0249	356239.3951	356322.7081	356399.0784
86.00	359891.2811	359974.5941	360050.9644	360134.2773	360217.5903	360293.9606	360370.3308	360453.6438	360536.9568	360613.3270
87.00	364105.5298	364188.8428	364272.1558	364348.5260	364424.8962	364508.2092	364591.5222	364667.8925	364744.2627	364827.5757
88.00	368326.7212	368403.0914	368486.4044	368562.7747	368646.0876	368722.4579	368805.7709	368882.1411	368965.4541	369041.8243
89.00	372540.9698	372624.2828	372700.6531	372783.9661	372860.3363	372936.7065	373020.0195	373096.3898	373179.7028	373256.0730
90.00	376762.1613	376838.5315	376921.8445	376998.2147	377074.5850	377157.8979	377234.2682	377317.5812	377393.9514	377477.2644
91.00	380983.3527	381059.7229	381143.0359	381219.4061	381295.7764	381379.0894	381455.4596	381531.8298	381615.1428	381691.5131
92.00	385204.5441	385280.9143	385357.2845	385440.5975	385516.9678	385593.3380	385669.7083	385753.0212	385829.3915	385905.7617
93.00	389425.7355	389502.1057	389578.4760	389654.8462	389738.1592	389814.5294	389890.8997	389974.2126	390050.5829	390126.9531
94.00	393646.9269	393723.2971	393806.6101	393882.9803	393959.3506	394035.7208	394112.0911	394195.4041	394271.7743	394348.1445

T ,C	h(T, 1bar) J/kg	h(T, 2bar) J/kg	h(T, 3bar) J/kg	h(T, 4bar) J/kg	h(T, 5bar) J/kg	h(T, 6bar) J/kg	h(T, 7bar) J/kg	h(T, 8bar) J/kg	h(T, 9bar) J/kg	h(T,10bar) J/kg
95.00	397875.0610	397951.4313	398027.8015	398104.1718	398180.5420	398263.8550	398340.2252	398416.5955	398492.9657	398569.3359
96.00	402096.2524	402172.6227	402248.9929	402332.3059	402408.6761	402485.0464	402561.4166	402637.7869	402714.1571	402790.5273
97.00	406324.3866	406400.7568	406477.1271	406553.4973	406629.8676	406706.2378	406789.5508	406865.9210	406942.2913	407018.6615
98.00	410552.5208	410628.8910	410705.2612	410781.6315	410858.0017	410934.3719	411010.7422	411087.1124	411163.4827	411246.7957
99.00	414780.6549	414857.0251	414933.3954	415009.7656	415086.1359	415162.5061	415238.8763	415315.2466	415391.6168	415467.9871
100.0	419008.7891	419085.1593	419161.5295	419237.8998	419314.2700	419390.6403	419467.0105	419543.3807	419619.7510	419696.1212

5 Numbering the Outermost Fuel Tube as the First When Using the Radial Geometry Exact Method in PLTEMP – Implementation and Verification

5.1 Introduction

The verification work reported here was done in October 2007. The PLTEMP/ANL code [1] is used in the Reduced Enrichment for Research and Test Reactor (RERTR) Program to do thermal hydraulic analysis of experimental reactors having multi-tube fuel assemblies. To improve the accuracy and speed of the code, the Exact method for calculating the temperature distribution in a multi-tube fuel assembly was added to the code in version 3.2 (V3.2 for brevity) [see Appendix VIII in Ref. 1]. The radial geometry Exact method in the code version 3.2 restricted the user to number the innermost fuel tube as 1 during input data preparation. The Exact method available in V3.4 is improved to remove this restriction. The code has a radial geometry capability to calculate temperature distribution in a multi-tube fuel assembly, and a method based on the Broyden minimization method. The input data can now be prepared either numbering the innermost tube as 1, or numbering the outermost tube as 1, when using the Exact method and the Broyden method.

The purpose of this chapter is to document the technique used for this improvement, and the verification of the implemented technique by solving a modified benchmark problem. At the end, a historical perspective on the accuracy of the last five PLTEMP/ANL versions is also presented. The Exact method and Broyden method solutions obtained by the code version 3.4 agree when tubes are numbered in either direction.

5.2 Technique Used if Input Data Has the Outermost Tube First

The Exact method used in PLTEMP/ANL when the fuel tubes are numbered in the input data starting from the innermost tube as 1, has been described earlier [Appendix VIII in Ref. 1]. In order to handle an input data file having the outermost tube numbered as 1, the code internally rearranges the input data that depend on the *numbering* of fuel tubes and coolant channels, then solves the problem using the earlier method [1], and finally rearranges the solution obtained. The input data card types 307, 308, 308A, 309 and 310 contain all the tube-numbering-dependent input data, altogether 10 arrays. The calculated data that are saved in the direct access file written on logical units 19 and 20, are rearranged after the solution. All rearranging is done in the subroutine SLICE1, using variables that have the suffix _R (e.g., AFF_R, DFF_R). It is noted that the input data arrays read from the input file are never changed during the whole technique. This technique was recently implemented in V3.4 of the PLTEMP/ANL code.

5.3 Verification of the Implementation of the Technique

The implementation of the above technique for calculating temperature distribution in radial geometry problems in which the fuel tubes are numbered starting from the outermost tube as 1, was performed by analyzing such a problem, i.e., the Standard Problem 17 whose input data is given in Fig. 5.1. This input data file was obtained by modifying a three-tube benchmark problem so that the differences (in coolant, cladding and fuel meat temperatures, and heat transfer coefficients) among the channels are exaggerated so that any possible coding discrepancy can be easily identified in the code output. To obtain the Standard Problem 17 given in Fig. 5.1, three

changes were made to the older benchmark problem: (i) The cladding thermal conductivity was reduced from 206.0 W/m-°C to 6.0 W/m-°C, (ii) The fuel meat thermal conductivity was reduced from 180.0 W/m-°C to 4.0 W/m-°C, and (iii) The coolant flow rate in coolant channel 2 (the channel inside the outermost fuel tube) was increased 10 times, i.e., was changed from 0.70516 kg/s to 7.0516 kg/s. The changes (i) and (ii) will make the temperature drops across fuel and cladding thicknesses about 40 times larger in Problem 17 compared to those in the original benchmark problem. The change (iii) will make the cladding-to-coolant temperature drop in channel 2 of Problem 17 about one-sixth of that in the original KFKI benchmark problem. This is because the Reynolds number will be 10 times larger, making the heat transfer coefficient about 6 times larger ($10^{0.8} = 6.3$).

Fig. 5.2 shows the input data file of a companion problem (Standard Problem 18) obtained from Problem 17 by manually reversing the data on the input card types 307, 308, 308A, 309 and 310 that contain all the tube-numbering-dependent input data.

Six PLTEMP/ANL calculations were performed for these two input data files, using the older code V3.2 and the code V3.4 in which the technique was implemented. Table 5.1 briefly shows a comparison of these calculations and is discussed below. Tables 5.4 through 5.9 show the temperature distribution and heat fluxes obtained in the six calculations. The six calculations are:

(1) Solution of Problem 17 by the Broyden method using the code V3.2
(2) Solution of Problem 18 by the Broyden method using the code V3.2
(3) Solution of Problem 17 by the Broyden method using the code V3.4
(4) Solution of Problem 18 by the Broyden method using the code V3.4
(5) Solution of Problem 17 by the Exact method using the code V3.4
(6) Solution of Problem 18 by the Exact method using the code V3.4

The results in columns A through F of Table 5.1 are taken from Tables 5.4 to 5.9 respectively, and each column presents a solution of a single problem, Standard Problem 17. The results of Problem 18 (from Tables 5.5, 5.7, and 5.9) are given in Table 5.1 in the reversed order, thus inferring a solution of Problem 17 from each solution of Problem 18. *The objective is to verify the results in column E* obtained by the code V3.4 using the newly implemented technique, for Problem 17 (input data file in Fig. 5.1). The first four solutions by the Broyden method (columns A to D of Table 5.1) establish a solution by a verified existing method that is used to verify the newly implemented technique.

The following observations, specially item (iv), are made to provide a verification of the implementation of the technique:

(i) For each problem (Problem 17 or Problem 18), the Broyden solution obtained after 20 iterations was found to be identical (by the UNIX diff command) to the solution obtained after 200 iterations or 2000 iterations. This is true for both code versions 3.2 and 3.4.

(ii) In each Broyden solution, all Tdiff's (i.e., the mismatch between the peak fuel temperatures computed from the inner and outer surfaces of a tube) are zero, due to good initial guess for starting the Broyden iteration. This implies that each Broyden solution is reliable.

(iii) Table 5.1 compares the coolant channel temperatures and the location of the maximum temperature in meat thickness, at the channel exit. These quantities are found to be equal in the four Broyden solutions (columns A to D of Table 5.1). This comparison provides further confidence in the Broyden solutions. A more detailed comparison of these four solutions using Tables 5.4 to 5.7 is discussed below in item (v).

(iv) The solution of Problem 17 (column E of Table 5.1) by the newly-implemented technique is verified by its agreement with the solutions by the Broyden method shown in columns A to D. Furthermore, the column E agrees precisely with the column F which is the solution of Problem 18 obtained by the previously-implemented and verified Exact method. Table 5.6, the source of column E, was hand-compared with Table 5.7 in the reverse order (the source of column F), and it was found that all the output temperatures, heat fluxes, and heat transfer coefficients in the two tables agree *precisely*. This provides a verification of the newly-implemented technique.

(v) A detailed comparison of the Broyden solutions of Problems 17 and 18 by the code V3.2 (Tables 5.4 and 5.5) shows small differences in the fuel and cladding temperatures. The largest difference occurs in fuel assembly's innermost fuel tube (tube 3 of Problem 17, which corresponds to tube 1 of Problem 18) in the cladding surface temperature of axial node 4, and is 0.010 °C (shown underlined and in boldface in Tables 5.4 and 5.5). The largest difference between Tables 5.4 and 5.5 in tube 1 (of Problem 17) is 0.007 °C, and that in tube 2 is 0.008 °C (shown in boldface in Tables 5.4 and 5.5). The V3.2 Broyden solutions for the two companion problems are not exactly the same. *This minor discrepancy is present in the code V3.2 but not in the code V3.4 as discussed next.*

A detailed comparison of the V3.4 Broyden solutions of Problems 17 and 18 (Tables 5.6 and 5.7) shows no difference in the fuel and cladding temperatures, or in heat transfer coefficients. Turning to the Exact method, a detailed comparison of the V3.4 Exact solutions of Problems 17 and 18 (Tables 5.8 and 5.9) also shows no difference in the fuel and cladding temperatures, or in heat transfer coefficients. This improvement is probably due to calculating the coolant specific heat in the subroutines HCOEF1 and HCOEF at the actual coolant temperature, rather than using the value of the specific heat already available in the common block A1 (which is done in the code V3.2).

(vi) The Broyden solutions given in Tables 5.6 and 5.7 may be considered to be better than the Broyden solutions of Tables 5.4 and 5.5 because Tables 5.6 and 5.7 are precisely consistent with each other whereas Tables 5.4 and 5.5 are only approximately consistent, as discussed in item (v). The maximum temperature difference between the Exact solution given in Table 5.6 or 5.9 (precisely consistent with each other) and the Broyden solution given in Table 5.4 or 5.7 is 0.009 °C (65.802 °C versus 65.811 °C, occurring in channel 4 coolant temperature of node 8) as summarized in Table 5.1. The cause of this difference is not clear.

5.4 Historical Perspective on PLTEMP/ANL Code Versions

To get a historical perspective on the improvements made in PLTEMP/ANL, five code versions V3.0, V3.1, V3.2, V3.3, and V3.4 were run for Problems 17 and 18, using both the Broyden and the Exact methods. Out of the 20 runs, two did not produce a solution. These two are the runs of PLTEMP/ANL V3.2 and V3.3 for Problem 17 using the Exact method. This is because these versions do not have an Exact method to handle radial geometry problems in which the outermost fuel tube is numbered as the first. PLTEMP/ANL V3.2 and V3.3 do have the Exact method to handle radial geometry problems in which the innermost fuel tube is numbered as the first. It is noted that PLTEMP/ANL V3.0 and V3.1 do not have any radial geometry Exact method (although do have the slab geometry Exact method) but they run for both Problems 17 and 18 by using the slab geometry Exact method (which is acceptable in problems with high thermal conductivity solids and large fuel tube radii). PLTEMP/ANL V3.0 and V3.1 should not be used for problems with low thermal conductivity solids (e.g., Problems 17 and 18).

Altogether 18 solutions were obtained: 5 Broyden solutions for Problem 17, 5 Broyden solutions for Problem 18, 3 Exact solutions for Problem 17, and 5 Exact solutions for Problem 18. Fifteen iterations were used in the Broyden solutions, and each Tdiff was found to be zero in all 10 Broyden solutions.

The 18 solutions obtained are compared in Table 5.8. First, each version's Broyden solution is compared with the Broyden solution of the latest version, i.e., V3.4. Next, each version's Exact solution is compared with the Exact solution of V3.4 (see Table 5.8). Finally, each Exact solution is compared with the Broyden solution obtained by the same code version. All these comparisons were made using a program *differ.f* developed earlier to compare two PLTEMP/ANL output files and to find the maximum temperature difference for each fuel tube in the output file. The maximum difference is determined over all cladding, fuel, and adjacent coolant channel temperatures of a fuel tube (i.e., a table in the code output file).

Table 5.8 shows that the Problems 17 and 18 solutions by the V3.0 Broyden method are not good. There is an error of 10.0 °C in the innermost fuel tube for these problems (see Table 5.8). By running V3.0 for the original benchmark problems, it is found that this error is 3.2 °C (which is lower but still not acceptable). Also, the solutions by the (slab geometry) Exact method in V3.0 and V3.1 are not good for these radial geometry problems. Altogether, six solutions are not good. The remaining 12 solutions are good, and are listed below:

(i) The Broyden solutions of both problems by V3.1, V3.2, V3.3, and V3.4 (8 solutions)
(ii) The Exact solutions of Problem 18 by V3.2, V3.3, and V3.4 (3 solutions)
(iii) The Exact solution of Problem 17 by V3.4

In conclusion, the code V3.4 has a maximum difference of 0.009 °C between the solutions obtained by the Broyden and Exact methods for Problems 17 and 18. This provides an additional verification of the implementation of the technique.

5.5 REFERENCES

1. M. Kalimullah, A. P. Olson and E. E. Feldman, “A User’s Guide to the PLTEMP/ANL Code,” ANL/RTR/TM-18/17 Version 4.3, Revision 0, Argonne National Laboratory, 9700 South Cass Avenue, Argonne, IL 60439, USA (November 2018).

Figure 5.1 Input Data for Standard Problem 17 Having the Outermost Tube Numbered First in the Input Data

```
Stdproblem 17, Outermost Tube First, Based on Hungarian Reactor Benchmark; 90 kW Card 100
   0   0   5   1   0   0   0   0   1   0   0   0   0   0   1   1   0   0         Card 200
   1   3         0.0         1.0         1.0         1.0   0   0                 Card 300
   1   2         1.0                                                             Card 301
   1   1   1                                                                     Card 302
        1.53                                                                     Card 303
         1.0         1.0         1.0         1.0         1.0         1.0         Card 304
         1.0         1.0         1.0         1.0         1.0         1.0         Card 304
         1.0         1.0         1.0         1.0         1.0         1.0         Card 304
         0.0         0.0         0.0                                             Card 305
   4   0         0.0         0.58     0.76e-3        6.00     0.98e-3        4.00 Card 306
  1.8003E-04  6.6631E-03  1.0808E-01  1.0808E-01         1.0         1.0         Card 307
  2.5015E-04  6.1964E-03  1.6148E-01  1.6148E-01         1.0         1.0         Card 307
  1.3195E-04  6.0000E-03  8.7965E-02  8.7965E-02         1.0         1.0         Card 307
  2.8274E-05  6.0000E-03  1.8850E-02  1.8850E-02         1.0         1.0         Card 307
  1.0022E-01  6.1261E-02  2.6704E-02                                             Card 308
   0.0159511   0.0097500   0.0042500                                             Card 308A
         1.0         1.0         1.0                                             Card 309
  5.1356E-01  7.0516E-00  3.6415E-01  7.8065E-02                                 Card 310
       0.127       0.001       0.130      90.e-3         50.                     Card 500
         0.0         0.0                                                         Card 500
   1      0.0001        36.8         0.0         1.0                             Card 600
  -9                                                                             Card 700
       0.000      0.0625     0.30448                                             Card 701
       0.125      0.1875     0.86709                                             Card 701
       0.250      0.3125     1.29769                                             Card 701
       0.375      0.4375     1.53073                                             Card 701
       0.500      0.5625     1.53073                                             Card 701
       0.625      0.6875     1.29769                                             Card 701
       0.750      0.8125     0.86709                                             Card 701
       0.875      0.9375     0.30448                                             Card 701
       1.000                                                                     Card 701
   0                                                                             Card 702
```

Figure 5.2 Input Data for Standard Problem 18 Having the Innermost Tube Numbered First in the Input Data

```
Stdproblem 18, Innermost Tube First, Based on Hungarian Reactor Benchmark; 90 kW Card 100
   0   0   5   1   0   0   0   0   1   0   0   0   0   0   1   1   0   0         Card 200
   1   3         0.0         1.0         1.0         1.0   0   0                 Card 300
   1   2         1.0                                                             Card 301
   1   1   1                                                                     Card 302
        1.53                                                                     Card 303
         1.0         1.0         1.0         1.0         1.0         1.0         Card 304
         1.0         1.0         1.0         1.0         1.0         1.0         Card 304
         1.0         1.0         1.0         1.0         1.0         1.0         Card 304
         0.0         0.0         0.0                                             Card 305
   4   0         0.0         0.58     0.76e-3        6.00     0.98e-3        4.00 Card 306
  2.8274E-05  6.0000E-03  1.8850E-02  1.8850E-02         1.0         1.0         Card 307
  1.3195E-04  6.0000E-03  8.7965E-02  8.7965E-02         1.0         1.0         Card 307
  2.5015E-04  6.1964E-03  1.6148E-01  1.6148E-01         1.0         1.0         Card 307
  1.8003E-04  6.6631E-03  1.0808E-01  1.0808E-01         1.0         1.0         Card 307
  2.6704E-02  6.1261E-02  1.0022E-01                                             Card 308
   0.0042500   0.0097500   0.0159511                                             Card 308A
         1.0         1.0         1.0                                             Card 309
  7.8065E-02  3.6415E-01  7.0516E-00  5.1356E-01                                 Card 310
       0.127       0.001       0.130      90.e-3         50.                     Card 500
         0.0         0.0                                                         Card 500
   1      0.0001        36.8         0.0         1.0                             Card 600
  -9                                                                             Card 700
       0.000      0.0625     0.30448                                             Card 701
       0.125      0.1875     0.86709                                             Card 701
       0.250      0.3125     1.29769                                             Card 701
       0.375      0.4375     1.53073                                             Card 701
       0.500      0.5625     1.53073                                             Card 701
       0.625      0.6875     1.29769                                             Card 701
       0.750      0.8125     0.86709                                             Card 701
       0.875      0.9375     0.30448                                             Card 701
       1.000                                                                     Card 701
   0                                                                             Card 702
```

Table 5.1 Comparison of Six Solutions of Standard Problem 17 to Verify PLTEMP/ANL V3.4

	PLTEMP/ANL V3.2		PLTEMP/ANL V3.4			
	Problem 17 by Broyden Method	Solve Problem 18 by Broyden Method and then Reverse the Results	Problem17 by Broyden Method	Solve Problem 18 by Broyden Method and then Reverse the Results	Problem 17 by Exact Method	Solve Problem 18 by Exact Method and then Reverse the Results
	A	B	C	D	E	F
Table Showing Code Output	Table 5.2	Table 5.3	Table 5.4	Table 5.5	Table 5.6	Table 5.7
Channel Number	**Coolant Exit Temperature in Channel, °C**					
1	60.512	60.512	60.512	60.512	60.510	60.510
2	51.439	51.439	51.439	51.439	51.440	51.440
3	62.885	62.885	62.885	62.885	62.885	62.885
4	66.105	66.105	66.105	66.105	66.097	66.097
	Maximum Difference Between Code Runs in Coolant, Cladding and Fuel Temperatures, °C					
Table 5.6 or 5.9 vs. Table 5.2					0.012	
Table 5.6 or 5.9 vs. Table 5.3						0.017
Table 5.6 or 5.9 vs. Table 5.4					0.009	0.009
Table 5.6 or 5.9 vs. Table 5.5					0.009	0.009
Fuel Tube Number	**Location of Maximum Temperature in Meat At Exit, Outer Areal Fraction**					
1	0.4182	0.4182	0.4182	0.4182	0.4182	0.4182
2	0.6516	0.6516	0.6516	0.6516	0.6516	0.6516
3	0.6045	0.6045	0.6045	0.6045	0.6044	0.6044
Number of Broyden Iterations	20 (Note 1)	20 (Note 1)	20 (Note 1)	20 (Note 1)	-	-
Maximum T_{diff}, °C	0.0	0.0	0.0	0.0	-	-
Note 1. Using 20 iterations gave the same results as using 200 iterations.						

Table 5.2 PLTEMP V3.2 Output for Problem 17 Having the Outermost Tube First in Input Data – Broyden Method

FUEL PLATE 1 (BroydenSoln)

NODE	COOLANT outer(C)	CladSurf outer(C)	FUEL PEAK (C)	CladSurf inner(C)	COOLANT inner(C)	HCOFouter W/C-m^2	HCOFinner W/C-m^2	ONBRout [F Note 1]	ONBRin	ETAout K-cm^3/J	ETAin K-cm^3/J	COOLNT at outer(C)	NodeOutlet inner(C)
	50.000				50.000								
1	50.202	56.552	77.664	51.327	50.027	1.7498E+04	1.0952E+05	9.35	46.54	1.481E+03	1.143E+04	50.405	50.054
2	50.982	68.547	128.734	53.808	50.131	1.8029E+04	1.1023E+05	3.44	16.98	5.118E+02	4.003E+03	51.559	50.208
3	52.422	**78.024**	168.023	55.798	50.324	1.8499E+04	1.1086E+05	2.32	11.41	3.329E+02	2.660E+03	53.285	50.439
4	54.301	**83.819**	189.706	57.016	50.575	1.8889E+04	1.1135E+05	1.94	9.52	2.726E+02	2.238E+03	55.317	50.712
5	56.329	85.297	190.626	57.297	50.849	1.9171E+04	1.1162E+05	1.86	9.15	2.626E+02	2.215E+03	57.340	50.986
6	58.191	82.382	170.727	56.608	51.103	1.9307E+04	1.1164E+05	2.00	9.99	3.003E+02	2.579E+03	59.042	51.219
7	59.600	75.492	133.034	55.048	51.299	1.9259E+04	1.1140E+05	2.48	12.75	4.440E+02	3.775E+03	60.158	51.379
8	60.335	65.463	83.222	52.838	51.409	1.8987E+04	1.1093E+05	3.91	21.66	1.372E+03	9.913E+03	60.512	51.439
	60.512				51.439								

FUEL PLATE 2 (BroydenSoln)

	50.000				50.000								
1	50.027	51.203	77.794	57.207	50.248	1.0949E+05	1.7431E+04	51.16	8.52	1.264E+04	1.312E+03	50.054	50.495
2	50.131	53.459	129.104	70.396	51.201	1.1014E+05	1.8016E+04	18.59	3.14	4.426E+03	4.519E+02	50.208	51.906
3	50.324	55.280	168.601	80.847	52.961	1.1074E+05	1.8543E+04	12.45	2.12	2.941E+03	2.922E+02	50.439	54.016
4	50.575	56.409	190.441	**87.284**	55.258	1.1120E+05	1.8994E+04	10.35	1.77	2.474E+03	2.375E+02	50.712	56.500
5	50.849	56.691	191.462	89.030	57.739	1.1147E+05	1.9333E+04	9.91	1.69	2.448E+03	2.269E+02	50.986	58.977
6	51.103	56.094	171.613	86.010	60.021	1.1151E+05	1.9513E+04	10.76	1.81	2.847E+03	2.576E+02	51.219	61.064
7	51.299	54.703	133.919	78.666	61.751	1.1132E+05	1.9494E+04	13.61	2.22	4.161E+03	3.807E+02	51.379	62.438
8	51.409	52.716	84.086	67.878	62.661	1.1090E+05	1.9234E+04	22.55	3.38	1.084E+04	1.223E+03	51.439	62.885
	51.439				62.885								

FUEL PLATE 3 (BroydenSoln)

	50.000				50.000								
1	50.248	56.785	81.516	58.704	50.307	1.7415E+04	1.7501E+04	9.04	7.11	1.398E+03	1.084E+03	50.495	50.614
2	51.201	69.222	139.574	74.524	51.490	1.7978E+04	1.8188E+04	3.32	2.64	4.824E+02	3.718E+02	51.906	52.366
3	52.961	79.171	184.426	87.029	53.677	1.8495E+04	1.8805E+04	2.24	1.79	3.117E+02	2.382E+02	54.016	54.988
4	55.258	85.446	209.621	**94.755**	56.535	1.8944E+04	1.9353E+04	1.86	1.50	2.526E+02	1.908E+02	56.500	58.081
5	57.739	87.408	211.708	96.989	59.626	1.9289E+04	1.9778E+04	1.76	1.42	2.398E+02	1.789E+02	58.977	61.171
6	60.021	84.968	190.623	93.695	62.477	1.9483E+04	2.0013E+04	1.86	1.51	2.687E+02	1.984E+02	61.064	63.783
7	61.751	78.496	149.569	85.359	64.650	1.9488E+04	2.0021E+04	2.23	1.82	3.847E+02	2.838E+02	62.438	65.517
8	62.661	68.749	94.532	72.931	65.811	1.9266E+04	1.9759E+04	3.24	2.67	1.047E+03	8.114E+02	62.885	66.105
	62.885				66.105								

[1] The ONB ratio is here defined as (Tonb - Tinlet)/(Tsurf - Tinlet). If the heat flux is negative (the coolant is hotter than the adjacent cladding surface), then the ONB ratio is arbitrarily set to 99.99 .

Table 5-2 Contiune

FUEL PLATE 1 (BroydenSoln) AREAL FUEL-CLADinterface

NODE	FLUX outer MW/m^2	FLUX inner MW/m^2	FUEL X outer	Tsat (C)	Tdiff (C)	outer (C)	inner (C)	Pressure (bar)	Z-mid	Z-int
1	1.1111E-01	1.4241E-01	0.4772	107.091	0.00	70.947	68.915	1.29812	0.0625	0.1250
2	3.1667E-01	4.0525E-01	0.4776	107.006	0.00	109.572	103.856	1.29438	0.1875	0.2500
3	4.7362E-01	6.0686E-01	0.4773	106.921	0.00	139.382	130.746	1.29062	0.3125	0.3750
4	5.5759E-01	7.1712E-01	0.4764	106.836	0.00	156.055	145.580	1.28688	0.4375	0.5000
5	5.5537E-01	7.1972E-01	0.4745	106.751	0.00	157.245	146.183	1.28313	0.5625	0.6250
6	4.6703E-01	6.1457E-01	0.4707	106.666	0.00	142.886	132.508	1.27938	0.6875	0.7500
7	3.0608E-01	4.1765E-01	0.4616	106.580	0.00	115.144	106.628	1.27562	0.8125	0.8750
8	9.7362E-02	1.5850E-01	0.4182	106.495	0.00	78.076	72.412	1.27188	0.9375	1.0000

FUEL PLATE 2 (BroydenSoln)

1	1.2879E-01	1.2131E-01	0.5788	107.091	0.00	68.108	71.925	1.29812	0.0625	0.1250
2	3.6649E-01	3.4584E-01	0.5783	107.006	0.00	101.563	112.354	1.29438	0.1875	0.2500
3	5.4888E-01	5.1709E-01	0.5787	106.921	0.00	127.324	143.580	1.29062	0.3125	0.3750
4	6.4872E-01	6.0830E-01	0.5798	106.836	0.00	141.557	161.084	1.28688	0.4375	0.5000
5	6.5131E-01	6.0495E-01	0.5822	106.751	0.00	142.179	162.423	1.28313	0.5625	0.6250
6	5.5658E-01	5.0712E-01	0.5868	106.666	0.00	129.147	147.534	1.27938	0.6875	0.7500
7	3.7893E-01	3.2975E-01	0.5979	106.580	0.00	104.440	118.671	1.27562	0.8125	0.8750
8	1.4500E-01	1.0034E-01	0.6516	106.495	0.00	71.749	80.051	1.27188	0.9375	1.0000

FUEL PLATE 3 (BroydenSoln)

1	1.1385E-01	1.4695E-01	0.5869	107.091	0.00	72.305	75.295	1.29812	0.0625	0.1250
2	3.2398E-01	4.1892E-01	0.5864	107.006	0.00	113.386	121.822	1.29438	0.1875	0.2500
3	4.8475E-01	6.2718E-01	0.5863	106.921	0.00	145.252	157.840	1.29062	0.3125	0.3750
4	5.7187E-01	7.3970E-01	0.5863	106.836	0.00	163.402	178.269	1.28688	0.4375	0.5000
5	5.7228E-01	7.3894E-01	0.5867	106.751	0.00	165.420	180.418	1.28313	0.5625	0.6250
6	4.8607E-01	6.2477E-01	0.5879	106.666	0.00	151.228	164.234	1.27938	0.6875	0.7500
7	3.2634E-01	4.1460E-01	0.5907	106.580	0.00	122.982	132.169	1.27562	0.8125	0.8750
8	1.1727E-01	1.4068E-01	0.6045	106.495	0.00	84.735	88.814	1.27188	0.9375	1.0000

Table 5.3 PLTEMP V3.2 Output for Problem 18 Having the Innermost Tube First in Input Data – Broyden Method

FUEL PLATE 1 (BroydenSoln)

NODE	COOLANT inner(C)	CladSurf inner(C)	FUEL PEAK (C)	CladSurf outer(C)	COOLANT outer(C)	HCOFinner W/C-m^2	HCOFouter W/C-m^2	ONBRin [F Note 1]	ONBRout	ETAin K-cm^3/J	ETAout K-cm^3/J	COOLNT at inner(C)	NodeOutlet outer(C)
	50.000				50.000								
1	50.307	58.706	81.518	56.787	50.248	1.7496E+04	1.7411E+04	7.10	9.03	1.084E+03	1.398E+03	50.614	50.495
2	51.490	74.529	139.580	69.226	51.201	1.8183E+04	1.7973E+04	2.64	3.32	3.718E+02	4.824E+02	52.366	51.906
3	53.677	87.037	184.433	79.178	52.961	1.8800E+04	1.8490E+04	1.79	2.24	2.382E+02	3.117E+02	54.988	54.016
4	56.535	**94.765**	209.629	85.453	55.258	1.9349E+04	1.8939E+04	1.50	1.86	1.908E+02	2.526E+02	58.081	56.500
5	59.626	96.998	211.716	87.416	57.739	1.9773E+04	1.9284E+04	1.42	1.76	1.789E+02	2.398E+02	61.171	58.977
6	62.477	93.703	190.630	84.975	60.020	2.0008E+04	1.9479E+04	1.51	1.86	1.985E+02	2.687E+02	63.783	61.064
7	64.650	85.364	149.574	78.500	61.751	2.0016E+04	1.9483E+04	1.82	2.23	2.838E+02	3.847E+02	65.517	62.437
8	65.811	72.932	94.534	68.750	62.661	1.9754E+04	1.9261E+04	2.67	3.24	8.114E+02	1.047E+03	66.105	62.885
	66.105				62.885								

FUEL PLATE 2 (BroydenSoln)

	50.000				50.000								
1	50.248	57.209	77.796	51.204	50.027	1.7427E+04	1.0946E+05	8.52	51.14	1.312E+03	1.264E+04	50.495	50.054
2	51.201	70.401	129.107	53.460	50.131	1.8012E+04	1.1011E+05	3.14	18.58	4.519E+02	4.426E+03	51.906	50.208
3	52.961	80.854	168.605	55.282	50.324	1.8538E+04	1.1071E+05	2.12	12.44	2.923E+02	2.941E+03	54.016	50.439
4	55.258	**87.292**	190.446	56.411	50.575	1.8989E+04	1.1117E+05	1.77	10.35	2.375E+02	2.474E+03	56.500	50.712
5	57.739	89.037	191.467	56.693	50.849	1.9328E+04	1.1144E+05	1.69	9.91	2.269E+02	2.448E+03	58.977	50.986
6	60.020	86.016	171.617	56.095	51.103	1.9508E+04	1.1148E+05	1.81	10.76	2.576E+02	2.847E+03	61.064	51.220
7	61.751	78.670	133.922	54.704	51.299	1.9489E+04	1.1129E+05	2.22	13.61	3.807E+02	4.161E+03	62.437	51.379
8	62.661	67.879	84.087	52.717	51.409	1.9229E+04	1.1087E+05	3.38	22.55	1.223E+03	1.084E+04	62.885	51.439
	62.885				51.439								

FUEL PLATE 3 (BroydenSoln)

	50.000				50.000								
1	50.027	51.328	77.665	56.554	50.202	1.0949E+05	1.7493E+04	46.53	9.35	1.143E+04	1.481E+03	50.054	50.405
2	50.131	53.809	128.737	68.551	50.982	1.1020E+05	1.8024E+04	16.97	3.44	4.003E+03	5.118E+02	50.208	51.559
3	50.324	55.799	168.027	**78.030**	52.422	1.1084E+05	1.8494E+04	11.41	2.32	2.660E+03	3.329E+02	50.439	53.285
4	50.575	57.018	189.711	**83.826**	54.301	1.1132E+05	1.8885E+04	9.52	1.94	2.238E+03	2.726E+02	50.712	55.317
5	50.849	57.298	190.630	85.304	56.328	1.1159E+05	1.9166E+04	9.15	1.86	2.215E+03	2.627E+02	50.986	57.340
6	51.103	56.609	170.731	82.387	58.191	1.1161E+05	1.9302E+04	9.98	2.00	2.579E+03	3.003E+02	51.220	59.042
7	51.299	55.049	133.037	75.496	59.600	1.1137E+05	1.9255E+04	12.75	2.48	3.775E+03	4.440E+02	51.379	60.158
8	51.409	52.838	83.223	65.464	60.335	1.1090E+05	1.8982E+04	21.66	3.91	9.913E+03	1.372E+03	51.439	60.512
	51.439				60.512								

[1] The ONB ratio is here defined as (Tonb - Tinlet)/(Tsurf - Tinlet). If the heat flux is negative (the coolant is hotter than the adjacent cladding surface), then the ONB ratio is arbitrarily set to 99.99 .

Table 5-3 Continued

FUEL PLATE 1 (BroydenSoln) AREAL FUEL-CLADinterface

NODE	FLUX inner MW/m^2	FLUX outer MW/m^2	FUEL X inner	Tsat (C)	Tdiff (C)	inner (C)	outer (C)	Pressure (bar)	Z-mid	Z-int
1	1.4695E-01	1.1385E-01	0.4131	107.091	0.00	75.297	72.307	1.29812	0.0625	0.1250
2	4.1892E-01	3.2398E-01	0.4136	107.006	0.00	121.827	113.391	1.29438	0.1875	0.2500
3	6.2717E-01	4.8476E-01	0.4137	106.921	0.00	157.847	145.259	1.29062	0.3125	0.3750
4	7.3969E-01	5.7187E-01	0.4137	106.836	0.00	178.278	163.410	1.28688	0.4375	0.5000
5	7.3894E-01	5.7228E-01	0.4132	106.751	0.00	180.427	165.428	1.28313	0.5625	0.6250
6	6.2477E-01	4.8607E-01	0.4121	106.666	0.00	164.241	151.235	1.27938	0.6875	0.7500
7	4.1460E-01	3.2634E-01	0.4093	106.580	0.00	132.173	122.987	1.27562	0.8125	0.8750
8	1.4068E-01	1.1727E-01	0.3955	106.495	0.00	88.815	84.736	1.27188	0.9375	1.0000

FUEL PLATE 2 (BroydenSoln)

1	1.2131E-01	1.2880E-01	0.4212	107.091	0.00	71.926	68.109	1.29812	0.0625	0.1250
2	3.4583E-01	3.6650E-01	0.4217	107.006	0.00	112.357	101.564	1.29438	0.1875	0.2500
3	5.1708E-01	5.4889E-01	0.4213	106.921	0.00	143.585	127.326	1.29062	0.3125	0.3750
4	6.0829E-01	6.4873E-01	0.4201	106.836	0.00	161.090	141.560	1.28688	0.4375	0.5000
5	6.0494E-01	6.5132E-01	0.4178	106.751	0.00	162.429	142.182	1.28313	0.5625	0.6250
6	5.0711E-01	5.5659E-01	0.4132	106.666	0.00	147.539	129.150	1.27938	0.6875	0.7500
7	3.2974E-01	3.7893E-01	0.4021	106.580	0.00	118.674	104.441	1.27562	0.8125	0.8750
8	1.0033E-01	1.4501E-01	0.3484	106.495	0.00	80.051	71.750	1.27188	0.9375	1.0000

FUEL PLATE 3 (BroydenSoln)

1	1.4241E-01	1.1111E-01	0.5228	107.091	0.00	68.916	70.948	1.29812	0.0625	0.1250
2	4.0526E-01	3.1667E-01	0.5224	107.006	0.00	103.858	109.576	1.29438	0.1875	0.2500
3	6.0687E-01	4.7361E-01	0.5227	106.921	0.00	130.749	139.387	1.29062	0.3125	0.3750
4	7.1713E-01	5.5758E-01	0.5236	106.836	0.00	145.583	156.061	1.28688	0.4375	0.5000
5	7.1973E-01	5.5536E-01	0.5255	106.751	0.00	146.186	157.251	1.28313	0.5625	0.6250
6	6.1458E-01	4.6703E-01	0.5293	106.666	0.00	132.511	142.891	1.27938	0.6875	0.7500
7	4.1765E-01	3.0607E-01	0.5384	106.580	0.00	106.630	115.147	1.27562	0.8125	0.8750
8	1.5850E-01	9.7361E-02	0.5818	106.495	0.00	72.413	78.077	1.27188	0.9375	1.0000

Table 5.4 PLTEMP V3.4 Output for Problem 17 Having the Outermost Tube First in Input Data – Broyden Method

FUEL PLATE 1 (BroydenSoln)

NODE	COOLANT outer(C)	CladSurf outer(C)	FUEL PEAK (C)	CladSurf inner(C)	COOLANT inner(C)	HCOFouter W/C-m^2	HCOFinner W/C-m^2	ONBRout [F Note 1]	ONBRin	ETAout K-cm^3/J	ETAin K-cm^3/J	ONB Temp outer(C)	ONB Temp inner(C)
	50.000				50.000								
1	50.202	56.556	77.666	51.328	50.027	1.7488E+04	1.0946E+05	9.34	46.51	1.481E+03	1.143E+04	111.262	111.774
2	50.982	68.555	128.740	53.810	50.131	1.8019E+04	1.1017E+05	3.44	16.97	5.118E+02	4.003E+03	113.810	114.638
3	52.422	78.035	168.030	55.801	50.324	1.8491E+04	1.1080E+05	2.32	11.40	3.329E+02	2.660E+03	115.139	116.145
4	54.301	83.828	189.712	57.019	50.575	1.8883E+04	1.1129E+05	1.94	9.52	2.726E+02	2.238E+03	115.715	116.819
5	56.328	85.303	190.630	57.300	50.849	1.9167E+04	1.1156E+05	1.86	9.15	2.627E+02	2.215E+03	115.626	116.764
6	58.191	82.384	170.730	56.610	51.103	1.9305E+04	1.1158E+05	2.00	9.98	3.003E+02	2.579E+03	114.864	115.982
7	59.600	75.492	133.035	55.050	51.299	1.9260E+04	1.1135E+05	2.48	12.75	4.440E+02	3.775E+03	113.324	114.374
8	60.335	65.463	83.222	52.838	51.409	1.8988E+04	1.1087E+05	3.91	21.66	1.371E+03	9.913E+03	110.457	111.466
	60.512				51.439								

FUEL PLATE 2 (BroydenSoln)

	50.000				50.000								
1	50.027	51.204	77.797	57.211	50.248	1.0943E+05	1.7421E+04	51.12	8.52	1.264E+04	1.312E+03	111.560	111.437
2	50.131	53.461	129.109	70.405	51.201	1.1008E+05	1.8007E+04	18.58	3.14	4.426E+03	4.519E+02	114.289	114.095
3	50.324	55.283	168.607	80.857	52.961	1.1068E+05	1.8535E+04	12.44	2.12	2.941E+03	2.923E+02	115.723	115.482
4	50.575	56.412	190.447	87.292	55.258	1.1114E+05	1.8989E+04	10.35	1.77	2.474E+03	2.375E+02	116.364	116.083
5	50.849	56.695	191.465	89.034	57.739	1.1141E+05	1.9331E+04	9.90	1.69	2.448E+03	2.269E+02	116.309	115.986
6	51.103	56.096	171.614	86.009	60.020	1.1146E+05	1.9513E+04	10.75	1.81	2.847E+03	2.576E+02	115.562	115.185
7	51.299	54.705	133.919	78.664	61.751	1.1126E+05	1.9496E+04	13.61	2.22	4.161E+03	3.807E+02	114.029	113.562
8	51.409	52.717	84.086	67.877	62.661	1.1084E+05	1.9238E+04	22.55	3.38	1.084E+04	1.223E+03	111.264	110.513
	51.439				62.885								

FUEL PLATE 3 (BroydenSoln)

	50.000				50.000								
1	50.248	56.789	81.520	58.709	50.307	1.7406E+04	1.7491E+04	9.03	7.10	1.398E+03	1.084E+03	111.310	111.843
2	51.201	69.231	139.584	74.535	51.490	1.7969E+04	1.8179E+04	3.32	2.64	4.824E+02	3.718E+02	113.883	114.757
3	52.961	79.182	184.437	87.041	53.677	1.8488E+04	1.8798E+04	2.24	1.79	3.117E+02	2.382E+02	115.229	116.287
4	55.258	85.453	209.628	94.762	56.535	1.8939E+04	1.9350E+04	1.86	1.50	2.526E+02	1.908E+02	115.821	116.964
5	57.739	87.411	211.710	96.989	59.626	1.9286E+04	1.9778E+04	1.76	1.42	2.398E+02	1.789E+02	115.751	116.888
6	60.020	84.967	190.620	93.690	62.477	1.9484E+04	2.0017E+04	1.86	1.51	2.688E+02	1.984E+02	115.018	116.054
7	61.751	78.493	149.565	85.352	64.650	1.9491E+04	2.0028E+04	2.23	1.82	3.847E+02	2.838E+02	113.528	114.348
8	62.661	68.747	94.530	72.928	65.811	1.9270E+04	1.9768E+04	3.24	2.67	1.047E+03	8.114E+02	110.816	111.198
	62.885				66.105								

[1] The ONB ratio is here defined as (Tonb - Tinlet)/(Tsurf - Tinlet). If the heat flux is negative (the coolant is hotter than the adjacent cladding surface), then the ONB ratio is arbitrarily set to 99.99 .

Table 5-4 Continued

FUEL PLATE 1 (BroydenSoln) AREAL FUEL-CLADinterface

NODE	FLUX outer MW/m^2	FLUX inner MW/m^2	FUEL X outer	Tsat (C)	Tdiff (C)	outer (C)	inner (C)	Pressure (bar)	Z-mid	Z-int
1	1.1110E-01	1.4242E-01	0.4772	107.091	0.00	70.949	68.917	1.29812	0.0625	0.1250
2	3.1666E-01	4.0526E-01	0.4776	107.006	0.00	109.579	103.860	1.29438	0.1875	0.2500
3	4.7361E-01	6.0688E-01	0.4773	106.921	0.00	139.391	130.751	1.29062	0.3125	0.3750
4	5.5758E-01	7.1713E-01	0.4764	106.836	0.00	156.063	145.585	1.28688	0.4375	0.5000
5	5.5536E-01	7.1972E-01	0.4745	106.751	0.00	157.250	146.187	1.28313	0.5625	0.6250
6	4.6703E-01	6.1457E-01	0.4707	106.666	0.00	142.888	132.511	1.27938	0.6875	0.7500
7	3.0608E-01	4.1764E-01	0.4616	106.580	0.00	115.145	106.630	1.27562	0.8125	0.8750
8	9.7364E-02	1.5849E-01	0.4182	106.495	0.00	78.076	72.412	1.27188	0.9375	1.0000

FUEL PLATE 2 (BroydenSoln)

1	1.2880E-01	1.2131E-01	0.5788	107.091	0.00	68.110	71.928	1.29812	0.0625	0.1250
2	3.6650E-01	3.4583E-01	0.5783	107.006	0.00	101.566	112.361	1.29438	0.1875	0.2500
3	5.4889E-01	5.1707E-01	0.5787	106.921	0.00	127.328	143.589	1.29062	0.3125	0.3750
4	6.4873E-01	6.0829E-01	0.5799	106.836	0.00	141.561	161.091	1.28688	0.4375	0.5000
5	6.5131E-01	6.0495E-01	0.5822	106.751	0.00	142.182	162.426	1.28313	0.5625	0.6250
6	5.5657E-01	5.0713E-01	0.5868	106.666	0.00	129.149	147.535	1.27938	0.6875	0.7500
7	3.7892E-01	3.2975E-01	0.5979	106.580	0.00	104.440	118.670	1.27562	0.8125	0.8750
8	1.4500E-01	1.0034E-01	0.6516	106.495	0.00	71.749	80.050	1.27188	0.9375	1.0000

FUEL PLATE 3 (BroydenSoln)

1	1.1385E-01	1.4695E-01	0.5869	107.091	0.00	72.309	75.299	1.29812	0.0625	0.1250
2	3.2398E-01	4.1892E-01	0.5864	107.006	0.00	113.396	121.832	1.29438	0.1875	0.2500
3	4.8476E-01	6.2717E-01	0.5863	106.921	0.00	145.263	157.851	1.29062	0.3125	0.3750
4	5.7187E-01	7.3970E-01	0.5863	106.836	0.00	163.409	178.276	1.28688	0.4375	0.5000
5	5.7227E-01	7.3895E-01	0.5867	106.751	0.00	165.423	180.419	1.28313	0.5625	0.6250
6	4.8606E-01	6.2478E-01	0.5878	106.666	0.00	151.226	164.230	1.27938	0.6875	0.7500
7	3.2633E-01	4.1461E-01	0.5907	106.580	0.00	122.979	132.163	1.27562	0.8125	0.8750
8	1.1727E-01	1.4068E-01	0.6045	106.495	0.00	84.733	88.811	1.27188	0.9375	1.0000

Table 5.5 PLTEMP V3.4 Output for Problem 18 Having the Innermost Tube First in Input Data – Broyden Method

FUEL PLATE 1 (BroydenSoln)

NODE	COOLANT inner(C)	CladSurf inner(C)	FUEL PEAK (C)	CladSurf outer(C)	COOLANT outer(C)	HCOFinner W/C-m^2	HCOFouter W/C-m^2	ONBRin [F Note 1]	ONBRout	ETAin K-cm^3/J	ETAout K-cm^3/J	ONB Temp inner(C)	ONB Temp outer(C)
	50.000				50.000								
1	50.307	58.709	81.520	56.789	50.248	1.7491E+04	1.7406E+04	7.10	9.03	1.084E+03	1.398E+03	111.843	111.310
2	51.490	74.535	139.584	69.231	51.201	1.8179E+04	1.7969E+04	2.64	3.32	3.718E+02	4.824E+02	114.757	113.883
3	53.677	87.041	184.437	79.182	52.961	1.8798E+04	1.8488E+04	1.79	2.24	2.382E+02	3.117E+02	116.287	115.229
4	56.535	94.762	209.628	85.453	55.258	1.9350E+04	1.8939E+04	1.50	1.86	1.908E+02	2.526E+02	116.964	115.821
5	59.626	96.989	211.710	87.411	57.739	1.9778E+04	1.9286E+04	1.42	1.76	1.789E+02	2.398E+02	116.888	115.751
6	62.477	93.690	190.620	84.967	60.020	2.0017E+04	1.9484E+04	1.51	1.86	1.984E+02	2.688E+02	116.054	115.018
7	64.650	85.352	149.565	78.493	61.751	2.0028E+04	1.9491E+04	1.82	2.23	2.838E+02	3.847E+02	114.348	113.528
8	65.811	72.928	94.530	68.747	62.661	1.9768E+04	1.9270E+04	2.67	3.24	8.114E+02	1.047E+03	111.198	110.816
	66.105				62.885								

FUEL PLATE 2 (BroydenSoln)

	50.000				50.000								
1	50.248	57.211	77.797	51.204	50.027	1.7421E+04	1.0943E+05	8.52	51.12	1.312E+03	1.264E+04	111.437	111.560
2	51.201	70.405	129.109	53.461	50.131	1.8007E+04	1.1008E+05	3.14	18.58	4.519E+02	4.426E+03	114.095	114.289
3	52.961	80.857	168.607	55.283	50.324	1.8535E+04	1.1068E+05	2.12	12.44	2.923E+02	2.941E+03	115.482	115.723
4	55.258	87.292	190.447	56.412	50.575	1.8989E+04	1.1114E+05	1.77	10.35	2.375E+02	2.474E+03	116.083	116.364
5	57.739	89.034	191.465	56.695	50.849	1.9331E+04	1.1141E+05	1.69	9.90	2.269E+02	2.448E+03	115.986	116.309
6	60.020	86.009	171.614	56.096	51.103	1.9513E+04	1.1146E+05	1.81	10.75	2.576E+02	2.847E+03	115.185	115.562
7	61.751	78.664	133.919	54.705	51.299	1.9496E+04	1.1126E+05	2.22	13.61	3.807E+02	4.161E+03	113.562	114.029
8	62.661	67.877	84.086	52.717	51.409	1.9238E+04	1.1084E+05	3.38	22.55	1.223E+03	1.084E+04	110.513	111.264
	62.885				51.439								

FUEL PLATE 3 (BroydenSoln)

	50.000				50.000								
1	50.027	51.328	77.666	56.556	50.202	1.0946E+05	1.7488E+04	46.51	9.34	1.143E+04	1.481E+03	111.774	111.262
2	50.131	53.810	128.740	68.555	50.982	1.1017E+05	1.8019E+04	16.97	3.44	4.003E+03	5.118E+02	114.638	113.810
3	50.324	55.801	168.030	78.035	52.422	1.1080E+05	1.8491E+04	11.40	2.32	2.660E+03	3.329E+02	116.145	115.139
4	50.575	57.019	189.712	83.828	54.301	1.1129E+05	1.8883E+04	9.52	1.94	2.238E+03	2.726E+02	116.819	115.715
5	50.849	57.300	190.630	85.303	56.328	1.1156E+05	1.9167E+04	9.15	1.86	2.215E+03	2.627E+02	116.764	115.626
6	51.103	56.610	170.730	82.384	58.191	1.1158E+05	1.9305E+04	9.98	2.00	2.579E+03	3.003E+02	115.982	114.864
7	51.299	55.050	133.035	75.492	59.600	1.1135E+05	1.9260E+04	12.75	2.48	3.775E+03	4.440E+02	114.374	113.324
8	51.409	52.838	83.222	65.463	60.335	1.1087E+05	1.8988E+04	21.66	3.91	9.913E+03	1.371E+03	111.466	110.457
	51.439				60.512								

[1] The ONB ratio is here defined as (Tonb - Tinlet)/(Tsurf - Tinlet). If the heat flux is negative (the coolant is hotter than the adjacent cladding surface), then the ONB ratio is arbitrarily set to 99.99 .

Table 5-5 Continued

FUEL PLATE 1 (BroydenSoln) AREAL FUEL-CLADinterface

NODE	FLUX inner MW/m^2	FLUX outer MW/m^2	FUEL X inner	Tsat (C)	Tdiff (C)	inner (C)	outer (C)	Pressure (bar)	Z-mid	Z-int
1	1.4695E-01	1.1385E-01	0.4131	107.091	0.00	75.299	72.309	1.29812	0.0625	0.1250
2	4.1892E-01	3.2398E-01	0.4136	107.006	0.00	121.832	113.396	1.29438	0.1875	0.2500
3	6.2717E-01	4.8476E-01	0.4137	106.921	0.00	157.851	145.263	1.29062	0.3125	0.3750
4	7.3970E-01	5.7187E-01	0.4137	106.836	0.00	178.276	163.409	1.28688	0.4375	0.5000
5	7.3895E-01	5.7227E-01	0.4133	106.751	0.00	180.419	165.423	1.28313	0.5625	0.6250
6	6.2478E-01	4.8606E-01	0.4122	106.666	0.00	164.230	151.226	1.27938	0.6875	0.7500
7	4.1461E-01	3.2633E-01	0.4093	106.580	0.00	132.163	122.979	1.27562	0.8125	0.8750
8	1.4068E-01	1.1727E-01	0.3955	106.495	0.00	88.811	84.733	1.27188	0.9375	1.0000

FUEL PLATE 2 (BroydenSoln)

1	1.2131E-01	1.2880E-01	0.4212	107.091	0.00	71.928	68.110	1.29812	0.0625	0.1250
2	3.4583E-01	3.6650E-01	0.4217	107.006	0.00	112.361	101.566	1.29438	0.1875	0.2500
3	5.1707E-01	5.4889E-01	0.4213	106.921	0.00	143.589	127.328	1.29062	0.3125	0.3750
4	6.0829E-01	6.4873E-01	0.4201	106.836	0.00	161.091	141.561	1.28688	0.4375	0.5000
5	6.0495E-01	6.5131E-01	0.4178	106.751	0.00	162.426	142.182	1.28313	0.5625	0.6250
6	5.0713E-01	5.5657E-01	0.4132	106.666	0.00	147.535	129.149	1.27938	0.6875	0.7500
7	3.2975E-01	3.7892E-01	0.4021	106.580	0.00	118.670	104.440	1.27562	0.8125	0.8750
8	1.0034E-01	1.4500E-01	0.3484	106.495	0.00	80.050	71.749	1.27188	0.9375	1.0000

FUEL PLATE 3 (BroydenSoln)

1	1.4242E-01	1.1110E-01	0.5228	107.091	0.00	68.917	70.949	1.29812	0.0625	0.1250
2	4.0526E-01	3.1666E-01	0.5224	107.006	0.00	103.860	109.579	1.29438	0.1875	0.2500
3	6.0688E-01	4.7361E-01	0.5227	106.921	0.00	130.751	139.391	1.29062	0.3125	0.3750
4	7.1713E-01	5.5758E-01	0.5236	106.836	0.00	145.585	156.063	1.28688	0.4375	0.5000
5	7.1972E-01	5.5536E-01	0.5255	106.751	0.00	146.187	157.250	1.28313	0.5625	0.6250
6	6.1457E-01	4.6703E-01	0.5293	106.666	0.00	132.511	142.888	1.27938	0.6875	0.7500
7	4.1764E-01	3.0608E-01	0.5384	106.580	0.00	106.630	115.145	1.27562	0.8125	0.8750
8	1.5849E-01	9.7364E-02	0.5818	106.495	0.00	72.412	78.076	1.27188	0.9375	1.0000

Table 5.6 PLTEMP V3.4 Output for Problem 17 Having the Outermost Tube First in Input Data – Exact Method

FUEL PLATE 1 (ExactSoln)

NODE	COOLANT outer(C)	CladSurf outer(C)	FUEL PEAK (C)	CladSurf inner(C)	COOLANT inner(C)	HCOFouter W/C-m^2	HCOFinner W/C-m^2	ONBRout [F Note 1]	ONBRin	ETAout K-cm^3/J	ETAin K-cm^3/J	ONB Temp outer(C)	ONB Temp inner(C)
	50.000				50.000								
1	50.202	56.556	77.667	51.328	50.027	1.7488E+04	1.0946E+05	9.35	46.51	1.481E+03	1.143E+04	111.263	111.774
2	50.982	68.555	128.741	53.810	50.131	1.8019E+04	1.1017E+05	3.44	16.97	5.118E+02	4.003E+03	113.810	114.638
3	52.422	78.035	168.031	55.801	50.324	1.8491E+04	1.1080E+05	2.32	11.40	3.329E+02	2.660E+03	115.139	116.145
4	54.301	83.828	189.714	57.020	50.577	1.8884E+04	1.1129E+05	1.94	9.52	2.726E+02	2.238E+03	115.715	116.819
5	56.328	85.302	190.632	57.301	50.850	1.9167E+04	1.1156E+05	1.86	9.14	2.627E+02	2.215E+03	115.626	116.764
6	58.190	82.383	170.731	56.611	51.103	1.9305E+04	1.1158E+05	2.00	9.98	3.003E+02	2.579E+03	114.864	115.982
7	59.598	75.490	133.035	55.050	51.299	1.9259E+04	1.1135E+05	2.48	12.75	4.440E+02	3.775E+03	113.324	114.374
8	60.332	65.460	83.222	52.839	51.410	1.8988E+04	1.1087E+05	3.91	21.65	1.371E+03	9.913E+03	110.457	111.466
	60.510				51.440								

FUEL PLATE 2 (ExactSoln)

	50.000				50.000								
1	50.027	51.204	77.797	57.211	50.248	1.0943E+05	1.7421E+04	51.12	8.52	1.264E+04	1.312E+03	111.560	111.437
2	50.131	53.461	129.110	70.406	51.202	1.1008E+05	1.8008E+04	18.58	3.14	4.426E+03	4.519E+02	114.289	114.095
3	50.324	55.284	168.608	80.859	52.963	1.1068E+05	1.8536E+04	12.44	2.12	2.941E+03	2.922E+02	115.724	115.482
4	50.577	56.414	190.448	87.294	55.261	1.1114E+05	1.8989E+04	10.35	1.77	2.474E+03	2.374E+02	116.364	116.083
5	50.850	56.696	191.467	89.035	57.741	1.1141E+05	1.9331E+04	9.90	1.69	2.448E+03	2.269E+02	116.309	115.986
6	51.103	56.097	171.615	86.010	60.022	1.1146E+05	1.9514E+04	10.75	1.81	2.847E+03	2.576E+02	115.562	115.185
7	51.299	54.705	133.920	78.665	61.751	1.1126E+05	1.9496E+04	13.61	2.22	4.161E+03	3.807E+02	114.029	113.562
8	51.410	52.718	84.086	67.877	62.662	1.1084E+05	1.9238E+04	22.54	3.38	1.084E+04	1.223E+03	111.264	110.513
	51.440				62.885								

FUEL PLATE 3 (ExactSoln)

	50.000				50.000								
1	50.248	56.789	81.520	58.709	50.307	1.7406E+04	1.7491E+04	9.03	7.10	1.398E+03	1.084E+03	111.310	111.843
2	51.202	69.232	139.585	74.535	51.490	1.7969E+04	1.8179E+04	3.32	2.64	4.824E+02	3.718E+02	113.883	114.757
3	52.963	79.183	184.437	87.041	53.678	1.8488E+04	1.8799E+04	2.24	1.79	3.117E+02	2.382E+02	115.229	116.287
4	55.261	85.456	209.629	94.763	56.536	1.8939E+04	1.9350E+04	1.86	1.50	2.526E+02	1.908E+02	115.821	116.964
5	57.741	87.413	211.710	96.989	59.625	1.9287E+04	1.9778E+04	1.76	1.42	2.398E+02	1.789E+02	115.751	116.888
6	60.022	84.968	190.619	93.687	62.473	1.9484E+04	2.0016E+04	1.86	1.51	2.687E+02	1.985E+02	115.018	116.054
7	61.751	78.493	149.562	85.347	64.643	1.9491E+04	2.0026E+04	2.23	1.82	3.847E+02	2.838E+02	113.528	114.348
8	62.662	68.747	94.526	72.921	65.802	1.9270E+04	1.9767E+04	3.24	2.67	1.047E+03	8.115E+02	110.815	111.198
	62.885				66.097								

[1] The ONB ratio is here defined as (Tonb - Tinlet)/(Tsurf - Tinlet). If the heat flux is negative (the coolant is hotter than the adjacent cladding surface), then the ONB ratio is arbitrarily set to 99.99 .

Table 5-6 Continued

NODE	FUEL PLATE 1 (ExactSoln) FLUX outer MW/m^2	FLUX inner MW/m^2	AREAL FUEL X outer	Tsat (C)	Tdiff (C)	FUEL-CLADinterface outer (C)	inner (C)	Pressure (bar)	Z-mid	Z-int
1	1.1110E-01	1.4242E-01	0.4772	107.091		70.949	68.917	1.29812	0.0625	0.1250
2	3.1666E-01	4.0526E-01	0.4776	107.006		109.579	103.860	1.29438	0.1875	0.2500
3	4.7361E-01	6.0688E-01	0.4773	106.921		139.391	130.751	1.29062	0.3125	0.3750
4	5.5758E-01	7.1712E-01	0.4764	106.836		156.063	145.586	1.28688	0.4375	0.5000
5	5.5537E-01	7.1972E-01	0.4745	106.751		157.250	146.187	1.28313	0.5625	0.6250
6	4.6704E-01	6.1457E-01	0.4707	106.666		142.888	132.511	1.27938	0.6875	0.7500
7	3.0608E-01	4.1764E-01	0.4616	106.580		115.144	106.629	1.27562	0.8125	0.8750
8	9.7370E-02	1.5849E-01	0.4182	106.495		78.075	72.412	1.27188	0.9375	1.0000
FUEL PLATE 2 (ExactSoln)										
1	1.2880E-01	1.2131E-01	0.5788	107.091		68.110	71.928	1.29812	0.0625	0.1250
2	3.6651E-01	3.4582E-01	0.5783	107.006		101.567	112.362	1.29438	0.1875	0.2500
3	5.4890E-01	5.1707E-01	0.5787	106.921		127.329	143.590	1.29062	0.3125	0.3750
4	6.4873E-01	6.0829E-01	0.5799	106.836		141.562	161.093	1.28688	0.4375	0.5000
5	6.5131E-01	6.0495E-01	0.5822	106.751		142.183	162.428	1.28313	0.5625	0.6250
6	5.5658E-01	5.0713E-01	0.5868	106.666		129.150	147.536	1.27938	0.6875	0.7500
7	3.7892E-01	3.2975E-01	0.5979	106.580		104.441	118.671	1.27562	0.8125	0.8750
8	1.4500E-01	1.0034E-01	0.6516	106.495		71.750	80.051	1.27188	0.9375	1.0000
FUEL PLATE 3 (ExactSoln)										
1	1.1385E-01	1.4695E-01	0.5869	107.091		72.310	75.299	1.29812	0.0625	0.1250
2	3.2398E-01	4.1892E-01	0.5864	107.006		113.397	121.833	1.29438	0.1875	0.2500
3	4.8475E-01	6.2718E-01	0.5863	106.921		145.264	157.852	1.29062	0.3125	0.3750
4	5.7187E-01	7.3970E-01	0.5863	106.836		163.412	178.278	1.28688	0.4375	0.5000
5	5.7227E-01	7.3896E-01	0.5867	106.751		165.424	180.419	1.28313	0.5625	0.6250
6	4.8606E-01	6.2479E-01	0.5878	106.666		151.226	164.228	1.27938	0.6875	0.7500
7	3.2633E-01	4.1463E-01	0.5906	106.580		122.978	132.159	1.27562	0.8125	0.8750
8	1.1726E-01	1.4070E-01	0.6044	106.495		84.732	88.806	1.27188	0.9375	1.0000

Table 5.7 PLTEMP V3.4 Output for Problem 18 Having the Innermost Tube First in Input Data – Exact Method

FUEL PLATE 1 (ExactSoln)

NODE	COOLANT inner(C)	CladSurf inner(C)	FUEL PEAK (C)	CladSurf outer(C)	COOLANT outer(C)	HCOFinner W/C-m^2	HCOFouter W/C-m^2	ONBRin [F Note 1]	ONBRout	ETAin K-cm^3/J	ETAout K-cm^3/J	ONB Temp inner(C)	ONB Temp outer(C)
	50.000				50.000								
1	50.307	58.709	81.520	56.789	50.248	1.7491E+04	1.7406E+04	7.10	9.03	1.084E+03	1.398E+03	111.843	111.310
2	51.490	74.535	139.585	69.232	51.202	1.8179E+04	1.7969E+04	2.64	3.32	3.718E+02	4.824E+02	114.757	113.883
3	53.678	87.041	184.437	79.183	52.963	1.8799E+04	1.8488E+04	1.79	2.24	2.382E+02	3.117E+02	116.287	115.229
4	56.536	94.763	209.629	85.456	55.261	1.9350E+04	1.8939E+04	1.50	1.86	1.908E+02	2.526E+02	116.964	115.821
5	59.625	96.989	211.710	87.413	57.741	1.9778E+04	1.9287E+04	1.42	1.76	1.789E+02	2.398E+02	116.888	115.751
6	62.473	93.687	190.619	84.968	60.022	2.0016E+04	1.9484E+04	1.51	1.86	1.985E+02	2.687E+02	116.054	115.018
7	64.643	85.347	149.562	78.493	61.751	2.0026E+04	1.9491E+04	1.82	2.23	2.838E+02	3.847E+02	114.348	113.528
8	65.802	72.921	94.526	68.747	62.662	1.9767E+04	1.9270E+04	2.67	3.24	8.115E+02	1.047E+03	111.198	110.815
	66.097				62.885								

FUEL PLATE 2 (ExactSoln)

	50.000				50.000								
1	50.248	57.211	77.797	51.204	50.027	1.7421E+04	1.0943E+05	8.52	51.12	1.312E+03	1.264E+04	111.437	111.560
2	51.202	70.406	129.110	53.461	50.131	1.8008E+04	1.1008E+05	3.14	18.58	4.519E+02	4.426E+03	114.095	114.289
3	52.963	80.859	168.608	55.284	50.324	1.8536E+04	1.1068E+05	2.12	12.44	2.922E+02	2.941E+03	115.482	115.724
4	55.261	87.294	190.448	56.414	50.577	1.8989E+04	1.1114E+05	1.77	10.35	2.374E+02	2.474E+03	116.083	116.364
5	57.741	89.035	191.467	56.696	50.850	1.9331E+04	1.1141E+05	1.69	9.90	2.269E+02	2.448E+03	115.986	116.309
6	60.022	86.010	171.615	56.097	51.103	1.9514E+04	1.1146E+05	1.81	10.75	2.576E+02	2.847E+03	115.185	115.562
7	61.751	78.665	133.920	54.705	51.299	1.9496E+04	1.1126E+05	2.22	13.61	3.807E+02	4.161E+03	113.562	114.029
8	62.662	67.877	84.086	52.718	51.410	1.9238E+04	1.1084E+05	3.38	22.54	1.223E+03	1.084E+04	110.513	111.264
	62.885				51.440								

FUEL PLATE 3 (ExactSoln)

	50.000				50.000								
1	50.027	51.328	77.667	56.556	50.202	1.0946E+05	1.7488E+04	46.51	9.35	1.143E+04	1.481E+03	111.774	111.263
2	50.131	53.810	128.741	68.555	50.982	1.1017E+05	1.8019E+04	16.97	3.44	4.003E+03	5.118E+02	114.638	113.810
3	50.324	55.801	168.031	78.035	52.422	1.1080E+05	1.8491E+04	11.40	2.32	2.660E+03	3.329E+02	116.145	115.139
4	50.577	57.020	189.714	83.828	54.301	1.1129E+05	1.8884E+04	9.52	1.94	2.238E+03	2.726E+02	116.819	115.715
5	50.850	57.301	190.632	85.302	56.328	1.1156E+05	1.9167E+04	9.14	1.86	2.215E+03	2.627E+02	116.764	115.626
6	51.103	56.611	170.731	82.383	58.190	1.1158E+05	1.9305E+04	9.98	2.00	2.579E+03	3.003E+02	115.982	114.864
7	51.299	55.050	133.035	75.490	59.598	1.1135E+05	1.9259E+04	12.75	2.48	3.775E+03	4.440E+02	114.374	113.324
8	51.410	52.839	83.222	65.460	60.332	1.1087E+05	1.8988E+04	21.65	3.91	9.913E+03	1.371E+03	111.466	110.457
	51.440				60.510								

[1] The ONB ratio is here defined as (Tonb - Tinlet)/(Tsurf - Tinlet). If the heat flux is negative (the coolant is hotter than the adjacent cladding surface), then the ONB ratio is arbitrarily set to 99.99 .

Table 5-7 Continued

FUEL PLATE 1 (ExactSoln) NODE	FLUX inner MW/m^2	FLUX outer MW/m^2	AREAL FUEL X inner	Tsat (C)	Tdiff (C)	FUEL-CLADinterface inner (C)	outer (C)	Pressure (bar)	Z-mid	Z-int
1	1.4695E-01	1.1385E-01	0.4131	107.091		75.299	72.310	1.29812	0.0625	0.1250
2	4.1892E-01	3.2398E-01	0.4136	107.006		121.833	113.397	1.29438	0.1875	0.2500
3	6.2718E-01	4.8475E-01	0.4137	106.921		157.852	145.264	1.29062	0.3125	0.3750
4	7.3970E-01	5.7187E-01	0.4137	106.836		178.278	163.412	1.28688	0.4375	0.5000
5	7.3896E-01	5.7227E-01	0.4133	106.751		180.419	165.424	1.28313	0.5625	0.6250
6	6.2479E-01	4.8606E-01	0.4122	106.666		164.228	151.226	1.27938	0.6875	0.7500
7	4.1463E-01	3.2633E-01	0.4094	106.580		132.159	122.978	1.27562	0.8125	0.8750
8	1.4070E-01	1.1726E-01	0.3956	106.495		88.806	84.732	1.27188	0.9375	1.0000
FUEL PLATE 2 (ExactSoln)										
1	1.2131E-01	1.2880E-01	0.4212	107.091		71.928	68.110	1.29812	0.0625	0.1250
2	3.4582E-01	3.6651E-01	0.4217	107.006		112.362	101.567	1.29438	0.1875	0.2500
3	5.1707E-01	5.4890E-01	0.4213	106.921		143.590	127.329	1.29062	0.3125	0.3750
4	6.0829E-01	6.4873E-01	0.4201	106.836		161.093	141.562	1.28688	0.4375	0.5000
5	6.0495E-01	6.5131E-01	0.4178	106.751		162.428	142.183	1.28313	0.5625	0.6250
6	5.0713E-01	5.5658E-01	0.4132	106.666		147.536	129.150	1.27938	0.6875	0.7500
7	3.2975E-01	3.7892E-01	0.4021	106.580		118.671	104.441	1.27562	0.8125	0.8750
8	1.0034E-01	1.4500E-01	0.3484	106.495		80.051	71.750	1.27188	0.9375	1.0000
FUEL PLATE 3 (ExactSoln)										
1	1.4242E-01	1.1110E-01	0.5228	107.091		68.917	70.949	1.29812	0.0625	0.1250
2	4.0526E-01	3.1666E-01	0.5224	107.006		103.860	109.579	1.29438	0.1875	0.2500
3	6.0688E-01	4.7361E-01	0.5227	106.921		130.751	139.391	1.29062	0.3125	0.3750
4	7.1712E-01	5.5758E-01	0.5236	106.836		145.586	156.063	1.28688	0.4375	0.5000
5	7.1972E-01	5.5537E-01	0.5255	106.751		146.187	157.250	1.28313	0.5625	0.6250
6	6.1457E-01	4.6704E-01	0.5293	106.666		132.511	142.888	1.27938	0.6875	0.7500
7	4.1764E-01	3.0608E-01	0.5384	106.580		106.629	115.144	1.27562	0.8125	0.8750
8	1.5849E-01	9.7370E-02	0.5818	106.495		72.412	78.075	1.27188	0.9375	1.0000

Table 5.8 Comparison of Solutions by Different PLTEMP/ANL Versions for Standards Problems 17 and 18

	Maximum Temperature Difference in Cladding, Fuel, and Adjacent Coolant Channels of a Fuel Tube , °C						Comments
	Problem 17 Tube 1 is the outermost			**Problem 18 Tube 1 is innermost**			
Code Versions Compared	Tube 1	Tube 2	Tube 3	Tube 1	Tube 2	Tube 3	
	Broyden Solution History [Note 1, 2]						
Broyden V3.0 vs. Broyden V3.4	0.697	1.712	10.005	9.999	1.708	0.693	
Broyden V3.1 vs. Broyden V3.4	0.173	0.218	0.331	0.322	0.211	0.166	
Broyden V3.2 vs. Broyden V3.4	0.011	0.010	0.012	0.013	0.007	0.005	
Broyden V3.3 vs. Broyden V3.4	0.011	0.010	0.012	0.013	0.007	0.005	
	Exact Solution History [Note 1]						
Exact V3.0 vs. Exact V3.4	0.744	1.784	4.512	4.504	1.777	0.751	Note 3
Exact V3.1 vs. Exact V3.4	0.744	1.785	4.511	4.502	1.778	0.751	Note 3
Exact V3.2 vs. Exact V3.4				0.014	0.005	0.005	Note 4
Exact V3.3 vs. Exact V3.4				0.014	0.005	0.005	Note 4
	Exact vs. Broyden Solutions of a Code Version						
Exact V3.0 vs. Broyden V3.0	1.087	1.358	8.619	8.619	1.358	1.087	Note 3
Exact V3.1 vs. Broyden V3.1	2.178	4.004	11.511	4.179	1.565	0.917	Note 3
Exact V3.2 vs. Broyden V3.2				0.009	0.003	0.002	Note 4
Exact V3.3 vs. Broyden V3.3				0.009	0.003	0.002	Note 4
Exact V3.4 vs. Broyden V3.4	0.003	0.003	0.009	0.009	0.003	0.003	

Note 1. PLTEMP/ANL V3.4 is used as the base version in these comparisons because it is the first version to have the radial geometry exact method that allows fuel tube numbering in both directions (the innermost tube first or the outermost tube first).

Note 2. Each Tdiff iz zero in all 5 Broyden solutions of Problem 17, and in all 5 Broyden solutions of Problem 18.

Note 3. Only the slab geometry exact method was available in PLTEMP/ANL V3.0 and V3.1. So this difference is due to the use of the slab geometry exact method in a radial geometry problem.

Note 4. PLTEMP/ANL V3.2 and V3.3 have the radial geometry exact method for problems in which the innermost tube is numbered as the first, and therefore give the exact solution for Problem 18. These versions do not give an exact solution for Problem 17 because the outermost tube is numbered as the first.

6 Verification of Carnavos Correlation Implemented in PLTEMP/ANL for Heat Transfer Coefficient and Friction Factor in Finned Coolant Channels

6.1 Introduction

The verification work reported here was done in September 2007. The MIT Reactor coolant channels have straight longitudinal internal fins of rectangular cross section. In preparation for the thermal hydraulic analysis of this reactor, the PLTEMP/ANL code has been improved to handle heat transfer coefficient and friction factor in finned channels of rectangular cross section. The implementaton of fins in circular and annular coolant channels is discussed later in Chapter 18.

Fins of different cross sections (triangular and rectangular), with the fin axis parallel to the channel axis or making an angle (called helix angle) with the channel axis, are used in heat exchangers. The fins of trapezoidal cross section (that covers both triangular and rectangular cross sections) at a user-input helix angle (0 to 30°) were recently modeled in PLTEMP/ANL version 3.3.

Figure 6.1 shows reactor coolant channels with straight longitudinal inner fins of trapezoidal cross section. Channels of two cross-sectional shapes are shown: (i) the circular tube, and (ii) the channel between parallel plates. The detailed geometry of the fins used in calculating the heat transfer area and the coolant flow area is shown in Fig. 6.2. The correlations of Carnavos [1, 2] for heat transfer coefficient and friction factor in a tube having internal longitudinal fins (straight or helical) were implemented in the PLTEMP/ANL version 3.3 code, as described below. Although developed based on measured data for round tubes, the correlations are used for rectangular cross-section channels also, based on hydraulic diameter, flow area, and heated perimeter.

A verification of the implemented fin model by hand calculation is presented in this chapter. The friction factor, coolant flow rate, heat transfer coefficient, Groeneveld critical heat flux calculations were verified with and without fins. The Users Guide of the code has also been updated by describing the method and the new input card required. The older input files should work without any change. The onset-of-nucleate boiling (ONB) temperatures are also now printed in the code's main output in version 3.3 and all later versions. PLTEMP/ANL version 3.3 code was also verified for a standard set of 14 test problems without fins, and found to reproduce all coolant, cladding, and fuel temperatures saved earlier from the version 3.2 of the code. The flow instability edits are not revised in the code version 3.3 to include the effect of fins. This will be done in a future version.

6.2 Carnavos Correlation and its Implementation

Based on his experimental data for 14 tubes with and without fins, Carnavos obtained the following correlations for heat transfer coefficient and Darcy-Weisbach friction factor, each representing the data to within ±10%. The heat transfer coefficient correlation is basically the Dittus-Boelter correlation multiplied by a factor that is a function of the fin geometry. The friction factor correlation is basically the McAdams correlation multiplied by a factor that is a function of the fin geometry. Equations (6.1) and (6.2) give these correlations, assuming the fins to be of a trapezoidal cross section as shown in Fig. 6.2.

$$Nu = 0.023\, Re_a^{\;0.8}\, Pr^{0.4} \left(\frac{A_{fa}}{A_{fc}}\right)^{0.1} \left(\frac{P_n}{P_a}\right)^{0.5} \sec^3\alpha \tag{6.1}$$

$$f_a = \frac{0.184}{Re_a^{\;0.2}} \left(\frac{A_{fn}}{A_{fa}}\right)^{0.5} (\cos\alpha)^{0.75} \tag{6.2}$$

The variables are defined in the nomenclature at the end of the chapter. The adjective "actual" is used to refer to the geometrical parametes of the channel with the fins included in the channel geometry. The adjective "nominal" is used to refer to the geometrical parametes without the fins, i.e., as if the fins were cut off at their roots.

The actual and nominal heat transfer areas, the actual and nominal coolant flow areas, and the actual and nominal hydraulic diameters are given by Eqs. (6.3) to (6.8) based on the trapezoidal cross section of the fins. The equations for a rectangular channel are a theoretical extension of the experimental data for tubes. It should be noted that, in the implementation, the *nominal perimeters and flow areas input on Card type 0307 are used* rather than the values obtained from Eq. (6.3), Eq. (6.5), and the input channel width and thickness.

$$P_n = \begin{cases} \pi D_i & \text{for tube} \\ 2(W_{ch} + T_{ch}) & \text{for rectangular channel} \end{cases} \tag{6.3}$$

$$P_a = P_n + n\, P_{fin} \sec\alpha \tag{6.4}$$

$$A_{fn} = \begin{cases} \dfrac{\pi D_i^{\;2}}{4} & \text{for tube} \\ W_{ch} T_{ch} & \text{for rectangular channel} \end{cases} \tag{6.5}$$

$$A_{fa} = A_{fn} - n\, A_{fin} \sec\alpha \tag{6.6}$$

$$A_{fc} = \begin{cases} \dfrac{\pi (D_i - 2e - 2\delta)^2}{4} & \text{for tube} \\ W_{ch}\,(T_{ch} - 2e) & \text{for rectangular channel} \end{cases} \tag{6.7}$$

$$\begin{aligned} P_{fin} &= \text{Sides EB} + \text{BC} + \text{CF} - \text{Arc length EF (in Fig. 2)} \\ &= \begin{cases} t + 2\sqrt{e^2 + \{(b-t)/2\}^2} - \beta D_i/2 & \text{for tube} \\ t + 2\sqrt{e^2 + \{(b-t)/2\}^2} - b & \text{for rectangular channel} \end{cases} \end{aligned} \tag{6.8}$$

$$A_{fin} = \begin{cases} \dfrac{e(b+t)}{2} + \dfrac{\beta D_i^2}{8} - \dfrac{b\sqrt{D_i^2 - b^2}}{4} & \text{for tube} \\ \dfrac{e(b+t)}{2} & \text{for rectangular channel} \end{cases} \tag{6.9}$$

$$D_{ha} = \frac{4A_{fa}}{P_a}, \qquad D_{hn} = \frac{4A_{fn}}{P_n} \tag{6.10}$$

$$Re_a = \frac{W\,D_{ha}}{A_{fa}\,\mu}, \quad Re_n = \frac{W\,D_{hn}}{A_{fn}\,\mu} \tag{6.11}$$

$$Pr = \frac{\mu\,C_p}{K} \tag{6.12}$$

$$D_c = D_i - 2(6.e + \delta) \tag{6.13}$$

$$\delta = \frac{D_i - \sqrt{D_i^2 - b^2}}{2} \tag{6.14}$$

$$\beta = 2\sin^{-1}(b/D_i) \tag{6.15}$$

$$A_\delta = \frac{\beta D_i^2}{8} - \frac{b\sqrt{D_i^2 - b^2}}{4} \tag{6.16}$$

The range of applicability of correlations in Eqs. (6.1) and (6.2) is given below [1,2]. The last three restrictions on fin geometry are given in Refs. [3, 4].

Helix angle range:	$0 < \alpha < 30°$
Reynolds number range:	$10{,}000 < Re < 100{,}000$
Prandtl number range:	$0.7 < Pr < 30$
Fin pitch:	$3.3 < p/e < 5.6$
Fin height:	$e/D_i < 0.29$
Fin aspect ratio:	$\dfrac{e}{0.5(b+t)} < 3.5$

The Reynolds number and the other five above problem parameters are checked against their range. If the Reynolds number or any parameter is found to be out of range, then a warning message is printed, identifying the parameter which was found to be out of range. A maximum of 12 messages is printed. The solution is not stopped due to any number of warnings.

Equation (6.1) results in Eq. (6.17) below for the finned tube heat transfer coefficient h_a that is based on the *actual* heat transfer area (P_a). For use in the PLTEMP/ANL code, one needs to express the coefficient h_a given by Eq. (6.17) as a heat transfer coefficient h_{a_n} based on the *nominal* heat transfer area P_n , preserving the heat transfer rate as done by Eq. (6.18).

$$h_a = \frac{Nu\ K}{D_{ha}} \tag{6.17}$$

$$h_{a_n} = \frac{P_a\ h_a}{P_n} \tag{6.18}$$

Equation (6.2) gives the finned tube friction factor f_a that is based on the *actual* hydraulic diameter D_{ha}. For use in PLTEMP/ANL, one needs to express the friction factor f_a as a friction factor f_{a_n} based on the *nominal* hydraulic diameter (D_{hn}). To do this, one must equate the pressure drop due to friction. For a given flow rate W in the channel, the pressure drop due to the finned tube friction factor f_a over a length L of the channel can be written as Eq. (6.19). The first factor on the right hand side of Eq. (6.19) must be preserved because the second factor is the same whether the nominal or the actual hydraulic diameter is used. Equating the first factor on the right hand side of Eq. (6.19) results in Eq. (6.20), which is rewritten as Eq. (6.21) below.

$$\Delta p_a = \left(\frac{f_a}{A_{fa}^{\ 2}\ D_{ha}} \right) \left(\frac{LW^2}{2\rho} \right) \tag{6.19}$$

$$\frac{f_{a_n}}{A_{fn}^{\ 2}\ D_{hn}} = \frac{f_a}{A_{fa}^{\ 2}\ D_{ha}} \tag{6.20}$$

$$f_{a_n} = \frac{A_{fn}^{\ 2}\ D_{hn}\ f_a}{A_{fa}^{\ 2}\ D_{ha}} \tag{6.21}$$

A subroutine CARNAVOS was developed to calculate the results of Eqs. (6.18) and (6.21). The subroutine has been implemented into the PLTEMP/ANL version 3.3. The subroutine CARNAVOS is called by the existing multi-option heat transfer subroutine HCOEF1 of the code.

6.3 Verification of Carnavos Correlation Implemented in PLTEMP/ANL

The purpose here is to verify the heat transfer coefficient, friction factor, and coolant flow rate calculated by PLTEMP/ANL version 3.3 for a sample problem with finned coolant channels. Figure 6.3 shows a sample input file (Test Problem 16) to model the coolant channels of the MIT Reactor. The sample problem has two assemblies of a single type, each having 9 fuel plates and 10 coolant channels. The reactor core axial region (region 2) of each assembly has the fin geometry of the MIT Reactor. The first and third axial regions (the inlet and exit regions) are each made artificially short (0.01 mm), and the minor loss coefficients are set to zero, so that the coolant flow rate in a channel could be hand-calculated. The power produced is set artificially small so that there is a negligible coolant temperature rise in channels and the coolant properties only at the inlet

temperature are required in the hand calculation of friction factor, flow rate and heat transfer coefficient.

The newly developed PLTEMP/ANL version 3.3 code was run for this sample input file, *with the fins* (Run 1), for an input frictional pressure drop of 0.1 MPa. The code was also run *without the fins* (Run 2), by modifying the input cards 200 and 202 of the input file (i.e., setting option IH=1 and fin height to zero). Table 6.1 provides the geometry of the finned channel, the needed coolant properties, and some data from the debug outputs printed by the code (using input KPRINT = 2). The columns 1 and 2 of Table 6.1 show selected results from the run with fins, and the column 3 shows results from the run without fins.

6.3.1 Verification of Friction Factor and Flow Rate in Finned Coolant Channels

In the first run, the code calculated a flow rate of 0.58046 kg/s per coolant channel with fins. This flow rate is established by a frictional pressure drop of 0.1 MPa. In the second run, it calculated a flow rate of 1.11814 kg/s per coolant channel without fins, at the same frictional pressure drop (0.1 MPa). The actual Reynolds number and friction factor, f_a in the finned channel (column 1 of Table 6.1) were hand-calculated as follows. The value of f_a at the flow rate of 0.58046 kg/s per coolant channel is found using the Carnavos correlation, i.e., Eq. (6.2).

$$Re_a = \frac{D_{ha}\ W}{\mu\ A_{fa}} = \frac{0.0021817 \text{ x } 0.58046}{5.9309 \text{ x} 10^{-4} \text{ x } 1.13548 \text{ x} 10^{-4}} = 18805.2$$

$$f_a = \frac{0.184}{(18805.2)^{0.2}} \left(\frac{1.26451}{1.13548}\right)^{0.5} \text{ x } 1.0 = 0.027123$$

The frictional pressure drop in the finned channel can be hand-calculated as follows.

$$\Delta p_a = \left(\frac{f_a\ L}{D_{ha}}\right)\left(\frac{W^2}{2\ \rho\ A_{fa}{}^2}\right)$$

$$= \frac{0.027123 \text{ x } 0.61}{0.0021817} \text{ x } \frac{(0.58046)^2}{2 \text{ x } 991.148 \text{ x } (1.13548 \text{ x} 10^{-4})^2} = 0.099975 \quad \text{MPa}$$

The above values of actual Reynolds number, friction factor, and pressure drop agree with those printed by the code and shown in column 1 of Table 6.1.

The Reynolds number Re_n and friction factor, f_n in the un-finned channel at the same flow rate, 0.58046 kg/s, were hand-calculated using $Re_n = D_{hn}\ W/(\mu\ A_{fn})$ and $f_n = 0.184 / Re_n^{0.2}$.

$$Re_n = \frac{D_{hn}\ W}{\mu\ A_{fn}} = \frac{0.0047459 \text{ x } 0.58046}{5.9309 \text{ x} 10^{-4} \text{ x } 1.26451 \text{ x} 10^{-4}} = 36732.0$$

$$f_n = \frac{0.184}{(36732.0)^{0.2}} = 0.022481$$

These nominal values are shown in columns 2 of Table 6.1, and agree with those printed by the code. The frictional pressure drop, Δp_n in the un-finned channel at this flow rate (0.58046 kg/s) can be hand-calculated as follows.

$$\Delta p_n = \left(\frac{f_n\ L}{D_{hn}}\right)\left(\frac{W^2}{2\ \rho\ A_{fn}{}^2}\right)$$

$$= \frac{0.022481 \text{ x } 0.61}{0.0047459} \text{ x } \frac{(0.58046)^2}{2 \text{ x } 991.148 \text{ x } (1.26451 \text{x} 10^{-4})^2} = 0.0307156 \quad \text{MPa}$$

At the flow rate 0.58046 kg/s, the ratio of pressure drop in the finned channel to that in the un-finned channel is hand-calculated to be 3.25487, which agrees with the ratio printed by the code.

$$\frac{\Delta p_a}{\Delta p_n} = \frac{0.099975}{0.0307156} = 3.25487$$

The flow rate W_3 in the un-finned channel at the input pressure drop of 0.1 MPa (Run 2) should be about $\sqrt{3.25487}$ times 0.58046 kg/s = 1.04722 kg/s. Actually it will be more than this value because the un-finned friction factor will be lower than 0.022481, because of the increase in Reynolds number at the increased flow rate. The code-calculated W_3 is 1.11814 kg/s as shown in column 3 of Table 6.1. This flow rate is verified by hand-calculating the corresponding Reynolds number, friction factor, and pressure drop, as follows.

$$Re_3 = \frac{D_{hn}\ W_3}{\mu\ A_{fn}} = \frac{0.0047459 \text{ x } 1.11814}{5.9341 \text{x} 10^{-4} \text{ x } 1.26451 \text{x} 10^{-4}} = 70719.2$$

$$f_3 = \frac{0.184}{(70719.2)^{0.2}} = 0.019720$$

$$\Delta p_3 = \left(\frac{f_3\ L}{D_{hn}}\right)\left(\frac{W_3{}^2}{2\ \rho\ A_{fn}{}^2}\right)$$

$$= \frac{0.019720 \text{ x } 0.61}{0.0047459} \text{ x } \frac{(1.11814)^2}{2 \text{ x } 991.223 \text{ x } (1.26451 \text{x} 10^{-4})^2} = 0.099968 \quad \text{MPa}$$

The value of Δp_3 agrees with the input pressure drop of 0.1 MPa, and this agreement verifies the code calculated results shown in column 3 of Table 6.1. In summary, the hand-calculated values of friction factor and coolant flow rate in the three cases are found to agree with the code-calculated values shown in Table 6.1. This verifies the implementation of the Carnavos correlation for friction factor.

6.3.2 Verification of Heat Transfer Coefficient

The actual heat transfer coefficient in the finned channel (column 1 of Table 6.1) was hand-calculated as follows, using the Carnavos correlation, i.e., Eq. (6.1).

$$\frac{h_a D_{ha}}{K} = 0.023 \text{ x } (18805.2)^{0.8} \ (3.86247)^{0.4} \left(\frac{1.13548}{1.00645}\right)^{0.1} \left(\frac{0.10658}{0.20818}\right)^{0.5} \text{ x } 1.0 = 75.11963$$

$$h_a = \frac{75.11963 \text{ x } 0.64130}{0.0021817} = 22081.0 \quad \text{W/m}^2 - {}^\circ\text{C} \ \text{(based on actual heat transfer area)}$$

The above actual heat transfer coefficient (22081.0) is based on the heat transfer area with fins. This value agrees with the value (22080.4) printed by the code. Since the code has all along used un-finned coolant channels, the heat transfer coefficients and heat transfer areas used throughout the code are those of the un-finned coolant channel. Therefore, the above heat transfer coefficient must be expressed as an equivalent heat transfer coefficient, h_{a_n} that is based on the heat transfer area of the un-finned coolant channel (nominal heat transfer area), such that the heat transfer rate and the temperature difference between the bulk coolant and cladding surface remain unchanged. The equivalent heat transfer coefficient is found using Eq. (6.18), as follows.

$$h_{a_n} = \frac{h_a P_a}{P_n} = \frac{22081.0 \text{ x } 0.20818}{0.10658} = 43130.3 \quad \text{W/m}^2 - {}^\circ\text{C} \ \text{(based on nominal heat transfer area)}$$

This is the value that is printed in the main temperature edits of PLTEMP/ANL version 3.3. To evaluate the heat transfer enhancement caused by the fins, the actual heat transfer rate is compared below with the heat transfer rate without fins at the same coolant flow rate (0.58046 kg/s). The heat transfer coefficient, h_n in the un-finned channel is given by

$$\frac{h_n D_{hn}}{K} = 0.023 \text{ x } (36732.0)^{0.8} \text{ x } (3.86247)^{0.4} = 177.2187$$

$$h_n = \frac{177.2187 \text{ x } 0.64130}{0.0047459} = 23947.1 \quad \text{W/m}^2 - {}^\circ\text{C} \ \text{(based on nominal heat transfer area)}$$

This value of the nominal heat transfer coefficient (23947.1) agrees with the value printed by the code (shown in column 2). The heat transfer enhancement factor provided by the fins is given by

$$\text{Enhancement factor} = \frac{h_{a_n}}{h_n} = \frac{43130.3}{23947.1} = 1.8010$$

This value of the heat transfer enhancement factor agrees with the value printed by the code.

6.3.3 Comparison of Zero-Height Fin Option with No Fin Option

The output obtained by running the code with fins of zero height (using option IH = -1 on input card 200, and fin height EFIN = 0.0 on input card 202), and that obtained by running the code without fins (using option IH = 1 without providing the input card 202) were compared to verify that the code gave the same results in both cases. It was found that the code does give the same results. A previously-developed PLTEMP/ANL output comparing utility program *differ.x* was used to compare the two cases. The maximum temperature difference for coolant, cladding, and fuel peak was found to be 0.001 °C. Two points of detail are noted here:

(1) In the latter case (without fins), the selected coolant flow friction factor uses input values of FCOEF, FEXPF, and ROUGH (0.184, 0.2, and 0.0) on the card 305. This was done because the finned friction factor correlation (Carnavos correlation) implemented in the code, is based on the McAdams correlation ($f = 0.184/Re^{0.2}$) and reduces to it in the absence of fins.

(2) In the latter case (without fins), IH is selected to be 1, implying the Dittus-Boelter correlation (not one of the other correlations available in the code). The reason for this is that the finned heat transfer correlation (Carnavos correlation) implemented in the code, is based on the Dittus-Boelter correlation and reduces to it in the absence of fins.

Without these two input choices, the code may not give the same results in the two cases discussed above.

The case without fins of this problem (Test Problem 16) was also run using the older version of PLTEMP/ANL (version 3.2), and the results were compared with that obtained by version 3.3. This comparison was performed at two power levels: 0.0024 MW and 0.24 MW. Using the utility program *differ.x*, the maximum temperature difference for coolant, cladding, and fuel peak was found to be zero, in the comparison at each power level. This verifies the implementation of Carnavos correlations in the coolant flow rate and temperature calculations in the code.

6.4 Code Output for Finned Coolant Channels

The following should be accounted for when using the code output. The flow instability edits are *not yet revised* to include the effect of fins.

(1) The heat transfer area (when using the fin option IH = -1) in the code are left unchanged as the *nominal* area without fins (just as it was calculated before implementing the fin option). The code performs the temperature calculation using the enhanced heat transfer coefficients expressed based on the nominal heat transfer area, $2(W_{ch} + T_{ch})$ m^2 per meter, of the coolant channel. The calculated heat fluxes are therefore based on the nominal heat transfer area. The heat transfer coefficients printed in the temperature table of code output (see part of output in Table 6.2) are based on the nominal heat transfer area in the channel without fins.

(2) The heat fluxes printed by the code in the table of heat fluxes are based on the *nominal* heat transfer area, $2(W_{ch} + T_{ch})$ m^2 per meter, in the coolant channel without fins.

(3) The *actual* heat flux (not the *nominal* heat flux) is used in finding the ONB temperature used to calculate the ONB ratio in subroutines FINLED, FINLED6, FINLEDIT, and FINLEDIT6. The actual heat flux q_a equals the nominal heat flux q_n divided by the actual-to-nominal perimeter ratio (P_a / P_n). The ratio P_a/P_n is stored in the COMMON block FINGEOM.

$$q_a = \frac{q_n}{(P_a / P_n)}$$

(4) The *actual* heat flux is used in calculating the DNB ratio. All six critical heat flux correlations in the code (i.e., Mirshak-Durant-Towell, Bernath, Labuntsov, Mishima, and Weatherhead correlations, and the Groeneveld table) in the subroutines DNB and DNB2 were revised to use the actual (with fins) flow area, perimeter, hydraulic diameter, and coolant velocity. A hand calculation (shown below) of the Groeneveld critical heat flux (code input option ICHF = 5) was done to verify the code calculated value with fins. The code has the 1995 version of the Groeneveld critical heat flux (CHF) table described in [5]. The needed parts of the CHF table at pressures of 1000 kPa and 3000 kPa (that bracket the coolant outlet pressure of 1300 kPa in Test Problem 16) are given below. All interpolations are also shown.

	CHF, kW/m^2 At 1000 kPa		CHF, kW/m^2 At 3000 kPa		CHF, kW/m^2 At Outlet Pressure of 1300 kPa		
Quality →	-0.4	-0.3	-0.4	-0.3	-0.4	-0.3	-0.3173
Mass Flux, kg/m^2-s ↓							
5000.0	14574	12447	14778	13200	14604.6	12560.0	12913.7
5500.0	15273	13033	15454	13765	15300.2	13142.8	13516.0
5112.1							**13048.7**

As mentioned above, the coolant temperature rise is small (only 0.06 °C) (see the code output shown in Table 6.2), the coolant outlet temperature is 45.06 °C, and outlet pressure is 1300 kPa (=1.4 MPa inlet pressure – 0.1 MPa pressure drop). Using these values, the exit quality is found as follows:

$h_{f,sat}$ = Saturated liquid enthalpy at 1300 kPa = 814.70 kJ/kg
$h_{g,sat}$ = Saturated vapor enthalpy at 1300 kPa = 2785.43 kJ/kg
h_f = Liquid enthalpy at 45.06 °C (from ASME Steam Table) = 189.48 kJ/kg

Quality of the sub-cooled liquid, $x = \dfrac{189.48 - 814.70}{2785.42 - 814.70} = -0.3173$

Using the coolant flow rate and actual flow area in a single channel (shown in Table 6.1), the coolant mass flux *with fins* is found to be ($0.58046/1.13548 \times 10^{-4}$) = 5112.1 kg/m^2-s. The critical heat flux for the reference 8-mm diameter tube, and that for the finned channel are shown below.

CHF(1300 kPa, 5112.1 kg/m^2-s, -0.3171) for diameter 8 mm = 13048.7 kW/m^2

CHF(1300 kPa, 5112.1 kg/m^2-s, -0.3171) for hydraulic diameter 2.1817 mm

$$= 13048.7\left(\frac{8}{2.1817}\right)^{0.3333} = 20121.8 \text{ kW/m}^2$$

The above hand-calculated critical heat flux of 20121.8 kW/m^2 is in agreement with the code-calculated value of 20241 kW/m^2 (see part of code output in Table 6.2).

NOMENCLATURE

P_a = Actual perimeter, i.e., actual heat transfer area per unit length of the tube with fins, m^2 per meter

P_n = Nominal perimeter, i.e., nominal heat transfer area per unit length of the tube, based on tube ID as if the fins were not present, m^2 per meter

P_{fin} = *Additional* heated perimeter provided by a single fin. It is the additional is over the tube perimeter covered by the fin, m

A_{fa} = Actual flow area in the tube with fins, m^2

A_{fc} = Core flow area, i.e., the flow area inside the circle touching the fin tips, (see Fig. 6.2), m^2

A_{fn} = Nominal flow area in the tube, based on tube ID as if the fins were not present, m^2

b = Fin thickness at the bottom, m

A_{fin} = Cross sectional area of a single fin. m^2

C_p = Specific heat of the coolant, J/kg-°C

D_c = Core diameter of a channel, i.e., diameter inside the fin tips, m

D_i = Inner diameter of the tube, m

D_{ha} = Actual hydraulic diameter of the finned channel, m

D_{hn} = Nominal hydraulic diameter of the channel without fins, m

e = Height of fins, m

f_a = Finned tube Darcy-Weisbach friction factor based on the *actual* hydraulic diameter D_{ha}

f_{a_n} = Finned tube Darcy-Weisbach friction factor expressed as a friction factor based on the *nominal* flow area A_{fn} and hydraulic diameter D_{hn}

h_a = Finned tube heat transfer coefficient based on the *actual* heat transfer area, W/m^2-°C

h_{a_n} = Finned tube heat transfer coefficient expressed as a coefficient based on the *nominal* heat transfer area, W/m^2-°C

K = Thermal conductivity of the coolant, W/m-°C

L = Channel length, m

n = Number of fins in a channel

Nu = $\frac{h_a D_{ha}}{K}$ = Nusselt number based on P_a and A_{fa} (i.e., actual perimeter and actual flow area)

p = Circumferential pitch of fins = $\pi D_i/n$ for tube = $2W_{ch}/n$ for rectangular channel

Pr = Prandtl number of the coolant

Δp_a = Actual pressure drop due to friction in the finned channel, N/m^2

Re_a = $\frac{W D_{ha}}{\mu A_{fa}}$ = Reynolds number based on P_a and A_{fa} (i.e., actual perimeter and actual flow area)

Re_n = $\frac{W D_{hn}}{\mu A_{fn}}$ = Reynolds number based on P_n and A_{fn} (i.e., nominal perimeter and nominal flow area)

t = Fin thickness at the tip, m

T_{ch} = Channel thickness between the parallel plates, m

W_{ch} = Channel width of the channel between the parallel plates, m

W = Coolant flow rate in the channel, kg/s

α = Angle between the spiral fin's longitudinal axis and the tube axis (called helix angle)

ρ = Density of the coolant, kg/m^3

μ = Dynamic viscosity of the coolant, N-s/m^2

6.5 REFERENCES

1. T. C. Carnavos, "Heat Transfer Performance of Internally Finned Tubes in Turbulent Flow," AIChE Paper presented at the 18th National Heat Transfer Conference, San Diego, CA (Aug. 1979).
2. T. C. Carnavos, "Heat Transfer Performance of Internally Finned Tubes in Turbulent Flow," Heat Transfer Eng., Vol. 1, No. 4, pp. 32-37 (Apr-June 1980).
3. R. L. Webb and M. J. Scott, "A Parametric Analysis of the Performance of Internally Finned Tubes for Heat Exchanger Application," J. of Heat Transfer, Trans. of the ASME, Vol. 102, pp. 38-43 (Feb. 1980).
4. N. H. Kim and R. L. Web, "Analytic Prediction of the Friction and Heat Transfer for Turbulent Flow in Axial Internal Fin Tubes," J. of Heat Transfer, Trans. of the ASME, Vol. 115, pp. 553-559 (Aug. 1993).
5. D. C. Groeneveld, et. al., "The 1995 Look-up Table for Critical Heat Flux in Tubes," Nuclear Eng. Design, Vol. 163, pp. 1-28 (1996).

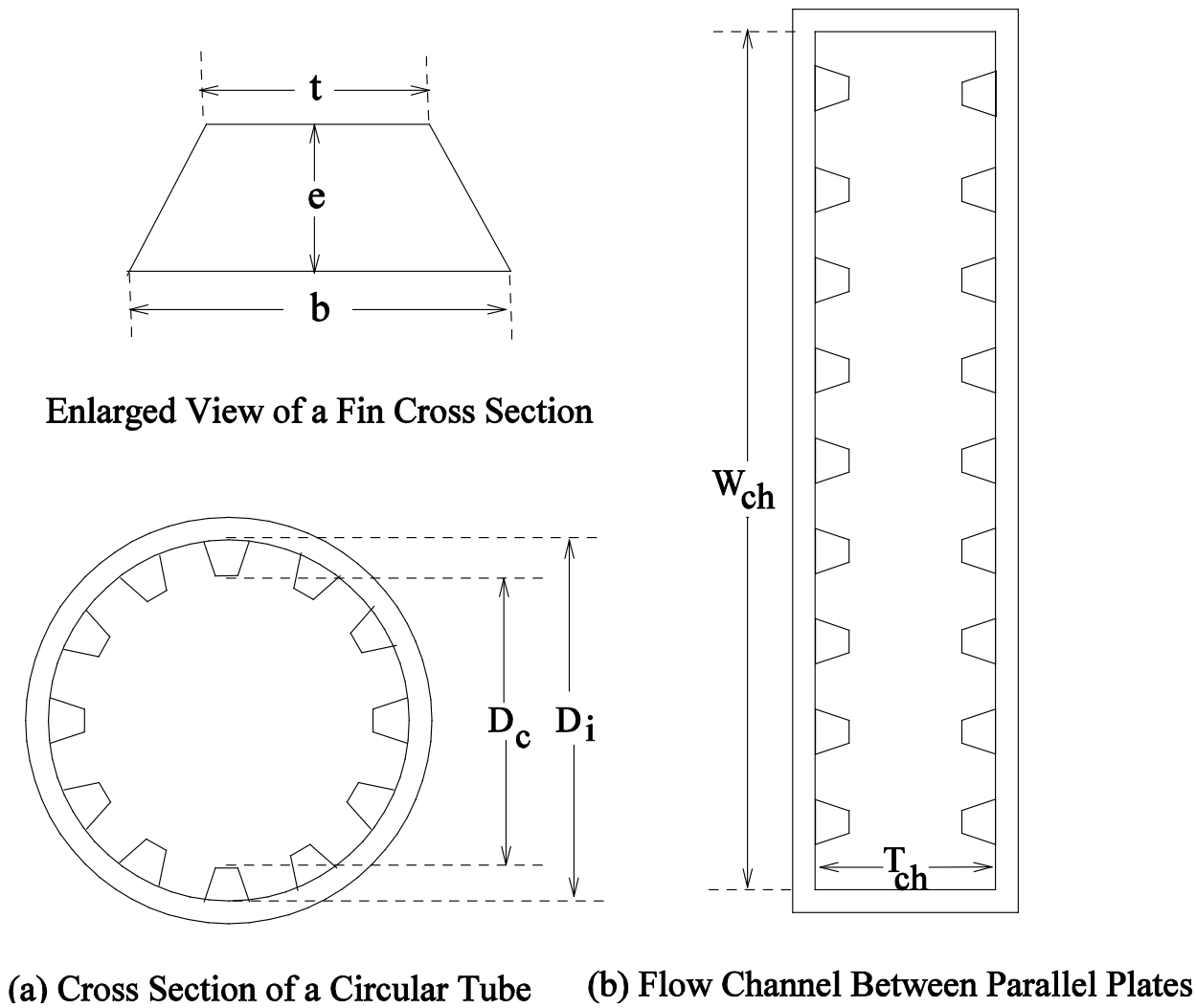

Figure 6.1 Reactor Coolant Channels with Longitudinal Inner Fins: (a) Circular Tube, and (b) Channel between Parallel Plates

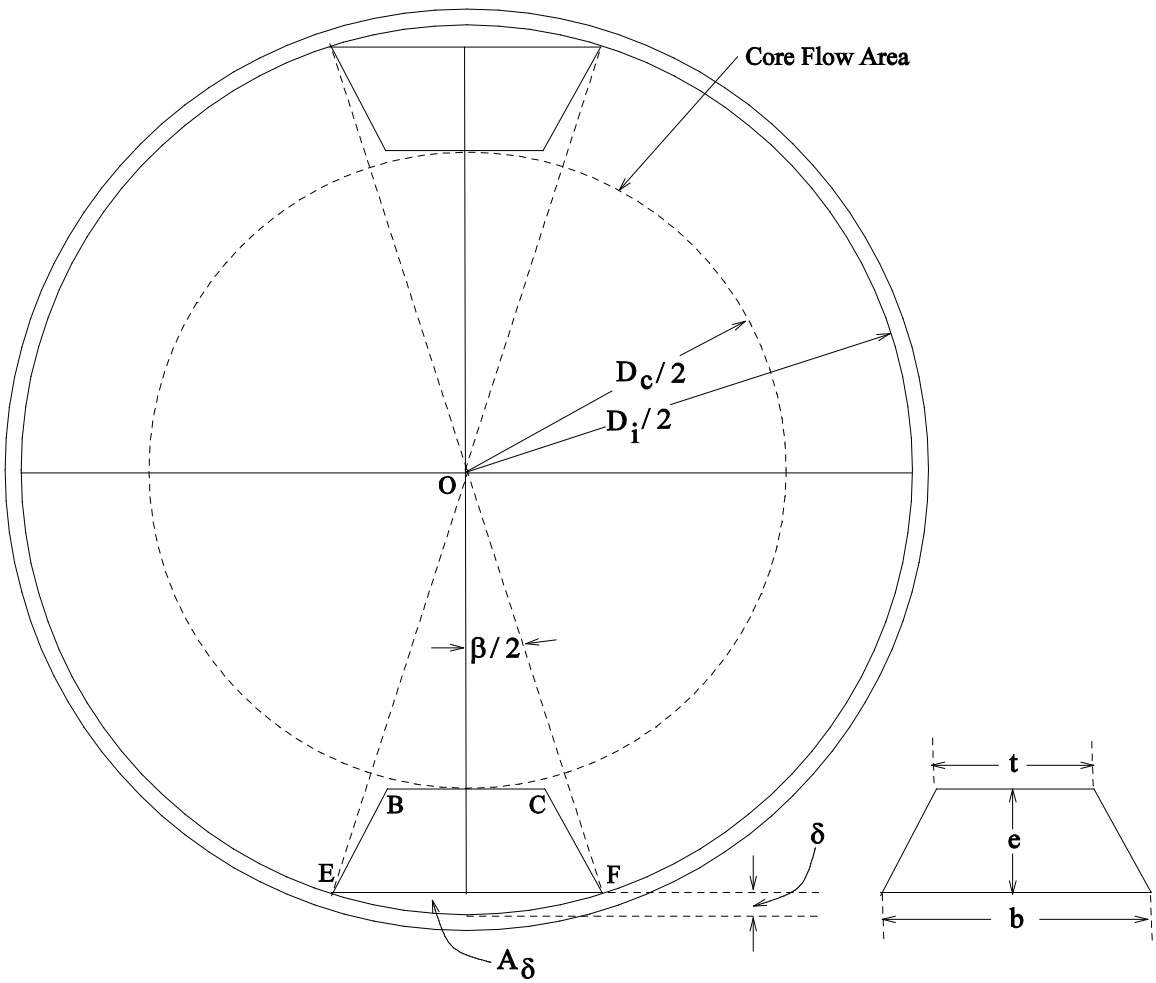

Figure 6.2 Fin Geometry Used in Calculating Coolant Flow Area in a Circular Tube Having Longitudinal Internal Fins

Figure 6.3 Input Data for Test Problem 16 Having MITR-Type Finned Coolant Channels

```
 Test Problem 16: MITR with fins
! 2 assemblies of one type, each producing 1.2 kWt
! Each assembly has 9 fuel plates and 10 coolant channels
! H2O coolant, Flow is calculated from input pressure drop
! All hot channel factors = 1.0
! No bypass flow, NCTYP=0
! 10 axial heat transfer nodes in the heated length of fuel plates
!  1   2   3   4   5   6   7   8   9  10  11  12  13  14  15  16  17  18        Indices
  -1   0   5   1   0   1   1   1   0   0   0   0   0       1   2      00        Card(1)0200
 0.000254   0.000254    0.000254    0.0         200                            Card(1)0202
   2   3 5.00       1.00        1.00        1.00           3                   Card(1)0300
! Using pressure driven mode
   1  20 1.00                                                                  Card(1)0301
   1   1   1                                                                   Card(1)0302
1.20        1.20                                                               Card(2)0303
12.645E-04  4.74585E-03 0.00001     0.00        0.0508      2.4892E-03         Card(3)0304
12.645E-04  4.74585E-03 0.61        0.00        0.0508      2.4892E-03         Card(3)0304
12.645E-04  4.74585E-03 0.00001     0.00        0.0508      2.4892E-03         Card(3)0304
! Use the code's biult-in correlation for friction factor
0.184       0.20        0.00                                                   Card(1)0305
  10   3 0.00       0.61        0.25E-03    0.00        0.55E-03    100.00     Card(1)0306
1.2645E-04  4.74585E-03 0.106578    0.0508      0.0508      2.4892E-03         Card(5)0307
1.2645E-04  4.74585E-03 0.106578    0.1016      0.0508      2.4892E-03         Card(5)0307
1.2645E-04  4.74585E-03 0.106578    0.1016      0.0508      2.4892E-03         Card(5)0307
1.2645E-04  4.74585E-03 0.106578    0.1016      0.0508      2.4892E-03         Card(5)0307
1.2645E-04  4.74585E-03 0.106578    0.1016      0.0508      2.4892E-03         Card(5)0307
1.2645E-04  4.74585E-03 0.106578    0.1016      0.0508      2.4892E-03         Card(5)0307
1.2645E-04  4.74585E-03 0.106578    0.1016      0.0508      2.4892E-03         Card(5)0307
1.2645E-04  4.74585E-03 0.106578    0.1016      0.0508      2.4892E-03         Card(5)0307
1.2645E-04  4.74585E-03 0.106578    0.1016      0.0508      2.4892E-03         Card(5)0307
1.2645E-04  4.74585E-03 0.106578    0.0508      0.0508      2.4892E-03         Card(5)0307
0.0508      0.0508      0.0508      0.0508      0.0508      0.0508             Card(1)0308
0.0508      0.0508      0.0508                                                 Card(1)0308
! Card 0308A not required in slab geometry
! Radial power peaking factor data by fuel plate for each assembly. Input flow data by
! channel for each assembly on Cards 0310 not required because WFGES(1) is non-zero
0.800       0.850       0.900       0.950       1.000       1.050              Card(2)0309
1.100       1.150       1.200                                                  Card(2)0309
0.801       0.851       0.901       0.951       1.001       1.051              Card(2)0309
1.101       1.151       1.201                                                  Card(2)0309
! DP0       DDP         DPMAX       POWER       TIN         PIN
0.10        0.04        0.10        2.4E-03     45.0        1.40               Card(1)0500
0.00        0.00                                                               Card(2)0500
  50 0.0001     25.0        0.50        2.0E-03                                Card(1)0600
  11                                                                           Card(1)0700
0.00        0.80                                                               Card(11)0701
0.10        0.88                                                               Card(11)0701
0.20        0.96                                                               Card(11)0701
0.30        1.04                                                               Card(11)0701
0.40        1.12                                                               Card(11)0701
0.50        1.20                                                               Card(11)0701
0.60        1.12                                                               Card(11)0701
0.70        1.04                                                               Card(11)0701
0.80        0.96                                                               Card(11)0701
0.90        0.88                                                               Card(11)0701
1.00        0.80                                                               Card(11)0701
   0                                                                           Card(11)0702
```

Table 6.1 Comparison of PLTEMP Calculations With and Without Fins in Internal Coolant Channels of Test Problem 16

Parameter	With Fins at 0.1 MPa Pressure Drop (Run 1)	Without Fins at Finned Channel Flow Rate (Run 1)	Without Fins at 0.1 MPa Pressure Drop (Run 2)
Column Number	1	2	3
PLTEMP/ANL Input			
Nominal thickness of channel, mm	2.4892		
Nominal width of channel, mm	50.8		
Channel Length, m	0.61		
Number of fins in a channel	200		
Fin height, mm	0.254		
Fin thickness (uniform), mm	0.254		
PLTEMP/ANL Output			
Core flow area (within fin tips), A_{fc} , m^2	1.00645×10^{-4}		
Flow area (A_{fa} and A_{fn}), m^2	1.13548×10^{-4}	1.26451×10^{-4}	
Perimeter (P_a and P_n) , m	0.20818	0.10658	
Hydraulic diameter (D_{ha} and D_{hn}) , m	0.0021817	0.0047459	
Coolant density, kg/m^3	991.148		991.223
Coolant specific heat, J/kg-°C	4176.421		
Coolant dynamic viscosity, N-s/m^2	5.9309×10^{-4}		5.9341×10^{-4}
Coolant thermal conductivity, W/m-°C	0.64130		
Prandtl number	3.86247		
Flow rate in a channel, kg/s	0.58046		1.11814
Reynolds number	18805.2	36732.0	70719.2
Darcy-Weisbach Friction Factor	0.027123	0.022481	0.019720
Pressure drop increase factor Δp_a / Δp_n	3.2548		
Actual heat transfer coefficient, W/m^2-°C	22080.4	23947.2	
Enhancement factor $h_a P_a$ / ($h_n P_n$)	1.8010		
Hand Calculation			
Pressure Drop (Δp), MPa	0.099975	0.030716	0.099968

Table 6.2 Portion of PLTEMP/ANL V3.3 Output for Test Problem 16 Having MITR-Type Finned Coolant Channels

FUEL PLATE 2 (ExactSoln)

NODE	COOLANTl (C)	CladSl (C)	FUEL PEAK (C)	CladSr (C)	COOLANTr (C)	HCOFl W/C-m^2 [F Note 2]	HCOFr W/C-m^2 [F Note 2]	ONBRl [F Note 1]	ONBRr	ETA'l K-cm^3/J	ETA'r K-cm^3/J	ONB Temp left(C)	ONB Temp right(C)
	45.000				45.000								
1	45.003	45.039	45.043	45.039	45.003	4.3130E+04	4.3130E+04	4.E+03	4.E+03	5.037E+05	5.034E+05	194.966	194.966
2	45.010	45.049	45.054	45.049	45.010	4.3132E+04	4.3132E+04	3.E+03	3.E+03	4.569E+05	4.604E+05	194.616	194.616
3	45.016	45.059	45.065	45.060	45.018	4.3134E+04	4.3135E+04	3.E+03	3.E+03	4.156E+05	4.264E+05	194.264	194.263
4	45.022	45.069	45.075	45.069	45.025	4.3137E+04	4.3138E+04	2.E+03	2.E+03	3.776E+05	4.007E+05	193.911	193.907
5	45.027	45.079	45.085	45.080	45.033	4.3138E+04	4.3140E+04	2.E+03	2.E+03	3.440E+05	3.799E+05	193.555	193.549
6	45.033	45.086	45.092	45.087	45.041	4.3140E+04	4.3143E+04	2.E+03	2.E+03	3.378E+05	3.857E+05	193.193	193.184
7	45.040	45.089	45.095	45.090	45.048	4.3143E+04	4.3146E+04	2.E+03	2.E+03	3.583E+05	4.181E+05	192.823	192.814
8	45.047	45.093	45.098	45.094	45.055	4.3145E+04	4.3149E+04	2.E+03	2.E+03	3.838E+05	4.534E+05	192.450	192.441
9	45.053	45.096	45.102	45.098	45.063	4.3148E+04	4.3151E+04	2.E+03	2.E+03	4.092E+05	5.016E+05	192.076	192.064
10	45.059	45.099	45.104	45.100	45.069	4.3150E+04	4.3153E+04	1.E+03	1.E+03	4.392E+05	5.602E+05	191.699	191.686
	45.061				45.071								

[1] The ONB ratio is here defined as (Tonb - Tinlet)/(Tsurf - Tinlet). If the heat flux is negative (the coolant is hotter than the adjacent cladding surface), then the ONB ratio is arbitrarily set to 99.99 .

[2] The finned heat transfer coeff is here expressed as an average over the nominal heat transfer area in the unfinned coolant channel. It equals (actual finned surface heat transfer coeff)X(1.9533 1.9533, finned-to-unfinned heat transfer area ratio).

Departure from Nucleate Boiling Ratio (DNBR) (ExactSoln)
Using Groeneveld Tables for CHF(Pressure, MassFlux, Quality)

NOTE: The coolant channel has fins. The CHF and peak heat flux are here based on the actual (not nominal) flow area, perimeter, and hydraulic diameter.

```
FUEL PLATE  1  LEFT SIDE: DNBR = 9.2017E+03, CHF = 2.0309E+01 MW/m**2, PEAK HEAT FLUX= 1.4947E-03 MW/m**2 of finned surface
FUEL PLATE  1 RIGHT SIDE: DNBR = 1.1195E+04, CHF = 2.0242E+01 MW/m**2, PEAK HEAT FLUX= 9.2567E-04 MW/m**2 of finned surface
FUEL PLATE  2  LEFT SIDE: DNBR = 8.9538E+03, CHF = 2.0242E+01 MW/m**2, PEAK HEAT FLUX= 1.1574E-03 MW/m**2 of finned surface
FUEL PLATE  2 RIGHT SIDE: DNBR = 1.0046E+04, CHF = 2.0241E+01 MW/m**2, PEAK HEAT FLUX= 1.0316E-03 MW/m**2 of finned surface
FUEL PLATE  3  LEFT SIDE: DNBR = 9.0431E+03, CHF = 2.0241E+01 MW/m**2, PEAK HEAT FLUX= 1.1459E-03 MW/m**2 of finned surface
FUEL PLATE  3 RIGHT SIDE: DNBR = 8.9510E+03, CHF = 2.0241E+01 MW/m**2, PEAK HEAT FLUX= 1.1577E-03 MW/m**2 of finned surface
FUEL PLATE  4  LEFT SIDE: DNBR = 8.4010E+03, CHF = 2.0241E+01 MW/m**2, PEAK HEAT FLUX= 1.2335E-03 MW/m**2 of finned surface
FUEL PLATE  4 RIGHT SIDE: DNBR = 8.6062E+03, CHF = 2.0241E+01 MW/m**2, PEAK HEAT FLUX= 1.2041E-03 MW/m**2 of finned surface
FUEL PLATE  5  LEFT SIDE: DNBR = 8.0426E+03, CHF = 2.0241E+01 MW/m**2, PEAK HEAT FLUX= 1.2885E-03 MW/m**2 of finned surface
FUEL PLATE  5 RIGHT SIDE: DNBR = 8.1786E+03, CHF = 2.0241E+01 MW/m**2, PEAK HEAT FLUX= 1.2670E-03 MW/m**2 of finned surface
FUEL PLATE  6  LEFT SIDE: DNBR = 7.5341E+03, CHF = 2.0241E+01 MW/m**2, PEAK HEAT FLUX= 1.3754E-03 MW/m**2 of finned surface
FUEL PLATE  6 RIGHT SIDE: DNBR = 7.8488E+03, CHF = 2.0241E+01 MW/m**2, PEAK HEAT FLUX= 1.3202E-03 MW/m**2 of finned surface
FUEL PLATE  7  LEFT SIDE: DNBR = 7.4072E+03, CHF = 2.0241E+01 MW/m**2, PEAK HEAT FLUX= 1.3990E-03 MW/m**2 of finned surface
FUEL PLATE  7 RIGHT SIDE: DNBR = 7.3034E+03, CHF = 2.0241E+01 MW/m**2, PEAK HEAT FLUX= 1.4188E-03 MW/m**2 of finned surface
FUEL PLATE  8  LEFT SIDE: DNBR = 6.9616E+03, CHF = 2.0241E+01 MW/m**2, PEAK HEAT FLUX= 1.4885E-03 MW/m**2 of finned surface
FUEL PLATE  8 RIGHT SIDE: DNBR = 7.1311E+03, CHF = 2.0241E+01 MW/m**2, PEAK HEAT FLUX= 1.4531E-03 MW/m**2 of finned surface
FUEL PLATE  9  LEFT SIDE: DNBR = 7.4507E+03, CHF = 2.0241E+01 MW/m**2, PEAK HEAT FLUX= 1.3908E-03 MW/m**2 of finned surface
FUEL PLATE  9 RIGHT SIDE: DNBR = 6.1030E+03, CHF = 2.0308E+01 MW/m**2, PEAK HEAT FLUX= 2.2535E-03 MW/m**2 of finned surface
```

7 Verification and Validation of Babelli-Ishii Flow Instability Criterion with 75 Tests Performed by Whittle and Forgan

The verification work reported here was done in February 2008. The PLTEMP/ANL code was improved to model heat transfer coefficient and friction factor in finned coolant channels. The routines used in the code to check for excursive flow instability criteria also needed to be modified to account for the fin geometry if the fuel plates had fins (i.e., the input option IH = -1). In this chapter, the Babelli-Ishii flow instability criterion [1] based on the Subcooling number and the Zuber number (available in the present code) is tested and verified for the purpose of modifying the criterion for use in the case of finned channels. A program has been developed to apply the Babelli-Ishii flow instability criterion of Eq. (7.1) and the simple criterion of Eq. (7.5) to 75 tests (using uniform heat flux) reported by Whittle and Forgan. The comparison of the measured and calculated (using either criterion) coolant inlet velocities at the onset of flow instability in these tests shows that both criteria are conservative. Based on this work, the following three improvements were made to the PLTEMP/ANL code.

(i) The older versions of the code (the version 3.3 and older) printed the results of the simplified Babelli-Ishii flow instability criterion of Eq. (7.5). Now, the version 3.4 of the code also prints the results of the main Babelli-Ishii flow instability criterion of Eq. (7.1).

(ii) An error in the implementation of the simplified Babelli-Ishii flow instability criterion was corrected. The error was related to the adjustment (to account for axially non-uniform heat flux) of the dimensionless non-boiling length. To adjust the uniform-heat-flux-based non-boiling length for heat flux non-uniformity, it may be divided by the peak/average heat flux ratio in the channel, but it was incorrectly divided by the peak heat flux. This has been corrected.

(iii) The coding in PLTEMP/ANL version 3.4 of the Babelli-Ishii criteria, both the main criterion and the simplified criterion, was improved to account for the fin geometry if the fuel plates have fins (i.e., if the input option IH = -1). Along with this, the coding of the other two flow instability criteria available in PLTEMP/ANL (i.e., the Whittle and Forgan criterion, and the ORNL criterion) was also improved to account for the fin geometry if the fuel plates have fins. The improvement was done simply by using the actual (i.e., with fins) geometry (flow area, heated and wetted perimeters, and hydraulic diameter) of the coolant channel instead of the nominal geometry.

7.1 Babelli-Ishii Criterion for Flow Instability

This section summarizes the Babelli-Ishii criterion [1] for excursive flow instability after boiling inception. Figure 7.1 shows a coolant channel with downward flow. The results are applicable to upward flow also. Babelli and Ishii obtained Eq. (7.1) given below as a criterion for excursive flow instability due to boiling inception in a coolant channel heated by a *uniform* wall heat flux, based on their theoretical and experimental work and the experimental data of Dougherty [2]. This equation is Eq. (7.5) of Babelli and Ishii [1], after substituting the value of $\rho_{in} V_{in} \Delta h_{nvg} / q''_w$ from Eq. (7.6) of Babelli and Ishii [1] which is basically the Saha-Zuber correlation [3] for net vapor

generation. The channel flow is *stable* if the ratio N_{sub}/N_{zu} on the left hand side of Eq. (7.1) is greater than the quantity on the right hand side, and *unstable* if the ratio N_{sub}/N_{zu} is smaller.

$$\frac{N_{sub}}{N_{zu}} = \left(\frac{L_{nvg}}{L}\right)_{critical} + \frac{A_F}{\zeta_H L}\left\{\begin{matrix} 0.0022\,Pe & \text{if} & Pe < 70000 \\ 154 & \text{if} & Pe > 70000 \end{matrix}\right\} \tag{7.1}$$

where

N_{sub} = Subcooling number = $\dfrac{\Delta h_{in}}{h_{fg}} \dfrac{(\rho_{f,nvg} - \rho_{g,nvg})}{\rho_{g,nvg}}$ (7.2)

N_{zu} = Zuber number = $\dfrac{q''_w \zeta_H L}{\rho_{in} V_{in} A_F h_{fg}} \dfrac{(\rho_{f,nvg} - \rho_{g,nvg})}{\rho_{g,nvg}}$ (7.3)

N_{sub}/N_{zu} = Ratio of Subcooling number to Zuber number = $\dfrac{\rho_{in} V_{in} A_F \Delta h_{in}}{q''_w \zeta_H L}$ (7.4)

Δh_{in} = Subcooling at the start of heated length, J/kg = $h_f(P_{in}) - h_{in} \approx h_f(P_{nvg}) - h_{in}$

Δh_{nvg} = Subcooling at the NVG position, J/kg = $h_f(P_{in}) - h_{nvg} \approx h_f(P_{nvg}) - h_{nvg}$

L = Channel heated length, m

L_{nvg} = Non-boiling length, i.e., the distance from the start of heated length of channel to the position of net vapor generation, m. It is determined by Δh_{nvg}.

L_{nvg}/L = Dimensionless non-boiling length

$(L_{nvg}/L)_{critical}$ = Critical value of the dimensionless non-boiling length. Based on experimental data for freon-113 and water, it is plotted in Fig. 7.4 of Ref. [1] as function of the Subcooling number, and the same data is tabulated here in Table 7.1.

A_F = Flow area of channel, m^2

ζ_H = Heated perimeter of channel, m

ρ_{in} = Coolant density at inlet, kg/m^3

V_{in} = Coolant velocity at inlet, m/s

q''_w = Wall heat flux, W/m^2

Pe = Peclet number = $\rho_{in} C_p V_{in} D_h / K$

The Peclet number dependent quantity inside the curly brackets on the right hand side of Eq. (7.1) can also be found in Ref. [4]. In the case of *upward flow*, the quantity is calculated as shown in Eq. (7.1) given above. However, in the case of *downward flow*, Babelli and Ishii suggest (based on the experimental data of Johnston [5]) that the quantity is always 154. Saha and Zuber [3] have discussed two regions, i.e., the region Pe < 70,000 and the region Pe > 70,000, as follows:

In the region Pe < 70,000 (i.e., at low mass flow rates), bubbles form attached to the wall downstream of the position at which the condition for the onset of nucleate boiling is satisfied, the local subcooling is still high, the bubbles that detach and move to the liquid core get immediately condensed, and the detached bubbles are forced to stay near the wall. The bubbles flow downstream while remaining close to the wall, until the local subcooling is low enough to initiate a rapid increase in void fraction. This is the position of net vapor generation. The region Pe < 70,000 is called the thermally controlled region.

In the region Pe > 70,000 (i.e., at high mass flow rates), the Stanton number $q''_w/\rho_{in}V_{in}\Delta h_{nvg}$ reaches the value of 0.0065, the bubbles attached to the wall grow in size acting like wall surface roughness, the bubbles detach due to hydrodynamic forces at the point where the surface roughness reaches a characteristic value of 0.02, the detached bubbles can move to the liquid core without being rapidly condensed, and this results in a rapid increase in vapor void fraction at the point of bubble detachment. The region Pe > 70,000 is called the hydrodynamically controlled region.

To calculate the Subcooling number using Eq. (7.2), the system reference pressure could be assumed equal to P_{in} or P_{nvg} , i.e., the coolant pressure at the start of the heated section or the pressure at the NVG position. The latter value is preferred as discussed in Appendix D.

A simpler criterion for flow instability due to boiling inception may also be inferred from Fig. 7.5 of Ref. [1] which is a plot on the N_{sub}-N_{zu} plane of several flow instability test data for Freon-113 and water. The plot suggests the following simple criterion for flow instability.

$$\frac{N_{sub}}{N_{zu}} = \begin{cases} > 1.36 & \text{clearly stable} \\ < 1.36 \text{ to } 1.0 & \text{may be stable or unstable} \\ < 1.0 & \text{clearly unstable} \end{cases} \tag{7.5}$$

To calculate the quantities in Eq. (7.1) for evaluating flow instability, one needs the channel exit temperature and pressure. The *first estimates* of the exit enthalpy h_{out}, and total pressure drop ΔP are calculated using Eqs. (7.6) and (7.7) where the thermally-induced change in coolant density is calculated using Eq. (7.8). The exit temperature T_{out} is estimated for use in Eq. (7.7), from h_{out} by assuming the exit pressure $P_{out} = P_{in}$. These estimates are improved by iteration.

$$h_{out} = h_{in} + \frac{q''_w \zeta_H L}{\rho_{in} V_{in} A_F} \tag{7.6}$$

$$\Delta P = \left\{ K_{orifice} + \frac{f L}{D_h} \right\} \frac{W^2}{2\rho_{ave} A_F^{\,2}} \pm \left(\rho_{in} - \frac{\Delta\rho}{2} \right) g L + \rho_{in} V_{in}^{\,2} (\rho_{in}/\rho_{out} - 1) ,$$

$$\text{use + for upflow, and – for downflow} \tag{7.7}$$

$$\Delta\rho = \rho_{in} - \rho_{out} = \frac{\beta_{ave} Q}{C_{p,in} V_{in} A_F} \tag{7.8}$$

In Eq. (7.7), the terms in the curly brackets are the orifice loss and frictional pressure drop, the terms (having ± sign) in the parentheses are the gravitational pressure drop, and the last term is the pressure drop due to velocity increase at exit caused by the coolant density decrease. In the absence of boiling at higher flow rates, the last term is negligible. ΔP *decreases* with decreasing inlet velocity V_{in} because the frictional pressure drop (the terms in the curly brackets of Eq. (7.7)) are then dominant, and these terms decrease with V_{in}. The term $\Delta\rho gL/2$ *increases* in magnitude with decreasing inlet velocity, and it is positive in downflow. Therefore, in the absence of boiling in downflow, there is a *minimum* in the ΔP versus V_{in} plot, i.e., $\partial(\Delta P)/\partial V_{in} = 0$ at a certain inlet velocity. At this minimum, the flow in the channel is unstable. In the absence of boiling in upflow, there is no such *minimum* in the ΔP versus V_{in} plot.

In the case of boiling and voiding, the last term may become as large as ~1000 times the inlet velocity head, and the frictional drop from the ONB position to the channel exit also becomes much greater than its liquid-phase value, thus increasing ΔP at low inlet velocities. This results in a *minimum* in the ΔP versus V_{in} plot, in both downflow and upflow.

7.2 Liquid-Phase Pressure Drop in a Channel Heated by a Given Power

Using the light water properties implemented in the PLTEMP/ANL code, the liquid-phase total pressure drop ΔP was calculated in a coolant channel removing a given power of 7 kW at an assumed value of inlet coolant velocity V_{in} (varied from 0.08 to 2.0 m/s). Both downflow and upflow cases were computed. The purpose here is to check if there exists a minimum in the ΔP versus V_{in} plot in the liquid-phase also, in addition to the minimum in the two-phase case discussed above. The channel data used in the computation are typical of a research reactor, and are given below.

Channel heated length	= 0.6 m
Gap between the surrounding fuel plates	= 5 mm
Hydraulic diameter based on heated perimeter	= 10 mm
Heated width of plate	= 50 mm
Coolant inlet temperature	= 35 °C
Coolant inlet pressure	= 1.5 bar
Power in the channel (uniform over length)	= 7 kW

The calculated total pressure drop ΔP and its components for the channel with downflow are shown in Table 7.2 and plotted in Fig. 7.2. It is noted that there is a minimum ΔP in this case at 0.2 m/s. This indicates a flow instability in liquid-phase in the case of a channel with downflow.

The calculated total pressure drop ΔP and its components for the channel with upflow are shown in Table 7.3 and plotted in Fig. 7.3. It is noted that there is no minimum ΔP in this case. This indicates an absence of flow instability in liquid-phase *before the onset of nucleation*, in the case of upflow.

7.3 Application of Babelli-Ishii Criterion to the Channel Heated by a Given Power

The Babelli-Ishii flow instability criterion of Eq. (7.1) or Eq. (7.5) was applied to the above coolant channel. The second part of Table 7.2 shows the results of applying the criterion of Eq. (7.1). This predicts flow instability at inlet velocities below 0.2 m/s. The flow instability results shown in the column titled 'Stable?' of Table 7.2 are based on this criterion. However, instead of Eq. (7.1), one may simply compare the ratio N_{sub}/N_{zu} with 1.36 as shown in Eq. (7.5), to check flow instability. Eq. (7.5) also predicts the same, i.e., flow instability at inlet velocities below 0.2 m/s.

The second part of Table 7.3 shows the results of applying the Babelli-Ishii criterion of Eq. (7.1). This predicts flow instability at inlet velocities below 0.1 m/s. The flow instability results shown in the column titled 'Stable?' of Table 7.3 are based on this criterion. However, instead of Eq. (7.1), one may simply compare the ratio N_{sub}/N_{zu} with 1.36 as shown in Eq. (7.5), to check flow instability. Eq. (7.5) also predicts the same, i.e., flow instability at inlet velocities below 0.1 m/s.

7.4 Application of Babelli-Ishii Flow Instability Criterion to Whittle and Forgan Tests

The Babelli-Ishii criterion for the onset of flow instability (OFI) was applied to all 75 tests performed by Whittle and Forgan at a uniform heat flux [6]. The geometry data used in the present calculation of these 75 tests are listed in Table 7.4. The last column of Table 7.4 is an operating data, i.e., the measured ratio $\Delta T_{sub,o}/\Delta T_c$ at OFI, which is used for comparison with the present calculation. Eight tests (Test Numbers 17 to 24) performed in Test Section 1A using non-uniform heat fluxes were not analyzed. A program *Babelli.WFtests.f* was developed (listed in Appendix E) to calculate for each test, the coolant exit temperature, single-phase pressure drop, Subcooling number, Zuber number, and other needed quantities, for an *assumed* coolant inlet velocity.

7.4.1 Application of Flow Instability Criterion of Equation (7.1)

The coolant inlet velocity was varied in steps of 0.001 m/s from a suitable low value to a higher value, in search of the inlet velocity at which the ratio N_{sub}/N_{zub}, the left hand side of Eq. (7.1) becomes higher than the right hand side, i.e., the flow becomes stable. The inlet velocity just before the flow becomes stable is the inlet velocity at OFI. Table 7.5 shows the exit coolant temperatures and pressure drops at different inlet velocities calculated for the application of the flow instability criterion of Eq. (7.1) to a typical Whittle and Forgan test (Test Number 1 for example). Using the data of Table 7.5, the application of Babelli-Ishii flow instability criterion of Eq. (7.1) to Test Number 1 is shown in Table 7.6. The data line shown in bold letters in Table 7.6, at the inlet velocity of 2.712 m/s, marks the onset of flow instability.

The inlet velocity at OFI was calculated for each test listed in Table 7.4, and the results are shown in Table 7.7. The results for all 75 tests remain unchanged irrespective of whether the upper or the lower limit of $(L_{nvg} / L)_{critical}$ (given in Table 7.1) is used in the calculation. This is because the upper and lower limits of $(L_{nvg} / L)_{critical}$, i.e., two limits exist only if the Subcooling number is less than 69.92. However, in all the 75 tests the Subcooling number is greater than 69.92, as shown in Table 7.7.

The measured coolant inlet velocity and flow rate at OFI are also shown in Table 7.7. The measured flow rate (W) and inlet velocity at OFI (V_{in}) were calculated from the measured exit coolant temperature using Eq. (7.7). This equation is obtained by equating the total power to the coolant enthalpy change times flow rate.

$$\rho_{in}\, V_{in}\, A_F = W = \frac{Q}{h(P_{out}, T_{out}) - h(P_{in}, T_{in})} \tag{7.7}$$

The measured exit temperature was itself calculated from the measured ratio $\Delta T_{sat,out}/\Delta T_c$ reported by Whittle and Forgan [6], using Eq. (7.8). To derive this equation, one substitutes the definitions $\Delta T_{sat,out} = T_{sat,out} - T_{out}$ and $\Delta T_c = T_{out} - T_{in}$ into the definition $\Delta T_{sat,out}/\Delta T_c = r$, obtains the relationship $(T_{sat,out} - T_{out})/(T_{out} - T_{in}) = r$, and then solves for T_{out}.

$$T_{out} = \frac{T_{sat,out} + r\, T_{in}}{1 + r} \tag{7.8}$$

where r = the measured ratio $\Delta T_{sat,out}/\Delta T_c$ at OFI reported by Whittle and Forgan, and shown in Table 7.4. See nomenclature for the other symbols.

The measured flow rates at OFI thus obtained were found to be in agreement with those obtained using a different approach during an earlier analysis of these tests [7]. The difference between the measured and calculated inlet velocities at OFI in a test determines the error in the Babelli-Ishii flow instability criterion. A statistical analysis was done to find the mean and the standard deviation of the difference between the calculated and measured inlet velocities (calculated – measured), and the results are shown below and in Table 7.7.

Mean error in the calculated inlet velocity at OFI	= 0.384 m/s
Standard deviation of the error in the calculated inlet velocity at OFI	= 0.242 m/s

The mean error is positive, implying that the criterion predicts flow instability at a higher inlet velocity (and hence higher flow rate) than that measured experimentally. Figure 7.4 shows a comparison of the calculated versus the measured coolant inlet velocity at OFI. The data points are generally above the line of slope 1, indicating that the criterion is conservative. The mean value of the Whittle and Forgan parameter η at OFI is found to be 37.55 with a standard deviation of 3.16.

In these tests, Table 7.7 shows that the calculated ratio $\Delta T_c/\Delta T_{sat}$ at OFI, i.e., coolant temperature change divided by the difference between the saturation temperature at exit and the inlet temperature, has a mean value of 0.7314 which is smaller than the measured value of about 0.8 reported by Whittle and Forgan. This implies that the Babelli-Ishii criterion predicts flow instability earlier than it should, i.e., at a smaller coolant temperature rise than that measured experimentally. This also indicates that the criterion is conservative.

7.4.2 Application of Flow Instability Criterion of Eq. (7.5)

The simple flow instability criterion of Eq. (7.5) was also applied to the above 75 tests reported by Whittle and Forgan. The coolant inlet velocity was varied in steps of 0.001 m/s from a suitable low value to a higher value, in search of the inlet velocity at which the ratio N_{sub}/N_{zub} becomes greater than 1.36, i.e., the flow becomes stable according to Eq. (7.5). The inlet velocity just before the ratio N_{sub}/N_{zub} becomes greater than 1.36 is the inlet velocity at OFI. Table 7.5 is independent of the flow instability criterion used, i.e., whether Eq. (7.1) or Eq. (7.5) is used. This table shows the exit coolant temperatures and pressure drops at different inlet velocities calculated for the application of the flow instability criterion of Eq. (7.5) to a typical Whittle and Forgan test (Test Number 1 for example). Using the data of Table 7.5, the application of the flow instability criterion of Eq. (7.5) to Test Number 1 is shown by the underlined line in Table 7.6. The data in the underlined line in Table 7.6, at the inlet velocity of 2.620 m/s, marks the onset of flow instability.

The inlet velocity at OFI was calculated for each test listed in Table 7.4, and the results are shown in Table 7.8. The last column of Table 7.8 gives the ratio N_{sub}/N_{zub} calculated at OFI and is 1.36 for all tests as required by the criterion. The difference between the measured and calculated inlet velocities at OFI in a test determines the error in this flow instability criterion. A statistical analysis was done to find the mean and standard deviation of the difference between the calculated and measured inlet velocities (calculated – measured). The results are shown below and in Table 7.8.

Mean error in the calculated inlet velocity at OFI	= 0.363 m/s
Standard deviation of the error in the calculated inlet velocity at OFI	= 0.319 m/s

Again, the mean error is positive, implying that the criterion predicts instability at a higher inlet velocity (and hence flow rate) than that measured experimentally. It is noted that the mean error for the criterion of Eq. (7.5) is somewhat smaller than that for the criterion of Eq. (7.1), and the standard deviation for the criterion of Eq. (7.5) is greater than that for the criterion of Eq. (7.1). Figure 7.5 shows a comparison of the calculated versus the measured coolant inlet velocity at OFI. The data points in Fig. 7.5 are generally above the line of slope 1, indicating that the criterion is conservative.

A comparison of the scatter of data points in Figs. 7.4 and 7.5 also shows that the standard deviation in Fig. 7.5 is greater than that in Fig. 7.4. For the 12 tests done by Whittle and Forgan in their test section number 3 (having a $L/D_H = 190.9$), the simple criterion finds the parameter η at OFI to be about 68.2 which is about two times the values of η at OFI found for all other tests. This happens because the parameter η at OFI *calculated based on Eq. (7.5)* equals $0.36(L/D_H)$, as explained in Section 5 below.

The average value of the calculated ratio $\Delta T_c/\Delta T_{sat}$ at OFI determined by the simple criterion is 0.7367 which is closer (compared to the former criterion) to the measured value of about 0.8 reported by Whittle and Forgan. This implies that the simple criterion also predicts flow instability earlier than it should, i.e., at a smaller coolant temperature rise than that measured experimentally. This criterion also is conservative.

7.4.3 Approach to Flow Instability

To understand how a research reactor approaches the flow instability condition in a typical channel, seven important quantities tabulated in Table 7.6 for Whittle and Forgan Test Number 1 are plotted in Fig. 7.6 as functions of the inlet velocity. These quantities include the left and right hand sides of Babelli-Ishii criterion given by Eq. (7.1). The program *Babelli.WFtests.f* developed to apply the flow instability criteria of Eq. (7.1) and Eq. (7.5) to Whittle and Forgan tests saves the data shown in Table 7.6 and Fig. 7.6 in an output file named *flow.instability.unit9*. If Eq. (7.1) is used to find flow instability as the coolant inlet velocity decreases from 7.5 m/s, the ratio $(L_{nvg}/L)_{critical}$ on the right hand side (RHS) of Eq. (7.1) is always 1.0 because the Subcooling number, 129.41, remains greater than 69.92 (see Table 7.1). Furthermore, the Peclet number is always greater than 70,000, thus making the quantity in the curly brackets on the RHS of Eq. (7.1) constant at 154. Therefore, using the channel thickness, width, and heated length given in Table 7.4, the RHS of Eq. (7.1) becomes constant at 1.407 $\left(=1.0+\frac{0.127}{2\times 24.0}\times 154\right)$ as shown in Fig. 7.6.

The ratio N_{sub}/N_{zub} on the left hand side of Eq. (7.1) decreases linearly with the coolant inlet velocity (from 3.891 at V_{in} = 7.5 m/s to 0.830 at V_{in} = 1.6 m/s). The ratio N_{sub}/N_{zub} at inlet velocity V_{in} is $3.891*V_{in}$ / 7.5. Therefore, the inlet velocity at which the ratio N_{sub}/N_{zub} equals 1.407 is 1.407x7.5/3.891 = 2.712 m/s. This is the calculated inlet velocity at OFI in Test Number 1, according to the Babelli-Ishii criterion of Eq. (7.1).

It is noted that the ratio N_{sub}/N_{zub} at OFI is 1.407, and not 1.36 as required by the simple instability criterion given by Eq. (7.5). From the above description it is seen that the ratio N_{sub}/N_{zub} at OFI equals 1.0 + 77x(channel thickness/heated length) for channels of rectangular cross section. The ratio N_{sub}/N_{zub} at OFI is therefore not constant. It depends on the channel thickness and length. The values of this ratio for the 75 tests are given in the last column of Table 7.7. They vary from 1.107 to 1.462.

7.5 Value of Parameter η According to the Instability Criterion of Equation (7.5)

It is shown in this section that the simple flow instability criterion of Eq. (7.5) implies that the parameter η at OFI is about 0.36(L / D_H). This explains why in Table 7.8 the values of parameter η at OFI for Test Numbers 63 to 74 are about twice the values of η at OFI found for all other tests. The reason is that Test Numbers 63 to 74 were performed in a test section having an L/D_H nearly twice the L/D_H in all other tests (see L/D_H of all tests in Table 7.4).

To show that the parameter η at OFI based on Eq. (7.5) is about 0.36(L / D_H), it is noted that the ratio N_{sub}/N_{zub} at OFI equals 1.36 according to this criterion. The ratio N_{sub}/N_{zub} is defined above by Eq. (7.4). The numerator of Eq. (7.4) can be written as Eq. (7.9), and the denominator of Eq. (7.4) is simply the total heat transferred, Q, to the coolant in the channel. Thus the ratio N_{sub}/N_{zub} equals $W\Delta h_{in}/Q$ as shown in Eq. (7.10). Noting that Q/W equals Δh_c (the coolant enthalpy rise in the channel), the ratio N_{sub}/N_{zub} is given by $\Delta h_{in}/\Delta h_c$ as shown in Eq. (7.10). Therefore, at OFI, the criterion of Eq. (7.5) implies Eq. (7.11).

$$\rho_{in} V_{in} A_F \Delta h_{in} = W \Delta h_{in} \tag{7.9}$$

$$\frac{N_{sub}}{N_{zub}} = \frac{W \Delta h_{in}}{Q} = \frac{\Delta h_{in}}{\Delta h_c} \tag{7.10}$$

$$\Delta h_{in} = 1.36 \Delta h_c \qquad \text{at OFI} \tag{7.11}$$

Noting that $\Delta h_{in} = \Delta h_{out} + \Delta h_c$, Eq. (7.11) gives Δh_{out} at the onset of flow instability.

$$\Delta h_{out} = 0.36 \Delta h_c \qquad \text{at OFI} \tag{7.12}$$

The purpose here is to find the value of the Whittle and Forgan parameter η at OFI which is defined by Eq. (7.13). In Eq. (7.13), the ratio of temperature differences, $\Delta T_{sub,o}/\Delta T_c$, can be estimated by the ratio of the corresponding enthalpy differences, as written below in Eq. (7.14).

$$\eta = \frac{\Delta T_{sub,o}}{\Delta T_c} \frac{L}{D_H} \qquad \text{at OFI} \tag{7.13}$$

$$\frac{\Delta T_{sub,o}}{\Delta T_c} = \frac{T_{sat,out} - T_{out}}{T_{out} - T_{in}} = \frac{(h_f - h_{out})/C_p}{(h_{out} - h_{in})/C_p} = \frac{\Delta h_{out}}{\Delta h_c} \qquad \text{at OFI} \tag{7.14}$$

Using Eq. (7.14) in Eq. (7.13), the parameter η can be approximated by Eq. (7.15).

$$\eta = \frac{\Delta h_{out}}{\Delta h_c}\frac{L}{D_H} \qquad \text{at OFI} \tag{7.15}$$

Using the value of Δh_{out} at OFI obtained in Eq. (7.12), one gets from Eq. (7.15) the value of parameter η at OFI.

$$\eta = \frac{0.36\,\Delta h_c}{\Delta h_c}\frac{L}{D_H} = 0.36\frac{L}{D_H} \qquad \text{at OFI} \tag{7.16}$$

Equation (7.16) is the desired result of this section. It means that the Whittle and Forgan parameter η at OFI based on the simple flow instability criterion of Eq. (7.5) is not constant. It varies linearly with the heated length-to-hydraulic diameter ratio. That is why the parameter η at OFI calculated based on Eq. (7.5) is about 68.2 in Test Numbers 63 to 74 (having L/D_H = 190.9).

7.6 A Program for Applying the Instability Criteria to Whittle and Forgan Tests

A program *Babelli.WFtests.f* was developed to apply the flow instability criteria of Eq. (7.1) and Eq. (7.5) to the 75 tests reported by Whittle and Forgan. It reads an input file containing the geometry and operating data of the tests. The input data are shown in Table 7.4. It saves the output results shown in Tables 7.5, 7.6, and 7.7 (or 8 depending upon the criterion chosen) in three output files as listed below. The listing of the program is given in Appendix E.

(1) Input file	Babelli.WFtests.Input.Data	contains the data shown in Table 7.4.
(2) Output file	flow.instability.unit6	contains the results shown in Table 7.5.
(3) Output file	flow.instability.unit9	contains the results shown in Table 7.6.
(4) Output file	flow.instability.summary	contains the results shown in Table 7.7 or 7.8.

There is an internally set input variable IEQ (see the bold line in the source code of the program in Appendix E) to choose one of the two instability criteria, as defined below, and there is an internally set input variable DELVIN to define the step size for coolant inlet velocity (usually DELVIN = 0.001 m/s).

IEQ = 1, use Babelli-Ishii Eq. (7.1) to predict flow instability
= 2, use Nsub/Nzu > 1.36 for stability

7.7 Conclusions

A program has been developed to apply the Babelli-Ishii flow instability criterion of Eq. (7.1) or the simple criterion of Eq. (7.5) to 75 tests reported by Whittle and Forgan. The comparison of the calculated (using either criterion) and measured coolant inlet velocities at OFI in these tests shows that both criteria are conservative. Both criteria, Eqs. (7.1) and (7.5), are implemented in the PLTEMP/ANL version 3.4 code [7].

NOMENCLATURE

Symbols

A_F = Flow area of channel, m^2
C_p = Specific heat of the coolant, J/kg-°C
D_h = Hydraulic diameter based on the *wetted* perimeter of the channel, m
D_H = Hydraulic diameter based on the *heated* perimeter of the channel, m
h(P,T) = Liquid coolant enthalpy as a function of coolant pressure P and temperature T, J/kg
h_{in} = Coolant enthalpy at the heated length inlet = $h(P_{in}, T_{in})$, J/kg
h_{out} = Coolant enthalpy at the heated length exit = $h(P_{out}, T_{out})$, J/kg
$h_{f,in}$ = Saturated liquid enthalpy at the heated length inlet pressure = $h(P_{in})$, J/kg
$h_{f,out}$ = Saturated liquid enthalpy at the heated length exit pressure = $h(P_{out})$, J/kg
$h_{fg}(P)$ = Latent heat of vaporization as a function of coolant pressure P
Δh_c = $h_{out} - h_{in}$ = Coolant enthalpy rise in the channel, J/kg
Δh_{in} = $h_{f,out} - h_{in}$ = Inlet subcooling in terms of enthalpy, J/kg
Δh_{out} = $h_{f,out} - h_{out}$ = Exit subcooling in terms of enthalpy, J/kg
K = Coolant thermal conductivity, W/m-°C
L = Channel heated length, m
L_{nvg} = Non-boiling length, i.e., the distance from start of heated length of channel to the position of net vapor generation, m
N_{zu} = Zuber number
N_{sub} = Subcooling number
P = Coolant pressure, Pa
Pe = Peclet number = Re Pr = $\rho_{in} C_p V_{in} D_h / K$
Pr = Prandtl number = $\mu C_p / K$
P_{in} = Channel inlet pressure, Pa
P_{out} = Channel outlet pressure, Pa
q''_w = Wall heat flux (assumed uniform over the channel length), W/m^2
Q = $q''_w \zeta_H L$ = Total power input to the coolant, W
Re = Reynolds number = $\rho_{in} V_{in} D_h / \mu$
ρ = Coolant density, kg/m^3
T = Coolant temperature, °C
T_{in} = Coolant temperature at the channel inlet, °C
T_{out} = Coolant temperature at the channel outlet, °C
$T_{sat}(P)$ = Coolant saturation temperature at a specific pressure P, °C
$T_{sat,in}$ = Coolant saturation temperature at channel inlet , °C
$T_{sat,out}$ = Coolant saturation temperature at channel outlet, °C
ΔT_c = $T_{out} - T_{in}$ = Coolant temperature rise at OFI, °C
ΔT_{sat} = $T_{sat,out} - T_{in}$ = Saturation temperature at exit minus inlet temperature at OFI, °C
$\Delta T_{sub,o}$ = $T_{sat,out} - T_{out}$ = Exit subcooling at the onset of flow instability, °C
η = $\frac{T_{sat,out} - T_{out}}{T_{out} - T_{in}} \frac{L}{D_H}$ = A parameter used by Whittle and Forgan in their analysis of the flow instability tests
μ = Absolute viscosity of the coolant, Pa-s
V = Coolant velocity, m/s

W = $\rho_{in} V_{in} A_F$ = Coolant flow rate, kg/s
ζ_H = Heated perimeter, m

Subscripts

c = coolant
F = flow
f = saturated liquid
g = saturated vapor
fg = liquid to vapor phase change
H = heated
h = hydraulic
in = channel heated length inlet
nvg = position of net vapor generation
out = channel heated length outlet
sat = saturated

7.8 REFERENCES

1. I. Babelli and M. Ishii, "Flow Excursion Instability in Downward Flow Systems, Part II: Two-Phase Instability," Nuclear Engineering and Design, Vol. 206, pp. 97-104 (2001).
2. T. Dougherty, C. Fighetti, G. Reddy, B. Yang, E. McAssey Jr., and Z. Qureshi, "Flow Instability in Vertical Channels," ASME Heat Transfer Division, HTD-Vol. 159, pp. 177-186 (1991).
3. P. Saha and N. Zuber, "Point of Net Vapor Generation and Vapor Void Fraction in Subcooled Boiling," Proc. Fifth International Heat Transfer Conf., Vol. 4, pp. 175-179 (1974).
4. W. M. Rohsenow, J. P. Hartnett, and Y. I. Cho, "Handbook of Heat Transfer," McGraw-Hill, Washington D.C., Third Edition, p. 15.92, (1998).
5. B. S. Johnston, " Subcooled Boiling of Downward Flow in a Vertical Annulus," ASME Heat Transfer Division, HTD-Vol. 109, pp. 149-156 (1989).
6. W. H. Whittle and R. Forgan, "A Correlation for the Minima in the Pressure Drop Versus Flow-Rate Curves for Sub-cooled Water Flowing in Narrow Heated Channels," Nuclear Engineering and Design, Vol. 6, pp. 89-99 (1967).
7. A. P. Olson and M. Kalimullah, "A User's Guide to the PLTEMP/ANL Code," ANL/RERTR/TM-11-22, Version 4.1, Argonne National Laboratory, 9700 South Cass Avenue, Argonne, IL 60439, USA (April 6, 2011).

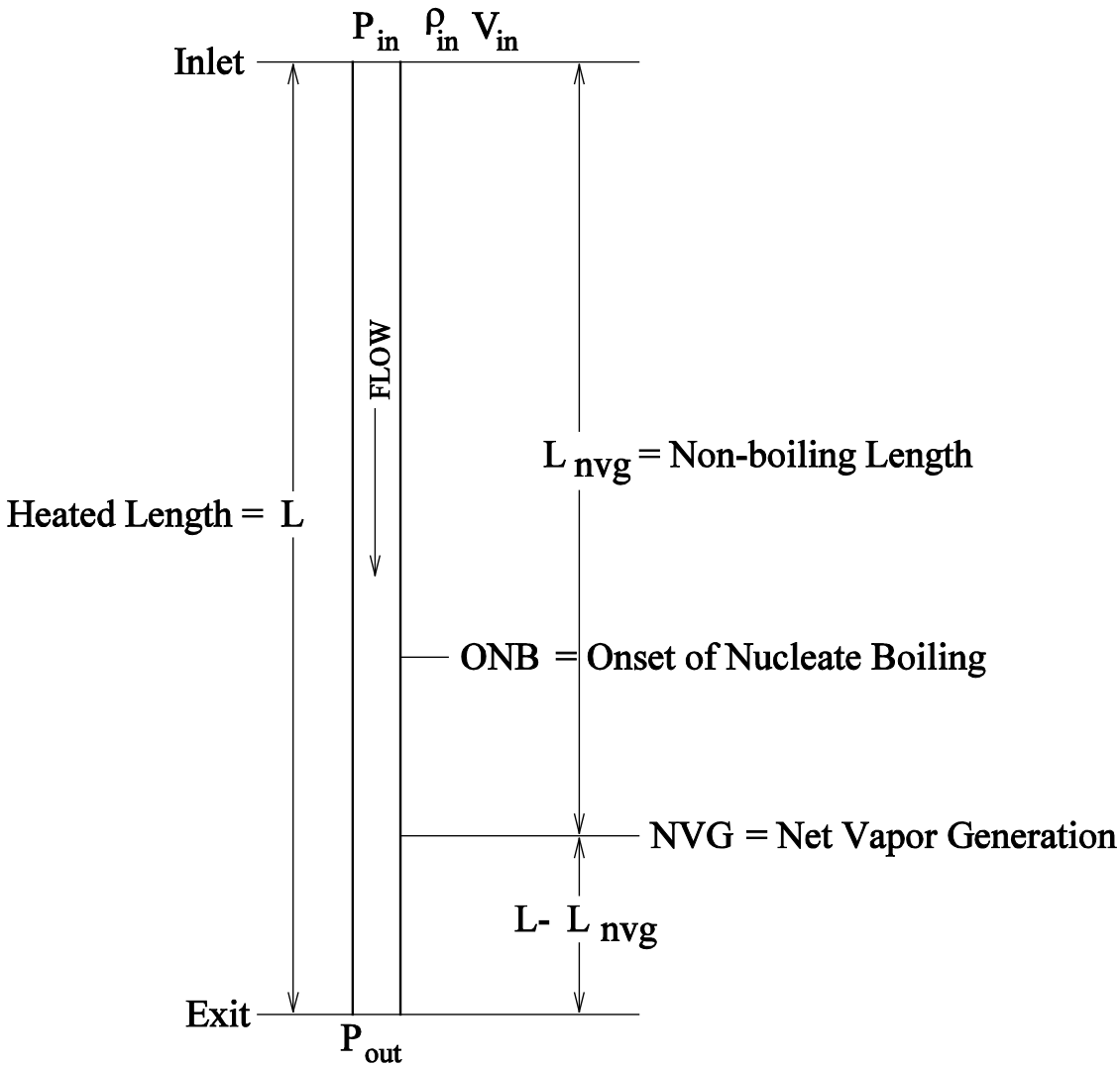

Figure 7.1 Schematic Diagram of a Heated Coolant Channel with Downward Flow

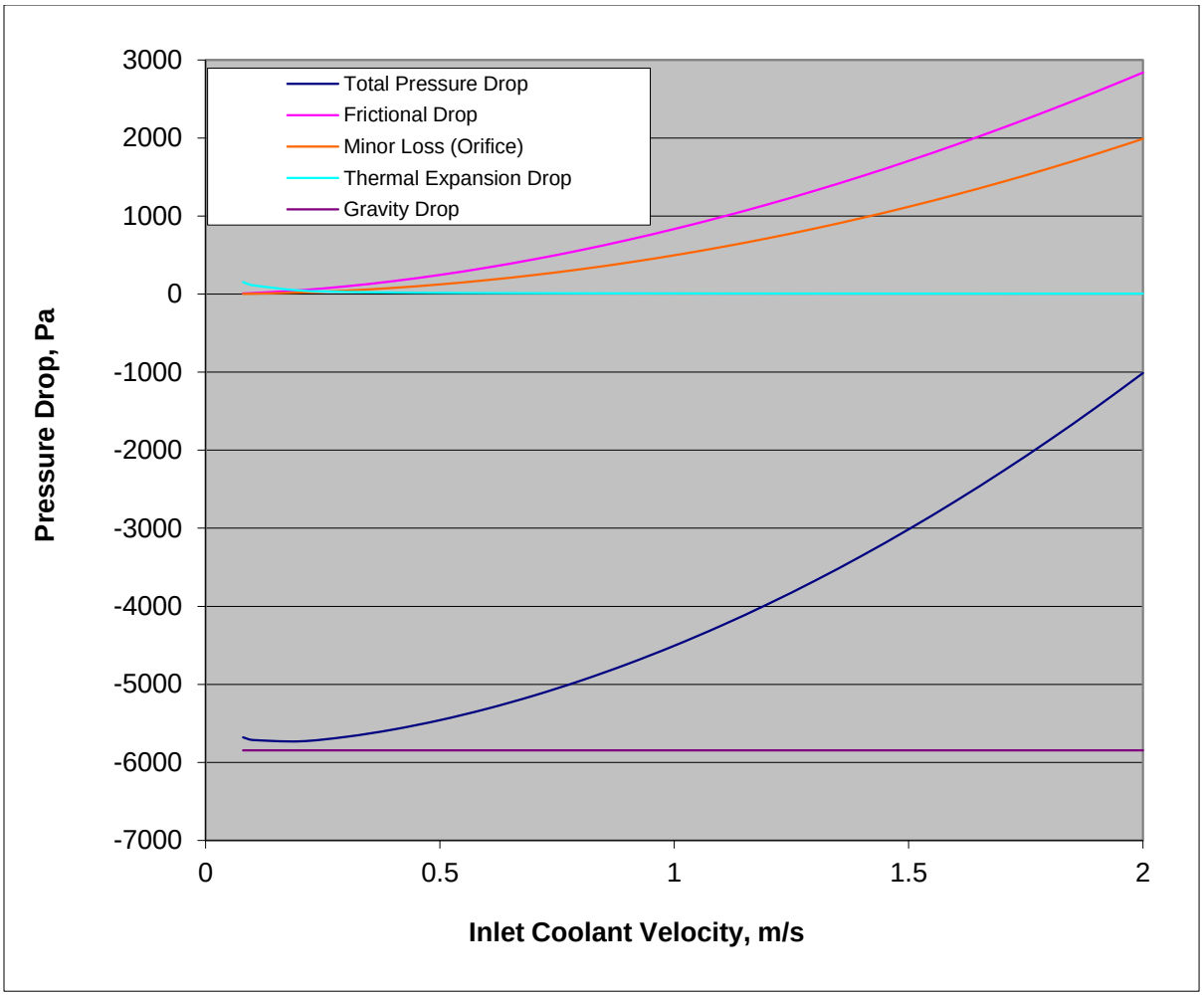

Figure 7.2 Dependence of Total Pressure Drop on Inlet Velocity for a Coolant Channel with Downflow of Water at a Given Power of 7 kW

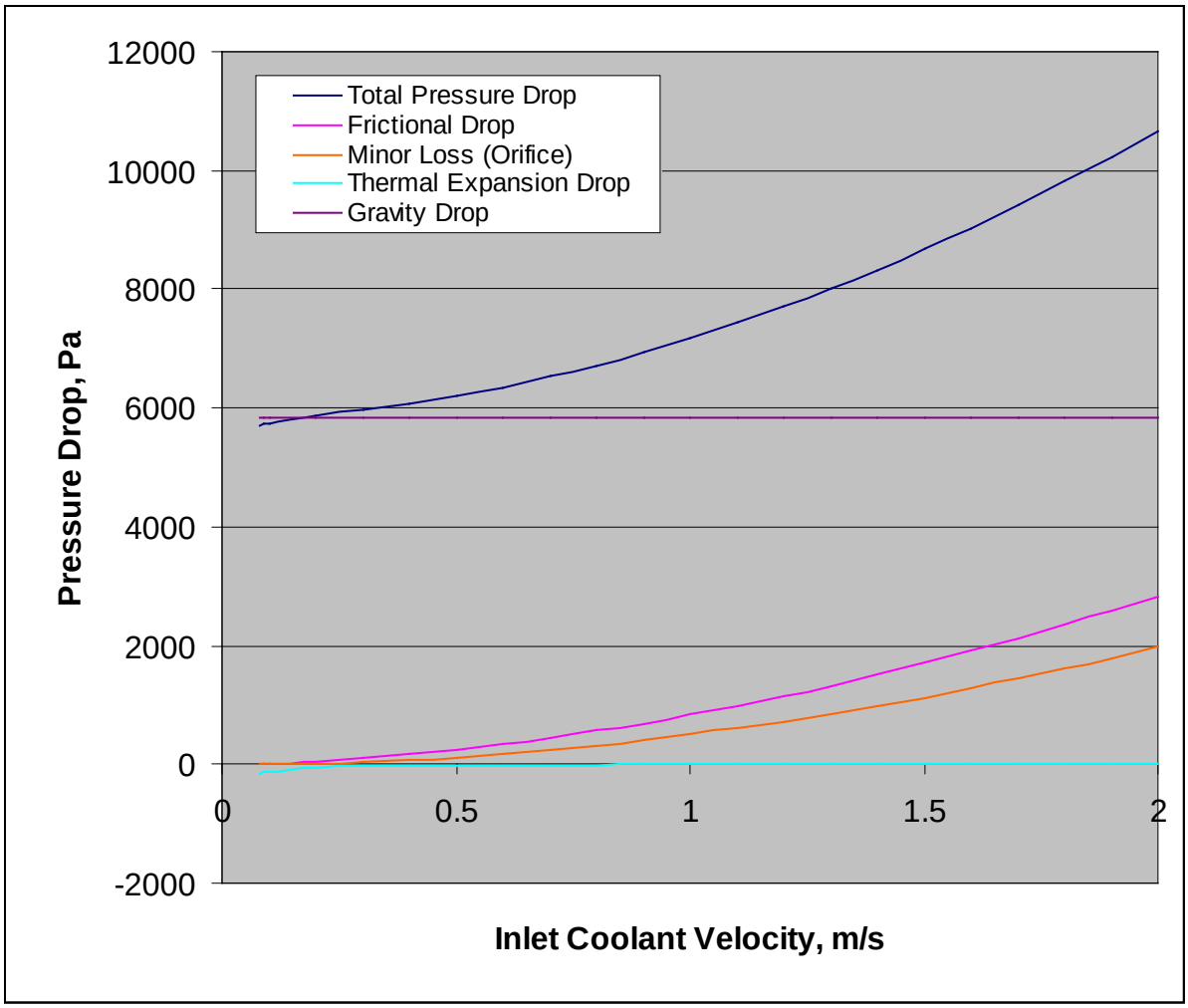

Figure 7.3 Dependence of Total Pressure Drop on Inlet Velocity for a Coolant Channel with Upflow of Water at a Given Power of 7 kW

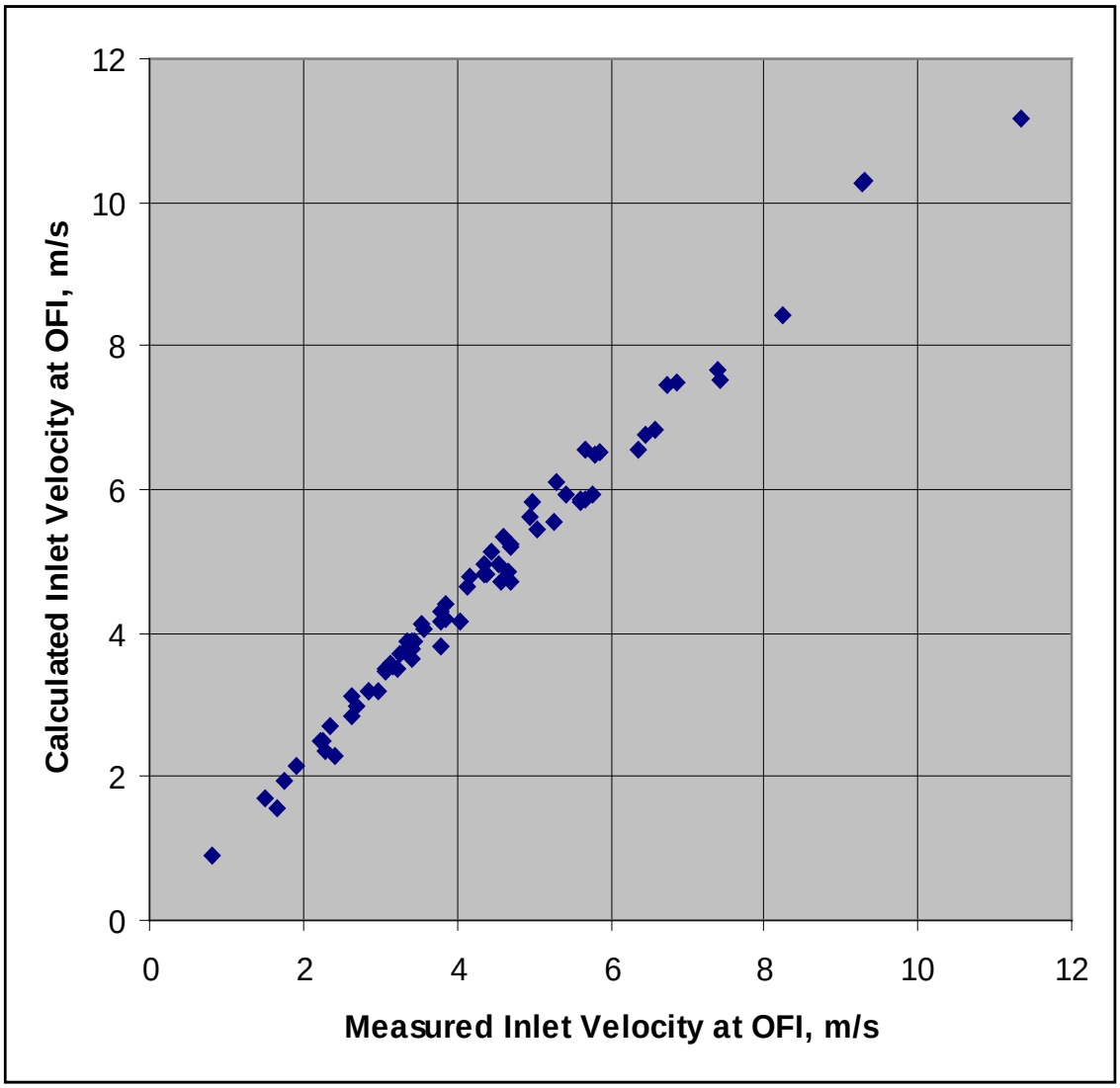

Figure 7.4 Comparison of Coolant Inlet Velocity at OFI Calculated Using Eq. (7.1) Versus its Measured Value in 75 Tests Reported by Whittle and Forgan

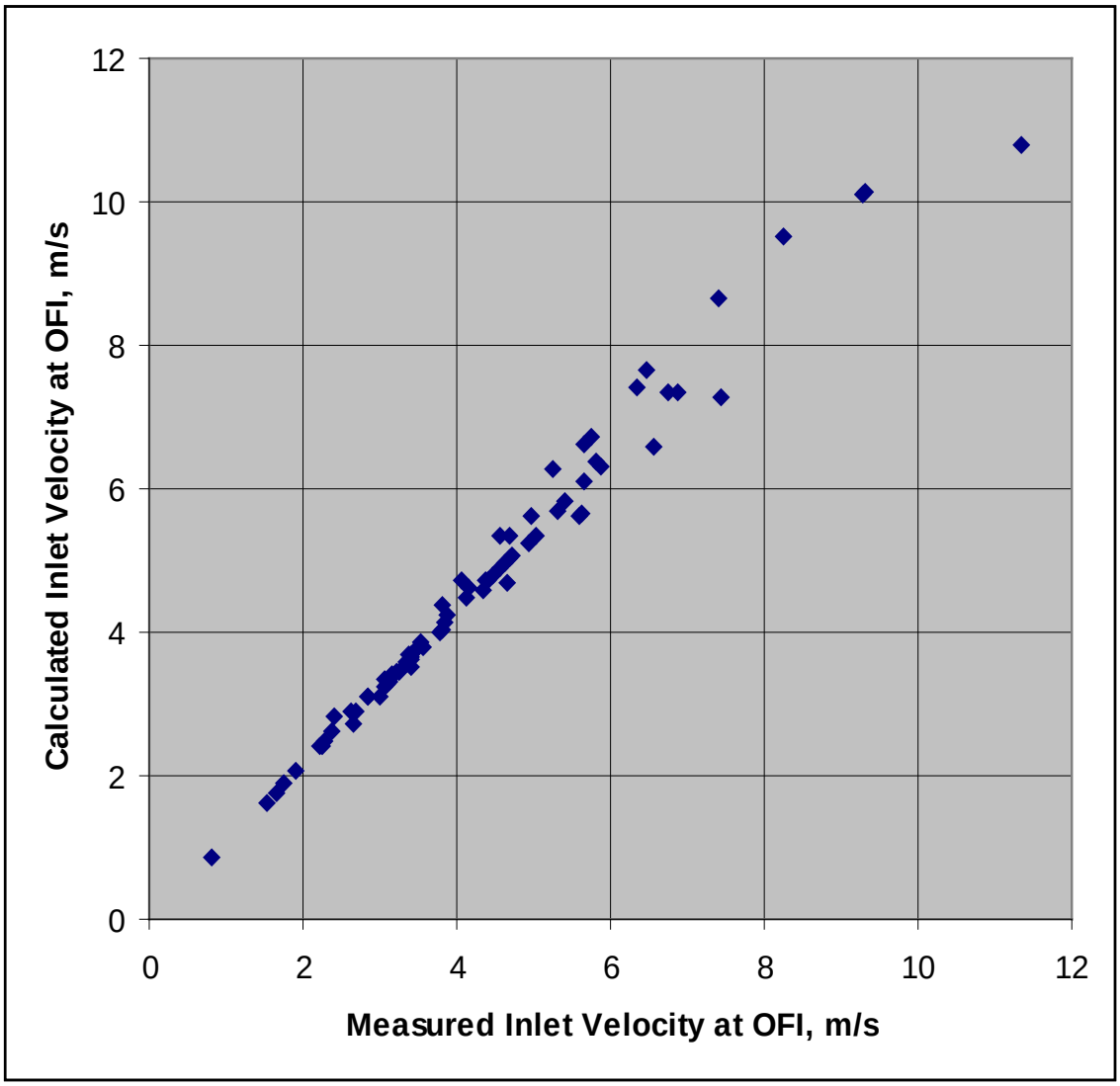

Figure 7.5 Comparison of Coolant Inlet Velocity at OFI Calculated Using Eq. (7.5) Versus its Measured Value in 75 Tests Reported by Whittle and Forgan

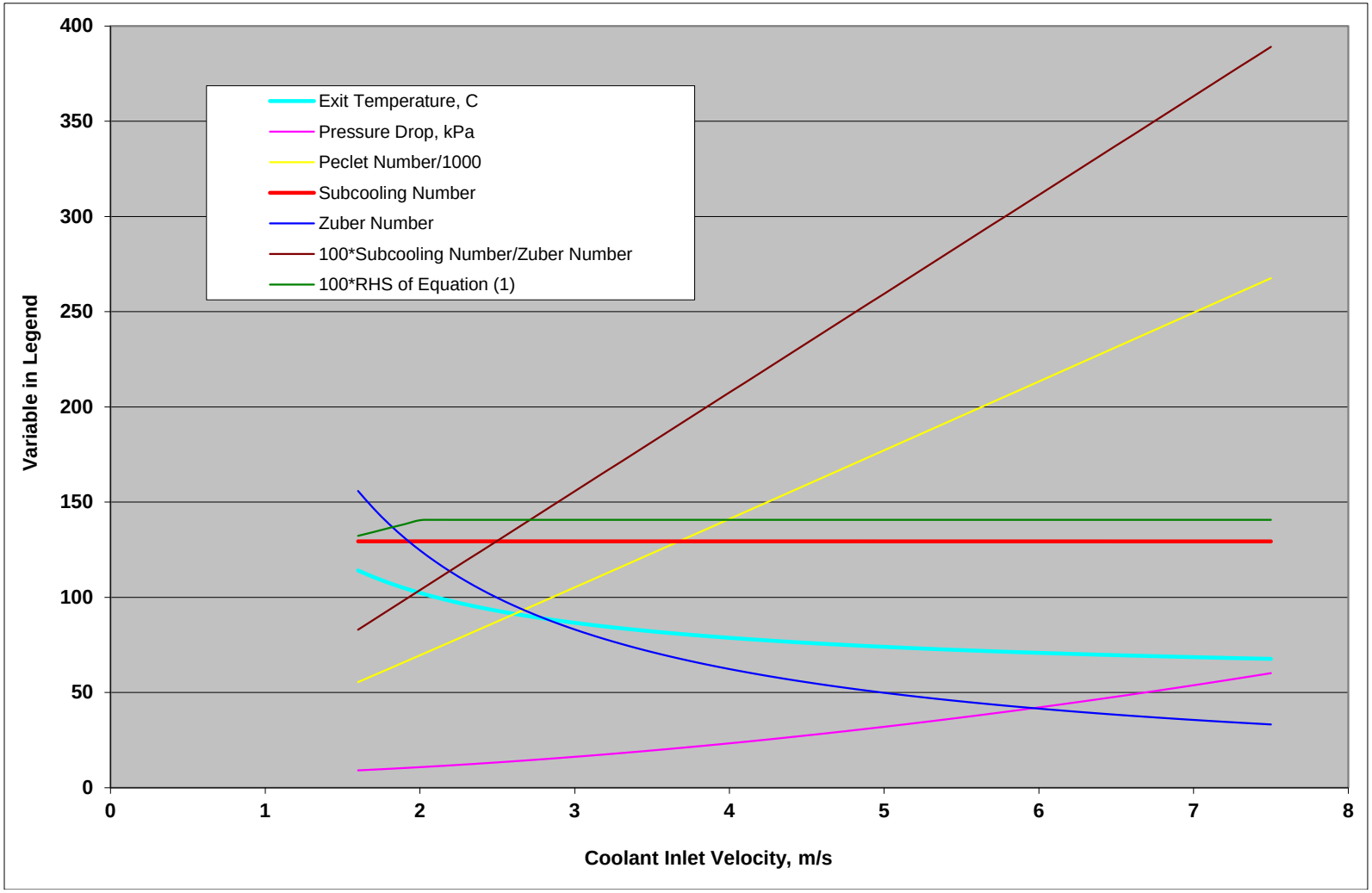

Figure 7.6 Variation of Ratio N_{sub}/N_{zub} and Right Hand Side of Eq. (7.1) Over the Heated Length of Channel in Whittle and Forgan Test 1.

Table 7.1 Critical Value of Dimensionless Non-boiling Length $(L_{nvg}/L)_{critical}$ as Function of Subcooling Number

Subcooling Number, N_{sub}	Experimental Value of $(L_{nvg}/L)_{critical}$	
	Lower Limit	Upper Limit
2.69	0.0232	0.0232
5.38	0.0684	0.414
8.07	0.141	0.594
10.76	0.256	0.756
21.51	0.440	1.083
32.27	0.527	1.222
43.03	0.594	1.297
53.78	0.711	1.222
64.54	0.905	1.083
69.92	1.00	1.00
160.00	1.00	1.00

Table 7.2 Application of Babelli and Ishii Flow Instability Criterion to a Channel With Downflow

```
Hydraulic diameter, mm               = 10
Channel heated length, m             = 0.6
Channel flow area, m**2              = 2.5E-04
Total minor loss coefficient         = 1.0
Pressure at heated section inlet, Pa = 1.5E+05
Inlet temperature, °C                = 35.0
Power removed by the channel, kW     = 7.0
```

EXIT TEMPERATURE AND PRESSURE DROP AT DIFFERENT INLET VELOCITIES

Inlet Vel, m/s	Exit Temp, C	Average Temp, C	Friction Factor	Beta per C	Total Press Drop, Pa	Friction Drop, Pa	Orifice Drop, Pa	Therm Exp Drop, Pa	Gravity Drop, Pa	Reynolds Number
0.08	118.65	76.83	0.0445	6.26E-04	-5679.17	8.67	3.25	154.61	-5845.70	2155.46
0.09	109.45	72.22	0.0442	6.00E-04	-5699.14	10.86	4.10	131.61	-5845.70	2294.36
0.10	102.06	68.53	0.0446	5.77E-04	-5713.08	13.49	5.05	114.08	-5845.70	2430.80
0.20	68.65	51.82	0.0406	4.67E-04	-5730.51	48.78	20.01	46.40	-5845.70	3777.67
0.30	57.46	46.23	0.0371	4.27E-04	-5672.22	100.06	44.92	28.50	-5845.70	5141.98
0.40	51.85	43.42	0.0347	4.06E-04	-5579.15	166.22	79.77	20.57	-5845.70	6510.81
0.50	48.48	41.74	0.0329	3.93E-04	-5458.72	246.24	124.56	16.18	-5845.70	7881.83
0.60	46.24	40.62	0.0316	3.85E-04	-5313.57	339.42	179.29	13.43	-5845.70	9254.71
0.70	44.63	39.82	0.0304	3.79E-04	-5144.98	445.20	243.96	11.56	-5845.70	10628.61
0.80	43.43	39.22	0.0295	3.74E-04	-4953.72	563.19	318.57	10.23	-5845.70	12002.96
0.90	42.49	38.75	0.0287	3.70E-04	-4740.32	693.01	403.13	9.24	-5845.70	13377.56
1.00	41.75	38.37	0.0279	3.67E-04	-4505.21	834.38	497.63	8.48	-5845.70	14752.78
1.10	41.13	38.07	0.0273	3.65E-04	-4248.70	987.05	602.07	7.89	-5845.70	16128.30
1.20	40.62	37.81	0.0268	3.63E-04	-3971.04	1150.78	716.45	7.43	-5845.70	17503.61
1.30	40.19	37.59	0.0263	3.61E-04	-3672.49	1325.38	840.77	7.06	-5845.70	18879.27
1.40	39.82	37.41	0.0258	3.60E-04	-3353.24	1510.66	975.04	6.76	-5845.70	20255.33
1.50	39.50	37.25	0.0254	3.59E-04	-3013.44	1706.50	1119.24	6.52	-5845.70	21630.90
1.60	39.22	37.11	0.0250	3.58E-04	-2653.27	1912.71	1273.39	6.33	-5845.70	23007.23
1.70	38.97	36.98	0.0247	3.57E-04	-2272.86	2129.19	1437.48	6.17	-5845.70	24382.89
1.80	38.75	36.87	0.0244	3.56E-04	-1872.36	2355.78	1611.51	6.05	-5845.70	25759.19
1.90	38.55	36.78	0.0241	3.55E-04	-1451.88	2592.39	1795.49	5.95	-5845.70	27135.59
2.00	38.37	36.69	0.0238	3.54E-04	-1011.51	2838.92	1989.40	5.87	-5845.70	28511.15

Table 7.2 Continued

APPLICATION OF BABELLI-ISHII FLOW INSTABILITY CRITERION

Inlet Vel, m/s	Exit Temp, C	Tot Press Drop, Pa	Exit Press Pa	Peclet Number	Inlet Subc J/kg	Subcool Number	Zuber Number	Nsub/Nzu	RHS of Eq. (7.1)	Stable?	Critical Lnvg/L	0.0022Pe or 154.0
0.08	118.65	-5679.17	155679.17	4883.42	325857.93	156.76	169.36	0.926	1.642	unstable	1.000	154.000
0.09	109.45	-5699.14	155699.14	5500.01	325871.81	156.75	150.53	1.041	1.642	unstable	1.000	154.000
0.10	102.06	-5713.08	155713.08	6124.39	325885.70	156.74	135.46	1.157	1.642	unstable	1.000	154.000
0.20	68.65	-5730.51	155730.51	12550.12	325899.58	156.73	67.73	2.314	1.642	stable	1.000	154.000
0.30	57.46	-5672.22	155672.22	19085.24	325850.98	156.77	45.17	3.471	1.642	stable	1.000	154.000
0.40	51.85	-5579.15	155579.15	25651.29	325774.61	156.82	33.89	4.627	1.642	stable	1.000	154.000
0.50	48.48	-5458.72	155458.72	32230.41	325677.41	156.88	27.13	5.782	1.642	stable	1.000	154.000
0.60	46.24	-5313.57	155313.57	38816.35	325559.39	156.96	22.63	6.936	1.642	stable	1.000	154.000
0.70	44.63	-5144.98	155144.98	45406.30	325413.59	157.05	19.42	8.088	1.642	stable	1.000	154.000
0.80	43.43	-4953.72	154953.72	51998.71	325253.91	157.15	17.01	9.239	1.642	stable	1.000	154.000
0.90	42.49	-4740.32	154740.32	58592.98	325080.34	157.27	15.14	10.388	1.642	stable	1.000	154.000
1.00	41.75	-4505.21	154505.21	65188.43	324885.94	157.39	13.64	11.535	1.642	stable	1.000	154.000
1.10	41.13	-4248.70	154248.70	71784.77	324670.72	157.53	12.42	12.681	1.642	stable	1.000	154.000
1.20	40.62	-3971.04	153971.04	78381.67	324441.60	157.68	11.41	13.824	1.642	stable	1.000	154.000
1.30	40.19	-3672.49	153672.49	84979.14	324191.67	157.85	10.55	14.964	1.642	stable	1.000	154.000
1.40	39.82	-3353.24	153353.24	91577.07	323927.84	158.02	9.81	16.102	1.642	stable	1.000	154.000
1.50	39.50	-3013.44	153013.44	98175.25	323643.19	158.21	9.18	17.237	1.642	stable	1.000	154.000
1.60	39.22	-2653.27	152653.27	104773.74	323344.65	158.41	8.62	18.369	1.642	stable	1.000	154.000
1.70	38.97	-2272.86	152272.86	111372.76	323025.28	158.62	8.14	19.498	1.642	stable	1.000	154.000
1.80	38.75	-1872.36	151872.36	117971.49	322685.09	158.84	7.70	20.623	1.642	stable	1.000	154.000
1.90	38.55	-1451.88	151451.88	124570.71	322331.01	159.07	7.32	21.745	1.642	stable	1.000	154.000
2.00	38.37	-1011.51	151011.51	131170.04	321963.04	159.32	6.97	22.863	1.642	stable	1.000	154.000

Table 7.3 Application of Babelli and Ishii Flow Instability Criterion to a Channel with Upflow

```
Hydraulic diameter, mm               = 10
Channel heated length, m             = 0.6
Channel flow area, m**2              = 2.5E-04
Total minor loss coefficient         = 1.0
Pressure at heated section inlet, Pa = 1.5E+05
Inlet temperature, C                 = 35.0
Power removed by the channel, kW     = 7.0
```

EXIT TEMPERATURE AND PRESSURE DROP AT DIFFERENT INLET VELOCITIES

Inlet Vel, m/s	Exit Temp, C	Average Temp, C	Friction Factor	Beta per C	Total Press Drop, Pa	Friction Drop, Pa	Orifice Drop, Pa	Therm Exp Drop, Pa	Gravity Drop, Pa	Reynolds Number
0.08	118.65	76.83	0.0445	6.26E-04	5703.35	8.67	3.25	-154.27	5845.70	2155.46
0.09	109.45	72.22	0.0442	6.00E-04	5729.41	10.86	4.10	-131.24	5845.70	2294.36
0.10	102.06	68.53	0.0446	5.77E-04	5750.54	13.49	5.05	-113.70	5845.70	2430.80
0.20	68.65	51.82	0.0406	4.67E-04	5868.72	48.78	20.01	-45.77	5845.70	3777.67
0.30	57.46	46.23	0.0371	4.27E-04	5963.04	100.06	44.92	-27.64	5845.70	5141.98
0.40	51.85	43.42	0.0347	4.06E-04	6072.20	166.22	79.77	-19.48	5845.70	6510.81
0.50	48.48	41.74	0.0329	3.93E-04	6201.64	246.24	124.56	-14.86	5845.70	7881.83
0.60	46.24	40.62	0.0316	3.85E-04	6352.53	339.42	179.29	-11.88	5845.70	9254.71
0.70	44.63	39.82	0.0304	3.79E-04	6525.09	445.20	243.96	-9.78	5845.70	10628.61
0.80	43.43	39.22	0.0295	3.74E-04	6719.25	563.19	318.57	-8.22	5845.70	12002.96
0.90	42.49	38.75	0.0287	3.70E-04	6934.85	693.01	403.13	-7.00	5845.70	13377.56
1.00	41.75	38.37	0.0279	3.67E-04	7171.70	834.38	497.63	-6.02	5845.70	14752.78
1.10	41.13	38.07	0.0273	3.65E-04	7429.62	987.05	602.07	-5.20	5845.70	16128.30
1.20	40.62	37.81	0.0268	3.63E-04	7708.43	1150.78	716.45	-4.51	5845.70	17503.61
1.30	40.19	37.59	0.0263	3.61E-04	8007.95	1325.38	840.77	-3.91	5845.70	18879.27
1.40	39.82	37.41	0.0258	3.60E-04	8328.02	1510.66	975.04	-3.38	5845.70	20255.33
1.50	39.50	37.25	0.0254	3.59E-04	8668.53	1706.50	1119.24	-2.91	5845.70	21630.90
1.60	39.22	37.11	0.0250	3.58E-04	9029.31	1912.71	1273.39	-2.49	5845.70	23007.23
1.70	38.97	36.98	0.0247	3.57E-04	9410.27	2129.19	1437.48	-2.10	5845.70	24382.89
1.80	38.75	36.87	0.0244	3.56E-04	9811.24	2355.78	1611.51	-1.75	5845.70	25759.19
1.90	38.55	36.78	0.0241	3.55E-04	10232.15	2592.39	1795.49	-1.42	5845.70	27135.59
2.00	38.37	36.69	0.0238	3.54E-04	10672.91	2838.92	1989.40	-1.12	5845.70	28511.15

Table 7.3 Continued

APPLICATION OF BABELLI-ISHII FLOW INSTABILITY CRITERION

Inlet Vel, m/s	Exit Temp, C	Tot Press Drop, Pa	Exit Press Pa	Peclet Number	Inlet Subc J/kg	Subcool Number	Zuber Number	Nsub/Nzu	RHS of Eq. (7.1)	Stable?	Critical Lnvg/L	0.0022Pe or 154.0
0.08	118.65	5703.35	144296.65	4883.46	316179.73	163.19	181.71	0.898	1.045	unstable	1.000	10.744
0.09	109.45	5729.41	144270.59	5500.05	316158.91	163.21	161.54	1.010	1.050	unstable	1.000	12.100
0.10	102.06	5750.54	144249.46	6124.44	316138.08	163.22	145.41	1.122	1.056	stable	1.000	13.474
0.20	68.65	5868.72	144131.28	12550.26	316033.94	163.29	72.76	2.244	1.115	stable	1.000	27.611
0.30	57.46	5963.04	144036.96	19085.42	315950.62	163.34	48.54	3.365	1.175	stable	1.000	41.988
0.40	51.85	6072.20	143927.80	25651.53	315853.42	163.41	36.43	4.486	1.235	stable	1.000	56.433
0.50	48.48	6201.64	143798.36	32230.82	315742.34	163.49	29.17	5.605	1.295	stable	1.000	70.908
0.60	46.24	6352.53	143647.47	38816.84	315610.43	163.58	24.33	6.724	1.356	stable	1.000	85.397
0.70	44.63	6525.09	143474.91	45406.88	315457.69	163.68	20.88	7.840	1.416	stable	1.000	99.895
0.80	43.43	6719.25	143280.75	51999.38	315284.12	163.80	18.29	8.956	1.477	stable	1.000	114.399
0.90	42.49	6934.85	143065.15	58593.74	315096.66	163.93	16.28	10.069	1.537	stable	1.000	128.906
1.00	41.75	7171.70	142828.30	65189.09	314888.38	164.07	14.67	11.180	1.598	stable	1.000	143.416
1.10	41.13	7429.62	142570.38	71785.49	314659.27	164.23	13.36	12.290	1.642	stable	1.000	154.000
1.20	40.62	7708.43	142291.57	78382.46	314409.33	164.39	12.27	13.396	1.642	stable	1.000	154.000
1.30	40.19	8007.95	141992.05	84980.00	314145.51	164.58	11.35	14.500	1.642	stable	1.000	154.000
1.40	39.82	8328.02	141671.98	91578.27	313860.86	164.77	10.56	15.602	1.642	stable	1.000	154.000
1.50	39.50	8668.53	141331.47	98176.54	313562.32	164.98	9.88	16.700	1.642	stable	1.000	154.000
1.60	39.22	9029.31	140970.69	104775.13	313236.01	165.20	9.28	17.795	1.642	stable	1.000	154.000
1.70	38.97	9410.27	140589.73	111373.89	312895.81	165.44	8.76	18.886	1.642	stable	1.000	154.000
1.80	38.75	9811.24	140188.76	117973.05	312534.79	165.68	8.29	19.974	1.642	stable	1.000	154.000
1.90	38.55	10232.15	139767.85	124571.99	312159.88	165.95	7.88	21.059	1.642	stable	1.000	154.000
2.00	38.37	10672.91	139327.09	131171.38	311757.20	166.22	7.51	22.138	1.642	stable	1.000	154.000

Table 7.4 Geometry and Operating Data for 75 Flow Instability Tests Performed by Whittle and Forgan

Test No.	Flow Direction*	Inlet Temp °C	Heat Flux W/cm²	Channel Thickness inch	Channel Width inch	Heated Length inch	Minor Loss Coeff	Exit Pressure psia	$\Delta T_{sub,o}/\Delta T_c$
1	1	55.0	104.0	0.127	1.0	24.0	0.0	17.0	0.224
2	1	55.0	145.0	0.127	1.0	24.0	0.0	17.0	0.266
3	1	55.0	184.0	0.127	1.0	24.0	0.0	17.0	0.220
4	1	55.0	250.0	0.127	1.0	24.0	0.0	17.0	0.266
5	1	55.0	82.0	0.127	1.0	24.0	0.0	17.0	0.250
6	1	55.0	136.0	0.127	1.0	24.0	0.0	17.0	0.250
7	1	55.0	160.0	0.127	1.0	24.0	0.0	17.0	0.282
8	1	55.0	200.0	0.127	1.0	24.0	0.0	17.0	0.266
9	1	45.0	160.0	0.127	1.0	24.0	0.0	17.0	0.250
10	1	45.0	180.0	0.127	1.0	24.0	0.0	17.0	0.250
11	1	45.0	204.0	0.127	1.0	24.0	0.0	17.0	0.234
12	1	60.0	110.0	0.127	1.0	24.0	0.0	17.0	0.250
13	1	60.0	160.0	0.127	1.0	24.0	0.0	17.0	0.250
14	1	60.0	180.0	0.127	1.0	24.0	0.0	17.0	0.266
15	1	60.0	200.0	0.127	1.0	24.0	0.0	17.0	0.204
16	1	35.0	136.0	0.127	1.0	24.0	0.0	17.0	0.250
25	0	45.0	78.0	0.127	1.0	24.0	0.0	17.0	0.266
26	0	45.0	116.0	0.127	1.0	24.0	0.0	17.0	0.266
27	0	45.0	148.0	0.127	1.0	24.0	0.0	17.0	0.250
28	0	55.0	115.0	0.127	1.0	24.0	0.0	17.0	0.266
29	0	55.0	75.0	0.127	1.0	24.0	0.0	17.0	0.266
30	0	55.0	146.0	0.127	1.0	24.0	0.0	17.0	0.250
31	0	45.0	42.0	0.127	1.0	24.0	0.0	17.0	0.282
32	1	55.0	147.0	0.096	1.0	16.0	0.0	17.0	0.282
33	1	55.0	170.0	0.096	1.0	16.0	0.0	17.0	0.282
34	1	55.0	180.0	0.096	1.0	16.0	0.0	17.0	0.282
35	1	55.0	215.0	0.096	1.0	16.0	0.0	17.0	0.266
36	1	45.0	196.0	0.096	1.0	16.0	0.0	17.0	0.282
37	1	45.0	250.0	0.096	1.0	16.0	0.0	17.0	0.282
38	1	45.0	180.0	0.096	1.0	16.0	0.0	17.0	0.282
39	1	65.0	177.0	0.096	1.0	16.0	0.0	17.0	0.266
40	1	65.0	203.0	0.096	1.0	16.0	0.0	17.0	0.266
41	1	65.0	218.0	0.096	1.0	16.0	0.0	17.0	0.261
42	1	65.0	123.0	0.096	1.0	16.0	0.0	17.0	0.282
43	1	45.0	250.0	0.096	1.0	16.0	0.0	25.0	0.250
44	1	65.0	242.0	0.096	1.0	16.0	0.0	25.0	0.282
45	1	65.0	134.0	0.096	1.0	16.0	0.0	25.0	0.234

Table 7.4 Continued

Test No.	Flow Direction	Inlet Temp °C	Heat Flux W/cm²	Channel Thickness inch	Channel Width inch	Heated Length inch	Minor Loss Coeff	Exit Pressure psia	$\Delta T_{sub,o}/\Delta T_c$
46	1	55.0	200.0	0.096	1.0	16.0	0.0	25.0	0.266
47	1	55.0	180.0	0.096	1.0	16.0	0.0	25.0	0.282
48	1	55.0	177.0	0.080	1.0	16.0	0.0	17.0	0.266
49	1	55.0	218.0	0.080	1.0	16.0	0.0	17.0	0.266
50	1	55.0	276.0	0.080	1.0	16.0	0.0	17.0	0.266
51	1	65.0	141.0	0.080	1.0	16.0	0.0	17.0	0.250
52	1	65.0	218.0	0.080	1.0	16.0	0.0	17.0	0.250
53	1	65.0	300.0	0.080	1.0	16.0	0.0	17.0	0.250
54	1	65.0	110.0	0.080	1.0	16.0	0.0	17.0	0.250
55	1	45.0	221.0	0.080	1.0	16.0	0.0	17.0	0.266
56	1	45.0	289.0	0.080	1.0	16.0	0.0	17.0	0.234
57	1	35.0	283.0	0.080	1.0	16.0	0.0	17.0	0.282
58	1	35.0	219.0	0.080	1.0	16.0	0.0	17.0	0.266
59	1	35.0	183.0	0.080	1.0	16.0	0.0	17.0	0.266
60	1	55.0	93.0	0.080	1.0	16.0	0.0	17.0	0.250
61	1	75.0	223.0	0.080	1.0	16.0	0.0	17.0	0.250
62	1	55.0	66.0	0.080	1.0	16.0	0.0	17.0	0.282
63	1	55.0	170.0	0.055	1.0	21.0	0.0	17.0	0.163
64	1	55.0	93.0	0.055	1.0	21.0	0.0	17.0	0.163
65	1	55.0	130.0	0.055	1.0	21.0	0.0	17.0	0.163
66	1	45.0	127.0	0.055	1.0	21.0	0.0	17.0	0.190
67	1	45.0	176.0	0.055	1.0	21.0	0.0	17.0	0.163
68	1	45.0	67.0	0.055	1.0	21.0	0.0	17.0	0.163
69	1	45.0	226.0	0.055	1.0	21.0	0.0	17.0	0.177
70	1	35.0	122.0	0.055	1.0	21.0	0.0	17.0	0.177
71	1	65.0	119.0	0.055	1.0	21.0	0.0	17.0	0.149
72	1	65.0	98.0	0.055	1.0	21.0	0.0	17.0	0.136
73	1	65.0	83.0	0.055	1.0	21.0	0.0	17.0	0.163
74	1	35.0	187.0	0.055	1.0	21.0	0.0	17.0	0.163
75	1	55.0	186.0	0.127	0.399	24.0	0.0	17.0	0.351
76	1	55.0	262.0	0.127	0.399	24.0	0.0	17.0	0.351
77	1	55.0	140.0	0.127	0.399	24.0	0.0	17.0	0.315
78	1	45.0	148.0	0.127	0.399	24.0	0.0	17.0	0.315
79	1	45.0	270.0	0.127	0.399	24.0	0.0	17.0	0.351
80	1	45.0	348.0	0.127	0.399	24.0	0.0	17.0	0.389
81	1	65.0	86.0	0.127	0.399	24.0	0.0	17.0	0.315
82	1	65.0	178.0	0.127	0.399	24.0	0.0	17.0	0.351
83	1	65.0	340.0	0.127	0.399	24.0	0.0	17.0	0.428

*** 1 implies upward flow, 0 implies downward flow.**

Table 7.5 Exit Temperature and Pressure Drop at Different Inlet Velocities Calculated in the Application ofBabelli and Ishii Flow Instability Criterion to a Typical Whittle and Forgan Test (Number 1)

```
Whittle & Forgan Test Numner                  =   1
Hydraulic diameter (heated), m                =     0.00645
Hydraulic diameter (wetted), m                =     0.00572
Channel heated length, m                      =      0.6096
Total minor loss coefficient                  =      0.0000
Inlet temperature, C                          =      55.000
Power removed by the channel, W               = 3.22064E+04
Pressure at heated section exit, Pa           = 1.17211E+05
Saturation temperature at exit, C             =     104.131
Channel flow area, m**2                       = 8.19353E-05
Heated perimeter, m                           =     0.05080
Measured ratio of exit subcooling-to-coolant
temp rise, at flow instability                =       0.224
Measured coolant velocity at OFI, m/s         =       2.361
Measured flow rate at OFI, kg/s               =       0.191
```

Inlet Vel, m/s	Inlet Temp, C	Exit Temp, C	Friction Factor	Beta per C	Total Press Drop, Pa	Friction Drop, Pa	Orifice Drop, Pa	Mom Change Drop, Pa	Gravity Drop, Pa	Reynolds Number	Inlet Press, Pa
2.500	55.00	92.92	0.0224	6.10E-04	13394.79	7423.94	0.00	146.79	5824.05	36997.61	130605.45
2.510	55.00	92.77	0.0224	6.09E-04	13449.43	7477.80	0.00	147.25	5824.37	37111.60	130660.09
2.520	55.00	92.62	0.0224	6.09E-04	13504.25	7531.84	0.00	147.71	5824.69	37225.56	130714.91
2.530	55.00	92.48	0.0223	6.08E-04	13559.23	7586.05	0.00	148.17	5825.01	37339.53	130769.90
2.540	55.00	92.33	0.0223	6.08E-04	13614.39	7640.44	0.00	148.63	5825.32	37453.46	130825.05
2.550	55.00	92.18	0.0223	6.08E-04	13669.72	7695.00	0.00	149.09	5825.63	37567.41	130880.38
2.560	55.00	92.04	0.0223	6.07E-04	13725.22	7749.73	0.00	149.55	5825.94	37681.32	130935.88
2.570	55.00	91.89	0.0223	6.07E-04	13780.88	7804.63	0.00	150.01	5826.25	37795.24	130991.55
2.580	55.00	91.75	0.0223	6.06E-04	13836.72	7859.70	0.00	150.47	5826.55	37909.12	131047.38
2.590	55.00	91.61	0.0222	6.06E-04	13892.73	7914.95	0.00	150.93	5826.85	38023.02	131103.39
2.600	55.00	91.47	0.0222	6.06E-04	13948.90	7970.38	0.00	151.38	5827.14	38136.90	131159.56
2.610	55.00	91.33	0.0222	6.05E-04	14005.25	8025.97	0.00	151.84	5827.44	38250.74	131215.91
2.620	55.00	91.19	0.0222	6.05E-04	14061.76	8081.73	0.00	152.30	5827.73	38364.60	131272.42
2.630	55.00	91.06	0.0222	6.04E-04	14118.53	8137.75	0.00	152.76	5828.02	38478.44	131329.19
2.640	55.00	90.92	0.0222	6.04E-04	14175.39	8193.86	0.00	153.22	5828.31	38592.26	131386.05
2.650	55.00	90.79	0.0222	6.04E-04	14232.41	8250.15	0.00	153.68	5828.59	38706.09	131443.08
2.660	55.00	90.65	0.0221	6.03E-04	14289.60	8306.60	0.00	154.13	5828.87	38819.89	131500.27
2.670	55.00	90.52	0.0221	6.03E-04	14346.97	8363.22	0.00	154.59	5829.15	38933.69	131557.62
2.680	55.00	90.39	0.0221	6.02E-04	14404.50	8420.02	0.00	155.05	5829.43	39047.47	131615.16
2.690	55.00	90.26	0.0221	6.02E-04	14462.20	8476.99	0.00	155.51	5829.70	39161.25	131672.86
2.700	55.00	90.13	0.0221	6.02E-04	14520.07	8534.13	0.00	155.97	5829.98	39275.00	131730.73
2.710	55.00	90.00	0.0221	6.01E-04	14578.11	8591.44	0.00	156.42	5830.25	39388.77	131788.78
2.711	55.00	89.98	0.0221	6.01E-04	14583.92	8597.18	0.00	156.47	5830.27	39400.14	131794.58
2.712	55.00	89.97	0.0221	6.01E-04	14589.74	8602.92	0.00	156.52	5830.30	39411.52	131800.41
2.713	55.00	89.96	0.0221	6.01E-04	14595.55	8608.67	0.00	156.56	5830.33	39422.89	131806.22
2.714	55.00	89.95	0.0221	6.01E-04	14601.37	8614.41	0.00	156.61	5830.35	39434.27	131812.03
2.715	55.00	89.93	0.0221	6.01E-04	14607.19	8620.16	0.00	156.65	5830.38	39445.64	131817.86

Table 7.5 Continued

Inlet Vel, m/s	Inlet Temp, C	Exit Temp, C	Friction Factor	Beta per C	Total Press Drop, Pa	Friction Drop, Pa	Orifice Drop, Pa	Mom Change Drop, Pa	Gravity Drop, Pa	Reynolds Number	Inlet Press, Pa
2.716	55.00	89.92	0.0221	6.01E-04	14613.01	8625.91	0.00	156.70	5830.41	39457.02	131823.67
2.717	55.00	89.91	0.0221	6.01E-04	14618.84	8631.66	0.00	156.75	5830.43	39468.39	131829.50
2.718	55.00	89.89	0.0221	6.01E-04	14624.66	8637.41	0.00	156.79	5830.46	39479.77	131835.33
2.719	55.00	89.88	0.0221	6.01E-04	14630.49	8643.17	0.00	156.84	5830.49	39491.13	131841.16
2.720	55.00	89.87	0.0220	6.01E-04	14636.31	8648.92	0.00	156.88	5830.51	39502.51	131846.98
2.730	55.00	89.74	0.0220	6.00E-04	14694.69	8706.57	0.00	157.34	5830.78	39616.23	131905.36
2.740	55.00	89.62	0.0220	6.00E-04	14753.23	8764.39	0.00	157.80	5831.04	39729.97	131963.89
2.750	55.00	89.49	0.0220	6.00E-04	14811.95	8822.39	0.00	158.25	5831.30	39843.68	132022.61
2.760	55.00	89.37	0.0220	5.99E-04	14870.82	8880.55	0.00	158.71	5831.56	39957.39	132081.48
2.770	55.00	89.24	0.0220	5.99E-04	14929.87	8938.88	0.00	159.17	5831.82	40071.08	132140.53
2.780	55.00	89.12	0.0220	5.99E-04	14989.09	8997.38	0.00	159.63	5832.08	40184.77	132199.75
2.790	55.00	89.00	0.0219	5.98E-04	15048.47	9056.06	0.00	160.08	5832.33	40298.44	132259.12
2.800	55.00	88.88	0.0219	5.98E-04	15108.02	9114.90	0.00	160.54	5832.58	40412.11	132318.69
2.810	55.00	88.76	0.0219	5.98E-04	15167.74	9173.91	0.00	161.00	5832.83	40525.75	132378.41
2.820	55.00	88.64	0.0219	5.97E-04	15227.62	9233.09	0.00	161.46	5833.08	40639.43	132438.28
2.830	55.00	88.52	0.0219	5.97E-04	15287.68	9292.44	0.00	161.91	5833.32	40753.07	132498.34
2.840	55.00	88.40	0.0219	5.96E-04	15347.90	9351.96	0.00	162.37	5833.56	40866.69	132558.56
2.850	55.00	88.28	0.0219	5.96E-04	15408.28	9411.65	0.00	162.83	5833.80	40980.31	132618.95

Table 7.6 Application of Babelli and Ishii Flow Instability Criterion to a Typical Whittle and Forgan Test (Number 1)

Inlet Vel, m/s	Exit Temp, C	Tot Press Drop, Pa	Exit Press Pa	Peclet Number	Inlet Subc J/kg	Subcool Number	Zuber Number	Nsub/Nzu	RHS of Eq. (7.1)	Stable?	Critical Lnvg/L	0.0022Pe or 154.0	
2.500	92.92	13394.79	117210.66	87332.46	206803.64	129.41	99.75	1.297	1.407	unstable	1.000	154.000	
2.510	92.77	13449.43	117210.66	87689.20	206803.64	129.41	99.35	1.303	1.407	unstable	1.000	154.000	
2.520	92.62	13504.25	117210.66	88046.04	206803.64	129.41	98.96	1.308	1.407	unstable	1.000	154.000	
2.530	92.48	13559.23	117210.66	88402.89	206803.64	129.41	98.57	1.313	1.407	unstable	1.000	154.000	
2.540	92.33	13614.39	117210.66	88759.84	206803.64	129.41	98.18	1.318	1.407	unstable	1.000	154.000	
2.550	92.18	13669.72	117210.66	89116.76	206803.64	129.41	97.79	1.323	1.407	unstable	1.000	154.000	
2.560	92.04	13725.22	117210.66	89473.73	206803.64	129.41	97.41	1.328	1.407	unstable	1.000	154.000	
2.570	91.89	13780.88	117210.66	89830.73	206803.64	129.41	97.03	1.334	1.407	unstable	1.000	154.000	
2.580	91.75	13836.72	117210.66	90187.84	206803.64	129.41	96.65	1.339	1.407	unstable	1.000	154.000	
2.590	91.61	13892.73	117210.66	90544.95	206803.64	129.41	96.28	1.344	1.407	unstable	1.000	154.000	
2.600	91.47	13948.90	117210.66	90902.08	206803.64	129.41	95.91	1.349	1.407	unstable	1.000	154.000	
2.610	91.33	14005.25	117210.66	91259.28	206803.64	129.41	95.54	1.354	1.407	unstable	1.000	154.000	
2.620	91.19	14061.76	117210.66	91616.52	206803.64	129.41	95.18	1.360	1.407	unstable	1.000	154.000	Eq. (7.5)
2.630	91.06	14118.53	117210.66	91973.76	206803.64	129.41	94.82	1.365	1.407	unstable	1.000	154.000	
2.640	90.92	14175.39	117210.66	92331.06	206803.64	129.41	94.46	1.370	1.407	unstable	1.000	154.000	
2.650	90.79	14232.41	117210.66	92688.41	206803.64	129.41	94.10	1.375	1.407	unstable	1.000	154.000	
2.660	90.65	14289.60	117210.66	93045.74	206803.64	129.41	93.75	1.380	1.407	unstable	1.000	154.000	
2.670	90.52	14346.97	117210.66	93403.16	206803.64	129.41	93.40	1.386	1.407	unstable	1.000	154.000	
2.680	90.39	14404.50	117210.66	93760.57	206803.64	129.41	93.05	1.391	1.407	unstable	1.000	154.000	
2.690	90.26	14462.20	117210.66	94118.10	206803.64	129.41	92.70	1.396	1.407	unstable	1.000	154.000	
2.700	90.13	14520.07	117210.66	94475.60	206803.64	129.41	92.36	1.401	1.407	unstable	1.000	154.000	
2.710	90.00	14578.11	117210.66	94833.12	206803.64	129.41	92.02	1.406	1.407	unstable	1.000	154.000	
2.710	90.00	14578.11	117210.66	94833.12	206803.64	129.41	92.02	1.406	1.407	unstable	1.000	154.000	
2.711	89.98	14583.92	117210.66	94868.88	206803.64	129.41	91.98	1.407	1.407	unstable	1.000	154.000	
2.712	**89.97**	**14589.74**	**117210.66**	**94904.67**	**206803.64**	**129.41**	**91.95**	**1.407**	**1.407**	**unstable**	**1.000**	**154.000**	**Eq. (7.1)**
2.713	89.96	14595.55	117210.66	94940.33	206803.64	129.41	91.92	1.408	1.407	stable	1.000	154.000	
2.714	89.95	14601.37	117210.66	94976.14	206803.64	129.41	91.88	1.408	1.407	stable	1.000	154.000	
2.715	89.93	14607.19	117210.66	95011.90	206803.64	129.41	91.85	1.409	1.407	stable	1.000	154.000	
2.716	89.92	14613.01	117210.66	95047.68	206803.64	129.41	91.82	1.409	1.407	stable	1.000	154.000	
2.717	89.91	14618.84	117210.66	95083.46	206803.64	129.41	91.78	1.410	1.407	stable	1.000	154.000	
2.718	89.89	14624.66	117210.66	95119.23	206803.64	129.41	91.75	1.410	1.407	stable	1.000	154.000	
2.719	89.88	14630.49	117210.66	95154.93	206803.64	129.41	91.71	1.411	1.407	stable	1.000	154.000	
2.720	89.87	14636.32	117210.66	95190.72	206803.64	129.41	91.68	1.412	1.407	stable	1.000	154.000	
2.720	89.87	14636.31	117210.66	95190.69	206803.64	129.41	91.68	1.412	1.407	stable	1.000	154.000	
2.730	89.74	14694.69	117210.66	95548.28	206803.64	129.41	91.34	1.417	1.407	stable	1.000	154.000	
2.740	89.62	14753.23	117210.66	95905.96	206803.64	129.41	91.01	1.422	1.407	stable	1.000	154.000	
2.750	89.49	14811.95	117210.66	96263.64	206803.64	129.41	90.68	1.427	1.407	stable	1.000	154.000	
2.760	89.37	14870.82	117210.66	96621.38	206803.64	129.41	90.35	1.432	1.407	stable	1.000	154.000	
2.770	89.24	14929.87	117210.66	96979.12	206803.64	129.41	90.03	1.437	1.407	stable	1.000	154.000	
2.780	89.12	14989.09	117210.66	97336.86	206803.64	129.41	89.70	1.443	1.407	stable	1.000	154.000	
2.790	89.00	15048.47	117210.66	97694.67	206803.64	129.41	89.38	1.448	1.407	stable	1.000	154.000	
2.800	88.88	15108.02	117210.66	98052.58	206803.64	129.41	89.06	1.453	1.407	stable	1.000	154.000	
2.810	88.76	15167.74	117210.66	98410.45	206803.64	129.41	88.74	1.458	1.407	stable	1.000	154.000	
2.820	88.64	15227.62	117210.66	98768.30	206803.64	129.41	88.43	1.463	1.407	stable	1.000	154.000	
2.830	88.52	15287.68	117210.66	99126.25	206803.64	129.41	88.12	1.469	1.407	stable	1.000	154.000	
2.840	88.40	15347.90	117210.66	99484.29	206803.64	129.41	87.81	1.474	1.407	stable	1.000	154.000	
2.850	88.28	15408.28	117210.66	99842.28	206803.64	129.41	87.50	1.479	1.407	stable	1.000	154.000	

The underlined line marks the flow instability predicted by the simple criterion of Eq. (7.5).

Table 7.7 Comparison of Coolant Inlet Velocity at OFI Calculated Using Eq. (7.1) Versus its Measured Value in 75 Tests Reported by Whittle and Forgan

Test No.	Calc. Inlet Vel,m/s	Inlet Temp C	Heat Flux W/cm^2	L/D_H Ratio	Exit Press psia	Exit Temp C	Ratio $\Delta T_c/\Delta T_{sat}$	η W&F	Measured at OFI Inlet Vel,m/s	Measured at OFI Flow kg/s	Peclet Number	Subcool Number	Zuber Number	Ratio N_{sub}/N_{zub}
1	2.712	55.000	104.000	94.488	17.000	89.971	0.712	38.260	2.361	0.1908	94905.	129.406	91.950	1.407
2	3.781	55.000	145.000	94.488	17.000	89.974	0.712	38.248	3.406	0.2752	132314.	129.402	91.954	1.407
3	4.798	55.000	184.000	94.488	17.000	89.975	0.712	38.244	4.164	0.3365	167903.	129.397	91.953	1.407
4	6.520	55.000	250.000	94.488	17.000	89.975	0.712	38.246	5.872	0.4745	228166.	129.384	91.938	1.407
5	2.138	55.000	82.000	94.488	17.000	89.976	0.712	38.240	1.902	0.1537	74818.	129.406	91.964	1.407
6	3.546	55.000	136.000	94.488	17.000	89.977	0.712	38.236	3.154	0.2549	124090.	129.402	91.962	1.407
7	4.172	55.000	160.000	94.488	17.000	89.977	0.712	38.238	3.806	0.3075	145996.	129.397	91.957	1.407
8	5.216	55.000	200.000	94.488	17.000	89.972	0.712	38.257	4.697	0.3796	182532.	129.393	91.939	1.407
9	3.455	45.000	160.000	94.488	17.000	87.105	0.712	38.210	3.073	0.2494	121664.	155.577	110.556	1.407
10	3.887	45.000	180.000	94.488	17.000	87.103	0.712	38.214	3.457	0.2806	136876.	155.577	110.552	1.407
11	4.405	45.000	204.000	94.488	17.000	87.107	0.712	38.201	3.868	0.3139	155117.	155.572	110.559	1.407
12	3.200	60.000	110.000	94.488	17.000	91.406	0.712	38.284	2.845	0.2293	111606.	116.295	82.629	1.407
13	4.654	60.000	160.000	94.488	17.000	91.412	0.712	38.262	4.138	0.3336	162317.	116.290	82.638	1.407
14	5.236	60.000	180.000	94.488	17.000	91.412	0.712	38.261	4.715	0.3801	182616.	116.286	82.634	1.407
15	5.818	60.000	200.000	94.488	17.000	91.410	0.712	38.267	4.982	0.4016	202915.	116.286	82.631	1.407
16	2.505	35.000	136.000	94.488	17.000	84.247	0.712	38.152	2.229	0.1816	88704.	181.713	129.155	1.407
25	1.684	45.000	78.000	94.488	17.000	87.108	0.712	38.200	1.517	0.1232	59299.	155.590	110.578	1.407
26	2.505	45.000	116.000	94.488	17.000	87.100	0.712	38.226	2.257	0.1832	88210.	155.585	110.551	1.407
27	3.196	45.000	148.000	94.488	17.000	87.100	0.712	38.225	2.843	0.2307	112543.	155.585	110.552	1.407
28	2.998	55.000	115.000	94.488	17.000	89.979	0.712	38.228	2.701	0.2183	104912.	129.410	91.977	1.407
29	1.955	55.000	75.000	94.488	17.000	89.982	0.712	38.219	1.762	0.1424	68413.	129.415	91.987	1.407
30	3.807	55.000	146.000	94.488	17.000	89.973	0.712	38.251	3.386	0.2736	133223.	129.406	91.956	1.407
31	0.907	45.000	42.000	94.488	17.000	87.097	0.712	38.233	0.827	0.0672	31939.	155.590	110.550	1.407
32	3.512	55.000	147.000	83.333	17.000	88.671	0.685	38.263	3.084	0.1884	95608.	129.402	88.514	1.462
33	4.061	55.000	170.000	83.333	17.000	88.675	0.685	38.249	3.566	0.2178	110553.	129.402	88.525	1.462
34	4.300	55.000	180.000	83.333	17.000	88.674	0.685	38.252	3.776	0.2307	117060.	129.402	88.522	1.462
35	5.136	55.000	215.000	83.333	17.000	88.676	0.685	38.244	4.454	0.2721	139819.	129.397	88.524	1.462
36	3.878	45.000	196.000	83.333	17.000	85.534	0.685	38.233	3.406	0.2090	106263.	155.577	106.414	1.462
37	4.946	45.000	250.000	83.333	17.000	85.539	0.686	38.218	4.344	0.2665	135528.	155.572	106.423	1.462
38	3.561	45.000	180.000	83.333	17.000	85.539	0.686	38.218	3.128	0.1919	97576.	155.577	106.427	1.462
39	5.331	65.000	177.000	83.333	17.000	91.812	0.685	38.288	4.621	0.2808	144098.	103.170	70.576	1.462
40	6.115	65.000	203.000	83.333	17.000	91.810	0.685	38.299	5.300	0.3221	165290.	103.166	70.566	1.462
41	6.566	65.000	218.000	83.333	17.000	91.813	0.685	38.284	5.669	0.3445	177481.	103.166	70.575	1.462
42	3.704	65.000	123.000	83.333	17.000	91.813	0.685	38.283	3.252	0.1976	100119.	103.179	70.588	1.462
43	4.137	45.000	250.000	83.333	25.000	93.422	0.686	38.159	3.543	0.2174	112790.	130.125	89.009	1.462
44	5.629	65.000	242.000	83.333	25.000	99.683	0.686	38.231	4.943	0.3004	151549.	93.463	63.930	1.462
45	3.116	65.000	134.000	83.333	25.000	99.690	0.686	38.207	2.634	0.1601	83891.	93.469	63.949	1.462

Table 7.7 Continued

Test No.	Calc. Inlet Vel,m/s	Inlet Temp C	Heat Flux W/cm^2	L/D_H Ratio	Exit Press psia	Exit Temp C	Ratio $\Delta T_c/\Delta T_{sat}$	η W&F	Measured at OFI Inlet Vel,m/s	Measured at OFI Flow kg/s	Peclet Number	Subcool Number	Zuber Number	Ratio N_{sub}/N_{zub}
46	3.868	55.000	200.000	83.333	25.000	96.556	0.686	38.180	3.355	0.2050	104826.	111.814	76.493	1.462
47	3.481	55.000	180.000	83.333	25.000	96.558	0.686	38.173	3.058	0.1868	94338.	111.814	76.497	1.462
48	4.807	55.000	177.000	100.000	17.000	90.538	0.723	38.249	4.400	0.2240	110537.	129.397	93.439	1.385
49	5.921	55.000	218.000	100.000	17.000	90.538	0.723	38.249	5.419	0.2759	136154.	129.389	93.430	1.385
50	7.497	55.000	276.000	100.000	17.000	90.540	0.723	38.244	6.861	0.3493	172396.	129.376	93.421	1.385
51	4.828	65.000	141.000	100.000	17.000	93.296	0.723	38.295	4.361	0.2209	110269.	103.170	74.495	1.385
52	7.466	65.000	218.000	100.000	17.000	93.296	0.723	38.291	6.743	0.3415	170522.	103.153	74.480	1.385
53	10.276	65.000	300.000	100.000	17.000	93.299	0.723	38.276	9.279	0.4699	234706.	103.131	74.466	1.385
54	3.766	65.000	110.000	100.000	17.000	93.298	0.723	38.283	3.402	0.1723	86013.	103.175	74.506	1.385
55	4.971	45.000	221.000	100.000	17.000	87.779	0.723	38.226	4.550	0.2327	115013.	155.568	112.326	1.385
56	6.500	45.000	289.000	100.000	17.000	87.785	0.724	38.205	5.799	0.2965	150390.	155.559	112.334	1.385
57	5.430	35.000	283.000	100.000	17.000	85.033	0.724	38.172	5.035	0.2584	126321.	181.699	131.215	1.385
58	4.202	35.000	219.000	100.000	17.000	85.032	0.724	38.175	3.848	0.1974	97753.	181.704	131.216	1.385
59	3.511	35.000	183.000	100.000	17.000	85.034	0.724	38.169	3.215	0.1650	81677.	181.708	131.226	1.385
60	2.369	55.000	93.000	100.000	17.000	92.875	0.771	29.718	2.282	0.1162	54400.	129.406	99.621	1.299
61	10.311	75.000	223.000	100.000	17.000	96.062	0.723	38.311	9.308	0.4686	233771.	76.856	55.494	1.385
62	1.546	55.000	66.000	100.000	17.000	96.172	0.838	19.331	1.661	0.0846	35439.	129.406	108.335	1.195
63	7.651	55.000	170.000	190.909	17.000	95.934	0.833	38.233	7.408	0.2593	123456.	129.341	107.638	1.202
64	4.154	55.000	93.000	190.909	17.000	96.226	0.839	36.608	4.053	0.1418	67016.	129.389	108.460	1.193
65	5.849	55.000	130.000	190.909	17.000	95.937	0.833	38.215	5.665	0.1983	94377.	129.367	107.673	1.201
66	4.732	45.000	127.000	190.909	17.000	94.269	0.833	38.214	4.691	0.1649	76753.	155.555	129.453	1.202
67	6.558	45.000	176.000	190.909	17.000	94.275	0.833	38.189	6.352	0.2233	106373.	155.533	129.445	1.202
68	2.300	45.000	67.000	190.909	17.000	98.442	0.904	20.323	2.418	0.0850	37229.	155.577	140.510	1.107
69	8.423	45.000	226.000	190.909	17.000	94.274	0.833	38.193	8.255	0.2902	136627.	155.503	129.412	1.202
70	3.803	35.000	122.000	190.909	17.000	93.738	0.850	33.779	3.803	0.1341	61920.	181.695	154.190	1.178
71	6.751	65.000	119.000	190.909	17.000	97.600	0.833	38.249	6.457	0.2248	108283.	103.131	85.836	1.201
72	5.559	65.000	98.000	190.909	17.000	97.597	0.833	38.266	5.257	0.1830	89163.	103.149	85.847	1.202
73	4.708	65.000	83.000	190.909	17.000	97.595	0.833	38.281	4.559	0.1587	75513.	103.157	85.850	1.202
74	5.945	35.000	187.000	190.909	17.000	92.610	0.833	38.178	5.759	0.2032	96859.	181.669	151.183	1.202
75	4.851	55.000	186.000	94.488	17.000	89.971	0.712	38.261	4.663	0.1504	145126.	129.393	91.936	1.407
76	6.833	55.000	262.000	94.488	17.000	89.976	0.712	38.241	6.569	0.2118	204422.	129.380	91.937	1.407
77	3.651	55.000	140.000	94.488	17.000	89.972	0.712	38.256	3.416	0.1102	109225.	129.397	91.944	1.407
78	3.196	45.000	148.000	94.488	17.000	87.103	0.712	38.215	2.991	0.0969	96212.	155.577	110.552	1.407
79	5.831	45.000	270.000	94.488	17.000	87.106	0.712	38.206	5.607	0.1816	175538.	155.559	110.542	1.407
80	7.517	45.000	348.000	94.488	17.000	87.102	0.712	38.218	7.431	0.2407	226297.	155.546	110.519	1.407
81	2.827	65.000	86.000	94.488	17.000	92.848	0.712	38.284	2.645	0.0848	83993.	103.179	73.321	1.407
82	5.853	65.000	178.000	94.488	17.000	92.846	0.712	38.295	5.624	0.1804	173901.	103.162	73.298	1.407
83	11.184	65.000	340.000	94.488	17.000	92.853	0.712	38.262	11.357	0.3643	332305.	103.114	73.268	1.407

Mean error in calculated inlet velocity at OFI, m/s = 0.384
Standard deviation of the error in calculated inlet velocity at OFI, m/s = 0.242

Table 7.8 Comparison of Coolant Inlet Velocity at OFI Calculated Using Eq. (7.5) Versus its Measured Value in 75 Tests Reported by Whittle and Forgan

Test No.	Calc. Inlet Vel,m/s	Inlet Temp C	Heat Flux W/cm^2	L/D_H Ratio	Exit Press psia	Exit Temp C	Ratio $\Delta T_c/\Delta T_{sat}$	η W&F	Measured at OFI Inlet Vel,m/s	Measured at OFI Flow kg/s	Peclet Number	Subcool Number	Zuber Number	Ratio N_{sub}/N_{zub}
1	2.620	55.000	104.000	94.488	17.000	91.194	0.737	33.775	2.361	0.1908	91617.	129.406	95.179	1.360
2	3.654	55.000	145.000	94.488	17.000	91.184	0.736	33.808	3.406	0.2752	127775.	129.402	95.150	1.360
3	4.637	55.000	184.000	94.488	17.000	91.184	0.736	33.808	4.164	0.3365	162149.	129.397	95.145	1.360
4	6.300	55.000	250.000	94.488	17.000	91.189	0.737	33.792	5.872	0.4745	220303.	129.389	95.149	1.360
5	2.066	55.000	82.000	94.488	17.000	91.190	0.737	33.789	1.902	0.1537	72244.	129.406	95.169	1.360
6	3.427	55.000	136.000	94.488	17.000	91.187	0.737	33.801	3.154	0.2549	119837.	129.402	95.155	1.360
7	4.032	55.000	160.000	94.488	17.000	91.186	0.737	33.802	3.806	0.3075	140993.	129.397	95.150	1.360
8	5.040	55.000	200.000	94.488	17.000	91.188	0.737	33.797	4.697	0.3796	176241.	129.393	95.149	1.360
9	3.339	45.000	160.000	94.488	17.000	88.560	0.737	33.776	3.073	0.2494	117464.	155.577	114.397	1.360
10	3.756	45.000	180.000	94.488	17.000	88.565	0.737	33.763	3.457	0.2806	132134.	155.577	114.408	1.360
11	4.257	45.000	204.000	94.488	17.000	88.562	0.737	33.769	3.868	0.3139	149759.	155.577	114.403	1.360
12	3.092	60.000	110.000	94.488	17.000	92.499	0.736	33.820	2.845	0.2293	107770.	116.295	85.515	1.360
13	4.497	60.000	160.000	94.488	17.000	92.504	0.737	33.801	4.138	0.3336	156741.	116.290	85.523	1.360
14	5.060	60.000	180.000	94.488	17.000	92.500	0.736	33.817	4.715	0.3801	176365.	116.286	85.508	1.360
15	5.622	60.000	200.000	94.488	17.000	92.501	0.736	33.812	4.982	0.4016	195954.	116.286	85.512	1.360
16	2.421	35.000	136.000	94.488	17.000	85.946	0.737	33.728	2.229	0.1816	85623.	181.713	133.636	1.360
25	1.627	45.000	78.000	94.488	17.000	88.576	0.737	33.729	1.517	0.1232	57236.	155.590	114.452	1.359
26	2.420	45.000	116.000	94.488	17.000	88.570	0.737	33.748	2.257	0.1832	85133.	155.590	114.434	1.360
27	3.088	45.000	148.000	94.488	17.000	88.565	0.737	33.761	2.843	0.2307	108633.	155.585	114.419	1.360
28	2.897	55.000	115.000	94.488	17.000	91.194	0.737	33.775	2.701	0.2183	101302.	129.410	95.183	1.360
29	1.889	55.000	75.000	94.488	17.000	91.199	0.737	33.757	1.762	0.1424	66054.	129.415	95.201	1.359
30	3.679	55.000	146.000	94.488	17.000	91.185	0.736	33.806	3.386	0.2736	128648.	129.406	95.155	1.360
31	0.876	45.000	42.000	94.488	17.000	88.578	0.737	33.723	0.827	0.0672	30816.	155.594	114.462	1.359
32	3.267	55.000	147.000	83.333	17.000	91.184	0.736	29.819	3.084	0.1884	88798.	129.406	95.152	1.360
33	3.778	55.000	170.000	83.333	17.000	91.187	0.737	29.809	3.566	0.2178	102688.	129.402	95.156	1.360
34	4.000	55.000	180.000	83.333	17.000	91.189	0.737	29.803	3.776	0.2307	108721.	129.402	95.162	1.360
35	4.778	55.000	215.000	83.333	17.000	91.189	0.737	29.803	4.454	0.2721	129868.	129.397	95.157	1.360
36	3.607	45.000	196.000	83.333	17.000	88.565	0.737	29.776	3.406	0.2090	98631.	155.577	114.410	1.360
37	4.601	45.000	250.000	83.333	17.000	88.563	0.737	29.782	4.344	0.2665	125812.	155.577	114.403	1.360
38	3.312	45.000	180.000	83.333	17.000	88.571	0.737	29.761	3.128	0.1919	90564.	155.581	114.429	1.360
39	4.959	65.000	177.000	83.333	17.000	93.815	0.736	29.837	4.621	0.2808	133891.	103.175	75.871	1.360
40	5.688	65.000	203.000	83.333	17.000	93.813	0.736	29.842	5.300	0.3221	153574.	103.170	75.863	1.360
41	6.108	65.000	218.000	83.333	17.000	93.816	0.736	29.830	5.669	0.3445	164914.	103.166	75.867	1.360
42	3.446	65.000	123.000	83.333	17.000	93.814	0.736	29.840	3.252	0.1976	93040.	103.179	75.873	1.360
43	3.848	45.000	250.000	83.333	25.000	97.037	0.737	29.720	3.543	0.2174	104716.	130.125	95.694	1.360
44	5.236	65.000	242.000	83.333	25.000	102.274	0.737	29.782	4.943	0.3004	140825.	93.463	68.729	1.360
45	2.899	65.000	134.000	83.333	25.000	102.274	0.737	29.781	2.634	0.1601	77969.	93.469	68.736	1.360

Table 7-8 Continued

Test No.	Calc. Inlet Vel,m/s	Inlet Temp C	Heat Flux W/cm^2	L/D_H Ratio	Exit Press psia	Exit Temp C	Ratio $\Delta T_c/\Delta T_{sat}$	η W&F	Measured at OFI Inlet Vel,m/s	Measured at OFI Flow kg/s	Peclet Number	Subcool Number	Zuber Number	Ratio N_{sub}/N_{zub}
46	3.598	55.000	200.000	83.333	25.000	99.657	0.737	29.741	3.355	0.2050	97372.	111.814	82.233	1.360
47	3.238	55.000	180.000	83.333	25.000	99.660	0.737	29.734	3.058	0.1868	87629.	111.814	82.238	1.360
48	4.720	55.000	177.000	100.000	17.000	91.190	0.737	35.758	4.400	0.2240	108494.	129.397	95.161	1.360
49	5.814	55.000	218.000	100.000	17.000	91.189	0.737	35.762	5.419	0.2759	133641.	129.389	95.150	1.360
50	7.362	55.000	276.000	100.000	17.000	91.187	0.737	35.772	6.861	0.3493	169225.	129.380	95.134	1.360
51	4.741	65.000	141.000	100.000	17.000	93.813	0.736	35.812	4.361	0.2209	108251.	103.170	75.862	1.360
52	7.331	65.000	218.000	100.000	17.000	93.814	0.736	35.808	6.743	0.3415	167391.	103.157	75.851	1.360
53	10.090	65.000	300.000	100.000	17.000	93.819	0.736	35.783	9.279	0.4699	230392.	103.131	75.839	1.360
54	3.698	65.000	110.000	100.000	17.000	93.816	0.736	35.795	3.402	0.1723	84436.	103.175	75.876	1.360
55	4.881	45.000	221.000	100.000	17.000	88.562	0.737	35.741	4.550	0.2327	112872.	155.572	114.397	1.360
56	6.383	45.000	289.000	100.000	17.000	88.565	0.737	35.730	5.799	0.2965	147606.	155.559	114.393	1.360
57	5.332	35.000	283.000	100.000	17.000	85.947	0.737	35.691	5.035	0.2584	123959.	181.699	133.627	1.360
58	4.126	35.000	219.000	100.000	17.000	85.948	0.737	35.689	3.848	0.1974	95921.	181.704	133.633	1.360
59	3.448	35.000	183.000	100.000	17.000	85.943	0.737	35.703	3.215	0.1650	80159.	181.708	133.624	1.360
60	2.480	55.000	93.000	100.000	17.000	91.187	0.737	35.769	2.282	0.1162	57005.	129.406	95.162	1.360
61	10.125	75.000	223.000	100.000	17.000	96.448	0.736	35.825	9.308	0.4686	229510.	76.856	56.514	1.360
62	1.760	55.000	66.000	100.000	17.000	91.187	0.737	35.769	1.661	0.0846	40455.	129.406	95.162	1.360
63	8.660	55.000	170.000	190.909	17.000	91.194	0.737	68.241	7.408	0.2593	140103.	129.324	95.096	1.360
64	4.735	55.000	93.000	190.909	17.000	91.193	0.737	68.245	4.053	0.1418	76600.	129.380	95.151	1.360
65	6.621	55.000	130.000	190.909	17.000	91.189	0.737	68.276	5.665	0.1983	107113.	129.358	95.118	1.360
66	5.355	45.000	127.000	190.909	17.000	88.568	0.737	68.195	4.691	0.1649	87154.	155.551	114.392	1.360
67	7.423	45.000	176.000	190.909	17.000	88.568	0.737	68.199	6.352	0.2233	120814.	155.520	114.360	1.360
68	2.825	45.000	67.000	190.909	17.000	88.562	0.737	68.232	2.418	0.0850	45977.	155.572	114.397	1.360
69	9.534	45.000	226.000	190.909	17.000	88.571	0.737	68.177	8.255	0.2902	155176.	155.481	114.330	1.360
70	4.389	35.000	122.000	190.909	17.000	85.942	0.737	68.168	3.803	0.1341	71813.	181.691	133.602	1.360
71	7.642	65.000	119.000	190.909	17.000	93.819	0.736	68.309	6.457	0.2248	122809.	103.118	75.827	1.360
72	6.292	65.000	98.000	190.909	17.000	93.818	0.736	68.322	5.257	0.1830	101113.	103.140	75.845	1.360
73	5.329	65.000	83.000	190.909	17.000	93.815	0.736	68.352	4.559	0.1587	85637.	103.149	75.845	1.360
74	6.728	35.000	187.000	190.909	17.000	85.947	0.737	68.138	5.759	0.2032	110086.	181.660	133.587	1.360
75	4.687	55.000	186.000	94.488	17.000	91.189	0.737	33.792	4.663	0.1504	140114.	129.393	95.153	1.360
76	6.603	55.000	262.000	94.488	17.000	91.189	0.737	33.793	6.569	0.2118	197394.	129.380	95.140	1.360
77	3.528	55.000	140.000	94.488	17.000	91.186	0.737	33.802	3.416	0.1102	105467.	129.397	95.150	1.360
78	3.088	45.000	148.000	94.488	17.000	88.568	0.737	33.752	2.991	0.0969	92870.	155.577	114.418	1.360
79	5.635	45.000	270.000	94.488	17.000	88.561	0.737	33.772	5.607	0.1816	169472.	155.564	114.387	1.360
80	7.263	45.000	348.000	94.488	17.000	88.565	0.737	33.761	7.431	0.2407	218436.	155.551	114.384	1.360
81	2.732	65.000	86.000	94.488	17.000	93.813	0.736	33.838	2.645	0.0848	81127.	103.179	75.871	1.360
82	5.655	65.000	178.000	94.488	17.000	93.817	0.736	33.819	5.624	0.1804	167928.	103.162	75.865	1.360
83	10.807	65.000	340.000	94.488	17.000	93.818	0.736	33.814	11.357	0.3643	320930.	103.118	75.824	1.360

Mean error in calculated inlet velocity at OFI, m/s = 0.363
Standard deviation of the error in calculated inlet velocity at OFI, m/s = 0.319

APPENDIX D Derivation of Babelli and Ishii Flow Instability Equation

Equation (2) of Ref. [1] is the starting point of Babelli and Ishii in obtaining the flow instability criterion. The purpose of this Appendix is to point out an inherent assumption or approximation in the derivation that affects the calculation of Subcooling number.

The coolant flow rate times the enthalpy change from channel inlet to the NVG position is related to the power generated in the fuel and transferred to the coolant over the non-boiling length, $q_w'' \zeta_H L_{nvg}$.

$$\left(h_{nvg} - h_{in}\right) = \frac{q_w'' \zeta_H L_{nvg}}{\rho_{in} V_{in} A_F} \tag{D.1}$$

Assume the coolant pressure P_{in} at the start of the heated section to be a *reference pressure* for calculating coolant subcooling at inlet and at the NVG position. Then the enthalpy difference between any pair of axial positions exactly equals the corresponding subcooling difference. The inlet subcooling $\Delta h_{in} = h_f(P_{in}) - h_{in}$, the subcooling at the NVG position $\Delta h_{nvg} = h_f(P_{in}) - h_{nvg}$, and the left hand side of Eq. (D.1) is

$$(h_{nvg} - h_{in}) = \Delta h_{in} - \Delta h_{nvg} \tag{D.2}$$

If the coolant pressure at the NVG position (instead of the pressure P_{in} at the start of the heated section) were used as the system *reference pressure*, then inlet subcooling $\Delta h_{in} = h_f(P_{nvg}) - h_{in}$, the subcooling at the NVG position $\Delta h_{nvg} = h_f(P_{nvg}) - h_{nvg}$, and Eq. (D.2) remains unchanged. With this assumption the subcooling at the NVG position is accurate and the subcooling at inlet is approximate, whereas with the former assumption, the subcooling at the NVG position is approximate and the subcooling at inlet is accurate (the reverse is true).

Substituting Eq. (D.2) into Eq. (D.1), and solving for the non-boiling length L_{nvg} , one gets

$$\frac{L_{nvg}}{L} = \frac{\rho_{in} V_{in} A_F \left(\Delta h_{in} - \Delta h_{nvg}\right)}{q_w'' \zeta_H L} \tag{D.3}$$

Equation (D.3) is the desired Eq. (D.2) of Ref. [1]. Using the Subcooling number and Zuber number defined above by Eqs. (D.2) and (D.3), Babelli and Ishii recast Eq. (D.3) as

$$\frac{N_{sub}}{N_{zu}} = \frac{L_{nvg}}{L} + \frac{A_F}{\zeta_H L}\left\{\frac{\rho_{in} V_{in} \Delta h_{nvg}}{q_w''}\right\} \tag{D.4}$$

The ratio inside the curly brackets on the right hand side of Eq. (D.4) is obtained from the Zuber correlation for the net vapor generation. For an accurate application of the Zuber correlation, it is preferred that the system *reference pressure* is assumed equal to the coolant pressure at the NVG position (rather than the pressure P_{in} at the start of the heated section), making the value of the subcooling at the NVG position accurate. This suggestion is the main purpose of this Appendix.

APPENDIX E *Babelli.WFtests.f* Program for Applying Flow Instability Criteria of Eq. (7.1) or Eq. (7.5) to Whittle and Forgan Tests.

(The thermal property subroutines of PLTEMP/ANL code were used with this program but are not listed here for brevity.)

```
C     Application of Babelli-Ishii Flow Instability Criterion
C     on Whittle and Forgan Tests. See Refs. [1, 2].
C     M. Kalimullah and A. P. Olson, November 27, 2007
C     Find when partial derivative of pressure drop (in a heated channel) with
C     respect to inlet coolant velocity is zero.
C     References:
C     (1) Babelli and Ishii, Nuclear Eng & Design, Vol. 96, pp. 91-96 (2001).
C     (2) Babelli and Ishii, Nuclear Eng & Design, Vol. 96, pp. 97-104 (2001).
C     (3) Whittle and Forgan, Nuclear Eng & Design, Vol. 6, pp. 89-99 (1967).
C
C     Friction Factor     =GETF(RE,ROUGH)
C     Tsat                =FUNCTION ZTSAT(P,IFLUID)
C     Liquid
C     Enthalpy            =FUNCTION ZHLIQ(P,T,IFLUID)
C     Density             =FUNCTION ZROLIQ(H,P,T,IFLUID)
C     Kinematic Viscosity =FUNCTION ZVISLIQ(H,P,T,RHO,IFLUID)
C     Cp                  =FUNCTION ZCPLIQ(H,P,T,IFLUID)
C     Thermal Conductivity=FUNCTION ZTHCL(H,P,T,IFLUID)
C     Temperature         =FUNCTION ZTLIQ(P,H,IFLUID,HFUNCL)
C     Vapor
C     Enthalpy            =FUNCTION ZHVAP(P,T,IFLUID)
C     Density             =FUNCTION ZROVAP(H,P,T,IFLUID)
      REAL LENGTH,KORIF,NSUB,NZUB,LENGTHI
      CHARACTER*8 STABLE
      EXTERNAL HFUNCL
C
C     Whittle and Forgan Tests Data in the Original Units
C     ---------------------------------------------------
C     ITEST   = Whittle and Forgan test number in Ref. [3]
C     HTFLXI  = Heat flux in the test, W/cm**2
C     GAPI    = Gap between plates (dimension 'A'), inch
C     WIDTHI  = Width of heated plates (dimension 'B'), inch
C     LENGTHI = Heated length, inch
C     KORIF   = Minor loss coefficient (if any)
C     POUTI   = Exit pressure in the test, psia
C
C     Whittle and Forgan Tests Data in MKS Units
C     ------------------------------------------
C     HTFLX   = Heat flux in the test, W/m**2
C     GAP     = Gap between plates (dimension 'A'), m
C     WIDTH   = Width of heated plates (dimension 'B'), m
C     LENGTH  = Heated length, m
C     POUT    = Exit pressure in the test, Pa
C     IFLUID  = 0 implies light water, IFLUID = 1 implies heavy water.
C     IFLOW   = 0 implies downflow, and IFLOW = 1 implies upflow.
C     LLP     = Number of iterations done to find the inlet pressure.
C     AAF     = Channel flow area, m**2
C     PPH     = Heated perimeter, m
C     QQ      = Power input per channel, W
C     TSATOUT = Saturation temperature at the exit pressure, C
C     HFOUT   = Saturated liquid enthalpy at the exit pressure, J/kg
C     WW      = Flow rate in channel, kg/s
C     IEQ     = 1, use Babelli-Ishii Eq. (1) to predict flow instability
C             = 2, use Nsub/Nzu > 1.36 for stability
C
      IEQ=1
```

```
      DELVIN=0.001
C     DELVIN = Step size for coolant inlet velocity, m/s
      IFLUID=0
      LLP=3
      GRAV=9.8
      ROUGH=0.0
      OPEN(UNIT=8,FILE='Babelli.WFtests.Input.Data',
     1 STATUS='OLD',FORM='FORMATTED')
      OPEN(UNIT=9,FILE='flow.instability.unit9',
     1 STATUS='UNKNOWN',FORM='FORMATTED')
      OPEN(UNIT=10,FILE='flow.instability.summary',
     1 STATUS='UNKNOWN',FORM='FORMATTED')
      WRITE(10,38)
      READ(8,*)
      READ(8,*)
C
C     Loop over the 75 tests of Whittle and Forgan.
C
      SUM1=0.0
      SUM2=0.0
      SUM3=0.0
  10  CONTINUE
      READ(8,8,END=9) ITEST,IFLOW,TIN,HTFLXI,GAPI,WIDTHI,
     1 LENGTHI,KORIF,POUTI,DTSUB0_DTC
      GO TO 11
   9  GO TO 45
  11  CONTINUE
      WRITE(6,8) ITEST,IFLOW,TIN,HTFLXI,GAPI,WIDTHI,
     1 LENGTHI,KORIF,POUTI,DTSUB0_DTC
   8  FORMAT(4X,I4,4X,I4,8F8.3)
      HTFLX=HTFLXI*1.0E+04
      GAP=GAPI*0.0254
      WIDTH=WIDTHI*0.0254
      LENGTH=LENGTHI*0.0254
      POUT=POUTI*1.0E+06/145.038
      AAF=GAP*WIDTH
      PPH=2.0*WIDTH
      DHH=4.0*AAF/PPH
      PPW=2.0*(WIDTH+GAP)
      DHW=4.0*AAF/PPW
C     DHH = Hydraulic diameter, based on heated perimeter
C     DHW = Hydraulic diameter, based on wetted perimeter
      QQ=HTFLX*PPH*LENGTH
      TSATOUT=ZTSAT(POUT,IFLUID)
      HFOUT=ZHLIQ(POUT,TSATOUT,IFLUID)
C     DTSUB0_DTC = Measured ratio of exit subcooling to coolant
C                  temp rise, at flow instability
      TOUT_MEAS=(TSATOUT+DTSUB0_DTC*TIN)/(DTSUB0_DTC+1.0)
      HOUT_MEAS=ZHLIQ(POUT,TOUT_MEAS,IFLUID)
      HIN=ZHLIQ(POUT,TIN,IFLUID)
      RHOIN=ZROLIQ(HIN,POUT,TIN,IFLUID)
      WW_MEAS=QQ/(HOUT_MEAS - HIN)
      VIN_MEAS=WW_MEAS/(RHOIN*AAF)
      WRITE(6,3) ITEST,DHH,DHW,LENGTH,KORIF,TIN,QQ,POUT,TSATOUT,AAF,
     1 PPH,DTSUB0_DTC,VIN_MEAS,WW_MEAS
   3  FORMAT(/,
     1 'Whittle & Forgan Test Numner                    =',I4,/,
     2 'Hydraulic diameter (heated), m                  =',F12.5,/,
     2 'Hydraulic diameter (wetted), m                  =',F12.5,/,
     3 'Channel heated length, m                        =',F12.4,/,
     4 'Total minor loss coefficient                    =',F12.4,/,
     5 'Inlet temperature, C                            =',F12.3,/,
     6 'Power removed by the channel, W                 =',1P,E12.5,/,
```

```
     7 'Pressure at heated section exit, Pa            =',E12.5,0P,/,
     8 'Saturation temperature at exit, C              =',F12.3,/,
     9 'Channel flow area, m**2                        =',1P,E12.5,0P,/,
     1 'Heated perimeter, m                            =',F12.5,/,
     2 'Measured ratio of exit subcooling-to-coolant',/,
     3 'temp rise, at flow instability                 =',F12.3,/,
     4 'Measured coolant velocity at OFI, m/s          =',F12.3,/,
     5 'Measured flow rate at OFI, kg/s                =',F12.3)
C
C     Tabulate Pressure drop vs. Inlet velocity
C
      WRITE(6,6) ITEST
   6  FORMAT(/,'W&F Test',I4,': EXIT TEMPERATURE AND PRESSURE DROP AT DI
     1FFERENT INLET VELOCITIES',/)
      WRITE(6,1)
   1  FORMAT(/,T4,'Inlet',T12,'Inlet',T20,'Exit',T27,
     1 'Friction',T37,'Beta',T44,'Total Press',T57,'Friction',
     2 T68,'Orifice',T78,'Mom Change',T90,'Gravity',T101,'Reynolds',
     3 T112,'Inlet', /,
     1 T2,'Vel, m/s',T11,'Temp, C',T19,'Temp, C',T27,'Factor',
     2 T36,'per C',T46,'Drop, Pa',T57,'Drop, Pa',T68,'Drop, Pa',
     3 T79,'Drop, Pa',T90,'Drop, Pa',T102,'Number',T111,'Press, Pa')
C
      WRITE(9,41) ITEST
  41  FORMAT(/,'W&F Test',I4,': APPLICATION OF BABELLI-ISHII FLOW INSTAB
     1ILITY CRITERION',/)
      WRITE(9,44)
  44  FORMAT(/,T4,'Inlet',T13,'Exit',T20,'Tot Press',T32,
     1 'Exit Press',T46,'Peclet',T55,'Inlet Subc',T66,'Subcool',
     2 T75,'Zuber',T82,'Nsub/Nzu',T92,'RHS of',T100,'Stable?',
     3 T108,'Critical',T118,'0.0022Pe',/,
     1 T2,'Vel, m/s',T11,'Temp, C',T21,'Drop, Pa',T35,'Pa',
     2 T46,'Number',T58,'J/kg',T67,'Number',T75,'Number',T91,
     3 'Eq. (1)',T109,'Lnvg/L',T118,'or 154.0')
C
C     Loop over VIN = Inlet coolant velocity, m/s
      IFLAG=0
      II=6.0/DELVIN
      VIN_MIN=QQ/(1000.0*AAF*4186.0*(115-TIN))
      MIN=VIN_MIN/DELVIN
      VIN_MIN=MIN*DELVIN
      DO 40 I=1,II
      VIN=DELVIN*FLOAT(I)+VIN_MIN
C     Guess PIN = POUT. Find guess values of coolant properties at inlet.
  31  PIN=POUT
      DO 35 LP=1,LLP
      TSATIN=ZTSAT(PIN,IFLUID)
      HFIN=ZHLIQ(PIN,TSATIN,IFLUID)
      HIN=ZHLIQ(PIN,TIN,IFLUID)
      RHOIN=ZROLIQ(HIN,PIN,TIN,IFLUID)
      CPIN=ZCPLIQ(HIN,PIN,TIN,IFLUID)
      CONDIN=ZTHCL(HIN,PIN,TIN,IFLUID)
C     WRITE(6,*) 'TSATIN =',TSATIN,' HIN    =',HIN,'  RHOIN  =',RHOIN
C     WRITE(6,*) 'CPIN   =',CPIN,' CONDIN =',CONDIN
      WW=RHOIN*VIN*AAF
      HOUT=HIN+QQ/WW
      TOUT=ZTLIQ(POUT,HOUT,IFLUID,HFUNCL)
C     TOUT = Exit coolant temperature. Its above value is an estimate because it
C            is based on the inlet pressure PIN, not the actual exit pressure.
      RHOOUT=ZROLIQ(HOUT,POUT,TOUT,IFLUID)
C     Find pressure drop in channel using the estimate TOUT and then refine.
      TAVE=0.5*(TIN+TOUT)
      HAVE=0.5*(HIN+HOUT)
```

```
      PAVE=0.5*(PIN+POUT)
      RHOAVE=ZROLIQ(HAVE,PAVE,TAVE,IFLUID)
      VISCAVE=ZVISLIQ(HAVE,PAVE,TAVE,RHOAVE,IFLUID)
C     VISCAVE  = Kinematic viscosity at the average temperature, m**2/s
C     VISCAVE*RHOAVE = Absolute viscosity at the average temperature, Pa-s
      REAVE=WW*DHW/(VISCAVE*RHOAVE*AAF)
      FRIC=GETF(REAVE,ROUGH)
      VELHEAD=0.5*(WW/AAF)**2/RHOAVE
      VELHEADI=0.5*(WW/AAF)**2/RHOIN
C     DPFRIC  = Frictional pressure drop, Pa
C     DPORIF  = Orifice (minor) loss, Pa
C     DPTHEXP = Thermal expansion pressure drop, Pa
C     DPGRAV  = Gravitational pressure drop, Pa
C     DPMFLX  = Pressure drop due to the change in momentum flux from
C               inlet to exit [i.e., the last term of Eq. (7)], Pa
      DPORIF=KORIF*VELHEAD
      DPFRIC=FRIC*LENGTH/DHW*VELHEAD
      BETA=0.28E-4 + 9.9E-6*TAVE - 2.75E-8*TAVE**2
C     This equation for BETA was fitted to the data on p. 2.36 of Rohsenow's
C     Handbook of Heat Transfer
      IF(IFLOW .EQ. 1) THEN
C     Upflow
      DPTHEXP=-BETA*QQ/(2.0*CPIN*VIN*AAF)*GRAV*LENGTH
      DPGRAV= RHOIN*GRAV*LENGTH + DPTHEXP
      ELSE
C     Downflow
      DPTHEXP= BETA*QQ/(2.0*CPIN*VIN*AAF)*GRAV*LENGTH
      DPGRAV=-RHOIN*GRAV*LENGTH + DPTHEXP
      ENDIF
      DPMFLX=2.0*VELHEADI*(RHOIN/RHOOUT-1.0)
      DELP=DPFRIC+DPORIF+DPGRAV+DPMFLX
      PIN=POUT+DELP
      IF(LP .EQ. LLP .AND. IFLAG .NE. 1)
     1 WRITE(6,2) VIN,TIN,TOUT,FRIC,BETA,DELP,DPFRIC,
     2 DPORIF,DPMFLX,DPGRAV,REAVE,PIN
   2  FORMAT(F8.3,2F8.2,F8.4,1P,E10.2,0P,7F11.2)
  35  CONTINUE
C
C     Find Subcooling Number and Zuber Number
C     Assume: System reference pressure  P3 = Pressure at exit
C
      P3=POUT
      T3=TOUT
      H3=ZHLIQ(P3,T3,IFLUID)
      RHO3 =ZROLIQ (H3,P3,T3,IFLUID)
      VISC3=ZVISLIQ(H3,P3,T3,RHO3,IFLUID)
      CP3=ZCPLIQ(H3,P3,T3,IFLUID)
      THC3=ZTHCL(H3,P3,T3,IFLUID)
      RE3=WW*DHW/(VISC3*RHO3*AAF)
      PR3=RHO3*VISC3*CP3/THC3
      PE3=RE3 * PR3
C     Get saturated fluid properties
      TSAT3=ZTSAT(P3,IFLUID)
      HF3=ZHLIQ(P3,TSAT3,IFLUID)
      HG3=ZHVAP(P3,TSAT3,IFLUID)
      HFG3=HG3 - HF3
      RHOF3=ZROLIQ(HF3,P3,TSAT3,IFLUID)
      RHOG3=ZROVAP(HG3,P3,TSAT3,IFLUID)
C
      NSUB=(HF3 - HIN)/HFG3 *(RHOF3 - RHOG3)/RHOG3
CX    NSUB=(HFIN - HIN)/HFG3 *(RHOF3 - RHOG3)/RHOG3
      NZUB=QQ/(WW*HFG3) *(RHOF3 - RHOG3)/RHOG3
C     Use Eq. (1) of the chapter
```

```
      PEFL=154.0
      IF(IFLOW .EQ. 1 .AND. PE3 .LT. 70000.0) PEFL=0.0022*PE3
      CRITL=CRITLNVG(NSUB)
      RATIO=CRITL+AAF/(LENGTH*2.0*WIDTH)*PEFL
      STABLE='stable'
      IF(NSUB/NZUB .LT. RATIO) STABLE='unstable'
      IF(IEQ .EQ. 2) THEN
C     Use Eq. (5) of the chapter
      STABLE='stable'
      IF(NSUB/NZUB .LT. 1.36) STABLE='unstable'
      ENDIF
      IF(IFLAG .NE. 1)
     1 WRITE(9,42) VIN,TOUT,DELP,P3,PE3,HF3-HIN,NSUB,NZUB,
     1 NSUB/NZUB,RATIO,STABLE,CRITL,PEFL
C     WRITE(9,43) VISC3,RE3,PR3,TSAT3,HF3,HFG3,RHOF3,RHOG3,PR3,RE3
C
C     Save inlet velocity and other quantities to find Whittle and Forgan ETA
C     at the onset of flow instability.
C     IFLAG  = 0, the onset of flow instability is not found
C            = 1, the onset of flow instability is found, stable VIN
C            = 2, the onset of flow instability is found, unstable VIN
C
      IF((STABLE .EQ. 'stable' .AND. IFLAG .EQ. 0) .OR.
     1 (STABLE .EQ. 'unstable' .AND. IFLAG .EQ. 1)) THEN
      IFLAG=IFLAG+1
C     Reduce VIN to its previous value, re-run, and print results.
      IF(IFLAG .EQ. 1) VIN=VIN-DELVIN
      IF(IFLAG .EQ. 1) GO TO 31
      DELTC=TOUT-TIN
      DELTSUB0=TSATOUT-TOUT
      ETA=(DELTSUB0/DELTC)*(LENGTH/DHH)
      WRITE(9,36) ITEST,VIN,TIN,HTFLXI,LENGTH/DHH,POUTI,TOUT,
     1 DELTC/(TSATOUT-TIN),ETA,VIN_MEAS,WW_MEAS,PE3,NSUB,NZUB,NSUB/NZUB
      WRITE(10,37) ITEST,VIN,TIN,HTFLXI,LENGTH/DHH,POUTI,TOUT,
     1 DELTC/(TSATOUT-TIN),ETA,VIN_MEAS,WW_MEAS,PE3,NSUB,NZUB,NSUB/NZUB
      SUM1=SUM1+1.0
      SUM2=SUM2+VIN-VIN_MEAS
      SUM3=SUM3+(VIN-VIN_MEAS)**2
C     WRITE(10,*) SUM1,SUM2,SUM3
      ENDIF
  40  CONTINUE
      WRITE(6,12)
      WRITE(9,12)
      GO TO 10
  12  FORMAT(126('-'))
  36  FORMAT('Test',I4,': Vin =',9F8.3,F8.4,F8.0,3F8.3)
  37  FORMAT(I4,9F8.3,F8.4,F8.0,3F8.3)
  42  FORMAT(F8.3,F8.2,4F12.2,2F8.2,2F8.3,A10,F8.3,3X,F8.3)
  43  FORMAT(12X,1P,10E12.4)
  38  FORMAT(T2,'Test',T8,'Inlet',T15,'Inlet',T22,'Heat',T31,'Lh/Dhh',
     1 T40,'Exit',T47,'Exit',T55,'delTc',T64,'ETA',T70,'Measured at OFI'
     2 ,T86,'Peclet',T94,'Subcool',T103,'Zuber',T112,'Nsub',/,
     3 T3,'No.',T9,'Vel',T15,'Temp',T22,'Flux',T31,'Ratio',
     4 T40,'Press',T47,'Temp',T54,'-------',T64,'W&F',T70,'Inlet',
     5 T80,'Flow',T86,'Number',T94,'Number',T103,'Number',T112,'----',/,
     6 T9,'m/s',T16,'C',T22,'W/cm^2',T40,'psia',T48,'C',T54,'delTsat',
     7 T70,'Vel,m/s',T80,'kg/s',T112,'Nzub')
  45  CONTINUE
      VIN_ERM=SUM2/SUM1
      VIN_RMS=SQRT(SUM3/SUM1)
      VIN_ERD=SQRT(VIN_RMS**2 - VIN_ERM**2)
C     VIN_ERM = Mean error in calculated inlet coolant velocity at OFI, m/s
C     VIN_RMS = RMS value of this error, m/s
```

```
C     VIN_ERD = Standard deviation of the error, m/s
      WRITE(10,39) VIN_ERM,VIN_ERD
C     WRITE(10,*) 'SUM1, SUM2, SUM3 =',SUM1,SUM2,SUM3
  39  FORMAT(/,
     1 'Mean error in calculated inlet velocity at OFI, m/s
     2         =',F8.3,/,
     3 'Standard deviation of the error in calculated inlet velocity at
     4OFI, m/s =',F8.3)
      END
      REAL FUNCTION CRITLNVG(NSUB)
      REAL NSUB
C     CRITLNVG  = (Lnvg/L)critical at an input Subcooling number NSUB,
C                 found by interpolating an experimentally determined table
C     SUBN(N)   = Subcooling numbers in an experimentally determined table
C                 of Subcooling number versus (Lnvg/L)critical
C     CRITLUP(N)= Corresponding values of (Lnvg/L)critical, its upper bound
C                 reported by Babelli and Ishii
C     CRITLOW(N)= Corresponding values of (Lnvg/L)critical, its lower bound
C                 reported by Babelli and Ishii
C     CRITLV(N) = Corresponding values of (Lnvg/L)critical, its value adjusted
C                 to fit 75 flow instability tests of Whittle & Forgan [Ref 3]
C
      DIMENSION SUBN(12),CRITLUP(12),CRITLOW(12),CRITLV(12)
      DATA NTAB/12/
      DATA SUBN/0.0,2.69,5.38,8.07,10.76,21.51,32.27,43.03,53.78,
     1 64.54,69.92,300.0/
      DATA CRITLUP/0.0,0.0232,0.414,0.594,0.756,1.083,1.222,1.297,
     1 1.222,1.083,1.0,1.0/
      DATA CRITLOW/0.0,0.0232,0.0684,0.141,0.256,0.440,0.527,0.594,
     1 0.711,0.905,1.0,1.0/
C     The above two tables are the upper and lower bounds reported by Babelli
C     and Ishii [Fig. 4 of Ref 2, listed at the top of the program]
      DO 1 N=1,NTAB
C     CRITLV(N)=CRITLOW(N)
      CRITLV(N)=CRITLUP(N)
C     CRITLV(N)=CRITLOW(N)+0.5*(CRITLUP(N)-CRITLOW(N))
   1  CONTINUE
      DO 10 N=2,NTAB
      IF(NSUB .LE. SUBN(N)) GO TO 11
C     WRITE(6,*) NSUB,N,SUBN(N)
  10  CONTINUE
      CRITLNVG=1.0
      WRITE(6,*) 'Subr CRITLNVG: Input Subcooling number is out of range
     1. (Lnvg/L)critical was assumed to be 1.0'
      RETURN
  11  CONTINUE
C
C     Interpolate (Lnvg/L)critical from array CRITLV
C     WRITE(6,*) NSUB,N,SUBN(N-1),SUBN(N),CRITLV(N-1),CRITLV(N)
      CRITLNVG=CRITLV(N-1)+(CRITLV(N)-CRITLV(N-1))/
     1 (SUBN(N)-SUBN(N-1))*(NSUB-SUBN(N-1))
      RETURN
      END
```

8 Verification of Colburn Heat Transfer Correlation

The verification work reported here was done in February 2008. PLTEMP/ANL version 3.4 fails to run in the case of Colburn heat transfer correlation because the variable VISC (i.e., the coolant viscosity at the mean of cladding surface and bulk coolant temperatures) in the routine HCOEF1 was left undefined. The variable VISC is defined in the case of all other heat transfer correlations, and the code version 3.4 runs correctly.

In the earlier versions of the code (i.e., versions 3.0, 3.1, 3.2, 3.3, 3.3.1), the variable VISC was passed to the routine HCOEF1 through the common block /A1/. The value passed was found to be incorrect, resulting in an incorrect heat transfer coefficient. Hence the common block /A1/ was discarded in the code V3.4, the variable VISC was locally defined in the heat transfer routine HCOEF, but the variable was left undefined in the case of Colburn correlation in the companion routine HCOEF1.

8.1 Verification of the Corrected Code

To correct the error, the variable VISC is locally defined in routine HCOEF1 using the coolant viscosity routine ZVISLIQ. The corrected code was run for a sample problem (input data listed in Fig. 8.1. A verification of the Colburn heat transfer coefficient calculated by the corrected version 3.4 is provided below, using the data taken from the code output and debug prints for axial node 11 of fuel plate 6 right hand side. After this, for comparison purposes, the heat transfer coefficient calculation by the code version 3.0 is shown using the data taken from the code output and debug prints for the same axial node of fuel plate 6. Note that the kinematic viscosity (46274×10^{-7} m^2/s) used to calculate the Colburn heat transfer coefficient is not correct in the code version 3.0. It should be 4.3490×10^{-7} m^2/s, i.e., the value at 65.6746 °C, the mean of cladding surface and bulk coolant temperatures (76.0920 °C and 55.2572 °C).

Both sets of data are summarized and compared in Table 8.1.

<u>Calculation of Heat Transfer Coefficient from the Right Surface of Fuel Plate 6 to Coolant Channel 7 in Axial Node 11, in PLTEMP/ANL Code V3.4</u>

T_m = 65.3211 °C
P = 101252.2 Pa
ν = Kinematic Viscosity at (T_m , P) = ν(65.3211 , 101252.2) = 4.3697×10^{-7} m^2/s
= Fortran Variable VISC locally defined in routine HCOEF1
Pr = $\rho\ \nu\ C_p / K$ = 1000.0 x 4.3697×10^{-7} x 4180.0 / 0.66216 = 2.7584
Re = $W\ D_h/(\rho\ \nu\ A)$ = 0.91358 x 4.2708×10^{-3} / (1000.0 x 4.3697×10^{-7} x 2.4641×10^{-4})
= 36236.5
Nu = $0.023\ Re^{0.8}\ Pr^{0.3}$ = 0.023 x $(36236.5)^{0.8}$ x $(2.7584)^{0.3}$ = 138.4337
= 138.4348 printed by code
h = $Nu\ K / D_h$ = 138.4348 x 0.66216 / 4.2708×10^{-3} = 21463.4 W/m^2-°C
= 21463.5 W/m^2-°C printed by code
T_w = $T_b + q''/h$ = 55.2198 + 0.43362×10^6/21463.5 = 55.2198 + 20.2027 = 75.4225 °C

<u>Calculation of Heat Transfer Coefficient from the Right Surface of Fuel Plate 6 to</u>

Coolant Channel 7 in Axial Node 11, in PLTEMP/ANL Code V3.0

T_m = 65.6746 °C
P = 101252.2 Pa
ν = Kinematic Viscosity at (T_m , P) = ν(65.6746 , 101252.2) = 4.3490×10^{-7} m^2/s
≠ Fortran Variable VISC in COMMON/A1/ = 4.6274×10^{-7} m^2/s
Pr = ρ ν C_p/ K = 1000.0 x 4.6274×10^{-7} x 4180.0 / 0.66248 = 2.9197
Re = W D_h/(ρ ν A) = 0.91358 x 4.2708×10^{-3} / (1000.0 x 4.6274×10^{-7} x 2.4641×10^{-4})
= 34218.5
Nu = 0.023 $Re^{0.8}$ $Pr^{0.3}$ = 0.023 x $(34218.5)^{0.8}$ x $(2.9197)^{0.3}$ = 134.5050
= 134.5050 printed by code
h = Nu K / D_h = 134.5050 x 0.66248 / 4.2708×10^{-3} = 20864.2 W/m^2-°C
= 20864.4 W/m^2-°C printed by code
T_w = T_b + q''/h = 55.2572 + 0.43470×10^6/20864.4 = 55.2572 + 20.8345 = 76.0917 °C

8.2 Conclusion

An error in the Colburn heat transfer coefficient in PLTEMP/ANL version 3.0 is fixed in the code version 3.4. Due to the error in the code version 3.0, there was a change in the cladding wall surface temperature although the bulk coolant temperature changed by a smaller amount. The wall surface temperature change was mainly due to the change in the temperature drop from cladding wall to bulk coolant, (T_w – T_b). The bulk coolant temperature changed due to the small change in the fraction of the fuel plate power transferred to each adjacent channel, due to the changes in heat transfer coefficient on each side of the plate.

Figure 8.1 Input Data File of the Sample Test Problem *input.file.sai.chi.inp3* Used in Verifying the Colburn Heat Transfer Coefficient

```
IRT-3M 36% Enr FA; 6 Tubes 0.58 m Height -           true->plate
! Colburn
   2   1   2   1   1   0   1   0   0   1                                        Card(1)0200
   1   3  0.0        1.00        1.000       1.00                              Card(1)0300
   7   7  1.000                                                                 Card(1)0301
   1   2   1                                                                    Card(1)0302
 1.3135                                                                         Card(1)0303
 0.0043433  0.038540    0.10        0.5                                         Card(3)0304
 0.0        0.0         0.580       0.0                                         Card(3)0304
 0.0043433  0.038540    0.035       1.0                                         Card(3)0304
 0.316      0.250                                                               Card(1)0305
   7  0 0.0         0.580         0.450E-03  170.        0.500E-03  100.       Card(1)0306
  6.0524E-04 4.46024E-03  0.27139    0.27139                                   Card(7)0307
  5.2931E-04 4.17778E-03  0.50679    0.50679                                   Card(7)0307
  4.7273E-04 4.18729E-03  0.45159    0.45159                                   Card(7)0307
  4.1615E-04 4.19944E-03  0.39639    0.39639                                   Card(7)0307
  3.5957E-04 4.21553E-03  0.34119    0.34119                                   Card(7)0307
  3.0299E-04 4.23783E-03  0.28599    0.28599                                   Card(7)0307
  2.4641E-04 4.27080E-03  0.23079    0.23079                                   Card(7)0307
 0.267193   0.239593    0.211993    0.184393    0.156793    0.129193           Card(1)0308
 1.1696     1.0901      1.0234      0.9579      0.90175     0.85731            Card(1)0309
1.94282     1.57675     1.54174     1.41065     1.16807     1.15058
0.91358
   1   1         1.0
  1.1545E-04    3.00E-03    0.680           1.4
       0.316    0.25
 .100633     .0005        .12540     0.82908      45.0        .135
 0.0        0.0                                                                 Card(2) 0501 NEW
 100 1.00000E-04   25.0        0.0000        0.82908
 -12
0.00000      0.025       0.52323
0.05000      0.100       0.62029
0.15         0.20        0.85886
0.25         0.30        1.06336
0.35         0.40        1.24058
0.45         0.50        1.34964
0.55         0.60        1.36328
0.65         0.70        1.27466
0.75         0.80        1.09062
0.85         0.90        0.85886
0.95         0.975       0.75662
1.00000
   0
```

Table 8.1 Comparison between Versions 3.4 and 3.0 of PLTEMP/ANL Code in Calculating Colburn Heat Transfer Coefficient

Variable	PLTEMP/ANL Code V3.4	PLTEMP/ANL Code V3.0	Comments
D_h , m	4.2708×10^{-3}	4.2708×10^{-3}	
A , m^2	2.4641×10^{-4}	2.4641×10^{-4}	
T_w , °C	75.4224	76.0920	
T_b, °C	55.2198	55.2572	
P , Pa	101252.2	101252.2	
T_{sat} , °C	99.9802	99.9802	
T_m , °C = $(T_w+T_b)/2$	65.3211	65.6746	
ν , m^2/s Variable VISC used to get Nu	4.3697×10^{-7} 4.3697×10^{-7}	4.3490×10^{-7} 4.6274×10^{-7}	Error in V3.0
W , kg/s	0.91358	0.91358	
ρ , kg/m^3	1000.0	1000.0	
C_p , J/kg-°C	4180.0	4180.0	
K , W/m-°C	0.66216	0.66248	
$Pr = \rho \nu C_p / K$	2.7584	2.9197	
$Re = W D_h/(\rho \nu A)$	36236.5	34218.5	
$Nu = 0.023 Re^{0.8} Pr^{0.3}$	138.4337	134.5050	
$h = Nu K / D_h$, W/m^2-°C Printed by Code	21463.5	20864.4	Error in V3.0
$h = Nu K / D_h$, W/m^2-°C By Hand Calculation	21463.4	20864.2	

9 Verification of the Natural Circulation Option Implemented in the PLTEMP/ANL V3.5 Code

The verification work reported here was done in June 2008. A natural circulation option was implemented in the PLTEMP/ANL version 3.5 code. For the verification of this option, a natural circulation test problem was solved by hand calculation, by *Mathematica*, by the NATCON code, by the RELAP5-3D code, and by the PLTEMP/ANL code. The *Mathematica* solution was performed three times, using the sets of coolant properties used in the three codes, i.e., the NATCON code, the PLTEMP/ANL code, and the RELAP5-3D code. The hand calculation and the *Mathematica* calculations were done starting from an assumed flow rate in the coolant channel, which was manually adjusted so that the buoyancy equals the frictional pressure drop in the channel. These seven solutions are summarized in columns 2 to 8 of Table 9.1. All these seven solutions assume that the laminar friction factor is 96 divided by Reynolds number. The PLTEMP/ANL solution in column 9 of Table 9.1 uses 94.7174 in place of 96, as explained below in Section 9.7. Five of these solutions agree well with the PLTEMP/ANL solution, and this provides a verification of the natural circulation calculation of PLTEMP/ANL. The RELAP5-3D solution is found to differ slightly from the PLTEMP/ANL and NATCON solutions because it (RELAP5-3D) uses coolant temperatures based on node exit to calculate buoyancy and frictional pressure drop, as discussed in Section 9.6. That is why the RELAP5-3D-calculated flow rate is about 5% higher than the PLTEMP/ANL- calculated flow rate.

9.1 Introduction

The PLTEMP/ANL code [1] was improved to model coolant flow by natural circulation upward through the fuel assemblies and downward in the reactor pool. The purpose of this chapter is to document the solution of a natural circulation test problem that is used in the verification of this model. The test problem is defined in Section 9.2, and referred to as Sample Problem 20. Its solution by seven methods/codes are reported and compared here:

(Sections 9.2 and 9.3)	hand calculation,
(Section 9.4)	three *Mathematica* calculations using the different sets of coolant properties used in the NATCON code, the PLTEMP/ANL code, and the RELAP5-3D code,
(Section 9.5)	the NATCON code [2],
(Section 9.6)	the RELAP5-3D code [3], and
(Section 9.7)	the PLTEMP/ANL version 3.5 code.

The solutions by codes/methods other than PLTEMP/ANL were obtained for a single coolant channel, and the PLTEMP/ANL solution was obtained for a four-plate fuel assembly.

9.2 Hand Calculation for a Natural Circulation Test Problem

<u>Problem Definition</u>: Calculate the coolant flow rate caused by natural circulation in a 1.05 m long vertical coolant channel with a 0.75 m long heated length. The lower unheated length is 0.15 m, and the upper unheated length is 0.15 m. The heated length has a power of 25 kW distributed uniformly over the 0.75 m length, with an inlet temperature of 25 °C. The channel has a rectangular cross section of thickness 3 mm, width 0.3 m, inlet pressure loss coefficient 0.5, and exit pressure

loss coefficient 1.0. The absolute pressure at the channel inlet is 5 bar, corresponding to the channel inlet being 40.81 m below the free surface of water in the pool.

The values of input variables (see nomenclature given at the end) for this problem are as follows:

D_h = 0.0059406 m,	g = 9.8 m/s^2,	H_{in} = 41.81 m,	K_{in} = 0.5,
K_{ex} = 1.0,	L_1 = 0.15 m,	L_2 = 0.75 m,	L_3 = 0.15 m,
L = 1.05 m,	Q = 25000 W,	P_{in} = 5.0 bar,	T_{in} = 25 °C,
T_{ch} = 0.003 m,	W_{ch} = 0.3 m,	f = 96/Re	
W = 0.1086 kg/s (*assumed value*)			

The assumed flow rate was adjusted in the hand calculation given below so that the buoyancy induced driving pressure head is equal to the frictional pressure drop plus the momentum flux term in the channel. The steps in the hand calculation are shown below for the finally obtained flow rate which makes the buoyancy equal to the frictional pressure drop. The results of hand calculation, and their comparison with other calculations are summarized in Table 9.1.

<u>Coolant Exit Temperature</u>: For the above assumed flow rate, the exit temperature is calculated as shown by Eq. (9.1) below, using a coolant specific heat C_p of 4188 J/kg-°C, obtained by averaging the temperature-dependent water specific heat over the coolant temperature range 25 to 80 °C that is expected in the problem.

$$T_{ex} = T_{in} + \frac{Q}{WC_p} = 25\,(^\circ C) + \frac{25000\ (J/s)}{0.1086\ (kg/s) \times 4188\ (J/kg-^\circ C)} = 79.967\ ^\circ C \tag{9.1}$$

<u>Average Coolant Density</u>: The coolant density difference between the cold liquid outside the channel (in the pool) and the hot liquid inside the coolant channel causes a pressure head (buoyancy) that drives the upward flow in the channel, i.e., natural circulation. The coolant density variation over the channel height is used to find the buoyancy pressure head as shown by Eq. (9.2) for the channel shown in Fig. 9.1.

$$\Delta P_{buoyancy} = \rho_1\ g\ L\ - \int_{z=0}^{z=L} \rho(z)\ g\ dz \tag{9.2a}$$

$$\Delta P_{buoyancy} = \rho_1\ g\ (L_1 + L_h + L_3) - g\left[\rho_1 L_1 + \int_{z=L_1}^{z=L_1+L_h} \rho(z)\ dz + \rho_3 L_3\right] \tag{9.2b}$$

where the symbols are defined in the nomenclature given at the end.

In Eqs. (9.2a) and (9.2b), the first term on the right hand side is the gravity head of cold liquid in the pool, and the second term is the gravity head in the heated channel. The second term is smaller than the first, and opposes the first. The difference between these terms gives the pressure head driving the natural circulation flow in the channel. Equation (9.2) is good irrespective of whether the power profile over the heated channel length is uniform or not. The power profile in the test problem is axially uniform, and this results in the simplification that the coolant temperature varies

linearly with position over the heated length, as shown by Eq. (9.3). The differential of Eq. (9.3) is given by Eq. (9.4).

$$T(z) = T_{in} + (T_{ex} - T_{in}) \frac{(z - L_1)}{L_h} \tag{9.3}$$

$$dT = \frac{(T_{ex} - T_{in})}{L_h} dz \tag{9.4}$$

Substituting Eq. (9.4) into Eq. (9.2b), the pressure head due to buoyancy is given by Eq. (9.5).

$$\Delta P_{buoyancy} = g \left[(\rho_1 - \rho_{ave}) L_h + (\rho_1 - \rho_3) L_3 \right] \tag{9.5}$$

where ρ_{ave} is the coolant density averaged over temperature from the inlet temperature to the exit temperature, as shown by Eq. (9.6). This simplification (i.e., averaging over temperature rather than axial position z as required by Eq. (9.2)) is not possible for non-uniform power profile.

$$\rho_{ave} = \frac{1}{(T_{ex} - T_{in})} \int_{T=T_{in}}^{T=T_{ex}} \rho(T)\, dT \tag{9.6}$$

The coolant density in the 0.15 m long unheated axial region 1 below the heated length does not vary with height. It equals the coolant density at the inlet temperature 25 °C. The coolant density in the 0.15 m long unheated axial region 3 above the heated length does not vary with height. It equals the coolant density at the exit temperature given by Eq. (9.1). The average coolant density over the heated length is calculated as follows, using *Mathematica*, by numerically integrating the temperature-dependent density data taken from the NATCON code. The coolant density and dynamic viscosity data used are given in Table 9.2.

$$\rho_{ave} = \frac{1}{(T_{ex} - T_{in})} \int_{T_{in}}^{T_{ex}} \rho(T)\, dT = \frac{1}{(79.967 - 25)} \int_{T=25}^{79.967} \rho(T)\, dT = 986.541 \text{ kg/m}^3 \tag{9.7}$$

<u>Pressure Head due to Buoyancy</u>: The pressure head due to buoyancy is calculated using Eq. (9.5). The densities at channel inlet and exit required in this calculation are interpolated from Table 9.2. For the assumed flow rate of 0.1086 kg/s in the channel, the pressure head due to buoyancy is found as follows.

ρ_1 = coolant density at inlet = ρ(25 °C) = 996.842 kg/m^3

ρ_3 = coolant density at exit = ρ(79.967 °C) = 972.325 kg/m^3

$$\begin{aligned} \Delta P_{buoy} &= 9.8\ [(996.842 - 986.541) \times 0.75 + (996.842 - 972.325) \times 0.15] \\ &= 75.716 + 36.040 \\ &= 111.756 \text{ Pa} \end{aligned} \tag{9.8}$$

Frictional Pressure Drops in Lower and Upper Unheated Lengths: The coolant in the whole lower unheated length (axial region 1) is at the inlet temperature 25 °C, and the coolant in the whole upper unheated length (axial region 3) is at the exit temperature 79.967 °C. The coolant dynamic viscosity required in calculating the frictional pressure drop ΔP_{fric1} in axial region 1 is found by interpolating the temperature-dependent viscosity data given in Table 9.2 for temperature 25 °C. The viscosity required in calculating the frictional pressure drop ΔP_{fric3} in axial region 3 is found by interpolating the viscosity data for temperature 79.967 °C.

$$\mu_1 = 9.0170\text{x}10^{-4} \text{ Pa-s} \tag{9.9a}$$

$$\mu_3 = 3.5606\text{x}10^{-4} \text{ Pa-s} \tag{9.9b}$$

The Reynolds numbers in axial regions 1 and 3 are calculated as follows.

$$Re_1 = \frac{\rho_1 V_1 D_h}{\mu_1} = \frac{WD_h}{\mu_1 W_{ch} T_{ch}} = \frac{0.1086 \times 0.0059406}{9.0170 \times 10^{-4} \times 0.3 \times 0.003} = 794.98 \tag{9.10a}$$

$$Re_3 = \frac{WD_h}{\mu_3 W_{ch} T_{ch}} = \frac{0.1086 \times 0.0059406}{3.5606 \times 10^{-4} \times 0.3 \times 0.003} = 2013.24 \tag{9.10b}$$

The width-to-thickness ratio of the rectangular cross section of the coolant channel is 100 which is large enough to calculate the laminar friction factor as 96/Re. Therefore, the friction factors in axial regions 1 and 3 are calculated as follows.

$$f_1 = 96/Re_1 = 96/794.98 = 0.120758 \tag{9.11a}$$

$$f_3 = 96/Re_3 = 96/2013.24 = 0.047684 \tag{9.11b}$$

The frictional pressure drop ΔP_{fric1} in axial region 1 (i.e., the lower unheated length) consists of two parts: (1) the pressure drop due to the input loss coefficient K_{in} of 0.5 at inlet, and (2) the pressure drop due to wall shear over the length 0.15 m, as shown below by Eq. (9.12).

$$\Delta P_{fric1} = \left(K_{in} + \frac{f_1 L_1}{D_h} \right) \frac{1}{2\rho_1} \left(\frac{W}{W_{ch} T_{ch}} \right)^2 \tag{9.12}$$

$$\Delta P_{fric1} = \left(0.5 + \frac{0.120758 \times 0.15}{0.0059406} \right) \frac{1}{2 \times 996.842} \left(\frac{0.1086}{0.3 \times 0.003} \right)^2 = 25.920 \text{ Pa} \tag{9.13}$$

The frictional pressure drop ΔP_{fric3} in axial region 3 (i.e., the upper unheated length) consists of two parts: (1) the pressure drop due to the input loss coefficient K_{ex} of 1.0 at exit, and (2) the pressure drop due to wall shear over the length 0.15 m, as shown below by Eq. (9.14).

$$\Delta P_{fric3} = \left(K_{ex} + \frac{f_3 L_3}{D_h} \right) \frac{1}{2\rho_3} \left(\frac{W}{W_{ch} T_{ch}} \right)^2 \tag{9.14}$$

$$\Delta P_{fric3} = \left(1.0 + \frac{0.047684 \times 0.15}{0.0059406} \right) \frac{1}{2 \times 972.325} \left(\frac{0.1086}{0.3 \times 0.003} \right)^2 = 16.502 \text{ Pa} \tag{9.15}$$

<u>Frictional Pressure Drop in Heated Section</u>: The pressure drop ΔP_{fric2} over the heated section (axial region 2) of length 0.75 m is calculated by dividing this length into 5 equal sub-sections (each 0.15 m long) to account for the temperature dependence of coolant viscosity. These sub-sections are numbered i = 1 to 5, starting from the lower end of the heated section. As pointed out above, the coolant temperature rises linearly with axial position in the heated length, and therefore, the average coolant temperature T_{2i} in the ith sub-section is calculated as follows.

$$T_{2i} = T_{in} + (T_{ex} - T_{in})(i - 0.5) / 5 \text{ , } i = 1, 2, 3, 4, 5 \tag{16a}$$

$$T_{2i} = 30.497, 41.490, 52.484, 63.477, 74.470 \text{ °C} \tag{16b}$$

In each of these 5 parts, the coolant density and dynamic viscosity are interpolated from Table 9.2. The Reynolds number, friction factor, and frictional pressure drop are calculated using formulas like Eqs. (9.10), (9.11) and (9.12) in *Mathematica*. The results are summarized below and in Table 9.1.

Frictional Pressure Drop Calculation in the Heated Section Using Five Sub-sections

Heated Sub-section Number	Coolant Temperature °C	Length m	Dynamic Viscosity Pa-s	Reynolds Number	Friction Factor	Density kg/m^3	Frictional Pressure Drop, Pa
Symbol →	T_{2i}	L_{2i}	μ_{2i}	Re_{2i}	f_{2i}	ρ_{2i}	ΔP_{fric2i}
1	30.497	0.15	7.9546x10^{-4}	901.154	0.10653	995.48	19.672
2	41.490	0.15	6.3381x10^{-4}	1130.99	0.084882	992.01	15.729
3	52.484	0.15	5.2097x10^{-4}	1375.95	0.069770	987.52	12.988
4	63.477	0.15	4.3925x10^{-4}	1631.95	0.058825	982.12	11.010
5	74.470	0.15	3.7934x10^{-4}	1889.70	0.050802	975.76	9.571
Total		**0.75**					**68.970**

The pressure drop ΔP_{fric2} over the heated section of length 0.75 m is found to be 68.970 Pa.

$$\Delta P_{fric2} = \Delta P_{fric21} + \Delta P_{fric22} + \Delta P_{fric23} + \Delta P_{fric24} + \Delta P_{fric25} = 68.970 \text{ Pa} \tag{9.17}$$

<u>Pressure Drop due to Momentum Flux</u>: The pressure drop due to momentum flux from the channel inlet to the exit is given by

$$\Delta P_{mom} = \rho_1 V_1^2 \left(\frac{\rho_1}{\rho_3} - 1 \right) \tag{9.18}$$

$$V_1 = \frac{W}{\rho_1 \, W_{ch} \, T_{ch}} = \frac{0.1086}{996.842 \times 0.3 \times 0.003} = 0.12105 \text{ m/s}$$

$$\Delta P_{mon} = 996.842 \text{ x } (0.12105)^2 \text{ x } (996.842/972.325 - 1) = 0.3683 \text{ Pa} \quad (9.19)$$

<u>Total Frictional Pressure Drop</u>: The total frictional pressure drop in the channel, including the small pressure drop due to momentum flux, is found by adding Eqs. (9.13), (9.15), (9.17), and (9.19).

$$\Delta P_{fric} = \Delta P_{fric1} + \Delta P_{fric2} + \Delta P_{fric3} + \Delta P_{mom} \quad (9.20)$$

$$\Delta P_{fric} = 25.920 + 16.502 + 68.970 + 0.3683$$

$$= 111.760 \text{ Pa} \quad (9.21)$$

9.3 Frictional Pressure Drop Calculation in the Heated Section Without Dividing it into Sub-sections

In Section 9.2, the heated section was divided into 5 sub-sections for calculating the frictional pressure drop, to account for the temperature dependence of water viscosity and density. In the current section, the frictional pressure drop in the heated section is calculated without dividing it into sub-sections, using a single set of water properties, i.e., viscosity and density at the mean of inlet and exit coolant temperatures. This calculation is done at the natural circulation flow rate of 0.1086 kg/s found in Section 9.2 because the purpose here is to get an estimate of the error in the frictional pressure drop if it is calculated using a single set of water properties. The results are summarized below. The subscript *2m* implies mean value for the whole heated length.

Coolant flow rate in channel, W	= 0.1086 kg/s
Coolant exit temperature, T_{ex}	= 79.967 °C
Coolant mean temperature, $T_{2m} = (T_{in} + T_{ex})/2$	= 52.484 °C
Heated length, L_2	= 0.75 m
Dynamic viscosity at the mean temperature, μ_{2m}	= 5.2097×10^{-4} Pa-s
Coolant density at the mean temperature, ρ_{2m}	= 987.53 kg/m^3
Reynolds number at the mean temperature, $Re_{2m} = W \, D_h/(\mu_{2m} \, W_{ch} \, T_{ch})$	= 1375.95
Friction factor, $f_{2m} = 96/Re_{2m}$	= 0.069770
Frictional pressure drop, $\Delta P_{fric2} = 0.5 \, (f_{2m} \, L_2/D_h) \, [W/(W_{ch} \, T_{ch})]^2$	= 64.938 Pa

The frictional drop in the heated section, based on this approximate calculation, is 64.938 Pa compared to 68.970 Pa calculated more accurately by dividing the heated section into five sub-sections (in Section 9.2). There is an error of 5.8 % in the approximate calculation. These results are useful for comparison with PLTEMP/ANL output because the *forced flow option* in the code is currently coded to use a single set of coolant properties in calculating the frictional pressure drop in the heated section. However, the coolant temperature rise of 54.967 °C in this example is much greater than is found in typical forced-flow situations in research reactors.

9.4 *Mathematica* Calculations Using Three Sets of Coolant Properties

The codes NATCON, RELAP5-3D, and PLTEMP/ANL have different built-in coolant properties. To account for the effect of the difference in coolant properties, solutions to the test problem were obtained by *Mathematica* calculations, using the coolant properties built in each code. A *Mathematica* program was written in which any set of coolant properties could be inserted. Appendix F gives a listing of this program with the coolant properties of the PLTEMP/ANL code.

The program uses 21 axial nodes (mesh intervals) of equal length in the total channel length of 1.05 m, with three each in the lower and upper unheated lengths of the channel, and 15 in the heated length. Starting from a guess flow rate, the program calculates the coolant enthalpy at each node exit, the coolant temperature at the node exit, and the temperature at the node center. Using the node-center temperatures, the program finds the nodal Reynolds number, friction factor, nodal frictional pressure drop, and the nodal contribution to buoyancy. It finds the inlet and outlet pressure losses. The calculation ends after printing the total buoyancy and the total frictional pressure drop in the channel. To find the steady-state natural circulation flow rate, the user reruns the program several times, each time using a more improved guess of the flow rate, in order to make the total buoyancy equal to the sum of the frictional and momentum flux pressure drops.

The *Mathematica* program uses coolant enthalpy as a function of temperature, as shown by the program listing in Appendix F. However, the NATCON code uses built-in coolant specific heat (rather than enthalpy), as shown in Table 9.2. When using the coolant properties of the NATCON code, some additional statements were added to the program to find the corresponding enthalpy by integrating the specific heat.

Using this program, three solutions to Sample Problem 20 were obtained, using the coolant properties of (1) the NATCON code, (2) the RELAP5-3D code, and (3) the PLTEMP/ANL code. These solutions are given in Tables 9.3, 9.4, and 9.5. It is noted that the flow rate of 0.1114 kg/s per channel, calculated using the coolant properties of RELAP5-3D, is 2.4 % higher than the flow rate based on the coolant properties of NATCON and PLTEMP/ANL. The three *Mathematica* calculations are summarized in Table 9.1.

9.5 NATCON Code Calculation

Fig. 9.2 shows the input data used in the NATCON calculation [3]. As the input data shows, the heated length was divided into 20 axial mesh intervals (or nodes). The code computes the coolant temperature, density, viscosity, Reynolds number, friction factor, buoyancy head, and frictional pressure drop for each axial node, for a guessed value of channel flow rate. The code finds the total buoyancy head and frictional pressure drop, and then adjusts the channel flow rate to make the total buoyancy head equal to the total frictional pressure drop. The momentum flux term is ignored in the code because it is small. The results obtained are summarized in Table 9.1.

9.6 RELAP5-3D Code Calculation

This calculation was performed using the RELAP5-3D code which uses liquid water properties from the 1967 ASME Steam Tables (see Appendix G). The channel length of 1.05 m was divided into 21 axial nodes (mesh intervals) of equal length, with three each in the lower and upper

unheated lengths of the channel, and 15 in the heated length. The natural circulation test problem (Sample Problem 20) was solved by running a thermal-hydraulic transient model of a single coolant channel for a long enough time to reach a steady-state, using a fixed channel inlet pressure of 5.0 bar and a fixed channel exit pressure of 4.897305 bar. This input exit pressure is equal to the inlet pressure minus the gravity head of water at the pool temperature of 25 °C.

$$\text{Input Pressure at Channel Exit} = 500000\ \text{Pa} - 997.340\ \text{kg/m}^3 \times 1.05\ \text{m} \times 9.80655\ \text{m/s}^2$$
$$= 4.897305\ \text{bar}$$

Here, the value 997.340 kg/m^3 is the coolant density at the pool temperature of 25 °C, and 9.80655 m/s^2 is the acceleration due to gravity used in the RELAP5-3D calculation.

The code finds a steady-state natural circulation flow rate of 0.11409 kg/s per channel and an exit temperature of 77.437 °C. The results differ noticeably from those obtained by PLTEMP/ANL and NATCON because the RELAP5-3D code computes nodal coolant temperatures at the node exit, but uses these nodal temperatures as *node-average* values in computing nodal gravity head, nodal buoyancy and nodal frictional pressure drop, as discussed below. The printed solution of the code is shown in Table 9.6, with two analyses of the solution for the purpose of pointing out this cause. The analyses were done by transferring the code-printed results to a Microsoft Spreadsheet. It is important to note that RELAP5-3D needs to make the above approximation because it is designed to model two-phase flow, rather than only single-phase liquid, and it simulates dynamic behavior, rather than only steady-state performance. So RELAP5-3D cannot assume that the average of the inlet and outlet temperatures of a coolant node is the average temperature of the node.

<u>RELAP5-3D-Printed Results</u>: Column 2 of Table 9.6 shows the code-printed nodal pressures, P_n . The pressure differences, P_{n-1}-P_n , are shown in column 6. The difference for the first node, P_0-P_1, is found to be 253.0 Pa, about half of the difference for other nodes (1 through 21). Based on this observation, the nodal pressures are inferred to be node-centered values. Column 3 of Table 9.6 shows the code-printed nodal coolant temperatures. The temperature for node 18, i.e., the last node in the heated length of the channel, is 350.589 K, equal to the nodal temperature of the nodes 19, 20 and 21 in the unheated length of the channel. If the temperature for node 18 were *node-centered*, it would be less than the nodal temperatures in the unheated length. Based on this observation, the nodal temperatures are inferred to be *node-exit* values. Based on similar observations in columns 4 and 5 of Table 9.6, the nodal Reynolds numbers and coolant densities are inferred to be *node-exit* values.

<u>Analyses of Printed Results</u>: Table 9.6 shows two analyses done on a Microsoft Spreadsheet to calculate the gravity head, the buoyancy and the frictional pressure drop due to each node, using the code-printed nodal densities, ρ_n , and Reynolds numbers, Re_n . The first analysis (shown in columns 7 to 9) was done by treating the code-printed nodal densities and Reynolds numbers to be node-exit values, as they actually are. The second analysis (shown in columns 10 to 12) was done treating the code-printed nodal densities and Reynolds numbers to be node-centered values. In each analysis, the channel gravity head and the channel buoyancy were found by summing the nodal values. The channel frictional pressure drop was determined by two techniques in each analysis: (i) Technique 1: The channel frictional pressure drop equals the sum of the nodal frictional pressure drops, and the inlet and outlet losses; (ii) Technique 2: The channel frictional

pressure drop equals the RELAP5-3D-printed pressure difference between the channel inlet and outlet minus the channel gravity head. This is based on the assumption that the pressure difference between any pair of axial positions is the sum of the gravity head and the frictional pressure drop between the two positions. The nodal equations used in the two analyses are given below.

<u>Equations Used on Spreadsheet in the First Analysis</u>:
Gravity head of node n $= 0.5(\rho_{n-1}+\rho_n)\ g\ \Delta z_n$

Buoyancy due to node n = $\{\rho_1 - 0.5(\rho_{n-1}+\rho_n)\}\ g\ \Delta z_n$

Frictional pressure drop over node n = $\dfrac{96\,\Delta z_n}{0.5(Re_{n-1}+Re_n)\,D_h}\dfrac{1}{(\rho_{n-1}+\rho_n)}\left(\dfrac{W}{W_{ch}T_{ch}}\right)^2$

<u>Equations Used on Spreadsheet in the Second Analysis</u>:
Gravity head of node n $= \rho_n\ g\ \Delta z_n$

Buoyancy due to node n = $(\rho_1 - \rho_n)\ g\ \Delta z_n$

Frictional pressure drop over node n = $\dfrac{96\,\Delta z_n}{Re_n\,D_h}\dfrac{1}{2\rho_n}\left(\dfrac{W}{W_{ch}T_{ch}}\right)^2$

The channel buoyancy is found to be 111.936 Pa by the first analysis, and 117.797 Pa by the second analysis, as noted in Table 9.6. There is a difference of 5.2 % between the two values. The channel frictional pressure drop is found by technique 1 to be 118.590 Pa in the first analysis, and 116.420 Pa in the second analysis. To determine the channel frictional pressure drop by technique 2, the RELAP5-3D-printed pressure difference between the channel inlet and outlet of 10269.0 Pa, as shown in column 6 of Table 9.6, is reduced by the total gravity head. This gravity head is 10157.657 Pa in the first analysis and10151.795 Pa in the second. The frictional pressure drops determined by technique 2 are as follows:

Technique 2 in the First Analysis:
Channel Frictional Pressure Drop = 10269.0 – 10157.657 =111.343 Pa

Technique 2 in the Second Analysis:
Channel Frictional Pressure Drop = 10269.0 – 10151.795 =117.205 Pa

The values of channel buoyancy and channel frictional pressure drop obtained by the two analyses for Sample Problem 20 are given in Table 9.6, and also summarized below.

Technique Used	First Analysis		Second Analysis	
	Channel Buoyancy, Pa	Channel Frictional Pressure Drop, Pa	Channel Buoyancy, Pa	Channel Frictional Pressure Drop, Pa
Technique 1	111.936	118.590	117.797	116.420
Technique 2		111.343		117.205

In the first analysis, there are two discrepancies: (i) The channel buoyancy (111.936 Pa) and the channel frictional pressure drop (118.590 Pa) are not equal as they should be in the steady-state natural circulation. (ii) The two techniques give different values of the channel frictional pressure drop, 118.590 Pa and 111.343 Pa. Hence it is inferred that RELAP5-3D does not use the assumption of the first analysis to calculate the buoyancy and the frictional pressure drop.

In the second analysis, the values of channel frictional pressure drop (116.420 and 117.205 Pa) found by the two techniques are nearly equal. The channel buoyancy (117.797 Pa) and the channel frictional pressure drop (117.205 Pa) are nearly equal as they should be in the steady-state natural circulation. Hence it is inferred that RELAP5-3D uses the assumption of the second analysis to calculate the buoyancy and the frictional pressure drop, i.e., *it treats the node-exit densities and Reynolds numbers as node-center values.* This assumption artificially increases the channel buoyancy which causes a higher flow rate.

Concluding Remarks: Using the node-exit densities and Re as node-centered values makes the RELAP5-3D solution slightly inaccurate. The RELAP5-3D solution can be used for only an approximate verification (within 6 %) of the PLTEMP/ANL V3.5 natural circulation calculation. The buoyancy and the frictional pressure drop obtained in the second analysis are shown in Table 9.1 because they are preferred over those obtained in the first analysis.

9.7 PLTEMP/ANL Version 3.5 Code Calculation

To solve Sample Problem 20 using the PLTEMP/ANL code, the problem defined above in Section 9.2 is turned into a problem for a research reactor fuel assembly consisting of (arbitrarily) four plates cooled by five coolant channels. Each fuel plate produces 25 kW as defined in Section 9.2, and the fuel assembly has a power of 100 kW. The internal channels (channels 2, 3, and 4) are of the thickness 3 mm as defined in Section 9.2. In order to have identical axial profiles of coolant temperature in each channel, the first and the last channels are of half thickness, i.e., 1.5 mm. Based on symmetry, it is noted that exactly half of each fuel plate's power goes to each coolant channel adjacent to the plate. Fig. 9.3 gives the input data used in the PLTEMP/ANL code. It is noted that there are two identical fuel assemblies in the PLTEMP/ANL problem, and hence the total power in the input data is 0.2 MW.

In the input data of Fig. 9.3, the friction factor is obtained using the code's built-in correlation which accounts for laminar, transition, or turbulent flow as the case may be. This input data produces the results shown in the last column (column 9) of Table 9.1. The flow is found to remain always laminar in this problem, and the friction factor is given by C/Re where C is 94.7174 based on the thickness-to-width ratio of the coolant channel.

To do a fair comparison, another PLTEMP/ANL calculation was done using the friction factor (i.e., f = 96/Re) that was used in all the other calculations shown in Table 9.1. The results of the PLTEMP/ANL calculation using the friction factor of 96/Re are shown in column 8 of Table 9.1. This calculation agrees well with the *Mathematica* solution obtained using the coolant properties of PLTEMP/ANL given in column 4 of Table 9.1. This comparison provides a verification of the natural circulation option of the PLTEMP/ANL version 3.5 code.

9.8 Conclusion

There is a good agreement among the following four solutions of Sample Problem 20, as shown in Table 9.1: (1) hand calculation, (2) *Mathematica* solution using the coolant properties of the NATCON code, (3) *Mathematica* solution using the coolant properties of the PLTEMP/ANL code, and (4) NATCON code solution. The natural circulation flow rate is 0.1088 kg/s and the channel frictional pressure drop is 111.8 Pa. These values are accurately equal to the flow rate and channel frictional pressure drop calculated by the PLTEMP/ANL version 3.5 code using the frictional factor 96/Re. This provides a verification of the recently implemented natural circulation calculation capability of PLTEMP/ANL.

The RELAP5-3D solution is found to differ noticeably from the PLTEMP/ANL and NATCON solutions because the coolant temperatures at each node exit are used by the RELAP5-3D code as *node-average* temperatures in calculating buoyancy and frictional pressure drop, as discussed in Section 9.6. That is why the RELAP5-3D-calculated flow rate is about 5% higher than the PLTEMP/ANL-calculated flow rate.

The only difference between the two solutions by PLTEMP/ANL (given in the last two columns of Table 9.1) is in the value of the constant C in the laminar friction factor C/Re. The solution in the last column of Table 9.1 uses C = 94.7174 (instead of 96 for parallel plates) based on the aspect ratio of the rectangular cross section of the coolant channel. This causes a difference of 0.5 % in the flow rate.

NOMENCLATURE

ΔP_{buoy}	Pressure head due to buoyancy, Pa
ΔP_{fric}	Total frictional pressure drop in the coolant channel, Pa
C_p	Coolant specific heat averaged over the temperature range 25 to 80 °C existing in the problem, J/kg-°C
D_h	Hydraulic diameter of the channel, m
g	Acceleration due to gravity, m/s^2
H_{in}	Water depth at the channel inlet, m
L_1	Unheated channel length below the heated section, m
L_2	Heated length of channel, m
L_3	Unheated channel length above the heated section, m
L	Channel height = $L_1 + L_2 + L_3$, m
K_{in}	Pressure loss coefficient at the channel inlet
K_{ex}	Pressure loss coefficient at the channel exit
P_{in}	Pressure at the channel inlet, Pa
Q	Power in the channel, W
V_1	Coolant velocity at channel inlet, m/s
V_3	Coolant velocity at channel exit, m/s
T	Coolant temperature at an axial location, °C
T_{in}	Coolant temperature at the channel inlet, °C
T_{ex}	Coolant temperature at the channel exit, °C
T_{ch}	Channel thickness, m
W	Coolant flow rate in the channel, kg/s

W_{ch}	Channel width, m
z	Axial position, m
$\rho(z)$	Coolant density at position z, kg/m^3
$\rho(T)$	Coolant density as a function of temperature T, kg/m^3
ρ_1	Coolant density at the channel inlet temperature, kg/m^3
ρ_{ave}	Coolant density averaged over the heated length of the channel, kg/m^3
ρ_3	Coolant density at the channel exit temperature, kg/m^3
$\mu(T)$	Coolant dynamic viscosity as a function of temperature T, Pa-s
μ_1	Coolant dynamic viscosity at channel inlet, Pa-s
μ_3	Coolant dynamic viscosity at channel exit, Pa-s

REFERENCES

1. A. P. Olson and M. Kalimullah, "A User's Guide to the PLTEMP/ANL Code," ANL/RERTR/TM-11-22, Version 4.1, Argonne National Laboratory, 9700 South Cass Avenue, Argonne, IL 60439, USA (April 6, 2011).
2. R. S. Smith and W. L. Woodruff, "A Computer Code, Natcon, for the Analyses of Steady-State Thermal-Hydraulics and Safety Margins in Plate-Type Research Reactors Cooled by Natural Convection," ANL/RERTR/TM-12, Argonne National Laboratory, Argonne, Illinois, USA (December 1988).
3. The RELAP5-3D© Code Development Team, RELAP5-3D© Code Manual, Version 2.3, INEEL-EXT-98-00834, Idaho National Laboratory, Idaho, USA (April 2005).

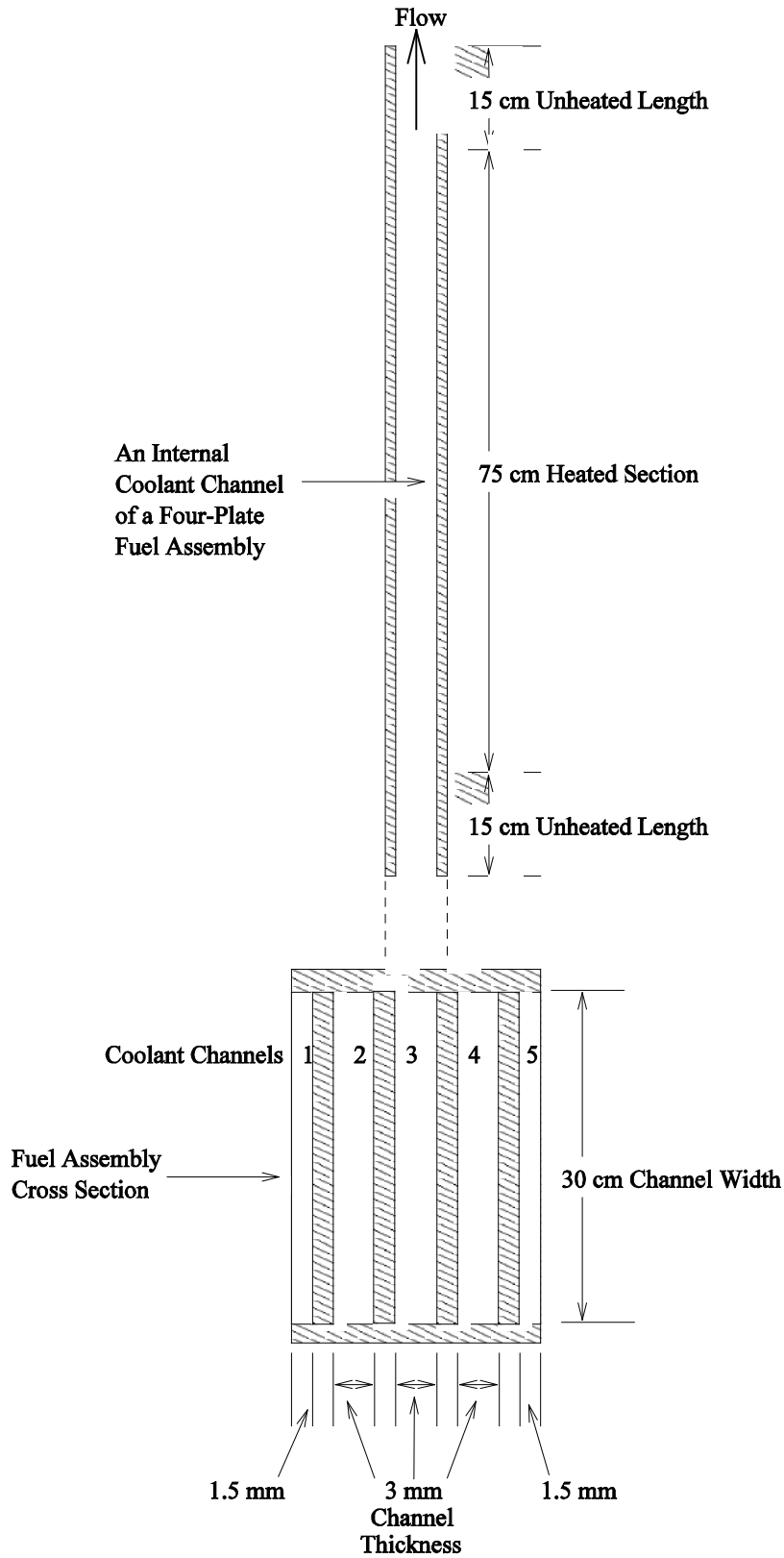

Figure 9.1 Geometry of a Coolant Channel in a Four-Plate Fuel Assembly Used in Sample Problem 20

Figure 9.2 NATCON Input Data for Sample Problem 20 Used in the Verification of Natural Circulation Calculation of PLTEMP/ANL Version 3.5

```
PLTEMP Sample Problem 20 on natural circulation modeled by NATCON          Card 0
    20     1     2     4     0     0     2     1     0                     Card 1
0.75        0.3         0.001       100.0       0.0005      180.0          Card 2
1.05        0.3         0.003       40.81       0.0         25.0           Card 3
0.0001      0.5         1.000       200.0                                  Card 4
1.000       1.000       1.000       1.000       1.000       1.000          Card 5
0.0         1.000                                                          Card 6
0.050       1.000                                                          Card 6
0.100       1.000                                                          Card 6
0.150       1.000                                                          Card 6
0.200       1.000                                                          Card 6
0.250       1.000                                                          Card 6
0.300       1.000                                                          Card 6
0.350       1.000                                                          Card 6
0.400       1.000                                                          Card 6
0.450       1.000                                                          Card 6
0.500       1.000                                                          Card 6
0.550       1.000                                                          Card 6
0.600       1.000                                                          Card 6
0.650       1.000                                                          Card 6
0.700       1.000                                                          Card 6
0.750       1.000                                                          Card 6
0.800       1.000                                                          Card 6
0.850       1.000                                                          Card 6
0.900       1.000                                                          Card 6
0.950       1.000                                                          Card 6
1.0         1.000                                                          Card
```

Figure 9.3 PLTEMP/ANL Input Data for Sample Problem 20 Used in the Verification of Natural Circulation Calculation by the Code

```
 Test Problem 20: Flow is calculated by natural circulation
! 2 assemblies, Total power = 0.20 MWt, Axially uniform power profile
! Each assembly has 4 fuel plates and 5 coolant channels
! H2O coolant, All hot channel factors = 1.0, No bypass flow, NCTYP=0
! 14 axial heat transfer nodes in the heated length of fuel plates
!  1   2   3   4   5   6   7   8   9  10  11  12  13  14  15  16  17  18  19    #  Card 200
   5   0   0   1   0   1   1   1   0   0   0   0   0   0   1   0   0   0   1    Card(1)0200
   2   3 0.50       1.00        1.00        1.00           0                   Card(1)0300
! Using pressure driven mode
   1   1 1.00                                                                   Card(1)0301
   1   1   1                                                                    Card(1)0302
1.00        1.00                                                                Card(2)0303
36.0E-04    5.94059E-03 0.15        0.50        0.30        3.00E-03            Card(3)0304
0.00        5.94059E-03 0.75        0.00        0.30        3.00E-03            Card(3)0304
36.0E-04    5.94059E-03 0.15        1.00        0.30        3.00E-03            Card(3)0304
! Use the code's biult-in correlation for friction factor
0.00        0.00        0.00                                                    Card(1)0305
   5   3 0.00       0.75        0.50E-03    180.00        1.00E-03    100.00    Card(1)0306
4.50E-04    5.94059E-03 0.3030      0.30        0.30        3.00E-03            Card(5)0307
9.00E-04    5.94059E-03 0.6060      0.60        0.30        3.00E-03            Card(5)0307
9.00E-04    5.94059E-03 0.6060      0.60        0.30        3.00E-03            Card(5)0307
9.00E-04    5.94059E-03 0.6060      0.60        0.30        3.00E-03            Card(5)0307
4.50E-04    5.94059E-03 0.3030      0.30        0.30        3.00E-03            Card(5)0307
0.30        0.30        0.30        0.30                                        Card(1)0308
! Card 0308A not required
! Radial power peaking factor data by fuel plate for each assembly. Input flow data by
! channel for each assembly on Cards 0310 not required because WFGES(1) is non-zero
1.000       1.000       1.000       1.000                                       Card(2)0309
1.000       1.000       1.000       1.000                                       Card(2)0309
! DP0       DDP         DPMAX       POWER       TIN         PIN
0.0003275   0.04        0.00        0.200       25.0        0.50                Card(1)0500
0.00        0.00                                                                Card(2)0500
  50 0.0001     25.0        0.00        0.00                                    Card(1)0600
  15                                                                            Card(1)0700
0.0         1.000                                                               Card(11)0701
0.100       1.000                                                               Card(11)0701
0.167       1.000                                                               Card(11)0701
0.233       1.000                                                               Card(11)0701
0.300       1.000                                                               Card(11)0701
0.367       1.000                                                               Card(11)0701
0.433       1.000                                                               Card(11)0701
0.5         1.000                                                               Card(11)0701
0.567       1.000                                                               Card(11)0701
0.633       1.000                                                               Card(11)0701
0.700       1.000                                                               Card(11)0701
0.767       1.000                                                               Card(11)0701
0.833       1.000                                                               Card(11)0701
0.900       1.000                                                               Card(11)0701
1.0         1.000                                                               Card(11)0701
   0                                                                            Card(11)0702
```

Table 9.1 Solution of Sample Problem 20 by Different Codes Used to Verify the Natural Circulation Option of PLTEMP/ANL Version 3.5

Input or Calculated Quantity	Hand Calculation Using NATCON Properties	*Mathematica* Calculation			NATCON Code Solution	RELAP5 Code Solution	PLTEMP/ANL V3.5 Solution	
		Using NATCON Coolant Properties	Using PLTEMP Coolant Properties	Using RELAP5 Coolant Properties			General Method, Friction Factor = 96/Re	General Method, Friction Factor = 94.7174/Re
Column Number	**2**	**3**	**4**	**5**	**6**	**7**	**8**	**9**
Inlet Temp, °C	25	25	25	25	25	25	25	25
Power per Channel, W	25000	25000	25000	25000	25000	25000	25000	25000
Loss Coeff. at Inlet	0.5	0.5	0.5	0.5	0.5	0.5	0.5	0.5
Loss Coeff. at Exit	1.0	1.0	1.0	1.0	1.0	1.0	1.0	1.0
CALCULATED QUANTITIES								
Flow per Channel, kg/s	0.1086	0.1088	0.1088	0.1114	0.1087	0.1141	0.1088	0.1093
Exit Temp, °C	79.967	79.900	79.891	78.660	79.970	77.44	79.891	79.646
BUOYANCY ΔP_{buoy}, Pa								
Axial Region 1	0.0	0.0	0.0	0.0	0.0	0.005	0.0	0.0
Axial Region 2 (Heated Section)	75.716	75.761	75.793	78.965	75.783	82.620	75.786	75.342
Axial Region 3	36.040	36.001	36.009	36.272	36.034	35.172	36.015	35.785
Channel ΔP_{buoy}	111.756	111.762	111.802	115.237	111.817	117.797	111.801	111.127
FRICTIONAL PRESSURE DROP ΔP_{fric}, Pa								
Inlet Loss	3.652	3.664	3.667	3.840	3.659	4.028	3.667	3.700
Axial Region 1	22.268	22.307	22.300	22.542	22.348	23.084	22.300	22.101
Axial Region 2 (Heated Length)	68.970	69.239	69.276	71.619	69.275	71.417	69.275	68.758
Axial Region 3	9.015	9.037	9.041	9.360	9.033	9.637	9.042	8.894
Exit Loss	7.487	7.513	7.518	7.875	7.503	8.254	7.518	7.585
Momentum Flux Term	0.368	0.0	0.0	0.0	0.0	0.0	0.0	0.0
Channel ΔP_{fric}	111.760	111.761	111.802	115.236	111.817	116.420	111.803	111.126

Note 1. Laminar friction factor = 96/Re, except as noted in the last column.

Note 2. The RELAP5-3D solution is not accurate because the nodal coolant temperatures at node exit are used as node-centered temperatures in calculating buoyancy and frictional pressure drop (as discussed in Section 9.5).

Table 9.2 Water Properties Used in the NATCON Code, RELAP5-3D Code, and PLTEMP/ANL Code

Water Properties Used in NATCON Code and Hand Calculation				Water Properties Used in in RELAP5-3D Code at 5.0 bar				Water Properties Used in in PLTEMP/ANL Code at 5.0 bar			
Temp °C	Specific Heat kJ/kg-°C	Water Density kg/m^3	Dynamic Viscosity µ Pa-s	Temp °C	Enthalpy kJ/kg	Water Density kg/m^3	Dynamic Viscosity µ Pa-s	Temp °C	Enthalpy kJ/kg	Water Density kg/m^3	Dynamic Viscosity µ Pa-s
21.718	4.165	997.54	974	20	84.33	998.505	1001.8	20	83.952	997.988	1014.5
27.301	4.168	996.30	855	25	105.23	997.339	890.3	25	104.773	996.982	901.17
32.879	4.171	994.81	755	30	126.12	995.930	797.6	30	125.608	995.759	804.50
38.450	4.175	993.08	673	35	147.00	994.300	719.6	35	146.457	994.321	722.29
44.022	4.179	991.06	604	40	167.89	992.466	653.3	40	167.327	992.672	652.48
49.583	4.183	988.79	547	45	188.78	990.443	596.4	45	188.211	990.815	593.26
55.144	4.187	986.30	499	50	209.68	988.244	547.1	50	209.116	988.754	542.91
60.694	4.192	983.57	458	55	230.58	985.879	504.2	55	230.034	986.495	499.92
66.239	4.196	980.62	422	60	251.49	983.357	466.6	60	250.973	984.042	462.93
71.778	4.201	977.39	392	65	272.42	980.685	433.5	65	271.934	981.403	430.75
77.311	4.206	974.00	367	70	293.36	977.871	404.1	70	292.915	978.583	401.28
82.839	4.212	970.46	345	75	314.31	974.922	377.9	75	313.923	975.590	377.03
88.356	4.217	966.66	326	80	335.28	971.843	354.5	80	334.946	972.432	355.98
93.867	4.223	962.76	309	85	356.26	968.638	333.4	85	356.003	969.117	337.40
99.370	4.230	958.67	292	90	377.27	965.313	314.5	90	377.075	965.655	320.63
104.867	4.236	954.44	277	95	398.30	961.871	297.3	95	398.181	962.055	304.97
110.356	4.244	950.09	263	100	419.36	958.315	281.8	100	419.314	958.326	290.21
115.828	4.251	945.66	250	105	440.45	954.647	267.6	105	440.476	954.482	276.41
121.294	4.259	941.16	238	110	461.57	950.869	254.7	110	461.672	950.532	263.52
127.190	4.268	936.20	226	115	482.73	946.983	242.9	115	482.896	946.490	251.49
132.340	4.276	931.85	216	120	503.93	942.990	232.0	120	504.162	942.367	240.27
				125	525.17	938.890	222.1	125	525.455	938.181	229.83
				130	546.46	934.684	212.9	130	546.797	933.940	220.10

Table 9.3 *Mathematica* Solution of Standard Problem 20, Using Coolant Properties of NATCON Code

Flow rate per coolant channel = 0.108788 kg/s

Node	Nodal Power W	Temp at Node Exit °C	Temp at Node Center, °C	Density at Node Center kg/m³	Buoyancy due to Node, Pa	Re at Node Center	Friction Factor at Node Center	Frictional Pressure Drop, Pa
Inlet				996,842				3.6643
1	0	25.	25.	996.842	0.	796.356	0.120549	7.43576
2	0	25.	25.	996.842	0.	796.356	0.120549	7.43576
3	0	25.	25.	996.842	0.	796.356	0.120549	7.43576
4	1666.67	28.676	26.838	996.413	0.210597	830.971	0.115527	7.12908
5	1666.67	32.3502	30.5131	995.472	0.671721	903.04	0.106308	6.56633
6	1666.67	36.0223	34.1862	994.428	1.1839	977.855	0.0981741	6.07031
7	1666.67	39.6923	37.8573	993.277	1.74805	1054.41	0.0910465	5.63612
8	1666.67	43.3599	41.5261	991.998	2.37497	1133.73	0.0846761	5.24852
9	1666.67	47.0252	45.1925	990.602	3.05961	1214.78	0.0790267	4.90526
10	1666.67	50.6882	48.8567	989.1	3.7963	1296.46	0.074048	4.60321
11	1666.67	54.3488	52.5185	987.505	4.57842	1379.1	0.0696094	4.33427
12	1666.67	58.0069	56.1779	985.809	5.40968	1462.77	0.0656287	4.09344
13	1666.67	61.6624	59.8347	984.008	6.29302	1547.65	0.0620294	3.87602
14	1666.67	65.3153	63.4888	982.115	7.22126	1635.06	0.0587134	3.67589
15	1666.67	68.9656	67.1405	980.11	8.20403	1723.08	0.0557142	3.49525
16	1666.67	72.6133	70.7895	977.982	9.24774	1808.92	0.0530702	3.33663
17	1666.67	76.2581	74.4357	975.781	10.3267	1892.18	0.0507351	3.197
18	1666.67	79.8997	78.0789	973.52	11.4355	1973.99	0.0486324	3.07162
19	0	79.8997	79.8997	972.368	12.0003	2015.2	0.0476379	3.01238
20	0	79.8997	79.8997	972.368	12.0003	2015.2	0.0476379	3.01238
21	0	79.8997	79.8997	972.368	12.0003	2015.2	0.0476379	3.01238
Outlet								7.5131
Total					111.762			111.761

Table 9.4 *Mathematica* Solution of Standard Problem 20, Using Coolant Properties of PLTEMP/ANL Code

Flow rate per coolant channel = 0.108838 kg/s

Node	Nodal Power W	Temp at Node Exit °C	Temp at Node Center, °C	Density at Node Center kg/m³	Buoyancy due to Node, Pa	Re at Node Center	Friction Factor at Node Center	Frictional Pressure Drop, Pa
Inlet		25.		996.982				3.6666
1	0	25.	25.	996.982	0.	797.13	0.120432	7.43323
2	0	25.	25.	996.982	0.	797.13	0.120432	7.43323
3	0	25.	25.	996.982	0.	797.13	0.120432	7.43323
4	1666.67	28.6755	26.8377	996.558	0.208068	831.596	0.115441	7.12818
5	1666.67	32.3492	30.5123	995.622	0.667042	903.077	0.106303	6.57014
6	1666.67	36.0207	34.185	994.57	1.18254	977.625	0.0981972	6.07556
7	1666.67	39.6895	37.8551	993.405	1.75386	1054.81	0.0910119	5.6376
8	1666.67	43.3566	41.523	992.128	2.38013	1134.12	0.0846472	5.2501
9	1666.67	47.0212	45.1889	990.74	3.06046	1215.06	0.0790086	4.90724
10	1666.67	50.6834	48.8523	989.244	3.794	1297.22	0.0740045	4.60339
11	1666.67	54.3439	52.5137	987.642	4.57954	1380.21	0.0695545	4.33359
12	1666.67	58.0018	56.1729	985.936	5.41603	1463.78	0.0655835	4.09325
13	1666.67	61.6569	59.8294	984.129	6.30224	1547.81	0.062023	3.87814
14	1666.67	65.3095	63.4832	982.223	7.23685	1632.13	0.0588188	3.68492
15	1666.67	68.9594	67.1344	980.221	8.21851	1719.81	0.0558203	3.50421
16	1666.67	72.6056	70.7825	978.126	9.24574	1808.57	0.0530806	3.33936
17	1666.67	76.2495	74.4276	975.941	10.3171	1892.35	0.0507304	3.19866
18	1666.67	79.8914	78.0704	973.67	11.4307	1974.73	0.0486142	3.07238
19	0	79.8914	79.8914	972.503	12.003	2015.52	0.0476303	3.01381
20	0	79.8914	79.8914	972.503	12.003	2015.52	0.0476303	3.01381
21	0	79.8914	79.8914	972.503	12.003	2015.52	0.0476303	3.01381
Outlet								7.5178
Total					111.802			111.802

Table 9.5 *Mathematica* Solution of Standard Problem 20, Using Coolant Properties of RELAP5-3D Code

Flow rate per coolant channel = 0.111395 kg/s

Node	Nodal Power W	Temp at Node Exit °C	Temp at Node Center, °C	Density at Node Center kg/m³	Buoyancy due to Node, Pa	Re at Node Center	Friction Factor at Node Center	Frictional Pressure Drop, Pa
Inlet				997.339				3.8401
1	0	25.	25.	997.339	0.	825.879	0.11624	7.51396
2	0	25.	25.	997.339	0.	825.879	0.11624	7.51396
3	0	25.	25.	997.339	0.	825.879	0.11624	7.51396
4	1666.67	28.5808	26.7904	996.861	0.234251	859.818	0.111652	7.22083
5	1666.67	32.1632	30.372	995.816	0.746781	929.173	0.103318	6.68886
6	1666.67	35.7457	33.9545	994.658	1.31466	1000.59	0.0959429	6.21865
7	1666.67	39.3268	37.5363	993.394	1.93444	1073.95	0.0893898	5.80127
8	1666.67	42.908	41.1174	992.03	2.60328	1149.18	0.0835381	5.42896
9	1666.67	46.4883	44.6982	990.571	3.31876	1226.28	0.0782855	5.0951
10	1666.67	50.0676	48.2779	989.021	4.07856	1305.32	0.0735454	4.79409
11	1666.67	53.6471	51.8573	987.385	4.88091	1386.08	0.0692602	4.52225
12	1666.67	57.2257	55.4364	985.665	5.7241	1468.45	0.0653751	4.27602
13	1666.67	60.8024	59.014	983.866	6.60621	1552.43	0.0618387	4.05211
14	1666.67	64.3766	62.5895	981.991	7.52554	1637.79	0.0586156	3.84824
15	1666.67	67.9495	66.163	980.043	8.48081	1724.59	0.0556653	3.66181
16	1666.67	71.5214	69.7354	978.024	9.47095	1812.95	0.0529524	3.49054
17	1666.67	75.0918	73.3066	975.936	10.4948	1902.7	0.0504546	3.33301
18	1666.67	78.6595	76.8757	973.782	11.5509	1993.6	0.0481541	3.18808
19	0	78.6595	78.6595	972.681	12.0908	2039.46	0.0470713	3.11992
20	0	78.6595	78.6595	972.681	12.0908	2039.46	0.0470713	3.11992
21	0	78.6595	78.6595	972.681	12.0908	2039.46	0.0470713	3.11992
Outlet								7.8749
Total					115.237			115.236

Table 9.6 RELAP5-3D-Calculated Solution of Sample Problem 20 and Two Analyses of the Solution

Flow rate per coolant channel = 0.11409 kg/s (practically constant at 400 s into the transient)

	RELAP5-3D Printed Output					**First Analysis**			**Second Analysis**		
1	2	3	4	5	6	7	8	9	10	11	12
Axial Node Number	P_n Pressure at Node Center, Pa	Coolant Temp at Node Exit, K	Reynolds Number at Node Exit	Density at Node Exit kg/m^3	P_{n-1} - P_n Pressure Drop Pa	Nodal Gravity Head Pa	Buoyancy Due to the Node Pa	Frictional Pressure Drop in the Node Pa	Nodal Gravity Head Pa	Buoyancy Due to the Node Pa	Frictional Pressure Drop in the Node Pa
	500000.00		845.83	997.340				4.0282			4.0282
1	499747.00	298.155	845.83	997.340	253.000	489.028	0.0000	7.6960	489.028	0.0000	7.6960
2	499251.00	298.162	845.96	997.340	496.000	489.028	0.0000	7.6954	489.028	0.0000	7.6948
3	498754.00	298.171	846.13	997.330	497.000	489.026	0.0025	7.6941	489.023	0.0049	7.6934
4	498258.00	301.669	914.80	996.370	496.000	488.788	0.2403	7.3969	488.553	0.4756	7.1227
5	497762.00	305.168	985.80	995.300	496.000	488.290	0.7380	6.8603	488.028	1.0003	6.6168
6	497268.00	308.667	1059.00	994.120	494.000	487.739	1.2896	6.3837	487.449	1.5789	6.1668
7	496775.00	312.166	1134.40	992.840	493.000	487.136	1.8927	5.9586	486.822	2.2065	5.7643
8	496283.00	315.664	1211.70	991.470	492.000	486.486	2.5424	5.5782	486.150	2.8783	5.4040
9	495792.00	319.162	1291.10	990.010	491.000	485.792	3.2362	5.2364	485.434	3.5941	5.0792
10	495302.00	322.659	1372.20	988.470	490.000	485.057	3.9717	4.9283	484.679	4.3492	4.7864
11	494813.00	326.155	1455.10	986.840	489.000	484.279	4.7489	4.6499	483.880	5.1485	4.5212
12	494325.00	329.650	1539.60	985.140	488.000	483.463	5.5653	4.3974	483.046	5.9821	4.2804
13	493838.00	333.144	1625.70	983.360	487.000	482.610	6.4185	4.1677	482.173	6.8548	4.0611
14	493353.00	336.636	1713.20	981.510	485.000	481.720	7.3084	3.9584	481.266	7.7620	3.8609
15	492868.00	340.127	1802.20	979.590	485.000	480.796	8.2327	3.7668	480.325	8.7034	3.6774
16	492385.00	343.616	1892.40	977.600	483.000	479.837	9.1913	3.5913	479.349	9.6792	3.5093
17	491902.00	347.103	1983.80	975.550	483.000	478.846	10.1818	3.4301	478.344	10.6843	3.3546
18	491421.00	350.589	2076.30	973.430	481.000	477.824	11.2041	3.2818	477.304	11.7239	3.2122
19	490941.00	350.589	2076.30	973.430	480.000	477.304	11.7239	3.2122	477.304	11.7239	3.2122
20	490460.00	350.589	2076.30	973.430	481.000	477.304	11.7239	3.2122	477.304	11.7239	3.2122
21	489980.00	350.587	2076.30	973.430	480.000	477.304	11.7239	3.2122	477.304	11.7239	3.2122
	489731.00				249.000			8.2542			8.2542
Total					10269.000	10157.657	**111.936**	**118.590**	10151.795	**117.797**	**116.420**
Channel Fric Press Drop given by Press Drop minus Gravity Head								**111.343**			**117.205**

APPENDIX F *Mathematica* Program for Solving Sample Problem 20, Using Coolant Properties of the PLTEMP/ANL Code

```
(" SOLUTION OF NATURAL CIRCULATION STANDARD PROBLEM 20, Using Water Properties of
the PLTEMP/ANL V3.5 Code ")
data={kin→0.5,kex→1.0,Dh→0.00594059,len1→0.15,len2→0.75,len3→0.15,wch→0.3,tch→0.003,grav
→9.80665,Cfric→96,tin→25.0,powr→25000.0};
flow=0.10883; ←———— This guess flow was adjusted and the program was rerun to achieve channel
                     channel buoyancy (buoy) equal to channel frictional pressure drop (delp).
(* power = 25 kW per plate, total power = 200 kW in 8 plates *)
Print["Subcooled water density, kg/m**3, at 5 bar absolute used in the PLTEMP/ANL V3.5 Code"];
rho={{20.,997.9875},{25.,996.9820},{30.,995.7591},{35.,994.3214},{40.,992.6718},{45.,990.8146},{5
0.,988.7536},{55.,986.4945},{60.,984.0422},{65.,981.4029},{70.,978.5832},{75.,975.5897},{80.,972.43
24},{85.,969.1167},{90.,965.6552},{95.,962.0546},{100.,958.3263},{105.,954.4819},{110.,950.5318},{
115.,946.4900},{120.,942.3674},{125.,938.1805},{130.,933.9403},{135.,929.6651},{140.,925.3685},{1
45.,921.0693},{150.,916.7842}};
Plot[Interpolation[rho][temp],{temp,20,150}];
Print["Subcooled water enthalpy, kJ/kg, at 5 bar absolute used in the PLTEMP/ANL V3.5 Code"];
enthalpy={{20.,83.9517},{25.,104.7730},{30.,125.6082},{35.,146.4573},{40.,167.3272},{45.,188.2110}
,{50.,209.1156},{55.,230.0341},{60.,250.9734},{65.,271.9336},{70.,292.9146},{75.,313.9233},{80.,334
.9460},{85.,356.0033},{90.,377.0746},{95.,398.1805},{100.,419.3143},{105.,440.4758},{110.,461.6720
},{115.0,482.8960},{120.,504.1616},{125.,525.4550},{130.,546.7970},{135.,568.1738},{140.,589.5991
},{145.,611.0661},{150.,632.5816}};
Plot[Interpolation[enthalpy][temp],{temp,20,150}];
Print["Dynamic viscosity, micro Pa-s, of water used in the PLTEMP/ANL V3.5 Code"];
visc={{20.,1014.5},{25.,901.17},{30.,804.50},{35.,722.29},{40.,652.48},{45.,593.26},{50.,542.91},{55
.,499.92},{60.,462.93},{65.,430.75},{70.,401.28},{75.,377.03},{80.,355.98},{85.,337.40},{90.,320.63},
{95.,304.97},{100.,290.21},{105.,276.41},{110.,263.52},{115.,251.49},{120.,240.27},{125.,229.83},{1
30.,220.10},{135.,211.05},{140.,202.64},{145.,194.82},{150.,187.56}};
Plot[Interpolation[visc][temp],{temp,20,150}];
Print["Inlet and Exit temperatures, C"];
tin=tin/.data
Cfric=Cfric/.data;
grav=grav/.data;
hin=1000*Interpolation[enthalpy][tin];
hout=hin+powr/flow/.data;
tout=tx/.FindRoot[hout==1000*Interpolation[enthalpy][tx],{tx,tin}]
rhoin=Interpolation[rho][tin];
rhoout=Interpolation[rho][tout];
Print["Density at inlet =",rhoin,", Density at exit =",rhoout];
rhoave=NIntegrate[Interpolation[rho][temp],{temp,tin,tout}]/(tout-tin);
Print["Integrated average coolant density over (",tin," to ",tout,") = ",rhoave];
buoy2=(rhoin-rhoave)*grav*len2 /.data;
buoy3=(rhoin-rhoout)*grav*len3 /.data;
buoy=buoy2+buoy3;
Print["DRIVING PRESSURE HEAD DUE TO BUOYANCY in Section 1 =0.0, Section 2 =",buoy2,",
Section 3 =",buoy3,", Total buoyancy (Pa) =",buoy];
velin=flow/(rhoin*wch*tch)/.data;
```

```
Print["Coolant inlet velocity, m/s = ",velin];
visc1=0.000001*Interpolation[visc][tin];
visc3=0.000001*Interpolation[visc][tout];
Print["Coolant dynamic viscosity, Pa-s, in axial regions 1 and 3 =",visc1," ",visc3]
reyn1=flow*Dh/(wch*tch*visc1)/.data;
reyn3=flow*Dh/(wch*tch*visc3)/.data;
Print["Reynolds numbers in axial regions 1 and 3 =",reyn1," ",reyn3];
fric2300=Cfric/2300.0;
fric4000=0.184/4000.0^0.2;
frica=If[reyn1<2300.0,Cfric/reyn1,fric2300+(fric4000-fric2300)*(reyn1-2300.0)/1700.0];
fric1=If[reyn1>4000.0,0.184/reyn1^0.2,frica];
frica=If[reyn3<2300.0,Cfric/reyn3,fric2300+(fric4000-fric2300)*(reyn3-2300.0)/1700.0];
fric3=If[reyn3>4000.0,0.184/reyn3^0.2,frica];
Print["Friction factors in Sections 1 and 3 =",fric1," ",fric3];
Print["FRICTIONAL PRESSURE DROP IN SECTION 1"]
delp1s=(fric1*len1/Dh)*0.5*(flow/(wch*tch))^2/rhoin/.data;
delp1m=kin*0.5*(flow/(wch*tch))^2/rhoin/.data;
delp1=delp1s+delp1m;
Print["Total pressure drop in Section 1 =",delp1,", Minor loss = ",delp1m,", Wall shear =",delp1s]
Print["FRICTIONAL PRESSURE DROP IN SECTION 3"]
delp3s=(fric3*len3/Dh)*0.5*(flow/(wch*tch))^2/rhoout/.data;
delp3m=kex*0.5*(flow/(wch*tch))^2/rhoout/.data;
delp3=delp3s+delp3m;
Print["Total pressure drop in Section 3 =",delp3,", Minor loss = ",delp3m,", Wall shear =",delp3s]
delp4=rhoin*velin*velin*(rhoin/rhoout-1.0)/.data;
Print["Pressure drop due to momentum flux (Pa) =",delp4];
Print["Flow =",flow,", g =",grav,", Temp at inlet and exit =",tin,", ",tout,", Density at inlet and exit =",rhoin,", ",rhoout,", Gravity head =",grav*(rhoin*len1+rhoave*len2+rhoout*len3)/.data,", Total buoyancy =",buoy,", Buoyancy in Section 2 =",buoy2,", Buoyancy in Section 3 =",buoy3,", Power into coolant (W) =",flow*(hout-hin)]
Print["LOOP OVER 21 AXIAL SEGMENTS"];
powr1=powr/15/.data;
delz=len2/15/.data;
enth1=hin;
temp1=tin;
delp2p=0;
buoy2p=0;
Do[powr2=powr1;
  If[j<4,powr2=0];
  If[j>18,powr2=0];
  enth2=enth1+powr2/flow;
  temp2=tx/.FindRoot[enth2==1000*Interpolation[enthalpy][tx],{tx,temp1}];
  tempj=0.5*(temp2+temp1);
  viscj=0.000001*Interpolation[visc][tempj];
  rhoj=Interpolation[rho][tempj];
  buoy2s=buoy2p+grav*(rhoin-rhoj)*delz;
  reynj=flow*Dh/(wch*tch*viscj)/.data;
  frica=If[reynj<2300.0,Cfric/reynj,fric2300+(fric4000-fric2300)*(reynj-2300.0)/1700.0];
  fricj=If[reynj>4000.0,0.184/reynj^0.2,frica];
  delpj=(fricj*delz/Dh)*0.5*(flow/(wch*tch))^2/rhoj/.data;
  delp2=delp2p+delpj;
```

```
  (*Print["Axial segment =",j,", Flow, kg/s =",flow,", delz (m) =",delz,"Power in segment (W) =",powr2,", Enthalpy at segment exit (J/kg) =",enth2,", Enthalpy at segment center (J/kg) =",0.5(enth1+enth2),", Temp at segment exit (C) =",temp2,", Segment mean temp (C) =",tempj,", Segment mean density (kg/m^3) =",rhoj,", Buoyancy due to segments 1 through ",j," (Pa) =",buoy2s,", Viscosity (Pa-s) =",viscj,", Reynolds number =",reynj,", Friction factor =",fricj,", fl/Dh of segment (Pa) =",delpj,", Cumulative sum fL/Dh of segments 1 through ",j", (Pa) =",delp2];*)
  Print[j," ",powr2," ",temp2," ",tempj," ",rhoj," ",grav*(rhoin-rhoj)*delz," ",reynj," ",fricj," ",delpj];
  buoy2p=buoy2s;
  delp2p=delp2;
  temp1=temp2;
  enth1=enth2,
  {j,1,21}]
Print["BALANCE OF BUOYANCY AND FRICTIONAL PRESSURE DROP:"]
delp=delp2+delp1m+delp3m;
buoy=buoy2s;
Print["Total buoyancy (Pa) =",buoy,", Total frictional pressure drop (Pa) =",delp];
```

APPENDIX G Natural Convective Test Case for PLEMP/ANL Solved with RELAP5

G.1 Introduction

There is an effort currently underway to expand the capabilities of the PLTEMP/ANL code[1] to include analysis where the core flow rate is driven solely by natural convection. Because the Natcon code[2], which does consider such flows, considers only a single fueled channel at a time, it can not include heat transfer through the fuel plates to adjacent coolant channels. Incorporating the capabilities of Natcon into PLTEMP/ANL would enable PLTEMP/ANL to consider both force flow and convective flow in all channels with a single model setup.

A single-channel test problem was devised to assist in the development and testing of the expanded capabilities of PLTEMP/ANL. This test problem was analyzed with the RELAP5 code[3] because RELAP5 was externally and independently developed, is well documented, and is widely used by reactor analysts. The test problem model was extremely easy to develop by adapting parts of two other similar natural-convective flow RELAP5 models that had been developed and successfully deployed in the immediate past.

G.2 The Test Problem

The test problem was designed to be extremely simple so that differences between RELAP5 and PLTEMP predictions would be easy to trace. This test problem is a vertical rectangular channel whose key parameters are provided in Table G.1. The duct is 3 mm thick by 0.3 m wide, yielding an aspect ratio of 0.01. The duct length is 1.05 m. The first and last 0.15-meter channel lengths are unheated. The middle 0.75-meter channel length is uniformly heated over the two 0.3-m wide opposing walls of the duct with a total power of 25 kW. Although there is a K-loss (or form-loss) at the inlet of 0.5 and a K-loss of 1.0 at the exit, it is assumed that there is no area change at either end of the duct.

The inlet temperature of the coolant is 25° C. The coolant pressure at the inlet it 5.0 bar. The pressure of the coolant at the inlet is greater than that at the outlet only because the coolant is 1.05 m deeper at the inlet than at the outlet. This pressure difference is equal to the water density (997.3390 kg/m^3) times the acceleration due to gravity (9.80655 m/s^2) times the elevation difference (1.05 m), or 10269.48 Pa = 0.1026948 bar. Thus, the outlet pressure is 4.8973052 bar. The density is based on the 1967 ASME Steam Tables, which are also used by RELAP5. There may be a few non-significant digits in the outlet pressure, but they were maintained in the model input since the entire buoyancy pressure drop, as will be shown later, is only 117.80 Pa.

Table G.1 Key Parameters

Parameter	Value
Channel Thickness, mm	3.0
Channel Width, m	0.30
Channel Length, m	1.05
Channel Heated Length, m	0.75
Channel Heated Width, m	0.30
Heated Length Below Channel, m	0.15
Heated Length Above Channel, m	0.15
Inlet Temperature, C	25
Power Shape	Uniform
Channel Power, kW	25
Inlet Form Loss (K-loss)	0.5
Outlet Form Loss (K-loss)	1.0
Hot Channel Factors (All)	1.0
Inlet Pressure, bar	5.0
Inlet − Outlet Press., m 25° C H_2O	1.05
Laminar Friction Factor × Rey. No.	96

In the RELAP5 model the 1.05 m channel length was divided into 21 layer, or nodes, of 0.05 m each. A RELAP5 time-dependent node was used at the inlet as a pressure and temperature source and another time-dependent node was used at the exit as a pressure sink. The steady-state solution was obtained via a 400-s pseudo-transient.

For laminar flow, RELAP5 assumes that the Moody friction factor is $64/(Re \times \Phi)$, where Re is the Reynolds number and Φ is an input parameter. For infinite parallel plates the laminar flow Moody friction factor is 96/Re. Since the duct aspect ratio is only 0.01, it behaves essentially like parallel plates. Because the PLTEMP/ANL code uses the infinite parallel plate model for this aspect ratio, Φ was set to 0.6667.

The flow area is the product of the channel width and thickness, or 9.0×10^{-4} m^2. The hydraulic diameter is 4 times the flow area divided by the wetted perimeter, or 5.940594 mm.

G.3 Results

RELAP5 predicted a flow rate of 0.1141 kg/s and an outlet temperature of 77.44° C. The code also provided a value of coolant density at each of the 21 axial levels. The buoyancy pressure drop, which is what drives the flow, can be obtained from these 21 density values. These 21 values were summed and then multiplied by the product of the acceleration due to gravity and the 0.05-m node thickness, to obtain a value of 10151.69 Pa. The buoyancy pressure drop is the difference between the 10269.48 Pa calculated above, due to 1.05 m of 25° C water, and 10151.69 Pa. Thus, the gravity pressure difference is 117.80 Pa.

G.4 REFERENCES

1. A. P. Olson and M. Kalimullah, "A User's Guide to the PLTEMP/ANL Code," ANL/RERTR/TM-11-22, Version 4.1, Argonne National Laboratory, 9700 South Cass Avenue, Argonne, IL 60439, USA (April 6, 2011).

2. R. S. Smith and W. L. Woodruff, "A Computer Code, Natcon, for the Analyses of Steady-State Thermal-Hydraulics and Safety Margins in Plate-Type Research Reactors Cooled by Natural Convection," ANL/RERTR/TM-12, Argonne National Laboratory, Argonne, Illinois, USA (December 1988).

3. The RELAP5-3D© Code Development Team, RELAP5-3D© Code Manual, Version 2.3, INEEL-EXT-98-00834, Idaho National Laboratory, Idaho, USA April 2005.

10 Verification of the Chimney Model in Natural Circulation Calculation Implemented in the PLTEMP/ANL V3.6 Code

The verification work reported here was done in December 2008. A natural circulation calculation implemented in the PLTEMP/ANL V3.5 code was verified earlier. A chimney model was added in the V3.6 code. For the verification of the chimney model, a natural circulation test problem for a 4-fuel-plate assembly entering a 2.0 m high chimney, was solved by *Mathematica*, by the NATCON code, and by PLTEMP/ANL V3.6. *Mathematica* solutions were performed using, in turn, the sets of coolant properties used in PLTEMP/ANL and NATCON. The *Mathematica* calculations were done starting from an assumed flow rate in a coolant channel which was manually adjusted so that the buoyancy equals the frictional pressure drop in the channel. All four solutions are summarized in Table 10.1. The *Mathematica* and NATCON code solutions agree well with the PLTEMP/ANL solution, and this provides a verification of the chimney model in PLTEMP/ANL.

10.1 Introduction

The PLTEMP/ANL code was improved to model a chimney of a user-specified height in the coolant flow calculation by natural circulation, upward through the fuel assemblies and downward in the reactor pool. All fuel assemblies in the problem or a group of fuel assemblies enter into a common chimney. In the latter case, the problem has more than one chimney. The schematic and physical geometries of the model are shown in Figs. 10.1 and 10.2. The thermal-hydraulic equations to model the chimney and the method of solution are described in the PLTEMP/ANL V4.3 Users Guide [1].

The purpose of this report is to document the solution of a natural circulation test problem that is used in the verification of this model. The test problem is defined in Section 10.2, and referred to as Test Problem 22. Its solution by four methods/codes are reported and compared here:

(1) *Mathematica* calculation using the coolant properties used in the PLTEMP/ANL code,
(2) *Mathematica* calculation using the coolant properties used in the NATCON code,
(3) Solution by the NATCON code [2], and
(4) Solution by the PLTEMP/ANL version 3.6 code.

The solutions by NATCON and by *Mathematica* were obtained for a single coolant channel, and the PLTEMP/ANL solution was obtained for a four-plate fuel assembly.

10.2 A Test Problem with Chimney

<u>Problem Definition</u>: Calculate the coolant flow rate caused by natural circulation in a 1.05 m long vertical coolant channel entering a chimney of height 2.0 m. The heated length of the channel is 0.75 m, the lower unheated length is 0.15 m, and the upper unheated length is 0.15 m. The heated length has a power of 25 kW distributed uniformly over the 0.75 m length, with an inlet temperature of 25 °C. The channel has a rectangular cross section of thickness 3 mm, width 0.3 m, inlet pressure loss coefficient 0.5, and exit pressure loss coefficient 1.0. The absolute pressure at the channel inlet is 5 bar, corresponding to the channel inlet being 40.81 m below the free surface of water in the pool.

The values of input variables (see nomenclature given at the end) for this problem are as follows:

D_h = 0.0059406 m,	g = 9.8 m/s^2,	H_{in} = 41.81 m,	K_{in} = 0.5,
K_{ex} = 1.0,	L_1 = 0.15 m,	L_2 = 0.75 m,	L_3 = 0.15 m,
L = 1.05 m,	L_{ch} = 2.00 m,	Q = 25000 W,	P_{in} = 5.0 bar,
T_{in} = 25 °C,	T_{ch} = 0.003 m,	W_{ch} = 0.3 m,	
W = 0.1980283 kg/s (*assumed value*)			

10.3 *Mathematica* Calculations

The codes NATCON and PLTEMP/ANL have slightly different built-in coolant properties, as shown in Table 10.2. To account for the effect of the difference between coolant properties, two solutions to the test problem were obtained by *Mathematica* calculations, using the coolant properties built in each code. In each *Mathematica* calculation, the same friction factor correlations were used, i.e., the correlations used in the PLTEMP/ANL code. A *Mathematica* program was written in which any set of coolant properties could be inserted. Appendix H gives a listing of this program with the coolant properties of the PLTEMP/ANL code.

The program uses 21 axial nodes (mesh intervals) of equal length in the total channel length of 1.05 m, with three each in the lower and upper unheated lengths of the channel, and 15 in the heated length. Starting from a guessed flow rate, the program calculates the coolant enthalpy at each node exit, the coolant temperature at the node exit, and the temperature at the node-center. Using the node-center temperature, the program finds the nodal Reynolds number, friction factor, nodal frictional pressure drop, and the nodal contribution to buoyancy. It finds the channel inlet and outlet pressure losses. It finds the buoyancy due to the chimney. The frictional pressure drop in the chimney is assumed to be negligible. The momentum flux term is ignored because it is small. The calculation ends after printing the total buoyancy and the total frictional pressure drop in the channel. To find the steady-state natural circulation flow rate, the user reruns the program several times, each time using a more improved guess of the flow rate, in order to make the total buoyancy equal to the total frictional pressure drop.

The *Mathematica* program uses coolant enthalpy as a function of temperature, as shown by the program listing in Appendix H. However, the NATCON code uses built-in coolant specific heat (rather than enthalpy), as shown in Table 10.2. When using the coolant properties of the NATCON code, some additional statements were added to the program to find the corresponding enthalpy by integrating the specific heat.

The two solutions to Test Problem 22, obtained using the coolant properties of PLTEMP/ANL and NATCON are given in Tables 10.3 and 10.4. The two *Mathematica* calculations are summarized in Table 10.1. It is noted that the two calculated flow rates, 0.19803 and 0.19796 kg/s, are in good agreement (with a small difference of 0.035 %).

10.4 NATCON Code Calculation

Fig. 10.4 shows the input data for Test Problem 22 used in the NATCON version 2.2 calculation [2]. As the input data shows, the heated length was divided into 15 axial mesh intervals (or nodes). The chimney height (2.0 m) is the fifth input datum on Card 3. The code computes the coolant

temperature, density, viscosity, Reynolds number, friction factor, buoyancy head, and frictional pressure drop for each axial node, for a guessed value of channel flow rate. The code finds the total buoyancy head and frictional pressure drop, and then adjusts the channel flow rate to make the total buoyancy head equal to the total frictional pressure drop. The momentum flux term is ignored in the code because it is small. The results obtained are given in Table 10.5 which is summarized in Table 10.1 for comparison with other solutions of the problem.

10.5 PLTEMP/ANL Version 3.6 Code Calculation

To solve Test Problem 22 using the PLTEMP/ANL V3.6 code, the problem defined above in Section 10.2 is turned into a problem for a research reactor fuel assembly consisting of (arbitrarily) four plates cooled by five coolant channels (Fig. 10.3). Each fuel plate produces 25 kW as specified in the problem definition, and the fuel assembly has a power of 100 kW. The internal channels (channels 2, 3, and 4) are of the thickness 3 mm as specified in the problem definition. In order to have identical axial profiles of coolant temperature in each channel, the first and the last channels are of half thickness, i.e., 1.5 mm. Based on symmetry, it is noted that exactly half of each fuel plate's power goes to each coolant channel adjacent to the plate. Fig. 10.5 gives the input data used in the PLTEMP/ANL V3.6 code. It is noted that there are two identical fuel assemblies in the PLTEMP/ANL problem, and hence the total power in the input data is 0.2 MW.

In the input data of Fig. 10.5, the friction factor is obtained using the PLTEMP/ANL V3.6 code's built-in correlations which accounts for laminar, transition, or turbulent flow as the case may be. The results obtained are given in Table 10.6 which is summarized in Table 10.1 for comparison with other solutions of the problem. The flow is laminar over the lower part of the channel, and then changes to the transition regime over the upper part of the channel. The Darcy-Weisbach friction factor is calculated using the following correlations.

$$f = \begin{cases} f_{lam}(Re, a) & \text{if } Re \le 2200 \\ \left(3.75 - \dfrac{8250}{Re}\right)\left(f_a - f_{2200}\right) + f_{2200} & \text{if } 2200 < Re < 3000 \end{cases} \tag{10.1}$$

where

$$f_{lam}(Re, a) = \frac{96\left(1 - 1.3553\,a + 1.9467\,a^2 - 1.7012\,a^3 + 0.9564\,a^4 - 0.2537\,a^5\right)}{Re} \tag{10.2}$$

$$f_{2200} = f_{lam}(2200, a) \tag{10.3}$$

$$f_a = \left[-2\,\mathrm{Log}_{10}\left\{\frac{E_{rel}}{3.7} + \frac{2.51}{Re}\left\{1.14 - 2\,\mathrm{Log}_{10}\left(E_{rel} + 21.25\,Re^{-0.9}\right)\right\}\right\}\right]^{-2} \tag{10.4}$$

a = Channel aspect ratio = Channel thickness/width ratio, always ≤ 1.0
E_{rel} = Relative roughness

The numerator of Eq. (10.2) for the laminar friction factor is found to be 94.7174/Re based on the thickness-to-width ratio of the coolant channel. The results of the PLTEMP/ANL calculation agree well with the *Mathematica* solution obtained using the coolant properties of PLTEMP/ANL given in column 2 of Table 10.1. This comparison provides a verification of the chimney model in the natural circulation calculation implemented in the PLTEMP/ANL V3.6 code.

10.6 Conclusion

There is a good agreement among the following four solutions of Test Problem 22, as shown in Table 10.1: (1) PLTEMP/ANL V3.6 calculation, (2) *Mathematica* solution using the coolant properties of the PLTEMP/ANL code, (3) *Mathematica* solution using the coolant properties of the NATCON code, and (4) NATCON code solution. The natural circulation flow rate per channel calculated by the PLTEMP/ANL V3.6 code is 0.19809 kg/s, compared to 0.19803 kg/s calculated by *Mathematica* using the PLTEMP/ANL coolant properties. This provides a verification of the chimney model implemented in the PLTEMP/ANL V3.6 code.

The flow rate 0.19967 kg/s calculated by the NATCON V2.2 code is 0.8 % higher than that calculated by PLTEMP/ANL V3.6. This is mainly due to the difference between the friction factors used in the two codes. NATCON V2.2 has no provision for transition-flow-regime friction factor whereas PLTEMP/ANL V3.6 provides for it as shown in Eq. (10.1) to Eq. (10.4). Only a small difference in the flow rate is caused by the coolant property differences between the two codes, as shown by a comparison between the two *Mathematica* solutions.

NOMENCLATURE

a	Channel aspect ratio = Channel thickness/width ratio, always ≤ 1.0
C_p	Coolant specific heat averaged over the temperature range 25 to 80 °C existing in the problem, J/kg-°C
D_h	Hydraulic diameter of the channel, m
E_{rel}	Relative roughness
g	Acceleration due to gravity, m/s^2
H_{in}	Water depth at the channel inlet, m
L_1	Unheated channel length below the heated section, m
L_2	Heated length of channel, m
L_3	Unheated channel length above the heated section, m
L	Channel height = $L_1 + L_2 + L_3$, m
L_{ch}	Effective chimney height, m
K_{in}	Pressure loss coefficient at the channel inlet
K_{ex}	Pressure loss coefficient at the channel exit
ΔP_{buoy}	Pressure head due to buoyancy, Pa
ΔP_{fric}	Total frictional pressure drop in the coolant channel, Pa
P_{in}	Pressure at the channel inlet, Pa
Q	Power in the channel, W
V_1	Coolant velocity at channel inlet, m/s
V_3	Coolant velocity at channel exit, m/s
T	Coolant temperature at an axial location, °C
T_{in}	Coolant temperature at the channel inlet, °C
T_{ex}	Coolant temperature at the channel exit, °C
T_{ch}	Channel thickness, m
W	Coolant flow rate in the channel, kg/s
W_{ch}	Channel width, m

10.7 REFERENCES

1. M. Kalimullah, A. P. Olson and E. E. Feldman, "A User's Guide to the PLTEMP/ANL Code," ANL/RTR/TM-18/17 Version 4.3, Revision 0, Argonne National Laboratory, 9700 South Cass Avenue, Argonne, IL 60439, USA (November 2018).
2. R. S. Smith and W. L. Woodruff, "A Computer Code, NATCON, for the Analysis of Steady-State Thermal-Hydraulics and Safety Margins in Plate-Type Research Reactors Cooled by Natural Convection," ANL/RERTR/TM-12, Argonne National Laboratory, Argonne, Illinois, USA (December 1988).

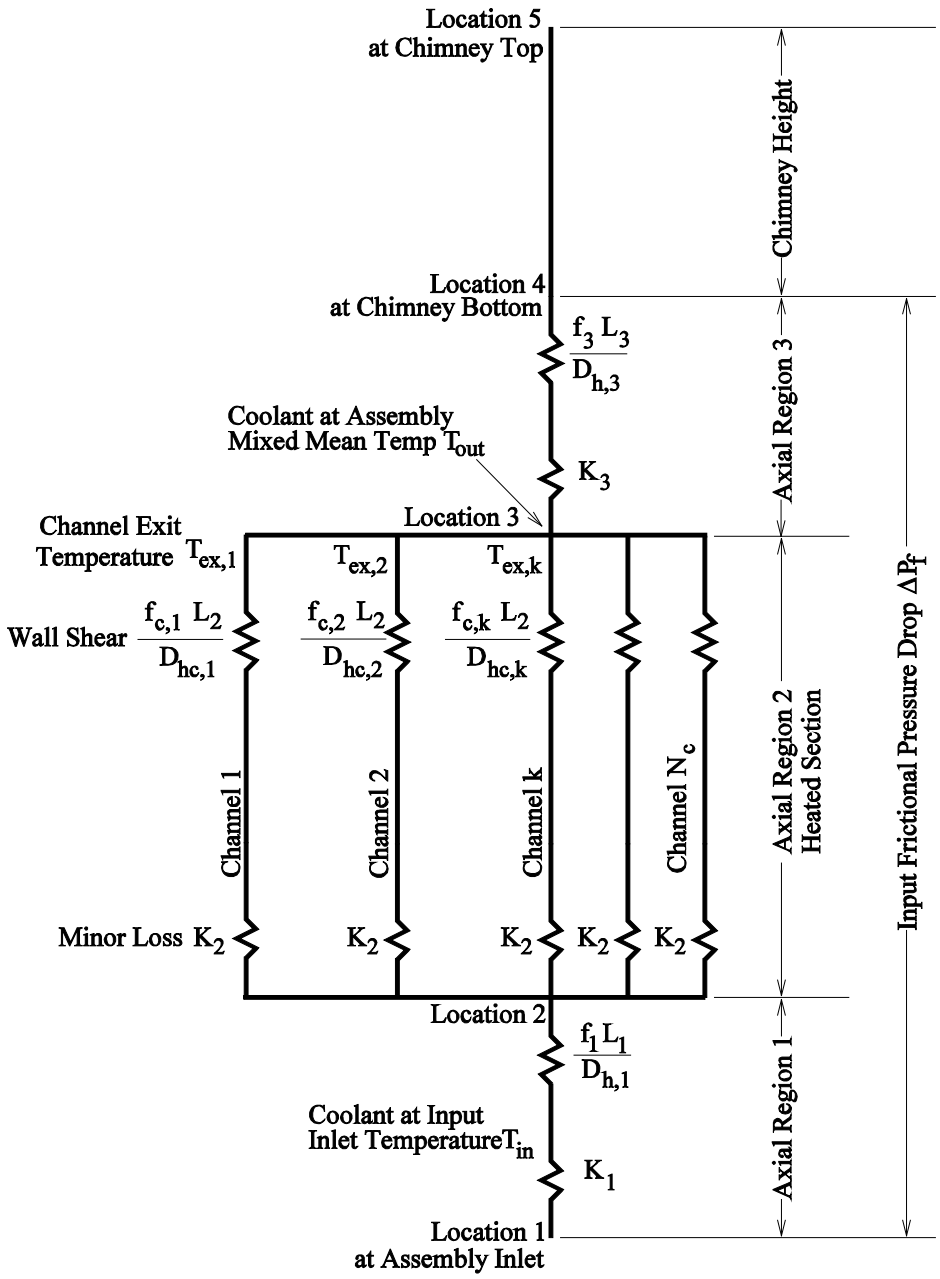

Figure 10.1 Coolant Flow Path in a Fuel Assembly and Chimney Modeled in PLTEMP/ANL (Multiple Axial Regions Downstream of the Heated Section Are Allowed)

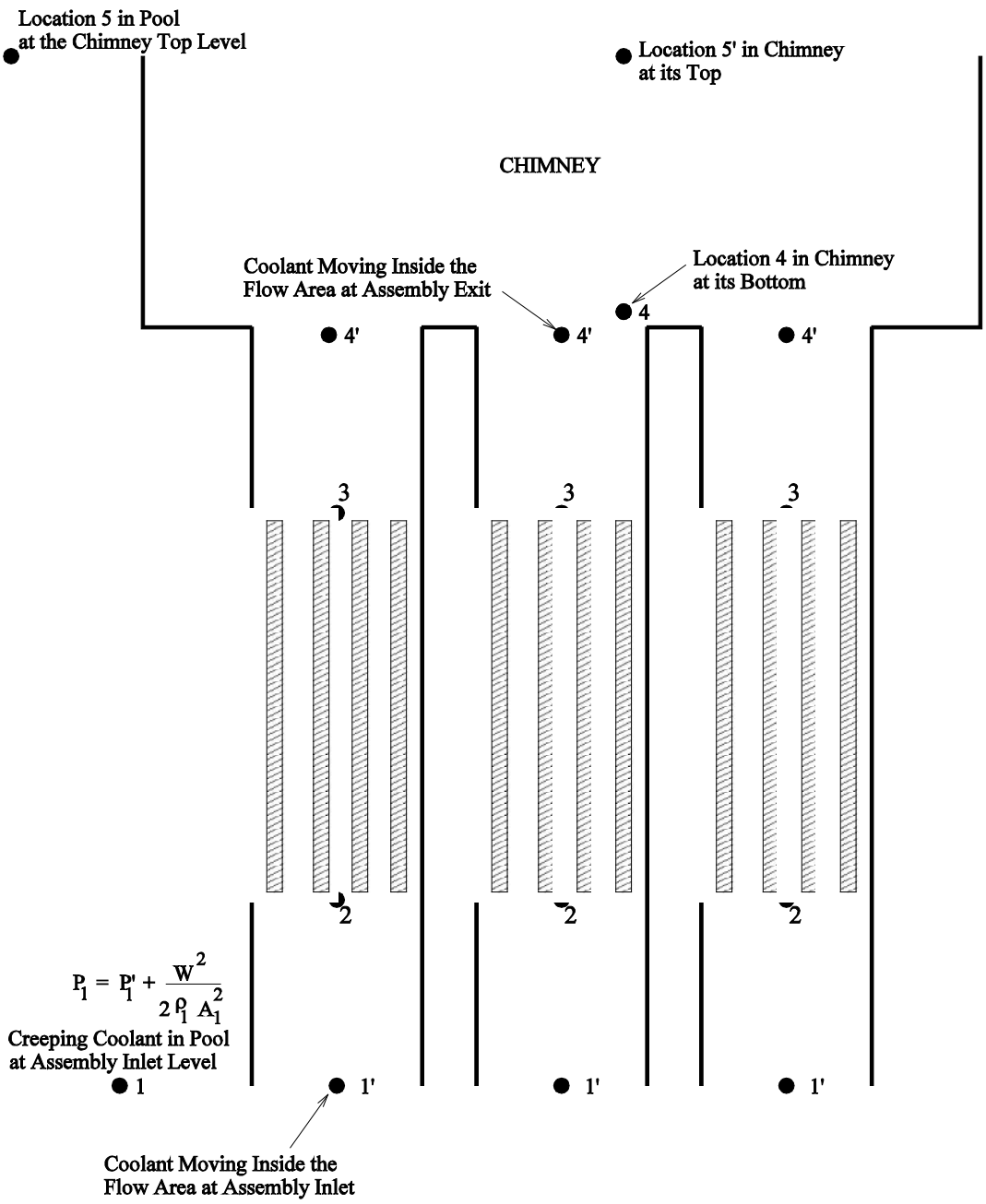

Figure 10.2 Locations of Coolant Pressure in a Group of Fuel Assemblies Exiting into a Common Chimney

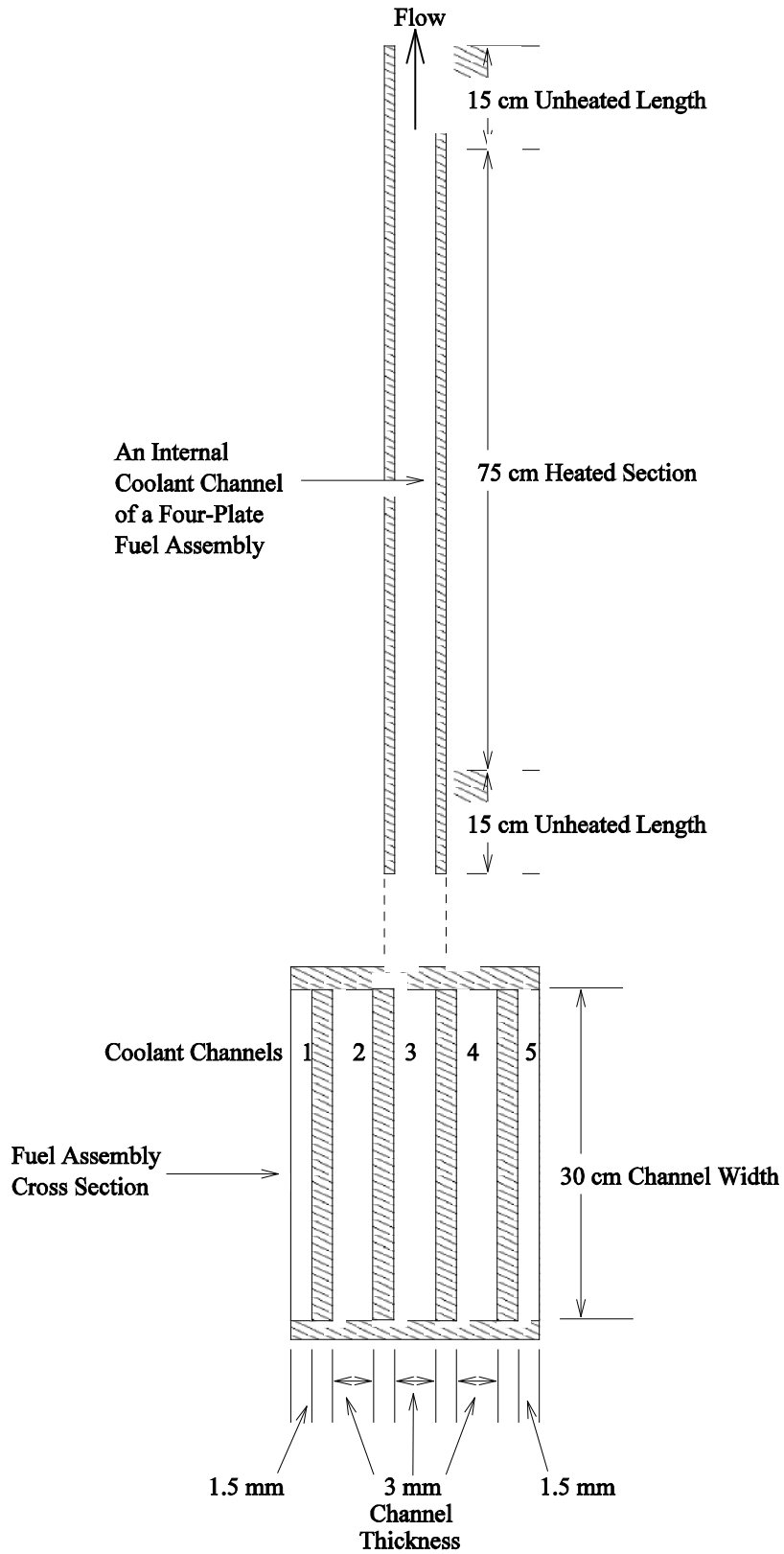

Figure 10.3 Geometry of a Coolant Channel in a Four-Plate Fuel Assembly Used in Test Problem 22

Figure 10.4 NATCON Input Data for Test Problem 22 Used in the Verification of the Chimney Model

```
PLTEMP Sample Problem 22 on natural circ with chimney modeled by NATCON         Card 0
    15     1     2     4     0     0     2     1     0                         Card 1
0.75        0.3         0.001       100.0       0.0005      180.0               Card 2
1.05        0.3         0.003       40.81       2.0         25.0                Card 3
0.0001      0.5         1.000       200.0                                       Card 4
1.000       1.000       1.000       1.000       1.000       1.000               Card 5
0.0         1.000                                                               Card 6
0.066667    1.000                                                               Card 6
0.133333    1.000                                                               Card 6
0.200000    1.000                                                               Card 6
0.266667    1.000                                                               Card 6
0.333333    1.000                                                               Card 6
0.400000    1.000                                                               Card 6
0.466667    1.000                                                               Card 6
0.533333    1.000                                                               Card 6
0.600000    1.000                                                               Card 6
0.666667    1.000                                                               Card 6
0.733333    1.000                                                               Card 6
0.800000    1.000                                                               Card 6
0.866667    1.000                                                               Card 6
0.933333    1.000                                                               Card 6
1.000000    1.000                                                               Card 6
```

Figure 10.5 PLTEMP/ANL Input Data for Test Problem 22 Used in the Verification of the Chimney Model

```
 Test Problem 22: Natural Circulation, 2.0 m chimney, f = 94.7174/Re
! 2 assemblies, Total power = 0.20 MWt, Axially uniform power profile
! Each assembly has 4 fuel plates and 5 coolant channels
! H2O coolant, All hot channel factors = 1.0, No bypass flow, NCTYP=0
! 14 axial heat transfer nodes in the heated length of fuel plates
!  1   2   3   4   5   6   7   8   9  10  11  12  13  14  15  16  17  18  19  20 # Card 200
   5   0   0   1   0   1   1   1   0   0   0   0   0   0   1   1   0   0   0   1   Card 200
   1                                                                                Card 200A
   2   3 0.50       1.00        1.00        1.00           0                     Card(1)0300
! Using pressure driven mode
   1   1 1.00                                                                      Card(1)0301
   1   1   1                                                                       Card(1)0302
1.00        1.00                                                                   Card(2)0303
36.0E-04    5.94059E-03 0.15        0.50        0.30        3.00E-03               Card(3)0304
0.00        5.94059E-03 0.75        0.00        0.30        3.00E-03               Card(3)0304
36.0E-04    5.94059E-03 0.15        1.00        0.30        3.00E-03               Card(3)0304
! Use the code's built-in correlation for friction factor
!                                   CHIMNY
0.00        0.00        0.00        2.0                                            Card(1)0305
   5   3 0.00       0.75        0.50E-03    180.00        1.00E-03    100.00       Card(1)0306
4.50E-04    5.94059E-03 0.3030      0.30        0.30        3.00E-03               Card(5)0307
9.00E-04    5.94059E-03 0.6060      0.60        0.30        3.00E-03               Card(5)0307
9.00E-04    5.94059E-03 0.6060      0.60        0.30        3.00E-03               Card(5)0307
9.00E-04    5.94059E-03 0.6060      0.60        0.30        3.00E-03               Card(5)0307
4.50E-04    5.94059E-03 0.3030      0.30        0.30        3.00E-03               Card(5)0307
0.30        0.30        0.30        0.30                                           Card(1)0308
! Card 0308A not required
! Radial power peaking factor data by fuel plate for each assembly. Input flow data by
! channel for each assembly on Cards 0310 not required because WFGES(1) is non-zero
1.000       1.000       1.000       1.000                                          Card(2)0309
1.000       1.000       1.000       1.000                                          Card(2)0309
! DP0       DDP         DPMAX       POWER       TIN         PIN
0.0003275   0.04        0.00        0.200       25.0        0.50                   Card(1)0500
0.00        0.00                                                                   Card(2)0500
  50 0.0001     25.0        0.00        0.00                                       Card(1)0600
  16                                                                               Card(1)0700
0.000000    1.000                                                                  Card(15)0701
0.066667    1.000                                                                  Card(15)0701
0.133333    1.000                                                                  Card(15)0701
0.200000    1.000                                                                  Card(15)0701
0.266667    1.000                                                                  Card(15)0701
0.333333    1.000                                                                  Card(15)0701
0.400000    1.000                                                                  Card(15)0701
0.466667    1.000                                                                  Card(15)0701
0.533333    1.000                                                                  Card(15)0701
0.600000    1.000                                                                  Card(15)0701
0.666667    1.000                                                                  Card(15)0701
0.733333    1.000                                                                  Card(15)0701
0.800000    1.000                                                                  Card(15)0701
0.866667    1.000                                                                  Card(15)0701
0.933333    1.000                                                                  Card(15)0701
1.000000    1.000                                                                  Card(15)0701
   0                                                                               Card(11)0702
```

Table 10.1 Solution of Test Problem 22 by Different Codes Used to Verify the Chimney Model in Natural Circulation Calculation in PLTEMP/ANL V3.6

Input or Calculated Quantity	PLTEMP/ANL Version 3.6 Solution	*Mathematica* Calculation Using PLTEMP/ANL Coolant Properties	*Mathematica* Calculation Using NATCON Coolant Properties	NATCON V2.2 Code Solution
Inlet Temp, °C	25			
Power per Channel, W	25000			
Loss Coeff. at Inlet	0.5			
Loss Coeff. at Exit	1.0			
	Calculated Quantities			
Flow per Channel, kg/s	0.19809	0.19803	0.19796	0.19967
Exit Temp, °C	55.225	55.235	55.253	54.990
	Buoyancy Head, Pa			
Axial Region 1	0.0	0.0	0.0	0.0
Axial Region 2 (Heated Section)	34.359	34.352	34.363	33.888
Axial Region 3	15.592	15.590	15.583	15.350
Chimney	207.984	207.871	207.768	204.670
Total Buoyancy	**257.935**	**257.813**	**257.715**	**253.904**
	Frictional Pressure Drop, Pa			
Inlet Loss	12.148	12.140	12.133	12.344
Axial Region 1	40.047	40.035	40.049	41.050
Axial Region 2 (Heated Length)	153.696	153.627	153.552	152.600
Axial Region 3	27.487	27.470	27.454	22.959
Exit Loss	24.557	24.541	24.527	24.949
Chimney	0.0	0.0	0.0	0.0
Total Pressure Drop	**257.935**	**257.813**	**257.715**	**253.904**

Table 10.2 Water Properties Used in the NATCON Code and PLTEMP/ANL Code

Water Properties Used in NATCON Code				Water Properties Used in in PLTEMP/ANL Code at 5.0 bar			
Temp °C	Specific Heat kJ/kg-°C	Water Density kg/m^3	Dynamic Viscosity μ Pa-s	Temp °C	Enthalpy kJ/kg	Water Density kg/m^3	Dynamic Viscosity μ Pa-s
21.718	4.165	997.54	974	20	83.952	997.988	1014.5
27.301	4.168	996.30	855	25	104.773	996.982	901.17
32.879	4.171	994.81	755	30	125.608	995.759	804.50
38.450	4.175	993.08	673	35	146.457	994.321	722.29
44.022	4.179	991.06	604	40	167.327	992.672	652.48
49.583	4.183	988.79	547	45	188.211	990.815	593.26
55.144	4.187	986.30	499	50	209.116	988.754	542.91
60.694	4.192	983.57	458	55	230.034	986.495	499.92
66.239	4.196	980.62	422	60	250.973	984.042	462.93
71.778	4.201	977.39	392	65	271.934	981.403	430.75
77.311	4.206	974.00	367	70	292.915	978.583	401.28
82.839	4.212	970.46	345	75	313.923	975.590	377.03
88.356	4.217	966.66	326	80	334.946	972.432	355.98
93.867	4.223	962.76	309	85	356.003	969.117	337.40
99.370	4.230	958.67	292	90	377.075	965.655	320.63
104.867	4.236	954.44	277	95	398.181	962.055	304.97
110.356	4.244	950.09	263	100	419.314	958.326	290.21
115.828	4.251	945.66	250	105	440.476	954.482	276.41
121.294	4.259	941.16	238	110	461.672	950.532	263.52
127.190	4.268	936.20	226	115	482.896	946.490	251.49
132.340	4.276	931.85	216	120	504.162	942.367	240.27
				125	525.455	938.181	229.83
				130	546.797	933.940	220.10

Table 10.3 Solution of Test Problem 22 with a Chimney by *Mathematica* Using PLTEMP/ANL Coolant Properties and Laminar and Transition Flow Friction Factor Correlations of PLTEMP/ANL

Flow rate per coolant channel = 0.19803 kg/s

Region or Axial Node	Nodal Power W	Temp at Node Exit, °C	Temp at Node Center, °C	Density at Node Center kg/m³	Buoyancy due to Node, Pa	Re at Node Center	Friction Factor at Node Center	Frictional Pressure Drop, Pa
Inlet				996.982				12.1401
Region 1	0.0	25.0	25.0	996.982	0.0	1450.47	0.0653014	40.0347
1	1666.67	27.0201	26.0101	996.752	0.112582	1484.74	0.0637941	13.0399
2	1666.67	29.0397	28.0299	996.267	0.350721	1554.72	0.0609225	12.459
3	1666.67	31.0588	30.0493	995.746	0.606063	1626.53	0.0582328	11.9151
4	1666.67	33.0774	32.0681	995.19	0.878518	1700.07	0.0557138	11.4061
5	1666.67	35.0952	34.0863	994.6	1.16795	1775.19	0.0533563	10.9299
6	1666.67	37.1121	36.1036	993.975	1.47425	1851.76	0.05115	10.4845
7	1666.67	39.1282	38.1201	993.317	1.79727	1929.64	0.0490854	10.068
8	1666.67	41.1439	40.136	992.624	2.13687	2008.67	0.0471542	9.67867
9	1666.67	43.1591	42.1515	991.898	2.49291	2088.71	0.0453473	9.31461
10	1666.67	45.1735	44.1663	991.139	2.86524	2169.59	0.0436569	8.97425
11	1666.67	47.187	46.1802	990.346	3.25371	2251.2	0.0434203	8.93277
12	1666.67	49.1997	48.1934	989.521	3.65815	2333.41	0.0438629	9.03134
13	1666.67	51.2121	50.2059	988.664	4.07837	2416.1	0.0441508	9.0985
14	1666.67	53.2239	52.218	987.776	4.51418	2499.21	0.0443059	9.13867
15	1666.67	55.235	54.2294	986.855	4.96541	2582.62	0.044347	9.15567
Region 2		55.235			34.3522			153.627
Region 3	0.0	55.235	55.235	986.384	15.5903	2624.43	0.04433	27.4696
Reg 3 Exit		55.235		986.384				24.5411
Chimney		55.235	55.235	986.384	207.871			
Total					257.813			257.813

Table 10.4 Solution of Test Problem 22 with a Chimney by *Mathematica* Using NATCON Coolant Properties and Laminar and Transition Flow Friction Factor Correlations of PLTEMP/ANL

Flow rate per coolant channel = 0.19796 kg/s

Region or Axial Node	Nodal Power W	Temp at Node Exit, °C	Temp at Node Center, °C	Density at Node Center kg/m³	Buoyancy due to Node, Pa	Re at Node Center	Friction Factor at Node Center	Frictional Pressure Drop, Pa
Inlet				996.842				12.1329
Region 1	0.0	25.0	25.0	996.842	0.0	1449.09	0.0653635	40.0491
1	1666.67	27.0211	26.0105	996.609	0.114119	1483.49	0.0638479	13.0432
2	1666.67	29.0416	28.0313	996.119	0.354515	1553.94	0.060953	12.4579
3	1666.67	31.0616	30.0516	995.596	0.610922	1626.41	0.0582372	11.9091
4	1666.67	33.0811	32.0714	995.041	0.883126	1700.58	0.055697	11.396
5	1666.67	35.1002	34.0906	994.456	1.16996	1775.77	0.0533387	10.9199
6	1666.67	37.1186	36.1094	993.839	1.4723	1851.84	0.0511476	10.4778
7	1666.67	39.1363	38.1275	993.188	1.79188	1929.06	0.0491004	10.065
8	1666.67	41.1533	40.1448	992.495	2.13167	2008.09	0.0471679	9.67564
9	1666.67	43.1696	42.1615	991.765	2.48965	2088.41	0.0453538	9.31037
10	1666.67	45.1852	44.1774	991.0	2.86461	2169.56	0.0436574	8.96904
11	1666.67	47.2001	46.1927	990.202	3.25569	2250.89	0.0434184	8.92712
12	1666.67	49.2144	48.2072	989.373	3.66212	2332.64	0.0438596	9.02539
13	1666.67	51.2279	50.2211	988.516	4.08255	2414.9	0.0441476	9.09255
14	1666.67	53.2407	52.2343	987.632	4.51603	2497.78	0.0443042	9.13296
15	1666.67	55.2528	54.2467	986.718	4.96427	2581.16	0.0443471	9.15027
Region 2		55.2528			34.3634			153.552
Region 3	0.0	55.2528	55.2528	986.249	15.5826	2623.05	0.0443309	27.4538
Reg 3 Exit		55.2528		986.249				24.5265
Chimney		55.2528	55.2528	986.249	207.768			
Total					257.715			257.7

Table 10.5 Solution of Test Problem 22 with Chimney by NATCON Code Using its Built-in Coolant Properties and Friction Factor.

Flow rate per channel = 0.19967 kg/s

Region or Axial Node of Heated Length, m	Axial Length, m	Coolant Temp at Node Exit, C	Coolant Temp at Node Center, C	Coolant Density, kg/m^3	Buoyancy Due to Node, Pa	Reynolds Number	Friction Factor	Frictional Pressure Drop, Pa
Inlet								12.3440
Region 1	0.1500				0.0000			41.0500
1	0.0500	27.003	26.002	996.590	0.1090	1493.100	0.06430	13.3630
2	0.0500	29.006	28.005	996.110	0.3425	1564.500	0.06136	12.7590
3	0.0500	31.009	30.008	995.580	0.6047	1634.200	0.05875	12.2220
4	0.0500	33.011	32.010	995.040	0.8668	1710.300	0.05613	11.6840
5	0.0500	35.012	34.012	994.460	1.1528	1785.000	0.05378	11.2010
6	0.0500	37.013	36.013	993.840	1.4574	1859.200	0.05164	10.7610
7	0.0500	39.013	38.013	993.220	1.7618	1939.800	0.04949	10.3210
8	0.0500	41.013	40.013	992.510	2.1059	2016.300	0.04761	9.9361
9	0.0500	43.012	42.012	991.790	2.4610	2095.700	0.04581	9.5669
10	0.0500	45.010	44.011	991.060	2.8160	2181.500	0.04401	9.1971
11	0.0500	47.007	46.009	990.250	3.2153	2258.100	0.04251	8.8922
12	0.0500	49.004	48.006	989.430	3.6148	2340.200	0.04102	8.5875
13	0.0500	51.000	50.002	988.600	4.0223	2425.400	0.03958	8.2928
14	0.0500	52.995	51.998	987.710	4.4601	2504.800	0.03833	8.0370
15	0.7500	54.990	53.993	986.820	4.8979	2589.600	0.03707	7.7812
Region 2	0.7500	54.990			33.8883			152.6000
Region 3	0.1500	54.990	54.990	986.370	15.3500	2634.100	0.03645	22.9590
Region 3 Exit		54.990		986.370				24.9490
Chimney	2.0000	54.990	54.990	986.370	204.6700			
Total	3.0500				253.9040			253.9040

Table 10.6 Solution of Test Problem 22 with a Chimney by PLTEMP/ANL V3.6 Code Using its Laminar and Transition Flow Friction Factor Correlations

Flow rate per coolant channel = 0.19809 kg/s

Region or Axial Node of Heated Length	Axial Length, m	Fraction of Left/Right Fuel Plate Power Going to Channel	Coolant Temp at Node Exit, °C	Coolant Temp at Node Center, °C	Coolant Density, kg/m^3	Buoyancy Due to Node, Pa	Reynolds Number	Friction Factor	Frictional Pressure Drop, Pa
Inlet			25.000		996.982				12.1478
Region 1	0.150		25.000	25.000	996.982	0.0000	1450.93	0.065281	40.0473
1	0.050	0.50/0.50		26.010	996.752	0.1130	1485.21	0.063774	13.0440
2	0.050	0.50/0.50		28.030	996.266	0.3512	1555.20	0.060904	12.4630
3	0.050	0.50/0.50		30.049	995.745	0.6066	1627.03	0.058215	11.9191
4	0.050	0.50/0.50		32.067	995.189	0.8791	1700.57	0.055697	11.4100
5	0.050	0.50/0.50		34.085	994.599	1.1686	1775.71	0.053341	10.9336
6	0.050	0.50/0.50		36.102	993.975	1.4747	1852.23	0.051137	10.4885
7	0.050	0.50/0.50		38.118	993.316	1.7977	1930.12	0.049073	10.0720
8	0.050	0.50/0.50		40.133	992.623	2.1373	2009.15	0.047143	9.6825
9	0.050	0.50/0.50		42.149	991.897	2.4934	2089.20	0.045337	9.3184
10	0.050	0.50/0.50		44.164	991.138	2.8657	2170.10	0.043647	8.9778
11	0.050	0.50/0.50		46.177	990.345	3.2542	2251.73	0.043424	8.9391
12	0.050	0.50/0.50		48.190	989.520	3.6587	2333.95	0.043865	9.0376
13	0.050	0.50/0.50		50.202	988.663	4.0789	2416.67	0.044152	9.1046
14	0.050	0.50/0.50		52.214	987.775	4.5147	2499.78	0.044307	9.1446
15	0.050	0.50/0.50	55.225	54.224	986.855	4.9655	2583.14	0.044347	9.1615
Region 2	0.750		55.225			34.3589			153.6962
Region 3	0.150		55.225	55.225	986.383	15.5918	2624.97	0.044330	27.4868
Region 3 Exit			55.225		986.383				24.5566
Chimney	2.000		55.225	55.225	986.383	207.9840			
Total	3.050					257.9347			257.9347

APPENDIX H *Mathematica* Program for Solving Test Problem 22

```
(" SOLUTION OF NATURAL CIRCULATION STANDARD PROBLEM 20, Using Water Properties of
the PLTEMP/ANL V3.5 Code ")
data={kin=0.5,kex=1.0,Dh=0.00594059,len1=0.15,len2=0.75,len3=0.15,wch=0.3,tch=0.003,grav=9.8066
5,erel=0.0,tin=25.0,powr=25000.0};
flow=0.1980283;
flow=0.1980283; ←——— This guess flow was adjusted and the program was rerun to achieve channel
                     channel buoyancy (buoy) equal to channel frictional pressure drop (delp).
chimny=2.0
(* power = 25 kW per plate, total power = 200 kW in 8 plates *)
Print["Subcooled water density, kg/m**3, at 5 bar absolute used in the PLTEMP/ANL V3.5 Code"];
rho={{20.,997.9875},{25.,996.9820},{30.,995.7591},{35.,994.3214},{40.,992.6718},{45.,990.8146},{5
0.,988.7536},{55.,986.4945},{60.,984.0422},{65.,981.4029},{70.,978.5832},{75.,975.5897},{80.,972.43
24},{85.,969.1167},{90.,965.6552},{95.,962.0546},{100.,958.3263},{105.,954.4819},{110.,950.5318},{
115.,946.4900},{120.,942.3674},{125.,938.1805},{130.,933.9403},{135.,929.6651},{140.,925.3685},{1
45.,921.0693},{150.,916.7842}};
Plot[Interpolation[rho][temp],{temp,20,150}];
Print["Subcooled water enthalpy, kJ/kg, at 5 bar absolute used in the PLTEMP/ANL V3.5 Code"];
enthalpy={{20.,83.9517},{25.,104.7730},{30.,125.6082},{35.,146.4573},{40.,167.3272},{45.,188.2110}
,{50.,209.1156},{55.,230.0341},{60.,250.9734},{65.,271.9336},{70.,292.9146},{75.,313.9233},{80.,334
.9460},{85.,356.0033},{90.,377.0746},{95.,398.1805},{100.,419.3143},{105.,440.4758},{110.,461.6720
},{115.0,482.8960},{120.,504.1616},{125.,525.4550},{130.,546.7970},{135.,568.1738},{140.,589.5991
},{145.,611.0661},{150.,632.5816}};
Plot[Interpolation[enthalpy][temp],{temp,20,150}];
Print["Dynamic viscosity, micro Pa-s, of water used in the PLTEMP/ANL V3.5 Code"];
visc={{20.,1014.5},{25.,901.17},{30.,804.50},{35.,722.29},{40.,652.48},{45.,593.26},{50.,542.91},{55
.,499.92},{60.,462.93},{65.,430.75},{70.,401.28},{75.,377.03},{80.,355.98},{85.,337.40},{90.,320.63},
{95.,304.97},{100.,290.21},{105.,276.41},{110.,263.52},{115.,251.49},{120.,240.27},{125.,229.83},{1
30.,220.10},{135.,211.05},{140.,202.64},{145.,194.82},{150.,187.56}};
Plot[Interpolation[visc][temp],{temp,20,150}];
Print["Inlet and Exit temperatures, C"];
tin=tin/.data
grav=grav/.data;
hin=1000*Interpolation[enthalpy][tin];
hout=hin+powr/flow/.data;
tout=tx/.FindRoot[hout==1000*Interpolation[enthalpy][tx],{tx,tin}]
rhoin=Interpolation[rho][tin];
rhoout=Interpolation[rho][tout];
Print["Density at inlet =",rhoin,", Density at exit =",rhoout];
rhoave=NIntegrate[Interpolation[rho][temp],{temp,tin,tout}]/(tout-tin);
Print["Integrated average coolant density over (",tin," to ",tout,") = ",rhoave];
buoy2=(rhoin-rhoave)*grav*len2 /.data;
buoy3=(rhoin-rhoout)*grav*len3 /.data;
buoychimny=(rhoin-rhoout)*grav*chimny /.data;
Print["Buoyancy due to chimney =",buoychimny];
buoy=buoy2+buoy3;
Print["DRIVING PRESSURE HEAD DUE TO BUOYANCY in Section 1 =0.0, Section 2 =",buoy2,",
Section 3 =",buoy3,", Total buoyancy (Pa) =",buoy];
velin=flow/(rhoin*wch*tch)/.data;
```

```
Print["Coolant inlet velocity, m/s = ",velin];
visc1=0.000001*Interpolation[visc][tin];
visc3=0.000001*Interpolation[visc][tout];
Print["Coolant dynamic viscosity, Pa-s, in axial regions 1 and 3 =",visc1," ",visc3]
reyn1=flow*Dh/(wch*tch*visc1)/.data;
reyn3=flow*Dh/(wch*tch*visc3)/.data;
Print["Reynolds numbers in axial regions 1 and 3 =",reyn1," ",reyn3];
aspect=tch/wch/.data;
erela=If[0<erel<0.00000001,0.00000001,erel]/.data;
Cfric=96*(1-1.3553*aspect+1.9467*aspect^2-1.7012*aspect^3+0.9564*aspect^4-0.2537*aspect^5)
fric2200=Cfric/2200.0;
reyn=reyn1;
fa=1/(-2*Log[10,erela/3.7+2.51/reyn*(1.14-2*Log[10,erela+21.25/reyn^0.9])])^2;
If[reyn>=3000 && erela==0,fb=4*fric/.FindRoot[fric==6.25002/(1-
8.68591*Log[reyn*fric^0.5]+18.8612*(Log[reyn*fric^0.5])^2),{fric,0.1}]];
If[reyn>=3000 && erela>=0.00000001,
   fb=4*fric/.FindRoot[fric==0.331369/(Log[0.27027*erela+1.255/(reyn*fric^0.5)])^2,{fric,0.1}]];
If[reyn>=3000,Print["Turbulent friction factor fb = ",fb,", Re = ",reyn,", Rel roughness = ",erela]];
frica=If[reyn<=2200.0,Cfric/reyn,fric2200+(fa-fric2200)*(3.75-8250/reyn)];
fric1=If[reyn>=3000.0,fb,frica];
reyn=reyn3;
fa=1/(-2*Log[10,erela/3.7+2.51/reyn*(1.14-2*Log[10,erela+21.25/reyn^0.9])])^2;
If[reyn>=3000 && erela==0,fb=4*fric/.FindRoot[fric==6.25002/(1-
8.68591*Log[reyn*fric^0.5]+18.8612*(Log[reyn*fric^0.5])^2),{fric,0.1}]];
If[reyn>=3000 && erela>=0.00000001,
   fb=4*fric/.FindRoot[fric==0.331369/(Log[0.27027*erela+1.255/(reyn*fric^0.5)])^2,{fric,0.1}]];
If[reyn>=3000,Print["Turbulent friction factor fb = ",fb,", Re = ",reyn,", Rel roughness = ",erela]];
frica=If[reyn<=2200.0,Cfric/reyn,fric2200+(fa-fric2200)*(3.75-8250/reyn)];
fric3=If[reyn>=3000.0,fb,frica];
Print["Friction factors in Sections 1 and 3 =",fric1," ",fric3];
Print["FRICTIONAL PRESSURE DROP IN SECTION 1"]
delp1s=(fric1*len1/Dh)*0.5*(flow/(wch*tch))^2/rhoin/.data;
delp1m=kin*0.5*(flow/(wch*tch))^2/rhoin/.data;
delp1=delp1s+delp1m;
Print["Total pressure drop in Section 1 =",delp1,", Minor loss = ",delp1m,", Wall shear =",delp1s]
Print["FRICTIONAL PRESSURE DROP IN SECTION 3"]
delp3s=(fric3*len3/Dh)*0.5*(flow/(wch*tch))^2/rhoout/.data;
delp3m=kex*0.5*(flow/(wch*tch))^2/rhoout/.data;
delp3=delp3s+delp3m;
Print["Total pressure drop in Section 3 =",delp3,", Minor loss = ",delp3m,", Wall shear =",delp3s]
delp4=rhoin*velin*velin*(rhoin/rhoout-1.0)/.data;
Print["Pressure drop due to momentum flux (Pa) =",delp4];
Print["Flow =",flow,", g =",grav,", Temp at inlet and exit =",tin,", ",tout,", Density at inlet and exit
=",rhoin,", ",rhoout,", Gravity head =",grav*(rhoin*len1+rhoave*len2+rhoout*len3)/.data,", Total
buoyancy =",buoy,", Buoyancy in Section 2 =",buoy2,", Buoyancy in Section 3 =",buoy3,", Power into
coolant (W) =",flow*(hout-hin)]
Print["LOOP OVER 21 AXIAL SEGMENTS"];
powr1=powr/15/.data;
delz=len2/15/.data;
enth1=hin;
temp1=tin;
```

```
delp2p=0;
buoy2p=0;
Do[powr2=powr1;
  If[j<4,powr2=0];
  If[j>18,powr2=0];
  enth2=enth1+powr2/flow;
  temp2=tx/.FindRoot[enth2==1000*Interpolation[enthalpy][tx],{tx,temp1}];
  tempj=0.5*(temp2+temp1);
  viscj=0.000001*Interpolation[visc][tempj];
  rhoj=Interpolation[rho][tempj];
  buoy2s=buoy2p+grav*(rhoin-rhoj)*delz;
  reynj=flow*Dh/(wch*tch*viscj)/.data;
  reyn=reynj;
  fa=1/(-2*Log[10,erela/3.7+2.51/reyn*(1.14-2*Log[10,erela+21.25/reyn^0.9])])^2;
  If[reyn>=3000 && erela==0,fb=4*fric/.FindRoot[fric==6.25002/(1-
8.68591*Log[reyn*fric^0.5]+18.8612*(Log[reyn*fric^0.5])^2),{fric,0.1}]];
  If[reyn>=3000 && erela>=0.00000001,
    fb=4*fric/.FindRoot[fric==0.331369/(Log[0.27027*erela+1.255/(reyn*fric^0.5)])^2,{fric,0.1}]];
  If[reyn>=3000,Print["Turbulent friction factor fb = ",fb,", Re = ",reyn,", Rel roughness = ",erela]];
  frica=If[reyn<=2200.0,Cfric/reyn,fric2200+(fa-fric2200)*(3.75-8250/reyn)];
  fricj=If[reyn>=3000.0,fb,frica];
  delpj=(fricj*delz/Dh)*0.5*(flow/(wch*tch))^2/rhoj/.data;
  delp2=delp2p+delpj;
  (*Print["Axial segment =",j,", Flow, kg/s =",flow,", delz (m) =",delz,"Power in segment (W) =",powr2,",
Enthalpy at segment exit (J/kg) =",enth2,", Enthalpy at segment center (J/kg) =",0.5(enth1+enth2),",
Temp at segment exit (C) =",temp2,", Segment mean temp (C) =",tempj,", Segment mean density
(kg/m^3) =",rhoj,", Buoyancy due to segments 1 through ",j," (Pa) =",buoy2s,", Viscosity (Pa-s)
=",viscj,", Reynolds number =",reynj,", Friction factor =",fricj,", fl/Dh of segment (Pa) =",delpj,",
Cumulative sum fL/Dh of segments 1 through ",j", (Pa) =",delp2];*)
  Print[j,"   ",powr2,"   ",temp2,"   ",tempj,"   ",rhoj,"   ",grav*(rhoin-rhoj)*delz,"   ",reynj,"   ",fricj,"
",delpj];
  buoy2p=buoy2s;
  delp2p=delp2;
  temp1=temp2;
  enth1=enth2,
  {j,1,21}]
Print["Pressure drop due to wall shear in region 2 = ",delp2-delp1s-delp3s]
Print["BALANCE OF BUOYANCY AND FRICTIONAL PRESSURE DROP:"]
delp=delp2+delp1m+delp3m;
buoy=buoy2s+buoychimny;
Print["Total buoyancy (Pa) =",buoy,", Total frictional pressure drop (Pa) =",delp];
```

11 Verification of the Hot Channel Factors Option in Natural Circulation Calculation by PLTEMP/ANL V3.6

The verification work reported here was done in January 2009. A natural circulation calculation was implemented in the PLTEMP/ANL V3.5 code. In V3.6 of the code, the treatment of uncertainties in fuel assembly geometry and in thermal-hydraulic data and methods that is available for forced flow calculations in V3.5 of the code (using six hot channel factors), was extended to the case of natural circulation calculations. For the verification of this extension of the six hot channel factors treatment, a natural circulation test problem for a 4-fuel-plate assembly was solved by PLTEMP/ANL V3.6 and verified by *Mathematica* calculations. *Mathematica* calculations were done for (i) the nominal case without applying any hot channel factors and (ii) with only the three global hot channel factors. These *Mathematica* solutions agree well with the PLTEMP/ANL solution as shown in Table 11.1. This provides a verification of the implementation of the six hot channel factors in the case of natural circulation calculation in PLTEMP/ANL V3.6. Table 11.2 summarizes the effect of global and local hot channel factors on the solution of the test problem.

11.1 Introduction

The PLTEMP/ANL code was improved to model natural circulation flow upward through the fuel assemblies and downward in the reactor pool. In the model, the flows of all fuel assemblies in the problem can enter into a common chimney, or the flows of a group of fuel assemblies enter into a common chimney. In the latter case, the problem will have more than one chimney. The schematic and physical geometries of the model are shown in Figs. 11.1 and 11.2. The thermal-hydraulic equations to model the chimney and the method of solution are described in the PLTEMP/ANL Users Guide [1]. There was a need for incorporating in the model hot channel factors for treating uncertainties in fuel assembly geometry and in thermal-hydraulic data and methods in research reactor conversion analyses. In the case of forced flow calculations, an option for treating the uncertainties using six hot channel factors was already available. This hot channel factors treatment was recently extended to the case of natural circulation calculation in the PLTEMP/ANL V3.6 code.

This chapter documents a verification of this extension of the six hot channel factors treatment to a natural circulation calculation, using a natural circulation test problem. The test problem is defined in Section 11.2, and referred to as Test Problem 21. Its solution by two methods/codes are reported and compared here: (1) *Mathematica* calculation using the coolant properties used in the PLTEMP/ANL code, and (2) Solution by the PLTEMP/ANL version 3.6 code. The solutions by *Mathematica* were obtained for a single coolant channel, and the PLTEMP/ANL solution was obtained for a four-plate fuel assembly.

11.2 Test Problem Used in Verification

Problem Definition: Calculate the coolant flow rate caused by natural circulation in a 1.05 m long vertical coolant channel having a heated length of 0.75 m. The lower unheated length is 0.15 m, and the upper unheated length is 0.15 m. The heated length has a power of 12.5 kW distributed uniformly over the 0.75 m length, with an inlet temperature of 25 °C. The channel has a rectangular cross section of thickness 3 mm, width 0.3 m, inlet pressure loss coefficient 0.5, and exit pressure loss coefficient 1.0. The absolute pressure at the channel inlet is 5 bar, corresponding to the channel inlet being 40.81 m below the free surface of water in the pool. Also calculate the effect of the following values of the six hot channel factors used in treatment option 2 (IHCF = 2) in PLTEMP/ANL input data[1].

System-wide hot channel factors: FPOWER = 1.20, FFLOW = 1.20, FNUSLT = 1.15,
Random or local hot channel factors: FBULK = 1.15, FFILM = 1.18, FFLUX = 1.22

where

FPOWER	= A factor to account for the uncertainty in total reactor power measurement
FFLOW	= A factor to account for the uncertainty in total reactor flow measurement
FNUSLT	= A factor to account for the uncertainty in Nusselt number correlation
FBULK	= A factor to account for the uncertainty in local bulk coolant temperature rise
FFILM	= A factor to account for the uncertainty in local temperature rise across the coolant film (from the bulk coolant to the cladding surface)
FFLUX	= A factor to account for the uncertainty in local heat flux from the cladding surface to the coolant.

The thermal-hydraulic input data (see nomenclature given at the end) for the problem are as follows:

D_h = 0.0059406 m,	g = 9.8 m/s^2,	H_{in} = 41.81 m,	K_{in} = 0.5,
K_{ex} = 1.0,	L_1 = 0.15 m,	L_2 = 0.75 m,	L_3 = 0.15 m,
L = 1.05 m,	L_{ch} = 2.00 m,	Q = 12500 W,	P_{in} = 5.0 bar,
T_{in} = 25 °C,	T_{ch} = 0.003 m,	W_{ch} = 0.3 m,	
W = 0.072086 kg/s (*assumed value*)			

11.3 *Mathematica* Calculations

A *Mathematica* program was written in which any set of coolant properties and friction factor correlations could be inserted. In the current calculations, the coolant properties and friction factor correlations of the PLTEMP/ANL code were inserted into the *Mathematica* program. The *Mathematica* program uses coolant enthalpy as a function of temperature, as shown by the program listing given in Appendix I.

The program uses 21 axial nodes (mesh intervals) of equal length in the total channel length of 1.05 m, with three each in the lower and upper unheated lengths of the channel, and 15 in the heated length. Starting from a guessed flow rate, the program calculates the coolant enthalpy at each node exit, the coolant temperature at the node exit, and the temperature at the node-center. Using the node-center temperature, the program finds the nodal Reynolds number, friction factor,

nodal frictional pressure drop, and the nodal contribution to buoyancy. It finds the channel inlet and outlet pressure losses. It finds the buoyancy due to the chimney. The frictional pressure drop in the chimney is assumed to be negligible. The momentum flux term is ignored because it is small. The calculation ends after printing the total buoyancy and the total frictional pressure drop in the channel. To find the steady-state natural circulation flow rate, the user reruns the program several times, each time using a more improved guess of the flow rate, in order to make the total buoyancy equal to the total frictional pressure drop.

The following three solutions to Test Problem 21 were obtained using the Mathematica program:

(1) A solution using the nominal power (12.5 kW) whose results are given in Table 11.3. This solution gives a flow rate of 0.072071 kg/s per channel.

(2) A solution using a power of 15.0 kW which is obtained by multiplying the nominal power by the global hot channel factor for power, i.e., 1.20x12.5 kW. This solution gives a flow rate of 0.080415 kg/s per channel. The results of this solution are given in Table 11.4.

(3) A coolant temperature distribution calculation at a channel flow rate of 0.0670128 kg/s which equals the flow rate found in the second calculation divided by the global hot channel factor FFLOW for flow, i.e., 0.080415/1.20 = 0.0670128 kg/s. The results of this calculation are given in Table 11.5.

The three *Mathematica* calculations given in Tables 11.3, 11.4 and 11.5 are summarized in Table 11.1 for comparison with PLTEMP/ANL calculation.

11.4 PLTEMP/ANL Version 3.6 Code Calculation

To solve Test Problem 21 using the PLTEMP/ANL V3.6 code, the problem defined above in Section 11.2 is turned into a research reactor problem of two geometrically identical and equal-power fuel assemblies, each consisting of (arbitrarily) four fuel plates cooled by five coolant channels (Fig. 11.3). Only the first fuel assembly in the test problem is relevant to the present verification. The second fuel assembly is not used in the verification. The purpose of the second fuel assembly is to illustrate the effect of unequal fuel plate powers on channel flow rates, the resulting unequal partitioning of each plate power into its two adjacent coolant channels, and the effect of hot channel factors on such a fuel assembly.

In the first fuel assembly, each fuel plate produces an equal nominal power of 12.5 kW as specified in the problem definition, and the fuel assembly has a power of 50 kW. The internal channels (channels 2, 3, and 4) are of the thickness 3 mm as specified in the problem definition. In order to have identical axial profiles of coolant temperature in each channel, the first and the last channels are of half thickness, i.e., 1.5 mm. Based on symmetry, it is noted that exactly half of each fuel plate's power goes to each coolant channel adjacent to the plate.

In the second fuel assembly, the fuel plates produce unequal powers as specified by the radial power factors input on Card 0309. The only difference between the two fuel assemblies is in the radial power factors. The fuel plates 1, 2, 3, and 4 produce nominal powers of 7.5 kW, 17.5 kW, 17.5 kW, and 7.5 kW respectively, and the fuel assembly has a power of 50 kW. Hence the total power in the input data is 0.1 MW. Figure 11.4 gives the input data used in the PLTEMP/ANL V3.6 code.

In the input data of Fig. 11.4, the friction factor is obtained using the PLTEMP/ANL V3.6 code's built-in correlations which accounts for laminar, transition, or turbulent flow as the case may be. The code calculates three solutions in one run: (1) the nominal power solution given in Fig. 11.5, (2) the solution with global hot channel factors applied, given in Fig. 11.6, and (3) the temperature distribution with both global and local hot channel factors applied, given in Fig. 11.7.

These results are summarized in Table 11.1 for comparison with the *Mathematica* solutions of the problem. The flow is laminar over the whole part of the channel. The Darcy-Weisbach friction factor is calculated using the following correlations.

$$f = \begin{cases} f_{lam}(Re, a) & \text{if } Re \le 2200 \\ \left(3.75 - \dfrac{8250}{Re}\right)\left(f_a - f_{2200}\right) + f_{2200} & \text{if } 2200 < Re < 3000 \end{cases} \tag{11.1}$$

where

$$f_{lam}(Re, a) = \frac{96\left(1 - 1.3553\,a + 1.9467\,a^2 - 1.7012\,a^3 + 0.9564\,a^4 - 0.2537\,a^5\right)}{Re} \tag{11.2}$$

$$f_{2200} = f_{lam}(2200, a) \tag{11.3}$$

$$f_a = \left[-2\,\mathrm{Log}_{10}\left\{\frac{E_{rel}}{3.7} + \frac{2.51}{Re}\left\{1.14 - 2\,\mathrm{Log}_{10}\left(E_{rel} + 21.25\,Re^{-0.9}\right)\right\}\right\}\right]^{-2} \tag{11.4}$$

a = Channel aspect ratio = Channel thickness/width ratio, always ≤ 1.0
E_{rel} = Relative roughness

The numerator of Eq. (11.2) for the laminar friction factor is found to be 94.7174/Re based on the thickness-to-width ratio of the coolant channel. The results of the PLTEMP/ANL calculation at the nominal power agree well with the corresponding *Mathematica* solution given in column 3 of Table 11.1. Also, the results of the PLTEMP/ANL calculation at the global hot channel factors applied power agree well with the corresponding *Mathematica* solution given in column 5 of Table 11.1. These comparisons provide a verification of the implementation of hot channel factors treatment in the natural circulation calculation implemented in the PLTEMP/ANL V3.6 code.

11.5 Conclusions

There is a good agreement between the PLTEMP/ANL V3.6 and *Mathematica* solutions of the test problem, as shown in Table 11.1. The flow rate per channel calculated by PLTEMP/ANL V3.6 at the nominal power is 0.072086 kg/s, compared to 0.072071 kg/s calculated by *Mathematica*. With the global hot channel factors applied, the flow rate per channel calculated by PLTEMP/ANL V3.6 is 0.067016 kg/s, compared to 0.067013 kg/s calculated by *Mathematica*. This provides a verification of the hot channel factors treatment in the natural circulation calculation in the PLTEMP/ANL V3.6 code.

NOMENCLATURE

a	Channel aspect ratio = Channel thickness/width ratio, always ≤ 1.0
C_p	Coolant specific heat averaged over the temperature range 25 to 80 °C existing in the problem, J/kg-°C
D_h	Hydraulic diameter of the channel, m
E_{rel}	Relative roughness
g	Acceleration due to gravity, m/s^2
H_{in}	Water depth at the channel inlet, m
L_1	Unheated channel length below the heated section, m
L_2	Heated length of channel, m
L_3	Unheated channel length above the heated section, m
L	Channel height = $L_1 + L_2 + L_3$, m
L_{ch}	Effective chimney height, m
K_{in}	Pressure loss coefficient at the channel inlet
K_{ex}	Pressure loss coefficient at the channel exit
ΔP_{buoy}	Pressure head due to buoyancy, Pa
ΔP_{fric}	Total frictional pressure drop in the coolant channel, Pa
P_{in}	Pressure at the channel inlet, Pa
Q	Power in the channel, W
V_1	Coolant velocity at channel inlet, m/s
V_3	Coolant velocity at channel exit, m/s
T	Coolant temperature at an axial location, °C
T_{in}	Coolant temperature at the channel inlet, °C
T_{ex}	Coolant temperature at the channel exit, °C
T_{ch}	Channel thickness, m
W	Coolant flow rate in the channel, kg/s
W_{ch}	Channel width, m

11.6 REFERENCES

1. M. Kalimullah, A. P. Olson and E. E. Feldman, “A User’s Guide to the PLTEMP/ANL Code,” ANL/RTR/TM-18/17 Version 4.3, Revision 0, Argonne National Laboratory, 9700 South Cass Avenue, Argonne, IL 60439, USA (November 2018).

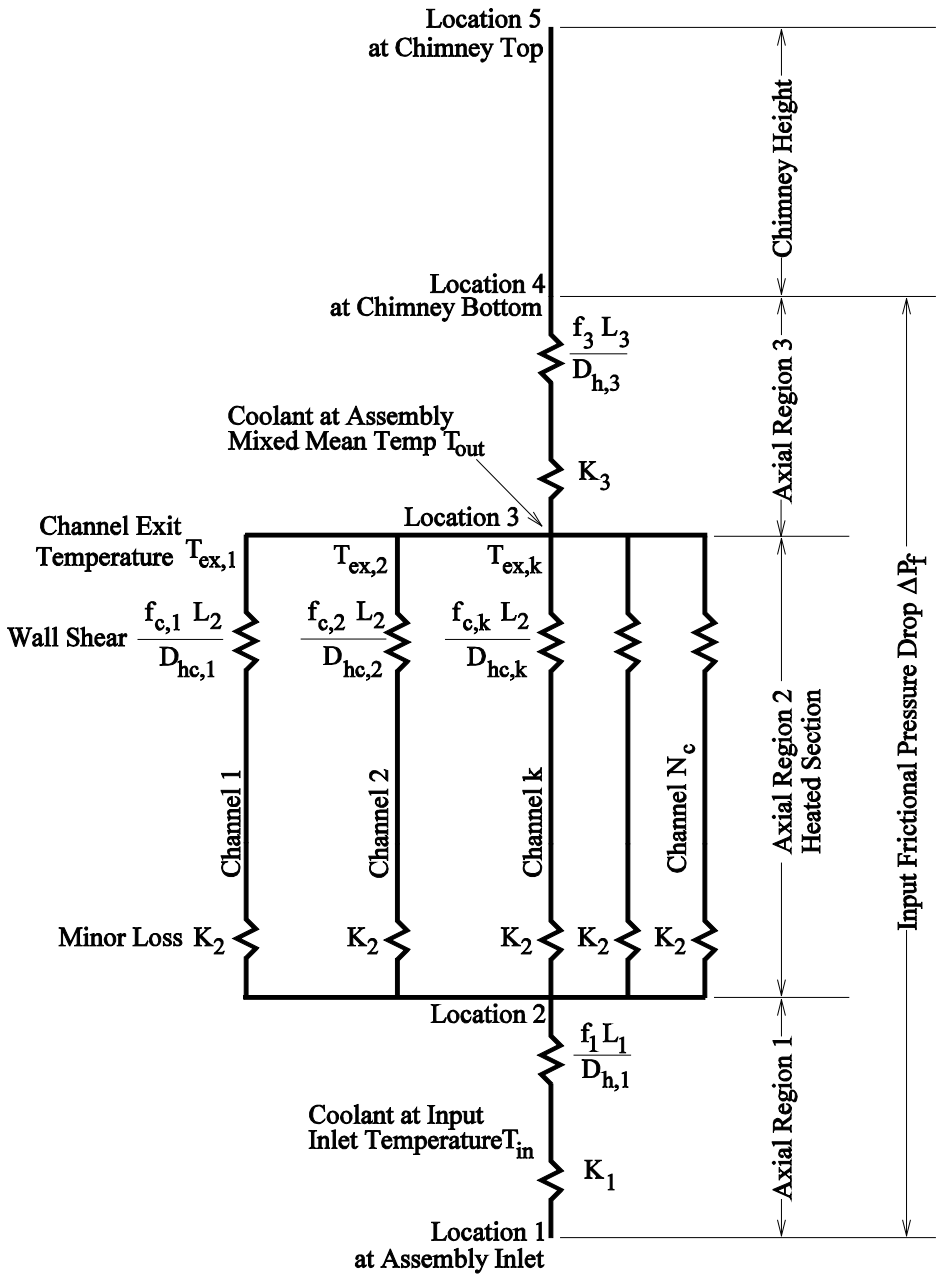

Figure 11.1 Coolant Flow Path in a Fuel Assembly and Chimney Modeled in PLTEMP/ANL (Multiple Axial Regions Downstream of the Heated Section Are Allowed)

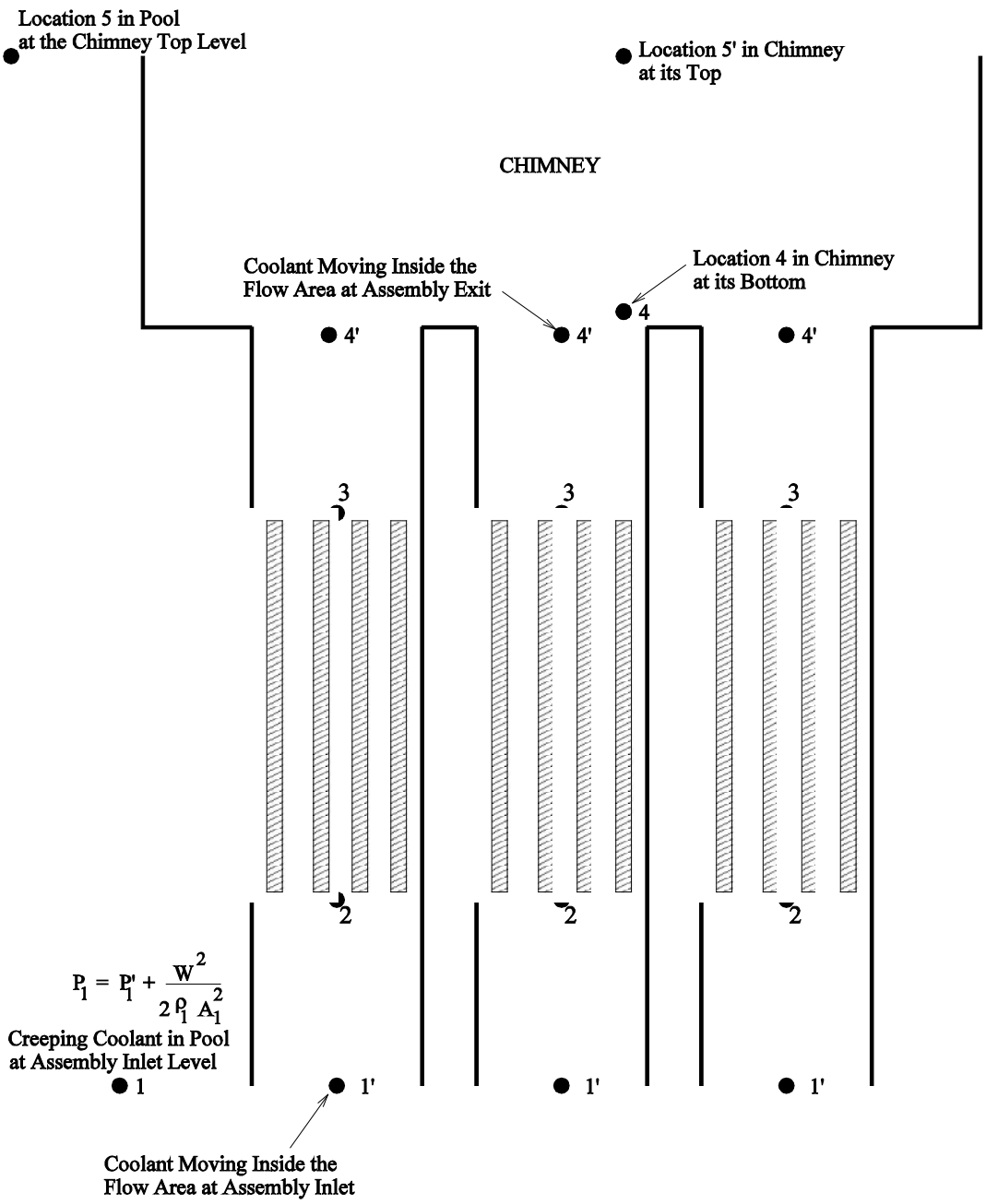

Figure 11.2 Locations of Coolant Pressure in a Group of Fuel Assemblies Exiting into a Common Chimney

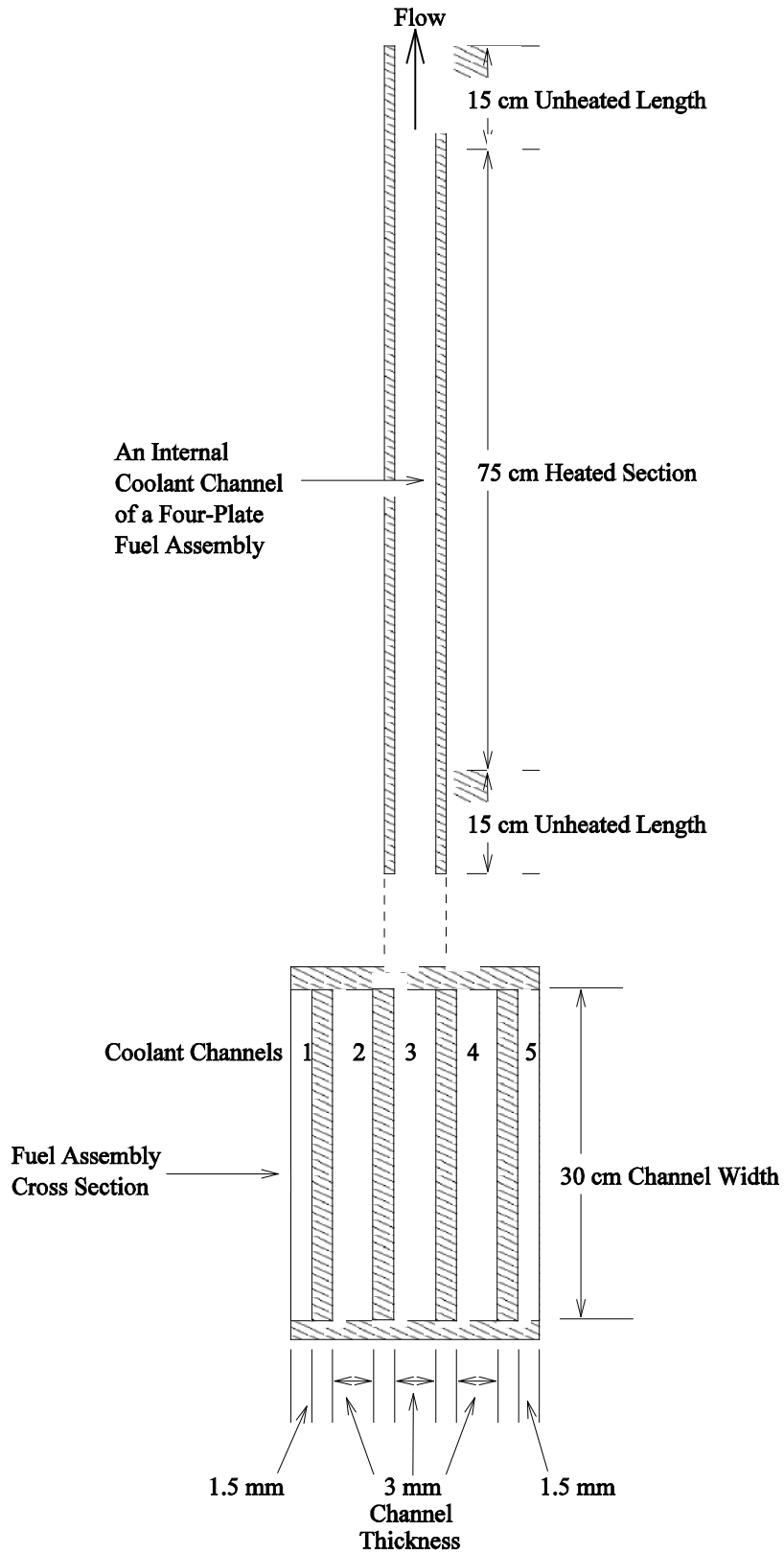

Figure 11.3 Geometry of a Coolant Channel in a Four-Plate Fuel Assembly Used in Test Problem 22

Figure 11.4 PLTEMP/ANL Input Data for Test Problem 21 Used in the Verification of Hot Channel Factors Treatment in Case of Natural Circulation

```
 Test Problem 21: Flow is calculated by natural circulation
! 2 assemblies, Each assembly has 4 fuel plates and 5 coolant channels
! H2O coolant, No bypass flow, NCTYP=0
! Total power = 0.10 MWt, Axially uniform power profile
! 14 axial heat transfer nodes in the heated length of fuel plates
!  1   2   3   4   5   6   7   8   9  10  11  12  13  14  15  16  17  18  19    #  Card 200
   5   0   1   1   0   1   1   1   0   0   0   0   0   0   2   0   0   0   0    Card(1)0200
1.20        1.20        1.15                                                   Card(1)0201
   2   3 0.50       1.00        1.00        1.00           0                   Card(1)0300
1.15        1.18        1.22                                                   Card(1)0300A
! Using pressure driven mode
1.00        1.00                                                               Card(2)0303
36.0E-04    5.94059E-03 0.15        0.50        0.30        3.00E-03           Card(3)0304
0.00        5.94059E-03 0.75        0.00        0.30        3.00E-03           Card(3)0304
36.0E-04    5.94059E-03 0.15        1.00        0.30        3.00E-03           Card(3)0304
! Use the code's biult-in correlation for friction factor
0.00        0.00        0.00                                                   Card(1)0305
! Use laminar friction factor
!94.7174     1.00        0.00                                                   Card(1)0305
   5   3 0.00       0.75        0.50E-03    180.00        1.00E-03    100.00    Card(1)0306
4.50E-04    5.94059E-03 0.3030      0.30        0.30        3.00E-03           Card(5)0307
9.00E-04    5.94059E-03 0.6060      0.60        0.30        3.00E-03           Card(5)0307
9.00E-04    5.94059E-03 0.6060      0.60        0.30        3.00E-03           Card(5)0307
9.00E-04    5.94059E-03 0.6060      0.60        0.30        3.00E-03           Card(5)0307
4.50E-04    5.94059E-03 0.3030      0.30        0.30        3.00E-03           Card(5)0307
0.30        0.30        0.30        0.30                                       Card(1)0308
! Card 0308A not required
! Radial power peaking factor data by fuel plate for each assembly. Input flow data by
! channel for each assembly on Cards 0310 not required because WFGES(1) is non-zero
1.000       1.000       1.000       1.000                                      Card(2)0309
0.600       1.400       1.400       0.600                                      Card(2)0309
! DP0       DDP         DPMAX       POWER       TIN         PIN
0.0000      0.04        0.00        0.100       25.0        0.50               Card(1)0500
0.00        0.00                                                               Card(2)0500
  50 1.E-04     25.0        0.00        0.00                                   Card(1)0600
  15                                                                           Card(1)0700
0.0         1.000                                                              Card(11)0701
0.100       1.000                                                              Card(11)0701
0.167       1.000                                                              Card(11)0701
0.233       1.000                                                              Card(11)0701
0.300       1.000                                                              Card(11)0701
0.367       1.000                                                              Card(11)0701
0.433       1.000                                                              Card(11)0701
0.5         1.000                                                              Card(11)0701
0.567       1.000                                                              Card(11)0701
0.633       1.000                                                              Card(11)0701
0.700       1.000                                                              Card(11)0701
0.767       1.000                                                              Card(11)0701
0.833       1.000                                                              Card(11)0701
0.900       1.000                                                              Card(11)0701
1.0         1.000                                                              Card(11)0701
   0                                                                           Card(11)0702
```

Figure 11.5 Solution of Test Problem 21 Assembly 1 by PLTEMP/ANL V3.6 Code – Nominal Case

Flow Rate in the Assembly = 2.8834E-01 kg/s

Channel	Flow Rate kg/s	Velocity m/s
1	3.60431E-02	8.03383E-02
2	7.20862E-02	8.03383E-02
3	7.20862E-02	8.03383E-02
4	7.20862E-02	8.03383E-02
5	3.60431E-02	8.03383E-02

NODE	COOLANTl (C)	CladSl (C)	FUEL PEAK (C)	CladSr (C)	COOLANTr (C)	HCOFl W/C-m^2	HCOFr W/C-m^2	ONBRl [F Note 1]	ONBRr	ETA'l K-cm^3/J [Note 3]	ETA'r K-cm^3/J [Note 3]	ONB Temp left(C)	ONB Temp right(C)
	25.000				25.000								
1	27.081	62.654	62.801	62.654	27.081	7.8086E+02	7.8086E+02	3.39	3.39	3.604E+02	3.604E+02	152.792	152.792
2	30.556	65.852	65.999	65.852	30.556	7.8700E+02	7.8700E+02	3.13	3.13	3.503E+02	3.503E+02	152.746	152.746
3	33.322	68.407	68.553	68.407	33.322	7.9174E+02	7.9174E+02	2.94	2.94	3.422E+02	3.422E+02	152.710	152.710
4	36.086	70.968	71.115	70.968	36.086	7.9634E+02	7.9634E+02	2.78	2.78	3.341E+02	3.341E+02	152.673	152.673
5	38.870	73.556	73.702	73.556	38.870	8.0084E+02	8.0084E+02	2.63	2.63	3.259E+02	3.259E+02	152.637	152.637
6	41.631	76.130	76.277	76.130	41.631	8.0517E+02	8.0517E+02	2.50	2.50	3.178E+02	3.178E+02	152.600	152.600
7	44.391	78.712	78.858	78.712	44.391	8.0937E+02	8.0937E+02	2.37	2.37	3.097E+02	3.097E+02	152.564	152.564
8	47.171	81.318	81.465	81.318	47.171	8.1347E+02	8.1347E+02	2.26	2.26	3.016E+02	3.016E+02	152.527	152.527
9	49.929	83.912	84.059	83.912	49.929	8.1741E+02	8.1741E+02	2.16	2.16	2.935E+02	2.935E+02	152.491	152.491
10	52.687	86.512	86.658	86.512	52.687	8.2122E+02	8.2122E+02	2.07	2.07	2.854E+02	2.854E+02	152.454	152.454
11	55.462	89.135	89.282	89.135	55.462	8.2492E+02	8.2492E+02	1.99	1.99	2.773E+02	2.773E+02	152.418	152.418
12	58.216	91.745	91.891	91.745	58.216	8.2847E+02	8.2847E+02	1.91	1.91	2.692E+02	2.692E+02	152.381	152.381
13	60.968	94.359	94.505	94.359	60.968	8.3189E+02	8.3189E+02	1.84	1.84	2.611E+02	2.611E+02	152.344	152.344
14	64.421	97.648	97.794	97.648	64.421	8.3601E+02	8.3601E+02	1.75	1.75	2.510E+02	2.510E+02	152.298	152.298
	66.488				66.488								

[1] The ONB ratio is here defined as (Tonb - Tinlet)/(Tsurf - Tinlet). If the heat flux is negative (the coolant is hotter than the adjacent cladding surface), then the ONB ratio is arbitrarily set to 99.99 .

[3] The column gives ETA' = (Coolant Velocity)*(Tsat - Coolant Temp)/(Heat Flux). ETA' in the units chosen here, equals Whittle and Forgan dimensionless ETA for water-cooled reactors: ETA = ETA'*Coolant Density*Cp/4. The last value in the colunm (at exit) should be greater than 32.5 to avoid excursive flow instability. ETA is also used in the equation R = 1/(1+ETA*Dh/Lh)

Figure 11.6 Solution of Test Problem 21 Assembly 1 by PLTEMP/ANL V3.6 Code – Global Hot Channel Factors Applied FPOWER = 1.20, FFLOW = 1.20, FNUSLT = 1.15

Flow Rate at Power 15 kW (i.e., FPOWER*12.5 kW)

Channel	Flow Rate kg/s	Velocity m/s
1	4.02097E-02	8.96262E-02
2	8.04195E-02	8.96262E-02
3	8.04195E-02	8.96262E-02
4	8.04195E-02	8.96262E-02
5	4.02097E-02	8.96262E-02
Total	3.21680E-01	

Flow Rate at Power 15.0 kW with Hot Channel Factor FFLOW Applied

Channel	Flow Rate kg/s	Velocity m/s
1	3.35081E-02	7.46885E-02
2	6.70162E-02	7.46885E-02
3	6.70162E-02	7.46885E-02
4	6.70162E-02	7.46885E-02
5	3.35081E-02	7.46885E-02
Total	2.68067E-01	

NODE	COOLANT ON LEFT (C)	CLAD SURF ON LEFT (C)	FUEL PEAK (C)	CLAD SURF ON RIGHT (C)	COOLANT ON RIGHT (C)	H ON LEFT W/C-m^2	H ON RIGHT W/C-m^2	ONBR LEFT [F Note 1]	ONBR RIGHT [F Note 1]	ETA LEFT K-cm^3/J [Note 3]	ETA RIGHT K-cm^3/J [Note 3]	ONB TEMP LEFT (C) [Note 1]	ONB TEMP RIGHT (C) [Note 1]
	25.000				25.000								
1	27.686	76.709	76.885	76.709	27.686	6.7995E+02	6.7995E+02	2.47	2.47	2.779E+02	2.779E+02	152.891	152.891
2	32.170	80.707	80.883	80.707	32.170	6.8676E+02	6.8676E+02	2.29	2.29	2.677E+02	2.677E+02	152.845	152.845
3	35.738	83.910	84.086	83.910	35.738	6.9197E+02	6.9197E+02	2.17	2.17	2.597E+02	2.597E+02	152.809	152.809
4	39.305	87.130	87.306	87.130	39.305	6.9698E+02	6.9698E+02	2.06	2.06	2.516E+02	2.516E+02	152.773	152.773
5	42.896	90.391	90.567	90.391	42.896	7.0183E+02	7.0183E+02	1.95	1.95	2.435E+02	2.435E+02	152.736	152.736
6	46.459	93.642	93.818	93.642	46.459	7.0646E+02	7.0646E+02	1.86	1.86	2.354E+02	2.354E+02	152.700	152.700
7	50.018	96.908	97.084	96.908	50.018	7.1090E+02	7.1090E+02	1.78	1.78	2.273E+02	2.273E+02	152.663	152.663
8	53.603	100.212	100.388	100.212	53.603	7.1518E+02	7.1518E+02	1.70	1.70	2.192E+02	2.192E+02	152.627	152.627
9	57.159	103.504	103.680	103.504	57.159	7.1924E+02	7.1924E+02	1.63	1.63	2.112E+02	2.112E+02	152.590	152.590
10	60.712	106.809	106.985	106.809	60.712	7.2311E+02	7.2311E+02	1.56	1.56	2.031E+02	2.031E+02	152.554	152.554
11	64.290	110.151	110.327	110.151	64.290	7.2683E+02	7.2683E+02	1.50	1.50	1.950E+02	1.950E+02	152.517	152.517
12	67.837	113.478	113.653	113.478	67.837	7.3034E+02	7.3034E+02	1.44	1.44	1.870E+02	1.870E+02	152.481	152.481
13	71.382	116.815	116.991	116.815	71.382	7.3367E+02	7.3367E+02	1.39	1.39	1.790E+02	1.790E+02	152.444	152.444
14	75.829	121.021	121.197	121.021	75.829	7.3760E+02	7.3760E+02	1.33	1.33	1.689E+02	1.689E+02	152.398	152.398
	78.491				78.491								

[1] The ONB ratio is here defined as (Tonb - Tinlet)/(Tsurf - Tinlet). If the heat flux is negative (the coolant is hotter than the adjacent cladding surface), then the ONB ratio is arbitrarily set to 99.99 .

[3] The column gives ETA' = (Coolant Velocity)*(Tsat - Coolant Temp)/(Heat Flux). ETA' in the units chosen here, equals Whittle and Forgan dimensionless ETA for water-cooled reactors: ETA = ETA'*Coolant Density*Cp/4. The last value in the colunm (at exit) should be greater than 32.5 to avoid excursive flow instability. ETA is also used in the equation R = 1/(1+ETA*Dh/Lh)

Figure 11.7 Solution of Test Problem 21 Assembly 1 by PLTEMP/ANL V3.6 Code – All Six Hot Channel Factors Applied FPOWER = 1.20, FFLOW = 1.20, FNUSLT = 1.15, FBULK = 1.15, FFILM = 1.18, FFLUX = 1.22

NODE	COOLANT ON LEFT (C)	CLAD SURF ON LEFT (C)	FUEL PEAK (C)	CLAD SURF ON RIGHT (C)	COOLANT ON RIGHT (C)	H ON LEFT W/C-m^2	H ON RIGHT W/C-m^2	ONBR LEFT [F Note 1]	ONBR RIGHT [F Note 1]
	25.000				25.000				
1	28.089	85.936	86.151	85.936	28.089	6.7995E+02	6.7995E+02	2.10	2.10
2	33.245	90.519	90.733	90.519	33.245	6.8676E+02	6.8676E+02	1.95	1.95
3	37.349	94.191	94.406	94.191	37.349	6.9197E+02	6.9197E+02	1.85	1.85
4	41.451	97.885	98.099	97.885	41.451	6.9698E+02	6.9698E+02	1.75	1.75
5	45.581	101.625	101.839	101.625	45.581	7.0183E+02	7.0183E+02	1.67	1.67
6	49.677	105.354	105.569	105.354	49.677	7.0646E+02	7.0646E+02	1.59	1.59
7	53.771	109.100	109.315	109.100	53.771	7.1090E+02	7.1090E+02	1.52	1.52
8	57.894	112.892	113.107	112.892	57.894	7.1518E+02	7.1518E+02	1.45	1.45
9	61.983	116.670	116.885	116.670	61.983	7.1924E+02	7.1924E+02	1.39	1.39
10	66.069	120.463	120.678	120.463	66.069	7.2311E+02	7.2311E+02	1.34	1.34
11	70.183	124.299	124.514	124.299	70.183	7.2683E+02	7.2683E+02	1.28	1.28
12	74.262	128.118	128.333	128.118	74.262	7.3034E+02	7.3034E+02	1.24	1.24
13	78.339	131.951	132.165	131.951	78.339	7.3367E+02	7.3367E+02	1.19	1.19
14	83.453	136.780	136.994	136.780	83.453	7.3760E+02	7.3760E+02	1.14	1.14
	86.515				86.515				

Table 11.1 Comparison of PLTEMP/ANL V3.6 and *Mathematica* Solutions of Test Problem 21 Fuel Assembly 1, With and Without Global Hot Channel Factors

	Nominal Solution		**Solution with Global Hot Channel Factors**	
Input or Calculated Quantity	PLTEMP/ANL V3.6 Solution	*Mathematica* Calculation	PLTEMP/ANL V3.6 Solution	*Mathematica* Calculation
Inlet Temp, °C	25	25	25	25
Power per Channel, kW	12.5	12.5	15.0	15.0
Loss Coeff. at Inlet	0.5	0.5	0.5	0.5
Loss Coeff. at Exit	1.0	1.0	1.0	1.0
	Calculated Quantities			
Flow per Channel, kg/s	0.072086	0.072071	0.067016	0.067013
Exit Temp, °C	66.488	66.497	78.491	78.494
	Buoyancy Head, Pa			
Axial Region 1	0.0	0.0	0.0	0.0
Axial Region 2 (Heated Section)	51.991	51.859	57.129	57.138
Axial Region 3	24.132	24.131	26.743	26.737
Total Buoyancy	**75.991**	**75.991**	**83.872**	**83.876**
	Frictional Pressure Drop, Pa			
Inlet Loss	16.182	1.608	18.260	2.002
Axial Region 1		14.570		16.257
Axial Region 2 (Heated Length)	49.623	49.613	54.123	54.126
Axial Region 3	10.186	6.929	11.490	7.412
		3.270		4.078
Total Pressure Drop	**75.991**	**75.991**	**83.873**	**83.876**

Table 11.2 PLTEMP/ANL Results for Sample Problem 21 with Six Hot Channel Factors

System-wide Factors: FPOWER = 1.20, FFLOW = 1.20, FNUSLT = 1.15,
Local Factors: FBULK = 1.15, FFILM = 1.18, FFLUX = 1.22

	Assembly 1, Nominal Case, Power = 50 kW								
Assembly Flow, kg/s	0.28834								
Channel Number	**1**		**2**		**3**		**4**		**5**
Plate Number		1		2		3		4	
Plate Power, kW		12.5		12.5		12.5		12.5	
Channel Flow, kg/s	0.036043		0.072086		0.072086		0.072086		0.036043
Ch Exit Temp, °C	66.488		66.488		66.488		66.488		66.488
ONBR[1] at Inlet, L/R	3.417		3.417, 3.417		3.417, 3.417		3.417, 3.417		3.417
ONBR[1] at Exit, L/R	1.757		1.757, 1.757		1.757, 1.757		1.757, 1.757		1.757
	Assembly 1 with Systemic Uncertainties, Power = 60 kW								
Assembly Flow, kg/s	0.32168 / 1.2 = 0.26806								
Plate Power, kW		15.0		15.0		15.0		15.0	
Channel Flow, kg/s	0.033508		0.067016		0.067016		0.067016		0.033508
Ch Exit Temp, °C	78.491		78.491		78.491		78.491		78.491
ONBR at Inlet, L/R	2.486		2.486, 2.486		2.486, 2.486		2.486, 2.486		2.486
ONBR at Exit, L/R	1.329		1.329, 1.329		1.329, 1.329		1.329, 1.329		1.329
	Assembly 1 with Systemic and Local Uncertainties, Power = 60 kW								
Assembly Flow, kg/s	0.26806								
Plate Power, kW		15.0		15.0		15.0		15.0	
Channel Flow, kg/s	0.033508		0.067016		0.067016		0.067016		0.033508
Ch Exit Temp, °C	86.515		86.515		86.515		86.515		86.515
ONBR at Inlet, L/R	2.110		2.110, 2.110		2.110, 2.110		2.110, 2.110		2.110
ONBR at Exit, L/R	1.142		1.142, 1.142		1.142, 1.142		1.142, 1.142		1.142
	Assembly 2, Nominal Case, Power = 50 kW								
Assembly Flow, kg/s	0.28687								
Plate Power, kW		7.5		17.5		17.5		7.5	
Channel Flow, kg/s	0.027193		0.072094		0.072094		0.072094		0.027193
Ch Exit Temp, °C	60.543		66.272		71.186		66.272		60.543
ONBR at Inlet, L/R	5.538		5.537, 2.474		2.474, 2.474		2.474, 5.537		5.538
ONBR at Exit, L/R	2.259		2.255, 1.453		1.451, 1.451		1.453, 2.255		2.259
	Assembly 2 with Systemic Uncertainties, Power = 60 kW								
Assembly Flow, kg/s	0.31999 / 1.2 = 0.26666								
Plate Power, kW		9.0		21.0		21.0		9.0	
Channel Flow, kg/s	0.025038		0.067056		0.082470		0.067056		0.025038
Ch Exit Temp, °C	70.991		78.205		84.408		78.205		70.991
ONBR at Inlet, L/R	4.034		4.033, 1.799		1.799, 1.799		1.799, 4.033		4.033
ONBR at Exit, L/R	1.716		1.713, 1.095		1.094, 1.094		1.095, 1.713		1.716
	Assembly 2 with Systemic and Local Uncertainties, Power = 60 kW								
Assembly Flow, kg/s	0.26666								
Plate Power, kW		9.0		21.0		21.0		9.0	
Channel Flow, kg/s	0.025038		0.067056		0.082470		0.067056		0.025038
Ch Exit Temp, °C	77.890		86.185		93.319		86.185		77.890
ONBR at Inlet, L/R	3.426		3.426, 1.526		1.526, 1.526		1.526, 3.426		3.426
ONBR at Exit, L/R	1.476		1.477, 0.939		0.939, 0.939		0.939, 1.477		1.476

1. Heat flux based ONB ratio on the left and right surfaces of the fuel plate

Table 11.3 Solution of Test Problem 21 Fuel Assembly 1 by *Mathematica* Using PLTEMP/ANL Coolant Properties, Nominal Case

Flow rate per coolant channel = 0.072071 kg/s

Region or Axial Node	Nodal Power W	Temp at Node Exit, °C	Temp at Node Center, °C	Density at Node Center kg/m³	Buoyancy due to Node, Pa	Re at Node Center	Friction Factor at Node Center	Frictional Pressure Drop, Pa
Inlet				996.982				1.60802
Region 1	0.0	25.0	25.0	996.982	0.0	527.889	0.179427	14.5704
1	833.333	27.7752	26.3876	996.664	0.155776	545.069	0.173771	4.70522
2	833.333	30.5494	29.1623	995.979	0.491785	580.407	0.163191	4.42178
3	833.333	33.3226	31.936	995.228	0.860166	616.961	0.153522	4.16294
4	833.333	36.0943	34.7085	994.411	1.26061	654.607	0.144694	3.92675
5	833.333	38.8645	37.4794	993.53	1.69282	693.229	0.136632	3.71127
6	833.333	41.6337	40.2491	992.584	2.1564	732.67	0.129277	3.51483
7	833.333	44.4018	43.0177	991.575	2.65098	772.795	0.122565	3.33573
8	833.333	47.1682	45.785	990.504	3.17619	813.462	0.116437	3.17239
9	833.333	49.9333	48.5507	989.372	3.73162	854.563	0.110837	3.02327
10	833.333	52.6976	51.3154	988.178	4.31676	895.989	0.105713	2.88697
11	833.333	55.4605	54.079	986.925	4.93114	937.657	0.101015	2.76218
12	833.333	58.2219	56.8412	985.614	5.57429	979.521	0.0966977	2.64765
13	833.333	60.9817	59.6018	984.244	6.24564	1021.55	0.0927196	2.54226
14	833.333	63.74	62.3608	982.819	6.94463	1063.62	0.0890523	2.44524
15	833.333	66.4969	65.1184	981.338	7.67068	1106.29	0.0856169	2.35446
Region 2		66.4969			51.85944			49.6129
Region 3	0.0	66.4969	66.4969	980.577	24.13116	1128.55	0.0839282	6.92943
Reg 3 Exit		66.4969		980.577				3.26985
Total					75.9906			75.9906

Table 11.4 Solution of Test Problem 21 Fuel Assembly 1 by *Mathematica* Using PLTEMP/ANL Coolant Properties, with Global Hot Channel Factors

Flow rate per coolant channel at 15 kW (FPOWER*12.5 kW) = 0.0804153 kg/s

Region or Axial Node	Nodal Power W	Temp at Node Exit, °C	Temp at Node Center, °C	Density at Node Center kg/m³	Buoyancy due to Node, Pa	Re at Node Center	Friction Factor at Node Center	Frictional Pressure Drop, Pa
Inlet				996.982				2.00191
Region 1	0.0	25.0	25.0	996.982	0.0	589.005	0.160809	16.25727
1	1000.	27.9846	26.4923	996.64	0.167865	609.636	0.155367	5.2375
2	1000.	30.9681	29.4764	995.897	0.531874	652.155	0.145238	4.89968
3	1000.	33.9504	32.4593	995.079	0.93329	696.228	0.136044	4.59329
4	1000.	36.9309	35.4407	994.184	1.37172	741.679	0.127707	4.31569
5	1000.	39.9097	38.4203	993.216	1.84678	788.34	0.120148	4.0642
6	1000.	42.8876	41.3986	992.173	2.35799	835.999	0.113299	3.83654
7	1000.	45.8638	44.3757	991.058	2.90487	884.458	0.107091	3.63042
8	1000.	48.8382	47.351	989.871	3.48697	933.554	0.101459	3.44362
9	1000.	51.8114	50.3248	988.613	4.10368	983.118	0.096344	3.27417
10	1000 .	54.7834	53.2974	987.286	4.75441	1033.04	0.091688	3.12013
11	1000.	57.7535	56.2685	985.89	5.43856	1083.22	0.0874407	2.9798
12	1000.	60.7219	59.2377	984.428	6.15548	1133.62	0.0835531	2.85155
13	1000.	63.6885	62.2052	982.901	6.90446	1184.1	0.0799913	2.73423
14	1000.	66.6535	65.171	981.309	7.68478	1235.31	0.0766748	2.62512
15	1000.	69.6165	68.135	979.656	8.49569	1288.97	0.0734829	2.52009
Region 2	15000.0	69.6165			57.1384			54.126
Region 3	0.0	69.6165	69.6165	978.806	26.7373	1315.84	0.0719824	7.41231
Reg 3 Exit		69.6165		978.806		1315.84		4.07818
Total	15000.0				83.8757			83.8757

Table 11.5 Temperature Distribution in Test Problem 21 Fuel Assembly 1 at the Channel Flow Rate Obtained byApplying Global Hot Channel Factors

Flow rate per coolant channel = 0.0804153/FFLOW = 0.0670128 kg/s

Region or Axial Node	Nodal Power W	Temp at Node Exit, °C	Temp at Node Center, °C
Inlet		25.0	
Region 1	0.0	25.0	25.0
1	1000.0.	28.5814	26.7907
2	1000.0.	32.1612	30.3713
3	1000.0.	35.739	33.9501
4	1000.0	39.3141	37.5265
5	1000.0.	42.8876	41.1008
6	1000.0.	46.4588	44.6732
7	1000.0.	50.0275	48.2432
8	1000.0.	53.5948	51.8112
9	1000.0.	57.1596	55.3772
10	1000.0.	60.7219	58.9408
11	1000.0.	64.2816	62.5018
12	1000.0.	67.8389	66.0603
13	1000.0.	71.3931	69.616
14	1000.0.	74.9441	73.1686
15	1000.0.	78.4939	76.719
Region 2	15000.0	78.4939	
Region 3	0.0	78.4939	78.4939
Reg 3 Exit		78.4939	

APPENDIX I *Mathematica* Program for Solving Test Problem 21

```
(" SOLUTION OF NATURAL CIRCULATION STANDARD PROBLEM 21, Fuel Assembly 1,
Nominal hcf case, Using Water Properties of the PLTEMP/ANL V3.5 Code ")
data={kin=0.5,kex=1.0,Dh=0.00594059,len1=0.15,len2=0.75,len3=0.15,wch=0.3,tch=0.003,grav=9.8066
5,erel=0.0,tin=25.0,powr=12500.0};
flow=0.072071323; ←—— This guess flow was adjusted and the program was rerun to achieve channel
                      channel buoyancy (buoy) equal to channel frictional pressure drop (delp).
chimny=0.0
(* power = 12.5 kW per plate, total power = 50 kW in 4 plates *)
Print["Subcooled water density, kg/m**3, at 5 bar absolute used in the PLTEMP/ANL V3.5 Code"];
rho={{20.,997.9875},{25.,996.9820},{30.,995.7591},{35.,994.3214},{40.,992.6718},{45.,990.8146},{5
0.,988.7536},{55.,986.4945},{60.,984.0422},{65.,981.4029},{70.,978.5832},{75.,975.5897},{80.,972.43
24},{85.,969.1167},{90.,965.6552},{95.,962.0546},{100.,958.3263},{105.,954.4819},{110.,950.5318},{
115.,946.4900},{120.,942.3674},{125.,938.1805},{130.,933.9403},{135.,929.6651},{140.,925.3685},{1
45.,921.0693},{150.,916.7842}};
Plot[Interpolation[rho][temp],{temp,20,150}];
Print["Subcooled water enthalpy, kJ/kg, at 5 bar absolute used in the PLTEMP/ANL V3.5 Code"];
enthalpy={{20.,83.9517},{25.,104.7730},{30.,125.6082},{35.,146.4573},{40.,167.3272},{45.,188.2110}
,{50.,209.1156},{55.,230.0341},{60.,250.9734},{65.,271.9336},{70.,292.9146},{75.,313.9233},{80.,334
.9460},{85.,356.0033},{90.,377.0746},{95.,398.1805},{100.,419.3143},{105.,440.4758},{110.,461.6720
},{115.0,482.8960},{120.,504.1616},{125.,525.4550},{130.,546.7970},{135.,568.1738},{140.,589.5991
},{145.,611.0661},{150.,632.5816}};
Plot[Interpolation[enthalpy][temp],{temp,20,150}];
Print["Dynamic viscosity, micro Pa-s, of water used in the PLTEMP/ANL V3.5 Code"];
visc={{20.,1014.5},{25.,901.17},{30.,804.50},{35.,722.29},{40.,652.48},{45.,593.26},{50.,542.91},{55
.,499.92},{60.,462.93},{65.,430.75},{70.,401.28},{75.,377.03},{80.,355.98},{85.,337.40},{90.,320.63},
{95.,304.97},{100.,290.21},{105.,276.41},{110.,263.52},{115.,251.49},{120.,240.27},{125.,229.83},{1
30.,220.10},{135.,211.05},{140.,202.64},{145.,194.82},{150.,187.56}};
Plot[Interpolation[visc][temp],{temp,20,150}];
Print["Inlet and Exit temperatures, C"];
tin=tin/.data
grav=grav/.data;
hin=1000*Interpolation[enthalpy][tin];
hout=hin+powr/flow/.data;
tout=tx/.FindRoot[hout==1000*Interpolation[enthalpy][tx],{tx,tin}]
rhoin=Interpolation[rho][tin];
rhoout=Interpolation[rho][tout];
Print["Density at inlet =",rhoin,", Density at exit =",rhoout];
rhoave=NIntegrate[Interpolation[rho][temp],{temp,tin,tout}]/(tout-tin);
Print["Integrated average coolant density over (",tin," to ",tout,") = ",rhoave];
buoy2=(rhoin-rhoave)*grav*len2 /.data;
buoy3=(rhoin-rhoout)*grav*len3 /.data;
buoychimny=(rhoin-rhoout)*grav*chimny /.data;
Print["Buoyancy due to chimney =",buoychimny];
buoy=buoy2+buoy3;
Print["DRIVING PRESSURE HEAD DUE TO BUOYANCY in Section 1 =0.0, Section 2 =",buoy2,",
Section 3 =",buoy3,", Total buoyancy (Pa) =",buoy];
velin=flow/(rhoin*wch*tch)/.data;
Print["Coolant inlet velocity, m/s = ",velin];
```

```
visc1=0.000001*Interpolation[visc][tin];
visc3=0.000001*Interpolation[visc][tout];
Print["Coolant dynamic viscosity, Pa-s, in axial regions 1 and 3 =",visc1," ",visc3]
reyn1=flow*Dh/(wch*tch*visc1)/.data;
reyn3=flow*Dh/(wch*tch*visc3)/.data;
Print["Reynolds numbers in axial regions 1 and 3 =",reyn1," ",reyn3];
aspect=tch/wch/.data;
erela=If[0<erel<0.00000001,0.00000001,erel]/.data;
Cfric=96*(1-1.3553*aspect+1.9467*aspect^2-1.7012*aspect^3+0.9564*aspect^4-0.2537*aspect^5)
fric2200=Cfric/2200.0;
reyn=reyn1;
fa=1/(-2*Log[10,erela/3.7+2.51/reyn*(1.14-2*Log[10,erela+21.25/reyn^0.9])])^2;
If[reyn>=3000 && erela==0,fb=4*fric/.FindRoot[fric==6.25002/(1-
8.68591*Log[reyn*fric^0.5]+18.8612*(Log[reyn*fric^0.5])^2),{fric,0.1}]];
If[reyn>=3000 && erela>=0.00000001,
   fb=4*fric/.FindRoot[fric==0.331369/(Log[0.27027*erela+1.255/(reyn*fric^0.5)])^2,{fric,0.1}]];
If[reyn>=3000,Print["Turbulent friction factor fb = ",fb,", Re = ",reyn,", Rel roughness = ",erela]];
frica=If[reyn<=2200.0,Cfric/reyn,fric2200+(fa-fric2200)*(3.75-8250/reyn)];
fric1=If[reyn>=3000.0,fb,frica];
reyn=reyn3;
fa=1/(-2*Log[10,erela/3.7+2.51/reyn*(1.14-2*Log[10,erela+21.25/reyn^0.9])])^2;
If[reyn>=3000 && erela==0,fb=4*fric/.FindRoot[fric==6.25002/(1-
8.68591*Log[reyn*fric^0.5]+18.8612*(Log[reyn*fric^0.5])^2),{fric,0.1}]];
If[reyn>=3000 && erela>=0.00000001,
   fb=4*fric/.FindRoot[fric==0.331369/(Log[0.27027*erela+1.255/(reyn*fric^0.5)])^2,{fric,0.1}]];
If[reyn>=3000,Print["Turbulent friction factor fb = ",fb,", Re = ",reyn,", Rel roughness = ",erela]];
frica=If[reyn<=2200.0,Cfric/reyn,fric2200+(fa-fric2200)*(3.75-8250/reyn)];
fric3=If[reyn>=3000.0,fb,frica];
Print["Friction factors in Sections 1 and 3 =",fric1," ",fric3];
Print["FRICTIONAL PRESSURE DROP IN SECTION 1"]
delp1s=(fric1*len1/Dh)*0.5*(flow/(wch*tch))^2/rhoin/.data;
delp1m=kin*0.5*(flow/(wch*tch))^2/rhoin/.data;
delp1=delp1s+delp1m;
Print["Total pressure drop in Section 1 =",delp1,", Minor loss = ",delp1m,", Wall shear =",delp1s]
Print["FRICTIONAL PRESSURE DROP IN SECTION 3"]
delp3s=(fric3*len3/Dh)*0.5*(flow/(wch*tch))^2/rhoout/.data;
delp3m=kex*0.5*(flow/(wch*tch))^2/rhoout/.data;
delp3=delp3s+delp3m;
Print["Total pressure drop in Section 3 =",delp3,", Minor loss = ",delp3m,", Wall shear =",delp3s]
delp4=rhoin*velin*velin*(rhoin/rhoout-1.0)/.data;
Print["Pressure drop due to momentum flux (Pa) =",delp4];
Print["Flow =",flow,", g =",grav,", Temp at inlet and exit =",tin,", ",tout,", Density at inlet and exit
=",rhoin,", ",rhoout,", Gravity head =",grav*(rhoin*len1+rhoave*len2+rhoout*len3)/.data,", Total
buoyancy =",buoy,", Buoyancy in Section 2 =",buoy2,", Buoyancy in Section 3 =",buoy3,", Power into
coolant (W) =",flow*(hout-hin)]
Print["LOOP OVER 21 AXIAL SEGMENTS"];
powr1=powr/15/.data;
delz=len2/15/.data;
enth1=hin;
temp1=tin;
delp2p=0;
```

```
buoy2p=0;
Do[powr2=powr1;
  If[j<4,powr2=0];
  If[j>18,powr2=0];
  enth2=enth1+powr2/flow;
  temp2=tx/.FindRoot[enth2==1000*Interpolation[enthalpy][tx],{tx,temp1}];
  tempj=0.5*(temp2+temp1);
  viscj=0.000001*Interpolation[visc][tempj];
  rhoj=Interpolation[rho][tempj];
  buoy2s=buoy2p+grav*(rhoin-rhoj)*delz;
  reynj=flow*Dh/(wch*tch*viscj)/.data;
  reyn=reynj;
  fa=1/(-2*Log[10,erela/3.7+2.51/reyn*(1.14-2*Log[10,erela+21.25/reyn^0.9])])^2;
  If[reyn>=3000 && erela==0,fb=4*fric/.FindRoot[fric==6.25002/(1-
8.68591*Log[reyn*fric^0.5]+18.8612*(Log[reyn*fric^0.5])^2),{fric,0.1}]];
  If[reyn>=3000 && erela>=0.00000001,
    fb=4*fric/.FindRoot[fric==0.331369/(Log[0.27027*erela+1.255/(reyn*fric^0.5)])^2,{fric,0.1}]];
  If[reyn>=3000,Print["Turbulent friction factor fb = ",fb,", Re = ",reyn,", Rel roughness = ",erela]];
  frica=If[reyn<=2200.0,Cfric/reyn,fric2200+(fa-fric2200)*(3.75-8250/reyn)];
  fricj=If[reyn>=3000.0,fb,frica];
  delpj=(fricj*delz/Dh)*0.5*(flow/(wch*tch))^2/rhoj/.data;
  delp2=delp2p+delpj;
  (*Print["Axial segment =",j,", Flow, kg/s =",flow,", delz (m) =",delz,"Power in segment (W) =",powr2,",
Enthalpy at segment exit (J/kg) =",enth2,", Enthalpy at segment center (J/kg) =",0.5(enth1+enth2),",
Temp at segment exit (C) =",temp2,", Segment mean temp (C) =",tempj,", Segment mean density
(kg/m^3) =",rhoj,", Buoyancy due to segments 1 through ",j," (Pa) =",buoy2s,", Viscosity (Pa-s)
=",viscj,", Reynolds number =",reynj,", Friction factor =",fricj,", fl/Dh of segment (Pa) =",delpj,",
Cumulative sum fL/Dh of segments 1 through ",j", (Pa) =",delp2];*)
  Print[j,"   ",powr2,"   ",temp2,"   ",tempj,"   ",rhoj,"   ",grav*(rhoin-rhoj)*delz,"   ",reynj,"   ",fricj,"
",delpj];
  buoy2p=buoy2s;
  delp2p=delp2;
  temp1=temp2;
  enth1=enth2,
  {j,1,21}]
Print["Pressure drop due to wall shear in region 2 = ",delp2-delp1s-delp3s]
Print["BALANCE OF BUOYANCY AND FRICTIONAL PRESSURE DROP:"]
delp=delp2+delp1m+delp3m;
buoy=buoy2s+buoychimny;
Print["Total buoyancy (Pa) =",buoy,", Total frictional pressure drop (Pa) =",delp];
```

12 Verification of the Search Capability in PLTEMP/ANL V3.7

12.1 Introduction

The verification work reported here was done in April 2009. To save the reactor analyst's time, a general search capability (input option ISRCH = 1) has been implemented in the PLTEMP/ANL V3.7 thermal-hydraulics code used for research reactors. The search capability gets a user-specified target value for a specified code output variable (e.g., reactor coolant flow rate) by adjusting a specified input datum (e.g., applied pressure drop). Two basic types of search are implemented: (1) Single search in which *one* input datum is adjusted to achieve a target value for *one* output variable; and (2) Double search in which *two* input data are adjusted to achieve target values for *two* output variables. The logic flow diagram of how a search is performed by the code, basically using the *interval-halving technique*, is given in the Users Guide [1].

Currently, 11 single searches and 5 double searches, listed in Table 12.1, are available. These searches adjust the input applied pressure drop or/and reactor power to get target values of any one or any two of these calculated quantities: core flow rate, minimum onset of nucleate boiling ratio (ONBR), minimum departure from nucleate boiling ratio (DNBR), minimum flow instability power ratio FIR), maximum cladding surface temperature ($T_{cs,max}$), and maximum coolant exit temperature ($T_{ex,max}$). The search capability is implemented such that new searches can be easily added.

The search capability also works for reactor problems using the hot channel factors option 2 (input IHCF = 2). When the option IHCF is 2, an input datum (depending on the search type) is adjusted so that the value of a code output quantity with *both* global and local hot channel factors applied equals an input target value. Using the search capability, a single run of the code generates all the data needed to plot a reactor operation diagram showing the relationship among three reactor parameters, e.g., nominal or true reactor power, nominal or true core flow, and the global minimum ONBR or minimum DNBR with all hot channel factors applied.

The purpose this chapter is to present a verification of the search capability, and an example of its application to research reactor analysis.

12.2 History Data and Search Capability

At the end of the output file on unit 6, the code prints one line of history data (a summary of the key results of the run) for a problem that does not use the hot channel factors option 2, and two lines of history data for a problem that uses the hot channel factors option 2. The first line is for the nominal case (without applying any hot channel factors), and the second line is for the case with global and local hot channel factors applied.

The history data is useful in plotting the results obtained by the search capability, as demonstrated herein. In a single run of the PLTEMP/ANL V3.7 code, one can make a diagram plotting the *nominal reactor power versus the nominal core flow* at a constant value of the minimum ONBR with global and local hot channel factors applied, parametrically varying the constant value of the

minimum ONBR. Using the results of the same run, one can also make another diagram plotting the *true reactor power versus the true core flow* at constant values of the minimum ONBR with global and local hot channel factors applied.

The following differences are noted between the history data outputs of PLTEMP/ANL V3.7 code and its earlier versions.

PLTEMP/ANL V3.7: When using the hot channel factors option IHCF = 2, both global and local hot channel factors are used in calculating the onset of nucleate boiling ratio (ONBR), the departure from nucleate boiling ratio (DNBR), and the flow instability power ratio (FIR). The calculation of the maximum cladding surface temperature ($T_{cs,max}$), and the maximum coolant temperature ($T_{ex,max}$) has been newly added. The code prints one line of HISTORY DATA at the end of the output file on unit 6 if the option IHCF is 1, and prints two lines of HISTORY DATA when using the option IHCF is 2. The first line shows results without incorporating any hot channel factor, and the second line shows results with *all six hot channel factors applied*. It is noted that the meaning of ONBR, DNBR, and FIR printed in the second line has changed.

PLTEMP/ANL Earlier Versions: When using the hot channel factors option IHCF = 2, both global and local hot channel factors are used in calculating ONBR. However, *only the global hot channel factors* are used in calculating DNBR and FIR. The maximum cladding surface temperature and the maximum coolant temperature are not calculated. The code prints one line of HISTORY DATA at the end of the output file if the option IHCF is 1, and prints two lines of HISTORY DATA when using the option IHCF is 2. The first line shows results without incorporating any hot channel factor, and the second line shows results with *only* the global hot channel factors applied.

12.3 Implementation of the Search Capability

Figure 12.1 shows a logic flow diagram of how a search is performed by the main program of the code. Basically, each search is performed using the *interval-halving technique*.

In a single search using this technique, the specified input datum is first set at its lower limit X1=XLOW (which is an input); an input data file is written on a scratch file; and the *pre-search* code is run to find the corresponding value Y1 for the specified output variable. The specified input datum is then reset at its upper limit X2=XHIGH (an input); another input data file is written over the scratch file; and the *pre-search* code is re-run to find the corresponding value Y2 for the output variable. The interval between X1 and X2 is then halved, and the specified input datum is reset at the arithmetic mean X3 of its lower and upper limits X1 and X2; a third input data file is written over the scratch file; and the *pre-search* code is re-run to find the corresponding value Y3 for the output variable. If the user-specified target value YTARGT of the output variable lies between Y1 and Y3, then X2 is set equal to X3; or if the target value YTARGT lies between Y3 and Y2, then X1 is set equal to X3. The interval between X1 and X2 is halved again, and the process (of writing an input data file and running the *pre-search* code) is repeated to get another pair of values, X3 and Y3, for the input datum and the output variable. This process is repeated to achieve a convergence, i.e., either the gap between X1 and X2 is a very small fraction of (XHIGH - XLOW), or Y3 is very close to YTARGT. This process is carried out in the subroutine

SEARCH1. A single search converges in about 15 to 30 iterations, i.e., passes through the pre-search code.

In a double search using this technique, the same process is carried out in the main program MAINSRCH (Fig. 12.1) in order to achieve a user-specified target value YTARGT2 of *the second* of the two output variables, by adjusting *the second* of the two specified input data (e.g., reactor power in the case of search type 21). In the main program, instead of running the pre-search code, the subroutine SEARCH1 is called each time to run a single search to adjust *the first* specified input datum (e.g., applied pressure drop in the case of search type 21) to achieve *the first* output variable's specified target value. The process in the main program is repeated till either the gap between the lower and upper limits of the second datum is a very small fraction of (XHIGH2 – XLOW2), or the value of the second output variable at the interval mid-point is very close to YTARGT2. A double search converges in about 300 to 400 iterations, i.e., passes through the pre-search code.

12.4 Verification for a Test Problem without Hot Channel Factors

In order to verify PLTEMP/ANL V3.7 for problems not using hot channel factors, Fig. 12.2 shows an input data file for a test problem (Test Problem 27) having 2 fuel assemblies of identical geometry, without any bypass channel. Each fuel assembly has 4 fuel plates and 5 coolant channels. The geometry and power distribution in the fuel assemblies are specified in the input data file. The flow through the coolant channels is determined by a pressure drop applied on the fuel assemblies. As specified on input cards 0203 and 0204 in Fig. 12.2, this problem exercises the double search type 21 with the objective of verifying the implementation of this search type. The input cards 0203 and 0204 specify that the applied pressure drop be adjusted in the range 0.1 to 0.5 MPa, and the nominal reactor power be adjusted in the range 0.5 to 2.5 MW so that the reactor achieves a core flow of 35.0 kg/s with a minimum ONBR of 5.0.

The following steps were taken in the verification of the code PLTEMP/ANL V3.7:

(1) PLTEMP/ANL V3.7 was run for Test Problem 27 (input file in Fig. 12.2). The code writes and saves the input data file (named *input.modified* and shown in Fig. 12.3) used in the last iteration of the search which has the converged values of the two input data that are adjusted during the search, i.e., the applied pressure drop (0.32109375 MPa) and the nominal reactor power (1.4580078 MW, both shown in boldface on the card 0500 in Fig. 12.3). The output file and the converged input data file were saved.

(2) The converged input data file saved in step 1 was converted into an input data file *without any search* for the older pre-search code PLTEMP/ANL V3.6, simply by commenting out the input cards 0203 and 0204, and by setting the search option ISRCH to zero on the input card 0200. Fig. 12.3 shows the converged input data file thus obtained. Then PLTEMP/ANL V3.6 was run for the converged input data file obtained, and the resulting output file was saved.

(3) The implementation of the search option 21 in PLTEMP/ANL V3.7 is verified if the two codes give the same results. The output files obtained by running the code versions V3.7 and V3.6 were compared. Fig. 12.4 shows a comparison of the key results. PLTEMP/ANL

V3.6 gives a core flow of 35.0 kg/s and a minimum ONBR of 5.0, the same results as PLTEMP/ANL V3.7. This provides a verification of the implementation of the search option 21.

It is noted that the history data of PLTEMP/ANL V3.6 does not have three key results: the minimum flow instability power ratio FIR_{min}, the maximum cladding surface temperature $T_{cs,max}$, and the maximum coolant temperature $T_{ex,max}$. This is because PLTEMP/ANL V3.6 calculates FIR_{min}, and prints it in the body of the output file but does not include it in the history data. Its value printed in the body of the output file is 9.1616, identical to that in the output of the code version V3.7. Furthermore, the code version V3.6 does not calculate the other two key data ($T_{cs,max}$ and $T_{ex,max}$) and hence they are not present in its history data. These two data were added in the code version V3.7 in the course of adding the search capability.

12.5 Verification for a Test Problem Using Hot Channel Factors

The same approach as used in Section 12.4 (for problems without hot channel factors) is used again to verify the implementation of the search type 21 for a problem with hot channel factors. To verify PLTEMP/ANL V3.7 for problems using the option 2 of hot channel factors, Fig. 12.5 shows the input data file for a test problem (Test Problem 28) having 2 fuel assemblies of identical geometry, without any bypass channel. Each fuel assembly has 4 fuel plates and 5 coolant channels. The geometry and power distribution in the fuel assemblies are specified in the input data file. The six hot channel factors that are used in the option 2 are defined in the Code Users Guide [1]. Their values, shown in boldface in Fig. 12.5, are:

Global Factors: FPOWER = 1.18, FFLOW = 1.25, FNUSLT = 1.20
Local Factors: FBULK = 1.05, FFILM = 1.06, FFLUX = 1.07

The flow through the coolant channels is determined by a pressure drop applied on the fuel assemblies. As specified on input cards 0203 and 0204 in Fig. 12.5, this problem exercises the double search type 21 with the objective of verifying the implementation of this search type. The input cards 0203 and 0204 specify that the applied pressure drop be adjusted in the range 0.1 to 0.5 MPa, and the nominal reactor power be adjusted in the range 0.5 to 3.0 MW so that the reactor achieves, with all hot channel factors applied, a core flow of 6.0 kg/s with a minimum ONBR of 1.2. The following steps were taken to verify the code:

(1) PLTEMP/ANL V3.7 was run for Test Problem 28 (input file in Fig. 12.5). The code writes and saves the input data file (named *input.modified* and shown in Fig. 12.6) used in the last iteration of the search which has the converged values of the two input data that are adjusted during the search, i.e., the applied pressure drop (0.11537476 MPa) and the nominal reactor power (0.95423889 MW, both shown in boldface on the card 0500 in Fig. 12.6). The output file and the converged input data file were saved.

(2) The converged input data file saved in step 1 was converted into an input data file *without any search* for the older pre-search code PLTEMP/ANL V3.6, simply by commenting out the input cards 0203 and 0204, and by setting the search option ISRCH to zero on the input card 0200. Fig. 12.6 shows the converged input data file thus obtained. Then

PLTEMP/ANL V3.6 was run for the converged input data file obtained, and the resulting output file was saved.

(3) The implementation of the search option 21 in PLTEMP/ANL V3.7 is verified if the two codes give the same results. The output files obtained by running the code versions V3.7 and V3.6 were compared. Fig. 12.7 shows a comparison of the key results printed as the history data at the end of the output file. *As discussed below*, PLTEMP/ANL V3.6 gives a core flow of 6.000 kg/s and a minimum ONBR of 1.200 with both global and local hot channel factors, the same results as PLTEMP/ANL V3.7. This provides a verification of the implementation of the search option 21 for problems using hot channel factors.

Discussion of ONBR with Hot Channel Factors: When using the hot channel factors option 2, PLTEMP/ANL V3.6 and the earlier code versions calculate (i) the minimum ONBR with only global hot channel factors, and also (ii) the minimum ONBR with both global and local hot channel factors. Both minima are printed in the main body of the output file. However, the history data printed at the end of the code version V3.6 output file contains the former, not the latter. This discrepancy is removed in PLTEMP/ANL V3.7, and the history data printed at the end of its output file contains the minimum ONBR with both global and local hot channel factors. As shown in Fig. 12.7, both code versions calculate a minimum ONBR of 1.268 with only global hot channel factors. Both code versions calculate a minimum ONBR of 1.200 with both global and local hot channel factors.

Discussion of DNBR with Hot Channel Factors: Regarding the DNBR using the hot channel factors option 2, PLTEMP/ANL V3.6 and the earlier code versions calculate the minimum DNBR with only global hot channel factors. The code versions V3.6 and V3.7 calculate a minimum DNBR of 14.092 with only global hot channel factors. The minimum DNBR with both global and local hot channel factors is not calculated by the code version V3.6 and the earlier versions. This discrepancy is removed in the code version V3.7. The minimum DNBR of 12.934 with both global and local hot channel factors is printed in the main body of the PLTEMP/ANL V3.7 output file, and also in the pass 2 of the history data.

Flow Instability Power Ratio (FIR) with Hot Channel Factors: Regarding the FIR using the hot channel factors option 2, PLTEMP/ANL V3.6 and the earlier code versions calculate the minimum FIR with only global hot channel factors. The code versions V3.6 and V3.7 calculate a minimum FIR of 1.807 with only global hot channel factors. The minimum FIR with both global and local hot channel factors is not calculated by the code version V3.6 and the earlier versions. This discrepancy is removed in the code version V3.7. The minimum FIR of 1.721 with both global and local hot channel factors is printed in the main body of the PLTEMP/ANL V3.7 output file, and also in the pass 2 of the history data.

12.6 Conclusions

A general search capability has been implemented in the PLTEMP/ANL V3.7 code for the thermal-hydraulics analysis of research reactors. The method used in the search capability has been described, and a verification of PLTEMP/ANL V3.7 has been performed by comparing it with a previous version of the code. PLTEMP/ANL V3.7 has also been verified for problems using hot channel factors. The utility of the search capability has been demonstrated by plotting some reactor

operation diagrams involving three reactor parameters (plotting different sets of three parameters), using data obtained by a single run of the code. This greatly reduces the reactor analyst's effort.

In the course of implementing the search capability, the calculation of minimum DNBR and minimum flow instability power ratio (FIR), with both global and local hot channel factors applied, were added to the code when using the hot channel factors option 2 (input IHCF = 2). The newly calculated ratios are used as target values in some searches available in the code.

12.7 REFERENCES

1. M. Kalimullah, A. P. Olson and E. E. Feldman, "A User's Guide to the PLTEMP/ANL Code," ANL/RTR/TM-18/17 Version 4.3, Revision 0, Argonne National Laboratory, 9700 South Cass Avenue, Argonne, IL 60439, USA (November 2018).

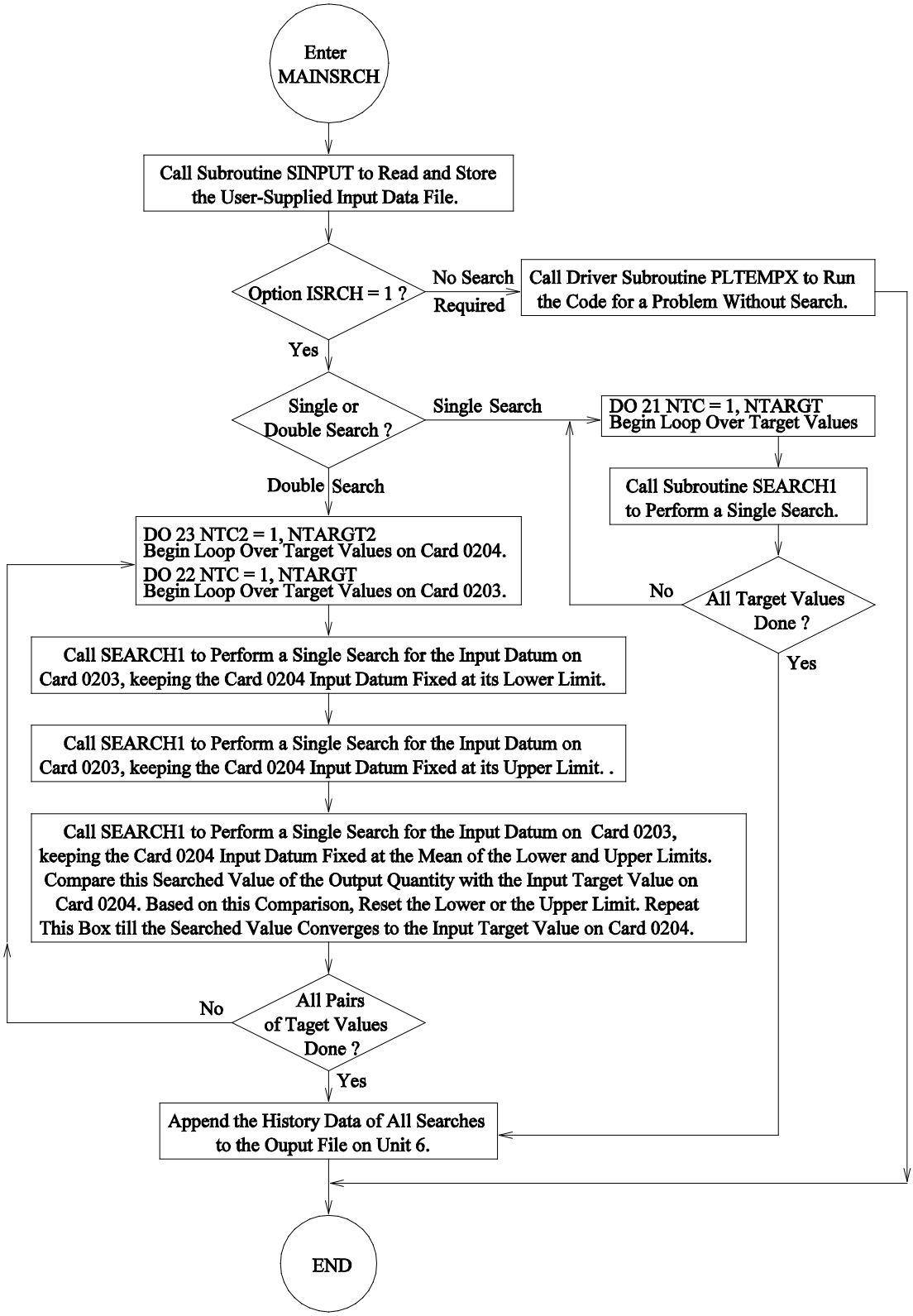

Figure 12.1 Logical Flow Diagram of the Main Program of PLTEMP/ANL V3.7 Code

Figure 12.2 Input File for Test Problem 27 without Hot Channel Factors That Uses Double Search Type 21

```
Test Problem: Using Search Option, 2 assy (of identical geometry) producing 1 MWt
! Each assembly has 4 fuel plates and 5 coolant channels
! H2O coolant, Flow is calculated from input pressure drop
! All hot channel factors = 1.0
! No bypass flow, NCTYP=0
! 10 axial heat transfer nodes in the heated length of fuel plates
!  1   2   3   4   5   6   7   8   9  10  11  12  13  14  15  16  17  18  19    # Card 0200
   0   0   0   1   0   1   1   1   0   0   0   0   0           0   1       0    Card(1)0200
  21 0.1         0.5           1 35.0                                          Card(1)0203
 0.5         2.5           1 5.00                                              Card(1)0204
   2   3 0.50       1.00        1.00        1.00           3                   Card(1)0300
! Using pressure driven mode
   1  20 1.00                                                                  Card(1)0301
   1   1   1                                                                   Card(1)0302
1.20        1.20                                                               Card(2)0303
30.0E-04    0.02955665  0.15        8.00        0.20        15.0E-03           Card(3)0304
30.0E-04    5.91133E-03 0.75        0.00        0.20        3.00E-03           Card(3)0304
30.0E-04    0.02955665  0.15        8.00        0.20        15.0E-03           Card(3)0304
! Use the code's biult-in correlation for friction factor
0.00        0.00        0.00                                                   Card(1)0305
   5   3 0.00       0.75        0.50E-03    0.00        1.00E-03    100.00     Card(1)0306
6.00E-04    5.91133E-03 0.4060      0.20        0.20        3.00E-03           Card(5)0307
6.00E-04    5.91133E-03 0.4060      0.40        0.20        3.00E-03           Card(5)0307
6.00E-04    5.91133E-03 0.4060      0.40        0.20        3.00E-03           Card(5)0307
6.00E-04    5.91133E-03 0.4060      0.40        0.20        3.00E-03           Card(5)0307
6.00E-04    5.91133E-03 0.4060      0.20        0.20        3.00E-03           Card(5)0307
0.20        0.20        0.20        0.20                                       Card(1)0308
! Card 0308a not required
! Radial power peaking factor data by fuel plate for each assembly. Input flow data by
! channel for each assembly on Cards 0310 not required because WFGES(1) is non-zero
0.900       0.950       1.050       1.100                                      Card(2)0309
0.901       0.951       1.049       1.099                                      Card(2)0309
! DP0       DDP         DPMAX       POWER       TIN         PIN
0.10        0.04        0.10        1.00        45.0        1.40               Card(1)0500
                                                                               Card(2)0500
  50 0.0001     25.0        0.00        1.00                                   Card(1)0600
  11                                                                           Card(1)0700
0.00        0.80                                                               Card(11)0701
0.10        0.88                                                               Card(11)0701
0.20        0.96                                                               Card(11)0701
0.30        1.04                                                               Card(11)0701
0.40        1.12                                                               Card(11)0701
0.50        1.20                                                               Card(11)0701
0.60        1.12                                                               Card(11)0701
0.70        1.04                                                               Card(11)0701
0.80        0.96                                                               Card(11)0701
0.90        0.88                                                               Card(11)0701
1.00        0.80                                                               Card(11)0701
   0                                                                           Card(11)0702
```

Figure 12.3 Converged Input File for Test Problem 27 without the Search Option

```
 Test Problem: Using Search Option, 2 assy (identical geometry) producing 1 MW  Card 100
   0   0   0   1   0   1   1   1   0   0   0   0   0   0   0   0   0   0   0Card 200
! 21 1.00000E-01 5.00000E-01   1 3.50000E+01
!5.00000E-01 2.50000E+00   1 5.00000E+00
   2   3 5.00000E-01 1.00000E+00 1.00000E+00 1.00000E+00   3   0 0.00000E+00    Card 300
   1  20 1.00000E+00                                                            Card 301
   1   1   1                                                                    Card 302
 1.20000E+00 1.20000E+00                                                        Card 303
 3.00000E-03 2.95567E-02 1.50000E-01 8.00000E+00 2.00000E-01 1.50000E-02        Card 304
 3.00000E-03 5.91133E-03 7.50000E-01 0.00000E+00 2.00000E-01 3.00000E-03        Card 304
 3.00000E-03 2.95567E-02 1.50000E-01 8.00000E+00 2.00000E-01 1.50000E-02        Card 304
 0.00000E+00 0.00000E+00 0.00000E+00 0.00000E+00                                Card 305
   5   3 0.00000E+00 7.50000E-01 5.00000E-04 0.00000E+00 1.00000E-03 1.00000E+02Card 306
 6.00000E-04 5.91133E-03 4.06000E-01 2.00000E-01 2.00000E-01 3.00000E-03        Card 307
 6.00000E-04 5.91133E-03 4.06000E-01 4.00000E-01 2.00000E-01 3.00000E-03        Card 307
 6.00000E-04 5.91133E-03 4.06000E-01 4.00000E-01 2.00000E-01 3.00000E-03        Card 307
 6.00000E-04 5.91133E-03 4.06000E-01 4.00000E-01 2.00000E-01 3.00000E-03        Card 307
 6.00000E-04 5.91133E-03 4.06000E-01 2.00000E-01 2.00000E-01 3.00000E-03        Card 307
 2.00000E-01 2.00000E-01 2.00000E-01 2.00000E-01                                Card 308
 9.00000E-01 9.50000E-01 1.05000E+00 1.10000E+00                                Card 309
 9.01000E-01 9.51000E-01 1.04900E+00 1.09900E+00                                Card 309
!-------------------------------------------------------------------------------
3.2109375E-1 4.00000E-02 1.00000E-011.4580078E+0 4.50000E+01 1.40000E+00        Card 500
.00000000000.00000000000                                                        Card 500
  10 1.00000E-04 2.50000E+01 0.00000E+00 1.00000E+00                            Card 600
  11                                                                            Card 700
 0.00000E+00 8.00000E-01                                                        Card 701
 1.00000E-01 8.80000E-01                                                        Card 701
 2.00000E-01 9.60000E-01                                                        Card 701
 3.00000E-01 1.04000E+00                                                        Card 701
 4.00000E-01 1.12000E+00                                                        Card 701
 5.00000E-01 1.20000E+00                                                        Card 701
 6.00000E-01 1.12000E+00                                                        Card 701
 7.00000E-01 1.04000E+00                                                        Card 701
 8.00000E-01 9.60000E-01                                                        Card 701
 9.00000E-01 8.80000E-01                                                        Card 701
 1.00000E+00 8.00000E-01                                                        Card 701
0
```

Figure 12.4 Comparison of Key Results for Test Problem 27 Obtained by PLTEMP/ANL V3.7 and V3.6

History Data for Test Problem 27 Calculated by
PLTEMP/ANL V3.7 Using Input File of Fig. 12.2

Pass No.	Power MW	Delta P MPa	Core Flow kg/s	Bypass kg/s	Total kg/s	ONBR Min	DNBR Min	Total m^3/hr	Total gpm	FIR Min	Max Clad Surf T(C)	Max Cool Temp(C)
1	1.45801	0.32109375	35.0000	0.0000	35.0000	5.000	23.799	127.11796	559.68352	9.162	74.489	58.035

History Data for Test Problem 27 Calculated by
PLTEMP/ANL V3.6 Using Converged Input File of Fig. 12.3

1	1.45801	0.32109375	35.0000	0.0000	35.0000	5.000	23.799	127.11796	559.68352

Figure 12.5 Input File for Test Problem 28 with Hot Channel Factors Option 2 That Uses Double Search Type 21

```
 Test Problem: 2 assemblies (of identical geometry) producing 1 MWt
! Each assembly has 4 fuel plates and 5 coolant channels
! H2O coolant, Flow is calculated from input pressure drop
! Uses Earl's hot channel factors, All Arnie's hot channel factors must be 1.0
! No bypass flow, NCTYP=0
! 10 axial heat transfer nodes in the heated length of fuel plates
!  1   2   3   4   5   6   7   8   9  10  11  12  13  14  15  16  17  18  19  20 #Card 0200
   0   0   0   1   0   1   1   1   0   0   0   0   0   0   2   0   1            Card(1)0200
 1.18       1.25        1.20                                                   Card(1)0201
  21 0.1          0.5          1 6.0                                           Card(1)0203
 0.2         3.0           1 1.2                                               Card(1)0204
   2   3 0.50       1.00        1.00        1.00           3                   Card(1)0300
! Using pressure driven mode
 1.05       1.06        1.07                                                   Card(1)0300A
   1  20 1.00                                                                  Card(1)0301
   1   1   1                                                                   Card(1)0302
1.20        1.20                                                               Card(2)0303
30.0E-04    0.02955665  0.15        8.00        0.20        15.0E-03           Card(3)0304
30.0E-04    0.02955665  0.75        0.00        0.20        15.0E-03           Card(3)0304
30.0E-04    0.02955665  0.15        8.00        0.20        15.0E-03           Card(3)0304
! Use the code's biult-in correlation for friction factor
0.00        0.00        0.00                                                   Card(1)0305
   5   3 0.00       0.75        0.50E-03    0.00        1.00E-03    100.00     Card(1)0306
6.00E-04    5.91133E-03 0.4060      0.20        0.20        3.00E-03           Card(5)0307
6.00E-04    5.91133E-03 0.4060      0.40        0.20        3.00E-03           Card(5)0307
6.00E-04    5.91133E-03 0.4060      0.40        0.20        3.00E-03           Card(5)0307
6.00E-04    5.91133E-03 0.4060      0.40        0.20        3.00E-03           Card(5)0307
6.00E-04    5.91133E-03 0.4060      0.20        0.20        3.00E-03           Card(5)0307
0.20        0.20        0.20        0.20                                       Card(1)0308
! Card 0308a not required
! Radial power peaking factor data by fuel plate for each assembly. Input flow data by
! channel for each assembly on Cards 0310 not required because WFGES(1) is non-zero
0.900       0.950       1.050       1.100                                      Card(2)0309
0.600       0.800       1.200       1.400                                      Card(2)0309
! DP0       DDP         DPMAX       POWER       TIN         PIN
0.10        0.04        0.10        1.00        45.0        1.40               Card(1)0500
                                                                               Card(2)0500
  50 0.0001     25.0        0.00        1.00                                   Card(1)0600
  11                                                                           Card(1)0700
0.00        0.80                                                               Card(11)0701
0.10        0.88                                                               Card(11)0701
0.20        0.96                                                               Card(11)0701
0.30        1.04                                                               Card(11)0701
0.40        1.12                                                               Card(11)0701
0.50        1.20                                                               Card(11)0701
0.60        1.12                                                               Card(11)0701
0.70        1.04                                                               Card(11)0701
0.80        0.96                                                               Card(11)0701
0.90        0.88                                                               Card(11)0701
1.00        0.80                                                               Card(11)0701
   0                                                                           Card(11)0702
```

Figure 12.6 Converged Input File for Test Problem 28 with Hot Channel Factors Option 2 Without the Search Option

```
 Test Problem: 2 assemblies (of identical geometry) producing 1 MWt            Card 100
   0   0   0   1   0   1   1   1   0   0   0   0   0   0   2   0   0   0   0   0Card 200
 1.18000E+00 1.25000E+00 1.20000E+00                                           Card 201
! 21 1.00000E-01 5.00000E-01   1 6.00000E+00
!2.00000E-01 3.00000E+00   1 1.20000E+00
   2   3 5.00000E-01 1.00000E+00 1.00000E+00 1.00000E+00   3   0 0.00000E+00    Card 300
 1.05000E+00 1.06000E+00 1.07000E+00                                           Card300A
   1  20 1.00000E+00                                                           Card 301
   1   1   1                                                                   Card 302
 1.20000E+00 1.20000E+00                                                       Card 303
 3.00000E-03 2.95567E-02 1.50000E-01 8.00000E+00 2.00000E-01 1.50000E-02        Card 304
 3.00000E-03 2.95567E-02 7.50000E-01 0.00000E+00 2.00000E-01 1.50000E-02        Card 304
 3.00000E-03 2.95567E-02 1.50000E-01 8.00000E+00 2.00000E-01 1.50000E-02        Card 304
 0.00000E+00 0.00000E+00 0.00000E+00 0.00000E+00                               Card 305
   5   3 0.00000E+00 7.50000E-01 5.00000E-04 0.00000E+00 1.00000E-03 1.00000E+02Card 306
 6.00000E-04 5.91133E-03 4.06000E-01 2.00000E-01 2.00000E-01 3.00000E-03        Card 307
 6.00000E-04 5.91133E-03 4.06000E-01 4.00000E-01 2.00000E-01 3.00000E-03        Card 307
 6.00000E-04 5.91133E-03 4.06000E-01 4.00000E-01 2.00000E-01 3.00000E-03        Card 307
 6.00000E-04 5.91133E-03 4.06000E-01 4.00000E-01 2.00000E-01 3.00000E-03        Card 307
 6.00000E-04 5.91133E-03 4.06000E-01 2.00000E-01 2.00000E-01 3.00000E-03        Card 307
 2.00000E-01 2.00000E-01 2.00000E-01 2.00000E-01                               Card 308
 9.00000E-01 9.50000E-01 1.05000E+00 1.10000E+00                               Card 309
 6.00000E-01 8.00000E-01 1.20000E+00 1.40000E+00                               Card 309
!-----------------------------------------------------------------------------
1.1537476E-1 4.00000E-02 1.00000E-019.5423889E-1 4.50000E+01 1.40000E+00        Card 500
.00000000000.00000000000                                                       Card 500
  17 1.00000E-04 2.50000E+01 0.00000E+00 1.00000E+00                           Card 600
  11                                                                           Card 700
 0.00000E+00 8.00000E-01                                                       Card 701
 1.00000E-01 8.80000E-01                                                       Card 701
 2.00000E-01 9.60000E-01                                                       Card 701
 3.00000E-01 1.04000E+00                                                       Card 701
 4.00000E-01 1.12000E+00                                                       Card 701
 5.00000E-01 1.20000E+00                                                       Card 701
 6.00000E-01 1.12000E+00                                                       Card 701
 7.00000E-01 1.04000E+00                                                       Card 701
 8.00000E-01 9.60000E-01                                                       Card 701
 9.00000E-01 8.80000E-01                                                       Card 701
 1.00000E+00 8.00000E-01                                                       Card 701
0
! end of input
```

Figure 12.7 Comparison of Key Results for Test Problem 28 Calculated by PLTEMP/ANL V3.7 and V3.6

Pass No.	Power MW	Delta P MPa	Core Flow kg/s	Bypass kg/s	Total kg/s	ONBR Min	DNBR Min	Total m^3/hr	Total gpm	FIR Min	Max Clad Surf T(C)	Max Cool Temp(C)
History Data for Test Problem 28 Calculated by PLTEMP/ANL V3.7 Using Input File of Fig. 12.5												
1	0.95424	0.11537476	7.5000	0.0000	7.5000	1.926	18.953	27.23946	119.93171	2.674	123.287	91.039
2*	1.12600	0.11537476	6.0000	0.0000	6.0000	1.200	12.934	21.79156	95.94537	1.721	170.848	116.556
With Only Global Hot Channel Factors						1.268	14.092			1.807		
History Data for Test Problem 28 Calculated by PLTEMP/ANL V3.6 Using Converged Input File of Fig. 12.6												
1	0.95424	0.11537476	7.5000	0.0000	7.5000	1.926	18.953	27.23946	119.93171			
2**	1.12600	0.11537476	6.0000	0.0000	6.0000	1.268	14.092	21.79156	95.94537			
With Global and Local Factors						1.200						

* With Global and Local Hot Channel Factors Applied
** With Only Global Hot Channel Factors Applied

Figure 12.8 Input File for Test Problem 29 Using Double Search Type 21 for 40 Target Values

```
 Test Problem: 2 assemblies (of identical geometry) producing 1 MWt
! Each assembly has 4 fuel plates and 5 coolant channels
! H2O coolant, Flow is calculated from input pressure drop
! Uses Earl's hot channel factors, All Arnie's hot channel factors must be 1.0
! No bypass flow, NCTYP=0
! 10 axial heat transfer nodes in the heated length of fuel plates
!  1   2   3   4   5   6   7   8   9  10  11  12  13  14  15  16  17  18  19  20 #Card 0200
   0   0   0   1   0   1   1   1   0   0   0   0   0   0   2   0   1            Card(1)0200
 1.18       1.25        1.20                                                   Card(1)0201
  21 0.1          0.5         10 6.0         6.5         7.0           7.5      Card(1)0203
 8.0          9.0        10.0        11.0        12.0        12.5               Card(1)0203
 0.2         3.0           4 1.2         1.5         2.0         2.5            Card(1)0204
   2   3 0.50       1.00        1.00        1.00           3                   Card(1)0300
! Using pressure driven mode
 1.05       1.06        1.07                                                   Card(1)0300A
   1  20 1.00                                                                  Card(1)0301
   1   1   1                                                                   Card(1)0302
1.20        1.20                                                               Card(2)0303
30.0E-04    0.02955665  0.15        8.00        0.20        15.0E-03           Card(3)0304
30.0E-04    0.02955665  0.75        0.00        0.20        15.0E-03           Card(3)0304
30.0E-04    0.02955665  0.15        8.00        0.20        15.0E-03           Card(3)0304
! Use the code's biult-in correlation for friction factor
0.00        0.00        0.00                                                   Card(1)0305
   5   3 0.00       0.75        0.50E-03    0.00        1.00E-03    100.00     Card(1)0306
6.00E-04    5.91133E-03 0.4060      0.20        0.20        3.00E-03           Card(5)0307
6.00E-04    5.91133E-03 0.4060      0.40        0.20        3.00E-03           Card(5)0307
6.00E-04    5.91133E-03 0.4060      0.40        0.20        3.00E-03           Card(5)0307
6.00E-04    5.91133E-03 0.4060      0.40        0.20        3.00E-03           Card(5)0307
6.00E-04    5.91133E-03 0.4060      0.20        0.20        3.00E-03           Card(5)0307
0.20        0.20        0.20        0.20                                       Card(1)0308
! Card 0308a not required
! Radial power peaking factor data by fuel plate for each assembly. Input flow data by
! channel for each assembly on Cards 0310 not required because WFGES(1) is non-zero
0.900       0.950       1.050       1.100                                      Card(2)0309
0.600       0.800       1.200       1.400                                      Card(2)0309
! DP0       DDP         DPMAX       POWER       TIN         PIN
0.10        0.04        0.10        1.00        45.0        1.40               Card(1)0500
                                                                               Card(2)0500
  50 0.0001     25.0        0.00        1.00                                   Card(1)0600
  11                                                                           Card(1)0700
0.00        0.80                                                               Card(11)0701
0.10        0.88                                                               Card(11)0701
0.20        0.96                                                               Card(11)0701
0.30        1.04                                                               Card(11)0701
0.40        1.12                                                               Card(11)0701
0.50        1.20                                                               Card(11)0701
0.60        1.12                                                               Card(11)0701
0.70        1.04                                                               Card(11)0701
0.80        0.96                                                               Card(11)0701
0.90        0.88                                                               Card(11)0701
1.00        0.80                                                               Card(11)0701
   0                                                                           Card(11)0702
```

Figure 12.9 History Data Printed by PLTEMP/ANL V3.7 for the Test Problem 29

====== BEGIN HISTORY RESULTS FOR ALL SEARCHES ======

I	Power MW	Delta P MPa	Core Flow kg/s	Bypass kg/s	Total kg/s	ONBR Min	DNBR Min	Total m^3/hr	Total gpm	FIR Min	Max Clad Surf T(C)	Max Cool Temp(C)
1	**0.95424**	0.11537476	**7.5000**	0.0000	7.5000	1.926	18.953	27.23946	119.93171	2.674	123.287	91.039
2	1.12600	0.11537476	6.0000	0.0000	6.0000	1.200	12.934	21.79156	95.94537	1.721	170.848	116.556
1	1.01809	0.13475037	8.1250	0.0000	8.1250	1.926	17.908	29.50959	129.92680	2.704	123.139	90.418
2	1.20135	0.13475037	6.5000	0.0000	6.5000	1.200	12.211	23.60767	103.94144	1.740	170.664	115.577
1	1.08051	0.15558472	8.7499	0.0000	8.7499	1.927	16.997	31.77929	139.91999	2.733	122.975	89.826
2	1.27500	0.15558472	7.0000	0.0000	7.0000	1.200	11.580	25.42343	111.93599	1.759	170.455	114.657
1	1.14156	0.17788086	9.3749	0.0000	9.3749	1.928	16.191	34.04927	149.91442	2.760	122.796	89.262
2	1.34705	0.17788086	7.5000	0.0000	7.5000	1.200	11.022	27.23942	119.93154	1.776	170.221	113.783
1	1.20127	0.20163574	10.0000	0.0000	10.0000	1.928	15.473	36.31941	159.90953	2.786	122.605	88.728
2	1.41750	0.20163574	8.0000	0.0000	8.0000	1.200	10.526	29.05553	127.92763	1.793	169.959	112.944
1	1.31616	0.25350342	11.2500	0.0000	11.2500	1.930	14.250	40.85949	179.89891	2.835	122.150	87.692
2	1.55307	0.25350342	9.0000	0.0000	9.0000	1.200	9.683	32.68759	143.91913	1.825	169.360	111.322
1	1.42617	0.31115723	12.5001	0.0000	12.5001	1.931	13.230	45.39956	199.88823	2.879	121.658	86.731
2	1.68289	0.31115723	10.0001	0.0000	10.0001	1.200	8.979	36.31965	159.91058	1.854	168.654	109.819
1	1.53079	0.37457275	13.7500	0.0000	13.7500	1.932	12.363	49.93915	219.87546	2.920	121.101	85.801
2	1.80633	0.37457275	11.0000	0.0000	11.0000	1.200	8.382	39.95132	175.90037	1.880	167.839	108.369
1	1.62986	0.44375000	15.0000	0.0000	15.0000	1.933	11.612	54.47921	239.86473	2.958	120.478	84.902
2	1.92324	0.44375000	12.0000	0.0000	12.0000	1.200	7.868	43.58337	191.89179	1.905	166.913	106.958
1	1.67690	0.48052979	15.6250	0.0000	15.6250	1.934	11.272	56.74902	249.85840	2.976	120.136	84.460
2	1.97875	0.48052979	12.5000	0.0000	12.5000	1.200	7.637	45.39922	199.88672	1.917	166.403	106.265
1	0.72682	0.11635742	7.5000	0.0000	7.5000	2.430	25.528	27.23974	119.93295	3.498	106.885	80.196
2	0.85764	0.11635742	6.0000	0.0000	6.0000	1.500	18.555	21.79179	95.94636	2.248	145.405	99.751
1	0.77537	0.13587036	8.1250	0.0000	8.1250	2.431	24.107	29.50968	129.92719	3.537	106.761	79.718
2	0.91494	0.13587036	6.5000	0.0000	6.5000	1.500	17.494	23.60774	103.94176	2.275	145.245	98.990
1	0.82284	0.15685425	8.7500	0.0000	8.7500	2.432	22.869	31.77954	139.92111	3.576	106.622	79.259
2	0.97095	0.15685425	7.0000	0.0000	7.0000	1.500	16.568	25.42363	111.93689	2.299	145.068	98.278
1	0.86929	0.17930298	9.3750	0.0000	9.3750	2.433	21.775	34.04949	149.91538	3.612	106.472	78.822
2	1.02576	0.17930298	7.5000	0.0000	7.5000	1.500	15.751	27.23959	119.93230	2.322	144.867	97.601
1	0.91470	0.20321655	10.0000	0.0000	10.0000	2.434	20.800	36.31951	159.90996	3.646	106.315	78.410
2	1.07934	0.20321655	8.0000	0.0000	8.0000	1.500	15.023	29.05560	127.92797	2.344	144.648	96.954
1	1.00245	0.25541992	11.2501	0.0000	11.2501	2.435	19.132	40.85967	179.89971	3.709	105.959	77.627
2	1.18290	0.25541992	9.0001	0.0000	9.0001	1.500	13.781	32.68774	143.91976	2.386	144.145	95.719
1	1.08615	0.31342773	12.5000	0.0000	12.5000	2.437	17.748	45.39935	199.88733	3.767	105.552	76.885
2	1.28166	0.31342773	10.0000	0.0000	10.0000	1.500	12.752	36.31948	159.90986	2.424	143.559	94.554
1	1.16569	0.37723389	13.7501	0.0000	13.7501	2.438	16.573	49.93941	219.87660	3.820	105.095	76.175
2	1.37552	0.37723389	11.0000	0.0000	11.0000	1.500	11.882	39.95153	175.90128	2.459	142.885	93.442
1	1.24103	0.44680176	14.9999	0.0000	14.9999	2.440	15.554	54.47894	239.86356	3.870	104.585	75.486
2	1.46441	0.44680176	12.0000	0.0000	12.0000	1.500	11.135	43.58315	191.89085	2.491	142.123	92.358
1	1.27702	0.48375244	15.6250	0.0000	15.6250	2.440	15.093	56.74909	249.85871	3.894	104.306	75.142
2	1.50689	0.48375244	12.5000	0.0000	12.5000	1.500	10.795	45.39927	199.88697	2.507	141.704	91.822
1	0.51669	0.11736755	7.5000	0.0000	7.5000	3.282	36.731	27.23963	119.93249	4.903	90.691	70.102
2	0.60970	0.11736755	6.0000	0.0000	6.0000	2.000	27.647	21.79171	95.94599	3.149	120.082	84.082
1	0.55119	0.13702087	8.1250	0.0000	8.1250	3.284	34.672	29.50950	129.92642	4.960	90.593	69.756
2	0.65041	0.13702087	6.5000	0.0000	6.5000	2.000	26.059	23.60760	103.94114	3.187	119.953	83.534

Figure 12.9 Continued

```
    1    0.58466  0.15815430    8.7500      0.0000     8.7500     3.286    32.892    31.77937   139.92033     5.017   90.467     69.415
    2    0.68990  0.15815430    7.0000      0.0000     7.0000     2.000    24.673    25.42349   111.93626     3.223  119.809     83.004
    1    0.61765  0.18076172    9.3750      0.0000     9.3750     3.287    31.303    34.04947   149.91531     5.067   90.351     69.102
    2    0.72883  0.18076172    7.5000      0.0000     7.5000     2.000    23.447    27.23958   119.93225     3.256  119.651     82.514
    1    0.64988  0.20483398   10.0000      0.0000    10.0000     3.289    29.891    36.31937   159.90935     5.116   90.225     68.804
    2    0.76686  0.20483398    8.0000      0.0000     8.0000     2.000    22.356    29.05549   127.92748     3.287  119.478     82.050
    1    0.71223  0.25737305   11.2500      0.0000    11.2500     3.291    27.472    40.85924   179.89779     5.204   89.953     68.246
    2    0.84043  0.25737305    9.0000      0.0000     9.0000     2.000    20.487    32.68739   143.91823     3.345  119.083     81.166
    1    0.77166  0.31574707   12.5000      0.0000    12.5000     3.293    25.465    45.39913   199.88633     5.284   89.643     67.723
    2    0.91055  0.31574707   10.0000      0.0000    10.0000     2.000    18.938    36.31930   159.90906     3.398  118.625     80.335
    1    0.82818  0.37993164   13.7500      0.0000    13.7500     3.295    23.761    49.93917   219.87554     5.359   89.294     67.214
    2    0.97725  0.37993164   11.0000      0.0000    11.0000     2.000    17.622    39.95134   175.90043     3.447  118.103     79.542
    1    0.88167  0.44990234   14.9999      0.0000    14.9999     3.297    22.286    54.47890   239.86336     5.427   88.905     66.728
    2    1.04037  0.44990234   11.9999      0.0000    11.9999     2.000    16.484    43.58312   191.89069     3.492  117.512     78.770
    1    0.90732  0.48706055   15.6250      0.0000    15.6250     3.298    21.615    56.74903   249.85847     5.459   88.696     66.490
    2    1.07063  0.48706055   12.5000      0.0000    12.5000     2.000    15.968    45.39923   199.88677     3.514  117.189     78.385
    1    0.39934  0.11798706    7.5001      0.0000     7.5001     4.142    48.102    27.23975   119.93302     6.333   81.145     64.434
    2    0.47122  0.11798706    6.0000      0.0000     6.0000     2.500    36.478    21.79180    95.94642     4.066  104.950     75.268
    1    0.42600  0.13772583    8.1250      0.0000     8.1250     4.144    45.395    29.50961   129.92691     6.406   81.063     64.166
    2    0.50268  0.13772583    6.5000      0.0000     6.5000     2.500    34.367    23.60769   103.94153     4.114  104.843     74.846
    1    0.45208  0.15894775    8.7500      0.0000     8.7500     4.145    43.031    31.77942   139.92058     6.476   80.976     63.911
    2    0.53345  0.15894775    7.0000      0.0000     7.0000     2.500    32.525    25.42354   111.93646     4.159  104.723     74.444
    1    0.47758  0.18165283    9.3751      0.0000     9.3751     4.147    40.943    34.04980   149.91673     6.538   80.883     63.678
    2    0.56355  0.18165283    7.5001      0.0000     7.5001     2.500    30.897    27.23984   119.93338     4.202  104.592     74.065
    1    0.50252  0.20581665   10.0000      0.0000    10.0000     4.148    39.085    36.31928   159.90896     6.602   80.783     63.444
    2    0.59298  0.20581665    8.0000      0.0000     8.0000     2.500    29.447    29.05542   127.92717     4.241  104.449     73.707
    1    0.55073  0.25855713   11.2499      0.0000    11.2499     4.151    35.905    40.85899   179.89669     6.715   80.561     63.012
    2    0.64986  0.25855713    8.9999      0.0000     8.9999     2.500    26.966    32.68719   143.91735     4.316  104.125     73.024
    1    0.59673  0.31715088   12.5000      0.0000    12.5000     4.153    33.267    45.39928   199.88702     6.819   80.313     62.605
    2    0.70414  0.31715088   10.0000      0.0000    10.0000     2.500    24.909    36.31943   159.90962     4.384  103.750     72.379
    1    0.64048  0.38156738   13.7500      0.0000    13.7500     4.155    31.029    49.93939   219.87651     6.913   80.034     62.218
    2    0.75577  0.38156738   11.0000      0.0000    11.0000     2.500    23.164    39.95151   175.90121     4.447  103.322     71.762
    1    0.68192  0.45178223   15.0001      0.0000    15.0001     4.158    29.087    54.47965   239.86667     6.998   79.724     61.846
    2    0.80467  0.45178223   12.0001      0.0000    12.0001     2.500    21.654    43.58372   191.89334     4.505  102.841     71.167
    1    0.70174  0.48905029   15.6250      0.0000    15.6250     4.158    28.207    56.74904   249.85849     7.039   79.558     61.660
    2    0.82805  0.48905029   12.5000      0.0000    12.5000     2.500    20.970    45.39923   199.88680     4.533  102.578     70.872
======= END OF HISTORY RESULTS FOR SEARCHES =======
Total Elapsed Time =   9351.06 sec
```

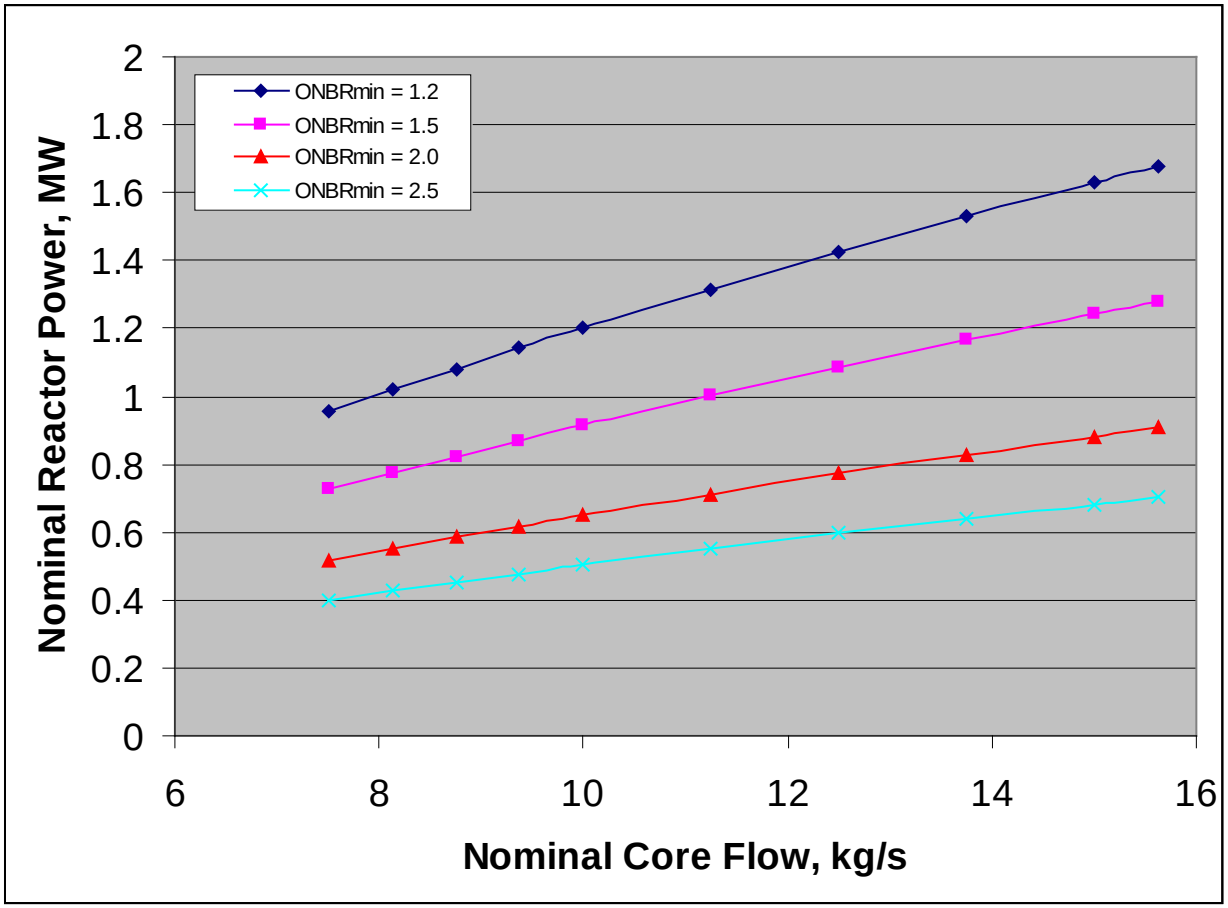

Figure 12.10 Reactor Operation Diagram Showing the Relationship among Nominal Reactor Power, Nominal Core Flow, and the Minimum ONBR with Global and Local Hot Channel Factors

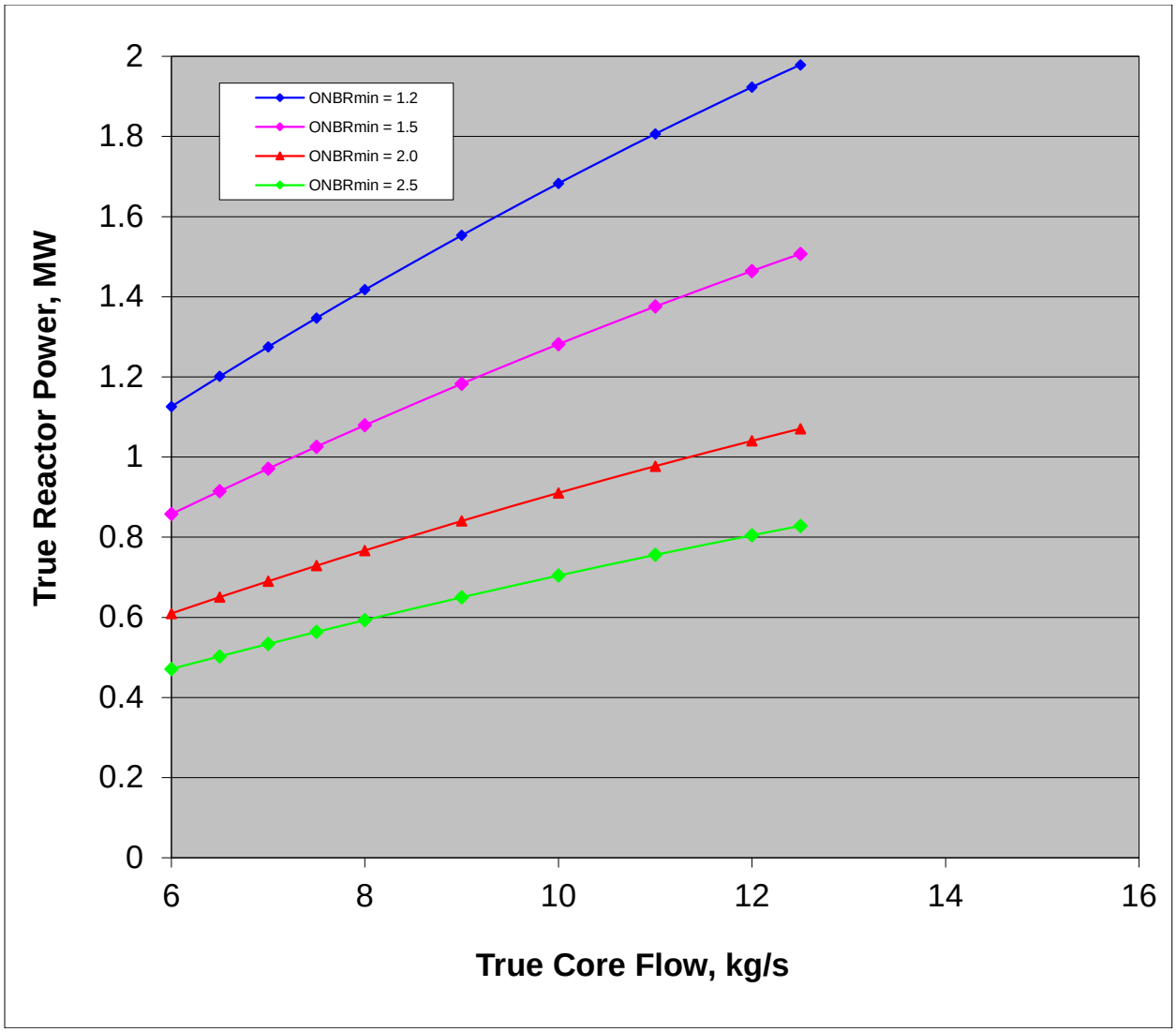

Figure 12.11 Reactor Operation Diagram Showing the Relationship among True Reactor Power, True Core Flow, and the Minimum ONBR with Global and Local Hot Channel Factors Applied

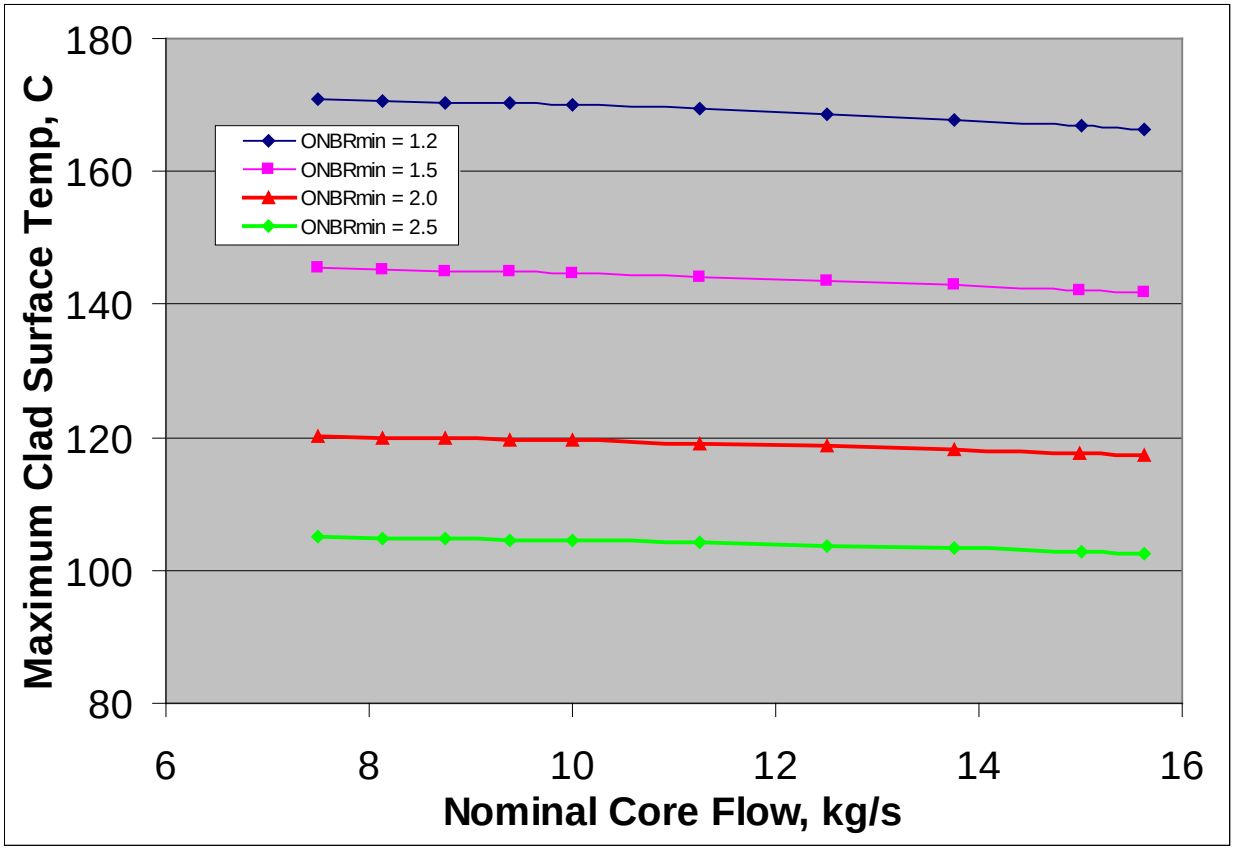

Figure 12.12 Reactor Operation Diagram Showing the Relationship among Nominal Core Flow, Maximum Cladding Surface Temperature, and the Minimum ONBR with Global and Local Hot Channel Factors Applied

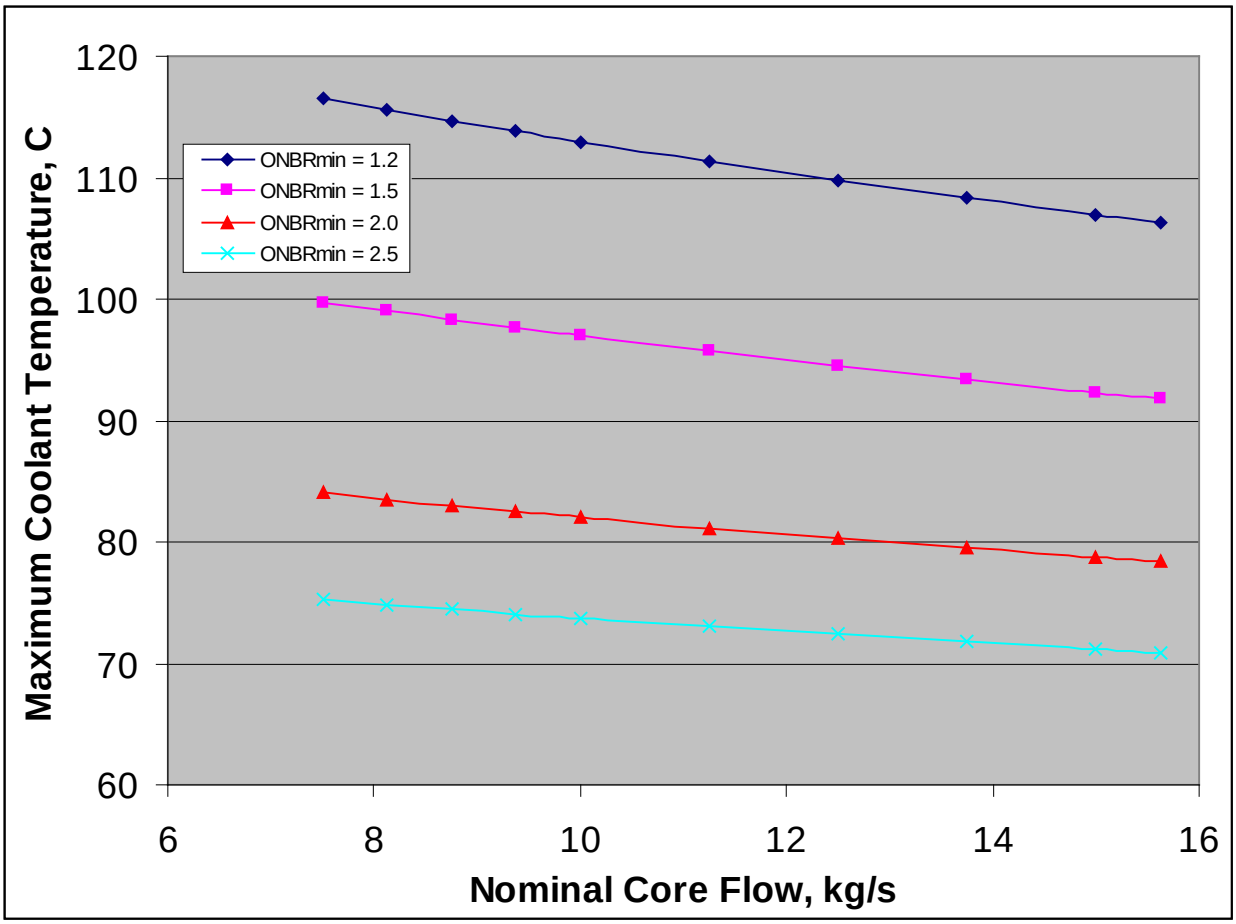

Figure 12.13 Reactor Operation Diagram Showing the Relationship among Nominal Core Flow, Maximum Coolant Temperature, and the Minimum ONBR with Global and Local Hot Channel Factors Applied

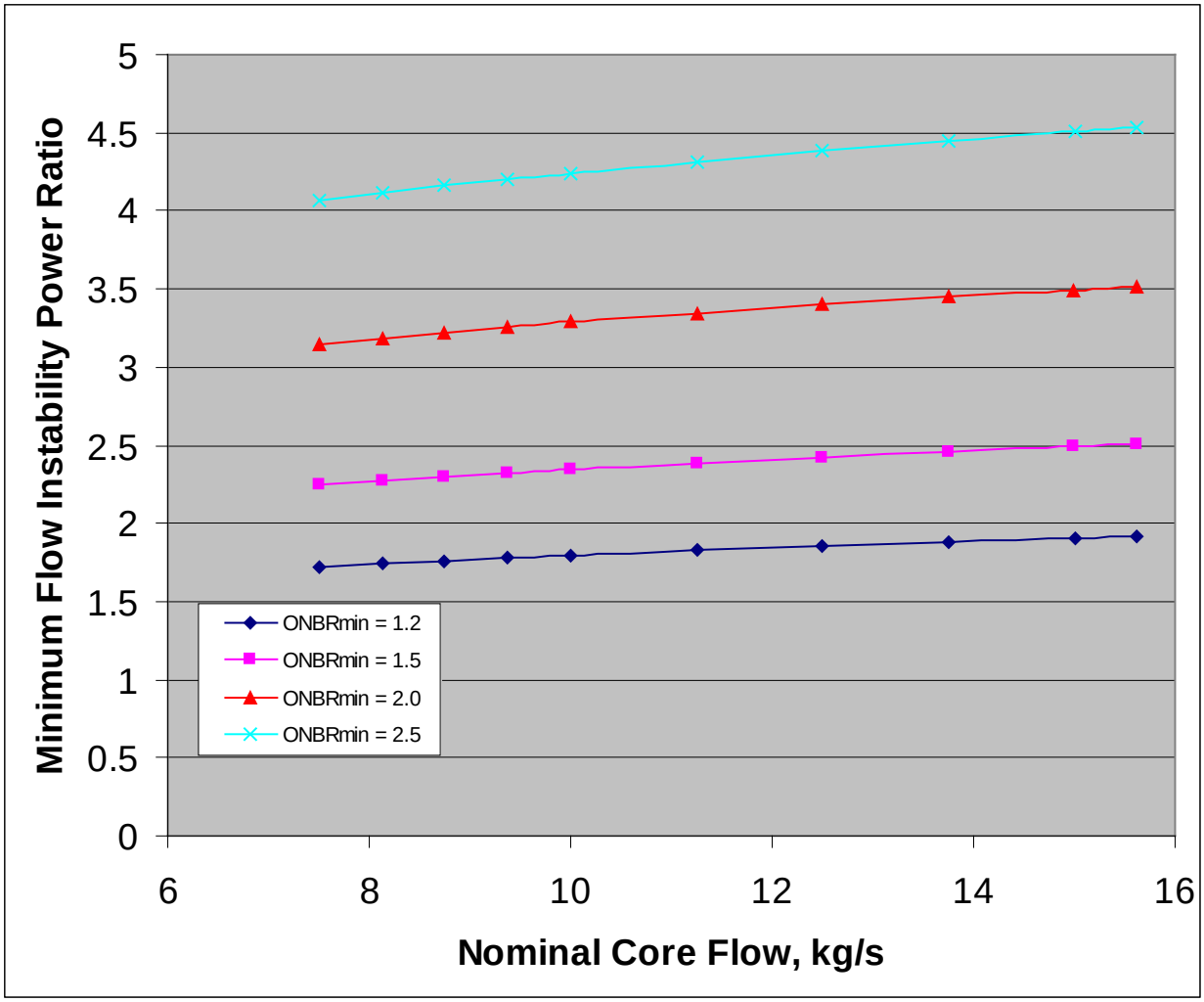

Figure 12.14 Reactor Operation Diagram Showing the Relationship among Nominal Core Flow, Minimum Flow Instability Power Ratio, and the Minimum ONBR with Global and Local Hot Channel Factors Applied

Table 12.1 List of Searches Implemented in PLTEMP/ANL V3.7

NSRCH, Search Type	Input Datum Being Adjusted	Output Quantity Whose Target Value is Searched	Comments
Single Searches			
1	Pressure Drop	Total flow through all fuel assemblies, WT	
2	Pressure Drop	Onset of nucleate boiling ratio, $ONBR_{min}$	Desired $ONBR_{min} \geq 1$
3	Pressure Drop	Minimum ratio of critical heat flux to reactor heat flux, $DNBR_{min}$	Desired $DNBR_{min} \geq 1$
4	Reactor Power	$ONBR_{min}$	
5	Reactor Power	$DNBR_{min}$	
6	Pressure Drop	Minimum flow instability power ratio FIR_{min}	Desired $FIR_{min} \geq 1.15$
7	Reactor Power	Minimum flow instability power ratio FIR_{min}	
8	Pressure Drop	Maximum cladding surface temperature $T_{cs,max}$	
9	Pressure Drop	Maximum coolant temperature $T_{ex,max}$	
10	Reactor Power	$T_{cs,max}$	
11	Reactor Power	$T_{ex,max}$	
Double Searches			
21	First Pressure Drop, Then Reactor Power	Total flow WT $ONBR_{min}$	Multiple values of each target may be be input in a run.
22	First Pressure Drop, Then Reactor Power	Total flow WT $DNBR_{min}$	
23	First Pressure Drop, Then Reactor Power	Total flow WT FIR_{min}	
24	First Pressure Drop, Then Reactor Power	Total flow WT Maximum cladding surface temperature $T_{cs,max}$	
25	First Pressure Drop, Then Reactor Power	Total flow WT Maximum coolant temperature $T_{ex,max}$	

13 Verification and Validation of the Sudo-Kaminaga CHF Correlation for Rectangular Channels as Implemented in the PLTEMP/ANL Code

13.1 Introduction

The verification and validation work reported here was done in May 2010. A thermal-hydraulic safety criterion commonly checked for in research reactors is a required minimum critical heat flux ratio (CHFR). Sudo and Kaminaga studied CHF experimentally and theoretically for more than a decade in the course of designing the Japanese research reactors JRR-3 and JRR-4. They proposed a correlation [1, 2] for CHF in rectangular coolant channels of research reactors using plate-type fuel, based on 596 CHF data points from 8 sources [3-10], including their own data [3, 4]. Sudo and Kaminaga included the CHF test data of Mishima [9], and their correlation used and improved upon CHF equations suggested by Mishima [11]. Most of the CHF data (586 out of the 596 data points) were measured at pressures in the range of 1 to 7.2 bars. Only 10 data points from one data source [8] were measured at pressures in the range of 11 to 40 bars, and these data points are not considered adequate to extend the pressure range of applicability of the correlation up to 40 bars. Therefore, the correlation is expected to cover the pressure range of 1 to 7.2 bars. Additional restrictions on the correlation are noted below in Section 13.2 based on the test ranges of other thermodynamic and geometrical variables. Although the correlation covers a mass velocity range of 25800 kg/m^2-s downflow to 6250 kg/m^2-s upflow of water, it specially focuses on CHF at low mass velocities ($G \leq 600$ kg/m^2-s, i.e., natural circulation flow) at near-atmospheric pressure. The correlation was recently implemented in the PLTEMP/ANL code [12] for steady-state thermal-hydraulic analysis of research reactors.

The purpose of this chapter is to document a validation of this CHF correlation as implemented in PLTEMP/ANL, by comparing the code with some experimental CHF data obtained by Sudo and Kaminaga [1], and by Mirshak, Durant, and Towell [7]. At the end, two parametric studies of the correlation are given to illustrate: (i) the effect of varying channel thickness on the CHF calculated by the correlation, and (ii) the effect of varying coolant mass velocity on the CHF calculated by the correlation.

13.2 Sudo-Kaminaga CHF Correlation

To calculate CHF in channels of rectangular cross section, Sudo and Kaminaga [1, 2] improved on Mishima's CHF work [11] at low mass velocities (i.e. $G \leq 600$ kg/m^2-s) and suggested a correlation for downflow and upflow over three mass velocity ranges (low, medium, and high) as shown in Fig. 13.1. The low mass velocity range is from 0.0 to G_3 kg/m^2-s for upflow (or 0.0 to G_2 kg/m^2-s for downflow). The medium mass velocity range is from G_3 to G_1 kg/m^2-s for upflow (or G_2 to G_1 kg/m^2-s for downflow). The high mass velocity range is above G_1 kg/m^2-s for both upflow and downflow. The Sudo-Kaminaga correlation[1] can be written as Eqs. (13.1) to (13.5):

$$q_c = \begin{cases} \mathrm{Max}(q_{c3}\,,\, q_{c2}) & \text{for } G < G_1 \quad \text{and} \quad \text{downflow} \\ \mathrm{Max}\left[q_{c3}\,,\, 5\,\mathrm{x}\,10^{-6}\; G^{*\;0.611}\; \lambda \left\{\sigma\, \rho_v^{\;2} (\rho_l - \rho_v)\, g\right\}^{0.25}\right] & \text{for } G < G_1 \quad \text{and} \quad \text{upflow} \\ \mathrm{Min}(q_{c1}\,,\, q_{c2}) & \text{for } G \geq G_1\,, \text{ upflow or downflow} \end{cases} \tag{13.1}$$

$$q_{c1} = 5\,\mathrm{x}\,10^{-6}\; G^{*\;0.611}\; \left\{1 + 5000\; \Delta h_o/(\lambda\, G^*)\right\} \lambda \left\{\sigma\, \rho_v^{\;2} (\rho_l - \rho_v)\, g\right\}^{0.25} \tag{13.2}$$

$$q_{c2} = 0.001\, A_f\ \Delta h_i\ G / A_h \tag{13.3}$$

$$q_{c3} = \frac{0.7\,x10^{-3}\, A_f\ \lambda \left\{ g \rho_v (\rho_l - \rho_v)\, w \right\}^{0.5}}{A_h \left\{ 1 + (\rho_v/\rho_l)^{0.25} \right\}^2} \left(1 + 3\,\Delta h_i/\lambda \right) \tag{13.4}$$

$$G_1 = \left(\frac{0.005\, A_h\ \lambda}{A_f\, \Delta h_i} \right)^{2.5707} \left\{ \sigma \rho_v{}^2 (\rho_l - \rho_v)\, g \right\}^{0.25} \tag{13.5}$$

where

A_f = Flow area, m^2
A_h = $P_h\ L_h$ = Heated area, m^2
G = Mass velocity, kg/m^2-s
G^* = $G \Big/ \left\{ \sigma \rho_v^2 (\rho_l - \rho_v)\, g \right\}^{0.25}$ = Dimensionless mass velocity corresponding to G
G_1 = Mass velocity at which Eq. (13.2) with Δh_o set to zero intersects Eq. (13.3), kg/m^2-s
G_2 = Mass velocity at which Eq. (13.3) intersects Eq. (13.4), kg/m^2-s
G_3 = Mass velocity at which Eq. (13.2) with Δh_o set to zero intersects Eq. (13.4), kg/m^2-s
G_1^* = $G_1 \Big/ \left\{ \sigma \rho_v^2 (\rho_l - \rho_v)\, g \right\}^{0.25}$ = Dimensionless mass velocity corresponding to G_1
G_2^* = $G_2 \Big/ \left\{ \sigma \rho_v^2 (\rho_l - \rho_v)\, g \right\}^{0.25}$ = Dimensionless mass velocity corresponding to G_2
G_3^* = $G_3 \Big/ \left\{ \sigma \rho_v^2 (\rho_l - \rho_v)\, g \right\}^{0.25}$ = Dimensionless mass velocity corresponding to G_3
g = Acceleration due to gravity = 9.80665 m/s^2
Δh_i = Coolant subcooling at inlet, kJ/kg
Δh_o = Coolant subcooling at outlet, kJ/kg
L_h = Heated Length, m
P_h = Heated perimeter of the channel, m
q_c = Critical heat flux obtained by the correlation, MW/m^2
q_{c1} = Critical heat flux obtained from Eq. (13.2), MW/m^2
q_{c2} = Critical heat flux obtained from Eq. (13.3), MW/m^2
q_{c3} = Critical heat flux obtained from Eq. (13.4), MW/m^2
w = Width (larger dimension) of the channel rectangular cross section, m
λ = Latent heat of vaporization at the system (exit) pressure, kJ/kg
ρ_l = Saturated liquid density at the system (exit) pressure, kg/m^3
ρ_v = Saturated vapor density at the system (exit) pressure, kg/m^3
σ = Surface tension of saturated coolant at the system (exit) pressure, N/m
2.5707 = Exponent in Eq. (13.8) which is related to the exponent 0.611 of Eq. (13.4) = 1/(1-0.611)

The mass velocities at region boundaries, G_3, G_2, and G_1, are determined by the intersection of an appropriate pair from Eqs. (13.2), (13.3), and (13.4). The boundary of the high mass velocity region, G_1, is given by Eq. (13.5). As shown in Fig. 13.1, the CHF in downward flow is given by Eq. (13.4) if the mass velocity $G \le G_2$; it is given by Eq. (13.3) if $G_2 \le G \le G_1$; it is given by the smaller of Eqs. (13.2) and (13.3) for $G \ge G_1$. The CHF in upward flow is given by Eq. (13.4) if the mass velocity $G \le G_3$; it is given by Eq. (13.2) with Δh_o set to zero [i.e., the quantity inside the

first pair of curly brackets of Eq. (13.2) set to 1] if $G_3 \leq G \leq G_1$; it is given by the smaller of Eqs. (13.2) and (13.3) for $G \geq G_1$. It is noted that the CHF in downward flow is smaller than that in upward flow in the mass velocity range $G_3 \leq G \leq G_1$, and outside this range the CHFs in downward flow and upward flow are equal. The correlation was tested with 596 CHF data for water from 8 sources covering the following geometrical and thermal-hydraulic conditions:

Channel gap: 2.25 to 5.0 mm
Ratio of heated length to hydraulic diameter: 8 to 240
Mass velocity: Downflow of 25,800 to stagnant flow to upflow of 6250 kg/m^2-s
System pressure: 0.1 to 0.72 MPa
Inlet subcooling: 1 to 213 °C
Outlet condition: From subcooling of 0 to 74 °C to quality of 0 to 1.0

By comparing with the 596 CHF data, Sudo and Kaminaga[2] found a root-mean-square (RMS) error of ±33 %, and recommended that when the CHF correlation is used in thermal-hydraulic analysis of reactors, the minimum critical heat flux ratio (CHFR) should be greater than 1.5 (which is equivalent to an error of -33 %, i.e., 1/(1 - 0.33) = 1.5). Based on a statistical analysis, Sudo and Kaminaga[1] also reported that the error in the correlation means that there is a 10% possibility of the occurrence of CHF condition even when the minimum CHFR is 1.5. This correlation was recently implemented in the PLTEMP/ANL version 3.9 code [12] which is used for thermal-hydraulic analysis and design of research reactors.

13.3 Validation of the Sudo-Kaminaga CHF Correlation Implemented in PLTEMP/ANL

13.3.1 Validation at Lower Coolant Velocities

To validate the implementation of the Sudo-Kaminaga CHF correlation in PLTEMP/ANL at coolant velocities less than 1.0 m/s, the code was compared with some of the CHF data measured and reported by Sudo and Kaminaga [4] in graphical form (in Fig. 13.3 of [4]). The geometry of the test section used in these measurements is shown in Fig. 13.2, and the test conditions are given in Table 13.1. Briefly, Sudo and Kaminaga used a single rectangular coolant channel of 2.25 mm thickness, heated on both sides by plates 750 mm long. Each plate had a wetted perimeter of 50 mm with a heated perimeter of 40 mm. The test section was modeled by PLTEMP/ANL, and the input data used is shown in Fig. 13.3. The code requires the number of channels to be one greater than the number of fuel plates. Therefore, the input data file of Fig. 13.3 assumes 2 plates and 3 coolant channels that are part of an infinite array of identical coolant channels and plates, as shown in Fig. 13.2. The first and third channels are artificially added half-channels, i.e., of half thickness compared to the actual channel 2 used in the test. The outer boundaries of the first and third channels in the *modeled* test section are lines of symmetry which are adiabatic due to symmetry. The flow in each channel is input to the code. The flow in a half-channel is half of the flow in channel 2 (the actual channel). This makes the temperature distributions in all three channels identical.

The measured CHF data were scaled from Fig. (1-3) of Reference 4, and are shown in Tables 13.2 and 13.3 for upflow and downflow respectively. For each CHF data, the code was run in the search mode to adjust the power to achieve a CHFR of 1.0. For some of the CHF data, the code ran past

boiling but these calculations were not acceptable because PLTEMP/ANL is a single-phase code that does not model two-phase flow. In these cases, the code was run several times for the same measured CHF data, using increasing values (greater than 1.0) of the CHFR. It was found that the critical heat flux did not change much from run to run. The practically unchanging CHF values are also included in the comparison. The PLTEMP/ANL-calculated CHF values are compared with the measured data in Tables 13.2 and 13.3. The calculated CHF values are found to be in the scatter range of the measured data. This provides a verification of the implementation of the Sudo-Kaminaga correlation in PLTEMP/ANL at coolant velocities less than 1.0 m/s.

13.3.2 Verification at Higher Coolant Velocities

To verify the Sudo-Kaminaga CHF correlation implemented in PLTEMP/ANL at coolant velocities greater than 1.0 m/s, the code was compared with 11 of the CHF data measured and reported by Mirshak, Durant, and Towell [7]. The test section geometry and test conditions in these measurements are given in Table 13.4. In these tests, Mirshak, Durant, and Towell used a single rectangular coolant channel of different thicknesses (3.18 to 6.48 mm), heated on only one side by a Type 304 stainless steel plate which was 2.06 inches (52.32 mm) wide and 19.25 inches (0.48895 m) long. The width of the coolant channel was 2.56 inches (65.02 mm). Some of the required input data were calculated from the reported quantities, using the equations given in Note 1 below Table 13.4. The calculated input data are shown in Table 13.4. The PLTEMP/ANL input data files prepared for the 11 tests are given in Appendix J. The code requires the number of channels to be one greater than the number of fuel plates. Therefore, the input data files of Appendix J assume one plate and two identical coolant channels. The outer boundary of each channel in the *modeled* test section is adiabatic. The power of the plate in this model is two times the actual power used in the test. The flow in each channel, equal to the actual flow used in the test, is input to the code. The temperature distributions in both channels are identical.

The measured values of CHF reported in Reference 7 are included in Tables 13.4 and 13.5. For each CHF test, the code was run twice, first using the Mirshak CHF correlation (ICHF = 0) and then using the Sudo-Kaminaga CHF correlation (ICHF = 8). The PLTEMP/ANL-calculated CHF values are compared with the measured data in Table 13.5. For the 11 tests analyzed, the errors in the CHF obtained using the Sudo-Kaminaga correlation (compared to the measured CHF) vary from -11.4 to 21.6 %, with an RMS error of 10.8%. This RMS error can be assessed in two ways:

(i) By comparing it with the RMS error of 6.7% in the CHF obtained using the Mirshak correlation. The errors in the CHF obtained using the Mirshak correlation (compared to the measured CHF) vary from -13.2 to 9.0 % as shown in Table 13.5.
(ii) By comparing it with the reported RMS error of 33 % in the Sudo-Kaminaga correlation [1,2].

The RMS error in the CHF values obtained using the Sudo-Kaminaga correlation is less than the reported RMS error of 33 % in the Sudo-Kaminaga correlation. This provides a validation of the Sudo-Kaminaga correlation as implemented in PLTEMP/ANL at coolant velocities used in the 11 tests, which are greater than 1.0 m/s.

13.4 Parametric Studies of Sudo-Kaminaga CHF Correlation

Two parametric studies were done using the Microsoft Spreadsheet shown in Fig. 13.4. These studies are presented in this section. First, the effect of varying channel thickness on the CHF calculated using the Sudo-Kaminaga correlation is presented to show that the correlation is sensitive to channel thickness and that it should not be used for channel thicknesses less than 2.25 mm as specified by Sudo and Kaminaga [1, 2]. Second, the effect of varying coolant mass velocity on the CHF calculated using the correlation is presented to illustrate how the correlation is a continuous function of mass velocity over the three regions of mass velocity (low, medium, and high) shown in Fig. 13.1. Both parametric studies were done using a half-channel model of a test section similar to those used in the 1964 Advanced Test Reactor (ATR) burnout heat transfer tests done by Croft [13]. The basic geometrical and thermal hydraulic quantities of the test section used in the Spreadsheet of Fig. 13.4 are:

Channel width	= 30.48 mm,	Channel length	= 1.2192 m (48 inches)
Heated width of plate	= 25.4 mm,	Channel thickness	= varies from 1.37 to 5.0 mm
Outlet pressure	= 15.6 bar,	Mass velocity	= varies from 5.0 to 20000.0 kg/m^2-s
Inlet temperature	= 54.4 °C,	Outlet temperature	= 188.3 °C

This outlet temperature corresponds to a flow instability power ratio (FIR) of 1.0.

13.4.1 Sensitivity of Sudo-Kaminaga CHF Correlation to Coolant Channel Thickness

The effect on CHF of varying the channel thickness from 1.37 to 5.0 mm was studied at a fixed coolant mass velocity of 10141.5 kg/m^2-s, and the results are shown in Table 13.6. The Sudo-Kaminaga CHF correlation is valid only for channel thicknesses in the range 2.25 to 5.00 mm, as noted in Section 13.2. Table 13.6 shows that the value of boundary mass velocity G_1 is very sensitive to the channel thickness. It rises very steeply from 10485.0 to 37424.0 kg/m^2-s as the channel thickness decreases from 2.25 to 1.37 mm, i.e., over the invalid range of channel thickness. The values of CHF shown in Table 13.6 over this range should not be used in reactor analysis.

13.4.2 Continuity of Sudo-Kaminaga CHF Correlation as a Function of Mass Velocity

The effect on CHF of varying the coolant mass velocity from 5.0 to 20000.0 kg/m^2-s was studied at a fixed channel thickness of 3.5 mm (the valid range is 2.25 to 5.0 mm), and the results are shown in Tables 13.7 and 13.8, for upflow and downflow respectively. The Sudo-Kaminaga CHF correlation is valid for both downflow and upflow (from a downflow of 25,800 to an upflow of 6250 kg/m^2-s), as noted in Section 13.2. Tables 13.7 and 13.8 show (i) the calculated values of the boundary mass velocities G_3, G_2, and G_1 in columns 2 to 4, and (ii) the results of Eqs. (13.1) to (13.4) in columns 5 to 9. The boundary mass velocities G_3, G_2, and G_1 do not depend on the mass velocity G at which the value of CHF is being calculated. The boundary mass velocities G_3, G_2, and G_1 are found to be 12.96, 112.7, and 3367.3 kg/m^2-s.

Table 13.7 shows in column 9 the CHF *for upflow* found from Eq. (13.1), using the heat fluxes found from Eqs. (13.2) to (13.4) and shown in columns 5 to 8. In upflow, according to Eq. (13.1), the CHF for mass velocities up to 12.96 kg/m^2-s is shaded in yellow in column 8; the CHF for mass velocities from 12.96 to 3367.3 kg/m^2-s is shaded in yellow in column 6; and the CHF for mass velocities above 3367.3 kg/m^2-s is given by the smaller of columns 5 and 7 that is shaded in

yellow. The columns 5 and 7 intersect at a mass velocity of 6068.5 kg/m^2-s. All the yellow-shaded values of CHF for upflow are collected in column 9 for mass velocities from 5.0 to 20000.0 kg/m^2-s. It is obvious that the values of CHF given in column 9 for upflow are continuous, i.e., there is not any jump in CHF at any mass velocity.

Table 13.8 shows in column 9 the CHF *for downflow* found from Eq. (13.1), using the heat fluxes found from Eqs. (13.2) to (13.4) and shown in columns 5 to 8 (same as Table 13.7). In downflow, according to Eq. (13.1), the CHF for mass velocities up to 112.7 kg/m^2-s is shaded in yellow in column 8; the CHF for mass velocities from 112.7 to 3367.3 kg/m^2-s is shaded in yellow in column 7; and the CHF for mass velocities above 3367.3 kg/m^2-s is given by the smaller of columns 5 and 7 that is shaded in yellow. All the yellow-shaded values of CHF for downflow are collected in column 9 for mass velocities from 5.0 to 20000.0 kg/m^2-s. It is obvious that the values of CHF given in column 9 for downflow are continuous, i.e., there is not any jump in CHF at any mass velocity.

13.5 Conclusions

The Sudo-Kaminaga CHF correlation has a root-mean-square (RMS) error of ±33 %. Sudo and Kaminaga recommend that when the correlation is used in thermal-hydraulic analysis of reactors, the minimum critical heat flux ratio (CHFR) should be greater than 1.5. The correlation was recently implemented in the PLTEMP/ANL code. To validate this implementation, the CHF values calculated by PLTEMP/ANL using the correlation were compared with measured CHF data for rectangular channels from two sources. The comparison provided a validation of the implementation of the correlation in the code. Parametric studies of the correlation showed that (i) the correlation is very sensitive to the channel thickness at channel thicknesses smaller than 2.25 mm, and (ii) the correlation is a continuous function of coolant mass velocity.

13.6 REFERENCES

1. M. Kaminaga, K. Yamamoto, and Y. Sudo, "Improvement of Critical Heat Flux Correlation for Research Reactors Using Plate-Type Fuel," J. Nuclear Sci. and Technol., Vol. 35, No. 12, pp. 943-951 (1998).
2. Y. Sudo and M. Kaminaga, "A New CHF Correlation Scheme Proposed for Vertical Rectangular Channels Heated From Both Sides in Nuclear Research Reactors," Transactions of the ASME, J. of Heat Transfer, Vol. 115, pp. 426-434 (1993).
3. Y. Sudo, K. Miyata, H. Ikawa, M. Kaminaga, and M. Ohkawara, "Experimental Study of Differences in DNB Heat Flux Between Upflow and Downflow in Vertical Rectangular Channel," J. Nucl. Sci. Technol., Vol. 22(8), pp. 604-618 (1985).
4. M. Kaminaga, Y. Sudo, Y. Murayama, and T. Usui, "Experimental Study of Critical Heat Flux in Narrow Vertical Rectangular Channel," Heat Transfer – Japanese Research, Vol. 20(1), pp. 72-85 (1991).
5. B. Yucel, and S. Kakac, "Forced Flow Boiling and Burnout in Rectangular Channels," Proc. 6th Int. Heat Transfer Conf., Vol. 1, pp. 387-392 (1978).
6. G. J. Kirby, R. Stanforth, and J. H. Kinneir, "A Visual Study of Forced Convection Boiling, Part 2: Flow Patterns and Burnout for a Round Tube Test Section," AEEW-R506 (1967).
7. S. Mirshak, W. S. Durant, and R. H. Towell, "Heat Flux at Burnout," DP-355, U.S. Atomic Energy Commission (1959).
8. W. R. Gambill, and R. D. Bundy, "HFIR Heat Transfer Studies of Turbulent Water Flow in Thin Rectangular Channels," ORNL-3079, Oak Ridge National Laboratory, Oak Ridge, Tennessee, USA (1961).
9. K. Mishima, "Boiling Burnout at Low Flow Rate and Low Pressure Conditions," Dissertation Thesis, Kyoto University, Japan (1984).
10. Y. Komori, M. Kaminaga, F. Sakurai, H. Ando, H. Nakata, Y. Sudo, and Y. Futamura, "Experimental Study on DNB Heat Flux Correlations for JMTR Safety Analysis," Proc. Int. Mtg. on Reduced Enrichment for Research and Test Reactors, Newport, Rhode Island, USA, September 23-27 (1990).
11. K. Mishima, H. Nishihara, and T. Shibata, "CHF Correlations Related to the Core Cooling of a Research Reactor," Proc. Int. Mtg. on Reduced Enrichment for Research and Test Reactors, October 24-27, 1983, Tokai, Japan, JAERI-M-84-073, pp. 311-320 (1983).
12. A. P. Olson and M. Kalimullah, Argonne National Laboratory, unpublished information, November 16, 2009.
13. M. W. Croft, "Advanced Test Reactor Burnout Heat Transfer Tests," ATR-FE-102, Babcock & Wilcox Company, Atomic Energy Division, Lynchburg, Virginia, USA (January 1964).

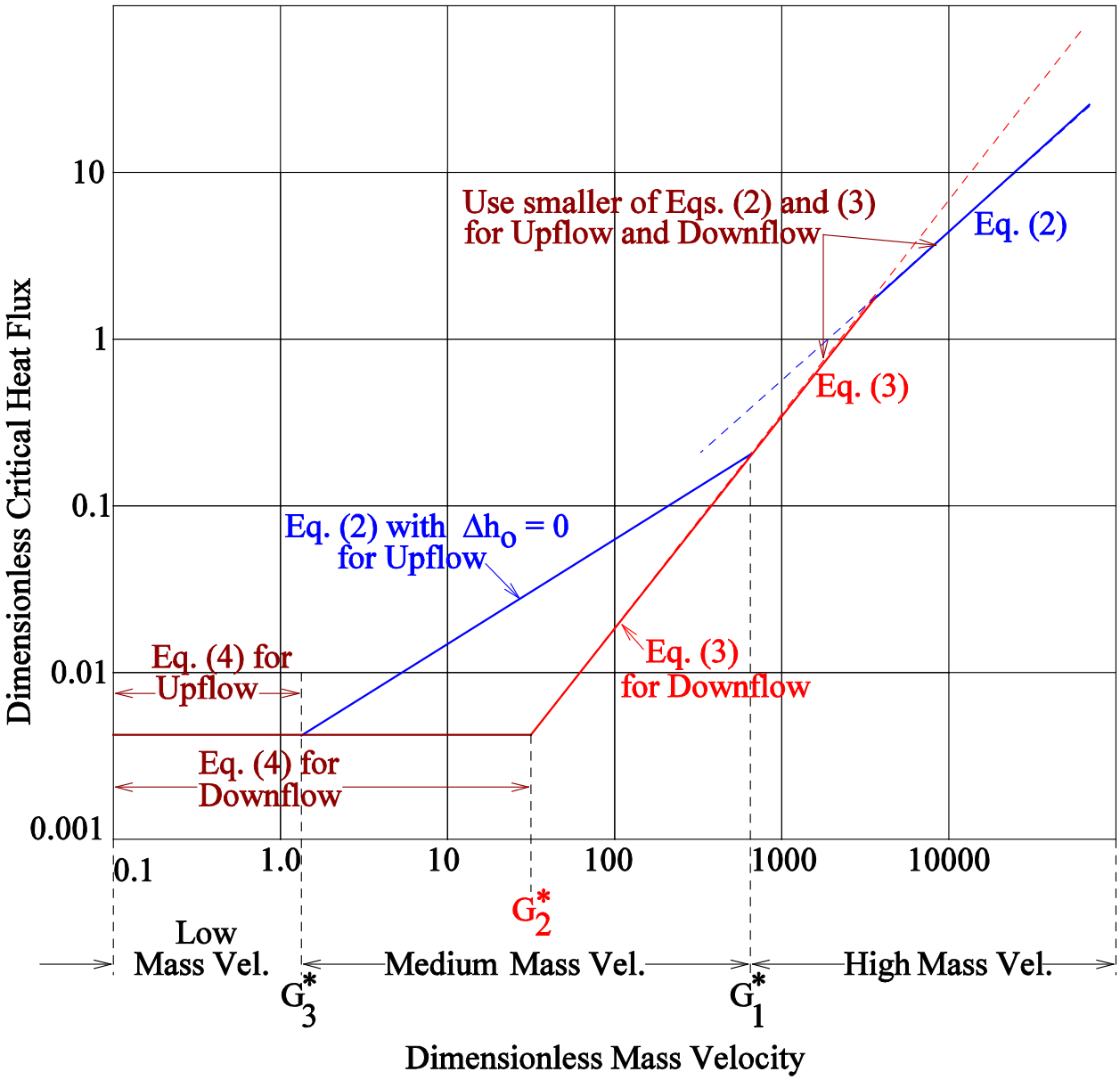

Figure 13.1 Illustration of Sudo-Kaminaga Correlation for Upward and Downward Flows

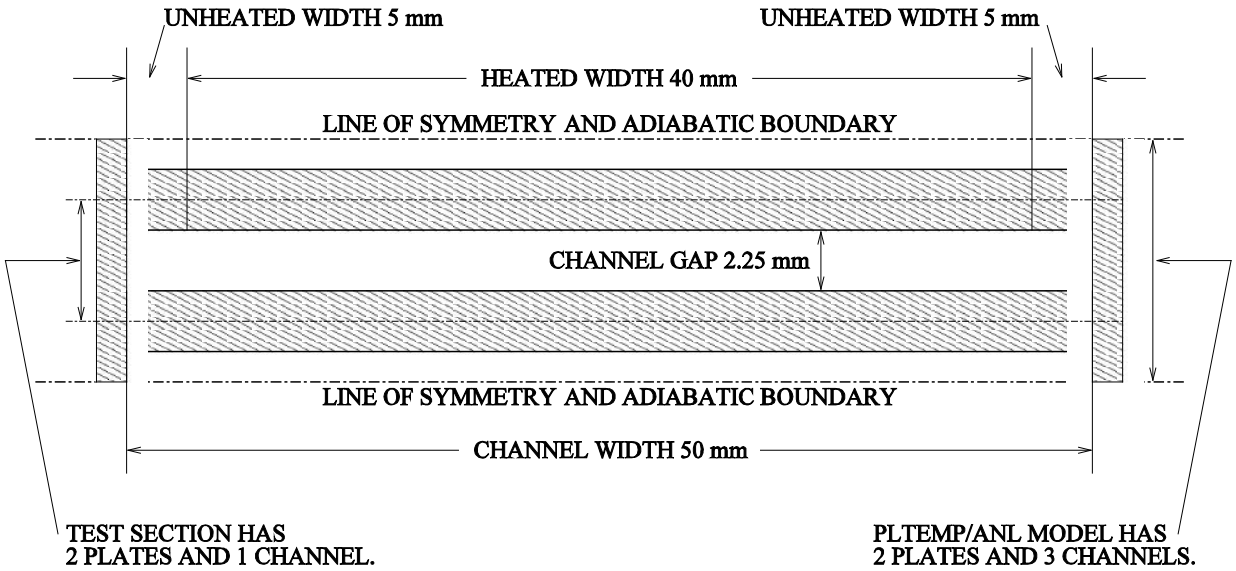

Figure 13.2 Geometry of the Test Section Used by Sudo and Kaminaga for Measuring CHF

Figure 13.3 PLTEMP/ANL Input Data for the Test Section Used by Sudo and Kaminaga for Measuring CHF

```
 Sudo-Kaminaga 1991 CHF Test Section
! 2 assemblies (of identical geometry)
! Each assembly has 1 fuel plate and 2 coolant channels
! H2O coolant, All hot channel factors = 1.0, No bypass flow, NCTYP=0
! 10 axial heat transfer nodes in the heated length of fuel plates
!234567890123456789012345678901234567890123456789012345678901234567890123456789 0
!  1   2   3   4   5   6   7   8   9  10  11  12  13  14  15  16  17  18  19  20    Indices
   0   0   8   1   0   1   1   0   0   0   0   0   0           1   1            Card(1)0200
! Search for CHFR = 1.0
   5 0.0005      1.000         1 1.000                                          Card(1)0203
! Search for ONBR = 1.0
!  4 0.020       1.000         1 1.000                                          Card(1)0203
   2   3 0.00       1.00        1.00        1.00           3                    Card(1)0300
! Using pressure driven mode
   1  20 1.00                                                                   Card(1)0301
   1   1   1                                                                    Card(1)0302
1.00        1.00                                                               Card(2)0303
2.25000E-04 4.3062E-03  0.15        8.00        0.050000    2.2500E-03         Card(3)0304
2.25000E-04 4.3062E-03  0.75        0.00        0.050000    2.2500E-03         Card(3)0304
2.25000E-04 4.3062E-03  0.15        8.00        0.050000    2.2500E-03         Card(3)0304
! Use the code's biult-in correlation for friction factor
0.00        0.00        0.00                                                   Card(1)0305
   3   3 5.00E-03   0.75000     0.50E-03    0.00        1.00E-03    100.00      Card(1)0306
0.56250E-04 4.3062E-03  0.05225     0.040000    0.050000    2.2500E-03         Card(5)0307
1.12500E-04 4.3062E-03  0.10450     0.080000    0.050000    2.2500E-03         Card(5)0307
0.56250E-04 4.3062E-03  0.05225     0.040000    0.050000    2.2500E-03         Card(5)0307
0.050000    0.050000                                                           Card(1)0308
! Card 0308a not required
! Radial power peaking factor data by fuel plate for each assembly. Input flow data by
! channel for each assembly on Cards 0310 not required because WFGES(1) is non-zero
! Input for G* = 200
1.00        1.00                                                               Card(2)0309
0.04402     0.08804     0.04402                                                Card(2)0310
1.00        1.00                                                               Card(2)0309
0.04402     0.08804     0.04402                                                Card(2)0310
! DP0       DDP         DPMAX       POWER       TIN         PIN
0.101325    0.001       0.101326    1.0         31.0        0.101325           Card(1)0500
                                                                               Card(1)0500
  50 0.0001     25.0        0.00        0.10                                   Card(1)0600
  11                                                                           Card(1)0700
0.00        1.00                                                               Card(11)0701
0.10        1.00                                                               Card(11)0701
0.20        1.00                                                               Card(11)0701
0.30        1.00                                                               Card(11)0701
0.40        1.00                                                               Card(11)0701
0.50        1.00                                                               Card(11)0701
0.60        1.00                                                               Card(11)0701
0.70        1.00                                                               Card(11)0701
0.80        1.00                                                               Card(11)0701
0.90        1.00                                                               Card(11)0701
1.00        1.00                                                               Card(11)0701
   0                                                                           Card(11)0702
```

Figure 13.4 Spreadsheet for Calculating the Effect of Varying Channel Thickness or Mass Velocity on the Sudo-Kaminaga CHF Correlation

Effect of Channel Thickness and Mass Velocity on Sudo-Kaminaga CHF Correlation by Spreadsheet Calculation for a Half Channel Model of a Test Section Like Those Used in the 1964 ATR Burnout Tests Done by Croft

INPUT QUANTITIES		
G, Mass Vel	kg/m^2-s	6068.543
Flow	kg/s	0.323696084
T inlet	C	54.4
T exit	C	188.34
Tsat	C	200.09
Cp	kJ/kg	4.266
Flow Area, AF	m^2	0.00005334
HeatedArea,AH	m^2	0.03096768
Ch Width	m	0.03048
Width Heated	m	0.0254
Length	m	1.2192
Ch Thickness	m	0.0035
RHO Vapor	kg/m^3	8.0525
RHO Liquid	kg/m^3	864.73
Hfg	kJ/kg	1920.16
SIGMA	N/m	0.037707
GRAVITY	m/s^2	9.80665

CALCULATED QUANTITIES			
G*	506.9079034		dimensionless
G*1	281.2757937		dimensionless
G*2	1.082288889	1.082289	dimensionless
G*3	9.41230914	9.412309	dimensionless
G1	3367.345897		kg/m^2-s
G2	12.95682434		kg/m^2-s
G3	112.6812235		kg/m^2-s
ZZG	11.97168748		kg/m^2-s
ZZQ	22987.55543		kW/m^2
C	3		dimensionless
LAMDA	0.002118566		m
DTSUBout	11.75		C
DTSUBin	145.69		C
DTSUB*out	0.026104856		dimensionless
DTSUB*in	0.323677996		dimensionless
ZZX	4.352224795		dimensionless
QCHF*1	0.282609388		dimensionless
QCHF*2	0.282609385		dimensionless
QCHF*3	0.005247515		dimensionless
QCHF1	6496.498983		kW/m^2
QCHF2	6496.498892		kW/m^2
QCHF3	120.6275449		kW/m^2
AF/AH	0.001722441		dimensionless
ZZ1	1.257491111		dimensionless
QCHF1(0)	5166.238493		kW/m^2

Table 13.1 Test Section Used by Sudo and Kaminaga for Measuring CHF [Ref. 1]

Flow Channel	750 mm long × 50 mm wide × 2.25 mm gap
Heating Plates	750 mm long × 40 mm wide
Heating Mode	Heated from both sides
Coolant	Water
Pressure	About 1 atmosphere

Table 13.2 Comparison of PLTEMP/ANL with the Sudo and Kaminaga Experimental CHF Data for Upflow (Inlet Subcooling is 20 to 36 °C)

Measured Data				Calculated by PLTEMP/ANL	
G^* Dimen-sionless Mass Velocity	Mass Velocity kg/m^2-s	Coolant Velocity m/s	q_c^* Dimensionless Critical Heat Flux [Note 1]	q_c^* Dimen-sionless Critical Heat Flux	Critical Heat Flux MW/m^2
4.0	15.7	0.016	0.00768 – 0.0124	0.0118	0.102
10.0	39.1	0.04	0.0129 – 0.0191	0.0207	0.178
20.0	78.3	0.08	0.0218 – 0.0308	0.0316	0.272
40.0	156.6	0.16	0.0308 – 0.0456	0.0483	0.416
60.0	234.8	0.24	0.0400 – 0.0618	0.0619	0.533
100.0	391.3	0.4		0.0845	0.728
200.0	782.6	0.8		0.129	1.11

(1) The data range was scaled from Fig. 3 of Reference 1.

Table 13.3 Comparison of PLTEMP/ANL with the Sudo and Kaminaga Experimental CHF Data for Downflow (Inlet Subcooling is 69 to 78 °C)

Measured Data				Calculated by PLTEMP/ANL	
G^* Dimen-sionless Mass Velocity	Mass Velocity kg/m^2-s	Coolant Velocity m/s	q_c^* Dimensionless Critical Heat Flux [Note 1]	q_c^* Dimen-sionless Critical Heat Flux	Critical Heat Flux MW/m^2
~ 0.0	~ 0.0	~ 0.0	0.00437 – 0.00619	0.0058	0.051 [2]
10.0	39.1	0.04	0.00339 – 0.00477	0.0058	0.051
20.0	78.3	0.08	0.00543 – 0.00803	0.0058	0.051
60.0	234.8	0.24	0.00803 – 0.00957	0.0146	0.128
100.0	391.3	0.4	0.0161 – 0.0296	0.0243	0.214
200.0	782.6	0.8	0.0367 – 0.0543	0.0486	0.428

(1) The data range was scaled from Fig. 3 of Reference 1.
(2) PLTEM/ANL was run at G^*= 2.0, mass velocity = 7.83 kg/m^2-s, velocity = 0.0082 m/s.

Table 13.4 Spreadsheet Calculation of 11 CHF Tests Done by Mirshak, Durant, and Towell to Find the Geometry, Power, and Flow Data Required for Preparing PLTEMP/ANL Input Data Files

	Run Number Assigned by Mirshak										
	#1	**#4**	**#21**	**#22**	**#23**	**#43**	**#24**	**#26**	**#27**	**#36**	**#48**
Hydraulic Dia, inch	0.247	0.247	0.464	0.458	0.455	0.253	0.453	0.243	0.239	0.247	0.254
Coolant Velocity, ft/s	18.8	18.6	18.8	18.9	18.9	33	19.2	33.4	33.6	33.7	38.5
Pressure, psia	38	35.6	50.1	50.7	51.4	24.5	51.2	50.4	60	52	55.3
Subcooling ΔT_{sub}, °C	46	44	44.7	54.5	62.7	43.5	71	45	55	65	54
Measured CHF, 10^3 pcu/hr.ft^2	875	883	1000	1206	1208	1208	1400	1412	1642	1633	1765
Measured CHF, MW/m^2	4.96825	5.01367	5.678	6.84767	6.85902	6.85902	7.9492	8.01734	9.32328	9.27217	10.02167
Calculated Power, MW	0.127107	0.128269	0.145265	0.17519	0.17548	0.17548	0.203371	0.205114	0.238525	0.237218	0.256393
Hydraulic Diameter D, m	0.006274	0.006274	0.011786	0.011633	0.011557	0.006426	0.011506	0.006172	0.006071	0.006274	0.006452
Coolant Velocity, m/s	5.73024	5.66928	5.73024	5.76072	5.76072	10.0584	5.85216	10.18032	10.24128	10.27176	11.7348
Pressure, bar	2.620003	2.454529	3.454267	3.495636	3.543899	1.689212	3.530109	3.474951	4.136847	3.585267	3.812794
Tsat, °C	128.5733	126.8451	137.2862	137.7183	138.2223	118.8522	138.0783	137.5022	144.415	138.6544	141.0306
Tout, °C	82.57327	82.84508	92.58621	83.21826	75.52231	75.35222	67.0783	92.50223	89.41498	73.65436	87.03062
Exit Density, kg/m^3	969.3074	969.1403	963.1495	968.9108	973.6438	973.7484	978.8368	963.2011	965.0998	974.7926	966.5662
Channel Thickness, mm	3.295901	3.295901	6.480055	6.388029	6.342105	3.380126	6.311522	3.239867	3.183925	3.295901	3.394183
Flow Area, 10^{-4} m^2	2.143127	2.143127	4.213591	4.153752	4.12389	2.197893	4.104004	2.106691	2.070315	2.143127	2.207034
Wetted Perimeter, m	0.13664	0.13664	0.143008	0.142824	0.142732	0.136808	0.142671	0.136528	0.136416	0.13664	0.136836
Flow Rate, kg/s	1.190371	1.177504	2.325514	2.318468	2.313044	2.152693	2.350901	2.065757	2.04627	2.145878	2.503319
Mass Velocity, kg/s.m^2	5554.364	5494.328	5519.078	5581.624	5608.889	9794.351	5728.31	9805.696	9883.857	10012.84	11342.46
Temp Rise Tout-Tin, °C	25.48429	25.9983	14.90829	18.03404	18.1063	19.45501	20.64622	23.69748	27.81999	26.38323	24.44416
Tin, °C	57.08898	56.84678	77.67792	65.18422	57.41601	55.89721	46.43208	68.80475	61.59499	47.27113	62.58645

Note 1. The geometry data common to all the 11 test sections are given first, followed by the equations used to find the required input data from the quantities reported by Mirshak, Durant, and Towell[7].

Channel Length, L = 19.25 inch = 0.48895 m
Heated Perimeter, P_h = 2.06 inch = 0.052324 m
Channel Width, w = 2.56 inch = 0.065024 m
Power, P = (Measured CHF*L P_h)
D = Hydraulic Diameter (reported for each test)
Channel Thickness, $t_c = D/(2 - D/w)$
Flow Area, $A_f = w\ t_c$
Exit Temp., T_o = (T_{sat} at Measured P) – (Measured ΔT_{sub})
Flow Rate, W = A_f (Measured Vel.)*(Density at CHF Location)
Average C_p = 4.19 kJ/kg-°C
Temp. Rise, $\Delta T = P/(W\ C_p)$
$T_{in} = T_o - \Delta T$

Table 13.5 Comparison of PLTEMP/ANL-Calculated CHF Using the Sudo-Kaminaga Correlation with Measured CHF for 11 CHF Tests Done by Mirshak, Durant, and Towell

	Run Number Assigned by Mirshak										
	#1	**#4**	**#21**	**#22**	**#23**	**#43**	**#24**	**#26**	**#27**	**#36**	**#48**
Coolant Velocity, ft/s	18.8	18.6	18.8	18.9	18.9	33	19.2	33.4	33.6	33.7	38.5
Measured CHF, MW/m^2	4.96825	5.01367	5.678	6.84767	6.85902	6.85902	7.9492	8.01734	9.32328	9.27217	10.02167
Mirshak Corr. CHF, MW/m^2	5.413	5.194	5.973	6.389	6.742	5.957	7.099	7.876	9.001	9.037	9.359
% Error in Mirshak CHF	9.0	3.6	5.2	-6.7	-1.7	-13.2	-10.7	-1.8	-3.5	-2.5	-6.6
Sudo-Kaminaga CHF, MW/m^2	6.040	5.818	6.490	7.004	7.436	6.520	7.854	7.860	8.605	8.754	8.882
% Error in Sudo-Kaminaga CHF	21.6	16.0	14.3	2.3	8.4	-4.9	-1.2	-2.0	-7.7	-5.6	-11.4

Table 13.6 Effect of Varying Channel Thickness for a Fixed Coolant Mass Velocity on the Sudo-Kaminaga CHF Correlation (Mass Velocity = 10141.5 kg/m^2-s downflow)

Outlet Pressure = 15.6 bar
Outlet Temperature = 188.3 °C
Heated Width of Plate = 25.4 mm
Inlet Temperature = 54.4 °C
Channel Width = 30.5 mm
Channel Length = 1.2192 m

Channel Thickness mm	G_2 kg/m^2-s	G_3 kg/m^2-s	G_1 kg/m^2-s	q_{c1} MW/m^2	q_{c1} at $\Delta T_{sub,o}$=0 MW/m^2	q_{c2} MW/m^2	q_{c3} MW/m^2	CHF[a] in Downflow MW/m^2
Column→1	2	3	4	5	6	7	8	9
1.37*	2.8	112.7	37424.0	8.16	7.07	4.25	0.0473	4.25*
1.4*	2.9	112.7	35503.4	8.16	7.07	4.34	0.0483	4.34*
1.5*	3.2	112.7	29733.3	8.16	7.07	4.65	0.0517	4.65*
1.6*	3.6	112.7	25187.8	8.16	7.07	4.96	0.0551	4.96*
1.8*	4.4	112.7	18607.7	8.16	7.07	5.58	0.0620	5.58*
2.0*	5.2	112.7	14192.7	8.16	7.07	6.20	0.0689	6.20*
2.25	6.3	112.7	10485.0	8.16	7.07	6.98	0.0775	6.98
2.5	7.5	112.7	7997.2	8.16	7.07	7.75	0.0862	7.74
2.75	8.7	112.7	6259.4	8.16	7.07	8.53	0.0948	8.16
3.0	10.1	112.7	5004.8	8.16	7.07	9.31	0.103	8.16
3.5	13.0	112.7	3367.3	8.16	7.07	10.86	0.121	8.16
4.0	16.1	112.7	2389.0	8.16	7.07	12.41	0.138	8.16
4.5	19.5	112.7	1764.9	8.16	7.07	13.96	0.155	8.16
5.0	23.2	112.7	1346.1	8.16	7.07	15.51	0.172	8.16

* The channel thickness is out of the test range 2.25 to 5.0 mm. The correlation is not applicable.
a CHF in downflow is given by column 8 for mass velocities up to G_3 (112.7 kg/m^2-s), then by column 7 for mass velocities up to G_1, and above G_1 by the smaller of columns 5 and 7.

Table 13.7 Effect of Varying Upward Mass Velocity for a Fixed Channel Thickness on the Sudo-Kaminaga CHF Correlation

Channel Thickness = 3.5 mm,
Inlet Temperature = 54.4 °C,
Channel Width = 30.5 mm,
Channel Length = 1.2192 m

Outlet Pressure = 15.6 bar
Outlet Temperature = 188.3 °C
Heated Width of Plate = 25.4 mm

Mass Velocity kg/m²-s	G_2 kg/m²-s	G_3 kg/m²-s	G_1 kg/m²-s	q_{c1} MW/m²	q_{c1} at $\Delta T_{sub,o}=0$ MW/m²	q_{c2} MW/m²	q_{c3} MW/m²	CHF[b] in Uplow MW/m²
Column→1	2	3	4	5	6	7	8	9
5.0				21.14	0.0674	0.0054	0.121	0.121
12.96				14.67	**0.121**	0.0139	**0.121**	**0.121**
20.0				12.44	0.157	0.0214	0.121	0.157
50.0				8.88	0.275	0.0535	0.121	0.275
75.0				7.70	0.353	0.0803	0.121	0.353
112.7				6.72	0.452	**0.121**	**0.121**	0.452
200.0	12.96	112.7	3367.3	5.66	0.642	0.214	0.121	0.642
500.0				4.64	1.124	0.535	0.121	1.124
1000.0				4.40	1.716	1.070	0.121	1.716
2000.0				4.67	2.622	2.141	0.121	2.622
3367.3				5.278	**3.605**	**3.605**	0.121	**3.605**
3368.0				5.278	3.605	3.606	0.121	3.606
5000.0				6.02	4.59	5.350	0.121	5.350
6000.0				6.467	5.139	6.423	0.121	6.423
6068.5				6.496	5.166	6.496	0.121	6.496
10000.0				8.11	7.01	10.71	0.121	8.11
15000.0				9.92	8.98	16.06	0.121	9.92
20000.0				11.54	10.71	21.41	0.121	11.54

a CHF in downflow is given by column 8 for mass velocities up to 112.7 kg/m²-s, then by column 7 for mass velocities up to 3367.3 kg/m²-s, and above 3367.3 kg/m²-s by the smaller of columns 5 and 7.

b CHF in upflow is given by column 8 for mass velocities up to 12.96 kg/m²-s, then by column 6 for mass velocities up to 3367.3 kg/m²-s, and above 3367.3 kg/m²-s by the smaller of columns 5 and 7.

Table 13.8 Effect of Varying Downward Mass Velocity for a Fixed Channel Thickness on the Sudo-Kaminaga CHF Correlation

Channel Thickness = 3.5 mm,
Inlet Temperature = 54.4 °C,
Channel Width = 30.5 mm,
Channel Length = 1.2192 m

Outlet Pressure = 15.6 bar
Outlet Temperature = 188.3 °C
Heated Width of Plate = 25.4 mm

Mass Velocity kg/m²-s	G_2 kg/m²-s	G_3 kg/m²-s	G_1 kg/m²-s	q_{c1} MW/m²	q_{c1} at $\Delta T_{sub,o}=0$ MW/m²	q_{c2} MW/m²	q_{c3} MW/m²	CHF[a] in Downflow MW/m²
Column→1	2	3	4	5	6	7	8	9
5.0				21.14	0.0674	0.0054	0.121	0.121
12.96				14.67	**0.121**	0.0139	**0.121**	0.121
20.0				12.44	0.157	0.0214	0.121	0.121
50.0				8.88	0.275	0.0535	0.121	0.121
75.0				7.70	0.353	0.0803	0.121	0.121
112.7				6.72	0.452	**0.121**	**0.121**	**0.121**
200.0	12.96	112.7	3367.3	5.66	0.642	0.214	0.121	0.214
500.0				4.64	1.124	0.535	0.121	0.535
1000.0				4.40	1.716	1.070	0.121	1.070
2000.0				4.67	2.622	2.141	0.121	2.141
3367.3				5.278	**3.605**	**3.605**	0.121	**3.605**
3368.0				5.278	3.605	3.606	0.121	3.606
5000.0				6.02	4.59	5.350	0.121	5.350
6000.0				6.467	5.139	6.423	0.121	6.423
6068.5				**6.496**	5.166	**6.496**	0.121	6.496
10000.0				8.11	7.01	10.71	0.121	8.11
15000.0				9.92	8.98	16.06	0.121	9.92
20000.0				11.54	10.71	21.41	0.121	11.54

a CHF in downflow is given by column 8 for mass velocities up to 112.7 kg/m²-s, then by column 7 for mass velocities up to 3367.3 kg/m²-s, and above 3367.3 kg/m²-s by the smaller of columns 5 and 7.
b CHF in upflow is given by column 8 for mass velocities up to 12.96 kg/m²-s, then by column 6 for mass velocities up to 3367.3 kg/m²-s, and above 3367.3 kg/m²-s by the smaller of columns 5 and 7.

APPENDIX J PLTEMP/ANL Input Data Files for 11 CHF Tests Done by Mirshak, Durant, and Towell

The following is a listing of all the PLTEMP/ANL input data files used to model 11 of the CHF tests done by Mirshak, Durant, and Towell[7]. The test number is given on the first card.

```
  CHF Run #1, Mirshak, Durant, & Towell, Ref. DP-355 (1959)
! Rectangular channel, down flow, 1-sided heating
!  1   2   3   4   5   6   7   8   9  10  11  12  13  14  15  16  17  18  19  20
   0   0   0   1   0           0   0   0   0   0   0   0   2   1   0   0   0   00200
          1.          1.          1.                                           0201
!  5        0.20         0.5   1         1.0                                   0203
   1   3          0.          1.          1.          1.   0   0               00300
          1.          1.          1.                                           0300A
         1.0                                                                   0303
          1.          1.          0.          0.                               0304
          0.          0.     0.48895          0.    0.065024   0.0032959        0304
          1.          1.          0.          0.                               0304
          0.          0.          0.                                           0305
   2   0     0.00635     0.48895      3.0e-5         10.      9.7e-4         10.0306
 2.143127e-4    6.274e-3     0.13664    0.052324    0.065024   0.0032959        0307
 2.143127e-4    6.274e-3     0.13664    0.052324    0.065024   0.0032959        0307
    0.065024                                                                   0308
          1.                                                                   0309
    1.190371    1.190371                                                       0310
! 2 x 0.127107 MW = 0.254214 MW
    0.262000          0.    0.262000    0.254214       57.09          0.        0500
          0.          0.                                                       0500
   0      0.0001        32.5          0.          0.                           0600
 -25                                                                           0700
     0.00000     0.02083          1.                                           0701
     0.04167     0.06250          1.                                           0701
     0.08333     0.10417          1.                                           0701
     0.12500     0.14583          1.                                           0701
     0.16667     0.18750          1.                                           0701
     0.20833     0.22917          1.                                           0701
     0.25000     0.27083          1.                                           0701
     0.29167     0.31250          1.                                           0701
     0.33333     0.35417          1.                                           0701
     0.37500     0.39583          1.                                           0701
     0.41667     0.43750          1.                                           0701
     0.45833     0.47917          1.                                           0701
     0.50000     0.52083          1.                                           0701
     0.54167     0.56250          1.                                           0701
     0.58333     0.60417          1.                                           0701
     0.62500     0.64583          1.                                           0701
     0.66667     0.68750          1.                                           0701
     0.70833     0.72917          1.                                           0701
     0.75000     0.77083          1.                                           0701
     0.79167     0.81250          1.                                           0701
     0.83333     0.85417          1.                                           0701
     0.87500     0.89583          1.                                           0701
     0.91667     0.93750          1.                                           0701
     0.95833     0.97917          1.                                           0701
     1.00000                                                                   0701
   0                                                                           0702


  CHF Run #4, Mirshak, Durant, & Towell, Ref. DP-355 (1959)
```

```
! Rectangular channel, down flow, 1-sided heating
!  1   2   3   4   5   6   7   8   9  10  11  12  13  14  15  16  17  18  19  20
   0   0   0   1   0           0   0   0   0   0   0   0   2   1   0   0   0   00200
          1.          1.          1.                                           0201
!  5        0.20         0.5   1         1.0                                   0203
   1   3          0.          1.          1.          1.   0   0               00300
          1.          1.          1.                                           0300A
         1.0                                                                   0303
          1.          1.          0.          0.                               0304
          0.          0.     0.48895          0.   0.0650244   0.0032959        0304
          1.          1.          0.          0.                               0304
          0.          0.          0.                                           0305
   2   0     0.00635      0.4890      3.0e-5         10.      9.7e-4         10.0306
 2.143127e-4    6.274e-3     0.13664    0.052324    0.065024   0.0032959        0307
 2.143127e-4    6.274e-3     0.13664    0.052324    0.065024   0.0032959        0307
    0.065024                                                                   0308
          1.                                                                   0309
    1.177504    1.177504                                                       0310
! 2 x 0.128269 MW = 0.256538 MW
    0.245453          0.    0.245453    0.256538       56.85          0.        0500
          0.          0.                                                       0500
   0      0.0001        32.5          0.          0.                           0600
 -25                                                                           0700
     0.00000     0.02083          1.                                           0701
     0.04167     0.06250          1.                                           0701
     0.08333     0.10417          1.                                           0701
     0.12500     0.14583          1.                                           0701
     0.16667     0.18750          1.                                           0701
     0.20833     0.22917          1.                                           0701
     0.25000     0.27083          1.                                           0701
     0.29167     0.31250          1.                                           0701
     0.33333     0.35417          1.                                           0701
     0.37500     0.39583          1.                                           0701
     0.41667     0.43750          1.                                           0701
     0.45833     0.47917          1.                                           0701
     0.50000     0.52083          1.                                           0701
     0.54167     0.56250          1.                                           0701
     0.58333     0.60417          1.                                           0701
     0.62500     0.64583          1.                                           0701
     0.66667     0.68750          1.                                           0701
     0.70833     0.72917          1.                                           0701
     0.75000     0.77083          1.                                           0701
     0.79167     0.81250          1.                                           0701
     0.83333     0.85417          1.                                           0701
     0.87500     0.89583          1.                                           0701
     0.91667     0.93750          1.                                           0701
     0.95833     0.97917          1.                                           0701
     1.00000                                                                   0701
   0                                                                           0702
```

CHF Run #21, Mirshak, Durant, & Towell, Ref. DP-355 (1959)

```
! Rectangular channel, down flow, 1-sided heating
!  1   2   3   4   5   6   7   8   9  10  11  12  13  14  15  16  17  18  19  20
   0   0   0   1   0           0   0   0   0   0   0   0   2   1   0   0   0   00200
          1.          1.          1.                                           0201
!  5        0.20         0.5   1         1.0                                   0203
   1   3          0.          1.          1.          1.   0   0               00300
          1.          1.          1.                                           0300A
         1.0                                                                   0303
          1.          1.          0.          0.                               0304
          0.          0.     0.48895          0.   0.0650244 0.006480055        0304
          1.          1.          0.          0.                               0304
```

```
          0.          0.          0.                                                  0305
   2   0     0.00635      0.4890      3.0e-5         10.      9.7e-4         10.0306
 4.213591e-4   11.786e-3    0.143008    0.052324    0.065024 0.006480055        0307
 4.213591e-4   11.786e-3    0.143008    0.052324    0.065024 0.006480055        0307
    0.065024                                                                      0308
          1.                                                                      0309
    2.325514    2.325514                                                          0310
! 2 x 0.145265 MW = 0.290530 MW
    0.345427          0.    0.345427    0.290530       77.68          0.         0500
          0.          0.                                                          0500
   0      0.0001        32.5          0.          0.                              0600
 -25                                                                              0700
     0.00000     0.02083          1.                                              0701
     0.04167     0.06250          1.                                              0701
     0.08333     0.10417          1.                                              0701
     0.12500     0.14583          1.                                              0701
     0.16667     0.18750          1.                                              0701
     0.20833     0.22917          1.                                              0701
     0.25000     0.27083          1.                                              0701
     0.29167     0.31250          1.                                              0701
     0.33333     0.35417          1.                                              0701
     0.37500     0.39583          1.                                              0701
     0.41667     0.43750          1.                                              0701
     0.45833     0.47917          1.                                              0701
     0.50000     0.52083          1.                                              0701
     0.54167     0.56250          1.                                              0701
     0.58333     0.60417          1.                                              0701
     0.62500     0.64583          1.                                              0701
     0.66667     0.68750          1.                                              0701
     0.70833     0.72917          1.                                              0701
     0.75000     0.77083          1.                                              0701
     0.79167     0.81250          1.                                              0701
     0.83333     0.85417          1.                                              0701
     0.87500     0.89583          1.                                              0701
     0.91667     0.93750          1.                                              0701
     0.95833     0.97917          1.                                              0701
     1.00000                                                                      0701
   0                                                                              0702
```

CHF Run #22, Mirshak, Durant, & Towell, Ref. DP-355 (1959)

```
! Rectangular channel, down flow, 1-sided heating
!  1   2   3   4   5   6   7   8   9  10  11  12  13  14  15  16  17  18  19  20
   0   0   0   1   0           0   0   0   0   0   0   0   2   1   0   0   0   00200
          1.          1.          1.                                              0201
!  5        0.20         0.5   1         1.0                                      0203
   1   3          0.          1.          1.          1.   0   0                00300
          1.          1.          1.                                              0300A
         1.0                                                                      0303
          1.          1.          0.          0.                                  0304
          0.          0.     0.48895          0.   0.0650244  0.00638803          0304
          1.          1.          0.          0.                                  0304
          0.          0.          0.                                              0305
   2   0     0.00635      0.4890      3.0e-5         10.      9.7e-4         10.0306
 4.153752e-4   11.633e-3    0.142824    0.052324    0.065024  0.00638803        0307
 4.153752e-4   11.633e-3    0.142824    0.052324    0.065024  0.00638803        0307
    0.065024                                                                      0308
          1.                                                                      0309
    2.318468    2.318468                                                          0310
! 2 x 0.17519 MW = 0.350389 MW
    0.349564          0.    0.349564    0.350389       65.18          0.         0500
          0.          0.                                                          0500
   0      0.0001        32.5          0.          0.                              0600
```

```
 -25                                                                    0700
     0.00000     0.02083          1.                                    0701
     0.04167     0.06250          1.                                    0701
     0.08333     0.10417          1.                                    0701
     0.12500     0.14583          1.                                    0701
     0.16667     0.18750          1.                                    0701
     0.20833     0.22917          1.                                    0701
     0.25000     0.27083          1.                                    0701
     0.29167     0.31250          1.                                    0701
     0.33333     0.35417          1.                                    0701
     0.37500     0.39583          1.                                    0701
     0.41667     0.43750          1.                                    0701
     0.45833     0.47917          1.                                    0701
     0.50000     0.52083          1.                                    0701
     0.54167     0.56250          1.                                    0701
     0.58333     0.60417          1.                                    0701
     0.62500     0.64583          1.                                    0701
     0.66667     0.68750          1.                                    0701
     0.70833     0.72917          1.                                    0701
     0.75000     0.77083          1.                                    0701
     0.79167     0.81250          1.                                    0701
     0.83333     0.85417          1.                                    0701
     0.87500     0.89583          1.                                    0701
     0.91667     0.93750          1.                                    0701
     0.95833     0.97917          1.                                    0701
     1.00000                                                            0701
   0                                                                    0702


  CHF Run #23, Mirshak, Durant, & Towell, Ref. DP-355 (1959)
! Rectangular channel, down flow, 1-sided heating
!  1   2   3   4   5   6   7   8   9  10  11  12  13  14  15  16  17  18  19  20
   0   0   0   1   0           0   0   0   0   0   0   0   2   1   0   0   0   00200
          1.          1.          1.                                        0201
!  5        0.20         0.5   1         1.0                                0203
   1   3          0.          1.          1.          1.   0   0            00300
          1.          1.          1.                                        0300A
         1.0                                                                0303
          1.          1.          0.          0.                            0304
          0.          0.     0.48895          0.   0.0650244 0.006342105    0304
          1.          1.          0.          0.                            0304
          0.          0.          0.                                        0305
   2   0     0.00635      0.4890      3.0e-5         10.      9.7e-4         10.0306
 4.123890e-4   11.557e-3    0.142732    0.052324    0.065024 0.006342105    0307
 4.123890e-4   11.557e-3    0.142732    0.052324    0.065024 0.006342105    0307
    0.065024                                                                0308
          1.                                                                0309
    2.313044    2.313044                                                    0310
! 2 x 0.17548 MW = 0.350960 MW
    0.354390          0.    0.354390    0.350960       57.42          0.     0500
          0.          0.                                                    0500
   0      0.0001        32.5          0.          0.                        0600
 -25                                                                        0700
     0.00000     0.02083          1.                                    0701
     0.04167     0.06250          1.                                    0701
     0.08333     0.10417          1.                                    0701
     0.12500     0.14583          1.                                    0701
     0.16667     0.18750          1.                                    0701
     0.20833     0.22917          1.                                    0701
     0.25000     0.27083          1.                                    0701
     0.29167     0.31250          1.                                    0701
     0.33333     0.35417          1.                                    0701
     0.37500     0.39583          1.                                    0701
```

```
     0.41667     0.43750          1.                                          0701
     0.45833     0.47917          1.                                          0701
     0.50000     0.52083          1.                                          0701
     0.54167     0.56250          1.                                          0701
     0.58333     0.60417          1.                                          0701
     0.62500     0.64583          1.                                          0701
     0.66667     0.68750          1.                                          0701
     0.70833     0.72917          1.                                          0701
     0.75000     0.77083          1.                                          0701
     0.79167     0.81250          1.                                          0701
     0.83333     0.85417          1.                                          0701
     0.87500     0.89583          1.                                          0701
     0.91667     0.93750          1.                                          0701
     0.95833     0.97917          1.                                          0701
     1.00000                                                                  0701
   0                                                                          0702


  CHF Run #24, Mirshak, Durant, & Towell, Ref. DP-355 (1959)
! Rectangular channel, down flow, 1-sided heating
!  1   2   3   4   5   6   7   8   9  10  11  12  13  14  15  16  17  18  19  20
   0   0   0   1   0           0   0   0   0   0   0   0   2   1   0   0   0   00200
         1.          1.          1.                                           0201
!  5        0.20         0.5   1         1.0                                  0203
   1   3          0.          1.          1.          1.   0   0              00300
         1.          1.          1.                                           0300A
        1.0                                                                   0303
         1.          1.          0.          0.                               0304
         0.          0.     0.48895          0.   0.0650244 0.006311522       0304
         1.          1.          0.          0.                               0304
         0.          0.          0.                                           0305
   2   0     0.00635      0.4890      3.0e-5         10.      9.7e-4         10.0306
 4.104004e-4   11.557e-3    0.136528    0.052324    0.065024 0.006311522        0307
 4.104004e-4   11.557e-3    0.136528    0.052324    0.065024 0.006311522        0307
    0.065024                                                                  0308
         1.                                                                   0309
    2.350901    2.350901                                                      0310
! 2 x 0.203371 MW = 0.406641 MW
    0.353011          0.    0.353011    0.406641       46.43          0.       0500
         0.          0.                                                       0500
   0      0.0001        32.5          0.          0.                          0600
 -25                                                                          0700
     0.00000     0.02083          1.                                          0701
     0.04167     0.06250          1.                                          0701
     0.08333     0.10417          1.                                          0701
     0.12500     0.14583          1.                                          0701
     0.16667     0.18750          1.                                          0701
     0.20833     0.22917          1.                                          0701
     0.25000     0.27083          1.                                          0701
     0.29167     0.31250          1.                                          0701
     0.33333     0.35417          1.                                          0701
     0.37500     0.39583          1.                                          0701
     0.41667     0.43750          1.                                          0701
     0.45833     0.47917          1.                                          0701
     0.50000     0.52083          1.                                          0701
     0.54167     0.56250          1.                                          0701
     0.58333     0.60417          1.                                          0701
     0.62500     0.64583          1.                                          0701
     0.66667     0.68750          1.                                          0701
     0.70833     0.72917          1.                                          0701
     0.75000     0.77083          1.                                          0701
     0.79167     0.81250          1.                                          0701
     0.83333     0.85417          1.                                          0701
```

```
     0.87500     0.89583          1.                                          0701
     0.91667     0.93750          1.                                          0701
     0.95833     0.97917          1.                                          0701
     1.00000                                                                  0701
   0                                                                          0702
```

CHF Run #26, Mirshak, Durant, & Towell, Ref. DP-355 (1959)

```
! Rectangular channel, down flow, 1-sided heating
!  1   2   3   4   5   6   7   8   9  10  11  12  13  14  15  16  17  18  19  20
   0   0   0   1   0           0   0   0   0   0   0   0   2   1   0   0   0   00200
          1.          1.          1.                                          0201
!  5        0.20         0.5   1         1.0                                  0203
   1   3          0.          1.          1.          1.   0   0              00300
          1.          1.          1.                                          0300A
         1.0                                                                  0303
          1.          1.          0.          0.                              0304
          0.          0.     0.48895          0.   0.0650244 0.003239867       0304
          1.          1.          0.          0.                              0304
          0.          0.          0.                                          0305
   2   0     0.00635      0.4890      3.0e-5         10.      9.7e-4         10.0306
 2.106691e-4   6.1720e-3    0.136528    0.052324    0.065024 0.003239867       0307
 2.106691e-4   6.1720e-3    0.136528    0.052324    0.065024 0.003239867       0307
    0.065024                                                                  0308
          1.                                                                  0309
    2.065757    2.065757                                                      0310
! 2 x 0.205114 MW = 0.410228 MW
    0.347495          0.    0.347495    0.410228       68.80          0.       0500
          0.          0.                                                      0500
   0      0.0001        32.5          0.          0.                          0600
 -25                                                                          0700
     0.00000     0.02083          1.                                          0701
     0.04167     0.06250          1.                                          0701
     0.08333     0.10417          1.                                          0701
     0.12500     0.14583          1.                                          0701
     0.16667     0.18750          1.                                          0701
     0.20833     0.22917          1.                                          0701
     0.25000     0.27083          1.                                          0701
     0.29167     0.31250          1.                                          0701
     0.33333     0.35417          1.                                          0701
     0.37500     0.39583          1.                                          0701
     0.41667     0.43750          1.                                          0701
     0.45833     0.47917          1.                                          0701
     0.50000     0.52083          1.                                          0701
     0.54167     0.56250          1.                                          0701
     0.58333     0.60417          1.                                          0701
     0.62500     0.64583          1.                                          0701
     0.66667     0.68750          1.                                          0701
     0.70833     0.72917          1.                                          0701
     0.75000     0.77083          1.                                          0701
     0.79167     0.81250          1.                                          0701
     0.83333     0.85417          1.                                          0701
     0.87500     0.89583          1.                                          0701
     0.91667     0.93750          1.                                          0701
     0.95833     0.97917          1.                                          0701
     1.00000                                                                  0701
   0                                                                          0702
```

CHF Run #27, Mirshak, Durant, & Towell, Ref. DP-355 (1959)

```
! Rectangular channel, down flow, 1-sided heating
!  1   2   3   4   5   6   7   8   9  10  11  12  13  14  15  16  17  18  19  20
   0   0   0   1   0           0   0   0   0   0   0   0   2   1   0   0   0   00200
          1.          1.          1.                                          0201
```

```
!  5        0.20         0.5   1         1.0                                    0203
   1   3          0.          1.          1.          1.   0   0               00300
          1.          1.          1.                                            0300A
         1.0                                                                     0303
          1.          1.          0.          0.                                0304
          0.          0.     0.48895          0.   0.0650244 0.003183925        0304
          1.          1.          0.          0.                                0304
          0.          0.          0.                                            0305
   2   0     0.00635      0.4890      3.0e-5         10.      9.7e-4         10.0306
 2.070315e-4   6.0710e-3    0.136416    0.052324    0.065024 0.003183925        0307
 2.070315e-4   6.0710e-3    0.136416    0.052324    0.065024 0.003183925        0307
    0.065024                                                                     0308
          1.                                                                     0309
    2.046270    2.046270                                                         0310
! 2 x 0.238525 MW = 0.477050 MW
   0.4136847          0.   0.4136847    0.477050       61.60          0.         0500
          0.          0.                                                         0500
   0      0.0001        32.5          0.          0.                            0600
 -25                                                                             0700
     0.00000     0.02083          1.                                            0701
     0.04167     0.06250          1.                                            0701
     0.08333     0.10417          1.                                            0701
     0.12500     0.14583          1.                                            0701
     0.16667     0.18750          1.                                            0701
     0.20833     0.22917          1.                                            0701
     0.25000     0.27083          1.                                            0701
     0.29167     0.31250          1.                                            0701
     0.33333     0.35417          1.                                            0701
     0.37500     0.39583          1.                                            0701
     0.41667     0.43750          1.                                            0701
     0.45833     0.47917          1.                                            0701
     0.50000     0.52083          1.                                            0701
     0.54167     0.56250          1.                                            0701
     0.58333     0.60417          1.                                            0701
     0.62500     0.64583          1.                                            0701
     0.66667     0.68750          1.                                            0701
     0.70833     0.72917          1.                                            0701
     0.75000     0.77083          1.                                            0701
     0.79167     0.81250          1.                                            0701
     0.83333     0.85417          1.                                            0701
     0.87500     0.89583          1.                                            0701
     0.91667     0.93750          1.                                            0701
     0.95833     0.97917          1.                                            0701
     1.00000                                                                     0701
   0                                                                             0702
```

CHF Run #36, Mirshak, Durant, & Towell, Ref. DP-355 (1959)

```
! Rectangular channel, down flow, 1-sided heating
!  1   2   3   4   5   6   7   8   9  10  11  12  13  14  15  16  17  18  19  20
   0   0   0   1   0           0   0   0   0   0   0   0   2   1   0   0   0   00200
          1.          1.          1.                                            0201
!  5        0.20         0.5   1         1.0                                    0203
   1   3          0.          1.          1.          1.   0   0               00300
          1.          1.          1.                                            0300A
         1.0                                                                     0303
          1.          1.          0.          0.                                0304
          0.          0.     0.48895          0.   0.0650244   0.0032959        0304
          1.          1.          0.          0.                                0304
          0.          0.          0.                                            0305
   2   0     0.00635      0.4890      3.0e-5         10.      9.7e-4         10.0306
 2.143127e-4    6.274e-3     0.13664    0.052324    0.065024   0.0032959        0307
 2.143127e-4    6.274e-3     0.13664    0.052324    0.065024   0.0032959        0307
```

```
    0.065024                                                                0308
          1.                                                                0309
    2.145878    2.145878                                                    0310
! 2 x 0.237218 MW = 0.474436 MW
    0.358527          0.    0.358527    0.474436       47.27          0.    0500
          0.          0.                                                    0500
   0      0.0001        32.5          0.          0.                        0600
 -25                                                                        0700
     0.00000     0.02083          1.                                        0701
     0.04167     0.06250          1.                                        0701
     0.08333     0.10417          1.                                        0701
     0.12500     0.14583          1.                                        0701
     0.16667     0.18750          1.                                        0701
     0.20833     0.22917          1.                                        0701
     0.25000     0.27083          1.                                        0701
     0.29167     0.31250          1.                                        0701
     0.33333     0.35417          1.                                        0701
     0.37500     0.39583          1.                                        0701
     0.41667     0.43750          1.                                        0701
     0.45833     0.47917          1.                                        0701
     0.50000     0.52083          1.                                        0701
     0.54167     0.56250          1.                                        0701
     0.58333     0.60417          1.                                        0701
     0.62500     0.64583          1.                                        0701
     0.66667     0.68750          1.                                        0701
     0.70833     0.72917          1.                                        0701
     0.75000     0.77083          1.                                        0701
     0.79167     0.81250          1.                                        0701
     0.83333     0.85417          1.                                        0701
     0.87500     0.89583          1.                                        0701
     0.91667     0.93750          1.                                        0701
     0.95833     0.97917          1.                                        0701
     1.00000                                                                0701
   0                                                                        0702
```

CHF Run #43, Mirshak, Durant, & Towell, Ref. DP-355 (1959)

```
! Rectangular channel, down flow, 1-sided heating
!  1   2   3   4   5   6   7   8   9  10  11  12  13  14  15  16  17  18  19  20
   0   0   0   1   0           0   0   0   0   0   0   0   2   1   0   0   0   00200
          1.          1.          1.                                          0201
!  5        0.20         0.5   1         1.0                                  0203
   1   3          0.          1.          1.          1.   0   0              00300
          1.          1.          1.                                          0300A
         1.0                                                                  0303
          1.          1.          0.          0.                              0304
          0.          0.     0.48895          0.   0.0650244 0.003380126      0304
          1.          1.          0.          0.                              0304
          0.          0.          0.                                          0305
   2   0     0.00635      0.4890      3.0e-5         10.      9.7e-4         10.0306
 2.197893e-4   6.4260e-3    0.136808    0.052324    0.065024 0.003380126      0307
 2.197893e-4   6.4260e-3    0.136808    0.052324    0.065024 0.003380126      0307
    0.065024                                                                0308
          1.                                                                0309
    2.152693    2.152693                                                    0310
! 2 x 0.17548 MW = 0.35096 MW
    0.168212          0.    0.168212     0.35096       55.90          0.    0500
          0.          0.                                                    0500
   0      0.0001        32.5          0.          0.                        0600
 -25                                                                        0700
     0.00000     0.02083          1.                                        0701
     0.04167     0.06250          1.                                        0701
     0.08333     0.10417          1.                                        0701
```

```
     0.12500     0.14583          1.                                          0701
     0.16667     0.18750          1.                                          0701
     0.20833     0.22917          1.                                          0701
     0.25000     0.27083          1.                                          0701
     0.29167     0.31250          1.                                          0701
     0.33333     0.35417          1.                                          0701
     0.37500     0.39583          1.                                          0701
     0.41667     0.43750          1.                                          0701
     0.45833     0.47917          1.                                          0701
     0.50000     0.52083          1.                                          0701
     0.54167     0.56250          1.                                          0701
     0.58333     0.60417          1.                                          0701
     0.62500     0.64583          1.                                          0701
     0.66667     0.68750          1.                                          0701
     0.70833     0.72917          1.                                          0701
     0.75000     0.77083          1.                                          0701
     0.79167     0.81250          1.                                          0701
     0.83333     0.85417          1.                                          0701
     0.87500     0.89583          1.                                          0701
     0.91667     0.93750          1.                                          0701
     0.95833     0.97917          1.                                          0701
     1.00000                                                                  0701
   0                                                                          0702


  CHF Run #48, Mirshak, Durant, & Towell, Ref. DP-355 (1959)
! Rectangular channel, down flow, 1-sided heating
!  1   2   3   4   5   6   7   8   9  10  11  12  13  14  15  16  17  18  19  20
   0   0   0   1   0           0   0   0   0   0   0   0   2   1   0   0   0   00200
         1.          1.          1.                                            0201
!  5        0.20         0.5   1         1.0                                   0203
   1   3          0.          1.          1.          1.   0   0               00300
         1.          1.          1.                                            0300A
        1.0                                                                    0303
         1.          1.          0.          0.                                0304
         0.          0.     0.48895          0.   0.0650244   0.0033942        0304
         1.          1.          0.          0.                                0304
         0.          0.          0.                                            0305
   2   0     0.00635     0.48895      3.0e-5         10.      9.7e-4         10.0306
 2.207034e-4    6.452e-3    0.136836    0.052324    0.065024   0.0033942        0307
 2.207034e-4    6.452e-3    0.136836    0.052324    0.065024   0.0033942        0307
    0.065024                                                                   0308
         1.                                                                    0309
    2.503319    2.503319                                                       0310
! 2 x 0.256393 MW = 0.512786 MW
    0.381279          0.    0.381279    0.512786       62.59          0.        0500
         0.          0.                                                        0500
   0      0.0001        32.5          0.          0.                           0600
 -25                                                                           0700
     0.00000     0.02083          1.                                          0701
     0.04167     0.06250          1.                                          0701
     0.08333     0.10417          1.                                          0701
     0.12500     0.14583          1.                                          0701
     0.16667     0.18750          1.                                          0701
     0.20833     0.22917          1.                                          0701
     0.25000     0.27083          1.                                          0701
     0.29167     0.31250          1.                                          0701
     0.33333     0.35417          1.                                          0701
     0.37500     0.39583          1.                                          0701
     0.41667     0.43750          1.                                          0701
     0.45833     0.47917          1.                                          0701
     0.50000     0.52083          1.                                          0701
     0.54167     0.56250          1.                                          0701
```

```
  0.58333     0.60417          1.                                          0701
  0.62500     0.64583          1.                                          0701
  0.66667     0.68750          1.                                          0701
  0.70833     0.72917          1.                                          0701
  0.75000     0.77083          1.                                          0701
  0.79167     0.81250          1.                                          0701
  0.83333     0.85417          1.                                          0701
  0.87500     0.89583          1.                                          0701
  0.91667     0.93750          1.                                          0701
  0.95833     0.97917          1.                                          0701
  1.00000                                                                  0701
0                                                                          0702
```

14 Comparison between PLTEMP/ANL and Hand Calculation for Interpolating the Groeneveld 2006 CHF Tables

14.1 Introduction

This verification work was reported in October 2018. In the critical heat flux (CHF) input options ICHF=5 and ICHF=9, the PLTEMP/ANL code interpolates the Groeneveld 2006 CHF Tables [1] to calculate the CHF at every axial node in all coolant channels of all fuel assemblies in the reactor. This chapter documents a comparison between the code-calculated and hand-calculated values of the CHF at a location in the Standard Problem 12 of the verification script (input file shown in Fig. 2.8, filename *input.Stdproblem12.HEATinCladandFuel*). The comparison gives a verification of the technique used in the code for interpolating the Groeneveld 2006 CHF Tables.

14.2 PLTEMP/ANL-Calculated CHF for a Standard Test Problem

The critical heat flux (CHF) for the Standard Problem 12 of the verification script is calculated using the Groeneveld 2006 CHF tables, by running the PLTEMP/ANL V4.2 code. Figure 14.1 is a portion of the output file, showing the temperature, pressure and CHF in fuel assembly 1 of the problem. The CHF at the exit (i.e., axial node 10) of channel 1 located on the left hand side of fuel plate 1, using option ICHF=5, is 4.511 MW/m^2 (marked in red in Fig. 14.1). For comparison with this code-calculated value, the CHF at this location is found below by hand calculation.

14.3 Hand Calculation of CHF

Interpolation of the CHF Tables for 8 mm Tube: In the Groeneveld 2006 CHF Tables, the critical heat flux is a function of three thermal-hydraulic parameters in the channel at the location of CHF occurrence: coolant pressure, mass flux and quality. These three parameters are determined below at coolant channel 1 exit, using the data in the test problem input data file, and the temperatures, pressures, and flow rates calculated and printed by PLTEMP/ANL. The required properties of the coolant are obtained from the code output and the NIST water properties available on the world wide web.

Flow rate in channel 1 (from PLTEMP/ANL output) = 0.25 kg/s
Flow area in channel 1 = 6.0×10^{-4} m^2
Coolant mass flux = $0.25/6.0\times10^{-4}$ = **416.67 kg/s-m^2**
Inlet temperature = 45 ºC
Channel 1 exit temperature (from PLTEMP/ANL output) = 96.074 ºC
Pressure in axial node 10 (from PLTEMP/ANL output) = 325.26 kPa
Exit pressure in channel 1 (from PLTEMP/ANL output) = **323.36 kPa**

Temperature, ºC	Coolant Enthalpy from PLTEMP/ANL Output, kJ/kg	Interpolated Enthalpy, kJ/kg
91.00	381.185	
98.00	410.754	
Channel 1 exit temperature, 96.074		402.618

Coolant enthalpy (H) at channel 1 exit = 381.185 + 5.074 ×(410.754 – 381.185)/7.00
= 402.618 kJ/kg
Saturation temperature = 136.10 ºC
Saturated liquid enthalpy (H_f) at the exit pressure (from NIST) = 572.44 kJ/kg
Saturated vapor enthalpy (H_g) at the exit pressure (from NIST) = 2728.3 kJ/kg
Enthalpy of evaporation (H_{fg}) at the exit pressure (from NIST) = 2728.3 – 572.44
= 2155.86 kJ/kg
Quality (X) of the coolant at channel 1 exit = $(H - H_{sat})/H_{fg}$ = (402.618 – 572.44)/2155.86
= **- 0.0787723**

As mentioned above, in the Groeneveld 2006 CHF Tables, the critical heat flux is a function of three parameters at the location of CHF occurrence: coolant pressure, mass flux and quality. These three parameters were calculated above, and they are:
P = 323.36 kPa,
G = 416.67 kg/s-m^2 and
X = -0.0787723 .
The pertinent part of the Groeneveld 2006 CHF Tables, required for interpolating the value of CHF at these values of the three parameters, are collected together in cases 1 to 4 of Table 14.1. Also shown in Table 14.1 are the results of interpolation obtained (cases 5 to 8) to get the final value of CHF (case 9) at pressure 323.36 kPa, mass flux 416.67 kg/s-m^2 and quality - 0.0787723.

Interpolate mass flux between cases 1 and 2 to get case 5, as follows.
q_c(P=300.00,G=416.67,X=-0.10) = 4107 + (4134 – 4107)*(416.67 – 300.0)/(500.0 – 300.0)
= 4107 + (4134 – 4107)*0.58335 = 4122.750 kW/m^2

q_c(P=300.00,G=416.67,X=-0.05) = 3429 + (3563 – 3429)*0.58335 = 3507.169 kW/m^2

Interpolate between the two qualities of case 5 to get case 6.
q_c(P=300.00,G=416.67,X=-0.07877)
= 4122.750 + (3507.169 – 4122.750)*(-0.0787723 + 0.10)/(-0.05 + 0.10)
= 4122.750 + (3507.169 – 4122.750)*0.424554 = 3861.403 kW/m^2

Interpolate mass flux between cases 3 and 4 to get case 7, as follows.
q_c(P=500.00,G=416.67,X=-0.10) = 4193 + (4281 – 4193)*(416.67 – 300.0)/(500.0 – 300.0)
= 4193 + (4281 – 4193)*0.58335 = 4244.335 kW/m^2

q_c(P=500.00,G=416.67,X=-0.05) = 3498 + (3671 – 3498)*0.58335 = 3598.920 kW/m^2

Interpolate between the two qualities of case 7 to get case 8.
q_c(P=500.00,G=416.67,X=-0.07877)

$= 4244.335 + (3598.920 – 4244.335)*0.424554 = 3970.321$ kW/m^2

Interpolate pressure between cases 6 and 8 to get case 9.
q_c(P=323.36,G=416.67,X=-0.07877)
$= 3861.403 + (3970.321 – 3861.403)*(323.36 – 300.0)/(500.0 – 300.0)$
$= 3861.403 + (3970.321 – 3861.403)*0.1168 =$ <u>3874.125 kW/m^2</u>
Diameter Correction: The above-calculated critical heat flux, 3874.125 kW/m^2, is for a circular tube of inner diameter 8 mm. In order to get the CHF for a coolant channel of a different hydraulic diameter D, the following diameter correction is applied to the above CHF.

CHF for hydraulic diameter D = $q_c(P, G, X)*(0.008/D)^{0.5}$

The hydraulic diameter of channel 1 is 5.91133×10^{-3} m, and the CHF at the exit of channel 1 is found to be

q_c(P=323.36, G=416.67, X=-0.07877, D=0.00591133)
$= q_c$(P=323.36,G=416.67,X=-0.07877)$*(0.008/0.00591133)^{0.5}$
$= 3874.125*(0.008/0.00591133)^{0.5} = 4506.880$ kW/m^2 = <u>4.507 MW/m^2</u>

14.4 Comparison between Hand and PLTEMP/ANL Calculations

There is a difference of 0.09% between the code-calculated CHF of 4.511 MW/m^2 in axial node 10 of channel 1 and the hand-calculated CHF of 4.507 MW/m^2 at channel 1 exit. This comparison provides a verification of the technique used in PLTEMP/ANL for interpolating the Groeneveld 2006 CHF Tables, for input options ICHF=5 and ICHF=9.

14.5 REFERENCES

1. D. C. Groeneveld et al., “The 2006 CHF Look-up Table,” Nuclear Engineering and Design, 237, pp. 1909-1922 (2007).

Figure 14.1. A Part of the PLTEMP/ANL Output File Showing the CHFs for Fuel Assembly 1 of Standard Problem 12

FUEL PLATE 1 (ExactSoln), Assembly = 1 of Type = 1

NODE	COOLANTl (C)	CladSl (C)	FUEL PEAK (C)	CladSr (C)	COOLANTr (C)	HCOFl W/C-m^2	HCOFr W/C-m^2	ONBRl [F Note 1]	ONBRr	ETA'l K-cm^3/J [Note 3]	ETA'r K-cm^3/J [Note 3]	ONB Temp left(C)	ONB Temp right(C)	Avg Meat Temp (C)
	45.000				45.000									
1	47.083	117.201	129.231	105.239	47.725	4.1386E+03	7.1254E+03	1.37	1.65	1.365E+02	1.919E+02	143.764	144.470	122.886
2	51.462	125.734	139.104	113.100	53.422	4.3107E+03	7.4819E+03	1.22	1.46	1.173E+02	1.645E+02	143.601	144.316	132.195
3	56.269	134.307	149.051	121.079	59.610	4.4918E+03	7.8544E+03	1.10	1.30	1.009E+02	1.405E+02	143.430	144.150	141.582
4	61.505	143.171	159.253	129.260	66.284	4.6585E+03	8.2501E+03	1.00	1.17	8.662E+01	1.190E+02	143.247	143.978	151.215
5	67.161	152.417	169.825	137.793	73.444	4.8116E+03	8.6473E+03	0.91	1.06	7.405E+01	9.954E+01	143.055	143.799	161.216
6	73.049	156.518	174.232	142.614	80.823	4.9577E+03	8.9472E+03	0.88	1.01	6.693E+01	8.818E+01	142.713	143.424	165.677
7	78.783	155.348	172.226	143.298	87.900	5.0905E+03	9.2104E+03	0.88	1.00	6.435E+01	8.305E+01	142.213	142.856	164.323
8	84.163	154.285	170.286	143.985	94.420	5.2076E+03	9.4456E+03	0.88	0.98	6.193E+01	7.790E+01	141.700	142.275	163.024
9	89.183	153.202	168.288	144.552	100.391	5.3123E+03	9.6595E+03	0.89	0.97	5.969E+01	7.274E+01	141.174	141.681	161.655
10	93.838	152.017	166.157	144.939	105.817	5.4077E+03	9.8508E+03	0.89	0.96	5.766E+01	6.760E+01	140.634	141.072	160.145
	96.074				108.394									152.392

……

……

CRITICAL HEAT FLUX RATIO (CHFR) BY NODE IN ASSEMBLY 1 OF TYPE 1 : NOMINAL CASE
Based on Groeneveld CHF Table

Axial Node	CHFR	CHF MW/m^2	Ht Flx MW/m^2	CHFR	CHF MW/m^2	Ht Flx MW/m^2	CHFR	CHF MW/m^2	Ht Flx MW/m^2	CHFR	CHF MW/m^2	Ht Flx MW/m^2	CHFR	CHF MW/m^2	Ht Flx MW/m^2	CHFR	CHF MW/m^2	Ht Flx MW/m^2
	<--Plate	1 Left Side--->		<--Plate	1 Right Side-->		<--Plate	2 Left Side--->		<--Plate	2 Right Side-->		<--Plate	3 Left Side--->		<--Plate	3 Right Side-->	
1	2.475E+1	7.182	0.2902	1.956E+1	8.014	0.4098	2.292E+1	8.014	0.3497	2.298E+1	8.048	0.3503	2.298E+1	8.048	0.3503	2.292E+1	8.014	0.3497
2	2.167E+1	6.938	0.3202	1.678E+1	7.494	0.4465	1.959E+1	7.494	0.3825	1.969E+1	7.563	0.3842	1.969E+1	7.563	0.3842	1.959E+1	7.494	0.3825
3	1.903E+1	6.672	0.3505	1.436E+1	6.933	0.4828	1.670E+1	6.933	0.4151	1.683E+1	7.038	0.4182	1.683E+1	7.038	0.4182	1.670E+1	6.933	0.4151
4	1.672E+1	6.360	0.3804	1.234E+1	6.411	0.5196	1.432E+1	6.411	0.4478	1.445E+1	6.534	0.4522	1.445E+1	6.534	0.4522	1.432E+1	6.411	0.4478
5	1.452E+1	5.956	0.4102	1.053E+1	5.858	0.5565	1.220E+1	5.858	0.4802	1.236E+1	6.013	0.4865	1.236E+1	6.013	0.4865	1.220E+1	5.858	0.4802
6	1.341E+1	5.548	0.4138	9.603E+0	5.309	0.5529	1.108E+1	5.309	0.4792	1.127E+1	5.492	0.4875	1.127E+1	5.492	0.4875	1.108E+1	5.309	0.4792
7	1.325E+1	5.163	0.3898	9.786E+0	4.993	0.5102	1.122E+1	4.993	0.4449	1.114E+1	5.070	0.4551	1.114E+1	5.070	0.4551	1.122E+1	4.993	0.4449
8	1.317E+1	4.811	0.3652	1.029E+1	4.817	0.4682	1.173E+1	4.817	0.4106	1.159E+1	4.899	0.4227	1.159E+1	4.899	0.4227	1.173E+1	4.817	0.4106
9	1.370E+1	4.659	0.3401	1.091E+1	4.653	0.4266	1.236E+1	4.653	0.3766	1.215E+1	4.741	0.3900	1.215E+1	4.741	0.3900	1.236E+1	4.653	0.3766
10	1.434E+1	4.511	0.3146	1.167E+1	4.497	0.3854	1.312E+1	4.497	0.3428	1.284E+1	4.587	0.3572	1.284E+1	4.587	0.3572	1.312E+1	4.497	0.3428

Axial Node	CHFR	CHF MW/m^2	Ht Flx MW/m^2	CHFR	CHF MW/m^2	Ht Flx MW/m^2	CHFR	CHF MW/m^2	Ht Flx MW/m^2	CHFR	CHF MW/m^2	Ht Flx MW/m^2	CHFR	CHF MW/m^2	Ht Flx MW/m^2	CHFR	CHF MW/m^2	Ht Flx MW/m^2
	<--Plate	4 Left Side--->		<--Plate	4 Right Side-->		<--Plate	5 Left Side--->		<--Plate	5 Right Side-->		<--Plate	6 Left Side--->		<--Plate	6 Right Side-->	
1	1.956E+1	8.014	0.4098	2.475E+1	7.182	0.2902												
2	1.678E+1	7.494	0.4465	2.167E+1	6.938	0.3202												
3	1.436E+1	6.933	0.4828	1.903E+1	6.672	0.3505												
4	1.234E+1	6.411	0.5196	1.672E+1	6.360	0.3804												
5	1.053E+1	5.858	0.5565	1.452E+1	5.956	0.4102												
6	9.603E+0	5.309	0.5529	1.341E+1	5.548	0.4138												
7	9.786E+0	4.993	0.5102	1.325E+1	5.163	0.3898												
8	1.029E+1	4.817	0.4682	1.317E+1	4.811	0.3652												
9	1.091E+1	4.653	0.4266	1.370E+1	4.659	0.3401												
10	1.167E+1	4.497	0.3854	1.434E+1	4.511	0.3146												

MINIMUM CHFR IN THIS ASSEMBLY = 9.603 OCCURS AT RIGHT SURFACE OF PLATE 1 IN AXIAL NODE 6 (FUEL ELEMENT 1 OF TYPE 1) FROM GROENEVELD CHF TABLE.

Figure 14.1. Continued

```
.................
.................
FUEL PLATE   1 (ExactSoln)   AREAL                          FUEL-CLADinterface                                                Assembly  1 of Type  1
NODE FLUX left  FLUX right  FUEL X   Tsat     Tdiff     left      right    Pressure  CHF (MW/m^2)     CHF RATIO       Z-mid   Z-int
       MW/m^2     MW/m^2     left    (C)       (C)       (C)       (C)      (bar)    left    right   left    right
                                                        [Note 2]  [Note 2]
   1 2.9019E-01 4.0981E-01  0.4146 139.815             117.201   105.239   3.59460   7.182   8.014 2.475E+1 1.956E+1  0.0500  0.1000
   2 3.2016E-01 4.4650E-01  0.4176 139.441             125.734   113.100   3.55660   6.938   7.494 2.167E+1 1.678E+1  0.1500  0.2000
   3 3.5053E-01 4.8281E-01  0.4206 139.063             134.307   121.079   3.51860   6.672   6.933 1.903E+1 1.436E+1  0.2500  0.3000
   4 3.8044E-01 5.1956E-01  0.4227 138.681             143.171   129.260   3.48060   6.360   6.411 1.672E+1 1.234E+1  0.3500  0.4000
   5 4.1021E-01 5.5645E-01  0.4244 138.296             152.417   137.793   3.44260   5.956   5.858 1.452E+1 1.053E+1  0.4500  0.5000
   6 4.1381E-01 5.5285E-01  0.4281 137.908             156.518   142.614   3.40460   5.548   5.309 1.341E+1 9.603E+0  0.5500  0.6000
   7 3.8975E-01 5.1025E-01  0.4331 137.516             155.348   143.299   3.36660   5.163   4.993 1.325E+1 9.786E+0  0.6500  0.7000
   8 3.6517E-01 4.6817E-01  0.4382 137.121             154.285   143.985   3.32860   4.811   4.817 1.317E+1 1.029E+1  0.7500  0.8000
   9 3.4009E-01 4.2658E-01  0.4436 136.722             153.202   144.552   3.29060   4.659   4.653 1.370E+1 1.091E+1  0.8500  0.9000
  10 3.1461E-01 3.8539E-01  0.4494 136.319             152.017   144.939   3.25260   4.511   4.497 1.434E+1 1.167E+1  0.9500  1.0000
```

Table 14.1. Part of Groeneveld 2006 CHF Table and Results of Interpolation by Hand Calculation of CHF at Channel 1 Exit

Case	Pressure kPa	Mass Flux kg/m^2-s	Quality = -0.10	Quality = -0.05	Quality = 0.0787723
			CHF, kW/m^2		
1	300.00	300.0	4107	3429	
2	300.00	500.0	4134	3563	
3	500.00	300.0	4193	3498	
4	500.00	500.0	4281	3671	
5	300.00	416.67	4122.750	3507.169	
6	300.00	416.67			3861.403
7	500.00	416.67	4244.335	3598.920	
8	500.00	416.67			3970.321
9	323.36	416.67			4506.880

15 Verification of Pressure Drops during Subcooled Nucleate Boiling by Comparison with the RELAP5 Code

The PLTEMP/ANL [1] code hydraulics model does not include the effects of boiling on the hydraulic resistance. A concern is that when these effects are included the power at which flow instability is predicted to first occur may be reduced. A single-channel test problem was analyzed with both PLTEMP/ANL V4.1 and RELAP5-3D [2]. Pressure drop as a function of flow rate for a fixed channel power of 200 kW and an exit pressure of 5 bar was predicted with both codes. A flow versus pressure drop relationship based on experimental data, that is independent of both codes and believed to be reasonably reliable, predicts the minimum stable flow rate to be about 0.63 kg/s for the channel of the test problem. The results show that for flow rates at or above the predicted minimum stable flow RELAP5 and PLTEMP/ANL pressure drops agree extremely well, with RELAP5 predicting 1.6% more pressure drop at the highest flow, which has no boiling, and 4.2% more at the flow expected to be the minimum stable flow. Thus, for this test case, the exclusion of the effects of boiling in the PLTEMP/ANL hydraulics model has only a minor adverse impact on the prediction of the power level at which flow instability is expected to first occur.

15.1 Background

The PLTEMP/ANL code hydraulics model is based on single-phase flow with no consideration for subcooled nucleate boiling. This model is completely appropriate for conditions from zero power up to conditions that lead to the onset of nucleate boiling. Subcooled nucleate boiling can cause increased hydraulic resistance in the fuel channels where this boiling is occurring and thereby lead to reduced flow rates in these potentially limiting channels. A lower channel flow rate would, in turn, result in higher coolant temperatures in the channel and cause flow instability to occur at a lower power level than it would otherwise occur. If flow instability occurs, fuel damage is highly likely. Thus, the potential increased hydraulic resistance between the onset of nucleate boiling and the onset of flow instability is of concern. Although there are plans to modify the PLTEMP/ANL code to include the effects of subcooled nucleate boiling on hydraulic resistance, in the interim it is highly desirable to obtain a quick assessment of the potential impact on past and ongoing analyses. Accordingly, it was decided to compare PLTEMP/ANL hydraulic results for a single channel operating at a fixed power with those obtained with RELAP5. Moreover, the exact data generated for this comparison could be used to aid the planned improvement to the PTEMP code.

Table 15.1 Key Parameters

Parameter	Value
Channel Thickness, in.	0.080
Channel Width, in.	2.00
Channel Length, in.	24.0
Heated Width, in.	2.00
Heated Length, in.	24.0
Flow Direction	Upward
Inlet Temperature, C	60
Outlet Pressure, bar	5.0
Power Shape	Uniform
Inlet & Outlet Form Losses	0.0
Hot Channel Factors (All)	1.0
Channel Power, kW	200

15.2 Test Case

The reactor conditions chosen for the test case are shown in Table 15.1. The coolant flow in the channel is in the upward direction rather than downward. A single heated channel that is symmetrically heated by two fuel plates is represented with each code. In both the PLTEMP/ANL and RELAP5 models, the 24-inch heated length was divided into 24 1-inch axial segments. The full 2-inch by 24-inch width of each fuel plate was assumed to be uniformly heated.

15.3 Solution Procedure and Results

The results are presented in Table 15.2 and Fig. 15.1. In all cases the channel power was assumed to be 200 kW. The analysis was performed by first selecting a friction pressure drop for PLTEMP/ANL and guessing an inlet pressure at the bottom of the channel that would produce an outlet pressure of exactly 5 bar at the top of the channel. If the desired exact outlet pressure was not achieved, the inlet pressure was adjusted and the case was rerun. The reason for this guesswork is that the pressure drop provided in the input does not include the gravity pressure drop portion of the pressure difference between the inlet and the outlet. For example, when a friction pressure drop of 60 kPa was requested, the difference between the inlet and outlet pressures was 65.756 kPa. The extra 5.765 kPa was caused by the inlet being 24 inches below the outlet, and is the gravity pressure drop from the inlet to the outlet. The code output provides the pressure at the center of each layer, or node, including the effects of gravity. A small modification to Reference 0 of the PLTEMP/ANL version 3.5 code was made by one of the code authors to enable it to output the pressure at the inlet of the first node and the outlet of the last node.

Table 15.2 Pressure Drop vs. Flow

	PLTEMP/ANL		RELAP5			
Flow, kg/s	Pressure Drop*, kPa	Boiling	Pressure Drop*, kPa	Boiling	Gravity Pressure Drop, kPa	Exit Void Fraction, %
1.1800	185.8	no	188.8	no	5.80	0.0
1.0285	145.8	no	148.5	yes	5.79	0.0
0.9454	125.8	no	128.3	yes	5.78	0.0
0.7576	85.8	yes	87.9	yes	5.75	0.0
0.6476	65.8	yes	67.6	yes	5.73	0.0
0.6264	62.2	yes	64.8	yes	5.72	2.0
0.6000			62.4	yes	5.69	7.2
0.5600			62.0	yes	5.61	22.5
0.5400			63.6	yes	5.54	32.9
0.5300			65.0	yes	5.49	38.5
0.5250			65.9	yes	5.47	41.5
0.5200			No Stable Solution			
0.5194	45.7	yes				

*Inlet pressure minus outlet pressure, including effects of differences in elevation.

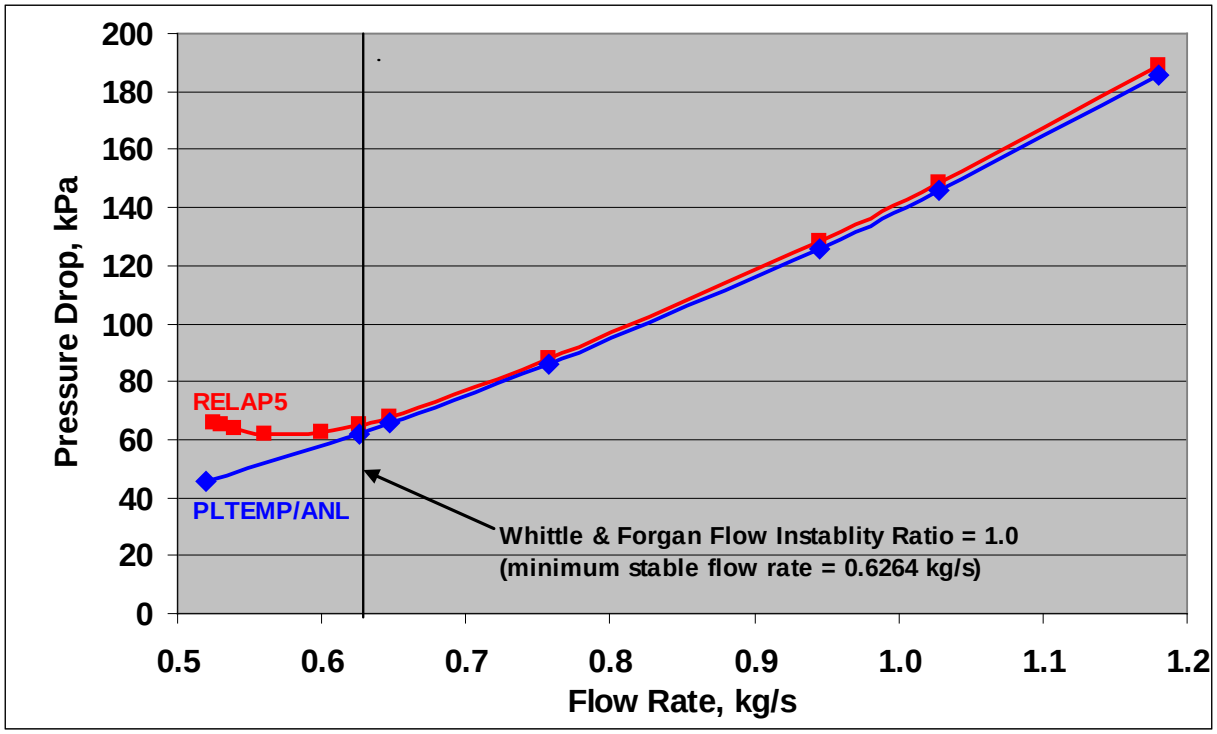

Figure 15.1 Pressure Drop vs. Flow at 200 kW per Channel and 5.0 bar Exit Pressure

The flow rate obtained from each PLTEMP/ANL solution was used as the input flow to the RELAP5 model. RELAP5 allows the exit pressure to be specified as 5 bar and determined the corresponding value of the inlet pressure, which was used to obtain the pressure difference between the inlet and the outlet. This pressure difference includes the effects of gravity. Since RELAP5 provides the coolant density at each of the 24 axial layers, it was a simple matter to calculate the gravity pressure drop as the sum over all 24 axial layers of the product of coolant density times the acceleration due to gravity (9.80655 m/s^2) times the thickness of the layer (1 inch). The gravity pressure drops are provided in the second to last column of Table 15.2.

The presence of boiling anywhere in the channel is also indicated in Table 15.2 for each of the two sets of results. The onset of nucleate boiling is predicted in the PLTEMP/ANL code by the Bergles and Rohsenow correlation [3]. The RELAP5 code outputs an integer to denote the flow region. A "yes" in Table 15.2 signifies the presence of boiling at at least one of the 24 axial nodes. Thus, there was no boiling predicted only for the highest flow when RELAP5 was used and only for the highest three flows when PLTEMP/ANL was used.

The lowest Reynolds number observed for the lowest flow rate studied is greater than 40,000. Thus, the flow is turbulent at all axial levels in all of the cases.

15.4 Analysis

The pressure drop in Fig. 15.1 is the difference between the inlet and outlet pressures, as tabulated in Table 15.2. The range of interest for the current comparison is from the highest flow down to the onset of flow instability. This limiting stability flow rate was predicted by the Whittle and

Forgan correlation [4] via PLTEMP/ANL, with the internal η parameter set to 32.5, as recommended by Reference 5. The 0.6264 kg/s instability flow value calculated by PLTEMP/ANL was carefully verified by hand. The hand calculation produced a value of 0.6282 kg/s, which demonstrates very good agreement with PLTEMP/ANL.

The PLTEMP/ANL flow decreases monotonically with pressure drop, as is expected when the boiling is not included in the model. The RELAP5 results between 0.5200 and 0.6000 kg/s, which have no PLTEMP/ANL counterpart, were included to study the behavior of RELAP5 in this region. As indicated in the last column of Table 15.2, RELAP5 predicts an increase in the exit void fraction as the flow is decreased from 0.6264 kg/s. The lowest flow rate for which RELAP5 provided a stable solution is 0.5250 kg/s. This case has an exit void fraction of 41.5 %. The increasing volume of vapor with decreasing flow rate causes the pressure drop to have a local minimum value at or near 0.5600 kg/s. Since past experience has shown the Reference 4 flow stability criterion to be reasonably reliable, there is good reason to question the stable flow results predicted by RELAP5 for flows below 0.6264 kg/s, the lowest stable flow predicted by PLTEMP/ANL. Moreover, RELAP5 is known to have difficulty accurately predicting flows at pressures far below the 70 to 140 bar range where water-cooled power reactors typically operate.

At the flow rate where Reference 4 predicts flow instability, the RELAP5 pressure drop is only 4.2% greater than the PLTEMP/ANL one. At the highest flow rate, where neither code predicts boiling, the RELAP5 pressure drop is 1.6% greater than the PLTEMP/ANL one. Thus, if the differences between the two codes that are not related to boiling are taken into account, then the RELAP5 results indicates that at the point of flow instability the PLTEMP/ANL pressure drop should be increased by 4.2% − 1.6%, or 2.6%. Since pressure drop is approximately proportional to the square of flow rate, increasing the pressure drop by 2.3% is approximately equivalent to increasing the flow rate by 2.6%/2, or 1.3%. Thus, flow instability would occur at a flow rate that is about 1.3% higher than PLTEMP/ANL is predicting. The precise value of this difference is not important. What is important and very encouraging is that the PLTEMP/ANL and RELAP5 pressure drops agree very well for all flows at or above the one where flow instability is predicted by Reference 4 to occur. Had there been a large increase in pressure drop due to subcooled nucleate boiling predicted by RELAP5 at flows above, but near, the instability flow predicted by Reference 4, there would be reason for considerable concern. The concern would have been that flow instability occurs at power levels much lower than those indicated by PLTEMP/ANL.

15.5 Conclusions

The very good agreement in pressure drop between RELAP5 and PLTEMP/ANL, shown in Fig. 15.1, for flow rates above the one where Reference 4 predicts flow instability to occur support the conclusion that the increased hydraulic resistance expected due to boiling probably will not have a major adverse impact on the power at which PLTEMP/ANL predicts flow instability to occur. Thus, plans to improve the PLTEMP/ANL code in this area are not on the critical path with regard to future reactor conversions from HEU to LEU fuel.

15.6 REFERENCES:

1. A. P. Olson and M. Kalimullah, "A User's Guide to the PLTEMP/ANL Code," ANL/RERTR/TM-11-22, Version 4.1, Argonne National Laboratory, 9700 South Cass Avenue, Argonne, IL 60439, USA (April 6, 2011).
2. The RELAP5-3D© Code Development Team, RELAP5-3D© Code Manual, Version 2.3, INEEL-EXT-98-00834, Idaho National Laboratory, April 2005.
3. A. E. Bergles and W. M. Rohsenow, "The Determination of Forced-Convection Surface-Boiling Heat Transfers," Trans. ASME, J. Heat Transfer **86**, 365 (1964).
4. R. H. Whittle and R. Forgan, "A Correlation for the Minima in the Pressure Drop Versus Flow-Rate Curves for Sub-Cooled Water Flowing in Narrow Heated Channels," *Nuclear Engineering and Design*, 1967.
5. A. P. Olson, "Analysis of Flow Excursion Experiments Relevant to Research Reactors," 2006 International Meeting on Reduced Enrichment for Research and Test Reactors, October 29-November 3, 2006, Cape Town, South Africa.

16 Verification of the PLTEMP/ANL Capability to Model a Solid Fuel Rod at the Center of a Fuel Assembly of Nested Fuel Tubes

16.1 Introduction

PLTEMP/ANL version 4.2 was verified for the 29 test problems in the verification script. The results for all 29 test problems in the script were found to be in good agreement with the stored results. Additional verification of this version for four test problems (listed below), with and without a pinhole at the fuel pellet center, is documented in this chapter. A good agreement is found in all comparisons.

(1) Comparison of the results of PLTEMP/ANL with Excel spreadsheet steady-state solution for a six-tube Test Problem 1 (input filename *problem1.without.pinhole.inp*).
(2) Comparison of the results of PLTEMP/ANL with Excel spreadsheet steady-state solution for a six-tube Test Problem 2 (input filename *problem2.with.pinhole.inp*).
(3) Comparison of the results of PLTEMP/ANL with Excel spreadsheet steady-state solution for a six-tube Test Problem 3 which is modeled by two input data files, with the tube radii in the increasing and the decreasing orders (input filenames *problem3.with.pinhole-20.inp* and *problem3.decRMID.with.pinhole-20.inp*).

The capability to model a solid fuel rod at the center of a fuel assembly of nested fuel tubes in two versions of the PLTEMP/ANL code, the version 42bta_r65_131030 and the version 4.2 under development, were verified. This capability is available in all later code versions, including the PLTEMP/ANL V4.3 code.

16.2 Comparison of PLTEMP with an Independent Method

The code's solution is verified against a solution obtained by an independent method of solving the problem. To do this, two simpler test problems (referred to as Problems 1 and 2 whose input data files are shown in Figs. 16.2 and 16.3) consisting of six fuel tubes are solved on the spreadsheet using a different method, which consists of minimizing the error in the areal fractions on the left side of the adiabatic point in each tube's fuel meat. In Problem 1, the innermost coolant channel inside the innermost fuel tube has a finite flow area whereas Problem 2 models a solid fuel rod at the center assuming the innermost coolant channel to be a pinhole. The independent method is described in Section 16.2.1. Section 16.2.2 describes the solution of these test problems by the independent method. PLTEMP input data files prepared for these problems are run and compared with the solutions by the independent method. The verification of two versions of the PLTEMP/ANL code, the version 42bta_r65_131030 and the version 4.2 under development, is described in Section 16.2.3.

For Problem 1 without pinhole, the RMS difference between the code-calculated and the spreadsheet-calculated temperatures (of the coolant at channel exit, the tube surface temperatures at mid-core height, and the meat maximum temperature at mid-core height) is 0.11 ºC. For Test Problem 2 with pinhole, the difference between the code-calculated and the spreadsheet-calculated temperatures (of the coolant at channel exit, the tube surface temperatures at mid-core height, and the meat maximum temperature at mid-core height) is 0.048 ºC.

These comparisons provide a verification of PLTEMP/ANL version 42bta_r65_131030 and the version 4.2.

16.2.1 An Independent Method of Calculating Steady-State Temperature Distribution in a Fuel Assembly Consisting of Six Fuel Tubes

Figure 16.1 shows a vertical section of a fuel assembly made of 6 nested fuel tubes, each made of a single material (fuel meat). The method assumes constant coolant thermal properties (specific heat and density), constant thermal conductivities of fuel and cladding, no axial conduction, and uniform power density in the meat of each fuel tube. The coolant flow rates in the 7 channels and the convective heat transfer coefficients at the surface of fuel tubes are assumed to be given constants. These assumptions provide a set of 6 linear algebraic thermal-hydraulic equations for the six variables f_i (i = 1, 2, 3 … 6) defined below. The temperatures of the coolant and fuel tube are calculated at the staggered points, as shown in Fig. 16.1. These equations are solved on the Excel spreadsheet to obtain an independent calculation of the steady-state temperature distribution.

f_i = Areal fraction on the left side or inside of the adiabatic point in the fuel meat of fuel tube i
K_i = Thermal conductivity of fuel tube i
W_i = Coolant flow rate in channel i
R_{1i} = Radius of the inner or left surface of fuel tube i
R_{2i} = Radius of the outer or right surface of fuel tube i
H_{1i} = Convective heat transfer coefficient at the inner or left surface of fuel tube i
H_{2i} = Convective heat transfer coefficient at the outer or right surface of fuel tube i
T_{fmi} = Fuel meat maximum temperature at the adiabatic point in tube i (i = 1, 2, 3 … 6)
T_{s1i} = Surface temperature on the left side of fuel plate i (i = 1, 2, 3 … 6)
T_{s2i} = Surface temperature on the right side of fuel plate i (i = 1, 2, 3 … 6)
T_0 = Coolant inlet temperature
$T_{i,1}$ = Coolant temperature at the exit of axial interval ΔZ of channel i (i = 1, 2, 3 … 7)
$T_{i,c1}$ = Coolant temperature at the center of axial interval ΔZ of channel i (i = 1, 2, 3 … 7)
q_i = Volumetric heat source in fuel tube i

The power generated Q_i in an axial interval ΔZ of fuel tube i is given by

$$Q_i = \pi(R_{2i}^2 - R_{1i}^2)\,\Delta Z\, q_i \quad (i = 1, 2, 3, \ldots 6) \tag{16.1}$$

The temperature rise in channel i is determined by the heat coming from the right surface of tube i-1 and the heat from the left surface of tube i.

$$T_{i,1} = T_0 + \frac{(1-f_{i-1})Q_{i-1} + f_i Q_i}{W_i\, C_p} \quad (i = 1, 2, 3 \ldots 7), \qquad \text{where } Q_0 = Q_7 = 0 \tag{16.2}$$

The coolant temperature in channel i at the *center* of the axial interval ΔZ is given by the average of the inlet temperature T_0 and the axial interval exit temperature $T_{i,1}$, as shown by Eq. (16.3).

$$T_{i,c1} = \frac{T_0 + T_{i,1}}{2} \quad (i = 1, 2, 3 \ldots 7) \tag{16.3}$$

The left surface temperature of tube i at the *center* of axial interval ΔZ is the sum of the coolant temperature at the center $T_{i,c1}$ and the surface-to-bulk coolant temperature difference. The latter equals the heat flux on the surface divided by the convective heat transfer coefficient. The heat flux on the left surface of tube i is given by Eq. (16.4), and the heat flux on the right surface of tube i is given by Eq. (16.5).

$$q''_{1i} = \frac{f_i q_i \left(R_{2i}{}^2 - R_{1i}{}^2\right)}{2 R_{1i}} \qquad (i = 1, 2, 3 \ldots 6) \tag{16.4}$$

$$q''_{2i} = \frac{(1 - f_i) q_i \left(R_{2i}{}^2 - R_{1i}{}^2\right)}{2 R_{2i}} \qquad (i = 1, 2, 3 \ldots 6) \tag{16.5}$$

Using Eqs. (16.3) to (16.5), the fuel tube temperature on the left and the right surfaces of tube i are given by Eqs. (16.6) and (16.7). These surface temperatures provide the two boundary conditions required below in the solution of the radial heat conduction equation in the fuel tube.

$$T_{s1i} = \frac{T_0 + T_{i,1}}{2} + \frac{f_i q_i \left(R_{2i}{}^2 - R_{1i}{}^2\right)}{2 R_{1i} H_{1i}} \qquad (i = 1, 2, 3 \ldots 6) \tag{16.6}$$

$$T_{s2i} = \frac{T_0 + T_{i+1,1}}{2} + \frac{(1 - f_i) q_i \left(R_{2i}{}^2 - R_{1i}{}^2\right)}{2 R_{2i} H_{2i}} \qquad (i = 1, 2, 3 \ldots 6) \tag{16.7}$$

Equation (16.8) is the radial heat conduction equation in fuel tube i, and Eq. (16.9) is its solution.

$$\frac{d}{dr}\left(r \frac{dT_{fi}}{dr}\right) = -\frac{r q_i}{K_i} \tag{16.8}$$

$$T_{f\,i}(r) = C_{1i} \ln(r) + C_{2i} - \frac{q_i^2}{4 K_i} \tag{16.9}$$

The arbitrary constants of integration C_{1i} and C_{2i} are found using the boundary conditions at the tube surface on the left and right sides, given by Eq. (16.10). The constants of integration C_{1i} and C_{2i} are given by Eqs. (16.11) and (16.12).

$$T_{fi}(R_{1i}) = T_{s1i}\,, \qquad \text{and} \qquad T_{fi}(R_{2i}) = T_{s2i} \tag{16.10}$$

$$C_{1i} = \frac{T_{s2i} - T_{s1i} + \frac{q_i}{4 K_1}\left(R_{2i}{}^2 - R_{1i}{}^2\right)}{\ln\left(R_{2i}/R_{1i}\right)} \tag{16.11}$$

$$C_{2i} = \frac{T_{s1i}\ln(R_{2i}) - T_{s2i}\ln(R_{1i}) + \frac{q_i}{4K_1}\left(R_{1i}^{\ 2}\ln(R_{2i}) - R_{2i}^{\ 2}\ln(R_{1i})\right)}{\ln\left(R_{2i}/R_{1i}\right)} \tag{16.12}$$

Setting the derivative $\frac{dT_{fi}}{dr}$ of meat temperature obtained from Eq. (16.9) to zero, the radial position $R_{m,i}$ of the maximum meat temperature is given by Eq. (16.13). Using Eq. (16.13), the areal fraction f_i is given by Eq. (16.14). The symbol $f_{calc,i}$ is used in Eq. (16.14) for the areal fractions, to recognize that its value will be different from that of the symbol f_i assumed at the beginning of the derivation of equations (see Eq. (16.2)).

$$R_{m,i}^{\ 2} = \frac{2K_i C_{1i}}{q_i} \tag{16.13}$$

$$f_{calc,i} = \frac{R_{m,i}^{\ 2} - R_{1,i}^{\ 2}}{R_{2,i}^{\ 2} - R_{1,i}^{\ 2}} = \frac{2K_i C_{1i} - q_i R_{1,i}^{\ 2}}{q_i\left(R_{2,i}^{\ 2} - R_{1,i}^{\ 2}\right)} \qquad (i = 1, 2, 3 \ldots 6) \tag{16.14}$$

Equation (16.14) is a set of six equations in the six variables f_1 , f_2 , f_3 ... f_6 where the value of C_{1i} is given by Eq. (16.11); T_{s1i} and T_{s2i} used in Eq. (16.11) are given by Eqs. (16.6) and (16.7); $T_{i,1}$ used in Eqs. (16.6) and (16.7) is given by Eq. (16.2). These six equations are solved with ΔZ set to the heated length (L_h) of the channel (0.58 m for the two problems solved here), using the calculation steps are outlined below.

Calculation steps:

(1) Assume guess values of 0.5 for the areal fraction f_i on the inner side (left side) of the adiabatic point (maximum meat temperature) in each fuel tube i (i = 1, 2, 3 ... 6).

(2) Calculate coolant temperature at axial node exit using f_i , fuel tube power density q_i , channel flow rate W_i and axial interval (node) length ΔZ.

(3) Calculate fuel tube surface temperatures on the inner and outer surfaces T_{s1i} and T_{s2i} using the coolant temperature at node center, nodal heat flux and given heat transfer coefficients.

(4) Calculate the arbitrary constants of integration C_{1i} and C_{2i} for each fuel tube using the surface temperatures. Calculate $f_{i,calc}$ using C_{1i}.

(5) Minimize the error $E = \sum_{i=1}^{6}\left(f_{i,calc} - f_i\right)^2$ to get the solution, using the solver of the spreadsheet.

The resulting solution gives the values of the six variables f_1 , f_2 , f_3 ... f_6 along with fuel tube surface temperatures and meat maximum temperatures at midpoint of core height ($Z = 0.5L_h$), and coolant temperatures at the channel exit ($Z = L_h$).

16.2.2 Solution of Test Problems with Six Fuel Tubes by an Independent Method

Based on the method described in Section 16.2.1, an Excel spreadsheet was developed to calculate steady-state temperature distribution in radial geometry problems consisting of 6 fuel tubes. The spreadsheet calculates the coolant temperature at the channel exit, the tube inner and outer surface

temperatures at axial node center, and the maximum fuel temperature across the meat thickness at midpoint of core height, as mentioned in Section 16.2.1. The spreadsheet was used to solve two test problems (referred to as Problem 1 and Problem 2). The innermost channel of Problem 1 is not a pinhole whereas the innermost channel of Problem 2 is a pinhole to model a solid fuel rod. The geometry and operating data for these problems, used in the spreadsheet calculation, are given in Tables 16.1 and 16.2. With the heat transfer coefficients and flow rates specified for all 7 coolant channels, the flow areas and hydraulic diameters of channels are not required in the spreadsheet calculation. The thickness of meat in each tube is 2 mm in Problem 1, and 5 mm in Problem 2. The cladding thickness is zero in both problems. The solution obtained for Test Problems 1 and 2 are given in Tables 16.3 and 16.5.

16.2.3 Verification of PLTEMP against Solution Obtained by an Independent Method

Two versions of the PLTEMP/ANL code, the version 42bta_r65_131030 and the version 4.2 under development, were verified by comparing the solutions calculated by the code with those obtained independently by the spreadsheet for Test Problems 1 and 2 (given in Tables 16.3 and 16.5). These two problems use the same set of given values of convective heat transfer coefficient (different in each channel). Therefore for this verification exercise, the two subroutines hcoef.f and hcoef1.f (which calculate heat transfer coefficient in the code) were modified to reset the heat transfer coefficient at the end of the subroutines, to the values given in Table 16.1 or Table 16.2 (which are 10000, 30000, 20000, 50000, 15000, 40000, and 25000 W/m^2-°C in channels 1 to 7).

The input data files to PLTEMP/ANL for Test Problems 1 and 2 are given in Figs. 16.2 and 16.3. In these input data files, the coolant properties option ICP is set to 1 to use constant specific heat and density. The output files obtained by running the two versions of the code were compared using the UNIX diff command, and were found to be identical. The code-calculated results are given in Tables 16.4 and 16.6.

The calculated coolant, tube surface, and meat maximum temperatures are plotted versus axial position in Figs. 16.4 and 16.5. *All these temperature plots for both problems are straight lines*. The calculated meat areal fractions f_i on the left side of the adiabatic in each fuel tube are plotted versus axial position in Fig. 16.6 for Test Problem 4. *All these plots are straight lines*.

For Test Problem 1 without pinhole, the difference between the code-calculated and the spreadsheet-calculated temperatures (of the coolant at channel exit, the tube surface temperatures at mid-core height, and the meat maximum temperature at mid-core height) is as follows:
Maximum Absolute Temperature Difference between Tables 16.3 and 16.4 = 0.28 ºC
RMS Temperature Difference between Tables 16.3 and 16.4 = 0.11 ºC

For Test Problem 2 with pinhole, the difference between the code-calculated and the spreadsheet-calculated temperatures (of the coolant at channel exit, the tube surface temperatures at mid-core height, and the meat maximum temperature at mid-core height) is as follows:
Maximum Absolute Temperature Difference between Tables 16.5 and 16.6 = 0.131 ºC
RMS Temperature Difference between Tables 16.5 and 16.6 = 0.048 ºC

These comparisons provide a verification of PLTEMP/ANL version 42bta_r65_131030 and the version 4.2.

16.3 Comparison of Two PLTEMP Solutions of a Six-Tube Test Problem 3 with its Spreadsheet Solution

The Test Problem 3 used here is the same as the Test Problem 2 described in Section 16.2.2 except for two differences: (1) the heat transfer coefficients in Problem 3 are calculated by the code whereas they were given and fixed in Problem 2, and (2) the cross-sectional area of the innermost pinhole channel in Problem 3 is less than 1.0×10^{-15} m^2 whereas it was more than 1.0×10^{-15} m^2 in Problem 2. This is done to verify a modification made in the code version 4.2. This modification sets the heat transfer coefficient in the innermost channel to 1.0 W/m^2-ºC if its flow area of less than 1.0×10^{-15} m^2. Besides these differences, Table 16.2 gives the geometry and operating data for Problem 3. Two input data files were prepared for Problem 3, the first with the fuel tubes numbered in the increasing order of radii and the second with the tubes numbered in the decreasing order of radii. The two input files are shown in Figs. 16.7 and 16.8, and are stored in the files *problem3.with.pinhole-20.inp* and *problem3.decRMID.with.pinhole-20.inp*). A portion of each output file obtained by running PLTEMP/ANL version 4.2 for the two input files is shown in Figs. 16.9 and 16.10.

A comparison of these two calculations is made in Table 16.7 for four quantities: (1) outlet temperatures of all 7 coolant temperatures, (2) heat transfer coefficients of all 7 coolant channels at the mid-height of core, (3) maximum fuel temperatures of fuel tubes at the mid-height of core, and (4) areal fractions on the inside of fuel tubes at the radial location of the maximum fuel temperature (at the mid-height of core). The two calculations give identical results.

The channel-wise heat transfer coefficients (at core mid-height) given in Table 16.7 was as input in the spreadsheet described in Section 16.2.1, and a third solution of Test Problem 3 was obtained independently. The heat transfer coefficient actually varies axially in each channel, as shown by Figs. 16.9 and 16.10. However, this spreadsheet solution ignores the axial variation and assumes a constant value of heat transfer coefficient in each channel over the entire core height. The spreadsheet solution is also included in Table 16.7 to show the comparison of the results of PLTEMP/ANL version 4.2 with the Excel spreadsheet steady-state solution.

There is a good agreement between the code and the spreadsheet. The maximum difference in coolant outlet temperatures and fuel temperatures shown in Table 16.7 is 0.048 ºC.

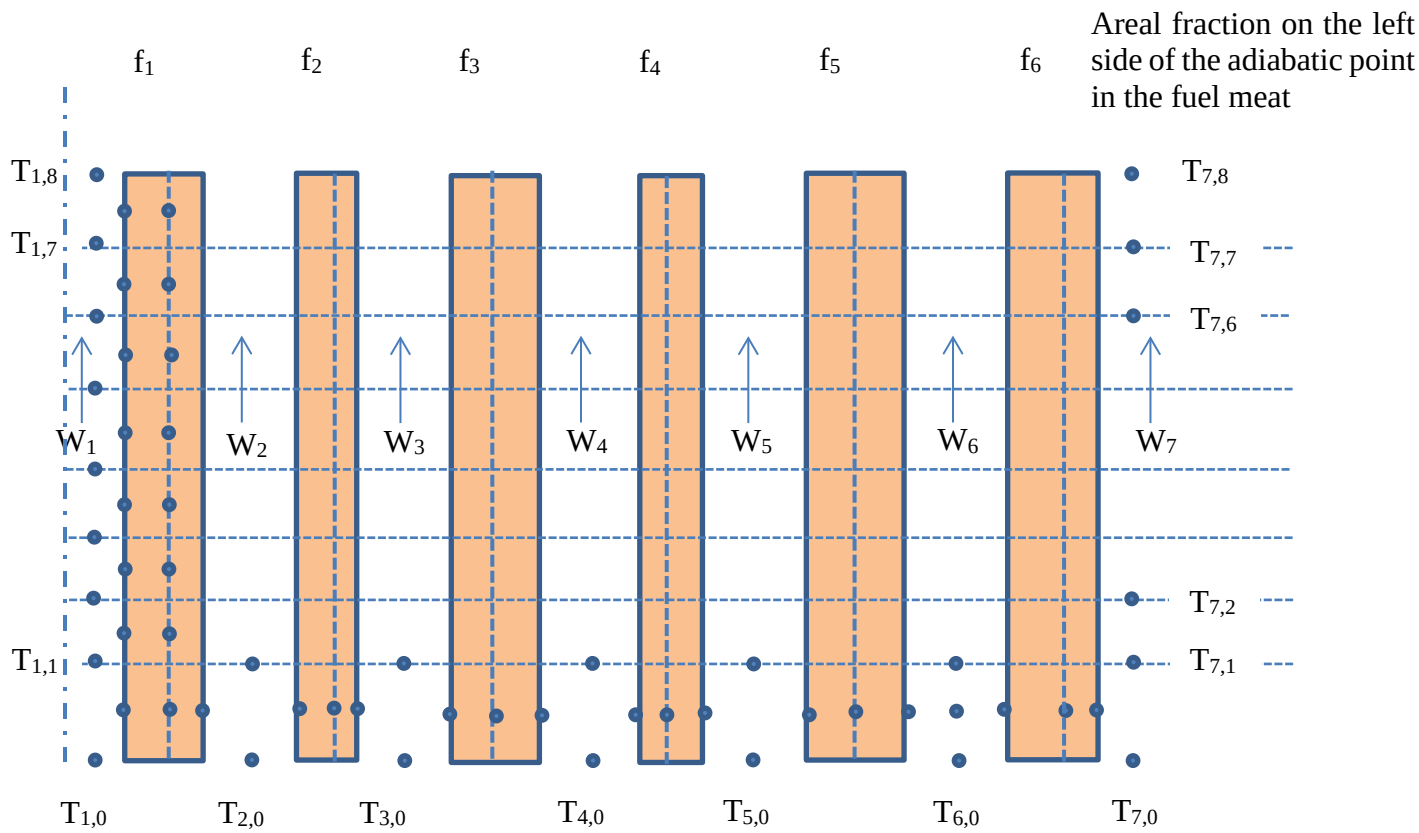

Figure 16.1 Vertical Section of an Experimental Reactor Fuel Assembly Consisting of Multiple Coaxial Fuel Tubes

Figure 16.2 PLTEMP Input Data File of Test Problem 1

```
A 6-fuel-tube Test Problem 1 Solved on Spreadsheet
!  1   2   3   4   5   6   7   8   9  10  11  12  13  14  15  16  17  18  19  20
   1   1   2   1   1   1   1   0   1   1   0   0   0   0   0   0   0   0   0   0Card(1)0200
! WFGES=0; flow-driven mode via card type 0310
   1   3  0.0        1.00        1.000       1.00                                Card(1)0300
   7   7  1.000                                                                   Card(1)0301
   1   2   1                                                                      Card(1)0302
 1.0000                                                                           Card(1)0303
 0.0043433  0.038540    0.10        0.5                                           Card(3)0304
 0.0        0.0         0.580       0.0                                           Card(3)0304
 0.0043433  0.038540    0.035       1.0                                           Card(3)0304
 0.316      0.250                                                                 Card(1)0305
   7  0 0.0         0.580         0.450E-08  170.        2.000E-03   10.         Card(1)0306
 9.07920E-04 3.40000E-02  0.106814   0.106814               0.017                Card(1)0307
 5.27788E-04 8.00000E-03  0.263894   0.263894                                    Card(2)0307
 6.78582E-04 8.00000E-03  0.339292   0.339292                                    Card(3)0307
 8.29380E-04 8.00000E-03  0.414690   0.414690                                    Card(4)0307
 9.80177E-04 8.00000E-03  0.490088   0.490088                                    Card(5)0307
 1.13097E-03 8.00000E-03  0.565487   0.565487                                    Card(6)0307
 1.28076E-03 1.66400E-02  0.307876   0.307876                                    Card(7)0307
 0.113097   0.150796    0.188496    0.226195    0.263894    0.301593            Card(1)0308
 0.018      0.024        0.030       0.036      0.042       0.048               Card(1)0308A
 0.813053   0.975664    1.409292    1.029867    0.921460    0.813053            Card(1)0309
!0.717522   0.903667    0.917400    1.10792     1.210880    1.23838             Card(1)0310
!1.663038                                                                        Card(2)0310
 0.85       1.15        1.25        1.46        1.44        1.40                Card(1)0310
 1.05                                                                            Card(2)0310
   1   1                                                                         Card 0400
  1.1545E-04    3.00E-03    0.680           1.4                                 Card 0401
       0.316    0.25                                                             Card 0402
!        DP0         DDP       DPMAX       POWER         TIN           P
     .100633       .0005      .12540    1.311929        45.0       0.135         Card 0500
!     QFCLAD      QFCOOL       EPSLN      EPSLNI       XCONV       YCONF
         0.0         0.0         0.6         0.5       1.E-8       1.E-5         Card 0500
!ITER       CONV         ETA        DPWR        PWRM
    100 1.00000E-04     25.0      0.0000     1.311929                            Card 0600
 -12                                                                             Card 0700
0.00000      0.025       1.0                                                     Card 0701
0.05         0.100       1.0                                                     Card 0701
0.15         0.20        1.0                                                     Card 0701
0.25         0.30        1.0                                                     Card 0701
0.35         0.40        1.0                                                     Card 0701
0.45         0.50        1.0                                                     Card 0701
0.55         0.60        1.0                                                     Card 0701
0.65         0.70        1.0                                                     Card 0701
0.75         0.80        1.0                                                     Card 0701
0.85         0.90        1.0                                                     Card 0701
0.95         0.975       1.0                                                     Card 0701
1.00000                                                                          Card 0701
```

Figure 16.3 PLTEMP Input Data File of Test Problem 2

```
A 6-fuel-tube Test Problem 2 Solved on Spreadsheet
!  1   2   3   4   5   6   7   8   9  10  11  12  13  14  15  16  17  18  19  20
   1   1   2   1   1   1   1   0   1   1   0   0   0   0   0   0   0   0   0   0Card(1)0200
! WFGES=0; flow-driven mode via card type 0310
   1   3  0.0        1.00        1.000       1.00                                Card(1)0300
   7   7  1.000                                                                  Card(1)0301
   1   2   1                                                                     Card(1)0302
 1.0000                                                                          Card(1)0303
 0.0043433  0.038540    0.10        0.5                                          Card(3)0304
 0.0        0.0         0.580       0.0                                          Card(3)0304
 0.0043433  0.038540    0.035       1.0                                          Card(3)0304
 0.316      0.250                                                                Card(1)0305
   7  0 0.0         0.580         0.450E-08  170.        5.000E-03   10.        Card(1)0306
  3.1416E-14  2.000E-07 0.000000628 0.000000628             1.0E-07             Card(1)0307
  1.7593E-04  8.000E-03 0.087965851 0.087965851                                  Card(2)0307
  4.0213E-04  8.000E-03 0.201063186 0.201063186                                  Card(3)0307
  6.2832E-04  8.000E-03 0.314160522 0.314160522                                  Card(4)0307
  8.5452E-04  8.000E-03 0.427257858 0.427257858                                  Card(5)0307
 10.8071E-04  8.000E-03 0.540355193 0.540355193                                  Card(6)0307
 13.0691E-04  1.664E-02 0.314159894 0.314159894                                  Card(7)0307
0.015708592 0.072257259 0.128805927 0.185354595 0.241903263 0.298451930         Card(1)0308
0.0025001   0.0115001   0.0205001   0.0295001   0.0385001   0.0475001           Card(1)0308A
!0.813053   0.975664    1.409292    1.029867    0.921460    0.813053            Card(1)0309
 0.679508   1.019262    1.472267    1.087212    0.860710    0.792759            Card(1)0309
 0.85       1.15        1.25        1.46        1.44        1.40                Card(1)0310
 1.05                                                                            Card(2)0310
   1   1                                                                         Card 0400
  1.1545E-04    3.00E-03    0.680           1.4                                 Card 0401
       0.316    0.25                                                             Card 0402
!        DP0         DDP       DPMAX       POWER         TIN           P
     .100633       .0005      .12540    1.178281        45.0       0.135        Card 0500
!     QFCLAD      QFCOOL       EPSLN      EPSLNI       XCONV       YCONF
         0.0         0.0         0.6         0.5       1.E-8       1.E-5        Card 0500
!ITER       CONV         ETA        DPWR        PWRM
    100 1.00000E-04     25.0      0.0000     1.311929                           Card 0600
 -12                                                                             Card 0700
0.00000      0.025       1.0                                                    Card 0701
0.05         0.100       1.0                                                    Card 0701
0.15         0.20        1.0                                                    Card 0701
0.25         0.30        1.0                                                    Card 0701
0.35         0.40        1.0                                                    Card 0701
0.45         0.50        1.0                                                    Card 0701
0.55         0.60        1.0                                                    Card 0701
0.65         0.70        1.0                                                    Card 0701
0.75         0.80        1.0                                                    Card 0701
0.85         0.90        1.0                                                    Card 0701
0.95         0.975       1.0                                                    Card 0701
1.00000                                                                         Card 0701
```

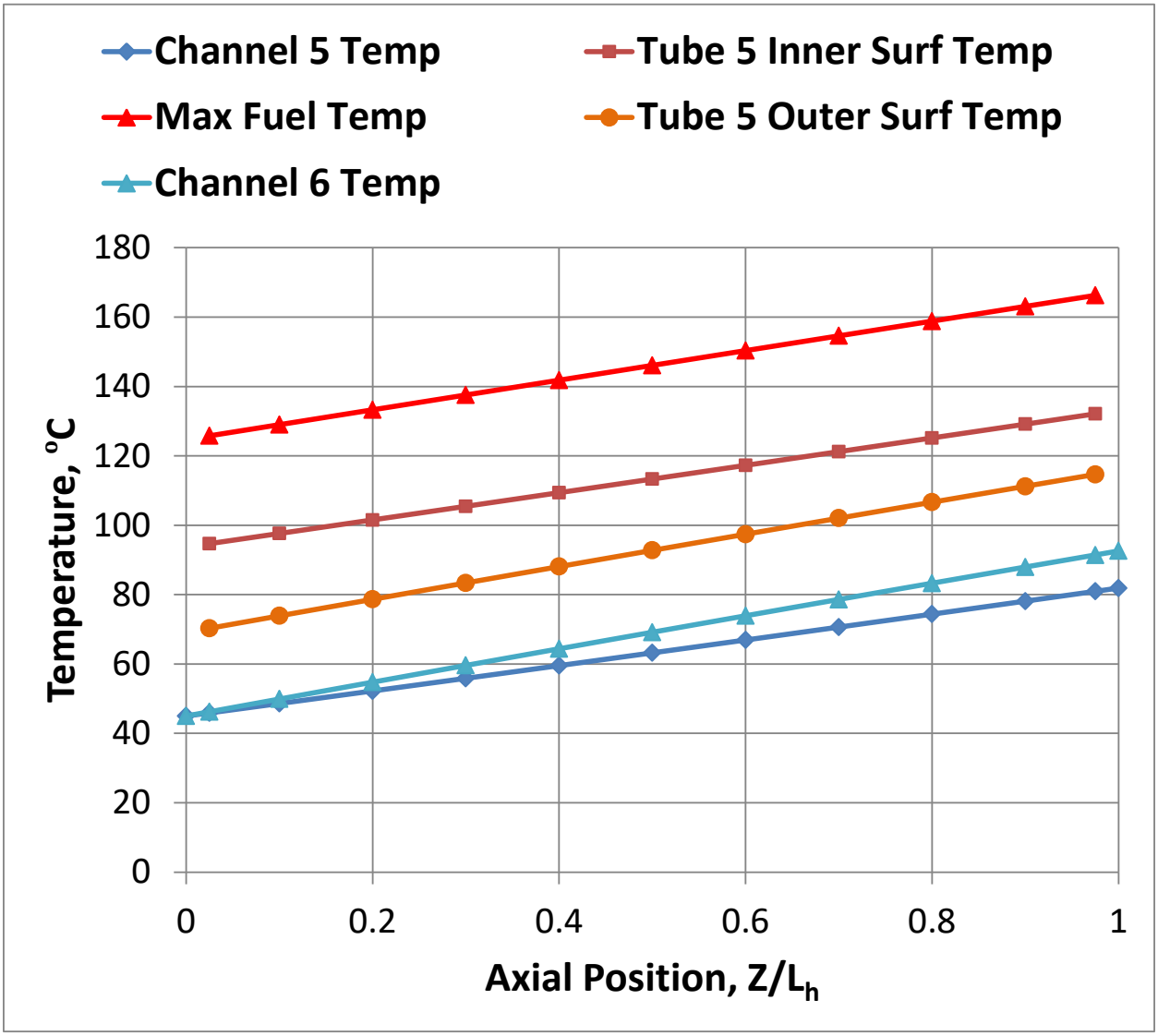

Figure 16.4 PLTEMP Version 42bta_r65_131030 Calculated Results for Problem 1 Without Pinhole

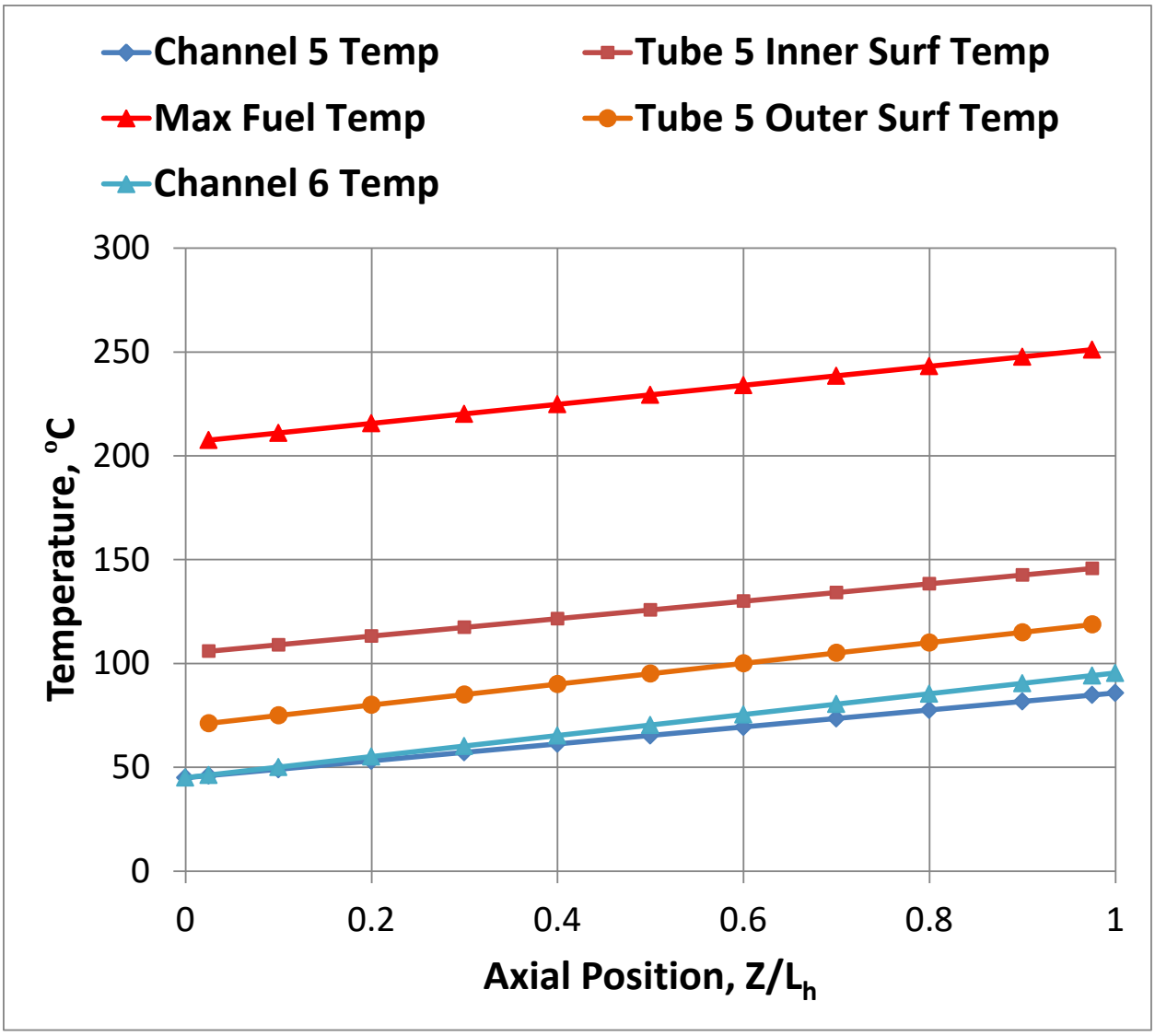

Figure 16.5 PLTEMP Version 42bta_r65_131030 Calculated Results for Problem 2 With a Pinhole

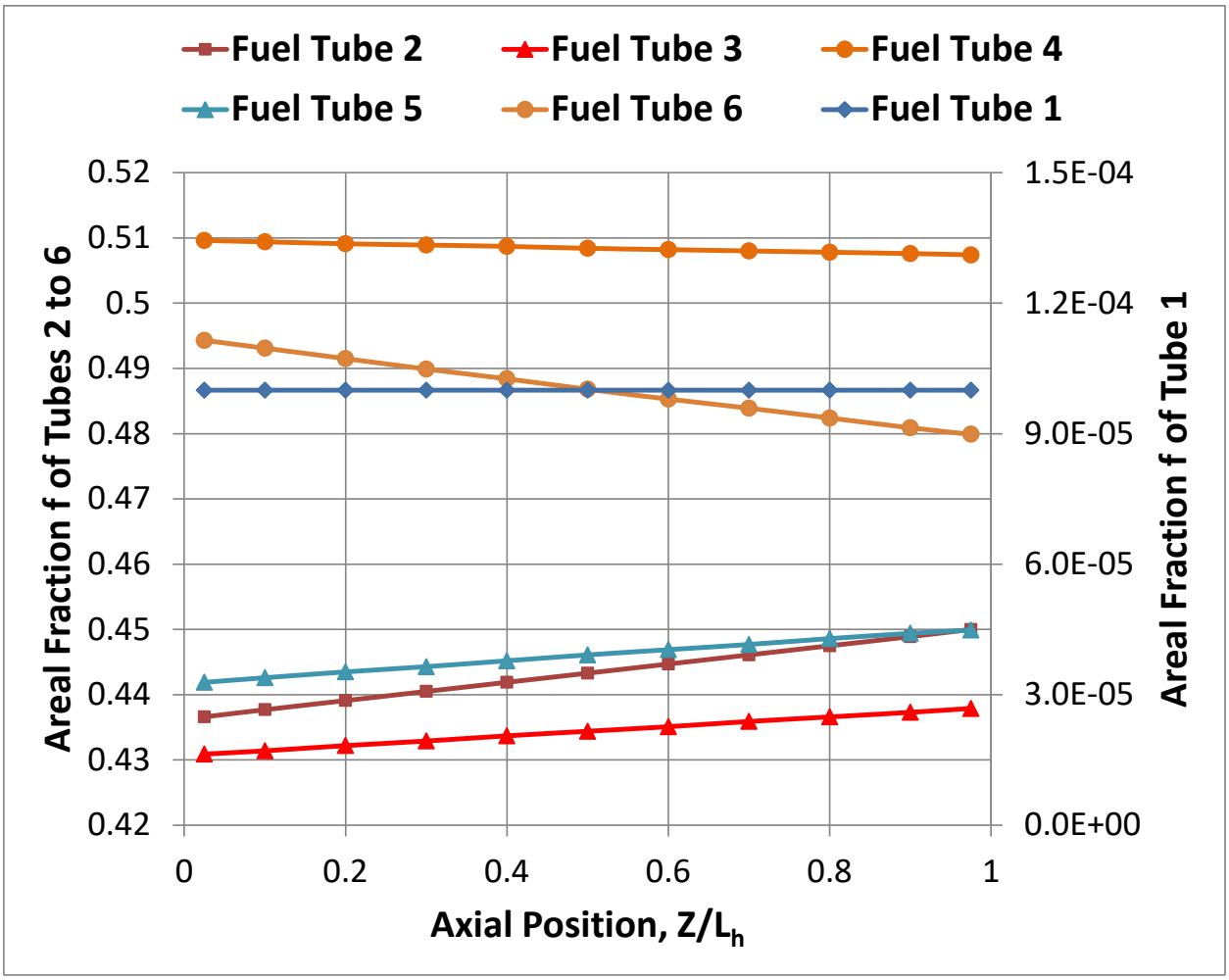

Figure 16.6 PLTEMP Version 42bta_r65_131030 Calculated Areal Fractions for Problem 2 With a Pinhole

Figure 16.7 PLTEMP Input Data File of Test Problem 3 with Increasing Tube Radii

```
A 6-fuel-tube Test Problem 3, Input File=problem3.with.pinhole-20.inp
!  1   2   3   4   5   6   7   8   9  10  11  12  13  14  15  16  17  18  19  20
   1   1   2   1   1   1   1   0   1   1   0   0   0   0   0   0   0   0   0   0Card(1)0200
! WFGES=0; flow-driven mode via card type 0310
   1   3  0.0        1.00        1.000       1.00                                Card(1)0300
   7   7  1.000                                                                  Card(1)0301
   1   2   1                                                                     Card(1)0302
 1.0000                                                                          Card(1)0303
 0.0043433  0.038540    0.10        0.5                                          Card(3)0304
 0.0        0.0         0.580       0.0                                          Card(3)0304
 0.0043433  0.038540    0.035       1.0                                          Card(3)0304
 0.316      0.250                                                                Card(1)0305
   7  0 0.0         0.580         0.450E-08  170.        5.000E-03   10.        Card(1)0306
  3.1416E-20  2.000E-07 0.000000628 0.000000628             1.0E-07             Card(1)0307
  1.7593E-04  8.000E-03 0.087965851 0.087965851                                  Card(2)0307
  4.0213E-04  8.000E-03 0.201063186 0.201063186                                  Card(3)0307
  6.2832E-04  8.000E-03 0.314160522 0.314160522                                  Card(4)0307
  8.5452E-04  8.000E-03 0.427257858 0.427257858                                  Card(5)0307
 10.8071E-04  8.000E-03 0.540355193 0.540355193                                  Card(6)0307
 13.0691E-04  1.664E-02 0.314159894 0.314159894                                  Card(7)0307
0.015708592 0.072257259 0.128805927 0.185354595 0.241903263 0.298451930         Card(1)0308
0.0025001   0.0115001   0.0205001   0.0295001   0.0385001   0.0475001           Card(1)0308A
!0.813053   0.975664    1.409292    1.029867    0.921460    0.813053            Card(1)0309
 0.679508   1.019262    1.472267    1.087212    0.860710    0.792759            Card(1)0309
 0.85       1.15        1.25        1.46        1.44        1.40                Card(1)0310
 1.05                                                                            Card(2)0310
   1   1                                                                         Card 0400
  1.1545E-04    3.00E-03    0.680           1.4                                 Card 0401
       0.316    0.25                                                             Card 0402
!        DP0         DDP       DPMAX       POWER         TIN           P
     .100633       .0005      .12540    1.178281        45.0       0.135        Card 0500
!     QFCLAD      QFCOOL       EPSLN      EPSLNI       XCONV       YCONF
         0.0         0.0         0.6         0.5       1.E-8       1.E-5        Card 0500
!ITER       CONV         ETA        DPWR        PWRM
    100 1.00000E-04     25.0      0.0000     1.311929                           Card 0600
 -12                                                                             Card 0700
0.00000      0.025       1.0                                                     Card 0701
0.05         0.100       1.0                                                     Card 0701
0.15         0.20        1.0                                                     Card 0701
0.25         0.30        1.0                                                     Card 0701
0.35         0.40        1.0                                                     Card 0701
0.45         0.50        1.0                                                     Card 0701
0.55         0.60        1.0                                                     Card 0701
0.65         0.70        1.0                                                     Card 0701
0.75         0.80        1.0                                                     Card 0701
0.85         0.90        1.0                                                     Card 0701
0.95         0.975       1.0                                                     Card 0701
1.00000                                                                          Card 0701
```

Figure 16.8 PLTEMP Input Data File of Test Problem 3 with Decreasing Tube Radii

```
A 6-fuel-tube Test Problem 3, Input File=problem3.decrRMID.with.pinhole-20.inp
!  1   2   3   4   5   6   7   8   9  10  11  12  13  14  15  16  17  18  19  20
   1   1   2   1   1   1   1   0   1   1   0   0   0   0   0   0   0   0   0   0Card(1)0200
! WFGES=0; flow-driven mode via card type 0310
   1   3  0.0        1.00        1.000       1.00                              Card(1)0300
   7   7  1.000                                                                 Card(1)0301
   1   2   1                                                                    Card(1)0302
 1.0000                                                                         Card(1)0303
 0.0043433  0.038540    0.10        0.5                                         Card(3)0304
 0.0        0.0         0.580       0.0                                         Card(3)0304
 0.0043433  0.038540    0.035       1.0                                         Card(3)0304
 0.316      0.250                                                               Card(1)0305
   7  0 0.0         0.580         0.450E-08  170.        5.000E-03   10.        Card(1)0306
 13.0691E-04  1.664E-02 0.314159894 0.314159894             4.160E-03           Card(7)0307
 10.8071E-04  8.000E-03 0.540355193 0.540355193                                 Card(6)0307
  8.5452E-04  8.000E-03 0.427257858 0.427257858                                 Card(5)0307
  6.2832E-04  8.000E-03 0.314160522 0.314160522                                 Card(4)0307
  4.0213E-04  8.000E-03 0.201063186 0.201063186                                 Card(3)0307
  1.7593E-04  8.000E-03 0.087965851 0.087965851                                 Card(2)0307
  3.1416E-20  2.000E-07 0.000000628 0.000000628             1.0E-07             Card(1)0307
0.298451930 0.241903263 0.185354595 0.128805927 0.072257259 0.015708592         Card(1)0308
0.0475001   0.0385001   0.0295001   0.0205001   0.0115001   0.0025001           Card(1)0308A
!0.813053   0.975664    1.409292    1.029867    0.921460    0.813053            Card(1)0309
 0.792759   0.860710    1.087212    1.472267    1.019262    0.679508            Card(1)0309
 1.05       1.40        1.44        1.46        1.25        1.15                Card(1)0310
 0.85                                                                           Card(2)0310
   1   1                                                                        Card 0400
  1.1545E-04    3.00E-03    0.680           1.4                                 Card 0401
       0.316    0.25                                                            Card 0402
!        DP0          DDP       DPMAX       POWER         TIN           P
     .100633       .0005      .12540    1.178281        45.0       0.135        Card 0500
!     QFCLAD      QFCOOL       EPSLN      EPSLNI       XCONV       YCONF
         0.0         0.0         0.6         0.5       1.E-8       1.E-5        Card 0500
!ITER       CONV         ETA        DPWR        PWRM
    100 1.00000E-04     25.0      0.0000     1.311929                           Card 0600
 -12                                                                            Card 0700
0.00000      0.025       1.0                                                    Card 0701
0.05         0.100       1.0                                                    Card 0701
0.15         0.20        1.0                                                    Card 0701
0.25         0.30        1.0                                                    Card 0701
0.35         0.40        1.0                                                    Card 0701
0.45         0.50        1.0                                                    Card 0701
0.55         0.60        1.0                                                    Card 0701
0.65         0.70        1.0                                                    Card 0701
0.75         0.80        1.0                                                    Card 0701
0.85         0.90        1.0                                                    Card 0701
0.95         0.975       1.0                                                    Card 0701
1.00000                                                                         Card 0701
```

Figure 16.9 PLTEMP/ANL V4.2 Output File for Test Problem 3 with Pinhole with Increasing RMID (Input File: problem3.with.pinhole-20.inp)

FUEL PLATE 1 (ExactSoln), Assembly = 1 of Type = 1

NODE	COOLANT inner(C)	CladSurf inner(C)	FUEL PEAK (C)	CladSurf outer(C)	COOLANT outer(C)	HCOFinner W/C-m^2	HCOFouter W/C-m^2	ONBRin [F Note 1]	ONBRout	ETAin K-cm^3/J [Note 3]	ETAout K-cm^3/J [Note 3]	ONB Temp inner(C)	ONB Temp outer(C)	Avg Meat Temp (C)
	45.000				45.000									
1	45.000	259.037	259.037	71.530	45.289	1.0000E+00	2.8583E+04	999.99	3.04	7.703E+21	5.286E+02	107.070	125.628	196.535
2	45.000	259.719	259.719	72.212	46.158	1.0000E+00	2.8787E+04	999.99	2.95	7.624E+21	5.172E+02	106.640	125.261	197.217
3	45.000	260.635	260.635	73.127	47.317	1.0000E+00	2.9059E+04	999.99	2.84	7.518E+21	5.020E+02	106.059	124.766	198.133
4	45.000	261.558	261.558	74.051	48.478	1.0000E+00	2.9328E+04	999.99	2.73	7.411E+21	4.867E+02	105.468	124.262	199.056
5	45.000	262.490	262.490	74.982	49.640	1.0000E+00	2.9595E+04	999.99	2.63	7.303E+21	4.712E+02	104.866	123.751	199.987
6	45.000	263.428	263.428	75.920	50.803	1.0000E+00	2.9861E+04	999.99	2.53	7.195E+21	4.557E+02	104.254	123.231	200.925
7	45.000	264.373	264.374	76.866	51.969	1.0000E+00	3.0124E+04	999.99	2.44	7.086E+21	4.400E+02	103.630	122.703	201.871
8	45.000	265.326	265.326	77.819	53.136	1.0000E+00	3.0386E+04	999.99	2.35	6.977E+21	4.242E+02	102.995	122.165	202.824
9	45.000	266.286	266.286	78.779	54.305	1.0000E+00	3.0646E+04	999.99	2.27	6.866E+21	4.083E+02	102.348	121.619	203.784
10	45.000	267.253	267.253	79.746	55.476	1.0000E+00	3.0904E+04	999.99	2.19	6.755E+21	3.923E+02	101.688	121.063	204.751
11	45.000	267.983	267.983	80.475	56.355	1.0000E+00	3.1095E+04	999.99	2.13	6.671E+21	3.802E+02	101.185	120.639	205.480
	45.000				56.649									200.955

FUEL PLATE 2 (ExactSoln), Assembly = 1 of Type = 1

NODE	COOLANT inner(C)	CladSurf inner(C)	FUEL PEAK (C)	CladSurf outer(C)	COOLANT outer(C)	HCOFinner W/C-m^2	HCOFouter W/C-m^2	ONBRin [F Note 1]	ONBRout	ETAin K-cm^3/J [Note 3]	ETAout K-cm^3/J [Note 3]	ONB Temp inner(C)	ONB Temp outer(C)	Avg Meat Temp (C)
	45.000				45.000									
1	45.289	90.071	242.619	110.541	45.794	2.8583E+04	1.5836E+04	1.88	1.26	3.097E+02	1.823E+02	129.679	127.906	195.555
2	46.158	90.665	243.493	111.641	48.174	2.8787E+04	1.6143E+04	1.85	1.24	3.028E+02	1.739E+02	129.334	127.540	196.427
3	47.317	91.474	244.720	113.202	51.346	2.9059E+04	1.6544E+04	1.80	1.20	2.934E+02	1.627E+02	128.870	127.046	197.648
4	48.478	92.300	246.011	114.865	54.517	2.9328E+04	1.6935E+04	1.76	1.17	2.840E+02	1.515E+02	128.400	126.543	198.933
5	49.640	93.144	247.363	116.621	57.687	2.9595E+04	1.7316E+04	1.72	1.13	2.745E+02	1.402E+02	127.924	126.032	200.278
6	50.803	94.004	248.769	118.461	60.856	2.9861E+04	1.7688E+04	1.68	1.10	2.649E+02	1.288E+02	127.441	125.511	201.675
7	51.969	94.878	250.225	120.377	64.023	3.0124E+04	1.8051E+04	1.64	1.06	2.553E+02	1.174E+02	126.952	124.982	203.121
8	53.136	95.761	251.686	122.294	67.190	3.0386E+04	1.8430E+04	1.60	1.03	2.457E+02	1.060E+02	126.454	124.443	204.570
9	54.305	96.664	253.234	124.350	70.357	3.0646E+04	1.8775E+04	1.57	0.99	2.359E+02	9.445E+01	125.950	123.894	206.106
10	55.476	97.580	254.831	126.479	73.523	3.0904E+04	1.9106E+04	1.53	0.96	2.261E+02	8.285E+01	125.438	123.335	207.687
11	56.355	98.276	256.058	128.119	75.898	3.1095E+04	1.9345E+04	1.50	0.94	2.188E+02	7.410E+01	125.048	122.909	208.901
	56.649				76.689									201.867

[1] The ONB ratio is here defined as (Tonb - Tinlet)/(Tsurf - Tinlet). If the heat flux is negative (the coolant is hotter than the adjacent cladding surface), then the ONB ratio is arbitrarily set to 99.99 .

[3] The column gives ETA' = (Coolant Velocity)*(Tsat - Coolant Temp)/(Heat Flux). ETA' in the units chosen here, equals Whittle and Forgan dimensionless ETA for water-cooled reactors: ETA = ETA'*Coolant Density*Cp/4. The last value in the colunm (at exit) should be greater than 32.5 to avoid excursive flow instability. ETA is also used in the equation R = 1/(1+ETA*Dh/Lh)

Figure 16.9 Continued

FUEL PLATE 3 (ExactSoln), Assembly = 1 of Type = 1

NODE	COOLANT inner(C)	CladSurf inner(C)	FUEL PEAK (C)	CladSurf outer(C)	COOLANT outer(C)	HCOFinner W/C-m^2	HCOFouter W/C-m^2	ONBRin [F Note 1]	ONBRout	ETAin K-cm^3/J [Note 3]	ETAout K-cm^3/J [Note 3]	ONB Temp inner(C)	ONB Temp outer(C)	Avg Meat Temp (C)
	45.000				45.000									
1	45.794	155.092	365.690	168.693	46.042	1.5836E+04	1.2573E+04	0.79	0.70	1.080E+02	9.025E+01	132.324	131.278	297.904
2	48.174	155.374	365.888	168.818	49.168	1.6143E+04	1.2891E+04	0.79	0.69	1.030E+02	8.487E+01	131.978	130.933	298.103
3	51.346	155.937	366.402	169.287	53.336	1.6544E+04	1.3304E+04	0.78	0.69	9.623E+01	7.770E+01	131.513	130.464	298.617
4	54.517	156.696	367.175	170.073	57.503	1.6935E+04	1.3703E+04	0.77	0.68	8.946E+01	7.052E+01	131.042	129.988	299.390
5	57.687	157.633	368.179	171.136	61.668	1.7316E+04	1.4089E+04	0.76	0.67	8.266E+01	6.334E+01	130.565	129.503	300.393
6	60.856	158.727	369.382	172.437	65.833	1.7688E+04	1.4464E+04	0.75	0.66	7.583E+01	5.614E+01	130.082	129.010	301.596
7	64.023	159.949	370.700	173.841	69.996	1.8051E+04	1.4845E+04	0.74	0.65	6.899E+01	4.893E+01	129.591	128.509	302.914
8	67.190	161.203	372.218	175.593	74.158	1.8430E+04	1.5189E+04	0.72	0.64	6.211E+01	4.171E+01	129.096	127.997	304.431
9	70.357	162.702	373.969	177.568	78.319	1.8775E+04	1.5515E+04	0.71	0.62	5.522E+01	3.446E+01	128.592	127.477	306.181
10	73.523	164.332	375.879	179.726	82.478	1.9106E+04	1.5825E+04	0.70	0.61	4.831E+01	2.720E+01	128.081	126.947	308.089
11	75.898	165.632	377.399	181.442	85.597	1.9345E+04	1.6049E+04	0.69	0.60	4.312E+01	2.173E+01	127.692	126.544	309.608
	76.689				86.636									302.347

FUEL PLATE 4 (ExactSoln), Assembly = 1 of Type = 1

NODE	COOLANT inner(C)	CladSurf inner(C)	FUEL PEAK (C)	CladSurf outer(C)	COOLANT outer(C)	HCOFinner W/C-m^2	HCOFouter W/C-m^2	ONBRin [F Note 1]	ONBRout	ETAin K-cm^3/J [Note 3]	ETAout K-cm^3/J [Note 3]	ONB Temp inner(C)	ONB Temp outer(C)	Avg Meat Temp (C)
	45.000				45.000									
1	46.042	147.203	305.663	163.217	46.096	1.2573E+04	9.7277E+03	0.83	0.71	1.094E+02	8.851E+01	129.626	128.731	255.592
2	49.168	147.789	306.104	163.528	49.384	1.2891E+04	9.9859E+03	0.82	0.70	1.030E+02	8.297E+01	129.269	128.378	256.035
3	53.336	148.846	306.993	164.267	53.768	1.3304E+04	1.0321E+04	0.81	0.70	9.433E+01	7.558E+01	128.788	127.901	256.927
4	57.503	150.188	308.193	165.339	58.153	1.3703E+04	1.0644E+04	0.79	0.68	8.565E+01	6.818E+01	128.300	127.416	258.129
5	61.668	151.777	309.664	166.703	62.539	1.4089E+04	1.0957E+04	0.78	0.67	7.695E+01	6.079E+01	127.805	126.923	259.601
6	65.833	153.562	311.296	168.199	66.926	1.4464E+04	1.1275E+04	0.76	0.66	6.822E+01	5.337E+01	127.301	126.423	261.236
7	69.996	155.464	313.170	170.046	71.315	1.4845E+04	1.1566E+04	0.74	0.65	5.945E+01	4.596E+01	126.793	125.912	263.110
8	74.158	157.676	315.327	172.155	75.704	1.5189E+04	1.1842E+04	0.72	0.63	5.066E+01	3.852E+01	126.275	125.393	265.268
9	78.319	160.072	317.686	174.480	80.095	1.5515E+04	1.2102E+04	0.70	0.62	4.184E+01	3.107E+01	125.750	124.865	267.627
10	82.478	162.624	320.213	176.985	84.487	1.5825E+04	1.2350E+04	0.68	0.60	3.300E+01	2.361E+01	125.215	124.327	270.155
11	85.597	164.621	322.197	178.956	87.782	1.6049E+04	1.2530E+04	0.67	0.59	2.635E+01	1.799E+01	124.809	123.917	272.139
	86.636				88.881									262.195

[1] The ONB ratio is here defined as (Tonb - Tinlet)/(Tsurf - Tinlet). If the heat flux is negative (the coolant is hotter than the adjacent cladding surface), then the ONB ratio is arbitrarily set to 99.99 .

[3] The column gives ETA' = (Coolant Velocity)*(Tsat - Coolant Temp)/(Heat Flux). ETA' in the units chosen here, equals Whittle and Forgan dimensionless ETA for water-cooled reactors: ETA = ETA'*Coolant Density*Cp/4. The last value in the colunm (at exit) should be greater than 32.5 to avoid excursive flow instability. ETA is also used in the equation R = 1/(1+ETA*Dh/Lh)

Figure 16.9 Continued

FUEL PLATE 5 (ExactSoln), Assembly = 1 of Type = 1

NODE	COOLANT inner(C)	CladSurf inner(C)	FUEL PEAK (C)	CladSurf outer(C)	COOLANT outer(C)	HCOFinner W/C-m^2	HCOFouter W/C-m^2	ONBRin [F Note 1]	ONBRout	ETAin K-cm^3/J [Note 3]	ETAout K-cm^3/J [Note 3]	ONB Temp inner(C)	ONB Temp outer(C)	Avg Meat Temp (C)
	45.000				45.000									
1	46.096	148.752	274.009	161.220	46.267	9.7277E+03	7.8929E+03	0.80	0.71	1.010E+02	8.520E+01	127.703	126.985	234.370
2	49.384	149.350	274.519	161.651	50.068	9.9859E+03	8.1341E+03	0.79	0.70	9.474E+01	7.912E+01	127.341	126.625	234.882
3	53.768	150.465	275.567	162.638	55.131	1.0321E+04	8.4449E+03	0.78	0.69	8.637E+01	7.104E+01	126.853	126.138	235.931
4	58.153	151.903	276.984	164.035	60.190	1.0644E+04	8.7433E+03	0.76	0.68	7.796E+01	6.296E+01	126.358	125.642	237.348
5	62.539	153.618	278.714	165.780	65.243	1.0957E+04	9.0304E+03	0.74	0.66	6.952E+01	5.488E+01	125.858	125.137	239.078
6	66.926	155.453	280.598	167.707	70.288	1.1275E+04	9.3177E+03	0.73	0.65	6.105E+01	4.681E+01	125.350	124.622	240.961
7	71.315	157.646	282.885	170.080	75.326	1.1566E+04	9.5761E+03	0.71	0.63	5.256E+01	3.873E+01	124.836	124.098	243.247
8	75.704	160.068	285.426	172.730	80.354	1.1842E+04	9.8181E+03	0.69	0.62	4.404E+01	3.065E+01	124.313	123.565	245.786
9	80.095	162.687	288.178	175.602	85.372	1.2102E+04	1.0046E+04	0.67	0.60	3.551E+01	2.256E+01	123.783	123.022	248.535
10	84.487	165.466	291.090	178.635	90.381	1.2350E+04	1.0266E+04	0.65	0.58	2.696E+01	1.446E+01	123.243	122.469	251.445
11	87.782	167.629	293.345	180.974	94.131	1.2530E+04	1.0429E+04	0.63	0.57	2.055E+01	8.366E+00	122.831	122.049	253.698
	88.881				95.381									242.125

FUEL PLATE 6 (ExactSoln), Assembly = 1 of Type = 1

NODE	COOLANT inner(C)	CladSurf inner(C)	FUEL PEAK (C)	CladSurf outer(C)	COOLANT outer(C)	HCOFinner W/C-m^2	HCOFouter W/C-m^2	ONBRin [F Note 1]	ONBRout	ETAin K-cm^3/J [Note 3]	ETAout K-cm^3/J [Note 3]	ONB Temp inner(C)	ONB Temp outer(C)	Avg Meat Temp (C)
	45.000				45.000									
1	46.267	170.697	303.094	213.802	45.808	7.8929E+03	4.6347E+03	0.66	0.48	7.871E+01	6.205E+01	127.577	125.888	265.690
2	50.068	170.662	302.745	213.204	48.235	8.1341E+03	4.7261E+03	0.65	0.48	7.321E+01	5.901E+01	127.207	125.531	265.367
3	55.131	171.066	302.653	212.718	51.475	8.4449E+03	4.8458E+03	0.65	0.48	6.587E+01	5.495E+01	126.706	125.052	265.316
4	60.190	171.921	302.942	212.553	54.723	8.7433E+03	4.9629E+03	0.64	0.47	5.852E+01	5.087E+01	126.195	124.567	265.649
5	65.243	173.160	303.560	212.672	57.979	9.0304E+03	5.0773E+03	0.63	0.47	5.113E+01	4.678E+01	125.674	124.077	266.315
6	70.288	174.624	304.404	213.015	61.244	9.3177E+03	5.1891E+03	0.62	0.47	4.371E+01	4.269E+01	125.146	123.578	267.206
7	75.326	176.555	305.606	213.625	64.519	9.5761E+03	5.2986E+03	0.61	0.46	3.626E+01	3.858E+01	124.605	123.074	268.461
8	80.354	178.759	306.967	214.296	67.805	9.8181E+03	5.4130E+03	0.59	0.46	2.877E+01	3.446E+01	124.051	122.566	269.881
9	85.372	181.238	308.653	215.328	71.103	1.0046E+04	5.5171E+03	0.58	0.45	2.123E+01	3.035E+01	123.490	122.047	271.620
10	90.381	183.901	310.530	216.553	74.412	1.0266E+04	5.6172E+03	0.56	0.45	1.364E+01	2.624E+01	122.920	121.518	273.548
11	94.131	185.977	312.033	217.580	76.900	1.0429E+04	5.6898E+03	0.55	0.44	7.910E+00	2.317E+01	122.485	121.115	275.086
	95.381				77.731									268.375

[1] The ONB ratio is here defined as (Tonb - Tinlet)/(Tsurf - Tinlet). If the heat flux is negative (the coolant is hotter than the adjacent cladding surface), then the ONB ratio is arbitrarily set to 99.99 .

[3] The column gives ETA' = (Coolant Velocity)*(Tsat - Coolant Temp)/(Heat Flux). ETA' in the units chosen here, equals Whittle and Forgan dimensionless ETA for water-cooled reactors: ETA = ETA'*Coolant Density*Cp/4. The last value in the colunm (at exit) should be greater than 32.5 to avoid excursive flow instability. ETA is also used in the equation R = 1/(1+ETA*Dh/Lh)

Figure 16.10 PLTEMP/ANL V4.2 Output File for Test Problem 3 with Pinhole with Decreasing RMID (Input File: problem3.decrRMID.with.pinhole-20.inp)

FUEL PLATE 1 (ExactSoln), Assembly = 1 of Type = 1

NODE	COOLANT outer(C)	CladSurf outer(C)	FUEL PEAK (C)	CladSurf inner(C)	COOLANT inner(C)	HCOFouter W/C-m^2	HCOFinner W/C-m^2	ONBRout [F Note 1]	ONBRin	ETAout K-cm^3/J [Note 3]	ETAin K-cm^3/J [Note 3]	ONB Temp outer(C)	ONB Temp inner(C)	Avg Meat Temp (C)
	45.000				45.000									
1	45.808	213.802	303.094	170.697	46.267	4.6347E+03	7.8929E+03	0.48	0.66	6.205E+01	7.871E+01	125.888	127.577	265.690
2	48.235	213.204	302.745	170.662	50.068	4.7261E+03	8.1341E+03	0.48	0.65	5.901E+01	7.321E+01	125.531	127.207	265.367
3	51.475	212.718	302.653	171.066	55.131	4.8458E+03	8.4449E+03	0.48	0.65	5.495E+01	6.587E+01	125.052	126.706	265.316
4	54.723	212.553	302.942	171.921	60.190	4.9629E+03	8.7433E+03	0.47	0.64	5.087E+01	5.852E+01	124.567	126.195	265.649
5	57.979	212.672	303.560	173.160	65.243	5.0773E+03	9.0304E+03	0.47	0.63	4.678E+01	5.113E+01	124.077	125.674	266.315
6	61.244	213.015	304.404	174.624	70.288	5.1891E+03	9.3177E+03	0.47	0.62	4.269E+01	4.371E+01	123.578	125.146	267.206
7	64.519	213.625	305.606	176.555	75.326	5.2986E+03	9.5761E+03	0.46	0.61	3.858E+01	3.626E+01	123.074	124.605	268.461
8	67.805	214.296	306.967	178.759	80.354	5.4130E+03	9.8181E+03	0.46	0.59	3.446E+01	2.877E+01	122.566	124.051	269.881
9	71.103	215.328	308.653	181.238	85.372	5.5171E+03	1.0046E+04	0.45	0.58	3.035E+01	2.123E+01	122.047	123.490	271.620
10	74.412	216.553	310.530	183.901	90.381	5.6172E+03	1.0266E+04	0.45	0.56	2.624E+01	1.364E+01	121.518	122.920	273.548
11	76.900	217.580	312.033	185.977	94.131	5.6898E+03	1.0429E+04	0.44	0.55	2.317E+01	7.910E+00	121.115	122.485	275.086
	77.731				95.381									268.375

FUEL PLATE 2 (ExactSoln), Assembly = 1 of Type = 1

NODE	COOLANT outer(C)	CladSurf outer(C)	FUEL PEAK (C)	CladSurf inner(C)	COOLANT inner(C)	HCOFouter W/C-m^2	HCOFinner W/C-m^2	ONBRout [F Note 1]	ONBRin	ETAout K-cm^3/J [Note 3]	ETAin K-cm^3/J [Note 3]	ONB Temp outer(C)	ONB Temp inner(C)	Avg Meat Temp (C)
	45.000				45.000									
1	46.267	161.220	274.009	148.752	46.096	7.8929E+03	9.7277E+03	0.71	0.80	8.520E+01	1.010E+02	126.985	127.703	234.370
2	50.068	161.651	274.519	149.350	49.384	8.1341E+03	9.9859E+03	0.70	0.79	7.912E+01	9.474E+01	126.625	127.341	234.882
3	55.131	162.638	275.567	150.465	53.768	8.4449E+03	1.0321E+04	0.69	0.78	7.104E+01	8.637E+01	126.138	126.853	235.931
4	60.190	164.035	276.984	151.903	58.153	8.7433E+03	1.0644E+04	0.68	0.76	6.296E+01	7.796E+01	125.642	126.358	237.348
5	65.243	165.780	278.714	153.618	62.539	9.0304E+03	1.0957E+04	0.66	0.74	5.488E+01	6.952E+01	125.137	125.858	239.078
6	70.288	167.707	280.598	155.453	66.926	9.3177E+03	1.1275E+04	0.65	0.73	4.681E+01	6.105E+01	124.622	125.350	240.961
7	75.326	170.080	282.885	157.646	71.315	9.5761E+03	1.1566E+04	0.63	0.71	3.873E+01	5.256E+01	124.098	124.836	243.247
8	80.354	172.730	285.426	160.068	75.704	9.8181E+03	1.1842E+04	0.62	0.69	3.065E+01	4.404E+01	123.565	124.313	245.786
9	85.372	175.602	288.178	162.687	80.095	1.0046E+04	1.2102E+04	0.60	0.67	2.256E+01	3.551E+01	123.022	123.783	248.535
10	90.381	178.635	291.090	165.466	84.487	1.0266E+04	1.2350E+04	0.58	0.65	1.446E+01	2.696E+01	122.469	123.243	251.445
11	94.131	180.974	293.345	167.629	87.782	1.0429E+04	1.2530E+04	0.57	0.63	8.366E+00	2.055E+01	122.049	122.831	253.698
	95.381				88.881									242.125

[1] The ONB ratio is here defined as (Tonb - Tinlet)/(Tsurf - Tinlet). If the heat flux is negative (the coolant is hotter than the adjacent cladding surface), then the ONB ratio is arbitrarily set to 99.99 .

[3] The column gives ETA' = (Coolant Velocity)*(Tsat - Coolant Temp)/(Heat Flux). ETA' in the units chosen here, equals Whittle and Forgan dimensionless ETA for water-cooled reactors: ETA = ETA'*Coolant Density*Cp/4. The last value in the colunm (at exit) should be greater than 32.5 to avoid excursive flow instability. ETA is also used in the equation R = 1/(1+ETA*Dh/Lh)

Figure 16.10 Continued

FUEL PLATE 3 (ExactSoln), Assembly = 1 of Type = 1

NODE	COOLANT outer(C)	CladSurf outer(C)	FUEL PEAK (C)	CladSurf inner(C)	COOLANT inner(C)	HCOFouter W/C-m^2	HCOFinner W/C-m^2	ONBRout [F Note 1]	ONBRin	ETAout K-cm^3/J [Note 3]	ETAin K-cm^3/J [Note 3]	ONB Temp outer(C)	ONB Temp inner(C)	Avg Meat Temp (C)
	45.000				45.000									
1	46.096	163.217	305.663	147.203	46.042	9.7277E+03	1.2573E+04	0.71	0.83	8.851E+01	1.094E+02	128.731	129.626	255.592
2	49.384	163.528	306.104	147.789	49.168	9.9859E+03	1.2891E+04	0.70	0.82	8.297E+01	1.030E+02	128.378	129.269	256.035
3	53.768	164.267	306.993	148.846	53.336	1.0321E+04	1.3304E+04	0.70	0.81	7.558E+01	9.433E+01	127.901	128.788	256.927
4	58.153	165.339	308.193	150.188	57.503	1.0644E+04	1.3703E+04	0.68	0.79	6.818E+01	8.565E+01	127.416	128.300	258.129
5	62.539	166.703	309.664	151.777	61.668	1.0957E+04	1.4089E+04	0.67	0.78	6.079E+01	7.695E+01	126.923	127.805	259.601
6	66.926	168.199	311.296	153.562	65.833	1.1275E+04	1.4464E+04	0.66	0.76	5.337E+01	6.822E+01	126.423	127.301	261.236
7	71.315	170.046	313.170	155.464	69.996	1.1566E+04	1.4845E+04	0.65	0.74	4.596E+01	5.945E+01	125.912	126.793	263.110
8	75.704	172.155	315.327	157.676	74.158	1.1842E+04	1.5189E+04	0.63	0.72	3.852E+01	5.066E+01	125.393	126.275	265.268
9	80.095	174.480	317.686	160.072	78.319	1.2102E+04	1.5515E+04	0.62	0.70	3.107E+01	4.184E+01	124.865	125.750	267.627
10	84.487	176.985	320.213	162.624	82.478	1.2350E+04	1.5825E+04	0.60	0.68	2.361E+01	3.300E+01	124.327	125.215	270.155
11	87.782	178.956	322.197	164.621	85.597	1.2530E+04	1.6049E+04	0.59	0.67	1.799E+01	2.635E+01	123.917	124.809	272.139
	88.881				86.636									262.195

FUEL PLATE 4 (ExactSoln), Assembly = 1 of Type = 1

NODE	COOLANT outer(C)	CladSurf outer(C)	FUEL PEAK (C)	CladSurf inner(C)	COOLANT inner(C)	HCOFouter W/C-m^2	HCOFinner W/C-m^2	ONBRout [F Note 1]	ONBRin	ETAout K-cm^3/J [Note 3]	ETAin K-cm^3/J [Note 3]	ONB Temp outer(C)	ONB Temp inner(C)	Avg Meat Temp (C)
	45.000				45.000									
1	46.042	168.693	365.690	155.092	45.794	1.2573E+04	1.5836E+04	0.70	0.79	9.025E+01	1.080E+02	131.278	132.324	297.904
2	49.168	168.818	365.888	155.374	48.174	1.2891E+04	1.6143E+04	0.69	0.79	8.487E+01	1.030E+02	130.933	131.978	298.103
3	53.336	169.287	366.402	155.937	51.346	1.3304E+04	1.6544E+04	0.69	0.78	7.770E+01	9.623E+01	130.464	131.513	298.617
4	57.503	170.073	367.175	156.696	54.517	1.3703E+04	1.6935E+04	0.68	0.77	7.052E+01	8.946E+01	129.988	131.042	299.390
5	61.668	171.136	368.179	157.633	57.687	1.4089E+04	1.7316E+04	0.67	0.76	6.334E+01	8.266E+01	129.503	130.565	300.393
6	65.833	172.437	369.382	158.727	60.856	1.4464E+04	1.7688E+04	0.66	0.75	5.614E+01	7.583E+01	129.010	130.082	301.596
7	69.996	173.841	370.700	159.949	64.023	1.4845E+04	1.8051E+04	0.65	0.74	4.893E+01	6.899E+01	128.509	129.591	302.914
8	74.158	175.593	372.218	161.203	67.190	1.5189E+04	1.8430E+04	0.64	0.72	4.171E+01	6.211E+01	127.997	129.096	304.431
9	78.319	177.568	373.969	162.702	70.357	1.5515E+04	1.8775E+04	0.62	0.71	3.446E+01	5.522E+01	127.477	128.592	306.181
10	82.478	179.726	375.879	164.332	73.523	1.5825E+04	1.9106E+04	0.61	0.70	2.720E+01	4.831E+01	126.947	128.081	308.089
11	85.597	181.442	377.399	165.632	75.898	1.6049E+04	1.9345E+04	0.60	0.69	2.173E+01	4.312E+01	126.544	127.692	309.608
	86.636				76.689									302.347

[1] The ONB ratio is here defined as (Tonb - Tinlet)/(Tsurf - Tinlet). If the heat flux is negative (the coolant is hotter than the adjacent cladding surface), then the ONB ratio is arbitrarily set to 99.99 .

[3] The column gives ETA' = (Coolant Velocity)*(Tsat - Coolant Temp)/(Heat Flux). ETA' in the units chosen here, equals Whittle and Forgan dimensionless ETA for water-cooled reactors: ETA = ETA'*Coolant Density*Cp/4. The last value in the colunm (at exit) should be greater than 32.5 to avoid excursive flow instability. ETA is also used in the equation R = 1/(1+ETA*Dh/Lh)

Figure 16.10 Continued

FUEL PLATE 5 (ExactSoln), Assembly = 1 of Type = 1

NODE	COOLANT outer(C)	CladSurf outer(C)	FUEL PEAK (C)	CladSurf inner(C)	COOLANT inner(C)	HCOFouter W/C-m^2	HCOFinner W/C-m^2	ONBRout [F Note 1]	ONBRin	ETAout K-cm^3/J [Note 3]	ETAin K-cm^3/J [Note 3]	ONB Temp outer(C)	ONB Temp inner(C)	Avg Meat Temp (C)
	45.000				45.000									
1	45.794	110.541	242.619	90.071	45.289	1.5836E+04	2.8583E+04	1.26	1.88	1.823E+02	3.097E+02	127.906	129.679	195.555
2	48.174	111.641	243.493	90.665	46.158	1.6143E+04	2.8787E+04	1.24	1.85	1.739E+02	3.028E+02	127.540	129.334	196.427
3	51.346	113.202	244.720	91.474	47.317	1.6544E+04	2.9059E+04	1.20	1.80	1.627E+02	2.934E+02	127.046	128.870	197.648
4	54.517	114.865	246.011	92.300	48.478	1.6935E+04	2.9328E+04	1.17	1.76	1.515E+02	2.840E+02	126.543	128.400	198.933
5	57.687	116.621	247.363	93.144	49.640	1.7316E+04	2.9595E+04	1.13	1.72	1.402E+02	2.745E+02	126.032	127.924	200.278
6	60.856	118.461	248.769	94.004	50.803	1.7688E+04	2.9861E+04	1.10	1.68	1.288E+02	2.649E+02	125.511	127.441	201.675
7	64.023	120.377	250.225	94.878	51.969	1.8051E+04	3.0124E+04	1.06	1.64	1.174E+02	2.553E+02	124.982	126.952	203.121
8	67.190	122.294	251.686	95.761	53.136	1.8430E+04	3.0386E+04	1.03	1.60	1.060E+02	2.457E+02	124.443	126.454	204.570
9	70.357	124.350	253.234	96.664	54.305	1.8775E+04	3.0646E+04	0.99	1.57	9.445E+01	2.359E+02	123.894	125.950	206.106
10	73.523	126.479	254.831	97.580	55.476	1.9106E+04	3.0904E+04	0.96	1.53	8.285E+01	2.261E+02	123.335	125.438	207.687
11	75.898	128.119	256.058	98.276	56.355	1.9345E+04	3.1095E+04	0.94	1.50	7.410E+01	2.188E+02	122.909	125.048	208.901
	76.689				56.649									201.867

FUEL PLATE 6 (ExactSoln), Assembly = 1 of Type = 1

NODE	COOLANT outer(C)	CladSurf outer(C)	FUEL PEAK (C)	CladSurf inner(C)	COOLANT inner(C)	HCOFouter W/C-m^2	HCOFinner W/C-m^2	ONBRout [F Note 1]	ONBRin	ETAout K-cm^3/J [Note 3]	ETAin K-cm^3/J [Note 3]	ONB Temp outer(C)	ONB Temp inner(C)	Avg Meat Temp (C)
	45.000				45.000									
1	45.289	71.530	259.037	259.037	45.000	2.8583E+04	1.0000E+00	3.04	999.99	5.286E+02	7.703E+21	125.628	107.070	196.535
2	46.158	72.212	259.719	259.719	45.000	2.8787E+04	1.0000E+00	2.95	999.99	5.172E+02	7.624E+21	125.261	106.640	197.217
3	47.317	73.127	260.635	260.635	45.000	2.9059E+04	1.0000E+00	2.84	999.99	5.020E+02	7.518E+21	124.766	106.059	198.133
4	48.478	74.051	261.558	261.558	45.000	2.9328E+04	1.0000E+00	2.73	999.99	4.867E+02	7.411E+21	124.262	105.468	199.056
5	49.640	74.982	262.490	262.490	45.000	2.9595E+04	1.0000E+00	2.63	999.99	4.712E+02	7.303E+21	123.751	104.866	199.987
6	50.803	75.920	263.428	263.428	45.000	2.9861E+04	1.0000E+00	2.53	999.99	4.557E+02	7.195E+21	123.231	104.254	200.925
7	51.969	76.866	264.374	264.373	45.000	3.0124E+04	1.0000E+00	2.44	999.99	4.400E+02	7.086E+21	122.703	103.630	201.871
8	53.136	77.819	265.326	265.326	45.000	3.0386E+04	1.0000E+00	2.35	999.99	4.242E+02	6.977E+21	122.165	102.995	202.824
9	54.305	78.779	266.286	266.286	45.000	3.0646E+04	1.0000E+00	2.27	999.99	4.083E+02	6.866E+21	121.619	102.348	203.784
10	55.476	79.746	267.253	267.253	45.000	3.0904E+04	1.0000E+00	2.19	999.99	3.923E+02	6.755E+21	121.063	101.688	204.751
11	56.355	80.475	267.983	267.983	45.000	3.1095E+04	1.0000E+00	2.13	999.99	3.802E+02	6.671E+21	120.639	101.185	205.480
	56.649				45.000									200.955

[1] The ONB ratio is here defined as (Tonb - Tinlet)/(Tsurf - Tinlet). If the heat flux is negative (the coolant is hotter than the adjacent cladding surface), then the ONB ratio is arbitrarily set to 99.99 .

[3] The column gives ETA' = (Coolant Velocity)*(Tsat - Coolant Temp)/(Heat Flux). ETA' in the units chosen here, equals Whittle and Forgan dimensionless ETA for water-cooled reactors: ETA = ETA'*Coolant Density*Cp/4. The last value in the colunm (at exit) should be greater than 32.5 to avoid excursive flow instability. ETA is also used in the equation R = 1/(1+ETA*Dh/Lh)

Table 16.1 Geometry and Operating Data for a 6-Tube Radial Geometry Problem without a Pinhole - Test Problem 1

Total Power = 1.31193 MW, Inlet temperature = 45 ºC, Heated length = 0.58 m,
Fuel tube thickness = 2 mm, C_p = 4180 J/kg-ºC (constant), Fuel thermal conductivity = 10 W/m-ºC

Fuel Tube No. or Channel No.	1	2	3	4	5	6	7
BASIC INPUT DATA USED IN THE SPREADSHEET CALCULATION							
Fuel Tube Inner Radius, m	0.017	0.023	0.029	0.035	0.041	0.047	
Fuel Tube Outer Radius, m	0.019	0.025	0.031	0.037	0.043	0.049	
Heat Trans. Coef. in Channel, W/m^2-ºC	10000	30000	20000	50000	15000	40000	25000
Power density, W/m^3	7.500E+08	9.000E+08	1.300E+09	9.500E+08	8.500E+08	7.500E+08	
Channel Flow Rate in Channel, kg/s	0.85	1.15	1.25	1.46	1.44	1.4	1.05
DERIVED DATA FOR PLTEMP INPUT PREPARATION							
RMID, m	0.018	0.024	0.03	0.036	0.042	0.048	
CIRCF, m	0.113097	0.150796	0.188496	0.226195	0.263894	0.301593	
Radial power factor	0.813053	0.975664	1.409292	1.029867	0.921460	0.813053	
Wetted Perimeter, m	0.106814	0.263894	0.339292	0.414690	0.490088	0.565487	0.307876
Heated Perimeter, m	0.106814	0.263894	0.339292	0.414690	0.490088	0.565487	0.307876

Table 16.2 Geometry and Operating Data for a 6-Tube Radial Geometry Problem with a Pinhole - Test Problem 2

Total Power = 1.17828 MW, Inlet temperature = 45 ºC, Heated length = 0.58 m,
Fuel tube thickness = 5 mm, C_p = 4180 J/kg-ºC (constant), Fuel thermal conductivity = 10 W/m-ºC

Fuel Tube No. or Channel No.	1	2	3	4	5	6	7
BASIC INPUT DATA USED IN THE SPREADSHEET CALCULATION							
Fuel Tube Inner Radius, m	0.00000010	0.00900010	0.01800010	0.02700010	0.03600010	0.04500010	0.05400010
Fuel Tube Outer Radius, m	0.00500010	0.01400010	0.02300010	0.03200010	0.04100010	0.05000010	
Heat Trans. Coef. in Channel, W/m^2-ºC	10000	30000	20000	50000	15000	40000	25000
Power density, W/m^3	3.000E+08	4.500E+08	6.500E+08	4.800E+08	3.800E+08	3.500E+08	
Channel Flow Rate, kg/s	0.85	1.15	1.25	1.46	1.44	1.4	1.05
DERIVED DATA FOR PLTEMP INPUT PREPARATION							
RMID, m	0.002500100	0.011500100	0.020500100	0.029500100	0.038500100	0.047500100	
CIRCF, m	0.015708592	0.072257259	0.128805927	0.185354595	0.241903263	0.298451930	
Radial power factor	0.679508	1.019262	1.472267	1.087212	0.860710	0.792759	
Flow area of channel, m^2	3.14159E-14	1.75932E-04	4.02126E-04	6.28321E-04	8.54516E-04	1.08071E-03	1.30691E-03
Hydraulic diameter, m	2.0000E-07	8.0000E-03	8.0000E-03	8.0000E-03	8.0000E-03	8.0000E-03	1.6640E-02
Wetted Perimeter, m	0.000000628	0.087965851	0.201063186	0.314160522	0.427257858	0.540355193	0.314159894
Heated Perimeter, m	0.000000628	0.087965851	0.201063186	0.314160522	0.427257858	0.540355193	0.314159894

Table 16.3 Excel Spreadsheet Calculated Results for Test Problem 1

			At Axial Location $Z/L_h = 0.5$			
Tube No. Or Chan No.	Fuel Tube Power	Coolant Channel Outlet Temp.	Tube Inner Surf Temp.	Fuel Max Temp	Tube Outer Surf Temp.	Areal Frac. on Inside of Adiabatic Point
	kW	ºC	ºC	ºC	ºC	
1	98.395	56.000	113.585	139.281	88.275	0.3972
2	157.431	74.443	92.418	144.260	105.435	0.5222
3	284.251	83.314	123.285	175.980	97.681	0.4397
4	249.267	93.968	91.368	153.045	117.657	0.5599
5	260.199	81.836	113.400	146.001	92.471	0.4305
6	262.386	92.663	87.915	126.211	89.485	0.4983
7	-	74.994	-	-	-	-

Table 16.4 Results for Test Problem 1 Calculated by PLTEMP Versions 42bta_r65_131030 and 4.2 with Hard-Coded Values of Heat Transfer Coefficients

The heat transfer coefficient in each coolant channel was set to a given value in subroutines hcoef.f and hcoef1.f of the code.

			At Axial Location $Z/L_h = 0.5$			
Tube No. Or Chan No.	Fuel Tube Power	Coolant Channel Outlet Temp.	Tube Inner Surf Temp.	Fuel Max Temp	Tube Outer Surf Temp.	Areal Frac. on Inside of Adiabatic Point
	kW	ºC	ºC	ºC	ºC	
1	98.394	56.005	113.506	139.239	88.280	0.3975
2	157.43	74.437	92.431	144.254	105.413	0.5222
3	284.25	83.326	123.296	176.064	97.851	0.4400
4	249.27	93.940	91.525	153.046	117.541	0.5592
5	260.20	81.884	113.319	146.080	92.753	0.4316
6	262.39	92.589	88.180	126.238	89.281	0.4967
7	-	75.053	-	-	-	-

Maximum Absolute Temperature Difference between Tables 16.3 and 16.4 = 0.28 ºC
RMS Temperature Difference between Tables 16.3 and 16.4 = 0.11 ºC

Table 16.5 Excel Spreadsheet Calculated Results for Test Problem 2 with Pinhole

			At Axial Location $Z/L_h = 0.5$			
Tube No. Or Chan No.	Fuel Tube Power	Coolant Channel Outlet Temp.	Tube Inner Surf Temp.	Fuel Max Temp	Tube Outer Surf Temp.	Areal Frac. on Inside of Adiabatic Point
	kW	ºC	ºC	ºC	ºC	
1	13.6665	45.000	263.040	263.159	75.769	0.0001
2	94.296	56.539	93.254	244.604	111.559	0.4433
3	242.799	75.231	140.504	323.280	99.771	0.4344
4	258.014	89.002	93.670	267.342	137.903	0.5085
5	266.577	85.816	125.811	229.351	94.943	0.4459
6	302.929	95.456	92.723	204.219	96.807	0.4871
7	-	80.399	-	-	-	-

Table 16.6 Results for Test Problem 2 Calculated by PLTEMP Versions 42bta_r65_131030 and 4.2 with Hard-Coded Values of Heat Transfer Coefficients

The heat transfer coefficient in each coolant channel was set to a given value in subroutines hcoef.f and hcoef1.f of the code.

			At Axial Location $Z/L_h = 0.5$			
Tube No. Or Chan No.	Fuel Tube Power	Coolant Channel Outlet Temp.	Tube Inner Surf Temp.	Fuel Max Temp	Tube Outer Surf Temp.	Areal Frac. on Inside of Adiabatic Point
	kW	ºC	ºC	ºC	ºC	
1	13.666	45.000	263.017	263.130	75.735	0.0001
2	94.296	56.539	93.222	244.583	111.547	0.4433
3	242.80	75.232	140.499	323.300	99.816	0.4344
4	258.01	89.000	93.712	267.337	137.858	0.5084
5	266.58	85.823	125.779	229.397	95.074	0.4461
6	302.93	95.442	92.849	204.226	96.700	0.4868
7	-	80.411	-	-	-	-

Maximum Absolute Temperature Difference between Tables 16.5 and 16.6 = 0.131 ºC
RMS Temperature Difference between Tables 16.5 and 16.6 = 0.048 ºC

Table 16.7 Comparison of PLTEMP/ANL Version 4.2 Results for Test Problem 3 with Increasing versus Decreasing Fuel Tube Radii

Channel Number or Tube Number	Channel Outlet Temp. ºC			Heat Transfer Coef. At Location Z/L_h=0.5 kW/m^2-ºC [Note 1]			Areal Frac. on Inside of Adiabatic Point At Location Z/L_h=0.5			Maximum Fuel Temperature At Location Z/L_h=0.5 ºC		
	RMID Incr'g	RMID Decr'g [Note 2]	Excel RMID Incr'g	RMID Incr'g	RMID Decr'g [Note 2]	Excel RMID Incr'g	RMID Incr'g	RMID Decr'g [Note 2]	Excel RMID Incr'g	RMID Incr'g	RMID Decr'g [Note 2]	Excel RMID Incr'g
1	45.000	45.000	45.000	0.001	0.001	0.001	0.0000	0.0000	0.0000	263.428	263.428	263.447
2	56.649	56.649	56.644	29.861	29.861	29.861	0.4487	0.4487	0.4487	248.769	248.769	248.770
3	76.689	76.689	76.683	17.688	17.688	17.688	0.4677	0.4677	0.4677	369.382	369.382	369.368
4	86.636	86.636	86.637	14.464	14.464	14.464	0.4839	0.4839	0.4839	311.296	311.296	311.295
5	88.881	88.881	88.874	11.275	11.275	11.275	0.4912	0.4912	0.4912	280.598	280.598	280.565
6	95.381	95.381	95.429	9.3177	9.3177	9.3177	0.5263	0.5263	0.5264	304.404	304.404	304.414
7	77.731	77.731	77.687	5.1891	5.1891	5.1891						

1. The Dittus-Boelter heat transfer correlation was used in the PLTEMP/ANL calculation. Then the heat transfer coefficient varies from channel to channel, and is independent of the plate surface temperature.
2. The values printed in the code output file are rearranged in the column in the order of the innermost to the outermost fuel tube.

17 Verification of H_2O and D_2O Coolant Properties Calculated by the Code Version 4.2

17.1 Introduction and Summary

The thermal properties of liquid H_2O and liquid D_2O coolant calculated by the PLTEMP/ANL version 4.2 code [1] are verified by comparison with the National Institute of Standards and Technology (NIST) data [2].

Table 17.15 summarizes the maximum percent difference in five properties of H_2O over the pressure range of 1 to 145 bar and temperature range of 4 to 339 ºC. The maximum difference in enthalpy is 0.6%, in thermal conductivity 2.2%, in density 0.12%, in dynamic viscosity 21.4%, and in specific heat 3.7%. All the properties are in reasonable agreement with the NIST data except for the dynamic viscosity near saturation temperature at pressures above 100 bar.

Table 17.30 summarizes the maximum percent difference in five properties of D_2O over the pressure range of 1 to 150 bar and temperature range of 5 to 341 ºC. The maximum difference is 2.8% in enthalpy, 4.8% in thermal conductivity, 3.4% in specific heat, 0.5% in density, and 1.8% in liquid D_2O dynamic viscosity.

The PLTEMP/ANL code is limited as follows:
The maximum pressure that can be used is 16.790 MPa for light or heavy water, provided that the maximum coolant temperature does not exceed the smaller of the saturation temperature (T_{sat}) and 340 ºC. The NIST value of saturation pressure at 340 C is 14.60 MPa. During power searches, the code will permit reaching T_{sat}. If the converged problem solution for coolant temperature reaches or exceeds T_{sat}, then the solution is in a two-phase regime that PLTEMP/ANL cannot evaluate correctly.

17.2 Verification of Coolant Thermal Properties

In order to verify the properties of light water and heavy water coolants, the PLPEMP/ANL version 4.2 code was run for a sample problem, changing the inlet pressure in the input data file to 14 selected values ranging from 1 to 150 bar. For light water, the code ran at 145 bar but did not at 150 bar. For heavy water, the code ran at 150 bar. The pressures at which the liquid H_2O properties were calculated by the code and compared with the NIST data are: 1, 2, 3, 4, 5, 10, 20, 30, 40, 50, 75, 100, 125, and 145 bar. The pressures at which the liquid D_2O properties were calculated by the code and compared with the NIST data are: 1, 2, 3, 4, 5, 10, 20, 30, 40, 50, 75, 100, 125, and 150 bar. The code prints five thermal properties (enthalpy, thermal conductivity, specific heat at constant pressure, density, and dynamic viscosity) of the coolant at the inlet pressure. Two sets of 14 problems were run, one for liquid H_2O (input option IFLUID = 0) and the other for liquid D_2O (input option IFLUID = 1). Figures 17.1 to 17.4 show the dependence of enthalpy of light water and heavy water on temperature at all 14 pressures.

17.2.1 Verification of Liquid H_2O Thermal Properties

The properties of liquid H_2O are compared in Tables 17.1 to 17.15 with the National Institute of Standards and Technology (NIST) properties data [2]. Tables 17.1 to 17.14 compare five code-calculated thermal properties (enthalpy, thermal conductivity, specific heat at constant pressure, density, and dynamic viscosity) of liquid H_2O with NIST data [2] over the pressure range of 1 to 145 bar and temperature range of 4 to 339 ºC. The percent difference in each thermal property at each (temperature, pressure) point is shown in the last five columns, with the maximum percent difference at a given pressure shown in the last row of Tables 17.1 to 17.14.

Table 17.15 summarizes the last rows of Tables 17.1 through 17.14, and shows the maximum percent difference in each H_2O property over the pressure range of 1 to 145 bar and temperature range of 4 to 339 ºC. The maximum difference in enthalpy is 0.6%, in thermal conductivity 2.2%, in density 0.12%, in dynamic viscosity 21.4%, and in specific heat 3.7%. All the properties are in reasonable agreement with the NIST data except for the dynamic viscosity near saturation temperature at pressures above 100 bar.

17.2.2 Verification of Liquid D_2O Thermal Properties

Tables 17.16 to 17.30 compare the code-calculated D_2O thermal properties with the NIST data. It is important to note that the D_2O enthalpy data on the NIST website [2] has a different reference compared to the reference used for the H_2O enthalpy data. The D_2O enthalpy on the NIST website is tabulated using a reference that the liquid D_2O enthalpy at its *boiling* point (101.41 ºC) at the normal atmospheric pressure (1.01325 bar) is zero, whereas the H_2O enthalpy is tabulated using the reference that the liquid H_2O enthalpy at its *freezing* point (0.0 ºC) at the normal atmospheric pressure (1.01325 bar) is zero. The liquid D_2O properties at 1.01325 bar obtained from the NIST website are tabulated below without changing the enthalpy reference. In this table, the liquid D_2O enthalpy is practically zero (-1.73×10^{-13} kJ/kg) at the normal boiling point of 101.41 ºC, and the enthalpy is -410.80 kJ/kg at the freezing point of 3.822 ºC (38.88 ºF).

Therefore, to change the enthalpy reference to “zero enthalpy at the freezing point”, one needs to add 410.80 kJ/kg to the D_2O enthalpy obtained from the NIST web site at all temperatures and pressures. This change in enthalpy reference has been made in the NIST enthalpy data given in Tables 17.16 to 17.29 for comparison with the code-calculated values.

Tables 17.16 to 17.29 compare five code-calculated thermal properties (enthalpy, thermal conductivity, specific heat at constant pressure, density, and dynamic viscosity) of liquid D_2O with NIST data [2] over the pressure range of 1 to 150 bar and temperature range of 5 to 341 ºC. The percent difference in each thermal property at each (temperature, pressure) point is shown in the last five columns, with the maximum percent difference at a given pressure shown in the last row of Tables 17.16 to 17.29.

NIST Isobaric Data for D_2O at 1.01325 bar Without Changing the Enthalpy Reference

Temp. (C)	Pressure (bar)	Density (kg/m^3)	Volume (m^3/kg)	Internal Energy (kJ/kg)	Enthalpy (kJ/kg)	Entropy (J/g*K)	Cv (J/g*K)	Cp (J/g*K)	Sound Spd. (m/s)	Viscosity (Pa*s)	Therm. Cond. (W/m*K)	Phase
3.8220	1.0132	1105.5	0.00090454	-410.89	**-410.80**	-1.2712	4.2031	4.2105	1324.5	0.0020851	0.56462	liquid
5.0000	1.0132	1105.7	0.00090442	-405.93	-405.84	-1.2533	4.2104	4.2156	1327.7	0.0019962	0.56660	liquid
15.000	1.0132	1105.9	0.00090424	-363.63	-363.54	-1.1040	4.2372	4.2390	1359.3	0.0014366	0.58196	liquid
25.000	1.0132	1104.5	0.00090539	-321.22	-321.12	-0.95924	4.2214	4.2423	1390.0	0.0010951	0.59487	liquid
35.000	1.0132	1101.8	0.00090763	-278.82	-278.72	-0.81937	4.1817	4.2364	1415.1	0.00086998	0.60563	liquid
45.000	1.0132	1098.0	0.00091078	-236.50	-236.41	-0.68423	4.1282	4.2261	1434.0	0.00071281	0.61448	liquid
55.000	1.0132	1093.2	0.00091472	-194.30	-194.21	-0.55363	4.0670	4.2136	1447.1	0.00059808	0.62163	liquid
65.000	1.0132	1087.7	0.00091936	-152.23	-152.14	-0.42734	4.0014	4.2003	1454.8	0.00051139	0.62721	liquid
75.000	1.0132	1081.5	0.00092463	-110.30	-110.20	-0.30512	3.9339	4.1872	1457.8	0.00044408	0.63134	liquid
85.000	1.0132	1074.7	0.00093051	-68.487	-68.393	-0.18672	3.8658	4.1752	1456.4	0.00039063	0.63414	liquid
95.000	1.0132	1067.3	0.00093697	-26.788	-26.693	-0.07188	3.7983	4.1651	1451.1	0.00034742	0.63568	liquid
101.41	1.0133	1062.2	0.00094142	-0.0954	**-1.73e-13**	-4.3e-17	3.7557	4.1600	1445.8	0.00032389	0.63604	liquid
101.41	1.0133	0.66194	1.5107	1917.3	2070.4	5.5275	1.4362	1.9028	446.70	1.2668e-05	0.024961	vapor
105.00	1.0132	0.65519	1.5263	1922.6	2077.2	5.5456	1.4322	1.8959	448.98	1.2806e-05	0.025242	vapor

Table 17.30 summarizes the last rows of Tables 17.16 through 17.29, and shows the maximum percent difference in each D_2O property over the pressure range of 1 to 150 bar and temperature range of 5 to 341 ºC. The maximum difference in enthalpy is 2.8%, in thermal conductivity 3.6%, in specific heat 3.8%, in density 0.5%, and in liquid D_2O dynamic viscosity 1.8%. All the properties are in reasonable agreement with the NIST data.

17.3 Conclusions

Five thermal properties (enthalpy, thermal conductivity, specific heat at constant pressure, density, and dynamic viscosity) of liquid light water and liquid heavy water calculated by the PLTEMP/ANL version 4.2 code are in good agreement with the NIST data over the pressure range of 1 to 145 bar.

17.4 REFERENCES

1. M. Kalimullah, A. P. Olson and E. E. Feldman, "A User's Guide to the PLTEMP/ANL Code," ANL/RTR/TM-18/17 Version 4.3, Revision 0, Argonne National Laboratory, 9700 South Cass Avenue, Argonne, IL 60439, USA (November 2018).
2. National Institute of Standards and Technology (NIST), webbook.nist.gov/chemistry/, 100 Bureau Drive, Gaithersburg, MD 20899, USA (2011).

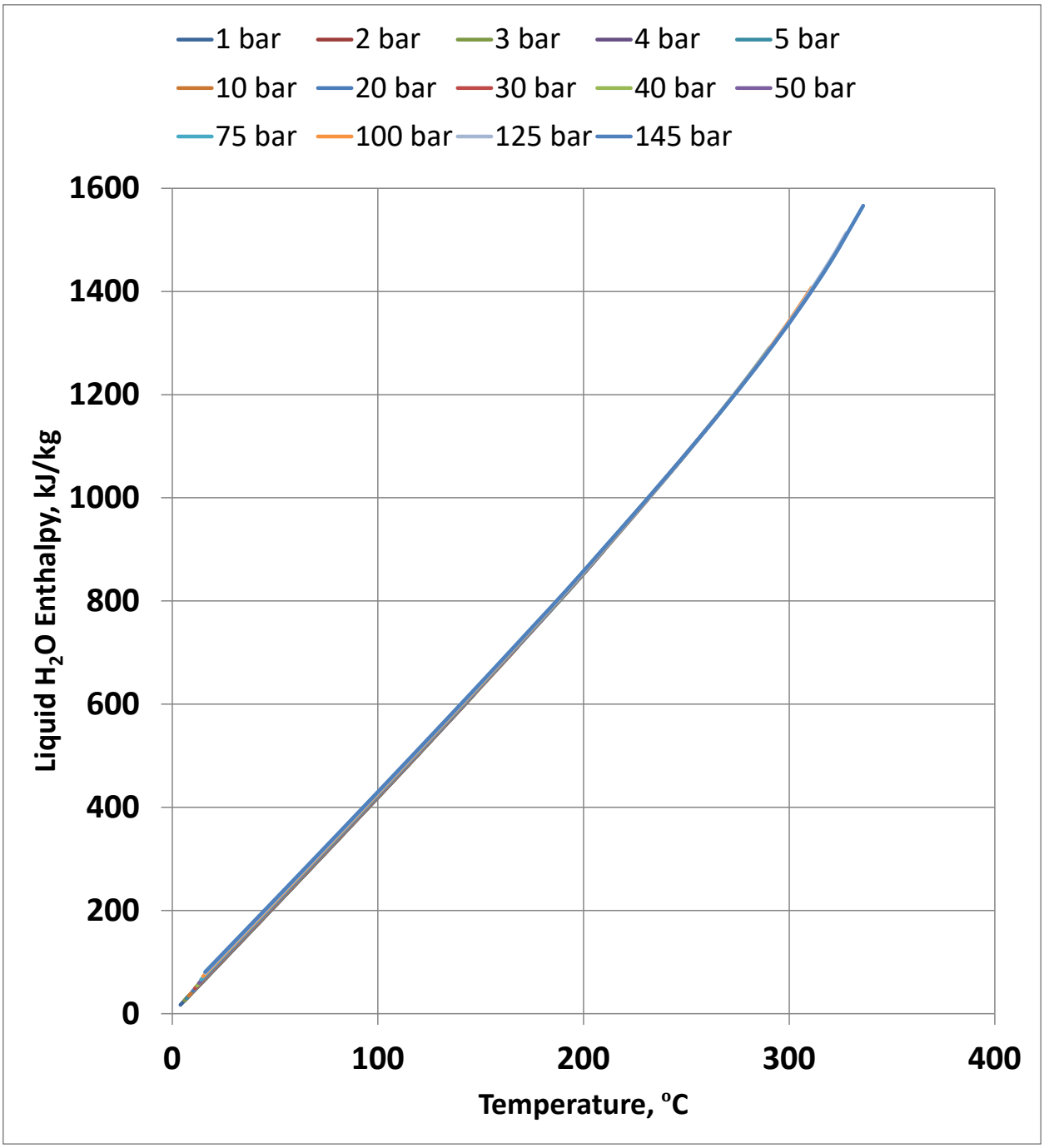

Figure 17.1 Liquid H_2O Enthalpy Calculated by PLTEMP/ANL Code as a Function of Temperature and Pressure

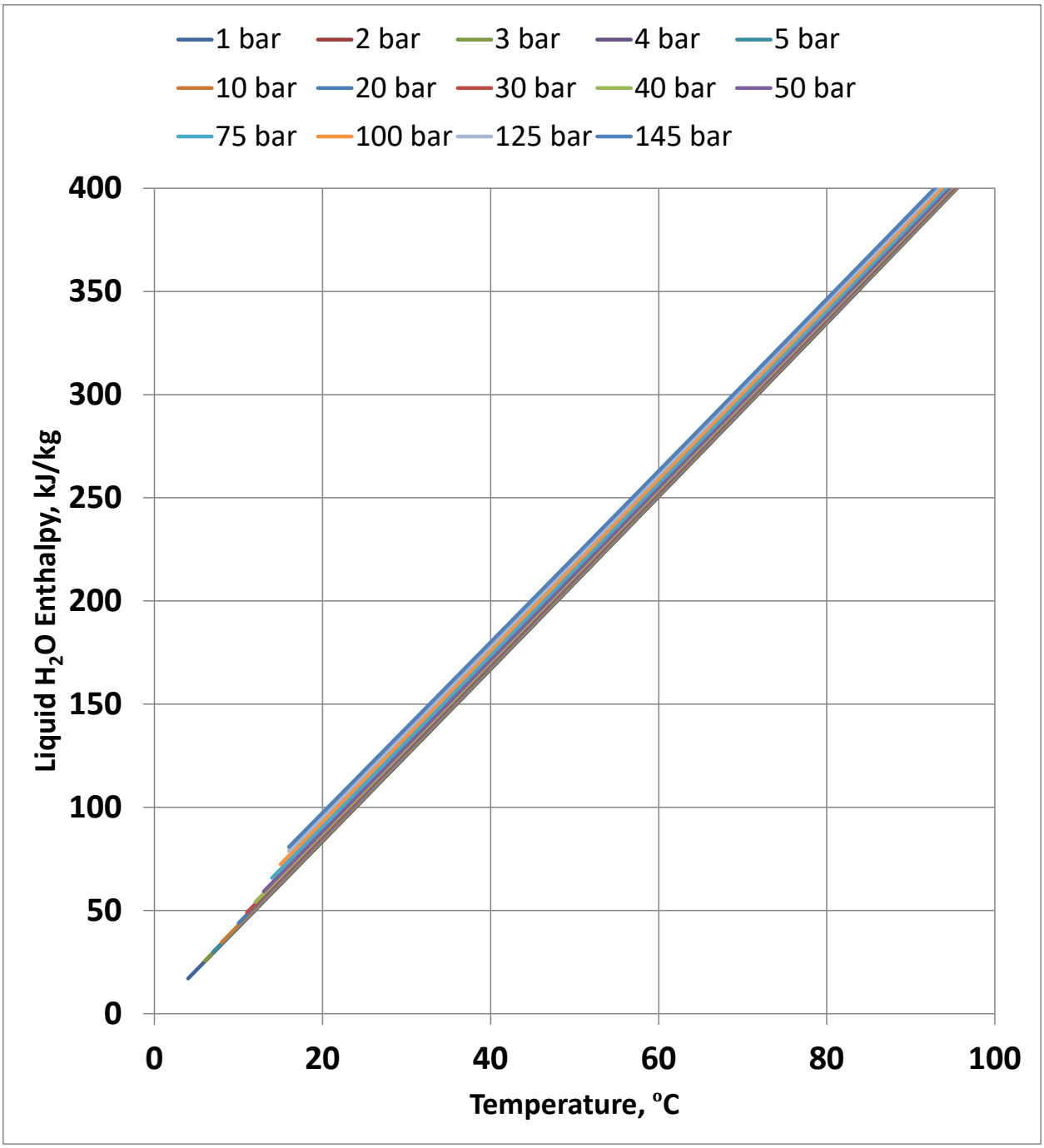

Figure 17.2 Liquid H_2O Enthalpy Calculated by PLTEMP/ANL Code as a Function of Temperature and Pressure (Enlarged View)

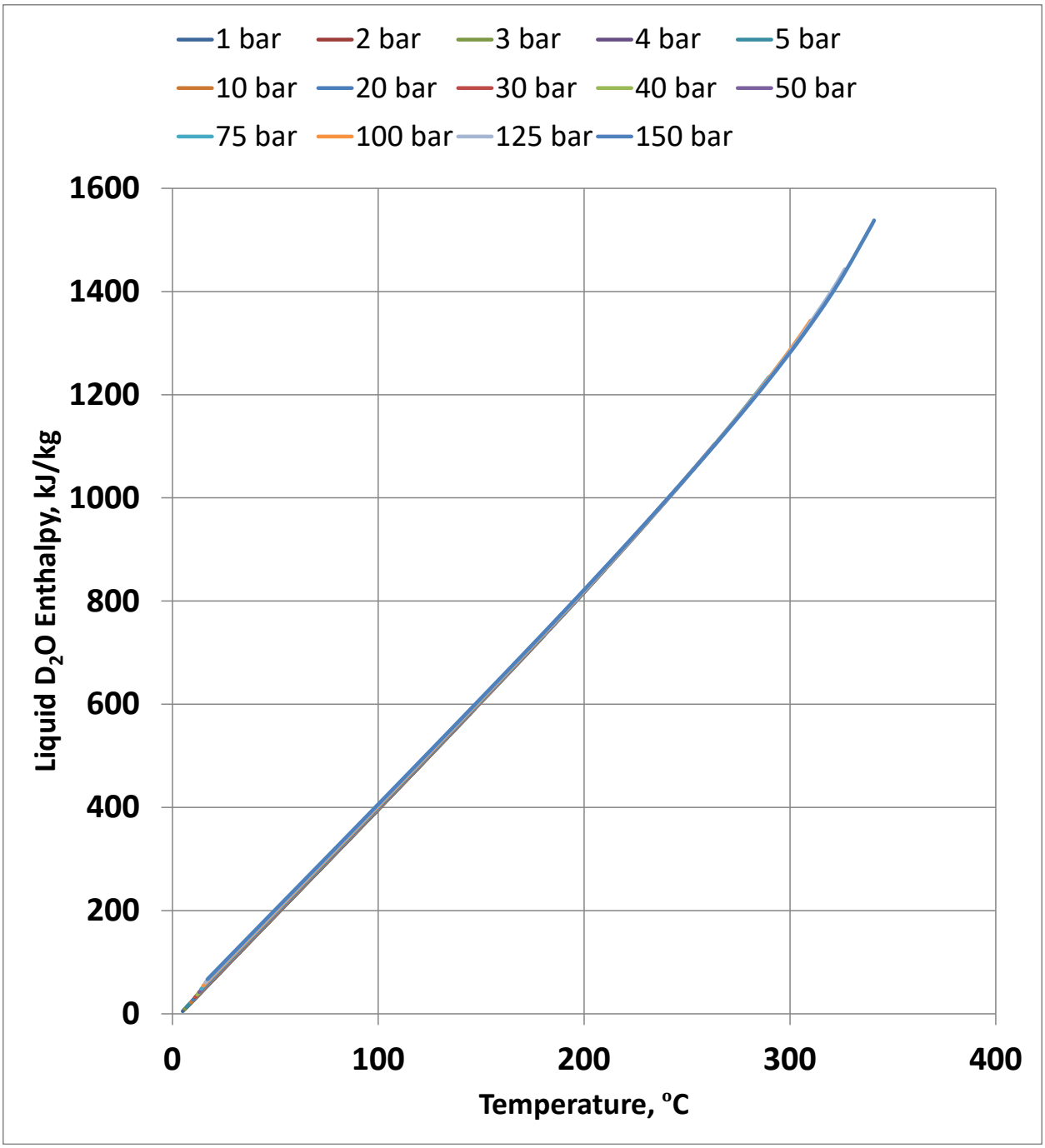

Figure 17.3 Liquid D_2O Enthalpy Calculated by PLTEMP/ANL Code as a Function of Temperature and Pressure

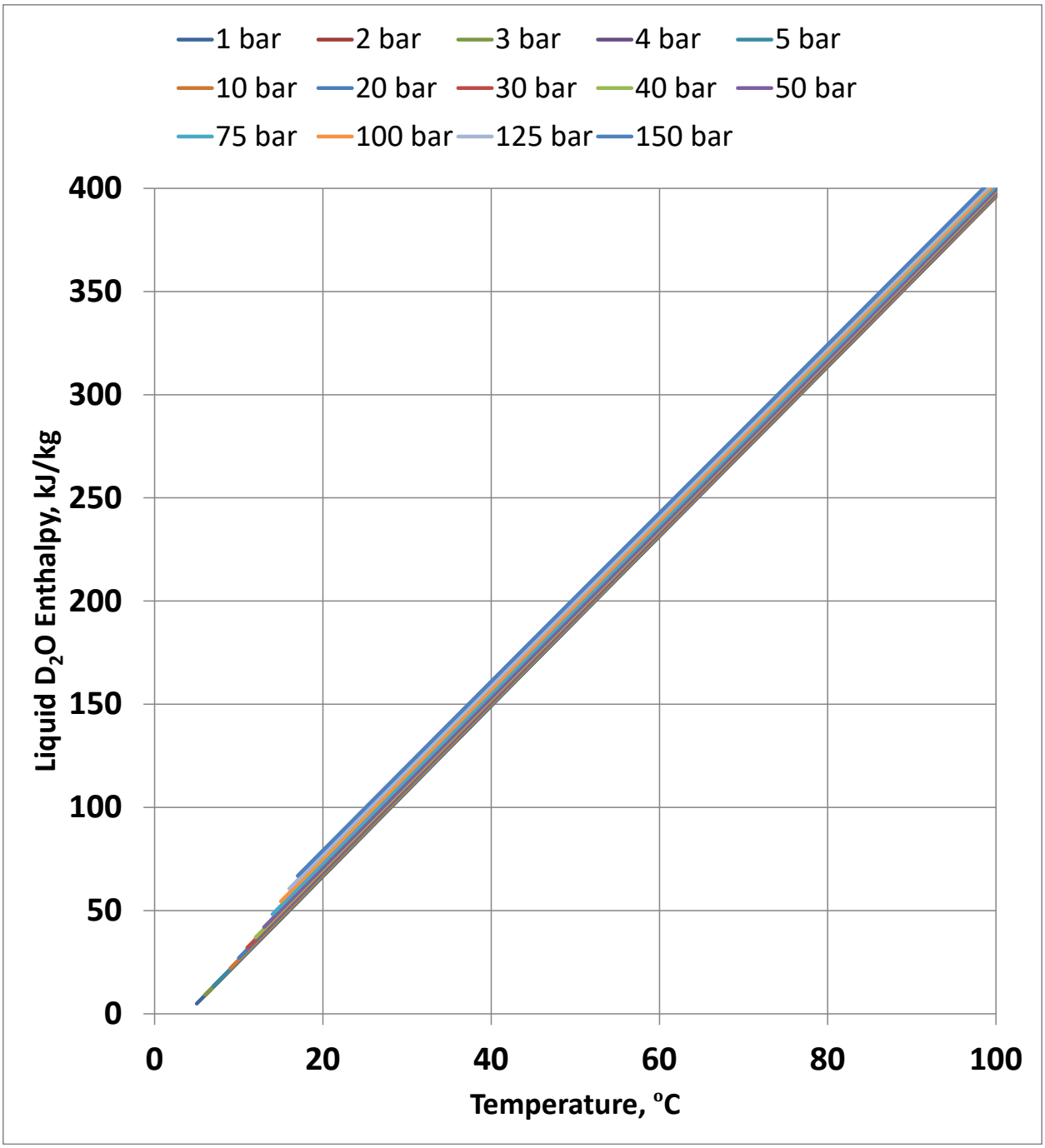

Figure 17.4 Liquid D_2O Enthalpy Calculated by PLTEMP/ANL Code as a Function of Temperature and Pressure (Enlarged View)

Table 17.1 Comparison of Liquid H_2O Properties at 1 bar between PLTEMP/ANL Version 4.2 and NIST Data

	PLTEMP	PLTEMP	PLTEMP	PLTEMP	PLTEMP	NIST	NIST	NIST	NIST	NIST	% Diff. H	% Diff. K	% Diff. Cp	% Diff. ρ	% Diff. μ
Temp, C	H, kJ/kg	K, W/m-C	Cp, kJ/kg-C	ρ, kg/m^3	μ, Pa-s	H, kJ/kg	K, W/m-C	Cp, kJ/kg-C	ρ, kg/m^3	μ, Pa-s					
4	17.017	0.581	4.155	999.527	1.518E-03	16.912	0.569	4.208	999.970	1.567E-03	0.619	2.175	1.251	0.044	3.160
8	33.645	0.588	4.157	999.309	1.369E-03	33.724	0.576	4.199	999.850	1.385E-03	0.235	2.023	0.994	0.054	1.136
12	50.272	0.595	4.159	998.949	1.237E-03	50.505	0.584	4.192	999.500	1.234E-03	0.461	1.848	0.790	0.055	0.205
16	66.914	0.601	4.161	998.447	1.119E-03	67.263	0.591	4.187	998.950	1.108E-03	0.519	1.657	0.623	0.050	0.968
20	83.563	0.607	4.164	997.803	1.015E-03	84.006	0.598	4.184	998.210	1.002E-03	0.527	1.464	0.490	0.041	1.296
24	100.226	0.613	4.166	997.019	9.225E-04	100.740	0.605	4.182	997.300	9.107E-04	0.510	1.275	0.379	0.028	1.288
28	116.895	0.619	4.168	996.094	8.413E-04	117.460	0.612	4.180	996.240	8.325E-04	0.481	1.098	0.285	0.015	1.060
32	133.572	0.624	4.171	995.032	7.700E-04	134.180	0.619	4.180	995.030	7.646E-04	0.453	0.937	0.206	0.000	0.706
36	150.262	0.630	4.174	993.832	7.073E-04	150.900	0.625	4.179	993.680	7.052E-04	0.423	0.795	0.136	0.015	0.302
40	166.959	0.635	4.176	992.497	6.524E-04	167.620	0.631	4.179	992.220	6.530E-04	0.394	0.676	0.077	0.028	0.089
44	183.670	0.640	4.179	991.029	6.042E-04	184.330	0.636	4.180	990.630	6.068E-04	0.358	0.580	0.025	0.040	0.419
48	200.396	0.644	4.182	989.429	5.620E-04	201.060	0.641	4.181	988.930	5.657E-04	0.330	0.507	0.025	0.050	0.663
52	217.128	0.649	4.185	987.701	5.248E-04	217.780	0.646	4.182	987.120	5.290E-04	0.299	0.458	0.070	0.059	0.798
56	233.873	0.653	4.188	985.847	4.919E-04	234.510	0.650	4.183	985.210	4.961E-04	0.272	0.429	0.110	0.065	0.832
60	250.626	0.657	4.191	983.871	4.628E-04	251.250	0.654	4.185	983.200	4.664E-04	0.248	0.419	0.145	0.068	0.773
64	267.400	0.661	4.194	981.773	4.367E-04	267.990	0.658	4.187	981.090	4.396E-04	0.220	0.430	0.181	0.070	0.650
68	284.181	0.665	4.198	979.560	4.119E-04	284.740	0.662	4.189	978.900	4.152E-04	0.196	0.457	0.213	0.067	0.802
72	300.982	0.668	4.201	977.234	3.911E-04	301.500	0.665	4.191	976.610	3.931E-04	0.172	0.498	0.240	0.064	0.513
76	317.797	0.671	4.205	974.798	3.726E-04	318.270	0.667	4.194	974.240	3.729E-04	0.149	0.552	0.266	0.057	0.080
80	334.627	0.674	4.209	972.257	3.560E-04	335.050	0.670	4.197	971.790	3.544E-04	0.126	0.618	0.288	0.048	0.470
84	351.470	0.677	4.213	969.616	3.411E-04	351.850	0.672	4.200	969.260	3.374E-04	0.108	0.691	0.309	0.037	1.098
Max % Diff.	**0.619**	**2.175**	**1.251**	**0.070**	**3.160**										

Table 17.2 Comparison of Liquid H_2O Properties at 2 bar between PLTEMP/ANL Version 4.2 and NIST Data

	PLTEMP	PLTEMP	PLTEMP	PLTEMP	PLTEMP	NIST	NIST	NIST	NIST	NIST	% Diff. H	% Diff. K	% Diff. Cp	% Diff. ρ	% Diff. μ
Temp, C	H, kJ/kg	K, W/m-C	Cp, kJ/kg-C	ρ, kg/m^3	μ, Pa-s	H, kJ/kg	K, W/m-C	Cp, kJ/kg-C	ρ, kg/m^3	μ, Pa-s					
6	25.431	0.585	4.156	999.484	1.441E-03	25.422	0.573	4.202	999.99	1.517E-03	0.037	2.102	1.110	0.051	4.978
12	50.377	0.595	4.159	998.997	1.236E-03	50.602	0.584	4.192	999.55	1.305E-03	0.445	1.846	0.786	0.055	5.247
18	75.336	0.604	4.162	998.189	1.065E-03	75.731	0.595	4.185	998.64	1.137E-03	0.522	1.559	0.552	0.045	6.318
24	100.323	0.613	4.166	997.064	9.224E-04	100.83	0.606	4.182	997.34	1.001E-03	0.503	1.272	0.377	0.028	7.866
30	125.324	0.622	4.169	995.625	8.045E-04	125.91	0.616	4.180	995.69	8.899E-04	0.465	1.012	0.244	0.007	9.594
36	150.352	0.630	4.173	993.876	7.073E-04	150.99	0.625	4.179	993.73	7.973E-04	0.423	0.793	0.137	0.015	11.278
42	175.402	0.637	4.177	991.823	6.276E-04	176.06	0.633	4.179	991.48	7.193E-04	0.374	0.622	0.050	0.035	12.756
48	200.479	0.644	4.182	989.473	5.620E-04	201.14	0.641	4.181	988.97	6.531E-04	0.329	0.504	0.024	0.051	13.942
54	225.584	0.651	4.186	986.833	5.079E-04	226.23	0.648	4.182	986.22	5.962E-04	0.286	0.437	0.088	0.062	14.809
60	250.717	0.657	4.191	983.913	4.628E-04	251.33	0.654	4.185	983.24	5.470E-04	0.244	0.416	0.146	0.068	15.389
66	275.877	0.663	4.196	980.724	4.247E-04	276.45	0.660	4.188	980.05	5.042E-04	0.207	0.437	0.197	0.069	15.762
72	301.065	0.668	4.201	977.277	3.911E-04	301.58	0.665	4.191	976.66	4.666E-04	0.171	0.494	0.239	0.063	16.185
78	326.288	0.673	4.207	973.584	3.641E-04	326.74	0.669	4.195	973.07	4.335E-04	0.138	0.578	0.277	0.053	16.012
84	351.546	0.677	4.213	969.661	3.410E-04	351.93	0.672	4.200	969.30	4.041E-04	0.109	0.686	0.307	0.037	15.608
90	376.839	0.681	4.219	965.522	3.208E-04	377.14	0.675	4.205	965.35	3.780E-04	0.080	0.808	0.330	0.018	15.128
96	402.173	0.684	4.226	961.184	3.021E-04	402.39	0.678	4.211	961.24	3.546E-04	0.054	0.941	0.345	0.006	14.801
102	427.548	0.687	4.233	956.665	2.847E-04	427.67	0.680	4.218	956.95	3.336E-04	0.029	1.077	0.351	0.030	14.646
108	452.966	0.690	4.240	951.984	2.687E-04	453	0.681	4.225	952.50	3.147E-04	0.008	1.216	0.349	0.054	14.603
114	478.432	0.692	4.248	947.163	2.540E-04	478.38	0.682	4.234	947.88	2.975E-04	0.011	1.352	0.334	0.076	14.644
120	503.946	0.693	4.257	942.223	2.404E-04	503.81	0.683	4.244	943.11	2.820E-04	0.027	1.480	0.312	0.094	14.752
Max % Diff.	**0.522**	**2.102**	**1.110**	**0.094**	**16.185**										

Table 17.3 Comparison of Liquid H_2O Properties at 3 bar between PLTEMP/ANL Version 4.2 and NIST Data

	PLTEMP	PLTEMP	PLTEMP	PLTEMP	PLTEMP	NIST	NIST	NIST	NIST	NIST	% Diff. H	% Diff. K	% Diff. Cp	% Diff. ρ	% Diff. μ
Temp, C	H, kJ/kg	K, W/m-C	Cp, kJ/kg-C	ρ, kg/m^3	μ, Pa-s	H, kJ/kg	K, W/m-C	Cp, kJ/kg-C	ρ, kg/m^3	μ, Pa-s					
6	25.528	0.585	4.155	999.533	1.441E-03	25.521	0.573	4.202	1000.00	1.471E-03	0.027	2.101	1.107	0.047	2.046
12	50.474	0.595	4.159	999.044	1.236E-03	50.698	0.584	4.191	999.59	1.234E-03	0.442	1.850	0.783	0.055	0.211
18	75.433	0.604	4.162	998.236	1.065E-03	75.826	0.595	4.185	998.69	1.053E-03	0.518	1.553	0.547	0.045	1.178
24	100.413	0.613	4.166	997.110	9.225E-04	100.920	0.606	4.181	997.39	9.107E-04	0.502	1.276	0.375	0.028	1.294
30	125.421	0.622	4.169	995.670	8.045E-04	126.000	0.616	4.179	995.74	7.973E-04	0.460	1.009	0.242	0.007	0.898
36	150.449	0.630	4.173	993.920	7.073E-04	151.080	0.625	4.179	993.77	7.052E-04	0.418	0.797	0.136	0.015	0.303
42	175.499	0.637	4.177	991.866	6.276E-04	176.150	0.633	4.179	991.52	6.292E-04	0.370	0.617	0.050	0.035	0.261
48	200.569	0.645	4.181	989.516	5.620E-04	201.230	0.641	4.180	989.01	5.657E-04	0.328	0.504	0.026	0.051	0.656
54	225.674	0.651	4.186	986.876	5.079E-04	226.320	0.648	4.182	986.26	5.121E-04	0.285	0.438	0.086	0.062	0.822
60	250.800	0.657	4.191	983.957	4.629E-04	251.420	0.654	4.185	983.28	4.664E-04	0.247	0.416	0.146	0.069	0.768
66	275.960	0.663	4.196	980.767	4.247E-04	276.530	0.660	4.187	980.09	4.272E-04	0.206	0.430	0.196	0.069	0.567
72	301.149	0.668	4.201	977.320	3.911E-04	301.670	0.665	4.191	976.70	3.931E-04	0.173	0.490	0.241	0.063	0.511
78	326.372	0.673	4.206	973.628	3.641E-04	326.820	0.669	4.195	973.12	3.635E-04	0.137	0.571	0.277	0.052	0.168
84	351.629	0.677	4.212	969.704	3.410E-04	352.000	0.672	4.200	969.35	3.374E-04	0.105	0.684	0.307	0.037	1.064
90	376.922	0.681	4.219	965.566	3.207E-04	377.220	0.675	4.205	965.40	3.145E-04	0.079	0.804	0.328	0.017	1.997
96	402.249	0.684	4.225	961.229	3.021E-04	402.460	0.678	4.211	961.28	2.941E-04	0.052	0.940	0.344	0.005	2.700
102	427.625	0.687	4.232	956.710	2.847E-04	427.750	0.680	4.218	956.99	2.760E-04	0.029	1.072	0.349	0.029	3.149
108	453.042	0.690	4.240	952.031	2.687E-04	453.080	0.681	4.225	952.54	2.598E-04	0.008	1.209	0.348	0.053	3.422
114	478.501	0.692	4.248	947.211	2.539E-04	478.450	0.682	4.234	947.93	2.452E-04	0.011	1.349	0.335	0.076	3.552
120	504.016	0.693	4.257	942.271	2.404E-04	503.880	0.683	4.243	943.16	2.321E-04	0.027	1.471	0.311	0.094	3.563
126	529.579	0.695	4.266	937.238	2.279E-04	529.370	0.684	4.254	938.23	2.202E-04	0.039	1.589	0.277	0.106	3.492
Max % Error	**0.518**	**2.101**	**1.107**	**0.106**	**3.563**										

Table 17.4 Comparison of Liquid H_2O Properties at 4 bar between PLTEMP/ANL Version 4.2 and NIST Data

	PLTEMP	PLTEMP	PLTEMP	PLTEMP	PLTEMP	NIST	NIST	NIST	NIST	NIST	% Diff. H	% Diff. K	% Diff. Cp	% Diff. ρ	% Diff. μ
Temp, C	H, kJ/kg	K, W/m-C	Cp, kJ/kg-C	ρ, kg/m^3	μ, Pa-s	H, kJ/kg	K, W/m-C	Cp, kJ/kg-C	ρ, kg/m^3	μ, Pa-s					
7	29.784	0.586	4.156	999.522	1.404E-03	29.820	0.575	4.199	1000.00	1.427E-03	0.121	2.050	1.041	0.048	1.563
14	58.888	0.598	4.160	998.857	1.176E-03	59.175	0.588	4.189	999.39	1.168E-03	0.485	1.741	0.695	0.053	0.659
21	88.020	0.609	4.164	997.758	9.904E-04	88.471	0.600	4.183	998.13	9.774E-04	0.510	1.402	0.454	0.037	1.324
28	117.180	0.619	4.168	996.229	8.413E-04	117.740	0.612	4.180	996.37	8.324E-04	0.476	1.099	0.282	0.014	1.066
35	146.367	0.629	4.172	994.277	7.223E-04	146.990	0.623	4.179	994.17	7.193E-04	0.424	0.824	0.153	0.011	0.409
42	175.589	0.637	4.177	991.910	6.276E-04	176.240	0.634	4.179	991.57	6.292E-04	0.369	0.611	0.050	0.034	0.257
49	204.839	0.646	4.182	989.139	5.523E-04	205.500	0.643	4.180	988.61	5.562E-04	0.322	0.478	0.033	0.054	0.696
56	234.137	0.653	4.187	985.976	4.920E-04	234.770	0.650	4.183	985.34	4.961E-04	0.270	0.420	0.108	0.065	0.824
63	263.463	0.660	4.193	982.437	4.431E-04	264.050	0.657	4.186	981.76	4.461E-04	0.222	0.417	0.170	0.069	0.679
70	292.831	0.666	4.199	978.540	4.013E-04	293.370	0.663	4.189	977.90	4.040E-04	0.184	0.457	0.224	0.065	0.673
77	322.248	0.672	4.205	974.303	3.683E-04	322.710	0.668	4.194	973.77	3.682E-04	0.143	0.557	0.269	0.055	0.030
84	351.706	0.677	4.212	969.749	3.410E-04	352.080	0.672	4.199	969.39	3.375E-04	0.106	0.677	0.305	0.037	1.046
91	381.219	0.681	4.220	964.901	3.175E-04	381.500	0.676	4.206	964.77	3.109E-04	0.074	0.818	0.333	0.014	2.107
98	410.782	0.685	4.227	959.787	2.960E-04	410.960	0.679	4.213	959.92	2.879E-04	0.043	0.974	0.347	0.014	2.842
105	440.399	0.688	4.236	954.436	2.765E-04	440.480	0.681	4.221	954.84	2.677E-04	0.018	1.133	0.351	0.042	3.280
112	470.087	0.691	4.245	948.878	2.587E-04	470.060	0.682	4.231	949.53	2.499E-04	0.006	1.288	0.338	0.069	3.493
119	499.836	0.693	4.255	943.149	2.425E-04	499.710	0.683	4.241	944.01	2.342E-04	0.025	1.448	0.316	0.091	3.540
126	529.648	0.695	4.265	937.287	2.279E-04	529.440	0.684	4.254	938.28	2.202E-04	0.039	1.578	0.280	0.106	3.465
133	559.551	0.695	4.277	931.328	2.146E-04	559.260	0.684	4.267	932.32	2.078E-04	0.052	1.705	0.227	0.106	3.307
140	589.530	0.696	4.289	925.317	2.027E-04	589.190	0.683	4.283	926.16	1.966E-04	0.058	1.826	0.161	0.091	3.109
143.628	605.102	0.696	4.296	922.196	1.969E-04	604.650	0.683	4.291	922.89	1.912E-04	0.075	1.883	0.126	0.075	2.986
Max % Error	**0.510**	**2.050**	**1.041**	**0.106**	**3.540**										

Table 17.5 Comparison of Liquid H_2O Properties at 5 bar between PLTEMP/ANL Version 4.2 and NIST Data

	PLTEMP	PLTEMP	PLTEMP	PLTEMP	PLTEMP	NIST	NIST	NIST	NIST	NIST	% Diff. H	% Diff. K	% Diff. Cp	% Diff. ρ	% Diff. μ
Temp, C	H, kJ/kg	K, W/m-C	Cp, kJ/kg-C	ρ, kg/m^3	μ, Pa-s	H, kJ/kg	K, W/m-C	Cp, kJ/kg-C	ρ, kg/m^3	μ, Pa-s					
7	29.882	0.586	4.155	999.570	1.404E-03	29.919	0.575	4.199	1000.10	1.427E-03	0.125	2.057	1.036	0.053	1.559
14	58.986	0.598	4.159	998.904	1.176E-03	59.271	0.588	4.188	999.43	1.168E-03	0.482	1.746	0.691	0.053	0.660
21	88.117	0.609	4.163	997.804	9.904E-04	88.565	0.600	4.182	998.18	9.774E-04	0.505	1.409	0.453	0.038	1.325
28	117.270	0.619	4.167	996.274	8.413E-04	117.830	0.612	4.179	996.41	8.324E-04	0.475	1.089	0.281	0.014	1.070
35	146.457	0.629	4.172	994.321	7.223E-04	147.080	0.624	4.178	994.21	7.193E-04	0.424	0.817	0.151	0.011	0.412
42	175.679	0.637	4.177	991.953	6.276E-04	176.330	0.634	4.179	991.61	6.292E-04	0.369	0.613	0.050	0.035	0.256
49	204.929	0.646	4.182	989.182	5.524E-04	205.580	0.643	4.180	988.66	5.562E-04	0.317	0.479	0.036	0.053	0.694
56	234.221	0.653	4.187	986.019	4.921E-04	234.850	0.651	4.182	985.38	4.962E-04	0.268	0.413	0.108	0.065	0.820
63	263.547	0.660	4.193	982.480	4.431E-04	264.140	0.657	4.186	981.80	4.461E-04	0.225	0.408	0.169	0.069	0.674
70	292.915	0.666	4.199	978.583	4.013E-04	293.450	0.663	4.189	977.94	4.040E-04	0.182	0.457	0.224	0.066	0.670
77	322.331	0.672	4.205	974.346	3.683E-04	322.790	0.668	4.194	973.82	3.682E-04	0.142	0.547	0.269	0.054	0.023
84	351.789	0.677	4.212	969.792	3.410E-04	352.160	0.673	4.199	969.44	3.375E-04	0.105	0.667	0.306	0.036	1.031
91	381.296	0.681	4.219	964.945	3.174E-04	381.580	0.676	4.205	964.82	3.110E-04	0.074	0.811	0.331	0.013	2.084
98	410.858	0.685	4.227	959.832	2.960E-04	411.040	0.679	4.213	959.96	2.879E-04	0.044	0.965	0.346	0.013	2.814
105	440.476	0.688	4.236	954.482	2.764E-04	440.550	0.681	4.221	954.88	2.677E-04	0.017	1.125	0.349	0.042	3.253
112	470.156	0.691	4.245	948.926	2.586E-04	470.130	0.682	4.230	949.58	2.499E-04	0.006	1.284	0.339	0.069	3.468
119	499.906	0.693	4.254	943.197	2.425E-04	499.780	0.683	4.241	944.06	2.342E-04	0.025	1.434	0.315	0.091	3.511
126	529.718	0.695	4.265	937.336	2.278E-04	529.510	0.684	4.253	938.33	2.203E-04	0.039	1.575	0.277	0.106	3.435
133	559.613	0.695	4.277	931.379	2.146E-04	559.330	0.684	4.267	932.38	2.078E-04	0.051	1.703	0.228	0.107	3.283
140	589.599	0.696	4.289	925.368	2.026E-04	589.250	0.683	4.282	926.21	1.966E-04	0.059	1.815	0.163	0.091	3.081
147	619.668	0.696	4.303	919.352	1.919E-04	619.280	0.683	4.299	919.82	1.865E-04	0.063	1.911	0.084	0.051	2.876
Max % Diff.	**0.505**	**2.057**	**1.036**	**0.107**	**3.511**										

Table 17.6 Comparison of Liquid H_2O Properties at 10 bar between PLTEMP/ANL Version 4.2 and NIST Data

	PLTEMP	PLTEMP	PLTEMP	PLTEMP	PLTEMP	NIST	NIST	NIST	NIST	NIST	% Diff. H	% Diff. K	% Diff. Cp	% Diff. ρ	% Diff. μ
Temp, C	H, kJ/kg	K, W/m-C	Cp, kJ/kg-C	ρ, kg/m^3	μ, Pa-s	H, kJ/kg	K, W/m-C	Cp, kJ/kg-C	ρ, kg/m^3	μ, Pa-s					
8	34.533	0.588	4.155	999.742	1.368E-03	34.608	0.577	4.195	1000.30	1.384E-03	0.216	2.008	0.960	0.056	1.099
16	67.789	0.601	4.159	998.867	1.118E-03	68.122	0.592	4.184	999.36	1.108E-03	0.489	1.641	0.602	0.049	0.992
24	101.079	0.614	4.164	997.428	9.224E-04	101.570	0.606	4.179	997.71	9.105E-04	0.483	1.256	0.366	0.028	1.308
32	134.412	0.625	4.169	995.432	7.701E-04	135.000	0.619	4.177	995.43	7.645E-04	0.436	0.914	0.200	0.000	0.725
40	167.785	0.635	4.174	992.890	6.526E-04	168.410	0.631	4.177	992.61	6.531E-04	0.371	0.649	0.076	0.028	0.070
48	201.201	0.645	4.180	989.818	5.622E-04	201.840	0.642	4.179	989.32	5.659E-04	0.317	0.477	0.023	0.050	0.641
56	234.658	0.653	4.186	986.234	4.922E-04	235.270	0.651	4.181	985.60	4.963E-04	0.260	0.392	0.105	0.064	0.807
64	268.171	0.661	4.192	982.159	4.370E-04	268.740	0.659	4.185	981.49	4.398E-04	0.212	0.390	0.176	0.068	0.629
72	301.732	0.668	4.199	977.622	3.913E-04	302.230	0.665	4.189	977.01	3.933E-04	0.165	0.453	0.234	0.063	0.514
80	335.356	0.674	4.207	972.649	3.559E-04	335.770	0.670	4.195	972.19	3.546E-04	0.123	0.568	0.282	0.047	0.376
88	369.042	0.680	4.215	967.277	3.269E-04	369.350	0.675	4.201	967.05	3.220E-04	0.083	0.717	0.317	0.023	1.533
96	402.791	0.684	4.223	961.543	3.017E-04	403.000	0.678	4.209	961.61	2.943E-04	0.052	0.887	0.339	0.007	2.504
104	436.616	0.688	4.233	955.489	2.789E-04	436.710	0.681	4.218	955.86	2.706E-04	0.022	1.067	0.346	0.039	3.066
112	470.524	0.691	4.243	949.161	2.584E-04	470.490	0.683	4.229	949.83	2.501E-04	0.007	1.245	0.336	0.070	3.326
120	504.516	0.693	4.255	942.609	2.401E-04	504.380	0.684	4.242	943.51	2.323E-04	0.027	1.415	0.309	0.095	3.372
128	538.605	0.695	4.267	935.889	2.237E-04	538.360	0.684	4.256	936.91	2.167E-04	0.046	1.570	0.267	0.109	3.261
136	572.791	0.696	4.281	929.063	2.092E-04	572.470	0.684	4.272	930.03	2.030E-04	0.056	1.706	0.204	0.104	3.066
144	607.095	0.696	4.295	922.192	1.962E-04	606.720	0.683	4.290	922.86	1.908E-04	0.062	1.823	0.124	0.072	2.837
152	641.524	0.695	4.312	915.349	1.847E-04	641.120	0.682	4.311	915.42	1.800E-04	0.063	1.918	0.026	0.008	2.610
160	676.085	0.694	4.330	907.734	1.745E-04	675.700	0.680	4.334	907.68	1.703E-04	0.057	1.990	0.086	0.006	2.431
168	710.813	0.692	4.351	899.664	1.654E-04	710.470	0.678	4.360	899.64	1.616E-04	0.048	2.043	0.213	0.003	2.321
Max % Diff.	**0.489**	**2.043**	**0.960**	**0.109**	**3.372**										

Table 17.7 Comparison of Liquid H_2O Properties at 20 bar between PLTEMP/ANL Version 4.2 and NIST Data

	PLTEMP	PLTEMP	PLTEMP	PLTEMP	PLTEMP	NIST	NIST	NIST	NIST	NIST	% Diff. H	% Diff. K	% Diff. Cp	% Diff. ρ	% Diff. μ
Temp, C	H, kJ/kg	K, W/m-C	Cp, kJ/kg-C	ρ, kg/m^3	μ, Pa-s	H, kJ/kg	K, W/m-C	Cp, kJ/kg-C	ρ, kg/m^3	μ, Pa-s					
10	43.830	0.592	4.154	1000.050	1.300E-03	43.969	0.581	4.188	1000.60	1.304E-03	0.317	1.904	0.823	0.055	0.328
20	85.396	0.608	4.159	998.677	1.014E-03	85.793	0.599	4.178	999.08	1.001E-03	0.463	1.428	0.457	0.040	1.329
30	127.011	0.622	4.165	996.429	8.046E-04	127.550	0.616	4.175	996.49	7.972E-04	0.423	0.970	0.230	0.006	0.930
40	168.695	0.635	4.172	993.328	6.528E-04	169.300	0.631	4.175	993.05	6.531E-04	0.357	0.620	0.076	0.028	0.049
50	210.449	0.647	4.179	989.401	5.434E-04	211.060	0.644	4.177	988.86	5.472E-04	0.289	0.411	0.041	0.055	0.699
60	252.272	0.658	4.186	984.686	4.634E-04	252.840	0.655	4.181	984.02	4.668E-04	0.225	0.340	0.134	0.068	0.729
70	294.178	0.667	4.195	979.228	4.017E-04	294.680	0.664	4.186	978.60	4.044E-04	0.170	0.383	0.214	0.064	0.658
80	336.168	0.674	4.204	973.085	3.558E-04	336.570	0.671	4.193	972.64	3.549E-04	0.119	0.512	0.275	0.046	0.260
90	378.262	0.681	4.214	966.319	3.198E-04	378.530	0.676	4.201	966.18	3.149E-04	0.071	0.696	0.317	0.014	1.555
100	420.460	0.686	4.226	959.007	2.894E-04	420.590	0.680	4.211	959.24	2.823E-04	0.031	0.908	0.339	0.024	2.546
110	462.776	0.690	4.238	951.234	2.629E-04	462.770	0.683	4.224	951.84	2.552E-04	0.001	1.125	0.335	0.064	3.010
120	505.224	0.693	4.252	943.094	2.397E-04	505.080	0.684	4.239	944.01	2.325E-04	0.029	1.332	0.308	0.097	3.098
130	547.825	0.695	4.268	934.692	2.196E-04	547.550	0.685	4.257	935.73	2.133E-04	0.050	1.517	0.252	0.111	2.956
140	590.585	0.696	4.285	926.150	2.023E-04	590.220	0.684	4.278	927.02	1.970E-04	0.062	1.671	0.171	0.094	2.693
150	633.533	0.695	4.305	917.594	1.873E-04	633.120	0.683	4.302	917.87	1.829E-04	0.065	1.793	0.061	0.030	2.410
160	676.689	0.694	4.327	908.212	1.743E-04	676.280	0.681	4.330	908.27	1.706E-04	0.060	1.881	0.070	0.006	2.182
170	720.088	0.691	4.353	898.123	1.631E-04	719.740	0.678	4.363	898.21	1.599E-04	0.048	1.935	0.224	0.010	2.062
180	763.765	0.687	4.383	887.611	1.535E-04	763.560	0.674	4.401	887.67	1.504E-04	0.027	1.962	0.395	0.007	2.067
190	807.768	0.683	4.418	876.636	1.451E-04	807.770	0.669	4.444	876.61	1.420E-04	0.000	1.965	0.575	0.003	2.203
200	852.236	0.677	4.610	865.133	1.377E-04	852.450	0.664	4.493	865.00	1.344E-04	0.025	1.951	2.606	0.015	2.460
210	898.294	0.670	4.605	852.755	1.311E-04	897.660	0.657	4.551	852.79	1.276E-04	0.071	1.898	1.202	0.004	2.693
Max % Diff.	**0.463**	**1.965**	**2.606**	**0.111**	**3.098**										

Table 17.8 Comparison of Liquid H_2O Properties at 30 bar between PLTEMP/ANL Version 4.2 and NIST Data

	PLTEMP	PLTEMP	PLTEMP	PLTEMP	PLTEMP	NIST	NIST	NIST	NIST	NIST	% Diff. H	% Diff. K	% Diff. Cp	% Diff. ρ	% Diff. μ
Temp, C	H, kJ/kg	K, W/m-C	Cp, kJ/kg-C	ρ, kg/m^3	μ, Pa-s	H, kJ/kg	K, W/m-C	Cp, kJ/kg-C	ρ, kg/m^3	μ, Pa-s					
11	48.960	0.594	4.152	1000.430	1.266E-03	49.13	0.583	4.183	1001.00	1.266E-03	0.335	1.843	0.748	0.057	0.006
22	94.664	0.611	4.158	998.754	9.666E-04	95.08	0.603	4.174	999.09	9.535E-04	0.438	1.311	0.388	0.034	1.377
33	140.438	0.627	4.165	996.031	7.538E-04	140.98	0.622	4.172	995.99	7.489E-04	0.384	0.825	0.172	0.004	0.658
44	186.288	0.641	4.172	992.289	6.050E-04	186.87	0.637	4.173	991.89	6.072E-04	0.311	0.487	0.027	0.040	0.358
55	232.228	0.653	4.180	987.569	5.007E-04	232.79	0.651	4.177	986.95	5.046E-04	0.241	0.320	0.085	0.063	0.767
66	278.252	0.663	4.189	981.927	4.243E-04	278.76	0.661	4.182	981.27	4.278E-04	0.182	0.308	0.177	0.067	0.832
77	324.386	0.672	4.199	975.430	3.683E-04	324.79	0.670	4.188	974.93	3.688E-04	0.124	0.413	0.250	0.051	0.150
88	370.632	0.680	4.210	968.160	3.259E-04	370.91	0.676	4.197	967.96	3.225E-04	0.075	0.596	0.302	0.021	1.056
99	417.002	0.686	4.222	960.214	2.918E-04	417.14	0.680	4.208	960.42	2.855E-04	0.033	0.818	0.331	0.021	2.194
110	463.512	0.690	4.235	951.702	2.624E-04	463.50	0.683	4.222	952.32	2.555E-04	0.003	1.051	0.330	0.065	2.733
121	510.188	0.694	4.251	942.749	2.372E-04	510.02	0.685	4.238	943.70	2.307E-04	0.033	1.269	0.301	0.101	2.821
132	557.038	0.695	4.268	933.498	2.157E-04	556.74	0.685	4.258	934.55	2.101E-04	0.054	1.461	0.238	0.113	2.646
143	604.096	0.696	4.288	924.106	1.973E-04	603.71	0.685	4.282	924.87	1.928E-04	0.064	1.613	0.145	0.083	2.353
154	651.383	0.695	4.311	914.643	1.817E-04	650.96	0.683	4.310	914.66	1.780E-04	0.065	1.726	0.024	0.002	2.062
165	698.940	0.693	4.337	903.724	1.684E-04	698.54	0.680	4.342	903.91	1.653E-04	0.057	1.798	0.127	0.021	1.860
176	746.811	0.689	4.368	892.418	1.571E-04	746.51	0.677	4.381	892.59	1.543E-04	0.040	1.832	0.299	0.019	1.806
187	795.049	0.684	4.404	880.578	1.474E-04	794.94	0.672	4.425	880.67	1.446E-04	0.014	1.835	0.483	0.010	1.908
198	843.516	0.678	4.603	868.201	1.391E-04	843.89	0.666	4.477	868.11	1.361E-04	0.044	1.817	2.821	0.010	2.191
209	894.094	0.670	4.596	854.740	1.316E-04	893.47	0.659	4.538	854.85	1.285E-04	0.070	1.749	1.284	0.013	2.420
220	944.728	0.661	4.615	840.670	1.251E-04	943.76	0.650	4.609	840.82	1.217E-04	0.103	1.687	0.118	0.018	2.815
231	995.715	0.651	4.661	825.860	1.193E-04	994.92	0.641	4.694	825.92	1.155E-04	0.080	1.649	0.713	0.007	3.288
Max % Diff.	**0.438**	**1.843**	**2.821**	**0.113**	**3.288**										

Table 17.9 Comparison of Liquid H_2O Properties at 40 bar between PLTEMP/ANL Version 4.2 and NIST Data

	PLTEMP	PLTEMP	PLTEMP	PLTEMP	PLTEMP	NIST	NIST	NIST	NIST	NIST	% Diff. H	% Diff. K	% Diff. Cp	% Diff. ρ	% Diff. μ
Temp, C	H, kJ/kg	K, W/m-C	Cp, kJ/kg-C	ρ, kg/m^3	μ, Pa-s	H, kJ/kg	K, W/m-C	Cp, kJ/kg-C	ρ, kg/m^3	μ, Pa-s					
12	54.091	0.596	4.150	1000.790	1.234E-03	54.272	0.586	4.178	1001.300	1.231E-03	0.334	1.778	0.677	0.051	0.301
24	103.933	0.614	4.157	998.790	9.220E-04	104.350	0.607	4.171	999.060	9.097E-04	0.400	1.194	0.331	0.027	1.348
36	153.858	0.631	4.164	995.550	7.079E-04	154.390	0.627	4.169	995.400	7.053E-04	0.345	0.690	0.126	0.015	0.367
48	203.874	0.645	4.172	991.116	5.631E-04	204.430	0.643	4.172	990.620	5.663E-04	0.272	0.372	0.014	0.050	0.578
60	253.994	0.658	4.182	985.545	4.641E-04	254.520	0.656	4.176	984.890	4.673E-04	0.207	0.255	0.123	0.067	0.688
72	304.238	0.669	4.192	978.916	3.919E-04	304.670	0.667	4.183	978.330	3.941E-04	0.142	0.302	0.210	0.060	0.551
84	354.601	0.677	4.203	971.327	3.397E-04	354.920	0.674	4.191	971.010	3.384E-04	0.090	0.465	0.278	0.033	0.390
96	405.116	0.685	4.216	962.892	3.000E-04	405.280	0.680	4.203	962.990	2.951E-04	0.040	0.690	0.317	0.010	1.664
108	455.792	0.690	4.230	953.751	2.670E-04	455.790	0.683	4.217	954.310	2.608E-04	0.000	0.935	0.326	0.059	2.398
120	506.647	0.693	4.247	944.063	2.390E-04	506.490	0.685	4.234	945.000	2.331E-04	0.031	1.169	0.301	0.099	2.559
132	557.718	0.695	4.265	934.004	2.154E-04	557.420	0.686	4.255	935.060	2.104E-04	0.053	1.371	0.240	0.113	2.382
144	609.032	0.696	4.287	923.781	1.955E-04	608.630	0.685	4.281	924.510	1.916E-04	0.066	1.528	0.142	0.079	2.066
156	660.623	0.694	4.312	913.089	1.789E-04	660.180	0.683	4.312	913.330	1.758E-04	0.067	1.635	0.008	0.026	1.770
168	712.541	0.692	4.342	901.215	1.650E-04	712.140	0.680	4.349	901.500	1.624E-04	0.056	1.695	0.154	0.032	1.587
180	764.848	0.687	4.377	888.750	1.533E-04	764.570	0.676	4.392	888.990	1.509E-04	0.036	1.711	0.336	0.027	1.582
192	816.433	0.681	4.607	875.934	1.436E-04	817.570	0.670	4.443	875.760	1.409E-04	0.139	1.713	3.687	0.020	1.911
204	871.565	0.674	4.587	861.622	1.348E-04	871.230	0.663	4.503	861.750	1.321E-04	0.038	1.634	1.860	0.015	2.045
216	926.635	0.665	4.597	846.649	1.274E-04	925.690	0.654	4.575	846.870	1.244E-04	0.102	1.549	0.489	0.026	2.417
228	982.010	0.654	4.638	830.860	1.208E-04	981.080	0.644	4.660	831.020	1.174E-04	0.095	1.481	0.486	0.019	2.897
240	1038.070	0.642	4.712	814.070	1.148E-04	1037.600	0.633	4.765	814.060	1.110E-04	0.045	1.457	1.104	0.001	3.418
250.3	1087.220	0.630	4.807	798.636	1.100E-04	1087.200	0.621	4.873	798.450	1.060E-04	0.002	1.485	1.365	0.023	3.825
Max % Diff.	**0.400**	**1.778**	**3.687**	**0.113**	**3.825**										

Table 17.10 Comparison of Liquid H_2O Properties at 50 bar between PLTEMP/ANL Version 4.2 and NIST Data

	PLTEMP	PLTEMP	PLTEMP	PLTEMP	PLTEMP	NIST	NIST	NIST	NIST	NIST	% Diff. H	% Diff. K	% Diff. Cp	% Diff. ρ	% Diff. μ
Temp, C	H, kJ/kg	K, W/m-C	Cp, kJ/kg-C	ρ, kg/m^3	μ, Pa-s	H, kJ/kg	K, W/m-C	Cp, kJ/kg-C	ρ, kg/m^3	μ, Pa-s					
13	59.215	0.598	4.148	1001.144	1.203E-03	59.409	0.588	4.174	1001.70	1.196E-03	0.327	1.718	0.616	0.056	0.552
26	113.188	0.618	4.156	998.787	8.802E-04	113.610	0.611	4.167	998.98	8.692E-04	0.371	1.078	0.281	0.019	1.264
39	167.265	0.635	4.164	994.990	6.664E-04	167.780	0.631	4.167	994.74	6.658E-04	0.307	0.564	0.089	0.025	0.086
52	221.453	0.650	4.173	989.813	5.262E-04	221.980	0.648	4.171	989.24	5.299E-04	0.237	0.276	0.048	0.058	0.698
65	275.766	0.663	4.183	983.337	4.322E-04	276.240	0.661	4.177	982.69	4.344E-04	0.172	0.216	0.156	0.066	0.518
78	330.218	0.673	4.195	975.670	3.638E-04	330.580	0.671	4.185	975.20	3.647E-04	0.110	0.320	0.239	0.048	0.255
91	384.837	0.682	4.208	966.946	3.149E-04	385.050	0.678	4.195	966.87	3.122E-04	0.055	0.531	0.298	0.008	0.868
104	439.629	0.688	4.223	957.329	2.769E-04	439.680	0.683	4.209	957.75	2.716E-04	0.012	0.779	0.321	0.044	1.955
117	494.629	0.693	4.240	947.008	2.452E-04	494.510	0.686	4.227	947.88	2.397E-04	0.024	1.025	0.308	0.092	2.290
130	549.873	0.695	4.259	936.202	2.188E-04	549.590	0.687	4.249	937.28	2.141E-04	0.051	1.250	0.252	0.115	2.162
143	605.394	0.696	4.282	925.162	1.968E-04	604.990	0.686	4.276	925.95	1.933E-04	0.067	1.426	0.157	0.085	1.842
156	661.227	0.694	4.309	913.578	1.787E-04	660.790	0.684	4.309	913.90	1.760E-04	0.066	1.525	0.021	0.035	1.522
169	717.457	0.691	4.342	900.735	1.638E-04	717.050	0.681	4.348	901.10	1.616E-04	0.057	1.587	0.149	0.041	1.343
182	774.144	0.686	4.380	887.201	1.514E-04	773.870	0.676	4.395	887.50	1.494E-04	0.035	1.585	0.337	0.034	1.366
195	830.776	0.680	4.588	873.050	1.412E-04	831.360	0.669	4.452	873.06	1.388E-04	0.070	1.556	3.057	0.001	1.671
208	890.317	0.671	4.578	857.443	1.322E-04	889.660	0.661	4.519	857.68	1.297E-04	0.074	1.450	1.303	0.028	1.905
221	949.956	0.660	4.603	841.007	1.245E-04	948.920	0.652	4.601	841.27	1.216E-04	0.109	1.351	0.041	0.031	2.360
234	1010.142	0.648	4.663	823.537	1.177E-04	1009.400	0.640	4.700	823.68	1.144E-04	0.074	1.286	0.791	0.017	2.902
247	1071.363	0.634	4.764	804.783	1.115E-04	1071.200	0.626	4.824	804.69	1.078E-04	0.015	1.271	1.236	0.012	3.431
260	1134.216	0.618	4.915	784.408	1.058E-04	1134.900	0.610	4.980	784.03	1.018E-04	0.060	1.348	1.317	0.048	3.911
263.914	1153.566	0.613	4.972	777.891	1.041E-04	1154.600	0.604	5.037	777.37	1.000E-04	0.090	1.415	1.285	0.067	4.050
Max % Error	**0.371**	**1.718**	**3.057**	**0.115**	**4.050**										

Table 17.11 Comparison of Liquid H_2O Properties at 75 bar between PLTEMP/ANL Version 4.2 and NIST Data

	PLTEMP	PLTEMP	PLTEMP	PLTEMP	PLTEMP	NIST	NIST	NIST	NIST	NIST	% Diff. H	% Diff. K	% Diff. Cp	% Diff. ρ	% Diff. μ
Temp, C	H, kJ/kg	K, W/m-C	Cp, kJ/kg-C	ρ, kg/m^3	μ, Pa-s	H, kJ/kg	K, W/m-C	Cp, kJ/kg-C	ρ, kg/m^3	μ, Pa-s					
14	65.789	0.601	4.143	1002.185	1.172E-03	65.969	0.591	4.165	1002.70	1.163E-03	0.273	1.621	0.523	0.051	0.774
28	123.845	0.621	4.151	999.417	8.410E-04	124.230	0.616	4.160	999.52	8.315E-04	0.310	0.929	0.226	0.010	1.135
42	182.018	0.639	4.160	995.006	6.290E-04	182.480	0.637	4.162	994.65	6.300E-04	0.253	0.396	0.055	0.036	0.156
56	240.323	0.655	4.170	989.031	4.942E-04	240.780	0.654	4.167	988.41	4.976E-04	0.190	0.136	0.067	0.063	0.695
70	298.774	0.668	4.181	981.604	4.030E-04	299.170	0.667	4.174	981.00	4.058E-04	0.132	0.111	0.170	0.062	0.683
84	357.406	0.678	4.194	972.867	3.383E-04	357.670	0.676	4.184	972.57	3.393E-04	0.074	0.265	0.249	0.031	0.318
98	416.225	0.686	4.209	963.004	2.923E-04	416.340	0.682	4.197	963.20	2.898E-04	0.028	0.491	0.293	0.020	0.877
112	475.273	0.691	4.226	952.232	2.557E-04	475.200	0.686	4.214	952.95	2.518E-04	0.015	0.746	0.301	0.075	1.553
126	534.578	0.695	4.246	940.807	2.256E-04	534.340	0.688	4.235	941.87	2.221E-04	0.045	0.972	0.264	0.113	1.576
140	594.188	0.696	4.270	929.025	2.009E-04	593.810	0.688	4.262	929.96	1.984E-04	0.064	1.148	0.188	0.101	1.291
154	654.153	0.695	4.298	916.800	1.808E-04	653.700	0.686	4.295	917.22	1.791E-04	0.069	1.255	0.063	0.046	0.949
168	714.548	0.692	4.331	903.109	1.645E-04	714.110	0.683	4.335	903.63	1.633E-04	0.061	1.298	0.092	0.058	0.753
182	775.470	0.686	4.373	888.706	1.511E-04	775.130	0.678	4.384	889.15	1.500E-04	0.044	1.263	0.267	0.050	0.773
196	836.664	0.679	4.559	873.520	1.402E-04	836.920	0.671	4.443	873.71	1.387E-04	0.031	1.200	2.602	0.022	1.074
210	900.447	0.669	4.559	856.865	1.308E-04	899.610	0.662	4.515	857.22	1.290E-04	0.093	1.068	0.968	0.041	1.372
224	964.473	0.658	4.595	839.230	1.228E-04	963.400	0.652	4.602	839.55	1.205E-04	0.111	0.918	0.161	0.038	1.875
238	1029.276	0.644	4.670	820.364	1.157E-04	1028.600	0.639	4.710	820.52	1.130E-04	0.066	0.800	0.845	0.019	2.425
252	1095.448	0.628	4.791	799.953	1.093E-04	1095.400	0.623	4.845	799.87	1.062E-04	0.004	0.756	1.114	0.010	2.920
266	1163.702	0.610	4.971	777.572	1.032E-04	1164.400	0.605	5.021	777.25	9.985E-05	0.060	0.822	1.000	0.041	3.345
280	1235.004	0.589	5.231	752.605	9.744E-05	1236.300	0.583	5.259	752.07	9.387E-05	0.105	1.031	0.546	0.071	3.805
290.512	1291.351	0.572	5.502	731.618	9.341E-05	1292.900	0.564	5.505	730.88	8.945E-05	0.120	1.321	0.064	0.101	4.420
Max % Error	**0.310**	**1.621**	**2.602**	**0.113**	**4.420**										

Table 17.12 Comparison of Liquid H_2O Properties at 100 bar between PLTEMP/ANL Version 4.2 and NIST Data

	PLTEMP	PLTEMP	PLTEMP	PLTEMP	PLTEMP	NIST	NIST	NIST	NIST	NIST	% Diff. H	% Diff. K	% Diff. Cp	% Diff. ρ	% Diff. μ
Temp, C	H, kJ/kg	K, W/m-C	Cp, kJ/kg-C	ρ, kg/m^3	μ, Pa-s	H, kJ/kg	K, W/m-C	Cp, kJ/kg-C	ρ, kg/m^3	μ, Pa-s					
15	72.343	0.603	4.138	1003.207	1.142E-03	72.506	0.594	4.156	1003.70	1.131E-03	0.225	1.527	0.445	0.049	0.937
30	134.467	0.625	4.146	1000.002	8.043E-04	134.820	0.620	4.154	1000.00	7.966E-04	0.262	0.777	0.185	0.000	0.965
45	196.730	0.643	4.156	994.942	5.953E-04	197.150	0.642	4.157	994.49	5.975E-04	0.213	0.227	0.036	0.045	0.360
60	259.152	0.659	4.167	988.130	4.658E-04	259.550	0.659	4.164	987.48	4.687E-04	0.153	0.002	0.079	0.066	0.615
75	321.748	0.672	4.180	979.713	3.772E-04	322.070	0.672	4.172	979.19	3.803E-04	0.100	0.024	0.175	0.053	0.810
90	384.545	0.682	4.194	969.884	3.152E-04	384.730	0.680	4.184	969.78	3.171E-04	0.048	0.194	0.249	0.011	0.587
105	447.578	0.689	4.211	958.879	2.720E-04	447.600	0.686	4.199	959.34	2.702E-04	0.005	0.446	0.283	0.048	0.648
120	510.889	0.694	4.231	946.986	2.369E-04	510.730	0.689	4.219	947.94	2.346E-04	0.031	0.685	0.275	0.101	0.968
135	574.519	0.696	4.254	934.543	2.085E-04	574.200	0.690	4.245	935.60	2.069E-04	0.056	0.868	0.217	0.113	0.773
150	638.539	0.695	4.282	921.943	1.857E-04	638.110	0.688	4.277	922.32	1.849E-04	0.067	0.980	0.117	0.041	0.427
165	703.023	0.692	4.316	907.468	1.673E-04	702.560	0.685	4.317	908.10	1.670E-04	0.066	1.005	0.023	0.070	0.180
180	768.069	0.687	4.359	892.342	1.526E-04	767.680	0.680	4.366	892.88	1.524E-04	0.051	0.970	0.181	0.060	0.171
195	833.421	0.679	4.534	876.349	1.407E-04	833.610	0.673	4.426	876.61	1.401E-04	0.023	0.881	2.426	0.030	0.471
210	901.405	0.669	4.538	858.796	1.307E-04	900.530	0.664	4.500	859.18	1.296E-04	0.097	0.692	0.851	0.045	0.795
225	969.749	0.657	4.580	840.128	1.222E-04	968.680	0.653	4.590	840.44	1.206E-04	0.110	0.507	0.205	0.037	1.319
240	1039.024	0.642	4.665	820.067	1.147E-04	1038.300	0.639	4.702	820.18	1.126E-04	0.070	0.332	0.800	0.014	1.874
255	1109.930	0.624	4.799	798.233	1.079E-04	1109.900	0.623	4.845	798.13	1.055E-04	0.003	0.228	0.958	0.013	2.342
270	1183.308	0.604	4.998	774.115	1.016E-04	1183.900	0.603	5.033	773.83	9.887E-05	0.050	0.249	0.707	0.037	2.708
285	1260.317	0.581	5.288	746.960	9.556E-05	1261.200	0.579	5.293	746.61	9.262E-05	0.070	0.397	0.094	0.047	3.175
300	1342.658	0.555	5.722	715.589	9.027E-05	1343.300	0.551	5.681	715.29	8.646E-05	0.048	0.714	0.725	0.042	4.408
310.96	1407.788	0.532	6.191	688.866	8.731E-05	1408.100	0.527	6.124	688.42	8.180E-05	0.022	0.981	1.092	0.065	6.747
Max % Error	**0.262**	**1.527**	**2.426**	**0.113**	**6.747**										

Table 17.13 Comparison of Liquid H_2O Properties at 125 bar between PLTEMP/ANL Version 4.2 and NIST Data

	PLTEMP	PLTEMP	PLTEMP	PLTEMP	PLTEMP	NIST	NIST	NIST	NIST	NIST	% Diff. H	% Diff. K	% Diff. Cp	% Diff. ρ	% Diff. μ
Temp, C	H, kJ/kg	K, W/m-C	Cp, kJ/kg-C	ρ, kg/m^3	μ, Pa-s	H, kJ/kg	K, W/m-C	Cp, kJ/kg-C	ρ, kg/m^3	μ, Pa-s					
16	78.884	0.606	4.132	1004.211	1.112E-03	79.020	0.597	4.148	1004.60	1.101E-03	0.172	1.422	0.381	0.039	1.054
32	145.069	0.628	4.141	1000.543	7.700E-04	145.380	0.624	4.148	1000.50	7.642E-04	0.214	0.625	0.157	0.004	0.758
48	211.407	0.647	4.152	994.801	5.649E-04	211.780	0.647	4.153	994.27	5.678E-04	0.176	0.076	0.024	0.053	0.518
64	277.932	0.663	4.164	987.118	4.391E-04	278.280	0.664	4.161	986.45	4.426E-04	0.125	0.136	0.084	0.068	0.789
80	344.666	0.676	4.178	977.683	3.529E-04	344.930	0.676	4.171	977.26	3.576E-04	0.077	0.075	0.177	0.043	1.314
96	411.643	0.685	4.194	966.745	2.955E-04	411.760	0.684	4.184	966.85	2.974E-04	0.028	0.133	0.244	0.011	0.649
112	478.897	0.692	4.213	954.613	2.537E-04	478.840	0.689	4.202	955.32	2.531E-04	0.012	0.373	0.267	0.074	0.225
128	546.485	0.695	4.236	941.655	2.202E-04	546.260	0.691	4.226	942.72	2.197E-04	0.041	0.572	0.241	0.113	0.264
144	614.475	0.696	4.264	928.311	1.936E-04	614.110	0.691	4.257	929.07	1.937E-04	0.059	0.708	0.164	0.082	0.041
160	682.951	0.693	4.297	913.694	1.726E-04	682.510	0.688	4.295	914.37	1.732E-04	0.065	0.739	0.047	0.074	0.346
176	752.025	0.688	4.339	897.993	1.559E-04	751.590	0.684	4.343	898.59	1.566E-04	0.058	0.687	0.094	0.066	0.428
192	821.188	0.681	4.510	881.412	1.428E-04	821.540	0.677	4.402	881.66	1.430E-04	0.043	0.583	2.456	0.028	0.140
208	893.330	0.670	4.514	863.125	1.318E-04	892.530	0.668	4.475	863.47	1.315E-04	0.090	0.352	0.885	0.040	0.160
224	965.854	0.657	4.558	843.628	1.226E-04	964.820	0.656	4.565	843.87	1.218E-04	0.107	0.110	0.151	0.029	0.698
240	1039.413	0.642	4.645	822.605	1.147E-04	1038.700	0.642	4.678	822.63	1.133E-04	0.069	0.118	0.712	0.003	1.254
256	1114.769	0.623	4.784	799.635	1.075E-04	1114.700	0.625	4.824	799.45	1.057E-04	0.006	0.282	0.823	0.023	1.693
272	1192.861	0.602	4.991	774.142	1.008E-04	1193.300	0.604	5.016	773.84	9.877E-05	0.037	0.358	0.510	0.039	2.013
288	1274.994	0.577	5.295	745.264	9.452E-05	1275.600	0.578	5.285	745.04	9.224E-05	0.048	0.287	0.187	0.030	2.480
304	1363.119	0.548	5.754	711.629	8.920E-05	1363.200	0.548	5.692	711.71	8.580E-05	0.006	0.104	1.103	0.011	3.964
320	1460.629	0.513	6.502	670.764	8.607E-05	1459.300	0.513	6.405	671.13	7.905E-05	0.091	0.010	1.513	0.055	8.883
327.78	1513.283	0.493	7.064	646.898	8.620E-05	1511.600	0.494	7.021	646.81	7.540E-05	0.111	0.083	0.602	0.014	14.332
Max % Error	**0.214**	**1.422**	**2.456**	**0.113**	**14.332**										

Table 17.14 Comparison of Liquid H_2O Properties at 145 bar between PLTEMP/ANL Version 4.2 and NIST Data

	PLTEMP	PLTEMP	PLTEMP	PLTEMP	PLTEMP	NIST	NIST	NIST	NIST	NIST	% Diff. H	% Diff. K	% Diff. Cp	% Diff. ρ	% Diff. μ
Temp, C	H, kJ/kg	K, W/m-C	Cp, kJ/kg-C	ρ, kg/m^3	μ, Pa-s	H, kJ/kg	K, W/m-C	Cp, kJ/kg-C	ρ, kg/m^3	μ, Pa-s					
16	80.793	0.606	4.128	1005.138	1.111E-03	80.903	0.598	4.142	1005.50	1.100E-03	0.136	1.380	0.348	0.036	1.027
32	146.909	0.629	4.137	1001.432	7.697E-04	147.170	0.625	4.143	1001.30	7.642E-04	0.177	0.558	0.154	0.013	0.728
48	213.170	0.648	4.147	995.670	5.652E-04	213.500	0.648	4.149	995.11	5.681E-04	0.155	0.006	0.036	0.056	0.525
64	279.619	0.664	4.159	987.985	4.396E-04	279.940	0.665	4.156	987.30	4.430E-04	0.115	0.221	0.065	0.069	0.785
80	346.277	0.676	4.173	978.565	3.521E-04	346.520	0.677	4.167	978.13	3.582E-04	0.070	0.182	0.156	0.044	1.692
96	413.163	0.686	4.189	967.659	2.944E-04	413.280	0.685	4.180	967.75	2.979E-04	0.028	0.006	0.222	0.009	1.182
112	480.341	0.692	4.208	955.569	2.529E-04	480.300	0.690	4.198	956.25	2.536E-04	0.009	0.222	0.248	0.071	0.296
128	547.845	0.695	4.231	942.666	2.196E-04	547.640	0.692	4.221	943.70	2.202E-04	0.037	0.410	0.230	0.110	0.241
144	615.745	0.696	4.258	929.383	1.932E-04	615.410	0.692	4.251	930.12	1.942E-04	0.054	0.519	0.167	0.079	0.525
160	684.132	0.693	4.291	914.828	1.723E-04	683.710	0.690	4.289	915.51	1.737E-04	0.062	0.536	0.061	0.074	0.812
176	753.108	0.688	4.333	899.245	1.557E-04	752.690	0.685	4.335	899.82	1.571E-04	0.056	0.452	0.060	0.064	0.878
192	822.278	0.681	4.488	882.774	1.426E-04	822.500	0.679	4.393	883.01	1.435E-04	0.027	0.314	2.174	0.027	0.606
208	894.122	0.670	4.498	864.695	1.316E-04	893.330	0.670	4.464	864.97	1.320E-04	0.089	0.073	0.766	0.032	0.288
224	966.403	0.657	4.544	845.420	1.226E-04	965.420	0.658	4.551	845.55	1.223E-04	0.102	0.202	0.163	0.015	0.229
240	1039.725	0.641	4.630	824.649	1.147E-04	1039.100	0.644	4.660	824.55	1.138E-04	0.060	0.473	0.657	0.012	0.773
256	1114.797	0.623	4.764	801.989	1.075E-04	1114.700	0.627	4.799	801.69	1.062E-04	0.009	0.682	0.744	0.037	1.177
272	1192.487	0.602	4.960	776.900	1.008E-04	1192.900	0.607	4.982	776.51	9.936E-05	0.035	0.829	0.440	0.050	1.443
288	1273.981	0.577	5.244	748.591	9.459E-05	1274.500	0.582	5.232	748.34	9.289E-05	0.041	0.852	0.220	0.034	1.834
304	1361.008	0.548	5.664	715.834	8.931E-05	1360.900	0.553	5.602	716.02	8.657E-05	0.008	0.784	1.110	0.026	3.159
320	1456.492	0.514	6.327	676.482	8.612E-05	1455.000	0.519	6.220	677.30	8.004E-05	0.103	0.804	1.724	0.121	7.601
336	1566.187	0.473	7.519	626.154	8.811E-05	1563.600	0.479	7.566	626.47	7.257E-05	0.165	1.373	0.620	0.050	21.414
Max % Error	**0.177**	**1.380**	**2.174**	**0.121**	**21.414**										

Table 17.15 Comparison of Thermal Properties of H_2O over 1 to 145 bar Pressure and 4 to 339 ºC Temperature between PLTEMP/ANL Version 4.2 and NIST Data

Phase & Pressure	% Diff. H	% Diff. K	% Diff. Cp	% Diff. ρ	% Diff. μ
Liquid, 1 bar	0.619	2.175	1.251	0.070	3.160
Liquid, 2 bar	0.522	2.110	1.109	0.096	3.590
Liquid, 3 bar	0.518	2.101	1.107	0.106	3.563
Liquid, 4 bar	0.510	2.050	1.041	0.106	3.540
Liquid, 5 bar	0.505	2.057	1.036	0.107	3.511
Liquid, 10 bar	0.489	2.043	0.960	0.109	3.372
Liquid, 20 bar	0.463	1.965	2.606	0.111	3.098
Liquid, 30 bar	0.438	1.843	2.821	0.113	3.288
Liquid, 40 bar	0.400	1.778	3.687	0.113	3.825
Liquid, 50 bar	0.371	1.718	3.057	0.115	4.050
Liquid, 75 bar	0.310	1.621	2.602	0.113	4.420
Liquid, 100 bar	0.262	1.527	2.426	0.113	6.747
Liquid, 125 bar	0.214	1.422	2.456	0.113	14.332
Liquid, 145 bar	0.177	1.380	2.174	0.121	21.414
Max. % Error All Pressures	**0.619**	**2.175**	**3.687**	**0.121**	**21.414**

Table 17.16 Comparison of Liquid D_2O Properties at 1 bar between PLTEMP/ANL Version 4.2 and NIST Data

	PLTEMP	PLTEMP	PLTEMP	PLTEMP	PLTEMP	NIST	NIST	NIST	NIST	NIST	% Diff. H	% Diff. K	% Diff. Cp	% Diff. ρ	% Diff. μ
Temp C	H kJ/kg	K W/m-C	Cp kJ/kg-C	ρ kg/m3	μ Pa-s	H kJ/kg	K W/m-C	Cp kJ/kg-C	P kg/m3	μ Pa-s					
5	4.921	0.578	4.072	1110.960	1.960E-03	4.960	0.567	4.216	1105.70	1.996E-03	0.779	1.941	3.411	0.476	1.793
10	25.381	0.583	4.109	1110.580	1.676E-03	26.080	0.575	4.231	1106.00	1.679E-03	2.680	1.539	2.892	0.414	0.188
15	45.979	0.589	4.128	1109.820	1.441E-03	47.260	0.582	4.239	1105.90	1.437E-03	2.710	1.194	2.615	0.354	0.317
20	66.643	0.594	4.136	1108.730	1.250E-03	68.460	0.589	4.242	1105.40	1.247E-03	2.654	0.899	2.507	0.301	0.261
25	87.325	0.599	4.136	1107.340	1.097E-03	89.680	0.595	4.242	1104.50	1.095E-03	2.626	0.650	2.506	0.257	0.142
30	107.996	0.603	4.132	1105.680	9.740E-04	110.880	0.601	4.240	1103.30	9.718E-04	2.601	0.443	2.554	0.216	0.233
35	128.640	0.607	4.126	1103.780	8.740E-04	132.070	0.606	4.236	1101.80	8.700E-04	2.597	0.272	2.615	0.180	0.457
40	149.251	0.611	4.119	1101.660	7.897E-04	153.240	0.610	4.232	1100.00	7.849E-04	2.603	0.135	2.658	0.151	0.615
45	169.832	0.615	4.113	1099.330	7.170E-04	174.390	0.614	4.226	1098.00	7.128E-04	2.614	0.025	2.667	0.121	0.589
50	190.388	0.618	4.109	1096.810	6.539E-04	195.500	0.618	4.220	1095.70	6.512E-04	2.615	0.061	2.629	0.101	0.408
55	210.925	0.621	4.106	1094.110	5.991E-04	216.590	0.622	4.214	1093.20	5.981E-04	2.616	0.125	2.546	0.083	0.166
60	231.454	0.624	4.105	1091.230	5.516E-04	237.640	0.625	4.207	1090.60	5.519E-04	2.603	0.170	2.417	0.058	0.050
65	251.981	0.626	4.106	1088.180	5.104E-04	258.660	0.627	4.200	1087.70	5.114E-04	2.582	0.200	2.248	0.044	0.196
70	272.515	0.628	4.108	1084.980	4.744E-04	279.640	0.629	4.194	1084.70	4.757E-04	2.548	0.218	2.049	0.026	0.267
75	293.061	0.630	4.111	1081.630	4.429E-04	300.600	0.631	4.187	1081.50	4.441E-04	2.508	0.222	1.827	0.012	0.270
80	313.623	0.632	4.114	1078.130	4.150E-04	321.516	0.633	4.181	1078.20	4.159E-04	2.455	0.218	1.594	0.006	0.216
85	334.205	0.633	4.118	1074.500	3.901E-04	342.406	0.634	4.175	1074.70	3.906E-04	2.395	0.206	1.360	0.019	0.124
90	354.808	0.634	4.123	1070.730	3.679E-04	363.269	0.635	4.170	1071.00	3.679E-04	2.329	0.186	1.131	0.025	0.008
95	375.432	0.635	4.127	1066.830	3.478E-04	384.106	0.636	4.165	1067.30	3.474E-04	2.258	0.162	0.914	0.044	0.116
100	396.078	0.635	4.131	1062.810	3.296E-04	404.921	0.636	4.161	1063.40	3.288E-04	2.184	0.133	0.718	0.055	0.241
Max % Diff.	**2.710**	**1.941**	**3.411**	**0.476**	**1.793**										

Table 17.17 Comparison of Liquid D_2O Properties at 2 bar between PLTEMP/ANL Version 4.2 and NIST Data

	PLTEMP	PLTEMP	PLTEMP	PLTEMP	PLTEMP	NIST	NIST	NIST	NIST	NIST	% Diff. H	% Diff. K	% Diff. Cp	% Diff. ρ	% Diff. μ
Temp C	H kJ/kg	K W/m-C	Cp kJ/kg-C	ρ kg/m3	μ Pa-s	H kJ/kg	K W/m-C	Cp kJ/kg-C	P kg/m3	μ Pa-s					
6	9.087	0.579	4.080	1110.970	1.899E-03	9.270	0.568	4.219	1105.800	1.925E-03	1.978	1.854	3.285	0.468	1.353
12	33.695	0.586	4.118	1110.370	1.576E-03	34.640	0.578	4.235	1106.100	1.575E-03	2.728	1.394	2.755	0.386	0.122
18	58.458	0.592	4.134	1109.250	1.322E-03	60.070	0.586	4.241	1105.700	1.317E-03	2.684	1.010	2.533	0.321	0.320
24	83.272	0.598	4.136	1107.690	1.125E-03	85.520	0.594	4.242	1104.800	1.123E-03	2.629	0.696	2.501	0.262	0.160
30	108.077	0.603	4.132	1105.730	9.740E-04	110.970	0.601	4.240	1103.300	9.717E-04	2.607	0.443	2.553	0.220	0.235
36	132.845	0.608	4.124	1103.430	8.560E-04	136.390	0.607	4.235	1101.500	8.518E-04	2.599	0.242	2.626	0.175	0.502
42	157.566	0.613	4.116	1100.810	7.594E-04	161.790	0.612	4.229	1099.300	7.546E-04	2.611	0.087	2.665	0.137	0.629
48	182.246	0.617	4.110	1097.890	6.781E-04	187.140	0.617	4.222	1096.700	6.748E-04	2.615	0.029	2.651	0.109	0.493
54	206.895	0.620	4.107	1094.710	6.094E-04	212.450	0.621	4.215	1093.800	6.081E-04	2.615	0.114	2.566	0.083	0.213
60	231.529	0.624	4.105	1091.280	5.516E-04	237.720	0.625	4.207	1090.600	5.519E-04	2.604	0.170	2.417	0.062	0.051
66	256.161	0.626	4.106	1087.610	5.028E-04	262.930	0.628	4.199	1087.200	5.039E-04	2.574	0.205	2.211	0.038	0.218
72	280.804	0.629	4.109	1083.710	4.614E-04	288.100	0.630	4.191	1083.500	4.627E-04	2.532	0.221	1.963	0.019	0.278
78	305.467	0.631	4.113	1079.600	4.258E-04	313.224	0.632	4.183	1079.600	4.268E-04	2.477	0.221	1.687	0.000	0.246
84	330.157	0.633	4.117	1075.290	3.949E-04	338.302	0.634	4.176	1075.400	3.955E-04	2.408	0.209	1.406	0.010	0.148
90	354.877	0.634	4.123	1070.790	3.679E-04	363.339	0.635	4.170	1071.100	3.680E-04	2.329	0.186	1.131	0.029	0.010
96	379.628	0.635	4.128	1066.090	3.441E-04	388.339	0.636	4.164	1066.500	3.436E-04	2.243	0.157	0.872	0.038	0.141
102	404.409	0.635	4.133	1061.220	3.228E-04	413.309	0.636	4.159	1061.800	3.219E-04	2.153	0.121	0.644	0.055	0.288
108	429.219	0.635	4.137	1056.160	3.038E-04	438.255	0.636	4.156	1056.900	3.025E-04	2.062	0.082	0.449	0.070	0.412
114	454.056	0.635	4.142	1050.930	2.866E-04	463.183	0.635	4.154	1051.700	2.851E-04	1.970	0.040	0.288	0.073	0.506
120	478.921	0.635	4.146	1045.530	2.710E-04	488.103	0.635	4.153	1046.400	2.695E-04	1.881	0.001	0.163	0.083	0.563
121.4	484.759	0.634	4.147	1044.240	2.675E-04	493.940	0.634	4.153	1045.200	2.660E-04	1.859	0.012	0.137	0.092	0.568
Max % Diff.	**2.728**	**1.854**	**3.285**	**0.468**	**1.353**										

Table 17.18 Comparison of Liquid D_2O Properties at 3 bar between PLTEMP/ANL Version 4.2 and NIST Data

	PLTEMP	PLTEMP	PLTEMP	PLTEMP	PLTEMP	NIST	NIST	NIST	NIST	NIST	% Diff. H	% Diff. K	% Diff. Cp	% Diff. ρ	% Diff. μ
Temp C	H kJ/kg	K W/m-C	Cp kJ/kg-C	ρ kg/m3	μ Pa-s	H kJ/kg	K W/m-C	Cp kJ/kg-C	P kg/m3	μ Pa-s					
6	9.176	0.579	4.080	1111.025	1.899E-03	9.360	0.568	4.219	1105.900	1.925E-03	1.966	1.853	3.283	0.463	1.346
12	33.782	0.586	4.118	1110.424	1.576E-03	34.730	0.578	4.234	1106.100	1.574E-03	2.730	1.395	2.754	0.391	0.133
18	58.543	0.592	4.133	1109.304	1.322E-03	60.150	0.586	4.241	1105.700	1.317E-03	2.672	1.010	2.533	0.326	0.319
24	83.355	0.598	4.136	1107.737	1.125E-03	85.600	0.594	4.242	1104.800	1.123E-03	2.623	0.694	2.497	0.266	0.160
30	108.159	0.603	4.131	1105.781	9.740E-04	111.050	0.601	4.240	1103.400	9.717E-04	2.603	0.450	2.552	0.216	0.238
36	132.925	0.608	4.124	1103.476	8.560E-04	136.470	0.607	4.235	1101.500	8.518E-04	2.598	0.247	2.623	0.179	0.502
42	157.645	0.613	4.116	1100.855	7.594E-04	161.870	0.612	4.229	1099.300	7.547E-04	2.610	0.095	2.665	0.141	0.629
48	182.323	0.617	4.110	1097.944	6.781E-04	187.220	0.617	4.222	1096.700	6.748E-04	2.616	0.032	2.648	0.113	0.493
54	206.972	0.620	4.106	1094.762	6.095E-04	212.530	0.621	4.214	1093.800	6.082E-04	2.615	0.111	2.565	0.088	0.214
60	231.604	0.624	4.105	1091.328	5.517E-04	237.790	0.625	4.207	1090.700	5.519E-04	2.601	0.176	2.415	0.058	0.051
66	256.235	0.627	4.106	1087.657	5.029E-04	263.010	0.628	4.199	1087.200	5.040E-04	2.576	0.204	2.208	0.042	0.220
72	280.877	0.629	4.108	1083.762	4.614E-04	288.180	0.630	4.191	1083.500	4.627E-04	2.534	0.214	1.962	0.024	0.279
78	305.539	0.631	4.112	1079.654	4.258E-04	313.296	0.632	4.183	1079.600	4.269E-04	2.476	0.225	1.688	0.005	0.246
84	330.227	0.633	4.117	1075.344	3.950E-04	338.373	0.634	4.176	1075.500	3.955E-04	2.407	0.208	1.406	0.015	0.149
90	354.946	0.634	4.122	1070.840	3.680E-04	363.408	0.635	4.170	1071.100	3.680E-04	2.329	0.183	1.132	0.024	0.014
96	379.695	0.635	4.128	1066.147	3.441E-04	388.408	0.636	4.164	1066.600	3.436E-04	2.243	0.153	0.872	0.042	0.140
102	404.475	0.635	4.132	1061.273	3.229E-04	413.376	0.636	4.159	1061.900	3.220E-04	2.153	0.119	0.644	0.059	0.286
108	429.284	0.636	4.137	1056.220	3.038E-04	438.321	0.636	4.156	1056.900	3.026E-04	2.062	0.085	0.448	0.064	0.413
114	454.120	0.635	4.142	1050.993	2.866E-04	463.248	0.636	4.154	1051.800	2.852E-04	1.970	0.035	0.289	0.077	0.508
120	478.983	0.635	4.146	1045.591	2.710E-04	488.166	0.635	4.153	1046.500	2.695E-04	1.881	0.003	0.164	0.087	0.560
126	503.874	0.634	4.151	1040.018	2.568E-04	513.090	0.633	4.154	1041.000	2.553E-04	1.796	0.039	0.070	0.094	0.580
Max % Diff.	**2.730**	**1.853**	**3.283**	**0.463**	**1.346**										

Table 17.19 Comparison of Liquid D_2O Properties at 4 bar between PLTEMP/ANL Version 4.2 and NIST Data

	PLTEMP	PLTEMP	PLTEMP	PLTEMP	PLTEMP	NIST	NIST	NIST	NIST	NIST	% Diff. H	% Diff. K	% Diff. Cp	% Diff. ρ	% Diff. μ
Temp C	H kJ/kg	K W/m-C	Cp kJ/kg-C	ρ kg/m3	μ Pa-s	H kJ/kg	K W/m-C	Cp kJ/kg-C	P kg/m3	μ Pa-s					
7	13.348	0.580	4.088	1111.019	1.840E-03	13.680	0.570	4.222	1106.000	1.858E-03	2.427	1.779	3.167	0.454	0.969
14	42.110	0.588	4.124	1110.157	1.484E-03	43.290	0.581	4.237	1106.100	1.480E-03	2.726	1.255	2.651	0.367	0.297
21	71.031	0.595	4.136	1108.623	1.216E-03	72.970	0.590	4.241	1105.400	1.214E-03	2.657	0.840	2.497	0.292	0.239
28	99.976	0.602	4.133	1106.524	1.020E-03	102.650	0.598	4.240	1104.000	1.018E-03	2.605	0.523	2.528	0.229	0.177
35	128.881	0.607	4.125	1103.933	8.740E-04	132.320	0.606	4.236	1101.900	8.700E-04	2.599	0.267	2.614	0.184	0.461
42	157.724	0.613	4.116	1100.905	7.594E-04	161.950	0.612	4.229	1099.400	7.547E-04	2.609	0.087	2.663	0.137	0.629
49	186.510	0.617	4.109	1097.482	6.659E-04	191.520	0.618	4.221	1096.300	6.629E-04	2.616	0.047	2.639	0.108	0.451
56	215.259	0.622	4.105	1093.695	5.891E-04	221.030	0.622	4.212	1092.900	5.884E-04	2.611	0.129	2.522	0.073	0.117
63	243.993	0.625	4.105	1089.572	5.263E-04	250.480	0.626	4.202	1089.000	5.271E-04	2.590	0.185	2.318	0.053	0.152
70	272.734	0.628	4.107	1085.135	4.745E-04	279.870	0.630	4.193	1084.800	4.758E-04	2.550	0.222	2.046	0.031	0.273
77	301.499	0.631	4.112	1080.405	4.314E-04	309.190	0.632	4.184	1080.300	4.325E-04	2.487	0.215	1.735	0.010	0.259
84	330.298	0.633	4.117	1075.397	3.950E-04	338.444	0.634	4.176	1075.500	3.956E-04	2.407	0.216	1.406	0.010	0.152
91	359.138	0.634	4.123	1070.124	3.638E-04	367.647	0.635	4.168	1070.500	3.638E-04	2.314	0.183	1.084	0.035	0.011
98	388.020	0.635	4.129	1064.597	3.368E-04	396.802	0.636	4.162	1065.100	3.362E-04	2.213	0.152	0.795	0.047	0.187
105	416.942	0.636	4.135	1058.825	3.131E-04	425.918	0.636	4.157	1059.500	3.120E-04	2.107	0.094	0.541	0.064	0.353
112	445.903	0.635	4.140	1052.812	2.922E-04	455.005	0.636	4.154	1053.600	2.908E-04	2.000	0.061	0.337	0.075	0.478
119	474.901	0.635	4.145	1046.562	2.735E-04	484.077	0.635	4.153	1047.500	2.720E-04	1.896	0.008	0.181	0.090	0.555
126	503.935	0.634	4.151	1040.078	2.568E-04	513.150	0.633	4.153	1041.100	2.553E-04	1.796	0.046	0.067	0.098	0.576
133	533.011	0.632	4.157	1033.360	2.417E-04	542.230	0.631	4.156	1034.400	2.404E-04	1.700	0.098	0.010	0.101	0.545
140	562.134	0.630	4.165	1026.405	2.280E-04	571.340	0.629	4.162	1027.500	2.270E-04	1.611	0.130	0.065	0.107	0.467
144.518	580.961	0.628	4.170	1021.790	2.199E-04	590.200	0.627	4.167	1022.900	2.190E-04	1.565	0.161	0.091	0.109	0.402
Max % Diff.	**2.726**	**1.779**	**3.167**	**0.454**	**0.969**										

Table 17.20 Comparison of Liquid D_2O Properties at 5 bar between PLTEMP/ANL Version 4.2 and NIST Data

	PLTEMP	PLTEMP	PLTEMP	PLTEMP	PLTEMP	NIST	NIST	NIST	NIST	NIST	% Diff. H	% Diff. K	% Diff. Cp	% Diff. ρ	% Diff. μ
Temp C	H kJ/kg	K W/m-C	Cp kJ/kg-C	ρ kg/m3	μ Pa-s	H kJ/kg	K W/m-C	Cp kJ/kg-C	P kg/m3	μ Pa-s					
7	13.437	0.580	4.088	1111.070	1.840E-03	13.77	0.570	4.221	1106.10	1.858E-03	2.420	1.770	3.167	0.449	0.957
14	42.196	0.588	4.124	1110.210	1.484E-03	43.38	0.581	4.236	1106.20	1.480E-03	2.728	1.256	2.649	0.363	0.305
21	71.115	0.595	4.135	1108.670	1.216E-03	73.05	0.590	4.241	1105.40	1.214E-03	2.649	0.844	2.496	0.296	0.240
28	100.058	0.602	4.133	1106.570	1.020E-03	102.74	0.599	4.240	1104.00	1.018E-03	2.610	0.520	2.528	0.233	0.180
35	128.961	0.607	4.125	1103.980	8.740E-04	132.40	0.606	4.235	1102.00	8.700E-04	2.597	0.271	2.611	0.180	0.464
42	157.803	0.613	4.116	1100.950	7.594E-04	162.03	0.612	4.229	1099.40	7.547E-04	2.609	0.087	2.665	0.141	0.631
49	186.588	0.617	4.109	1097.530	6.659E-04	191.60	0.618	4.220	1096.40	6.629E-04	2.616	0.046	2.639	0.103	0.452
56	215.335	0.622	4.105	1093.740	5.891E-04	221.11	0.622	4.211	1092.90	5.884E-04	2.612	0.135	2.522	0.077	0.116
63	244.068	0.625	4.105	1089.620	5.263E-04	250.56	0.626	4.202	1089.10	5.271E-04	2.591	0.191	2.318	0.048	0.152
70	272.807	0.628	4.107	1085.190	4.746E-04	279.94	0.630	4.193	1084.90	4.759E-04	2.548	0.218	2.047	0.027	0.273
77	301.570	0.631	4.111	1080.460	4.314E-04	309.26	0.632	4.184	1080.40	4.326E-04	2.487	0.222	1.735	0.006	0.260
84	330.368	0.633	4.117	1075.450	3.950E-04	338.52	0.634	4.176	1075.60	3.956E-04	2.407	0.208	1.406	0.014	0.153
91	359.207	0.634	4.123	1070.180	3.638E-04	367.72	0.635	4.168	1070.50	3.638E-04	2.314	0.182	1.085	0.030	0.011
98	388.087	0.635	4.129	1064.650	3.368E-04	396.87	0.636	4.162	1065.10	3.362E-04	2.213	0.145	0.792	0.042	0.186
105	417.008	0.636	4.134	1058.880	3.132E-04	425.99	0.636	4.157	1059.50	3.121E-04	2.107	0.101	0.542	0.059	0.349
112	445.968	0.635	4.140	1052.870	2.922E-04	455.07	0.636	4.154	1053.60	2.908E-04	2.000	0.054	0.337	0.069	0.477
119	474.964	0.635	4.145	1046.620	2.736E-04	484.14	0.635	4.152	1047.50	2.721E-04	1.896	0.005	0.181	0.084	0.555
126	503.997	0.634	4.150	1040.140	2.568E-04	513.21	0.633	4.153	1041.10	2.554E-04	1.795	0.043	0.069	0.092	0.578
133	533.070	0.632	4.157	1033.420	2.417E-04	542.29	0.632	4.156	1034.50	2.404E-04	1.700	0.091	0.009	0.104	0.544
140	562.192	0.630	4.164	1026.470	2.281E-04	571.40	0.629	4.162	1027.60	2.270E-04	1.611	0.135	0.065	0.110	0.463
147	591.373	0.627	4.174	1019.280	2.156E-04	600.56	0.626	4.169	1020.40	2.149E-04	1.530	0.174	0.107	0.110	0.349
Max % Diff.	**2.728**	**1.770**	**3.167**	**0.449**	**0.957**										

Table 17.21 Comparison of Liquid D_2O Properties at 10 bar between PLTEMP/ANL Version 4.2 and NIST Data

	PLTEMP	PLTEMP	PLTEMP	PLTEMP	PLTEMP	NIST	NIST	NIST	NIST	NIST	% Diff. H	% Diff. K	% Diff. Cp	% Diff. ρ	% Diff. μ
Temp C	H kJ/kg	K W/m-C	Cp kJ/kg-C	ρ kg/m3	μ Pa-s	H kJ/kg	K W/m-C	Cp kJ/kg-C	P kg/m3	μ Pa-s					
9	22.065	0.583	4.100	1111.170	1.728E-03	22.67	0.574	4.225	1106.50	1.734E-03	2.670	1.608	2.965	0.422	0.339
18	59.136	0.592	4.131	1109.660	1.321E-03	60.77	0.587	4.238	1106.10	1.317E-03	2.688	1.005	2.521	0.322	0.353
27	96.337	0.601	4.132	1107.160	1.044E-03	98.92	0.598	4.239	1104.50	1.043E-03	2.611	0.559	2.510	0.241	0.180
36	133.486	0.609	4.122	1103.830	8.561E-04	137.05	0.607	4.233	1101.90	8.518E-04	2.601	0.240	2.619	0.175	0.511
45	170.536	0.615	4.111	1099.780	7.172E-04	175.11	0.615	4.224	1098.40	7.130E-04	2.612	0.023	2.662	0.126	0.592
54	207.505	0.621	4.105	1095.110	6.096E-04	213.07	0.621	4.213	1094.20	6.084E-04	2.612	0.115	2.562	0.083	0.208
63	244.440	0.625	4.104	1089.870	5.264E-04	250.94	0.627	4.201	1089.30	5.273E-04	2.590	0.191	2.316	0.052	0.157
72	281.386	0.629	4.107	1084.120	4.616E-04	288.69	0.631	4.189	1083.90	4.629E-04	2.530	0.220	1.961	0.020	0.289
81	318.376	0.632	4.113	1077.890	4.101E-04	326.34	0.634	4.178	1077.90	4.109E-04	2.441	0.215	1.547	0.001	0.215
90	355.430	0.634	4.121	1071.210	3.682E-04	363.90	0.636	4.168	1071.50	3.683E-04	2.327	0.186	1.129	0.027	0.024
99	392.553	0.636	4.129	1064.120	3.334E-04	401.37	0.636	4.160	1064.60	3.327E-04	2.197	0.138	0.754	0.045	0.206
108	429.742	0.636	4.136	1056.620	3.040E-04	438.78	0.636	4.154	1057.30	3.028E-04	2.060	0.081	0.447	0.064	0.402
117	466.993	0.635	4.142	1048.720	2.789E-04	476.16	0.636	4.151	1049.60	2.774E-04	1.924	0.018	0.220	0.084	0.532
126	504.303	0.634	4.149	1040.440	2.570E-04	513.52	0.634	4.152	1041.40	2.555E-04	1.795	0.046	0.066	0.092	0.573
135	541.681	0.632	4.157	1031.770	2.378E-04	550.90	0.631	4.156	1032.80	2.366E-04	1.673	0.105	0.029	0.100	0.523
144	579.142	0.629	4.168	1022.720	2.210E-04	588.34	0.628	4.164	1023.80	2.201E-04	1.563	0.160	0.091	0.105	0.397
153	616.716	0.625	4.182	1013.260	2.060E-04	625.87	0.624	4.177	1014.40	2.056E-04	1.463	0.206	0.141	0.112	0.222
162	654.439	0.621	4.201	1003.400	1.928E-04	663.53	0.619	4.193	1004.60	1.927E-04	1.370	0.242	0.202	0.119	0.015
171	692.358	0.615	4.226	993.108	1.810E-04	701.36	0.614	4.214	994.25	1.813E-04	1.284	0.267	0.280	0.115	0.192
180	730.523	0.609	4.256	982.370	1.704E-04	739.40	0.607	4.240	983.47	1.711E-04	1.201	0.284	0.379	0.112	0.365
180.4	732.084	0.609	4.257	981.923	1.700E-04	741.00	0.607	4.241	983.01	1.707E-04	1.203	0.285	0.383	0.111	0.368
Max % Diff.	**2.688**	**1.608**	**2.965**	**0.422**	**0.592**										

Table 17.22 Comparison of Liquid D_2O Properties at 20 bar between PLTEMP/ANL Version 4.2 and NIST Data

	PLTEMP	PLTEMP	PLTEMP	PLTEMP	PLTEMP	NIST	NIST	NIST	NIST	NIST	% Diff. H	% Diff. K	% Diff. Cp	% Diff. ρ	% Diff. μ
Temp C	H kJ/kg	K W/m-C	Cp kJ/kg-C	ρ kg/m3	μ Pa-s	H kJ/kg	K W/m-C	Cp kJ/kg-C	P kg/m3	μ Pa-s					
10	27.040	0.584	4.102	1111.590	1.675E-03	27.81	0.576	4.223	1107.10	1.676E-03	2.770	1.526	2.869	0.406	0.054
20	68.242	0.595	4.130	1109.700	1.250E-03	70.12	0.590	4.236	1106.40	1.245E-03	2.678	0.887	2.482	0.298	0.342
30	109.545	0.604	4.127	1106.630	9.741E-04	112.47	0.602	4.235	1104.30	9.715E-04	2.601	0.435	2.535	0.211	0.276
40	150.757	0.612	4.115	1102.610	7.900E-04	154.78	0.611	4.227	1100.90	7.851E-04	2.599	0.129	2.644	0.155	0.629
50	191.853	0.619	4.105	1097.760	6.543E-04	197.00	0.619	4.216	1096.60	6.517E-04	2.613	0.063	2.620	0.106	0.402
60	232.880	0.624	4.102	1092.180	5.521E-04	239.09	0.626	4.203	1091.50	5.525E-04	2.597	0.172	2.410	0.062	0.068
70	273.903	0.629	4.104	1085.950	4.750E-04	281.05	0.630	4.190	1085.60	4.764E-04	2.543	0.218	2.045	0.032	0.293
80	314.974	0.632	4.111	1079.120	4.156E-04	322.88	0.634	4.177	1079.10	4.166E-04	2.450	0.217	1.592	0.002	0.245
90	356.121	0.635	4.119	1071.750	3.685E-04	364.60	0.636	4.166	1072.00	3.686E-04	2.325	0.184	1.127	0.023	0.037
100	397.353	0.636	4.127	1063.850	3.302E-04	406.21	0.637	4.157	1064.40	3.295E-04	2.180	0.131	0.714	0.052	0.217
110	438.665	0.636	4.135	1055.460	2.984E-04	447.75	0.637	4.151	1056.20	2.972E-04	2.028	0.065	0.386	0.070	0.427
120	480.051	0.636	4.142	1046.590	2.716E-04	489.24	0.636	4.149	1047.50	2.701E-04	1.879	0.007	0.159	0.087	0.545
130	521.511	0.634	4.150	1037.250	2.485E-04	530.74	0.633	4.151	1038.20	2.471E-04	1.739	0.075	0.015	0.092	0.553
140	563.060	0.631	4.160	1027.430	2.285E-04	572.27	0.630	4.157	1028.50	2.275E-04	1.609	0.140	0.069	0.104	0.454
150	604.728	0.627	4.174	1017.130	2.111E-04	613.90	0.626	4.169	1018.20	2.106E-04	1.494	0.195	0.129	0.105	0.276
160	646.561	0.622	4.194	1006.330	1.959E-04	655.67	0.621	4.186	1007.50	1.958E-04	1.389	0.239	0.189	0.116	0.058
170	688.620	0.617	4.219	995.017	1.825E-04	697.63	0.615	4.208	996.13	1.828E-04	1.292	0.270	0.273	0.112	0.173
180	730.970	0.610	4.252	983.159	1.707E-04	739.84	0.608	4.236	984.23	1.714E-04	1.199	0.290	0.381	0.109	0.375
190	773.679	0.602	4.291	970.722	1.604E-04	782.36	0.601	4.270	971.74	1.612E-04	1.110	0.295	0.503	0.105	0.513
200	816.814	0.594	4.337	957.658	1.512E-04	825.26	0.592	4.311	958.61	1.520E-04	1.023	0.292	0.612	0.099	0.564
210	860.436	0.585	4.388	943.910	1.430E-04	868.60	0.583	4.359	944.80	1.438E-04	0.940	0.280	0.674	0.094	0.524
Max % Diff.	**2.770**	**1.526**	**2.869**	**0.406**	**0.629**										

Table 17.23 Comparison of Liquid D_2O Properties at 30 bar between PLTEMP/ANL Version 4.2 and NIST Data

	PLTEMP	PLTEMP	PLTEMP	PLTEMP	PLTEMP	NIST	NIST	NIST	NIST	NIST	% Diff. H	% Diff. K	% Diff. Cp	% Diff. ρ	% Diff. μ
Temp C	H kJ/kg	K W/m-C	Cp kJ/kg-C	ρ kg/m3	μ Pa-s	H kJ/kg	K W/m-C	Cp kJ/kg-C	P kg/m3	μ Pa-s					
11	32.013	0.586	4.104	1111.990	1.624E-03	32.93	0.578	4.221	1107.60	1.621E-03	2.786	1.444	2.783	0.396	0.183
22	77.340	0.597	4.129	1109.680	1.184E-03	79.45	0.593	4.233	1106.60	1.181E-03	2.656	0.779	2.459	0.278	0.310
33	122.730	0.607	4.121	1106.020	9.120E-04	126.00	0.605	4.230	1103.90	9.083E-04	2.595	0.326	2.563	0.192	0.413
44	167.991	0.615	4.108	1101.250	7.313E-04	172.48	0.615	4.220	1099.80	7.268E-04	2.603	0.038	2.649	0.132	0.617
55	213.131	0.622	4.100	1095.550	5.998E-04	218.83	0.623	4.207	1094.70	5.989E-04	2.604	0.128	2.534	0.078	0.145
66	258.229	0.628	4.100	1089.020	5.036E-04	265.03	0.629	4.193	1088.60	5.049E-04	2.566	0.205	2.203	0.039	0.253
77	303.363	0.632	4.106	1081.750	4.322E-04	311.07	0.633	4.179	1081.60	4.335E-04	2.479	0.221	1.730	0.014	0.297
88	348.581	0.635	4.115	1073.790	3.774E-04	356.97	0.636	4.166	1074.00	3.778E-04	2.349	0.192	1.215	0.020	0.101
99	393.900	0.637	4.124	1065.210	3.341E-04	402.73	0.637	4.156	1065.70	3.335E-04	2.193	0.136	0.749	0.046	0.176
110	439.316	0.637	4.133	1056.030	2.988E-04	448.40	0.637	4.149	1056.70	2.975E-04	2.027	0.063	0.384	0.063	0.415
121	484.820	0.636	4.141	1046.270	2.694E-04	494.02	0.636	4.146	1047.10	2.680E-04	1.863	0.015	0.138	0.079	0.540
132	530.414	0.634	4.149	1035.940	2.446E-04	539.64	0.633	4.149	1036.90	2.433E-04	1.710	0.092	0.007	0.093	0.532
143	576.118	0.630	4.161	1025.030	2.234E-04	585.32	0.629	4.157	1026.10	2.225E-04	1.572	0.161	0.091	0.104	0.400
154	621.979	0.626	4.178	1013.550	2.051E-04	631.13	0.625	4.172	1014.60	2.047E-04	1.450	0.218	0.153	0.103	0.189
165	668.064	0.620	4.202	1001.460	1.893E-04	677.12	0.619	4.192	1002.50	1.894E-04	1.337	0.261	0.232	0.104	0.067
176	714.455	0.613	4.234	988.735	1.756E-04	723.39	0.612	4.220	989.79	1.761E-04	1.235	0.288	0.339	0.107	0.307
187	761.244	0.606	4.274	975.336	1.636E-04	769.99	0.604	4.254	976.34	1.645E-04	1.136	0.301	0.468	0.103	0.487
198	808.516	0.597	4.322	961.206	1.532E-04	817.01	0.595	4.297	962.14	1.541E-04	1.040	0.301	0.593	0.097	0.576
209	856.353	0.587	4.377	946.275	1.441E-04	864.54	0.585	4.348	947.13	1.449E-04	0.947	0.288	0.670	0.090	0.545
220	904.831	0.576	4.439	930.449	1.361E-04	912.70	0.574	4.409	931.25	1.366E-04	0.862	0.269	0.666	0.086	0.391
231	954.034	0.564	4.509	913.610	1.289E-04	961.60	0.563	4.484	914.37	1.291E-04	0.787	0.241	0.555	0.083	0.133
Max % Diff.	**2.786**	**1.444**	**2.783**	**0.396**	**0.617**										

Table 17.24 Comparison of Liquid D_2O Properties at 40 bar between PLTEMP/ANL Version 4.2 and NIST Data

	PLTEMP	PLTEMP	PLTEMP	PLTEMP	PLTEMP	NIST	NIST	NIST	NIST	NIST	% Diff. H	% Diff. K	% Diff. Cp	% Diff. ρ	% Diff. μ
Temp C	H kJ/kg	K W/m-C	Cp kJ/kg-C	ρ kg/m3	μ Pa-s	H kJ/kg	K W/m-C	Cp kJ/kg-C	P kg/m3	μ Pa-s					
12	36.983	0.588	4.105	1112.370	1.575E-03	38.05	0.580	4.219	1108.10	1.569E-03	2.805	1.366	2.703	0.385	0.367
24	86.427	0.600	4.126	1109.610	1.124E-03	88.77	0.596	4.230	1106.70	1.121E-03	2.640	0.676	2.450	0.263	0.285
36	135.889	0.610	4.115	1105.310	8.565E-04	139.51	0.609	4.225	1103.40	8.518E-04	2.596	0.231	2.591	0.173	0.547
48	185.191	0.619	4.102	1099.780	6.789E-04	190.14	0.619	4.213	1098.60	6.756E-04	2.603	0.037	2.630	0.107	0.487
60	234.381	0.625	4.098	1093.180	5.526E-04	240.61	0.627	4.199	1092.50	5.531E-04	2.589	0.174	2.405	0.062	0.088
72	283.566	0.631	4.101	1085.650	4.624E-04	290.90	0.632	4.183	1085.40	4.640E-04	2.521	0.220	1.955	0.023	0.331
84	332.830	0.635	4.110	1077.280	3.961E-04	341.01	0.636	4.168	1077.40	3.969E-04	2.398	0.205	1.400	0.011	0.204
96	382.210	0.637	4.120	1068.150	3.453E-04	390.95	0.638	4.156	1068.50	3.450E-04	2.235	0.151	0.865	0.033	0.088
108	431.707	0.638	4.129	1058.300	3.050E-04	440.77	0.638	4.148	1058.90	3.039E-04	2.055	0.074	0.441	0.057	0.366
120	481.309	0.637	4.138	1047.760	2.722E-04	490.51	0.637	4.144	1048.60	2.708E-04	1.876	0.011	0.154	0.080	0.524
132	531.015	0.634	4.147	1036.550	2.449E-04	540.25	0.634	4.147	1037.50	2.437E-04	1.709	0.095	0.011	0.092	0.526
144	580.851	0.631	4.160	1024.660	2.219E-04	590.05	0.630	4.156	1025.70	2.211E-04	1.559	0.170	0.100	0.101	0.379
156	630.875	0.626	4.179	1012.080	2.024E-04	640.01	0.624	4.172	1013.10	2.021E-04	1.427	0.231	0.170	0.101	0.138
168	681.178	0.619	4.207	998.781	1.857E-04	690.21	0.617	4.196	999.83	1.860E-04	1.309	0.275	0.261	0.105	0.140
180	731.870	0.611	4.244	984.723	1.714E-04	740.74	0.610	4.227	985.73	1.720E-04	1.197	0.301	0.386	0.102	0.388
192	783.065	0.602	4.290	969.848	1.590E-04	791.70	0.601	4.268	970.78	1.599E-04	1.091	0.308	0.528	0.096	0.549
204	834.871	0.592	4.345	954.080	1.484E-04	843.20	0.590	4.318	954.94	1.493E-04	0.988	0.303	0.643	0.090	0.583
216	887.385	0.581	4.408	937.317	1.392E-04	895.37	0.579	4.379	938.10	1.398E-04	0.892	0.285	0.676	0.083	0.474
228	940.707	0.568	4.480	919.424	1.311E-04	948.35	0.567	4.454	920.15	1.314E-04	0.806	0.258	0.591	0.079	0.229
240	994.961	0.555	4.565	900.218	1.239E-04	1002.33	0.553	4.547	900.93	1.237E-04	0.735	0.223	0.390	0.079	0.122
250.1	1041.480	0.542	4.652	882.857	1.182E-04	1048.59	0.541	4.644	883.64	1.177E-04	0.678	0.177	0.176	0.089	0.430
Max % Diff.	**2.805**	**1.366**	**2.703**	**0.385**	**0.583**										

Table 17.25 Comparison of Liquid D_2O Properties at 50 bar between PLTEMP/ANL Version 4.2 and NIST Data

	PLTEMP	PLTEMP	PLTEMP	PLTEMP	PLTEMP	NIST	NIST	NIST	NIST	NIST	% Diff. H	% Diff. K	% Diff. Cp	% Diff. ρ	% Diff. μ
Temp C	H kJ/kg	K W/m-C	Cp kJ/kg-C	ρ kg/m3	μ Pa-s	H kJ/kg	K W/m-C	Cp kJ/kg-C	P kg/m3	μ Pa-s					
13	41.950	0.589	4.106	1112.731	1.527E-03	43.160	0.582	4.217	1108.700	1.520E-03	2.804	1.298	2.630	0.364	0.507
26	95.502	0.602	4.123	1109.490	1.070E-03	98.080	0.599	4.227	1106.800	1.067E-03	2.628	0.578	2.451	0.243	0.291
39	149.023	0.613	4.110	1104.531	8.063E-04	152.990	0.612	4.220	1102.800	8.012E-04	2.593	0.147	2.611	0.157	0.637
52	202.361	0.622	4.098	1098.183	6.321E-04	207.760	0.622	4.206	1097.100	6.303E-04	2.599	0.101	2.580	0.099	0.287
65	255.610	0.628	4.096	1090.650	5.117E-04	262.340	0.630	4.190	1090.100	5.130E-04	2.565	0.202	2.236	0.050	0.257
78	308.900	0.633	4.103	1082.078	4.272E-04	316.699	0.635	4.173	1082.000	4.286E-04	2.463	0.221	1.680	0.007	0.317
91	362.310	0.637	4.114	1072.573	3.653E-04	370.855	0.638	4.159	1072.800	3.655E-04	2.304	0.177	1.077	0.021	0.055
104	415.860	0.638	4.124	1062.211	3.178E-04	424.842	0.639	4.148	1062.700	3.170E-04	2.114	0.099	0.564	0.046	0.268
117	469.536	0.638	4.133	1051.035	2.802E-04	478.719	0.638	4.142	1051.800	2.788E-04	1.918	0.009	0.210	0.073	0.491
130	523.330	0.636	4.143	1039.069	2.495E-04	532.570	0.635	4.143	1040.000	2.482E-04	1.735	0.087	0.007	0.090	0.528
143	577.266	0.632	4.156	1026.315	2.241E-04	586.470	0.631	4.152	1027.300	2.232E-04	1.569	0.173	0.096	0.096	0.390
156	631.412	0.626	4.176	1012.758	2.027E-04	640.550	0.625	4.169	1013.800	2.025E-04	1.427	0.234	0.173	0.103	0.133
169	685.881	0.619	4.206	998.366	1.847E-04	694.900	0.617	4.194	999.390	1.850E-04	1.298	0.285	0.272	0.102	0.168
182	740.810	0.611	4.247	983.086	1.695E-04	749.640	0.609	4.229	984.050	1.702E-04	1.178	0.315	0.411	0.098	0.429
195	796.342	0.601	4.298	966.845	1.565E-04	804.900	0.599	4.274	967.730	1.575E-04	1.063	0.317	0.564	0.091	0.578
208	852.609	0.589	4.360	949.543	1.455E-04	860.820	0.588	4.331	950.340	1.463E-04	0.954	0.300	0.667	0.084	0.574
221	909.730	0.577	4.430	931.044	1.360E-04	917.560	0.575	4.401	931.760	1.365E-04	0.853	0.280	0.657	0.077	0.403
234	967.831	0.563	4.511	911.163	1.277E-04	975.320	0.561	4.489	911.840	1.278E-04	0.768	0.246	0.501	0.074	0.094
247	1027.097	0.547	4.611	889.643	1.202E-04	1034.370	0.546	4.600	890.320	1.199E-04	0.703	0.205	0.233	0.076	0.309
260	1087.856	0.530	4.744	866.115	1.134E-04	1095.070	0.529	4.746	866.860	1.126E-04	0.659	0.134	0.032	0.086	0.693
263.542	1104.737	0.525	4.789	859.290	1.115E-04	1111.800	0.524	4.793	860.130	1.107E-04	0.635	0.111	0.069	0.098	0.750
Max % Diff.	**2.804**	**1.298**	**2.630**	**0.364**	**0.750**										

Table 17.26 Comparison of Liquid D_2O Properties at 75 bar between PLTEMP/ANL Version 4.2 and NIST Data

	PLTEMP	PLTEMP	PLTEMP	PLTEMP	PLTEMP	NIST	NIST	NIST	NIST	NIST	% Diff. H	% Diff. K	% Diff. Cp	% Diff. ρ	% Diff. μ
Temp C	H kJ/kg	K W/m-C	Cp kJ/kg-C	ρ kg/m3	μ Pa-s	H kJ/kg	K W/m-C	Cp kJ/kg-C	P kg/m3	μ Pa-s					
14	48.196	0.592	4.102	1113.848	1.482E-03	49.600	0.585	4.210	1109.900	1.471E-03	2.831	1.204	2.547	0.356	0.693
28	105.791	0.605	4.116	1110.071	1.020E-03	108.630	0.602	4.219	1107.600	1.017E-03	2.613	0.497	2.446	0.223	0.354
42	163.313	0.616	4.101	1104.405	7.607E-04	167.650	0.616	4.211	1102.900	7.557E-04	2.587	0.068	2.615	0.136	0.658
56	220.642	0.625	4.091	1097.215	5.908E-04	226.500	0.626	4.196	1096.300	5.905E-04	2.586	0.139	2.498	0.083	0.059
70	277.922	0.632	4.093	1088.724	4.765E-04	285.120	0.633	4.178	1088.300	4.783E-04	2.525	0.215	2.034	0.039	0.370
84	335.293	0.636	4.103	1079.094	3.971E-04	343.498	0.638	4.161	1079.100	3.982E-04	2.389	0.199	1.396	0.001	0.259
98	392.820	0.639	4.115	1068.438	3.391E-04	401.651	0.640	4.147	1068.800	3.387E-04	2.199	0.131	0.781	0.034	0.092
112	450.499	0.639	4.125	1056.830	2.945E-04	459.640	0.640	4.138	1057.400	2.934E-04	1.989	0.044	0.321	0.054	0.392
126	508.309	0.638	4.134	1044.310	2.591E-04	517.550	0.637	4.136	1045.100	2.578E-04	1.786	0.056	0.048	0.076	0.516
140	566.263	0.634	4.146	1030.892	2.303E-04	575.490	0.633	4.142	1031.800	2.294E-04	1.603	0.161	0.087	0.088	0.414
154	624.428	0.629	4.165	1016.564	2.066E-04	633.580	0.627	4.158	1017.500	2.062E-04	1.444	0.233	0.168	0.092	0.160
168	682.930	0.621	4.195	1001.294	1.868E-04	691.960	0.620	4.183	1002.200	1.871E-04	1.305	0.286	0.270	0.090	0.166
182	741.934	0.612	4.237	985.024	1.702E-04	750.760	0.610	4.219	985.910	1.710E-04	1.176	0.318	0.417	0.090	0.444
196	801.613	0.602	4.291	967.671	1.564E-04	810.140	0.600	4.266	968.470	1.573E-04	1.053	0.337	0.579	0.083	0.610
210	862.120	0.590	4.355	949.118	1.447E-04	870.270	0.588	4.326	949.820	1.455E-04	0.936	0.317	0.675	0.074	0.598
224	923.593	0.576	4.429	929.202	1.347E-04	931.330	0.574	4.401	929.820	1.352E-04	0.831	0.307	0.629	0.066	0.385
238	986.179	0.560	4.515	907.701	1.261E-04	993.590	0.559	4.496	908.270	1.261E-04	0.746	0.261	0.416	0.063	0.024
252	1050.116	0.544	4.624	884.296	1.183E-04	1057.350	0.542	4.619	884.880	1.179E-04	0.684	0.221	0.108	0.066	0.399
266	1115.855	0.525	4.777	858.521	1.111E-04	1123.110	0.524	4.783	859.180	1.103E-04	0.646	0.135	0.121	0.077	0.734
280	1184.239	0.504	5.010	829.652	1.040E-04	1191.570	0.504	5.011	830.480	1.031E-04	0.615	0.010	0.018	0.100	0.853
289.846	1234.691	0.488	5.252	806.868	9.894E-05	1241.770	0.488	5.232	807.950	9.820E-05	0.570	0.199	0.384	0.134	0.751
Max % Diff.	**2.831**	**1.204**	**2.615**	**0.356**	**0.853**										

Table 17.27 Comparison of Liquid D_2O Properties at 100 bar between PLTEMP/ANL Version 4.2 and NIST Data

	PLTEMP	PLTEMP	PLTEMP	PLTEMP	PLTEMP	NIST	NIST	NIST	NIST	NIST	% Diff. H	% Diff. K	% Diff. Cp	% Diff. ρ	% Diff. μ
Temp C	H kJ/kg	K W/m-C	Cp kJ/kg-C	ρ kg/m3	μ Pa-s	H kJ/kg	K W/m-C	Cp kJ/kg-C	P kg/m3	μ Pa-s					
15	54.426	0.594	4.098	1114.935	1.438E-03	56.010	0.587	4.202	1111.200	1.426E-03	2.828	1.134	2.468	0.336	0.828
30	116.050	0.608	4.108	1110.598	9.745E-04	119.150	0.606	4.211	1108.300	9.704E-04	2.602	0.401	2.443	0.207	0.428
45	177.559	0.620	4.093	1104.201	7.189E-04	182.260	0.619	4.202	1102.800	7.147E-04	2.579	0.002	2.603	0.127	0.593
60	238.880	0.628	4.086	1096.142	5.541E-04	245.180	0.630	4.186	1095.400	5.549E-04	2.570	0.183	2.387	0.068	0.151
75	300.199	0.635	4.092	1086.666	4.457E-04	307.820	0.636	4.167	1086.400	4.476E-04	2.476	0.222	1.809	0.024	0.413
90	361.660	0.639	4.104	1075.948	3.710E-04	370.196	0.640	4.150	1076.100	3.715E-04	2.306	0.173	1.113	0.014	0.156
105	423.301	0.641	4.115	1064.108	3.162E-04	432.336	0.641	4.137	1064.500	3.155E-04	2.090	0.081	0.522	0.037	0.228
120	485.099	0.640	4.125	1051.215	2.742E-04	494.327	0.640	4.130	1051.900	2.729E-04	1.867	0.019	0.140	0.065	0.465
135	547.042	0.637	4.135	1037.302	2.408E-04	556.290	0.636	4.133	1038.100	2.397E-04	1.662	0.130	0.056	0.077	0.455
150	609.180	0.632	4.152	1022.368	2.137E-04	618.360	0.631	4.145	1023.200	2.132E-04	1.485	0.225	0.152	0.081	0.230
165	671.646	0.625	4.179	1006.387	1.915E-04	680.700	0.623	4.169	1007.300	1.917E-04	1.330	0.283	0.252	0.091	0.104
180	734.625	0.616	4.220	989.300	1.732E-04	743.480	0.614	4.204	990.120	1.739E-04	1.191	0.324	0.400	0.083	0.431
195	798.324	0.604	4.275	971.017	1.580E-04	806.870	0.602	4.251	971.750	1.590E-04	1.059	0.339	0.572	0.075	0.623
210	862.928	0.592	4.341	951.410	1.454E-04	871.070	0.590	4.312	952.030	1.463E-04	0.935	0.329	0.675	0.065	0.629
225	928.590	0.577	4.416	930.299	1.348E-04	936.300	0.575	4.389	930.820	1.353E-04	0.823	0.310	0.617	0.056	0.414
240	995.474	0.561	4.505	907.429	1.256E-04	1002.840	0.559	4.488	907.900	1.257E-04	0.735	0.283	0.368	0.052	0.024
255	1063.860	0.543	4.619	882.434	1.175E-04	1071.100	0.541	4.618	882.910	1.170E-04	0.676	0.244	0.028	0.054	0.419
270	1134.311	0.522	4.786	854.767	1.099E-04	1141.610	0.522	4.794	855.330	1.091E-04	0.639	0.153	0.161	0.066	0.724
285	1207.909	0.500	5.048	823.556	1.024E-04	1215.260	0.500	5.042	824.300	1.017E-04	0.605	0.010	0.117	0.090	0.738
300	1286.584	0.474	5.479	787.289	9.477E-05	1293.530	0.476	5.424	788.320	9.430E-05	0.537	0.368	1.014	0.131	0.497
310.074	1343.901	0.453	5.931	758.683	8.942E-05	1349.870	0.458	5.824	760.040	8.917E-05	0.442	0.953	1.837	0.179	0.276
Max % Diff.	**2.828**	**1.134**	**2.603**	**0.336**	**0.828**										

Table 17.28 Comparison of Liquid D_2O Properties at 125 bar between PLTEMP/ANL Version 4.2 and NIST Data

	PLTEMP	PLTEMP	PLTEMP	PLTEMP	PLTEMP	NIST	NIST	NIST	NIST	NIST	% Diff. H	% Diff. K	% Diff. Cp	% Diff. ρ	% Diff. μ
Temp C	H kJ/kg	K W/m-C	Cp kJ/kg-C	ρ kg/m3	μ Pa-s	H kJ/kg	K W/m-C	Cp kJ/kg-C	P kg/m3	μ Pa-s					
16	60.638	0.596	4.094	1115.993	1.396E-03	62.400	0.590	4.195	1112.400	1.383E-03	2.824	1.057	2.396	0.323	0.926
32	126.280	0.611	4.101	1111.073	9.326E-04	129.630	0.609	4.204	1108.900	9.279E-04	2.584	0.323	2.450	0.196	0.514
48	191.765	0.623	4.085	1103.922	6.806E-04	196.830	0.623	4.194	1102.700	6.775E-04	2.573	0.053	2.585	0.111	0.461
64	257.079	0.632	4.082	1094.970	5.214E-04	263.790	0.633	4.176	1094.300	5.231E-04	2.544	0.204	2.253	0.061	0.325
80	322.447	0.638	4.091	1084.484	4.186E-04	330.443	0.639	4.156	1084.300	4.203E-04	2.420	0.208	1.576	0.017	0.402
96	388.001	0.641	4.104	1072.653	3.479E-04	396.797	0.642	4.139	1072.800	3.480E-04	2.217	0.145	0.850	0.014	0.032
112	453.749	0.642	4.115	1059.596	2.961E-04	462.917	0.642	4.127	1060.100	2.951E-04	1.980	0.031	0.310	0.048	0.339
128	519.657	0.640	4.124	1045.378	2.563E-04	528.920	0.640	4.125	1046.000	2.551E-04	1.751	0.080	0.010	0.059	0.470
144	585.740	0.636	4.138	1030.021	2.247E-04	594.960	0.635	4.132	1030.800	2.239E-04	1.550	0.202	0.126	0.076	0.322
160	652.112	0.629	4.161	1013.508	1.992E-04	661.210	0.627	4.152	1014.300	1.992E-04	1.376	0.271	0.222	0.078	0.000
176	718.975	0.620	4.199	995.788	1.785E-04	727.890	0.618	4.184	996.560	1.791E-04	1.225	0.324	0.363	0.077	0.368
192	786.568	0.609	4.252	976.771	1.615E-04	795.170	0.606	4.229	977.450	1.626E-04	1.082	0.355	0.544	0.069	0.621
208	855.115	0.595	4.318	956.325	1.476E-04	863.300	0.593	4.289	956.880	1.486E-04	0.948	0.349	0.671	0.058	0.673
224	924.793	0.580	4.394	934.259	1.361E-04	932.520	0.578	4.366	934.710	1.368E-04	0.829	0.329	0.625	0.048	0.475
240	995.775	0.563	4.482	910.299	1.264E-04	1003.140	0.561	4.466	910.680	1.265E-04	0.734	0.299	0.361	0.042	0.079
256	1068.359	0.544	4.597	884.051	1.178E-04	1075.600	0.543	4.598	884.430	1.173E-04	0.673	0.267	0.009	0.043	0.375
272	1143.179	0.523	4.768	854.912	1.098E-04	1150.510	0.522	4.777	855.370	1.090E-04	0.637	0.180	0.178	0.054	0.660
288	1221.499	0.499	5.045	821.922	1.019E-04	1228.860	0.499	5.034	822.550	1.012E-04	0.599	0.038	0.223	0.076	0.622
304	1305.580	0.471	5.505	783.382	9.388E-05	1312.330	0.473	5.433	784.300	9.356E-05	0.514	0.357	1.323	0.117	0.338
320	1399.427	0.437	6.309	735.761	8.547E-05	1404.380	0.444	6.158	737.060	8.540E-05	0.353	1.579	2.452	0.176	0.083
326.689	1443.361	0.419	6.863	711.246	8.158E-05	1447.100	0.431	6.693	712.810	8.156E-05	0.258	2.699	2.541	0.219	0.023
Max % Diff.	**2.824**	**2.699**	**2.585**	**0.323**	**0.926**										

Table 17.29 Comparison of Liquid D_2O Properties at 150 bar between PLTEMP/ANL Version 4.2 and NIST Data

	PLTEMP	PLTEMP	PLTEMP	PLTEMP	PLTEMP	NIST	NIST	NIST	NIST	NIST	% Diff. H	% Diff. K	% Diff. Cp	% Diff. ρ	% Diff. μ
Temp C	H kJ/kg	K W/m-C	Cp kJ/kg-C	ρ kg/m3	μ Pa-s	H kJ/kg	K W/m-C	Cp kJ/kg-C	P kg/m3	μ Pa-s					
17	66.835	0.599	4.090	1117.024	1.356E-03	68.770	0.593	4.188	1113.600	1.342E-03	2.814	0.987	2.333	0.307	0.983
34	136.481	0.614	4.094	1111.500	8.940E-04	140.080	0.612	4.197	1109.500	8.887E-04	2.569	0.263	2.459	0.180	0.595
51	205.933	0.626	4.079	1103.574	6.455E-04	211.350	0.626	4.185	1102.400	6.437E-04	2.563	0.096	2.549	0.106	0.281
68	275.244	0.635	4.079	1093.707	4.923E-04	282.340	0.636	4.166	1093.200	4.945E-04	2.513	0.219	2.100	0.046	0.447
85	344.668	0.640	4.090	1082.189	3.946E-04	352.985	0.642	4.146	1082.100	3.960E-04	2.356	0.193	1.339	0.008	0.346
102	414.314	0.643	4.103	1069.218	3.275E-04	423.307	0.644	4.129	1069.500	3.272E-04	2.124	0.103	0.618	0.026	0.095
119	484.159	0.643	4.113	1054.913	2.783E-04	493.403	0.643	4.119	1055.400	2.771E-04	1.874	0.033	0.146	0.046	0.408
136	554.172	0.640	4.124	1039.331	2.404E-04	563.430	0.639	4.121	1040.000	2.394E-04	1.643	0.152	0.080	0.064	0.409
153	624.420	0.634	4.142	1022.478	2.104E-04	633.580	0.632	4.135	1023.200	2.101E-04	1.446	0.248	0.184	0.071	0.143
170	695.096	0.625	4.175	1004.317	1.865E-04	704.090	0.623	4.162	1005.000	1.870E-04	1.277	0.319	0.310	0.068	0.246
187	766.469	0.614	4.224	984.768	1.672E-04	775.180	0.612	4.204	985.410	1.682E-04	1.124	0.366	0.492	0.065	0.583
204	838.809	0.601	4.288	963.700	1.516E-04	847.100	0.599	4.261	964.220	1.527E-04	0.979	0.364	0.653	0.054	0.708
221	912.331	0.585	4.363	940.923	1.388E-04	920.130	0.583	4.335	941.310	1.396E-04	0.848	0.352	0.648	0.041	0.573
238	987.213	0.568	4.449	916.158	1.282E-04	994.610	0.566	4.432	916.460	1.285E-04	0.744	0.325	0.397	0.033	0.195
255	1063.741	0.548	4.560	889.001	1.190E-04	1070.990	0.546	4.560	889.280	1.187E-04	0.677	0.289	0.002	0.031	0.278
272	1142.562	0.526	4.726	858.833	1.105E-04	1149.910	0.525	4.735	859.170	1.099E-04	0.639	0.229	0.199	0.039	0.582
289	1225.034	0.501	5.000	824.662	1.023E-04	1232.420	0.501	4.988	825.160	1.018E-04	0.599	0.082	0.251	0.060	0.531
306	1313.608	0.473	5.460	784.745	9.402E-05	1320.270	0.474	5.379	785.510	9.380E-05	0.505	0.264	1.489	0.097	0.226
323	1412.445	0.437	6.243	735.511	8.543E-05	1417.000	0.444	6.085	736.650	8.542E-05	0.321	1.472	2.605	0.155	0.011
340	1530.944	0.389	8.061	666.295	7.505E-05	1533.000	0.408	7.965	667.850	7.506E-05	0.134	4.674	1.207	0.233	0.017
340.852	1537.887	0.387	8.250	661.704	7.439E-05	1539.900	0.406	8.161	663.290	7.441E-05	0.131	4.839	1.086	0.239	0.024
Max % Diff.	**2.814**	**4.839**	**2.605**	**0.307**	**0.983**										

Table 17.30 Comparison of Thermal Properties of D_2O over 1 to 150 bar Pressure and 5 to 341 ºC Temperature between PLTEMP/ANL Version 4.2 and NIST Data

Phase & Pressure	% Diff. H	% Diff. K	% Diff. Cp	% Diff. ρ	% Diff. μ
Liquid, 1 bar	2.710	1.941	3.411	0.476	1.793
Liquid, 2 bar	2.728	1.854	3.285	0.468	1.353
Liquid, 3 bar	2.730	1.853	3.283	0.463	1.346
Liquid, 4 bar	2.726	1.779	3.167	0.454	0.969
Liquid, 5 bar	2.728	1.770	3.167	0.449	0.957
Liquid, 10 bar	2.688	1.608	2.965	0.422	0.592
Liquid, 20 bar	2.770	1.526	2.869	0.406	0.629
Liquid, 30 bar	2.786	1.444	2.783	0.396	0.617
Liquid, 40 bar	2.805	1.366	2.703	0.385	0.583
Liquid, 50 bar	2.804	1.298	2.630	0.364	0.750
Liquid, 75 bar	2.831	1.204	2.615	0.356	0.853
Liquid, 100 bar	2.828	1.134	2.603	0.336	0.828
Liquid, 125 bar	2.824	2.699	2.585	0.323	0.926
Liquid, 150 bar	2.814	4.839	2.605	0.307	0.983
Max. % Diff., All Pressures	2.831	4.839	3.411	0.476	1.793

18 Implementation and Verification of Carnavos Correlations for Heat Transfer Coefficient and Friction Factor in Channels Having Longitudinal Fins in the Radial Geometry Option of PLTEMP/ANL Code

18.1 Introduction and Summary

The verification work reported here was done in July 2016. The Carnavos correlations [1] for calculating heat transfer coefficient and friction factor in coolant channels of rectangular cross section with longitudinal fins were implemented and verified in 2007 in the sab geometry option (IGOM = 0) of the PLTEMP/ANL Code. This is documented in Appendix IX of the code user's guide [2]. The same correlations were implemented in finned channels of annular cross section in a multi-tube fuel assembly, in the radial geometry option (IGOM = 1) of the PLTEMP/ANL version 4.2_r80_160720 code dated July 20, 2016, and are available in all later versions of the code including PLTEMP/ANL V4.3. The purpose of this chapter is to document this implementation and its verification using test problems for a six-tube fuel assembly.

Section 18.2 describes the derivation of the equations for the geometrical parameters of fins in the radial geometry, and Section 18.3 describes the verification of the implementation of these equations in the code.

All geometrical parameters related to fins in the radial geometry option, calculated by the code for a test problem (input data file of Fig. 18.3) were compared with the values calculated on a Microsoft spreadsheet developed for this purpose. The two calculations agree to six significant digits. This agreement verifies that the equations for calculating the geometrical parameters are implemented correctly.

The coolant and cladding temperatures calculated by the code were compared for two models of the same problem, one with the fuel tube radii entered in the input data file in the increasing order and the other with the radii entered in the decreasing order. The two calculations agree to all digits printed by the code. This provides a verification that the Carnavos correlation for heat transfer coefficient in finned channels in the radial geometry option of the code is correctly implemented.

The coolant and cladding temperatures for a test problem having no fins were calculated by the code in two ways: first using the Carnavos correlation with fins of zero size, and the other using the Dittus-Boelter correlation without fins. The agreement between these two calculations provides a verification that the Carnavos correlation for heat transfer coefficient in finned channels in the radial geometry option of the code is correctly implemented.

The hand-calculated heat transfer coefficient of 97.651 kW/m^2-ºC at the exit of coolant channel 1 of a test problem (input data file shown in Fig. 18.3) agrees with the code-calculated value of 97.878 kW/m^2-ºC (shown in Table 18.3). The hand-calculated heat transfer coefficient of 1072.2 kW/m^2-ºC at the exit of coolant channel 2 of the same test problem agrees with the code-calculated value of 1070.4 kW/m^2-ºC (shown in Table 18.3). This agreement provides a verification that the Carnavos correlation for heat transfer coefficient in finned channels in the radial geometry option of the code is correctly implemented.

18.2 Carnavos Correlation and its Implementation

The subroutine CARNAVOS in the code (versions 3.3 and later) has the capability to calculate the results of Eqs. (18.28) and (18.31) for Carnavos correlations and related geometrical parameters, only for the slab geometry option (input option IGOM = 0). The radial geometry legs of these equations have been developed and implemented recently. The subroutine CARNAVOS can now calculate the same results also for the radial geometry option (input option IGOM = 1). This section develops equations for calculating the 24 needed geometrical parameters used in Section 18.3.2. The equations are implemented in such a manner that all the channel-dependent geometry parameters ($D_{i,k}$, $D_{o,k}$, $D_{ci,k}$, $D_{co,k}$, etc.) are calculated and printed only once (during the first call to subroutine CARNAVOS) and stored in a COMMON/FINGOM2/ for use in all later calculations. The following describes the Carnavos correlations Nu number and friction factor, and related geometrical parameters, for both geometry options (IGOM = 0 or 1).

Based on his experimental data for 14 tubes with and without fins, Carnavos obtained the following correlations for heat transfer coefficient and Darcy-Weisbach friction factor, each representing the data to within ±10%. The heat transfer coefficient correlation is basically the Dittus-Boelter correlation multiplied by a factor F_{nu} that is a function of the fin geometry. The friction factor correlation is basically the McAdams correlation multiplied by a factor F^* that is a function of the fin geometry. Equations (18.1) and (18.2) give these correlations, assuming the fins to be of a trapezoidal cross section as shown in Fig. 18.1. This figure has fuel tube radii in the increasing order. The equations given below are based on Figs. 18.1 and 18.2.

$$Nu = 0.023\, Re_a^{\,0.8}\, Pr^{0.4} \left(\frac{A_{fa}}{A_{fc}}\right)^{0.1} \left(\frac{P_n}{P_a}\right)^{0.5} \sec^3\alpha \tag{18.1}$$

$$f_a = \frac{0.184}{Re_a^{\,0.2}} \left(\frac{A_{fn}}{A_{fa}}\right)^{0.5} (\cos\alpha)^{0.75} \tag{18.2}$$

where the subscript a = actual, n = nominal (see nomenclature at the end). Note that P_n and P_a are heated (*finned*) nominal and actual perimeters of the channel whereas the Reynolds number Re_a is calculated using the actual *wetted* perimeter P_{a_wt}. Note that the correlations were developed for channels having fins on the whole wetted perimeter ($P_n = P_{n_wt}$), and their application to a channel with fins on only a part of the wetted perimeter ($P_n < P_{n_wt}$) is an extension.

$$F_{nu} = \left(\frac{A_{fa}}{A_{fc}}\right)^{0.1} \left(\frac{P_n}{P_a}\right)^{0.5} \sec^3\alpha \tag{18.1a}$$

$$F^* = \left(\frac{A_{fn}}{A_{fa}}\right)^{0.5} (\cos\alpha)^{0.75} \tag{18.2a}$$

Here, the actual and nominal heat transfer areas, the actual and nominal coolant flow areas, and the actual and nominal hydraulic diameters of coolant channel k are given by the following equations based on the trapezoidal cross section of the fins. The equations for a rectangular channel are a theoretical extension of the experimental data for tubes. It should be noted that, in the

implementation, the *nominal perimeters and flow areas input on Card type 0307 are used* in Eq. (18.3) and Eq. (18.5). See nomenclature at the end.

$P_{n,k}$ = Input PERF(i,k) where i = fuel type number (18.3)

$$P_{a,k} = P_{n,k} + n\,P_{fin}\sec\alpha \tag{18.4}$$

$A_{fn,k}$ = Input AFF(i,k) where i = fuel type number (18.5)

$$A_{fa,k} = A_{fn,k} - n\,A_{fin}\sec\alpha \tag{18.6}$$

The *core flow area* (*core* is here used in the sense of Carnavos[1]) in a coolant channel (e.g., channels 1 and 2) of a fuel assembly made of multiple fuel tubes having longitudinal fins is shown in Fig. 18.1. The core flow area in a coolant channel is calculated by subtracting the *finned area* (fin cross-section plus flow area in-between fins) on the two surrounding fuel tubes, from the input nominal flow area of the channel. In the slab geometry (input option IGOM = 0), *the finned area* is simply $2eW_{ch}$ as shown in Fig. IX-1(b) of the code users guide[2] (copied below Eq. (18.31a) of this V&V report) here on page 432). In the radial geometry (option IGOM = 1), as shown in Fig. 18.2, *the finned area* has two parts in all intermediate channels, i.e., $2 \le k \le$ NCHNF(i)-1 where the channel NCHNF(i) is the last or outermost channel. The innermost channel (k = 1) is assumed to have fins only on the inner surface of fuel tube 1, and therefore has only one *the finned area*. The outermost channel (k = NCHNF(i)) is assumed to have fins only on the outer surface of fuel tube NCHNF(i)-1, and therefore has only one *the finned area*. Equation (18.7) accounts for all these cases.

$$A_{fc,k} = A_{fn,k} - A_{fnon-core,k} \tag{18.7a}$$

$$A_{fnon-core,k} = \begin{cases} 2\,e\,W_{ch} & \text{if IGOM} = 0 \\ 0.25\pi\left(D_{i,k}^{\ 2} - D_{co,k}^{\ 2}\right)F_w & \text{if IGOM} = 1,\ k = 1 \\ 0.25\pi\left\{\left(D_{ci,k}^{\ 2} - D_{o,k-1}^{\ 2}\right) - \left(D_{i,k}^{\ 2} - D_{co,k}^{\ 2}\right)\right\}F_w & \text{if IGOM} = 1, \text{ and} \\ \qquad 2 \le k \le \text{NCHNF(i)} - 1 & \\ 0.25\pi\left(D_{ci,k}^{\ 2} - D_{o,k-1}^{\ 2}\right)F_w & \text{if IGOM} = 1,\ k = \text{NCHNF(i)} \end{cases} \tag{18.7b}$$

$$F_w = \begin{cases} \dfrac{\text{CIRCF(i,k)}}{2\pi * \text{RMID(i,k)}} & \text{if} \quad k = 1 \\ 0.5\left(\dfrac{\text{CIRCF(i,k-1)}}{2\pi * \text{RMID(i,k-1)}} + \dfrac{\text{CIRCF(i,k)}}{2\pi * \text{RMID(i,k)}}\right) & \text{if} \quad 2 \le k \le \text{NCHNF(i)} - 1 \\ \dfrac{\text{CIRCF(i,k-1)}}{2\pi * \text{RMID(i,k-1)}} & \text{if} \quad k = \text{NCHNF(i)} \end{cases} \tag{18.7c}$$

where

$A_{fnon\text{-}core,k}$ = Flow area in channel k that is outside the core flow area of the channel.
$D_{i,k}$ = Inner diameter of fuel tube k
$D_{o,k}$ = Outer diameter of fuel tube k
$D_{ci,k}$ = Diameter of the inner boundary of the core flow area in channel k
$D_{co,k}$ = Diameter of the outer boundary of the core flow area in channel k
F_w = Fraction of circular arc spanned by channel k

Equations for $D_{i,k}$ and $D_{o,k}$: The inner and outer diameters of a fuel tube can be obtained from the input values of fuel meat centerline radius RMID(i,k), cladding thickness CLAD(i), and meat thickness TAEM(i) on the input cards 306 and 308A (in input option IEND = 0). The values of inner and outer cladding thicknesses CLAD1(i,k), CLAD2(i,k), and meat thickness TAEM0(i,k) on the input cards 306B are used in input option IEND = 1.

$$D_{i,k} = \begin{cases} 2\left[\mathrm{RMID}(i,k) - 0.5 * \mathrm{TAEM}(i) - \mathrm{CLAD}(i)\right] & \text{if option IEND} = 0 \\ 2\left[\mathrm{RMID}(i,k) - 0.5 * \mathrm{TAEM0}(i,k) - \mathrm{GAP1}(i,k) - \mathrm{CLAD1}(i,k)\right] & \text{if option IEND} = 1 \end{cases} \quad \ldots\ldots\ldots\ldots \tag{18.8}$$

$$D_{o,k} = \begin{cases} 2\left[\mathrm{RMID}(i,k) + 0.5 * \mathrm{TAEM}(i) + \mathrm{CLAD}(i)\right] & \text{if option IEND} = 0 \\ 2\left[\mathrm{RMID}(i,k) + 0.5 * \mathrm{TAEM0}(i,k) + \mathrm{GAP2}(i,k) - \mathrm{CLAD2}(i,k)\right] & \text{if option IEND} = 1 \end{cases} \quad \ldots\ldots\ldots\ldots \tag{18.9}$$

Equations for $D_{ci,k}$ and $D_{co,k}$: In Fig. 18.2, the coolant channels (and fuel tubes) are assumed to be numbered in the increasing order, starting from the innermost to the outermost. In the right-angled triangle OLG in Fig. 18.2, side GL = 0.5t, and side OL = ($0.5D_{o,k-1}$ + e), and the hypotenuse GO is the radius ($0.5D_{ci,k}$\ ) of the inner boundary of the core flow area in coolant channel k. The Pythagorean rule gives Eq. (18.10). Equation (18.10) can be rewritten as Eq. (18.10a).

$$0.5\,D_{ci,k} = \sqrt{(0.5\,t)^2 + (0.5\,D_{o,k-1} + e)^2} \tag{18.10}$$

$$D_{ci,k} = 2\sqrt{(0.5\,t)^2 + (0.5\,D_{o,k-1} + e)^2} = \sqrt{t^2 + (D_{o,k-1} + 2\,e)^2} \tag{18.10a}$$

In the right-angled triangle ONE in Fig. 18.2, side EN = 0.5b, and hypotenuse OE = $D_{i,k}/2$, and the side ON = PN + OP= e + $0.5D_{co,k}$ where $D_{co,k}$ is the radius of the outer boundary of the core flow area in coolant channel k. The Pythagorean rule gives Eq. (18.11) which is solved as Eq. (18.11a).

$$e + 0.5\,D_{co,k} = \sqrt{(0.5\,D_{i,k})^2 - (0.5\,b)^2} \tag{18.11}$$

$$D_{co,k} = 2\left(\sqrt{(0.5\,D_{i,k})^2 - (0.5\,b)^2} - e\right) = \sqrt{D_{i,k}{}^2 - b^2} - 2\,e \tag{18.11a}$$

Equation for P_{fin}: The quantity P_{fin} is the *additional* heated perimeter provided by a single fin. It is required in Eq. (18.4). It is noted in Fig. 18.2 that in channel k the *additional* heated perimeter provided by an internal fin (on the tube surface of radius $0.5D_{i,k}$) is slightly different from that

provided by an external fin (on the tube surface of radius $0.5D_{o,k-1}$). Each *additional* heated perimeter ($P_{fin,in}$ and $P_{fin,ex}$) is separately calculated below. The total additional heated perimeter nP_{fin}, required in Eq. (18.4), could then be calculated if the number of internal and external fins in the channel were separately user-specified. However, the number of internal and external fins in the channel are assumed to be equal in the current modeling, and this is tantamount to basically averaging $P_{fin,in}$ and $P_{fin,ex}$ which is written as Eq. (18.12). The values of $P_{fin,in}$ and $P_{fin,ex}$ are given by Eqs. (18.13) and (18.14) as follows.

$$P_{fin} = 0.5(P_{fin,in} + P_{fin,ex}) \tag{18.12}$$

$$\begin{aligned} P_{fin,in} &= \text{Sides EB} + \text{BC} + \text{CF} - \text{Arc length EMF (in Fig. IX} - 2\text{b)} \\ &= \begin{cases} t + 2\sqrt{e^2 + \{0.5(b-t)\}^2} - 0.5\beta_{i,k} D_{i,k} & \text{if IGOM} = 1 \\ t + 2\sqrt{e^2 + \{0.5(b-t)\}^2} - b & \text{if IGOM} = 0 \end{cases} \end{aligned} \tag{18.13}$$

$$\begin{aligned} P_{fin,ex} &= \text{Sides QI} + \text{IG} + \text{GH} + \text{HJ} + \text{JR} - \text{Arc length QSR (in Fig. IX} - 2\text{b)} \\ &= \begin{cases} t + 2\sqrt{e^2 + \{0.5(b-t)\}^2} + 2\delta_o - 0.5\beta_{o,k} D_{o,k-1} & \text{if IGOM} = 1 \\ t + 2\sqrt{e^2 + \{0.5(b-t)\}^2} - b & \text{if IGOM} = 0 \end{cases} \end{aligned} \tag{18.14}$$

<u>Equation for A_{fin}</u>: The cross-sectional of a single fin A_{fin} is required in Eq. (18.6). The cross-sectional area of an internal fin in channel k, i.e., area EBCFME in Fig. 18.2, is slightly different from the cross-sectional area of an external fin in the same channel, i.e., area QIGHJRSQ. Each cross-sectional area ($A_{fin,in}$ and $A_{fin,ex}$) is separately calculated below. The total cross-sectional area nA_{fin}, required in Eq. (18.6), could then be calculated if the number of internal and external fins (i.e., fins on the concave and convex sides of fuel tube, respectively) in the channel were separately user-specified. However, the number of internal and external fins in the channel are assumed to be equal in the current modeling, and this is tantamount to basically averaging $A_{fin,in}$ and $A_{fin,ex}$ which is written as Eq. (18.15). The value of $A_{fin,in}$ is calculated as follows by Eqs. (18.16) through (18.18).

$$A_{fin} = 0.5(A_{fin,in} + A_{fin,ex}) \tag{18.15}$$

$$\begin{aligned} A_{fin,in} &= \text{Area of trapezoid EBCF} + \text{Area of segment ENFME (in Fig. 18.2)} \\ &= \text{Area of trapezoid EBCF} + (\text{Area of sector OEMF} - \text{Area of triangle OENF}) \end{aligned} \tag{18.16}$$

where

$$\text{Area of trapezoid EBCF} = \frac{e(b+t)}{2} \tag{17a}$$

$$\text{Area of sector OEMF} = \frac{\beta_{i,k} D_{i,k}^{\ 2}}{8} \tag{17b}$$

Area of triangle OENF = 2(Area of right-angled triangle OEN) = $\dfrac{b\sqrt{D_{i,k}^{\ 2}-b^2}}{4}$ (17c)

$$A_{fin,in} = \begin{cases} \dfrac{e(b+t)}{2} + \dfrac{\beta_{i,k}\ D_{i,k}^{\ 2}}{8} - \dfrac{b\sqrt{D_{i,k}^{\ 2}-b^2}}{4} & \text{if IGOM} = 1 \\ \dfrac{e(b+t)}{2} & \text{if IGOM} = 0 \end{cases} \tag{18.18}$$

The value of $A_{fin,ex}$ is calculated as follows by Eqs. (18.19) through (18.21).

$A_{fin,ex}$ = Area of trapezoid IGHJ + Area of isosceles triangle ORQ
+ Area of rectangle RJIQ - Area of sector ORSQ (in Fig. 18.2) (18.19)

where

Area of trapezoid IGHJ = $\dfrac{e(b+t)}{2}$ (18.20a)

Area of sector ORSQ = $\dfrac{\beta_{o,k}\ D_{o,k-1}^{\ 2}}{8}$ (18.20b)

Area of isosceles triangle ORQ = $\dfrac{b\sqrt{D_{o,k-1}^{\ 2}-b^2}}{4}$ (18.20c)

Area of rectangle RJIQ = $b\delta_o$ (18.20d)

$$A_{fin,ex} = \begin{cases} \dfrac{e(b+t)}{2} - \dfrac{\beta_{o,k}\ D_{o,k-1}^{\ 2}}{8} + \dfrac{b\sqrt{D_{o,k-1}^{\ 2}-b^2}}{4} + b\delta_{o,k} & \text{if IGOM} = 1 \\ \dfrac{e(b+t)}{2} & \text{if IGOM} = 0 \end{cases} \tag{18.21}$$

<u>Equation for Parameters δ_i , δ_o , β_i , and β_o:</u>

$$\delta_{i,k} = \frac{D_{i,k} - \sqrt{D_{i,k}^{\ 2}-b^2}}{2} \tag{18.22a}$$

$$\delta_{o,k} = \frac{D_{o,k-1} - \sqrt{D_{o,k-1}^{\ 2}-b^2}}{2} \tag{18.22b}$$

$$\beta_{i,k} = 2\sin^{-1}(b/D_{i,k}) \tag{18.23a}$$

$$\beta_{o,k} = 2\tan^{-1}(b/D_{o,k-1}) \tag{18.23b}$$

The actual and nominal hydraulic diameters and Reynolds numbers are then calculated using Eqs. (18.24) and (18.25). The Prandtl number is calculated using Eq. (18.26).

$$D_{ha} = \frac{4 A_{fa}}{P_a}, \qquad D_{hn} = \frac{4 A_{fn}}{P_n} \tag{18.24}$$

$$Re_a = \frac{W\, D_{ha}}{A_{fa}\, \mu}, \quad Re_n = \frac{W\, D_{hn}}{A_{fn}\, \mu} \tag{18.25}$$

$$Pr = \frac{\mu\, C_p}{K} \tag{18.26}$$

Equation (18.1) results in Eq. (18.27) below for the finned tube heat transfer coefficient h_a that is based on the *actual* heat transfer area (P_a). For use in the PLTEMP/ANL code, one needs to express the coefficient h_a given by Eq. (18.27) as a heat transfer coefficient h_{a_n} based on the *nominal* heat transfer area P_n , preserving the heat transfer rate, as done by Eq. (18.28).

$$h_a = \frac{Nu\, K}{D_{ha}} \tag{18.27}$$

$$h_{a_n} = \frac{P_a\, h_a}{P_n} \tag{18.28}$$

Equation (18.2) gives the finned tube friction factor f_a that is based on the *actual* hydraulic diameter D_{ha}. For use in PLTEMP/ANL, one needs to express the friction factor f_a as a friction factor f_{a_n} based on the *nominal* hydraulic diameter (D_{hn}). To do this, one must equate the pressure drop due to friction. For a given flow rate W in the channel, the pressure drop due to the finned tube friction factor f_a over a length L of the channel can be written as Eq. (18.29). The first factor on the right hand side of Eq. (18.29) must be preserved because the second factor is the same whether the nominal or the actual hydraulic diameter is used. Equating the first factor on the right hand side of Eq. (18.29) results in Eq. (18.30), which is rewritten as Eq. (18.31) below.

$$\Delta p_a = \left(\frac{f_a}{A_{fa}^{\ 2}\, D_{ha}} \right) \left(\frac{L W^2}{2 \rho} \right) \tag{18.29}$$

$$\frac{f_{a_n}}{A_{fn}^{\ 2}\, D_{hn}} = \frac{f_a}{A_{fa}^{\ 2}\, D_{ha}} \tag{18.30}$$

$$f_{a_n} = \frac{A_{fn}^{\ 2}\, D_{hn}\, f_a}{A_{fa}^{\ 2}\, D_{ha}} \qquad \text{(Also see Eq. (18.31a) below, } \textit{an extension of the correlation}\text{)} \tag{18.31}$$

It is important to note here that Eq. (18.29) is based on experimental data on channels (tubes) having fins on the whole perimeter, with the friction factor f_a applicable on the whole perimeter. However sometimes, a part of the wetted perimeter in the first or last coolant channel of a fuel assembly is not finned (and not heated) as shown in Fig. IX-3 of [2] copied below. For example, in the first or last coolant channel of an MTR-type fuel assembsly made of flat fuel plates, the outermost end plates may be smooth and not finned while the fuel plates are finned. In such cases, the friction factor f_a should apply only on the finned perimeter of the channel (with a tacit assumption discussed below) while the friction factor f_{smooth} for smooth wall should apply to the unfinned perimeter. The friction factor f_{smooth} can be calculated using the McAdams correlation that forms the basis of the Carnavos correlation Eq. (18.2).

The tacit assumption is that *the friction factor f_a is not sensitive to the pitch of fins*. This assumption is made here because the Carnavos correlation is itself independent of fin pitch. With this assumption, it can be shown that the effective friction factor f_{a_avg} in a channel with partly finned perimeter is given by the perimeter-weighted average of f_a and f_{smooth}, as in Eq. (18.32). Equation (18.31) is then rewritten as Eq. (18.31a).

$$f_{a_avg} = \frac{P_{a_finned}\, f_a + (P_{a_wt} - P_{a_finned})\, f_{smooth}}{P_{a_wt}} \qquad \text{(finned = heated)} \qquad (18.32)$$

$$f_{a_n} = \frac{A_{fn}^{\ 2}\, D_{hn}\, f_{a_avg}}{A_{fa}^{\ 2}\, D_{ha}} \qquad (18.31a)$$

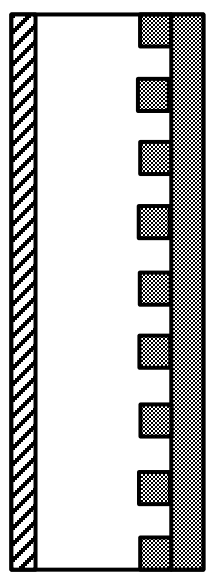

A Coolant Channel with Partly Finned and Partly Smooth Perimeter - Fig. IX-3 of [2]

Equation (32) for the effective friction factor f_{a_avg} in a channel with partly finned perimeter can be derived as follows. The shear stress τ applied on the channel wall by coolant flow in a channel is related to the Darcy-Weisbach friction factor, f, as $\tau = f\rho V^2/8$ where ρ is coolant density and V is coolant velocity. If the whole wetted perimeter of the channel is alike, the total force applied on

the wall by the coolant flow is given by τ L P_{wt} where L is channel length and P_{wt} is wetted perimeter of the channel. The coolant pressure drop ΔP is given by τ L P_{wt}/A_f where A_f is coolant flow area in the channel. The pressure drop ΔP can be rewritten as Eq. (18.33) below.

$$\Delta P = \frac{\tau L P_{wt}}{A_f} = \frac{f \rho V^2}{8} \frac{L P_{wt}}{A_f} = \frac{f L \rho V^2}{2 D_h} \quad \text{where} \quad D_h = \frac{4 A_f}{P_{wt}} \tag{18.33}$$

If the whole wetted perimeter of the channel is not alike, let us assume that a part P_{wt1} of the wetted perimeter has friction factor f_1, and the other part P_{wt2} of the perimeter has friction factor f_2. The shear stress τ_1 applied on the channel perimeter P_{wt1} is related to the Darcy-Weisbach friction factor f_1 as $\tau_1 = f_1 \rho V^2/8$, and the shear stress τ_2 applied on the channel perimeter P_{wt2} is related to the Darcy-Weisbach friction factor f_2 as $\tau_2 = f_2 \rho V^2/8$. Then the total force applied on the channel wall is the sum of the two shear forces (τ_1 L P_{wt1} + τ_2 L P_{wt2}). The coolant pressure drop ΔP is given by (τ_1 L P_{wt1} + τ_2 L P_{wt2})/A_f which can be rewritten as Eq. (18.34) below. Equation (18.35) shows that the effective friction factor f_{a_avg} equals the perimeter-weighted average of the two friction factors f_1 and f_2.

$$\Delta P = \frac{(\tau_1 L P_{wt1} + \tau_2 L P_{wt2})}{A_f} = \frac{\left(\frac{f_1 \rho V^2}{8} L P_{wt1} + \frac{f_2 \rho V^2}{8} L P_{wt2}\right)}{A_f} = \frac{f_{a_avg} L \rho V^2}{2 D_{ha}} \tag{18.34}$$

$$\text{where} \quad f_{a_avg} = \frac{f_1 P_{wt1} + f_2 P_{wt2}}{P_{wt1} + P_{wt2}} \quad \text{and} \quad D_{ha} = \frac{4 A_f}{(P_{wt1} + P_{wt2})} \tag{18.35}$$

18.3 Verification of Carnavos Correlation in Radial Geometry

18.3.1 Plan of Testing and Verification

The following four comparisons were done to verify the implementation of the Carnavos heat transfer coefficient in the radial geometry option of the PLTEMP/ANL version 4.2_r80_160720 code. These comparisons were done for a fuel assembly consisting of six coaxial fuel tubes with a specified flow rate in each of the seven coolant channels.

(1) All geometrical parameters calculated by the code for the above-mentioned six-tube fuel assembly (input data file of Fig. 18.3, filename *input.Stdproblem34.6tubes.RMIDincr.fins*) were compared with a spreadsheet calculation of these parameters. This comparison is described in Section 18.3.2. It verifies that the code correctly calculates (to 6 significant digits) the nominal and actual perimeters and flow areas and other geometrical parameters (altogether 24 parameters).

(2) Comparison of the code results for two models of the same problem, one with the fuel tube radii entered in the input data file in the increasing order and other with the radii entered in the decreasing order. The two input data files prepared to perform this comparison are listed in Figs. 18.3 and 18.4. The filenames are:

input.Stdproblem34.6tubes.RMIDincr.fins, and
input.Stdproblem34.6tubes.RMIDdecr.fins.
This comparison is described in Section 18.3.3. The coolant and cladding temperatures, and coolant-cladding heat transfer coefficients of all channels are in agreement to all digits printed by the code. It verifies that the Carnavos correlation for calculating heat transfer coefficients in finned channels in the radial geometry option are correctly implemented in the code.

(3) The code results for the implemented fin option using zero size fins (using the input option IH = -1, filename *input.Stdproblem34.6tubes.RMIDincr.e=b=t=0.fins*) were compared with the code results obtained using the Dittus-Boelter correlation without fins (using the input option IH = 1, filename *input.Stdproblem34.6tubes.RMIDdecr.no_fins*). The two input data files prepared to perform this comparison are listed in Figs. 18.5 and 18.6.
This comparison is described in Section 18.3.4. The maximum temperature difference is 0.001 ºC, and the maximum difference in the heat transfer coefficient is 0.001 kW/m^2-ºC. This provides another verification that the Carnavos correlation for calculating heat transfer coefficient in finned channels in the radial geometry option is correctly implemented in the code.

(4) The heat transfer coefficients (i) at the midpoint of the heat transfer node at channel 1 exit (ii) at the midpoint of the heat transfer node at channel 2 exit, calculated by the code using the input file of Fig. 18.3 (filename *input.Stdproblem34.6tubes.RMIDincr.fins*) are compared with hand-calculated values. This comparison is described in Section 18.3.5. There is a difference of 0.2 % between the code-calculated and hand-calculated values. This provides yet another verification that the Carnavos correlation for calculating heat transfer coefficient in finned channels in the radial geometry option is correctly implemented in the code.

The code input data file of the test problem used for verifying geometrical parameters (Standard Test Problem 34) is given in Fig. 18.3. The input data file shown in Fig. 18.4 also models the same problem with the modification that the fuel tubes are numbered starting from the *outermost* tube in Fig. 18.4 (decreasing tube radii) whereas they are numbered starting from the *innermost* tube in Fig. 18.3 (increasing tube radii). When this modification is done, the input data on the card types 307, 308, 308A, 309 and 310 must be entered in the reversed order.

Two more input data files (Figs. 18.5 and 18.6) were used in these comparisons. Fig. 18.5 is obtained by modifying the input data file of Test Problem 34 of Fig. 18.3, to set the fin size to zero while using the finned channels heat transfer correlation. Note in Fig. 18.5 that the input data on card type 202 (shown in red) are all set to zero except the number of fins. Fig. 18.6 is obtained by modifying the input data file of Test Problem 34 of Fig. 18.3 to have no fins (IH = 1) while using the Dittus-Boelter heat transfer correlation. Note in Fig. 18.6 that the input option IH for heat transfer correlation on card type 200 in changed and the card type 202 (shown in red) is not needed and hence commented out. The three comparisons are described below.

18.3.2 Verification of Geometrical Parameters for Test Problem 34

All geometrical parameters related to fins in the radial geometry option, calculated by the PLTEMP/ANL code for Test Problem 34 (input data file of Fig. 18.3), were compared with the values calculated on a Microsoft spreadsheet developed for this purpose. The spreadsheet was developed using the equations given in Section 18.2. The fin dimensions are entered on the card type 202 of Fig. 18.3. Table 18.1 shows a part of the spreadsheet, and Table 18.2 shows a part of the code output file that shows the values of 24 geometrical parameters defined in Section 18.2. These parameters are calculated by the code only once, and stored in a common block for later use. In Table 18.2, the algebraic symbols in red have been added above the FORTRAN variables at the top of data columns in order to identify the data and facilitate comparison with Table 18.1. The 24 geometrical parameters in Table 18.2 were compared with the values in Table 18.1. There is agreement to all six significant digits shown in the tables. This verifies that the equations for calculating all geometrical parameters are correctly implemented in the code.

18.3.3 Comparison of Code Results for Two Models of Test Problem 34

The coolant and cladding temperatures calculated by the PLTEMP/ANL version 4.2_r80_160720 code were compared for two models of the same problem (Standard Test Problem 34), one with the fuel tube radii entered in the input data file in the increasing order and the other with the radii entered in the decreasing order. The two input data files prepared to perform this comparison are listed in Figs. 18.3 and 18.4. Fig. 18.7 shows a part of the code output file (temperature tables for all fuel tubes) calculated using the input file with the tube radii in the increasing order, and Table 18.2 shows a part of the code output file calculated using the input file with the tube radii in the decreasing order.

Some of the results shown in Figs. 18.7 and 18.8 (coolant and cladding temperatures, and coolant-cladding heat transfer coefficients of all channels) are compared in Table 18.3. It is noted during the comparison that the results for the input file of Fig. 18.4 are in the reverse order of channel number, compared to that for the input file of Fig. 18.3, i.e., channel 1 results of the former should be compared with channel 7 results of the latter; channel 2 results of the former should be compared with channel 6 results of the latter, and so on. Table 18.3 shows that there is agreement to all digits printed by the code. This provides a verification that the Carnavos correlation for calculating heat transfer coefficients in finned channels in the radial geometry option are correctly implemented in the code. Additional verification of the same is described below in Sections 18.3.4 and 18.3.5.

18.3.4 Comparison of Code Results for Test Problem 34 Modified to Have No Fins

The coolant and cladding temperatures calculated by the PLTEMP/ANL version 4.2_r80_160720 code were compared for two models of the same problem, i.e., Test Problem 34 of Fig. 18.3 was modified to have no fins in two different ways: first using zero size fins (using the input option IH = -1 for the Carnavos correlation) by setting the fin dimensions to zero in Fig. 18.3, and the other using the Dittus-Boelter correlation without fins (instead of the Carnavos correlation) by removing the input card type 202 and setting the input option IH = 1 in Fig. 18.3. The two modified input data files used in this comparison are listed in Figs. 18.5 and 18.6. Fig. 18.9 shows a part of the code output file (temperature tables for all fuel tubes) calculated using the input file with the

Carnavos correlation with the fin size set to zero, and Fig. 18.10 shows a part of the code output file calculated using the input file with the Dittus-Boelter correlation without fins. Both input files (Figs. 18.5 and 18.6) have the fuel tube radii in the increasing order.

Some of the results shown in Figs. 18.9 and 18.10 (coolant and cladding temperatures, and coolant-cladding heat transfer coefficients of all channels) are compared in Table 18.4. Table 18.4 shows that there is a very good agreement between the two calculations. The maximum temperature difference is 0.001 ºC (e.g., 54.773 compared to 57.772 ºC), and the maximum difference in the heat transfer coefficient is 0.001 kW/m^2-ºC (22.251 compared to 22.251 kW/m^2-ºC). As expected for fins of zero size, the Carnavos heat transfer correlation gives the same results as the Dittus-Boelter correlation. This provides another verification that the Carnavos correlation for calculating heat transfer coefficient in finned channels in the radial geometry option is correctly implemented in the code.

18.3.5 Hand Calculation of Heat Transfer Coefficient for Test Problem 34 with Fins

The heat transfer coefficients for channels 1 and 2 (shown in Table 18.3) calculated by the code using the input file of Fig. 18.3 are obtained here by hand calculation for comparison with the code-calculated values.

<u>Heat Transfer Coefficient at Exit of Channel 1</u>:

The Nusselt number, Nu, at the midpoint of the heat transfer node at channel 1 exit is calculated using Eq. (18.1) of Section 2. Then the actual heat transfer coefficient, h_a, is obtained by Eq. (18.27). The heat transfer coefficient used and edited by the code that is based on the nominal heat transfer area, is calculated using Eq. (18.28) of Section 2.

$$Nu = 0.023\, Re_a^{0.8}\, Pr^{0.4} \left(\frac{A_{fa}}{A_{fc}}\right)^{0.1} \left(\frac{P_n}{P_a}\right)^{0.5} \sec^3\alpha \tag{18.1}$$

$$h_a = \frac{Nu\, K}{D_{ha}} \tag{18.27}$$

$$h_{a_n} = \frac{P_a\, h_a}{P_n} \tag{18.28}$$

The data required for this calculation are accumulated below from earlier tables.

Actual flow area, A_{fa}	= 1.00750E-04 m^2 (obtained from Table 18.1)
Core flow area, A_{fc}	= 1.97049E-04 m^2
Nominal heated perimeter, P_n	= 0.230790 m
Actual heated perimeter, P_a	= 0.586353 m
Actual hydraulic diameter, D_{ha}	= 6.87296E-04 m
Helix angle, α	= 0.0

Flow rate, W = 0.91358 kg/s (from input card type 310 in Fig. 18.3)

Coolant temperature at the midpoint of the node

at the channel exit = 54.758 ºC (from code output for input of Fig. 18.3)
Viscosity, μ(50.0 ºC) = 5.4279E-04 Pa-s (from code output for input of Fig. 18.3)
Viscosity, μ(55.0 ºC) = 4.9979E-04 Pa-s (from code output for input of Fig. 18.3)
Viscosity, μ(54.758 ºC) = 5.4279E-04 + (54.758 – 50.0)*(4.9979E-04 - 5.4279E-04)/5.0
= 5.01871E-04 Pa-s

Thermal conductivity, K(50.0 ºC) = 0.6467 W/m-ºC
Thermal conductivity, K(55.0 ºC) = 0.6521 W/m-ºC
Thermal conductivity, K(54.758 ºC) = 0.6467 + (54.758 – 50.0)*(0.6521 – 0.6467)/5.0
= 0.651839 W/m-ºC

Specific heat, C_p(50.0 ºC) = 4183.3 J/kg-ºC
Specific heat, C_p(55.0 ºC) = 4187.0 J/kg-ºC
Specific heat, C_p(54.758 ºC) = 4183.3 + (54.758 – 50.0)*(4187.0 – 4183.3)/5.0
= 4186.8209 J/kg-ºC

Prandtl number, Pr = $\mu C_p/K$ = 5.01871E-04*4186.8209/0.651839 = 3.223563

Reynolds number, $Re_a = \dfrac{W\,D_{ha}}{\mu\,A_{fa}} = \dfrac{0.91358*6.87296\,E-04}{5.01871\,E-04*1.00750\,E-04} = 12418.05$

$$Nu = 0.023\,Re_a^{0.8}\,Pr^{0.4}\left(\frac{A_{fa}}{A_{fc}}\right)^{0.1}\left(\frac{P_n}{P_a}\right)^{0.5}\sec^3\alpha$$

$$= 0.023\,(12418.05)^{0.8}\,(3.223563)^{0.4}\left(\frac{1.00750\,E-04}{1.97049\,E-04}\right)^{0.1}\left(\frac{0.230790}{0.586353}\right)^{0.5}*1.0$$

= 0.023*1884.70*1.593570*0.935119*0.627377
Nu = 40.526

$$h_a = \frac{Nu\,K}{D_{ha}} = \frac{40.526*0.651839}{6.87296\,E-04} = 38435.56\ W/m^2\text{-}^oC$$

$$h_{a_n} = \frac{P_a\,h_a}{P_n} = \left(\frac{0.586353}{0.230790}\right)*38435.56 = 97650.70\ W/m^2\text{-}^oC = \mathbf{\underline{97.651\ kW/m^2\text{-}^oC}}$$

This hand-calculated value, 97.651 kW/m^2-ºC, agrees with the code-calculated value of 97.878 kW/m^2-ºC shown in Table 18.3. There is a difference of 0.2 % between the two values. This provides a verification that the Carnavos correlation for calculating heat transfer coefficient in finned channels in the radial geometry option is correctly implemented in the code.

<u>Heat Transfer Coefficient at Exit of Channel 2</u>:

The data required for this calculation are accumulated below from earlier tables.

Actual flow area, A_{fa} = 1.26270E-05 m^2 (obtained from Table 18.1)
Core flow area, A_{fc} = 1.88099E-04 m^2
Nominal heated perimeter, P_n = 0.285990 m
Actual heated perimeter, P_a = 1.00240 m
Actual hydraulic diameter, D_{ha} = 5.03871E-05 m
Helix angle, α = 0.0

Flow rate, W = 1.15058 kg/s (from input card type 310 in Fig. 18.3)
Exit coolant temperature = 64.451 ºC (from Table 18.3)
Viscosity, μ(60.0 ºC) = 4.6281E-04 Pa-s (from code output for input of Fig. 18.3)
Viscosity, μ(65.0 ºC) = 4.3062E-04 Pa-s (from code output for input of Fig. 18.3)
Viscosity, μ(64.451 ºC) = 4.6281E-04 + (64.451 – 60.0)*(4.3062E-04 - 4.6281E-04)/5.0
= 4.34154E-04 Pa-s

Thermal conductivity, K(60.0 ºC) = 0.6571 W/m-ºC
Thermal conductivity, K(65.0 ºC) = 0.6619 W/m-ºC
Thermal conductivity, K(64.451 ºC) = 0.6571 + (65.451 – 60.0)*(0.6619 – 0.6571)/5.0
= 0.66137 W/m-ºC

Specific heat, C_p(60.0 ºC) = 4191.0 J/kg-ºC
Specific heat, C_p(65.0 ºC) = 4195.2 J/kg-ºC
Specific heat, C_p(64.451 ºC) = 4191.0 + (64.451 – 55.0)*(4195.2 – 4191.0)/5.0
= 4194.7388 J/kg-ºC

Prandtl number, Pr = $\mu C_p/K$ = 4.34154E-04*4194.7388/0.66137 = 2.753621

Reynolds number, $Re_a = \dfrac{W\,D_{ha}}{\mu\,A_{fa}} = \dfrac{1.15058*5.03871E-05}{4.34154E-04*1.26270E-05} = 10575.29$

$$Nu = 0.023\,Re_a^{0.8}\,Pr^{0.4}\left(\frac{A_{fa}}{A_{fc}}\right)^{0.1}\left(\frac{P_n}{P_a}\right)^{0.5}\sec^3\alpha$$

$$= 0.023\,(10575.29)^{0.8}\,(2.753621)^{0.4}\left(\frac{1.26270\,E-05}{1.88099\,E-04}\right)^{0.1}\left(\frac{0.28599}{1.00240}\right)^{0.5}*1.0$$

= 0.023*1657.425*1.499552*0.763293*0.534140
Nu = 23.3061

$$h_a = \frac{Nu\,K}{D_{ha}} = \frac{23.3061*0.66137}{5.03871\,E-05} = 305910.8\ W/m^2\text{-}^oC$$

$$h_{a_n} = \frac{P_a\,h_a}{P_n} = \left(\frac{1.00240}{0.28599}\right)*305910.8 = 1072222.6\ W/m^2\text{-}^oC = \underline{\mathbf{1072.2\ kW/m^2\text{-}^oC}}$$

This hand-calculated value, 1072.2 kW/m^2-ºC, is in agreement with the code-calculated value of 1070.4 kW/m^2-ºC shown in Table 18.3. There is a difference of 0.17 % between the two values. This provides a verification that the Carnavos correlation for calculating heat transfer coefficient in finned channels in the radial geometry option is correctly implemented in the code.

NOMENCLATURE

Input data is shown in red.

i = Fuel assembly type index
k = Fuel tube index
A_{fa} = Actual flow area in the tube with fins, m^2
A_{fc} = Core flow area, i.e., the flow area between the circles touching the tips of fins on the inner and outer fuel tubes, (see Fig. 18.2), m^2
$A_{fn,k}$ = Nominal flow area in channel k, based on tube ID as if the fins were not present, m^2
A_{fin} = Cross sectional area of a single fin. m^2
$A_{fin,in}$ = Cross sectional area of a single internal fin. m^2
$A_{fin,ex}$ = Cross sectional area of a single external fin. m^2
b = Fin thickness at the bottom, m
C_p = Specific heat of the coolant, J/kg-°C
$D_{ci,k}$ = Diameter of the inner boundary of the core flow area in channel k
$D_{co,k}$ = Diameter of the outer boundary of the core flow area in channel k
$D_{i,k}$ = Inner diameter of fuel tube k
$D_{o,k}$ = Outer diameter of fuel tube k
$D_{ha,k}$ = Actual hydraulic diameter of the finned channel k, m
$D_{hn,k}$ = Nominal hydraulic diameter of channel k without fins, m
e = Height of fins, m
F_{nu} = Nusselt number with fins divided by that without fins, defined by Eq. (18.1a)
F^* = Friction factor with fins divided by that without fins, defined by Eq. (18.2a)
f_a = Finned tube Darcy-Weisbach friction factor based on the *actual* hydraulic diameter D_{ha}
f_{a_n} = Finned tube Darcy-Weisbach friction factor expressed as a friction factor based on the *nominal* flow area A_{fn} and hydraulic diameter D_{hn}
h_a = Finned tube heat transfer coefficient based on the *actual* heat transfer area, W/m^2-°C
h_{a_n} = Finned tube heat transfer coefficient expressed as a coefficient based on the *nominal* heat transfer area, W/m^2-°C
K = Thermal conductivity of the coolant, W/m-°C
L = Channel length, m
n = Number of fins in a channel
Nu = $\frac{h_a D_{ha}}{K}$ = Nusselt number based on P_a and A_{fa} (i.e., actual perimeter and actual flow area)
P_a = Actual perimeter, i.e., actual heat transfer area per unit length of the tube with fins, m^2 per meter
P_n = Nominal perimeter, i.e., nominal heat transfer area per unit length of the tube, based on tube ID as if the fins were not present, m^2 per meter
P_{fin} = *Additional* heated perimeter provided by a single fin. It is the additional is over the tube

perimeter covered by the fin, m

$P_{fin,in}$ = *Additional* heated perimeter provided by a single internal fin. It is the additional is over the tube perimeter covered by the fin, m

$P_{fin,ex}$ = *Additional* heated perimeter provided by a single external fin. It is the additional is over the tube perimeter covered by the fin, m

p = Circumferential pitch of fins = $\pi D_i/n$ for tube, = $2W_{ch}$ / n for rectangular channel

Pr = Prandtl number of the coolant

Δp_a = Actual pressure drop due to friction in the finned channel, N/m^2

Re_a = $\frac{W D_{ha}}{\mu A_{fa}}$ = Reynolds number based on P_a and A_{fa} (i.e., actual perimeter and actual flow area)

Re_n = $\frac{W D_{hn}}{\mu A_{fn}}$ = Reynolds number based on P_n and A_{fn} (i.e., nominal perimeter and nominal flow area)

t = Fin thickness at the tip, m

T_{ch} = Channel thickness between the parallel plates, m

W_{ch} = Channel width of the channel between the parallel plates, m

W = Coolant flow rate in the channel, kg/s

α = Angle between the spiral fin's longitudinal axis and the tube axis (called helix angle)

ρ = Density of the coolant, kg/m^3

μ = Dynamic viscosity of the coolant, $N\text{-}s/m^2$

18.4 REFERENCES

1. T. C. Carnavos, "Heat Transfer Performance of Internally Finned Tubes in Turbulent Flow," Heat Transfer Eng., Vol. 1, No. 4, pp. 32-37 (April- June 1980).
2. M. Kalimullah, A. P. Olson and E. E. Feldman, "A User's Guide to the PLTEMP/ANL Code," ANL/RERTR/TM-18/17 Version 4.3, Revision 0, Argonne National Laboratory, 9700 South Cass Avenue, Argonne, IL 60439, USA (November 2018).

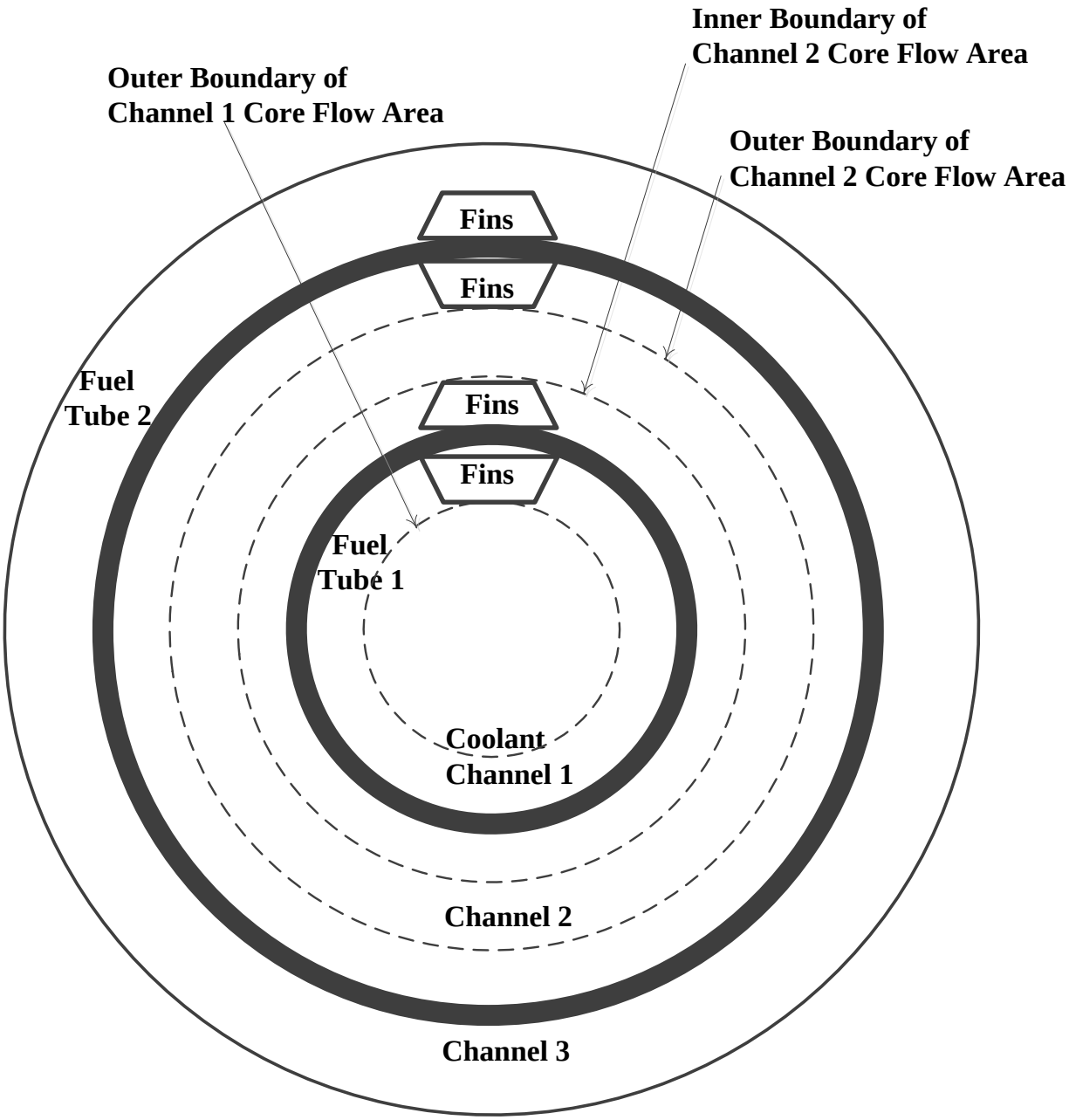

Figure 18.1 A Typical Fuel Assembly Made of Two Fuel Tubes Having Longitudinal Fins on the Inside and Outside of the Tubes (Input Option IGOM = 1)

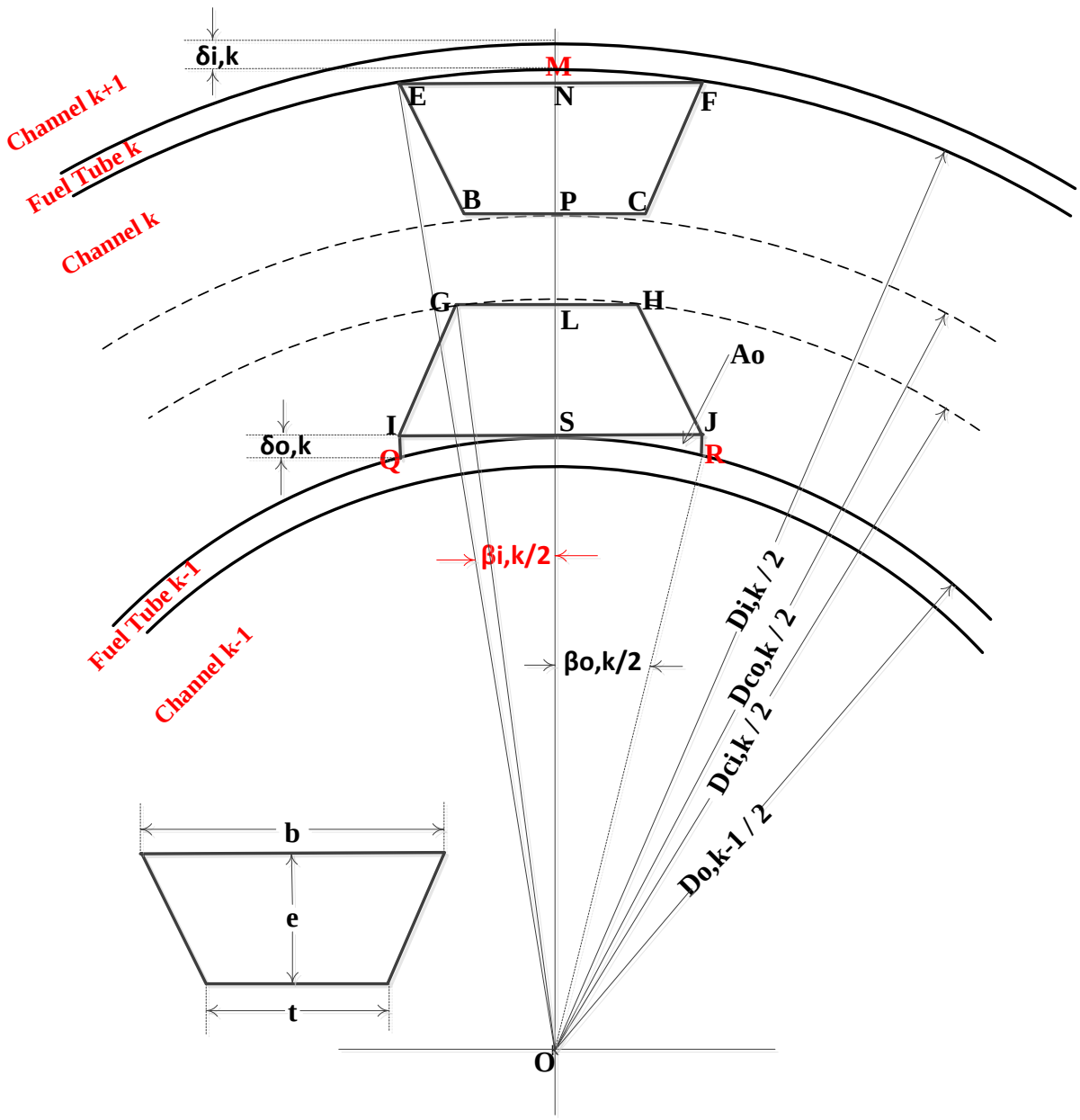

OP = Dco,k / 2 = Radius of the outer boundary of core flow area in channel k
OG = Dci,k / 2 = Radius of the inner boundary of core flow area in channel k

Figure 18.2 Radial Geometry Used in Calculating Coolant Flow Area in an Assembly Made of Multiple Fuel Tubes Having Longitudinal Fins (Fuel tube radii entered in increasing order)

Figure 18.3 Input Data File of Standard Test Problem 34 Having Finned Channels with Fuel Tubes Radii in the Increasing Order

```
Test Problem with Fins; 6 Tubes 0.58 m high, Tube radii in increasing order
! August 7, 2015
! Only one type of assembly in the problem; A single assembly in type 1
!  1   2   3   4   5   6   7   8   9  10  11  12  13  14  15  16  17  18  19  20
  -1   2   2   1   1   0   1   0   1   0                                        Card(1)0200
  4.00000E-4  7.00000E-4  2.62164E-4  0.00000   1500                           Card(1)0202
   1   3  0.0        1.00        1.000       1.00                              Card(1)0300
   7   7  1.000                                                                Card(1)0301
   1   2   1                                                                   Card(1)0302
 1.3135                                                                        Card(1)0303
 0.0043433  0.038540    0.10        0.5                                        Card(3)0304
 0.0        0.0         0.580       0.0                                        Card(3)0304
 0.0043433  0.038540    0.035       1.0                                        Card(3)0304
 0.316      0.250                                                              Card(1)0305
   7  0 0.0         0.580         0.450E-03  170.        0.500E-03  100.      Card(1)0306
  2.4641E-04 4.27181E-03  0.23079    0.23079                                   Card(7)0307
  3.0299E-04 4.23777E-03  0.28599    0.28599                                   Card(6)0307
  3.5957E-04 4.21548E-03  0.34119    0.34119                                   Card(5)0307
  4.1615E-04 4.19940E-03  0.39639    0.39639                                   Card(4)0307
  4.7273E-04 4.18725E-03  0.45159    0.45159                                   Card(3)0307
  5.2931E-04 4.17775E-03  0.50679    0.50679                                   Card(2)0307
  6.0524E-04 8.92059E-03  0.27139    0.27139                                   Card(1)0307
 0.129193   0.156793    0.184393    0.211993    0.239593    0.267193           Card(1)0308R
  .01675     .02020      .02365       .02710     .03055      .0340             Card(1)308AR
 0.85731    0.90175     0.9579      1.0234      1.0901      1.1696             Card(1)0309R
 0.91358    1.15058     1.16807     1.41065     1.54174     1.57675            Card(1)0310R
 1.94282                                                                       Card(2)0310R
   1   1         1.0                                                           Card(1)0400
  1.1545E-04    3.00E-03    0.680           1.4                                Card(1)0401
       0.316    0.25                                                           Card(1)0402
 .100633     .0005        .12540     0.80811      45.0        .135             Card(1)0500
                                                                               Card(2)0500
 100 1.00000E-04   25.0        0.0000        0.80811                           Card(1)0600
 -12                                                                           Card(1)0700
0.00000      0.025       0.52323                                              Card(1)0701
0.05000      0.100       0.62029                                              Card(2)0701
0.15         0.20        0.85886                                              Card(3)0701
0.25         0.30        1.06336                                              Card(4)0701
0.35         0.40        1.24058                                              Card(5)0701
0.45         0.50        1.34964                                              Card(6)0701
0.55         0.60        1.36328                                              Card(7)0701
0.65         0.70        1.27466                                              Card(8)0701
0.75         0.80        1.09062                                              Card(9)0701
0.85         0.90        0.85886                                              Card(10)0701
0.95         0.975       0.75662                                              Card(11)0701
1.00000                                                                       Card(12)0701
   0                                                                          Card(1)0702
```

Figure 18.4 Input Data File of Standard Test Problem 34 Having Finned Channels with Fuel Tubes Radii in the Decreasing Order

```
Test Problem with Fins; 6 Tubes 0.58 m high, Tube radii in decreasing order
! August 7, 2015
! Only one type of assembly in the problem; A single assembly in type 1
!  1   2   3   4   5   6   7   8   9  10  11  12  13  14  15  16  17  18  19  20
  -1   2   2   1   1   0   1   0   1   0                                       Card(1)0200
  4.00000E-4  7.00000E-4  2.62164E-4  0.00000   1500                          Card(1)0202
   1   3  0.0        1.00        1.000       1.00                             Card(1)0300
   7   7  1.000                                                               Card(1)0301
   1   2   1                                                                  Card(1)0302
 1.3135                                                                       Card(1)0303
 0.0043433  0.038540    0.10        0.5                                       Card(3)0304
 0.0        0.0         0.580       0.0                                       Card(3)0304
 0.0043433  0.038540    0.035       1.0                                       Card(3)0304
 0.316      0.250                                                             Card(1)0305
   7  0 0.0         0.580         0.450E-03  170.        0.500E-03  100.     Card(1)0306
  6.0524E-04 8.92059E-03  0.27139    0.27139                                  Card(7)0307
  5.2931E-04 4.17775E-03  0.50679    0.50679                                  Card(7)0307
  4.7273E-04 4.18725E-03  0.45159    0.45159                                  Card(7)0307
  4.1615E-04 4.19940E-03  0.39639    0.39639                                  Card(7)0307
  3.5957E-04 4.21548E-03  0.34119    0.34119                                  Card(7)0307
  3.0299E-04 4.23777E-03  0.28599    0.28599                                  Card(7)0307
  2.4641E-04 4.27181E-03  0.23079    0.23079                                  Card(7)0307
 0.267193   0.239593    0.211993    0.184393    0.156793    0.129193         Card(1)0308
  .0340      .03055      .02710       .02365      .02020      .01675          Card(1)0308A
 1.1696     1.0901      1.0234      0.9579      0.90175     0.85731          Card(1)0309
1.94282     1.57675     1.54174     1.41065     1.16807     1.15058          Card(1)0310
0.91358                                                                       Card(2)0310
   1   1         1.0                                                          Card(1)0400
  1.1545E-04    3.00E-03    0.680           1.4                               Card(1)0401
       0.316    0.25                                                          Card(1)0402
 .100633     .0005        .12540     0.80811      45.0        .135            Card(1)0500
                                                                              Card(2)0500
 100 1.00000E-04   25.0        0.0000        0.80811                          Card(1)0600
 -12                                                                          Card(1)0700
0.00000      0.025       0.52323                                             Card(1)0701
0.05000      0.100       0.62029                                             Card(2)0701
0.15         0.20        0.85886                                             Card(3)0701
0.25         0.30        1.06336                                             Card(4)0701
0.35         0.40        1.24058                                             Card(5)0701
0.45         0.50        1.34964                                             Card(6)0701
0.55         0.60        1.36328                                             Card(7)0701
0.65         0.70        1.27466                                             Card(8)0701
0.75         0.80        1.09062                                             Card(9)0701
0.85         0.90        0.85886                                             Card(10)0701
0.95         0.975       0.75662                                             Card(11)0701
1.00000                                                                       Card(12)0701
   0                                                                          Card(1)0702
```

Figure 18.5 Input Data File of Test Problem 34 of Fig. 18.3 Modified to Set the Fin Size to Zero While Using the Finned Channels Heat Transfer Correlation

The changes in this file compared to Fig. 18.3 are shown in red.

```
Test Problem with Fins; 6 Tubes 0.58 m high, Tube radii in increasing order
! Fin size e=b=t=0.0, August 7, 2015
! Only one type of assembly in the problem; A single assembly in type 1
!  1   2   3   4   5   6   7   8   9  10  11  12  13  14  15  16  17  18  19  20
  -1   2   2   1   1   0   1   0   1   0                                        Card(1)0200
  0.00000E-4  0.00000E-4  0.00000E-4  0.00000   1500                           Card(1)0202
   1   3  0.0        1.00        1.000       1.00                              Card(1)0300
   7   7  1.000                                                                Card(1)0301
   1   2   1                                                                   Card(1)0302
 1.3135                                                                        Card(1)0303
 0.0043433  0.038540    0.10        0.5                                        Card(3)0304
 0.0        0.0         0.580       0.0                                        Card(3)0304
 0.0043433  0.038540    0.035       1.0                                        Card(3)0304
 0.316      0.250                                                              Card(1)0305
   7  0 0.0         0.580         0.450E-03  170.        0.500E-03  100.      Card(1)0306
  2.4641E-04 4.27181E-03  0.23079    0.23079                                   Card(7)0307
  3.0299E-04 4.23777E-03  0.28599    0.28599                                   Card(6)0307
  3.5957E-04 4.21548E-03  0.34119    0.34119                                   Card(5)0307
  4.1615E-04 4.19940E-03  0.39639    0.39639                                   Card(4)0307
  4.7273E-04 4.18725E-03  0.45159    0.45159                                   Card(3)0307
  5.2931E-04 4.17775E-03  0.50679    0.50679                                   Card(2)0307
  6.0524E-04 8.92059E-03  0.27139    0.27139                                   Card(1)0307
 0.129193   0.156793    0.184393    0.211993    0.239593    0.267193           Card(1)0308R
  .01675     .02020      .02365      .02710      .03055      .0340             Card(1)308AR
 0.85731    0.90175     0.9579      1.0234      1.0901      1.1696             Card(1)0309R
 0.91358    1.15058     1.16807     1.41065     1.54174     1.57675            Card(1)0310R
 1.94282                                                                       Card(2)0310R
   1   1         1.0                                                           Card(1)0400
  1.1545E-04    3.00E-03    0.680           1.4                                Card(1)0401
       0.316    0.25                                                           Card(1)0402
 .100633     .0005        .12540     0.80811      45.0        .135             Card(1)0500
                                                                               Card(2)0500
 100 1.00000E-04   25.0        0.0000        0.80811                           Card(1)0600
 -12                                                                           Card(1)0700
0.00000      0.025       0.52323                                              Card(1)0701
0.05000      0.100       0.62029                                              Card(2)0701
0.15         0.20        0.85886                                              Card(3)0701
0.25         0.30        1.06336                                              Card(4)0701
0.35         0.40        1.24058                                              Card(5)0701
0.45         0.50        1.34964                                              Card(6)0701
0.55         0.60        1.36328                                              Card(7)0701
0.65         0.70        1.27466                                              Card(8)0701
0.75         0.80        1.09062                                              Card(9)0701
0.85         0.90        0.85886                                              Card(10)0701
0.95         0.975       0.75662                                              Card(11)0701
1.00000                                                                       Card(12)0701
   0                                                                          Card(1)0702
```

Figure 18.6 Input Data File of Test Problem 34 of Fig. 18.3 Modified to Have No Fins While Using the Dittus-Boelter Heat Transfer Correlation

The changes in this file compared to Fig. 18.3 are shown in red.

```
Test Problem with Fins; 6 Tubes 0.58 m high, Tube radii in increasing order
! No fins, August 7, 2015
! Only one type of assembly in the problem; A single assembly in type 1
!  1   2   3   4   5   6   7   8   9  10  11  12  13  14  15  16  17  18  19  20
   1   2   2   1   1   0   1   0   1   0                                       Card(1)0200
! 0.63000E-4  7.00000E-4  2.62164E-4  0.00000   1500                          Card(1)0202
   1   3  0.0        1.00        1.000       1.00                             Card(1)0300
   7   7  1.000                                                               Card(1)0301
   1   2   1                                                                  Card(1)0302
 1.3135                                                                       Card(1)0303
 0.0043433  0.038540    0.10        0.5                                       Card(3)0304
 0.0        0.0         0.580       0.0                                       Card(3)0304
 0.0043433  0.038540    0.035       1.0                                       Card(3)0304
 0.316      0.250                                                             Card(1)0305
   7  0 0.0         0.580         0.450E-03  170.        0.500E-03  100.     Card(1)0306
  2.4641E-04 4.27181E-03  0.23079    0.23079                                  Card(7)0307
  3.0299E-04 4.23777E-03  0.28599    0.28599                                  Card(6)0307
  3.5957E-04 4.21548E-03  0.34119    0.34119                                  Card(5)0307
  4.1615E-04 4.19940E-03  0.39639    0.39639                                  Card(4)0307
  4.7273E-04 4.18725E-03  0.45159    0.45159                                  Card(3)0307
  5.2931E-04 4.17775E-03  0.50679    0.50679                                  Card(2)0307
  6.0524E-04 8.92059E-03  0.27139    0.27139                                  Card(1)0307
 0.129193   0.156793    0.184393    0.211993    0.239593    0.267193          Card(1)0308R
  .01675     .02020      .02365      .02710      .03055      .0340            Card(1)308AR
 0.85731    0.90175     0.9579      1.0234      1.0901      1.1696            Card(1)0309R
 0.91358    1.15058     1.16807     1.41065     1.54174     1.57675           Card(1)0310R
 1.94282                                                                      Card(2)0310R
   1   1         1.0                                                          Card(1)0400
  1.1545E-04    3.00E-03    0.680           1.4                               Card(1)0401
       0.316    0.25                                                          Card(1)0402
 .100633     .0005        .12540     0.80811      45.0        .135            Card(1)0500
                                                                              Card(2)0500
 100 1.00000E-04   25.0        0.0000        0.80811                          Card(1)0600
 -12                                                                          Card(1)0700
0.00000      0.025       0.52323                                             Card(1)0701
0.05000      0.100       0.62029                                             Card(2)0701
0.15         0.20        0.85886                                             Card(3)0701
0.25         0.30        1.06336                                             Card(4)0701
0.35         0.40        1.24058                                             Card(5)0701
0.45         0.50        1.34964                                             Card(6)0701
0.55         0.60        1.36328                                             Card(7)0701
0.65         0.70        1.27466                                             Card(8)0701
0.75         0.80        1.09062                                             Card(9)0701
0.85         0.90        0.85886                                             Card(10)0701
0.95         0.975       0.75662                                             Card(11)0701
1.00000                                                                       Card(12)0701
   0                                                                          Card(1)0702
```

Figure 18.7 Part of Code Output Showing the Temperature Distribution Calculated Using the Input Data File of Fig. 18.3 (Radii of Fuel Tubes in the Increasing Order)

FUEL PLATE 1 (ExactSoln), Assembly = 1 of Type = 1

NODE	COOLANT inner(C)	CladSurf inner(C)	FUEL PEAK (C)	CladSurf outer(C)	COOLANT outer(C)	HCOFinner W/C-m^2 [F Note 2]	HCOFouter W/C-m^2 [F Note 2]	ONBRin [F Note 1]	ONBRout	ETAin K-cm^3/J [Note 3]	ETAout K-cm^3/J [Note 3]	ONB Temp inner(C)	ONB Temp outer(C)	Avg Meat Temp (C)
	45.000				45.000									
1	45.069	46.696	47.184	45.653	45.288	9.0611E+04	9.2971E+05	40.65	108.01	9.621E+03	5.785E+04	113.935	115.503	47.026
2	45.331	47.580	48.281	46.635	46.234	9.0813E+04	9.3715E+05	26.94	43.09	6.863E+03	5.114E+04	114.500	115.447	48.120
3	45.820	49.280	50.392	48.294	47.778	9.1190E+04	9.4923E+05	16.46	21.52	4.364E+03	3.779E+04	115.444	115.884	50.192
4	46.520	51.181	52.724	50.325	49.732	9.1726E+04	9.6434E+05	11.50	13.33	3.149E+03	3.089E+04	116.088	115.960	52.495
5	47.428	53.262	55.251	52.660	52.018	9.2420E+04	9.8181E+05	8.66	9.25	2.432E+03	2.655E+04	116.542	115.817	54.997
6	48.532	55.344	57.743	55.170	54.529	9.3259E+04	1.0007E+06	6.94	6.92	2.001E+03	2.453E+04	116.754	115.334	57.476
7	49.789	57.247	59.977	57.671	57.092	9.4207E+04	1.0197E+06	5.85	5.48	1.747E+03	2.484E+04	116.692	114.429	59.706
8	51.137	58.829	61.782	59.971	59.505	9.5213E+04	1.0372E+06	5.16	4.54	1.612E+03	2.833E+04	116.339	113.035	61.508
9	52.503	59.989	63.044	61.891	61.580	9.6226E+04	1.0521E+06	4.72	3.91	1.574E+03	3.913E+04	115.684	111.005	62.751
10	53.815	60.769	63.843	63.339	63.190	9.7191E+04	1.0635E+06	4.43	3.44	1.609E+03	7.647E+04	114.780	108.165	63.490
11	54.758	61.420	64.503	64.242	64.161	9.7878E+04	1.0704E+06	4.21	3.18	1.616E+03	1.333E+05	114.156	106.237	64.100
	55.064				64.451									56.630

[1] The ONB ratio is here defined as (Tonb - Tinlet)/(Tsurf - Tinlet). If the heat flux is negative (the coolant is hotter than the adjacent cladding surface), then the ONB ratio is arbitrarily set to 99.99 .
[2] The finned heat transfer coeff is here expressed as an average over the nominal heat transfer area in the unfinned coolant channel. It equals (actual finned surface heat transfer coeff)X(2.5406 3.5050, finned-to-unfinned heat transfer area ratio).
[3] The column gives ETA' = (Coolant Velocity)*(Tsat - Coolant Temp)/(Heat Flux). ETA' in the units chosen here, equals Whittle and Forgan dimensionless ETA for water-cooled reactors: ETA = ETA'*Coolant Density*Cp/4. The last value in the colunm (at exit) should be greater than 32.5 to avoid excursive flow instability. ETA is also used in the equation R = 1/(1+ETA*Dh/Lh)

FUEL PLATE 2 (ExactSoln), Assembly = 1 of Type = 1

NODE	COOLANT inner(C)	CladSurf inner(C)	FUEL PEAK (C)	CladSurf outer(C)	COOLANT outer(C)	HCOFinner W/C-m^2 [F Note 2]	HCOFouter W/C-m^2 [F Note 2]	ONBRin [F Note 1]	ONBRout	ETAin K-cm^3/J [Note 3]	ETAout K-cm^3/J [Note 3]	ONB Temp inner(C)	ONB Temp outer(C)	Avg Meat Temp (C)
	45.000				45.000									
1	45.288	45.643	47.002	46.289	45.261	9.2971E+05	1.8942E+05	109.51	53.65	5.944E+04	1.645E+04	115.413	114.164	46.877
2	46.234	46.648	48.238	47.375	46.146	9.3715E+05	1.9085E+05	42.82	29.18	4.949E+04	1.336E+04	115.561	114.315	48.091
3	47.778	48.342	50.532	49.330	47.639	9.4923E+05	1.9323E+05	21.32	16.13	3.458E+04	9.260E+03	116.230	114.859	50.330
4	49.732	50.418	53.132	51.645	49.586	9.6434E+05	1.9630E+05	13.21	10.55	2.667E+04	7.151E+03	116.575	115.085	52.881
5	52.018	52.808	55.990	54.267	51.922	9.8181E+05	1.9994E+05	9.19	7.57	2.157E+04	5.833E+03	116.731	115.111	55.695
6	54.529	55.378	58.872	57.022	54.548	1.0007E+06	2.0396E+05	6.90	5.81	1.850E+04	5.079E+03	116.605	114.853	58.549
7	57.092	57.943	61.527	59.702	57.296	1.0197E+06	2.0810E+05	5.50	4.71	1.692E+04	4.764E+03	116.152	114.253	61.195
8	59.505	60.303	63.742	62.102	59.963	1.0372E+06	2.1205E+05	4.60	3.99	1.655E+04	4.873E+03	115.356	113.274	63.422
9	61.580	62.275	65.351	64.046	62.347	1.0521E+06	2.1553E+05	4.01	3.51	1.752E+04	5.596E+03	114.204	111.855	65.061
10	63.190	63.762	66.376	65.480	64.297	1.0635E+06	2.1833E+05	3.61	3.17	1.985E+04	7.404E+03	112.794	110.010	66.120
11	64.161	64.685	67.141	66.451	65.525	1.0704E+06	2.2009E+05	3.40	2.97	2.066E+04	8.930E+03	111.997	108.784	66.890
	64.451				65.897									57.823

[1] The ONB ratio is here defined as (Tonb - Tinlet)/(Tsurf - Tinlet). If the heat flux is negative (the coolant is hotter than the adjacent cladding surface), then the ONB ratio is arbitrarily set to 99.99 .
[2] The finned heat transfer coeff is here expressed as an average over the nominal heat transfer area in the unfinned coolant channel. It equals (actual finned surface heat transfer coeff)X(3.5050 3.0973, finned-to-unfinned heat transfer area ratio).
[3] The column gives ETA' = (Coolant Velocity)*(Tsat - Coolant Temp)/(Heat Flux). ETA' in the units chosen here, equals Whittle and Forgan dimensionless ETA for water-cooled reactors: ETA = ETA'*Coolant Density*Cp/4. The last value in the colunm (at exit) should be greater than 32.5 to avoid excursive flow instability. ETA is also used in the equation R = 1/(1+ETA*Dh/Lh)

Figure 18.7 Continued

FUEL PLATE 3 (ExactSoln), Assembly = 1 of Type = 1

NODE	COOLANT inner(C)	CladSurf inner(C)	FUEL PEAK (C)	CladSurf outer(C)	COOLANT outer(C)	HCOFinner W/C-m^2 [F Note 2]	HCOFouter W/C-m^2 [F Note 2]	ONBRin [F Note 1]	ONBRout	ETAin K-cm^3/J [Note 3]	ETAout K-cm^3/J [Note 3]	ONB Temp inner(C)	ONB Temp outer(C)	Avg Meat Temp (C)
	45.000				45.000									
1	45.261	46.920	48.170	47.253	45.279	1.8942E+05	1.2192E+05	36.81	31.12	1.020E+04	8.008E+03	115.662	115.110	48.050
2	46.146	48.109	49.603	48.526	46.221	1.9085E+05	1.2290E+05	22.80	19.92	8.367E+03	6.649E+03	115.883	115.249	49.461
3	47.639	50.336	52.417	50.937	47.805	1.9323E+05	1.2452E+05	13.42	11.94	5.804E+03	4.653E+03	116.625	115.870	52.220
4	49.586	52.888	55.479	53.660	49.868	1.9630E+05	1.2661E+05	9.13	8.22	4.460E+03	3.603E+03	117.021	116.160	55.234
5	51.922	55.722	58.764	56.659	52.345	1.9994E+05	1.2909E+05	6.73	6.11	3.600E+03	2.931E+03	117.210	116.248	58.477
6	54.548	58.625	61.962	59.695	55.137	2.0396E+05	1.3184E+05	5.29	4.83	3.083E+03	2.535E+03	117.099	116.037	61.648
7	57.296	61.368	64.780	62.524	58.068	2.0810E+05	1.3467E+05	4.38	4.02	2.814E+03	2.351E+03	116.640	115.471	64.460
8	59.963	63.751	66.999	64.938	60.928	2.1205E+05	1.3738E+05	3.78	3.49	2.752E+03	2.358E+03	115.811	114.516	66.696
9	62.347	65.605	68.467	66.773	63.503	2.1553E+05	1.3978E+05	3.38	3.13	2.919E+03	2.618E+03	114.592	113.126	68.202
10	64.297	66.923	69.289	68.043	65.637	2.1833E+05	1.4174E+05	3.11	2.88	3.335E+03	3.248E+03	113.076	111.356	69.069
11	65.525	67.882	70.044	69.006	66.999	2.2009E+05	1.4317E+05	2.94	2.72	3.508E+03	3.646E+03	112.189	110.262	69.842
	65.897				67.416									60.441

[1] The ONB ratio is here defined as (Tonb - Tinlet)/(Tsurf - Tinlet). If the heat flux is negative (the coolant is hotter than the adjacent cladding surface), then the ONB ratio is arbitrarily set to 99.99 .

[2] The finned heat transfer coeff is here expressed as an average over the nominal heat transfer area in the unfinned coolant channel. It equals (actual finned surface heat transfer coeff)X(3.0973 2.8037, finned-to-unfinned heat transfer area ratio).

[3] The column gives ETA' = (Coolant Velocity)*(Tsat - Coolant Temp)/(Heat Flux). ETA' in the units chosen here, equals Whittle and Forgan dimensionless ETA for water-cooled reactors: ETA = ETA'*Coolant Density*Cp/4. The last value in the colunm (at exit) should be greater than 32.5 to avoid excursive flow instability. ETA is also used in the equation R = 1/(1+ETA*Dh/Lh)

FUEL PLATE 4 (ExactSoln), Assembly = 1 of Type = 1

NODE	COOLANT inner(C)	CladSurf inner(C)	FUEL PEAK (C)	CladSurf outer(C)	COOLANT outer(C)	HCOFinner W/C-m^2 [F Note 2]	HCOFouter W/C-m^2 [F Note 2]	ONBRin [F Note 1]	ONBRout	ETAin K-cm^3/J [Note 3]	ETAout K-cm^3/J [Note 3]	ONB Temp inner(C)	ONB Temp outer(C)	Avg Meat Temp (C)
	45.000				45.000									
1	45.279	47.970	49.268	48.257	45.313	1.2192E+05	8.9716E+04	23.96	21.71	5.875E+03	5.069E+03	116.160	115.689	49.142
2	46.221	49.415	50.973	49.791	46.369	1.2290E+05	9.0518E+04	16.18	14.79	4.799E+03	4.216E+03	116.428	115.852	50.823
3	47.805	52.205	54.386	52.769	48.145	1.2452E+05	9.1857E+04	10.03	9.21	3.313E+03	2.952E+03	117.254	116.532	54.177
4	49.868	55.268	57.997	56.021	50.457	1.2661E+05	9.3577E+04	7.08	6.52	2.530E+03	2.284E+03	117.720	116.857	57.737
5	52.345	58.574	61.794	59.518	53.229	1.2909E+05	9.5608E+04	5.38	4.96	2.030E+03	1.854E+03	117.969	116.966	61.488
6	55.137	61.837	65.385	62.949	56.345	1.3184E+05	9.7846E+04	4.33	4.00	1.725E+03	1.597E+03	117.906	116.758	65.050
7	58.068	64.778	68.424	66.016	59.606	1.3467E+05	1.0014E+05	3.66	3.39	1.561E+03	1.474E+03	117.476	116.171	68.082
8	60.928	67.188	70.679	68.496	62.772	1.3738E+05	1.0233E+05	3.23	2.99	1.511E+03	1.472E+03	116.659	115.171	70.353
9	63.503	68.909	72.006	70.228	65.601	1.3978E+05	1.0424E+05	2.95	2.72	1.583E+03	1.628E+03	115.429	113.710	71.718
10	65.637	70.007	72.581	71.287	67.918	1.4174E+05	1.0593E+05	2.75	2.54	1.788E+03	2.015E+03	113.880	111.853	72.341
11	66.999	70.912	73.264	72.187	69.376	1.4317E+05	1.0689E+05	2.62	2.42	1.871E+03	2.249E+03	112.967	110.728	73.043
	67.416				69.819									63.286

[1] The ONB ratio is here defined as (Tonb - Tinlet)/(Tsurf - Tinlet). If the heat flux is negative (the coolant is hotter than the adjacent cladding surface), then the ONB ratio is arbitrarily set to 99.99 .

[2] The finned heat transfer coeff is here expressed as an average over the nominal heat transfer area in the unfinned coolant channel. It equals (actual finned surface heat transfer coeff)X(2.8037 2.5822, finned-to-unfinned heat transfer area ratio).

[3] The column gives ETA' = (Coolant Velocity)*(Tsat - Coolant Temp)/(Heat Flux). ETA' in the units chosen here, equals Whittle and Forgan dimensionless ETA for water-cooled reactors: ETA = ETA'*Coolant Density*Cp/4. The last value in the colunm (at exit) should be greater than 32.5 to avoid excursive flow instability. ETA is also used in the equation R = 1/(1+ETA*Dh/Lh)

Figure 18.7 Continued

FUEL PLATE 5 (ExactSoln), Assembly = 1 of Type = 1

NODE	COOLANT inner(C)	CladSurf inner(C)	FUEL PEAK (C)	CladSurf outer(C)	COOLANT outer(C)	HCOFinner W/C-m^2 [F Note 2]	HCOFouter W/C-m^2 [F Note 2]	ONBRin [F Note 1]	ONBRout [F Note 1]	ETAin K-cm^3/J [Note 3]	ETAout K-cm^3/J [Note 3]	ONB Temp inner(C)	ONB Temp outer(C)	Avg Meat Temp (C)
	45.000				45.000									
1	45.313	49.189	50.566	49.483	45.392	8.9716E+04	6.9109E+04	17.11	15.87	3.850E+03	3.448E+03	116.675	116.171	50.432
2	46.369	50.991	52.657	51.403	46.688	9.0518E+04	6.9866E+04	12.02	11.14	3.121E+03	2.876E+03	117.001	116.337	52.497
3	48.145	54.520	56.859	55.152	48.821	9.1857E+04	7.1100E+04	7.66	7.10	2.141E+03	2.007E+03	117.914	117.062	56.636
4	50.457	58.274	61.205	59.122	51.537	9.3577E+04	7.2647E+04	5.53	5.13	1.626E+03	1.542E+03	118.441	117.422	60.927
5	53.229	62.225	65.680	63.280	54.728	9.5608E+04	7.4431E+04	4.28	3.97	1.296E+03	1.239E+03	118.735	117.565	65.353
6	56.345	65.987	69.788	67.214	58.241	9.7846E+04	7.6352E+04	3.51	3.26	1.094E+03	1.054E+03	118.694	117.384	69.430
7	59.606	69.216	73.107	70.550	61.823	1.0014E+05	7.8268E+04	3.03	2.81	9.832E+02	9.580E+02	118.259	116.817	72.742
8	62.772	71.673	75.371	73.030	65.181	1.0233E+05	8.0029E+04	2.71	2.53	9.466E+02	9.391E+02	117.403	115.838	75.025
9	65.601	73.194	76.425	74.478	68.036	1.0424E+05	8.1605E+04	2.52	2.35	9.920E+02	1.014E+03	116.086	114.413	76.124
10	67.918	73.922	76.537	75.061	70.201	1.0593E+05	8.2695E+04	2.40	2.25	1.131E+03	1.214E+03	114.400	112.627	76.294
11	69.376	74.646	76.967	75.680	71.465	1.0689E+05	8.3320E+04	2.31	2.17	1.200E+03	1.307E+03	113.372	111.610	76.752
	69.819				71.833									66.862

[1] The ONB ratio is here defined as (Tonb - Tinlet)/(Tsurf - Tinlet). If the heat flux is negative (the coolant is hotter than the adjacent cladding surface), then the ONB ratio is arbitrarily set to 99.99 .

[2] The finned heat transfer coeff is here expressed as an average over the nominal heat transfer area in the unfinned coolant channel. It equals (actual finned surface heat transfer coeff)X(2.5822 2.4091, finned-to-unfinned heat transfer area ratio).

[3] The column gives ETA' = (Coolant Velocity)*(Tsat - Coolant Temp)/(Heat Flux). ETA' in the units chosen here, equals Whittle and Forgan dimensionless ETA for water-cooled reactors: ETA = ETA'*Coolant Density*Cp/4. The last value in the colunm (at exit) should be greater than 32.5 to avoid excursive flow instability. ETA is also used in the equation R = 1/(1+ETA*Dh/Lh)

FUEL PLATE 6 (ExactSoln), Assembly = 1 of Type = 1

NODE	COOLANT inner(C)	CladSurf inner(C)	FUEL PEAK (C)	CladSurf outer(C)	COOLANT outer(C)	HCOFinner W/C-m^2 [F Note 2]	HCOFouter W/C-m^2 [F Note 2]	ONBRin [F Note 1]	ONBRout [F Note 1]	ETAin K-cm^3/J [Note 3]	ETAout K-cm^3/J [Note 3]	ONB Temp inner(C)	ONB Temp outer(C)	Avg Meat Temp (C)
	45.000				45.000									
1	45.392	51.407	53.120	52.158	45.128	6.9109E+04	3.7315E+04	11.34	9.92	2.345E+03	2.296E+03	117.648	116.038	52.961
2	46.688	53.526	55.472	54.264	45.572	6.9866E+04	3.7457E+04	8.54	7.71	1.983E+03	1.823E+03	117.843	116.436	55.291
3	48.821	57.885	60.486	58.734	46.344	7.1100E+04	3.7700E+04	5.72	5.27	1.402E+03	1.242E+03	118.687	117.383	60.241
4	51.537	62.244	65.357	63.094	47.381	7.2647E+04	3.8026E+04	4.30	4.03	1.093E+03	9.438E+02	119.103	117.978	65.060
5	54.728	66.613	70.123	67.374	48.662	7.4431E+04	3.8427E+04	3.44	3.28	8.916E+02	7.582E+02	119.257	118.361	69.782
6	58.241	70.461	74.124	70.992	50.151	7.6352E+04	3.8888E+04	2.91	2.83	7.740E+02	6.469E+02	119.016	118.451	73.758
7	61.823	73.366	76.865	73.509	51.773	7.8268E+04	3.9386E+04	2.58	2.57	7.243E+02	5.864E+02	118.293	118.204	76.499
8	65.181	75.101	78.116	74.722	53.432	8.0029E+04	3.9889E+04	2.39	2.44	7.431E+02	5.643E+02	117.035	117.606	77.771
9	68.036	75.559	77.823	74.577	55.025	8.1605E+04	4.0368E+04	2.30	2.42	8.688E+02	5.789E+02	115.152	116.641	77.512
10	70.201	75.103	76.528	73.542	56.469	8.2695E+04	4.0797E+04	2.25	2.47	1.203E+03	6.260E+02	112.663	115.398	76.243
11	71.465	75.229	76.298	73.414	57.465	8.3320E+04	4.1091E+04	2.19	2.45	1.464E+03	6.425E+02	111.158	114.640	76.012
	71.833				57.783									69.664

[1] The ONB ratio is here defined as (Tonb - Tinlet)/(Tsurf - Tinlet). If the heat flux is negative (the coolant is hotter than the adjacent cladding surface), then the ONB ratio is arbitrarily set to 99.99 .

[2] The finned heat transfer coeff is here expressed as an average over the nominal heat transfer area in the unfinned coolant channel. It equals (actual finned surface heat transfer coeff)X(2.4091 2.3200, finned-to-unfinned heat transfer area ratio).

[3] The column gives ETA' = (Coolant Velocity)*(Tsat - Coolant Temp)/(Heat Flux). ETA' in the units chosen here, equals Whittle and Forgan dimensionless ETA for water-cooled reactors: ETA = ETA'*Coolant Density*Cp/4. The last value in the colunm (at exit) should be greater than 32.5 to avoid excursive flow instability. ETA is also used in the equation R = 1/(1+ETA*Dh/Lh)

Figure 18.8 Part of Code Output Showing the Temperature Distribution Calculated Using the Input Data File of Fig. 18.4 (Radii of Fuel Tubes in the Decreasing Order)

FUEL PLATE 1 (ExactSoln), Assembly = 1 of Type = 1

NODE	COOLANT outer(C)	CladSurf outer(C)	FUEL PEAK (C)	CladSurf inner(C)	COOLANT inner(C)	HCOFouter W/C-m^2 [F Note 2]	HCOFinner W/C-m^2 [F Note 2]	ONBRout [F Note 1]	ONBRin [1]	ETAout K-cm^3/J [Note 3]	ETAin K-cm^3/J [Note 3]	ONB Temp outer(C)	ONB Temp inner(C)	Avg Meat Temp (C)
	45.000				45.000									
1	45.128	52.158	53.120	51.407	45.392	3.7315E+04	6.9109E+04	9.92	11.34	2.296E+03	2.345E+03	116.038	117.648	52.961
2	45.572	54.264	55.472	53.526	46.688	3.7457E+04	6.9866E+04	7.71	8.54	1.823E+03	1.983E+03	116.436	117.843	55.291
3	46.344	58.734	60.486	57.885	48.821	3.7700E+04	7.1100E+04	5.27	5.72	1.242E+03	1.402E+03	117.383	118.687	60.241
4	47.381	63.094	65.357	62.244	51.537	3.8026E+04	7.2647E+04	4.03	4.30	9.438E+02	1.093E+03	117.978	119.103	65.060
5	48.662	67.374	70.123	66.613	54.728	3.8427E+04	7.4431E+04	3.28	3.44	7.582E+02	8.916E+02	118.361	119.257	69.782
6	50.151	70.992	74.124	70.461	58.241	3.8888E+04	7.6352E+04	2.83	2.91	6.469E+02	7.740E+02	118.451	119.016	73.758
7	51.773	73.509	76.865	73.366	61.823	3.9386E+04	7.8268E+04	2.57	2.58	5.864E+02	7.243E+02	118.204	118.293	76.499
8	53.432	74.722	78.116	75.101	65.181	3.9889E+04	8.0029E+04	2.44	2.39	5.643E+02	7.431E+02	117.606	117.035	77.771
9	55.025	74.577	77.823	75.559	68.036	4.0368E+04	8.1605E+04	2.42	2.30	5.789E+02	8.688E+02	116.641	115.152	77.512
10	56.469	73.542	76.528	75.103	70.201	4.0797E+04	8.2695E+04	2.47	2.25	6.260E+02	1.203E+03	115.398	112.663	76.243
11	57.465	73.414	76.298	75.229	71.465	4.1091E+04	8.3320E+04	2.45	2.19	6.425E+02	1.464E+03	114.640	111.158	76.012
	57.783				71.833									69.664

[1] The ONB ratio is here defined as (Tonb - Tinlet)/(Tsurf - Tinlet). If the heat flux is negative (the coolant is hotter than the adjacent cladding surface), then the ONB ratio is arbitrarily set to 99.99 .
[2] The finned heat transfer coeff is here expressed as an average over the nominal heat transfer area in the unfinned coolant channel. It equals (actual finned surface heat transfer coeff)X(2.3200 2.4091, finned-to-unfinned heat transfer area ratio).
[3] The column gives ETA' = (Coolant Velocity)*(Tsat - Coolant Temp)/(Heat Flux). ETA' in the units chosen here, equals Whittle and Forgan dimensionless ETA for water-cooled reactors: ETA = ETA'*Coolant Density*Cp/4. The last value in the colunm (at exit) should be greater than 32.5 to avoid excursive flow instability. ETA is also used in the equation R = 1/(1+ETA*Dh/Lh)

FUEL PLATE 2 (ExactSoln), Assembly = 1 of Type = 1

NODE	COOLANT outer(C)	CladSurf outer(C)	FUEL PEAK (C)	CladSurf inner(C)	COOLANT inner(C)	HCOFouter W/C-m^2 [F Note 2]	HCOFinner W/C-m^2 [F Note 2]	ONBRout [F Note 1]	ONBRin [1]	ETAout K-cm^3/J [Note 3]	ETAin K-cm^3/J [Note 3]	ONB Temp outer(C)	ONB Temp inner(C)	Avg Meat Temp (C)
	45.000				45.000									
1	45.392	49.483	50.566	49.189	45.313	6.9109E+04	8.9716E+04	15.87	17.11	3.448E+03	3.850E+03	116.171	116.675	50.432
2	46.688	51.403	52.657	50.991	46.369	6.9866E+04	9.0518E+04	11.14	12.02	2.876E+03	3.121E+03	116.337	117.001	52.497
3	48.821	55.152	56.859	54.520	48.145	7.1100E+04	9.1857E+04	7.10	7.66	2.007E+03	2.141E+03	117.062	117.914	56.636
4	51.537	59.122	61.205	58.274	50.457	7.2647E+04	9.3577E+04	5.13	5.53	1.542E+03	1.626E+03	117.422	118.441	60.927
5	54.728	63.280	65.680	62.225	53.229	7.4431E+04	9.5608E+04	3.97	4.28	1.239E+03	1.296E+03	117.565	118.735	65.353
6	58.241	67.214	69.788	65.987	56.345	7.6352E+04	9.7846E+04	3.26	3.51	1.054E+03	1.094E+03	117.384	118.694	69.430
7	61.823	70.550	73.107	69.216	59.606	7.8268E+04	1.0014E+05	2.81	3.03	9.580E+02	9.832E+02	116.817	118.259	72.742
8	65.181	73.030	75.371	71.673	62.772	8.0029E+04	1.0233E+05	2.53	2.71	9.391E+02	9.466E+02	115.838	117.403	75.025
9	68.036	74.478	76.425	73.194	65.601	8.1605E+04	1.0424E+05	2.35	2.52	1.014E+03	9.920E+02	114.413	116.086	76.124
10	70.201	75.061	76.537	73.922	67.918	8.2695E+04	1.0593E+05	2.25	2.40	1.214E+03	1.131E+03	112.627	114.400	76.294
11	71.465	75.680	76.967	74.646	69.376	8.3320E+04	1.0689E+05	2.17	2.31	1.307E+03	1.200E+03	111.610	113.372	76.752
	71.833				69.819									66.862

[1] The ONB ratio is here defined as (Tonb - Tinlet)/(Tsurf - Tinlet). If the heat flux is negative (the coolant is hotter than the adjacent cladding surface), then the ONB ratio is arbitrarily set to 99.99 .
[2] The finned heat transfer coeff is here expressed as an average over the nominal heat transfer area in the unfinned coolant channel. It equals (actual finned surface heat transfer coeff)X(2.4091 2.5822, finned-to-unfinned heat transfer area ratio).
[3] The column gives ETA' = (Coolant Velocity)*(Tsat - Coolant Temp)/(Heat Flux). ETA' in the units chosen here, equals Whittle and Forgan dimensionless ETA for water-cooled reactors: ETA = ETA'*Coolant Density*Cp/4. The last value in the colunm (at exit) should be greater than 32.5 to avoid excursive flow instability. ETA is also used in the equation R = 1/(1+ETA*Dh/Lh)

Figure 18.8 Continued

FUEL PLATE 3 (ExactSoln), Assembly = 1 of Type = 1

NODE	COOLANT outer(C)	CladSurf outer(C)	FUEL PEAK (C)	CladSurf inner(C)	COOLANT inner(C)	HCOFouter W/C-m^2 [F Note 2]	HCOFinner W/C-m^2 [F Note 2]	ONBRout [F Note 1]	ONBRin [F Note 1]	ETAout K-cm^3/J [Note 3]	ETAin K-cm^3/J [Note 3]	ONB Temp outer(C)	ONB Temp inner(C)	Avg Meat Temp (C)
	45.000				45.000									
1	45.313	48.257	49.268	47.970	45.279	8.9716E+04	1.2192E+05	21.71	23.96	5.069E+03	5.875E+03	115.689	116.160	49.142
2	46.369	49.791	50.973	49.415	46.221	9.0518E+04	1.2290E+05	14.79	16.18	4.216E+03	4.799E+03	115.852	116.428	50.823
3	48.145	52.769	54.386	52.205	47.805	9.1857E+04	1.2452E+05	9.21	10.03	2.952E+03	3.313E+03	116.532	117.254	54.177
4	50.457	56.021	57.997	55.268	49.868	9.3577E+04	1.2661E+05	6.52	7.08	2.284E+03	2.530E+03	116.857	117.720	57.737
5	53.229	59.518	61.794	58.574	52.345	9.5608E+04	1.2909E+05	4.96	5.38	1.854E+03	2.030E+03	116.966	117.969	61.488
6	56.345	62.949	65.385	61.837	55.137	9.7846E+04	1.3184E+05	4.00	4.33	1.597E+03	1.725E+03	116.758	117.906	65.050
7	59.606	66.016	68.424	64.778	58.068	1.0014E+05	1.3467E+05	3.39	3.66	1.474E+03	1.561E+03	116.171	117.476	68.082
8	62.772	68.496	70.679	67.188	60.928	1.0233E+05	1.3738E+05	2.99	3.23	1.472E+03	1.511E+03	115.171	116.659	70.353
9	65.601	70.228	72.006	68.909	63.503	1.0424E+05	1.3978E+05	2.72	2.95	1.628E+03	1.583E+03	113.710	115.429	71.718
10	67.918	71.287	72.581	70.007	65.637	1.0593E+05	1.4174E+05	2.54	2.75	2.015E+03	1.788E+03	111.853	113.880	72.341
11	69.376	72.187	73.264	70.912	66.999	1.0689E+05	1.4317E+05	2.42	2.62	2.249E+03	1.871E+03	110.728	112.967	73.043
	69.819				67.416									63.286

[1] The ONB ratio is here defined as (Tonb - Tinlet)/(Tsurf - Tinlet). If the heat flux is negative (the coolant is hotter than the adjacent cladding surface), then the ONB ratio is arbitrarily set to 99.99 .

[2] The finned heat transfer coeff is here expressed as an average over the nominal heat transfer area in the unfinned coolant channel. It equals (actual finned surface heat transfer coeff)X(2.5822 2.8037, finned-to-unfinned heat transfer area ratio).

[3] The column gives ETA' = (Coolant Velocity)*(Tsat - Coolant Temp)/(Heat Flux). ETA' in the units chosen here, equals Whittle and Forgan dimensionless ETA for water-cooled reactors: ETA = ETA'*Coolant Density*Cp/4. The last value in the colunm (at exit) should be greater than 32.5 to avoid excursive flow instability. ETA is also used in the equation R = 1/(1+ETA*Dh/Lh)

FUEL PLATE 4 (ExactSoln), Assembly = 1 of Type = 1

NODE	COOLANT outer(C)	CladSurf outer(C)	FUEL PEAK (C)	CladSurf inner(C)	COOLANT inner(C)	HCOFouter W/C-m^2 [F Note 2]	HCOFinner W/C-m^2 [F Note 2]	ONBRout [F Note 1]	ONBRin [F Note 1]	ETAout K-cm^3/J [Note 3]	ETAin K-cm^3/J [Note 3]	ONB Temp outer(C)	ONB Temp inner(C)	Avg Meat Temp (C)
	45.000				45.000									
1	45.279	47.253	48.170	46.920	45.261	1.2192E+05	1.8942E+05	31.12	36.81	8.008E+03	1.020E+04	115.110	115.662	48.050
2	46.221	48.526	49.603	48.109	46.146	1.2290E+05	1.9085E+05	19.92	22.80	6.649E+03	8.367E+03	115.249	115.883	49.461
3	47.805	50.937	52.417	50.336	47.639	1.2452E+05	1.9323E+05	11.94	13.42	4.653E+03	5.804E+03	115.870	116.625	52.220
4	49.868	53.660	55.479	52.888	49.586	1.2661E+05	1.9630E+05	8.22	9.13	3.603E+03	4.460E+03	116.160	117.021	55.234
5	52.345	56.659	58.764	55.722	51.922	1.2909E+05	1.9994E+05	6.11	6.73	2.931E+03	3.600E+03	116.248	117.210	58.477
6	55.137	59.695	61.962	58.625	54.548	1.3184E+05	2.0396E+05	4.83	5.29	2.535E+03	3.083E+03	116.037	117.099	61.648
7	58.068	62.524	64.780	61.368	57.296	1.3467E+05	2.0810E+05	4.02	4.38	2.351E+03	2.814E+03	115.471	116.640	64.460
8	60.928	64.938	66.999	63.751	59.963	1.3738E+05	2.1205E+05	3.49	3.78	2.358E+03	2.752E+03	114.516	115.811	66.696
9	63.503	66.773	68.467	65.605	62.347	1.3978E+05	2.1553E+05	3.13	3.38	2.618E+03	2.919E+03	113.126	114.592	68.202
10	65.637	68.043	69.289	66.923	64.297	1.4174E+05	2.1833E+05	2.88	3.11	3.248E+03	3.335E+03	111.356	113.076	69.069
11	66.999	69.006	70.044	67.882	65.525	1.4317E+05	2.2009E+05	2.72	2.94	3.646E+03	3.508E+03	110.262	112.189	69.842
	67.416				65.897									60.441

[1] The ONB ratio is here defined as (Tonb - Tinlet)/(Tsurf - Tinlet). If the heat flux is negative (the coolant is hotter than the adjacent cladding surface), then the ONB ratio is arbitrarily set to 99.99 .

[2] The finned heat transfer coeff is here expressed as an average over the nominal heat transfer area in the unfinned coolant channel. It equals (actual finned surface heat transfer coeff)X(2.8037 3.0973, finned-to-unfinned heat transfer area ratio).

[3] The column gives ETA' = (Coolant Velocity)*(Tsat - Coolant Temp)/(Heat Flux). ETA' in the units chosen here, equals Whittle and Forgan dimensionless ETA for water-cooled reactors: ETA = ETA'*Coolant Density*Cp/4. The last value in the colunm (at exit) should be greater than 32.5 to avoid excursive flow instability. ETA is also used in the equation R = 1/(1+ETA*Dh/Lh)

Figure 18.8 Continued

FUEL PLATE 5 (ExactSoln), Assembly = 1 of Type = 1

NODE	COOLANT outer(C)	CladSurf outer(C)	FUEL PEAK (C)	CladSurf inner(C)	COOLANT inner(C)	HCOFouter W/C-m^2 [F Note 2]	HCOFinner W/C-m^2 [F Note 2]	ONBRout [F Note 1]	ONBRin	ETAout K-cm^3/J [Note 3]	ETAin K-cm^3/J [Note 3]	ONB Temp outer(C)	ONB Temp inner(C)	Avg Meat Temp (C)
	45.000				45.000									
1	45.261	46.289	47.002	45.643	45.288	1.8942E+05	9.2971E+05	53.65	109.51	1.645E+04	5.944E+04	114.164	115.413	46.877
2	46.146	47.375	48.238	46.648	46.234	1.9085E+05	9.3715E+05	29.18	42.82	1.336E+04	4.949E+04	114.315	115.561	48.091
3	47.639	49.330	50.532	48.342	47.778	1.9323E+05	9.4923E+05	16.13	21.32	9.260E+03	3.458E+04	114.859	116.230	50.330
4	49.586	51.645	53.132	50.418	49.732	1.9630E+05	9.6434E+05	10.55	13.21	7.151E+03	2.667E+04	115.085	116.575	52.881
5	51.922	54.267	55.990	52.808	52.018	1.9994E+05	9.8181E+05	7.57	9.19	5.833E+03	2.157E+04	115.111	116.731	55.695
6	54.548	57.022	58.872	55.378	54.529	2.0396E+05	1.0007E+06	5.81	6.90	5.079E+03	1.850E+04	114.853	116.605	58.549
7	57.296	59.702	61.527	57.943	57.092	2.0810E+05	1.0197E+06	4.71	5.50	4.764E+03	1.692E+04	114.253	116.152	61.195
8	59.963	62.102	63.742	60.303	59.505	2.1205E+05	1.0372E+06	3.99	4.60	4.873E+03	1.655E+04	113.274	115.356	63.422
9	62.347	64.046	65.351	62.275	61.580	2.1553E+05	1.0521E+06	3.51	4.01	5.596E+03	1.752E+04	111.855	114.204	65.061
10	64.297	65.480	66.376	63.762	63.190	2.1833E+05	1.0635E+06	3.17	3.61	7.404E+03	1.985E+04	110.010	112.794	66.120
11	65.525	66.451	67.141	64.685	64.161	2.2009E+05	1.0704E+06	2.97	3.40	8.930E+03	2.066E+04	108.784	111.997	66.890
	65.897				64.451									57.823

[1] The ONB ratio is here defined as (Tonb - Tinlet)/(Tsurf - Tinlet). If the heat flux is negative (the coolant is hotter than the adjacent cladding surface), then the ONB ratio is arbitrarily set to 99.99 .
[2] The finned heat transfer coeff is here expressed as an average over the nominal heat transfer area in the unfinned coolant channel. It equals (actual finned surface heat transfer coeff)X(3.0973 3.5050, finned-to-unfinned heat transfer area ratio).
[3] The column gives ETA' = (Coolant Velocity)*(Tsat - Coolant Temp)/(Heat Flux). ETA' in the units chosen here, equals Whittle and Forgan dimensionless ETA for water-cooled reactors: ETA = ETA'*Coolant Density*Cp/4. The last value in the colunm (at exit) should be greater than 32.5 to avoid excursive flow instability. ETA is also used in the equation R = 1/(1+ETA*Dh/Lh)

FUEL PLATE 6 (ExactSoln), Assembly = 1 of Type = 1

NODE	COOLANT outer(C)	CladSurf outer(C)	FUEL PEAK (C)	CladSurf inner(C)	COOLANT inner(C)	HCOFouter W/C-m^2 [F Note 2]	HCOFinner W/C-m^2 [F Note 2]	ONBRout [F Note 1]	ONBRin	ETAout K-cm^3/J [Note 3]	ETAin K-cm^3/J [Note 3]	ONB Temp outer(C)	ONB Temp inner(C)	Avg Meat Temp (C)
	45.000				45.000									
1	45.288	45.653	47.184	46.696	45.069	9.2971E+05	9.0611E+04	108.01	40.65	5.785E+04	9.621E+03	115.503	113.935	47.026
2	46.234	46.635	48.281	47.580	45.331	9.3715E+05	9.0813E+04	43.09	26.94	5.114E+04	6.863E+03	115.447	114.500	48.120
3	47.778	48.294	50.392	49.280	45.820	9.4923E+05	9.1190E+04	21.52	16.46	3.779E+04	4.364E+03	115.884	115.444	50.192
4	49.732	50.325	52.724	51.181	46.520	9.6434E+05	9.1726E+04	13.33	11.50	3.089E+04	3.149E+03	115.960	116.088	52.495
5	52.018	52.660	55.251	53.262	47.428	9.8181E+05	9.2420E+04	9.25	8.66	2.655E+04	2.432E+03	115.817	116.542	54.997
6	54.529	55.170	57.743	55.344	48.532	1.0007E+06	9.3259E+04	6.92	6.94	2.453E+04	2.001E+03	115.334	116.754	57.476
7	57.092	57.671	59.977	57.247	49.789	1.0197E+06	9.4207E+04	5.48	5.85	2.484E+04	1.747E+03	114.429	116.692	59.706
8	59.505	59.971	61.782	58.829	51.137	1.0372E+06	9.5213E+04	4.54	5.16	2.833E+04	1.612E+03	113.035	116.339	61.508
9	61.580	61.891	63.044	59.989	52.503	1.0521E+06	9.6226E+04	3.91	4.72	3.913E+04	1.574E+03	111.005	115.684	62.751
10	63.190	63.339	63.843	60.769	53.815	1.0635E+06	9.7191E+04	3.44	4.43	7.647E+04	1.609E+03	108.165	114.780	63.490
11	64.161	64.242	64.503	61.420	54.758	1.0704E+06	9.7878E+04	3.18	4.21	1.333E+05	1.616E+03	106.237	114.156	64.100
	64.451				55.064									56.630

[1] The ONB ratio is here defined as (Tonb - Tinlet)/(Tsurf - Tinlet). If the heat flux is negative (the coolant is hotter than the adjacent cladding surface), then the ONB ratio is arbitrarily set to 99.99 .
[2] The finned heat transfer coeff is here expressed as an average over the nominal heat transfer area in the unfinned coolant channel. It equals (actual finned surface heat transfer coeff)X(3.5050 2.5406, finned-to-unfinned heat transfer area ratio).
[3] The column gives ETA' = (Coolant Velocity)*(Tsat - Coolant Temp)/(Heat Flux). ETA' in the units chosen here, equals Whittle and Forgan dimensionless ETA for water-cooled reactors: ETA = ETA'*Coolant Density*Cp/4. The last value in the colunm (at exit) should be greater than 32.5 to avoid excursive flow instability. ETA is also used in the equation R = 1/(1+ETA*Dh/Lh)

Figure 18.9 Part of Code Output Showing the Temperature Distribution Calculated Using the Input Data File of Fig. 18.5 (Fin Size Set to Zero While Using the Carnavos Correlation)

```
 FUEL PLATE   1 (ExactSoln), Assembly =  1 of Type =  1
 NODE    COOLANT  CladSurf FUEL PEAK  CladSurf  COOLANT  HCOFinner HCOFouter  ONBRin   ONBRout   ETAin   ETAout    ONB Temp  ONB Temp  Avg Meat
        inner(C)  inner(C)    (C)     outer(C)  outer(C) W/C-m^2    W/C-m^2     [F Note 1]     K-cm^3/J  K-cm^3/J  inner(C)  outer(C)  Temp (C)
                                                         [F Note 2] [F Note 2]                [Note 3]  [Note 3]
         45.000                                  45.000
    1    45.116    57.061    57.992    56.995    45.226 2.0635E+04 2.1087E+04    6.15    6.19 9.253E+02 9.413E+02   119.204   119.236    57.888
    2    45.510    59.769    60.888    59.721    45.990 2.0705E+04 2.1224E+04    5.06    5.07 7.620E+02 7.857E+02   119.687   119.623    60.765
    3    46.176    65.969    67.535    65.935    47.268 2.0821E+04 2.1451E+04    3.62    3.62 5.345E+02 5.539E+02   120.936   120.776    67.365
    4    47.047    71.562    73.521    71.560    48.923 2.0973E+04 2.1743E+04    2.89    2.88 4.177E+02 4.330E+02   121.718   121.454    73.311
    5    48.098    76.668    78.975    76.710    50.903 2.1155E+04 2.2088E+04    2.44    2.42 3.450E+02 3.564E+02   122.220   121.844    78.731
    6    49.291    80.363    82.904    80.469    53.124 2.1360E+04 2.2470E+04    2.19    2.17 3.040E+02 3.129E+02   122.320   121.808    82.638
    7    50.554    82.037    84.649    82.232    55.442 2.1576E+04 2.2863E+04    2.08    2.05 2.865E+02 2.953E+02   121.954   121.260    84.380
    8    51.801    81.529    84.034    81.835    57.688 2.1787E+04 2.3238E+04    2.08    2.04 2.896E+02 3.026E+02   121.097   120.153    83.782
    9    52.947    78.950    81.183    79.383    59.689 2.1980E+04 2.3568E+04    2.20    2.14 3.163E+02 3.438E+02   119.723   118.419    80.965
   10    53.928    75.249    77.124    75.808    61.323 2.2144E+04 2.3834E+04    2.41    2.31 3.698E+02 4.365E+02   117.957   116.145    76.947
   11    54.572    73.875    75.600    74.502    62.350 2.2251E+04 2.4000E+04    2.49    2.37 3.964E+02 4.964E+02   116.956   114.805    75.439
         54.773                                  62.663                                                                                   75.555
[1] The ONB ratio is here defined as (Tonb - Tinlet)/(Tsurf - Tinlet). If the heat flux is negative (the coolant is hotter
    than the adjacent cladding surface), then the ONB ratio is arbitrarily set to 99.99 .
[2] The finned heat transfer coeff is here expressed as an average over the nominal heat transfer area in the unfinned coolant
    channel. It equals (actual finned surface heat transfer coeff)X(  1.0000  1.0000, finned-to-unfinned heat transfer area ratio).
[3] The column gives ETA' = (Coolant Velocity)*(Tsat - Coolant Temp)/(Heat Flux). ETA' in the units chosen here, equals Whittle
    and Forgan dimensionless ETA for water-cooled reactors: ETA = ETA'*Coolant Density*Cp/4. The last value in the colunm (at exit)
    should be greater than 32.5 to avoid excursive flow instability. ETA is also used in the equation R = 1/(1+ETA*Dh/Lh)

 FUEL PLATE   2 (ExactSoln), Assembly =  1 of Type =  1
 NODE    COOLANT  CladSurf FUEL PEAK  CladSurf  COOLANT  HCOFinner HCOFouter  ONBRin   ONBRout   ETAin   ETAout    ONB Temp  ONB Temp  Avg Meat
        inner(C)  inner(C)    (C)     outer(C)  outer(C) W/C-m^2    W/C-m^2     [F Note 1]     K-cm^3/J  K-cm^3/J  inner(C)  outer(C)  Temp (C)
                                                         [F Note 2] [F Note 2]                [Note 3]  [Note 3]
         45.000                                  45.000
    1    45.226    58.319    59.389    58.428    45.263 2.1087E+04 1.8637E+04    5.61    5.52 8.461E+02 8.148E+02   119.741   119.183    59.280
    2    45.990    61.455    62.728    61.593    46.149 2.1224E+04 1.8776E+04    4.57    4.50 6.976E+02 6.744E+02   120.223   119.598    62.599
    3    47.268    68.504    70.271    68.705    47.635 2.1451E+04 1.9010E+04    3.26    3.20 4.869E+02 4.712E+02   121.508   120.777    70.092
    4    48.923    74.922    77.117    75.184    49.564 2.1743E+04 1.9309E+04    2.58    2.53 3.770E+02 3.647E+02   122.305   121.484    76.895
    5    50.903    80.831    83.400    81.152    51.875 2.2088E+04 1.9663E+04    2.17    2.13 3.073E+02 2.966E+02   122.810   121.907    83.141
    6    53.124    85.227    88.032    85.598    54.471 2.2470E+04 2.0055E+04    1.94    1.89 2.665E+02 2.566E+02   122.889   121.912    87.751
    7    55.442    87.454    90.305    87.861    57.187 2.2863E+04 2.0458E+04    1.82    1.78 2.472E+02 2.377E+02   122.469   121.420    90.020
    8    57.688    87.338    90.027    87.765    59.824 2.3238E+04 2.0842E+04    1.81    1.76 2.464E+02 2.376E+02   121.519   120.393    89.761
    9    59.689    84.984    87.320    85.416    62.183 2.3568E+04 2.1181E+04    1.88    1.83 2.676E+02 2.610E+02   119.999   118.776    87.091
   10    61.323    81.383    83.267    81.808    64.122 2.3834E+04 2.1456E+04    2.01    1.95 3.152E+02 3.158E+02   118.035   116.672    83.085
   11    62.350    80.133    81.823    80.564    65.350 2.4000E+04 2.1628E+04    2.05    1.98 3.392E+02 3.467E+02   116.918   115.444    81.662
         62.663                                  65.725                                                                                   80.091
[1] The ONB ratio is here defined as (Tonb - Tinlet)/(Tsurf - Tinlet). If the heat flux is negative (the coolant is hotter
    than the adjacent cladding surface), then the ONB ratio is arbitrarily set to 99.99 .
[2] The finned heat transfer coeff is here expressed as an average over the nominal heat transfer area in the unfinned coolant
    channel. It equals (actual finned surface heat transfer coeff)X(  1.0000  1.0000, finned-to-unfinned heat transfer area ratio).
[3] The column gives ETA' = (Coolant Velocity)*(Tsat - Coolant Temp)/(Heat Flux). ETA' in the units chosen here, equals Whittle
    and Forgan dimensionless ETA for water-cooled reactors: ETA = ETA'*Coolant Density*Cp/4. The last value in the colunm (at exit)
    should be greater than 32.5 to avoid excursive flow instability. ETA is also used in the equation R = 1/(1+ETA*Dh/Lh)
```

Figure 18.9 Continued

FUEL PLATE 3 (ExactSoln), Assembly = 1 of Type = 1

NODE	COOLANT inner(C)	CladSurf inner(C)	FUEL PEAK (C)	CladSurf outer(C)	COOLANT outer(C)	HCOFinner W/C-m^2 [F Note 2]	HCOFouter W/C-m^2 [F Note 2]	ONBRin [F Note 1]	ONBRout	ETAin K-cm^3/J [Note 3]	ETAout K-cm^3/J [Note 3]	ONB Temp inner(C)	ONB Temp outer(C)	Avg Meat Temp (C)
	45.000				45.000									
1	45.263	59.881	60.916	59.796	45.283	1.8637E+04	1.9300E+04	5.02	5.06	7.338E+02	7.446E+02	119.677	119.811	60.800
2	46.149	63.376	64.606	63.281	46.238	1.8776E+04	1.9456E+04	4.09	4.12	6.046E+02	6.145E+02	120.148	120.276	64.469
3	47.635	71.225	72.930	71.099	47.839	1.9010E+04	1.9716E+04	2.91	2.93	4.208E+02	4.279E+02	121.417	121.547	72.740
4	49.564	78.355	80.469	78.206	49.921	1.9309E+04	2.0050E+04	2.31	2.33	3.245E+02	3.298E+02	122.200	122.325	80.234
5	51.875	84.903	87.374	84.737	52.415	1.9663E+04	2.0445E+04	1.95	1.96	2.630E+02	2.669E+02	122.691	122.807	87.100
6	54.471	89.762	92.456	89.594	55.220	2.0055E+04	2.0881E+04	1.74	1.75	2.263E+02	2.293E+02	122.758	122.855	92.158
7	57.187	92.220	94.951	92.069	58.158	2.0458E+04	2.1330E+04	1.64	1.64	2.081E+02	2.106E+02	122.323	122.387	94.650
8	59.824	92.101	94.667	91.985	61.015	2.0842E+04	2.1758E+04	1.62	1.63	2.056E+02	2.082E+02	121.355	121.366	94.386
9	62.183	89.532	91.746	89.469	63.580	2.1181E+04	2.2137E+04	1.68	1.68	2.217E+02	2.255E+02	119.811	119.741	91.505
10	64.122	85.606	87.373	85.604	65.697	2.1456E+04	2.2445E+04	1.79	1.79	2.599E+02	2.677E+02	117.812	117.624	87.184
11	65.350	84.259	85.831	84.287	67.043	2.1628E+04	2.2669E+04	1.83	1.82	2.790E+02	2.897E+02	116.667	116.405	85.664
	65.725				67.455									83.766

[1] The ONB ratio is here defined as (Tonb - Tinlet)/(Tsurf - Tinlet). If the heat flux is negative (the coolant is hotter than the adjacent cladding surface), then the ONB ratio is arbitrarily set to 99.99 .

[2] The finned heat transfer coeff is here expressed as an average over the nominal heat transfer area in the unfinned coolant channel. It equals (actual finned surface heat transfer coeff)X(1.0000 1.0000, finned-to-unfinned heat transfer area ratio).

[3] The column gives ETA' = (Coolant Velocity)*(Tsat - Coolant Temp)/(Heat Flux). ETA' in the units chosen here, equals Whittle and Forgan dimensionless ETA for water-cooled reactors: ETA = ETA'*Coolant Density*Cp/4. The last value in the colunm (at exit) should be greater than 32.5 to avoid excursive flow instability. ETA is also used in the equation R = 1/(1+ETA*Dh/Lh)

FUEL PLATE 4 (ExactSoln), Assembly = 1 of Type = 1

NODE	COOLANT inner(C)	CladSurf inner(C)	FUEL PEAK (C)	CladSurf outer(C)	COOLANT outer(C)	HCOFinner W/C-m^2 [F Note 2]	HCOFouter W/C-m^2 [F Note 2]	ONBRin [F Note 1]	ONBRout	ETAin K-cm^3/J [Note 3]	ETAout K-cm^3/J [Note 3]	ONB Temp inner(C)	ONB Temp outer(C)	Avg Meat Temp (C)
	45.000				45.000									
1	45.283	60.831	61.985	60.837	45.314	1.9300E+04	1.8729E+04	4.75	4.74	6.950E+02	6.903E+02	120.150	119.993	61.862
2	46.238	64.560	65.932	64.575	46.372	1.9456E+04	1.8896E+04	3.87	3.86	5.716E+02	5.691E+02	120.655	120.466	65.786
3	47.839	72.915	74.819	72.944	48.149	1.9716E+04	1.9176E+04	2.76	2.75	3.969E+02	3.952E+02	121.990	121.759	74.617
4	49.921	80.499	82.861	80.544	50.456	2.0050E+04	1.9534E+04	2.19	2.18	3.051E+02	3.033E+02	122.823	122.552	82.611
5	52.415	87.460	90.221	87.524	53.222	2.0445E+04	1.9957E+04	1.85	1.84	2.462E+02	2.441E+02	123.356	123.045	89.929
6	55.220	92.630	95.643	92.717	56.332	2.0881E+04	2.0423E+04	1.65	1.64	2.107E+02	2.083E+02	123.449	123.097	95.325
7	58.158	95.270	98.326	95.384	59.587	2.1330E+04	2.0902E+04	1.55	1.54	1.924E+02	1.897E+02	123.026	122.625	98.006
8	61.015	95.202	98.078	95.345	62.754	2.1758E+04	2.1358E+04	1.53	1.52	1.886E+02	1.857E+02	122.054	121.590	97.778
9	63.580	92.564	95.051	92.738	65.593	2.2137E+04	2.1760E+04	1.59	1.57	2.014E+02	1.993E+02	120.490	119.939	94.794
10	65.697	88.493	90.485	88.695	67.936	2.2445E+04	2.2116E+04	1.69	1.67	2.338E+02	2.347E+02	118.456	117.787	90.282
11	67.043	87.128	88.906	87.351	69.424	2.2669E+04	2.2320E+04	1.72	1.69	2.487E+02	2.528E+02	117.305	116.540	88.727
	67.455				69.879									86.442

[1] The ONB ratio is here defined as (Tonb - Tinlet)/(Tsurf - Tinlet). If the heat flux is negative (the coolant is hotter than the adjacent cladding surface), then the ONB ratio is arbitrarily set to 99.99 .

[2] The finned heat transfer coeff is here expressed as an average over the nominal heat transfer area in the unfinned coolant channel. It equals (actual finned surface heat transfer coeff)X(1.0000 1.0000, finned-to-unfinned heat transfer area ratio).

[3] The column gives ETA' = (Coolant Velocity)*(Tsat - Coolant Temp)/(Heat Flux). ETA' in the units chosen here, equals Whittle and Forgan dimensionless ETA for water-cooled reactors: ETA = ETA'*Coolant Density*Cp/4. The last value in the colunm (at exit) should be greater than 32.5 to avoid excursive flow instability. ETA is also used in the equation R = 1/(1+ETA*Dh/Lh)

Figure 18.9 Continued

FUEL PLATE 5 (ExactSoln), Assembly = 1 of Type = 1

NODE	COOLANT inner(C)	CladSurf inner(C)	FUEL PEAK (C)	CladSurf outer(C)	COOLANT outer(C)	HCOFinner W/C-m^2 [F Note 2]	HCOFouter W/C-m^2 [F Note 2]	ONBRin [F Note 1]	ONBRout	ETAin K-cm^3/J [Note 3]	ETAout K-cm^3/J [Note 3]	ONB Temp inner(C)	ONB Temp outer(C)	Avg Meat Temp (C)
	45.000				45.000									
1	45.314	62.712	63.975	62.786	45.366	1.8729E+04	1.7435E+04	4.27	4.23	6.159E+02	6.036E+02	120.565	120.210	63.844
2	46.372	66.873	68.377	66.972	46.593	1.8896E+04	1.7616E+04	3.48	3.44	5.053E+02	4.967E+02	121.102	120.692	68.221
3	48.149	76.179	78.267	76.328	48.641	1.9176E+04	1.7915E+04	2.49	2.46	3.496E+02	3.434E+02	122.497	122.010	78.051
4	50.456	84.591	87.182	84.788	51.291	1.9534E+04	1.8296E+04	1.98	1.96	2.674E+02	2.619E+02	123.375	122.821	86.915
5	53.222	92.277	95.308	92.522	54.451	1.9957E+04	1.8743E+04	1.67	1.65	2.144E+02	2.089E+02	123.943	123.328	94.997
6	56.332	97.955	101.262	98.242	57.982	2.0423E+04	1.9231E+04	1.49	1.47	1.821E+02	1.763E+02	124.061	123.386	100.924
7	59.587	100.820	104.177	101.142	61.650	2.0902E+04	1.9727E+04	1.41	1.39	1.647E+02	1.585E+02	123.648	122.912	103.835
8	62.754	100.689	103.852	101.035	65.171	2.1358E+04	2.0193E+04	1.39	1.37	1.596E+02	1.531E+02	122.669	121.866	103.531
9	65.593	97.707	100.441	98.059	68.268	2.1760E+04	2.0622E+04	1.44	1.42	1.685E+02	1.620E+02	121.077	120.198	100.167
10	67.936	93.156	95.349	93.509	70.740	2.2116E+04	2.0934E+04	1.54	1.51	1.932E+02	1.889E+02	119.007	118.016	95.131
11	69.424	91.612	93.564	91.961	72.257	2.2320E+04	2.1122E+04	1.56	1.53	2.042E+02	2.016E+02	117.823	116.770	93.372
	69.879				72.711									91.038

[1] The ONB ratio is here defined as (Tonb - Tinlet)/(Tsurf - Tinlet). If the heat flux is negative (the coolant is hotter than the adjacent cladding surface), then the ONB ratio is arbitrarily set to 99.99 .
[2] The finned heat transfer coeff is here expressed as an average over the nominal heat transfer area in the unfinned coolant channel. It equals (actual finned surface heat transfer coeff)X(1.0000 1.0000, finned-to-unfinned heat transfer area ratio).
[3] The column gives ETA' = (Coolant Velocity)*(Tsat - Coolant Temp)/(Heat Flux). ETA' in the units chosen here, equals Whittle and Forgan dimensionless ETA for water-cooled reactors: ETA = ETA'*Coolant Density*Cp/4. The last value in the colunm (at exit) should be greater than 32.5 to avoid excursive flow instability. ETA is also used in the equation R = 1/(1+ETA*Dh/Lh)

FUEL PLATE 6 (ExactSoln), Assembly = 1 of Type = 1

NODE	COOLANT inner(C)	CladSurf inner(C)	FUEL PEAK (C)	CladSurf outer(C)	COOLANT outer(C)	HCOFinner W/C-m^2 [F Note 2]	HCOFouter W/C-m^2 [F Note 2]	ONBRin [F Note 1]	ONBRout	ETAin K-cm^3/J [Note 3]	ETAout K-cm^3/J [Note 3]	ONB Temp inner(C)	ONB Temp outer(C)	Avg Meat Temp (C)
	45.000				45.000									
1	45.366	65.498	66.863	65.596	45.158	1.7435E+04	1.5875E+04	3.71	3.67	5.223E+02	6.086E+02	120.951	120.544	66.722
2	46.593	69.984	71.581	70.059	45.694	1.7616E+04	1.5948E+04	3.06	3.04	4.327E+02	5.001E+02	121.443	121.119	71.414
3	48.641	80.261	82.451	80.324	46.601	1.7915E+04	1.6070E+04	2.21	2.20	3.007E+02	3.496E+02	122.823	122.548	82.221
4	51.291	89.371	92.060	89.404	47.786	1.8296E+04	1.6228E+04	1.77	1.77	2.303E+02	2.720E+02	123.670	123.460	91.775
5	54.451	97.536	100.646	97.520	49.216	1.8743E+04	1.6417E+04	1.51	1.51	1.846E+02	2.233E+02	124.196	124.066	100.313
6	57.982	103.259	106.604	103.163	50.835	1.9231E+04	1.6630E+04	1.36	1.36	1.568E+02	1.951E+02	124.238	124.233	106.241
7	61.650	105.619	108.936	105.400	52.548	1.9727E+04	1.6852E+04	1.30	1.31	1.424E+02	1.821E+02	123.695	123.893	108.569
8	65.171	104.435	107.446	104.047	54.241	2.0193E+04	1.7070E+04	1.30	1.32	1.399E+02	1.818E+02	122.512	123.024	107.101
9	68.268	99.929	102.380	99.340	55.798	2.0622E+04	1.7268E+04	1.38	1.41	1.525E+02	1.960E+02	120.609	121.594	102.080
10	70.740	93.717	95.488	92.919	57.136	2.0934E+04	1.7436E+04	1.50	1.56	1.872E+02	2.258E+02	118.072	119.748	95.242
11	72.257	91.359	92.824	90.452	58.019	2.1122E+04	1.7547E+04	1.54	1.62	2.080E+02	2.396E+02	116.588	118.713	92.600
	72.711				58.295									94.462

[1] The ONB ratio is here defined as (Tonb - Tinlet)/(Tsurf - Tinlet). If the heat flux is negative (the coolant is hotter than the adjacent cladding surface), then the ONB ratio is arbitrarily set to 99.99 .
[2] The finned heat transfer coeff is here expressed as an average over the nominal heat transfer area in the unfinned coolant channel. It equals (actual finned surface heat transfer coeff)X(1.0000 1.0000, finned-to-unfinned heat transfer area ratio).
[3] The column gives ETA' = (Coolant Velocity)*(Tsat - Coolant Temp)/(Heat Flux). ETA' in the units chosen here, equals Whittle and Forgan dimensionless ETA for water-cooled reactors: ETA = ETA'*Coolant Density*Cp/4. The last value in the colunm (at exit) should be greater than 32.5 to avoid excursive flow instability. ETA is also used in the equation R = 1/(1+ETA*Dh/Lh)

Figure 18.10 Part of Code Output Showing the Temperature Distribution Calculated Using the Input Data File of Fig. 18.6 (Without Fins While Using the Dittus-Boelter Correlation)

FUEL PLATE 1 (ExactSoln), Assembly = 1 of Type = 1

NODE	COOLANT inner(C)	CladSurf inner(C)	FUEL PEAK (C)	CladSurf outer(C)	COOLANT outer(C)	HCOFinner W/C-m^2	HCOFouter W/C-m^2	ONBRin [F Note 1]	ONBRout	ETAin K-cm^3/J [Note 3]	ETAout K-cm^3/J [Note 3]	ONB Temp inner(C)	ONB Temp outer(C)	Avg Meat Temp (C)
	45.000				45.000									
1	45.116	57.061	57.992	56.995	45.227	2.0634E+04	2.1087E+04	6.15	6.19	9.254E+02	9.413E+02	119.204	119.236	57.889
2	45.510	59.769	60.888	59.721	45.990	2.0703E+04	2.1224E+04	5.06	5.07	7.621E+02	7.857E+02	119.687	119.623	60.766
3	46.176	65.969	67.535	65.936	47.268	2.0820E+04	2.1451E+04	3.62	3.62	5.345E+02	5.539E+02	120.936	120.776	67.366
4	47.047	71.563	73.521	71.560	48.924	2.0972E+04	2.1743E+04	2.89	2.88	4.177E+02	4.330E+02	121.718	121.454	73.312
5	48.098	76.669	78.976	76.710	50.903	2.1154E+04	2.2088E+04	2.44	2.42	3.450E+02	3.564E+02	122.220	121.844	78.732
6	49.289	80.363	82.904	80.469	53.124	2.1359E+04	2.2470E+04	2.19	2.17	3.040E+02	3.129E+02	122.320	121.808	82.638
7	50.551	82.037	84.649	82.232	55.443	2.1574E+04	2.2863E+04	2.08	2.05	2.865E+02	2.953E+02	121.954	121.260	84.380
8	51.797	81.529	84.034	81.835	57.689	2.1785E+04	2.3239E+04	2.08	2.04	2.896E+02	3.026E+02	121.097	120.153	83.782
9	52.944	78.949	81.183	79.383	59.689	2.1978E+04	2.3568E+04	2.20	2.14	3.163E+02	3.438E+02	119.723	118.419	80.965
10	53.926	75.248	77.123	75.807	61.322	2.2142E+04	2.3834E+04	2.41	2.31	3.698E+02	4.365E+02	117.957	116.145	76.946
11	54.571	73.874	75.599	74.501	62.349	2.2250E+04	2.4000E+04	2.49	2.37	3.965E+02	4.964E+02	116.956	114.805	75.438
	54.772				62.661									75.555

[1] The ONB ratio is here defined as (Tonb - Tinlet)/(Tsurf - Tinlet). If the heat flux is negative (the coolant is hotter than the adjacent cladding surface), then the ONB ratio is arbitrarily set to 99.99 .

[3] The column gives ETA' = (Coolant Velocity)*(Tsat - Coolant Temp)/(Heat Flux). ETA' in the units chosen here, equals Whittle and Forgan dimensionless ETA for water-cooled reactors: ETA = ETA'*Coolant Density*Cp/4. The last value in the colunm (at exit) should be greater than 32.5 to avoid excursive flow instability. ETA is also used in the equation R = 1/(1+ETA*Dh/Lh)

FUEL PLATE 2 (ExactSoln), Assembly = 1 of Type = 1

NODE	COOLANT inner(C)	CladSurf inner(C)	FUEL PEAK (C)	CladSurf outer(C)	COOLANT outer(C)	HCOFinner W/C-m^2	HCOFouter W/C-m^2	ONBRin [F Note 1]	ONBRout	ETAin K-cm^3/J [Note 3]	ETAout K-cm^3/J [Note 3]	ONB Temp inner(C)	ONB Temp outer(C)	Avg Meat Temp (C)
	45.000				45.000									
1	45.227	58.319	59.389	58.428	45.263	2.1087E+04	1.8637E+04	5.61	5.52	8.461E+02	8.148E+02	119.741	119.183	59.280
2	45.990	61.455	62.728	61.593	46.149	2.1224E+04	1.8776E+04	4.57	4.50	6.976E+02	6.744E+02	120.223	119.598	62.599
3	47.268	68.504	70.271	68.705	47.635	2.1451E+04	1.9010E+04	3.26	3.20	4.869E+02	4.712E+02	121.508	120.777	70.092
4	48.924	74.922	77.117	75.184	49.564	2.1743E+04	1.9309E+04	2.58	2.53	3.770E+02	3.647E+02	122.305	121.484	76.895
5	50.903	80.831	83.400	81.152	51.875	2.2088E+04	1.9663E+04	2.17	2.13	3.073E+02	2.966E+02	122.810	121.907	83.142
6	53.124	85.227	88.032	85.598	54.471	2.2470E+04	2.0055E+04	1.94	1.89	2.665E+02	2.566E+02	122.889	121.912	87.751
7	55.443	87.454	90.305	87.862	57.187	2.2863E+04	2.0458E+04	1.82	1.78	2.472E+02	2.377E+02	122.469	121.421	90.021
8	57.689	87.338	90.028	87.766	59.824	2.3239E+04	2.0842E+04	1.81	1.76	2.464E+02	2.376E+02	121.519	120.393	89.761
9	59.689	84.985	87.321	85.417	62.184	2.3568E+04	2.1181E+04	1.88	1.83	2.676E+02	2.609E+02	119.999	118.776	87.092
10	61.322	81.383	83.267	81.808	64.124	2.3834E+04	2.1456E+04	2.01	1.95	3.152E+02	3.158E+02	118.035	116.671	83.085
11	62.349	80.133	81.823	80.564	65.351	2.4000E+04	2.1628E+04	2.05	1.98	3.392E+02	3.467E+02	116.918	115.444	81.661
	62.661				65.725									80.091

[1] The ONB ratio is here defined as (Tonb - Tinlet)/(Tsurf - Tinlet). If the heat flux is negative (the coolant is hotter than the adjacent cladding surface), then the ONB ratio is arbitrarily set to 99.99 .

[3] The column gives ETA' = (Coolant Velocity)*(Tsat - Coolant Temp)/(Heat Flux). ETA' in the units chosen here, equals Whittle and Forgan dimensionless ETA for water-cooled reactors: ETA = ETA'*Coolant Density*Cp/4. The last value in the colunm (at exit) should be greater than 32.5 to avoid excursive flow instability. ETA is also used in the equation R = 1/(1+ETA*Dh/Lh)

Figure 18.10 Continued

FUEL PLATE 3 (ExactSoln), Assembly = 1 of Type = 1

NODE	COOLANT inner(C)	CladSurf inner(C)	FUEL PEAK (C)	CladSurf outer(C)	COOLANT outer(C)	HCOFinner W/C-m^2	HCOFouter W/C-m^2	ONBRin [F Note 1]	ONBRout	ETAin K-cm^3/J [Note 3]	ETAout K-cm^3/J [Note 3]	ONB Temp inner(C)	ONB Temp outer(C)	Avg Meat Temp (C)
	45.000				45.000									
1	45.263	59.881	60.916	59.796	45.283	1.8637E+04	1.9300E+04	5.02	5.06	7.338E+02	7.446E+02	119.677	119.811	60.800
2	46.149	63.376	64.606	63.281	46.238	1.8776E+04	1.9456E+04	4.09	4.12	6.046E+02	6.145E+02	120.148	120.276	64.469
3	47.635	71.225	72.930	71.099	47.839	1.9010E+04	1.9716E+04	2.91	2.93	4.208E+02	4.279E+02	121.417	121.547	72.740
4	49.564	78.355	80.469	78.206	49.921	1.9309E+04	2.0050E+04	2.31	2.33	3.245E+02	3.298E+02	122.200	122.325	80.234
5	51.875	84.903	87.374	84.738	52.415	1.9663E+04	2.0445E+04	1.95	1.96	2.630E+02	2.669E+02	122.691	122.807	87.100
6	54.471	89.762	92.456	89.594	55.220	2.0055E+04	2.0881E+04	1.74	1.75	2.263E+02	2.293E+02	122.758	122.855	92.158
7	57.187	92.220	94.951	92.069	58.158	2.0458E+04	2.1330E+04	1.64	1.64	2.081E+02	2.106E+02	122.323	122.387	94.650
8	59.824	92.101	94.667	91.985	61.015	2.0842E+04	2.1758E+04	1.62	1.63	2.056E+02	2.082E+02	121.355	121.366	94.386
9	62.184	89.532	91.746	89.469	63.579	2.1181E+04	2.2137E+04	1.68	1.68	2.217E+02	2.255E+02	119.811	119.741	91.505
10	64.124	85.606	87.373	85.604	65.696	2.1456E+04	2.2445E+04	1.79	1.79	2.599E+02	2.677E+02	117.811	117.624	87.184
11	65.351	84.259	85.831	84.287	67.042	2.1628E+04	2.2669E+04	1.83	1.82	2.790E+02	2.897E+02	116.667	116.405	85.664
	65.725				67.455									83.766

[1] The ONB ratio is here defined as (Tonb - Tinlet)/(Tsurf - Tinlet). If the heat flux is negative (the coolant is hotter than the adjacent cladding surface), then the ONB ratio is arbitrarily set to 99.99 .

[3] The column gives ETA' = (Coolant Velocity)*(Tsat - Coolant Temp)/(Heat Flux). ETA' in the units chosen here, equals Whittle and Forgan dimensionless ETA for water-cooled reactors: ETA = ETA'*Coolant Density*Cp/4. The last value in the colunm (at exit) should be greater than 32.5 to avoid excursive flow instability. ETA is also used in the equation R = 1/(1+ETA*Dh/Lh)

FUEL PLATE 4 (ExactSoln), Assembly = 1 of Type = 1

NODE	COOLANT inner(C)	CladSurf inner(C)	FUEL PEAK (C)	CladSurf outer(C)	COOLANT outer(C)	HCOFinner W/C-m^2	HCOFouter W/C-m^2	ONBRin [F Note 1]	ONBRout	ETAin K-cm^3/J [Note 3]	ETAout K-cm^3/J [Note 3]	ONB Temp inner(C)	ONB Temp outer(C)	Avg Meat Temp (C)
	45.000				45.000									
1	45.283	60.831	61.985	60.837	45.314	1.9300E+04	1.8729E+04	4.75	4.74	6.950E+02	6.903E+02	120.150	119.993	61.862
2	46.238	64.560	65.932	64.575	46.372	1.9456E+04	1.8896E+04	3.87	3.86	5.716E+02	5.691E+02	120.655	120.466	65.786
3	47.839	72.915	74.819	72.944	48.149	1.9716E+04	1.9176E+04	2.76	2.75	3.969E+02	3.952E+02	121.990	121.759	74.617
4	49.921	80.499	82.861	80.544	50.456	2.0050E+04	1.9534E+04	2.19	2.18	3.051E+02	3.033E+02	122.823	122.552	82.611
5	52.415	87.460	90.221	87.524	53.222	2.0445E+04	1.9957E+04	1.85	1.84	2.462E+02	2.441E+02	123.356	123.045	89.929
6	55.220	92.630	95.643	92.718	56.332	2.0881E+04	2.0423E+04	1.65	1.64	2.107E+02	2.083E+02	123.449	123.097	95.325
7	58.158	95.270	98.326	95.384	59.587	2.1330E+04	2.0902E+04	1.55	1.54	1.924E+02	1.897E+02	123.026	122.625	98.006
8	61.015	95.202	98.078	95.345	62.754	2.1758E+04	2.1358E+04	1.53	1.52	1.886E+02	1.857E+02	122.054	121.590	97.778
9	63.579	92.563	95.051	92.738	65.593	2.2137E+04	2.1760E+04	1.59	1.57	2.014E+02	1.993E+02	120.490	119.938	94.794
10	65.696	88.493	90.484	88.694	67.936	2.2445E+04	2.2116E+04	1.69	1.67	2.338E+02	2.347E+02	118.456	117.787	90.281
11	67.042	87.127	88.905	87.350	69.424	2.2669E+04	2.2320E+04	1.72	1.69	2.487E+02	2.528E+02	117.306	116.540	88.726
	67.455				69.879									86.442

[1] The ONB ratio is here defined as (Tonb - Tinlet)/(Tsurf - Tinlet). If the heat flux is negative (the coolant is hotter than the adjacent cladding surface), then the ONB ratio is arbitrarily set to 99.99 .

[3] The column gives ETA' = (Coolant Velocity)*(Tsat - Coolant Temp)/(Heat Flux). ETA' in the units chosen here, equals Whittle and Forgan dimensionless ETA for water-cooled reactors: ETA = ETA'*Coolant Density*Cp/4. The last value in the colunm (at exit) should be greater than 32.5 to avoid excursive flow instability. ETA is also used in the equation R = 1/(1+ETA*Dh/Lh)

Figure 18.10 Continued

FUEL PLATE 5 (ExactSoln), Assembly = 1 of Type = 1

NODE	COOLANT inner(C)	CladSurf inner(C)	FUEL PEAK (C)	CladSurf outer(C)	COOLANT outer(C)	HCOFinner W/C-m^2	HCOFouter W/C-m^2	ONBRin [F Note 1]	ONBRout	ETAin K-cm^3/J [Note 3]	ETAout K-cm^3/J [Note 3]	ONB Temp inner(C)	ONB Temp outer(C)	Avg Meat Temp (C)
	45.000				45.000									
1	45.314	62.712	63.975	62.786	45.366	1.8729E+04	1.7435E+04	4.27	4.23	6.159E+02	6.036E+02	120.565	120.210	63.844
2	46.372	66.873	68.377	66.972	46.593	1.8896E+04	1.7616E+04	3.48	3.44	5.053E+02	4.967E+02	121.102	120.692	68.221
3	48.149	76.179	78.267	76.328	48.641	1.9176E+04	1.7915E+04	2.49	2.46	3.496E+02	3.434E+02	122.497	122.010	78.051
4	50.456	84.591	87.182	84.788	51.291	1.9534E+04	1.8296E+04	1.98	1.96	2.674E+02	2.619E+02	123.375	122.821	86.915
5	53.222	92.277	95.308	92.522	54.451	1.9957E+04	1.8743E+04	1.67	1.65	2.144E+02	2.089E+02	123.943	123.328	94.997
6	56.332	97.955	101.262	98.242	57.982	2.0423E+04	1.9231E+04	1.49	1.47	1.821E+02	1.763E+02	124.061	123.386	100.924
7	59.587	100.820	104.177	101.142	61.650	2.0902E+04	1.9727E+04	1.41	1.39	1.647E+02	1.585E+02	123.648	122.912	103.835
8	62.754	100.689	103.852	101.035	65.171	2.1358E+04	2.0193E+04	1.39	1.37	1.596E+02	1.531E+02	122.669	121.866	103.531
9	65.593	97.707	100.441	98.059	68.268	2.1760E+04	2.0622E+04	1.44	1.42	1.685E+02	1.620E+02	121.077	120.198	100.167
10	67.936	93.156	95.349	93.508	70.740	2.2116E+04	2.0934E+04	1.54	1.51	1.932E+02	1.889E+02	119.007	118.016	95.131
11	69.424	91.612	93.564	91.961	72.257	2.2320E+04	2.1122E+04	1.56	1.53	2.042E+02	2.016E+02	117.823	116.770	93.372
	69.879				72.711									91.038

[1] The ONB ratio is here defined as (Tonb - Tinlet)/(Tsurf - Tinlet). If the heat flux is negative (the coolant is hotter than the adjacent cladding surface), then the ONB ratio is arbitrarily set to 99.99 .

[3] The column gives ETA' = (Coolant Velocity)*(Tsat - Coolant Temp)/(Heat Flux). ETA' in the units chosen here, equals Whittle and Forgan dimensionless ETA for water-cooled reactors: ETA = ETA'*Coolant Density*Cp/4. The last value in the colunm (at exit) should be greater than 32.5 to avoid excursive flow instability. ETA is also used in the equation R = 1/(1+ETA*Dh/Lh)

FUEL PLATE 6 (ExactSoln), Assembly = 1 of Type = 1

NODE	COOLANT inner(C)	CladSurf inner(C)	FUEL PEAK (C)	CladSurf outer(C)	COOLANT outer(C)	HCOFinner W/C-m^2	HCOFouter W/C-m^2	ONBRin [F Note 1]	ONBRout	ETAin K-cm^3/J [Note 3]	ETAout K-cm^3/J [Note 3]	ONB Temp inner(C)	ONB Temp outer(C)	Avg Meat Temp (C)
	45.000				45.000									
1	45.366	65.498	66.863	65.596	45.158	1.7435E+04	1.5875E+04	3.71	3.67	5.223E+02	6.086E+02	120.951	120.544	66.722
2	46.593	69.984	71.581	70.059	45.694	1.7616E+04	1.5948E+04	3.06	3.04	4.327E+02	5.001E+02	121.443	121.119	71.414
3	48.641	80.261	82.451	80.324	46.601	1.7915E+04	1.6070E+04	2.21	2.20	3.007E+02	3.496E+02	122.823	122.548	82.221
4	51.291	89.371	92.060	89.404	47.786	1.8296E+04	1.6228E+04	1.77	1.77	2.303E+02	2.720E+02	123.670	123.460	91.775
5	54.451	97.536	100.646	97.520	49.216	1.8743E+04	1.6417E+04	1.51	1.51	1.846E+02	2.232E+02	124.196	124.066	100.313
6	57.982	103.259	106.604	103.163	50.835	1.9231E+04	1.6630E+04	1.36	1.36	1.568E+02	1.951E+02	124.238	124.233	106.241
7	61.650	105.619	108.936	105.400	52.548	1.9727E+04	1.6852E+04	1.30	1.31	1.424E+02	1.821E+02	123.695	123.893	108.569
8	65.171	104.435	107.446	104.047	54.241	2.0193E+04	1.7070E+04	1.30	1.32	1.399E+02	1.818E+02	122.512	123.024	107.101
9	68.268	99.929	102.380	99.340	55.798	2.0622E+04	1.7268E+04	1.38	1.41	1.525E+02	1.960E+02	120.609	121.594	102.080
10	70.740	93.717	95.488	92.919	57.136	2.0934E+04	1.7436E+04	1.50	1.56	1.872E+02	2.258E+02	118.072	119.748	95.242
11	72.257	91.359	92.824	90.452	58.019	2.1122E+04	1.7547E+04	1.54	1.62	2.080E+02	2.396E+02	116.588	118.713	92.600
	72.711				58.295									94.462

[1] The ONB ratio is here defined as (Tonb - Tinlet)/(Tsurf - Tinlet). If the heat flux is negative (the coolant is hotter than the adjacent cladding surface), then the ONB ratio is arbitrarily set to 99.99 .

[3] The column gives ETA' = (Coolant Velocity)*(Tsat - Coolant Temp)/(Heat Flux). ETA' in the units chosen here, equals Whittle and Forgan dimensionless ETA for water-cooled reactors: ETA = ETA'*Coolant Density*Cp/4. The last value in the colunm (at exit) should be greater than 32.5 to avoid excursive flow instability. ETA is also used in the equation R = 1/(1+ETA*Dh/Lh)

Table 19.1 Geometry Data Calculated on Spreadsheet from the Input Data for Standard Test Problem 34

Tube No., k	RMID	CIRCF	D_i	D_o	$D_{ci,k}$	$D_{co,k}$	$\beta_{i,k}$	$\beta_{o,k}$	$\delta_{o,k}$	$P_{fin,in}$	$P_{fin,ex}$	$A_{fin,in}$	$A_{fin,ex}$	$P_{fin,k}$	$A_{fin,k}$
	m	m	m	m	m	m	radian	radian	m	m	m	m^2	m^2	m	m^2
1	0.01675	0.129193	0.032100	0.034900		0.031292	0.043617			4.74085E-04		1.94214E-07		4.74085E-04	1.94214E-07
2	0.02020	0.156793	0.039000	0.041800	0.035701	0.038194	0.035899	0.040117	3.5104E-06	4.74102E-04	4.81114E-04	1.93899E-07	1.93252E-07	4.77608E-04	1.93575E-07
3	0.02365	0.184393	0.045900	0.048700	0.042601	0.045095	0.030502	0.033494	2.9308E-06	4.74113E-04	4.79969E-04	1.93678E-07	1.93117E-07	4.77041E-04	1.93397E-07
4	0.02710	0.211993	0.052800	0.055600	0.049501	0.051995	0.026516	0.028748	2.5155E-06	4.74120E-04	4.79147E-04	1.93516E-07	1.93020E-07	4.76633E-04	1.93268E-07
5	0.03055	0.239593	0.059700	0.062500	0.056401	0.058896	0.023451	0.025181	2.2033E-06	4.74124E-04	4.78528E-04	1.93390E-07	1.92947E-07	4.76326E-04	1.93169E-07
6	0.03400	0.267193	0.066600	0.069400	0.063301	0.065796	0.021021	0.022400	1.9601E-06	4.74127E-04	4.78046E-04	1.93291E-07	1.92890E-07	4.76086E-04	1.93091E-07
7					0.070200			0.020173	1.7652E-06		4.77659E-04		1.92845E-07	4.77659E-04	1.92845E-07
Chan. No., k	Flow Rate	P_n	A_{fn}	$D_{hn,k}$	n_k	$n_k A_{fin,k}$	$n_k P_{fin,k}$	A_{fa}	P_a	$D_{ha,k}$	F_w Eq. (18.7c)	$A_{fnon\text{-}core}$ Eq. (18.7b)	A_{fc}	F_{nu} Eq. (18.1a)	F^* Eq. (18.2a)
	kg/s	m	m^2	m	-	m^2	m	m^2	m	m	-	m^2	m^2	-	-
0 (total)	9.70419	2.484130	2.9324E-03	4.72181E-03	9000	1.74004E-03	4.28935	1.19236E-03	6.77348	7.04132E-04		9.54494E-04	1.97791E-03	0.575707	1.56823
1	0.91358	0.230790	2.4641E-04	4.27072E-03	750	1.45660E-04	0.355563	1.00750E-04	0.586353	6.87296E-04	1.227564	4.93612E-05	1.97049E-04	0.586672	1.56390
2	1.15058	0.285990	3.0299E-04	4.23777E-03	1500	2.90363E-04	0.716412	1.26270E-05	1.00240	5.03871E-05	1.231465	1.14891E-04	1.88099E-04	0.407705	4.89850
3	1.16807	0.341190	3.5957E-04	4.21548E-03	1500	2.90096E-04	0.715561	6.94738E-05	1.05675	2.62971E-04	1.238128	1.36985E-04	2.22585E-04	0.505760	2.27500
4	1.41065	0.396390	4.1615E-04	4.19940E-03	1500	2.89901E-04	0.714950	1.26249E-04	1.11134	4.54401E-04	1.242950	1.59075E-04	2.57075E-04	0.556230	1.81556
5	1.54174	0.451590	4.7273E-04	4.18725E-03	1500	2.89753E-04	0.714489	1.82977E-04	1.16608	6.27666E-04	1.246603	1.81161E-04	2.91569E-04	0.593983	1.60734
6	1.57675	0.506790	5.2931E-04	4.17775E-03	1500	2.89636E-04	0.714130	2.39674E-04	1.22092	7.85225E-04	1.249467	2.03246E-04	3.26064E-04	0.624744	1.48609
7	1.94282	0.271390	6.0524E-04	8.92059E-03	750	1.44634E-04	0.358244	4.60606E-04	0.629634	2.92619E-03	1.250738	1.09774E-04	4.95466E-04	0.651755	1.14630

Table 18.2 Geometry Data Calculated on PLTEMP/ANL from the Input Data for Standard Test Problem 34

CARNAVOS: Fuel Tube Inner & Outer Diameters

k	D_i	D_o
KA	DDI(KA)	DDO(KA)
1	3.2100E-02	3.4900E-02
2	3.9000E-02	4.1800E-02
3	4.5900E-02	4.8700E-02
4	5.2800E-02	5.5600E-02
5	5.9700E-02	6.2500E-02
6	6.6600E-02	6.9400E-02

CARNAVOS: Coolant Channel Geometrical Parameters Used in Calculating Fin Perimeter and Cross-Sectional Area

k	$D_{ci,k}$	$D_{co,k}$	$\beta_{i,k}$	$\beta_{o,k}$	$\delta_{o,k}$	$P_{fin,in}$	$P_{fin,ex}$	$A_{fin,in}$	$A_{fin,ex}$	$P_{fin,k}$	$A_{fin,k}$
KA	DDCI(KA)	DDCO(KA)	BETA_I(KA)	BETA_O(KA)	DELTA_O(KA)	PFIN_IN(KA)	PFIN_EX(KA)	AFIN_IN(KA)	AFIN_EX(KA)	PFIN1(KA)	AFIN1(KA)
1	-1.00000E+15	3.12924E-02	4.36172E-02	-1.00000E+15	-1.00000E+15	4.74085E-04	-1.00000E+15	1.94214E-07	-1.00000E+15	4.74085E-04	1.94214E-07
2	3.57010E-02	3.81937E-02	3.58994E-02	4.01173E-02	3.51038E-06	4.74102E-04	4.81114E-04	1.93899E-07	1.93252E-07	4.77608E-04	1.93575E-07
3	4.26008E-02	4.50947E-02	3.05023E-02	3.34944E-02	2.93083E-06	4.74113E-04	4.79969E-04	1.93678E-07	1.93117E-07	4.77041E-04	1.93397E-07
4	4.95007E-02	5.19954E-02	2.65159E-02	2.87484E-02	2.51553E-06	4.74120E-04	4.79147E-04	1.93516E-07	1.93020E-07	4.76633E-04	1.93268E-07
5	5.64006E-02	5.88959E-02	2.34511E-02	2.51805E-02	2.20332E-06	4.74124E-04	4.78528E-04	1.93390E-07	1.92947E-07	4.76326E-04	1.93169E-07
6	6.33005E-02	6.57963E-02	2.10214E-02	2.24005E-02	1.96006E-06	4.74127E-04	4.78046E-04	1.93291E-07	1.92890E-07	4.76086E-04	1.93091E-07
7	7.02005E-02	-1.00000E+15	-1.00000E+15	2.01733E-02	1.76517E-06	-1.00000E+15	4.77659E-04	-1.00000E+15	1.92845E-07	4.77659E-04	1.92845E-07

NOTE: A value of -1.0000E+15 for a parameter implies that the parameter is not used and hence left undefined.

CARNAVOS: Coolant Channel Geometrical Parameters Usedn Calculating Heat Transfer Coefficient & Friction Factor

k	n_k	$A_{fnon\text{-}core}$	A_{fn}	A_{fa}	A_{fc}	P_n	P_a	$D_{hn,k}$	$D_{ha,k}$	F_{nu}	F^*
KA	MFIN1(KA)	AANONC(KA)	AAFN1(KA)	AAFA1(KA)	AAFC1(KA)	PTRN1(KA)	PTRA1(KA)	DH_N1(KA)	DH_A1(KA)	FF_NU(KA)	FF_STR(KA)
0	9000	9.54494E-04	2.93240E-03	1.19236E-03	1.97791E-03	2.48413E+00	6.77348E+00	4.72181E-03	7.04132E-04	5.75707E-01	1.56823E+00
1	750	4.93612E-05	2.46410E-04	1.00750E-04	1.97049E-04	2.30790E-01	5.86353E-01	4.27072E-03	6.87296E-04	5.86672E-01	1.56390E+00
2	1500	1.14891E-04	3.02990E-04	1.26270E-05	1.88099E-04	2.85990E-01	1.00240E+00	4.23777E-03	5.03871E-05	4.07705E-01	4.89850E+00
3	1500	1.36985E-04	3.59570E-04	6.94738E-05	2.22585E-04	3.41190E-01	1.05675E+00	4.21548E-03	2.62971E-04	5.05760E-01	2.27500E+00
4	1500	1.59075E-04	4.16150E-04	1.26249E-04	2.57075E-04	3.96390E-01	1.11134E+00	4.19940E-03	4.54401E-04	5.56230E-01	1.81556E+00
5	1500	1.81161E-04	4.72730E-04	1.82977E-04	2.91569E-04	4.51590E-01	1.16608E+00	4.18725E-03	6.27666E-04	5.93983E-01	1.60734E+00
6	1500	2.03246E-04	5.29310E-04	2.39674E-04	3.26064E-04	5.06790E-01	1.22092E+00	4.17775E-03	7.85225E-04	6.24744E-01	1.48609E+00
7	750	1.09774E-04	6.05240E-04	4.60606E-04	4.95466E-04	2.71390E-01	6.29634E-01	8.92059E-03	2.92619E-03	6.51755E-01	1.14630E+00

Note: The symbols in red are added to identify the columns of data printed by the code, in order to compare them with the spreadsheet-calculated data in Table 18.1.

Table 18.3 Comparison of Channel Coolant Exit Temperatures Calculated Using the Input File of Fig. 18.3 with Those Calculated Using the Input File of Fig. 18.4

Channel or Tube No.	Code Calculation Using Input File of Fig. 18.3 (Increasing Tube Radii)				Code Calculation Using Input File of Fig. 18.4 (Decreasing Tube Radii) [1]			
	Exit Coolant Temp.	Heat Transfer Coef. at Exit	Tube Inner Surf. Temp. at Exit	Tube Outer Surf. Temp. at Exit	Exit Coolant Temp.	Heat Transfer Coef. at Exit	Tube Inner Surf. Temp. at Exit	Tube Outer Surf. Temp. at Exit
	°C	kW/m^2-°C	°C	°C	°C	kW/m^2-°C	°C	°C
1	55.064	97.878	61.420	64.242	57.783	41.091	75.229	73.414
2	64.451	1070.4	64.685	66.451	71.833	83.320	74.646	75.680
3	65.897	220.09	67.882	69.006	69.819	106.89	70.912	72.187
4	67.416	143.17	70.912	72.187	67.416	143.17	67.882	69.006
5	69.819	106.89	74.646	75.680	65.897	220.09	64.685	66.451
6	71.833	83.320	75.229	73.414	64.451	14	61.420	64.242
7	57.783	41.091			55.064	97.878		

1. It should be noted during comparison that the results for the input file of Fig. 18.4 are in the reverse order of channel number, compared to that for the input file of Fig. 18.3.

Table 18.4 Comparison of Channel Coolant Exit Temperatures Calculated Using the Input File of Fig. 18.5 with Those Calculated Using the Input File of Fig. 18.6

Channel or Tube No.	Code Calculation Using Input File of Fig. 18.5				Code Calculation Using Input File of Fig. 18.6			
	Exit Coolant Temp.	Heat Transfer Coef. at Exit	Tube Inner Surf. Temp. at Exit	Tube Outer Surf. Temp. at Exit	Exit Coolant Temp.	Heat Transfer Coef. at Exit	Tube Inner Surf. Temp. at Exit	Tube Outer Surf. Temp. at Exit
	ºC	kW/m^2-ºC	ºC	ºC	ºC	kW/m^2-ºC	ºC	ºC
1	54.773	22.251	73.875	74.502	54.772	22.250	73.874	74.501
2	62.663	24.000	80.133	80.564	62.661	24.000	80.133	80.564
3	65.725	21.628	84.259	84.287	65.725	21.628	84.259	84.287
4	67.455	22.669	87.128	87.351	67.455	22.669	87.127	87.350
5	69.879	22.320	91.612	91.961	69.879	22.320	91.612	91.961
6	72.711	21.122	91.359	90.452	72.711	21.122	91.359	90.452
7	58.295	17.547			58.295	17.547		

19 Comparison of PLTEMPANL_4.2_r80_160720 Calculation with Carnavos' Experimental Data of Internally Finned Tubes

19.1 Introduction

The verification work reported here was done in August 2016. The Carnavos correlation [1] was implemented in PLTEMP/ANL to handle heat transfer coefficient and friction factor in finned channels. However, the implementation of this correlation has been verified only by the comparison between the hand calculation and the output generated by the code for hypothetical test cases documented in Chapters 6 and 18. This enhancement was implemented initially in patch version PLTEMPANL _4.2_r80_160720, and is included in all later versions of the code including PLTEMP/ANL V4.3. To fulfill the verification and validation (V&V) requirement, the simulation of Carnavos' experiment with patch PLTEMPANL _4.2_r80_160720 is performed and presented in this chapter.

Four test cases of the experiment are selected for the comparison purpose. Each test-section is modeled by using circular geometry with the fin option and an adiabatic boundary condition at the outer tube surface. The comparison between the code calculation, hand calculation, and experimental data shows the following points:

- The Carnavos correlation has been implemented correctly in PLTEMPANL_4.2_r80 _160720.
- The code successfully predicts the experiment data of $Nu/Pr^{0.4}$ within 10%.
- The differences up to 19% between the calculation and experiment data of friction factors indicate that the uncertainty surpasses the 10% value declared in the description of Carnavos correlation [1].

19.2 Carnavos Experiment

Based on the information provided in [1], the Carnavos heat transfer experiment of finned tubes can be described by the diagram presented in Fig. 19.1. The heat generated at the heater was transferred to the test-section by the outer loop. The heat received by the coolant flowing inside the test-section was in turn removed by the city water line.

Due to the low quality of the image presenting experiment data in [1], only four test cases can be recognized and used in this V&V. The channel geometry parameters of the four corresponding finned tubes are provided in Table 19.1. Although the Carnavos correlation uses these channel parameters directly, PLTEMP/ANL firstly determines them based on the trapezoid fin dimensions given in the input file. Therefore, the fin parameters are approximately estimated by using the channel parameters provided in [1]. This approximation meets the requirement that the error of the channel parameters calculated based on the fin parameters is less than 0.1%.

The experimental data of the Fanning friction factor and ratio $Nu/Pr^{0.4}$ are shown in Fig. 19.2 with the digitization performed by Engauge Digitizer software.

19.3 PLTEMP/ANL Modeling

The modeling is based on the following assumptions:

- All the power (9 kW) generated at the heater is assumed to be transferred to the coolant flowing inside the tube.
- The lengths of test-sections which were not provided in [1] are arbitrarily set to 1.83 m. This parameter does not affect the calculation of the ratio $Nu/Pr^{0.4}$ and friction factor.

Figure 19.3 shows how an internally finned tube test-section of Carnavos experiment is modeled in PLTEMP/ANL. The original finned tube keeps the role of inner cladding, while virtual layers of fuel, outer cladding, and outer coolant are added to simulate the fuel geometry type allowed by the code. Because the model focuses on the test-section only, the heat provided by the heater is now considered to be generated equally in the fuel meat volume.

Additionally, the heat transfer coefficient at the boundary between the outer cladding and outer coolant channel is set to a very low value (10^{-5} W/m^2C) to simulate the adiabatic boundary condition. This arrangement assures that all generated heat is transferred to the inner coolant as what happened in the experiment.

19.4 Comparison of Calculation Results and Experimental Data

Eight PLTEMP/ANL input files (an example is provided in Fig. 19.4) are built for the four test sections and two mass flow rates. These flow rates are calculated from two Reynolds numbers of 17000 and 30000 and thermal hydraulic properties of water generated by the code by using the equation $\dot{m} = \mu \mathrm{Re} A / D_h$

where $\dot{m}$: mass flow rate μ : absolute viscosity Re : Reynolds number
A : flow area D_h : hydraulic diameter

The comparison is performed between the followings:

- Experiment data,
- Hand calculation using channel parameters provided in [1] and code's water properties,
- PLTEMP/ANL calculation using channel and fin parameters at the middle axial node.

19.4.1 Data of $Nu/Pr^{0.4}$

The obtained data of $Nu/Pr^{0.4}$ are presented in Table 19.2 and Fig. 19.5. The code calculation agrees well with the hand calculation. The small differences of less than 0.3% are caused by the approximate determination of the fin parameters. This agreement confirms that the implementation of Carnavos correlation of heat transfer has been correctly performed in PLTEMPANL_4.2_r80_160720.

In comparison with the experiment data, it should be noticed that the Carnavos' equations were claimed to correlate these data to within 10% [1]. With this point of view, the code predicts well the experiment data of $Nu/Pr^{0.4}$ for all selected test cases with relative differences less than 7.5%.

19.4.2 Friction Factor

Table 19.3 and Fig. 19.6 show the obtained data of friction factor. The Darcy friction factors printed in the PLTEMP/ANL output are multiplied by 0.25 to obtain the Fanning friction factors which were used in [1].

Similar to the prediction of $Nu/Pr^{0.4}$, the code output of friction factor is mostly identical to the hand calculation with differences less than 0.3% for all test cases. However, both the code and hand calculations cannot predict all experiment data points with the accuracy of ±10%. Particularly, the relative difference reaches 19% in the case of Tube #34 with Reynolds number equals to 17000.

Based on this fact, the Carnavos correlation hardly predicts all experimental data of friction factor within 10% as claimed in [1]. Instead, the data of four selected test cases indicate that the correlation and so the PLTEM/ANL V4.2_r80_160720 should have the uncertainty up to 19% in the prediction of friction factor.

19.5 Conclusion

The Carnavos heat transfer experiment with internally finned tubes has been simulated by PLTEMPANL_4.2_r80_160720 to verify and validate the implementation of Carnavos correlation. The agreement of the code output and hand calculation for both $Nu/Pr^{0.4}$ and friction factor confirms that the correlation has been programed correctly.

Comparing to the four selected test cases, the code has successfully predicted the experiment data of $Nu/Pr^{0.4}$ within 10% as expected by the setting up of Carnavos correlation. However, the differences up to 19% between the calculation and experiment data of friction factor indicate that the correlation actually could not predict this parameter to within 10% as claimed in [1]. The application of the code needs to take this point into account by tolerating the uncertainty of 19%.

19.6 REFERENCE

1. T. C. Carnavos, “Heat Transfer Performance of Internally Finned Tubes in Turbulent Flow”, Heat Transfer Eng., Vol. 1, No. 4, pp. 32-37 (Apr-June 1980).

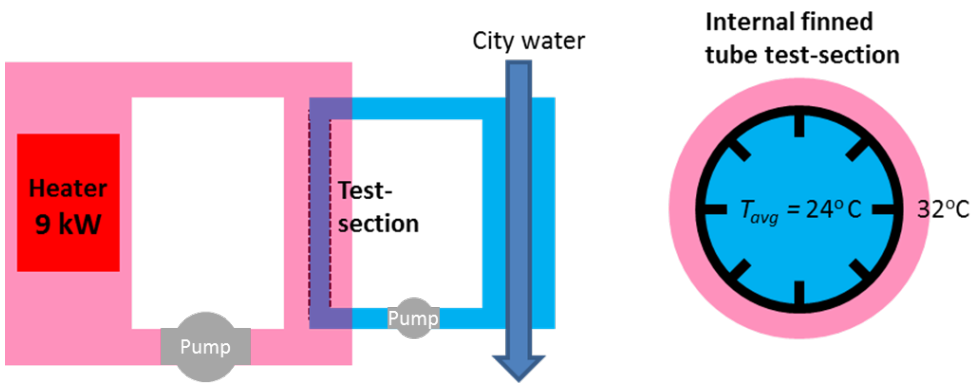

Figure 19.1 Diagram of Carnavos Heat Transfer Experiment

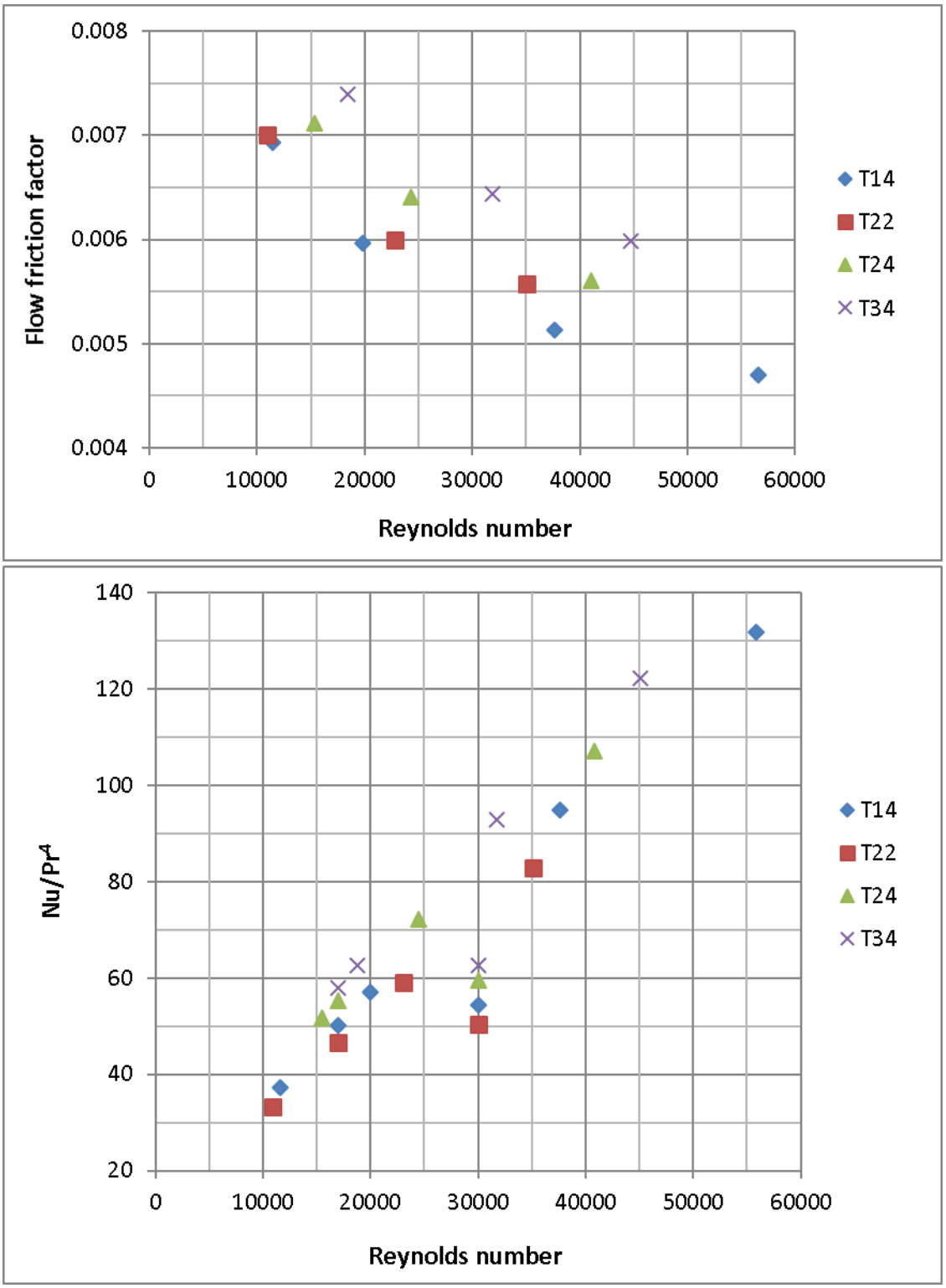

Figure 19.2 Experimental Data Plot

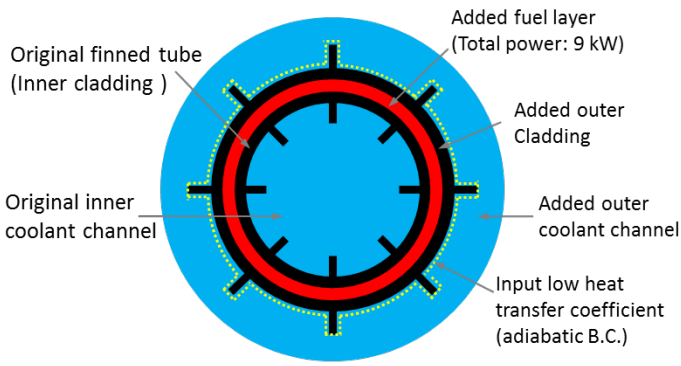

Figure 19.3 PLTEMP/ANL Model of Carnavos Experiment Test-section

Figure 19.4 Sample Input Data (Tube #10 and Re = 17000)

```
Simulation of Carnavos Experiment ,  Tube 14    Re = 17000
  -1   0   0   1   0   0   1   1   1   0   0   0   0   1   0   2   0   0   0   0 Card(1)0200
  1.47141E-3  1.25940E-3  6.43531E-4  0.00000E+0  20                            Card(1)0202
   1   3  0.00000E-0  1.00000E-0  1.00000E-0  1.00000E-0   3   2  1.00000E+0     Card(1)0300
   1   10  1.00000E-0                                                           Card(1)0301
   1   1   1                                                                   Card(1)0302
  1.00000E-0                                                                   Card(2)0303
  4.37336E-4  1.34539E-2  1.00000E-5  0.00000E+0  2.18341E-2  6.95000E-3         Card(3)0304
  4.37336E-4  1.34539E-2  1.83000E+0  0.00000E+0  2.18341E-2  6.95000E-3         Card(3)0304
  4.37336E-4  1.34539E-2  1.00000E-5  0.00000E+0  2.18341E-2  6.95000E-3         Card(3)0304
  0.00000E+0  0.00000E+0  0.00000E+0  0.00000E+0                                 Card(1)0305
   2   0  0.00000E-0  1.83000E+0  1.00000E-3  4.00000E+1  1.00000E-3  1.00000E+2 Card(1)0306
  1.51000E-4  1.39000E-2  4.36000E-2  4.36000E-2  2.18341E-2  6.95000E-3         Card(5)0307
  2.86336E-4  1.32525E-2  8.64248E-2  8.64248E-2  7.50841E-2  4.00000E-3         Card(5)0307
  5.30929E-2                                                                   Card(1)0308
  8.45000E-3                                                                   Card(1)0308A
         1.0                                                                   Card(2)0309
  2.64709E-1  5.01959E-1                                                       Card(1)0310
  1.00000E-1  0.00000E+0  1.20000E-1  9.00000E-3  1.99193E+1  1.20000E-1         Card(1)0500
         0.0         0.0                                                       Card(2)0500
  50  1.00000E-4  3.25000E+1  0.00000E+0  0.00000E+0                            Card(1)0600
  12                                                                           Card(1)0700
  0.00000E-0        1.00                                                       Card(11)0701
  9.09091E-2        1.00                                                       Card(11)0701
  1.81818E-1        1.00                                                       Card(11)0701
  2.72727E-1        1.00                                                       Card(11)0701
  3.63636E-1        1.00                                                       Card(11)0701
  4.54545E-1        1.00                                                       Card(11)0701
  5.45455E-1        1.00                                                       Card(11)0701
  6.36364E-1        1.00                                                       Card(11)0701
  7.27273E-1        1.00                                                       Card(11)0701
  8.18182E-1        1.00                                                       Card(11)0701
  9.09091E-1        1.00                                                       Card(11)0701
  1.00000E-0        1.00                                                       Card(11)0701
    0                                                                          Card(11)0702
```

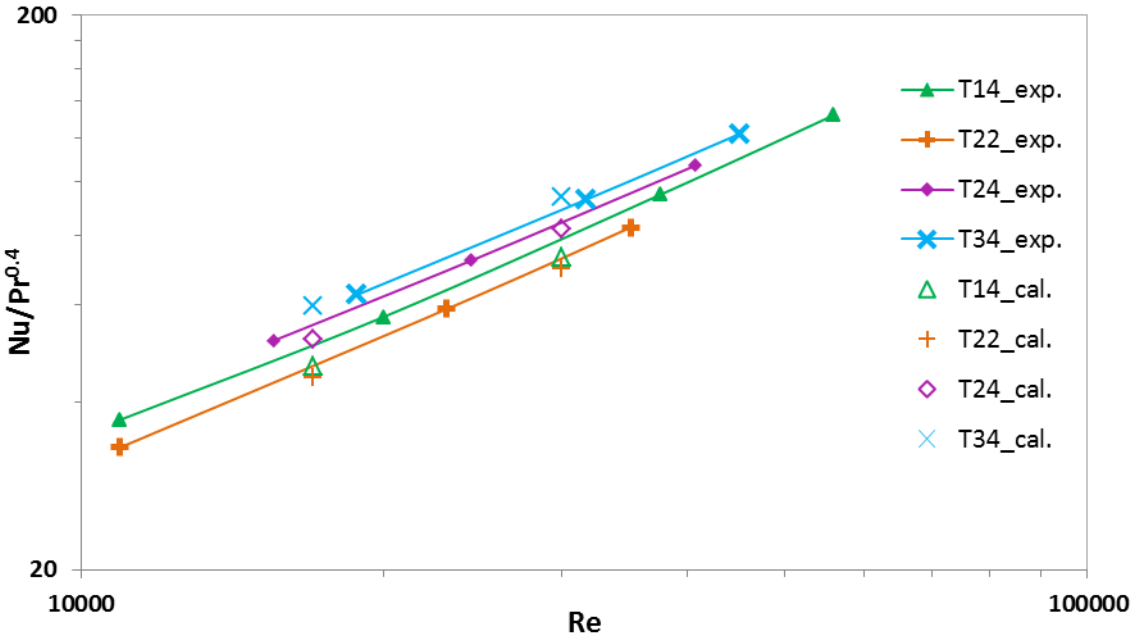

Figure 19.5 Data of $Nu/Pr^{0.4}$

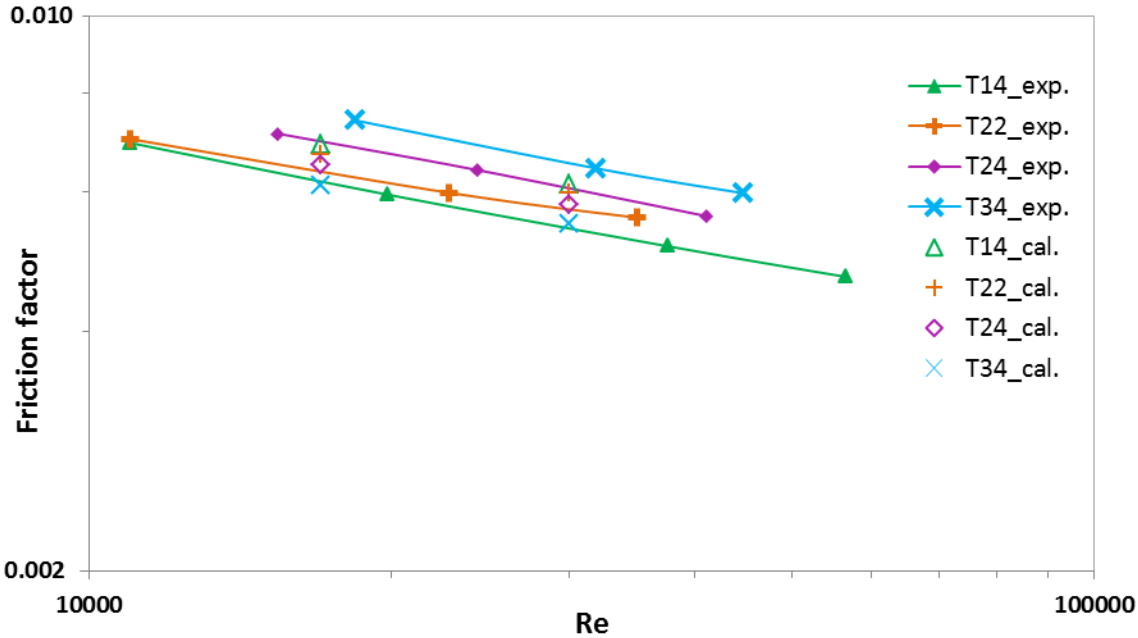

Figure 19.6 Data of Friction Factor

Table 19.1 Internally Finned Tube Dimension

Tube number	#14	#22	#24	#34	Comment
Tube outer diameter (mm)	15.90	19.10	25.40	19.10	Channel parameters provided in [1]
Tube inner diameter (mm)	13.90	17.00	23.80	17.40	
Fin tip diameter (mm)	10.90	13.60	19.80	16.20	
Number of fins	10.00	16.00	16.00	38.00	
Helix angle (degrees)	0.00	11.00	20.00	27.00	
Actual flow area (mm^2)	137.00	212.00	415.00	229.00	
Nominal flow area (mm^2)	151.00	227.00	444.00	237.00	
Core flow area (mm^2)	93.70	146.00	309.00	206.00	
Actual wetted perimeter (mm)	67.30	102.00	132.00	97.00	
Nominal wetted perimeter (mm)	43.60	53.50	74.70	54.50	
Hydraulic diameter (mm)	8.15	8.32	12.60	9.45	
Fin height (mm)	1.47141E-03	1.69500E-03	1.96511E-03	6.20000E-04	Approximately estimated
Top fin width (mm)	6.43531E-04	3.36195E-04	5.89680E-04	1.99117E-04	
Base fin width (mm)	1.25940E-03	7.70000E-04	1.25500E-03	4.80000E-04	

Table 19.2 Comparison of $Nu/Pr^{0.4}$

Reynold number	**17000**				**30000**			
Tube number	**#14**	**#22**	**#24**	**#34**	**#14**	**#22**	**#24**	**#34**
Experimental data	5.02E+1	4.66E+1	5.53E+1	5.80E+1	7.93E+1	7.30E+1	8.47E+1	8.92E+1
Hand calculation	4.66E+1	4.43E+1	5.20E+1	5.97E+1	7.34E+1	6.98E+1	8.20E+1	9.40E+1
PLTEMPANL_4.2_r80_160720	4.65E+1	4.43E+1	5.21E+1	5.97E+1	7.33E+1	6.98E+1	8.21E+1	9.41E+1
Relative difference (%)								
Code cal. vs. Hand cal.	-0.03	-0.02	0.27	0.18	-0.04	-0.02	0.27	0.18
Code cal. vs. Experiment	-7.30	-5.03	-5.62	3.02	-7.43	-4.44	-2.96	5.59
Hand cal. vs. Experiment	-7.27	-5.01	-5.87	2.84	-7.39	-4.42	-3.22	5.40

Table 19.3 Comparison of Friction Factor

Reynold number	**17000**				**30000**			
Tube number	**#14**	**#22**	**#24**	**#34**	**#14**	**#22**	**#24**	**#34**
Experimental data	6.22E-3	6.39E-3	6.96E-3	7.55E-3	5.41E-3	5.72E-3	6.07E-3	6.53E-3
Hand calculation	6.88E-3	6.69E-3	6.47E-3	6.12E-3	6.14E-3	5.97E-3	5.78E-3	5.46E-3
PLTEMPANL_4.2_r80_160720	6.89E-3	6.70E-3	6.49E-3	6.13E-3	6.15E-3	5.98E-3	5.79E-3	5.47E-3
Relative difference (%)								
Code cal. vs. Hand cal.	0.09	0.09	0.25	0.24	0.09	0.08	0.25	0.22
Code cal. vs. Experiment	10.73	4.87	-6.76	-18.78	13.69	4.47	-4.54	-16.25
Hand cal. vs. Experiment	10.63	4.78	-7.00	-18.97	13.59	4.38	-4.78	-16.44

20 Testing of Carnavos Correlations for Heat Transfer Coefficient and Friction Factor with Longitudinal Fins over a Part of the Coolant Channel Perimeter in the PLTEMP/ANL Version 4.2_r80_160720 Code

20.1 Introduction and Summary

The verification work reported here was done in August 2016. The Carnavos correlations [1] for calculating heat transfer coefficient and friction factor in coolant channels with longitudinal fins were implemented and verified earlier in the slab geometry and radial geometry options (IGOM = 0 and 1) of the PLTEMP/ANL code, as documented above in Chapters 6, 18 and 19. The earlier implementation of the Carnavos correlations did not account for the situation in which only a part of the coolant channel perimeter is finned. The first and the last coolant channel in a fuel assembly may be finned on one side and un-finned on the other side (resulting in partly finned channels). The modeling of finned channels in the code has now been improved to account for this, and the improvement is documented in Appendix IX of the code user's guide [2]. The purpose of this chapter is to document a verification of this improvement.

The new code was verified for a new standard test problem 36 (as described in Section 20.2) and for the set of 33 standard test problems in the verification script. It reproduces the past results for all 33 test problems. The code was also verified for a pair of radial geometry problems with the fuel tube radii input in the increasing order and then in decreasing order. The outputs of these two problems were compared to verify that they were identical except that the coolant channels are in the reversed order of each other.

20.2 Verification for Standard Test Problem 36

The design parameters of the fuel assembly used in this test problem are given in Table 20.1. The fuel assembly consists of 4 fuel plates (see Fig. 20.1). The coolant channel 1 is surrounded on the left side by a side plate without any fin and on the right side by a fuel plate having 100 longitudinal fins. Each of the coolant channels 2, 3, and 4 is each surrounded by a fuel plate on both sides and has 200 fins (100 fins on each surrounding fuel plate). The last channel (channel 5) is surrounded on the left side by a fuel plate having 100 fins, without a side plate on the right side. The input data file for this test problem with partly finned channel 1 is shown in Fig. 20.2. A comparison of the PLTEMP/ANL results (heat transfer coefficients and friction factors in all 5 channels) for axial segment 10 with the results of a Microsoft spreadsheet calculation is shown in Table 20.2. This Microsoft spreadsheet was developed for this purpose. The coolant temperatures and flow rates calculated by the code were used as input to the spreadsheet. There is a good agreement (the difference being less than 0.1%) between the two calculations. The agreement in channel 1 provides a verification of the Carnavos correlations in a partly finned channel.

All geometrical parameters related to fins, calculated by the code, were compared with the values calculated on the Microsoft spreadsheet developed for this purpose. The two calculations agree to six significant digits. This agreement verifies that the equations for calculating the geometrical parameters are implemented correctly.

20.3 Conclusion

The Carnavos correlations for heat transfer coefficient and friction factor implemented in the PLTEMP/ANL code version 4.2_r80_160720 is verified for a coolant channel with longitudinal fins on part or whole of the channel parameter.

20.4 REFERENCES

1. T. C. Carnavos, "Heat Transfer Performance of Internally Finned Tubes in Turbulent Flow," Heat Transfer Eng., Vol. 1, No. 4, pp. 32-37 (April- June 1980).

2. M. Kalimullah, A. P. Olson and E. E. Feldman, "A User's Guide to the PLTEMP/ANL Code," ANL/RTR/TM-18/17 Version 4.3, Revision 0, Argonne National Laboratory, 9700 South Cass Avenue, Argonne, IL 60439, USA (November 2018).

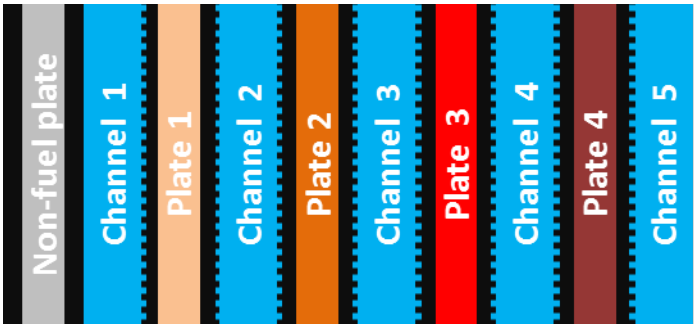

Figure 20.1 Geometry of the Fuel Assembly in Standard Test Problem 36

Figure 20.2 PLTEMP/ANL Input Data File of Standard Test Problem 36 Used in Verification

```
 VnV STAT7 - using Carnavos
! IH  IB CHF FTYP  5   6   7   8 IGOM 10  11 IEND 13  14 ICHF 16  17  18  19  MORE
  -1   0   0   1   0   0   1   1   0   0   0   0   0   1   0   0   1   0   0   0 Card(1)0200
!    EFIN         BFIN       TFIN       AHELIX   NFIN
  2.00000E-3  2.00000E-3  2.00000E-3  0.00000E+0 200                              Card(1)0202
! NSRCH   X-LOW    X-HIGH    NTARGT  YTARGT
   1  1.00000E-4  1.00000E-2   1  3.00000E+1                                      Card(1)0203
! NELF NF   WFGES         FB          FQ          FH     IBC IBCA   HBC
   1   3  2.85000E+1  1.00000E+0  1.00000E+0  1.00000E+0   3   0  1.00000E+0     Card(1)0300
!IQNODS,IQNODF,FQL
   1  11  1.00000E+0                                                             Card(1)0301
!IEFLFHF,ICHNHF,IPLTHF
   1   1   1                                                                     Card(1)0302
!   FZ(I,J)
  1.06474E-1                                                                     Card(1)0303
!     AF          DF          LF          ZF        WIDTH       THICK
  4.00000E-2  4.44444E-2  0.00000E+0  0.00000E+0  4.00000E-1  2.00000E-2         Card(1)0304
  4.00000E-2  4.44444E-2  1.00000E+0  0.00000E+0  4.00000E-1  2.00000E-2         Card(1)0304
  4.00000E-2  4.44444E-2  0.00000E+0  0.00000E+0  4.00000E-1  2.00000E-2         Card(1)0304
!    FCOEF       FEXPF       ROUGH     CHIMNY
  0.00000E+0  0.00000E+0  0.00000E+0                                             Card(1)0305
! NCHNF,IDC  UNFUEL       L          CLAD       TCCLAD       TAEM       TCFUEL
   5   0  0.00000E+0  1.00000E+0  5.00000E-3  1.00000E+2  1.00000E-2  5.00000E+1 Card(1)0306
!     AFF         DFF         PERF         XIF       WIDTHH      THICKH
  8.00000E-3  4.00000E-2  8.00000E-1  4.00000E-1  4.00000E-1  2.00000E-2         Card(4)0307
  8.00000E-3  4.00000E-2  8.00000E-1  8.00000E-1  4.00000E-1  2.00000E-2         Card(4)0307
  8.00000E-3  4.00000E-2  8.00000E-1  8.00000E-1  4.00000E-1  2.00000E-2         Card(4)0307
  8.00000E-3  4.00000E-2  8.00000E-1  8.00000E-1  4.00000E-1  2.00000E-2         Card(4)0307
  8.00000E-3  8.00000E-2  4.00000E-1  4.00000E-1  4.00000E-1  2.00000E-2         Card(4)0307
! CIRCF(I,K)
  4.00000E-1  4.00000E-1  4.00000E-1  4.00000E-1  0.00000E+0  0.00000E+0         Card(1)0308
! FACTF(I,J,K)
  4.00000E-1  8.00000E-1  1.20000E+0  1.60000E+0  0.00000E+0  0.00000E+0         Card(1)0309
!    DP0         DDP         DPMAX      POWER         TIN         P
  5.00000E-4  5.00000E-5  0.00000E+0  2.00000E+0  3.40500E+1  1.11400E-1         Card(2)0500
!   QFCLAD      QFCOOL     EPSLN     EPSLNI
  0.00000E+0  0.00000E+0                                                         Card(2)0500
! ITER   CONV         ETA         DPWR       PWRM
  20  1.00000E-4  3.25000E+1  0.00000E+0  0.00000E+0                              Card(1)0600
! NN
  11                                                                             Card(1)0700
!     ZR         QVZ
  0.00000E+0  5.19976E-2                                                         Card(11)0701
  1.00000E-1  6.59156E-2                                                         Card(11)0701
  2.00000E-1  7.77884E-2                                                         Card(11)0701
  3.00000E-1  8.76159E-2                                                         Card(11)0701
  4.00000E-1  9.53982E-2                                                         Card(11)0701
  5.00000E-1  1.01135E-1                                                         Card(11)0701
  6.00000E-1  1.04827E-1                                                         Card(11)0701
  7.00000E-1  1.06474E-1                                                         Card(11)0701
  8.00000E-1  1.06075E-1                                                         Card(11)0701
  9.00000E-1  1.03631E-1                                                         Card(11)0701
  1.00000E+0  9.91420E-2                                                         Card(11)0701
  0                                                                              Card(11)0702
```

Table 20.1 Fuel Assembly Design in Standard Test Problem 36 Used in PLTEMP/ANL Verification

	Design Parameter	Value
FUEL	Number of fuel assemblies	1
	Number of fuel plates /fuel assembly	4
	Number of axial nodes	10
	Number of stripe/plate	1
	Side plate on the left	Unfueled and un-finned
	Side plate on the right	No side plate
	Fuel length in the plate, m	1
	Fuel width in the plate, m	0.4
	Fuel thickness, m	0.01
	Fuel thermal conductivity, W/m-ºC	50
	Cladding thickness (one side), m	0.005
	Cladding thermal conductivity, W/m-ºC	100
FIN	Number of fins on each side of fuel plate	100
	Fin height, m	0.002
	Fin width at bottom, m	0.002
	Fin width at tip, m	0.002
COOLANT	Number of coolant channels	5
	Coolant thickness (without fins), m	0.02
	Total flow rate, kg/s	30
	Inlet temperature, ºC	34.05
	Coolant height above the core	0
	Bypass flow area	0
	Inlet pressure, MPa	0.1114
POWER	Total power, MW	2.0

Table 20.2 Comparison between PLTEMP/ANL and Spreadsheet Calculations of Heat Transfer Coefficient and Friction Factor in Finned Channels for Standard Test Problem 36

SPREADSHEET INPUT DATA IN GREEN BOXES					
PLTEMP axial node 10					
Channel	1	2	3	4	5
Flow,kg/s	6.55372	4.90182	4.9456	4.98536	8.61365
# fins	100	200	200	200	100
Nominal Wetted Perim, m	8.00E-01	8.00E-01	8.00E-01	8.00E-01	4.00E-01
Nominal Heated Perim, m	4.00E-01	8.00E-01	8.00E-01	8.00E-01	4.00E-01
Fin height, m	2.00E-03	2.00E-03	2.00E-03	2.00E-03	2.00E-03
BFIN, m	2.00E-03	2.00E-03	2.00E-03	2.00E-03	2.00E-03
TFIN, m	2.00E-03	2.00E-03	2.00E-03	2.00E-03	2.00E-03
AHELIX, radian	0.0000	0.0000	0.0000	0.0000	0.0000
Additional area Afin, m^2	4.00E-06	4.00E-06	4.00E-06	4.00E-06	4.00E-06
Additional Perim Pfin, m	4.00E-03	4.00E-03	4.00E-03	4.00E-03	4.00E-03
Afn, m^2	0.0080	0.0080	0.0080	0.0080	0.0080
Dhn, m	0.0400	0.0400	0.0400	0.0400	0.0800
Afa, m^2	7.6000E-03	7.2000E-03	7.2000E-03	7.2000E-03	7.6000E-03
Afc, m^2	7.2000E-03	6.4000E-03	6.4000E-03	6.4000E-03	7.2000E-03
Wetted Pa, m	1.2000E+00	1.6000E+00	1.6000E+00	1.6000E+00	8.0000E-01
Heated Pa, m	8.0000E-01	1.6000E+00	1.6000E+00	1.6000E+00	8.0000E-01
Coolant Temp, C	37.669	47.690	56.877	64.801	45.145
Viscosity, Pa-s	6.8495E-04	5.6606E-04	4.8590E-04	4.3190E-04	5.9170E-04
Th. cond, W/m-C	6.3192E-01	6.4407E-01	6.5398E-01	6.6171E-01	6.4117E-01
Sp. Heat, W/kg-C	4.1746E+03	4.1816E+03	4.1886E+03	4.1950E+03	4.1797E+03
Dha, m	2.5333E-02	1.8000E-02	1.8000E-02	1.8000E-02	3.8000E-02
Re,a	3.1894E+04	2.1649E+04	2.5446E+04	2.8857E+04	7.2787E+04
Pr	4.5250	3.6751	3.1121	2.7381	3.8572
Nu	119.887	81.430	86.704	91.099	217.629
ha, W/m^2-C	2.9905E+03	2.9137E+03	3.1501E+03	3.3489E+03	3.6720E+03
ha-n, W/m^2-C	5.9810E+03	5.8274E+03	6.3002E+03	6.6979E+03	7.3440E+03
PLTEMP-calc ha-n, W/m^2-C	5.9861E+03	5.8316E+03	6.3037E+03	6.6983E+03	7.3444E+03
% difference	0.086	0.072	0.055	0.007	0.005
Factor F*	1.0259784	1.0540926	1.0540926	1.0540926	1.0259784
fsmooth	0.0231247	0.0249880	0.0241933	0.0235921	0.0196068
fa	0.0237254	0.0263396	0.0255020	0.0248683	0.0201161
fa_avg	0.0235252	0.0263396	0.0255020	0.0248683	0.0201161
fa_n	0.0411580	0.0722624	0.0699643	0.0682258	0.0469250
PLTEMP-calculated fa-avg, Eq. (18.32)	0.0235166	0.0263333	0.0254983	0.0248692	0.0201177
% difference	-0.037	-0.024	-0.014	0.004	0.008

21 Verification of PLTEMPANL_4.2_r80_160720 for Finned Pin Problems

21.1 Introduction

The verification work reported here was done in August 2016. The Carnavos correlations [1] were implemented in PLTEMP/ANL to handle heat transfer and friction factor in nested tubes having longitudinal fins at both sides of the fuel tube [2]. However, the code could not be applied in finned solid pin problems because the fins existing on the inner surface of the tube geometry have restricted the shrinking of inner channel of the tube to approach the solid pin geometry. To resolve this problem, the code has been upgraded to the Version 4.2_r80_160720 so that if the inner flow area is set to a number smaller than 10^{-15} m^2, the number of fins in the inner channel is set to zero.

This chapter presents the verification of the applicability of PLTEMPANL _4.2_r80_160720 in finned pin problems by comparing the code's results with the hand calculations. Three test problems are set up for the comparison purpose:

(A) Pin diameter of 26 mm, fin height of 2 mm, and zero helix angle,

(B) Pin diameter of 90 mm, fin height of 10 mm, and helix angle of 30°, and

(C) Similar to case A but the coolant is bounded by an unfinned solid surface.

While the smaller size case A can be more similar to the reality, the larger size case B helps to evaluate the geometry processing related to the fins. Finally, case C is to check the code performance when one side of the coolant channel is a finned surface and the other is a smooth surface.

Using the water properties generated by the code, the differences in temperatures obtained by hand and code calculations for problems A, B and C are 0.003 %, 0.006 %, and 0.003 %, respectively. These very good agreements confirm that the PLTEMPANL_4.2_r80_160720 can handle longitudinal finned fuel pin problems appropriately.

21.2 Finned Fuel Pin Test Problems

Three test cases of longitudinal finned fuel pin are set up. The representative cross section of finned pin with the coolant is provided in Fig. 21.1 and the detail specifications of the current test problems are given in Table 21.1.

21.3 PLTEMP/ANL Model

The finned fuel pin is modeled by the tube geometry allowed in the code with the following approach (Fig. 21.2):

- Set the inner channel flow area (AFF_1) of the tube to a value smaller than 10^{-15} m^2 so that the number of fins belonging to this channel is set to zero by the code.
- Use 5-layer option (IEND = 1) and set the thickness of inner and outer clads of the tube as: $CLAD_1 = 10^{-15}$ m and $CLAD_2$ equals to the clad thickness of the fuel pin without fins.

- Arrange a very small inner radius of the tube $R_i = 10^{-6}$ m by specifying the input fuel meat centerline radius RMID $=(R_f + R_i)/2 = (R_c - \text{CLAD}_2 + R_i)/2$, where R_f, R_c are the outer radii of fuel meat and pin's clad without the fins, respectively.
- Set a low value for heat transfer coefficient at the inner interface of the tube (HBC = 1 W/m^{2}K) to make sure all the heat is transferred through the outer surface of the tube only.
- Use zero values for the thermal resistance and thickness of gaps between fuel and clad.

It should also be noticed that the input NFIN stands for the total number of fins belonging to a two-side heated coolant channel and therefore, it needs to be the double of the actual number of fins of the fuel pin.

With these settings, the inner surface temperature of the tube can be considered as the centerline temperature of the fuel pin. The PLTEMP/ANL model (input deck shown in Fig. 21.3) consists of 11 axial nodes and the data of the middle node (#6) will be used for the comparison with the hand calculation presented in the next section.

21.4 Hand Calculation Procedure

The objective of the hand calculation is to obtain the temperatures of fuel center line, fuel-clad interface, clad surface, and bulk coolant at the middle length of the fuel pin or channel. This procedure is performed through the following steps:

(1) All geometry parameters of the fuel pin and coolant channel with and without fins are determined.

(2) Bulk coolant temperature at the middle length (T_w) equals the coolant average temperature (T_{avg}) which is calculated by:

$$T_w = T_{avg} = 0.5 * (T_{in} + T_{out}) \tag{21.1}$$

$$T_{out} = T_{in} + \frac{P}{W\,Cp} \tag{21.2}$$

where T_{in}, T_{out} : inlet and outlet coolant temperatures
P : power of the fuel pin
W: coolant flow rate
Cp : coolant specific heat capacity obtained by NIST table (webbook.nist.gov).

Two-step iteration is performed for Cp and T_{out}.

(3) As will be seen in the Tables 21.2 and 21.3, the hand-calculated average temperatures agree very well with the code results and therefore, the water properties generated by the code are used in the hand calculation to facilitate the comparison between these methods.

(4) Heat transfer coefficient, h, is calculated using Carnavos correlation.

(5) Clad surface temperature is calculated based on T_{avg} and h:

$$T_c = T_w + \frac{P}{A_{ht}\,h} \tag{21.3}$$

where A_{ht} is the actual area of heated surface including fins.

(6) Fuel-clad interface temperature is:

$$T_{fc} = T_c + \frac{P}{2\pi\, L\, K_c} ln\left(\frac{R_c}{R_f}\right) \tag{21.4}$$

where L : length of fuel meat
K_f: clad thermal conductivity
R_f , R_c : outer radii of the fuel meat and clad without the fins

(7) Fuel centerline temperature is obtained based on the solution provided in [3]:

$$T_f = T_{fc} + \frac{P}{4\pi\, L\, K_f} \tag{21.5}$$

where K_f is the fuel thermal conductivity.

21.5 Comparison between Code and Hand Calculations

This section presents the comparison between the hand-calculated data and code results including the geometry parameters, heat transfer coefficients, and temperatures at the middle length of the fuel pin or coolant channel. The obtained data are given in Tables 21.2, 21.3 and 21.4 for the test cases A, B and C, respectively.

The very small differences in the geometry data point out that the geometry of the finned fuel pin can be modeled correctly by the tube geometry allowed by the code when the 5-layer of material option is used.

The excellent agreements in the obtained temperatures for the cases A, B, and C lead to the conclusion that the PLTEMPANL_4.2_r80_160720 is suitable to simulate the finned fuel pin problems.

21.6 REFERENCE

1. T. C. Carnavos, “Heat Transfer Performance of Internally Finned Tubes in Turbulent Flow”, Heat Transfer Eng., Vol. 1, No. 4, pp. 32-37 (Apr-June 1980).
2. A.P. Olson, M. Kalimullah, and E. E. Feldman, “A User’s Guide to the PLTEMP/ANL Code,” ANL/RERTR/TM-11-22, Version 4.2, Argonne National Laboratory, 9700 South Cass Avenue, Argonne, IL 60439, USA (July 25, 2016).
3. F. P. Incropera et al., *Introduction to Heat Transfer*, Fifth edition, pp. 133. (2007).

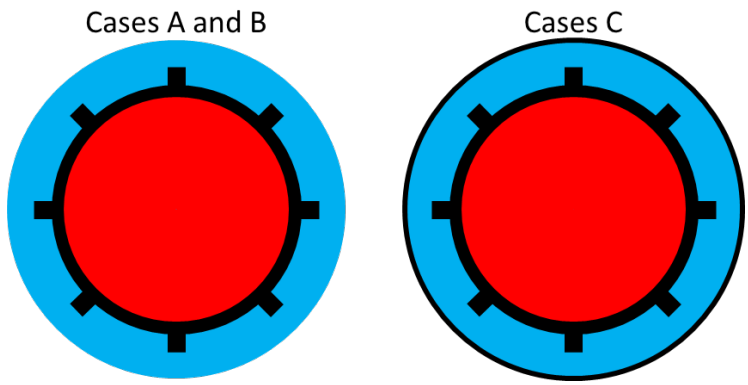

Figure 21.1 Representative Cross Section of Finned Fuel Pin Geometry

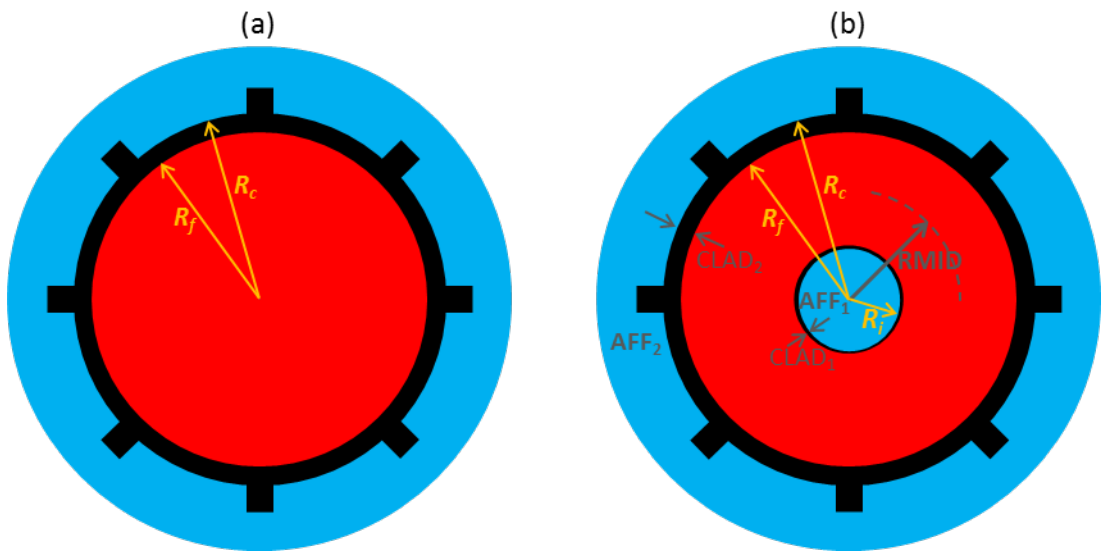

Figure 21.2 Original Finned Fuel Pin (a) is Simulated by Tube Geometry of PLTEMP/ANL (b)

Figure 21.3 Sample Input Data (Case A)

Input data deck:

```
VnV Finned Pin - Case A
  -1   0   0   1   0   0   2   1   1   0   0   1   0   1   0   2   0   0   0   0 Card(1)0200
  2.00000E-3  2.00000E-3  2.00000E-3  0.00000E+0 40                              Card(1)0202
   1   3  0.00000E+0  1.00000E+0  1.00000E+0  1.00000E+0   3   1  1.00000E+0     Card(1)0300
   1  12  1.00000E+0                                                             Card(1)0301
   1   1   1                                                                     Card(1)0302
  1.00000E+0                                                                     Card(1)0303
  1.13104E-3  5.53834E-2  1.00000E-1  0.00000E+0  1.13104E-1  1.00000E-2         Card(1)0304
  1.13104E-3  5.53834E-2  1.20000E+0  0.00000E+0  1.13104E-1  1.00000E-2         Card(1)0304
  1.13104E-3  5.53834E-2  1.00000E-1  0.00000E+0  1.13104E-1  1.00000E-2         Card(1)0304
  0.00000E+0  0.00000E+0  0.00000E+0                                             Card(1)0305
   2  0.00000E+0  1.20000E+0                                                     Card(1)0306A
   0  0.00000E+0  1.0000E-15  1.00000E+2  0.00000E+0  0.00000E+0  1.00000E+6     Card(1)0306B
   0  0.00000E+0  3.00000E-3  1.00000E+2  0.00000E+0  0.00000E+0  1.00000E+6     Card(1)0306B
  1.00000E-2  5.00000E+1                                                         Card(1)0306B
  1.0000E-16  2.00000E-6  6.28319E-6  0.00000E+0  3.14159E-6  1.00000E-6         Card(4)0307
  1.13104E-3  5.53834E-2  8.16877E-2  8.16877E-2  1.13104E-1  1.00000E-2         Card(4)0307
  3.14222E-2                                                                     Card(1)0308
  5.00100E-3                                                                     Card(1)0308A
  1.00000E+0                                                                     Card(1)0309
  1.00000E-4  2.00000E+0                                                         Card(4)0310
  1.00000E-1  0.00000E+0  1.20000E-1  5.00000E-2  4.00000E+1  1.20000E-1         Card(2)0500
  0.00000E+0  0.00000E+0                                                         Card(2)0500
  0.00000E+0  0.00000E+0                                                         Card(2)0501
  20  1.00000E-4  3.25000E+1  0.00000E+0  0.00000E+0                             Card(1)0600
axial.power.VnV.Finned.pin                                                       Card 702A
  1   1   1   1  1                                                              Card 702
```

Axial power profile:

```
  Axial power shapes for Finned pin VnV                                          Card703
  12                                                                             Card704
  0.00000E+0  9.09091E-2  1.81818E-1  2.72727E-1  3.63636E-1  4.54545E-1         Card704
  5.45455E-1  6.36364E-1  7.27273E-1  8.18182E-1  9.09091E-1  1.00000E+0         Card704
   1   1                                                                         Card705
    1.0                                                                          Card705
   1   1   1   1   1   1   1                                                     Card706
  1.00000E+0  1.00000E+0  1.00000E+0  1.00000E+0  1.00000E+0  1.00000E+0         Card706
  1.00000E+0  1.00000E+0  1.00000E+0  1.00000E+0  1.00000E+0  1.00000E+0         Card706
```

Table 21.1 Specifications of Finned Pin Test Problems

Parameter	Test case	
	A, C	B
Power (generated uniformly in fuel meat), kW	50	100
Total length of fuel pin, m	1.2	1.2
Length of the non-fuel part at each end, m	0.1	0.1
Outer diameter of pin without the fin, mm	26	90
Clad thickness, mm	3	5
Number of fins	20	10
Fin height, mm	2	10
Fin width at base, mm	2	15
Fin width at top, mm	2	12
Helix angle, ^{o}	0	30
Fuel thermal conductivity, W/mK	50	50
Clad thermal conductivity, W/mK	100	100
Thickness of the coolant channel, mm	10	15
Water mass flowrate, kg/s	2	3
Inlet temperature, ^{o}C	40	40
Flow direction	Upward	Upward
Inlet pressure, MPa	0.12	0.12

Table 21.2. Comparison between Hand Calculation and Code Results for Test Case A

Parameters	Hand calculation	PLTEMP v42_r80_160720	Relative difference (%)
Geometry			
Nominal heated perimeter without fins, m	0.08169	0.08169	0.00001
Heated perimeter with fins, m	0.16319	0.16319	0.00002
Flow area without fins, cm^2	11.31036	11.31040	0.00034
Actual flow area with fins, cm^2	10.50523	10.50527	0.00036
Core flow area within fin tips, cm^2	9.51953	9.51957	0.00041
Heat transfer coefficient at middle length			
Based on actual heated surface area, W/m^2K	5929.696	5929.700	0.0001
Temperature at the middle length			
Bulk coolant, ^{o}C	42.991	42.992	0.003
Clad surface, ^{o}C	86.050	86.052	0.002
Fuel-clad interface , ^{o}C	103.447	103.449	0.002
Fuel centerline, ^{o}C	169.761	169.763	0.001

Table 21.3. Comparison between Hand Calculation and Code Results for Test Case B

Parameters	Hand calculation	PLTEMP v42_r80_160720	Relative difference (%)
Geometry			
Nominal heated perimeter without fins, m	0.28275	0.28275	0.00013
Heated perimeter with fins, m	0.49536	0.49536	0.00008
Flow area without fins, cm^2	49.48103	49.48100	0.00005
Actual flow area with fins, cm^2	33.53022	33.53019	0.00008
Core flow area within fin tips, cm^2	16.93350	16.93347	0.00017
Heat transfer coefficient at middle length			
Based on actual heated surface area, W/m^2K	5641.540	5641.500	0.0007
Temperature at the middle length			
Bulk coolant, ^oC	43.987	43.990	0.006
Clad surface, ^oC	79.771	79.773	0.002
Fuel-clad interface , ^oC	98.516	98.519	0.003
Fuel centerline, ^oC	257.671	257.673	0.001

Table 21.4. Comparison between Hand Calculation and Code Results for Test Case C

Parameters	Hand calculation	PLTEMP v42_r80_160720	Relative difference (%)
Geometry			
Nominal heated perimeter without fins, m	0.08169	0.08169	0.00001
Heated perimeter with fins, m	0.16319	0.16319	0.00002
Flow area without fins, cm^2	11.31036	11.31040	0.00034
Actual flow area with fins, cm^2	10.50523	10.50527	0.00036
Core flow area within fin tips, cm^2	9.51953	9.51957	0.00041
Actual Reynolds number with fins	42003.1	42003.3	0.00052
Prandtl number	4.05196	4.05192	0.00100
Heat transfer coefficient at middle length			
Based on actual heated surface area, W/m^2K	6731.661	6731.700	0.0006
Temperature at the middle length			
Bulk coolant, ^oC	42.991	42.992	0.003
Clad surface, ^oC	80.920	80.922	0.003
Fuel-clad interface , ^oC	98.317	98.319	0.002
Fuel centerline, ^oC	164.632	164.634	0.002

22 Verification of the Heat Transfer Method for Fuel Assemblies Made of Multiple Five-Layer Plates and the Calculation of ONBR and OFIR in PLTEMP/ANL

22.1 Introduction and Executive Summary

The verification work reported here was done in January 2017. The verification of three PLTEMP/ANL code capabilities is documented here: the capabilities 2, 7 and 8 listed in Section 1.2 of Chapter 1. The PLTEMP/ANL capability 2, i.e., the heat transfer method for calculating temperature distribution in a fuel assembly made of multiple five-layer fuel plates, with plate-by-plate axial power shape (described in Appendix XIII of the Code User's Guide [1]), is verified in Section 22.3 by comparing the code with solutions obtained by a spreadsheet developed for this purpose (see Section 22.2).

The PLTEMP/ANL code calculates the safety margin to onset of nucleate boiling ratio (ONBR) using the Bergles-Rohsenow correlation[2] by two approaches[1], the first based on the cladding-surface-to-coolant-inlet temperature difference, and the second based on the cladding-surface heat flux. The code calculates the safety margin to onset of Ledinegg flow instability ratio (OFIR) using the Whittle and Forgan criterion[3]. The spreadsheet developed for calculating temperature distribution was further developed to calculate the ONBR (by both approaches) and the OFIR. The ONBR calculation (PLTEMP/ANL capability 7) and the OFIR calculation (PLTEMP/ANL capability 8) are also verified here (in Sections 22.4 and 22.5) by comparing the code with their values obtained by the spreadsheet developed for this purpose.

The temperature distributions calculated by the code and the spreadsheet are compared for five test problems (Problems 38, 39, 40, 41, and 42), exercising an increasing number of code features. The input data common to all these problems is given in Table 22.1. The input data varying from problem to problem (i.e., the thickness and thermal conductivity of fuel plate material layers and coolant channels, and the radial power factors of fuel plates) are given in Figs. 22.1 to 22.5. These figures show top views of fuel assemblies that have vertical flow. Each problem has two types of fuel assembly, with two flat plates (with the fuel meat shown in red, the cladding shown in orange, and the yellow interlayer between the meat and cladding) and three coolant channels (D_2O coolant shown in green) in each fuel assembly. The flow rate in each coolant channel is specified. There is an unfueled width on each edge of the fuel plate, and therefore each coolant channel is divided into three sub-channels as shown in Figs. 22.1 to 22.5.

The coolant thermal properties in the spreadsheet are calculated using equations fitted to the temperature-dependent property values in the PLTEMP/ANL code (see Table 22.2). The coolant thermal properties in the spreadsheet are close but not identical to those in PLTEMP/ANL. The axial power shapes by fuel plate for each problem are given in Tables 22.3 and 22.4. The method of calculating coolant, cladding, and fuel meat temperatures on the spreadsheet is described in Section 22.2. The test problems, the calculated temperature distributions, and their comparisons are described in Section 22.3. Because the PLTEMP/ANL model of the fuel plates assumes that heat transfer is only in the direction from the fuel meat to the bulk coolant, the unfueled width on each edge of the fuel plate is not included in the heat transfer solution on the spreadsheet. The temperature distributions obtained by the spreadsheet and the PLTEMP/ANL code for the five test

problems (Problems 38, 39, 40, 41, and 42) are given in 15 tables (Tables 22.5 to 22.19). These tables also include the values of heat transfer coefficient at the cladding-coolant interfaces.

Verification of the Heat Transfer Method: For verifying the PLTEMP/ANL heat transfer method for a fuel assembly made of multiple five-layer plates, the steady-state temperature distributions obtained by the code and the spreadsheet were compared for each problem. The temperature difference between the code and the spreadsheet is summarized below.

Test Problem	Max Absolute Temperature Difference, ºC	RMS Temperature Difference, ºC	Max Absolute Difference in Heat Transfer Coefficient, W/m^2-ºC	RMS Difference in Heat Transfer Coef., W/m^2-ºC
Problem 38	0.18	0.14	25.3	19.2
Problem 39	0.20	0.12	39.5	20.7
Problem 40	0.20	0.12	41.5	20.0
Problem 41	0.61	0.18	60.6	27.4
Problem 42	0.61	0.14	44.3	18.3

The temperature differences are small. They are mainly due to the difference in the coolant thermal properties used in the spreadsheet and the PLTEMP/ANL code which gives rise to slightly different heat transfer coefficients in the two calculations (see Tables 22.5 to 22.19). This comparison provides a verification of the PLTEMP/ANL heat transfer method for calculating temperature distribution in a fuel assembly made of multiple five-layer fuel plates, i.e., capability 2 listed in Section 1.2 of Chapter 1.

Verification of the ONBR: For verifying the PLTEMP/ANL-calculated safety margin of ONBR, its values obtained by the code and the spreadsheet were compared for all 10 axial segments of all 8 fuel plate surfaces in the test Problem 42 (see Tables 22.22 to 22.27). As mentioned above, the code calculates ONBR using two approaches (defined in Fig. 22.6), the first based on the cladding-surface-to-coolant-inlet temperature difference, and the second based on the cladding-surface heat flux. The ONBR calculated by each approach is verified. The maximum absolute difference in the ONBR obtained by the first approach, between the code and the spreadsheet is 0.83%.

During the verification of the ONBR, it was found that the PLTEMP/ANL subprogram ONBRATIO used for calculating the ONBR by the second approach always used the light water saturation temperature (T_{sat}) for heavy water T_{sat}. This discrepancy of the code was corrected, and both the incorrect and correct code versions are verified here. The maximum absolute difference in the ONBR obtained by the second approach, between the spreadsheet and the code *before correction* is 1.32%. The maximum absolute difference in the ONBR obtained by the second approach, between the spreadsheet and the code *after correction* is 0.57%. The difference in the safety margins between the code and the spreadsheet is summarized below for Problem 42.

Test Problem	Safety Margin Verified	Max Absolute Difference
Problem 42	ONBR by first approach	0.83 %
Problem 42	ONBR by second approach, before correction (using H_2O T_{sat})	1.32 %
Problem 42	ONBR by second approach, after code correction (using D_2O T_{sat})	0.57 %
Problem 42	OFIR	0.00445

The small differences in the corrected code are mainly due to the difference in the coolant thermal properties used in the spreadsheet and the code. These comparisons provide a verification of the PLTEMP/ANL calculation of the safety margin ONBR, i.e., capability 7 listed in Section 1.2 of Chapter 1.

Verification of the OFIR: For verifying the PLTEMP/ANL-calculated safety margin of OFIR, its values obtained by the code and the spreadsheet were compared for all six coolant channels in the test Problem 42 (see Table 22.28). The maximum absolute difference in OFIR between the code and the spreadsheet is 0.00445. This small difference is mainly due to the difference in the coolant thermal properties used in the spreadsheet and the code. The comparison provides a verification of the PLTEMP/ANL calculation of the safety margin OFIR, i.e., capability 8 listed in Section 1.2 of Chapter 1.

The PLTEMP/ANL code with the saturation temperature in subprogram ONBRATIO corrected is saved in the code version *pltempv42_r82_170131*.

22.2 Development of a Spreadsheet for Calculating Temperature Distribution in Fuel Assemblies Made of Five-Layer Plates with Plate-by-Plate Axial Power Shape

A spreadsheet was developed to calculate the temperature distribution in a fuel assembly made of two five-layer flat fuel plates by assuming a position ($X_{left,1}$ and $X_{left,2}$) of the peak temperature in the meat thickness of each plate of the fuel assembly, and then iteratively minimizing the difference between (1) the peak temperature in the meat thickness of a plate calculated from the left side of the plate, and (2) that calculated from the right side of the plate. This is the Broyden method implemented in PLTEMP/ANL, which is described in Section 22.2.1.

The plate width is divided into only 3 sub-channels: (1) the nearer unfueled width of the fuel plate defines the width of sub-channel 1 (see Fig. 22.1), (2) the whole fueled width of the plate defines the width of sub-channel 2, and (3) the farther unfueled width of the plate defines the width of sub-channel 3. The fuel plate is divided axially into ten segments in the spreadsheet to account for the axial power shape. The D_2O thermal properties used in the spreadsheet are given in Section 22.2.2.

22.2.1 Method Used in the Spreadsheet to Calculate Temperature Distribution

The axial conduction is ignored in the solid and liquid regions, in both the PLTEMP/ANL code solution and the spreadsheet solution. This allows the inlet axial node to be solved independently of the downstream axial nodes. The outlet coolant temperature of inlet axial node is the inlet coolant temperature of the second axial node. Thus, it is possible to solve each axial node in succession, independently of the axial nodes that are downstream of the axial node being solved.

The following steps are used in the spreadsheet to calculate the meat peak temperature from the left and right sides in each plate *k* at the mid-height of each axial segment *j*.

Step 1. Calculate the average power density q_{avg} in the meat of the two-assembly problem, starting from the input geometry and the total power in the problem, as shown by Eq. (22.1). Using the average power density q_{avg} in the problem and the input radial power factors, calculate the power density $q_{k,j}$ in the meat of each plate k, as shown by Eq. (22.2). Calculate the power $P_{k,j}$ in an axial segment j of fuel plate k, as shown by Eq. (22.3a) which simplifies to Eq. (22.3b). The symbols are defined in the nomenclature given at the end.

$$\text{Fuel meat volume} = L_h P_h \sum_{\text{k, all assemblies}} t_k$$

$$q_{avg} = \frac{POW}{L_h P_h \sum_{\text{k, all assemblies}} t_k} \tag{22.1}$$

$$q_{k,j} = \frac{p_j * POW * FACTF_{i,k}}{L_h P_h \left(\sum_{\text{k, all assemblies}} t_k \right)} \tag{22.2}$$

$$P_{k,j} = (z_{j+1} - z_j) L_h P_h t_k * \frac{p_j * POW * FACTF_{i,k}}{L_h P_h \left(\sum_{\text{k, all assemblies}} t_k \right)} \tag{22.3a}$$

$$P_{k,j} = \frac{p_j * POW * FACTF_{i,k} * (z_{j+1} - z_j) t_k}{\left(\sum_{\text{k, all assemblies}} t_k \right)} \tag{22.3b}$$

Step 2. Initialize all 40 elements of array $X_{left,k,j}$ to 0.5 (k = 1 and 2, and j = 1, 2, 3, … 10).

Step 3. Stating with $P_{k,j}$ and an assumed value of the peak meat temperature position $X_{left,k,j}$ in axial segment j of plate k, calculate the heat flux $Q_{k,j,flux,left}$ going to the left of the meat in plate k (into coolant channel k) and the heat flux $Q_{k,j,flux,right}$ going to the right of the meat in the plate (into coolant channel k+1). The heat flux $Q_{k,j,flux,left}$ is given by Eq. (22.4) and the heat flux $Q_{k,j,flux,right}$ is given by Eq. (22.5).

$$Q_{k,j,flux,left} = \frac{P_{k,j} X_{left,k,j}}{(z_{j+1} - z_j) L_h P_h} \tag{22.4}$$

$$Q_{k,j,flux,right} = \frac{P_{k,j} (1 - X_{left,k,j})}{(z_{j+1} - z_j) L_h P_h} \tag{22.5}$$

Step 4. Calculate the total power $P_{chan,k,j}$ to axial segment j of sub-channel 2 of channel k from fuel plates on both sides. In general, sub-channel 2 of channel k gets the power $P_{k,j}X_{left,k,j}$ from fuel plate k and the power $P_{k-1,j}$ $(1-X_{left,k-1,j})$ from fuel plate k-1. In particular, it means that sub-channel 2 of channel 1 gets the power $P_{1,j}X_{left,1,j}$ from fuel plate 1; sub-channel 2 of channel 2 gets the power $P_{2,j}X_{left,2,j}$ from fuel plate 2 and the power $P_{1,j}$ $(1-X_{left,1,j})$ from fuel plate 1; and sub-channel 2 of channel 3 gets the power $P_{2,j}$ $(1-X_{left,2,j})$ from fuel plate 2, as shown by Eq. (22.6). Using the power $P_{chan,k,j}$, calculate the sub-channel 2 coolant temperature at the axial segment exit in each channel, as shown by Eq. (22.7). Calculate the sub-channel 2 coolant temperature at axial segment mid-height by Eq. (22.8).

$$P_{chan,k,j} = \begin{cases} P_{1,j}\ X_{left,1,j} & \text{if} \quad k=1 \\ P_{2,j}\ X_{left,2,j} + P_{1,j}\ (1-X_{left,1,j}) & \text{if} \quad k=2 \\ P_{2,j}\ (1-X_{left,2,j}) & \text{if} \quad k=3 \end{cases} \tag{22.6}$$

$$T_{k,j,c,exit} = T_{k,j,c,inlet} + \frac{P_{chan,k,j}}{W_{sub\,2,k}\ C_p(T_{k,c,inlet})} \tag{22.7}$$

$$T_{k,j,c} = 0.5(T_{k,j,c,inlet} + T_{k,j,c,exit}) \tag{22.8}$$

Step 5. Use Eqs. (22.9), (22.10), and (22.11) to calculate the coolant viscosity μ(T), specific heat $C_p(T)$, and thermal conductivity K(T), at the coolant temperature at the axial segment j inlet, in sub-channels 2 of each coolant channel. Using Eq. (22.12), calculate the corresponding Reynolds number Re, Prandtl number Pr, and Nusselt number using the Dittus-Boelter correlation. The subscripts k and j have been dropped from Eqs. (22.9) to (22.12) for clarity. Using Eqs. (22.13) and (22.14), calculate the cladding-to-coolant convective heat transfer coefficients, $h_{k,j,left}$ and $h_{k,j,right,}$ on the left and right sides of fuel plate k in axial segment j.

$$\mu(T) = \exp\left(\frac{a_1 + a_2 T}{1 + a_3 T + a_4 T^2}\right) \quad \text{Pa}-\text{s} \tag{22.9}$$

$$C_p(T) = 1000\left(a_1 + a_2 T + a_3 T^2 + a_4 T^3 + a_5 T^4 + a_6 T^5\right) \quad \text{J/kg}-{}^\circ\text{C} \tag{22.10}$$

$$K(T) = a_1 + a_2 T + a_3 T^2 + \frac{a_4}{1 + a_5 T} \quad \text{W/m}-{}^\circ\text{C} \tag{22.11}$$

$$Re = \frac{W_k\ D_{h,k}}{\mu\ A_{f,k}} \quad , \quad Pr = \frac{\mu\ C_p}{K} \tag{22.12}$$

$$h_{k,j,left} = 0.023\ Re^{0.8}\ Pr^{0.4}\ \frac{K}{D_{h,k}} \qquad (k = 1, 2) \tag{22.13}$$

$$h_{k,j,right} = 0.023\ Re^{0.8}\ Pr^{0.4}\ \frac{K}{D_{h,k+1}} \qquad (k = 1, 2) \tag{22.14}$$

Step 6. Calculate the peak meat temperature $T_{k,j,peak,left}$ in fuel plate k (k = 1 and 2) at mid-height of axial segment j, starting from the coolant temperature $T_{k,j,c}$ in sub-channel 2 on the left side of the plate k, as shown by Eq. (22.15). Calculate the peak meat temperature $T_{k,j,peak,right}$ in fuel plate k starting from the coolant temperature $T_{k+1,j,c}$ in sub-channel 2 on the right side of the plate k, as shown by Eq. (22.16).

$$T_{k,j,peak,left} = T_{k,j,c} + Q_{k,j,flux,left}\left\{\frac{1}{h_{k,j,left}} + \frac{t_{k,left,c}}{K_{k,left,c}} + \frac{t_{k,left,g}}{K_{k,left,g}}\right\} + \frac{q_{k,j}\left\{X_{left,k,j}\ t_{k,m}\right\}^2}{2\,K_{k,m}} \tag{22.15}$$

$$T_{k,j,peak,right} = T_{k+1,j,c} + Q_{k,j,flux,right}\left\{\frac{1}{h_{k,j,right}} + \frac{t_{k,right,c}}{K_{k,right,c}} + \frac{t_{k,right,g}}{K_{k,right,g}}\right\} + \frac{q_{k,j}\left\{(1 - X_{left,k,j})\ t_{k,m}\right\}^2}{2\,K_{k,m}} \tag{22.16}$$

Step 7. Using the SOLVER capability of spreadsheet, adjust the assumed values of $X_{left.k,j}$ in order to minimize the following quantity where the peak meat temperatures are given by Eqs. (22.15) and (22.16).

$$\textbf{\$BO\$50} = \sum_{\text{all assemblies}} \sum_{k=\text{all plates}} \sum_{j=\text{all segments}} \left(T_{k,j,peak,left} - T_{k,j,peak,right}\right)^2$$

This solves the coupled set of 40 equations in 40 unknowns $X_{left,k,j}$. The solution obtained gives the temperature distribution in the coolant, cladding and meat of the fuel assembly.

22.2.2 D_2O Coolant Thermal Properties Used in the Spreadsheet

The data for heavy water (D_2O) density, absolute viscosity, specific heat, enthalpy, and thermal conductivity at a selected pressure of 0.36 MPa were obtained from the PLTEMP/ANL code in tabular form as functions of temperature. The data for D_2O saturation temperature as a function of pressure was also obtained from the PLTEMP/ANL code in tabular form. Simple correlations were

fitted to the tabular data for use in the spreadsheet for calculating temperature distribution in fuel assemblies. These correlations are given in Table 22.2.

22.3 Verification of PLTEMP/ANL Heat Transfer Method for an Assembly of Five-Layer Fuel Plates

The heat transfer method in the PLTEMP/ANL version 4.2 code for calculating temperature distribution in a fuel assembly made of multiple five-layer fuel plates, is verified here by comparing the code with the spreadsheet described in Section 22.2. The temperature distributions calculated by the code and the spreadsheet are compared for five test problems, i.e., test Problems 38, 39, 40, 41, and 42 whose input data is given in Tables 22.1, 22.3 and 22.4. These problems exercise an increasing number of code features as shown in Figs. 22.1 to 22.5. For the first problem, Number 38, the fuel plate geometry and thermal conductivities are symmetric about the fuel meat and the same axial power shape and power are used for each fuel plate. With succeeding problems these symmetries and similarities are gradually removed. In the fifth problem, Number 42, the fuel plate geometry and thermal conductivities are asymmetric about the fuel meat and the axial power shape and power differ from plate to plate. Atypical extremes in problem parameters are used to uncover potential errors of the code.

Each problem has two types of fuel assembly, with two flat fuel plates and three coolant channels (D_2O coolant) in each fuel assembly. Each fuel plate is made of 5 material layers (left cladding, left cladding-meat interlayer, fuel meat, right cladding-meat interlayer, and right cladding). The thickness and thermal conductivity of each layer, and the radial power factor ($FACTF_{i,k}$) of each fuel plate are given in Figs. 22.1 to 22.5. There is an unfueled width on each edge of the fuel plate, and therefore each coolant channel is divided into three sub-channels. The flow rate in each coolant channel is specified.

The temperature difference between the code and the spreadsheet for each problem is described below in Sections 22.3.1 to 22.3.5. The files of the spreadsheet solutions of these five test problems, the PLTEMP/ANL input data files, the input axial power shape files, and the PLTEMP/ANL output files are named as follows:

Spreadsheet Solutions

Test Problem	Spreadsheet Filename
Problem 38	spreadsheet.solution.stdprob38.5-layers.xlsx
Problem 39	spreadsheet.solution.stdprob39.5-layers.xlsx
Problem 40	spreadsheet.solution.stdprob40.5-layers.xlsx
Problem 41	spreadsheet.solution.stdprob41.5-layers.xlsx
Problem 42	(1) spreadsheet.solution.stdprob42.5-layers.with.ONBR.and.OFIR.compared.to. PLTEMP.with.corrected.subr.onbratio.xlsx (2) spreadsheet.solution.stdprob42.5-layers.with.ONBR.and.OFIR.compared.to. PLTEMP.with.incorrect.subr.onbratio.xlsx

PLTEMP/ANL Input and Output Files

Test Problem	PLTEMP/ANL Input	PLTEMP/ANL Output
Problem 38	input.stdprob38.5-layers.linear-axial axial.power.stdprob38.linear	output.stdprob38.5-layers.linear-axial
Problem 39	input.stdprob39.5-layers.linear-axial axial.power.stdprob39.linear	output.stdprob39.5-layers.linear-axial
Problem 40	input.stdprob40.5-layers.linear-axial axial.power.stdprob40.linear	output.stdprob40.5-layers.linear-axial
Problem 41	input.stdprob41.5-layers.axial.by.plate axial.power.stdprob41	output.stdprob41.5-layers.axial.by.plate
Problem 42	input.stdprob42.5-layers.axial.by.plate axial.power.stdprob42	output.stdprob42.5-layers.axial.by.plate

22.3.1 Problem 38 with Symmetrical Fuel Plates and Linear Axial Power Shape

The test Problem 38 has the following features, as shown in Fig. 22.1.
(1) The thicknesses of the five material layers in each fuel plate are symmetrical.
(2) The thermal conductivities of the five material layers in each fuel plate are symmetrical.
(3) The power of each plate is the same (one-fourth of the input total power in the problem).
(4) The two fuel plates in a fuel assembly are identical.
(5) The fuel plates of assembly 1 are different from those of assembly 2, and
(6) The axial power shape is the same for all fuel plates, and varies linearly from 0.550 to 1.450, as shown in Table 22.3.

The results of the spreadsheet and PLTEMP/ANL calculations for test Problem 38 are given in Tables 22.5, 22.6, and 22.7. The meat thickness fraction measured from the left side of the meat at which the meat temperature peaks across its thickness, $X_{left,1,j}$, is compared in Table 22.5 for all four fuel plates for all 10 axial segments. The comparison is good (0.5000 versus 0.4999).

For problem 38, Table 22.6 shows the spreadsheet-calculated distributions of heat transfer coefficients in all coolant channels, coolant temperatures in all coolant channels, left and right cladding surface temperatures of all fuel plates, left and right meat surface temperatures of all fuel plates, and meat peak temperatures of all fuel plates. Table 22.7 shows the code-calculated distributions of the same quantities. The maximum absolute difference between the temperature distributions calculated by PLTEMP/ANL and the spreadsheet is 0.18 ºC. The RMS difference between the temperature distributions is 0.14 ºC. The comparison between the two temperature distributions is good.

22.3.2 Problem 39 with Unsymmetrical Plate 1 in Assembly 1 and Linear Axial Power Shape

The test Problem 39 has the following features, as shown in Fig. 22.2.
(1) The thicknesses of the five material layers in each fuel plate are symmetrical.
(2) The thermal conductivities of the five material layers in fuel plate 1 of assembly 1 are unsymmetrical. The thermal conductivities of the five material layers in fuel plate 2 of assembly 1 and in each plate of assembly 2 are symmetrical.
(3) The power of each plate is the same (one-fourth of the input total power in the problem).

(4) The two fuel plates in assembly 1 differ from each other. The two fuel plates in assembly 2 are identical.
(5) The fuel plates of assembly 1 are different from those of assembly 2, and
(6) The axial power shape is the same for all fuel plates, and varies linearly from 0.550 to 1.450, as shown in Table 22.3.

The results of the spreadsheet and PLTEMP/ANL calculations for test Problem 39 are given in Tables 22.8, 22.9, and 22.10. The meat thickness fraction measured from the left side of the meat at which the meat temperature peaks across its thickness, $X_{left,1,j}$, is compared in Table 22.8 for all four fuel plates for all 10 axial segments. The comparison is good (0.2351 versus 0.22350).

For problem 39, Table 22.9 shows the spreadsheet-calculated distributions of heat transfer coefficients in all coolant channels, coolant temperatures in all coolant channels, left and right cladding surface temperatures of all fuel plates, left and right meat surface temperatures of all fuel plates, and meat peak temperatures of all fuel plates. Table 22.10 shows the code-calculated distributions of the same quantities. The maximum absolute difference between the temperature distributions calculated by PLTEMP/ANL and the spreadsheet is 0.20 ºC. The RMS difference between the temperature distributions is 0.12 ºC. The comparison between the two temperature distributions is good.

22.3.3 Problem 40 with Unsymmetrical Plates in Assembly 1 and Linear Axial Power Shape

The test Problem 40 has the following features, as shown in Fig. 22.3.
(1) The thicknesses of the five material layers in fuel plate 2 of assembly 1 are unsymmetrical. The thicknesses of the five material layers in fuel plate 1 of assembly 1 and in each fuel plate of assembly 2 are symmetrical.
(2) The thermal conductivities of the five material layers in each fuel plate of assembly 1 are unsymmetrical. The thermal conductivities of the five material layers in each plate of assembly 2 are symmetrical.
(3) The power of each plate is the same (one-fourth of the input total power in the problem).
(4) The two fuel plates in assembly 1 differ from each other. The two fuel plates in assembly 2 are identical.
(5) The fuel plates of assembly 1 are different from those of assembly 2, and
(6) The axial power shape is the same for all fuel plates, and varies linearly from 0.550 to 1.450, as shown in Table 22.3.

The results of the spreadsheet and PLTEMP/ANL calculations for test Problem 40 are given in Tables 22.11, 22.12, and 22.13. The meat thickness fraction measured from the left side of the meat at which the meat temperature peaks across its thickness, $X_{left,1,j}$, is compared in Table 22.11 for all four fuel plates for all 10 axial segments. The comparison is good (0.199969 versus 0.1996).

For problem 40, Table 22.12 shows the spreadsheet-calculated distributions of heat transfer coefficients in all coolant channels, coolant temperatures in all coolant channels, left and right cladding surface temperatures of all fuel plates, left and right meat surface temperatures of all fuel plates, and meat peak temperatures of all fuel plates. Table 22.13 shows the code-calculated

distributions of the same quantities. The maximum absolute difference between the temperature distributions calculated by PLTEMP/ANL and the spreadsheet is 0.20 ºC. The RMS difference between the temperature distributions is 0.12 ºC. The comparison between the two temperature distributions is good.

22.3.4 Problem 41 with Unsymmetrical Plates in Both Assemblies and Plate-by-Plate Axial Power Shape

The test Problem 41 has the following features, as shown in Fig. 22.4.

(1) The thicknesses of the five material layers in each fuel plate in both assemblies are unsymmetrical.
(2) The thermal conductivities of the five material layers in each fuel plate in both assemblies are unsymmetrical.
(3) The power of each plate is the same (one-fourth of the input total power in the problem).
(4) The two fuel plates in assembly 1 differ from each other. Also, the two fuel plates in assembly 2 differ from each other.
(5) The fuel plates of assembly 1 are different from those of assembly 2, and
(6) The axial power shape is linear and changes from plate to plate, as shown in Table 22.4.

The results of the spreadsheet and PLTEMP/ANL calculations for test Problem 41 are given in Tables 22.14, 22.15, and 22.16. The meat thickness fraction measured from the left side of the meat at which the meat temperature peaks across its thickness, $X_{left,1,j}$ **,** is compared in Table 22.14 for all four fuel plates for all 10 axial segments. The comparison is good (0.25186 versus 0.2518).

For problem 41, Table 22.15 shows the spreadsheet-calculated distributions of heat transfer coefficients in all coolant channels, coolant temperatures in all coolant channels, left and right cladding surface temperatures of all fuel plates, left and right meat surface temperatures of all fuel plates, and meat peak temperatures of all fuel plates. Table 22.16 shows the code-calculated distributions of the same quantities. The maximum absolute difference between the temperature distributions calculated by PLTEMP/ANL and the spreadsheet is 0.61 ºC. The RMS difference between the temperature distributions is 0.18 ºC. The comparison between the two temperature distributions is good.

22.3.5 Problem 42 with Unsymmetrical and Unequal Power Plates in Both Assemblies and Plate-by-Plate Axial Power Shape

The test Problem 42 has the following features, as shown in Fig. 22.5.

(1) The thicknesses of the five material layers of a fuel plate are unsymmetrical,
(2) The thermal conductivities of the five material layers of a fuel plate are unsymmetrical,
(3) The power of each plate is different from that of others,
(4) The two fuel plates in a fuel assembly are different,
(5) The fuel plates of assembly 1 are different from those of assembly 2, and
(6) The axial power shape is linear and changes from plate to plate, as shown in Table 22.4.

The results of the spreadsheet and PLTEMP/ANL calculations for the test Problem 42 are given in Tables 22.17, 22.18, and 22.19. The meat thickness fraction measured from the left side of the

meat at which the meat temperature peaks across its thickness, $X_{left,1,j}$, is compared in Table 22.17 for all four fuel plates for all 10 axial segments. The comparison is good (0.2490 versus 0.2489).

For problem 42, Table 22.18 shows the spreadsheet-calculated distributions of heat transfer coefficients in all coolant channels, coolant temperatures in all coolant channels, left and right cladding surface temperatures of all fuel plates, left and right meat surface temperatures of all fuel plates, and meat peak temperatures of all fuel plates. Table 22.19 shows the code-calculated distributions of the same quantities. The maximum absolute difference between the temperature distributions calculated by PLTEMP/ANL and the spreadsheet is 0.61 ºC. The RMS difference between the temperature distributions is 0.14 ºC. The comparison between the two temperature distributions is good.

22.4 Verification of Onset of Nucleate Boiling Ratio

The safety margin, onset of nucleate boiling ratio (ONBR), is calculated by the PLTEMP/ANL code, using the Bergles-Rohsenow correlation that is written as follows. The correlation is based on experiments conducted with water on stainless steel and nickel surfaces, covering a range of pressures from 1.02 to 138 bar.

$$q_{onb}\ (\mathrm{MW/m^2}) = 1.0829\times10^{-3}\ P^{1.156}\left[1.8(T_{onb}-T_{sat})\right]^{(2.16/P^{0.0234})} \tag{22.17}$$

where

P	= Coolant absolute pressure, bar
q_{onb}	= Cladding-to-coolant heat flux (MW/m^2) that causes onset of nucleate boiling at a location with cladding surface temperature T_{onb} (ºC) and absolute pressure P (bar)
T_{sat}	= Coolant saturation temperature at the ONB location, °C
T_{onb}	= Cladding surface temperature (ºC) at which the designed operating heat flux q_{op} will cause onset of nucleate boiling at the axial location.

Equation (22.17) can be rewritten as:

$$T_{onb} = T_{sat} + \frac{1}{1.8}\left[\frac{q_{onb}}{0.0010829\ \ P^{1.156}}\right]^{(P^{0.0234}/2.16)} \tag{22.18}$$

As defined in Fig. 22.6, two approaches for calculating ONBR are implemented in the code, yielding *slightly different* values: one good for the onset of nucleate boiling at constant heat flux, i.e., when the flow (or the film coefficient) is decreased in a series of reactor designs at constant reactor power and assumes that ONB is reached by going from Point A to Point D in Fig. 22.6. The other is good for the onset of nucleate boiling when the reactor power is increased in a series of reactor designs at constant core flow and assumes that ONB is reached by going from Point A to Point E in Fig. 22.6.

Verification of ONBR by the First Approach

The ONBR calculated using the first approach is commonly used by reactor analysts; is printed in the main temperature table in the code output file; and is used in searches performed by the code. This ONBR is defined as

$$\mathrm{ONBR} = \frac{T_{onb,D} - T_{in}}{T_{w,op} - T_{in}} \tag{22.19}$$

where the ONB temperature $T_{onb,D}$ is calculated using Eq. (22.18) by setting q_{onb} to q_{op} and taking T_{onb} to be $T_{onb,D}$ for a given design operating condition being considered:

T_{in} = Coolant inlet temperature, ºC
$T_{w,op}$ = Designed operating cladding surface temperature at the axial location where ONBR is being calculated, ºC
q_{op} = Designed operating heat flux at the axial location where ONBR is being calculated, MW/m^2
$T_{onb,D}$ = Cladding surface temperature (ºC) at which the designed operating heat flux q_{op} will cause onset of nucleate boiling at the axial location. This cladding surface temperature is represented by the point D in Fig. 22.6.

For verifying the ONBR by the first approach, the code-calculated ONBRs on the left and right sides of all four fuel plates at each axial segment center in the test Problem 42, were compared with those calculated on the Excel spreadsheet. The spreadsheet uses Eq. (22.19) to calculate the ONB temperature $T_{onb,D}$ corresponding to the operating heat flux at the *center* of each axial segment. The operating cladding surface temperatures and heat fluxes (q_{op} and $T_{w,op}$) needed for this calculation are shown in Tables 22.20 and 22.21 for fuel assemblies 1 and 2 of Problem 42. These data were calculated during the verification of temperature distribution, and are already available on the spreadsheet. The axial distribution of pressure is not calculated on the spreadsheet; it is just copied to the spreadsheet from the PLTEMP/ANL code output. The spreadsheet then calculates the ONBR using Eq. (22.18).

Tables 22.22 and 22.23 show a comparison between the ONBRs calculated by the PLTEMP/ANL code and the spreadsheet for fuel assemblies 1 and 2 of Problem 42. The comparison is done at each axial segment center, on the left and right sides of all four fuel plates in Problem 42 (altogether 80 pairs of ONBR values). Figure 24.7 shows the comparison graphically for fuel assembly 1, and Fig. 22.8 shows the same for fuel assembly 2. The maximum absolute difference between the two calculations is 0.83 %, and this provides a verification of the ONBR calculation of the code.

Verification of ONBR by the Second Approach

In this approach, the reactor power is in effect increased in a series of reactor designs at constant core flow. When the reactor power increases at constant flow, the convective heat transfer coefficient remains practically constant (except for small changes due to temperature dependence of coolant properties). If the total reactor power is increased by a factor r, the heat flux at each segment center increases by the same factor r, the bulk coolant temperature rise gets multiplied by

the factor r, and the film temperature rise gets multiplied by the factor r. The operating condition of the segment in effect moves in Fig. 22.6 from Point A to Point E on the ONB line at some value of the factor r. The margin to ONB can be quantified in this approach by the value of factor r corresponding to point E in Fig. 22.6. This value for the factor r is sought for each segment of fuel plate surface.

To calculate the ONBR at an axial segment center, a value of factor r is guessed (say, 1.0). Then the operating heat flux at the segment center is multiplied by r as is the temperature rise from the coolant channel inlet to the fuel plate surface temperature at the segment center. This yields new values of heat flux, q, and wall temperature, T_w. This is described by Eqs. (22.20) and (22.21).

$$q = r\, q_{op} \tag{22.20}$$

$$T_w = T_{in} + r\,(T_{w,op} - T_{in}) \tag{22.21}$$

The new heat flux is substituted into Eq. (22.18), giving a new value for T_{onb}. Setting the segment center wall temperature of Eq. (22.21) equal to the new ONB temperature corresponding to the heat flux $r\, q_{op}$ (in MW/m^2), one gets the following equation for the factor r .

$$T_{in} + r(T_{w,op} - T_{in}) = T_{sat} + \frac{1}{1.8}\left[\frac{r\, q_{op}}{0.0010829\, P^{1.156}}\right]^{(P^{0.0234}/2.16)} \tag{22.22}$$

where P is coolant pressure in bar. The value of r obtained by solving Eq. (22.22) is the ONBR for the axial segment under consideration.

On the Excel spreadsheet developed for the purpose of verifying PLTEMP/ANL, the solution of Eq. (22.22) is carried out by starting from a guessed value for the factor r, and then minimizing the square of the residual of Eq. (22.22), i.e. the difference between the left and right sides of the equation, with the aid of the built-in SOLVER capability of the spreadsheet. As a matter of convenience, a spreadsheet cell was created, which is the sum of the squares of the residual of Eq. (22.22) for all axial segments of all fuel plate surfaces in the test Problem 42. The Excel SOLVER is used to minimize this sum by adjusting all of the values of r simultaneously.

For verifying the ONBR by the second approach, the code-calculated ONBRs on the left and right sides of all four fuel plates at each axial segment *center* in the test Problem 42, were compared with those calculated on the Excel spreadsheet. The heat flux is evaluated at the *center* of each axial segment. The operating cladding surface temperatures and heat fluxes (q_{op} and $T_{w,op}$) needed

for this calculation are shown in Tables 22.20 and 22.21 for fuel assemblies 1 and 2 of Problem 42. These data were calculated during the verification of temperature distribution, and are already available on the spreadsheet. The axial distribution of pressure is not calculated on the spreadsheet; it is just copied to the spreadsheet from the PLTEMP/ANL code output.

In PLTEMP/ANL, the function subprogram ONBRATIO calculates the ONBR by the second approach based on heat flux, and it was found during the verification that the subprogram did not to have the coolant selection flag IFLUID. As a result, it erroneously used the H_2O coolant saturation temperature (T_{sat}) for D_2O coolant, and the ONBR for D_2O coolant was calculated to be slightly lower (conservative) than the correct value. This discrepancy of the code has now been corrected by adding the coolant selection flag IFLUID and using the FORTRAN statement TSAT=ZTSAT(PPASC,IFLUID) instead of TSAT=TSAT11(PPASC) in the subprogram ONBRATIO. *Both the incorrect and correct code versions were verified.* It should be noted that the heat-flux-based ONBR is calculated and printed by the code only for comparison with the temperature-based ONBR that is commonly used in searches and reported by analysts.

Tables 22.24 and 22.25 show comparison of the ONBRs by the second approach, between the *code before correction* (using light water T_{sat} in the subprogram ONBRATIO) and the spreadsheet (correctly using heavy water T_{sat}). The comparison is done at each axial segment center, on the left and right sides of all four fuel plates in Problem 42 (altogether 80 pairs of ONBR values). Figure 24.9 shows the comparison graphically for fuel assembly 1, and Fig. 22.10 shows the same for fuel assembly 2. The maximum absolute difference between the two calculations is 1.32 %, and this provides a verification of the ONBR calculation of the *code before correction*.

Tables 22.26 and 22.27 show comparison of the ONBRs by the second approach, between the code *after correction* (using heavy water T_{sat} in the subprogram ONBRATIO) and the spreadsheet (correctly using heavy water T_{sat}). The comparison is done at each axial segment center, on the left and right sides of all four fuel plates in Problem 42 (altogether 80 pairs of ONBR values). Figure 24.11 shows the comparison graphically for fuel assembly 1, and Fig. 22.12 shows the same for fuel assembly 2. The maximum absolute difference between the two calculations is 0.57 %, and this provides a verification of the ONBR calculation of the *code after correction*.

22.5 Verification of Onset of Flow Instability Ratio

The safety margin, onset of Ledinegg flow instability ratio (OFIR), is calculated by the PLTEMP/ANL code using the Whittle and Forgan correlation[3]. According to this correlation, the flow instability occurs when the ratio of the bulk coolant temperature rise ($T_{out} - T_{in}$) to the difference (T_{sat} - T_{in}) between the inlet temperature and the saturation temperature at the exit, equals a value determined purely by the channel geometry, as shown below by Eq. (22.23).

$$\frac{T_{out,OFI} - T_{in}}{T_{sat} - T_{in}} = \frac{1}{1 + \left(\eta D_h / L_h\right)} \tag{22.23}$$

where

T_{in} = Coolant inlet temperature, ºC

$T_{out,op}$ = Designed operating coolant exit temperature at the axial location where OFIR is being calculated, ºC

$T_{out,OFI}$ = Coolant exit temperature (at the axial location where OFIR is being calculated) that will cause onset of flow instability, ºC

T_{sat} = Saturation temperature at the axial location where OFIR is being calculated, ºC

D_h = Heated diameter of the coolant channel, calculated for the *whole* channel, not only

for sub-channel 2 in the channel, m
= 4(Flow area in a channel)/(Heated perimeter in the channel).

L_h = Heated length to the axial location where OFIR is being calculated, m

η = An experimentally determined dimensionless parameter in Whittle and Forgan correlation for OFIR. The parameter η was set to 32.5 in this verification work.

The correlation is based on experiments conducted with water flowing in rectangular channels in the following range:

0.61 m/s	≤ coolant velocity	≤ 9.1 m/s
35 ºC	≤ inlet temperature	≤ 75 ºC
0.42 MW/m^2	≤ heat flux	≤ 3.49 MW/m^2
0.1172 MPa	≤ exit pressure	≤ 0.1724 MPa
1.4 mm	≤ channel thickness	≤ 3.2 mm
0.41 m	≤ heated length	≤ 0.61 m

This OFIR is defined by Eq. (22.24) which can be written as Eq. (22.25) with the aid of Eq. (22.23).

$$\mathrm{OFIR} = \frac{T_{out,OFI} - T_{in}}{T_{out,op} - T_{in}} \tag{22.24}$$

$$\mathrm{OFIR} = \frac{(T_{sat} - T_{in})}{\left(T_{out,op} - T_{in}\right)(1 + \eta D_h / L_h)} \tag{22.25}$$

For verifying this OFIR, the code-calculated OFIRs of each channel (at its exit) of each fuel assembly in Problem 42, were compared with those calculated on the Excel spreadsheet. The spreadsheet calculates the OFIR using Eq. (22.25). The saturation temperature T_{sat} is calculated at the channel exit pressure 0.36 MPa specified in Table 22.1, and the bulk coolant exit temperatures in all channels ($T_{out,op}$) needed for this calculation were calculated during the verification of the temperature distribution, and are already available on the spreadsheet.

Fig. 22.13 shows a part of the PLTEMP/ANL output file, and Table 22.28 shows a comparison between the OFIRs calculated by the code and the spreadsheet for each coolant channel in fuel assemblies 1 and 2 of Problem 42 (altogether 6 OFIRs). The maximum absolute difference between the two calculations is 0.00445, and this provides a verification of the OFIR calculation of the code.

22.6 Conclusions

(1) To verify the PLTEMP/ANL heat transfer method for a fuel assembly made of multiple five-layer fuel plates, the steady-state temperature distributions obtained by the code and the spreadsheet were compared for test Problems 38, 39, 40, 41, and 42. Also, the heat transfer coefficients obtained by the code and the spreadsheet were compared. The maximum absolute and root-mean-square differences are tabulated below for each problem.

Test Problem	Maximum Absolute Temperature Difference, ºC	RMS Temperature Difference, ºC	Max Absolute Difference in Heat Transfer Coef., W/m^2-ºC	RMS Difference in Heat Transfer Coef., W/m^2-ºC
Problem 38	0.18	0.14	25.3	19.2
Problem 39	0.20	0.12	39.5	20.7
Problem 40	0.20	0.12	41.5	20.0
Problem 41	0.61	0.18	60.6	27.4
Problem 42	0.61	0.14	44.3	18.3

The temperature differences are small. They are mainly due to the difference in the coolant thermal properties used in the spreadsheet and the PLTEMP/ANL code which gives rise to slightly different heat transfer coefficients in the two calculations. This comparison provides a verification of the heat transfer method in PLTEMP/ANL for calculating temperature distribution in a fuel assembly made of multiple five-layer fuel plates, i.e., capability 2 listed in Section 1.2 of Chapter 1.

(2) Tables 22.22 through 22.27 show comparison between the ONBRs calculated by the PLTEMP/ANL code and the spreadsheet, at each axial segment center, on the left and right sides of all four fuel plates in Problem 42. The code calculates ONBR by the Bergles-Rohnow correlation, using two approaches, the first based on the cladding-surface-to-coolant-inlet temperature difference, and the second based on the cladding-surface heat flux. The ONBR calculated by each approach is verified. The maximum absolute difference between the two calculations is 0.83% for ONBR by the first approach and 0.57% for ONBR by the second approach. This provides a verification of the ONBR calculation of the code, i.e., capability 7 listed in Section 1.2 of Chapter 1.

Test Problem	Safety Margin Verified	Max Absolute Difference
Problem 42	ONBR by first approach	0.83 %
Problem 42	ONBR by second approach, before correction (using H_2O T_{sat})	1.32 %
Problem 42	ONBR by second approach, after code correction (using D_2O T_{sat})	0.57 %
Problem 42	OFIR	0.00445

(3) Table 22.28 shows a comparison between the OFIRs calculated by the code and the spreadsheet using the Whittle and Forgan correlation for each coolant channel in fuel assemblies 1 and 2 of Problem 42 (altogether 6 OFIRs). The maximum absolute difference between the two calculations is 0.00445, and this provides a verification of the OFIR calculation of the code, i.e., capability 8 listed in Section 1.2 of Chapter 1.

NOMENCLATURE

i = Fuel assembly index
k = Fuel plate index

j	= Axial segment index
$A_{f,k}$	= Flow area in sub-channel 2 of coolant channel k (k = 1, 2, 3), m^2
$D_{h.k}$	= Hydraulic diameter of sub-channel 2 of coolant channel k (k = 1, 2, 3), m
D_h	= Heated diameter of the coolant channel, m = 4(Flow area in a channel)/(Heated perimeter in the channel)
$FACTF_{i,k}$	= Radial power factor of plate k of fuel assembly i
$h_{k,j,left}$	= Cladding-to-coolant heat transfer coefficient on the left side of fuel plate k in axial segment j, W/m^2-ºC
$h_{k,j,left}$	= Cladding-to-coolant heat transfer coefficient on the right side of fuel plate k in axial segment j, W/m^2-ºC
$K_{k,left,c}$	= Thermal conductivity of left cladding in plate k, W/m-ºC (k = 1, 2)
$K_{k,left,g}$	= Thermal conductivity of left cladding-meat interlayer in plate k, W/m-ºC (k = 1, 2)
$K_{k,right,c}$	= Thermal conductivity of right cladding in plate k, W/m-ºC (k = 1, 2)
$K_{k,right,g}$	= Thermal conductivity of right cladding-meat interlayer in plate k, W/m-ºC (k = 1, 2)
$K_{k,m}$	= Thermal conductivity of fuel meat in plate k, W/m-ºC (k = 1, 2)
L_h	= Heated length of fuel plates, m
ONBR	= Onset of nucleate boiling ratio, calculated using the Bergles-Rohsenow correlation for each axial segment of each fuel plate
OFIR	= Onset of Ledinegg flow instability ratio, calculated using the Whittle and Forgan criterion for each axial segment of each coolant channel
P	= Coolant absolute pressure, bar
P_h	= Heated width of fuel plates, m
POW	= Total power of the two fuel assemblies, W
$P_{k,j}$	= Power in axial segment j of plate k, W
$P_{chan,k,j}$	= Total power to sub-channel 2 of channel k from fuel plates on both sides, W
p_j	= Normalized axial power shape for axial segment j from relative height z_j to z_{j+1}
z_j	= Relative axial position of segment j inlet, dimensionless
z_{j+1}	= Relative axial position of segment j exit, dimensionless
$Q_{k,j,flux,left}$	= Heat flux to the left side from the meat in plate k in segment j, W/m^2 (k = 1, 2)
$Q_{k,j,flux,right}$	= Heat flux to the right side from the meat in plate k in segment j, W/m^2 (k = 1, 2)
$q_{1,j}$	= Power density in plate 1 meat in axial segment j, W/m^3
$q_{2,j}$	= Power density in plate 2 meat in axial segment j, W/m^3
q_{op}	= Designed operating heat flux at the axial location where ONBR is being calculated, MW/m^2
q_{ONB}	= Cladding-to-coolant heat flux (MW/m^2) that causes ONB at a location with cladding surface temperature T_{onb} (ºC) and absolute pressure P (bar)
$T_{1,j,peak,left}$	= Peak temperature in plate 1 meat thickness, calculated from the left side, ºC
$T_{1,j,peak,rigjt}$	= Peak temperature in plate 1 meat thickness, calculated from the right side, ºC
$T_{2,j,peak,left}$	= Peak temperature in plate 2 meat thickness, calculated from the left side, ºC
$T_{2,j,peak,rigjt}$	= Peak temperature in plate 2 meat thickness, calculated from the right side, ºC
$T_{k,j,c}$	= Coolant temperature in channel k at axial segment j mid-height, ºC
$T_{k,j,c,inlet}$	= Coolant temperature in channel k at axial segment j inlet, ºC (k =1, 2, 3)

$T_{k,j,c,exit}$ = Coolant temperature in channel k at axial segment j exit, ºC (k =1, 2, 3)
$t_{k,left,c}$ = Thickness of left cladding in plate k, m (k = 1, 2)
$t_{k,left,g}$ = Thickness of left cladding-meat interlayer in plate k, m (k = 1, 2)
$t_{k,right,c}$ = Thickness of right cladding in plate k, m (k = 1, 2)
$t_{k,right,g}$ = Thickness of right cladding-meat interlayer in plate k, m (k = 1, 2)
$t_{k,m}$ = Thickness of fuel meat in plate k, m (k = 1, 2)
T_{sat} = Coolant saturation temperature at the ONB location, °C
T_{onb} = Cladding surface temperature (ºC) at which the designed operating heat flux q_{op} will cause onset of nucleate boiling at the axial location.
T_{in} = Coolant inlet temperature, ºC
$T_{w,op}$ = Designed operating cladding surface temperature at the axial location where ONBR is being calculated, ºC
$T_{onb,D}$ = Cladding surface temperature (ºC) at which the designed operating heat flux q_{op} will cause onset of nucleate boiling at the axial location. This cladding surface temperature is represented by the point D in Fig. 22.6.
$T_{out,op}$ = Designed operating coolant exit temperature at the axial location where OFIR is being calculated, ºC
$T_{out,OFI}$ = Coolant exit temperature (at the axial location where OFIR is being calculated) that will cause onset of flow instability, ºC
T_{sat} = Saturation temperature at the axial location where OFIR is being calculated, ºC
W_k = Coolant flow rate in sub-channel 2 of coolant channel k (k = 1, 2, 3), kg/s
$X_{left,1,j}$ = Meat thickness fraction from the left side at which the meat temperature peaks in fuel plate 1 in axial segment j
$X_{left,2,j}$ = Meat thickness fraction from the left side at which the meat temperature peaks in fuel plate 2 in axial segment j
η = An experimentally determined dimensionless parameter in Whittle and Forgan correlation for OFIR. The parameter η was set to 32.5 in this verification work.

22.7 REFERENCES

1. A. P. Olson, M. Kalimullah, and E. E. Feldman, "A User's Guide to the PLTEMP/ANL Code," ANL/RERTR/TM-11-22, Version 4.2, Argonne National Laboratory, 9700 South Cass Avenue, Argonne, IL 60439, USA (July 25, 2016).
2. A. E. Bergles and W. M. Rohsenow, "The Determination of Forced-Convection Surface-Boiling Heat Transfers," Trans. ASME, J. Heat Transfer **86**, 365 (1964).
3. R. H. Whittle and R. Forgan, "A Correlation for the Minima in the Pressure Drop Versus Flow-Rate Curves for Sub-Cooled Water Flowing in Narrow Heated Channels," Nuclear Engineering and Design 6, pp. 89-99 (1967).

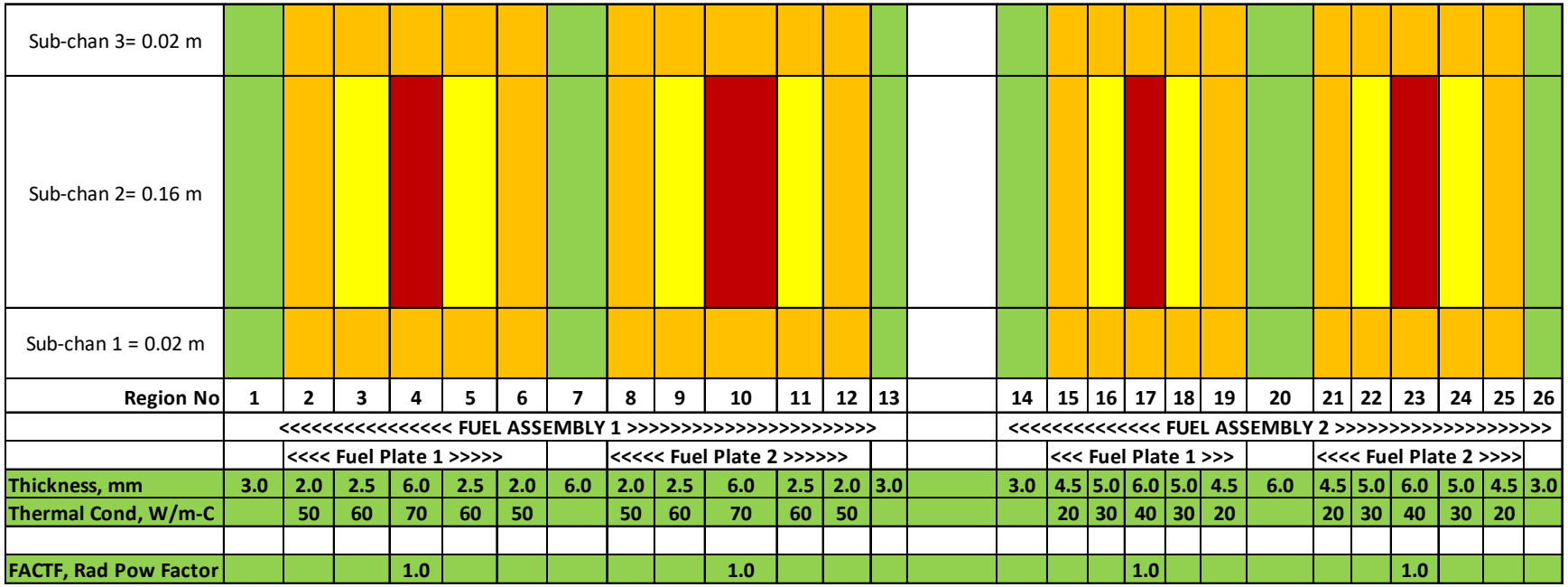

Region No	1	2	3	4	5	6	7	8	9	10	11	12	13		14	15	16	17	18	19	20	21	22	23	24	25	26
	<<<<<<<<<<<<<<<< FUEL ASSEMBLY 1 >>>>>>>>>>>>>>>>>>>>>>>														<<<<<<<<<<<<<<< FUEL ASSEMBLY 2 >>>>>>>>>>>>>>>>>>>>												
		<<<< Fuel Plate 1 >>>>>						<<<<< Fuel Plate 2 >>>>>>								<<< Fuel Plate 1 >>>						<<<< Fuel Plate 2 >>>>					
Thickness, mm	3.0	2.0	2.5	6.0	2.5	2.0	6.0	2.0	2.5	6.0	2.5	2.0	3.0		3.0	4.5	5.0	6.0	5.0	4.5	6.0	4.5	5.0	6.0	5.0	4.5	3.0
Thermal Cond, W/m-C		50	60	70	60	50		50	60	70	60	50				20	30	40	30	20		20	30	40	30	20	
FACTF, Rad Pow Factor				1.0						1.0								1.0						1.0			

Figure 22.1 Geometry and Thermal Conductivity of Fuel Assemblies in Problem 38 - Symmetrical Plates and Linear Axial Power Shape

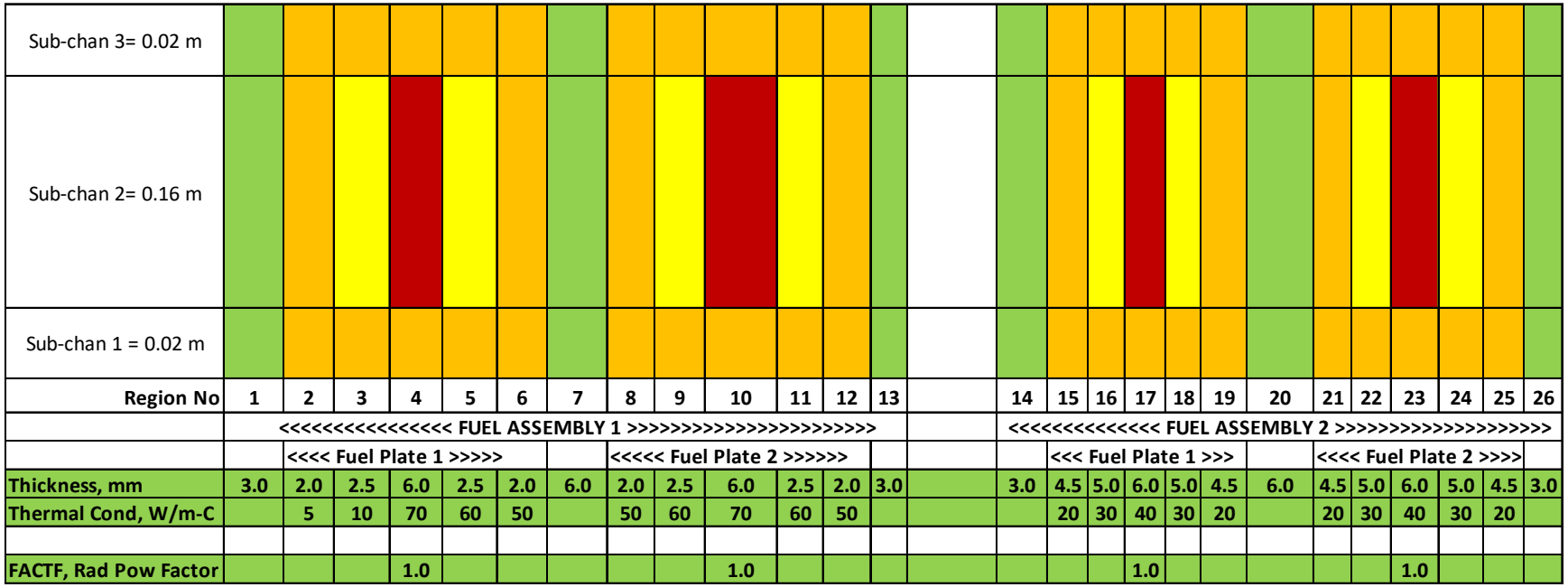

Region No	1	2	3	4	5	6	7	8	9	10	11	12	13		14	15	16	17	18	19	20	21	22	23	24	25	26
	<<<<<<<<<<<<<<<< FUEL ASSEMBLY 1 >>>>>>>>>>>>>>>>>>>>>>>														<<<<<<<<<<<<<< FUEL ASSEMBLY 2 >>>>>>>>>>>>>>>>>>>												
		<<<< Fuel Plate 1 >>>>>						<<<<< Fuel Plate 2 >>>>>>								<<< Fuel Plate 1 >>>						<<<< Fuel Plate 2 >>>>					
Thickness, mm	3.0	2.0	2.5	6.0	2.5	2.0	6.0	2.0	2.5	6.0	2.5	2.0	3.0		3.0	4.5	5.0	6.0	5.0	4.5	6.0	4.5	5.0	6.0	5.0	4.5	3.0
Thermal Cond, W/m-C		5	10	70	60	50		50	60	70	60	50				20	30	40	30	20		20	30	40	30	20	
FACTF, Rad Pow Factor				1.0						1.0								1.0						1.0			

Figure 22.2 Geometry and Thermal Conductivity of Fuel Assemblies in Problem 39 - Unsymmetrical Plate 1 in Assembly 1 and Linear Axial Power Shape

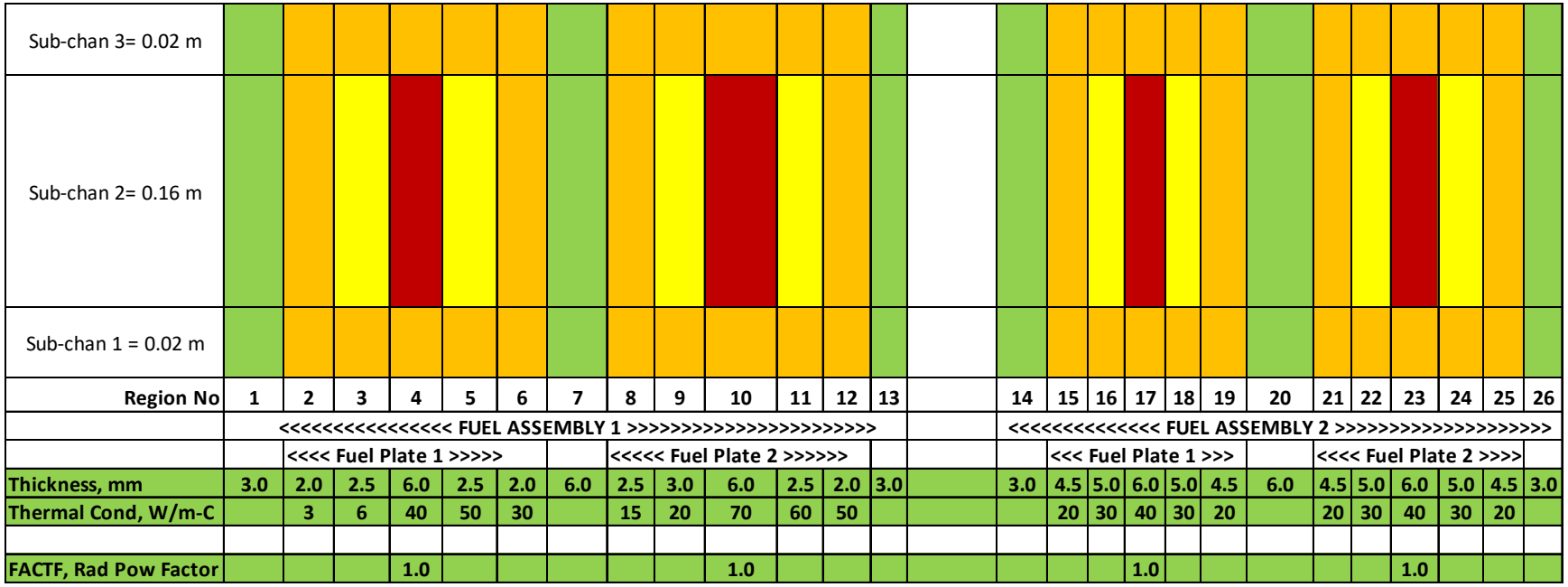

Region No	1	2	3	4	5	6	7	8	9	10	11	12	13		14	15	16	17	18	19	20	21	22	23	24	25	26
	<<<<<<<<<<<<<<<< FUEL ASSEMBLY 1 >>>>>>>>>>>>>>>>>>>>>>>														<<<<<<<<<<<<<<< FUEL ASSEMBLY 2 >>>>>>>>>>>>>>>>>>>>												
		<<<< Fuel Plate 1 >>>>>						<<<<< Fuel Plate 2 >>>>>>								<<< Fuel Plate 1 >>>						<<<< Fuel Plate 2 >>>>					
Thickness, mm	3.0	2.0	2.5	6.0	2.5	2.0	6.0	2.5	3.0	6.0	2.5	2.0	3.0		3.0	4.5	5.0	6.0	5.0	4.5	6.0	4.5	5.0	6.0	5.0	4.5	3.0
Thermal Cond, W/m-C		3	6	40	50	30		15	20	70	60	50				20	30	40	30	20		20	30	40	30	20	
FACTF, Rad Pow Factor				1.0						1.0								1.0						1.0			

Figure 22.3 Geometry and Thermal Conductivity of Fuel Assemblies in Problem 40 - Unsymmetrical Plates in Assembly 1 and Linear Axial Power Shape

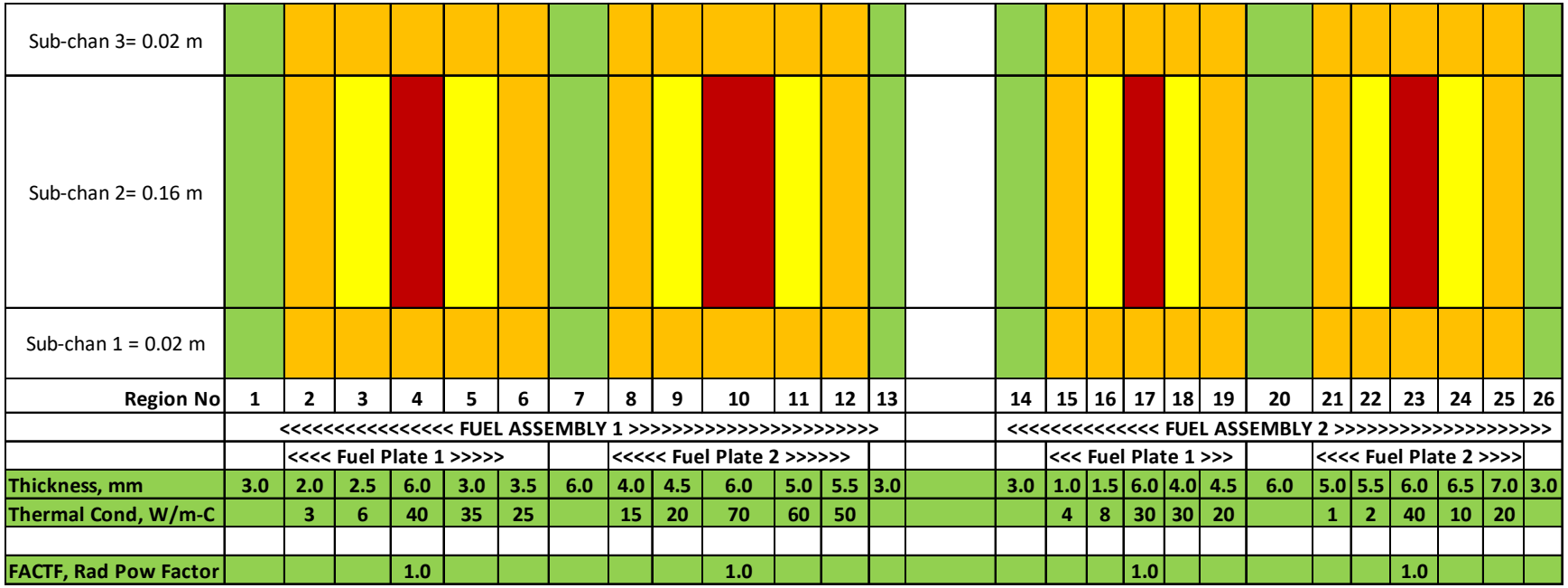

Region No	1	2	3	4	5	6	7	8	9	10	11	12	13		14	15	16	17	18	19	20	21	22	23	24	25	26
	<<<<<<<<<<<<<<<< FUEL ASSEMBLY 1 >>>>>>>>>>>>>>>>>>>>>>>>														<<<<<<<<<<<<<<< FUEL ASSEMBLY 2 >>>>>>>>>>>>>>>>>>>>												
		<<<< Fuel Plate 1 >>>>>						<<<<< Fuel Plate 2 >>>>>>								<<< Fuel Plate 1 >>>						<<<< Fuel Plate 2 >>>>					
Thickness, mm	3.0	2.0	2.5	6.0	3.0	3.5	6.0	4.0	4.5	6.0	5.0	5.5	3.0		3.0	1.0	1.5	6.0	4.0	4.5	6.0	5.0	5.5	6.0	6.5	7.0	3.0
Thermal Cond, W/m-C		3	6	40	35	25		15	20	70	60	50				4	8	30	30	20		1	2	40	10	20	
FACTF, Rad Pow Factor				1.0						1.0								1.0						1.0			

Figure 22.4 Geometry and Thermal Conductivity of Fuel Assemblies in Problem 41 - Unsymmetrical Plates in Both Assemblies and Plate-by-Plate Axial Power Shape

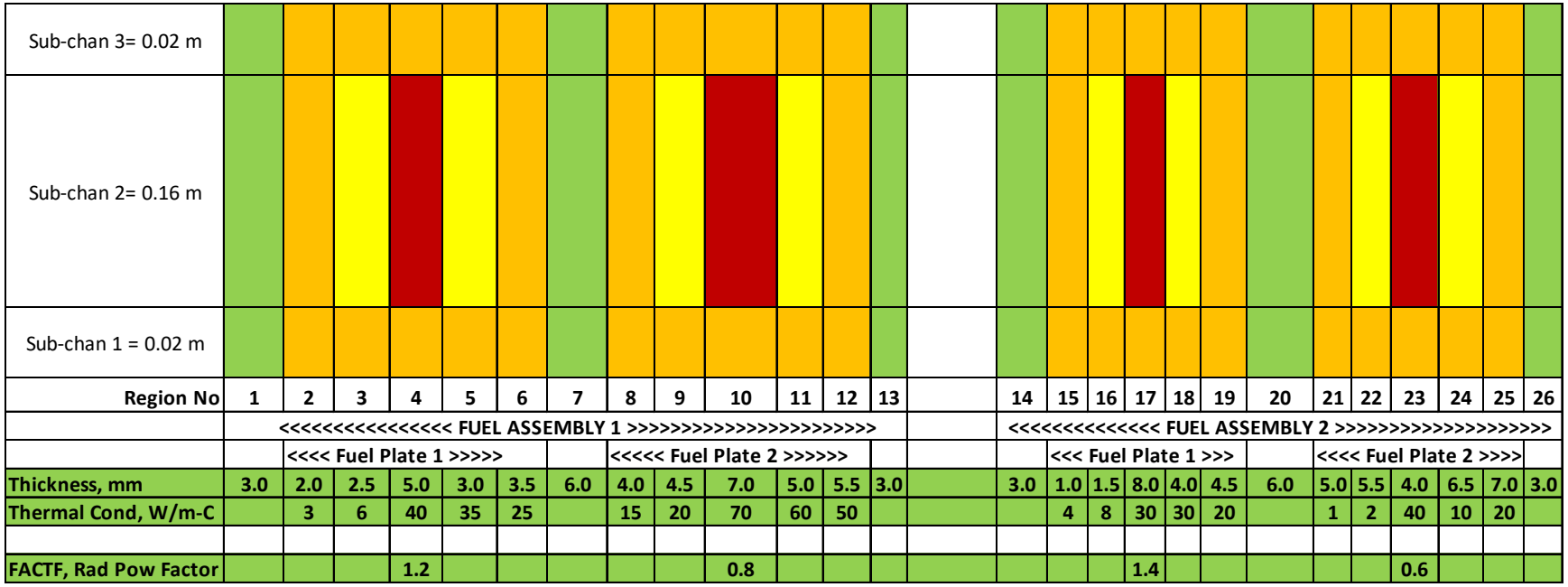

Region No	1	2	3	4	5	6	7	8	9	10	11	12	13		14	15	16	17	18	19	20	21	22	23	24	25	26
	<<<<<<<<<<<<<<<< FUEL ASSEMBLY 1 >>>>>>>>>>>>>>>>>>>>>>>														<<<<<<<<<<<<<<< FUEL ASSEMBLY 2 >>>>>>>>>>>>>>>>>>>>												
		<<<< Fuel Plate 1 >>>>>						<<<<< Fuel Plate 2 >>>>>>								<<< Fuel Plate 1 >>>						<<<< Fuel Plate 2 >>>>					
Thickness, mm	3.0	2.0	2.5	5.0	3.0	3.5	6.0	4.0	4.5	7.0	5.0	5.5	3.0		3.0	1.0	1.5	8.0	4.0	4.5	6.0	5.0	5.5	4.0	6.5	7.0	3.0
Thermal Cond, W/m-C		3	6	40	35	25		15	20	70	60	50				4	8	30	30	20		1	2	40	10	20	
FACTF, Rad Pow Factor				1.2						0.8								1.4						0.6			

Figure 22.5 Geometry and Thermal Conductivity of Fuel Assemblies in Problem 42 - Unsymmetrical and Unequal Power Plates in Both Assemblies and Plate-by-Plate Axial Power Shape

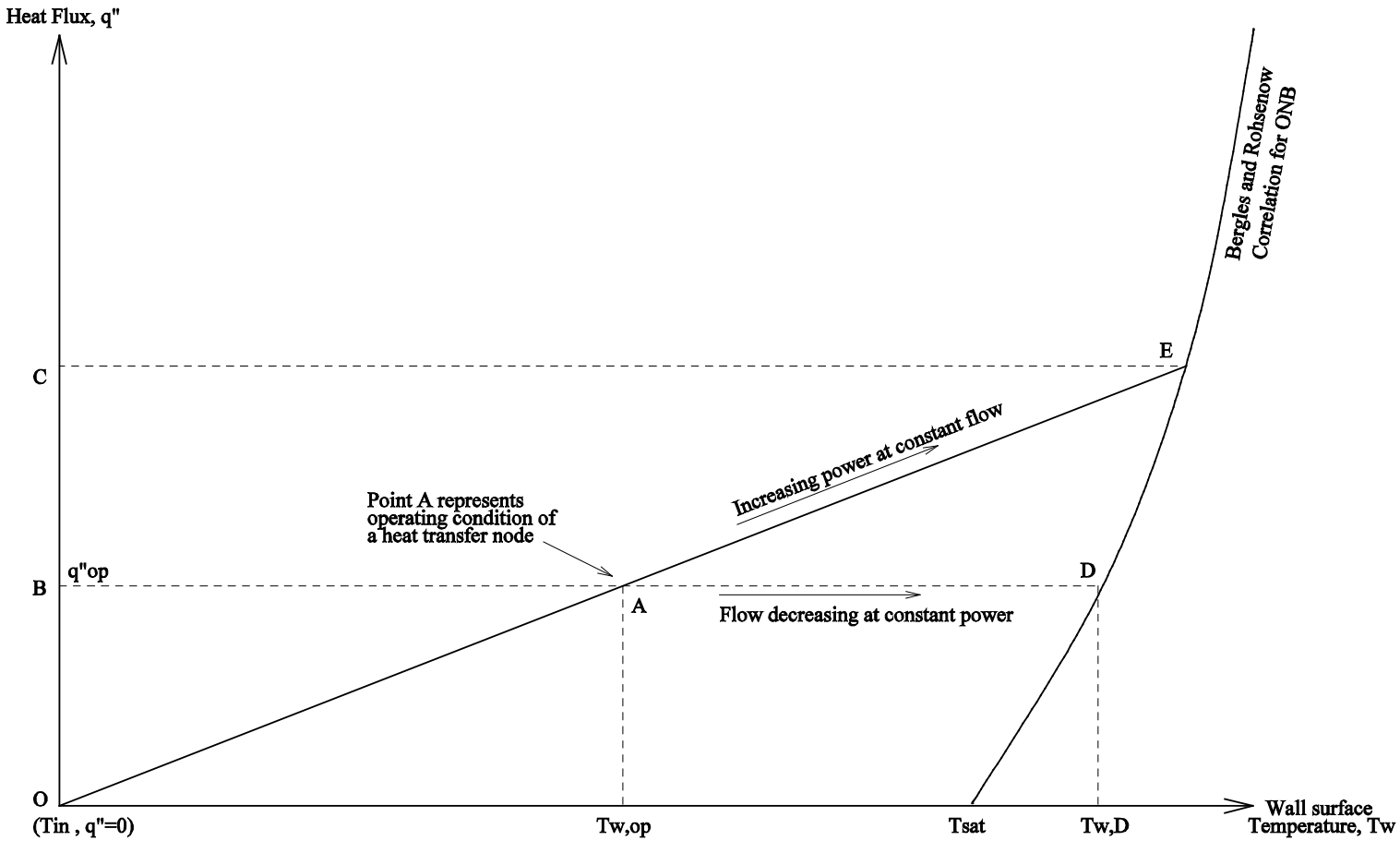

For decreasing flow at constant power, ONB Ratio = $(T_{w,D} - T_{in}) / (T_{w,op} - T_{in})$
For increasing power at constant flow, ONB Ratio = q''_E / q''_{op} = CO/BO

Figure 22.6 Geometrical Representation of ONB Ratio for a Fuel Plate Axial Node in PLTEMP/ANL Code.

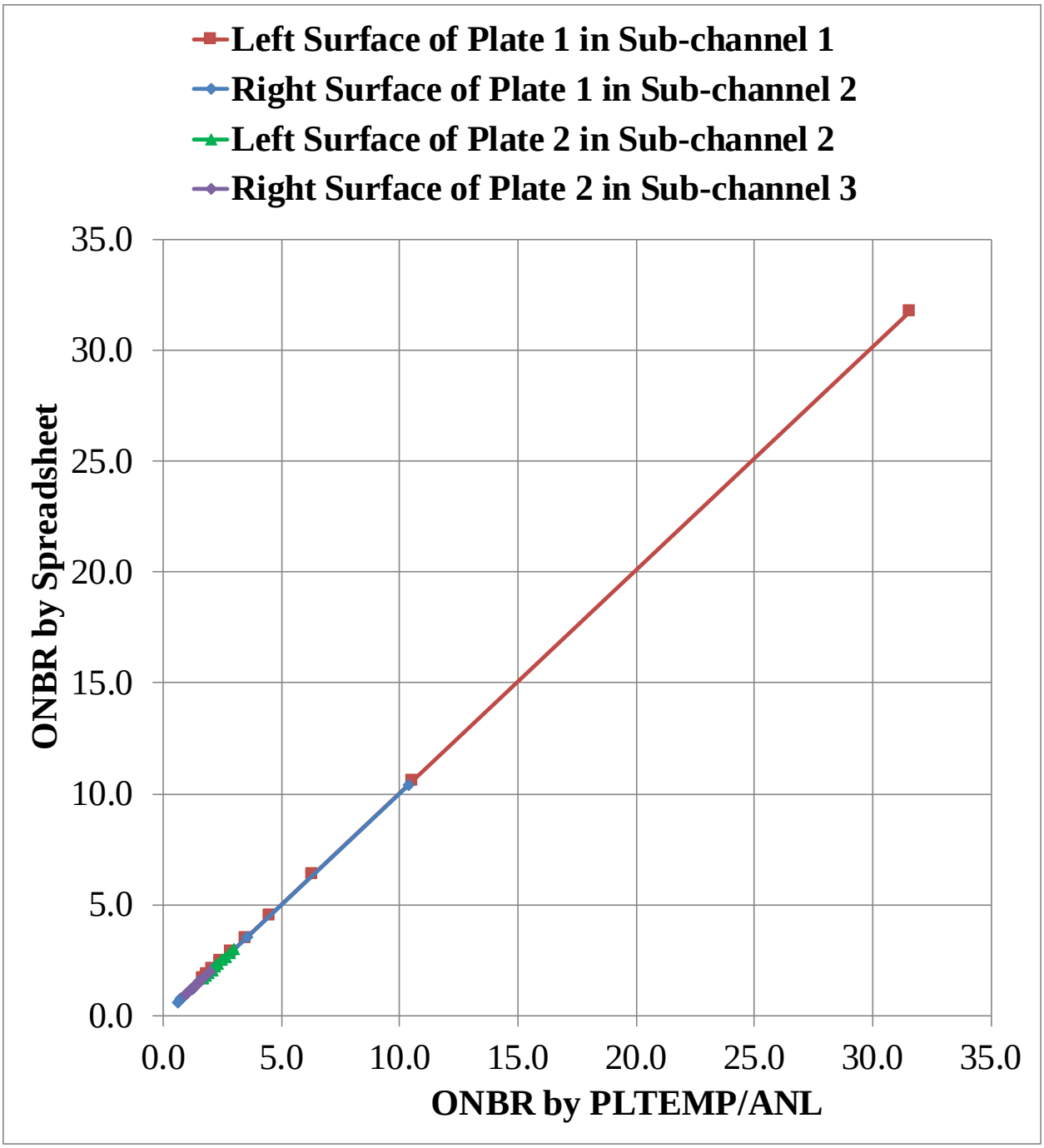

Figure 22.7 Comparison between PLTEMP/ANL- and Spreadsheet-Calculated ONBR by the First Approach for Fuel Assembly 1 of Problem 42

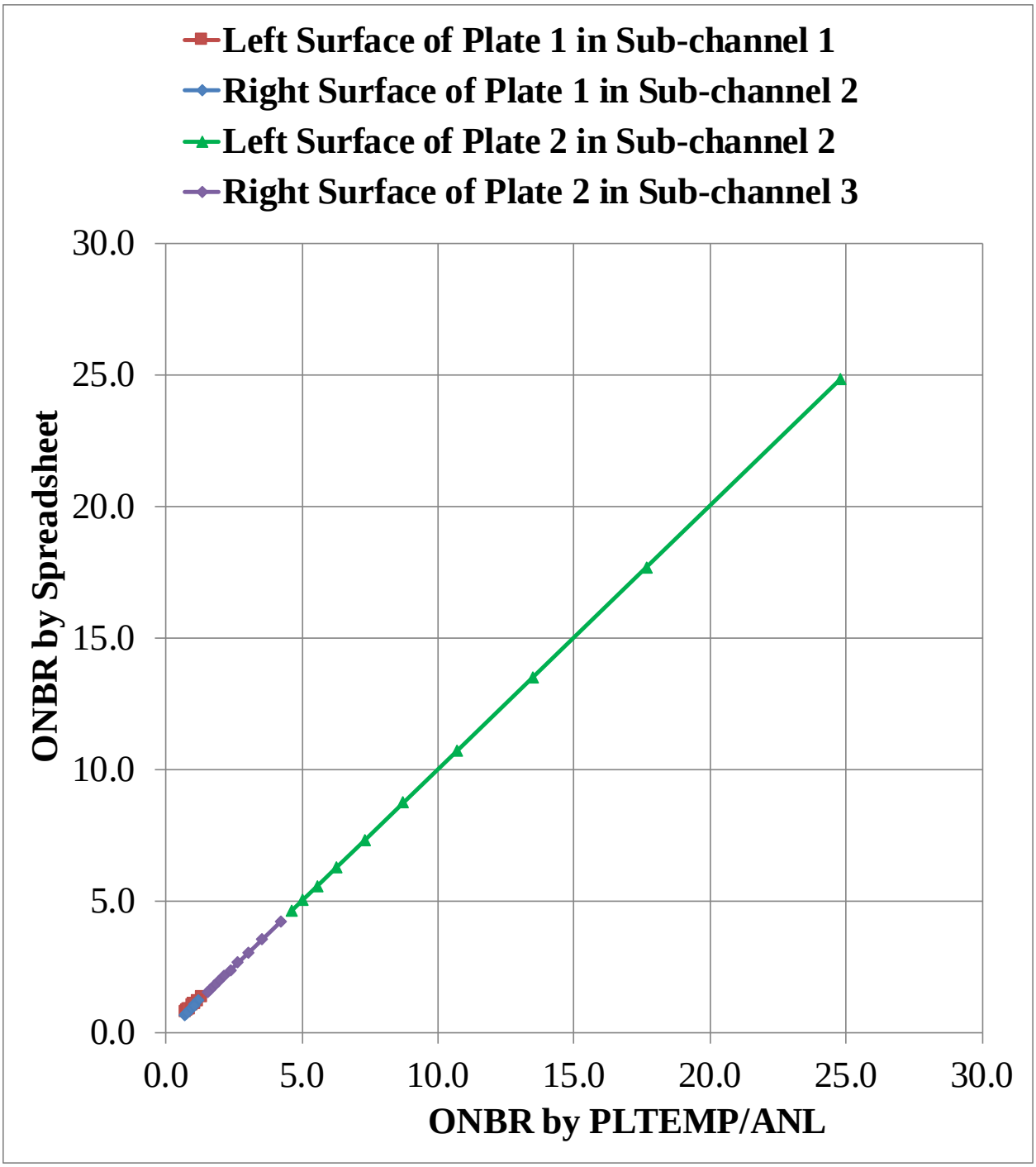

Figure 22.8 Comparison between PLTEMP/ANL- and Spreadsheet-Calculated ONBR by the First Approach for Fuel Assembly 2 of Problem 42

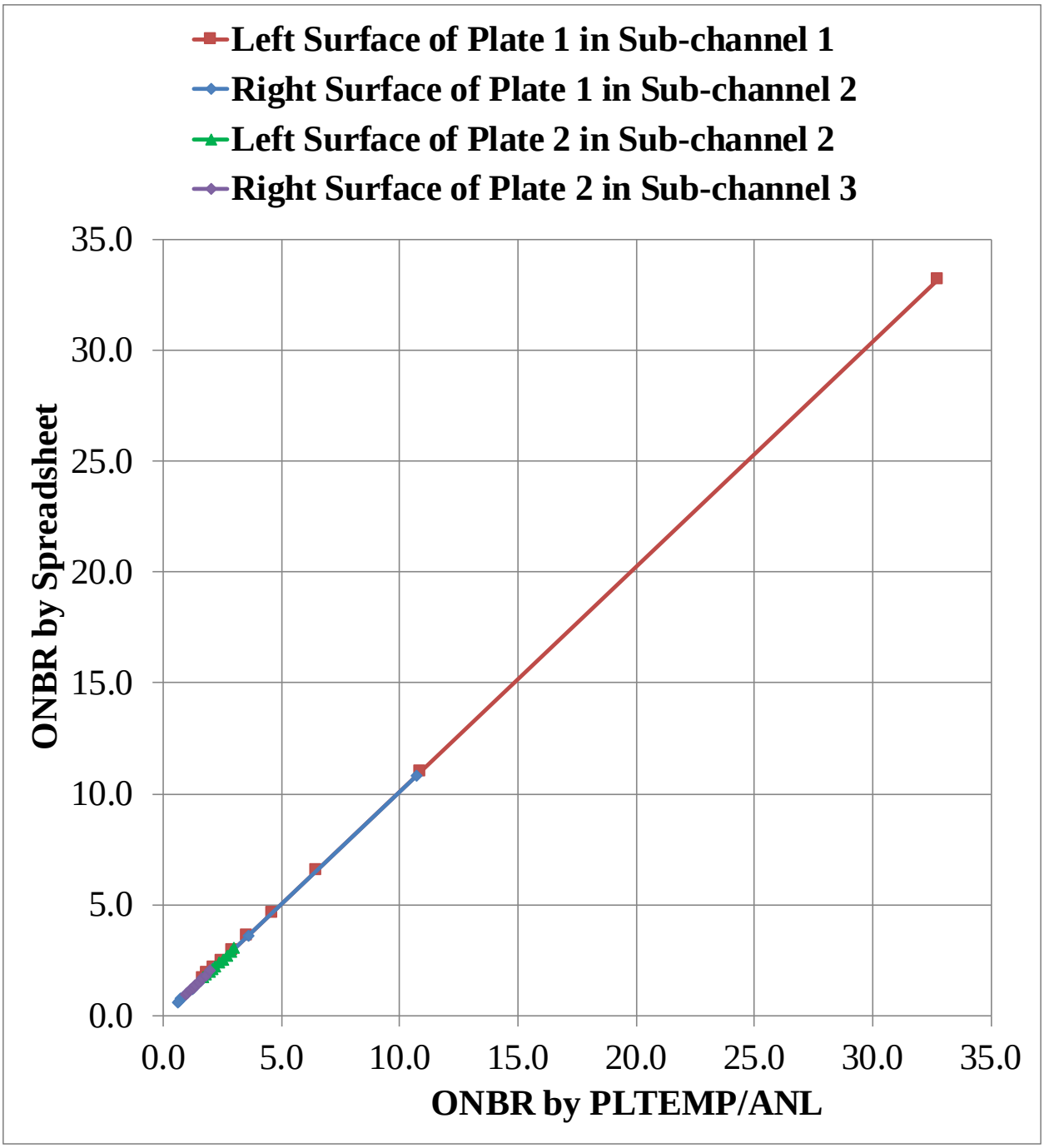

Figure 22.9 Comparison between PLTEMP/ANL- and Spreadsheet-Calculated ONBR by the Second Approach *before Code Correction* for Fuel Assembly 1 of Problem 42

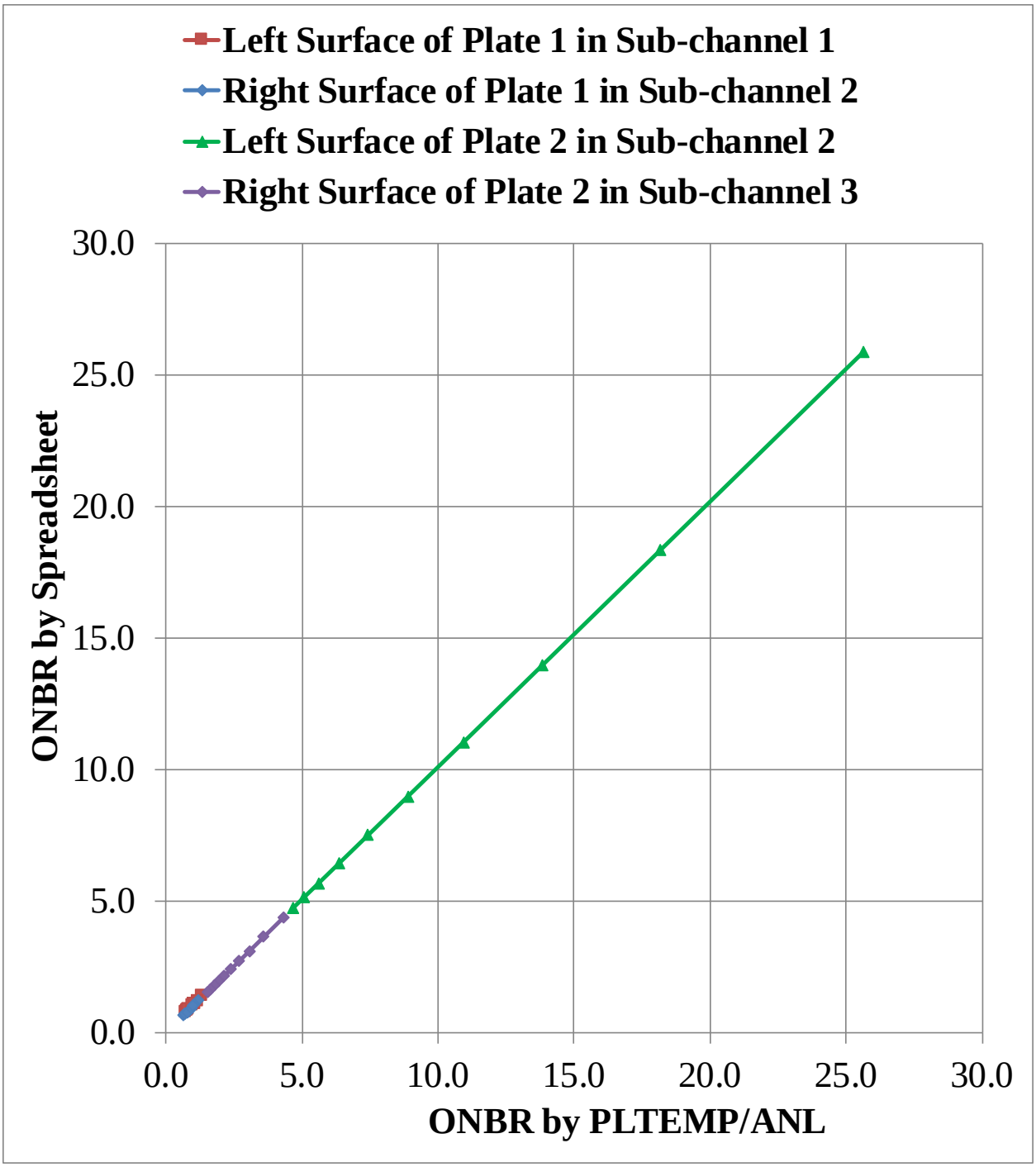

Figure 22.10 Comparison between PLTEMP/ANL- and Spreadsheet-Calculated ONBR by the Second Approach *before Code Correction* for Fuel Assembly 2 of Problem 42

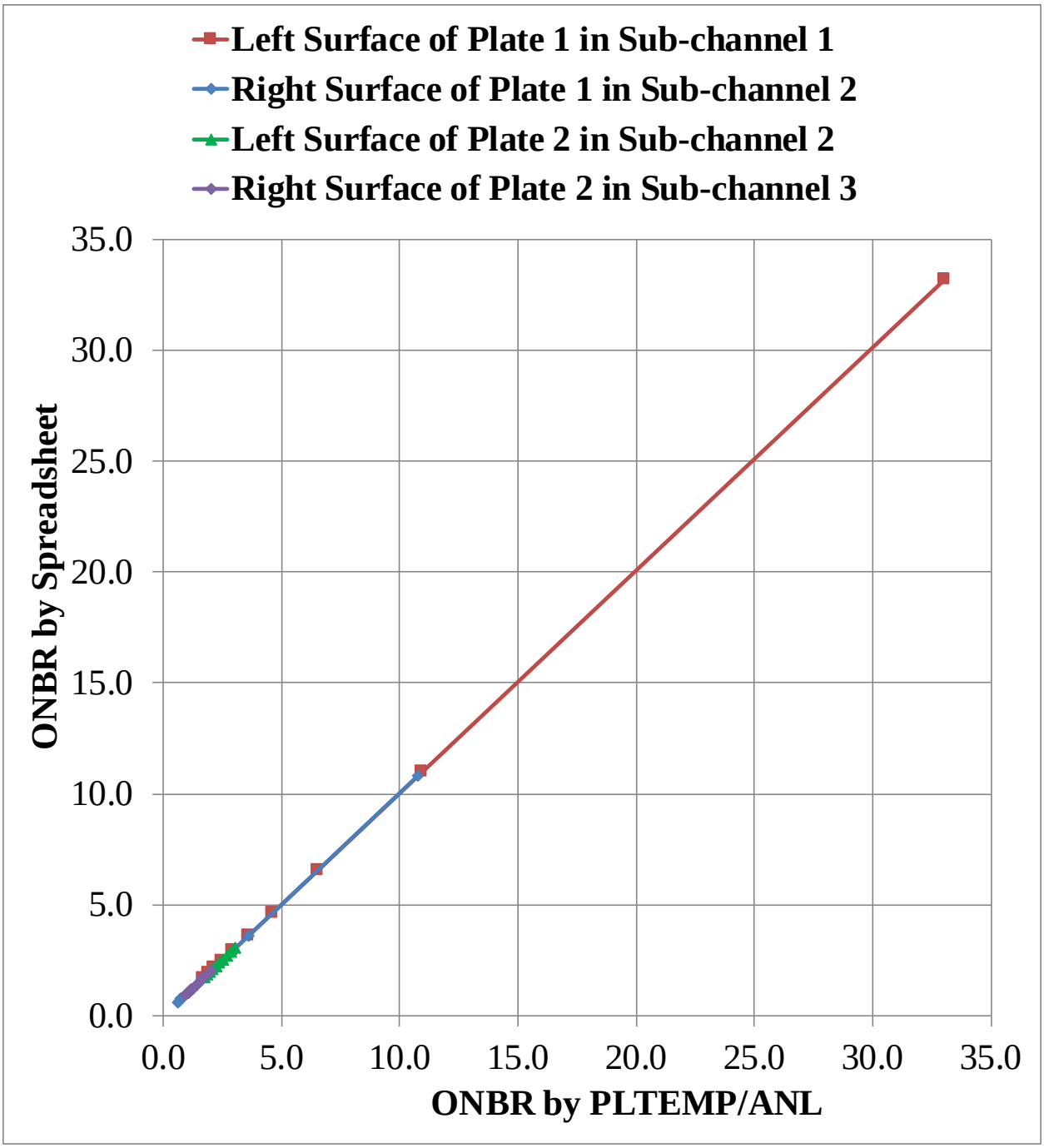

Figure 22.11 Comparison between PLTEMP/ANL- and Spreadsheet-Calculated ONBR by the Second Approach *after Code Correction* for Fuel Assembly 1 of Problem 42

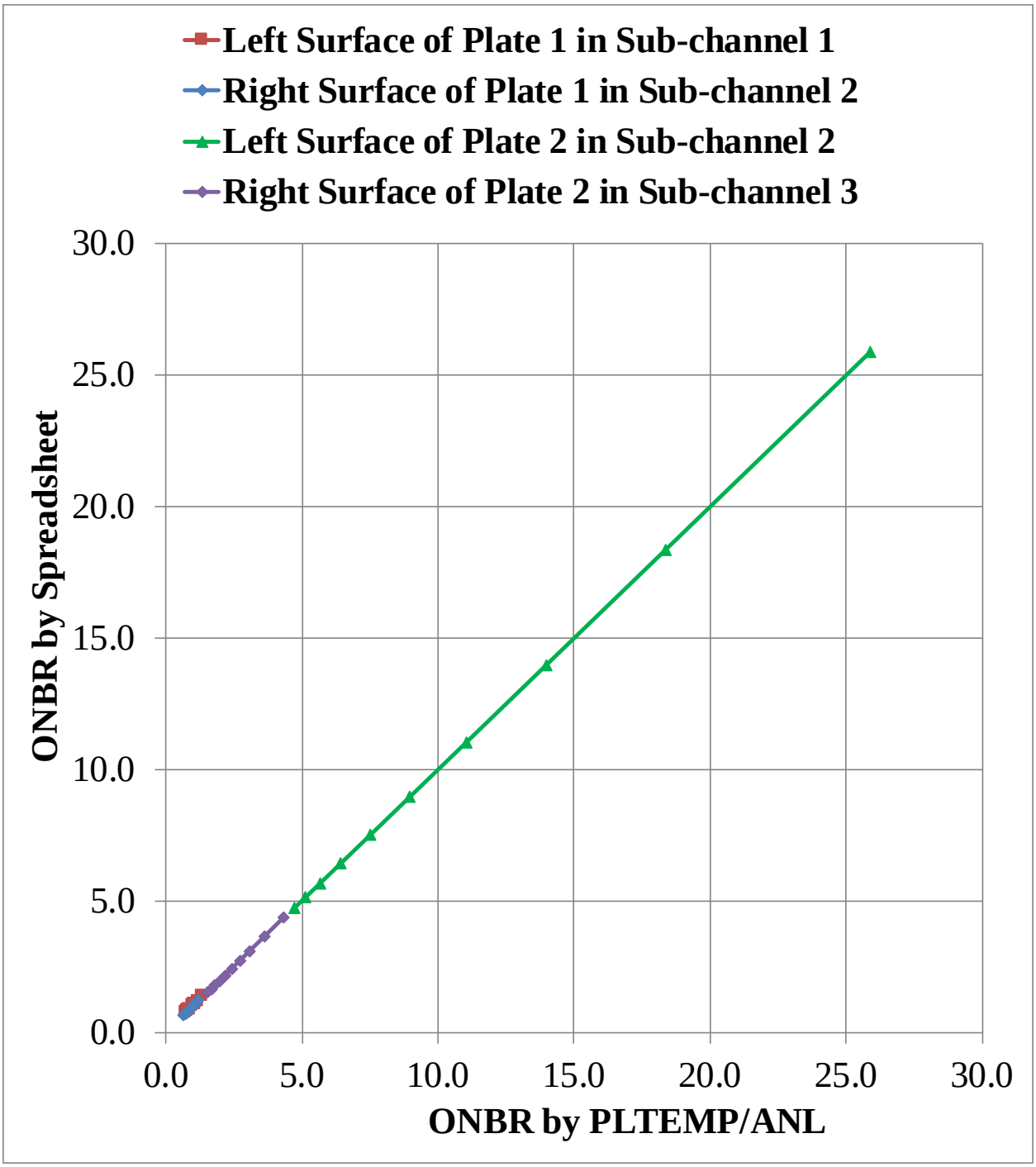

Figure 22.12 Comparison between PLTEMP/ANL- and Spreadsheet-Calculated ONBR by the Second Approach *after Code Correction* for Fuel Assembly 2 of Problem 42

Figure 22.13 Part of PLTEMP/ANL Output File Showing the Values of OFIR for Test Problem 42

```
…… output continued ……
Assembly =  1 of Type =  1, Stripe No.  2
FLOW INSTABILITY POWER RATIO BY CHANNEL (NOMINAL CASE WITHOUT HCF):
8.1640E+00  3.7113E+00  3.3725E+00
…… output continued ……
Assembly =  2 of Type =  2, Stripe No.  2
FLOW INSTABILITY POWER RATIO BY CHANNEL (NOMINAL CASE WITHOUT HCF):
2.2998E+00  3.8758E+00  5.7956E+00
…… output continued ……
HISTORY DATA FOR PRESSURE SWEEP
  I   Power      Delta P  Core Flow  Bypass   Total   Min   FUEL  DNBR Min  FUEL  Tot Flow   Tot Flow  FIR Min  Max Clad     Max Cool    H Flux       Max Fuel
      MW         MPa      kg/s       kg/s     kg/s    ONBR  TYPE          TYPE  m^3/hr     gpm          Surf T(C) Pl  Temp(C) Ch   MW/m^2    Pl  Temp(C) Pl
  1 4.0000E-01 2.00000E-02  8.0000  0.0000  8.0000  0.611  1    5.292   1   26.08878  114.8654   2.300  222.172  1  60.382  1  1.4217E+00  1  753.281  1
  2 4.0000E-01 2.00000E-02  8.0000  0.0000  8.0000  0.611  1    5.292   1   26.08878  114.8654   2.300  222.172  1  60.382  1  1.4217E+00  1  753.281  1

 PLTEMP/ANL     Version=V4.2_r80 Version Date=Jul 20, 2016       Run Date= 1/25/2017, Time=17:25:39

 ###### END OF PROBLEM ######
 ##### END OF INPUT FILE #####
```

Table 22.1 Fuel Assembly Input Data for Test Problems 37, 38, 39, and 40 Used in Verification of Capability 2 of PLTEMP/ANL

Reactor Power, MW	0.4
Number of Fuel Assemblies	2
Number of fuel plates in each assembly	2
Power of Each Fuel Plate, MW	0.1
Coolant	D2O
Flow rate in channel 1, kg/s	1.0
Flow rate in channel 2, kg/s	2.0
Flow rate in channel 3, kg/s	1.0
Heated length, m	0.6
No of axial segments	10
Inlet temperature, C	35
Plate width, m	0.20
Plate heated perimeter, m	0.16
System pressure, MPa	0.36
Heated diameter* of each channel of assembly 1, m	0.01500
Heated diameter* of each channel of assembly 2, m	0.01500

$$* \text{ Heated diameter} = \frac{4 \times (\text{Flow area of the full width of the channel})}{\text{Heated perimeter of the full width of the channel}}$$

Table 22.2 Coefficients of Fitted Equations for D_2O Coolant Thermal Properties at 0.36 MPa System pressure Used in the Spreadsheet

Fitted Coef.	Tsat, ºC	ρ (kg/m³)	h (kJ/kg)	Cp (J/g-ºC)	μ (Pa*s)	K (W/m-ºC)
a1	5.195270E+00	1.11185E+03	-1.56032E+01	4.14000E+00	-6.07159E+00	5.36341E-01
a2	2.381542E-01	-2.09000E-01	4.14222E+00	2.29510E-03	-8.88400E-02	1.73802E-03
a3	-3.439351E-03	-2.77000E-03	-5.48945E-04	-1.51312E-04	8.69800E-03	-7.68733E-06
a4	1.018878E-03		3.13190E-06	2.67539E-06	-5.15000E-07	5.92950E-01
a5				-1.86273E-08		1.61291E+00
a6				4.61798E-11		

$$T_{sat} = \exp\left(a_1 + a_2 X + a_3 X^2 + a_4 X^3\right) \quad {}^\circ C, \quad \text{where} \quad X = \ln(P, \text{MPa})$$

$$h(T) = 1000\left(a_1 + a_2 T + a_3 T^2\right) \quad \text{J/kg}$$

$$\rho(T) = a_1 + a_2 T + a_3 T^2 \quad \text{kg/m}^3$$

$$\mu(T) = \exp\left(\frac{a_1 + a_2 T}{1 + a_3 T + a_4 T^2}\right) \quad \text{Pa} - \text{s}$$

$$C_p(T) = 1000\left(a_1 + a_2 T + a_3 T^2 + a_4 T^3 + a_5 T^4 + a_6 T^5\right) \quad \text{J/kg} - {}^\circ C$$

$$K(T) = a_1 + a_2 T + a_3 T^2 + \frac{a_4}{1 + a_5 T} \quad \text{W/m} - {}^\circ C$$

Table 22.3 Axial Power Shape by Fuel Plate in Problems 38, 39, and 40

		Normalized Power Density Shape			
Axial Segment No	Segment Exit Relative Position	Assembly 1 Plate 1	Assembly 1 Plate 2	Assembly 2 Plate 1	Assembly 2 Plate 2
	0.000				
1	0.100	0.550	0.550	0.550	0.550
2	0.200	0.650	0.650	0.650	0.650
3	0.300	0.750	0.750	0.750	0.750
4	0.400	0.850	0.850	0.850	0.850
5	0.500	0.950	0.950	0.950	0.950
6	0.600	1.050	1.050	1.050	1.050
7	0.700	1.150	1.150	1.150	1.150
8	0.800	1.250	1.250	1.250	1.250
9	0.900	1.350	1.350	1.350	1.350
10	1.000	1.450	1.450	1.450	1.450

Table 22.4 Axial Power Shape by Fuel Plate in Problems 41 and 42

		Normalized Power Density Shape			
Axial Segment No	Segment Exit Relative Position	Assembly 1 Plate 1	Assembly 1 Plate 2	Assembly 2 Plate 1	Assembly 2 Plate 2
	0.000				
1	0.100	0.10	1.45	0.7	0.55
2	0.200	0.30	1.35	0.8	0.65
3	0.300	0.50	1.25	0.9	0.75
4	0.400	0.70	1.15	1.1	0.85
5	0.500	0.90	1.05	1.2	0.95
6	0.600	1.10	0.95	1.3	1.05
7	0.700	1.30	0.85	1.2	1.15
8	0.800	1.50	0.75	1.1	1.25
9	0.900	1.70	0.65	0.9	1.35
10	1.000	1.90	0.55	0.8	1.45

Table 22.5 Comparison of PLTEMP/ANL and Spreadsheet-Calculated Position (X_{left}) of Peak Meat Temperature in Meat Thickness - Problem 38

	Spreadsheet-Calculated X_{left}				PLTEMP/ANL-Calculated X_{left}			
Segment Number	Assembly 1 Plate 1	Assembly 1 Plate 2	Assembly 2 Plate 1	Assembly 2 Plate 2	Assembly 1 Plate 1	Assembly 1 Plate 2	Assembly 2 Plate 1	Assembly 2 Plate 2
1	0.50000	0.50000	0.50000	0.50000	0.4999	0.4999	0.4999	0.4999
2	0.50000	0.50000	0.50000	0.50000	0.4999	0.4999	0.4999	0.4999
3	0.50000	0.50000	0.50000	0.50000	0.4999	0.4999	0.4999	0.4999
4	0.50000	0.50000	0.50000	0.50000	0.4999	0.4999	0.4999	0.4999
5	0.50000	0.50000	0.50000	0.50000	0.4999	0.4999	0.4999	0.4999
6	0.50000	0.50000	0.50000	0.50000	0.4999	0.4999	0.4999	0.4999
7	0.50000	0.50000	0.50000	0.50000	0.4999	0.4999	0.4999	0.4999
8	0.50000	0.50000	0.50000	0.50000	0.4999	0.4999	0.4999	0.4999
9	0.50000	0.50000	0.50000	0.50000	0.4999	0.4999	0.4999	0.4999
10	0.50000	0.50000	0.50000	0.50000	0.4999	0.4999	0.4999	0.4999

Table 22.6 Spreadsheet-Calculated Temperature Distribution in Problem 38

Fuel Assembly 1

Axial Seg. No	Chan 1 coolant	Heat trans coef.	Plate 1 clad left surf	Plate 1 meat left surf	Plate 1 meat peak temp	Plate 1 meat right surf	Plate 1 clad right surf	Heat trans coef.	Chan 2 coolant	Heat trans coef.	Plate 2 clad left surf	Plate 2 meat left surf	Plate 2 meat peak temp	Plate 2 meat right surf	Plate 2 clad right surf	Heat trans coef.	Chan 3 coolant
	ºC	W/m^2-ºC	ºC	ºC	ºC	ºC	ºC	W/m^2-ºC	ºC	W/m^2-ºC	ºC	ºC	ºC	ºC	ºC	W/m^2-ºC	ºC
	35.00								35.00								35.00
1	35.42	7347.7	74.40	97.80	103.94	97.80	74.40	7347.7	35.42	7347.7	74.40	97.80	103.94	97.80	74.40	7347.7	35.42
2	36.33	7404.8	82.05	109.69	116.95	109.69	82.05	7404.8	36.33	7404.8	82.05	109.69	116.95	109.69	82.05	7404.8	36.33
3	37.39	7472.1	89.67	121.57	129.94	121.57	89.67	7472.1	37.39	7472.1	89.67	121.57	129.94	121.57	89.67	7472.1	37.39
4	38.60	7549.6	97.	133.40	142.88	133.40	97.24	7549.6	38.60	7549.6	97.24	133.40	142.88	133.40	97.24	7549.6	38.60
5	39.97	7637.1	104.75	145.16	155.76	145.16	104.75	7637.1	39.97	7637.1	104.75	145.16	155.76	145.16	104.75	7637.1	39.97
6	41.48	7734.6	112.19	156.85	168.57	156.85	112.19	7734.6	41.48	7734.6	112.19	156.85	168.57	156.85	112.19	7734.6	41.48
7	43.15	7842.0	119.53	168.45	181.28	168.45	119.53	7842.0	43.15	7842.0	119.53	168.45	181.28	168.45	119.53	7842.0	43.15
8	44.98	7959.0	126.78	179.94	193.90	179.94	126.78	7959.0	44.98	7959.0	126.78	179.94	193.90	179.94	126.78	7959.0	44.98
9	46.95	8085.6	133.91	191.33	206.40	191.34	133.91	8085.6	46.95	8085.6	133.91	191.33	206.40	191.34	133.91	8085.6	46.95
10	49.08	8221.4	140.94	202.61	218.80	202.62	140.94	8221.4	49.08	8221.4	140.94	202.61	218.80	202.62	140.94	8221.4	49.08
	50.18								50.18								50.18

Fuel Assembly 2

Axial Seg. No	Chan 1 coolant	Heat trans coef.	Plate 1 clad left surf	Plate 1 meat left surf	Plate 1 meat peak temp	Plate 1 meat right surf	Plate 1 clad right surf	Heat trans coef.	Chan 2 coolant	Heat trans coef.	Plate 2 clad left surf	Plate 2 meat left surf	Plate 2 meat peak temp	Plate 2 meat right surf	Plate 2 clad right surf	Heat trans coef.	Chan 3 coolant
	ºC	W/m^2-ºC	ºC	ºC	ºC	ºC	ºC	W/m^2-ºC	ºC	W/m^2-ºC	ºC	ºC	ºC	ºC	ºC	W/m^2-ºC	ºC
	35.00								35.00								35.00
1	35.42	7347.7	74.40	186.60	197.34	186.60	74.40	7347.7	35.42	7347.7	74.40	186.60	197.34	186.60	74.40	7347.7	35.42
2	36.33	7404.8	82.05	214.64	227.34	214.64	82.05	7404.8	36.33	7404.8	82.05	214.64	227.34	214.64	82.05	7404.8	36.33
3	37.39	7472.1	89.67	242.66	257.31	242.66	89.67	7472.1	37.39	7472.1	89.67	242.66	257.31	242.66	89.67	7472.1	37.39
4	38.60	7549.6	97.24	270.63	287.24	270.63	97.24	7549.6	38.60	7549.6	97.24	270.63	287.24	270.64	97.24	7549.6	38.60
5	39.97	7637.1	104.75	298.55	317.10	298.55	104.75	7637.1	39.97	7637.1	104.75	298.55	317.10	298.55	104.75	7637.1	39.97
6	41.48	7734.6	112.19	326.38	346.89	326.38	112.19	7734.6	41.48	7734.6	112.19	326.38	346.89	326.38	112.19	7734.6	41.48
7	43.15	7842.0	119.53	354.12	376.58	354.12	119.53	7842.0	43.15	7842.0	119.53	354.12	376.59	354.12	119.53	7842.0	43.15
8	44.98	7959.0	126.78	381.77	406.18	381.77	126.78	7959.0	44.98	7959.0	126.78	381.77	406.18	381.77	126.78	7959.0	44.98
9	46.95	8085.6	133.91	409.30	435.67	409.30	133.91	8085.6	46.95	8085.6	133.91	409.30	435.67	409.30	133.91	8085.6	46.95
10	49.08	8221.4	140.94	436.73	465.05	436.73	140.94	8221.4	49.08	8221.4	140.94	436.73	465.05	436.73	140.94	8221.4	49.08
	50.18								50.18								50.18

Table 22.7 PLTEMP/ANL-Calculated Temperature Distribution in Problem 38

Fuel Assembly 1

Axial Seg. No	Chan 1 coolant	Heat trans coef.	Plate 1 clad left surf	Plate 1 meat left surf	Plate 1 meat peak temp	Plate 1 meat right surf	Plate 1 clad right surf	Heat trans coef.	Chan 2 coolant	Heat trans coef.	Plate 2 clad left surf	Plate 2 meat left surf	Plate 2 meat peak temp	Plate 2 meat right surf	Plate 2 clad right surf	Heat trans coef.	Chan 3 coolant
	ºC	W/m^2-ºC	ºC	ºC	ºC	ºC	ºC	W/m^2-ºC	ºC	W/m^2-ºC	ºC	ºC	ºC	ºC	ºC	W/m^2-ºC	ºC
	35.00								35.00								35.00
1	35.42	7322.40	74.5	97.93	104.07	97.93	74.54	7322.40	35.42	7322.40	74.54	97.93	104.07	97.93	74.54	7322.4	35.42
2	36.33	7382.00	82.2	109.84	117.09	109.83	82.19	7382.00	36.33	7382.00	82.19	109.84	117.09	109.83	82.19	7382.0	36.33
3	37.39	7451.20	89.8	121.71	130.08	121.71	89.81	7451.20	37.39	7451.20	89.81	121.71	130.08	121.71	89.81	7451.2	37.39
4	38.60	7530.10	97.4	133.55	143.03	133.55	97.39	7530.10	38.60	7530.10	97.39	133.55	143.03	133.55	97.39	7530.1	38.60
5	39.97	7618.60	104.9	145.32	155.92	145.32	104.91	7618.70	39.97	7618.70	104.91	145.32	155.92	145.32	104.91	7618.7	39.97
6	41.48	7716.80	112.4	157.01	168.73	157.01	112.35	7716.90	41.48	7716.90	112.35	157.02	168.73	157.01	112.35	7716.9	41.48
7	43.15	7824.70	119.7	168.62	181.45	168.61	119.70	7824.80	43.15	7824.80	119.70	168.62	181.45	168.61	119.70	7824.9	43.16
8	44.98	7942.30	127.0	180.12	194.07	180.11	126.95	7942.40	44.98	7942.40	126.95	180.12	194.07	180.11	126.95	7942.5	44.98
9	46.95	8069.50	134.1	191.51	206.58	191.51	134.08	8069.50	46.95	8069.50	134.09	191.51	206.58	191.51	134.08	8069.6	46.96
10	49.08	8206.00	141.1	202.79	218.97	202.79	141.11	8206.10	49.08	8206.10	141.12	202.79	218.97	202.79	141.11	8206.2	49.08
	50.18								50.19								50.19

Fuel Assembly 2

Axial Seg. No	Chan 1 coolant	Heat trans coef.	Plate 1 clad left surf	Plate 1 meat left surf	Plate 1 meat peak temp	Plate 1 meat right surf	Plate 1 clad right surf	Heat trans coef.	Chan 2 coolant	Heat trans coef.	Plate 2 clad left surf	Plate 2 meat left surf	Plate 2 meat peak temp	Plate 2 meat right surf	Plate 2 clad right surf	Heat trans coef.	Chan 3 coolant
	ºC	W/m^2-ºC	ºC	ºC	ºC	ºC	ºC	W/m^2-ºC	ºC	W/m^2-ºC	ºC	ºC	ºC	ºC	ºC	W/m^2-ºC	ºC
	35.00								35.00								35.00
1	35.42	7322.40	74.5	186.74	197.48	186.73	74.53	7322.40	35.42	7322.40	74.54	186.74	197.48	186.73	74.53	7322.4	35.42
2	36.33	7382.00	82.2	214.79	227.48	214.78	82.18	7382.00	36.33	7382.00	82.19	214.79	227.48	214.78	82.18	7382.0	36.33
3	37.39	7451.20	89.8	242.81	257.46	242.80	89.81	7451.20	37.39	7451.20	89.82	242.81	257.46	242.80	89.81	7451.2	37.39
4	38.60	7530.10	97.4	270.79	287.39	270.78	97.39	7530.10	38.60	7530.10	97.40	270.79	287.39	270.78	97.39	7530.1	38.60
5	39.97	7618.60	104.9	298.71	317.26	298.70	104.91	7618.70	39.97	7618.70	104.92	298.71	317.26	298.70	104.91	7618.7	39.97
6	41.48	7716.80	112.4	326.55	347.05	326.54	112.35	7716.90	41.48	7716.90	112.36	326.55	347.05	326.54	112.35	7717.0	41.49
7	43.15	7824.70	119.7	354.30	376.75	354.29	119.69	7824.80	43.15	7824.80	119.71	354.30	376.75	354.29	119.70	7824.9	43.16
8	44.98	7942.30	127.0	381.95	406.35	381.93	126.94	7942.40	44.98	7942.40	126.96	381.95	406.35	381.93	126.94	7942.5	44.98
9	46.95	8069.40	134.1	409.48	435.84	409.47	134.08	8069.50	46.95	8069.50	134.09	409.48	435.85	409.47	134.08	8069.7	46.96
10	49.08	8205.90	141.1	436.91	465.22	436.90	141.11	8206.10	49.08	8206.10	141.12	436.91	465.22	436.90	141.11	8206.2	49.08
	50.18								50.19								50.19

Maximum absolute difference between the temperature distributions calculated by PLTEMP/ANL and the spreadsheet = 0.18 ºC
RMS difference between the temperature distributions calculated by PLTEMP/ANL and the spreadsheet = 0.14 ºC

Table 22.8 Comparison of PLTEMP/ANL and Spreadsheet-Calculated Position (X_{left}) of Peak Meat Temperature in Meat Thickness - Problem 39

	Spreadsheet-Calculated X_{left}				PLTEMP/ANL-Calculated X_{left}			
Segment Number	Assembly 1 Plate 1	Assembly 1 Plate 2	Assembly 2 Plate 1	Assembly 2 Plate 2	Assembly 1 Plate 1	Assembly 1 Plate 2	Assembly 2 Plate 1	Assembly 2 Plate 2
1	0.23972	0.49964	0.50000	0.50000	0.2397	0.4997	0.4999	0.4999
2	0.23979	0.49928	0.50000	0.50000	0.2398	0.4994	0.4999	0.4999
3	0.23964	0.49902	0.50000	0.50000	0.2396	0.4991	0.4999	0.4999
4	0.23932	0.49883	0.50000	0.50000	0.2393	0.4989	0.4999	0.4999
5	0.23886	0.49869	0.50000	0.50000	0.2388	0.4988	0.4999	0.4999
6	0.23827	0.49859	0.50000	0.50000	0.2382	0.4987	0.4999	0.4999
7	0.23759	0.49851	0.50000	0.50000	0.2375	0.4986	0.4999	0.4999
8	0.23682	0.49844	0.50000	0.50000	0.2367	0.4986	0.4999	0.4999
9	0.23599	0.49837	0.50000	0.50000	0.2359	0.4985	0.4999	0.4999
10	0.23511	0.49831	0.50000	0.50000	0.2350	0.4984	0.4999	0.4999

Table 22.9 Spreadsheet-Calculated Temperature Distribution in Problem 39

Fuel Assembly 1

Axial Seg. No	Chan 1 coolant	Heat trans coef.	Plate 1 clad left surf	Plate 1 meat left surf	Plate 1 meat peak temp	Plate 1 meat right surf	Plate 1 clad right surf	Heat trans coef.	Chan 2 coolant	Heat trans coef.	Plate 2 clad left surf	Plate 2 meat left surf	Plate 2 meat peak temp	Plate 2 meat right surf	Plate 2 clad right surf	Heat trans coef.	Chan 3 coolant
	ºC	W/m^2-ºC	ºC	ºC	ºC	ºC	ºC	W/m^2-ºC	ºC	W/m^2-ºC	ºC	ºC	ºC	ºC	ºC	W/m^2-ºC	ºC
	35.00								35.00								35.00
1	35.20	7347.7	53.89	143.16	144.57	130.38	94.81	7347.7	35.53	7347.7	74.48	97.86	103.99	97.84	74.43	7347.7	35.42
2	35.64	7375.1	57.65	163.18	164.85	148.08	106.04	7419.6	36.67	7419.6	82.23	109.84	117.07	109.80	82.11	7404.8	36.33
3	36.14	7407.4	61.42	183.11	185.04	165.68	117.17	7504.3	38.01	7504.3	89.96	121.80	130.14	121.73	89.77	7472.2	37.39
4	36.73	7444.7	65.19	202.92	205.10	183.14	128.14	7601.7	39.54	7601.7	97.64	133.71	143.15	133.62	97.38	7549.9	38.61
5	37.38	7486.7	68.95	222.59	225.01	200.44	138.93	7711.7	41.26	7711.7	105.25	145.55	156.10	145.44	104.93	7637.6	39.98
6	38.10	7533.6	72.69	242.09	244.75	217.56	149.52	7834.2	43.17	7834.2	112.78	157.31	168.97	157.18	112.39	7735.4	41.50
7	38.90	7585.2	76.42	261.42	264.31	234.47	159.89	7968.8	45.28	7968.8	120.21	168.98	181.74	168.83	119.77	7843.0	43.17
8	39.76	7641.5	80.11	280.55	283.68	251.18	170.02	8115.5	47.58	8115.5	127.55	180.55	194.41	180.38	127.04	7960.4	45.00
9	40.69	7702.3	83.78	299.49	302.84	267.67	179.92	8273.9	50.07	8273.9	134.78	192.01	206.98	191.82	134.21	8087.3	46.98
10	41.69	7767.6	87.41	318.23	321.81	283.94	189.59	8443.6	52.76	8443.6	141.90	203.37	219.44	203.15	141.26	8223.6	49.12
	42.21								54.15								50.22

Fuel Assembly 2

Axial Seg. No	Chan 1 coolant	Heat trans coef.	Plate 1 clad left surf	Plate 1 meat left surf	Plate 1 meat peak temp	Plate 1 meat right surf	Plate 1 clad right surf	Heat trans coef.	Chan 2 coolant	Heat trans coef.	Plate 2 clad left surf	Plate 2 meat left surf	Plate 2 meat peak temp	Plate 2 meat right surf	Plate 2 clad right surf	Heat trans coef.	Chan 3 coolant
	ºC	W/m^2-ºC	ºC	ºC	ºC	ºC	ºC	W/m^2-ºC	ºC	W/m^2-ºC	ºC	ºC	ºC	ºC	ºC	W/m^2-ºC	ºC
	35.00								35.00								35.00
1	35.42	7347.7	74.40	186.60	197.34	186.60	74.40	7347.7	35.42	7347.7	74.40	186.60	197.34	186.60	74.40	7347.7	35.42
2	36.33	7404.8	82.05	214.64	227.34	214.64	82.05	7404.8	36.33	7404.8	82.05	214.64	227.34	214.64	82.05	7404.8	36.33
3	37.39	7472.1	89.67	242.66	257.31	242.66	89.67	7472.1	37.39	7472.1	89.67	242.66	257.31	242.66	89.67	7472.1	37.39
4	38.60	7549.6	97.24	270.63	287.24	270.63	97.24	7549.6	38.60	7549.6	97.24	270.63	287.24	270.64	97.24	7549.6	38.60
5	39.97	7637.1	104.75	298.55	317.10	298.55	104.75	7637.1	39.97	7637.1	104.75	298.55	317.10	298.55	104.75	7637.1	39.97
6	41.48	7734.6	112.19	326.38	346.89	326.38	112.19	7734.6	41.48	7734.6	112.19	326.38	346.89	326.38	112.19	7734.6	41.48
7	43.15	7842.0	119.53	354.12	376.58	354.12	119.53	7842.0	43.15	7842.0	119.53	354.12	376.59	354.12	119.53	7842.0	43.15
8	44.98	7959.0	126.78	381.77	406.18	381.77	126.78	7959.0	44.98	7959.0	126.78	381.77	406.18	381.77	126.78	7959.0	44.98
9	46.95	8085.6	133.91	409.30	435.67	409.30	133.91	8085.6	46.95	8085.6	133.91	409.30	435.67	409.30	133.91	8085.6	46.95
10	49.08	8221.4	140.94	436.73	465.05	436.73	140.94	8221.4	49.08	8221.4	140.94	436.73	465.05	436.73	140.94	8221.4	49.08
	50.18								50.18								50.18

Table 22.10 PLTEMP/ANL-Calculated Temperature Distribution in Problem 39

Fuel Assembly 1

Axial Seg. No	Chan 1 coolant	Heat trans coef.	Plate 1 clad left surf	Plate 1 meat left surf	Plate 1 meat peak temp	Plate 1 meat right surf	Plate 1 clad right surf	Heat trans coef.	Chan 2 coolant	Heat trans coef.	Plate 2 clad left surf	Plate 2 meat left surf	Plate 2 meat peak temp	Plate 2 meat right surf	Plate 2 clad right surf	Heat trans coef.	Chan 3 coolant
	ºC	W/m^2-ºC	ºC	ºC	ºC	ºC	ºC	W/m^2-ºC	ºC	W/m^2-ºC	ºC	ºC	ºC	ºC	ºC	W/m^2-ºC	ºC
	35.00								35.00								35.00
1	35.20	7308.2	54.00	143.29	144.70	130.51	94.94	7329.5	35.53	7329.5	74.59	97.97	104.11	97.96	74.56	7322.5	35.42
2	35.64	7336.8	57.77	163.31	164.98	148.21	106.18	7404.5	36.67	7404.5	82.34	109.96	117.19	109.92	82.24	7382.0	36.33
3	36.14	7370.1	61.55	183.24	185.16	165.80	117.29	7491.6	38.01	7491.6	90.06	121.91	130.25	121.85	89.90	7451.4	37.39
4	36.73	7408.0	65.33	203.05	205.22	183.26	128.26	7590.8	39.54	7590.8	97.74	133.82	143.27	133.74	97.51	7530.4	38.61
5	37.38	7450.6	69.10	222.71	225.13	200.56	139.04	7702.2	41.26	7702.2	105.35	145.67	156.22	145.56	105.06	7619.2	39.97
6	38.10	7497.6	72.85	242.21	244.87	217.67	149.63	7825.9	43.17	7825.9	112.88	157.43	169.09	157.31	112.53	7717.7	41.50
7	38.89	7549.2	76.59	261.53	264.42	234.58	159.99	7961.7	45.28	7961.7	120.31	169.09	181.86	168.95	119.91	7825.9	43.17
8	39.76	7605.1	80.29	280.65	283.78	251.27	170.11	8109.7	47.58	8109.7	127.64	180.66	194.53	180.50	127.18	7943.8	45.00
9	40.69	7665.5	83.97	299.58	302.93	267.75	180.00	8269.5	50.08	8269.5	134.86	192.11	207.09	191.93	134.34	8071.3	46.98
10	41.69	7730.2	87.61	318.31	321.89	284.00	189.65	8440.7	52.77	8440.7	141.97	203.46	219.54	203.26	141.40	8208.3	49.12
	42.21								54.16								50.22

Fuel Assembly 2

Axial Seg. No	Chan 1 coolant	Heat trans coef.	Plate 1 clad left surf	Plate 1 meat left surf	Plate 1 meat peak temp	Plate 1 meat right surf	Plate 1 clad right surf	Heat trans coef.	Chan 2 coolant	Heat trans coef.	Plate 2 clad left surf	Plate 2 meat left surf	Plate 2 meat peak temp	Plate 2 meat right surf	Plate 2 clad right surf	Heat trans coef.	Chan 3 coolant
	ºC	W/m^2-ºC	ºC	ºC	ºC	ºC	ºC	W/m^2-ºC	ºC	W/m^2-ºC	ºC	ºC	ºC	ºC	ºC	W/m^2-ºC	ºC
	35.00								35.00								35.00
1	35.42	7322.4	74.54	186.74	197.48	186.73	74.53	7322.4	35.42	7322.4	74.54	186.74	197.48	186.73	74.53	7322.4	35.42
2	36.33	7382.0	82.19	214.79	227.48	214.78	82.18	7382.0	36.33	7382.0	82.19	214.79	227.48	214.78	82.18	7382.0	36.33
3	37.39	7451.2	89.82	242.81	257.46	242.80	89.81	7451.2	37.39	7451.2	89.82	242.81	257.46	242.80	89.81	7451.2	37.39
4	38.60	7530.1	97.40	270.79	287.39	270.78	97.39	7530.1	38.60	7530.1	97.40	270.79	287.39	270.78	97.39	7530.1	38.60
5	39.97	7618.6	104.92	298.71	317.26	298.70	104.91	7618.7	39.97	7618.7	104.92	298.71	317.26	298.70	104.91	7618.7	39.97
6	41.48	7716.8	112.36	326.55	347.05	326.54	112.35	7716.9	41.48	7716.9	112.36	326.55	347.05	326.54	112.35	7717.0	41.49
7	43.15	7824.7	119.71	354.30	376.75	354.29	119.69	7824.8	43.15	7824.8	119.71	354.30	376.75	354.29	119.70	7824.9	43.16
8	44.98	7942.3	126.95	381.95	406.35	381.93	126.94	7942.4	44.98	7942.4	126.96	381.95	406.35	381.93	126.94	7942.5	44.98
9	46.95	8069.4	134.09	409.48	435.84	409.47	134.08	8069.5	46.95	8069.5	134.09	409.48	435.85	409.47	134.08	8069.7	46.96
10	49.08	8205.9	141.12	436.91	465.22	436.90	141.11	8206.1	49.08	8206.1	141.12	436.91	465.22	436.90	141.11	8206.2	49.08
	50.18								50.19								50.19

Maximum absolute difference between the temperature distributions calculated by PLTEMP/ANL and the spreadsheet = 0.20 ºC
RMS difference between the temperature distributions calculated by PLTEMP/ANL and the spreadsheet = 0.12 ºC

Table 22.11 Comparison of PLTEMP/ANL and Spreadsheet-Calculated Position (X_{left}) of Peak Meat Temperature in Meat Thickness - Problem 40

	Spreadsheet-Calculated X_{left}				PLTEMP/ANL-Calculated X_{left}			
Segment Number	Assembly 1 Plate 1	Assembly 1 Plate 2	Assembly 2 Plate 1	Assembly 2 Plate 2	Assembly 1 Plate 1	Assembly 1 Plate 2	Assembly 2 Plate 1	Assembly 2 Plate 2
1	0.20238	0.34479	0.50000	0.50000	0.2024	0.3448	0.4999	0.4999
2	0.20240	0.34442	0.50000	0.50000	0.2024	0.3444	0.4999	0.4999
3	0.20229	0.34392	0.50000	0.50000	0.2023	0.3439	0.4999	0.4999
4	0.20205	0.34331	0.50000	0.50000	0.2021	0.3433	0.4999	0.4999
5	0.20172	0.34261	0.50000	0.50000	0.2017	0.3426	0.4999	0.4999
6	0.20130	0.34182	0.50000	0.50000	0.2013	0.3418	0.4999	0.4999
7	0.20082	0.34095	0.50000	0.50000	0.2008	0.3409	0.4999	0.4999
8	0.20028	0.34002	0.50000	0.50000	0.2002	0.3399	0.4999	0.4999
9	0.19969	0.33904	0.50000	0.50000	0.1996	0.3389	0.4999	0.4999
10	0.19906	0.33801	0.50000	0.50000	0.1990	0.3379	0.4999	0.4999

Table 22.12 Spreadsheet-Calculated Temperature Distribution in Problem 40

Fuel Assembly 1

Axial Seg. No	Chan 1 coolant	Heat trans coef.	Plate 1 clad left surf	Plate 1 meat left surf	Plate 1 meat peak temp	Plate 1 meat right surf	Plate 1 clad right surf	Heat trans coef.	Chan 2 coolant	Heat trans coef.	Plate 2 clad left surf	Plate 2 meat left surf	Plate 2 meat peak temp	Plate 2 meat right surf	Plate 2 clad right surf	Heat trans coef.	Chan 3 coolant
	ºC	W/m^2-ºC	ºC	ºC	ºC	ºC	ºC	W/m^2-ºC	ºC	W/m^2-ºC	ºC	ºC	ºC	ºC	ºC	W/m^2-ºC	ºC
	35.00								35.00								35.00
1	35.17	7347.7	50.95	176.56	178.32	150.98	97.67	7347.7	35.48	7347.7	62.36	124.91	127.83	117.29	86.63	7347.7	35.55
2	35.54	7370.8	54.13	202.60	204.68	172.37	109.37	7412.9	36.51	7412.9	67.97	141.82	145.26	132.79	96.54	7422.5	36.74
3	35.97	7398.1	57.33	228.53	230.93	193.64	120.94	7489.7	37.73	7489.7	73.60	158.69	162.65	148.23	106.38	7510.6	38.13
4	36.46	7429.6	60.54	254.34	257.05	214.77	132.34	7578.1	39.11	7578.1	79.22	175.48	179.96	163.59	116.11	7612.1	39.72
5	37.01	7465.1	63.75	280.00	283.02	235.72	143.56	7677.9	40.67	7677.9	84.83	192.19	197.17	178.84	125.71	7726.8	41.52
6	37.62	7504.8	66.96	305.48	308.80	256.47	154.56	7789.0	42.40	7789.0	90.40	208.79	214.27	193.96	135.17	7854.5	43.52
7	38.29	7548.4	70.16	330.77	334.39	277.01	165.32	7911.1	44.31	7911.1	95.93	225.27	231.24	208.94	144.47	7995.0	45.72
8	39.02	7596.0	73.35	355.86	359.78	297.32	175.84	8044.1	46.39	8044.1	101.42	241.62	248.08	223.77	153.59	8148.1	48.12
9	39.81	7647.6	76.53	380.74	384.95	317.39	186.09	8187.7	48.64	8187.7	106.87	257.85	264.77	238.45	162.54	8313.5	50.73
10	40.66	7702.9	79.69	405.41	409.90	337.23	196.09	8341.6	51.06	8341.6	112.27	273.94	281.33	252.97	171.31	8490.9	53.55
	41.09								52.32								55.01

Fuel Assembly 2

Axial Seg. No	Chan 1 coolant	Heat trans coef.	Plate 1 clad left surf	Plate 1 meat left surf	Plate 1 meat peak temp	Plate 1 meat right surf	Plate 1 clad right surf	Heat trans coef.	Chan 2 coolant	Heat trans coef.	Plate 2 clad left surf	Plate 2 meat left surf	Plate 2 meat peak temp	Plate 2 meat right surf	Plate 2 clad right surf	Heat trans coef.	Chan 3 coolant
	ºC	W/m^2-ºC	ºC	ºC	ºC	ºC	ºC	W/m^2-ºC	ºC	W/m^2-ºC	ºC	ºC	ºC	ºC	ºC	W/m^2-ºC	ºC
	35.00								35.00								35.00
1	35.42	7347.7	74.40	186.60	197.34	186.60	74.40	7347.7	35.42	7347.7	74.40	186.60	197.34	186.60	74.40	7347.7	35.42
2	36.33	7404.8	82.05	214.64	227.34	214.64	82.05	7404.8	36.33	7404.8	82.05	214.64	227.34	214.64	82.05	7404.8	36.33
3	37.39	7472.1	89.67	242.66	257.31	242.66	89.67	7472.1	37.39	7472.1	89.67	242.66	257.31	242.66	89.67	7472.1	37.39
4	38.60	7549.6	97.24	270.64	287.24	270.64	97.24	7549.6	38.60	7549.6	97.24	270.64	287.24	270.64	97.24	7549.6	38.60
5	39.97	7637.1	104.75	298.55	317.10	298.55	104.75	7637.1	39.97	7637.1	104.75	298.55	317.10	298.55	104.75	7637.1	39.97
6	41.48	7734.6	112.19	326.38	346.89	326.38	112.19	7734.6	41.48	7734.6	112.19	326.38	346.89	326.38	112.19	7734.6	41.48
7	43.15	7842.0	119.53	354.12	376.59	354.12	119.53	7842.0	43.15	7842.0	119.53	354.12	376.59	354.12	119.53	7842.0	43.15
8	44.98	7959.0	126.78	381.77	406.18	381.77	126.78	7959.0	44.98	7959.0	126.78	381.77	406.18	381.77	126.78	7959.0	44.98
9	46.95	8085.6	133.91	409.30	435.67	409.30	133.91	8085.6	46.95	8085.6	133.91	409.30	435.67	409.30	133.91	8085.6	46.95
10	49.08	8221.4	140.94	436.73	465.05	436.73	140.94	8221.4	49.08	8221.4	140.94	436.73	465.05	436.73	140.94	8221.4	49.08
	50.18								50.18								50.18

Table 22.13 PLTEMP/ANL-Calculated Temperature Distribution in Problem 40

Fuel Assembly 1

Axial Seg. No	Chan 1 coolant	Heat trans coef.	Plate 1 clad left surf	Plate 1 meat left surf	Plate 1 meat peak temp	Plate 1 meat right surf	Plate 1 clad right surf	Heat trans coef.	Chan 2 coolant	Heat trans coef.	Plate 2 clad left surf	Plate 2 meat left surf	Plate 2 meat peak temp	Plate 2 meat right surf	Plate 2 clad right surf	Heat trans coef.	Chan 3 coolant
	ºC	W/m^2-ºC	ºC	ºC	ºC	ºC	ºC	W/m^2-ºC	ºC	W/m^2-ºC	ºC	ºC	ºC	ºC	ºC	W/m^2-ºC	ºC
	35.00								35.00								35.00
1	35.17	7306.20	51.0	176.71	178.47	151.14	97.84	7326.30	35.48	7326.30	62.45	125.01	127.93	117.39	86.74	7330.9	35.55
2	35.54	7330.30	54.2	202.75	204.83	172.53	109.54	7394.30	36.52	7394.30	68.06	141.92	145.36	132.89	96.64	7408.9	36.74
3	35.97	7358.40	57.4	228.69	231.09	193.80	121.10	7473.30	37.73	7473.30	73.68	158.78	162.74	148.32	106.47	7499.6	38.13
4	36.46	7390.50	60.7	254.50	257.21	214.93	132.51	7563.30	39.11	7563.30	79.31	175.57	180.04	163.67	116.19	7603.0	39.72
5	37.01	7426.40	63.9	280.16	283.18	235.88	143.73	7664.20	40.67	7664.20	84.91	192.27	197.25	178.92	125.79	7719.2	41.52
6	37.62	7466.20	67.1	305.64	308.96	256.64	154.73	7776.20	42.40	7776.20	90.48	208.86	214.34	194.03	135.24	7848.2	43.52
7	38.29	7509.90	70.3	330.93	334.55	277.17	165.49	7899.20	44.31	7899.20	96.01	225.33	231.30	209.00	144.52	7990.2	45.72
8	39.02	7557.20	73.5	356.02	359.94	297.48	176.00	8033.00	46.39	8033.00	101.50	241.68	248.13	223.81	153.63	8144.8	48.13
9	39.81	7608.40	76.7	380.89	385.10	317.54	186.25	8177.60	48.64	8177.60	106.93	257.89	264.81	238.47	162.56	8311.9	50.74
10	40.65	7663.20	79.9	405.56	410.04	337.37	196.23	8332.60	51.06	8332.60	112.33	273.96	281.36	252.98	171.32	8490.7	53.56
	41.09								52.32								55.02

Fuel Assembly 2

Axial Seg. No	Chan 1 coolant	Heat trans coef.	Plate 1 clad left surf	Plate 1 meat left surf	Plate 1 meat peak temp	Plate 1 meat right surf	Plate 1 clad right surf	Heat trans coef.	Chan 2 coolant	Heat trans coef.	Plate 2 clad left surf	Plate 2 meat left surf	Plate 2 meat peak temp	Plate 2 meat right surf	Plate 2 clad right surf	Heat trans coef.	Chan 3 coolant
	ºC	W/m^2-ºC	ºC	ºC	ºC	ºC	ºC	W/m^2-ºC	ºC	W/m^2-ºC	ºC	ºC	ºC	ºC	ºC	W/m^2-ºC	ºC
	35.00								35.00								35.00
1	35.42	7322.40	74.5	186.74	197.48	186.73	74.53	7322.40	35.42	7322.40	74.54	186.74	197.48	186.73	74.53	7322.4	35.42
2	36.33	7382.00	82.2	214.79	227.48	214.78	82.18	7382.00	36.33	7382.00	82.19	214.79	227.48	214.78	82.18	7382.0	36.33
3	37.39	7451.20	89.8	242.81	257.46	242.80	89.81	7451.20	37.39	7451.20	89.82	242.81	257.46	242.80	89.81	7451.2	37.39
4	38.60	7530.10	97.4	270.79	287.39	270.78	97.39	7530.10	38.60	7530.10	97.40	270.79	287.39	270.78	97.39	7530.1	38.60
5	39.97	7618.60	104.9	298.71	317.26	298.70	104.91	7618.70	39.97	7618.70	104.92	298.71	317.26	298.70	104.91	7618.7	39.97
6	41.48	7716.80	112.4	326.55	347.05	326.54	112.35	7716.90	41.48	7716.90	112.36	326.55	347.05	326.54	112.35	7717.0	41.49
7	43.15	7824.70	119.7	354.30	376.75	354.29	119.69	7824.80	43.15	7824.80	119.71	354.30	376.75	354.29	119.70	7824.9	43.16
8	44.98	7942.30	127.0	381.95	406.35	381.93	126.94	7942.40	44.98	7942.40	126.96	381.95	406.35	381.93	126.94	7942.5	44.98
9	46.95	8069.40	134.1	409.48	435.84	409.47	134.08	8069.50	46.95	8069.50	134.09	409.48	435.85	409.47	134.08	8069.7	46.96
10	49.08	8205.90	141.1	436.91	465.22	436.90	141.11	8206.10	49.08	8206.10	141.12	436.91	465.22	436.90	141.11	8206.2	49.08
	50.18								50.19								50.19

Maximum absolute difference between the temperature distributions calculated by PLTEMP/ANL and the spreadsheet = 0.20 ºC
RMS difference between the temperature distributions calculated by PLTEMP/ANL and the spreadsheet = 0.12 ºC

Table 22.14 Comparison of PLTEMP/ANL and Spreadsheet-Calculated Position (X_{left}) of Peak Meat Temperature in Meat Thickness - Problem 41

	Spreadsheet-Calculated X_{left}				PLTEMP/ANL-Calculated X_{left}			
Segment Number	Assembly 1 Plate 1	Assembly 1 Plate 2	Assembly 2 Plate 1	Assembly 2 Plate 2	Assembly 1 Plate 1	Assembly 1 Plate 2	Assembly 2 Plate 1	Assembly 2 Plate 2
1	0.25459	0.35758	0.46861	0.13211	0.2546	0.3569	0.4687	0.1321
2	0.25413	0.35706	0.46841	0.13208	0.2541	0.3566	0.4685	0.1320
3	0.25363	0.35678	0.46826	0.13201	0.2536	0.3565	0.4683	0.1320
4	0.25308	0.35670	0.46820	0.13192	0.2531	0.3566	0.4682	0.1319
5	0.25249	0.35676	0.46808	0.13179	0.2525	0.3567	0.4681	0.1317
6	0.25186	0.35690	0.46798	0.13165	0.2518	0.3570	0.4680	0.1316
7	0.25120	0.35704	0.46765	0.13151	0.2512	0.3572	0.4677	0.1314
8	0.25050	0.35706	0.46725	0.13136	0.2505	0.3573	0.4673	0.1313
9	0.24979	0.35682	0.46648	0.13122	0.2498	0.3572	0.4665	0.1312
10	0.24906	0.35604	0.46586	0.13108	0.2490	0.3565	0.4659	0.1310

Table 22.15 Spreadsheet-Calculated Temperature Distribution in Problem 41

Fuel Assembly 1

Axial Seg. No	Chan 1 coolant	Heat trans coef.	Plate 1 clad left surf	Plate 1 meat left surf	Plate 1 meat peak temp	Plate 1 meat right surf	Plate 1 clad right surf	Heat trans coef.	Chan 2 coolant	Heat trans coef.	Plate 2 clad left surf	Plate 2 meat left surf	Plate 2 meat peak temp	Plate 2 meat right surf	Plate 2 clad right surf	Heat trans coef.	Chan 3 coolant
	ºC	W/m^2-ºC	ºC	ºC	ºC	ºC	ºC	W/m^2-ºC	ºC	W/m^2-ºC	ºC	ºC	ºC	ºC	ºC	W/m^2-ºC	ºC
	35.00								35.00								35.00
1	35.04	7347.7	38.65	67.38	67.88	63.54	46.02	7347.7	35.45	7347.7	108.95	374.50	382.78	356.06	168.47	7347.7	36.41
2	35.19	7353.0	45.99	132.03	133.54	120.50	67.89	7409.2	36.43	7409.2	104.20	351.07	358.76	333.84	159.04	7540.5	39.14
3	35.50	7368.8	53.43	196.53	199.05	177.29	89.54	7482.3	37.59	7482.3	99.68	328.08	335.19	312.10	150.18	7719.1	41.68
4	35.96	7395.1	60.92	260.83	264.33	233.82	110.89	7566.9	38.92	7566.9	95.39	305.47	312.01	290.76	141.77	7883.4	44.02
5	36.57	7431.9	68.42	324.86	329.34	290.05	131.87	7662.9	40.42	7662.9	91.34	283.19	289.16	269.77	133.75	8033.6	46.17
6	37.34	7478.9	75.93	388.56	394.01	345.91	152.42	7770.3	42.10	7770.3	87.55	261.20	266.60	249.06	126.02	8169.8	48.13
7	38.25	7536.1	83.39	451.90	458.31	401.36	172.49	7888.9	43.95	7888.9	84.02	239.45	244.29	228.60	118.54	8292.3	49.89
8	39.32	7603.5	90.80	514.83	522.18	456.36	192.02	8018.6	45.98	8018.6	80.77	217.92	222.19	208.35	111.24	8401.3	51.45
9	40.53	7680.8	98.12	577.33	585.61	510.87	211.01	8159.0	48.18	8159.0	77.79	196.58	200.27	188.27	104.07	8496.9	52.82
10	41.90	7767.8	105.36	639.37	648.57	564.87	229.41	8310.1	50.56	8310.1	75.11	175.40	178.51	168.33	97.00	8579.5	54.00
	42.62								51.79								54.53

Fuel Assembly 2

Axial Seg. No	Chan 1 coolant	Heat trans coef.	Plate 1 clad left surf	Plate 1 meat left surf	Plate 1 meat peak temp	Plate 1 meat right surf	Plate 1 clad right surf	Heat trans coef.	Chan 2 coolant	Heat trans coef.	Plate 2 clad left surf	Plate 2 meat left surf	Plate 2 meat peak temp	Plate 2 meat right surf	Plate 2 clad right surf	Heat trans coef.	Chan 3 coolant
	ºC	W/m^2-ºC	ºC	ºC	ºC	ºC	ºC	W/m^2-ºC	ºC	W/m^2-ºC	ºC	ºC	ºC	ºC	ºC	W/m^2-ºC	ºC
	35.00								35.00								35.00
1	35.50	7347.7	82.00	231.49	247.50	226.91	88.07	7347.7	35.34	7347.7	45.64	632.24	632.99	600.62	103.39	7347.7	35.72
2	36.56	7415.8	89.20	259.98	278.26	254.71	95.97	7393.8	36.06	7393.8	48.16	741.24	742.12	703.87	116.22	7446.7	37.30
3	37.77	7493.3	96.35	288.41	308.97	282.46	103.83	7446.8	36.89	7446.8	50.74	850.04	851.06	806.92	128.80	7563.3	39.14
4	39.19	7580.3	109.96	344.67	369.79	337.38	119.03	7506.5	37.85	7506.5	53.41	958.61	959.77	909.73	141.11	7697.2	41.25
5	40.82	7686.3	116.95	372.93	400.32	364.95	126.70	7578.5	38.96	7578.5	56.17	1066.92	1068.21	1012.26	153.10	7848.1	43.62
6	42.60	7801.3	123.83	401.09	430.74	392.42	134.26	7657.1	40.17	7657.1	58.97	1174.94	1176.36	1114.50	164.75	8015.8	46.26
7	44.38	7925.3	118.14	373.88	401.22	365.80	127.35	7742.2	41.40	7742.2	61.75	1282.64	1284.20	1216.43	176.05	8199.6	49.17
8	46.01	8039.2	112.61	346.84	371.86	339.34	120.60	7823.0	42.57	7823.0	64.43	1390.03	1391.72	1318.04	187.00	8399.2	52.34
9	47.43	8142.9	101.14	292.47	312.87	286.18	106.95	7899.5	43.64	7899.5	67.00	1497.11	1498.93	1419.32	197.61	8613.9	55.77
10	48.63	8227.3	95.82	265.67	283.75	259.98	100.48	7966.3	44.61	7966.3	69.46	1603.90	1605.84	1520.32	207.89	8843.0	59.48
	49.20								45.07								61.40

Table 22.16 PLTEMP/ANL-Calculated Temperature Distribution in Problem 41

Fuel Assembly 1

Axial Seg. No	Chan 1 coolant	Heat trans coef.	Plate 1 clad left surf	Plate 1 meat left surf	Plate 1 meat peak temp	Plate 1 meat right surf	Plate 1 clad right surf	Heat trans coef.	Chan 2 coolant	Heat trans coef.	Plate 2 clad left surf	Plate 2 meat left surf	Plate 2 meat peak temp	Plate 2 meat right surf	Plate 2 clad right surf	Heat trans coef.	Chan 3 coolant
	ºC	W/m^2-ºC	ºC	ºC	ºC	ºC	ºC	W/m^2-ºC	ºC	W/m^2-ºC	ºC	ºC	ºC	ºC	ºC	W/m^2-ºC	ºC
	35.00								35.00								35.00
1	35.04	7297.60	38.7	67.41	67.91	63.57	46.05	7324.50	35.45	7324.50	109.06	374.15	382.39	355.62	167.86	7387.7	36.41
2	35.19	7307.70	46.1	132.10	133.61	120.58	67.97	7388.90	36.43	7388.90	104.31	350.89	358.56	333.61	158.71	7565.4	39.15
3	35.50	7327.90	53.5	196.64	199.15	177.39	89.66	7464.20	37.59	7464.20	99.79	328.04	335.13	312.02	150.06	7729.8	41.68
4	35.96	7358.10	61.0	260.96	264.46	233.95	111.04	7550.50	38.92	7550.50	95.50	305.53	312.06	290.80	141.80	7881.3	44.03
5	36.57	7398.20	68.6	325.01	329.49	290.20	132.04	7647.90	40.42	7647.90	91.45	283.32	289.28	269.89	133.89	8019.8	46.18
6	37.34	7448.00	76.1	388.72	394.18	346.07	152.60	7756.40	42.10	7756.40	87.65	261.37	266.77	249.24	126.23	8145.5	48.14
7	38.25	7507.50	83.6	452.07	458.48	401.53	172.68	7876.00	43.95	7876.00	84.11	239.64	244.49	228.81	118.80	8258.1	49.90
8	39.32	7576.70	91.0	515.00	522.36	456.53	192.22	8006.60	45.98	8006.60	80.85	218.13	222.40	208.57	111.52	8357.9	51.46
9	40.53	7655.40	98.3	577.50	585.78	511.03	211.20	8148.30	48.18	8148.30	77.87	196.78	200.48	188.49	104.36	8444.7	52.83
10	41.90	7743.50	105.6	639.53	648.74	565.03	229.59	8300.50	50.56	8300.50	75.17	175.59	178.71	168.54	97.27	8518.9	54.00
	42.61								51.80								54.54

Fuel Assembly 2

Axial Seg. No	Chan 1 coolant	Heat trans coef.	Plate 1 clad left surf	Plate 1 meat left surf	Plate 1 meat peak temp	Plate 1 meat right surf	Plate 1 clad right surf	Heat trans coef.	Chan 2 coolant	Heat trans coef.	Plate 2 clad left surf	Plate 2 meat left surf	Plate 2 meat peak temp	Plate 2 meat right surf	Plate 2 clad right surf	Heat trans coef.	Chan 3 coolant
	ºC	W/m^2-ºC	ºC	ºC	ºC	ºC	ºC	W/m^2-ºC	ºC	W/m^2-ºC	ºC	ºC	ºC	ºC	ºC	W/m^2-ºC	ºC
	35.00								35.00								35.00
1	35.50	7327.70	82.1	231.66	247.67	227.09	88.27	7317.20	35.34	7317.20	45.68	632.205	632.96	600.588	103.42	7342.5	35.72
2	36.56	7397.40	89.3	260.15	278.44	254.89	96.19	7364.60	36.06	7364.60	48.20	741.161	742.05	703.792	116.21	7445.7	37.30
3	37.77	7476.10	96.5	288.59	309.16	282.65	104.06	7418.50	36.89	7418.50	50.79	849.92	850.94	806.793	128.75	7565.5	39.15
4	39.19	7568.40	110.1	344.85	369.97	337.57	119.27	7481.50	37.85	7481.50	53.46	958.447	959.60	909.556	141.02	7702.0	41.25
5	40.82	7674.20	117.1	373.12	400.51	365.15	126.96	7553.40	38.96	7553.40	56.22	1066.709	1068.00	1012.047	152.97	7855.3	43.63
6	42.60	7789.10	124.0	401.29	430.95	392.63	134.54	7631.80	40.17	7631.80	59.03	1174.678	1176.10	1114.24	164.58	8025.3	46.27
7	44.38	7903.70	118.4	374.14	401.48	366.06	127.67	7711.30	41.40	7711.30	61.82	1282.336	1283.89	1216.115	175.83	8211.8	49.17
8	46.01	8009.00	112.9	347.14	372.16	339.64	120.94	7786.90	42.57	7786.90	64.53	1389.678	1391.36	1317.669	186.74	8413.9	52.34
9	47.43	8100.20	101.4	292.77	313.18	286.49	107.29	7855.90	43.64	7855.90	67.12	1496.716	1498.53	1418.916	197.31	8630.5	55.78
10	48.64	8177.50	96.1	265.97	284.06	260.28	100.81	7918.30	44.60	7918.30	69.60	1603.478	1605.42	1519.884	207.58	8860.2	59.49
	49.20								45.07								61.40

Maximum absolute difference between the temperature distributions calculated by PLTEMP/ANL and the spreadsheet = 0.61 ºC
RMS difference between the temperature distributions calculated by PLTEMP/ANL and the spreadsheet = 0.18 ºC

Table 22.17 Comparison of PLTEMP/ANL and Spreadsheet-Calculated Position (X_{left}) of Peak Meat Temperature in Meat Thickness - Problem 42

	Spreadsheet-Calculated X_{left}				PLTEMP/ANL-Calculated X_{left}			
Segment Number	Assembly 1 Plate 1	Assembly 1 Plate 2	Assembly 2 Plate 1	Assembly 2 Plate 2	Assembly 1 Plate 1	Assembly 1 Plate 2	Assembly 2 Plate 1	Assembly 2 Plate 2
1	0.25094	0.35957	0.47014	0.12992	0.2509	0.3589	0.4702	0.1299
2	0.25053	0.35924	0.47003	0.12968	0.2505	0.3588	0.4701	0.1297
3	0.25007	0.35909	0.46997	0.12945	0.2500	0.3588	0.4701	0.1294
4	0.24956	0.35909	0.47004	0.12922	0.2495	0.3589	0.4701	0.1292
5	0.24900	0.35918	0.47005	0.12898	0.2489	0.3591	0.4701	0.1290
6	0.24840	0.35929	0.47006	0.12876	0.2483	0.3593	0.4702	0.1287
7	0.24777	0.35933	0.46976	0.12857	0.2477	0.3595	0.4698	0.1286
8	0.24710	0.35919	0.46933	0.12844	0.2470	0.3594	0.4694	0.1284
9	0.24641	0.35868	0.46837	0.12836	0.2463	0.3590	0.4684	0.1283
10	0.24569	0.35747	0.46754	0.12833	0.2456	0.3578	0.4675	0.1283

Table 22.18 Spreadsheet-Calculated Temperature Distribution in Problem 42

Fuel Assembly 1

Axial Seg. No	Chan 1 coolant	Heat trans coef.	Plate 1 clad left surf	Plate 1 meat left surf	Plate 1 meat peak temp	Plate 1 meat right surf	Plate 1 clad right surf	Heat trans coef.	Chan 2 coolant	Heat trans coef.	Plate 2 clad left surf	Plate 2 meat left surf	Plate 2 meat peak temp	Plate 2 meat right surf	Plate 2 clad right surf	Heat trans coef.	Chan 3 coolant
	ºC	W/m^2-ºC	ºC	ºC	ºC	ºC	ºC	W/m^2-ºC	ºC	W/m^2-ºC	ºC	ºC	ºC	ºC	ºC	W/m^2-ºC	ºC
	35.00								35.00								35.00
1	35.04	7333.2	38.43	65.40	65.79	62.31	45.54	7333.2	35.41	7333.2	101.24	338.59	347.27	319.74	153.50	7333.2	36.25
2	35.18	7338.2	45.34	126.12	127.28	116.84	66.49	7388.6	36.30	7388.6	97.07	317.85	325.92	300.26	145.41	7503.9	38.67
3	35.47	7353.0	52.34	186.72	188.66	171.22	87.26	7455.3	37.36	7455.3	93.11	297.45	304.92	281.14	137.73	7661.9	40.91
4	35.90	7377.7	59.39	247.14	249.84	225.40	107.77	7533.3	38.59	7533.3	89.35	277.35	284.21	262.34	130.40	7807.4	42.99
5	36.48	7412.1	66.47	307.32	310.78	279.31	127.96	7622.5	39.99	7622.5	85.81	257.50	263.77	243.81	123.35	7940.6	44.89
6	37.20	7456.2	73.55	367.22	371.43	332.90	147.77	7722.7	41.56	7722.7	82.49	237.87	243.55	225.50	116.54	8061.5	46.63
7	38.06	7509.9	80.61	426.78	431.73	386.12	167.14	7834.0	43.31	7834.0	79.41	218.45	223.53	207.38	109.90	8170.2	48.18
8	39.06	7573.1	87.61	485.97	491.65	438.92	186.04	7956.1	45.22	7956.1	76.57	199.21	203.69	189.43	103.40	8267.1	49.57
9	40.20	7645.6	94.55	544.75	551.15	491.29	204.42	8088.9	47.30	8088.9	73.99	180.12	184.00	171.62	97.00	8352.2	50.78
10	41.48	7727.3	101.41	603.11	610.23	543.20	222.27	8232.1	49.56	8232.1	71.67	161.18	164.43	153.92	90.66	8425.7	51.82
	42.15								50.73							79523.8	52.30

Fuel Assembly 2

Axial Seg. No	Chan 1 coolant	Heat trans coef.	Plate 1 clad left surf	Plate 1 meat left surf	Plate 1 meat peak temp	Plate 1 meat right surf	Plate 1 clad right surf	Heat trans coef.	Chan 2 coolant	Heat trans coef.	Plate 2 clad left surf	Plate 2 meat left surf	Plate 2 meat peak temp	Plate 2 meat right surf	Plate 2 clad right surf	Heat trans coef.	Chan 3 coolan t
	ºC	W/m^2-ºC	ºC	ºC	ºC	ºC	ºC	W/m^2-ºC	ºC	W/m^2-ºC	ºC	ºC	ºC	ºC	ºC	W/m^2-ºC	ºC
	35.00								35.00								35.00
1	35.89	7333.2	118.99	385.63	423.83	375.30	129.18	7333.2	35.52	7333.2	39.39	259.15	259.33	251.07	61.17	7333.2	35.28
2	37.79	7454.3	131.20	435.85	479.49	424.01	142.67	7404.3	36.64	7404.3	41.15	300.38	300.59	290.82	66.33	7371.0	35.88
3	39.94	7592.0	143.11	485.80	534.89	472.46	155.91	7485.5	37.90	7485.5	43.05	341.64	341.89	330.61	71.52	7415.6	36.58
4	42.48	7746.1	166.09	584.99	645.00	568.71	181.88	7576.6	39.39	7576.6	45.14	382.94	383.23	370.44	76.72	7467.0	37.39
5	45.40	7933.1	177.07	634.05	699.52	616.30	194.30	7687.3	41.10	7687.3	47.43	424.27	424.59	410.29	81.93	7525.1	38.29
6	48.57	8135.4	187.67	682.75	753.68	663.53	206.37	7807.5	42.97	7807.5	49.84	465.61	465.96	450.15	87.13	7590.0	39.30
7	51.75	8352.5	176.73	633.44	698.83	615.52	193.29	7937.2	44.84	7937.2	52.23	506.94	507.32	489.99	92.31	7661.5	40.41
8	54.67	8550.7	166.48	584.75	644.58	568.09	180.74	8057.2	46.57	8057.2	54.48	548.23	548.64	529.80	97.48	7739.7	41.62
9	57.21	8730.3	146.62	488.14	536.89	474.09	156.59	8167.7	48.11	8167.7	56.53	589.46	589.91	569.56	102.61	7824.4	42.93
10	59.36	8875.7	137.40	440.43	483.61	427.61	144.94	8259.4	49.43	8259.4	58.37	630.65	631.12	609.26	107.70	7915.5	44.34
	60.37								50.06								45.07

Table 22.19 PLTEMP/ANL-Calculated Temperature Distribution in Problem 42

Fuel Assembly 1

Axial Seg. No	Chan 1 coolant	Heat trans coef.	Plate 1 clad left surf	Plate 1 meat left surf	Plate 1 meat peak temp	Plate 1 meat right surf	Plate 1 clad right surf	Heat trans coef.	Chan 2 coolant	Heat trans coef.	Plate 2 clad left surf	Plate 2 meat left surf	Plate 2 meat peak temp	Plate 2 meat right surf	Plate 2 clad right surf	Heat trans coef.	Chan 3 coolant
	ºC	W/m^2-ºC	ºC	ºC	ºC	ºC	ºC	W/m^2-ºC	ºC	W/m^2-ºC	ºC	ºC	ºC	ºC	ºC	W/m^2-ºC	ºC
	35.00								35.00								35.00
1	35.04	7297.50	38.45	65.41	65.81	62.33	45.55	7321.60	35.41	7321.60	101.24	338.20	346.85	319.27	152.89	7377.2	36.25
2	35.18	7307.00	45.38	126.15	127.31	116.86	66.52	7380.10	36.30	7380.10	97.08	317.61	325.65	299.96	145.02	7534.8	38.67
3	35.47	7325.90	52.40	186.75	188.69	171.25	87.29	7449.40	37.36	7449.40	93.12	297.32	304.77	280.98	137.52	7680.5	40.92
4	35.90	7354.20	59.46	247.17	249.87	225.43	107.80	7529.40	38.59	7529.40	89.36	277.30	284.16	262.28	130.33	7814.7	43.00
5	36.48	7391.90	66.55	307.35	310.80	279.33	127.98	7620.20	39.99	7620.20	85.82	257.51	263.78	243.82	123.38	7937.5	44.90
6	37.20	7438.70	73.63	367.23	371.43	332.90	147.77	7721.90	41.56	7721.90	82.50	237.93	243.61	225.56	116.63	8049.0	46.63
7	38.06	7494.60	80.68	426.77	431.72	386.10	167.13	7834.40	43.30	7834.40	79.42	218.54	223.63	207.49	110.04	8149.0	48.19
8	39.06	7559.60	87.69	485.94	491.62	438.88	186.00	7957.80	45.22	7957.80	76.59	199.32	203.80	189.56	103.57	8237.8	49.58
9	40.20	7633.50	94.62	544.70	551.10	491.23	204.36	8091.90	47.30	8091.90	74.01	180.24	184.12	171.75	97.18	8315.2	50.79
10	41.48	7716.30	101.48	603.04	610.14	543.10	222.17	8236.50	49.56	8236.50	71.69	161.30	164.56	154.06	90.84	8381.4	51.83
	42.15								50.73								52.31

Fuel Assembly 2

Axial Seg. No	Chan 1 coolant	Heat trans coef.	Plate 1 clad left surf	Plate 1 meat left surf	Plate 1 meat peak temp	Plate 1 meat right surf	Plate 1 clad right surf	Heat trans coef.	Chan 2 coolant	Heat trans coef.	Plate 2 clad left surf	Plate 2 meat left surf	Plate 2 meat peak temp	Plate 2 meat right surf	Plate 2 clad right surf	Heat trans coef.	Chan 3 coolant
	ºC	W/m^2-ºC	ºC	ºC	ºC	ºC	ºC	W/m^2-ºC	ºC	W/m^2-ºC	ºC	ºC	ºC	ºC	ºC	W/m^2-ºC	ºC
	35.00								35.00								35.00
1	35.89	7353.30	118.80	385.51	423.7	375.23	129.19	7329.20	35.52	7329.20	39.39	259.181	259.37	251.104	61.24	7313.2	35.28
2	37.79	7477.30	130.95	435.69	479.4	423.90	142.66	7402.20	36.64	7402.20	41.16	300.409	300.63	290.857	66.40	7352.7	35.88
3	39.94	7617.20	142.81	485.60	534.7	472.31	155.88	7484.70	37.90	7484.70	43.05	341.673	341.92	330.645	71.59	7398.7	36.58
4	42.48	7781.30	165.57	584.62	644.7	568.41	181.72	7581.40	39.39	7581.40	45.14	382.973	383.26	370.467	76.79	7451.2	37.39
5	45.40	7969.70	176.51	633.65	699.2	615.98	194.13	7692.20	41.10	7692.20	47.43	424.302	424.62	410.315	82.00	7510.1	38.29
6	48.58	8173.80	187.07	682.32	753.3	663.18	206.19	7812.60	42.96	7812.60	49.83	465.642	465.99	450.174	87.21	7575.5	39.30
7	51.76	8376.60	176.42	633.25	698.7	615.40	193.30	7933.30	44.84	7933.30	52.23	506.969	507.35	490.018	92.40	7647.3	40.41
8	54.68	8561.30	166.38	584.75	644.6	568.14	180.89	8045.10	46.57	8045.10	54.49	548.258	548.67	529.827	97.56	7725.5	41.62
9	57.22	8720.00	146.75	488.34	537.1	474.30	156.88	8143.50	48.11	8143.50	56.55	589.495	589.94	569.586	102.70	7810.2	42.93
10	59.37	8853.10	137.62	440.69	483.9	427.88	145.27	8228.50	49.43	8228.50	58.41	630.678	631.15	609.292	107.80	7901.3	44.34
	60.38								50.06								45.07

Maximum absolute difference between the temperature distributions calculated by PLTEMP/ANL and the spreadsheet = 0.61 ºC
RMS difference between the temperature distributions calculated by PLTEMP/ANL and the spreadsheet = 0.14 ºC

Table 22.20 Wall Temperatures and Heat Fluxes Calculated by Spreadsheet for Fuel Assembly 1 of Problem 42

Axial Seg. No.	Cladding Surface Temperatures and Heat Fluxes Used for Calculating ONBR							
	Left Surf of Plate 1		Right Surf of Plate 1		Left Surf of Plate 2		Right Surf of Plate 2	
	Operating Wall Temp	Operating Heat Flux	Operating Wall Temp	Operating Heat Flux	Operating Wall Temp	Operating Heat Flux	Operating Wall Temp	Operating Heat Flux
	$T_{w,op}$	q_{op}	$T_{w,op}$	q_{op}	$T_{w,op}$	q_{op}	$T_{w,op}$	q_{op}
	ºC	MW/m^2	ºC	MW/m^2	ºC	MW/m^2	ºC	MW/m^2
1	38.43	0.024895	45.54	0.074311	101.24	0.482756	153.50	0.859836
2	45.34	0.074562	66.49	0.223057	97.07	0.449044	145.41	0.800956
3	52.34	0.124042	87.26	0.371990	93.11	0.415615	137.73	0.741793
4	59.39	0.173305	107.77	0.521140	89.35	0.382365	130.40	0.682450
5	66.47	0.222324	127.96	0.670533	85.81	0.349201	123.35	0.623021
6	73.55	0.271076	147.77	0.820193	82.49	0.316041	116.54	0.563588
7	80.61	0.319544	167.14	0.970139	79.41	0.282809	109.90	0.504228
8	87.61	0.367712	186.04	1.120384	76.57	0.249439	103.40	0.445005
9	94.55	0.415570	204.42	1.270938	73.99	0.215870	97.00	0.385982
10	101.41	0.463111	222.27	1.421809	71.67	0.182047	90.66	0.327212

Table 22.21 Wall Temperatures and Heat Fluxes Calculated by Spreadsheet for Fuel Assembly 2 of Problem 42

Axial Seg. No.	Cladding Surface Temperatures and Heat Fluxes Used for Calculating ONBR							
	Left Surf of Plate 1		Right Surf of Plate 1		Left Surf of Plate 2		Right Surf of Plate 2	
	Operating Wall Temp	Operating Heat Flux	Operating Wall Temp	Operating Heat Flux	Operating Wall Temp	Operating Heat Flux	Operating Wall Temp	Operating Heat Flux
	$T_{w,op}$	q_{op}	$T_{w,op}$	q_{op}	$T_{w,op}$	q_{op}	$T_{w,op}$	q_{op}
	ºC	MW/m^2	ºC	MW/m^2	ºC	MW/m^2	ºC	MW/m^2
1	118.99	0.609445	129.18	0.686852	39.387	0.028356	61.17	0.189898
2	131.20	0.696345	142.67	0.785137	41.154	0.033448	66.33	0.224489
3	143.11	0.783289	155.91	0.883378	43.050	0.038528	71.52	0.259091
4	166.09	0.957488	181.88	1.079549	45.145	0.043587	76.72	0.293715
5	177.07	1.044544	194.30	1.177678	47.429	0.048625	81.93	0.328359
6	187.67	1.131618	206.37	1.275789	49.837	0.053649	87.13	0.363018
7	176.73	1.043910	193.29	1.178312	52.229	0.058673	92.31	0.397677
8	166.48	0.956049	180.74	1.080988	54.481	0.063709	97.48	0.432322
9	146.62	0.780622	156.59	0.886045	56.525	0.068766	102.61	0.466948
10	137.40	0.692646	144.94	0.788835	58.373	0.073842	107.70	0.501555

Table 22.22 Comparison of ONBR Calculated by the *First Approach* between PLTEMP/ANL and Spreadsheet for Fuel Assembly 1 of Problem 42

Axial Seg. No.	PLTEMP/ANL				Spreadsheet								
	ONBR				ONBR				T_{sat}	T_{onb} , ºC			
	Left Surf of Plate 1	Right Surf of Plate 1	Left Surf of Plate 2	Right Surf of Plate 2	Left Surf of Plate 1	Right Surf of Plate 1	Left Surf of Plate 2	Right Surf of Plate 2	ºC	Left Surf of Plate 1	Right Surf of Plate 1	Left Surf of Plate 2	Right Surf of Plate 2
1	31.56	10.39	1.70	0.9700	31.72	10.41	1.70	0.9639	142.60	143.82	144.66	147.63	149.23
2	10.54	3.52	1.81	1.03	10.59	3.52	1.81	1.03	142.41	144.48	145.89	147.27	148.82
3	6.31	2.13	1.92	1.1	6.34	2.14	1.93	1.10	142.23	144.86	146.67	146.91	148.40
4	4.50	1.54	2.05	1.18	4.51	1.54	2.05	1.18	142.04	145.12	147.26	146.54	147.97
5	3.50	1.21	2.19	1.27	3.51	1.21	2.19	1.27	141.85	145.32	147.73	146.16	147.53
6	2.86	1.00	2.33	1.37	2.87	1.00	2.33	1.37	141.66	145.48	148.14	145.77	147.07
7	2.42	0.86	2.48	1.49	2.43	0.86	2.49	1.49	141.47	145.60	148.49	145.37	146.60
8	2.10	0.75	2.64	1.62	2.10	0.75	2.64	1.62	141.27	145.69	148.79	144.95	146.11
9	1.86	0.67	2.81	1.78	1.86	0.67	2.81	1.78	141.08	145.77	149.07	144.51	145.60
10	1.67	0.61	2.97	1.97	1.67	0.61	2.97	1.98	140.89	145.82	149.31	144.05	145.07

Maximum Absolute Difference in ONBR Calculated by PLTEMP/ANL and Spreadsheet = 0.63 %

Table 22.23 Comparison of ONBR Calculated by the *First Approach* between PLTEMP/ANL and Spreadsheet for Fuel Assembly 2 of Problem 42

Axial Seg. No.	PLTEMP/ANL				Spreadsheet								
	ONBR				ONBR				T_{sat}	T_{onb} , ºC			
	Left Surf of Plate 1	Right Surf of Plate 1	Left Surf of Plate 2	Right Surf of Plate 2	Left Surf of Plate 1	Right Surf of Plate 1	Left Surf of Plate 2	Right Surf of Plate 2	ºC	Left Surf of Plate 1	Right Surf of Plate 1	Left Surf of Plate 2	Right Surf of Plate 2
1	1.35	1.20	24.80	4.22	1.35	1.21	24.82	4.23	142.60	148.22	148.55	143.90	145.82
2	1.18	1.06	17.67	3.53	1.18	1.06	17.68	3.54	142.41	148.41	148.76	143.82	145.90
3	1.05	0.94	13.50	3.03	1.05	0.94	13.51	3.04	142.23	148.56	148.94	143.73	145.96
4	0.87	0.78	10.71	2.65	0.87	0.78	10.71	2.66	142.04	149.01	149.42	143.63	146.01
5	0.8100	0.72	8.73	2.36	0.8033	0.72	8.73	2.37	141.85	149.12	149.55	143.53	146.03
6	0.75	0.67	7.31	2.13	0.75	0.67	7.31	2.13	141.66	149.21	149.66	143.42	146.05
7	0.80	0.72	6.28	1.93	0.80	0.72	6.29	1.94	141.47	148.74	149.17	143.31	146.05
8	0.86	0.78	5.55	1.77	0.86	0.78	5.55	1.78	141.27	148.25	148.67	143.19	146.05
9	1.01	0.93	5.01	1.64	1.01	0.93	5.02	1.64	141.08	147.41	147.80	143.07	146.03
10	1.09	1.02	4.61	1.52	1.09	1.02	4.62	1.53	140.89	146.87	147.25	142.94	146.01

Maximum Absolute Difference in ONBR Calculated by PLTEMP/ANL and Spreadsheet = 0.83 %

Table 22.24 Comparison of ONBR Calculated by the *Second Approach* between PLTEMP/ANL and Spreadsheet for Fuel Assembly 1 of Problem 42 – Using H_2O Saturation Temperature

Axial Seg. No.	PLTEMP/ANL				Spreadsheet								
	ONBR				ONBR				T_{sat}	T_{onb} , ºC			
	Left Surf of Plate 1	Right Surf of Plate 1	Left Surf of Plate 2	Right Surf of Plate 2	Left Surf of Plate 1	Right Surf of Plate 1	Left Surf of Plate 2	Right Surf of Plate 2	ºC	Left Surf of Plate 1	Right Surf of Plate 1	Left Surf of Plate 2	Right Surf of Plate 2
1	32.775	10.7	1.706	0.959	33.209	10.803	1.720	0.961	142.60	148.94	148.85	148.95	148.94
2	10.863	3.577	1.817	1.026	10.998	3.610	1.833	1.030	142.41	148.74	148.69	148.75	148.76
3	6.471	2.153	1.938	1.099	6.548	2.172	1.954	1.106	142.23	148.54	148.53	148.54	148.57
4	4.595	1.544	2.067	1.179	4.647	1.558	2.085	1.188	142.04	148.34	148.37	148.31	148.37
5	3.557	1.208	2.206	1.27	3.595	1.218	2.225	1.281	141.85	148.15	148.21	148.07	148.14
6	2.9	0.994	2.355	1.372	2.930	1.003	2.375	1.385	141.66	147.96	148.06	147.79	147.90
7	2.448	0.847	2.511	1.489	2.473	0.854	2.533	1.504	141.47	147.77	147.91	147.48	147.65
8	2.119	0.741	2.674	1.625	2.140	0.747	2.697	1.643	141.27	147.58	147.77	147.13	147.36
9	1.869	0.659	2.84	1.787	1.887	0.665	2.865	1.807	141.08	147.40	147.62	146.72	147.05
10	1.674	0.596	3.007	1.983	1.690	0.601	3.034	2.007	140.89	147.21	147.48	146.24	146.71

Maximum Absolute Difference in ONBR Calculated by PLTEMP/ANL and Spreadsheet = 1.32 %

Table 22.25 Comparison of ONBR Calculated by the *Second Approach* between PLTEMP/ANL and Spreadsheet for Fuel Assembly 2 of Problem 42 - Using H_2O Saturation Temperature

Axial Seg. No.	PLTEMP/ANL				Spreadsheet								
	ONBR				ONBR				T_{sat}	T_{onb} , ºC			
	Left Surf of Plate 1	Right Surf of Plate 1	Left Surf of Plate 2	Right Surf of Plate 2	Left Surf of Plate 1	Right Surf of Plate 1	Left Surf of Plate 2	Right Surf of Plate 2	ºC	Left Surf of Plate 1	Right Surf of Plate 1	Left Surf of Plate 2	Right Surf of Plate 2
1	1.349	1.200	25.663	4.307	1.357	1.210	25.892	4.354	142.60	148.94	148.96	148.59	148.94
2	1.176	1.048	18.195	3.592	1.182	1.057	18.352	3.629	142.41	148.76	148.78	147.93	148.73
3	1.045	0.932	13.848	3.077	1.051	0.940	13.965	3.108	142.23	148.58	148.61	147.42	148.52
4	0.862	0.767	10.949	2.689	0.865	0.772	11.037	2.716	142.04	148.43	148.45	146.97	148.32
5	0.794	0.706	8.905	2.387	0.797	0.711	8.977	2.411	141.85	148.28	148.30	146.57	148.12
6	0.738	0.655	7.435	2.145	0.741	0.660	7.496	2.166	141.66	148.13	148.14	146.21	147.93
7	0.792	0.708	6.381	1.948	0.797	0.714	6.437	1.967	141.47	147.93	147.96	145.90	147.74
8	0.851	0.766	5.627	1.784	0.857	0.774	5.679	1.802	141.27	147.71	147.77	145.63	147.55
9	0.997	0.915	5.079	1.646	1.007	0.926	5.129	1.662	141.08	147.41	147.53	145.40	147.37
10	1.083	1.010	4.667	1.528	1.095	1.022	4.714	1.543	140.89	147.12	147.30	145.19	147.18

Maximum Absolute Difference in ONBR Calculated by PLTEMP/ANL and Spreadsheet = 1.15 %

Table 22.26 Comparison of ONBR Calculated by the *Second Approach* between PLTEMP/ANL and Spreadsheet for Fuel Assembly 1 of Problem 42 – Using D_2O Saturation Temperature

Axial Seg. No.	PLTEMP/ANL				Spreadsheet								
	ONBR				ONBR				T_{sat}	T_{onb} , ºC			
	Left Surf of Plate 1	Right Surf of Plate 1	Left Surf of Plate 2	Right Surf of Plate 2	Left Surf of Plate 1	Right Surf of Plate 1	Left Surf of Plate 2	Right Surf of Plate 2	ºC	Left Surf of Plate 1	Right Surf of Plate 1	Left Surf of Plate 2	Right Surf of Plate 2
1	33.048	10.789	1.720	0.967	33.209	10.803	1.720	0.961	142.60	148.94	148.85	148.95	148.94
2	10.953	3.607	1.832	1.034	10.998	3.610	1.833	1.030	142.41	148.74	148.69	148.75	148.76
3	6.526	2.171	1.954	1.108	6.548	2.172	1.954	1.106	142.23	148.54	148.53	148.54	148.57
4	4.633	1.557	2.085	1.189	4.647	1.558	2.085	1.188	142.04	148.34	148.37	148.31	148.37
5	3.587	1.218	2.225	1.280	3.595	1.218	2.225	1.281	141.85	148.15	148.21	148.07	148.14
6	2.924	1.003	2.375	1.383	2.930	1.003	2.375	1.385	141.66	147.96	148.06	147.79	147.90
7	2.469	0.855	2.532	1.501	2.473	0.854	2.533	1.504	141.47	147.77	147.91	147.48	147.65
8	2.137	0.747	2.696	1.639	2.140	0.747	2.697	1.643	141.27	147.58	147.77	147.13	147.36
9	1.885	0.665	2.865	1.802	1.887	0.665	2.865	1.807	141.08	147.40	147.62	146.72	147.05
10	1.688	0.601	3.033	2.000	1.690	0.601	3.034	2.007	140.89	147.21	147.48	146.24	146.71

Maximum Absolute Difference in ONBR Calculated by PLTEMP/ANL and Spreadsheet = 0.57 %

Table 22.27 Comparison of ONBR Calculated by the *Second Approach* between PLTEMP/ANL and Spreadsheet for Fuel Assembly 2 of Problem 42 – Using D_2O Saturation Temperature

Axial Seg. No.	PLTEMP/ANL				Spreadsheet								
	ONBR				ONBR				T_{sat}	T_{onb} , ºC			
	Left Surf of Plate 1	Right Surf of Plate 1	Left Surf of Plate 2	Right Surf of Plate 2	Left Surf of Plate 1	Right Surf of Plate 1	Left Surf of Plate 2	Right Surf of Plate 2	ºC	Left Surf of Plate 1	Right Surf of Plate 1	Left Surf of Plate 2	Right Surf of Plate 2
1	1.360	1.210	25.876	4.343	1.357	1.210	25.892	4.354	142.60	148.94	148.85	148.95	148.94
2	1.186	1.057	18.347	3.622	1.182	1.057	18.352	3.629	142.41	148.74	148.69	148.75	148.76
3	1.054	0.940	13.964	3.102	1.051	0.940	13.965	3.108	142.23	148.54	148.53	148.54	148.57
4	0.869	0.773	11.042	2.711	0.865	0.772	11.037	2.716	142.04	148.34	148.37	148.31	148.37
5	0.801	0.712	8.981	2.407	0.797	0.711	8.977	2.411	141.85	148.15	148.21	148.07	148.14
6	0.744	0.661	7.498	2.163	0.741	0.660	7.496	2.166	141.66	147.96	148.06	147.79	147.90
7	0.799	0.714	6.436	1.964	0.797	0.714	6.437	1.967	141.47	147.77	147.91	147.48	147.65
8	0.858	0.773	5.676	1.799	0.857	0.774	5.679	1.802	141.27	147.58	147.77	147.13	147.36
9	1.006	0.923	5.123	1.660	1.007	0.926	5.129	1.662	141.08	147.40	147.62	146.72	147.05
10	1.093	1.018	4.708	1.541	1.095	1.022	4.714	1.543	140.89	147.21	147.48	146.24	146.71

Maximum Absolute Difference in ONBR Calculated by PLTEMP/ANL and Spreadsheet = 0.45 %

Table 22.28 Comparison of OFIR between PLTEMP/ANL and Spreadsheet for Fuel Assemblies 1 and 2 of Problem 42

Fuel Assembly Exit	PLTEMP/ANL			Spreadsheet						
	OFIR			OFIR			T_{sat}	$T_{out,op}$, ºC		
	Channel 1	Channel 2	Channel 3	Channel 1	Channel 2	Channel 3	ºC	Channel 1	Channel 2	Channel 3
1	8.1640	3.7113	3.3725	8.1596	3.7111	3.3735	140.79	42.15	50.73	52.30
2	2.2998	3.8758	5.7956	2.3005	3.8751	5.7949	140.79	60.37	50.06	45.07

Maximum Absolute Difference in OFIR Calculated by PLTEMP/ANL and Spreadsheet = 0.00445

23 Verification of Flow Rate Calculation for a Specified Frictional Pressure Drop

The verification work reported here was done in August 2017. Section 23.1 describes the flow rate calculation method implemented in the PLTEMP/ANL code. Table 23.3 discussed in Section 23.3.1 provides a verification of the method by comparing the code-calculated flow rates for three standard problems (Problems 3, 3B, and 3C described in Section 23.2) with those of a spreadsheet developed for this purpose The filenames of all input and output files and spreadsheets are given in Section 23.5. The development and checking of the spreadsheet itself is documented in Appendix K at the end of this chapter. The conclusions given in Sectiom 23.6 are also stated below.

The maximum absolute difference in the flow rate of any of the five coolant channels in each of the two fuel assemblies of Problem 3B is 0.074%. The maximum absolute difference in the flow rate of any of the five coolant channels in each of the two fuel assemblies of Problem 3 is 0.097%. The maximum absolute difference in the flow rate of any of the five coolant channels in assembly 1 of Problem 3C is 0.097%. These are good agreements. The maximum absolute difference in the flow rate of any of the five coolant channels in assembly 2 of Problem 3C is 1.361%. This is an acceptable agreement. These comparisons provide a verification of the flow rate calculation implemented in the PLTEMP/ANL code.

The hydraulic calculation for determining the coolant channel flow rates is done by PLTEMP/ANL before the thermal calculation is performed. For this hydraulic calculation the power produced in each fuel plate is assumed to be divided equally between its two adjacent coolant channels. The thermal calculation performed using these coolant flow rates, determines the actual division of each fuel plate's power that could be utilized in a subsequent hydraulic calculation to improve the flow rate predictions. The subsequent hydraulic calculation (i.e., thermal-hydraulic iteration) is not done to speed up the code. The possible improvement in channel flow rates by performing thermal-hydraulic iteration in the PLTEMP/ANL code is studied and found to be about 0.15% or less. This much improvement is not significant enough to slow down the code by performing the thermal-hydraulic iteration.

23.1 Flow Rate Calculation Method in PLTEMP/ANL

The PLTEMP/ANL code calculates the flow rate in each fuel assembly and in its coolant channels for a user-input frictional pressure drop (not the total pressure drop including the gravity head) in the assembly[1] (see input data on the input card type 500 in Appendix I of Reference 1). The model is described in Appendix L at the end of this chapter. Basically, as shown in Fig. 23.1, in the hydraulics model the fuel assembly is divided into an inlet region (region 1), a fueled region (region 2), and a series of one or more consecutive outlet regions (regions 3, 4, etc.). Only one outlet region is shown in Fig. 23.1. The fueled region actually consists of a number of parallel coolant channels (flow paths) of equal length. Every hydraulic path – region 1, each individual coolant channel of region 2, region 3, and any region if present beyond region 3 – is characterized by a flow area, a hydraulic diameter, a form-loss factor, and an axial length. In region 2 of an assembly, every coolant channel is assumed to have the same form-loss factor, equal to that of the equivalent flow channel obtained by combining all the parallel coolant channels in region 2.

PLTEMP/ANL calculates flow rates in two steps. In the first step, all the parallel channels in region 2 of an assembly are represented by a single equivalent channel having an equivalent hydraulic diameter, the total flow area and total flow rate of all the parallel channels. The first step produces a frictional pressure drop in each region of the assembly. Then in the second step the code uses the region 2 frictional pressure drop (found in step 1) to determine the flow rate in each individual channel of region 2. Details of this two-step process are provided below.

In the first step, a starting guess for the assembly flow rate is used to get the coolant exit temperature in the assembly; the coolant temperature in the assembly inlet region (e.g., region 1 in Fig. 23.1) is axially uniform and equals the inlet temperature; the coolant temperature in the fueled length is assumed to be the average of the inlet temperature and the calculated assembly exit temperature; the coolant temperature in the assembly outlet regions (e.g., region 3 in Fig. 23.1) is axially uniform and equals the mixed-mean exit temperature for the assembly. An equivalent hydraulic diameter of all coolant channels in the fueled length (region 2 in Fig. 23.1) is obtained by combining the flow areas of all channels, and the wetted perimeters of all channels [equivalent hydraulic diameter = 4*(total flow area)/(total wetted permeter)]. For each axial region in the assembly, the code then calculates the coolant properties, the Reynolds number, the friction factor, and the frictional pressure drop. Finally, a new value for the assembly flow rate is obtained by equating the input assembly frictional pressure drop ΔP_{fric} to the sum of the frictional pressure drops in all axial regions of the assembly, as shown by Eq. (23.1) where the subscript n is region number. The guessed assembly flow rate is adjusted iteratively to arrive at a converged flow-rate solution. The converged assembly flow rate is used to determined the region-wise frictional pressure drops ($\Delta P_{fric,1}$, $\Delta P_{fric,2}$, $\Delta P_{fric,3}$, etc.) in the assembly.

$$\Delta P_{fric} = \frac{W_f^2}{2} \sum_{n=1}^{3} \frac{K_n + f_n \, L_n / D_{h,n}}{\rho_n \, A_{f,n}^2} \tag{23.1}$$

In the second step, the flow rate in each coolant channel in the fueled length (region 2) is obtained by equating the frictional pressuire drop for region 2, $\Delta P_{fric,2}$, determined in the first step, to the frictional pressure drop for the individal channel. This is done by solving Eq. (23.2) for the flow rate, $W_{ch,\,k}$, in the individual channel k.

$$W_{ch,k} = A_{ff,k} \left[\frac{2 \rho_{ch,k} \Delta P_{fric,2}}{\left(K_2 + f_{ch,k} L_2 / D_{ch,k} \right)} \right]^{0.5} \tag{23.2}$$

The coolant thermal properties used in this calculation are evaluated at the average of the channel inlet and outlet temperatures. Since the outlet temperature of channel is not known at the outset, some iteration is required. The initial guess is that the region 2 flow is divided equally among all of its channels. After obtaining the solution for all channels, the converged flow rates of all channels are summed to obtain the assembly flow rate.

23.2 Problems Used in Verification of the PLTEMP/ANL Flow Rate Calculation

The code-calculated flow rate for a specified frictional pressure drop in a fuel assembly is verified here by comparison with an Excel spreadsheet developed for this purpose (described in Appendix K), for an earlier standard Problem 3 described in Chapter 1, and two other similar problems (Problem 3B and Problem 3C). All three problems have upflow. Figure 23.1 shows the three axial regions of each fuel assembly in these problems. The three problems differ only in the input total power and the radial power factors of fuel plates in the two fuel assemblies in each problem. These input differences are shown below in Table 23.1. The PLTEMP/ANL input data files for these problems are shown in Figs. 23.3, 23.4, and 23.5. The radial power factors affect the relative distribution of the total core power among the fuel plates in the core, but not the total power itself.

The development and checking of the spreadsheet is described in Appendix K. The thermal properties of the coolant (light water) were calculated on the spreadsheet using simple correlations developed and reported by ORNL[2]. The comparison between the spreasheet and the PLTEMP/ANL code calculations for the problems is given in Section 23.4.

<u>Description of Standard Problem 3:</u> This input file shown in Fig. 23.3 models 2 fuel assemblies of a single fuel type in *slab geometry*, with a total power of 1.0 MW. The coolant inlet temperature is 45 ºC. Each assembly has 4 fuel plates (made of 1.0 mm thick fuel meat with 0.5 mm thick cladding on both sides) and 5 coolant channels (each 3.0 mm thick and 20.0 cm wide). Each fuel assembly has three axial regions as shown in Fig. 23.1. The fuel assembly has an un-fueled length of 0.15 meter above (minor loss factor 8.0) and an un-fueled length of 0.15 meter below (minor loss factor 8.0) the fueled length of 0.75 meter, which is divided into 10 equal-length axial segments in heat transfer calculation but treated as a single region in flow calculation. The code was run to calculate the flow rate (the pressure-drop-driven mode of the code) for a frictional pressure drop of 0.10 MPa and an inlet pressure of 1.4 MPa. The input roughness is zero in all three regions of the assembly. Bypass channel or hot channel factors are not used. The thermal-hydraulic data of the problem is given in Table 23.1.

23.3 Verification of Code-Calculated Flow Rates by Comparison with the Spreadsheet

Table 23.2 shows a comparison of PLTEMP/ANL- and spreadsheet-calculated coolant channel exit temperatures. The purpose of this table is to present the coolant temperatures used in the spreadsheet calculation of flow, in order to show that only rough estimates of coolant temperatures are needed to calculate an accurate coolant flow rate (discussed in Section 23.3.2).

Table 23.3 shows the main comparison of PLTEMP/ANL- and spreadsheet-calculated coolant channel flow rates. This comparison provides a verification of the flow rate calculation implemented in PLTEMP/ANL (discussed in Section 23.3.1).

Table 23.4 shows the inter-problem flow rate differences between Problems 3 vs 3B, and between Problems 3C vs 3B. It is used to obtain an estimate of the error in PLTEMP/ANL-calculated channel flow rates due to the lack of repeating the hydraulic calculation after doing the thermal calculation using flow rates calculated based on an assumption that each fuel plate's power is deposited equally into the two contacting channels (discussed in Section 23.3.2).

Tables 23.5 to 23.13 show the spreadsheet calculation in three parts for each standard problem (Problems 3B, 3, and 3C), from which the flow rates shown in Table 23.3 are summarized.

23.3.1 Verification of Code-Calculated Flow Rates

Table 23.3 shows a comparison between the spreadsheet- and PLTEMP/ANL-calculated flow rates for three standard problems, Problems 3, 3B, and 3C. The percent difference between the two calculations is separately discussed below for each problem, beginning with Problem 3B which is the simplest of the three problems.

Comparison for Standard Problem 3B: Problem 3B is the simplest of three problems in the sense that the coolant is practically at a uniform temperature in the whole fuel assembly (including the heated and the unheated axial regions, shown in Fig. 23.1) since the input total power in the problem is nearly zero (10^{-4} MW). The uniformity of coolant temperature removes the effect on flow rate caused by viscosity variation along the whole fuel assembly length. Table 23.3 shows that the maximum absolute difference in the flow rate of any of the 5 coolant channels in each of the two fuel assemblies of Problem 3B is 0.074%. This is a good agreement. This comparison provides a verification of the flow rate calculation implemented in the PLTEMP/ANL code.

Comparison for Standard Problem 3: In this problem, the power generated in each of the two fuel assemblies is 0.5 MW, and the largest coolant temperature rise in a channel is 16.5 ºC, comparable to the coolant temperature rise in experimental and test reactors. Table 23.3 shows that the maximum absolute difference in the flow rate of any of the 5 coolant channels in each of the two fuel assemblies of Problem 3 is 0.097%. This is a good agreement. This comparison provides a verification of the flow rate calculation implemented in the PLTEMP/ANL code.

Comparison for Standard Problem 3C**:** In this problem, the power of fuel assembly 1 is 0.5 MW, comparable to the assembly power in experimental and test reactors, and the power of assembly 2 is 3.5 MW, much greater than the assembly power in experimental and test reactors. Table 23.3 shows that the maximum absolute difference in the flow rate of any of the 5 coolant channels in assembly 1 of Problem 3C is 0.097%. This is a good agreement. The maximum absolute difference in the flow rate of any of the 5 coolant channels in assembly 2 of Problem 3C is 1.36%. This is an acceptable agreement. This comparison provides a verification of the flow rate calculation implemented in the PLTEMP/ANL code.

The spreadsheet- and PLTEMP/ANL-calculated flow rates differ slightly possibly due to two reasons: (1) The code uses the Colebrook[3] implicit correlation for friction factor whereas the spreadsheet uses the explicit correlation of Zigrang-Sylvester[3,4]. The difference between the Colebrook and Zigrang-Sylvester correlations is 0.11% in the Reynolds number range of the three problems, and (2) The code uses coolant properties obtained by the FORTRAN subroutines obtained from IAPS[5] whereas the spreadsheet uses simple fitted correlations reported by ORNL[2].

23.3.2 Comparison of Channel Exit Temperatures

Table 23.2 shows the difference between the spreadsheet- and PLTEMP/ANL-calculated coolant exit temperatures in each channel of both fuel assemblies of the three standard problems (Problems 3, 3B and 3C). The code-calculated coolant temperatures are of course more accurate than the spreadsheet-calculated values because the latter are based on an assumption that every fuel plate's power is split equally between the two adjacent channels whereas the former are obtained by a simultaneous solution of coolant and plate temperatures. *However, this error does not contribute to the difference (reported in Table 23.3 and discussed Section 23.3.1) between the spreadsheet- and code-calculated flow rates because, during the flow calculation, both calculations make this assumption.*
Table 23.2 shows that the maximum error in the spreadsheet-calculated channel exit temperature is 0.0073 ºC in Problem 3B (each assembly power = 50 W), 0.56 ºC in Problem 3 (each assembly power = 0.5 MW) and the same error in assembly 1 of Problem 3C (assembly 1 power = 0.5 MW). The maximum error increases to 5.0 ºC in assembly 2 of Problem 3C (assembly 2 power = 3.5 MW) in which the channel exit temperature is extremely high (within 3 ºC of the saturation temperature of 195 ºC). The assembly 2 of Problem 3C is an extreme test case because of (i) extremely high power causing near-saturation channel exit temperature, and (ii) extremely *unequal* fuel plate powers (powers of the 4 plates bear the ratio 1.0 : 2.5 : 2.5 : 1.0). Unequal fuel plate powers tend to cause unequal splits of plate power.

It is concluded from the above comparison that the assumption made on the spreadsheet regarding fuel plate power splitting is acceptable up to an assembly power of 0.5 M W, but gets worse with increasing assembly power (to near-saturation coolant temperature) causing unequal plate powers. Therefore, an estimate is here made of the flow rate error due to not repeating the hydraulic calculation after doing the thermal calculation in PLTEMP/ANL.

23.4 Channel Flow Rate Error due to Lack of Thermal-Hydraulic Iteration

The PLTEMP/ANL code calculates channel flow rates using an assumption that each fuel plate power is split equally into the two adjacent channels, but the code does not recalculate the flow rates after performing the coupled plate-channel heat transfer calculation for a fuel assembly (the equal-split assumption is not made in the heat transfer calculation). The absence of recalculation, i.e., lack of thermal-hydraulic (T/H) iteration, causes a small error. The channel flow rate error due to the lack of T/H iteration in the PLTEMP/ANL code, is found here using two methods:

(1) The first method finds the error due to lack of T/H iteration by actually carrying out one T/H iteration for a multi-channel problem and then comparing the channel flow rates obtained with those found without the T/H iteration. The iteration is carried out on the spreadsheet, using the actual plate power split fractions calculated by PLTEMP/ANL for the problem.
(2) The second method finds the error due to lack of T/H iteration based on the error in coolant temperature rise due to the assumption that each plate power is split equally into the two adjacent channels, and

The channel flow rate error due to the lack of T/H iteration is found to be ~0.15 % or less by both methods.

First Method: In the first method, the error ($E_{T\text{-}H}$) due to lack of T/H iteration is found by actually carrying out a T/H iteration and then comparing the channel flow rates obtained, with those found without the T/H iteration. The iteration is carried out on the spreadsheet, using the actual plate power split fractions calculated by PLTEMP/ANL for the problem. This comparison is done for four standard problems, i.e., Problems 3, 43, 44, and 45. These problems cover the typical ranges of hydraulic diameter, coolant velocity, assembly pressure drop, and plate-to-plate variation of power factors in a fuel assembly of experimental and test reactor designs. The PLTEMP/ANL input data files of these problems are given in Figs. 23.3, 23.6 to 23.8. The important features of these problems that affect the error to be estimated are shown below in Table 23.14.

The key data required to carry out a T/H iteration are the plate power split fractions obtained after the heat transfer calculation. The power split fraction in each fuel plate varies axially over the fueled length, in the PLTEMP/ANL code thermal calculation. It is averaged axially for input to the spreadsheet in order to make a T/H iteration on the flow rate calculation. The average power split fraction is shown in Table 23.15. The table shows the PLTEMP/ANL-calculated fraction of fuel plate power deposited to the coolant channel on the left hand side of the plate. For each of the four problems, the channel flow rates calculated before and after a T/H iteration is shown in Tables 23.16 to 23.19. The column 7 of these tables shows the channel flow rates *before the T/H iteration*. The column 10 of these tables shows the channel flow rates *after the T/H iteration*. The column 11of these four tables shows the channel flow rate error due to the lack of T/H iteration. The maximum error for each problem is summarized here in Table 23.14.

The maximum error due to the lack of T/H iteration is ~ 0.14% or less. This implies that the possible improvement in channel flow rates by performing T/H iteration is ~ 0.14% or less. This much improvement is not significant enough to slow down the code by doing the iteration.

Second Method: The PLTEMP/ANL code calculates channel flow rates using an assumption that each fuel plate power is split equally into the two adjacent channels, but the code does not recalculate the flow rates after performing the coupled plate-channel heat transfer calculation for a fuel assembly (the equal-split assumption is not made in the heat transfer calculation). The absence of recalculation is referred to here as a lack of thermal-hydraulic iteration. An estimate of the channel flow rate error ($E_{T\text{-}H}$) due to the lack of thermal-hydraulic iteration, can be obtained by comparing the flow solution of Problem 3C with that of Problem 3B, using the following equation based on the reasoning given below.

$$E_{T-H} = \frac{\text{Error in } \Delta T \text{ in Problem 3C due to the assumption}}{\Delta T \text{ in Problem 3C}} \times (\text{Flow rate error in Problem 3C}) \quad (23.3)$$

where ΔT is the largest coolant temperature rise in a channel of a fuel assembly,

Since Problem 3B has nearly zero power, the coolant temperature rise ΔT in each channel is nearly zero, the coolant is uniformly at the input inlet temperature, and hence any assumption regarding fuel plate power splitting makes no difference in the coolant temperature distribution and flow solution. It is therefore certain that the flow solution of Problem 3B (obtained by the spreadsheet or the code) does not have any error due to the assumption regarding fuel plate power splitting.

The effect of the higher fuel assembly power (when the assumption to split each plate power into two halves matters) on the calculated channel flow rates can be obtained by comparing the solution of Problem 3 or 3C with the solution of Problem 3B. Using the flow rates given in Table 23.3, Table 23.4 shows the inter-problem channel flow rate differences between Problems 3 vs 3B, and between Problems 3C vs 3B. A part of Table 23.4 is repeated below to show the *maximum* absolute difference in channel flow rate between Problems 3 vs 3B, and between Problems 3C vs 3B. These differences can be found either based on spreadsheet calculations or based on PLTEMP/ANL calculations. Both calculations give nearly the same results.

Flow Rate Difference between Problems 3 vs 3B, and between Problems 3C vs 3B
(Part of Table 23.4)

	Maximum Absolute % Difference in Flow Rate			
	Problem 3 vs 3B		Problem 3C vs 3B	
	Spreadsheet	PLTEMP/ANL	Spreadsheet	PLTEMP/ANL
Difference in Fuel Assembly 1	0.492	0.469	0.494	0.469
Difference in Fuel Assembly 2	0.491	0.468	4.019	3.679

Based on Problem 3 versus 3B, the maximum difference in channel flow rates is about 0.5% when each assembly power in Problem 3 is 0.5 MW, and the largest coolant channel temperature rise ΔT is 16 ºC (= 61.0 – 45.0 ºC, in channel 4, see Table 23.2). Based on Problem 3C versus 3B, the maximum difference in channel flow rates is about 4.0% when the power of assembly 2 in Problem 3C is 3.5 MW, and the largest coolant channel temperature rise ΔT is 143.7 ºC (= 188.7 – 45.0 ºC, in channel 3, see Table 23.2). Fuel assembly 2 in Problem 3C has an extremely high power because it has a near-saturation channel exit temperature.

We know that it is through its influence on the channel temperature distribution that the assumption (to split each plate power into two halves matters) causes difference in channel flow rates. The largest coolant channel temperature rise ΔT in a given fuel assembly is the most obvious quantity to measure of the extent of the channel temperature distribution in the assembly. So the difference in channel flow rates due to the assumption can be scaled in proportion to the largest channel ΔT in an assembly, e.g., assembly 2 of Problem 3C. To do the scaling, one needs to find the magnitude of the error in channel ΔT that the assumption causes in assembly 2 of Problem 3C. This error equals the difference between the PLTEMP/ANL-calculated channel ΔT (done without using the assumption) and the spreadsheet-calculated channel ΔT (done using the assumption). Using Table 23.2, the largest error in channel ΔT due to the assumption is 5.0383 ºC in fuel assembly 2 of Problem 3C. Substituting these values in Eq. (23.3) gives the flow rate error due to lack of thermal-hydraulic iteration, as shown in Eqs (23.4a) and (23.4b).

$$E_{T-H} = \frac{5.0383}{143.7} \times (4.019\ \%) = 0.141\ \% \qquad \text{based on Problem 3C vs 3B} \qquad (23.4a)$$

$$E_{T-H} = \frac{0.5549}{60.984 - 45.0} \times (3.546\ \%) = 0.123\ \% \qquad \text{based on Problem 3 vs 3B} \qquad (23.4b)$$

It is concluded that the possible improvement in channel flow rates by performing thermal-hydraulic iteration is ~ 0.14%. This much improvement is not significant enough to slow down the code by performing the iteration.

23.5 Conclusions

It is concluded in Section 23.3.1 (see Table 23.3) that the maximum absolute difference in the flow rate of any of the 5 coolant channels in each of the two fuel assemblies of Problem 3B is 0.074%. The maximum absolute difference in the flow rate of any of the 5 coolant channels in each of the two fuel assemblies of Problem 3 is 0.097%. The maximum absolute difference in the flow rate of any of the 5 coolant channels in assembly 1 of Problem 3C is 0.097%. This are good agreements. The maximum absolute difference in the flow rate of any of the 5 coolant channels in assembly 2 of Problem 3C is 1.361%. This is an acceptable agreement. These comparisons provide a verification of the flow rate calculation implemented in the PLTEMP/ANL code.

It is concluded in Section 23.4 that the possible improvement in channel flow rates by performing thermal-hydraulic iteration in the code is studied and found to be ~ 0.15% or less. This amount of improvement is not significant enough to slow down the code by performing the thermal-hydraulic iteration.

APPENDIX K Spreadsheet for Calculating Flow Rate to Verify PLTEMP/ANL

K.1. Development of Spreadsheet for Calculating Flow Rate at a Given Frictional Pressure Drop

The spreadsheet uses the following steps to calculate the flow rate in a fuel assembly of standard Problem 3 that consists of 3 axial regions, each having its own hydraulic diameter, flow area, form loss coefficients, and axial length. The fuel assembly axial region 1 models the assembly length from the inlet to the assembly to the fueled length inlet, the assembly axial region 2 models the fueled length, and the axial region 3 models the fuel assembly length from the exit of the fueled length to the assembly outlet.

Calculation Steps:

Step 1: First calculate the power generated in each fuel assembly of the problem, by splitting the total input power in the proportion of the radial power factors specified on the input card type 309 (which are shown in columns 8 to11 of Table 23.1). The problem consists of 2 assemblies of the same fuel type. All fuel plates have the same fuel meat volume (same meat thickness, same meat width, and same meat height) in the three standard problems used in this verification work. So, for Problem 3, the power of fuel plate k of assembly j is calculated using Eqs. (K-1) and (K-2), by splitting the total power of 1.0 MW in the proportion of the input radial power factors $FACT_{j,k}$. Note that the sum of radial power factors all 4 plates in each fuel assembly is 4.0. The calculated power of each fuel plate and each assembly is tabulated below.

$$Q_{j,k} = \frac{Q * FACT_{j,k}}{(\text{Sum of all radial power factors in the problem})} = \frac{Q * FACT_{j,k}}{8.0} \qquad \text{(K-1)}$$

$$\text{Power in fuel assembly 1} = \sum_{k=1}^{4} Q_{j,k} = \frac{Q * \sum_{k=1}^{4} FACT_{j,k}}{8.0} \qquad \text{(K-2a)}$$

$$\text{Power in fuel assembly 1} = \frac{1.0 \times 10^6 \times 4.0}{8.0} = 5.0 \times 10^5 \text{ W} \qquad \text{(K-2b)}$$

Power for Each Fuel Plate and Each Fuel Assembly in Standard Problem 3

Fuel Plate	**Power, W**	
	Assembly 1	Assembly 2
1	$1.0\times10^6\times0.90/8.0 = 1.1250\times10^5$	$1.0\times10^6\times0.901/8.0 = 1.12625\times10^5$
2	$1.0\times10^6\times0.95/8.0 = 1.1875\times10^5$	$1.0\times10^6\times0.951/8.0 = 1.18875\times10^5$
3	$1.0\times10^6\times1.05/8.0 = 1.3125\times10^5$	$1.0\times10^6\times1.049/8.0 = 1.31125\times10^5$
4	$1.0\times10^6\times1.10/8.0 = 1.3750\times10^5$	$1.0\times10^6\times1.099/8.0 = 1.37375\times10^5$
Total	5.0×10^5	5.0×10^5

Step 2: Calculate the equivalent hydraulic diameter for all the coolant channels in heated length (axial region 2) of the fuel assembly. The symbols are defined in the nomenclature below.

$$D_{h,2} = 4 \sum_{k=1}^{NCHNF} A_{ff,k} \Big/ \sum_{k=1}^{NCHNF} P_{w,k} \tag{K-3}$$

Step 3: Using an initial guess of flow rate W_{gues1} in the fuel assembly and coolant specific heat at the input inlet temperature, the spreadsheet uses Eq. (K-4) to calculate an initial guess of the coolant bulk temperature rise over the heated length (fueled length) of the assembly. Equation (K-5) is used to get an initial guess of the average coolant temperature T_{avg0} over the heated length.

$$\Delta T_{gues0} = \frac{Q}{W_{gues1}\, C_p(T_{in}, P_{in})}, \quad \text{if } T_{in} + \Delta T_{gues0} > T_{sat}, \text{ then set } \Delta T_{gues0} = T_{sat} - T_{in} \tag{K-4}$$

$$T_{avg0} = T_{in} + 0.5\,\Delta T_{gues0} \tag{K-5}$$

Step 4: Using the initial guess of the flow rate W_{gues1} in the fuel assembly and coolant specific heat at the average temperature T_{avg0} and, the spreadsheet uses Eq. (K-6) to calculate an improved initial guess of the coolant bulk temperature rise over the heated length of the assembly. Use Eq. (K-7) to get an improved guess of the average coolant temperature T_{avg} over the heated length.

$$\Delta T_{gues1} = \frac{Q}{W_{gues1}\, C_p(T_{avg}, P_{in})}, \quad \text{if } T_{in} + \Delta T_{gues1} > T_{sat}, \text{ then } \Delta T_{gues1} = \Delta T_{sat} - T_{in} \tag{K-6}$$

$$T_{avg} = T_{in} + 0.5\,\Delta T_{gues1} \tag{K-7}$$

Step 5: Use Eq. (K-8) to calculate the friction loss coefficient, C_{fric}, of the whole fuel assembly from inlet to outlet, accounting for both minor and Moody pressure drops, summed over all axial regions. This calculation uses the input geometrical data (flow area, hydraulic diameter, axial length, form loss coefficient, and Moody friction factor of each axial region of the assembly) of the assembly. Use the equivalent hydraulic diameter of axial region 2 (heated length) calculated in Step 1 for all the coolant channels. The friction factor in each axial region of the fuel assembly is calculated on the spreadsheet using the explicit Zigrang-Sylvester correlation[3,4] Eq. (K-9), although the PLTEMP/ANL code uses the classical implicit Colebrook correlation Eq. (K-10). Equation (K-11) is used to calculate the Reynolds number Re.

The Zigrang-Sylvester correlation was found to be the most accurate among 19 explicit correlations studied[3,4] in 2011, and is easier than the Colebrook implicit correlation to use on the spreadsheet. The Colebrook correlation will require an iteration to find the friction factor within the iteration to find the flow rate in the assembly. The Romeo-Royo-Monzon correlation Eq. (K-12) and the Fang correlation Eq. (K-13) were used only for comparison to check for typing error on the spreadsheet.

$$C_{fric} = \sum_{n=1}^{NF} \left(K_n + \frac{f_n L_n}{D_{h,n}} \right) \frac{1}{\rho_n A_{f,n}^{\ 2}} \tag{K-8}$$

Zigrang-Sylvester friction factor correlation (1982):

$$f = \left\{ -2\log\left[\frac{\varepsilon}{3.7} - \frac{5.02}{Re}\log\left\langle \varepsilon - \frac{5.02}{Re}\log\left(\frac{\varepsilon}{3.7} + \frac{13}{Re} \right) \right\rangle \right] \right\}^{-2}$$

where $4000 < Re < 10^8$, $0.00004 < \varepsilon < 0.05$ (K-9)

Colebrook friction factor correlation (1939):

$$1/\sqrt{f} = -2\log\left(\frac{2.51}{Re\sqrt{f}} + \frac{\varepsilon}{3.7} \right)$$

where $4000 < Re < 10^8$, $0.0 < \varepsilon < 0.05$ (K-10)

$$Re = \frac{D_h W_{gues1}}{A_f \mu(T_{avg,n})}$$

where $T_{avg1,n} = T_{in}$, $T_{in}+0.5\Delta T_{gues1}$, $T_{in}+\Delta T_{gues1}$ for axial region n = 1, 2, 3 (K-11)

Romeo-Royo-Monzon correlation (2002):

$$f = \left\{ -2\log\left[\frac{\varepsilon}{3.7065} - \frac{5.0272}{Re}\log\left(\frac{\varepsilon}{3.827} - \frac{4.567}{Re}\log\left\langle \left(\frac{\varepsilon}{7.7918} \right)^{0.9924} + \left(\frac{5.3326}{208.815 + Re} \right)^{0.9345} \right\rangle \right) \right] \right\}^{-2}$$

where $3000 < Re < 10^8$, $0.0 < \varepsilon < 0.05$ (K-12)

Fang friction factor correlation (2011):

$$f = 1.613\left[\ln\left(0.234\varepsilon^{1.1007} - \frac{60.525}{Re^{1.1105}} + \frac{56.291}{Re^{1.0712}} \right) \right]^{-2}$$

where $3000 < Re < 10^8$, $0.0 < \varepsilon < 0.05$ (K-13)

Step 6: The frictional pressure drops in all axial regions of a fuel assembly are modeled as tabulated below. The axial region 1 in the assembly inlet section, the axial region 2 is the heated section, and the axial region 3 is the assembly exit section. The fuel assembly heated section consists of several coolant channels (5 in this problem). However it is modeled as a single flow path having the combined flow area of all coolant channels, as a first approximation to be refined later. The last row of this table is the sum of all axial regions of the fuel assembly. It represents the user-specified assembly frictional pressure drop, and is written as Eqs. (K-14a) and (K-14b). Using Eq. (K-14b), calculate an improved value W_f of the flow rate in the assembly.

$$\Delta P_{fric} = \frac{W_f^2}{2} C_{fric} \quad \text{where } C_{fric} = \sum_{n=1}^{3} \frac{K_n + f_n L_n / D_{h,n}}{\rho_n A_{f,n}^2} \tag{K-14a}$$

$$W_f = \left(\frac{2\,\Delta P_{fric}}{C_{fric}} \right)^{0.5} \qquad \text{(K-14b)}$$

Equation for Frictional Pressure Drop and Total Pressure Drop in Each Axial Region of a Fuel Assembly

Axial Region	Coolant Temperature	Frictional Pressure Drop, ΔP_{fric}	Total Pressure Drop, ΔP
1	T_{in}	$\Delta P_{fric,1} = \left(K_1 + \frac{f_1 L_1}{D_{h,1}} \right) \frac{W_f^2}{2\rho_1 A_{f,1}^2}$	$\Delta P_1 = \Delta P_{fric,1} + g\rho_1 L_1$
2	$T_{in}+0.5\Delta T_{gues1}$	$\Delta P_{fric,2} = \left(K_2 + \frac{f_2 L_2}{D_{h,2}} \right) \frac{W_f^2}{2\rho_2 A_{f,2}^2}$	$\Delta P_2 = \Delta P_{fric,2} + g\rho_2 L_2$
3	$T_{in}+\Delta T_{gues1}$	$\Delta P_{fric,3} = \left(K_3 + \frac{f_3 L_3}{D_{h,3}} \right) \frac{W_f^2}{2\rho_3 A_{f,3}^2}$	$\Delta P_3 = \Delta P_{fric,3} + g\rho_3 L_3$
Fuel Assembly		$\Delta P_{fric} = \frac{W_f^2}{2} \sum_{n=1}^{3} \frac{K_n + f_n L_n / D_{h,n}}{\rho_n A_{f,n}^2}$	

Step 7: Go to Step 4 and use W_f instead of W_{gues1} as the starting guess flow rate in the assembly. Repeat Steps 4 to 6 until the square of difference between the starting guess of flow rate and the calculated improved flow rate, $(W_f - W_{gues1})^2$, becomes negligible. This is done by minimizing the cell containing $(W_f - W_{gues1})^2$ using the SOLVER capability of the Excel spreadsheet, When $(W_f - W_{gues1})^2$ is negligible, W_f is the desired flow rate in the fuel assembly.

Calculation of Flow Rates in Coolant Channels: The spreadsheet finds the flow rates in each coolant channel in axial region 2 of the fuel assembly, based on the total pressure drop (frictional + gravitational) between two common points at the inlet and exit of all the coolant channels (axial region 2) in an assembly. The following calculation steps are used to do this.

Step 8: Use the radial power factors of the fuel plates in an assembly to split the assembly power into powers generated in different fuel plates. Assuming that each plate power is split equally between the two adjacent coolant channels, calculate the power deposited in each channel.

$$Q_{ch,k} = 0.5\, Q_{1,k-1} + 0.5\, Q_{1,k} \;,\; k=1,2,\ldots 5 \;,\; Q_{1,k} = 0 \text{ for } k = 0 \text{ or } 5 \qquad \text{(K-15)}$$

Step 9: The solution method is iterative. To start the iteration, set the channel flow rates by splitting the W_f obtained in Step 6 based on channel flow areas.

$$W_{ch,k} = \frac{A_{ff,k}}{A_{f,2}} W_f \quad , \quad k = 1,...,5$$

Step 10: To calculate the coolant channel flow rates $W_{ch,k}$ accounting for the different powers deposited in the channels, **solve the following 7 coupled equations in 7 unknowns $W_{ch,k}$ (k = 1 to 5), W_f and ΔP_2.**

$$W_f = \sum_{k=1}^{5} W_{ch,k} \tag{K-16}$$

$$\Delta P_2 = \frac{K_2 W_f^2}{2\rho_2 A_{f,2}^2} + \frac{f_{ch,k} L_2 W_{ch,k}^2}{2\rho_{ch,k} D_{ck,k} A_{ff,k}^2} + g\rho_{ch,k} L_2 \quad , \; k = 1, 2, \ldots 5 \tag{K-17}$$

$$\Delta P_{fric} = \left(K_1 + \frac{f_1 L_1}{D_{h,1}}\right)\frac{W_f^2}{2\rho_1 A_{f,1}^2} + \left(K_3 + \frac{f_3 L_3}{D_{h,3}}\right)\frac{W_f^2}{2\rho_3 A_{f,3}^2} + \left[\Delta P_2 - g\rho_2 L_2\right] \tag{K-18}$$

Equation (K-16) simply states that the assembly flow rate equals the sum of all channel flow rates. Equation (K-17) is an equation for each channel flow rate based on the total pressure drop in the heated length. In Eq. (K-17) that the form loss coefficient K_2 for pressure drop in the heated length is based on the total flow area of all coolant channels. Equation (K-18) states that the sum of *frictional* pressure drops in all three axial regions of the assembly equals the *input* frictional pressure drop ΔP_{fric}. The first term of Eq. (K-18) gives the frictional pressure drop in the fuel assembly axial region 1, the second term of Eq. (K-18) gives the frictional pressure drop in the axial region 3, and the last term of Eq. (K-18), i.e., the quantity inside the square brackets, gives the frictional pressure drop in the fueled length of the assembly.

Step 11: Set the coolant average temperature $T_{avg1,k}$ in each channel at which the coolant properties will be evaluated in different channels.

$$H(T_{out,k}) = H(T_{in}) + \frac{Q_{ch,k}}{W_{ch,k}} \quad , \quad \text{Find } T_{out,k} \text{ at the enthalpy } H(T_{out,k})$$

$$T_{avg1,k} = T_{in} + 0.5 T_{out,k}$$

Step 12: Calculate $\mu_{ck,k}$, $Re_{ch,k}$, $f_{ch,k}$, $\rho_{ch,k}$. Here $\rho_{ch,k}$ is coolant density at $T_{avg1,k}$ and $f_{ch,k}$ is friction factor in channel k at the Reynolds number at flow rate $W_{ch,k}$

Step 13: Calculate the following sum of squares of the residues of Eqs. (K-16), (K-17) and (K-18).

$$S = \left(RHS_{17,1} - \Delta P_2\right)^2 + \left(RHS_{17,2} - \Delta P_2\right)^2 + \left(RHS_{17,3} - \Delta P_2\right)^2 + \left(RHS_{17,4} - \Delta P_2\right)^2 + \left(RHS_{17,5} - \Delta P_2\right)^2 + \left(RHS_{18} - \Delta P_{fric}\right)^2 \quad \text{(K-19)}$$

Here $RHS_{19,k}$ implies the right hand side of Eq. (K-17) for coolant channel k. The residue of an equation is the difference between the left and right hand sides of the equation. Repeat Steps 9 to 13, adjusting ΔP_2 and the channel flow rates $W_{ch,k}$ to minimize the sum of squares of the residues. Use the SOLVER capability on the spreadsheet to do this. The minimization solves the above 7 equations in 7 unknowns. This gives the channel flow rates $W_{ch,k}$ in the assembly and the pressure drop ΔP_2 in the heated length.

The channel flow rates $W_{ch,k}$ thus obtained are used in the heat transfer calculation. After the heat transfer calculation, in the forced flow option, there is no overall iteration between the heat transfer calculation and the hydraulic calculation.

K.2. Checking the Spreadsheet

The spreadsheet described in Section 23.2 was checked in two ways: (1) by comparing the spreadsheet solution of Problem 3C with that of the same problem with the modification that the two fuel assemblies interchanged, and (2) by examining the variation trend of the fuel assembly 2 flow rate in Problem 3C as the total input power in the problem (and hence the coolant average temperature) changes from 0.0 to 4 MW.

K.2.1. Spreadsheet Solution of Problem 3C Compared with That of this Problem with the Fuel Assemblies Interchanged

In order to check the spreadsheet, the spreadsheet solution for Problem 3C was compared with the spreadsheet solution for this problem with one modification that the two fuel assemblies are interchanged. The fuel assembly 1 in the modified problem is identical to assembly 2 of Problem 3C, and the assembly 2 in the modified problem is identical to assembly 1 of Problem 3C. Both spreadsheets are named and saved in the directory noted in Section 23.1. The fow rates calculated by the spreadsheet are shown below. The maximum difference in the assembly 1 flow is 0.0001 kg/s, and the maximum difference in the assembly 2 flow is 0.0002 kg/s. This difference is negligible in reactor analysis. The spreadsheet is found to be correct.

Problem	Reactor Power, W	Flow in Fuel Assembly 1		Flow in Fuel Assembly 2	
		Calculated By Assembly	Calculated By Channel	Calculated By Assembly	Calculated by Channel
Problem 3C	4.0×10^6	9.66262	9.66254	9.62270	9.61921
Prob. 3C [a]	4.0×10^6	9.62270	9.61920	9.66260	9.66252

[a] Modified problem 3C with the fuel assemblies interchanged.

K.2.2. Trend of Assembly Flow Rate in Problem 3C with Increasing Total Input Power

Problem 3C has a total power of 4.0 MW. This problem has a very high power, with the power of fuel assembly 2 being 7 times that of assembly 1. At a total power of 4.0 MW, the assembly 1 generates 0.5 MW and the assembly 2 generates 3.5 MW, with the coolant temperature approaching within 3 ºC of the saturation temperature of 195 ºC. Therefore, this problem is suitable for checking the effect of coolant temperature on the behavior of the spreadsheet-calculated flow rate at a fixed frictional pressure drop in the fuel assembly. In order to check the spreadsheet, the input total power in Problem 3C was modified to 11 values from 0.0 to 4.0 MW (i.e., 0.0, 10 W, 100 W, 1 kW, 10 kW, 100 kW, 0.5 MW, 1.0 MW, 2.0 MW, 3.0 MW and 4.0 MW), and the modified problem in each case was solved by the spreadsheet. All the eleven spreadsheets are saved in the directory noted in Section 23.1.

The spreadsheet-calculated flow rate in each assembly of Problem 3C is shown in Table 23.20 as a function of the input total power. As described in Section 23.2, the assembly flow rate is calculated by two methods: (1) using Eq. (K-14b) based on the total flow area in the fuel assembly (refferred to as "By Assembly" in Table 23.20), and (2) using Eqs. (K-16) to (K-18) based on the calculation of channel flow rates (refferred to as "By Channel" in Table 23.20). The flow rate in each fuel assembly is plotted in Fig. 23.2 as function of the case number. Figure 23.2 shows that the flow rate in assembly 1 is practically identical (max difference is 0.00083%), irrespective of the method used. The flow rate in assembly 2 is practically the same (max difference is 0.036%), irrespective of the method used. Assembly 1 has lower power (i.e., 0.5 MW) than the assembly 2 (i.e., 3.5 MW) when the total power is 4.0 MW. It should be noted that assembly 2 represents an extreme case because the coolant exit temperature is ~192 ºC (i.e., 3 ºC below the saturation temperature of ~195 ºC). In this extreme case, the maximum difference between the flow rates obtained by the two methods is only 0.036%.

Figure 23.2 shows that the assembly 1 flow rate monotonically increases as its power increases from zero to 0.5 MW, where as the assembly 2 flow rate goes through a maximum as its power increases from zero to 3.5 MW. The behavior of assembly 2 is not inconsistent with assembly 1 because the assembly 2 flow rate also increases as its power increases from zero to 1.0 MW. The assembly 2 flow rate begins to decrease only after an assembly power of 1.0 MW.
The trend of the assembly 2 flow rate going through a maximum as its power increases from zero to 3.5 MW is also expected due to the following reason. The reason for this trend in an axial region of any duct is as follows: If the form loss coefficient K were zero, the flow rate is expected to increase with coolant temperature because as the water gets warmer it can flow more easily for the same frictional pressure drop. It can be shown for turbulent flow that the flow rate is proportional to $\left(\rho/\mu^{0.25}\right)^{4/7}$, which increases with temperature for liquid water. If the flow resistance were all K-loss and no friction factor, the flow rate would be proportional to the square-root of coolant density, which means that flow rate would decrease as rising temperature causes density to decrease. When the hydraulic resistance is due to a combination of K-loss and friction factor (of comparable magnitudes), the two effects compete, the flow rate first increases, goes through a maximum, and then decreases. This trend has been numerically studied and verified for a pipe. Therefore, the trend shown by assembly 2 flow rate in Fig. 23.2 provides a verification of the spreadsheet.

Nomenclature

Subscripts

avg = Average value
gues = Guessed value
in = Value at inlet to the fuel assembly

Symbols

$A_{ff,k}$ = Flow area in coolant channel k in the fueled length of the fuel assembly, m^2
$A_{f,n}$ = Flow area in axial region n of the fuel assembly, m^2
$C_p(T, P)$ = Specific heat of the coolant at temperature T ºC and pressure P Pa, kJ/kg-°C
$D_{h,n}$ = Hydraulic diameter of axial region n of the fuel assembly, m
$D_{ch,k}$ = Hydraulic diameter of coolant channel k in the fueled length of the assembly, m
D_{fric} = Friction loss coefficient of the fuel assembly from inlet to outlet, accounting for both minor and Moody pressure drops, summed over all axial regions.
$D_{h,2}$ = Equivalent hydraulic diameter (m) of all coolant channels in the fuel assembly which is calculated by Eq. (23.1).
f_n = Moody friction factor of axial region n of the fuel assembly. The friction factor depends on the Reynolds number (Re). To calculate the friction factor in axial region 1 (n = 1), the coolant properties used in calculating Re are evaluated at the inlet temperature. To calculate the friction factor in axial region 2 (fueled length, n = 2), the coolant properties used in calculating Re are evaluated at the arithmetic mean of the fuel assembly inlet and outlet temperatures. To calculate the friction factor in axial region 3 (n = 3), the coolant properties used in calculating Re are evaluated at the fuel assembly outlet temperature.
k = Coolant channel index in the fuel assembly
K_n = Minor loss coefficient of axial region n of the fuel assembly
L_n = Length of axial region n of the fuel assembly, m
NF = Number of axial regions in the fuel assembly
n = Axial region index in the fuel assembly
P = Coolant pressure, Pa
$P_{w,k}$ = Wetted perimeter in coolant channel k in the fueled length of the fuel assembly, m
ΔP_{fric} = Frictional pressure drop from the fuel assembly inlet to outlet, Pa
Q = Power generated in the fuel assembly in which flow is being calculated, W
$Q_{i,k}$ = Power generated in fuel plate k of assembly I , W
$Q_{ch,k}$ = Power deposited in coolant channel k of assembly I , W
ρ = Coolant density (kg/m^3)at the average of core inlet and outlet temperature
T_{sat} = Coolant saturation temperature (ºC) at the inlet pressure
T = Coolant bulk temperature, ºC
ΔT = Coolant temperature rise over the heated length, °C
W_f = Coolant flow rate in the fuel assembly i, kg/s
$W_{ch,k}$ = Coolant flow rate (kg/s) in channel k of the fuel assembly i being solved. The sum of $W_{ch,k}$ over all channels in the fuel assembly equals W_i .

APPENDIX L Calculation of Channel Flow Rates in the PLTEMP/ANL Code

PLTEMP/ANL is a single-phase (liquid) code for experimental reactors with light or heavy water coolant. The code discretizes the coolant channels and fuel plates into a number of axial slices (called nodes). A 1-D "radial" thermal calculation across all fuel plates and coolant channels is performed for the first axial slice downstream of the inlet (using channel flow rates obtained as described below). This thermal calculation gives the coolant, cladding, and fuel temperatures at the center of the first slice, and the exit of the first slice (i.e., the inlet of the second slice). This "radial" thermal calculation is then repeated for the second slice, and so on for each axial slice from inlet to outlet, yielding a "pseudo-2D" solution.

The above thermal calculation depends on the coolant flow rates through the channels between the fuel plates. There are two options in the code for obtaining the *liquid* coolant flow rates through the channels in the reactor core: (1) user-specified channel flow rates, and (2) channel flow rates are calculated based on a user-specified frictional pressure drop from the inlet to outlet of a fuel assembly. In the second option, the flow calculation is *done before* the above-mentioned heat transfer calculation. In this option, the fuel assembly is hydraulically modeled as a series of a user-specified number of axial regions of specified hydraulic diameters, flow areas and lengths, with the fueled length of the assembly represented by the second axial region. The second axial region is modeled as having a user-specified number of hydraulically parallel coolant channels with specified geometrical parameters (hydraulic diameter, flow area, etc.). The flow rate W in a fuel assembly is calculated from the input frictional pressure drop ΔP from the inlet to outlet of the fuel assembly, using Eq. (L.1). Equation (L.1) is solved iteratively because the assembly loss coefficient DENOF and the coolant density ρ depend on the flow rate W which is to be calculated. The first iteration is started with $W_{gues,1}$ as an initial guess value, resulting in a calculated value of W_1 at the end of the iteration. The second iteration is started with a guessed value of

$$W_{gues,2} = 0.5(W_{gues,1} + W_1)$$

The iterations are repeated to convergence within a user-specified fractional error (CONV) for the flow rate in the fuel assembly. This calculation is performed in subroutine WORK.

The flow rates in the coolant channels in the fueled length (axial region 2) of the fuel assembly are obtained in the subroutine CNLFLO, by splitting the fuel assembly flow rate W using Eq. (23.2). (see . These channel flow rates W_k are used in the heat transfer calculation. After the heat transfer calculation, in the forced flow option, there is no overall iteration between the heat transfer calculation and the hydraulic calculation.

$$\Delta P = \text{DENOF} * \frac{W^2}{2\rho} \tag{L.1}$$

where

W = Coolant flow rate in a fuel assembly

W_k = Coolant flow rate in channel k of the fuel assembly. The sum of W_k over all channels in the fuel assembly equals W.

ΔP = Frictional pressure drop from the fuel assembly inlet to outlet

ρ = Coolant density at the average of core inlet and outlet temperature

DENOF = Friction loss coefficient summed over all axial regions from the fuel assembly inlet to outlet, accounting for both minor and Moody pressure drops. DENOF is calculated in subroutine RESIST using Eq. (L.2). In Eq. (L.2), $D_{h,2}$ is the hydraulic diameter of all coolant channels in a fuel assembly, which is calculated by Eq. (L.3).

NF = Number of axial regions in the fuel assembly

n = Axial region index in the fuel assembly

k = Coolant channel index in the fuel assembly

K_n = Minor loss coefficient of axial region n of the fuel assembly

L_n = Length of axial region n of the fuel assembly

$A_{f,n}$ = Flow area in axial region n of the fuel assembly

$D_{h,n}$ = Hydraulic diameter of axial region n of the fuel assembly

$D_{ch,k}$ = Hydraulic diameter of coolant channel k in the fueled length of the fuel assembly

$A_{ff,k}$ = Flow area in coolant channel k in the fueled length of the fuel assembly

$P_{w,k}$ = Wetted perimeter in coolant channel k in the fueled length of the fuel assembly

f_n = Moody friction factor of axial region n of the fuel assembly. The friction factor depends on the Reynolds number (Re). To calculate the friction factor in axial region 1, the coolant properties used in calculating Re are evaluated at the inlet temperature. To calculate the friction factor in axial region 2 (fueled length), the coolant properties used in calculating Re are evaluated at the arithmetic mean of the fuel assembly inlet and outlet temperatures. To calculate the friction factor in axial region n (n = 3 to NF), the coolant properties used in calculating Re are evaluated at the fuel assembly outlet temperature.

$$\mathrm{DENOF} = \sum_{n=1}^{NF}\left(K_n + \frac{f_n L_n}{D_{h,n}}\right)\frac{1}{A_{f,n}^{\ 2}} \tag{L.2}$$

$$D_{h,2} = \frac{4\sum_{k=1}^{NCHNF} A_{ff,k}}{\sum_{k=1}^{NCHNF} P_{w,k}} \tag{L.3}$$

Both turbulent and laminar flow regimes can be modeled. The correlations for the Moody friction factor are given in Section 3.7 of [1]. The modeling and calculation of natural circulation flow rate is documented in Appendix XI of [1].

L. 1 REFERENCES

1. A. P. Olson, M. Kalimullah, and E. E. Feldman, "A User's Guide to the PLTEMP/ANL Code," ANL/RERTR/TM-11-22, Version 4.2, Argonne National Laboratory, 9700 South Cass Avenue, Argonne, IL, USA (July 25, 2016).
2. A. Crabtree and M. Siman-Tov, "Thermophysical Properties of Saturated Light and Heavy Water for Advanced Neutron Source Applications," ORNL/TM-12322, Oak Ridge National Laboratory, Oak Ridge, Tennessee 37831 (May 1993).
3. U. H. Offor, and S. B. Alabi, "An Accurate and Computationally Efficient Explicit Friction Factor Model," Advances in Chemical Engineering and Science, 6, 237-245 (2016). http://dx.doi.org/10.4236/aces.2016.63024
4. S. Genic, I. Arandjelovic, P. Kolendic, M. Jaric, N. Budimir, and V. Genic, "A Review of Explicit Approximations of Colebrook's Equation," Faculty of Mechanical Engineering, Belgrade 35, Serbia, FME Transactions 39, 67-71 (2011). Correspondence to: Marko Jaric Innovation Center of Faculty of Mechanical Engineering, Kraljice Marije 16, 11120 E-mail: mjaric@mas.bg.ac.rs
5. "International Association of the Properties of Steam (IAPS)," H. J. White, Secretary, National Bureau of Standards, Washington, D. C., 1977 (revised 1983).

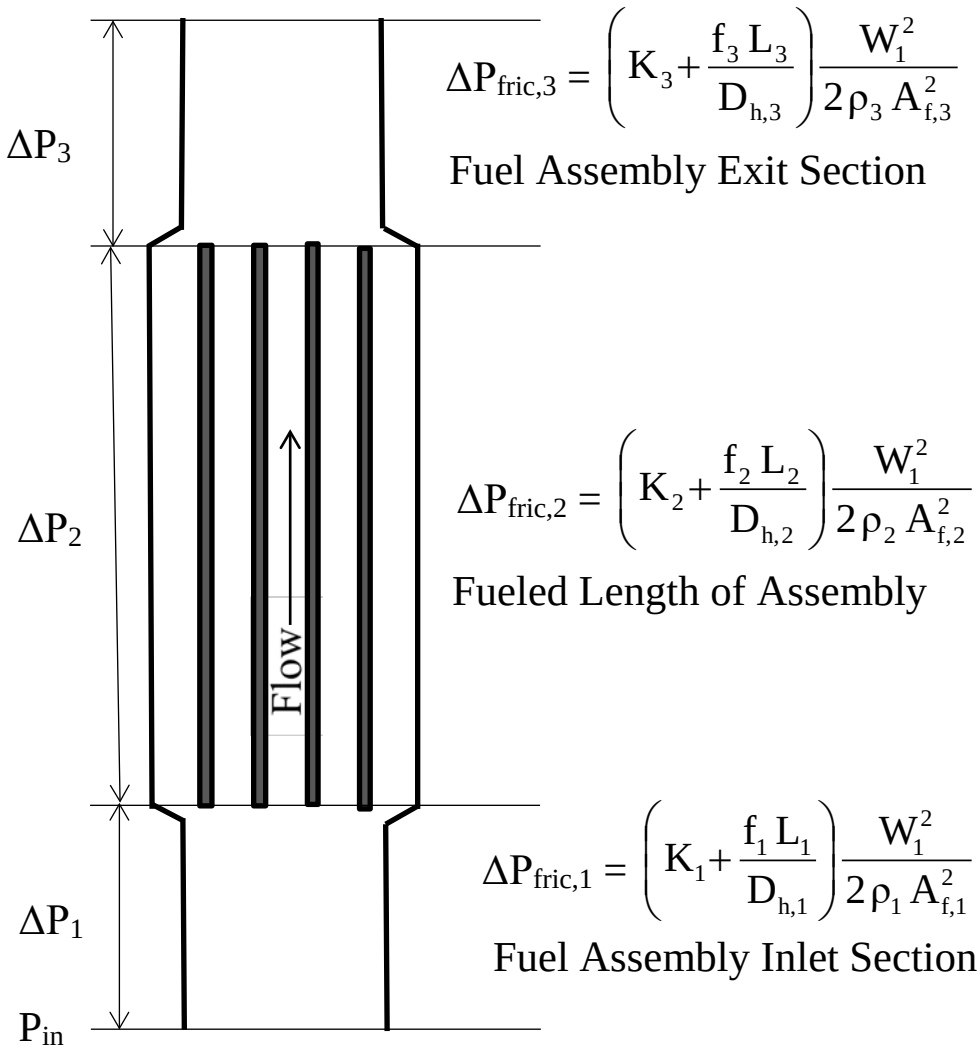

Figure 23.1 Pressure Drop and its Frictional Component in Several Axial Regions of a Fuel Assembly.
Region 1 is the Assembly Inlet Section, Region 2 is the Fueled Length, and Region 3 is the Assembly Exit Section

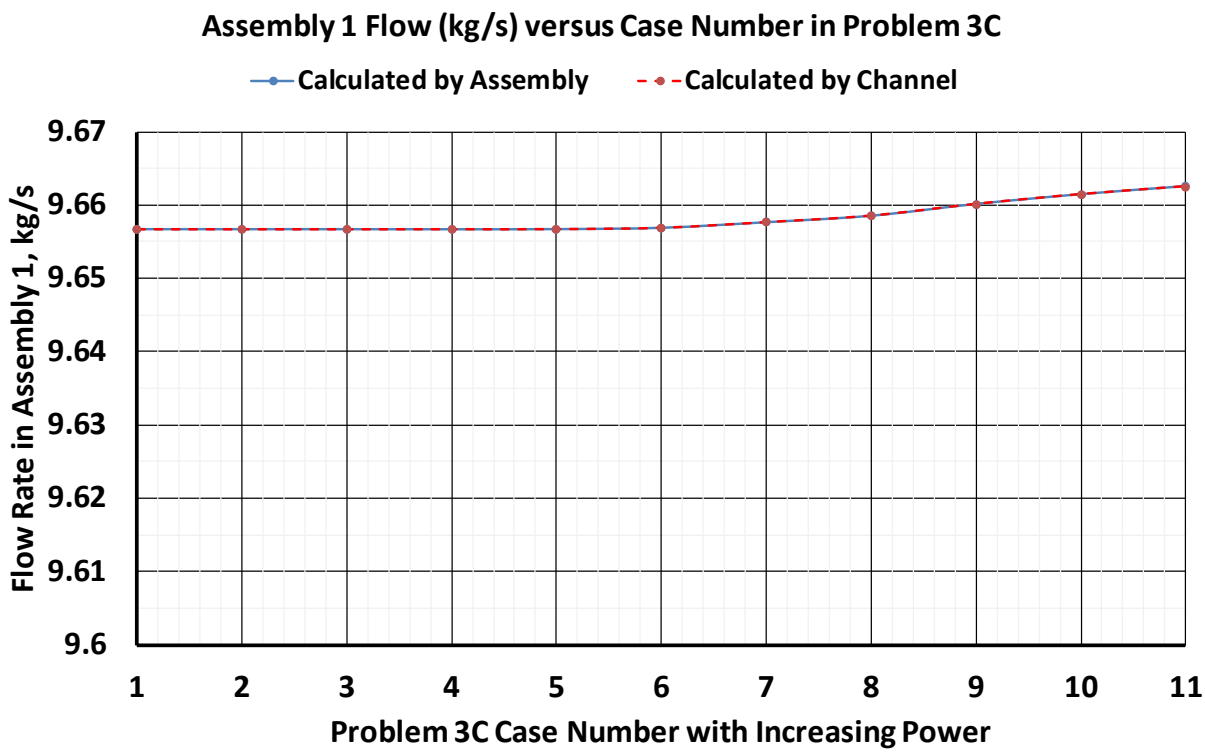

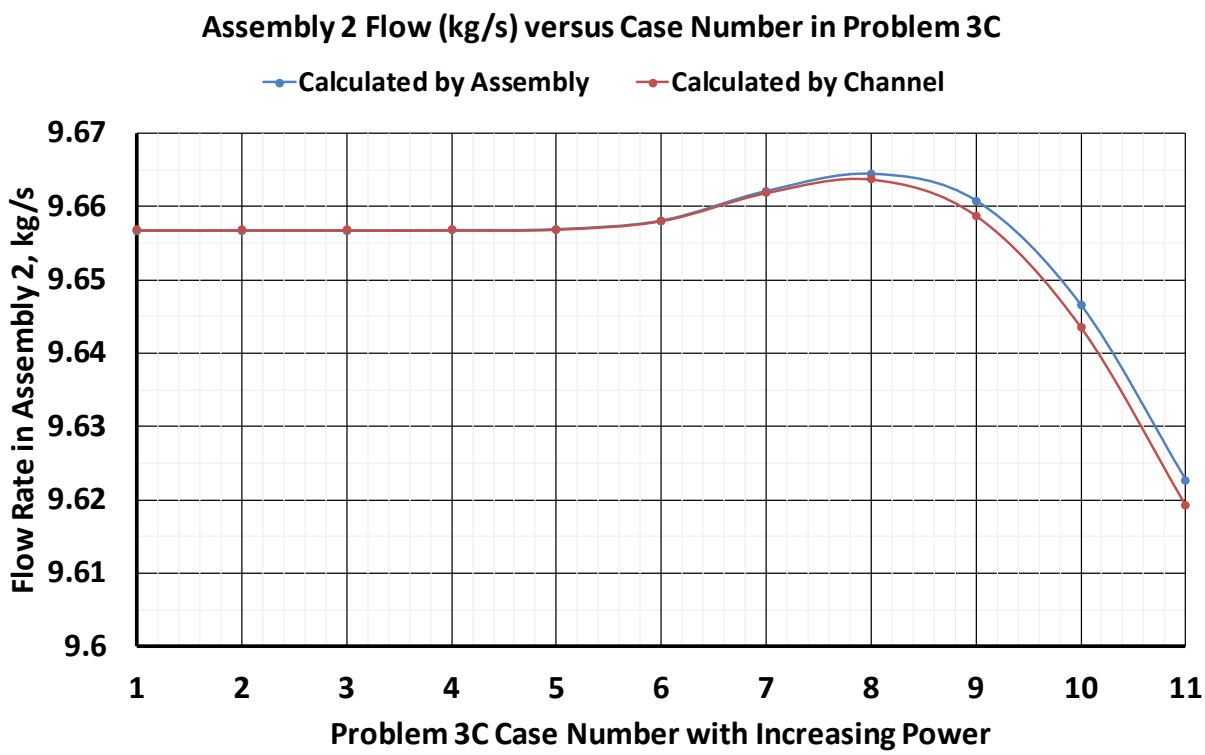

Figure 23.2 Dependence of the Spreadsheet-Calculated Flow Rate in Fuel Assemblies of Problem 3C with Increasing Power

Figure 23.3 PLTEMP/ANL Input File *input.2Assemblies.stdprob3* for Standard Problem 3 Used to Verify the Flow Calculation Method Implemented in the Code

```
Test Problem: 2 assemblies (of identical geometry) producing 1 MWt
! Each assembly has 4 fuel plates and 5 coolant channels
! H2O coolant, Flow is calculated from input pressure drop
! All hot channel factors = 1.0
! No bypass flow, NCTYP=0
! 10 axial heat transfer nodes in the heated length of fuel plates
!  1   2   3   4   5   6   7   8   9  10  11  12  13  14  15  16  17  18  19    # Card 0200
   0   0   0   1   0   1   1   1   0   0   0   0   0                       0    Card(1)0200
   2   3 0.50       1.00        1.00        1.00           3                  Card(1)0300
! Using pressure driven mode
   1  20 1.00                                                                  Card(1)0301
   1   1   1                                                                   Card(1)0302
1.20        1.20                                                              Card(2)0303
30.0E-04    0.02955665  0.15        8.00        0.20        15.0E-03          Card(3)0304
30.0E-04    5.91133E-03 0.75        0.00        0.20        3.00E-03          Card(3)0304
30.0E-04    0.02955665  0.15        8.00        0.20        15.0E-03          Card(3)0304
! Use the code's biult-in correlation for friction factor
0.00        0.00        0.00                                                  Card(1)0305
   5   3 0.00       0.75        0.50E-03    0.00        1.00E-03    100.00    Card(1)0306
6.00E-04    5.91133E-03 0.4060      0.20        0.20        3.00E-03          Card(5)0307
6.00E-04    5.91133E-03 0.4060      0.40        0.20        3.00E-03          Card(5)0307
6.00E-04    5.91133E-03 0.4060      0.40        0.20        3.00E-03          Card(5)0307
6.00E-04    5.91133E-03 0.4060      0.40        0.20        3.00E-03          Card(5)0307
6.00E-04    5.91133E-03 0.4060      0.20        0.20        3.00E-03          Card(5)0307
0.20        0.20        0.20        0.20                                      Card(1)0308
! Card 0308a not required
! Radial power peaking factor data by fuel plate for each assembly. Input flow data by
! channel for each assembly on Cards 0310 not required because WFGES(1) is non-zero
0.900       0.950       1.050       1.100                                     Card(2)0309
0.901       0.951       1.049       1.099                                     Card(2)0309
! DP0       DDP         DPMAX       POWER       TIN         PIN
0.10        0.04        0.10        1.00        45.0        1.40              Card(1)0500
                                                                              Card(2)0500
  50 0.0001     25.0        0.50        1.00                                  Card(1)0600
  11                                                                          Card(1)0700
0.00        0.80                                                              Card(11)0701
0.10        0.88                                                              Card(11)0701
0.20        0.96                                                              Card(11)0701
0.30        1.04                                                              Card(11)0701
0.40        1.12                                                              Card(11)0701
0.50        1.20                                                              Card(11)0701
0.60        1.12                                                              Card(11)0701
0.70        1.04                                                              Card(11)0701
0.80        0.96                                                              Card(11)0701
0.90        0.88                                                              Card(11)0701
1.00        0.80                                                              Card(11)0701
   0                                                                          Card(11)0702
```

Figure 23.4 PLTEMP/ANL Input File *input.2Assemblies.stdprob3B* for Standard Problem 3B Used to Verify the Flow Calculation Method Implemented in the Code

```
Test Problem: 2 assemblies (of identical geometry) producing 1 MWt
! Each assembly has 4 fuel plates and 5 coolant channels
! H2O coolant, Flow is calculated from input pressure drop
! All hot channel factors = 1.0
! No bypass flow, NCTYP=0
! 10 axial heat transfer nodes in the heated length of fuel plates
!  1   2   3   4   5   6   7   8   9  10  11  12  13  14  15  16  17  18  19    # Card 0200
   0   0   0   1   0   1   1   1   0   0   0   0   0                       0    Card(1)0200
   2   3 0.50       1.00        1.00        1.00           3                  Card(1)0300
! Using pressure driven mode
   1  20 1.00                                                                  Card(1)0301
   1   1   1                                                                   Card(1)0302
1.20        1.20                                                              Card(2)0303
30.0E-04    0.02955665  0.15        8.00        0.20        15.0E-03          Card(3)0304
30.0E-04    5.91133E-03 0.75        0.00        0.20        3.00E-03          Card(3)0304
30.0E-04    0.02955665  0.15        8.00        0.20        15.0E-03          Card(3)0304
! Use the code's biult-in correlation for friction factor
0.00        0.00        0.00                                                  Card(1)0305
   5   3 0.00       0.75        0.50E-03    0.00        1.00E-03    100.00    Card(1)0306
6.00E-04    5.91133E-03 0.4060      0.20        0.20        3.00E-03          Card(5)0307
6.00E-04    5.91133E-03 0.4060      0.40        0.20        3.00E-03          Card(5)0307
6.00E-04    5.91133E-03 0.4060      0.40        0.20        3.00E-03          Card(5)0307
6.00E-04    5.91133E-03 0.4060      0.40        0.20        3.00E-03          Card(5)0307
6.00E-04    5.91133E-03 0.4060      0.20        0.20        3.00E-03          Card(5)0307
0.20        0.20        0.20        0.20                                      Card(1)0308
! Card 0308a not required
! Radial power peaking factor data by fuel plate for each assembly. Input flow data by
! channel for each assembly on Cards 0310 not required because WFGES(1) is non-zero
0.900       0.950       1.050       1.100                                     Card(2)0309
0.901       0.951       1.049       1.099                                     Card(2)0309
! DP0       DDP         DPMAX       POWER       TIN         PIN
0.10        0.04        0.10        1.00E-4     45.0        1.40              Card(1)0500
                                                                              Card(2)0500
  50 0.0001     25.0        0.50        1.00                                  Card(1)0600
  11                                                                          Card(1)0700
0.00        0.80                                                              Card(11)0701
0.10        0.88                                                              Card(11)0701
0.20        0.96                                                              Card(11)0701
0.30        1.04                                                              Card(11)0701
0.40        1.12                                                              Card(11)0701
0.50        1.20                                                              Card(11)0701
0.60        1.12                                                              Card(11)0701
0.70        1.04                                                              Card(11)0701
0.80        0.96                                                              Card(11)0701
0.90        0.88                                                              Card(11)0701
1.00        0.80                                                              Card(11)0701
   0                                                                          Card(11)0702
```

Figure 23.5 PLTEMP/ANL Input File *input.2Assemblies.stdprob3C* for Standard Problem 3C Used to Verify the Flow Calculation Method Implemented in the Code

```
 Test Problem: 2 assemblies (of identical geometry) producing 1 MWt
! Each assembly has 4 fuel plates and 5 coolant channels
! H2O coolant, Flow is calculated from input pressure drop
! All hot channel factors = 1.0
! No bypass flow, NCTYP=0
! 10 axial heat transfer nodes in the heated length of fuel plates
!  1   2   3   4   5   6   7   8   9  10  11  12  13  14  15  16  17  18  19    # Card 0200
   0   0   0   1   0   1   1   1   0   0   0   0   0                       0    Card(1)0200
   2   3 0.50       1.00        1.00        1.00           3                  Card(1)0300
! Using pressure driven mode
   1  20 1.00                                                                  Card(1)0301
   1   1   1                                                                   Card(1)0302
1.20        1.20                                                              Card(2)0303
30.0E-04    0.02955665  0.15        8.00        0.20        15.0E-03          Card(3)0304
30.0E-04    5.91133E-03 0.75        0.00        0.20        3.00E-03          Card(3)0304
30.0E-04    0.02955665  0.15        8.00        0.20        15.0E-03          Card(3)0304
! Use the code's biult-in correlation for friction factor
0.00        0.00        0.00                                                  Card(1)0305
   5   3 0.00       0.75        0.50E-03    0.00        1.00E-03    100.00    Card(1)0306
6.00E-04    5.91133E-03 0.4060      0.20        0.20        3.00E-03          Card(5)0307
6.00E-04    5.91133E-03 0.4060      0.40        0.20        3.00E-03          Card(5)0307
6.00E-04    5.91133E-03 0.4060      0.40        0.20        3.00E-03          Card(5)0307
6.00E-04    5.91133E-03 0.4060      0.40        0.20        3.00E-03          Card(5)0307
6.00E-04    5.91133E-03 0.4060      0.20        0.20        3.00E-03          Card(5)0307
0.20        0.20        0.20        0.20                                      Card(1)0308
! Card 0308a not required
! Radial power peaking factor data by fuel plate for each assembly. Input flow data by
! channel for each assembly on Cards 0310 not required because WFGES(1) is non-zero
0.2250      0.2375      0.2625      0.2750                                    Card(2)0309
1.0000      2.5000      2.5000      1.0000                                    Card(2)0309
! DP0       DDP         DPMAX       POWER       TIN         PIN
0.10        0.04        0.10        4.00        45.0        1.40              Card(1)0500
                                                                              Card(2)0500
  50 0.0001     25.0        0.50        1.00                                  Card(1)0600
  11                                                                          Card(1)0700
0.00        0.80                                                              Card(11)0701
0.10        0.88                                                              Card(11)0701
0.20        0.96                                                              Card(11)0701
0.30        1.04                                                              Card(11)0701
0.40        1.12                                                              Card(11)0701
0.50        1.20                                                              Card(11)0701
0.60        1.12                                                              Card(11)0701
0.70        1.04                                                              Card(11)0701
0.80        0.96                                                              Card(11)0701
0.90        0.88                                                              Card(11)0701
1.00        0.80                                                              Card(11)0701
   0                                                                          Card(11)0702
```

Figure 23.6 PLTEMP/ANL Input File *input.2Assemblies.stdprob43* for Standard Problem 43 Used to Verify the Flow Calculation Method Implemented in the Code

```
 Test Problem 43: 2 assemblies (of identical geometry) producing 4 MWt
! Each assembly has 4 fuel plates and 5 coolant channels
! H2O coolant, Flow is calculated from input pressure drop
! All hot channel factors = 1.0
! No bypass flow, NCTYP=0
! 10 axial heat transfer nodes in the heated length of fuel plates
!  1   2   3   4   5   6   7   8   9  10  11  12  13  14  15  16  17  18  19    # Card 0200
   0   0   0   1   0   1   1   1   0   0   0   0   0                       0    Card(1)0200
   2   3 0.50       1.00        1.00        1.00           3                  Card(1)0300
! Using pressure driven mode
   1  20 1.00                                                                  Card(1)0301
   1   1   1                                                                   Card(1)0302
1.20        1.20                                                               Card(2)0303
2.03E-03    2.00E-02    0.15        0.50        0.20        10.15E-3           Card(3)0304
2.03E-03    4.00E-03    0.75        0.00        0.20        2.03E-03           Card(3)0304
2.03E-03    2.00E-02    0.15        0.50        0.20        10.15E-3           Card(3)0304
! Use the code's biult-in correlation for friction factor
0.00        0.00        0.00                                                   Card(1)0305
   5   3 0.00       0.75        0.50E-03    0.00        1.00E-03    100.00     Card(1)0306
4.06E-04    4.00E-03    0.4060      0.20        0.20        2.03E-03           Card(5)0307
4.06E-04    4.00E-03    0.4060      0.40        0.20        2.03E-03           Card(5)0307
4.06E-04    4.00E-03    0.4060      0.40        0.20        2.03E-03           Card(5)0307
4.06E-04    4.00E-03    0.4060      0.40        0.20        2.03E-03           Card(5)0307
4.06E-04    4.00E-03    0.4060      0.20        0.20        2.03E-03           Card(5)0307
0.20        0.20        0.20        0.20                                       Card(1)0308
! Card 0308a not required
! Radial power peaking factor data by fuel plate for each assembly. Input flow data by
! channel for each assembly on Cards 0310 not required because WFGES(1) is non-zero
0.900       0.950       1.050       1.100                                      Card(2)0309
0.901       0.951       1.049       1.099                                      Card(2)0309
! DP0       DDP         DPMAX       POWER       TIN         PIN
0.30        0.04        0.10        4.00        45.0        1.40               Card(1)0500
                                                                               Card(2)0500
  50 0.0001     25.0        0.50        1.00                                   Card(1)0600
  11                                                                           Card(1)0700
0.00        0.80                                                               Card(11)0701
0.10        0.88                                                               Card(11)0701
0.20        0.96                                                               Card(11)0701
0.30        1.04                                                               Card(11)0701
0.40        1.12                                                               Card(11)0701
0.50        1.20                                                               Card(11)0701
0.60        1.12                                                               Card(11)0701
0.70        1.04                                                               Card(11)0701
0.80        0.96                                                               Card(11)0701
0.90        0.88                                                               Card(11)0701
1.00        0.80                                                               Card(11)0701
   0                                                                           Card(11)0702
```

Figure 23.7 PLTEMP/ANL Input File *input.2Assemblies.stdprob44* for Standard Problem 44 Used to Verify the Flow Calculation Method Implemented in the Code

```
 Test Problem 44: 2 assemblies (of identical geometry) producing 4 MWt
! Each assembly has 4 fuel plates and 5 coolant channels
! H2O coolant, Flow is calculated from input pressure drop
! All hot channel factors = 1.0
! No bypass flow, NCTYP=0
! 10 axial heat transfer nodes in the heated length of fuel plates
!  1   2   3   4   5   6   7   8   9  10  11  12  13  14  15  16  17  18  19    # Card 0200
   0   0   0   1   0   1   1   1   0   0   0   0   0                       0    Card(1)0200
   2   3 0.50       1.00        1.00        1.00           3                  Card(1)0300
! Using pressure driven mode
   1  20 1.00                                                                  Card(1)0301
   1   1   1                                                                   Card(1)0302
1.20        1.20                                                               Card(2)0303
2.03E-03    2.00E-02    0.15        0.50        0.20        10.15E-3           Card(3)0304
2.03E-03    4.00E-03    0.75        0.00        0.20        2.03E-03           Card(3)0304
2.03E-03    2.00E-02    0.15        0.50        0.20        10.15E-3           Card(3)0304
! Use the code's biult-in correlation for friction factor
0.00        0.00        0.00                                                   Card(1)0305
   5   3 0.00       0.75        0.50E-03    0.00        1.00E-03    100.00     Card(1)0306
4.06E-04    4.00E-03    0.4060      0.20        0.20        2.03E-03           Card(5)0307
4.06E-04    4.00E-03    0.4060      0.40        0.20        2.03E-03           Card(5)0307
4.06E-04    4.00E-03    0.4060      0.40        0.20        2.03E-03           Card(5)0307
4.06E-04    4.00E-03    0.4060      0.40        0.20        2.03E-03           Card(5)0307
4.06E-04    4.00E-03    0.4060      0.20        0.20        2.03E-03           Card(5)0307
0.20        0.20        0.20        0.20                                       Card(1)0308
! Card 0308a not required
! Radial power peaking factor data by fuel plate for each assembly. Input flow data by
! channel for each assembly on Cards 0310 not required because WFGES(1) is non-zero
0.700       0.900       1.100       1.300                                      Card(2)0309
0.700       0.900       1.100       1.300                                      Card(2)0309
! DP0       DDP         DPMAX       POWER       TIN         PIN
0.30        0.04        0.10        4.00        45.0        1.40               Card(1)0500
                                                                               Card(2)0500
  50 0.0001     25.0        0.50        1.00                                   Card(1)0600
  11                                                                           Card(1)0700
0.00        0.80                                                               Card(11)0701
0.10        0.88                                                               Card(11)0701
0.20        0.96                                                               Card(11)0701
0.30        1.04                                                               Card(11)0701
0.40        1.12                                                               Card(11)0701
0.50        1.20                                                               Card(11)0701
0.60        1.12                                                               Card(11)0701
0.70        1.04                                                               Card(11)0701
0.80        0.96                                                               Card(11)0701
0.90        0.88                                                               Card(11)0701
1.00        0.80                                                               Card(11)0701
   0                                                                           Card(11)0702
```

Figure 23.8 PLTEMP/ANL Input File *input.2Assemblies.stdprob45* for Standard Problem 45 Used to Verify the Flow Calculation Method Implemented in the Code

```
 Test Problem 45: 2 assemblies (of identical geometry) producing 4 MWt
! Each assembly has 4 fuel plates and 5 coolant channels
! H2O coolant, Flow is calculated from input pressure drop
! All hot channel factors = 1.0
! No bypass flow, NCTYP=0
! 10 axial heat transfer nodes in the heated length of fuel plates
!  1   2   3   4   5   6   7   8   9  10  11  12  13  14  15  16  17  18  19    # Card 0200
   0   0   0   1   0   1   1   1   0   0   0   0   0                       0    Card(1)0200
   2   3 0.50       1.00        1.00        1.00           3                   Card(1)0300
! Using pressure driven mode
   1  20 1.00                                                                  Card(1)0301
   1   1   1                                                                   Card(1)0302
1.20        1.20                                                               Card(2)0303
2.03E-03    2.00E-02    0.15        0.50        0.20        10.15E-3           Card(3)0304
2.03E-03    4.00E-03    0.75        0.00        0.20        2.03E-03           Card(3)0304
2.03E-03    2.00E-02    0.15        0.50        0.20        10.15E-3           Card(3)0304
! Use the code's biult-in correlation for friction factor
0.00        0.00        0.00                                                   Card(1)0305
   5   3 0.00       0.75        0.50E-03    0.00        1.00E-03    100.00     Card(1)0306
4.06E-04    4.00E-03    0.4060      0.20        0.20        2.03E-03           Card(5)0307
4.06E-04    4.00E-03    0.4060      0.40        0.20        2.03E-03           Card(5)0307
4.06E-04    4.00E-03    0.4060      0.40        0.20        2.03E-03           Card(5)0307
4.06E-04    4.00E-03    0.4060      0.40        0.20        2.03E-03           Card(5)0307
4.06E-04    4.00E-03    0.4060      0.20        0.20        2.03E-03           Card(5)0307
0.20        0.20        0.20        0.20                                       Card(1)0308
! Card 0308a not required
! Radial power peaking factor data by fuel plate for each assembly. Input flow data by
! channel for each assembly on Cards 0310 not required because WFGES(1) is non-zero
0.400       0.800       1.200       1.600                                      Card(2)0309
0.400       0.800       1.200       1.600                                      Card(2)0309
! DP0       DDP         DPMAX       POWER       TIN         PIN
0.30        0.04        0.10        4.00        45.0        1.40               Card(1)0500
                                                                               Card(2)0500
  50 0.0001     25.0        0.50        1.00                                   Card(1)0600
  11                                                                           Card(1)0700
0.00        0.80                                                               Card(11)0701
0.10        0.88                                                               Card(11)0701
0.20        0.96                                                               Card(11)0701
0.30        1.04                                                               Card(11)0701
0.40        1.12                                                               Card(11)0701
0.50        1.20                                                               Card(11)0701
0.60        1.12                                                               Card(11)0701
0.70        1.04                                                               Card(11)0701
0.80        0.96                                                               Card(11)0701
0.90        0.88                                                               Card(11)0701
1.00        0.80                                                               Card(11)0701
   0                                                                           Card(11)0702
```

Table 23.1 Fuel Assembly Geometry and Fuel Plate Radial Power Factrors in Standard Problems 3, 3B and 3C

Total Power in Problem 3 = 1 MW, Problem 3B = 100 W, Problem 3C = 4 MW

1	2	3	4	5	6	7	8	9	10	11
							Radial Power Factor by Fuel Plate			
Axial Region in Fig. 23.1	Axial Length	Form Loss Coef. in Region	Coolant Channel	Flow Area	Hydraulic Diameter	Wetted Peri-meter	Problems 3 and 3B		Problem 3C	
	m			m^2	m	m	Assem-bly 1	Assem-bly 2	Assem-bly 1	Assem-bly 2
1	0.15	8.0		30.0E-4	29.55665E-3					
2	0.75	0.0	1	6.0E-4	5.91133E-3	0.4060	0.900	0.901	0.2250	1.000
			2	6.0E-4	5.91133E-3	0.4060	0.950	0.951	0.2375	2.500
			3	6.0E-4	5.91133E-3	0.4060	1.050	1.049	0.2625	2.500
			4	6.0E-4	5.91133E-3	0.4060	1.100	1.099	0.2750	1.000
			5	6.0E-4	5.91133E-3	0.4060				
3	0.15	8.0		30.0E-4	29.55665E-3					
Total							4.000	4.000	1.000	7.000

Table 23.2 Comparison of PLTEMP/ANL- and Spreadsheet-Calculated Channel Exit Temperatures for Three Problems

Input Data	Standard Problem 3B Flow Rate, kg/s				Standard Problem 3 Flow Rate, kg/s				Standard Problem 3C Flow Rate, kg/s			
Reactor Power, MW	0.0001				1.0				4.0			
Fuel Plate No.	1	2	3	4	1	2	3	4	1	2	3	4
Radial Power Factors of Plates in Assembly 1	0.900	0.950	1.050	1.100	0.900	0.950	1.050	1.100	0.2250	0.2375	0.2625	0.2750
Radial Power Factors of Plates in Assembly 2	0.901	0.951	1.049	1.099	0.901	0.951	1.049	1.099	1.0000	2.5000	2.5000	1.0000
	Comparison of Results											
Geometrical Region	PLTEMP Channel Exit Temp °C	Spread-sheet Channel Exit Temp °C	Exit Temp. Diff. °C		PLTEMP Channel Exit Temp °C	Spread-sheet Channel Exit Temp °C	Exit Temp. Diff. °C		PLTEMP Channel Exit Temp °C	Spread-sheet Channel Exit Temp °C	Exit Temp. Diff. °C	
Assembly 1, Estimate		45.0012				57.374				57.374		
Assembly 1	45.006	45.0012	0.0048		57.371	57.374	0.003		57.393	57.374	0.019	
Assembly 1, Channel 1	45.005	45.0007	0.0043		52.471	52.0004	0.4706		52.471	52.0004	0.4706	
Assembly 1, Channel 2	45.006	45.0014	0.0046		58.906	59.2780	0.3720		58.906	59.2780	0.3720	
Assembly 1, Channel 3	45.007	45.0015	0.0055		60.370	60.4173	0.0473		60.37	60.4173	0.0473	
Assembly 1, Channel 4	45.009	45.0017	0.0073		60.999	61.5541	0.5551		60.999	61.5541	0.5551	
Assembly 1, Channel 5	45.004	45.0009	0.0031		54.042	53.5417	0.5003		54.042	53.5417	0.5003	
Max. Diff. Assembly 1			0.0073				0.5551				0.5551	
Assembly 2, Estimate		45.0012				57.374				131.487		
Assembly 2	45.006	45.0012	0.0048		57.372	57.374	0.002		131.36	131.518	0.158	
Assembly 2, Channel 1	45.005	45.0007	0.0043		52.479	52.0082	0.4708		82.205	77.1667	5.0383	
Assembly 2, Channel 2	45.006	45.0014	0.0046		58.921	59.2932	0.3722		149.457	151.1219	1.6649	
Assembly 2, Channel 3	45.007	45.0015	0.0055		60.373	60.4173	0.0443		188.698	192.5837	3.8857	
Assembly 2, Channel 4	45.009	45.0017	0.0073		60.984	61.5389	0.5549		149.455	151.1219	1.6669	
Assembly 2, Channel 5	45.004	45.0009	0.0031		54.036	53.534	0.502		82.204	77.1667	5.0373	
Max. Diff. Assembly 2			0.0073				0.5549				5.0383	

Table 23.3 Comparison of PLTEMP/ANL- and Spreadsheet-Calculated Flow Rates for Three Problems

Input Data	Standard Problem 3B Flow Rate, kg/s				Standard Problem 3 Flow Rate, kg/s				Standard Problem 3C Flow Rate, kg/s			
Reactor Power, MW	0.0001				1.0				4.0			
Fuel Plate No.	1	2	3	4	1	2	3	4	1	2	3	4
Radial Power Factors of Plates in Assembly 1	0.900	0.950	1.050	1.100	0.900	0.950	1.050	1.100	0.2250	0.2375	0.2625	0.2750
Radial Power Factors of Plates in Assembly 2	0.901	0.951	1.049	1.099	0.901	0.951	1.049	1.099	1.0000	2.5000	2.5000	1.0000
	Comparison of Results											
Geometrical Region	Power Deposited in Channels W	Spread-sheet Flow kg/s	PLTEMP Flow kg/s	% Diff. in Flow	Power Deposited in Channels W	Spread-sheet Flow kg/s	PLTEMP Flow kg/s	% Diff. in Flow	Power Deposited in Channels W	Spread-sheet Flow kg/s	PLTEMP Flow kg/s	% Diff. in Flow
Assembly 1, Estimate	50	9.66577	9.6634	0.025	500000	9.66262	9.6697	0.073	500000	9.66262	9.6697	0.073
Assembly 1	50	9.65676	9.6639	0.074	500000	9.66254	9.6694	0.071	500000	9.66254	9.6694	0.071
Assembly 1, Channel 1	6	1.93135	1.93277	0.073	56250	1.92185	1.92371	0.097	56250	1.92185	1.92371	0.097
Assembly 1, Channel 2	12	1.93135	1.93278	0.074	115625	1.93636	1.93758	0.063	115625	1.93636	1.93758	0.063
Assembly 1, Channel 3	13	1.93135	1.93278	0.074	125000	1.93857	1.93966	0.056	125000	1.93857	1.93966	0.056
Assembly 1, Channel 4	13	1.93135	1.93278	0.074	134375	1.94076	1.94172	0.049	134375	1.94076	1.94172	0.049
Assembly 1, Channel 5	7	1.93135	1.93277	0.073	68750	1.92498	1.92673	0.091	68750	1.92498	1.92673	0.091
Max. Absolute % Diff.				**0.074**				**0.097**				**0.097**
Assembly 2, Estimate	50	9.65676	9.6634	0.069	500000	9.66262	9.6697	0.073	3500000	9.6227	9.6169	0.060
Assembly 2	50	9.65676	9.6639	0.074	500000	9.66254	9.6694	0.071	3500000	9.61921	9.5705	0.509
Assembly 2, Channel 1	6	1.93135	1.93277	0.073	56313	1.92187	1.92372	0.096	250000	1.85672	1.86167	0.266
Assembly 2, Channel 2	12	1.93135	1.93278	0.074	115750	1.9364	1.93761	0.062	875000	1.95561	1.93968	0.821
Assembly 2, Channel 3	13	1.93135	1.93278	0.074	125000	1.93858	1.93966	0.056	1250000	1.99455	1.96776	1.361
Assembly 2, Channel 4	13	1.93135	1.93278	0.074	134250	1.94073	1.94169	0.049	875000	1.95561	1.93969	0.821
Assembly 2, Channel 5	7	1.93135	1.93277	0.073	68688	1.92497	1.92671	0.090	250000	1.85672	1.86167	0.266
Max. Absolute % Diff.				**0.074**				**0.096**				**1.361**

Table 23.4 Flow Rate Difference between Problems 3 vs 3B, and between Problems 3C vs 3B

	Absolute % Difference in Flow Rate					
	Problem 3 vs 3B		**Problem 3C vs 3**		**Problem 3C vs 3B**	
	Spreadsheet	PLTEMP/ANL	Spreadsheet	PLTEMP/ANL	Spreadsheet	PLTEMP/ANL
Assembly 1, Estimate	0.033	0.065	0.000	0.000	0.033	0.065
Assembly 1	0.060	0.057	0.000	0.000	0.060	0.057
Assembly 1, Channel 1	0.492	0.469	0.000	0.000	0.494	0.469
Assembly 1, Channel 2	0.259	0.248	0.000	0.000	0.259	0.248
Assembly 1, Channel 3	0.374	0.356	0.000	0.000	0.372	0.356
Assembly 1, Channel 4	0.487	0.463	0.000	0.000	0.485	0.463
Assembly 1, Channel 5	0.330	0.313	0.000	0.000	0.331	0.313
Max. Absolute % Diff.	**0.492**	**0.469**	**0.000**	**0.000**	**0.494**	**0.469**
Assembly 2, Estimate	0.061	0.065	0.413	0.546	0.354	0.481
Assembly 2	0.060	0.057	0.448	1.023	0.390	0.966
Assembly 2, Channel 1	0.491	0.468	3.390	3.226	4.019	3.679
Assembly 2, Channel 2	0.261	0.250	0.992	0.107	1.241	0.357
Assembly 2, Channel 3	0.374	0.356	2.887	1.449	3.169	1.810
Assembly 2, Channel 4	0.486	0.461	0.767	0.103	1.241	0.358
Assembly 2, Channel 5	0.330	0.314	3.546	3.376	4.019	3.679
Max. Absolute % Diff.	**0.491**	**0.468**	**3.546**	**3.376**	**4.019**	**3.679**

Table 23.5 Spreadsheet Calculation of Parameters in Eq. (K.12) to Find the Assembly Flow Rate for Problem 3B

Assem-bly 1	$\frac{K_n + f_n L_n / D_{h,n}}{A_{f,n}^2}$	$\frac{K_n + f_n L_n / D_{h,n}}{\rho_n A_{f,n}^2}$	$K_n + f_n L_n / D_{h,n}$	Bulk Coolant	Viscosity μ	Sp. Heat		Density	f, Zigrang-Sylvester	f, Romeo for checking
Axial Region	m^{-2}	m/kg		Temp, °C	Pa-s	J/kg-°C	Re	kg/m³		
1	8.9809E+05	9.0774E+02	8.082851	45.000	5.9466E-04	4.1800E+03	1.5999E+05	989.377	0.016325	0.016359
2	3.2573E+05	3.2923E+02	2.931554	45.001	5.9465E-04	4.1800E+03	3.1999E+04	989.377	0.023106	0.023158
3	8.9809E+05	9.0774E+02	8.082851	45.001	5.9464E-04	4.1800E+03	1.6000E+05	989.377	0.016325	0.016359
D_{fric}	2.1219E+06	2.1447E+03								

Assem-bly 2	$\frac{K_n + f_n L_n / D_{h,n}}{A_{f,n}^2}$	$\frac{K_n + f_n L_n / D_{h,n}}{\rho_n A_{f,n}^2}$	$K_n + f_n L_n / D_{h,n}$	Bulk Coolant	Viscosity μ	Sp. Heat		Density	f, Zigrang-Sylvester	f, Romeo for checking
Axial Region	m^{-2}	m/kg		Temp, °C	Pa-s	J/kg-°C	Re	kg/m³		
1	8.9809E+05	9.0774E+02	8.082851	45.000	5.9466E-04	4.1800E+03	1.5999E+05	989.377	0.016325	0.016359
2	3.2573E+05	3.2923E+02	2.931555	45.001	5.9465E-04	4.1800E+03	3.1999E+04	989.377	0.023106	0.023158
3	8.9809E+05	9.0774E+02	8.082851	45.001	5.9464E-04	4.1800E+03	1.6000E+05	989.377	0.016325	0.016359
D_{fric}	2.1219E+06	2.1447E+03								

Table 23.6 Spreadsheet Solution of Equations (K.16) to (K.18) to Find Channel Flow Rates in Assembly 1 of Problem 3B

	Channel No	**1**	**2**	**3**	**4**	**5**	**Sum**
	Fuel plate No	1	2	3	4		
	Radial power factor	0.9000	0.9500	1.0500	1.1000		4.0000
	Qch,k , W	6	12	13	13	7	50
	Aff,k , m^2	6.00E-04	6.00E-04	6.00E-04	6.00E-04	6.00E-04	3.00E-03
	Wetted perimeter, m	0.4060	0.4060	0.4060	0.4060	0.4060	2.0300
	Dch,k , m	5.91133E-03	5.91133E-03	5.91133E-03	5.91133E-03	5.91133E-03	5.91133E-03
Solution from 1st. Minimization	Channel flow W1,k , kg/s	1.931353	1.931353	1.931353	1.931353	1.931353	9.656766
ASSUMED VALUES OF	Channel flow W1,k , kg/s	1.93135	1.93135	1.93135	1.93135	1.93135	**9.65676**
UNKNOWNS IN RED	ΔP2 , Pa	2.26275E+04					
	ΔPfric , Pa	1.0000E+05					
	Tchavg0,k	45.0003	45.0007	45.0008	45.0008	45.0004	45.0006
	Cp,chavg,k , J/kg-ºC	4.1800E+03	4.1800E+03	4.1800E+03	4.1800E+03	4.1800E+03	4.1800E+03
	Tchavg,k	45.0003	45.0007	45.0008	45.0008	45.0004	45.0006
	μ,ch,k , kg/m^3	5.9465E-04	5.9465E-04	5.9465E-04	5.9465E-04	5.9465E-04	
	ρ,ch,k , kg/m^3	989.3772	989.3770	989.3770	989.3770	989.3771	
	$Re_{ch,k}$	3.1999E+04	3.1999E+04	3.1999E+04	3.1999E+04	3.1999E+04	
	$f_{ch,k}$	0.023106	0.023106	0.023106	0.023106	0.023106	
	RHS of Eq. (K.17)	2.26275E+04	2.26275E+04	2.26275E+04	2.26275E+04	2.26275E+04	
	RHS of Eq. (K.18)	1.00000E+05					
	Tch,out , ºC	45.0007	45.0014	45.0015	45.0017	45.0009	45.0012
	Axial Region No	1	2	3			
	Length Ln, m	0.15	0.75	0.15			
	Dh,n , m	2.95567E-02	5.91133E-03	2.95567E-02			
	Af,n , m^2	3.00000E-03	3.00000E-03	3.00000E-03			
	Form loss factor Kn	8.00	0.00	8.00			
	Tavg0 , C	45.0000	45.0006	45.0012			
	Cp,avg,n , J/kg-ºC	4.1800E+03	4.1800E+03	4.1800E+03			
	Tavg,n	45.0000	45.0006	45.0012			
	μ,n , kg/m^3	5.9466E-04	5.9465E-04	5.9464E-04			
	ρ,n , kg/m^3	989.3773	989.3771	989.3768			
	Re,n	1.5999E+05	3.1999E+04	1.6000E+05			
	Friction factor fn	0.016325	0.023106	0.016325			
	$K_n + f_n L_n/D_{h,n}$	8.08285E+00	2.93155E+00	8.08285E+00			1.90973E+01
	$(K_n + f_n L_n/D_{h,n})/(\rho_n A_{f,n}^2)$	9.07737E+02	3.29226E+02	9.07738E+02			2.14470E+03
Sum of Square of Residue of Eqs (K.17) and (K.18)							9.380E-03

Table 23.7 Spreadsheet Solution of Equations (K.16) to (K.18) to Find Channel Flow Rates in Assembly 2 of Problem 3B

	Channel No	**1**	**2**	**3**	**4**	**5**	**Sum**
	Fuel plate No	1	2	3	4		
	Radial power factor	0.9010	0.9510	1.0490	1.0990		4.0000
	Qch,k , W	6	12	13	13	7	50
	Aff,k , m^2	6.00E-04	6.00E-04	6.00E-04	6.00E-04	6.00E-04	3.00E-03
	Wetted perimeter, m	0.4060	0.4060	0.4060	0.4060	0.4060	2.0300
	Dch,k , m	5.91133E-03	5.91133E-03	5.91133E-03	5.91133E-03	5.91133E-03	5.91133E-03
Solution from 1st. Minimization	Channel flow W1,k , kg/s	1.931352	1.931352	1.931352	1.931352	1.931352	9.656762
ASSUMED VALUES OF	Channel flow W1,k , kg/s	**1.93135**	**1.93135**	**1.93135**	**1.93135**	**1.93135**	**9.65676**
UNKNOWNS IN RED	ΔP2 , Pa	**2.26275E+04**					
	ΔPfric , Pa	1.0000E+05					
	Tchavg0,k	45.0003	45.0007	45.0008	45.0008	45.0004	45.0006
	Cp,chavg,k , J/kg-ºC	4.1800E+03	4.1800E+03	4.1800E+03	4.1800E+03	4.1800E+03	4.1800E+03
	Tchavg,k	45.0003	45.0007	45.0008	45.0008	45.0004	45.0006
	μ,ch,k , kg/m^3	5.9465E-04	5.9465E-04	5.9465E-04	5.9465E-04	5.9465E-04	
	ρ,ch,k , kg/m^3	989.3772	989.3770	989.3770	989.3770	989.3771	
	$Re_{ch,k}$	3.1999E+04	3.1999E+04	3.1999E+04	3.1999E+04	3.1999E+04	
	$f_{ch,k}$	0.023106	0.023106	0.023106	0.023106	0.023106	
	RHS of Eq. (K.17)	2.26275E+04	2.26275E+04	2.26275E+04	2.26275E+04	2.26275E+04	
	RHS of Eq. (K.18)	1.00000E+05					
	Tch,out , ºC	45.0007	45.0014	45.0015	45.0017	45.0009	45.0012
	Axial Region No	**1**	**2**	**3**			
	Length Ln, m	0.15	0.75	0.15			
	Dh,n , m	2.95567E-02	5.91133E-03	2.95567E-02			
	Af,n , m^2	3.00000E-03	3.00000E-03	3.00000E-03			
	Form loss factor Kn	8.00	0.00	8.00			
	Tavg0 , C	45.0000	45.0006	45.0012			
	Cp,avg,n , J/kg-ºC	4.1800E+03	4.1800E+03	4.1800E+03			
	Tavg,n	45.0000	45.0006	45.0012			
	μ,n , kg/m^3	5.9466E-04	5.9465E-04	5.9464E-04			
	ρ,n , kg/m^3	989.3773	989.3771	989.3768			
	Re,n	1.5999E+05	3.1999E+04	1.6000E+05			
	Friction factor fn	0.016325	0.023106	0.016325			
	$K_n + f_n L_n/D_{h,n}$	8.08285E+00	2.93155E+00	8.08285E+00			1.90973E+01
	$(K_n + f_n L_n/D_{h,n})/(\rho_n A_{f,n}^2)$	9.07737E+02	3.29226E+02	9.07738E+02			2.14470E+03
Sum of Square of Residue of Eqs (K.17) and (K.18)							4.633E-03

Table 23.8 Spreadsheet Calculation of Parameters in Eq. (K.12) to Find the Assembly Flow Rate for Problem 3

Assem-bly 1	$\frac{K_n + f_n L_n / D_{h,n}}{A_{f,n}^2}$	$\frac{K_n + f_n L_n / D_{h,n}}{\rho_n A_{f,n}^2}$	$K_n + f_n L_n / D_{h,n}$	Bulk Coolant	Viscosity μ	Sp. Heat		Density	f, Zigrang-Sylvester	f, Romeo for checking
Axial Region	m^{-2}	m/kg		Temp, °C	Pa-s	J/kg-°C	Re	kg/m³		
1	8.9809E+05	9.0774E+02	8.082841	45.000	5.9466E-04	4.1800E+03	1.6009E+05	989.377	0.016323	0.016358
2	3.1772E+05	3.2198E+02	2.859479	51.187	5.3453E-04	4.1818E+03	3.5620E+04	986.756	0.022538	0.022588
3	8.9773E+05	9.1238E+02	8.079531	57.374	4.8396E-04	4.1842E+03	1.9671E+05	983.937	0.015671	0.015703
D_{fric}	2.1135E+06	2.1421E+03								

Assem-bly 2	$\frac{K_n + f_n L_n / D_{h,n}}{A_{f,n}^2}$	$\frac{K_n + f_n L_n / D_{h,n}}{\rho_n A_{f,n}^2}$	$K_n + f_n L_n / D_{h,n}$	Bulk Coolant	Viscosity μ	Sp. Heat		Density	f, Zigrang-Sylvester	f, Romeo for checking
Axial Region	m^{-2}	m/kg		Temp, °C	Pa-s	J/kg-°C	Re	kg/m³		
1	8.9809E+05	9.0774E+02	8.082841	45.000	5.9466E-04	4.1800E+03	1.6009E+05	989.377	0.016323	0.016358
2	3.1772E+05	3.2198E+02	2.859479	51.187	5.3453E-04	4.1818E+03	3.5620E+04	986.756	0.022538	0.022588
3	8.9773E+05	9.1238E+02	8.079531	57.374	4.8396E-04	4.1842E+03	1.9671E+05	983.937	0.015671	0.015703
D_{fric}	2.1135E+06	2.1421E+03								

Table 23.9 Spreadsheet Solution of Equations (K.16) to (K.18) to Find Channel Flow Rates in Assembly 1 of Problem 3

	Channel No	**1**	**2**	**3**	**4**	**5**	**Sum**
	Fuel plate No	1	2	3	4		
	Radial power factor	0.9000	0.9500	1.0500	1.1000		4.0000
	Qch,k , W	56250	115625	125000	134375	68750	500000
	Aff,k , m^2	6.00E-04	6.00E-04	6.00E-04	6.00E-04	6.00E-04	3.00E-03
	Wetted perimeter, m	0.4060	0.4060	0.4060	0.4060	0.4060	2.0300
	Dch,k , m	5.91133E-03	5.91133E-03	5.91133E-03	5.91133E-03	5.91133E-03	5.91133E-03
Solution from 1st. Minimization	Channel flow W1,k , kg/s	1.932524	1.932524	1.932524	1.932524	1.932524	9.662622
ASSUMED VALUES OF	Channel flow W1,k , kg/s	**1.92185**	**1.93636**	**1.93857**	**1.94076**	**1.92498**	**9.66254**
UNKNOWNS IN RED	ΔP2 , Pa	**2.22903E+04**					
	ΔPfric , Pa	1.0000E+05					
	Tchavg0,k	48.5010	52.1426	52.7129	53.2821	49.2721	51.1897
	Cp,chavg,k , J/kg-ºC	4.1810E+03	4.1821E+03	4.1823E+03	4.1825E+03	4.1812E+03	4.1818E+03
	Tchavg,k	48.5002	52.1390	52.7086	53.2770	49.2709	51.1871
	μ,ch,k , kg/m^3	5.5933E-04	5.2618E-04	5.2129E-04	5.1648E-04	5.5202E-04	
	ρ,ch,k , kg/m^3	987.9187	986.3352	986.0811	985.8259	987.5890	
	$Re_{ch,k}$	3.3852E+04	3.6257E+04	3.6639E+04	3.7021E+04	3.4356E+04	
	$f_{ch,k}$	0.022805	0.022446	0.022392	0.022338	0.022727	
	RHS of Eq. (K.17)	2.22903E+04	2.22903E+04	2.22903E+04	2.22903E+04	2.22903E+04	
	RHS of Eq. (K.18)	9.99999E+04					
	Tch,out , ºC	52.0004	59.2780	60.4173	61.5541	53.5417	57.3741
	Axial Region No	**1**	**2**	**3**			
	Length Ln, m	0.15	0.75	0.15			
	Dh,n , m	2.95567E-02	5.91133E-03	2.95567E-02			
	Af,n , m^2	3.00000E-03	3.00000E-03	3.00000E-03			
	Form loss factor Kn	8.00	0.00	8.00			
	Tavg0 , C	45.0000	51.1897	57.3794			
	Cp,avg,n , J/kg-ºC	4.1800E+03	4.1818E+03	4.1842E+03			
	Tavg,n	45.0000	51.1871	57.3671			
	μ,n , kg/m^3	5.9466E-04	5.3453E-04	4.8401E-04			
	ρ,n , kg/m^3	989.3773	986.7561	983.9403			
	Re,n	1.6009E+05	3.5619E+04	1.9668E+05			
	Friction factor fn	0.016323	0.022538	0.015671			
	$K_n + f_n L_n/D_{h,n}$	8.08284E+00	2.85948E+00	8.07953E+00			1.90219E+01
	$(K_n + f_n L_n/D_{h,n})/(\rho_n A_{f,n}^2)$	9.07736E+02	3.21985E+02	9.12378E+02			2.14210E+03
Sum of Square of Residue of Eqs (K.17) and (K.18)							4.332E-03

Table 23.1 Spreadsheet Solution of Equations (K.16) to (K.18) to Find Channel Flow Rates in Assembly 2 of Problem 3

	Channel No	**1**	**2**	**3**	**4**	**5**	**Sum**
	Fuel plate No	1	2	3	4		
	Radial power factor	0.9010	0.9510	1.0490	1.0990		4.0000
	Qch,k , W	56313	115750	125000	134250	68688	500000
	Aff,k , m^2	6.00E-04	6.00E-04	6.00E-04	6.00E-04	6.00E-04	3.00E-03
	Wetted perimeter, m	0.4060	0.4060	0.4060	0.4060	0.4060	2.0300
	Dch,k , m	5.91133E-03	5.91133E-03	5.91133E-03	5.91133E-03	5.91133E-03	5.91133E-03
Solution from 1st. Minimization	Channel flow W1,k , kg/s	1.932523	1.932523	1.932523	1.932523	1.932523	9.662616
ASSUMED VALUES OF	Channel flow W1,k , kg/s	**1.92187**	**1.93640**	**1.93858**	**1.94073**	**1.92497**	**9.66254**
UNKNOWNS IN RED	ΔP2 , Pa	**2.22903E+04**					
	ΔPfric , Pa	1.0000E+05					
	Tchavg0,k	48.5049	52.1502	52.7129	53.2745	49.2682	51.1897
	Cp,chavg,k , J/kg-ºC	4.1810E+03	4.1821E+03	4.1823E+03	4.1825E+03	4.1812E+03	4.1818E+03
	Tchavg,k	48.5041	52.1466	52.7086	53.2695	49.2670	51.1871
	μ,ch,k , kg/m^3	5.5929E-04	5.2611E-04	5.2129E-04	5.1655E-04	5.5206E-04	
	ρ,ch,k , kg/m^3	987.9170	986.3318	986.0811	985.8293	987.5907	
	$Re_{ch,k}$	3.3855E+04	3.6262E+04	3.6639E+04	3.7016E+04	3.4354E+04	
	$f_{ch,k}$	0.022805	0.022445	0.022392	0.022339	0.022727	
	RHS of Eq. (K.17)	2.22903E+04	2.22903E+04	2.22903E+04	2.22903E+04	2.22903E+04	
	RHS of Eq. (K.18)	1.00000E+05					
	Tch,out , ºC	52.0082	59.2932	60.4173	61.5389	53.5340	57.3741
	Axial Region No	**1**	**2**	**3**			
	Length Ln, m	0.15	0.75	0.15			
	Dh,n , m	2.95567E-02	5.91133E-03	2.95567E-02			
	Af,n , m^2	3.00000E-03	3.00000E-03	3.00000E-03			
	Form loss factor Kn	8.00	0.00	8.00			
	Tavg0 , C	45.0000	51.1897	57.3794			
	Cp,avg,n , J/kg-ºC	4.1800E+03	4.1818E+03	4.1842E+03			
	Tavg,n	45.0000	51.1871	57.3671			
	μ,n , kg/m^3	5.9466E-04	5.3453E-04	4.8401E-04			
	ρ,n , kg/m^3	989.3773	986.7561	983.9403			
	Re,n	1.6009E+05	3.5619E+04	1.9668E+05			
	Friction factor fn	0.016323	0.022538	0.015671			
	$K_n + f_n L_n/D_{h,n}$	8.08284E+00	2.85948E+00	8.07953E+00			1.90219E+01
	$(K_n + f_n L_n/D_{h,n})/(\rho_n A$	9.07736E+02	3.21985E+02	9.12378E+02			2.14210E+03
Sum of Square of Residue of Eqs (K.17) and (K.18)							9.888E-04

Table 23.2 Spreadsheet Calculation of Parameters in Eq. (K.12) to Find the Assembly Flow Rate for Problem 3C

Assem-bly 1	$\frac{K_n + f_n L_n / D_{h,n}}{A_{f,n}^2}$	$\frac{K_n + f_n L_n / D_{h,n}}{\rho_n A_{f,n}^2}$	$K_n + f_n L_n / D_{h,n}$	Bulk Coolant	Viscosity μ	Sp. Heat	Re	Density	f, Zigrang-Sylvester	f, Romeo for checking
Axial Region	m^{-2}	m/kg		Temp, °C	Pa-s	J/kg-°C		kg/m³		
1	8.9809E+05	9.0774E+02	8.082841	45.000	5.9466E-04	4.1800E+03	1.6009E+05	989.377	0.016323	0.016358
2	3.1772E+05	3.2198E+02	2.859479	51.187	5.3453E-04	4.1818E+03	3.5620E+04	986.756	0.022538	0.022588
3	8.9773E+05	9.1238E+02	8.079531	57.374	4.8396E-04	4.1842E+03	1.9671E+05	983.937	0.015671	0.015703
D_{fric}	2.1135E+06	2.1421E+03								

Assem-bly 2	$\frac{K_n + f_n L_n / D_{h,n}}{A_{f,n}^2}$	$\frac{K_n + f_n L_n / D_{h,n}}{\rho_n A_{f,n}^2}$	$K_n + f_n L_n / D_{h,n}$	Bulk Coolant	Viscosity μ	Sp. Heat	Re	Density	f, Zigrang-Sylvester	f, Romeo for checking
Axial Region	m^{-2}	m/kg		Temp, °C	Pa-s	J/kg-°C		kg/m³		
1	8.9810E+05	9.0774E+02	8.082910	45.000	5.9466E-04	4.1800E+03	1.5943E+05	989.377	0.016337	0.016371
2	2.8349E+05	2.9319E+02	2.551373	88.243	3.2079E-04	4.2053E+03	5.9107E+04	966.917	0.020109	0.020154
3	8.9645E+05	9.5898E+02	8.068046	131.487	2.1146E-04	4.2675E+03	4.4833E+05	934.793	0.013408	0.013434
D_{fric}	2.0780E+06	2.1599E+03								

Table 23.3 Spreadsheet Solution of Equations (K.16) to (K.18) to Find Channel Flow Rates in Assembly 1 of Problem 3C

	Channel No	**1**	**2**	**3**	**4**	**5**	Sum
	Fuel plate No	1	2	3	4		
	Radial power factor	0.2250	0.2375	0.2625	0.2750		1.0000
	Qch,k , W	56250	115625	125000	134375	68750	500000
	Aff,k , m^2	6.00E-04	6.00E-04	6.00E-04	6.00E-04	6.00E-04	3.00E-03
	Wetted perimeter, m	0.4060	0.4060	0.4060	0.4060	0.4060	2.0300
	Dch,k , m	5.91133E-03	5.91133E-03	5.91133E-03	5.91133E-03	5.91133E-03	5.91133E-03
Solution from 1st. Minimization	Channel flow W1,k , kg/s	1.932524	1.932524	1.932524	1.932524	1.932524	9.662622
ASSUMED VALUES OF	Channel flow W1,k , kg/s	**1.92185**	**1.93636**	**1.93857**	**1.94076**	**1.92498**	**9.66254**
UNKNOWNS IN RED	ΔP2 , Pa	**2.22903E+04**					
	ΔPfric , Pa	1.0000E+05					
	Tchavg0,k	48.5010	52.1426	52.7129	53.2821	49.2721	
	Cp,chavg,k , J/kg-ºC	4.1810E+03	4.1821E+03	4.1823E+03	4.1825E+03	4.1812E+03	
	Tchavg,k	48.5002	52.1390	52.7086	53.2770	49.2709	
	μ,ch,k , kg/m^3	5.5933E-04	5.2618E-04	5.2129E-04	5.1648E-04	5.5202E-04	
	ρ,ch,k , kg/m^3	987.9187	986.3352	986.0811	985.8259	987.5890	
	$Re_{ch,k}$	3.3852E+04	3.6257E+04	3.6639E+04	3.7021E+04	3.4356E+04	
	$f_{ch,k}$	0.022805	0.022446	0.022392	0.022338	0.022727	
	RHS of Eq. (K.17)	2.22903E+04	2.22903E+04	2.22903E+04	2.22903E+04	2.22903E+04	
	RHS of Eq. (K.18)	9.99999E+04					
	Tch,out , ºC	52.0004	59.2780	60.4173	61.5541	53.5417	
	Axial Region No	**1**	**2**	**3**			
	Length Ln, m	0.15	0.75	0.15			
	Dh,n , m	2.95567E-02	5.91133E-03	2.95567E-02			
	Af,n , m^2	3.00000E-03	3.00000E-03	3.00000E-03			
	Form loss factor Kn	8.00	0.00	8.00			
	Tavg0 , C	45.0000	51.1897	57.3794			
	Cp,avg,n , J/kg-ºC	4.1800E+03	4.1818E+03	4.1842E+03			
	Tavg,n	45.0000	51.1871	57.3671			
	μ,n , kg/m^3	5.9466E-04	5.3453E-04	4.8401E-04			
	ρ,n , kg/m^3	989.3773	986.7561	983.9403			
	Re,n	1.6009E+05	3.5619E+04	1.9668E+05			
	Friction factor fn	0.016323	0.022538	0.015671			
	$K_n + f_n L_n/D_{h,n}$	8.08284E+00	2.85948E+00	8.07953E+00			1.90219E+01
	$(K_n + f_n L_n/D_{h,n})/(\rho_n A_{f,n}^2)$	9.07736E+02	3.21985E+02	9.12378E+02			2.14210E+03
Sum of Square of Residue of Eqs (K.17) and (K.18) for Fuel Assembly 1							4.030E-03

Table 23.4 Spreadsheet Solution of Equations (K.16) to (K.18) to Find Channel Flow Rates in Assembly 2 of Problem 3C

	Channel No	**1**	**2**	**3**	**4**	**5**	**Sum**
	Fuel plate No	1	2	3	4		
	Radial power factor	1.0000	2.5000	2.5000	1.0000		7.0000
	Qch,k , W	250000	875000	1250000	875000	250000	3500000
	Aff,k , m^2	6.00E-04	6.00E-04	6.00E-04	6.00E-04	6.00E-04	3.00E-03
	Wetted perimeter, m	0.4060	0.4060	0.4060	0.4060	0.4060	2.0300
	Dch,k , m	5.91133E-03	5.91133E-03	5.91133E-03	5.91133E-03	5.91133E-03	5.91133E-03
Solution from 1st. Minimization	Channel flow W1,k , kg/s	1.924540	1.924540	1.924540	1.924540	1.924540	9.622702
ASSUMED VALUES OF	Channel flow W1,k , kg/s	**1.85672**	**1.95561**	**1.99455**	**1.95561**	**1.85672**	**9.61921**
UNKNOWNS IN RED	ΔP2 , Pa	**2.07981E+04**					
	ΔPfric , Pa	1.0000E+05					
	Tchavg0,k	61.1059	98.5202	119.9646	98.5202	61.1059	
	Cp,chavg,k , J/kg-ºC	4.1859E+03	4.2162E+03	4.2465E+03	4.2162E+03	4.1859E+03	
	Tchavg,k	61.0834	98.0610	118.7918	98.0610	61.0834	
	μ,ch,k , kg/m^3	4.5740E-04	2.8802E-04	2.3562E-04	2.8802E-04	4.5740E-04	
	ρ,ch,k , kg/m^3	982.1521	960.4714	945.2258	960.4714	982.1521	
	$Re_{ch,k}$	3.9993E+04	6.6896E+04	8.3400E+04	6.6896E+04	3.9993E+04	
	$f_{ch,k}$	0.021946	0.019574	0.018669	0.019574	0.021946	
	RHS of Eq. (K.17)	2.07981E+04	2.07981E+04	2.07981E+04	2.07981E+04	2.07981E+04	
	RHS of Eq. (K.18)	1.00000E+05					
	Tch,out , ºC	77.1667	151.1219	192.5837	151.1219	77.1667	
	Axial Region No	**1**	**2**	**3**			
	Length Ln, m	0.15	0.75	0.15			
	Dh,n , m	2.95567E-02	5.91133E-03	2.95567E-02			
	Af,n , m^2	3.00000E-03	3.00000E-03	3.00000E-03			
	Form loss factor Kn	8.00	0.00	8.00			
	Tavg0 , C	45.0000	88.5232	132.0464			
	Cp,avg,n , J/kg-ºC	4.1800E+03	4.2055E+03	4.2686E+03			
	Tavg,n	45.0000	88.2590	130.2400			
	μ,n , kg/m^3	5.9466E-04	3.2073E-04	2.1363E-04			
	ρ,n , kg/m^3	989.3773	966.9067	935.8549			
	Re,n	1.5937E+05	5.9096E+04	4.4562E+05			
	Friction factor fn	0.016338	0.020110	0.013423			
	$K_n + f_n L_n/D_{h,n}$	8.08292E+00	2.55148E+00	8.06812E+00			1.87025E+01
	$(K_n + f_n L_n/D_{h,n})/(\rho_n A_{f,n}^2)$	9.07744E+02	2.93200E+02	9.57903E+02			2.15885E+03
Sum of Square of Residue of Eqs (K.17) and (K.18) for Fuel Assembly 2							6.602E-05

Table 23.14 Key Differences among Standard Problems 3, 43, 44, and 45

Problem ID	Frictional Pressure Drop, MPa	Coolant Velocity m/s	K-Loss Factor of Assembly	Channel Hydraulic Diameter, mm	Range of Fuel Plate Power Factor	% Error in Channel Flow Rate due to Lack of T/H Iteration
Problem 3	0.1	~ 3	16.0	5.9	0.9 to 1.1	0.066
Problem 43	0.3	~ 11	1.0	4.0	0.9 to 1.1	0.084
Problem 44	0.3	~ 11	1.0	4.0	0.7 to 1.3	0.102
Problem 45	0.3	~ 11	1.0	4.0	0.4 to 1.6	0.131

Table 23.5 PLTEMP/ANL-Calculated Fraction of Fuel Plate Power Deposited in the Left Coolant Channel

	Standard Problem 3		**Standard Problem 43**		**Standard Problem 44**		**Standard Problem 45**	
Fuel Plate No.	Plate Power Fraction Deposited in Left Channel	Axially Averaged Plate Power Fraction	Plate Power Fraction Deposited in Left Channel	Axially Averaged Plate Power Fraction	Plate Power Fraction Deposited in Left Channel	Axially Averaged Plate Power Fraction	Plate Power Fraction Deposited in Left Channel	Axially Averaged Plate Power Fraction
1	0.5023 to 0.5788	0.5406	0.5020 to 0.5779	0.5400	0.5029 to 0.5977	0.5503	0.5057 to 0.6597	0.5827
2	0.5004 to 0.5173	0.5089	0.5003 to 0.5172	0.5088	0.5009 to 0.5400	0.5205	0.5021 to 0.5846	0.5434
3	0.5003 to 0.5070	0.5036	0.5002 to 0.5071	0.5036	0.5006 to 0.5251	0.5128	0.5010 to 0.5497	0.5254
4	0.4982 to 0.4305	0.4643	0.4985 to 0.4313	0.4649	0.4990 to 0.4403	0.4696	0.4994 to 0.4484	0.4739

Table 23.6 Change in Channel Flow Rates due to the Second T/H Iteration in Problem 3 (Coolant Velocity ~ 3 m/s)

			Assuming Plate Power Splitting Fraction = 0.50				Second Thermal-Hydraulic Iteration			
1	**2**	3	4	5	6	7	8*	9	10	11
Fuel Plate No.	Radial Power Factor of Plate	Plate Power kW	Fraction of Plate Power Deposited in Left Channel	Coolant Channel No.	Power Deposited in Channels kW	Channel Flow Rate kg/s	Fraction of Plate Power Deposited in Left Channel	Power Deposited in Channels kW	Channel Flow Rate kg/s	% Diff. in Flow Rate
1	0.900	112.50	0.5	1	56.250	1.92185	0.5406	60.818	1.92298	-0.0585
2	0.950	118.75	0.5	2	115.625	1.93637	0.5089	112.114	1.93551	0.0443
3	1.050	131.25	0.5	3	125.000	1.93858	0.5036	124.416	1.93841	0.0084
4	1.100	137.50	0.5	4	134.375	1.94076	0.4643	128.994	1.93949	0.0659
				5	68.750	1.92498		73.659	1.92618	-0.0620
Total		500.00			500.00	9.66254		500.00	9.66256	-0.0002

* The data of column 8 was obtained from PLTEMP/ANL output of standard Problem 45, by axially averaging the power splitting fraction of each fuel plate.

Table 23.7 Change in Channel Flow Rates due to the Second T/H Iteration in Problem 43 (Coolant Velocity ~11 m/s)

			Assuming Plate Power Splitting Fraction = 0.50				Second Thermal-Hydraulic Iteration			
1	**2**	3	4	5	6	7	8*	9	10	11
Fuel Plate No.	Radial Power Factor of Plate	Plate Power kW	Fraction of Plate Power Deposited in Left Channel	Coolant Channel No.	Power Deposited in Channels kW	Channel Flow Rate kg/s	Fraction of Plate Power Deposited in Left Channel	Power Deposited in Channels kW	Channel Flow Rate kg/s	% Diff. in Flow Rate
1	0.900	450.0	0.5	1	225.0	4.54609	0.5400	243.000	4.54974	-0.0804
2	0.950	475.0	0.5	2	462.5	4.59231	0.5088	448.680	4.58973	0.0563
3	1.050	525.0	0.5	3	500.0	4.59915	0.5036	497.710	4.59870	0.0098
4	1.100	550.0	0.5	4	537.5	4.60588	0.4649	516.305	4.60205	0.0830
				5	275.0	4.55626		294.305	4.56008	-0.0840
Total		2000.0				22.89969		2000.00	22.90031	-0.0027

* The data of column 8 was obtained from PLTEMP/ANL output of standard Problem 45, by axially averaging the power splitting fraction of each fuel plate.

Table 23.8 Change in Channel Flow Rates due to the Second T/H Iteration in Problem 44 (Coolant Velocity ~ 11 m/s)

			Assuming Plate Power Splitting Fraction = 0.50				Second Thermal-Hydraulic Iteration			
1	**2**	3	4	5	6	7	8*	9	10	11
Fuel Plate No.	Radial Power Factor of Plate	Plate Power kW	Fraction of Plate Power Deposited in Left Channel	Coolant Channel No.	Power Deposited in Channels kW	Channel Flow Rate kg/s	Fraction of Plate Power Deposited in Left Channel	Power Deposited in Channels kW	Channel Flow Rate kg/s	% Diff. in Flow Rate
1	0.700	350.0	0.5	1	175.00	4.53574	0.5503	192.605	4.53940	-0.0806
2	0.900	450.0	0.5	2	400.00	4.58071	0.5205	391.620	4.57908	0.0357
3	1.100	550.0	0.5	3	500.00	4.59922	0.5128	497.815	4.59878	0.0095
4	1.300	650.0	0.5	4	600.00	4.61689	0.4696	573.200	4.61219	0.1018
				5	325.00	4.56626		344.760	4.57007	-0.0835
Total		2000.0			2000.00	22.89883		2000.00	22.89952	-0.0030

* The data of column 8 was obtained from PLTEMP/ANL output of standard Problem 45, by axially averaging the power splitting fraction of each fuel plate.

Table 23.9 Change in Channel Flow Rates due to the Second T/H Iteration in Problem 45 (Coolant Velocity ~11 m/s)

**			Assuming Plate Power Splitting Fraction = 0.50				Second Thermal-Hydraulic Iteration			
1	**2**	3	4	5	6	7	8*	9	10	11
Fuel Plate No.	Radial Power Factor of Plate	Plate Power kW	Fraction of Plate Power Deposited in Left Channel	Coolant Channel No.	Power Deposited in Channels kW	Channel Flow Rate kg/s	Fraction of Plate Power Deposited in Left Channel	Power Deposited in Channels kW	Channel Flow Rate kg/s	% Diff. in Flow Rate
1	0.400	200.0	0.5	1	100.0	4.51986	0.5827	116.54	4.52340	-0.0783
2	0.800	400.0	0.5	2	300.0	4.56155	0.5434	300.82	4.56164	-0.0021
3	1.200	600.0	0.5	3	500.0	4.59945	0.5254	497.88	4.59900	0.0098
4	1.600	800.0	0.5	4	700.0	4.63401	0.4739	663.88	4.62793	0.1312
				5	400.0	4.58094		420.88	4.58481	-0.0844
Total		2000.0			2000.0	22.89582		2000.00	22.89679	-0.0042

* The data of column 8 was obtained from PLTEMP/ANL output of standard Problem 45, by axially averaging the power splitting fraction of each fuel plate.

Table 23.10 Spreadsheet-Calculated Flow in Standard Problem 3C at Different Reactor Powers

Case	Reactor Power, W	Flow in Fuel Assembly 1		Flow in Fuel Assembly 2	
		Calculated By Assembly	Calculated By Channel	Calculated By Assembly	Calculated by Channel
1	0.0	9.65677	9.65676	9.65676	9.65677
2	10	9.65677	9.65676	9.65676	9.65677
3	100	9.65677	9.65676	9.65676	9.65677
4	1000	9.65676	9.65677	9.65677	9.65678
5	10000	9.65678	9.65678	9.65690	9.65690
6	1.0×10^5	9.65696	9.65696	9.65808	9.65807
7	5.0×10^5	9.65772	9.65772	9.66211	9.66190
8	1.0×10^6	9.65860	9.65860	9.66446	9.66374
9	2.0×10^6	9.66020	9.66017	9.66079	9.65877
10	3.0×10^6	9.66153	9.66148	9.64656	9.64354
11	4.0×10^6	9.66262	9.66254	9.62270	9.61921

24 Verification of the Bernath and the Labuntsov CHF Correlations in PLTEMP/ANL

24.1 Introduction

The verification work reported here was done in July 2017. The Bernath and the Labuntsov critical heat flux (CHF) correlations were recently verified by comparing the PLTEMP/ANL code-calculated values of CHF with those calculated by an Excel spreadsheet that was developed for this purpose. Any CHF correlation can be used in two ways, referred to in the literature as the Direct Substitution Method (DSM) and the Heat Balance Method (HBM), the HBM being the preferred method. Both methods are implemented in the code, and both methods were verified. A flag in the code input allows the user to select one method or the other.

In the Direct Substitution Method (DSM), the operating values of the thermal-hydraulic parameters (at the location where the CHF needs to be calculated) are simply substituted in the CHF correlation, and the value of CHF thus obtained is taken to be the critical heat flux. This is only roughly correct. The actual CHF value may be hundereds of percent different from the value obtained by the DSM. This is because a CHF correlation is obtained by correlating a set of experimemtally measured CHF values in terms of measured values of a few (usually 3 to 5) experimenter-chosen thermal-hydraulic parameters. Since the operating condition of a reactor is by design far removed from a CHF condition (i.e., the operating condition is more sub-cooled than the CHF condition), the reactor operating condition does not belong to the set of data points from which the CHF correlation was derived. *The DSM always gives a higher value of CHF than the actual CHF* bucause the CHF increases with sub-cooling and all CHF correlations account for the sub-cooling.

The Heat Balance Method (HBM) provides the correct method of using a CHF correlation as pointed out by Celata [1], and Hejzlar and Todreas[2]. This is an iterative method of raising the reactor power from the operating power P_{op} to a power P, thus raising the heat flux of the axial segment where CHF needs to be found, from the operating value q_{op} to a value q [with the consequent coolant bulk temperature of the axial segment rising from the operating value T_{op} to the value $T_{in}+(T_{op} - T_{in})*(q/q_{op})$] such that the CHF obtained from the correlation at the *raised* bulk temperature equals the *raised* nodal heat flux q. This method is correct because when it has converged, it uses the CHF correlation at a thermal-hydraulic condition belonging to the set of experimental data points from which the CHF correlation was derived.

24.2 Verification of Bernath Critical Heat Flux Correlation

The Bernath CHF correlation is verified here by comparing the PLTEMP/ANL-calculated CHF values with those obtained by an Excel spreadsheet developed to calculate CHF by the DSM and the HBM using the Bernath correlation. The comparison is done for the standard Problem 38 described above in Section 22.3.

<u>An Improvement Made in PLTEMP/ANL Version 4.2:</u> In the course of verification of the Bernath CHF correlation, PLTEMP/ANL version 4.2 was found to fail to converge during CHF calculation by the HBM using the Bernath correlation. It was determined that the failure occurred due to zero heat flux in the *unheated* longitudinal stripe 1 of Problem 38. This discrepancy was fixed simply

by avoiding iteration (doing one iteration only) if the nodal heat flux is zero or negligible ($\leq 10^{-6}$ MW/m^2). In the course of verification of the Labuntsov CHF correlation, PLTEMP/ANL version 4.2 was found to use the critical pressure of light water for both light and heavy waters. This discrepancy was fixed by setting the heavy water critical pressure to 216.71 bar. The version *pltempv42_r82_170630* contains the improved source code, and the file 7 listed above is the improved executable.

Spreadsheet to Calculate CHF Using the Bernath Correlation : The spreadsheet first calculates the distributions of coolant, cladding, and fuel temperatures and cladding surface heat flux as described in Section 22.2. These temperature and heat flux distributions, along with the axial pressure distribution calculated by PLTEMP/ANL and copied into the spreadsheet, are used by the spreadsheet in the Bernath correlation shown below.

$$q_c = 5.679 \times 10^{-6} \underbrace{\left(\frac{10890\,D}{D + \xi/\pi} + \frac{48\,V}{D^{0.6}} \right)}_{\text{Factor 1}} \underbrace{\left\{ 57 \ln(P) - \frac{54\,P}{P+15} - \frac{V}{4} - T_b \right\}}_{\text{Factor 2}}$$

<---------- Factor 1 ----------> <------ Factor 2 ------>

where

q_c	= Critical heat flux, MW/m^2
V	= Coolant velocity, ft/s
P	= Coolant pressure, psia
D	= Hydraulic diameter, ft
ξ	= Heated perimeter, ft
T_b	= Local bulk coolant temperature (at axial segment exit), °C

The PLTEMP/ANL-calculated CHF values calculated by the DSM and by the HBM are copied to the spreadsheet for comparison and plotting purposes. Problem 38 has two fuel assemblies each consisting of two fuel plates and three coolant channels. Each fuel plate is divided into three longitudinal stripes and correspondingly each coolant channel is divided into three sub-channels. Only the second plate stripe is fueled and has a heat source, and therefore the spreadsheet calculates, compares, and plots the CHF values for the second plate stripe only. The spreadsheet uses the coolant temperature at the segment exit, and finds CHF at each axial segment exit.

In calculating CHF by the HBM, all 40 equations (for 10 axial segments × 4 plate surfaces) are solved by minimizing a single quantity using the Excel spreadsheet built-in SOLVER capability. This quantity is the sum of squares of the difference between each segment's heat flux assumed at the beginning of an iteration and the value of CHF calculated using the correlation.

Comparison of CHF Values Calculated by PLTEMP/ANL and Spreadsheet: Table 24.1 shows a comparison of CHF values calculated by the DSM using the Bernath correlation for the standard Problem 38. The mean absolute difference in CHF over all 40 axial segments is 0.161%. Table 24.2 shows a similar comparison of CHF values calculated by the HBM using the Bernath correlation. Figures 24.1 and 24.2 show the same comparison graphically for fuel assemblies 1 and 2, respectively. A detailed comparison of all thermal-hydraulic parameters required to calculate the Bernath CHF by the HBM for one axial segment (segment 10) is given in Table 24.3. The

maximum absolute difference in CHF over all 40 axial segments is 0.185%. There is a good agreement in all these comparisons. This comparison provides a verification of the Bernath CHF correlation as implemented in the PLTEMP/ANL code.

24.3 Verification of Labuntsov Critical Heat Flux Correlation

The Labuntsov CHF correlation is verified here by comparing the PLTEMP/ANL-calculated CHF values with those obtained by an Excel spreadsheet developed to calculate CHF by the DSM and the HBM using the Labuntsov correlation. The comparison is done for the standard Problem 38 described above in Section 22.3.

Spreadsheet to Calculate CHF Using the Labuntsov Correlation : The spreadsheet first calculates the distributions of coolant, cladding, and fuel temperatures and cladding surface heat flux as described in Section 22.2. These temperature and heat flux distributions, along with the axial pressure distribution calculated by PLTEMP/ANL and copied into the spreadsheet, are used by the spreadsheet in the Labuntsov correlation shown below.

$$q_c = 1.454\ \theta(P)[1+2.5\ U^2 / \theta(P)]^{1/4}\ [1 + (15.1/ P^{1/2})\ (Cp\ \Delta T_{sub} / \lambda)],$$

where

$\theta(P)$ = $0.99531\ P^{1/3}(1 - P/P_c)^{4/3}$

C_p = Specific heat of the coolant, kJ/kg-°C

λ = Latent heat of vaporization, kJ/kg

= An average value of 1959.35 kJ/kg, over the pressure range 3.6 to 3.8 bar in the problem, was obtained from PLTEMP/ANL output and used in the spreadsheet.

P = Pressure at the axial location of CHF, bar

P_c = Critical pressure of the coolant, bar

= 221.14 bar is hard-coded in PLTEMP/ANL and used in the spreadsheet.

ΔT_{sub} = Coolant subcooling at the axial location of CHF (i.e., the heated length exit), °C

U = Coolant velocity, m/s

The PLTEMP/ANL-calculated CHF values calculated by the DSM and by the HBM are copied to the spreadsheet for comparison and plotting purposes. Problem 38 was analyzed with a spreadsheet in an analogous manner to that employed for the verification of the Bernath CHF correlation in the previous section.

Comparison of CHF Values Calculated by PLTEMP/ANL and Spreadsheet: Table 24.4 shows a comparison of CHF values calculated by the DSM using the Labuntsov correlation for the standard Problem 38. The mean absolute difference in CHF over all 40 axial segments is 0.181%. Table 24.5 shows a similar comparison of CHF values calculated by the HBM using the Labuntsov correlation. Figures 24.3 and 24.4 show the same comparison graphically for fuel assemblies 1 and 2, respectively. The maximum absolute difference in CHF over all 40 axial segments is 0.211%. There is a good agreement in all these comparisons. This comparison provides a verification of the Labuntsov CHF correlation as implemented in the PLTEMP/ANL code.

24.4 REFERENCES

1. G. P. Celata, “On the Application Method of Critical Heat Flux Correlations,” Letter to the Editor, Nuclear Engineering and Design, Vol. 163, pp. 241-242, (1996).
2. P. Hejzlar and N. E. Todreas, “Consideration of Critical Hat Flux Margin Prediction by Subcooled or Low Quality Critical Heat Flux Correlations,” Nuclear Engineering and Design, Vol. 163, pp. 215-223 (June 1996).

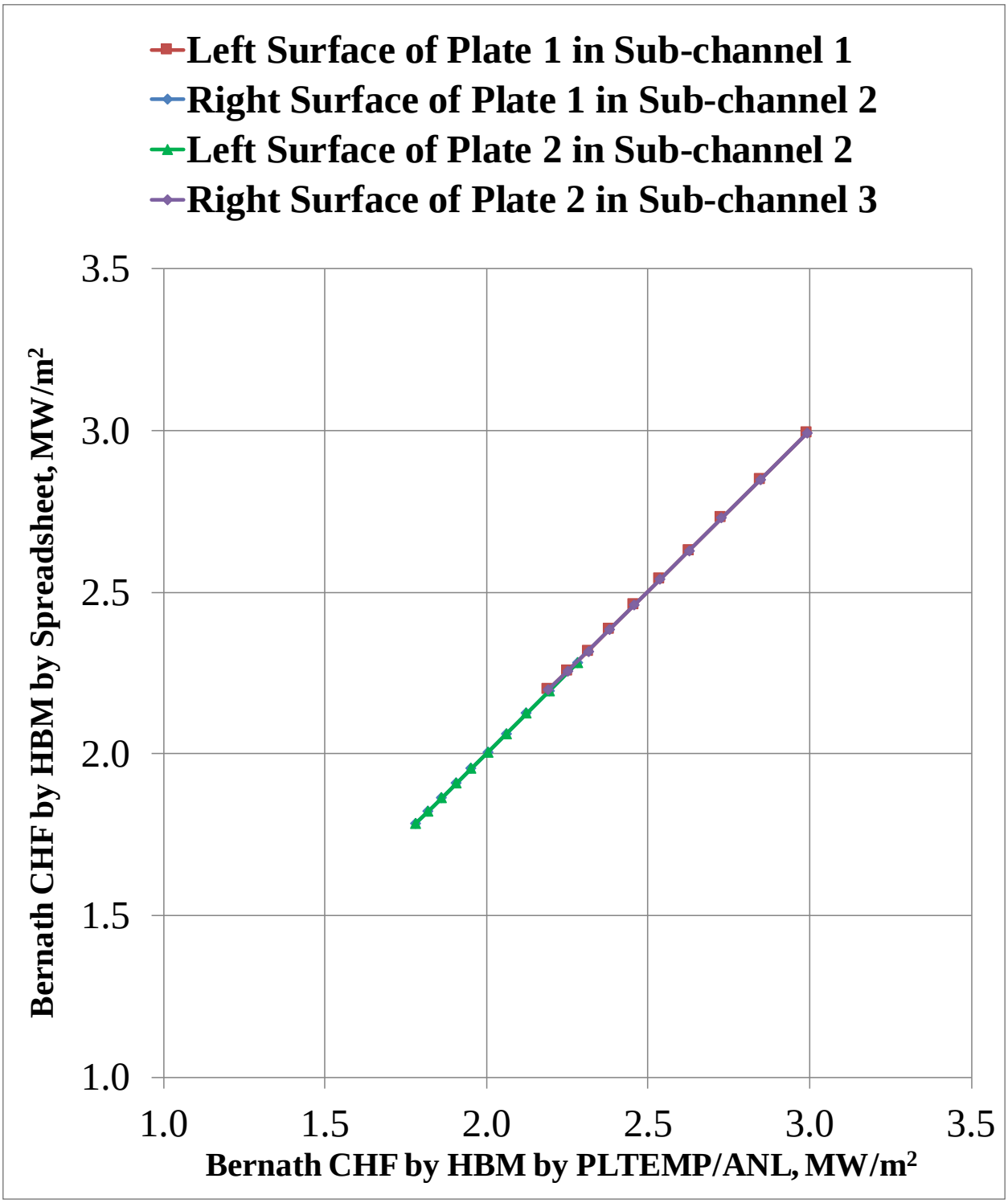

Figure 24.1 Comparison between PLTEMP/ANL- and Spreadsheet-Calculated Critical Heat Flux by Heat Balance Method using the Bernath Correlation for Fuel Assembly 1 of Problem 38

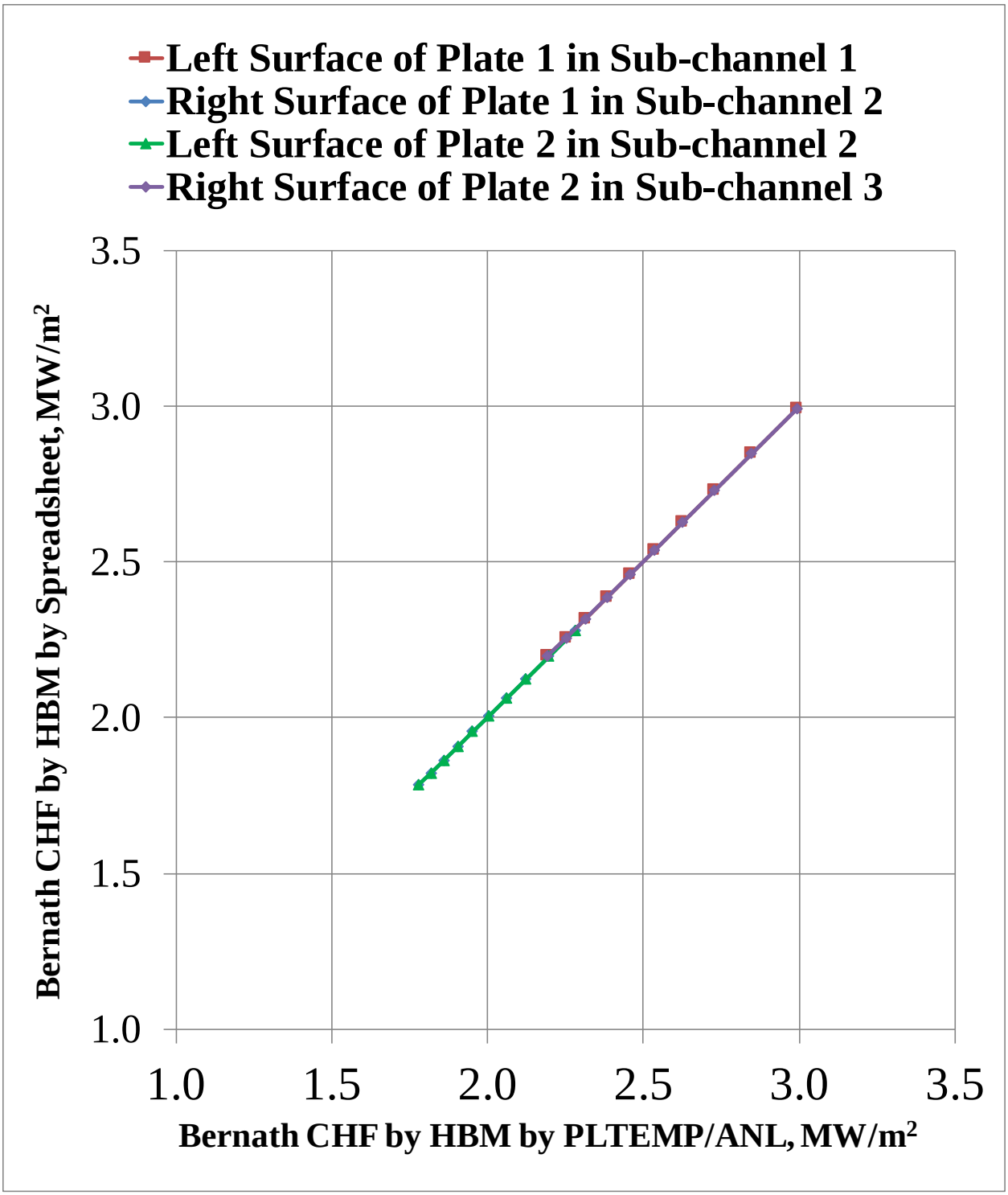

Figure 24.2 Comparison between PLTEMP/ANL- and Spreadsheet-Calculated Critical Heat Flux by Heat Balance Method using the Bernath Correlation for Fuel Assembly 2 of Problem 38

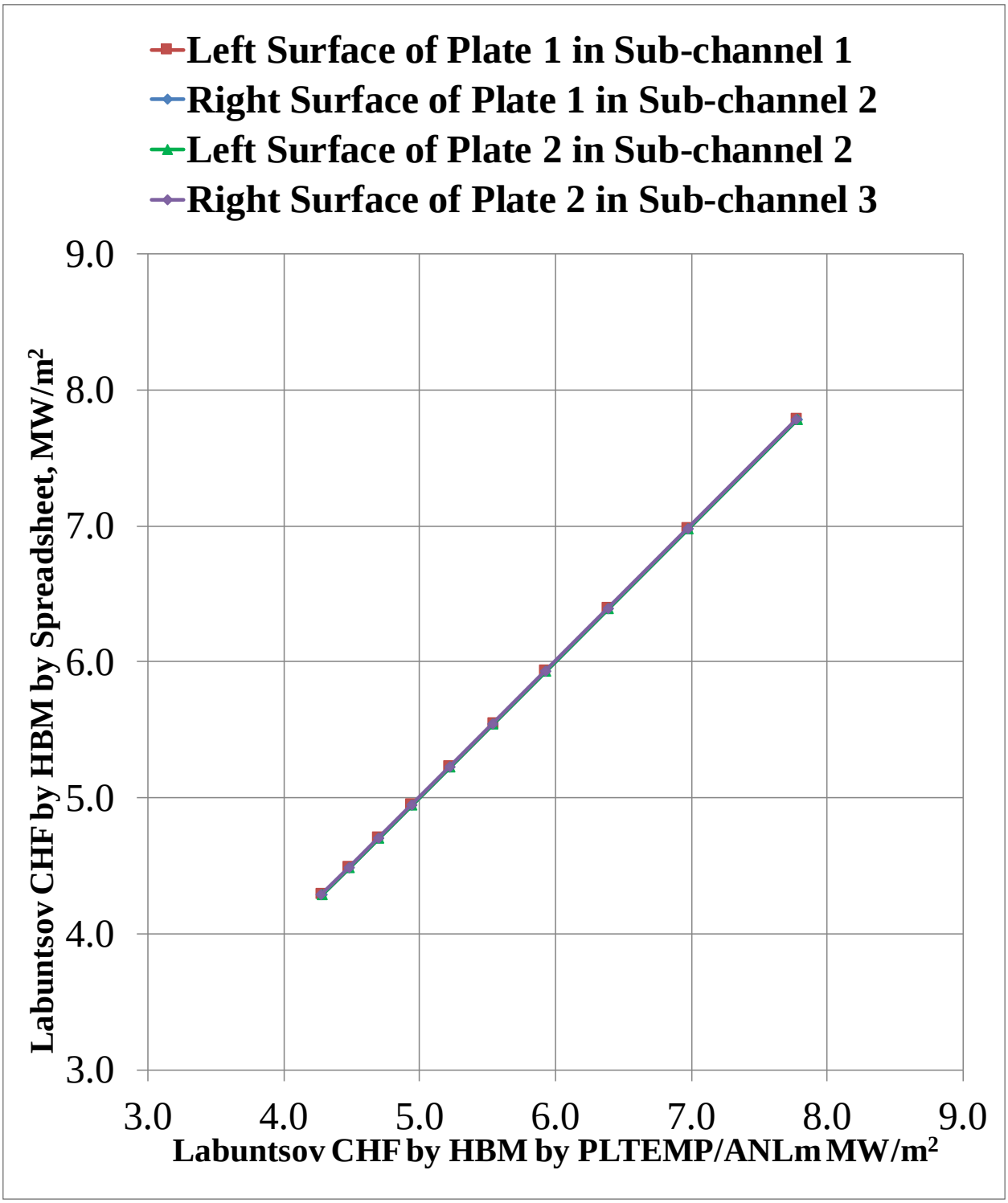

Figure 24.3 Comparison between PLTEMP/ANL- and Spreadsheet-Calculated Critical Heat Flux by Direct Substitution Method using the Labuntsov Correlation for Fuel Assembly 2 of Problem 38

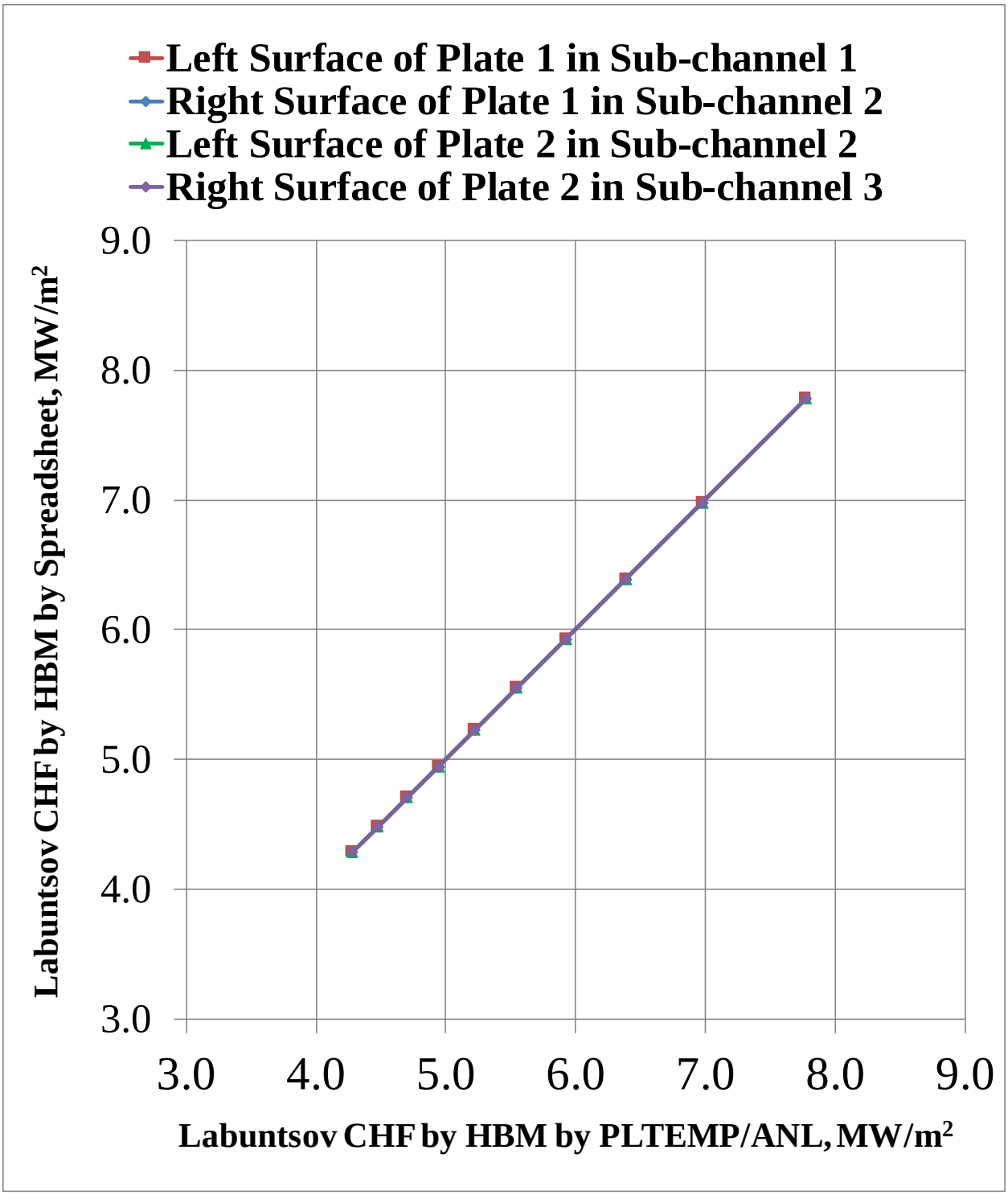

Figure 24.4 Comparison between PLTEMP/ANL- and Spreadsheet-Calculated Critical Heat Flux by Direct Substitution Method using the Labuntsov Correlation for Fuel Assembly 2 of Problem 38

Table 24.1 Comparison between PLTEMP/ANL and Spreadsheet of CHF by Direct Substitution Method Using the Bernath Correlation for Problem 38

D = Hydraulic diameter, ft ξ = Heated perimeter, ft V = Coolant velocity, ft/s P = Coolant pressure, psia

Axial Seg.	D	ξ	V	P	CHF by DSM by Bernath Correlation by Spreadsheet, MW/m²				CHF by DSM by Bernath Correlation by PLTEMP/ANL, MW/m²				% Absolute Error in CHF by Direct Substitution Method			
	ft	ft	ft/s	psia	Plate 1	Plate 1	Plate 2	Plate 2	Plate 1	Plate 1	Plate 2	Plate 2	Plate 1	Plate 1	Plate 2	Plate 2
					Left Surf	Right Surf	Left Surf	Right Surf	Left Surf	Right Surf	Left Surf	Right Surf	Left Surf	Right Surf	Left Surf	Right Surf
Fuel Assembly 1																
1	0.03937	0.5249	4.967	54.970	3.160	2.375	2.375	3.160	3.159	2.374	2.374	3.159	0.030	0.023	0.023	0.030
2	0.03937	0.5249	4.969	54.680	3.134	2.355	2.355	3.134	3.133	2.354	2.354	3.133	0.037	0.055	0.055	0.037
3	0.03937	0.5249	4.971	54.390	3.105	2.334	2.334	3.105	3.103	2.332	2.332	3.103	0.070	0.072	0.072	0.070
4	0.03937	0.5249	4.974	54.100	3.073	2.310	2.310	3.073	3.071	2.307	2.307	3.071	0.067	0.116	0.116	0.067
5	0.03937	0.5249	4.977	53.810	3.038	2.283	2.283	3.038	3.035	2.280	2.280	3.035	0.090	0.146	0.146	0.090
6	0.03937	0.5249	4.980	53.520	2.999	2.255	2.255	2.999	2.995	2.251	2.251	2.995	0.141	0.159	0.159	0.141
7	0.03937	0.5249	4.983	53.230	2.958	2.223	2.223	2.958	2.953	2.219	2.219	2.953	0.153	0.202	0.202	0.153
8	0.03937	0.5249	4.987	52.940	2.913	2.190	2.190	2.913	2.907	2.184	2.184	2.907	0.193	0.274	0.274	0.193
9	0.03937	0.5249	4.992	52.650	2.865	2.154	2.154	2.865	2.858	2.147	2.147	2.858	0.228	0.330	0.330	0.228
10	0.03937	0.5249	4.996	52.359	2.813	2.116	2.116	2.813	2.803	2.106	2.106	2.802	0.364	0.465	0.465	0.400
Fuel Assembly 2																
1	0.03937	0.5249	4.967	54.970	3.160	2.375	2.375	3.160	3.159	2.374	2.374	3.159	0.030	0.023	0.023	0.030
2	0.03937	0.5249	4.969	54.680	3.134	2.355	2.355	3.134	3.133	2.354	2.354	3.133	0.037	0.055	0.055	0.037
3	0.03937	0.5249	4.971	54.390	3.105	2.334	2.334	3.105	3.103	2.332	2.332	3.103	0.070	0.072	0.072	0.070
4	0.03937	0.5249	4.974	54.100	3.073	2.310	2.310	3.073	3.071	2.307	2.307	3.071	0.067	0.116	0.116	0.067
5	0.03937	0.5249	4.977	53.810	3.038	2.283	2.283	3.038	3.035	2.280	2.280	3.035	0.090	0.146	0.146	0.090
6	0.03937	0.5249	4.980	53.520	2.999	2.255	2.255	2.999	2.995	2.251	2.251	2.995	0.141	0.159	0.159	0.141
7	0.03937	0.5249	4.983	53.230	2.958	2.223	2.223	2.958	2.953	2.219	2.219	2.953	0.153	0.202	0.202	0.153
8	0.03937	0.5249	4.987	52.940	2.913	2.190	2.190	2.913	2.907	2.184	2.184	2.907	0.193	0.274	0.274	0.193
9	0.03937	0.5249	4.992	52.650	2.865	2.154	2.154	2.865	2.858	2.147	2.147	2.858	0.228	0.330	0.330	0.228
10	0.03937	0.5249	4.996	52.359	2.813	2.116	2.116	2.813	2.803	2.106	2.106	2.802	0.364	0.465	0.465	0.400

Mean Absolute Difference in CHF = 0.161 %

Table 24.2 Comparison between PLTEMP/ANL and Spreadsheet of CHF by Heat Balance Method Using the Bernath Correlation for Problem 38

Fuel Assembly 1																
Axial Seg.	Coolant temp. at axial segment exit, using the last assumed CHF during HBM iteration, ºC				CHF by HBM by Bernath Correlation by Spreadsheet, MW/m^2				CHF by HBM by Bernath Correlation by PLTEMP/ANL, MW/m^2				% Absolute Error in CHF by Heat Balance Method			
	Plate 1	Plate 1	Plate 2	Plate 2	Plate 1	Plate 1	Plate 2	Plate 2	Plate 1	Plate 1	Plate 2	Plate 2	Plate 1	Plate 1	Plate 2	Plate 2
	Left Surf	Right Surf	Left Surf	Right Surf	Left Surf	Right Surf	Left Surf	Right Surf	Left Surf	Right Surf	Left Surf	Right Surf	Left Surf	Right Surf	Left Surf	Right Surf
1	43.708	41.640	41.640	43.708	2.993	2.282	2.282	2.993	2.992	2.281	2.281	2.992	0.027	0.041	0.041	0.027
2	50.301	46.799	46.799	50.301	2.848	2.196	2.196	2.848	2.847	2.195	2.195	2.847	0.034	0.050	0.050	0.034
3	55.655	51.076	51.076	55.655	2.729	2.124	2.124	2.729	2.728	2.123	2.123	2.728	0.052	0.063	0.063	0.052
4	60.202	54.772	54.772	60.202	2.628	2.062	2.062	2.628	2.626	2.060	2.060	2.626	0.077	0.090	0.090	0.077
5	64.179	58.056	58.056	64.179	2.539	2.006	2.006	2.539	2.537	2.004	2.004	2.537	0.068	0.100	0.100	0.068
6	67.731	61.030	61.030	67.731	2.458	1.955	1.955	2.458	2.456	1.952	1.952	2.456	0.101	0.160	0.160	0.101
7	70.950	63.759	63.759	70.950	2.385	1.908	1.908	2.385	2.382	1.905	1.905	2.382	0.138	0.167	0.167	0.138
8	73.900	66.291	66.291	73.900	2.318	1.864	1.864	2.318	2.315	1.861	1.861	2.314	0.123	0.184	0.184	0.166
9	76.626	68.656	68.656	76.626	2.255	1.823	1.823	2.255	2.251	1.819	1.819	2.251	0.185	0.240	0.240	0.185
10	79.161	70.879	70.879	79.161	2.197	1.785	1.785	2.197	2.190	1.778	1.778	2.190	0.300	0.371	0.371	0.300
Fuel Assembly 2																
1	43.708	41.640	41.640	43.708	2.993	2.282	2.282	2.993	2.992	2.281	2.281	2.992	0.027	0.041	0.041	0.027
2	50.301	46.799	46.799	50.301	2.848	2.196	2.196	2.848	2.847	2.195	2.195	2.847	0.034	0.050	0.050	0.034
3	55.655	51.076	51.076	55.655	2.729	2.124	2.124	2.729	2.728	2.123	2.123	2.728	0.052	0.063	0.063	0.052
4	60.202	54.772	54.772	60.202	2.628	2.062	2.062	2.628	2.626	2.060	2.060	2.626	0.077	0.090	0.090	0.077
5	64.179	58.056	58.056	64.179	2.539	2.006	2.006	2.539	2.537	2.004	2.004	2.537	0.068	0.100	0.100	0.068
6	67.731	61.030	61.030	67.731	2.458	1.955	1.955	2.458	2.456	1.952	1.952	2.456	0.101	0.160	0.160	0.101
7	70.950	63.759	63.759	70.950	2.385	1.908	1.908	2.385	2.382	1.905	1.905	2.382	0.138	0.167	0.167	0.138
8	73.900	66.291	66.291	73.900	2.318	1.864	1.864	2.318	2.315	1.861	1.861	2.314	0.123	0.184	0.184	0.166
9	76.626	68.656	68.656	76.626	2.255	1.823	1.823	2.255	2.251	1.819	1.819	2.251	0.185	0.240	0.240	0.185
10	79.161	70.879	70.879	79.161	2.197	1.785	1.785	2.197	2.190	1.778	1.778	2.190	0.300	0.371	0.371	0.300

Maximum Absolute Difference in CHF = 0.371 %

Table 24.3 Detailed Comparison between PLTEMP/ANL and Spreadsheet of CHF by Heat Balance Method Using the Bernath Correlation For Axial Segment 10, Problem 38, Fuel Assembly 1, Plate 1 Left Side

Serial No.	Quantity	PLTEMP/ANL	Spreadsheet
1	Heated perimeter, ft	0.5249	0.5249
2	Coolant velocity, ft/s	4.9646	4.9964
3	Pressure, psia	52.213	52.3594
4	Operating heat flux in the axial segment, MW/m^2	0.7552	0.7552
5	Operating bulk temperature at segment exit, T_b, ºC	50.183	50.183
6	Segment heat flux assumed during iteration, MW/m^2	2.1902	2.1886
7	Adjusted (during iteration) bulk temperature at segment exit, T_b, ºC	79.032	79.161
8	CHF from correlation, MW/m^2	2.1904	2.197
9	Factor 1 of the correlation	0.021218	0.021279
10	Factor 2 of the correlation except the term T_b	182.264	182.389

Table 24.4 Comparison between PLTEMP/ANL and Spreadsheet of CHF by Direct Substitution Method Using the Labuntsov Correlation for Problem 38

λ = Latent heat of vaporization, jK/kg U = Coolant velocity, m/s P_c = Critical pressure, bar P = Coolant pressure, bar

Axial Seg.	λ	U	P_c	P	CHF by DSM by Labuntsov Correlation by Spreadsheet, MW/m²				CHF by DSM by Labuntsov Correlation by PLTEMP/ANL, MW/m²				% Absolute Error in CHF by Direct Substitution Method			
	kJ/kg	m/s	bar	bar	Plate 1	Plate 1	Plate 2	Plate 2	Plate 1	Plate 1	Plate 2	Plate 2	Plate 1	Plate 1	Plate 2	Plate 2
					Left Surf	Right Surf	Left Surf	Right Surf	Left Surf	Right Surf	Left Surf	Right Surf	Left Surf	Right Surf	Left Surf	Right Surf
Fuel Assembly 1																
1	1959.35	1.5140	216.71	3.790	8.939	8.939	8.939	8.939	8.941	8.941	8.941	8.941	0.013	0.013	0.013	0.013
2	1959.35	1.5146	216.71	3.770	8.880	8.880	8.880	8.880	8.885	8.885	8.885	8.885	0.025	0.025	0.025	0.025
3	1959.35	1.5153	216.71	3.750	8.812	8.812	8.812	8.812	8.821	8.821	8.821	8.821	0.066	0.066	0.066	0.066
4	1959.35	1.5160	216.71	3.730	8.736	8.736	8.736	8.736	8.749	8.749	8.749	8.749	0.112	0.112	0.112	0.112
5	1959.35	1.5169	216.71	3.710	8.652	8.652	8.652	8.652	8.669	8.669	8.669	8.669	0.161	0.161	0.161	0.161
6	1959.35	1.5178	216.71	3.690	8.560	8.560	8.560	8.560	8.580	8.580	8.580	8.580	0.204	0.204	0.204	0.204
7	1959.35	1.5189	216.71	3.670	8.459	8.459	8.459	8.459	8.483	8.483	8.483	8.483	0.250	0.250	0.250	0.250
8	1959.35	1.5201	216.71	3.650	8.350	8.350	8.350	8.350	8.377	8.377	8.377	8.377	0.289	0.289	0.289	0.289
9	1959.35	1.5214	216.71	3.630	8.233	8.233	8.233	8.233	8.263	8.263	8.263	8.263	0.331	0.331	0.331	0.331
10	1959.35	1.5229	216.71	3.610	8.107	8.107	8.107	8.107	8.139	8.139	8.139	8.139	0.353	0.353	0.353	0.353
Fuel Assembly 2																
1	1959.35	1.5140	216.71	3.790	8.939	8.939	8.939	8.939	8.941	8.941	8.941	8.941	0.013	0.013	0.013	0.013
2	1959.35	1.5146	216.71	3.770	8.880	8.880	8.880	8.880	8.885	8.885	8.885	8.885	0.025	0.025	0.025	0.025
3	1959.35	1.5153	216.71	3.750	8.812	8.812	8.812	8.812	8.821	8.821	8.821	8.821	0.066	0.066	0.066	0.066
4	1959.35	1.5160	216.71	3.730	8.736	8.736	8.736	8.736	8.749	8.749	8.749	8.749	0.112	0.112	0.112	0.112
5	1959.35	1.5169	216.71	3.710	8.652	8.652	8.652	8.652	8.669	8.669	8.669	8.669	0.161	0.161	0.161	0.161
6	1959.35	1.5178	216.71	3.690	8.560	8.560	8.560	8.560	8.580	8.580	8.580	8.580	0.204	0.204	0.204	0.204
7	1959.35	1.5189	216.71	3.670	8.459	8.459	8.459	8.459	8.483	8.483	8.483	8.483	0.250	0.250	0.250	0.250
8	1959.35	1.5201	216.71	3.650	8.350	8.350	8.350	8.350	8.377	8.377	8.377	8.377	0.289	0.289	0.289	0.289
9	1959.35	1.5214	216.71	3.630	8.233	8.233	8.233	8.233	8.263	8.263	8.263	8.263	0.331	0.331	0.331	0.331
10	1959.35	1.5229	216.71	3.610	8.107	8.107	8.107	8.107	8.139	8.139	8.139	8.139	0.353	0.353	0.353	0.353

Mean Absolute Difference in CHF = 0.181 %

Table 24.5 Comparison between PLTEMP/ANL and Spreadsheet of CHF by Heat Balance Method Using the Labuntsov Correlation for Problem 38

Fuel Assembly 1																
Axial Seg.	Coolant temp. at axial segment exit, using the last assumed CHF during HBM iteration, ºC				CHF by HBM by Labuntsov Correlation by Spreadsheet, MW/m^2				CHF by HBM by Labuntsov Correlation by PLTEMP/ANL, MW/m^2				% Absolute Error in CHF by Heat Balance Method			
	Plate 1	Plate 1	Plate 2	Plate 2	Plate 1	Plate 1	Plate 2	Plate 2	Plate 1	Plate 1	Plate 2	Plate 2	Plate 1	Plate 1	Plate 2	Plate 2
	Left Surf	Right Surf	Left Surf	Right Surf	Left Surf	Right Surf	Left Surf	Right Surf	Left Surf	Right Surf	Left Surf	Right Surf	Left Surf	Right Surf	Left Surf	Right Surf
1	57.635	57.635	57.635	57.635	7.779	7.779	7.779	7.779	7.779	7.779	7.779	7.779	0.029	0.029	0.029	0.042
2	72.496	72.496	72.496	72.496	6.979	6.979	6.979	6.979	6.979	6.979	6.979	6.979	0.033	0.033	0.033	0.047
3	83.361	83.361	83.361	83.361	6.391	6.391	6.391	6.391	6.390	6.390	6.390	6.389	0.041	0.041	0.041	0.056
4	91.844	91.844	91.844	91.844	5.928	5.928	5.928	5.928	5.927	5.927	5.927	5.926	0.045	0.045	0.045	0.062
5	98.760	98.760	98.760	98.760	5.547	5.547	5.547	5.547	5.546	5.546	5.546	5.545	0.044	0.062	0.062	0.062
6	104.570	104.570	104.570	104.570	5.226	5.226	5.226	5.226	5.224	5.224	5.224	5.223	0.048	0.067	0.067	0.067
7	109.559	109.559	109.559	109.559	4.947	4.947	4.947	4.947	4.945	4.945	4.945	4.944	0.059	0.080	0.080	0.080
8	113.911	113.911	113.911	113.911	4.702	4.702	4.702	4.702	4.699	4.699	4.699	4.698	0.082	0.082	0.082	0.104
9	117.757	117.757	117.757	117.757	4.484	4.484	4.484	4.484	4.480	4.480	4.480	4.480	0.078	0.101	0.101	0.101
10	121.189	121.189	121.189	121.189	4.287	4.287	4.287	4.287	4.280	4.280	4.280	4.279	0.164	0.187	0.187	0.211
Fuel Assembly 2																
1	57.635	57.635	57.635	57.635	7.779	7.779	7.779	7.779	7.780	7.779	7.779	7.779	0.029	0.029	0.029	0.042
2	72.497	72.497	72.497	72.497	6.979	6.979	6.979	6.979	6.979	6.979	6.979	6.978	0.033	0.033	0.033	0.047
3	83.361	83.361	83.361	83.361	6.391	6.391	6.391	6.391	6.390	6.389	6.390	6.389	0.041	0.041	0.041	0.056
4	91.844	91.844	91.844	91.844	5.928	5.928	5.928	5.928	5.927	5.926	5.926	5.926	0.045	0.045	0.045	0.062
5	98.760	98.760	98.760	98.760	5.547	5.547	5.547	5.547	5.546	5.545	5.546	5.545	0.044	0.062	0.062	0.062
6	104.571	104.570	104.571	104.570	5.226	5.226	5.226	5.226	5.224	5.223	5.223	5.223	0.048	0.067	0.067	0.067
7	109.559	109.559	109.559	109.559	4.947	4.947	4.947	4.947	4.945	4.944	4.944	4.944	0.059	0.080	0.080	0.080
8	113.912	113.912	113.912	113.912	4.702	4.702	4.702	4.702	4.699	4.699	4.699	4.698	0.082	0.082	0.082	0.104
9	117.758	117.758	117.758	117.758	4.484	4.484	4.484	4.484	4.481	4.480	4.480	4.479	0.078	0.101	0.101	0.101
10	121.189	121.189	121.189	121.189	4.287	4.287	4.287	4.287	4.280	4.279	4.280	4.279	0.164	0.187	0.187	0.211

Maximum Absolute Difference in CHF = 0.211 %

25 Verification of Newly Implemented Hot Channel Factors for Coolant Velocity and Channel Heated Diameter

The verification work reported here was done in April 2018. Two hot channel factors (HCFs), not used previously in thermal-hydraulic analysis of research reactors, were implemented in the PLTEMP/ANL code. These HCFs may be used as a refinement of the thermal-hydraulic analysis of *specific* research reactors. The first factor is a hot channel factor on channel coolant velocity, and also a hot channel factor on mass flux because mass flux is the product of coolant velocity and density, and the density is nearly constant. This factor is intended to appropriately add a small amount of conservatism to the calculation of critical heat flux (CHF). The inclusion of this factor will not affect the predicted allowed power of a reactor limited by flow instability rather than CHF.

The thermal-hydraulic analysis of *specific* research reactors by PLTEMP/ANL employs reduced coolant channel flow rates to account for reduced channel thicknesses due to dimensional tolerances and fuel burnup. In addition to accounting for the coolant channel flow rates, it is appropriate to use the reduced channel thicknesses (rather than the nominal channel thicknesses) in calculating the channel heated diameters used in the correlations used to predict margins to flow instability and CHF. The second new factor accomplishes this and thereby eliminates small amounts of unnecessary conservatism in the predictions of margins to flow instability and CHF. This was not done previously in thermal-hydraulic analyses by PLTEMP/ANL.

For purposes of verification, the input file for the limiting Low-Enriched Uranium (CD-35) PLTEMP/ANL flow instability case for the MURR reactor [1] was revised and rerun with the revised PLTEMP/ANL code, whose executable name is “pltempv42_r86_180215.x”. This is an internal patch version of the code utilized in the verification.

The particular case studied for this verification is the entire core for the proposed MURR CD-35 (LEU) core state 8A1. The reactor inlet temperature, flow rate, and pressurizer pressure are 145 °F, 3300 gpm, and 75 psia, respectively.

The key files used in the verification are listed in Table 25.1. The only revisions to the main code input file were to include a value of each of the two new factors for each of the 192 coolant channels in the model, as explained in the Step 1 Verification section, below. The replacement input file is File No. 1 in Table 25.1. File No. 2 is a PLTEMP/ANL input that describes the power distribution within the core and is unchanged from the original analysis. File No. 3 is the new PLTEMP/ANL output file.

Verification was accomplished in the following three steps:

1. Verify that all six hot channel and heated diameter factors for each channel/plate in the entire core model has been read by the code correctly.
2. Manually, with the aid of a spreadsheet, verify that the flow instability ratio (FIR) of each coolant channels in the entire core model has been calculated correctly.
3. Use the existing Checker program (spreadsheet) to verify CHF and CHF ratio (CHFR) in the flow-instability-limiting channel of the core and also in the CHF-limiting channel of the core.

The MURR reactor has eight fuel assemblies of the same manufactured design. Each assembly has 23 curved fuel plates and, when in the reactor, 24 coolant channels. The model predicts a FIR for each of the 192 (i.e., 8 × 24) coolant channels.

25.1 Step 1 - Verification of Correct Reading of Input Data for the Two New HCFs

For each of the 192 coolant channels in the core, the PLTEMP/ANL input file has a line of hot channel factor data in the 306C series of input lines. A sample line after the code modification is as follows:

```
  1     2.253      1.63      1.53      1.32      0.770     0.721     0306C m2p (  0 MWd)
```

The same sample line before the modification is as follows:

```
  1     2.253      1.63      1.53      1.32                          0306C m2p (  0 MWd)
```

The "0306C m2p (0 MWd)" at the end of line is ignored by the code, but provides information that is helpful to the user. These lines are grouped into eight groups of 24 to correspond to the eight assemblies. The integer at the beginning of the line is the channel number and is a value between 1 and 24, as appropriate. The first floating-point factor on each line is the hot channel factor on bulk coolant temperature for the channel. The next floating point numbers are hot channel factors that correspond to the fuel plate that is located immediately after that channel (on the curved channel's convex side). The 24th line of each group does not have these three plate hot channel factors because there is no fuel plate after the last (24th) channel. After the code modification, two new floating-point factors were added at the end of each line to correspond to the heated diameter factor and the velocity factor, respectively. For the 24th line of each group, the FORTRAN Format statement adds 36 blank spaces between the first floating-point factor and the two new ones so that all of the new factors on all 192 lines are aligned the same.

There is complete compatibility with previous versions of the code since previous versions of the code will ignore the two added factors on each line. Also, when old input without the two added factors is used with the revised code, blank input is treated as has having a value of zero and the PLTEMP/ANL code logic converts these values of zero to factors of 1.0.

The PLTEMP/ANL code writes out the values for each group of 24 lines one line at a time. The 24 lines corresponding to the first fuel assembly starts on line 97 of the output. The group for the second assembly starts 137 lines after the start of the first and each succeeding group starts 137 lines after its predecessor. The code reads the data in each line of input into the code and prints it out. It does this as data, not as merely character strings. Thus, this output is not a result of echoing each line of input as a long character string without regard to the numerical values in the string. Although the code does not label the values, all of them for each fuel assembly are in one large block of output, with one integer and six floating-point values for each of the 24 channels on a line. The last line of each group has three values of 0.00000E+00 to correspond to the 36 blank spaces needed for alignment.

Comparison of the input data and PLTEMP/ANL output file clearly showed that all of the factors and channel numbers on the eight sets of 24 lines were correctly interpreted by the code. In all instances, both new factors are considerably less than 1.000. Each value is between 0.671 and 0.914. It is important for verification purposed that they not be close to the default value of 1.000.

25.2 Step 2 - Verification of Correct Calculation of Flow Instability Ratio for Each Channel

The Whittle and Forgan relationship for flow instability is:

$$\frac{T_{allowed} - T_{inlet}}{T_{sat} - T_{inlet}} = \frac{1}{1+\eta \frac{D_h}{L_h}} \qquad (1)$$

where $T_{allowed}$ is the bulk coolant exit temperature at which flow instability is predicted to be initiated; T_{sat} is the coolant saturation temperature at the channel exit; T_{inlet} is the coolant inlet temperature; D_h and L_h are the heated diameter (4 times the flow area divided by the heated perimeter) and heated length of the channel, respectively. η is an adjustable parameter, for which a value of 32.5 is used.

By definition, the flow instability ratio, FIR, is:

$$FIR = \frac{T_{allowed} - T_{inlet}}{T_{outlet} - T_{inlet}} \qquad (2)$$

where T_{outlet} is the channel bulk coolant outlet temperature.

Combining equations (1) and (2), one obtains:

$$FIR = \frac{T_{sat} - T_{inlet}}{T_{outlet} - T_{inlet}} \frac{1}{1+\eta \frac{D_h}{L_h}} \qquad (3)$$

Equation (3) was used to manually calculate FIR for all 192 coolant channels.

The code output indicates the channel outlet pressure for the core is 3.88650 bar (56.37 psia). The NIST steam tables indicate that the saturation temperature for this pressure, T_{sat}, is 142.6 °C.

The inlet temperature, T_{inlet}, is 145 °F, which equals 62.778 °C.

As defined above, the heated diameter is 4 times the ratio of the flow area to the heated perimeter of the coolant channel. Values for flow area (m^2) and heated perimeter (m) are the first and fourth entries, respectively, on the 307 series of input cards. In the model, these vary from channel to channel within a fuel assembly, but do not vary from assembly to assembly. However, in the analysis, these values of heated diameter are multiplied by the new heated diameter factors, which are entered for each channel in the core. These factors, all being less than 1, decrease the value of D_h used in equation (3) and thereby increase the values of FIR being calculated.

The 192 values of new heated diameter factors were copied to a spreadsheet from the 306C series of lines in the input file.

The heated length of all 192 channels is 0.6096 m (24 inches).

Each of the 192 values of flow instability ratio calculated by the spreadsheet was compared with its counterpart from the PLTEMP/ANL code output. In each instance, the value calculated by the spreadsheet was slightly greater than the one obtained from the PLTEMP/ANL code output, but by no more than 0.014%. The detailed results of comparison are given in an Excel spreadsheet, the 8th. file of Table 25.1 (filename Ticket_15_verification_032218.xlsx). Hence, all 192 PLTEMP/ANL output values of flow instability ratio were calculated correctly by the code.

25.3 Step 3 - Verification of CHF and CHFR by the Checker Program for the Limiting FIR Channel and the Limiting CHF Channel

The focus of this phase of the verification is the calculation of CHF and CHF ratio with the Extended Groeneveld CHF correlation. The new hot channel factor on velocity (or mass flux) is included in this analysis. That is the reason for the first part of the code modification. In addition, the second new factor in this work affects the heated diameter in a manner that is beneficial to CHF and CHF ratio.

The Checker program is a spreadsheet in which many thermal-hydraulic quantities within a single coolant channel, including values of CHF and CHF ratio at all 24 axial levels in the model, are calculated and compared with their counterparts in the PLTEMP/ANL output. In this analysis only the fuel plate or plates that bound the channel are included. The fraction of power that each fuel plate contributes to the channel at each of its 24 axial levels is taken from the PLTEMP/ANL code output and is not verified. These values are typically close to 0.500, which corresponds to half of the fuel plate power exiting each side of the plate. Independent verification of these factors is beyond the scope of the Checker program. Similarly, the channel flow rate is taken from the PLTEMP/ANL code output and is not verified.

The Checker program was applied twice – first to the channel having the minimum FIR, which is 1.00 in this instance, and next to the channel having the smallest CHF ratio. The analysis of these two channels with the Checker program verifies CHF ratio calculations at one surface and 24 axial levels of three different fuel plates in the MURR PLTEMP/ANL core model and CHF at 24 levels of two coolant channels. Hence, 72 values of CHF ratio and 48 values of CHR were verified. Many other quantities were also checked. Each Checker program worksheet (or tab) is electronically (or digitally) linked to the “G2006CHF_table” worksheet, which contains all of the data for the Groeneveld 2006 CHF Look-Up Table. When a Checker program worksheet is copied to another Excel file, the “G2006CHF_table” worksheet must also be copied to maintain proper linkage.

Power distribution data that is need for the Checker program was manually extracted from File No. 12 of Table 25.1 and copied to cells B41, C41, and B80 through C103. Cells B41 and C41 contain the azimuthal peak-to-average power ratios for two fuel plates that bound the channel. When only one fuel plate bounds the channel, the same value must be entered into both cells. Cells

B80 through B103 contains the axial power distribution of the plate on the concave side to the channel. Cells C80 through C103 contains the axial power distribution of the plate on the convex side of the channel. When there is only one fuel plate that bounds the channel, only the column of values for that plate is needed and the other column is ignored. File No. 12 was generated by separate neutron physics analysis. The data in this file is used to generate File No. 2, which is a PLTEMP/ANL input file. Because the power distribution is extracted directly for File No. 12, the Checker program also helps to verify that the data in File No. 2 was assembled correctly.

The Checker program input also includes 1) for each fuel plate that bounds the channel, a film temperature rise hot channel factor and a fuel plate heat flux hot channel factor, 2) a bulk coolant temperature hot channel factor, 3) the new velocity hot channel factor, and 4) the new heated diameter factor. Note that the five values of items 1 and 2 that are used in the Checker program do not include the fuel plate azimuthal peak-to-average heat flux factor that is included in the PLTEMP/ANL code hot channel input. These peak-to-average factors are included separately in cells B41 and C41 of the Checker program. Items 1 through 4 are obtained with the aid of the "Hot Chan Factor CD-35 (2018)" worksheet of File No. 8 of Table 25.1. The channel number (select from 1 through 24) is entered in cell B35. The burnup is entered in cell B36. (For core state 8A1, assembly 7, with 77 MW days of burnup, has the FIR limiting channel, channel 23, and assembly 1, with 0 MW days of burnup, has the CHF ratio limiting channel, channel 24.) In two steps, the seven values that are needed for each application of the Checker program are copied from cells D32 through I32 of the "Hot Chan Factor CD-35 (2018)" worksheet. For six of the seven values needed for the FIR-limiting case, set cell B35 to 23 and cell B36 to 77 and then copy cells F5 through K5 to cells F5 through K5, respectively, of the Checker program application worksheet. Note that the velocity hot channel factor in the "Hot Chan Factor CD-35 (2018)" worksheet and copied to cell J5 of the Checker program is the reciprocal of what is defined in the PLTEMP/ANL code. However, it is used in the Checker program in cell B63, which is the reciprocal of cell J5 in the Checker program. For the seventh parameter, set cell B35 in the "Hot Chan Factor CD-35 (2018)" worksheet to 22 instead of 23 and copy cell G32 to cell I4 of the Checker program. For the CHF limiting channel application of the Checker program, the process is repeated with cell B36 of the "Hot Chan Factor CD-35 (2018)" worksheet set to 0 and cell B35 first set to 24 and then to 23.

The Checker program calculates the ratio of its prediction for each of the CHF and CHFR quantities to its counterpart from the PLTEMP/ANL output. Among the 72 ratios of CHFR, the smallest is 0.996 and the largest is 1.003. Among the 48 ratios CHF, the smallest is 0.998 and the largest is 1.002. The detailed results of comparison are given in an Excel spreadsheet, the 8th. file of Table 25.1 (filename Ticket_15_verification_032218.xlsx). Thus, there is very good agreement between the Checker program predictions and the PLTEMP/ANL predictions for CHF and CHFR.

25.4 Conclusions

All of the values of the two new input factors are correctly represented in the PLTEMP/ANL output, flow instability ratio is calculated correctly for all 192 coolant channels in the model, and CHF and CHF ratio are calculated correctly. Thus, it can be concluded with reasonable certainty that the two new factors are implemented in the PLTEMP/ANL code correctly.

25.5 REFERENCES

1. E. E. Feldman, et al., Technical Basis in Support of the Conversion of the University o Missouri Research Reactor (MURR) Core from Highly-Enriched to Low-Enriched Uranium – Steady-State Thermal-Hydraulic Analysis, ANL/RERTR/TM-12-37, Rev. 1, January 2013.

Table 25.1 Key Files Used in the Verification of Two New HCFs

File No.	File Description	File Name
1	PLTEMP/ANL main input file	C35_8A1_t145_f3300_p75_fir_6_Local_HCFs.inp
2	PLTEMP/ANL input power distribution	C35_8A1_t145_f3300_p75_fir.power
3	PLTEMP/ANL output file	C35_8A1_t145_f3300_p75_fir_6_Local_HCFs.out
4	Python3 script to extract channel exit temperatures from File No. 3	Find_Channel_Exit_Temps_020918.py
5	Python3 script to extract flow instability ratios from File No. 3	Find_FIRs_021518.py
6	Extracted channel exit coolant temperatures	Tout.inp
7	Extracted flow instability ratios	FIRs.inp
8	Excel Spreadsheet (contains Checker program)	Ticket_15_verification_032218.xlsx
9	Python2 script to extract data from File No. 3 to use in Checker program	pltemp_hotchan_analyzer
10	Data for FIR-limiting channel extracted from File No. 3 by File No. 9 to use in Checker program.	C35_8A1_t145_f3300_p75_fir_6_Local_HCFs_py_hca_fir.out
11	Data for CHF-limiting channel extracted from File No. 3 by File No. 9 to use in Checker program.	C35_8A1_t145_f3300_p75_fir_6_Local_HCFs_py_hca_chf.out
12	Neutron physics file used to obtain power distributions for input to PLTEMP/ANL code.	C35_8A1_processed_tallies

26 Verification and Validation of Heat Transfer with Lateral Conduction Option in PLTEMP/ANL Code V4.3

26.1 Introduction

The verification and validation work reported here was done in October 2018. A new capability of lateral heat conduction has been implemented in PTLEMP/ANL V4.3 code to be released. The verification of the numerical method for calculating temperature distribution with lateral heat conduction in fuel plates was already completed and reported in [1]. To fulfill the verification and validation requirement, a comparison between PLTEMP/ANL and COMSOL calculations of a test case is performed and presented in this memorandum. In addition, the PLTEMP/ANL model is run with the search option to confirm that the new capability of lateral heat conduction works correctly under this option.

26.2 Test Problem and Models

The test problem includes a typical high performance research reactor (HPRR) fuel plate that is cooled by two adjacent coolant channels as shown in Figure 26.1. The heat generated in fuel meat is described by the combination of an axial distribution and a symmetric lateral power distribution. The geometry parameters, thermal conductivities of solid materials, and flow conditions of the test problem are provided in Table 26.1.

Figure 26.2a presents the cross-section of PLTEMP/ANL model. The meshing includes 10 axial and 72 lateral nodes. The Dittus Boelter correlation improved to handle large film temperature rise is used for the heat transfer coefficient. On the other hand, COMSOL model (Figure 26.2b) simulates only a quarter of test problem using about 1.6 million mesh elements and K-ε turbulent model.

To evaluate the performance of the new lateral conduction capability under the search option of the code, a new PLTEMP/ANL model is created by modifying the original model with the search option activated. This new model will be run to search for the plate power that provides the same maximum cladding temperature as predicted by the original model. Table 26.2 presents the input parameters used for the search option.

26.3 Comparison between PLTEMP/ANL and COMSOL Calculations

First, it is necessary to confirm that the energy depositions in both models are the same. This can be done by checking the heat balance (Table 26.3) and power density profiles (Figure 26.3). The presented data show that the heat balance is correct and the power distribution is similar in both models.

Secondly, the comparisons between the obtained temperatures profiles are performed. Table 26.4 presents the value and location of peak fuel temperatures obtained with PLTEMP/ANL and COMSOL. It can be seen that the obtained peak temperatures agree to each other within 1.4%. The location data include a difference of 5 cm in the axial direction but this is actually because of the coarse axial mesh size of 10 cm used by PLTEMP/ANL model as can be seen in Figure 26.3.

Accepting the difference in axial location, the 3D temperature profiles including these peak fuel temperatures are compared. Figure 26.4 shows that PLTEMP/ANL and COMSOL results agree very well to each other.

26.4 Checking the Search Option of the Code

As shown in Table 26.5, the PLTEMP/ANL model using search option finds the same plate power as specified in the original model to match the maximum clad surface temperature. The very good agreements between two models in other limiting thermal hydraulic data as well as their corresponding locations help to confirm that the new lateral conduction capability works correctly under the search option.

26.5 Conclusion

A validation of temperature distribution calculated by the new lateral heat conduction capability of PLTEMP/ANL has been performed using COMSOL calculation. The obtained data show very good agreements between these two codes. This confirms that the new lateral heat conduction capability can provide high accurate temperatures that are comparable to the CFD calculations. The comparison between PLTEMP/ANL calculation with and without using the search option also shows that the new capability works correctly under this option. The reactor safety margins like ONBR, OFIR, and CHFR, without and with hot channel factors, remain to be verified.

26.6 REFERENCE

1. M. Kalimullah, A. P. Olson, and E. E. Feldman, unpublished work, Argonne National Laboratory, Argonne, IL, USA (May 28, 2016).

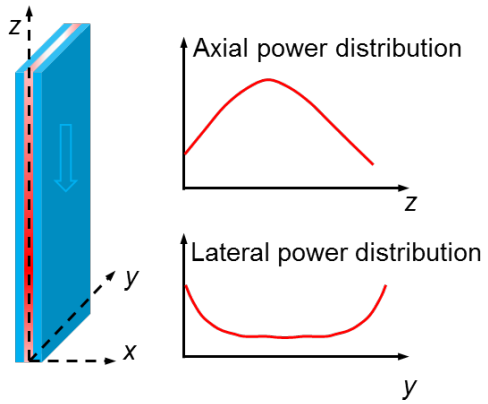

Figure 26.1. Test Problem Geometry

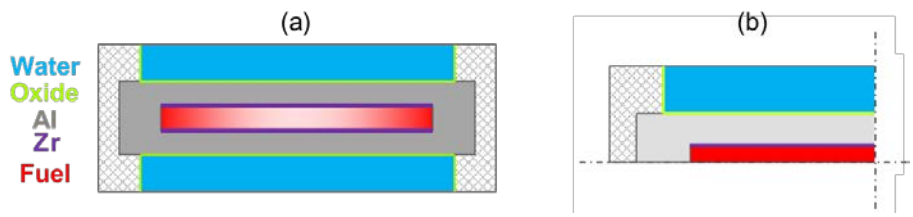

Figure 26.2. Cross-sections of (a) PLTEMP/ANL Model and (b) COMSOL Model

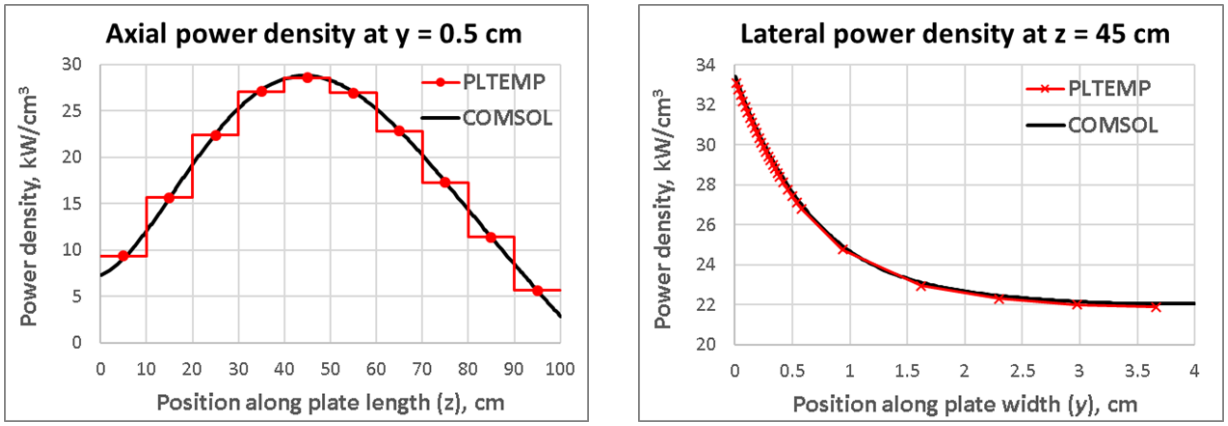

Figure 26.3. Power Distribution

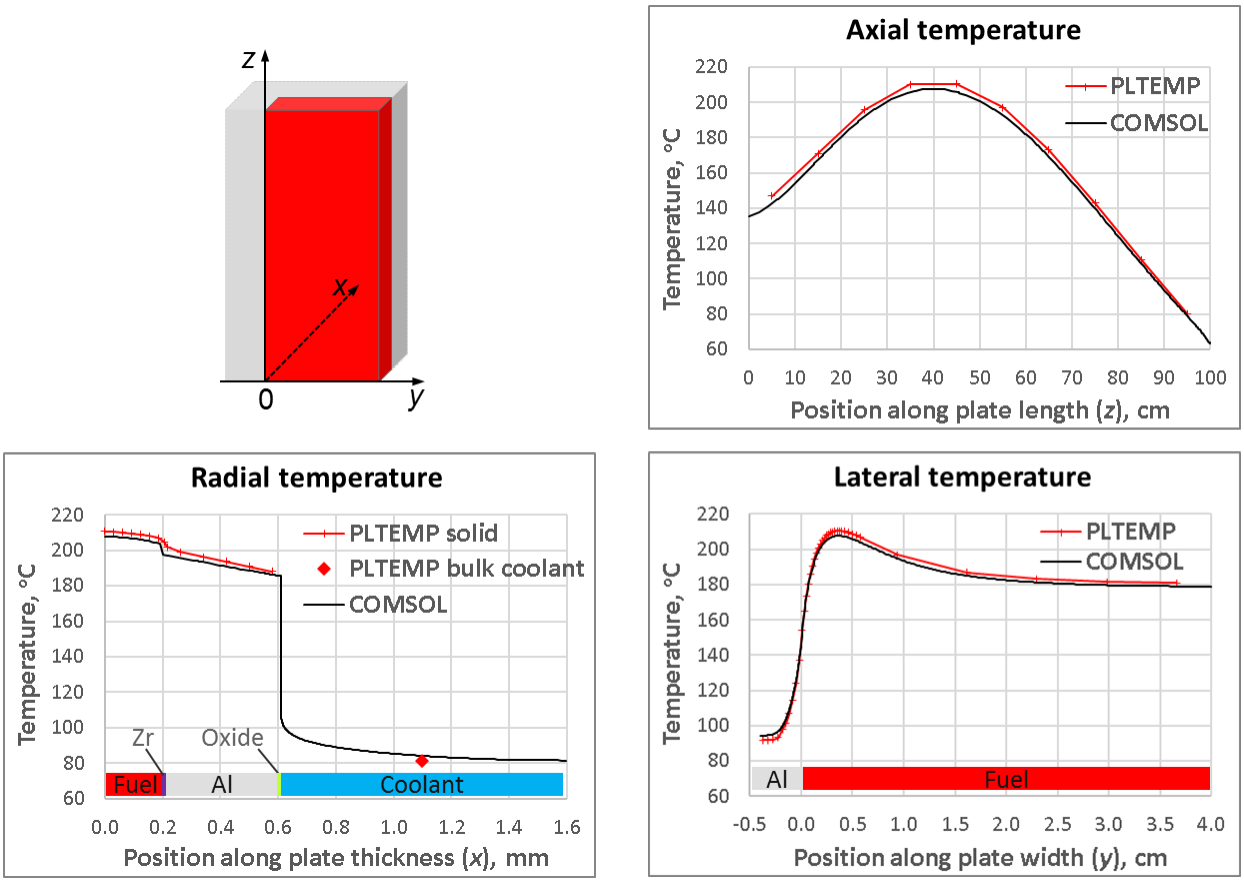

Figure 26.4. Comparison of Temperature Profiles

Table 26.1. Test Problem Specifications

Geometry Parameters [m]	
Fuel thickness	4.0E-4
Zr thickness	2.0E-5
Clad thickness	4.0E-4
Oxide layer thickness	2.0E-5
Channel thickness, m	1.0E-3
Side plate width	6.0E-3
Unfuel part width	2.0E-3
Fuel width	8.0E-2
Fueled length	1.0E+0
Solid Thermal Conductivity [W/m-ºC]	
Fuel meat	130.0
Zirconium	20.0
Aluminum	180.0
Oxide layer	2.5
Side plate (Aluminum)	180.0
Flow Conditions	
Inlet temperature, ºC	50.0
Inlet pressure, kPa	2.5
Channel flow rate, kg/s	1.2
Plate power, MW	0.5

Table 26.2. Input Parameter Used for the Search Option of PLTEMP/ANL Model

Lowest power of the code input datum varied in the search, MW	0.001
Highest power of the code input datum varied in the search, MW	1.000
Target maximum clad temperature (predicted by original model), ºC	189.009

Table 26.3. Heat balance

Parameters	PLTEMP/ANL	COMSOL
Model power, kW	500	125.0
Model flowrate, kg/s	2.4	0.6
Average inlet temp., ^{o}C	50.0	50.0
Average outlet temp., ^{o}C	99.6	99.7

Table 26.4. Comparison Between the Peak Fuel Temperatures and its Locations

Location	PLTEMP	COMSOL
x, cm	0.0	0.0
y, cm	0.37	0.37
z, cm	40.0	45.0
Temp., ^{o}C	207.6	210.5

Table 26.5. Comparison Between PLTEMP/ANL Models With and Without the Search Option

Parameter	PLTEMP Model	Value	Lateral Mesh	Axial Mesh
Max. coolant temperature, ^{o}C	Original	109.224	30	11
	Search option	109.224	30	11
Max. cladding surface temperature, ^{o}C	Original	189.009	30	7
	Search option	189.009	30	7
Max. fuel temperature, ^{o}C	Original	210.507	29	6
	Search option	210.506	29	6
Max. heat flux, MW/m^2	Original	9.259	30	6
	Search option	9.259	30	6
Min. ONBR	Original	1.790	30	7
	Search option	1.790	30	7
Min. OFIR	Original	2.412	11	11
	Search option	2.412	11	11
Min. CHFR	Original	3.672	30	7
	Search option	3.672	30	7
Plate power, MW	Original	0.50000	-	-
	Search option	0.50000	-	-

27 Closing Remarks

The verification and validation (V&V) work documented in this report was performed over several years, as the code development progressed. Not all verification work done by the developers was ever documented. The report is a collection of the V&V work done and documented for 16 frequently used capabilities of the code. The latest version of the code is PLTEMP/ANL V4.3 to be released shortly. Throughout the code development, in order to verify the code after a code modification, an automated UNIX script was used to routinely run dozens (now 46) of standard test problems, for the purpose of comparing each problem's new results with the older saved results of an earlier version of the code. After briefly describing (in Section 1.1) the code and its limitations, Section 1.2 provides a thermal-hydraulic analysis procedure recommended to guard against modeling error, followed by an overview of the verification and validation of the 16 frequently used code capabilities. On the basis of this document, these 16 capabilities of the code are believed to be adequately verified and validated.

Nuclear Engineering Division
Argonne National Laboratory
9700 South Cass Avenue, Bldg 208
Argonne, IL 60439
www.anl.gov

Argonne National Laboratory is a U.S. Department of Energy
laboratory managed by UChicago Argonne, LLC